AD-A166 176 UNITED STATES AIR FORCE SUMMER FACULTY RESEARCH PROGRAM 1/13
1985 TECHNICAL RE (U) UNIVERSAL ENERGY SYSTEMS INC
DAYTON OH R C DARRAH ET AL. DEC 85 AFOSR-TR-86-0139
UNCLASSIFIED F49620-85-C-0013 F/G 5/9 NL

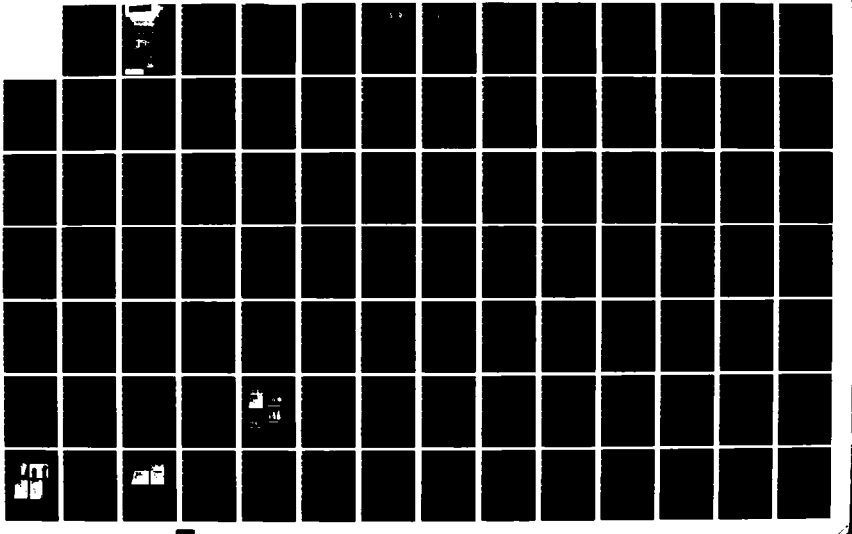

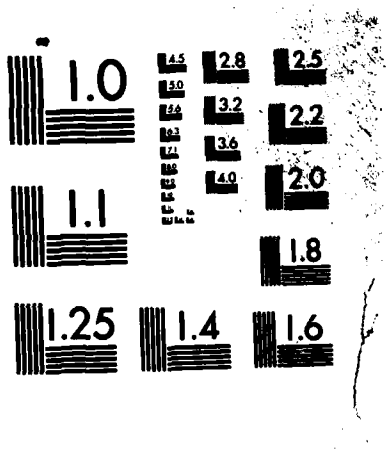

MICROCOPY RESOLUTION TEST CHART
NATIONAL BUREAU OF STANDARDS-1963-A

AFOSR-TR-86-0139

(1)

AIR FORCE OFFICE OF SCIENTIFIC RESEARCH

AD-A166 176

UNITED STATES AIR FORCE

SUMMER FACULTY RESEARCH PROGRAM

CONDUCTED BY
UNIVERSAL ENERGY SYSTEMS
U.E.S.

DTIC
ELECTE
APR 0 5 1986

1985 TECHNICAL REPORT

VOLUME 1 OF 3

RODNEY C. DARRAH
PROGRAM DIRECTOR, UES

SUSAN K. ESPY
PROGRAM ADMINISTRATOR

DISTRIBUTION STATEMENT A
Approved for public release;
Distribution Unlimited

86 4 1 140

UNCLASSIFIED

SECURITY CLASSIFICATION OF THIS PAGE

REPORT DOCUMENTATION PAGE

1a. REPORT SECURITY CLASSIFICATION: UNCLASSIFIED	1b. RESTRICTIVE MARKINGS
2a. SECURITY CLASSIFICATION AUTHORITY	3. DISTRIBUTION/AVAILABILITY OF REPORT: APPROVED FOR PUBLIC RELEASE; DISTRIBUTION UNLIMITED
2b. DECLASSIFICATION/DOWNGRADING SCHEDULE	
4. PERFORMING ORGANIZATION REPORT NUMBER(S)	5. MONITORING ORGANIZATION REPORT NUMBER(S): AFOSR-TR- 86-0139
6a. NAME OF PERFORMING ORGANIZATION: Universal Energy Systems; 6b. OFFICE SYMBOL (If applicable)	7a. NAME OF MONITORING ORGANIZATION: AFOSR/XOT
6c. ADDRESS (City, State and ZIP Code): 4401 Dayton-Xenia Rd. Dayton Ohio 45432	7b. ADDRESS (City, State and ZIP Code): Building 410 Bolling AFB, DC 20332-6448
8a. NAME OF FUNDING/SPONSORING ORGANIZATION: AFOSR; 8b. OFFICE SYMBOL (If applicable): XOT	9. PROCUREMENT INSTRUMENT IDENTIFICATION NUMBER: F49620-85-C-0013
8c. ADDRESS (City, State and ZIP Code): Building 410 Bolling AFB, DC 20332	10. SOURCE OF FUNDING NOS.

PROGRAM ELEMENT NO.	PROJECT NO.	TASK NO.	WORK UNIT NO.
61102F	2301	D5	

11. TITLE (Include Security Classification): United States Air Force Summer Faculty Research Program - Volume 1 - 1985

12. PERSONAL AUTHOR(S): Rodney C. Darrah, Susan K. Espy

13a. TYPE OF REPORT	13b. TIME COVERED	14. DATE OF REPORT (Yr., Mo., Day)	15. PAGE COUNT
Annual	FROM _____ TO _____	December 1985	

16. SUPPLEMENTARY NOTATION

17. COSATI CODES			18. SUBJECT TERMS (Continue on reverse if necessary and identify by block number)
FIELD	GROUP	SUB. GR.	

19. ABSTRACT (Continue on reverse if necessary and identify by block number)

See Attached

20. DISTRIBUTION/AVAILABILITY OF ABSTRACT: UNCLASSIFIED/UNLIMITED ☒ SAME AS RPT. ☐ DTIC USERS ☐	21. ABSTRACT SECURITY CLASSIFICATION: UNCLASSIFIED

22a. NAME OF RESPONSIBLE INDIVIDUAL	22b. TELEPHONE NUMBER (Include Area Code)	22c. OFFICE SYMBOL
Major Amos Otis , Program Manager	(202) 767-4970	XOT

DD FORM 1473, 83 APR EDITION OF 1 JAN 73 IS OBSOLETE.

Unclassified

SECURITY CLASSIFICATION OF THIS PAGE

TR-86-0135

The United States Air Force Graduate Student Summer Support Program (USAF-GSSSP) is conducted under the United States Air Force Summer Faculty Research Program. The program provides funds for selected graduate students to work at an appropriate Air Force Facility with a supervising professor who holds a concurrent Summer Faculty Research Program appointment or with a supervising Air Force Engineer. This is accomplished by the students being selected on a nationally advertised competitive basis for a ten-week assignment during the summer intersession period to perform research at Air Force laboratories/centers. Each assignment is in a subject area and at an Air Force facility mutually agreed upon by the students and the Air Force. In addition to compensation, travel and cost of living allowances are also paid. The USAF-GSSSP is sponsored by the Air Force Office of Scientific Research, Air Force Systems Command, United States Air Force, and is conducted by Universal Energy Systems, Inc.

The specific objectives of the 1985 USAF-GSSSP are:

(1) To provide a productive means for the graduate students to participate in research at the Air Force Weapons Laboratory;

(2) To stimulate continuing professional association among the Scholars and their professional peers in the Air Force;

(3) To further the research objectives of the United States Air Force;

(4) To enhance the research productivity and capabilities of the graduate students especially as these relate to Air Force technical interests.

During the summer of 1985, 92 graduate students participated. These researchers were assigned to 25 USAF laboratories/centers across the country. This two volume document is a compilation of the final reports written by the assigned students members about their summer research efforts.

UNCLASSIFIED

AFOSR-TR- 86-0139

Approved for public release;
distribution unlimited.

DTIC
ELECTE
APR 0 3 1986
S D
D

UNITED STATES AIR FORCE

SUMMER FACULTY RESEARCH PROGRAM

1985

PROGRAM TECHNICAL REPORT

UNIVERSAL ENERGY SYSTEMS, INC.

VOLUME I of III

Program Director, UES
Rodney C. Darrah

Program Administrator, UES
Susan K. Espy

Program Manager, AFOSR
Major Amos L. Otis

Submitted to

Air Force Office of Scientific Research

Bolling Air Force Base

Washington, DC

December 1985

DISTRIBUTION STATEMENT A
Approved for public release;
Distribution Unlimited

PREFACE

The United States Air Force Summer Faculty Research Program (USAF-SFRP) is a program designed to introduce university, college, and technical institute faculty members to Air Force research. This is accomplished by the faculty members being selected on a nationally advertised competitive basis for a ten-week assignment during the summer intersession period to perform research at Air Force laboratories/centers. Each assignment is in a subject area and at an Air Force facility mutually agreed upon by the faculty members and the Air Force. In addition to compensation, travel and cost of living allowances are also paid. The USAF-SFRP is sponsored by the Air Force Office of Scientific Research, Air Force Systems Command, United States Air Force, and is conducted by Universal Energy Systems, Inc.

The specific objectives of the 1985 USAF-SFRP are:

(1) To provide a productive means for Scientists and Engineers holding Ph.D. degrees to participate in research at the Air Force Weapons Laboratory;

(2) To stimulate continuing professional association among the Scholars and their professional peers in the Air Force;

(3) To further the research objectives of the United States Air Force;

(4) To enhance the research productivity and capabilities of Scientists and Engineers especially as these relate to Air Force technical interests.

During the summer of 1985, 154-faculty members participated. These researchers were assigned to 25 USAF laboratories/centers across the country. This three volume document is a compilation of the final reports written by the assigned faculty members about their summer research efforts.

LIST OF PARTICIPANTS

NAME/ADDRESS	DEGREE, SPECIALTY, LABORATORY ASSIGNED
Dr. Phillip Ackerman Assistant Professor University of Minnesota Dept. of Psychology Elliott Hall 75 E. River Rd. Minneapolis, Minnesota 55455 (612) 376-3139	Degree: Ph.D., Philosophy in Psychology, 1984 Specialty: Human Abilities, Cognitive Processes, Research Methodology Assigned: HRL/MO
Dr. Samuel Adams Associate Professor Iowa State University Dept. of Industrial Engineering 212 Marston Hall Ames, Iowa 50011 (515) 294-5065	Degree: Ph.D., Industrial Engineering 1966 Specialty: Human Factors Engineering (Ergonomics), Biomechanics Assigned: AMRL
Dr. Vernon Allen Professor Tennessee Technological Univ. Dept. of Chemistry Box 5055 Cookeville, Tennessee 38505 (615) 528-3425	Degree: Ph.D., Polymer Science, 1960 Specialty: Polymer Structure - Property Relationship Assigned: AFWAL/ML
Dr. Jihad Alsadek Assistant Professor & Chairman Tougaloo College Department of Economics Tougaloo, Mississippi 39174 (601) 956-4941	Degree: Ph.D., Economics, 1983 Specialty: Economics Assigned: HRL/OT
Dr. Deborah Armstrong Assistant Professor University of Texas Division of Life Sciences San Antonio, Texas 78285 (512) 691-4458	Degree: Ph.D., Neuroscience, 1982 Specialty: Neurophysiology Assigned: SAM

Accesion For
NTIS CRA&I
DTIC TAB
Unannounced
Justification
By
Dist ibution/
Availability Codes
Dist Avail and/or Special
A-1

Dr. Lucia Babcock
Assistant Professor
Louisiana State University
Department of Chemistry
Baton Rouge, Louisiana 70803
(504) 388-4694

Degree: Ph.D., Inorganic Chemistry, 1978
Specialty: Ion-Molecule Chemistry, Kinetics
Assigned: AFGL

Dr. Francesco Bacchialoni
Associate Professor
University of Lowell
Dept. of Electrical Engr.
1 University Avenue
Lowell, Massachusetts 01854
(617) 452-5000

Degree: Ph.D., Engineering, 1946
Specialty: Control Systems, Digital Signal Processing, Microprocessors
Assigned: AFGL

Dr. Mukul Banerjee
Professor
Meharry Medical College
Physiology Department
Nashville, Tennessee 37208
(615) 327-6288

Degree: Ph.D., Animal Physiology, 1964
Specialty: Respiratory Physiology, Environmental Physiology
Assigned: SAM

Dr. Rex Berney
Associate Professor
University of Dayton
Physics Department
300 College Park
Dayton, Ohio 45469
(513) 229-3012

Degree: Ph.D., Solid State Physics, 1978
Specialty: Digital Electronics, Photochromic Materials
Assigned: AFWAL/AL

Dr. Richard Bertrand
Professor of Chemistry
University of Colorado
Department of Chemistry
P. O. Box 7150
Colorado Springs, Colorado 80933-7150
(303) 593-3139

Degree: Ph.D., Chemistry, 1969
Specialty: NMR Spectroscopy, Atomic Spectroscopy
Assigned: FJSRL

Dr. Peter Binkert
Associate Professor
Oakland University
Linguistics and Classics
Department of Linguistics
Rochester, Michigan 48063
(313) 370-2175

Degree: Ph.D., Linguistics, 1970
Specialty: Linguistic Theory, Natural Language Understanding by Computers
Assigned: HRL/IO

Dr. Zinny Bond
Associate Professor
Ohio University
Linguistics Department
204C Gordy Hall
Athens, Ohio 45701
(614) 594-6539

Degree: Ph.D., Linguistics, 1971
Specialty: Speech Acoustics, Speech Perception
Assigned: AMRL

Dr. Kevin Bowyer
Assistant Professor
University of South Florida
Computer Science & Engr. Dept.
Tampa, Florida 33620
(813) 974-3032

Degree: Ph.D., Computer Science, 1980
Specialty: Software Engineering, Computer Architecture, Computer Networks
Assigned: AD

Dr. Eugene Brown
Associate Professor
Virginia Polytech Institute and State University
Blacksburg, Virginia 24060
(703) 961-7199

Degree: Ph.D., Mechanical Engineering, 1968
Specialty: Fluid Mechanics, Computational Fluid Dynamics
Assigned: WL

Dr. Linda Buehner
Assistant Professor
Wittenberg University
Education Department
P. O. Box 720
Springfield, Ohio 45501
(513) 327-6421

Degree: Ed. D., Curriculum and Instruction, 1983
Specialty: Learning and Developmental Handicaps, Reading
Assigned: HRL/LR

Dr. Connie Carrington
Assistant Professor
University of South Carolina
Mechanical Engineering Dept.
College of Engineering
Columbia, South Carolina 29208
(803) 777-7144

Degree: Ph.D., Engineering Mechanics, 1983
Specialty: Dynamics and Controls
Assigned: AFWAL/FDL

Dr. Robert Chamberlain
Assistant Professor
University of Alabama
Dept. of Aerospace Engr.
241 Hardaway Hall
University, Alabama 35486
(205) 348-7300

Degree: Ph.D., Aeronautical and Astronautical Engineering, 1984
Specialty: Computational Fluid Dynamics
Assigned: AFWAL/FDL

Dr. Jharna Chaudhuri
Assistant Professor
Wichita State University
Mechanical Engr. Department
Box 35
Wichita, Kansas 67208
(316) 689-3402

Degree: Ph.D., Materials Science, 1982
Specialty: Materials Science, Metallurgy, Thin Films, Electronic Materials
Assigned: AFWAL/AL

Dr. Lea Chen
Assistant Professor
The University of Iowa
Dept. Mechanical Engineering
2206 EB
Iowa City, Iowa 52242
(319) 353-5695

Degree: Ph.D., Mechanical Engineering, 1981
Specialty: Combustion
Assigned: AFWAL/APL

Dr. David Choate
Assistant Professor
Xavier University
Mathematics Department
New Orleans, Louisiana 70125
(504) 486-7411

Degree: Ph.D., Mathematics, 1982
Specialty: Algebra and Number Theory
Assigned: RADC

Dr. Karen Chou
Assistant Professor
Syracuse University
Dept. of Civil Engr.
Syracuse, New York 13210
(315) 423-3314

Degree: Ph.D., Philosophy, Structural Engineering, 1983
Specialty: Structural Engineering, Structural Reliability, Application of Probability and Statistics in Chemical Engineering
Assigned: ESC

Dr. Louis Chow
Assistant Professor
Washington State University
Mechanical Engineering Dept.
Pullman, Washington 99164-2920
(509) 335-1327

Degree: Ph.D., Mechanical Engineering, 1978
Specialty: Heat and Mass Transfer, Fluid Mechanics
Assigned: AFWAL/APL

Dr. Derald Chriss
Instructor
Southern University
Department of Chemistry
Baton Rouge, Louisiana 70813
(504) 771-3990

Degree: M.S., Chemistry, 1981
Specialty: NMR Spectroscopy, X-Ray Crystallography, Gas Chromatography, Magnetic Susceptibility Studies
Assigned: AFWAL/ML

Dr. David Chung Professor Howard University Department of Physics Washington, D.C. 20059 (202) 636-7903	Degree: Specialty: Assigned:	Ph.D., Solid State Physics, 1966 Fiber Optics Sensors, Ultrasound, Solid State Electronics RADC
Dr. Gale Clark Associate Professor Middle Tennessee State Univ. Chemistry Department P. O. Box 137 Murfreesboro, Tennessee 37132 (615) 898-2300	Degree: Specialty: Assigned:	Ph.D., Analytical Chemistry, 1968 HPLC using Electrochemical and Fluorescent Detection ESC
Dr. David Cochran Assistant Professor Clemson University Electrical and Computer Engineering Department Clemson, South Carolina 29631 (803) 656-3190	Degree: Specialty: Assigned:	Ph.D., Electrical Engineering, 1981 Solid State RADC
Dr. Alvin Compaan Professor Kansas State University Department of Physics Cardwell Hall Manhattan, Kansas 66506 (913) 532-6786	Degree: Specialty: Assigned:	Ph.D., Physics, 1971 Laser Interaction with Semiconductors AFWAL/AL
Dr. Thomas Connolly Professor Embry-Riddle Aeronautical University Aeronautical Science Regional Airport Daytona Beach, Florida 32014 (904) 252-5561	Degree: Specialty: Assigned:	Ed.D., Technical Education, 1979 Aviation Education, Instructional Technology HRL/OT
Dr. Hobert Corley Instructor Davis and Elkins College Computer Science Dept. Elkins, West Virginia 26241 (304) 636-1900	Degree: Specialty: Assigned:	M.S. Computer Science, 1980 Computer Science HRL/LR

Dr. Billy Covington
Assistant Professor
Sam Houston State University
Physics Department
Hunstville, Texas 77341
(409) 294-1606

Degree: Ph.D., Physics, 1978
Specialty: Solid State Physics
Assigned: AFWAL/ML

Dr. Dennis Cravens
Instructor
Vernon Regional Jr. College
Science and Math. Dept.
4400 College Drive
Vernon, Texas 76384
(817) 552-6291

Degree: Ph.D., Molecular Biophysics, 1977
Specialty: Mathematic Models, (numerical calculations)
Assigned: RPL

Dr. Parviz Dadras
Associate Professor
Wright State University
Mechanics Systems Engineering
Dayton, Ohio 45435
(513) 873-2944

Degree: Ph.D., Mechanical Engineering, 1972
Specialty: Mechanics, Deformation Processing, Material Properties
Assigned: AFWAL/ML

Dr. Charles Davis
Assistant Professor
University of Toledo
Department of Math.
Toledo, Ohio 43606
(419) 537-2297

Degree: Ph.D. Statistics, 1976
Specialty: Statistics
Assigned: AMRL

Dr. Vito DelVecchio
Professor of Biology
University of Scranton
Scranton, Pennsylvania 18510
(717) 961-6117

Degree: Ph.D., Biochemical Genetics, 1967
Specialty: Immunochemistry and Recombinant DNA Probes
Assigned: SAM

Dr. Hermann Donnert
Professor
Kansas State University
Department of Nuclear Engineering
Ward Hall
Manhattan, Kansas 66506-7039
(913) 532-5960

Degree: Ph.D., Mathematics and Physics, 1951
Specialty: Radiation Physics, Nuclear Weapon Effects, Plasma Physics
Assigned: FJSRL

Dr. Melvin Druelinger
Professor
University of Southern Colorado
Chemistry Department
2200 N. Bonforte Blvd.
Pueblo, Colorado 81001
(303) 549-2166

Degree: Ph.D. Chemistry, 1967
Specialty: Organic Chemistry (Mechanisms, Synthesis, Photochemistry, Energetic Materials Fluorinations)
Assigned: RPL

Dr. Charles Drummond, III
Associate Professor
The Ohio State University
Dept. of Ceramic Engineering
2041 College Road
Columbus, Ohio 43210
(614) 422-2960

Degree: Ph.D., Applied Physics, 1974
Specialty: Glass Structure and Properties and Composites
Assigned: AFWAL/ML

Dr. Leroy Eimers
Associate Professor
Cedarville College
Dept. of Science and Math.
Cedarville, Ohio 45314
(513) 766-2211

Degree: Ph.D., Theoretical Physics, 1970
Specialty: Mathematics, Physics
Assigned: AFWAL/APL

Dr. Hudson Eldridge
University of Central Arkansas
Physics Department, LSC 149
Conway, Arkansas 72032
(501) 450-3146

Degree: Ph.D., Nuclear Physics, 1967
Specialty: Experimental Nuclear Physics, Computing, Digital Electronics
Assigned: WL

Dr. Harry Emrick
Associate Professor
Colorado School of Mines
Dept. of Engineering
Golden, Colorado 80401
(303) 273-3675

Degree: Ph.D., Geodetic/Computer Science, 1973
Specialty: Positional Geodesy - Computer Applications
Assigned: FJSRL

Dr. John Erdei
Assistant Professor
University of Dayton
Dept. of Physics
300 College Park
Dayton, Ohio 45469
(513) 229-2318

Degree: Ph.D., Condensed Matter Theory, 1983
Specialty: Critical Phenomena and Field Theory
Assigned: AFWAL/APL

Dr. Dah-Nien Fan
Professor
Howard University
Dept. of Mechanical Engr.
Washington, D.C. 22059
(202) 636-6607

Degree: Ph.D., Aerospace Engineering, 1966
Specialty: Fluid Mechanics, Aerodynamics, Tensor Theory, Applied Mathematics
Assigned: AFWAL/FDL

Dr. Mack Felton
Chairman and Professor
Southern University at New Orleans
Biology Department
6400 Press Drive
New Orleans, Louisiana 70126
(504) 282-4401

Degree: Ph.D., Microbiology, 1973
Specialty: Virus Adsorption, Microbial Ecology, Physiology
Assigned: SAM

Dr. Edna Fiedler
St. Mary's University
Department Head - Psychology
One Camino Santa Maria
San Antonio, Texas 78284
(512) 436-3314

Degree: Ph.D., Psychology, 1972
Specialty: Social and Clinical Psychology
Assigned: HRL/MO

Dr. John Flach
Assistant Professor
University of Illinois at Urbana-Champaign
Aviation Research Laboratory
Willard Airport
Savoy, Illinois 61874
(217) 333-7749

Degree: Ph.D., Psychology, 1984
Specialty: Human Performance and Engineering Psychology
Assigned: AMRL

Dr. John Fleming
Assistant Professor
Texas A&M University
Dept. of Electrical Engr.
College Station, Texas 77843
(409) 845-7441

Degree: Ph.D. Electrical Engineering, 1977
Specialty: Systems, Control, Applied Mathematics, and Digital Signal Processing
Assigned: RADC

Dr. Dennis Flentge
Assistant Professor
Cedarville College
Math and Science Dept.
Cedarville, Ohio 45314
(513) 766-2211

Degree: Ph.D., Physical Chemistry, 1974
Specialty: Catalysis, Infrared Spectroscopy
Assigned: AFWAL/APL

Dr. Bessie Foster Professor Grambling State University Department of Physics Grambling, Louisiana 71245 (318) 274-2574	Degree: Specialty: Assigned:	Ph.D., Science, Radiological Science, 1968 Radiological Science (Health Physics and Radiation Biology) WL
Dr. James Gallas Assistant Professor University of Texas 1604 Loop/Rt. 10 San Antonio, Texas 78250 (512) 691-5446	Degree: Specialty: Assigned:	Ph.D., Physics, 1981 Interaction of Light (lasers) with Biological and Polymeric Materials SAM
Dr. Chester Gardner Professor University of Illinois Electrical and Computer Engr. 1406 W. Green Urbana, Illinois 61801 (217) 333-4682	Degree: Specialty: Assigned:	Ph.D., Electrical Engineering, 1973 Laser Remote Sensing, Optical Communications, Fiber Optics AFGL
Dr. Doris Ginn Associate Professor Jackson State University English Department 1400 John R. Lynch Street Jackson, Mississippi 39217 (601) 968-2116	Degree: Specialty: Assigned:	Ph.D., Linguistics, 1979 English as a Second Language and Sociolinguistics WL
Dr. Ramana Grandhi Assistant Professor Wright State University Mechanical Systems Engineering School of Engineering Dayton, Ohio 45435 (513) 873-2079	Degree: Specialty: Assigned:	Ph.D., Engineering Mechanics, 1984 Structural Optimization AFWAL/FDL
Dr. Alwin Green Associate Professor State University College - Buffalo Mathematics Department 1300 Elmwood Avenue Buffalo, New York 14222 (716) 878-4420	Degree: Specialty: Assigned:	Ph.D., Mathematics, 1972 Graph Theory, Networks, Combinatorics, Mathematics Modeling RADC

Mr. Mahesh Greywall
Professor
Wichita State University
Mechanical Engineering Dept.
Box 35
Wichita, Kansas 67208
(316) 689-3402

Degree: Ph.D., Mechanical Engineering, 1962
Specialty: Fluid Mechanics
Assigned: AFWAL/APL

Dr. Vijay Gupta
Associate Professor
Central State University
Chemistry Department
Wilberforce, Ohio 45384
(513) 376-6423

Degree: Ph.D., Chemistry, 1969
Specialty: Physical Chemistry
Assigned: AFWAL/ML

Dr. Barry Haack
Associate Professor
Ball State University
Dept. of Geography
Muncie, Indiana 47306
(317) 285-1776

Degree: Ph.D. Geography, 1977
Specialty: Digital Processing of Remotely Sensed Data
Assigned: RADC

Dr. Je-Chin Han
Associate Professor
Texas A&M University
Mechanical Engr. Department
College Station, Texas 77843
(409) 845-3738

Degree: Sc.D., Mechanical Engineering Heat Transfer, 1976
Specialty: Heat Transfer
Assigned: AFWAL/APL

Dr. Donald Hanson
Associate Professor
University of Mississippi
Electrical Engineering Dept.
University, Mississippi 38677
(601) 232-5389

Degree: Ph.D., Electromagnetics, 1976
Specialty: Electromagnetic Field Theory and MOSFET VLSI Design
Assigned: RADC

Dr. David Hart
Assistant Professor
University of Florida
Dept. of Mathematics
201 Walker Hall
Gainesville, Florida 32611
(904) 392-6162

Degree: Ph.D., Mathematics, 1980
Specialty: Nonlinear Differential Equations
Assigned: AFWAL/FDL

Dr. Albert Heaney
Professor
California State University
Electrical Engineering Dept.
Shaw and Cedar Avenues
Fresno, California 93740
(209) 294-2157

Degree: Ph.D. Electrical Engineering, 1972
Specialty: Computer Engineering
Assigned: RADC

Dr. Carolyn Heising
Associate Professor
Northeastern University
Industrial Engineering Dept.
360 Huntington Ave.
Boston, Massachusetts 02115
(617) 437-4948

Degree: Ph.D., Mechanical Engineering, 1978
Specialty: Reliability Analysis/Risk Assessment
Assigned: ESD

Dr. Troy Henson
Associate Professor
Louisiana Tech University
Electrical Engr. Dept.
Tech Station
Ruston, Louisiana 71272
(318) 257-4715

Degree: Ph.D. Electrical Engineering, 1975
Specialty: Communications and Control Systems Theory, Digital Signal Processing
Assigned: AMRL

Dr. Astor Herrell
Professor and Chairman
Winston-Salem State University
P. O. Box 13236
Winston-Salem, North Carolina 27110
(919) 761-2098

Degree: Ph.D., Inorganic Chemistry, 1973
Specialty: Chemistry and Physical Science
Assigned: AEDC

Dr. Albert Hsui
Associate Professor
University of Illinois
Dept. of Geology
245 Nat. Hist. Bldg.
1301 W. Green Street
Urbana, Illinois 61801
(217) 333-7732

Degree: Ph.D., Geophysics and Mechanics, 1972
Specialty: Geophysics, Applied Mathematics, Computer Simulation
Assigned: AFGL

Dr. Clifford Johnston
Assistant Professor
University of Florida
Soil Science
2169 McCarty Hall
Gainesville, Florida 32611
(904) 392-1951

Degree: Ph.D., Soil Physical Chemistry, 1983
Specialty: Vibrational Spectroscopy (laser Raman and FTIR)
Assigned: ESC

Dr. Betty Jones
Associate Professor and
Director of the Institute
of Electron Microscopy
Morehouse College
Department of Biology
830 Westview Drive, S.W.
Atlanta, Georgia 30314
(404) 681-2800

Degree: Ph.D., Biology, 1978
Specialty: Medical Parasitology
Tropical Medicine and
Electron Microscopy
Assigned: SAM

Dr. Jeremy Jones
Assistant Professor
The University of West Florida
Systems Science Department
Pensacola, Florida 32514-0103
(904) 474-2551

Degree: M.S., Physics, 1970
Specialty: Artificial Intelligence,
Computer Science Department
Assigned: AFWAL/AL

Dr. Patrick Jones
Assistant Professor
The Ohio State University
Chemistry Department
140 W. 18th Avenue
Columbus, Ohio 43210
(614) 422-9489

Degree: Ph.D., Chemical Physics,
1980
Specialty: Chemical Dynamics
Assigned: AFWAL/AL

Dr. Walter Jones
Assistant Professor
University of Tennessee
Dept. of Engineering Science
and Mechanics
310 Perkins Hall
Knoxville, Tennessee 37996-2030
(615) 974-7684

Degree: Ph.D., Engineering
Mechanics, 1982
Specialty: Mechanics of Composite
Materials
Assigned: AFWAL/FDL

Dr. Prasad Kadaba
Professor
University of Kentucky
Electrical Engineering Dept.
Room 453 Anderson Hall
Lexington, Kentucky 40506
(606) 257-2966

Degree: Ph.D., Physics, 1950
Specialty: Dielectric Relaxation
and Magnetic Resonance:
Microwave and Millimet
Wave Measurements
Assigned: AFWAL/ML

Dr. James Kane
Associate Professor
Wright State University
Chemistry Department
Dayton, Ohio 45435
(513) 873-2352

Degree: Ph.D., Chemistry, 1960
Specialty: Organic, Physical Organic,
Polymer Chemistry
Assigned: AFWAL/ML

Dr. Amir Karimi Assistant Professor University of Texas San Antonio Division of Engineering San Antonio, Texas 78285 (512) 691-5514	Degree: Specialty: Assigned:	Ph.D. Mechanical Engineering, 1982 Thermal Sciences, Condensation, Heat Exchanger Design, Heat Transfer, Phase Change Processes, Metastable Thermodynamics SAM
Dr. Daisy Kimble Instructor Southern University Chemistry Department P. O. Box S.U. Baton Rouge, Louisiana 70813 (504) 771-3990	Degree: Specialty: Assigned:	B.S., Chemistry, 1974 Chemistry-Analytical FJSRL
Dr. David Kohfeld Professor Southern Illinois University at Edwardsville Edwardsville, Illinois 62026 (618) 692-2582	Degree: Specialty: Assigned:	Ph.D., Experimental Psychology, 1966 Human Performance and Reaction Time, Math Models HRL/OT
Dr. Stephan Kolitz Assistant Professor University of Massachusetts Boston Harbor Campus Boston, Massachusetts 02125 (617) 929-8051	Degree: Specialty: Assigned:	Ph.D. Industrial Engineering, 1983 Operations Research ESD
Dr. Lawrence Koons Professor Tuskegee Institute Chemistry Department Tuskegee Institute, Alabama 36088 (205) 727-8835	Degree: Specialty: Assigned:	Ph.D., Physical Chemistry, 1956 Electrochemistry FJSRL
Dr. Arthur Kovitz Professor Northwestern University Mechanical and Nuclear Engr. 2145 Sheridan Road Evanston, Illinois 60201 (312) 491-7066	Degree: Specialty: Assigned:	Ph.D., Aerospace Engineering, 1957 Fluid Mechanics, (Interfaces, Combustion, Computation) WL

Dr. Kurt Kraiger Assistant Professor University of Colorado at Denver Department of Psychology 1100 14th Street Denver, Colorado 80202 (303) 556-8351	Degree: Specialty: Assigned:	Ph.D., Industrial/ Organizational Psychology, 1983 I/O Psychology, Performance Appraisal, Job Attitudes, Meta-Analysis HRL/MO
Dr. Madakasira Krishna Professor South Carolina State College Mathematics and Computer Science Box 1814, State College Orangeburg, Souch Carolina 29117 (803) 536-7120	Degree: Specialty: Assigned:	Ph.D., Numerical Analysis, Fluid Mechanics Computer Science, 1974 Computational Fluid Mechanics, Numerical Analysis, Pde AD
Dr. Paul Lee Associate Professor North Carolina A&T State Univ. Dept. of Business Administration Greensboro, North Carolina 27411 (919) 379-7744	Degree: Specialty: Assigned:	Ph.D., Resource Economics, 1973 Statistics, Management Science and Computer Sciences LMDC
Dr. Benjamin Lev Professor and Chairman Temple University Department of Management School of Business Admin. Philadelphia, Pennsylvania 19122 (215) 787-8188	Degree: Specialty: Assigned:	Ph.D., Operations Research, 1970 Production Management, Mathematical Programming RADC
Dr. Edward Lewis Professor Belmont College Computer Information Systems/ Management Science 1900 Belmont Blvd. Nashville, Tennessee 37203 (615) 383-7001	Degree: Specialty: Assigned:	Ph.D., Met. Science (Opera- tions Research and Statistics), 1978 Mathematical Modeling, Decision Support, Statistical Analysis LMC
Dr. Michael Lewis Assistant Professor Troy State University CIS Department Troy, Alabama 36082 (205) 566-3000	Degree: Specialty: Assigned:	M.S., Computer and Information Science, 1985 Advanced Microcomputer Applications LMC

Dr. Philip Lewis
Professor
Auburn University
Department of Psychology
Auburn University, Alabama 36849
(205) 826-4424

Degree: Ph.D., Clinical Psychology, 1968
Specialty: Marital Dynamics, Personality Development, Leadership
Assigned: LMDC

Dr. Irene Little-Marenin
Assistant Professor
Wellesley College
Astronomy Department
Whitin Observatory
Wellesley, Massachusetts 02181
(617) 325-0320

Degree: Ph.D., Astrophysics, 1970
Specialty: Astrophysics, Cool Stars
Assigned: AFGL

Dr. Dar-Biau Liu
Associate Professor
Old Dominion University
Dept. of Computer Sciences
Norfolk, Virginia 23508
(804) 440-3901

Degree: Ph.D., Applied Mathematics and Computer Sciences, 1972
Specialty: Computer Science
Assigned: RADC

Dr. Carl Looney
Associate Professor
University of Nevada
EE/Computer Science Dept.
Reno, Nevada 89557-0030
(702) 784-6918

Degree: Ph.D., Mathematic Analysis, 1972
Specialty: Artifical Intelligence, Tracking, Filtering
Assigned: AFWAL/AL

Dr. James Marsh
Associate Professor
University of West Florida
Department of Physics
Pensacola, Florida 32514
(904) 474-2270

Degree: Ph.D., Physics, 1966
Specialty: Optics (Physical), Electromagnetic Theory
Assigned: AD

Dr. Charles Mastin
Professor
Mississippi State University
Mathematics and Stat. Dept.
Drawer MA
Mississippi State, Mississippi 39762
(601) 325-3414

Degree: Ph.D., Mathematics, 1969
Specialty: Computational Fluid Dynamics
Assigned: AEDC

Dr. Odis McDuff
Professor
The University of Alabama
Electrical Engineering
P. O. Box 6169
University, Alabama 35486
(205) 348-6351

Degree: Ph.D., Electrical Engineering, 1966
Specialty: Lasers and Optics, Electromagnetics
Assigned: SAM

Mr. Bernard McIntyre
Associate Professor
University of Houston
Electrical Electronics Dept.
University Park
4800 Calhoun St.
Houston, Texas 77004
(713) 749-4753

Degree: Ph.D., Solid State Physics, 1970
Specialty: Space Plasma Physics
Assigned: AFGL

Dr. Leathem Mehaffey
Associate Professor
Vassar College
Biology Department
Box 410
Poughkeepsie, New York 12601
(914) 452-7000

Degree: Ph.D., Biophysics, 1971
Specialty: Neurobiology and Physiology of Vision
Assigned: SAM

Dr. Ivor Mitchell
Professor
Marketing Department
Atlanta University
223 Chestnut Street, S.W.
Atlanta, Georgia 30337
(404) 681-0251

Degree: Ph.D., Marketing and Statistics, 1977
Specialty: Marketing, Statistics
Assigned: LMDC

Dr. James Moore
Professor
University of Arkansas
Civil Engineering Dept.
Fayetteville, Arizona 72701
(501) 575-6027

Degree: Ph.D., Environmental Health Engineering, 1972
Specialty: Environmental Engineering
Assigned: ESC

Dr. Osoma Mostafa
Associate Professor
California State University
Electronics Engineering Dept.
C. S. U. C. #930
Chico, California 95929
(916) 895-5374

Degree: Ph.D., Electrical Engineering, 1975
Specialty: Systems, Automation, Artificial Intelligence
Assigned: AD

Dr. Rex Moyer
Associate Professor
Trinity University
Biology Department
715 Stadium Drive
San Antonio, Texas 78284
(512) 736-7242

Degree: Ph.D., Microbiology, 1965
Specialty: Molecular Biology, Experimental Oncology
Assigned SAM

Dr. James Mrotek
Associate Professor
Meharry Medical College
Department of Physiology
1005 D. B. Todd Blvd.
Nashville, Tennessee 37208
(615) 327-6979

Degree: Ph.D., Biology, 1973
Specialty: Environmental Influences on Cultured Mammalian Cells, Endocrine Cell Intracellular Exchanges
Assigned: SAM

Dr. Maurice Neveu
Associate Professor
State University College of N.Y.
Chemistry Department
Fredonia, New York 14063
(716) 673-3285

Degree: Ph.D., Physical-Organic Chemistry, 1959
Specialty: Physical-Organic Chemistry, Synthetic Organic Chemistry, Chemical Kinetics, Reaction Mechanisms, Explosives, Aviation Fuels
Assigned: AD

Dr. Robert Niebuhr
Associate Professor
Auburn University
Dept. of Management
Auburn, Alabama 36849
(205) 826-4591

Degree: Ph.D., Management, 1977
Specialty: Management Processes, Organizational Behavior
Assigned: LMDC

Dr. Marion Noble
Professor
Kansas State University
Physical Education Dept.
203 Ahearn Gym
Manhattan, Kansas 66506
(913) 532-6765

Degree: Ph.D., Biomechanics, 1970
Specialty: Biomechanics
Assigned: AMRL

Dr. Robert O'Connell
Assistant Professor
University of Missouri-Columbia
Electrical and Engr. Dept.
Columbia, Missouri 65211
(314) 882-8373

Degree: Ph.D., Electrical Engineering, 1975
Specialty: Applied Optics, Laser Effects
Assigned: FJSRL

Dr. Ralph Oberly
Professor and Chairman
Marshall University
Physics Department
Huntington, West Virginia 25701
(304) 696-6738

Degree: Ph.D., Physics (Molecular Spectra), 1970
Specialty: Molecular Spectroscopy, Optical Devices
Assigned: AFWAL/APL

Dr. Won Park
Professor
Wright State University
Mathematics and Statistics Dept.
Dayton, Ohio 45435
(513) 873-2837

Degree: Ph.D., Mathematics, 1969
Specialty: Stochastic Processes, Time Series, Reliability
Assigned: AFWAL/AL

Dr. Desmond Penny
Assistant Professor
Southern Utah State College
Physical Science Department
Cedar City, Utah 84720
(801) 586-7708

Degree: Ph.D., Civil Engineering, 1975
Specialty: Continuum Mechanics
Assigned: ESC

Dr. John Pierce
Associate Professor
University of North Alabama
Department of Chemistry
Florence, Alabama 35632
(205) 766-4100

Degree: Ph.D., Environmental Health, 1978
Specialty: Thermal Absorption of Toxicants, Analytical Methods Development
Assigned: OEHL

Dr. Boake Plessy
Professor
Dillard University
Division of Natural Science
2601 Gentilly Blvd.
New Orleans, Louisiana 70122
(504) 283-8822

Degree: Ph.D., Physical Chemistry, 1974
Specialty: Biopolymers, Proteoglycans from Corneal Tissue
Assigned: SAM

Dr. Arnold Polak
Professor
University of Cincinnati
Dept. of Aerospace Engr. and Engr. Mechanics
ML 70
Cincinnati, Ohio 45221
(513) 475-5133

Degree: Ph.D., Aerospace Engineering, 1966
Specialty: Fluid Mechanics
Assigned: AFWAL/APL

Dr. Justin Poland
Associate Professor
University of Maine Orono
Mechanical Engineering Dept.
209 Boardman Hall
Orono, Maine 04469
(207) 581-2123

Degree: Ph.D., Mechanical Engineering, 1979
Specialty: Thermal Sciences, Thermodynamics, Heat Transfer, Fluid Mechanics
Assigned: AEDC

Dr. Kuldip Rattan
Associate Professor
Wright State University
Electrical Systems Engineering Department
Fawcett Hall, Room 354
Dayton, Ohio 45435
(513) 873-2497

Degree: Ph.D., Electrical Engineering, 1975
Specialty: Digital Control Systems
Assigned: AFWAL/FDL

Dr. Hemen Ray
Assistant Professor
North Carolina A&T State Univ.
Mechanical Engr. Dept.
112 Cherry Hall
Greensboro, North Carolina 27411
(919) 379-7621

Degree: Ph.D., Engineering Mechanics, 1979
Specialty: Advanced Composites
Assigned: AFWAL/FDL

Dr. John Renie
Assistant Professor
University of Illinois
Dept. of Mechanical and Industrial Engineering
1206 W. Green Street
Urbana, Illinois 61801
(217) 333-6199

Degree: Ph.D., Combustion/Engineering, 1982
Specialty: Combustion and Fluid Dynamics
Assigned: RPL

Dr. Michael Rhodes
Instructor
Clark College
Department of Physics
240 Brawley Drive, S.W.
Atlanta, Georgia 30314
(404) 681-3080

Degree: Ph,D., Physics, 1983
Specialty: Plasma Physics, Numerical Analysis
Assigned: AFGL

Dr. Robert Ricci
Professor and Chairman
Holy Cross College
Chemistry Department
Worcester, Massachusetts 01610
(617) 793-3380

Degree: Ph.D., Chemistry, 1961
Specialty: Physical Chemistry, Analytical Chemistry
Assigned: AFGL

Dr. James Riehl
Associate Professor
University of Missouri
Department of Chemistry
8001 Natural Bridge Road
St. Louis, Missouri 63121
(314) 553-5328

Degree: PH.D., Physical Chemistry, 1975
Specialty: Physical Chemistry, Theoretical Chemistry, Laser, Spectroscopy
Assigned: AFGL

Dr. Michael Ross
Associate Professor
Slippery Rock University
Computer Science Department
Slippery Rock, Pennsylvania 16057
(412) 794-7133

Degree: Ph.D., Applied Mathematics,
Specialty: Computer Simulation, Operating Systems, Numerical Analysis
Assigned: AMRL

Dr. Samuel Russell
Assistant Professor
University of South Carolina
Mechanical Engineering Dept.
Columbia, South Carolina 29208
(803) 777-3241

Degree: Ph.D., Engrineering Mechanics, 1982
Specialty: Nondestructive Testing of Composite Materials
Assigned: AFWAL/ML

Dr. Sally Sage
Assistant Professor
West Georgia College
Department of Math
and Computer Science
Carrollton, Georgia 30118
(404) 834-1380

Degree: M.S., Computer Science, 1979
Specialty: Programming Languages and Computer Simulation
Assigned: AD

Dr. Joseph Saliba
Assistant Professor
University of Dayton
Civil Engr. Dept.
300 College Park
Dayton, Ohio 45469
(513) 229-3847

Degree: Ph.D., Solid Mechanics, 1983
Specialty: Solid Mechanics - Structures
Assigned: AFWAL/FDL

Dr. Gordon Schrank
Associate Professor
St. Cloud State University
Dept. of Biology Sciences
St. Cloud, Minnesota 56301
(612) 255-2036

Degree: Ph.D., Medical Microbiology, 1974
Specialty: General Microbiology, Medical Microbiology, Electron Microscopy
Assigned: SAM

Dr. Ronald Sega
Assistant Professor
University of Colorado
Department of Electrical Engr.
Colorado Springs, Colorado 80933-7150
(303) 593-3510

Degree: Ph.D., Electrical Engineering, 1982
Specialty: Electromagnetics
Assigned: FJSRL

Dr. Paul Seybold
Professor
Wright State University
Chemistry Department
Dayton, Ohio 45435
(513) 873-2407

Degree: Ph.D., Biophysics, 1968
Specialty: Structure-Activity Relations
Assigned: AMRL

Dr. Shawky Shamma
Professor
University of West Florida
Pensacola, Florida 32504
(904) 474-2281

Degree: Ph.D., Applied Mathematics,
Specialty: Applied Mathematics
Assigned: AD

Dr. Ralph Sheets
Professor
Southwest Missouri State Univ.
Department of Chemistry
Springfield, Missouri 65804
(417) 836-5611

Degree: Ph.D., Physical Chemistry, 1971
Specialty: Chemistry (surface chemistry and catalysis environmental)
Assigned: OEHL

Dr. Kyle Siegrist
Assistant Professor
University of Alabama
Mathematics Department
Huntsville, Alabama 35899
(205) 895-6470

Degree: Ph.D., Applied Mathematics, 1979
Specialty: Probability and Stochastic Processes
Assigned: RADC

Dr. Ricardo Silva
Professor
California State University
18111 Nordhoff Street
Northridge, California 91330
(818) 885-3378

Degree: Ph.D., Chemistry, 1961
Specialty: Organic Chemistry, Synthesis and Analysis
Assigned: RPL

Dr. S. Ballou Skinner
Professor
University of South Carolina
Coastal Carolina College
Physics Department
P. O. Box 1954
Conway, South Carolina 29526
(803) 347-3161

Degree: Ph.D., Physics, 1970
Specialty: Nuclear and Radiation Physics, Gamma Ray Spectroscopy, Neutron Activation Analysis
Assigned: AEDC

Dr. Terrill Smith
Professor
Central State University
Chemistry Department
100 N. University Drive
Edmond, Oklahoma 73034
(405) 341-2980

Degree: Ph.D., Organic Chemistry, 1959
Specialty: Organic, Polymer, Fluorine, Industrial Chemistry
Assigned: AFWAL/ML

Dr. Siavash Sohrab
Assistant Professor
Northwestern University
MNE Department
Technical Institute
Evanston, Illinois 60201
(312) 491-3572

Degree: Ph.D., Engineering Physics, 1981
Specialty: Combustion
Assigned: RPL

Dr. Richard Stebbins
Assistant Professor
University of Southern Maine
Chemistry Department
96 Falmouth Street
360 Science Building
Portland, Maine 04103
(207) 780-4232

Degree: Ph.D., Physical Chemistry, 1970
Specialty: Analysis of Trace Organics by ECD Gas Chromatography
Assigned: OEHL

Dr. Bob Stewart
Assistant Professor
University of Cincinnati
Dept. of Mechanical Engr.
M.L. #72
Cincinnati, Ohio 45221
(513) 475-4781

Degree: Ph.D., Physics, 1981
Specialty: General Relativity, Thermodynamics, Biomechanics
Assigned: WL

Dr. Lowell Stockstill
Assistant Professor
Wittenberg University
Dept. of Business Administration
P. O. Box 720
Springfield, Ohio 45501
(513) 327-7903

Degree: J.D./MBA, Law, 1982
Specialty: Small Business Law
Assigned: BRMC

Dr. William Stone
Assistant Professor
Meharry Medical College
Dept. of Pediatrics
Nashville, Tennessee 37208
(615) 327-6506

Degree: Ph.D., Molecular and Cellular Biology, 1973
Specialty: Lipid Biochemistry, Nutrition, Hyperbaric Medicine
Assigned: SAM

Dr. James Sturm
Professor
Lehigh University
Department of Chemistry #6
Bethlehem, Pennsylvania 18015
(215) 861-3477

Degree: Ph.D., Physical Chemistry, 1957
Specialty: Photochemical Kinetics
Assigned: AFGL

Dr. Thomas Sudkamp
Assistant Professor
Wright State University
Computer Science Department
Dayton, Ohio 45435
(513) 873-2491

Degree: Ph.D., Mathematics, 1978
Specialty: Computer Science, Mathematics
Assigned: AFWAL/AL

Dr. William Sutton
Assistant Professor
University of Oklahoma
School of Aerospace
Mechanical and Nuclear Engr. Department
865 Asp Ave., Rm. 212
Norman, Oklahoma 73019
(405) 325-5011

Degree: Ph.D., Mechanical Engineering, 1981
Specialty: Heat Transfer, Thermal Radiation
Assigned: AEDC

Dr. Robert Swanson
Assistant Professor
Virginia Polytechnic Institute and State University
Materials Engineering Dept.
Blacksburg, Virginia 24061
(703) 961-5600

Degree: Ph.D., Metallurgical Engineering and Materials Science, 1983
Specialty: Fracture Mechanics, Environmental Cracking, Corrosion
Assigned: AFWAL/ML

Dr. Patrick Sweeney
Professor
University of Dayton
Engineering Management and Systems Dept.
KL 361
Dayton, Ohio 45469
(513) 229-2238

Degree: Ph.D., Mechanical Engineering, 1977
Specialty: Simulation, Costing, Management Systems
Assigned: BRMC

Dr. Charles Taylor
Professor
University of Florida
Dept. of Engineering Science
231 Aerospace Eng. Building
Gainesville, Florida 32611
(904) 392-0961

Degree: Ph.D., Theory and Application Mechanics, 1953
Specialty: Optical Methods of Experimental Stress Analysis
Assigned: AD

Dr. Joseph Tedsco
Assistant Professor
Auburn University
Dept. of Civil Engineering
210 Ramsay Hall
Auburn, Alabama 36849
(205) 826-4320

Degree: Ph.D., Civil Engineering, 1982
Specialty: Structural Dynamics; Concrete Structures
Assigned: ESC

Dr. Walter Trafton
Associate Professor
Gallaudet College
Chemistry Department
Kendall Green
Washington D.C. 20002
(202) 651-5536

Degree: Ph.D., Chemistry, 1973
Specialty: Physical Chemistry, Kinetics and Gas Phase Reactions
Assigned: FJSRL

Dr. Larry Vardiman
Associate Professor and
Dept. Chairman
Christian Heritage College
Physical Sciences Dept.
2100 Greenfield Drive
El Cajon, California 92021
(619) 440-3043

Degree: Ph.D., Atmospheric Science, 1974
Specialty: Cloud Physics and Weather Modification
Assigned: AFGL

Dr. Daniel Voss
Assistant Professor
Wright State University
Dept. of Math and Stat.
Dayton, Ohio 45435
(513) 873-2958

Degree: Ph.D., Statistics, 1984
Specialty: Experimental Design, Confounding in Factorial Exper's
Assigned: LC

Dr. Christian Wagner
Assistant Professor
Oakland University
School of Engineering and
Computer Science
138 Dodge Hall
Rochester, Michigan 48063
(313) 370-2215

Degree: Ph.D., Educational Psychology and Artificial Intelligence, 1982
Specialty: Artificial Intelligence, Cognitive Psychology
Assigned: HRL/IO

Dr. Richard Walker
Chairman
Miami University
Aeronautics Department
219 Culler Hall
Oxford, Ohio 45056
(513) 529-5919

Degree: Ph.D., Aerospace Engineering, 1970
Specialty: Aircraft Design, Performance Analysis, Propulsion Aerodynamics
Assigned: AFWAL/FDL

Dr. Doris Walker-Dalhouse
Director of Independent/Home Study Programs
Associate Professor of Reading
Jackson State University
P. O. Box 17120
Jackson, Mississippi 39217
(601) 968-2378

Degree: Ph.D., Reading Education, 1977
Specialty: Education
Assigned: WL

Dr. Yin-min Wei
Professor
Ohio University
Computer Science Dept.
Morton Hall 573
Athens, Ohio 45701
(614) 594-6574

Degree: Ph.D., Electrical Engineering, 1966
Specialty: Signal Processing
Assigned: AMRL

Dr. Isaac Weiss
Associate Professor
Wright State University
School of Engineering
Dayton, Ohio 45435
(513) 873-3021

Degree: Ph.D., Metallurgy, 1978
Specialty: Thermomechanical Processing, Deformation Processing
Assigned: AFWAL/ML

Dr. Shih-sung Wen
Professor
Jackson State University
Psychology Department
1325 J. R. Lynch Street
Jackson, Mississippi 39217
(601) 968-2371

Degree: Ph.D., Educational Psychology, 1971
Specialty: Cognitive Psychology, Psychological Testing, Statistics
Assigned: SAM

Dr. David Wilson
Associate Professor
University of Florida
Mathematics Department
311 Walker Hall
Gainesville, Florida 32611
(904) 392-6035

Degree: Ph.D., Mathematics, Rutgers, 1969
Specialty: Geometric Topology, Grid Generation (Computer Flight Dynamics)
Assigned: AD

Dr. Jesse Williams
Associate Professor
Cheyney University
Math/CIS Department
Cheyney, Pennsylvania 19319
(215) 399-2348

Degree: M.B.A., Computer Science, 1975
Specialty: Computer Science
Assigned: LMC

Dr. Arthur Woodrum
Head, Dept. of Physics
Georgia Southern College
Landrum Box 8031
Statesboro, Georgia 30460
(912) 681-5292

Degree: Ph.D., Physics, 1968
Specialty: Atmospheric Physics
Assigned: SAM

Dr. Billy Wooten
Associate Professor
Brown University
Psychology Department
89 Waterman Street
Providence, Rhode Island 02912
(401) 863-2330

Degree: Ph.D., Experimental Psychology, 1970
Specialty: Color Vision
Assigned: HRL/OT

Dr. Carl Wulfman
Chairman
University of the Pacific
Department of Physics
Stockton, California 95211
(209) 946-2220

Degree: Ph.D., Organic Chemistry, 1957
Specialty: Chemical Physics
Assigned: FJSRL

Dr. Hsi-Han Yeh
Associate Professor
University of Kentucky
Dept. of E.E.
Lexington, Kentucky 40506
(606) 257-4289

Degree: Ph.D., Electrical Engineering, 1967
Specialty: Multivariable Control
Assigned: AFWAL/FDL

Dr. Juin Yu
Professor
West Virginia Institute
of Technology
Mechanical Engineering Department
Montgomery, West Virginia 25136
(304) 442-3248

Degree: Ph.D., Mechanical Engineering
Specialty: Thermofluid Processes
Assigned: AEDC

APPENDIX II C

PARTICIPANT LABORATORY ASSIGNMENT

C. PARTICIPANT LABORATORY ASSIGNMENT (Page 1)

1985 USAF/UES SUMMER FACULTY RESEARCH PROGRAM

AERO PROPULSION LABORATORY (AFWAL/APL)
(Wright-Patterson Air Force Base)

1. Lea Der Chen
2. Louis C. Chow
3. Leroy E. Eimers
4. John E. Erdei
5. Dennis R. Flentge
6. Mahesh S. Greywall
7. Je-Chen Han
8. Ralph E. Oberly
9. Arnold Polak

AEROSPACE MEDICAL RESEARCH LABORATORY (AMRL)
(Wright-Patterson Air Force Base)

1. Samuel K. Adams
2. Zinny S. Bond
3. Charles B. Davis
4. John M. Flach
5. Troy F. Henson
6. Marion L. Noble
7. Michael D. Ross
8. Paul G. Seybold
9. Yin-min Wei

ARMAMENT LABORATORY (AD)
(Eglin Air Force Base)

1. Kevin W. Bowyer
2. Madakasira V. Krishna
3. James S. Marsh
4. Osana M. Mostafa
5. Maurice C. Neveu
6. Sally A. Sage
7. Shawky E. Shamma
8. Charles E. Taylor
9. David C. Wilson

ARNOLD ENGINEERING DEVELOPMENT CENTER (AEDC)
(Arnold Air Force Station)

1. Astor Y. Herrell
2. Charles W. Mastin
3. Justin H. Poland
4. S. Ballou Skinner
5. William H. Sutton
6. Juin S. Yu

AVIONICS LABORATORY (AFWAL/AL)
(Wright-Patterson Air Force Base)

1. Rex Barney
2. Jharna Chaudhuri
3. Alvin Compaan
4. Patrick Jones
5. Jeremy Jones
6. Carl Looney
7. Won Park
8. Thomas Sudkamp

BUSINESS RESEARCH MANAGEMENT CENTER (BRMC)
(Wright-Patterson Air Force Base)

1. Lowell E. Stockstill
2. Patrick J. Sweeney

C. PARTICIPANT LABORATORY ASSIGNMENT (Page 2)

ELECTRONICS SYSTEMS DIVISION (ESD)
(Hanscom Air Force Base)

1. Carolyn D. Heising
2. Stephan E. Kolitz

ENGINEERING AND SERVICES CENTER (ESC)
(Tyndall Air Force Base)

1. Karen Chai-Kwan Chou
2. Gale J. Clark
3. Clifford T. Johnston
4. Desmond N. Penny
5. Joseph W. Tedesco

FLIGHT DYNAMICS LABORATORY (AFWAL/FDL)
(Wright-Patterson Air Force Base)

1. Connie K. Carrington
2. Robert R. Chamberlain
3. Dah-Nien Fan
4. ramana V. Grandhi
5. David C. Hart
6. Walter F. Jones
7. Kuldip S. Rattan
8. Hemen Ray
9. Joseph E. Saliba
10. Richard C. Walker
11. Hsi-Han Yeh

FRANK J. SEILER RESEARCH LABORATORY (FJSRL)
(USAF Academy)

1. Richard D. Bertrand
2. Hermann J. Donnert
3. Harry W. Emrick
4. Daisy W. Kimble
5. Lawrence F. Koons
6. Ronald M. Sega
7. Walter E. Trafton, Jr.
8. Carl E. Wulfman

GEOPHYSICS LABORATORY (AFGL)
(Hanscom Air Force Base)

1. Lucia M. Babcock
2. Francesco L. Bacchialoni
3. Chester S. Gardner
4. Albert Tong-Kwan Hsui
5. Irene R. Little-Marenin
6. Bernard McIntyre
7. Michael B. Rhodes
8. Robert W. Ricci
9. James P. Riehl
10. James E. Strum
11. Larry Vardiman

HUMAN RESOURCES LABORATORY/LR (HRL/LR)
(Wright-Patterson Air Force Base)

1. Linda J. Buehner
2. Hobert H. Corley

HUMAN RESOURCES LABORATORY/OT (HRL/OT)
(Williams Air Force Base)

1. Thomas J. Connolly
2. David L. Kohfeld
3. Billy R. Wooten

C. PARTICIPANT LABORATORY ASSIGNMENT (Page 3)

HUMAN RESOURCES LABORATORY/MO (HRL/MO)
(Brooks Air Force Base)

1. Phillip L. Ackerman
2. Jihad A. Alsadek
3. Edna R. Fiedler
4. Kurt Kraiger

HUMAN RESOURCES LABORATORY/ID (HRL/ID)
(Lowry Air Force Base)

1. Peter J. Binkert
2. Christian C. Wagner

LEADERSHIP AND MANAGEMENT DEVELOPMENT CENTER (LMDC)
(Maxwell Air Force Base)

1. Paul S.T. Lee
2. Philip M. Lewis
3. Ivor S. Mitchell
4. Robert E. Niebuhr

LOGISTICS COMMAND (LC)
(Wright-Patterson Air Force Base)

1. Daniel T. Voss

LOGISTICS MANAGEMENT CENTER (LMC)
(Gunter Air Force Base)

1. Michael M. Lewis
2. Edward N. Lewis
3. Jesse Williams

MATERIALS LABORATORY (AFWAL/ML)
(Wright-Patterson Air Force Base)

1. Vernon R. Allen
2. Derald Chriss
3. Billy C. Covington
4. Parviz Dadras
5. Charles H. Drummond, III
6. Vijay K. Gupta
7. Prasad K. Kadaba
8. James J. Kane
9. Samuel S. Russell
10. Terrill D. Smith
11. Robert E. Swanson
12. Isaac Weiss

OCCUPATIONAL AND ENVIRONMENTAL HEALTH LABORATORY (OEHL)
(Brooks Air Force Base)

1. John T. Pierce
2. Ralph W. Sheets
3. Richard G. Stebbins

C. PARTICIPANT LABORATORY ASSIGNMENT (Page 4)

ROCKET PROPULSION LABORATORY (RPL)
(Edwards Air Force Base)

1. Dennis J. Cravens
2. Melvin L. Druelinger
3. John P. Renie
4. Ricardo A. Silva
5. Siavash H. Sohrab

ROME AIR DEVELOPMENT CENTER (RADC)
(Griffiss Air Force Base)

1. David B. Choate
2. David Y. Chung
3. David R. Cochran
4. John A. Fleming
5. Alwin C. Green
6. Barry N. Haack
7. Donald F. Hanson
5. Albert A. Heaney
6. Benjamin Lev
7. Dar-Biau Liu
8. Kyle T. Siegrist

SCHOOL OF AEROSPACE MEDICINE (SAM)
(Brooks Air Force Base)

1. Deborah L. Armstrong
2. Mukul R. Banerjee
3. Vito G. DelVecchio
4. Mack Felton
5. James M. Gallas
6. Betty R. Jones
7. Amir Karimi
8. Odis P. McDuff
9. Leathem Mehaffey
10. Rex C. Moyer
11. James J. Mrotek
12. Boake L. Plessy
13. Gordon D. Schrank
14. William L. Stone
15. Shih-sung Wen
16. Arthur Woodrum

WEAPONS LABORATORY (WL)
(Kirtland Air Force Base)

1. Eugene F. Brown
2. Hudson B. Eldridge
3. Bessie R. Foster
4. Doris O. Ginn
5. Arthur A. Kovitz
6. Robert M. O'Connell
7. Bob W. Stewart
8. Doris Walker-Dalhouse

RESEARCH REPORTS

1985 SUMMER FACULTY RESEARCH PROGRAM

Technical Report Number	Title	Professor
Volume I		
1	Individual Differences in Abilities, Learning, and Cognitive Processes	Dr. Phillip L. Ackerman
2	Maximum Voluntary Hand Grip Torque for Circular Electrical Connectors	Dr. Samuel Adams
3	Properties and Processing of a Perfluorinated Polyalkylene Linked Polyimide	Dr. Vernon R. Allen
4	Quantifying Experience in the Cost of Human Capital	Dr. Jihad A. Alsadek
5	The Effects of Raphe Stimulation and Iontophoresis of Serotonergic Agents on Granule Cell Activity in Rat Lateral Cerebellar Cortex	Dr. Deborah Armstrong
6	Temperature Dependence of Ion-Molecule Association Reactions: Halide Ion Addition Reactions	Dr. Lucia Badcock
7	Active Control of Flexible Structures	Dr. Francesco Bacchialoni
8	Gas Exchange in the Rabbit Using High Frequency Ventilation in High Altitude	Dr. Mukul R. Banerjee
9	Computer Automated Test Mirror Registration System for the Ring Laser Gyro	Dr. Rex L. Berney
10	^{27}Al Spin Lattic Relaxation Measurements in Alkylammonium-Chloroaluminate Room-Temperature Electrolytes	Dr. Richard Bertrand
11	Natural Language Understanding Using Residential Grammar and It's Use in Automatic Programming	Dr. Peter J. Binkert
12	Speech Effects of High Sustained Acceleration: A Preliminary Study	Dr. Zinny S. Bond

13	Automatic Determination of Object Orientation in 2-D Images	Dr. Kevin W. Bowyer
14	Stimulation of Jet Injection Using RAVEN	Dr. Eugene F. Brown
15	The Impact of Cognitive Styles & Subject Matter on Instructional Design	Dr. Linda J. Buehner
16	Polynomial Feedback Control for Robotic Manipulators	Dr. Connie K. Carrington
17	Modification and Evaluation of Heat Transfer Calculations Using the AFWAL PNS Code	Dr. Robert R. Chamberlain
18	Optical and X-Ray Topographic Characterization of Undoped Simi-Insulating GaAs	Dr. Jharna Chaudhuri
19	Visualization of Jet Flames	Dr. Lea D. Chen
20	Splines and the Fourier Transform	Dr. David B. Choate
21	Protection From Nonnuclear Weapons: A Probabilistic Approach	Dr. Karen C. Chou
22	Fluid Recirculation, Deployment, and Retraction of the Expandable Radiator	Dr. Louis Chow
23	Applications of Internal Reflection Spectroscopy to the Characterization of Thermoset Polymers	Dr. Derald Chriss
24	Applications of Fiber Optics of Low Temperatures	Dr. David Y. Chung
25	Evaluation of Selected Parameters Which Affect K_d When Measured Using HPLC Instrumentation	Dr. Gale J. Clark
26	Dipole Moment of InP in the Melt	Dr. David R. Cochran
27	Laser Raman Laboratory Research	Dr. Alvin D. Compaan
28	Aeronautical Decision-Making for Air Force Pilots	Dr. Thomas J. Connolly
29	Feasibility Study on the Logistics Operational Assessment Model	Dr. Hobert H. Corley
30	Photo-Hall Study of Doped and Undoped Semi-Insulating GaAs.	Dr. Billy C. Covington

31	Spin Formed Mirrors	Dr. Dennis J. Cravens
32	High-Temperature Across-Ply Testing of C/C Composites	Dr. Parviz Dadras
33	Statistical Descriptions of Shape in R^2 and R^3	Dr. Charles B. Davis
34	An Assessment of the Development of a DNA Probe for Mycoplasma hominis and Ureaplasma urealyticum	Dr. Vito G. DelVecchio
35	Effects of Nuclear Radiation on the Optical Characteristics of Laser Components	Dr. Hermann J. Donnert
36	Energetic Materials via Alkoxy-fluorinations of Alkenes with Xenon Difluoride	Dr. Me'vin Druelinger
37	Metal Alkoxide Synthesis of High Temperature Matrices	Dr. Charles H. Drummond
38	Computer Modeling of GaAs and AlAs-GaAs Solar Cells	Dr. Leroy E. Eimers
39	Analyzing Gamma Ray and Neutron Emission Spectra	Dr. Hudson B. Eldridge
40	Geophysical Perturbing Forces on the Frank J. Seiler Large Passive Resonant Ring Laser Gyro	Dr. Harry W. Emrick
41	Quasiparticles and the Transition to Turbulence	Dr. John E. Erdei
42	Statistical Biases in IRLV Measurements of Turbulent Flows	Dr. Dah-Nien Fan
43	Analytical Methods for the Determination of Cholesterol and Cholesterol Esters in Salivary Fluids	Dr. Mack Felton
44	Personality Correlates of Pilot Performance	Dr. Edna Fiedler
45	Transfer of Training Between Alternative Motion Simulators	Dr. John Flach
46	Control of Adaptive Optical Systems	Dr. John A. Fleming

47	Electrochemical Analysis of the Degradation of Synthetic Lubricants	Dr. Dennis R. Flentge
48	Induced Nuclear Radiation Dose in a Simulated Standard Man with Implications on Aircrew Survivability	Dr. Bessie Ruth Foster
49	Determination of Thermal Properties of Melanin Using Photoacoustic Techniques	Dr. James M. Gallas
50	Lidar Measurements of the Mesospheric Sodium Layer at the Air Force Geophysics Laboratory	Dr. Chester S. Gardner
51	AFWL History	Dr. Doris O. Ginn
Volume II		
52	Optimum Design of Structures with Multiple Constraints	Dr. Ramana Grandhi
53	Descriptive Exploration of Patterns in Optical Turbulence Profiles	Dr. Alwin C. Green
54	Modular Modeling of Solid-Fuel Ramjet Combustor Flow	Dr. Mahesh S. Greywall
55	Thermal Stability Characteristics of Some Advanced Synthetic Base Fluids	Dr. Vijay K. Gupta
56	Use of Texture Measures in Multispectral Scanner Data Numerical Classifications	Dr. Barry N. Haack
57	Effect of High Free-Stream Turbulence From a Free Jet on Flat Plate Turbulent Boundary Layer Flow and Heat Transfer	Dr. Je-chin Han
58	A Study of Coplanar Waveguide and its Application to Phased Arrays of Integrated Circuit Antennas	Dr. Donald F. Hanson
59	Three-Dimensional Grid Generation for High-Performance Aircraft	Dr. David Hart
60	Analysis of the Report on Filan Performance Metrics	Dr. Albert A. Heaney
61	Methods for Reliability Warranty Verification	Dr. Carolyn D. Heising

62	Artificial Intelligence and Robotics Perception System	Dr. Troy Henson
63	The Thermodynamic, Physical and Optical Properties of Aluminum Oxide	Dr. Astor Y. Herrell
64	Geoid Modelling and Interpretation	Dr. Albert T. Hsui
65	FTIR Spectroscopic Study of Hydrazine Interactions with Clay Minerals	Dr. Clifford T. Johnston
66	Experimental Studies Related to III-V Semiconductor Growth and Characterization	Dr. Patrick L. Jones
67	A Preliminary Study of Learning Nets and Massive Parallelism	Dr. Jeremy Jones
68	Approximate Mathematical Solutions for Unidirectional Composites Containing Broken Fibers	Dr. Walter F. Jones
69	Long Term Life Expectancy Radiation Effects: An Ultrastructural Study of Brain Tumors Developed in Macaca Mulatta following Exposure to Proton Radiation	Dr. Betty Jones
70	Design Considerations for Phase Dependent Voltage Contrast Technique for Application to SEM Analysis and Electrical and Optical and Characterization of Certain Doped Organic Polymers	Dr. Prasad K. Kadaba
71	Synthesis of Novel Polybenzimidazole Monomers	Dr. James J. Kane
72	A Thermal Evaluation of a Portable, Battery-Powered Vapor-Compression Colling System	Dr. Amir Karimi
73	Mechanistic Studies of Energetic Materials: Analysis of 2,4,6-Trinitrotoluene Thermal Decomposition Products	Dr. Daisy W. Kimble
74	Role of Stimulus Uncertainty in Visual Contrast Sensitivity	Dr. David Kohfeld
75	The Multi-Weapon Multi-Target Multi-Phase Assignment Problem	Dr. Stephan E. Kolitz

76	A Study of the Electrochemical Behavior of the Bromine/Bromide Couple in Melts Composed of Aluminum Chloride and 1-Methyl-3-Ethylimidazolium Chloride	Dr. Lawrence F. Koons
77	The Thermal Layer: A Simplified Model	Dr. Arthur Kovitz
78	Analysis of Relationships Among Self, Peer, and Supervisory Ratings of Performance	Dr. Kurt Kraiger
79	Numerical Study of Detonation Near a Barrier	Dr. Madakasira V. Krishna
80	Sampling Plan for the Organizational Assessment Package Survey	Dr. Paul S. T. Lee
81	Route Planning Problem	Dr. Benjamin Lev
82	Statistical Performance Measures: Relating Air Force Mission Capability to Base Supply Measures	Dr. Edward Lewis
83	Testing the Effectiveness of some User Friendly Algorithms	Dr. Michael Lewis
84	Family Factors and the Career Intent of Air Force Enlisted Personnel	Dr. Philip M. Lewis
85	An Analysis of Low Dispersion IRAS Spectra of Carbon Stars, S Stars and M Variable Stars	Dr. Irene R. Little-Marenin
86	Preliminary Investigation on Resource Control Strategies on Distributed Computer Systems Real-Time vs. Non-Real Time	Dr. Dar-Biau Liu
87	Modelling/Analysis of Space Based Kinetic Energy Weapon Projectile Elyouts	Dr. Carl G. Looney
88	Image Formation and Processing in Superposition Eyes: Precision Location of Point Objects Using the Moire Effect	Dr. James S. Marsh
89	Control Functions in Grid Generation	Dr. C. Wayne Mastin
90	Active Mode-Locking Techniques for Ultra-Short Pulses in Nd:YAG Lasers	Dr. Odis P. McDuff

91	Plasma Parameter Data for BERT I Chamber Testing	Dr. Bernard McIntyre
92	Fourier Analysis of the Pattern Electroretinogram	Dr. Leathem Mehaffey
93	Profiling Air Force Family Work Groups to Optimize Service Satisfaction and Career Commitment Impact	Dr. Ivor Mitchell
94	No Report Submitted	Dr. Osoma Mostafa
95	Chlamydomonas Photoaxis as a Simple System for Vision Research	Dr. Rex Moyer
96	Normobaric Oxygen Concentration Effects on Cultured Mouse Macrophage Responses	Dr. James Mrotek
97	Isothermal Differential Scanning Calorimetric Studies of Thermal Decomposition of 1,4-Butanediammontium Dinitrate	Dr. Maurice C. Neveu
98	A Study of the Relationship Between Leadership and Job Satisfaction/Career Commitment Among Air Force Personnel	Dr. Robert E. Niebuhr
99	A Review of Research Literature on the Measurement of Forces/Pressure on the Plantar Surface of the Foot During Gait Using Ambulatory Transducers	Dr. Marion L. Noble
100	A Silicon Vidicon System for Profiling 1.06 μm Laser Pulses	Dr. Robert O'Connell
101	Free Radical Spectra of PO	Dr. Ralph Oberly
102	ATR Performance vs Image Measurements	Dr. Won J. Park
Volume III		
103	Blast Propagation Through a Composite Wall Section	Dr. Desmond Penny
104	Novel Means of Formaldehyde Analysis Adapted to USAF Laboratory Needs	Dr. Thomas Pierce
105	Raman Spectroscopy of Glycosaminoglycans from Cornea	Dr. Boake Plessy
106	Prediction of Surface Roughness Effects on Heat Transfer and Skin Friction	Dr. Arnold Polak

107	The Influence of Condensed Water Revaporization on Wind Tunnel Test Results	Dr. Justin H. Poland
108	Study of System Impairment Detection and Classification Algorithm for Unmanned Research Vehicle	Dr. Kuldip S. Rattan
109	Nonlinear Analysis of Composite Supports for Armor	Dr. Hemen Ray
110	Diagnostics of Solid Propellant Combustion	Dr. John P. Renie
111	Construction of Approximate Formulae for the Calculation of Conductivity Coefficients in Partially Ionized Gases	Dr. Michael B. Rhodes
112	A Literature Survey on the Formation and LUminescence of $NO(A^2\Sigma)$ in a Hydrazine N_2O_4 Propellant System	Dr. Robert W. Ricci
113	Numerical Modeling and Inversion of 63 μm Earthlimb Emission From Atomic Oxygen	Dr. James P. Riehl
114	No Report Submitted	Dr. Michael Ross
115	Nondestructive Evaluation of Advanced Composites by Strain Field Analysis Acquired Through Correlation of X-Radiographs	Dr. Samuel S. Russell
116	Infrared Radiation Target Modeling System	Dr. Sally Sage
117	Modeling of Tire/Soil Interaction	Dr. Joseph E. Saliba
118	Bacteriologic Techniques for the Isolation of Legionellae From Aquatic Environments	Dr. Gordon D. Schrank
119	Chemical Laser Research on the Iodine Monoflouride (IF) System	Dr. Ronald Sega
120	Modeling the Tissue Solubilities of Halogenated Methanes, Ethanes, and Ethylenes	Dr. Paul G. Seybold
121	Digital Simulation of Surface-to-Air Missiles and Smoothing of Cinetheodolite and Radar Data	Dr. Shawky E. Shamma

122	Indoor Radon Pollution	Dr. Ralph W. Sheets
123	Reliability of Systems with Markov Transfer of Control	Dr. Kyle Siegrist
124	The Synthesis of Reactive Intermediates	Dr. Ricardo Silva
125	Possible Targets for Testing the Neutral Particle Beam at Low Energies in the Mark I Aerospace Chamber	Dr. S. Ballou Skinner
126	Preparation of Non-Flammable Model Compounds	Dr. Terrill D. Smith
127	Studies on Combustion of Liquid Fuel Sprays in Stagnation Flows	Dr. Siavash H. Sohrab
128	Monitoring Environmental Quality by Metabolite Analysis	Dr. Richard G. Stebbins
129	Analysis of Geometric Attenuation in Ground Motion Testing	Dr. Bob W. Stewart
130	Competition Guide for Base-Level Buyers 1985	Dr. Lowell E. Stockstill
131	The Role of Antioxidants in Hyperbaric Oxygen Toxicity to the Retina	Dr. William L. Stone
132	Assessment of Maximum Entropy Method Software for Treatment of Data From the AFGL Labcede Facility	Dr. James E. Sturm
133	Inference Propagation in Emitter, System Hierarchies	Dr. Thomas A. Sudkamp
134	Particle Scattering in Plumes	Dr. William Holt Sutton
135	Thermal Stability of Aluminum-Iron-Cerium Alloys	Dr. Robert Swanson
136	The F-15 SPO Support Equipment "Tiger Team"	Dr. Patrick J. Sweeney
137	Studies in Holographic Procedures	Dr. Charles E. Taylor
138	Dynamic Stress Analysis of Layered Structures	Dr. Joseph W. Tedesco
139	An EPR Study of the Decomposition of Various Dinitrotoluenes and the Synthesis of Azo Compounds	Dr. Walter E. Trafton

140	A Comparison of Measured and Calculated Attenuation of 28 GHZ Beacon Signals in Three California Storms	Dr. Larry Vardiman
141	Allocation and Assessemnt of Logistics Resources	Dr. Daniel T. Voss
142	Natural Language Understanding Using Residential Grammar and Its Use in Automatic Programming	Dr. Christian C. Wagner
143	Stability and Control Computer Program for Conceptual Aircraft Design	Dr. Richard C. Walker
144	Compilation of Select Aspects of the Air Force Weapons Laboratory's 1984 History	Dr. Doris J. Walker-Dalhouse
145	The Planning of A R & D Office Information System	Dr. Yin-min Wei
146	Development of High Strength Titanium Alloys VIA Rapid Solidification Processing	Dr. Isaac Weiss
147	"POPCORN" As a Tool for Future Cognitive Workload Assessment: A Conceptual Analysis	Dr. Shih-sun Wen
148	Labeling the Topographic Features of a Gray-Level Image	Dr. David C. Wilson
149	The Warehouse Layout Program	Dr. Jesse Williams
150	A Summer's Study on Nuclear Debris Cloud Radiation and Laser Transmission in the Atmosphere	Dr. Arthur Woodrum
151	The Effect of Wavelength on Light Scatter in the Human Eye	Dr. Billy Wooten
152	Molecular Operators That Move Nuclei Along Paths of Constant Orbital Energy	Dr. Carl Wulfman
153	The LQG/LTR Design Via H_2-Optimization	Dr. Hsi-Han Yeh
154	Heat Transfer Correlation for Nosetips With Stagnation-Point Gas Injection	Dr. Juin S. Yu

1985 USAF-UES SUMMER FACULTY RESEARCH PROGRAM/

GRADUATE STUDENT SUMMER SUPPORT PROGRAM

Sponsored by the

AIR FORCE OFFICE OF SCIENTIFIC RESEARCH

Conducted by the

UNIVERSAL ENERGY SYSTEMS, INC.

FINAL REPORT

INDIVIDUAL DIFFERENCES IN ABILITIES, LEARNING, AND COGNITIVE PROCESSES

Prepared by:	Phillip L. Ackerman	Lori L. Case
Academic Rank:	Assistant Professor	Graduate Student
Department and University:	Department of Psychology, University of Minnesota	
Research Location:	Air Force Human Resources Laboratory, Manpower and Personnel Division, Test and Training Branch (AFHRL/MOEL)	
USAF Research	Dr. William Tirre	
Date:	September 2, 1985	
Contract No:	F59620-85-C-0013	

INDIVIDUAL DIFFERENCES IN ABILITIES, LEARNING, AND COGNITIVE PROCESSES

by

Phillip L. Ackerman

ABSTRACT

This paper represents the final report of my participation in the 1985 Summer Faculty Research Program in the Test and Training Branch of the Air Force Human Resources Laboratory (AFHRL) located at Brooks AFB. This research program has a combined focus of a) the determination of the basic causes and manifestations of individual differences in learning during skill acquisition and knowledge acquisition task practice; and b) refinement of a theoretical/empirical approach to interrelating cognitive abilities with individual differences in learning -- that provides a foundation for improved predictors of present and future performance in learning and training environments. The approach to these issues involves an integration of information processing theories of learning, practice, and skill acquisition with intellectual/cognitive ability constructs. During this summer research period several experiments have been completed that converge on the derivation of information about individual differences in learning and the relations between cognitive/intellectual abilities and learning.

I. INTRODUCTION:

As a psychologist interested in the relations between cognitive/intellectual abilities and cognitive processes, especially with respect to individual differences in learning (e.g., see Ackerman, 1984a; Ackerman & Schneider, 1985), it has been difficult for me to collect generalizable data in the relatively limited University environment. The reasons for this difficulty are as follows: a) the limited availability of experimental subjects from a normative population; b) the lack of equipment and other facilities to allow for collection of data from sufficient numbers of subjects; and c) a lack of funds for recruitment of subjects for experiments. In addition to providing an atmosphere of intellectual stimulation (in particular, the environment of the Test and Training Branch (AFHRL/MOEL) -- namely, Drs. Christal, Kyllonen, Tirre, and Woltz), this research branch of AFHRL has the capability of collecting learning data that encounter none of the above difficulties. In my initial contact with these scientists, I learned of the exemplary facilities available at AFHRL/MOEL as well as about the commitment of the research group towards pursuit of scientific goals in the Learning Abilities Measurement Program. It was this program and the caliber of the scientists directing the program that attracted me to apply to the Summer Faculty Research Program (SFRP). Furthermore, the prospects of beginning a continuing cooperative research initiative between myself and the Air Force Office of Scientific Research also seemed promising. I felt that this element of the program reinforced the idea that such an effort started during the SFRP might be continued, to the benefit of the research aims embodied in my program of study.

II. OBJECTIVES OF THE RESEARCH EFFORT:

Two broad objectives have served as the foundation of this SFR P research effort. The first objective has been to design and implement experiments that converge on the determination of the basic causes and manifestations of individual differences in learning, during skill acquisition and knowledge acquisition. The second objective of this program has been to refine a theoretical/empirical approach to interrelating cognitive abilities with individual differences in learning (that will ultimately provide for improved predictors of pre-training and post-training performance in learning environments). Secondary objectives towards these goals are discussed below in the relevant experimental contexts.

III. SCIENTIFIC BACKGROUND FOR THE RESEARCH PROGRAM:

A two-pronged approach to understanding and predicting individual differences in learning has been used in this research program. The first approach, or focus, concerns identification of the specific characteristics of individual differences in learning. This approach partly builds on the theory described in Ackerman (1984a), but also includes more basic descriptive and quantitative modeling contributions to the understanding of individual differences in learning. The work in this part of the research program has been mostly data-driven and empirically based, though the variables actually chosen for investigation are decided on the basis of information processing theories of learning, skill acquisition, and performance.

The second approach taken here represents a continuation and extension of the research described in Ackerman & Schneider (1985). This line of inquiry is used to determine the intellectual/cognitive abilities which predict individual differences in the information processing components that are integral to

performance of novel tasks, maintenance of post-practice performance, and that determine performance levels at intermediate levels of task practice/training. Ultimately, this focus is expected to yield assessment measures that predict task performance at all points during practice/training programs. (Several measures are currently under study such as: a) strategy generation and use, b) attentional resource capacity, c) task component integration rate, and so on.) Some progress had been made (prior to the SFRP) through a limited examination of verbal and spatial content tasks. However, there was a special need for extrapolating these findings to the perceptual/motor domain; where skill acquisition, rather than knowledge acquisition is emphasized. Further, data were needed to address the general aspects of task content and constraints of information processing consistency.

The basis for this approach is based on research from several domains. One major research impetus has been the Theory of Ability/Skill Relations during learning (Ackerman, 1984a). The initial domain of tasks considered by this theory are novel, resource-limited (i.e., tasks that demand attention, see Norman & Bobrow, 1975 for a more explicit discussion of resource-limited tasks) at the beginning of practice, and which allow all subjects to achieve a greater-than-chance (or greater than zero) performance level. Three main principles provide for the major effects in the theory. These are as follows: (1) Broad and general ability individual differences are equated with individual differences in amount or efficiency of attentional resources; (2) The transition from controlled (or attentional) to automatic processing (see Schneider & Shiffrin, 1977 for a description of automatic and controlled processing concepts) is equated with the transition from resource- to data-limited performance characteristics; and (3) The ability determinants of performance are associated with the extent and type of attentional resources

required by the task.

From those basic principles, one can predict which cognitive/intellectual abilities will be associated with naive and practiced performance for tasks containing either consistent on inconsistent information processing characteristics. For consistent tasks, general and content-relevant abilities will be associated with the initial performance individual differences (because attentional resources are required for processing new information). As time-on-task increases, these abilities will be less associated with performance (as the task becomes more "automatic"). Finally, only specific abilities which tap the skills/processes that overlap with task automatic processing components are expected to correlate with late, well-practiced performance. For predominantly inconsistent tasks, initial, intermediate, and late performance individual differences will be associated with both the general and content-relevant abilities (because attentional resources are required for both novel and familiar inconsistent information).

A second background source for this investigation regards the specific study of individual differences in learning. A study that illustrates individual differences in learning is one by Adams (1957). The ramifications of this study are important for any attempt at predicting (or modeling) how individual differences in performance change over practice. As the data from the Adams' study demonstrate, subjects "learn" quite different amounts over a period of task practice, depending on their initial performance levels. Adams divided his subjects into decile groups, based on a rank-ordering of performance on the first task trial. The results indicate that (for a relatively simple psychomotor task) subjects with initial performance falling in the highest decile, on the average, show only marginal improvements in performance (relative to the normative population) over practice trials.

Subjects in the lowest decile, though, show substantial performance increments over time (for these data, mean performance improvement for the lowest decile exceeded improvement in the highest decile by a factor of six). However, as Adams points out, the different decile group performance means appear to asymptote at different levels (which means that high ability individuals "learn" less during practice, but still perform at the highest levels).

It is essential to note that the group means data do not tell the whole story. The high decile groups are relatively homogeneous from beginning to the end of training. The low decile groups, while relatively homogeneous at trial one, are greatly heterogeneous in performance at the last practice trial. In fact, the heterogeneity is so pronounced that many of the subjects in the lowest group actually attain performance scores in the top performance categories after practice. The major implication is that some subjects can make up for poor initial performance and ultimately perform as well as the subjects that are in the upper deciles.

In general, subjects that begin a task with superior performance ultimately maintain their relative superiority in performance subsequent to practice. The converse is true for many subjects that begin the task with clearly inferior performance. However, there is a substantial asymmetry between the initial and final performance distributions for low and high performance groups. The important concerns for theories of individual differences in learning are to identify the subjects who will: a) perform well initially, and b) not necessarily perform the task with distinction early in the training sequence, but that ultimately will perform well (relative to the sample) subsequent to practice. Merely being concerned with initial scores, final scores, or "gains" in performance obscures these differential effects that occur during the practice sequence.

The Adams data concern a relatively simple psychomotor task; before this SFRP investigation no data have been available that allow for generalization to more complex, or different content (i.e., spatial, verbal, etc.) domains. In order to predict or model initial performance levels and learning functions for subjects of differing ability, though, sufficient groundwork must be laid that describes the basic data under consideration. Therefore, several experiments have been implemented that measure these performance and ability measures in the key content and task complexity areas.

IV. EXPERIMENTS COMPLETED DURING THE SFRP PERIOD:

The identification of the crucial conditions to be examined has been derived from consideration of a broad theory of individual differences in performance described above. The variables of concern include: 1) Task content (Verbal, Spatial, Perceptual/Motor); 2) The degree of task dependence on attentional (versus automatic) processing components; 3) Task complexity (this variable pertains to the dependence of initial task performance on general intellectual abilities, or equivalently, on initial attentional resource demand); and 4) The role of transfer of training on task performance and learning. By the end of the summer on-site period, data collection will have been completed for four studies. These studies mainly concern derivation of the parameters of individual differences in learning in the above context. The studies are as follows:

Study 1. Task content: Individual differences in learning were examined for (consistent task versions of) three major ability/task content groups: Verbal, Spatial, and Perceptual/Motor Speed. Subjects practiced on one of the tasks for 2.75 hours (with breaks). Pilot work in two of the areas (verbal and spatial) had indicated similarities in the mean learning curves of tasks that

share many of the basic information processing requirements, but differ in terms of task content (Ackerman, 1984a). However, little has been known about the nature of individual differences in learning that are found during practice in these task domains. Further, the three content domains specified here have been considered fundamentally different by most ability theorists. Any general theory of individual differences in learning must be able to account for differences in learning patterns across these major divisions (for example, contrasting the learning of facts or words (in the verbal domain) with the learning of procedures (such as in the spatial domain), and the learning of perceptual/motor programs).

Results. Each of the different content tasks provide sufficient data for deriving the relevant performance-ability functions necessary for describing the patterns of individual differences in learning. For consistent versions of the verbal and perceptual/motor tasks, post-practice performance has been shown to be predominantly data-limited throughout almost the total range of abilities. However, given the special nature of spatial processing, it is possible that, without specific instructional training, a significant portion of the sample may be found in a resource-limited situation at the end of practice. (These latter data have not been analyzed yet.) Significance. The significance of this study is that the data allow for a descriptive assessment of the range of individual differences in learning, and paths of improvement taken by individual subjects (and identifiable subgroups of subjects). These data permit modeling of individual learning curves and families of learning curves, as opposed to modeling a single mean learning curve (see Estes, 1974, on the spurious nature of averaged learning curves).

Study 2. Task Consistency: Three levels of task consistency were examined for the verbal content domain. The levels are a) Predominant use of

attentional processing resources; b) Consistent processing for development and predominant use of automatic process components; and c) Mixed information processing requirements (a moderate degree of consistency (70%), see Schneider & Fisk, 1982). These experiments have utilized between-subjects designs; that is, each subject receives practice/training on one level of consistency. Results. The tasks which require attentional processing throughout practice show similar initial and final performance-ability functions (which are resource-limited throughout most of the range of abilities). While these data have not been completely analyzed, it is expected that variability of the lower decile groups will ultimately be much smaller in these tasks than in the completely consistent tasks. Significance. Tasks that require continual allocations of attentional processing resources permit evaluation of the type of information processing crucial in the initial stages of most learning tasks. The completely inconsistent and moderately consistent tasks allow for unbiased measurements of these processes whereas consistent tasks do not. That is, most learning tasks have consistent components, and measurements taken early in learning confound the degree of attentional processing involvement with the speed of development of automatic processing components. Tasks which only require attentional processing are not confounded in this way.

Study 3. Task Complexity: One major aspect of task complexity, that is, memory load, has been explored in this study. The investigation of memory load involved a version of the verbal task used in Study 1 (above) with an increase on the demands made on short-term memory in performing the task. Results. By increasing task complexity, performance is more resource-limited throughout the ability range. In addition, it appears that fewer of the subjects that start at the lower decile level will achieve to higher levels during practice, given the level of initial attentional processing demands made on the subjects. This

inference was based on findings of Frederiksen, et al. (1983) on the characteristic distinctions between good and poor readers. Significance. The significance of this experiment, in addition to mapping out the range and variance of individual differences, regards a conceptual validation of the equating of performance-resource functions with ability-performance functions, given that difficulty/complexity are generally hypothesized to change the initial slope of the task performance-resource function (for details, see Navon & Gopher, 1979; Norman & Bobrow, 1975).

Study 4. Transfer of Training: The investigation of the differential effects of transfer of training (and subsequent effects on post-transfer training) results from the study of the perceptual/motor task considered above (Study 1). The initial task was enlarged to include a broader class of responses, which continue to require a subset of identical stimulus-response components. For this study, subjects received an intermediate amount of training on the first task, and then were transferred and trained on the enlarged task.

Results. Given what had already been observed regarding the influence of general and content abilities on initial task performance (Ackerman, 1984a), it was expected that a similar distribution at the point of transfer would be found in comparison to initial task performance. It is unclear, though, whether those subjects that "learn" more (i.e., start in the lowest decile at trial one, but reach much higher performance levels before transfer) will learn faster -- or transfer at a significantly better level than their peers (at trial one). (These data have yet to be analyzed.) Significance. In accordance with Ferguson's theory of learning, transfer and abilities (Ferguson, 1954), it is reasonable to assume that transfer of training is the norm for learning situations, and that learning in the absence of transfer is a quite special

case. To the degree that these results describe the characteristics of individual differences in a transfer/learning environment, a precise, general model of the individual learning functions may be derived. Pragmatic interest in individual differences in learning implies a concern with the broader learning environment, rather than just the artificial circumstances that are often obtained in a laboratory environment. Understanding individual differences in transfer of training helps in building a generalizable theory of individual differences in learning.

V. RECOMMENDATIONS:

The summer research period has allowed for collection of data that focus directly on those issues discussed above. However, given the massive amount of data collected and the need for intensive analyses of such data for final conclusions to be reached, it is necessary to follow-up the SFRP effort with a continued research initiative. Specifically, the proposed effort for follow-up (see Ackerman, 1985 -- Research Initiation Program proposal) regards the reduction and assessment of much of the data collected this summer. Specifically, the following objectives of the follow-up period are as follows:

Phase 1 Objectives:

Initial data reduction/analysis for studies 3 and 4 (plus second stage analyses for studies 1 and 2): Because of the rate at which experiment programming and data collection has been implemented this summer (i.e., one experimental task was administered per week), it has been impossible to perform much of the initial data reduction and analysis for the later two studies before completion of the summer effort. Therefore it will be necessary for data reduction to be implemented at some point subsequent to the end of the SFRP period. While many of the initial analyses are limited to computing

relatively basic statistics that require little programming; several techniques involving maximum likelihood modeling of the learning data, and simulation/evaluation of prototypical learning curves (utilizing three-mode factor-analytic procedures) will require a substantial effort from programming and substantive research domains. (In fact, it has not been possible to undertake these latter analysis for the earlier studies, either, since the requisite computer software has not been available at the data site.)

Phase 2 Objectives:

Empirical evaluation and extension of the theory of ability/performance relations: In addition to the focus on identifying the patterns of individual differences in learning, the data from all four studies should be used, in conjunction with ASVAB scores (Armed Services Vocational Aptitude Battery), for comparison with predictions from the Ackerman (1984a) Ability/Performance Theory. That is, the theory discussed above is used to make predictions regarding the relations between cognitive/intellectual abilities on the one hand (as measured by the ASVAB and other similar aptitude/ability batteries), and individual differences in performance in tasks of differing content, complexity, and consistency on the other hand. In order to test and improve the theory, the ASVAB scores must be submitted to hierarchical factor analysis (Schmid-Leiman technique, 1957), and then task performance loadings may be derived by the Dwyer Extension Technique (see Dwyer, 1937; or Ackerman, under review, for a detailed justification and description of these methods).

This type of data analysis requires a great deal of interactive computing and data-base management. Programming support will be needed for the initial stages of this procedure, and the work of a graduate student assistant is necessary to prepare the appropriate graphical representations of the data analyses, including the planning and implementation of multivariate tests of

equivalence for the different data samples collected. Because of a lag between task data collection and the availability of ASVAB scores (two or more weeks after completion of the experiment), only the initial stages of analysis in this phase of the research will be completed before the end of the on-site summer research period.

Phase 3 Objectives:

As described in the Plan for Summer Faculty Research Program (see Series 2), subsequent to the investigation of 1) the effects of task characteristics on the nature of individual differences in learning, and 2) the relations between cognitive/intellectual abilities, task characteristics, and task performance; the next phase (3) concerns a theoretically motivated search for assessment procedures that predict and/or diagnose individual differences in specific cognitive processes necessary to knowledge and skill acquisition. With the information derived from previous research and refined from data analyzed during phases (1) and (2) of this research program, the planning, programming, and initial implementation of several studies comprise the objectives of phase (3).

The task of planning and programming these experiments can be undertaken at the University of Minnesota, in collaboration with research scientists at the Test and Training Branch, AFHRL/MOEL. Subsequent to task preparation and final planning stages, the data may be collected at the Brooks/Lackland AFB facilities, with data to be returned to the University of Minnesota for reduction and analysis. It is expected that this part of a research effort will specifically reflect the initial phase of future (i.e., follow-on research efforts after the one-year research effort) collaborative research involving this investigator and the staff directing the AFHRL - Learning Abilities Research Project. Draft descriptions and potential value of these studies are presented in the RIP proposal under consideration by AFOSR.

ACKNOWLEDGMENTS

I would like to acknowledge the sponsorship of the Air Force Systems Command, Air Force Office of Scientific Research, the Air Force Human Resources Laboratory, and the Manpower and Personnel Division of AFHRL. In addition, the scientific and logistic assistance of the following individuals and organizations is gratefully acknowledged: AFHRL/MOEL - Test and Training Branch, Dr. Raymond E. Christal, Dr. Patrick C. Kyllonen, Dr. William C. Tirre, Dr. Dan J. Woltz, Ms. Gloria Koenig, and Ms. Christine Rancourt. I also would like to acknowledge the dedication of the test proctors and support staff at Lackland (AFHRL/MOET) and the programming/data reduction assistance of Mr. Richard Walker and Ms. Janice Hereford (OAO Corporation under contract to AFHRL).

REFERENCES

1. Ackerman, P. L. (1984). A theoretical and empirical investigation of individual differences in learning: A synthesis of cognitive ability and information processing perspectives. Unpublished doctoral dissertation, University of Illinois, Urbana.

2. Ackerman, P. L. (1984b). Multivariate evaluation of workload, resources, and performance in dual task data. Proceedings of the 28th Annual Meeting of the Human Factors Society. 210-214.

3. Ackerman, P. L. (Under review). Individual differences in learning and practice: An integration of psychometric and information processing perspectives. Manuscript submitted to Psychological Bulletin.

4. Ackerman, P. L., & Schneider, W. (1985) Individual differences in automatic and controlled information processing. In R. F. Dillon (Ed.), Individual differences in cognition, Vol. 2. New York: Academic Press.

5. Adams, J. A. (1957). The relationship between certain measures of ability and acquisition of a psychomotor response. Journal of General Psychology, 56, 121-134.

6. Dwyer, P. S. (1937). The determination of the factor loadings of a given test from the known factor loadings of other tests. Psychometrika, 2, 173-178.

7. Estes, W. K. (1974). Learning theory and intelligence. American Psychologist, 29, 740-749.

8. Ferguson, G. A. (1954). On learning and human ability. Canadian Journal of Psychology, 8, 95-112.

9. Frederiksen, J. R., Weaver, P. A., Warren, B. M., Gillotte, H. P., Rosebery, A. S., Freeman, B., & Goodman, L. (1983). A componential approach to training reading skills, (Report No. 5295, Final Report). Cambridge, MA: Bolt, Beranek, and Newman, Inc.

10. Navon, D., & Gopher, D. (1979). On the economy of the human processing system. Psychological Review, 86, 214-255.

11. Norman, D. A., & Bobrow, D. B. (1975). On data-limited and resource-limited processes. Cognitive Psychology, 7, 44-64.

12. Schmid, J., & Leiman, J. M. (1957). The development of hierarchical factor solutions. Psychometrika, 22, 53-61.

13. Schneider, W., & Fisk, A. D. (1982). Degree of consistent training: Improvements in search performance and automatic process development. Perception & Psychophysics, 31, 160-168.

14. Schneider, W., & Shiffrin, R. M. (1977). Controlled and automatic human information processing: I. Detection, search, and attention. Psychological Review, 84, 1-66.

1985 USAF-UES SUMMER FACULTY RESEARCH PROGRAM/

GRADUATE STUDENT SUMMER SUPPORT PROGRAM

Sponsored by the

AIR FORCE OFFICE OF SCIENTIFIC RESEARCH

Conducted by the

UNIVERSAL ENERGY SYSTEMS, INC.

FINAL REPORT

MAXIMUM VOLUNTARY HAND GRIP TORQUE FOR CIRCULAR ELECTRICAL CONNECTORS

Prepared by:	Dr. S. Keith Adams and Philip J. Peterson
Academic Rank:	Associate Professor and Graduate Assistant
Department and University:	Department of Industrial Engineering, Iowa State University
Research Location:	Aerospace Medical Research Laboratory Human Engineering Group
USAF Research Colleague:	Dr. Joe McDaniel
Date:	October 4, 1985
Contract No.:	F49620-85-C-0013

ERI-86140

MAXIMUM VOLUNTARY HAND GRIP TORQUE FOR CIRCULAR ELECTRICAL CONNECTORS

Dr. S. Keith Adams
and
Philip J. Peterson

ABSTRACT

A study employing twenty male and eleven female subjects was performed to determine maximum hand grip torque that can be exerted when tightening or loosening circular electrical connectors. A static, sustained three-second exertion was used as the strength criterion. Torque was applied to simulated connector rings with diameters of 0.9, 1.5, and 2.0 inches and was measured by means of a single bridge torsional load cell. Other variables tested included the type of grip employed (full or fingertip), orientation of the connector (front, right side, or rear facing behind a barrier), the use of work gloves and chemical defense gloves, the height of the connectors (60% and 85% of the maximum reach height) and the direction of rotation. Hand grip torque strength was found to be directly related to connector diameters with similar strength patterns exhibited for tightening and loosening. Higher torque was exerted when the connectors were on the subject's right side, and tightening and loosening effort corresponded to flexing and extending the wrist parallel to the forearms. The use of gloves resulted in higher torque in most situations. Connector height and direction of rotation had little effect on torque strength.

I. INTRODUCTION

Aircraft maintainability is currently recognized as a major problem area by the U.S. Air Force. Approximately 35% of the lifetime cost of military systems is spent for maintenance [1]. Modern aircraft are extremely complex in design and function, and physical demands and trouble-shooting skill requirements for maintenance personnel have grown with this complexity. A recent development, which has complicated the problem even more, has been the introduction of computer-aided designs that permit hardware choices and configurations to be generated rapidly with little regard for maintainability problems that may arise. The result has been an increase in ergonomic problems in maintainability stemming from inadequate work space, restricted vision, and strength or body position requirements that exceed the capabilities of many maintenance personnel.

A three-dimensional, computerized representation of human anthropometry, strength, mobility, manual material-handling capability, and visual limitations supported by a strong ergonomic data base was needed to handle these problems. This concept had worked well in cockpit design through the development and use of COMBIMAN [1,2]. It was thought that a similar model for maintenance could be developed; except that for this application, multiple body positions would have to be accounted for with strength and mobility considered in each position. Thus the concept of a CREW CHIEF model evolved that, when fully developed, will represent the maintenance technician performing many basic tasks in a simulated, computer-aided, design-compatible image.

It was quickly realized that a great deal of supporting ergonomic data based on experiments on strength testing, manual handling and hand tool usage would be needed. In addition, information was needed on how arctic and chemical defense clothing and gloves affected the performance of basic maintenance tasks. This broad research effort was broken down into a number of subtasks. The study of electrical connectors is representative of a unit problem area.

The principal investigator, S. Keith Adams, and a graduate assistant, Philip J. Peterson, became aware of the opportunity to participate in the Summer Faculty Research/Graduate Student Summer Support Program through announcements provided by the Air Force Office of Scientific Research (AFOSR). The principal investigator selected the Aerospace Medical Research Laboratory (AMRL) at Wright-Patterson Air Force Base as his first choice because of prior knowledge of the research in biomechanics that had been completed there and the desire to participate in these new developments.

The principal investigator's background includes includes teaching, research, industrial summer employment, and consulting in many areas of basic and applied ergonomics. Organizations have included Western Electric Co., Eastman Kodak, Employers Insurance of Wausau, NIOSH, the U.S. Army Human Engineering Laboratory, Science Applications Inc., Rockwell International, Essex Corporation and others. Research and application problems related to this summer's work have included: uses of the force platform in analyzing human effort, development of criteria and standards for manual material handling, development of

standards and criteria for combat vehicle evaluation, and evaluation of maintenance tasks in nuclear power plants.

II. OBJECTIVES

The purpose of this study was to define and quantify the relationship between hand grip torque applied from a standing posture and six independent variables affecting static torque strength when performing the task of attaching or removing circular multi-pin electrical connectors. An overall objective of this research was to add more information to the data base being used to quantify ergonomic requirements for aircraft maintenance under the CREW CHIEF program being conducted by the U.S. Air Force.

The six variables selected for study were connector size, grip type, orientation, glove usage, connector height, and direction of torque. At the conclusion of the study, it was decided that additional research should be conducted concerning the effect of crowding by adjacent connectors. Research on the effects of using right-angled connectors was also proposed. The overall goal of these studies was to quantify all important ergonomic variables affecting the attachment and detachment of electrical connectors so that these factors may be incorporated into computer-aided design models for aircraft hardware configuration. As an end result, aircraft should be better designed for the capabilities of those who will maintain them, thus improving maintainability and aircraft readiness.

A. Electrical Connectors

This study was focused entirely on simulating the tightening and loosening of circular electrical connectors. These devices are used to connect and disconnect multi-wired electrical cables linking one electrical device to another by means of a threaded, female, connector ring that rotates onto a threaded, male shaft, thereby forcing connector pins into their respective sockets. The ring is knurled to reduce hand slippage. In addition to the ring and cylindrical socket mounting assembly, the connector includes a backshell that fits over the assembly behind the rotating connector ring. This houses the cable connections entering the connector. It is also knurled to permit holding while the ring is rotated. A cable clamp with tightening bolts is used behind the backshell to provide rigid support for the entering cable and its sheathing. A sample of typical circular connectors used by the U.S. Air Force is shown in Fig. 1(d).

III. LITERATURE REVIEW

Only a few studies have been conducted on the measurement of hand grip torque strength. No published studies were found that involved the use of electrical connectors. Results of other studies were found to be useful in suggesting a theoretical basis for interpreting some of

(a)

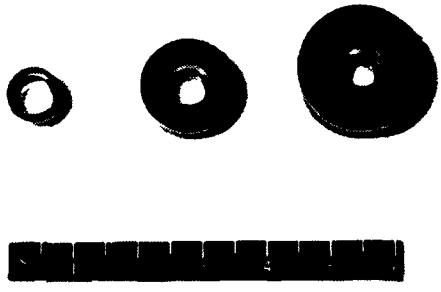

(b)

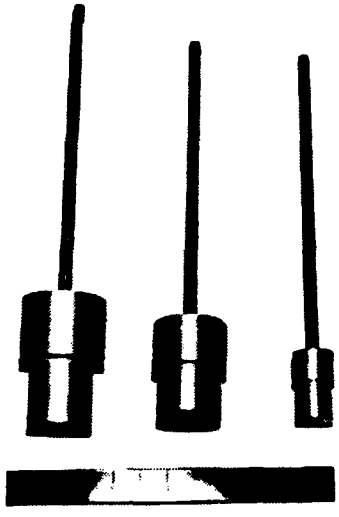

(c)

(d)

Fig. 1. Experimental apparatus. (a) Frame with movable mounting plate and mounted load cell. (b) Simulated connector rings. (c) Backshells for simulated connectors. (d) Electrical connectors.

the findings and in suggesting future extensions of the present investigation.

The need for computer-aided design models to support ergonomics in equipment design has been expressed in a number of publications [1-3]. The development of the CREW CHIEF computer-aided design model of an aircraft maintenance technician is of particular interest for maintainability [1]. When completed, this model will provide an aircraft or missile system designer with the ability to simulate maintenance operations and to predetermine limitations imposed by technician anthropometry, mobility, strength, and visibility under defined field conditions. The present study is one of many that will provide the ergonomic data needed as a basis for development the CREW CHIEF model.

A recent study of hand torque strength using smooth phenolic cylindrical handles with diameters from 0.95 cm to 8.89 cm was reported by Replogle [4]. A theoretical model for predicting torque as a function of handle diameter, gripped area, and relative grip force (proportional to the gripped circumferential angle) was proposed. Torque strength was found to increase up to about 2.5 cm (grip span diameter) with the square of the handle diameter, then to increase at a decreasing rate beyond that diameter up to a maximum of about 5 cm. Pheasant and O'Neill [5] conducted a study of screwdriver handles and the effect of size (diameter), shape, and quality of interface upon grip torque strength. They also made torque strength comparisons between the various screwdriver handles and smooth and rough steel cylinders. Handle shape was found to be unimportant. Handle diameter and the quality of interface (affected by friction and contact area) were important. Maximum torque

occurred at a diameter of 4 cm. Recommendations included the maximization of hand/handle contact area and the use of a 5-cm diameter knurled cylindrical handle as a basic simple design.

Swain, Shelton, and Rigby conducted an experiment to determine the maximum torque generated by men who were standing while operating small, diamond-shaped, knurled knobs [6]. The knobs were 3/8, 1/2, and 3/4 inches in diameter. Subjects represented urban and military nuclear maintenance personnel. Overall mean torque was approximately 10 in.-lbs for the 3/4 in. knob, 5.6 in.-lbs for the 1/2 in. knob and 4.3 in.-lbs for the 3/8 in. knob. Standard deviations for the three knob sizes were approximately 2.3, 1.2, and 1.1 in.-lbs, respectively.

A study conducted by Rohles, Moldrup, and Laviana investigated the jar opening capability of elderly men and women [7]. Eight common sizes of jar lids were tested, ranging in diameter from 27 mm to 123 mm (1 in. to 4.8 in.). Torque values for men ranged from (0.5-1) to (3-11) N-m or (4.4-8.8) to (26-97) in.-lbs for the smallest and largest diameters, respectively.

The effect of the handgrip span upon isometric strength and strength endurance was investigated by Petrofsky et al. [8]. An optimum handgrip length was found to exist for each subject. On the average, this was approximately 5-6 cm (2-2.4 in.) for males and females.

The procedures used for measuring maximum voluntary handgrip torque in the present investigation were based on those recommended by Caldwell and others [9] with slight modifications. This method produced results that were consistent throughout the data and could be compared with the results of the other studies cited.

IV. APPARATUS

The subject test apparatus used in this study, shown in Fig. 1(a), consisted of a c-sectioned steel frame supported by a steel platform. The frame held a quarter-inch aluminum, traveling mounting plate used to hold the load cell and simulated electrical connectors. The plate was held to the rounded edges on the open sides of the vertical frame members by means of aluminum inserts attached to flanged twist knobs on threaded shafts.

V. INSTRUMENTATION

Instrumentation for the experiment included the following items:

load cell (torque measuring)

bridge amplifier

analog to digital converter

digital computer

printer

signal tone generator

test signal generator

The system diagram for the instrumentation used in the experiment is given in Fig. 2.

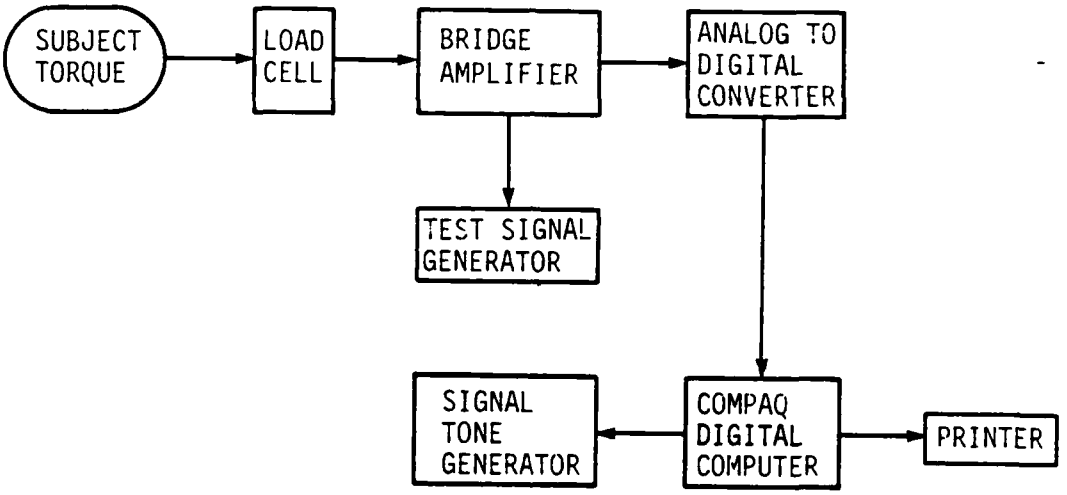

Figure 2. System diagram of instrumentation.

A. Simulated Connectors

A set of three simulated connectors was designed to provide an effective method of accurately measuring hand torque strength using a muscular effort closely matching that required to loosen or tighten similarly-sized electrical connectors. Each simulated connector consisted of a knurled aluminum ring and backshell. The three sizes chosen were typical of many actual connectors. They also provided for a representative set of hand grip styles by the subjects as well as an opportunity to investigate the effect of connector size upon hand torque strength. A solid aluminum backshell with a steel shaft was designed for each connector ring to simulate the backshell and attached cable on actual connectors. This facilitated full and fingertip grasping by fulfilling the requirement that the hand be positioned over or to the side of the simulated connector since a cable prevents the hand from covering the backshell on an actual connector. The three simulated torque rings and backshells are shown in Figs. 1(b) and 1(c). Detailed design features of the simulated connectors are given in Figs. A.1. through A.6. in Appendix II.

VI. EXPERIMENTAL TEST PROCEDURE

A. Subject Selection and Orientation

Thirty-one subjects (20 males and 11 females) participated in the experiment. Their ages ranged from 18 to 32 years for males and from 19 to 40 years for females. The mean age for all subjects was 23 years.

All subjects were measured with respect to height, weight, reach height, and maximum grip range. The latter measurements were used to compute the 60% and 85% reach height and the average grip range (half of the maximum). These values were used (1) to position chalk lines that the subjects stood behind while exerting torque on the connector ring and (2) to set magnetic markers used to indicate the proper height of the mounting plate holding the simulated connector and the load cell.

Subjects were classified according to height and weight into predefined height/weight categories used by the U.S. Air Force for classifying personnel anthropometrically. Each subject was assigned a number designating his or her category. Using the Air Force's categories for classifying subjects makes it possible to relate civilian subject data to a defined military population.

Instructions provided for the subjects are given in Appendix I.

B. Test Procedure

Subjects served in pairs during most of the tests, alternating on each combination of conditions. Each subject served in three sessions, performing 40 exertions in the main sequence plus eight benchmark exertions, four before and four after the main sequence during each session. Sessions on consecutive days were not permitted. Thus in the entire experiment, each subject performed 120 exertions in the main sequence and 24 benchmark exertions. A two-minute rest period was provided between exertions. The purpose of the benchmark exertions was to note basic torque strength characteristics of the subject and to detect any

decrement in strength from the beginning to the end of a session. All benchmark sequences were done bare handed with the medium-sized connector (1.5 in.) at a medium height (60% of the reach height) from the front. Each subject's benchmarks were identical and were performed in the following order:

1. Full grip, clockwise
2. Fingertip grip, clockwise
3. Full grip, counter clockwise
4. Fingertip grip, counter clockwise

Following the four initial benchmark exertions, subjects performed the first, second, or third set of 40 exertions in the main sequence.

Each pair of subjects (or individual if the subject served alone) followed a predefined computer-generated sequence of trials over the 120 combinations in the main sequence. Sequences were also generated in complementary pairs so that gloved and ungloved exertions were equally represented over all test conditions. Subject and test conditions were keyed into the data format on the Compaq computer. During the four-second exertions, torque in inch-lbs was sampled every 0.1 second using the Compaq computer for a total of 40 readings. The criteria for acceptance of a sample were as follows:

> Accept if up to eight 0.1 second torque values were plus or minus 10% of the mean value during the last three seconds (sec 1-4). Accept if applied torque during the first second (sec 0-1) was greater than 80% or less than 120% of the mean torque during the last three seconds (sec 1-4).

All other samples were rejected and the subject was required to repeat the test for that particular combination of conditions. If the

second trial also failed to pass acceptance, the subject was given a three-minute rest break and then tested a third time. The third trial was accepted. Very few third trials were necessary. All exertions in the benchmark series at the start and end of the sessions and the 40 exertions sequenced in the main series were separated by a two-minute rest break for each subject. Subjects were dismissed at the end of the session, having performed 48 exertions in a period of 2-2 1/2 hours.

C. Trial Sequence Generation

Two computer programs were written and run on the Compaq microcomputer to produce test sequences for each pair of subjects. To limit the total number of exertions each subject had to complete, the chemical defense glove conditions and work glove conditions were used in a total of 60 trials for each subject (30 chemical defense glove trials and 30 work glove trials). One BASIC program assigned a set of conditions with the chemical defense gloves and the remaining set of conditions with the work gloves. The other BASIC program assigned the same sets of conditions with the other gloved condition (i.e., chemical defense glove conditions were scheduled with work gloves and work glove conditions were scheduled with chemical defense gloves). By doing this, all possible conditions were tested with both chemical defense gloves and work gloves.

D. Gloves

The two types of gloves, work gloves and chemical defense gloves, were used. These are shown in Figs. 3(a) and 3(b). Since the study was conducted only for right-hand strength using right-handed subjects, only the right-hand glove was worn. The work glove consisted of two layers: an inner wool liner and an outer layer of sewn leather. These were available in five sizes and were fitted to each subject. The chemical defense glove consisted of three layers: an inner cotton liner to absorb perspiration, a smooth rubber layer with a sleeve that covered the lower forearm, and the leather work glove (without the wool liner) worn directly over the rubber glove. This was done to keep the rubber glove from being torn by projecting bolts, pins, or sharp edges during actual maintenance work. The chemical defense rubber gloves were available in four sizes, and the inner cotton liners were available in three sizes. These gloves and liners were also fitted to each subject.

E. Grasping Methods

Two types of grasp were employed. The first was a full or wrap-around grasp in which the thumb and forefinger encircled the knurled ring on the simulated connector during static clockwise or counter-clockwise torque exertions. In some cases when using the small connector, the tip of the thumb was pressed against the side of the forefinger. In others, the forefinger was wrapped around the small connector ring. The second grasp was a fingertip grasp formed between the tip of the thumb and tip of the forefinger, and in some cases, with additional

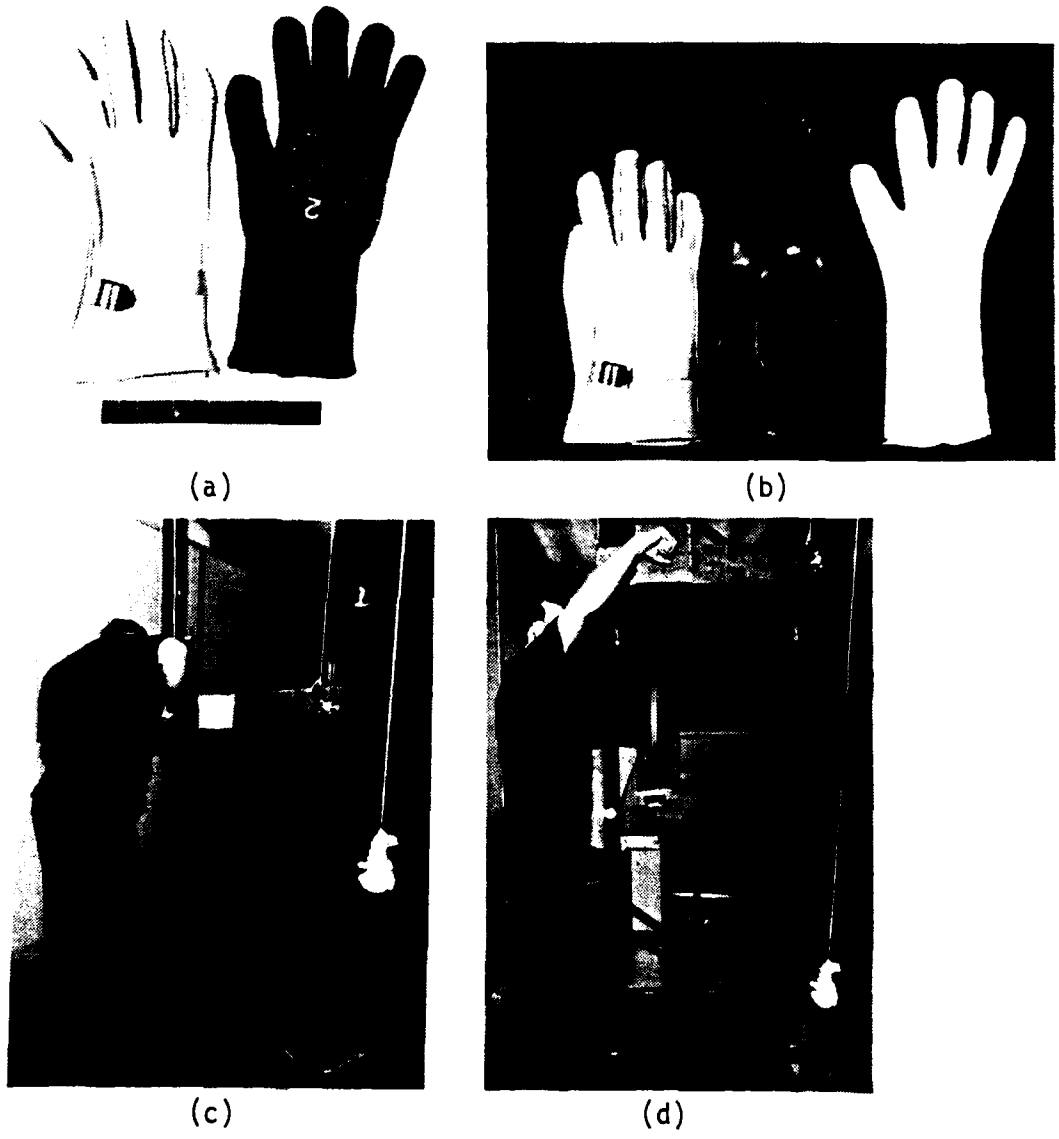

Fig. 3. (a) Work glove with leather shell (l) and wool insert (r). (b) Chemical defense glove with leather shell (l), rubber glove (c), and cotton inner liner (r). (c) Subject position from the front at 60% reach height. (d) Subject position from the right at 85% reach height.

opposing fingertips. Each subject was instructed to employ any style of grip, within each of the two specified categories, that maximized his or her torque strength and seemed most natural.

F. Working Positions

Subjects exerted torque from three different orientations around the simulated connector and two different work heights. With respect to the subject's body, orientations included from the front (the simulated connector was located ahead of the right edge of the right foot for an erect standing position), from the right (the connector again was located directly ahead of the right edge of the right foot for an erect standing position), and from the back (the connector was located similarly ahead of the subject but behind the mounting plate and load cell cover box so that the subject had to reach over the mounting plate to grasp the simulated connector). The three working positions are shown in Figs. 3(c), 4(a) and 4(b).

The centerline of the connector was set at 60% and 85% of the subject's maximum reach height (maximum fingertip reach height above the floor) for the front and right orientations. For the back-facing orientation the centerline was set at 60% of the maximum reach height. Grasping at these two heights is shown in Figs. 3(d) and 4(b). The distance from the subject's sternum to the forward surface of the connector torque ring was kept constant at the average grip range, which is defined as one half of the maximum grip distance. The maximum grip distance was found by determining the displacement range between the

(a) (b)

Fig. 4. (a) Subject position from the back at 60% reach height.
(b) Subject position from the right at 60% reach height.

centerlines of two cylindrical handles, one held by a full grip at arm's length and the other held by a full grip against the subject's sternum.

VII. ANALYSIS

All data recorded during the experiment were summarized by collecting the final three-second mean value (the last 30 torque values) and the peak torque (the greatest of the 30 torque values) for each exertion by each subject. This was done for all benchmark tests (eight per subject per session for three sessions) and all tests in the main sequence (40 per subject per session for three sessions) resulting in a total of 144 data points per subject of which 120 were a part of the data for the main experiment.

All data from the main experiment were analyzed to determine significant differences in torque resulting from the effect of each of the six independent variables tested: connector size, grip type, orientation, glove usage, height, and direction of torque. Male and female data were combined in examining these effects. Because of the unequal number of male and female subjects (20 and 11, respectively), meaningful comparisons between male and female data could not be made. (It is recommended that this comparison be made when an equivalent number of female subjects have completed the experiment.)

Statistical Procedures

Following collection and summarization of the three-second mean and peak data on separate Compaq micro-computer discs, the data were transferred to disc storage on the NAS-6 main frame computer facility at the Iowa State University Computation Center. Here, analysis employing SAS (Statistical Analysis System) was employed using the GLM (General Linear Models) procedure. The Duncan Multiple Range Test was employed in analyzing each of the six independent variables because of its suitability for two- and three-way comparisons. The overall test procedure was organized as follows.

First a t-test was used to compare loosening (counter clockwise) and tightening (clockwise) data for all subjects. No significant difference was found. In this case, the number of degrees of freedom was estimated as

$$f = \frac{\left[s_1^2/n_1 + s_2^2/n_2\right]^2}{\frac{\left(s_1^2/n_1\right)^2}{n_1 - 1} + \frac{\left(s_2^2/n_2\right)^2}{n_2 - 1}}$$

For this experiment, f was 3683 (or infinity when using tables). The calculated value of t was 0.703, insignificant at an alpha level of 0.1.

Following this test, each of the other five independent variables was analyzed with respect to mean torque occurring under each level at which it was tested using the Duncan Multiple Range Test. These levels

represented three sizes, three orientations, two grip types, two heights, and three gloved conditions. In addition the mean value for all male and female subjects were calculated for each combination of all six independent variables. These mean values were combined and summarized.

Results

Ranked in order of highest to lowest in terms of the effect upon grip torque strength, the six independent variables are presented as follows:

1. Size of connector
2. Type of grip employed
3. Orientation of connector
4. Use of gloves
5. Height of connector
6. Direction of torque

Of these, the first four indicated high levels of significance in an overall analysis of variance (beyond 0.01). The first three indicated levels of significance at or below the 0.05 alpha level, using the Duncan Multiple Range test. Male and female data were combined in making these analyses. Data for loosening and tightening were analyzed separately.

VIII. RESULTS

A. Graphical Analysis

The effects of the six independent variables upon hand grip torque strengths when tightening or loosening electrical connectors are best understood when viewed graphically. Figures 5 and 6 show grip torque strengths as a function of connector ring diameter for the two heights, three gloved conditions, three orientations, and two types of grip.

B. Connector Size

Connector size had the greatest effect on grip torque strength. This is logical since size affects the area of gripped surface as well as the torque moment. Data averaged among males and females for the three sizes tested were as follows:

Torque (in. lbs) (-) counter-clockwise in.-lbs
(+) clockwise in.-lbs

Size	Loosening	Tightening
Small (0.9 in.)	- 5.13	4.35
Medium (1.5 in.)	-15.70	15.16
Large (2.0 in.)	-26.13	28.36

The ratio of strength for the medium (1.5 in.) connector to the small (0.9 in.) connector is more than three to one, and between the

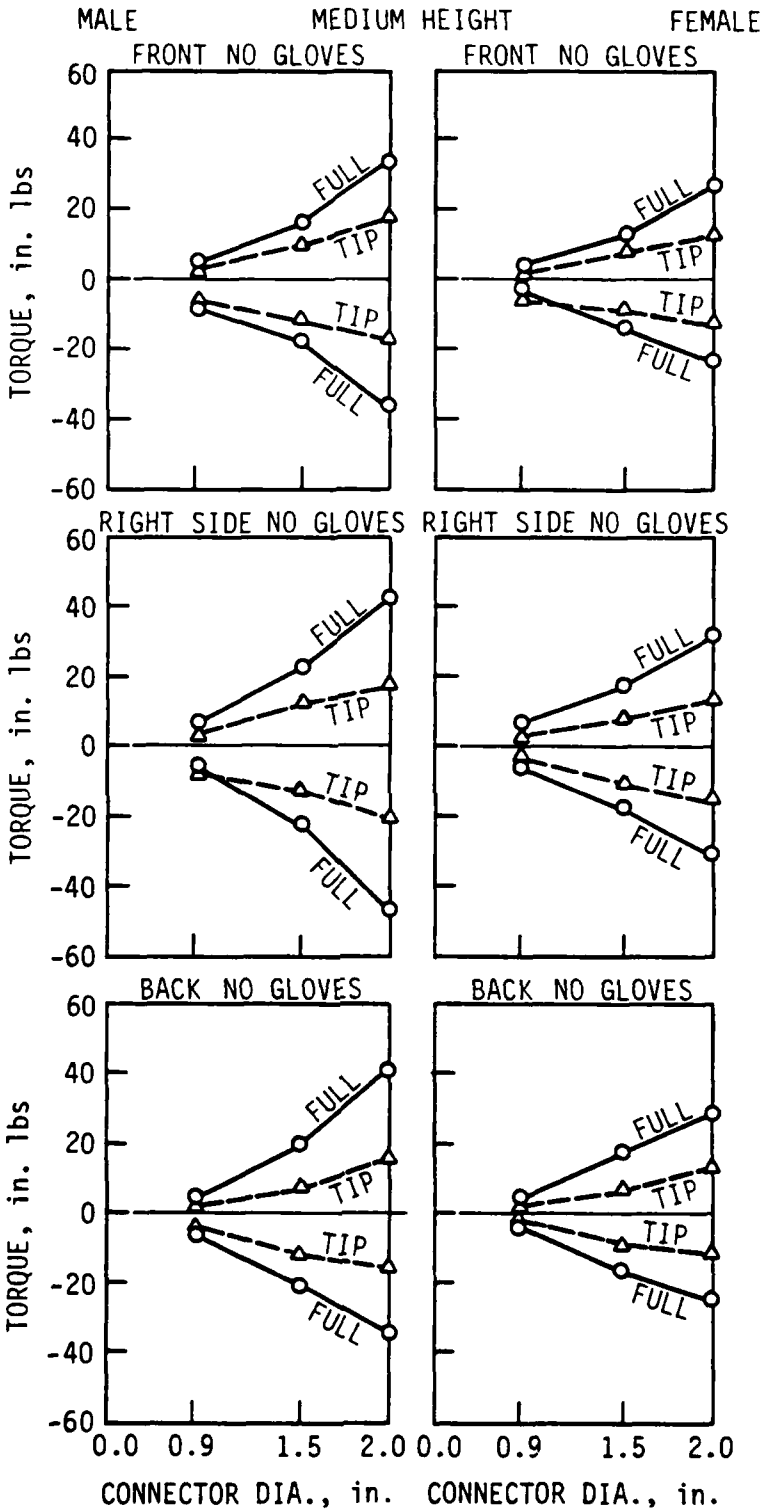

Fig. 5(a). Grip torque strengths at medium height from all three orientations when the subjects did not wear gloves.

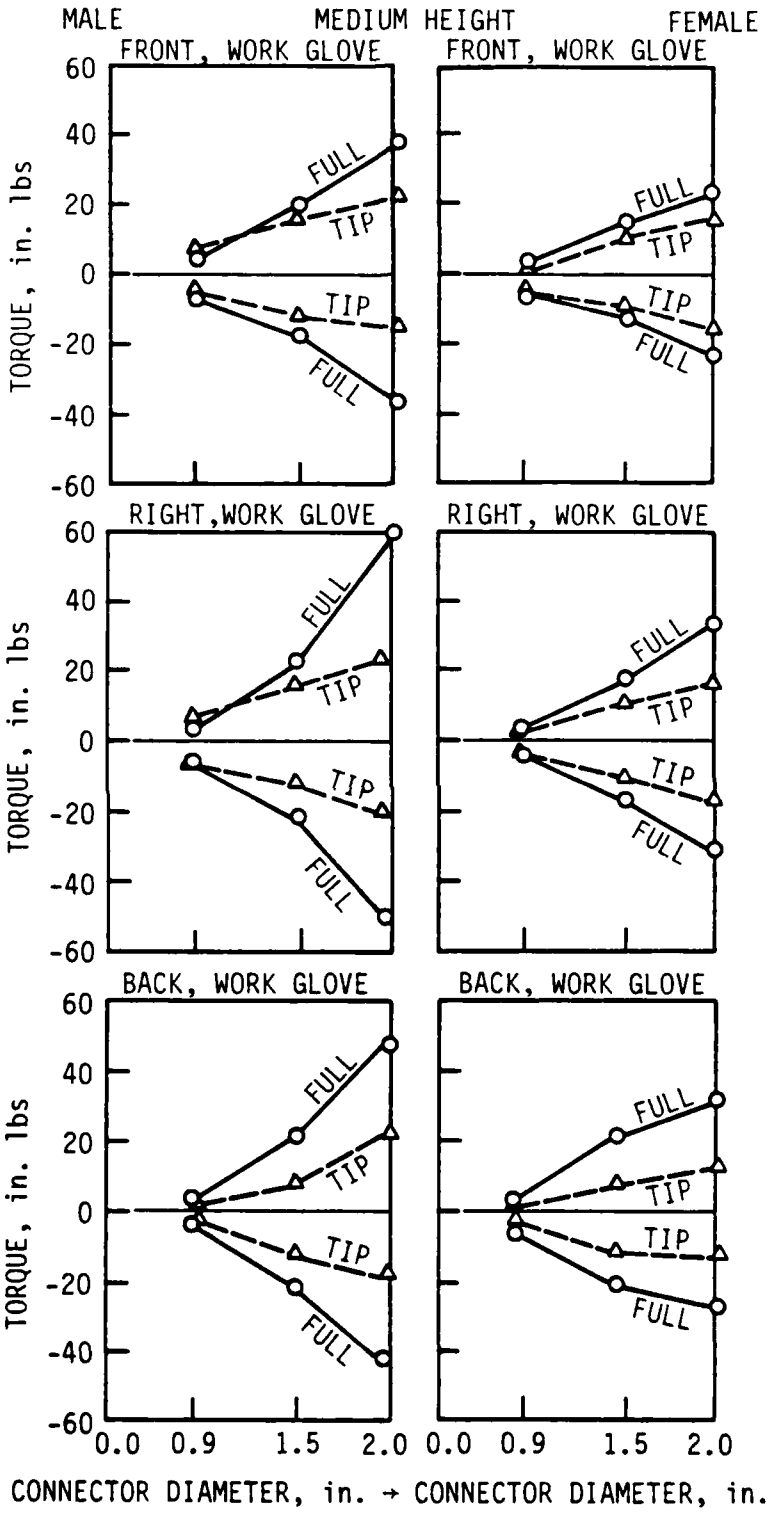

Fig. 5(b). Grip torque strengths at medium height from all three orientations when the subjects wore a work glove.

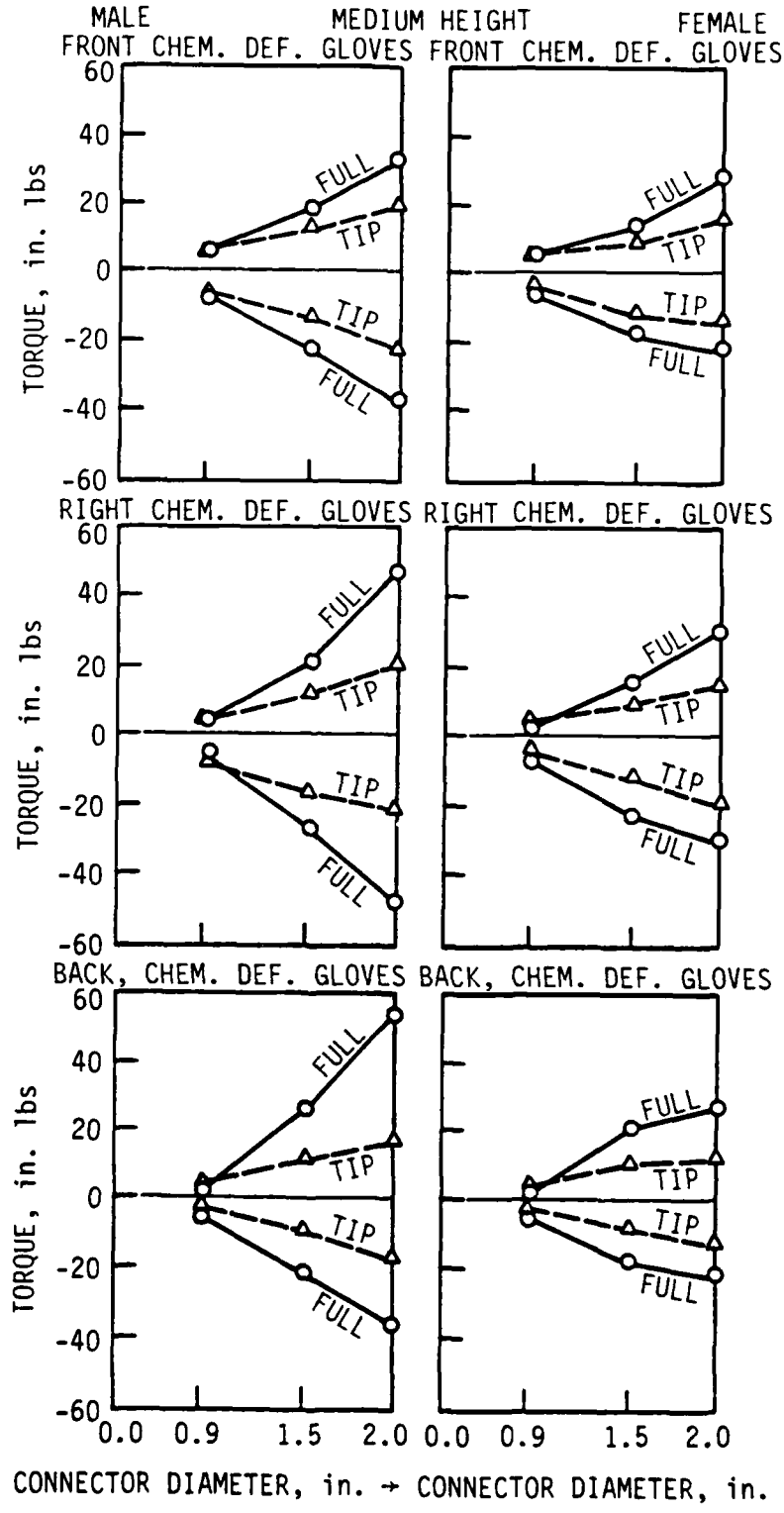

Fig. 5(c). Grip torque strengths at medium height from all three orientations when the subjects wore chemical defense gloves.

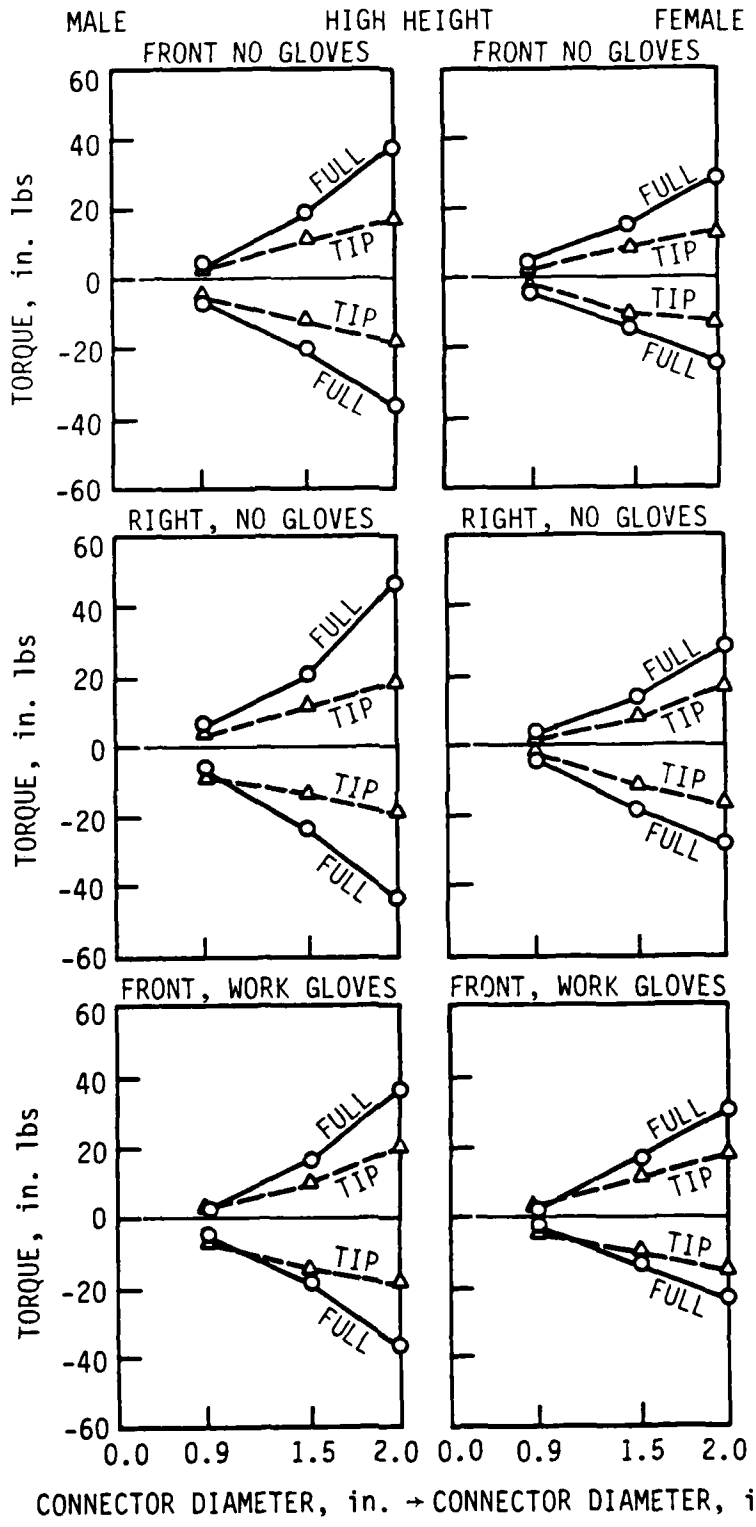

Fig. 6(a). Grip torque strengths at high height from front and right orientations.

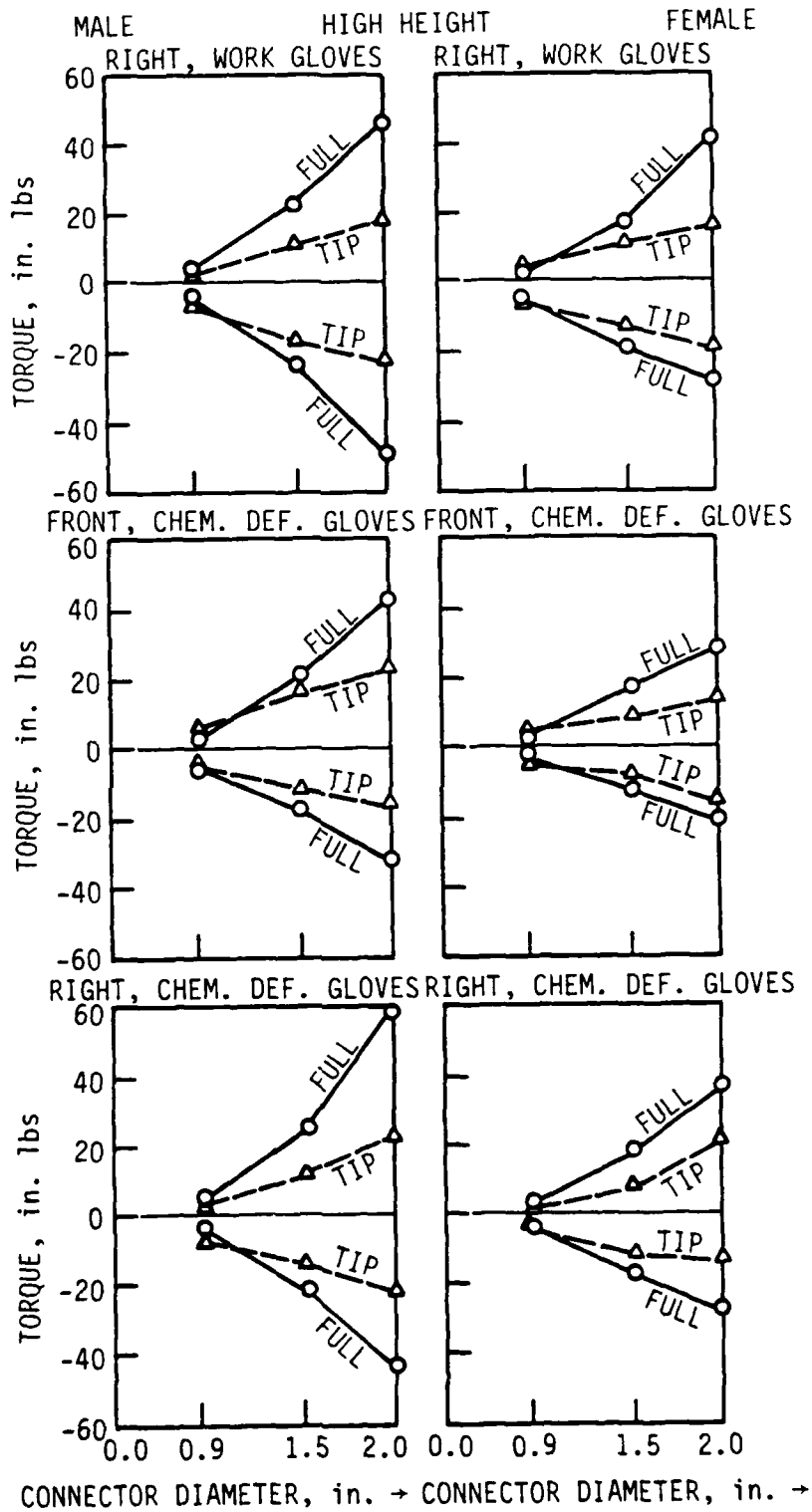

Fig. 6(b). Grip torque strengths at high height from front and right orientations.

large (2.0 in.) and medium connectors the ratio is nearly two to one. Differences in torque strength due to connector size were significant for loosening and tightening at an alpha level below 0.05. Direction of torque had practically no effect on torque strength.

C. Type of Grip

Full grip torque strength was approximately twice as large as fingertip torque strength for loosening and tightening. Averaged strength for males and females for the two directions was as follows:

Torque (in.-lbs)

Grip Type	Loosening	Tightening
Fingertip	-11.40	11.02
Full grip	-19.91	20.90

As in the previous case, no significant directional effects are evident. Difference due to grip type was significant at an alpha level below 0.05.

D. Orientation

Orientation also has a significant effect upon grip torque strength. The greatest strength occurred when the connector was grasped on the subject's right side with the wrist performing a forward flexion for

tightening or backward extension for loosening. The resulting data, averaged for males and females, were as follows:

Torque (in.-lbs)

Orientation	Loosening	Tightening
Front	-14.58	14.66
Right side	-17.53	17.20
Back	-14.06	16.07

Working from the back of the connector mounting plate did not produce a decrement compared with working from the front and side. In fact, tightening strength from behind the connector was higher than from the front. Loosening from the back was very difficult because of the orientation of the hand and the resulting inability to utilize forearm muscles effectively for wrist action in that position. Direction again had no significant effect except for a slight advantage of tightening over loosening from the back. For loosening, torque exerted from the right side was significantly higher (alpha equal to 0.05) than from the front or back, no other differences being statistically significant. For tightening, all differences due to orientation were significant at the 0.05 level.

AD-A166 176 UNITED STATES AIR FORCE SUMMER FACULTY RESEARCH PROGRAM 02/13
1985 TECHNICAL RE (U)UNIVERSAL ENERGY SYSTEMS INC
DAYTON OH R C DARRAH ET AL DEC 85 AFOSR-TR-86-0139
UNCLASSIFIED F49620-85-C-0013 F/G 5/9 NL

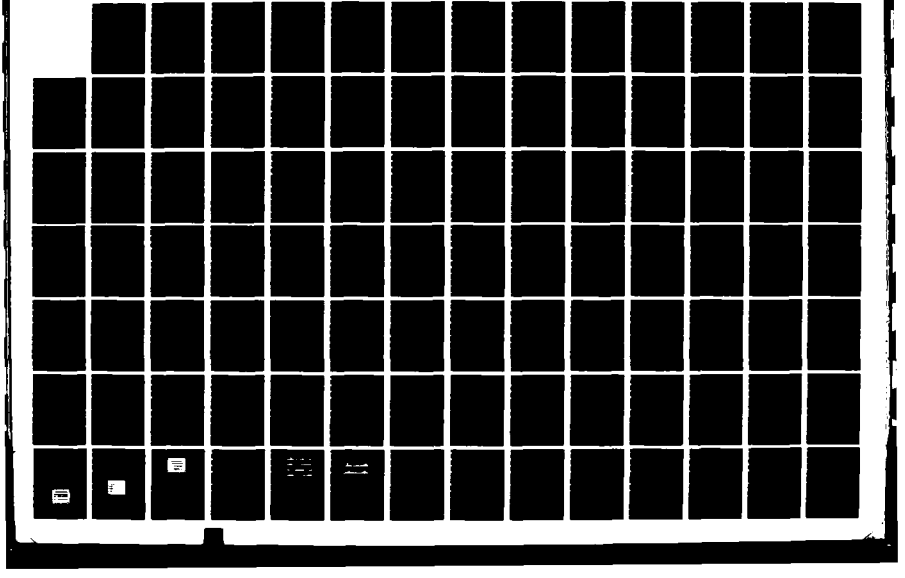

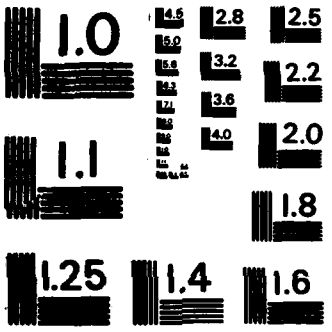

MICROCOPY RESOLUTION TEST CHART
NATIONAL BUREAU OF STANDARDS - 1963 - A

2. A fingertip grasp on small connectors can result in higher torque than a full grip because of reduced slippage.

3. Stronger hand grip torque can be exerted from the right than from the front or back because of more effective use of flexors and extensors affecting wrist and forearm motion and also because of additional torque provided by the upper arm.

4. The use of gloves increases hand grip torque strength beyond bare-handed strength in most situations. Approximately the same torque can be exerted using either a work glove or a chemical defense glove.

5. Connector height and the direction of rotation have little effect on grip torque strength between 60% and 85% of the reach height.

6. Males are significantly stronger than females for tightening and for loosening.

X. RECOMMENDATIONS

1. The effect of obstructions (adjacent connectors) upon grip type and torque strengths should be investigated for the three orientations employed in the present study.

2. The effect of restricted hand and/or arm motions and positions upon hand grip torque strength should be investigated.

3. A comparison should be made between straight connectors and L-shaped connectors of equivalent size with respect to the torque strength that can be applied to them.

4. Classifications and levels of hand mobility/obstruction need to be defined in order to relate grip posture and torque strength.

5. A flexible mock-up enclosure should be designed that would permit simulating problems in real maintenance tasks resulting from constricted work areas that limit grasping and hand/arm movement.

XI. ACKNOWLEDGMENTS

The principal investigator is grateful to the U.S. Air Force Systems Command, the U.S. Air Force Office of Scientific Research, the Aerospace Medical Research Laboratory, the Biodynamics Laboratory (sub unit), the University of Dayton Research Institute, and Universal Energy Systems for providing the research program, laboratory, equipment, technical support, funding, and program management that made this research possible.

The principal investigator and his assistant are especially grateful to certain key individuals without whose knowledge, skills, and efforts the project could not have been completed in ten weeks. First, the guidance and advice of Dr. Joe McDaniel, Director of the Biodynamics Laboratory, was invaluable in planning the study. Van Thai should be credited with developing the analog to digital/computer interface and the necessary software to permit direct processing of raw data using a minicomputer. Nilss Aume designed the simulated connectors and torque measuring system used in the study. Thanks are also given to Tom Garver and Morris Milton for building and maintaining the research apparatus. Glenn Robbins provided much needed support in assisting with the recruitment, interviewing, and measurement of subjects. Finally, thanks are expressed to all who helped out in any way, through personal effort or encouragement to see that the research was performed with the kind of professional dedication that has so long been traditional at the Aerospace Medical Research Laboratory and has established its reputation worldwide as a leader in human factors research.

Thanks are also expressed to the Department of Industrial Engineering (Dr. Keith L. McRoberts, chairman) and to the Engineering Research Institute Office of Editorial Services at Iowa State University for typing, editing, and assembling the final report. The authors would also like to thank Wayne Barkema, manager of Data Preparation at the ISU Computation Center for preparing the initial draft on a word processor.

REFERENCES

1. McDaniel, J. W. and Askren, W. B. "Computer-Aided Design Models to Support Ergonomics," Reports submitted to U.S. Air Force Aersopace Medical Research Laboratory, Wright Patterson AFB, Ohio, 1985.
2. Bapu, P. T., Korna, M. and McDaniel, J. W. "User's Guide for COMBIMAN Programs Version 6," Air Force Aerospace Medical Research Laboratory Technical Report 83-097, Dec. 1983, Wright-Patterson AFB, Ohio, AD139139.
3. McDaniel, J. W. "Computerized Biomechanical Man-Model," Air Force Aerospace Medical Research Laboratory Technical Report 76-30, July 1976, Wright Patterson AFB, Ohio, AD A032402.
4. Replogle, J. O. "Hand Torque Strength with Cylindrical Handles," Proceedings of the Human Factors Society 27th Annual Meeting, Oct. 10-14, 1983, Norfolk, Va., pp. 412-416.
5. Pheasant, S. and O'Neill, D. "Performance in Gripping and Turning--A Study in Hand/Handle Effectiveness," Applied Ergonomics, Vol. 6, No. 4, 1975, pp. 205-208.
6. Swain, A. D., Shelton, G. C. and L. V. Rigby. "Maximum Torque for Small Knobs Operated With and Without Gloves," Ergonomics, Vol. 13, No. 2, 1970, pp. 201-208.
7. Rohles, F. H., Moldrup, K. L. and Laviana, J. E. "Opening Jars: An Anthropometric Study of the Wrist-Twisting Strength of the Elderly," Proceedings of the Human Factors Society, 27th Annual Meeting, Oct. 10-14, 1983, Norfolk, Va., pp. 112-116.

8. Petrofsky, J. S., Williams, C., Kamin, G., and Lind, A. "The Effect of Handgrip Span on Isometric Exercise Performance," Ergonomics, Vol. 23, No. 12, 1980, pp. 1129-1135.

9. Caldwell, L. S. et al. "A Proposed Standard Procedure for Static Muscle Strength Testing," American Industrial Hygiene Association Journal, Vol. 35, April 1974, pp. 201-206.

APPENDIX I

Instructions for Subjects for Maximum Voluntary Hand Grip Torque for Standard Circular Electrical Connectors

This test is designed to measure the maximum torque that you can exert over a four-second interval in tightening and loosening standard circular multi-pin electrical connectors. You will be exerting torque, with your right hand without a glove and with work and chemical gloves, upon various sizes of simulated electrical connectors located at specified heights and angles. The torque that you apply will be measured by an electric load cell. The connector will not turn, regardless of how much torque you apply. You will be exerting torque using two types of grip: a fingertip grip and a full wrap-around grip. It is important that you use the type of grip specified during each exertion and that you apply torque in the proper direction (clockwise as in tightening or counter clockwise as in loosening) as instructed.

When exerting a torque, twist as hard as you can with a single sustained twist for four seconds. Start twisting when told to do so. A tone will sound when the four-second interval is over. You may relax and let go of the simulated connector at that time. You will then be given a two-minute rest period during which another subject will perform a torque exertion. You will alternate with this other subject until the test sequence is completed.

You will be permitted to dry your hands with a paper towel during the rest periods. You should wipe your fingertips before each trial.

APPENDIX II

Design Features of the Simulated Connectors

MATERIAL: MEDIUM ALUMINUM, BLACK ANODIZED

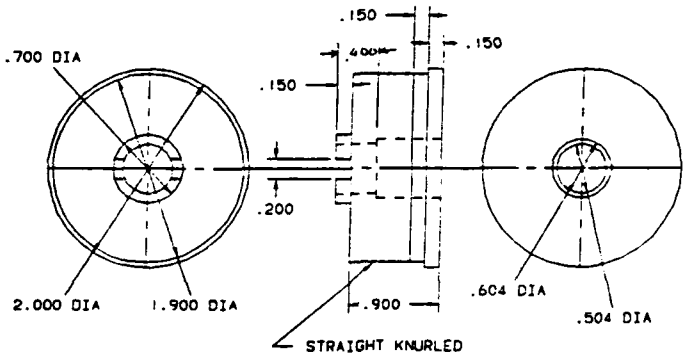

Fig. A.4. Large connector ring.

MATERIAL: MEDIUM ALUMINUM, BLACK ANODIZED

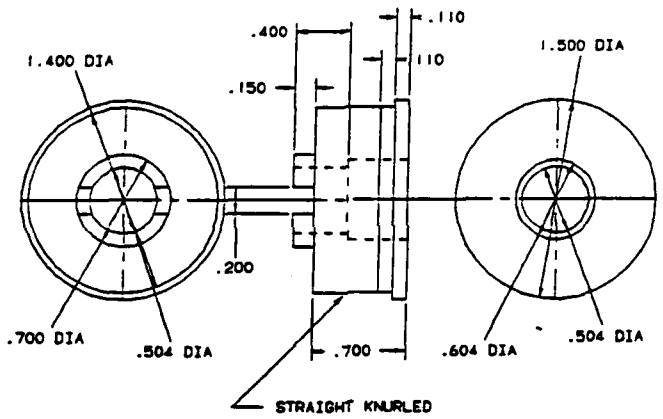

Fig. A.5. Medium connector ring.

MATERIAL: MEDIUM ALUMINUM, BLACK ANODIZED

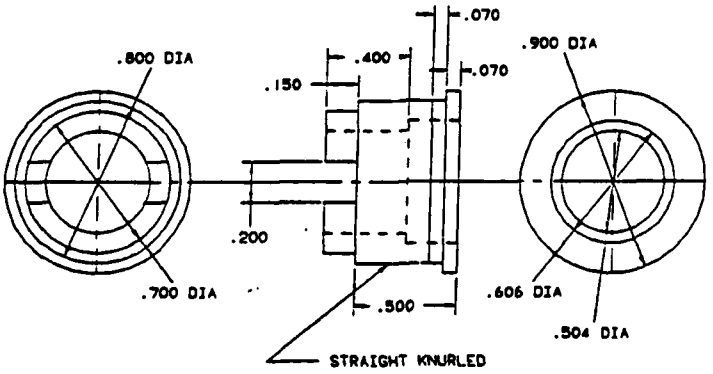

Fig. A.6. Small connector ring.

MATERIAL: MEDIUM ALUMINUM, CLEAR ANODIZED

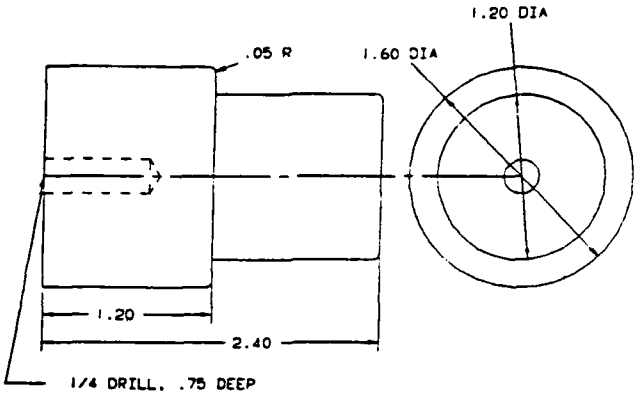

Fig. A.1. Large backshell.

MATERIAL: MEDIUM ALUMINUM, CLEAR ANODIZED

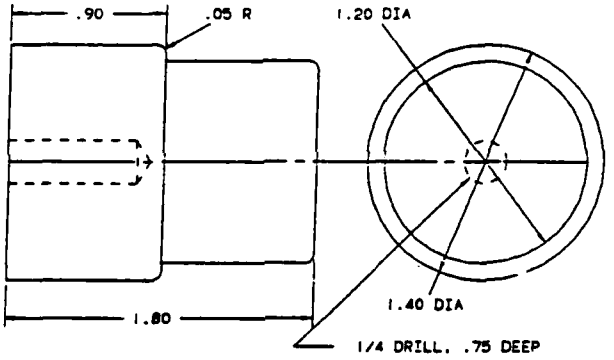

Fig. A.2. Medium backshell.

MATERIAL: MEDIUM ALUMINUM, CLEAR ANODIZED

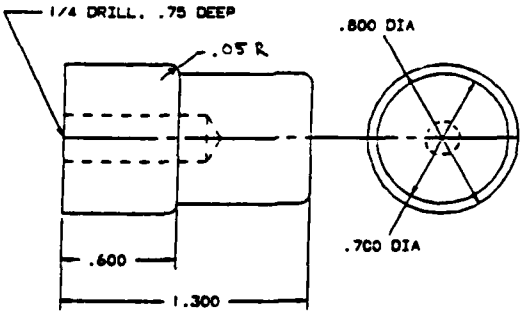

Fig. A.3. Small backshell.

1985 USAF-UES SUMMER FACULTY RESEARCH PROGRAM/

GRADUATE STUDENT SUMMER SUPPORT PROGRAM

Sponsored by the

AIR FORCE OFFICE OF SCIENTIFIC RESEARCH

Conducted by the

UNIVERSAL ENERGY SYSTEMS, INC.

FINAL REPORT

PROPERTIES AND PROCESSING OF A PERFLUORINATED POLYALKYLENE LINKED POLYIMIDE

Prepared by:	Vernon R. Allen
Academic Rank:	Professor
Department and	Chemistry Department
University:	Tennessee Technological University
Research Location:	Polymer Branch AFWAL/MLBP ASD
	Wright-Patterson, Ohio 45433
USAF Research	Ivan J. Goldfarb
Date:	6 September 1985
Contract No:	F49620-85-C-0013

PROPERTIES AND PROCESSING OF A PERFLUORINATED POLYALKYLENE LINKED POLYIMIDE

by

Vernon R. Allen

ABSTRACT

The chemical and physical properties of a thermoplastic aromatic polyimide were examined with regard to cure conditions by IR and DSC techniques. Reaction by-product evolution and thermal stability were also examined by TGA and by GC-MS. In the absence of activating catalysts such as pyridine or dimethylacetamide and moisture scavengers such as acetic anhydride, the reaction of the monomers proceeds slowly in the 100°C - 200°C range. Final imidization with H_2O release occurs very slowly above 150°C due to the concomitant increase in the glass transition temperature. Complete reaction required extended cure periods above the glass transition temperature of 350°-370°C. In the absence of (the plasticizing agent) N-methylpyrrolidone, compression molding with sample compaction (flow) of a partially cured molding powder required molding pressures in excess of 200 psi at 380°-400°C. The 130°-140°C "consolidation window" was not found for this sample of polyimide.

ACKNOWLEDGEMENTS

Sponsorship by the Air Force Systems Command and the Air Force Office of Scientific Research made this research project possible. The writer wishes especially to acknowledge the AFWAL/MLRB Materials Laboratory and its staff for the techinical assistance and for the spirit of friendly cooperation. A heart felt thank you is included.

I. INTRODUCTION: Although my academic job description is professor of chemistry, my research experience and specialties training are best described as materials scientist. The areas of specialty training include:

i. thesis research in elastomer theory and mechanism of rubber degradation,

ii. post-graduate research in viscous behavior of polymeric systems,

iii. summer applications of (classroom) macromolecular theory in copolymerization, polymer modification, fluorinated elastomers, polymides, and viscoelastomeric analysis of epoxy systems.

This varied experience involved summer programs with NSF, ASEE (NASA) and industry (AVCO, Gulf, duPont, and Carbide).

During the early part of my academic career, I was involved in the direction of (MS) thesis research with publications in the area of polymer structure-polymer properties correlation. Materials research in high temperature polymeric systems has produced a variety of promising resins including infusible themosets, addition-cured acetylene-terminated sulfones, and aromatic/heterocylic themoplastics. Even though each exhibits excellent chemical and thermal stability, as required for application in the thermooxidative environment of high-performance aircraft, each also exhibits rheological restraints, such as high glass-

transition temperatures and/or void-formation in some polycondensates, which create distinctive processing difficulties. The evaluation of processing variables and the relation of polymerization condition and cure behavior to these variables is an area in which my varied experience appears ideally suited and in an area in which the "Processing and Properties" section of the Polymer Branch of AFWAL is continually engaged.

II. OBJECTIVES OF THE RESEARCH EFFORT: A sample of a high temperature polymeric system, a perfluoroakylene linked polyimide, was available for testing at the start of the research period. Outstanding physical and mechanical properties were submitted by the supplier for this system. It was deemed of importance to identify the polymerization variables, especially with regard to the extent of solvent release and its resultant effect on the glass transition temperature. Also, it appeared necessary that the role of the polycondensation by-product, water, in auto-catalysis of depolymerization and in void formation during processing be studied.

As the research proceeded it was decided that an effort be made to establish the system composition in order to better interpret obtained data and to help establish a more complete understanding of the processing variables.

The major objective of the program, substantiation of supplier reported physical and mechanical properties, was not completed but a more in-depth understanding of the prime variables in process control of this system was arrived at during this period.

III. HISTORICAL BACKGROUND: Aromatic polymidies for high temperature applications possess outstanding thermooxidative stability due to the presence of the imide-aromatic fused cyclic groups in the chain backbone. The past several decades have seen extensive research effort designed to evaluate the prime variables in the polymerization process, e.g. nature of the monomers, order of monomer introduction, influence of solvents as reaction activators and as moisture scavengers, as reported in the review article by Sroog (1). A general two-step method was developed for formation of polyimides from aromatic diamines because of the excessive temperature required for melt-fusion reaction with aromatic systems. This two-stage polymerization usually incorporates pyromellitic dianhydride (or tetra-acid or diacid-diester) in an activating solvent such as DMAc with an aromatic diamine to produce a polyamic acid precusor at ambient temperature (eqn. 1) with subsequent conversion to the imide form at elevated temperature (eqn. 2).

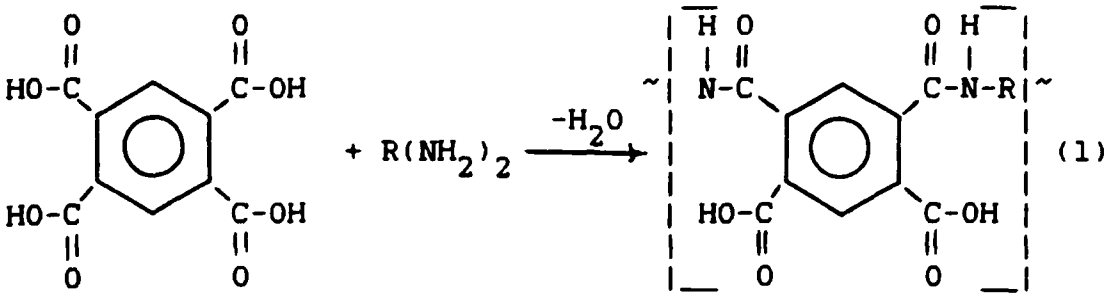

(1)

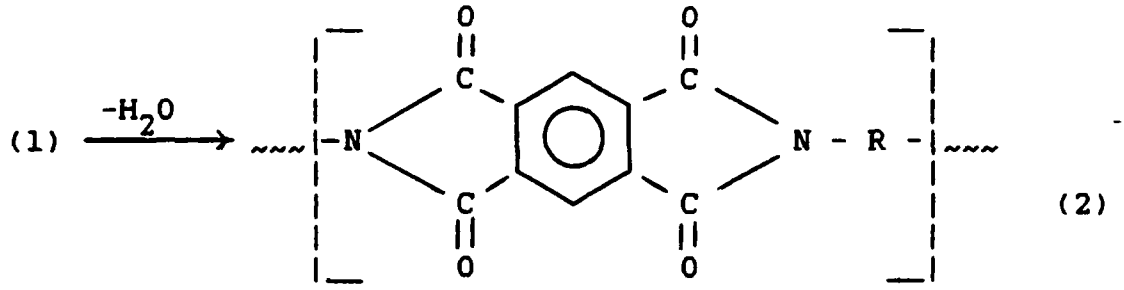

(2)

The obtainment of high molecular weight product is dependent on temperature control and moisture exclusion during amic acid formation. A kinetic study by Kaas (2) established autocatalysis in amic acid formation by carboxylic acid groups. The influence of the solvent (3,4) and Lewis base strength of the amine (5) have been reported to have a controlling effect on the value of the equilibrium constant for amic acid formation.

Sroog reports (ref. 1, p. 168) that poly(amic acid) films may be prepared by casting the polymerization mixture directly into glass or metal plates with vacuum drying at 80°C and may be used for IR determination of the extent of imidation. Assignment of spectral bands for various polyimides have been made by Dine-Hart and Wright (6) and by T. Mastsuo (7). The

amide 3.08 μ N-H band disappearance and appearance of the cyclic imide bands at 5.63 and 13.85 μ have been used to measure the degree of conversion to the imide form (8). Thermal conversion of poly(amic acid) film to the polyimide form was followed by Lusheikin (9) with tan delta measurement. Endrey (10) and Vinogradova et al. (11) reported on the catalyzed conversion of poly(amic acid) to polyimide using a combination of dehydrating agents and a strong Lewis base.

The observed decrease in rate of imide formation with extent of reaction was interupted by Kreuz et al. (12) to be related to chain stiffening with conversion. They also suggested that DMAc accelerates the reaction by favorable orientation for ring closure. Thus, as DMAc is lost during heating, the initation reaction is retarded.

IV. EXPERIMENTAL PROCEDURES AND RESULTS: The sample supplied for this study was a NR-150 polyimide precursor solution containing a proprietary aromatic tetracarboxylic acid, 2,2-bis(3',4'-dicarboxyphenyl) hexafluoropropane (6FTA) (13). This monomer was dissolved in ethyl alcohol with a stoiciometric quantity of various amines, including m-phenylene and p-phenylenediamine (MPD and PPD). On heating the monomers are reported to be converted into a thermoplastic polyimide with excellent thermal stability and outstanding toughness. Polyimides containing perfluoroalkylene bridging units have been reported by Critchley et al. (14) to exhibit low glass transition temperatures but still retain the

thermooxidative stability which is typical of aromatic polyimides.

A brief outline of the procedure followed in the evaluation of the properties of this novel polyimide precursor system is presented:

A. Preparation of poly(amic acid) films for imidation rate studies;
   1. Casting of original solution.
   2. Casting of curved solutions.
   3. Identification of 6FTA structure.

B. DSC, IR and TICA analyses of heat-treated samples;
   1. Relation of DSC endotherms with spectral changes.
   2. Determination of Tg as function of state of cure.
   3. Molding behavior versus state of cure.

A-1: Following the film preparation technique described by Sroog (1), efforts were made to obtain films with dimensional stability for subsequent cure studies. THe original precursor solution was cast onto glass, steel, teflon and cellophane substrates without success, even though heated under N_2 to 150°C for 72 hours. The product was brittle however infra-red analysis showed strong imide formation for comparable films cast directly onto NaCl plates (Figure 1). Attempts to produce KBr pellets for IR studies of the glassy (brittle) cured samples indicated a strong hygroscopic character with rapid clouding of the pellet on exposure

to air (Figure 2-A). [This property is discussed in more detail in the next section.]

A-2: Unable to obtain a film from the prescursor solution, a sample of the ethanol-solution was "dried" in a stream of N_2 at ambient temperature. This viscous system foamed on slow heating in N_2/vacuum (5 in Hg) in the 60^{o}-80^{o}C range. Both IR analysis (Figure 2-A) and DSC examination (Figure 3) suggested polyamic acid formation. It was later established that the broad band in the 3.6-3.0 μ range of Figure 2-A and the 60^{o}-100^{o}C endotherm in all DSC curves was due to the hygroscopic nature of the cured polyimide. This conclusion was based on two pieces of evidence:

first, a sample of polyimide cured by heating 2 hours each at 80^{o}C and 142^{o}C and one hour at 300^{o}C was dissolved in DMAc and cast as a 1 mil film. The IR spectrum of this film (Figure 2-curve B), dried 104 hours at 150^{o}C with N_2 flush, showed no evidence of the strong 3.6-3.0 absorption observed using KBr pellets on comparably cured samples, and second, the DSC curve A of Figure 3 showed no low temperature endotherm when cooled in N_2 atmosphere (curve B) but the original endotherm reappeared when the top of the sample holder was pierced and the sample allowed to stand overnight in 35-50% humidity (ambient) (curve C).

Numerous efforts were made to obtain thicker (20-30 mil.) films by dissolving partially-cured samples in DMF, DMAc, THF and NMP with no success. Two weeks in vacuo at 120^{o}C with continual N_2 flush produced either brittle flakes (from THF and DMF) or remained viscous under a tack-free surface.

A-3: As mentioned in the "Objectives" section, several weeks into the project it was considered that the 6FTA may have become partially esterified, resulting in the difficulties experienced in formation of a poly(amic acid) film. This hypothesis was based primarily on the slow release of ethanol during GC-MS analysis (Figure 4). A limited effort using NMR analysis was made without definitive results. Using the technique of thin layer chromatography, TLC, it was found that the supposed polyamic acid, cured at 120°C for 16 hours, contained principally three ingredients. Gas chromatography on the dried precursor solution contained only two major ingredients, the 6FTA and diamine mixture. Titration of the original precursor solution and of a dried sample against freshly-standardized ethanolic KOH yielded data indicative of four moles of carboxylic acid per mole of sample.

B-1: Scanning calorimetric analysis at 10°C/min. heat-up rate produced foaming unless the sample had been cured at temperatures above 80°C (Figure 5-A). A slower rate of 2°C/min. eliminated foam formation even for samples dried at 66°C (Figure 5-B). Also, when the sample had been cured one hour at 140°C, the DSC heating cycle yielded a cured sample with no endotherms on reheating and allowed clear determination of Tg at 355°C (Figure 5-C). When the same sample had been futher heated to

300°C for one hour with overnight oven cool-down, the 150°-200°C endotherm was not in evidence. An attempt was made to correlate spectral changes with state of curve using the heated cell but the slow rate of solid-state reaction and high temperature involved voided this technique (to prevent equipment damage).

B-2: A THF solution of a cured sample was used for preparation of TICA samples in the method described by Lee et al. (15). Torsional mechanical spectrometry of the impregnated cloth specimen is presented in (Figure 6) as obtained showing storage modulus (G'), loss modulus (G") and tan delta (G"/G') at 0.16, 1.6 and 16 Hz. Microscopic examination of the impregnated cloth after cool-down showed numerous resin patches of a foamy character (Figure 7-A). Similar examination of a resin-cloth specimen, prepared from the original precursor solution in ethanol without prior drying or heating, resulted in foamed resin-areas with poor glass filament wetting and, more importantly, the resin coating was mottled with dark-brown spots (Figure 7-B). Additional TICA analysis on a sample soaked in DMF (to improve resin dispersion) and on a sample cured at 300°C for one hour after glass-cloth impregnation were made with the results in modified form presented (Figure 8).

C: A study of molding characteristics of samples heated to 120°C for 72 hours in N_2/vacuum (30 in Hg) was made to

take advantage of the "consolidation window" discussed in reference 13 (p. 10). The foamed sample was ground in a mortar and pestle, screened through 144 μ sieve, and this molding powder placed in stainless-steel "dog-bone" molds, dried overnight at 100°C and placed directly in a stainless-steel vacuum bag, evacuated and flushed with N_2. Molding conditions were six hours heat-up to 400°C at 200 psi with a one hour ramp at 130°C. Effort was made to obtain level sample in the mold with vibration. Insufficient flow failed to yield a homogeneous section though some sections (thicker) did exhibit the desired characteristics of consolidation. One sample, heated to 415°C at 600 psi, gave desired flow but showed evidence of decomposition (black color, sublimed solid and stainless-steel coloration).

The best molded product was subjected to torsional mechanical spectrometry with the results presented in (Figure 9). Two other samples were subjected to Instron "tensile testing" under ambient conditions at 0.02 in./min. cross head speed without extensometer. Tensile moduli of 2.3×10^5 ksi and 3.2×10^5 ksi were obtained at 2% extension. Failure data were not calculated due to less than perfect samples.

V. DISCUSSION OF RESULTS: In the absence of an activating "plasticizer" such as DMAc (see Ref. 12 p. 170), both poly(amic acid) and polyimide formation occurs slowly in the

solid state for this special sample of NR-150-B252X as evidenced by comparison of IR spectra in Figure 2, the 150°-200°C endotherm corresponding to water loss on imidation, and increased Tg and G' on cool-down for the TICA and Torsion spectrometry data in Figures 6 and 9. The solvent, ethanol, is too volatile and does not have the Lewis-base strength of the solvents normally used in poly(amic acid) formation under ambient conditions (see Table II of Ref. 1) to both catalyze the amidation and imidation reactions and to retard the formation of the glassy solid state. The sample heated in the solid state for two hours at 80°C, two hours at 142°C and one hour at 300°C was incompletely curved as shown by the increase in Tg and G' on cool-down of curve B in Figure 8 and the sample molded at 400°C in Figure 9.

The hygroscopic character of the partially-cured polyimide and the deleterious effect of water on product molecular weight (Ref. 10) make infrared analysis of extent of reaction qualitative at best except with specialized equipment (see Ref. 2 p. 2259). The broad absorption in the 3.6-3.0 μ region due to absorbed moisture and subsequent clouding of KBr pellets makes difficult the quantitative measure of the amide N-H absorption at 3.02 μ, as presented in curve A of Figure 2.

The appearance of brown spots on the TICA sample - see curve B of Figure 7 - were very pronounced and may indicate phase separation of the amine(s) on solvent evaporation in that this spotting was not observed on the DMAc treated sample

or an the TICA sample preheated to 300°C. It was also evident, based on microscopic examination, that DMF treatment of the THF-cast TICA sample produced better "wetting" of the fiber bundles and also produced an order of magnitude increase in the storage modulus, as evidenced by the comparison of Figures 6 and 8.

The character of the TICA sample preheated at 300°C for one hour - curve B of Figure 8 - was strikingly different from the other samples, being tough and flexible with no fiber breakage or resin separation on cloth-folding. Thus, consideration of the absence of the 3.02 μ band in Figure 2 of curve B, the absence of an endotherm in curve C of Figure 5 and the high Tg as determined from the data of curve B of Figure 8, it may be concluded that polymerization of this system begins above 100°C and proceeds slowly as a solid-state reaction until above Tg in the 350°-400°C region. Because decomposition begins around 400°C - see Figures 4 and 10 - it has not been established that an optimum cure has been attained during this study although much background data has resulted in a clearer picture of the system and its cure characterists.

VI. RECOMMENDATIONS: The thermoplastic perfluoroalkylene linked polyimide was submitted to the Air Force for structural application as a composite matrix, having excellent thermo-oxidative stability and outstanding flexural strength and fracture energy. Verification of these properties was not

established during the course of this project but information concerning the chemical and physical properties of the system and cure characteristics was developed. It is obvious that further effort to achieve the original project goals requires application of this obtained information by:

1. Consideration of the primary difference between the researched system and the material for which the aforementioned properties were claimed - the absence of suitable "orienting" solvent (plasticizer) in the studied NR150-B252X system.
2. Initiation of a study to examine the influence of such a plasticizing solvent on cure behavior, especially as it affects separation of poly(amic acid) formation and subsequent ring-closing imidation to allow optimization of cure control and product properties.
3. Augmentation of reaction by-product (water) removal during the cure cycle by combination of thermal and microwave heating.
4. Examination of the molding cycle of precured molding powder as affected by plasticizer nature and content. Specifically, can the "consolidation window" be utilized in molding of structural shapes with controlled plasticizer content.

REFERENCES

1. Sroog, C. E., JPS Macromol. Rev. 11. 161 (1976).
2. Kaas, R. L., JPS Chem. Ed. 19, 2255 (1981).
3. Solomin, V. A. et al., Dokl. Chem. (Engl. Transl.) 236, 139 (1977).
4. A. Ya. Ardashnikov et al., Polym. Sci. USSR A13, 2092 (1971).
5. A. N. Pravednikov et al., Polym. Sci. USSR A15, 399 (1973).
6. Dine-Hart, R. A. and Wright, W. W., Makromol. Chem. 143, 189, (1971).
7. Matsuo, T., Bull. Chem. Soc. Japan 37, 1844 (1964).
8. Sroog, C. E. et al., JPS Part A 3, 1393 (1965).
9. Lusheikin, G. A. et al., Soviet Plastics 8, 31 (1972).
10. Endrey, A. L., Can. Pat. 645, 073 (1962).
11. Vinogradova, S. V. et al., Polym. Sci. USSR 16, 584 (1974).
12. Kreuz, J. A. et al., JPS A-1 4, 2607 (1966).
13. Private Communication to F. Hedberg, AFWAL/MLRB, Feb. 1985.
14. Critchley, J. P. et al., JPS A-1 10, 1789 (1972).
15. Lee, C. Y-C. and Goldfarb, I. J., AFWAL-TR-80-4159.

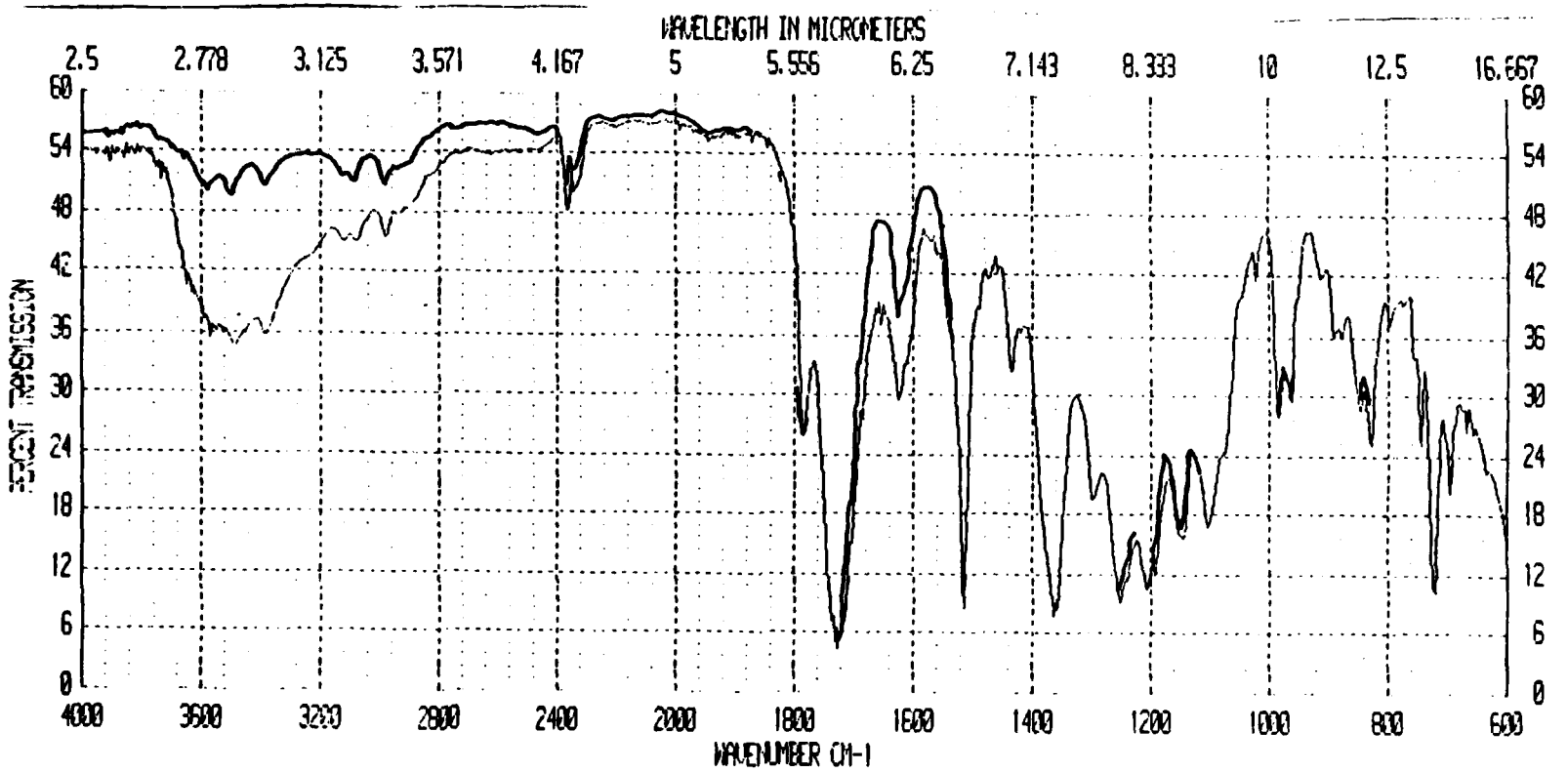

FIGURE 1. Infrared spectra of NR150B252X sample solution cast onto a NaCl plate, dried in vacuum - 5 in Hg - with N_2 flush and mounted in heated-cell assembley. The lower (lighter) curve represents the sample heated slowly to 150° at 3°C/min. The upper (darker) tracing is of the same sample heated to 200°C and held at that temperature for 15 minutes.

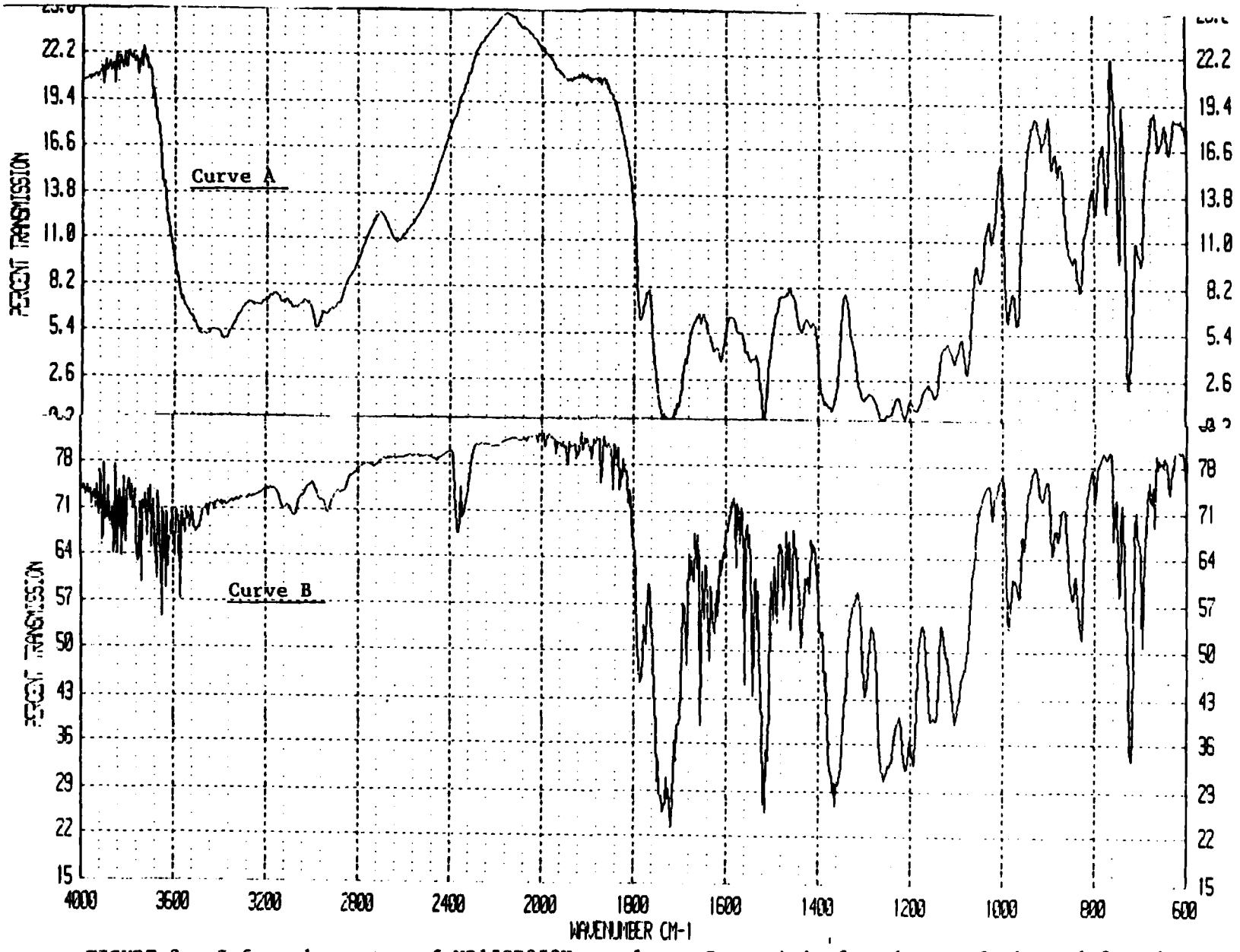

FIGURE 2. Infrared spectra of NR150B252X samples. Curve A is for the sample heated four hours at 120°C and made into a KBr pellet. Curve B is for a sample heated to 300°C in six hours, dissolved in DMAc and cast as a thin film.

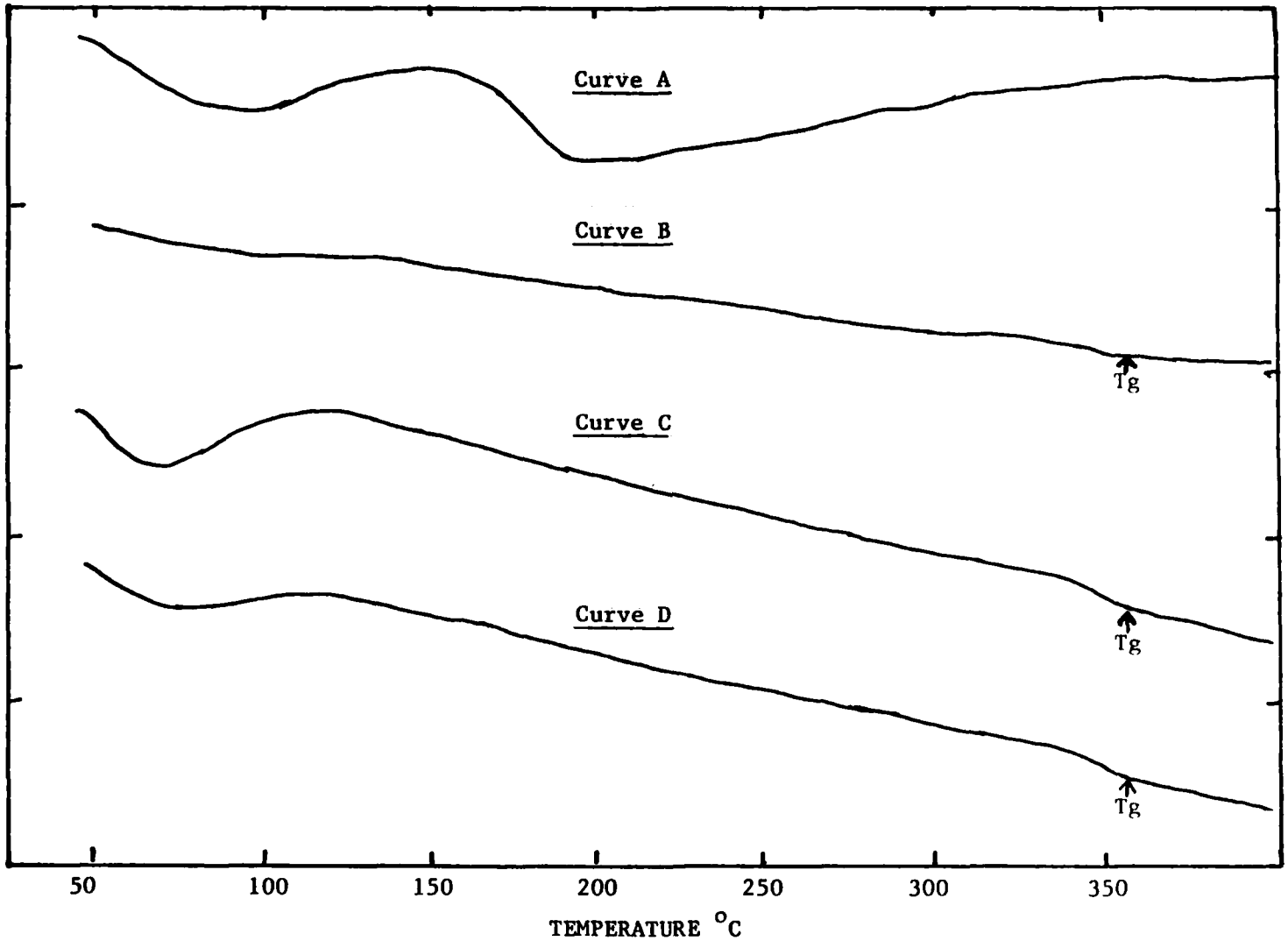

FIGURE 3. Tracings of DSC curves of NR150B252X sample preheated 66 hours at 120°C.
Curve A - 1st heatup. Curve B - reheat after N_2 cooldown in instrument.
Curve C - sample from B removed from pan and ground in air.
Curve D - sample cover pierced (4 holes) and allowed to stand in air four hours.

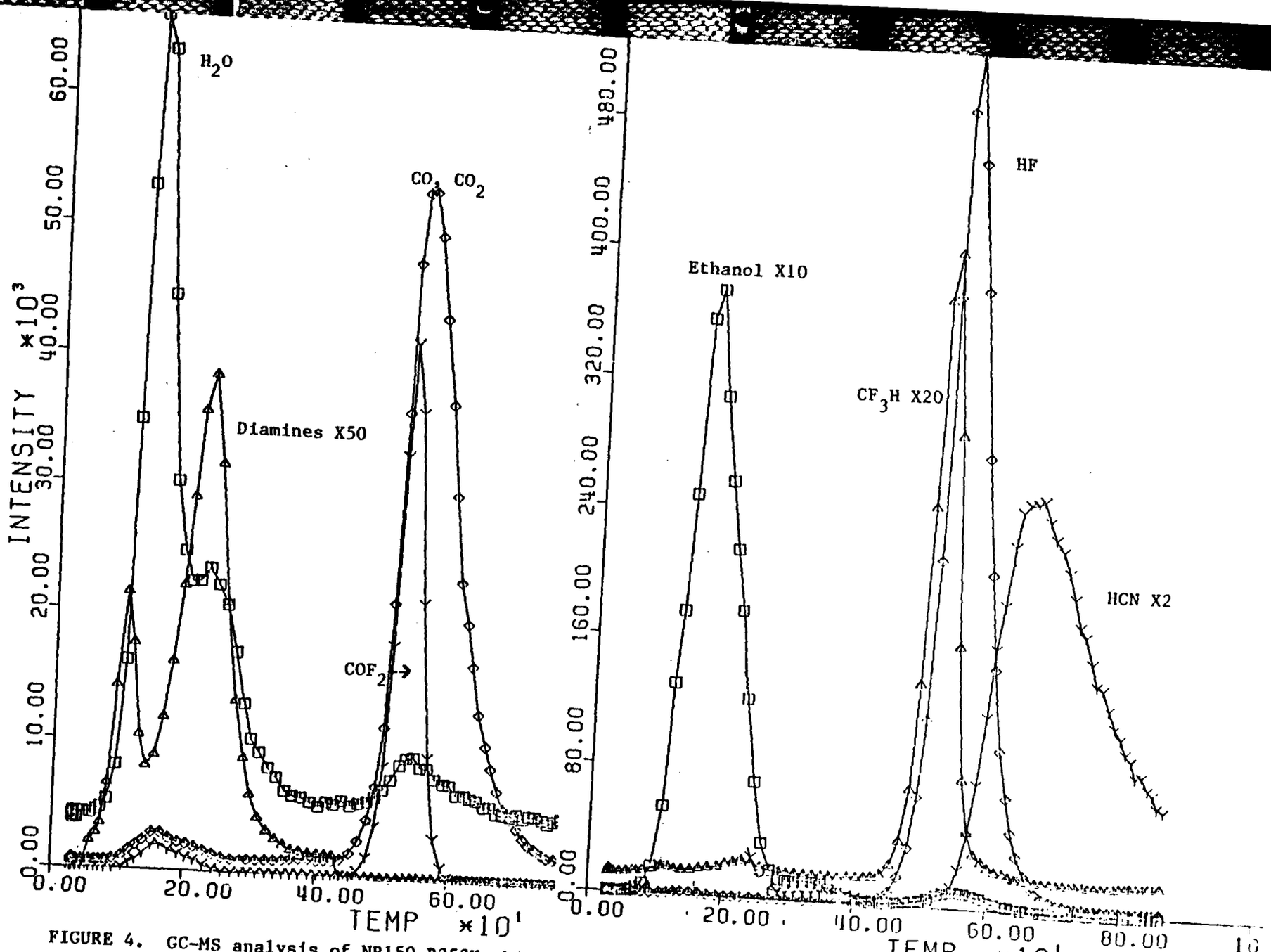

FIGURE 4. GC-MS analysis of NR150 B252X which had been preheated sixteen hours at 66°C with foaming. Area under peaks not connected for specific ion absorptivity.

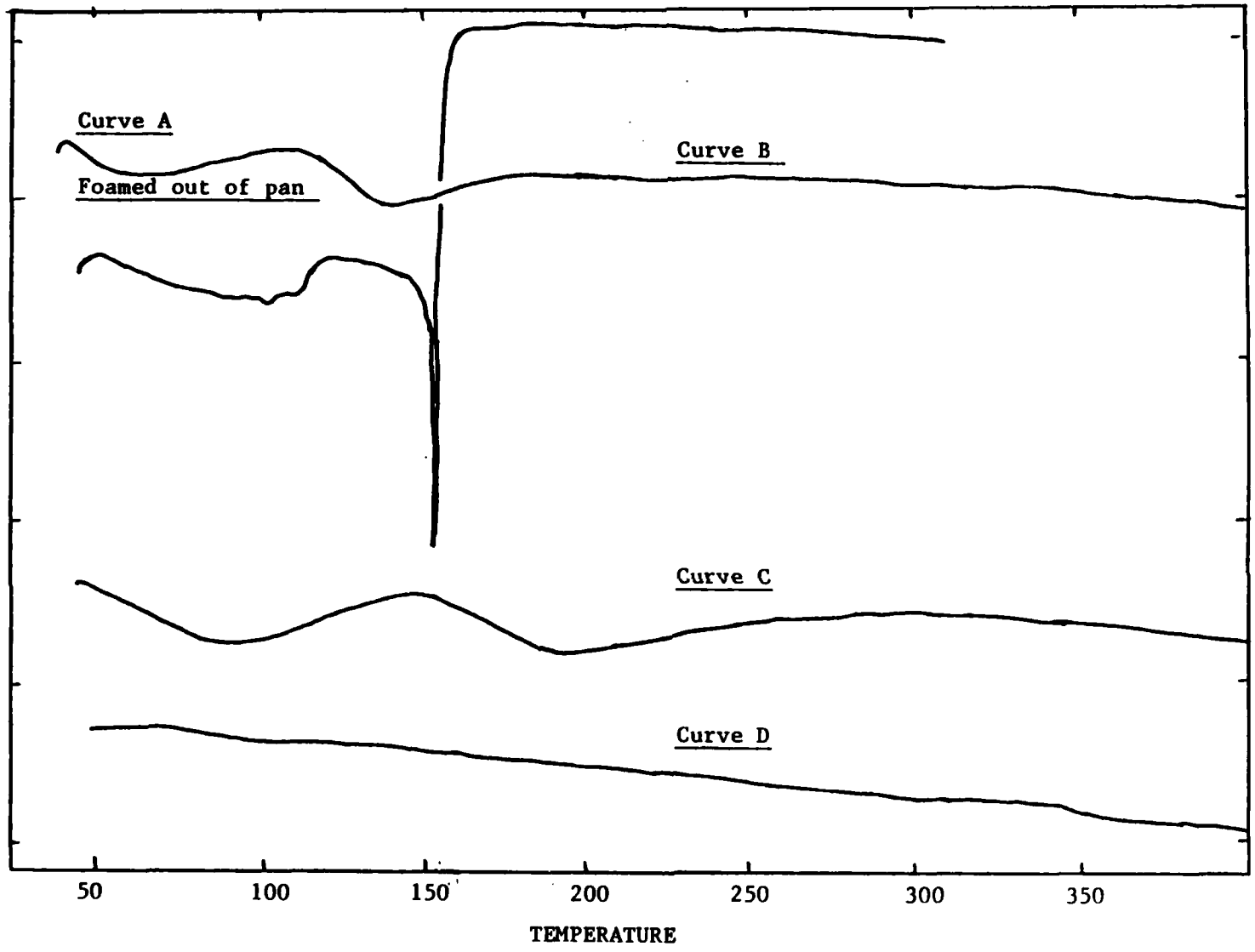

FIGURE 5. Tracings of DSC curves of NR150B252X sample.
Curve A - preheated 1 hour at 80°C - 10°C/min. heatup.
Curve B - same sample as Curve A with 2°C/min. heatup rate.
Curve C - preheated 2 hours at 80°C and 1 hour at 140°C with 10°C/min. heatup.
Curve D - reheat of sample C after instrument cool-down under N_2.

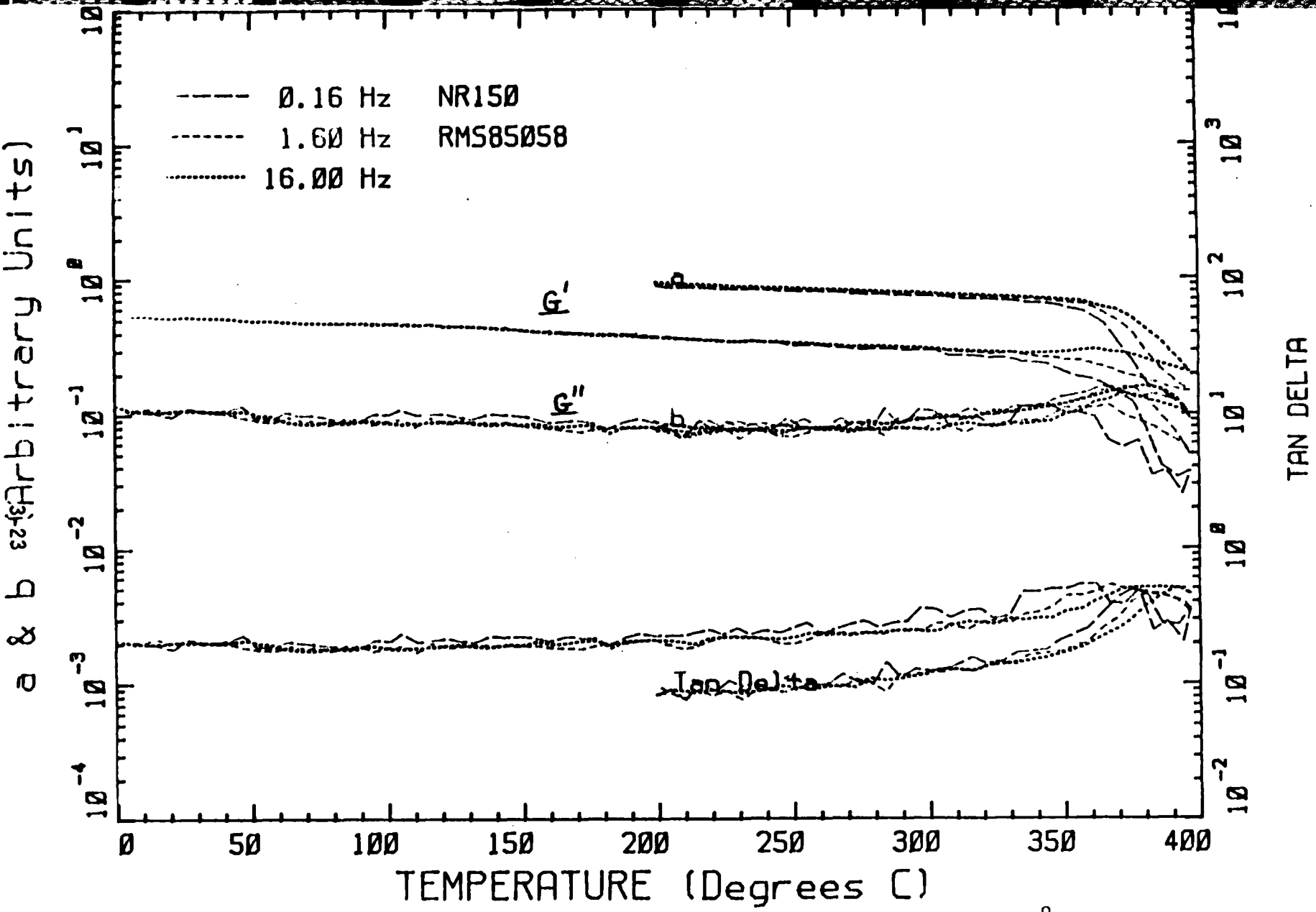

FIGURE 6. TICA curves for NR150B252X sample which had been heated 16 hours at 100°C, dissolved in THF soaked into fiber-glass cloth. The impregnated cloth was dried in vacuo.

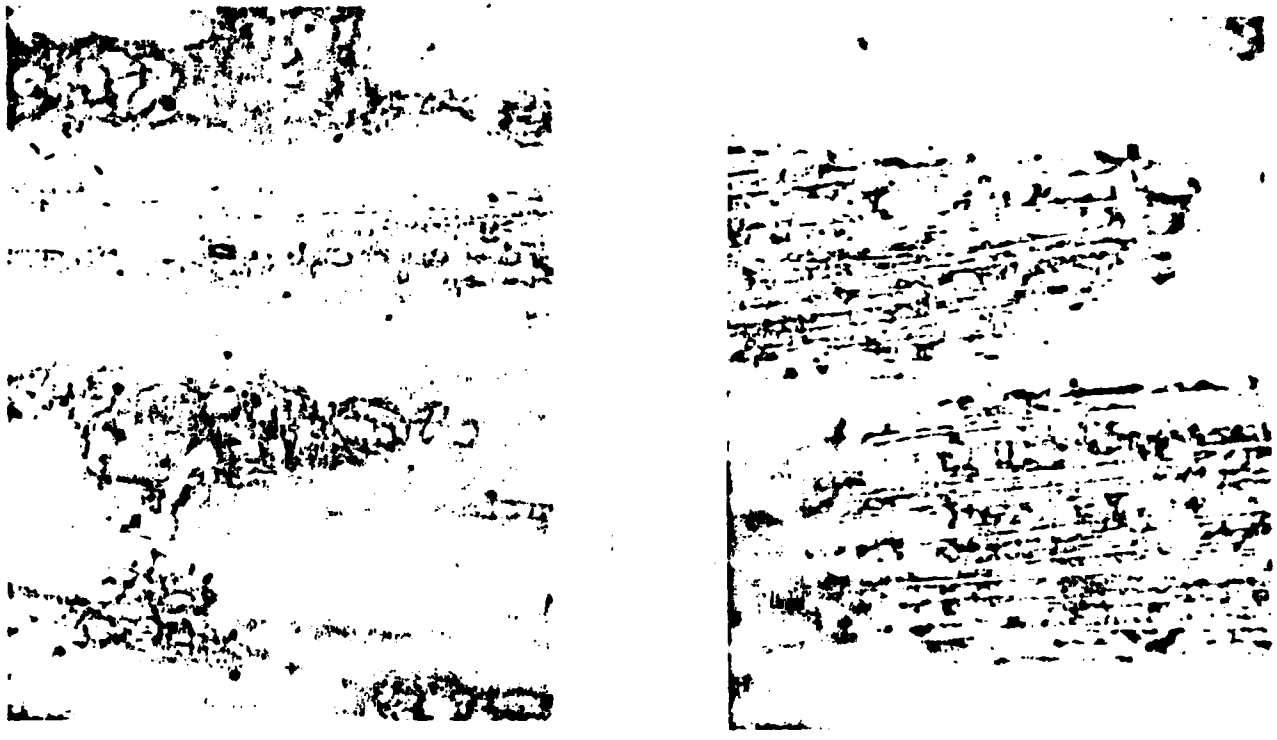

FIGURE 7. Polaroid pictures of TICA samples of NR150B252X after testing. Picture A at right (x 70) shows the brown spots for the test specimen cast from alcohol. Curve B at left patches of resin (from THF) which foamed on being put in the hot oven at 200°C.

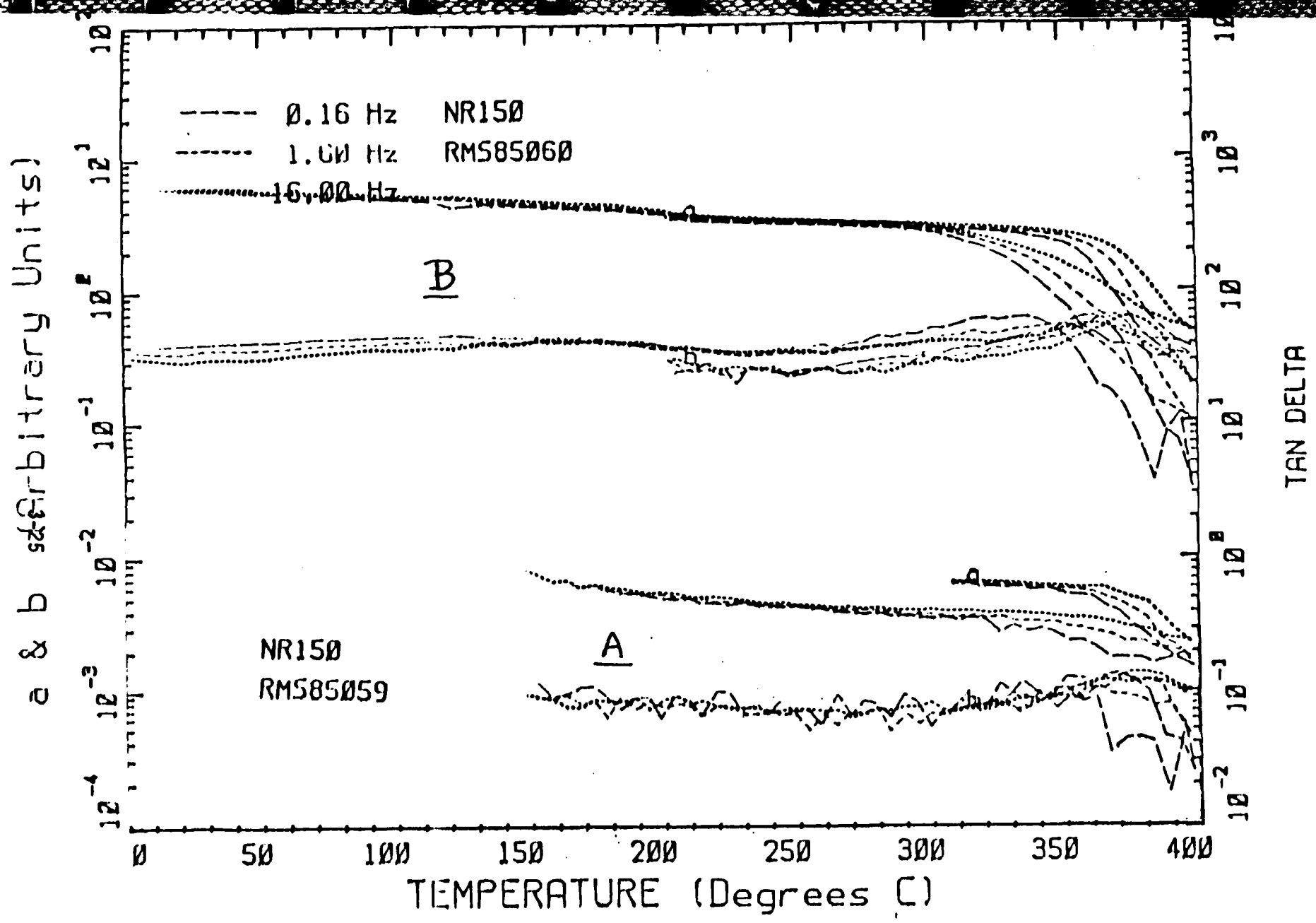

FIGURE 8. TICA curves for NR150B252X sample showing G' and G" only.
Curve A - impregnated cloth wet with DMF and dried in vacuo.
Curve B - impregnated cloth placed in 200°C oven and heated one hour.

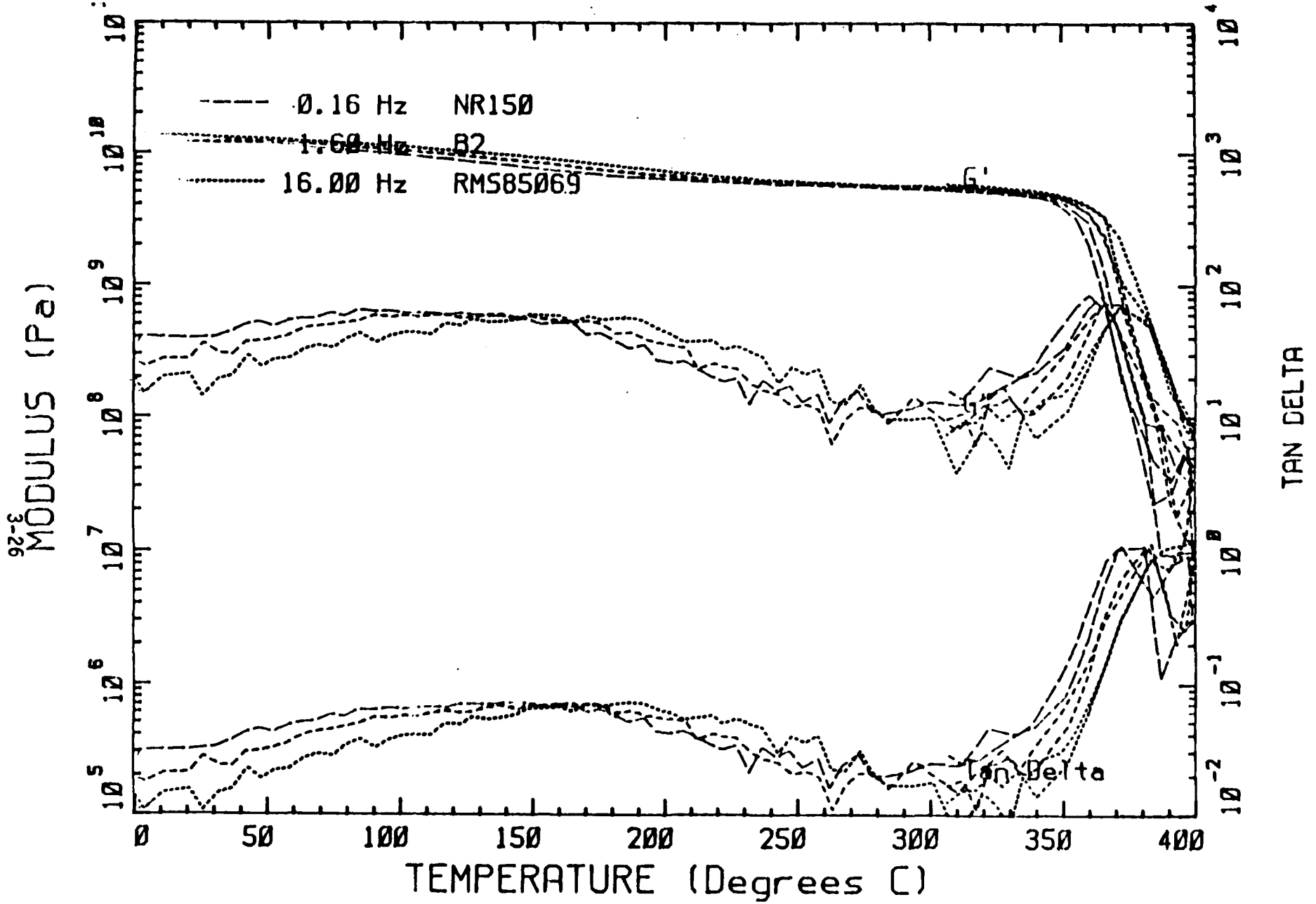

FIGURE 9. Torsion Bar Mechanical Spectrometry of NR150B252X sample molded from cured molding powder. Precured at 120°C for 72 hours and molded at 15-600 psi with slow heating to 400°C.

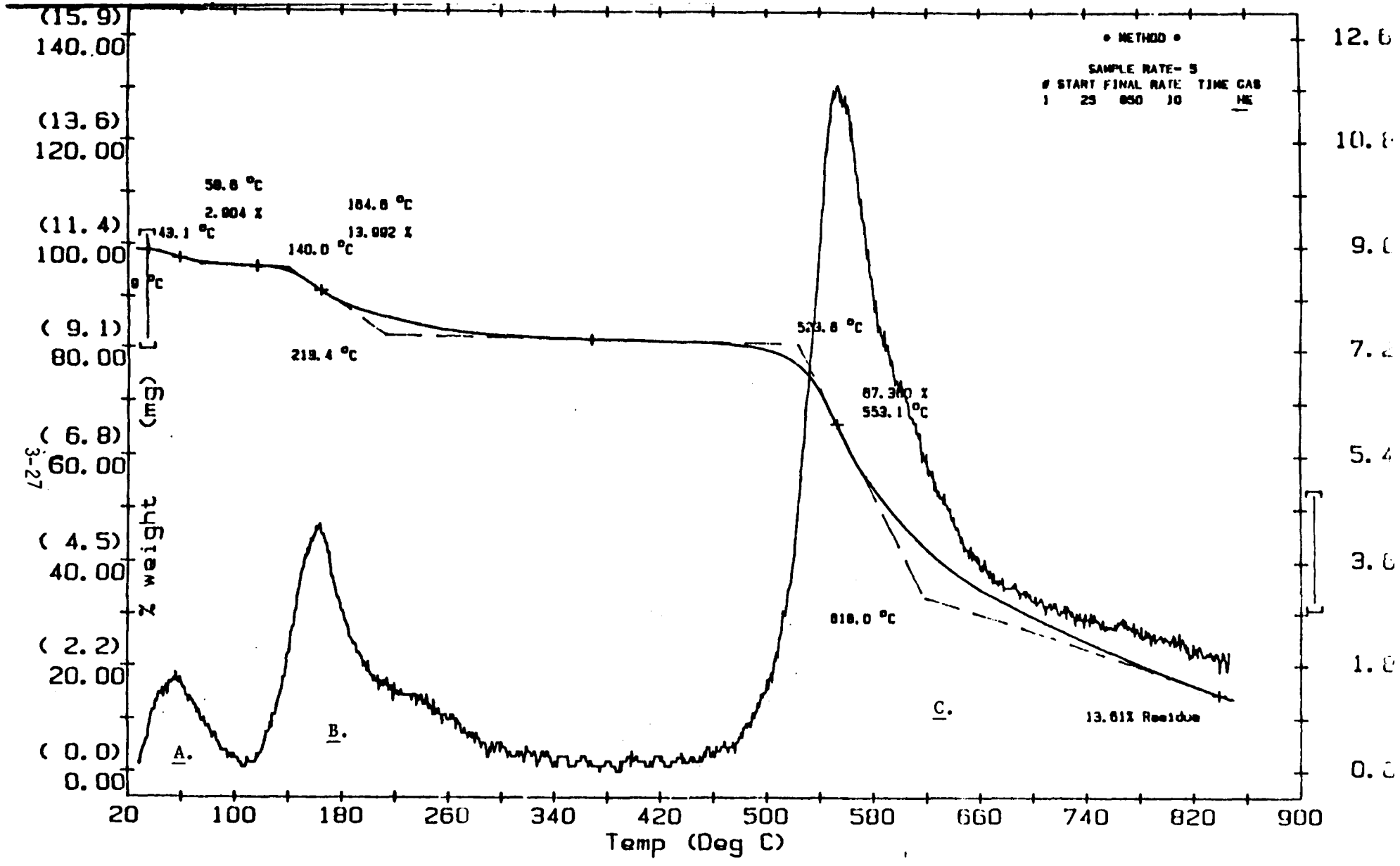

FIGURE 10. Thermogravimetric analysis of NR150B252X which had been preheated sixteen hours at 66°C with foaming. A. Absorbed water and residual solvent. B. Four moles of water released on polymerization and imidation. C. Decomposition.

1985 USAF-UES Summer Faculty Research Program/
Graduate Student Summer Support Program

Sponsored by the
Air Force Office of Scientific Research

Conducted by the
Universal Energy Systems, Inc.

Final Report

Quantifying Experience in the Cost of Human Capital

Prepared by: Jihad A. Alsadek

Academic Rank: Assistant Professor

Department and University: Department of Economics, Tougaloo College

Research Location: AFHRL/MOM

USAF Research Contact: Major Robert Rue

Date: 25 July 1985

Contract No: F49620-85-C-0013

Quantifying Experience in the Cost of Human Capital

by

Jihad A. Alsadek

ABSTRACT

The literature search led to the identification of a Historical Cost Model, a Replacement Cost Model, and a Present Discounted Value Model as tools to put a price (cost) on human experience. The Present Discounted Value, or Discounted Cash Flow Model, lends more credibility and accuracy to pricing human experience than the other two models. The civilian sector uses three approaches (the Economic Approach, the Accounting Approach, and the Alternative Investment Approach) and three techniques (the Key Man Insurance Technique, the Causal-Intervening Variable Technique, and the Investment Quantification Technique) to cost human experience. The military costing practices are nothing more than different versions of the Accounting Approach to personnel costing in the civilian sector. Singling out a model or an approach that is capable of quantifying the work experience in the cost of human capital and testing it with some AFSC data is the next step in research for this project.

ACKNOWLEDGEMENTS

I extend my deep appreciation to the Air Force Systems Command, the Air Force Office of Scientific Research, and the Universal Energy Systems, Inc., for granting me the opportunity to spend a nice and productive summer with the Air Force Human Resources Laboratory at Brooks AFB in Texas.

The laboratory, in particular the Manpower and Force Management Systems Branch, provided me with a delightful and stimulating working atmosphere.

Major (Dr) Robert Rue, the Branch Chief, facilitated my research tremendously through his competent management and his offering of invaluable insights and thoughts to the progress of the research.

I owe special thanks to Messrs John Taylor and Larry Looper, the economics team at the Branch, for all the help they provided. Thanks to the secretary of the branch, Mrs Virginia Weems, for her typing.

Many thanks to the AFHRL library team; the librarian, Mrs Orrine Woinowsk, and the technician, Mrs Millie Jones, for their help and quick service in ordering the material for the research.

Thanks are due to many people in the laboratory whose names I cannot mention for reasons of limited space.

QUANTIFYING EXPERIENCE IN THE COST OF HUMAN CAPITAL

I. INTRODUCTION

The investigation of Human Resources Accounting (HRA) is very essential for quantifying work experience in the cost of human capital. HRA is sometimes referred to as Human Asset Accounting (HAA). If a resource is used during the period when benefits are realized by the organization, then it is considered an expense; if it is used for benefits accruing in the future, then it is counted as an asset. HRA is a method or set of methods used to identify and calculate data about human resources or assets. HRA moves financial abstraction closer to reality. It can give management a very important indicator of each person's ability. HRA was conceptualized, as a theory, in 1964. It helps in recognizing and defining problems, such as the human asset investment ratio, which may be a beneficial predictor of future profit performance, and the rate of personnel turnover in the organization. One of the tough problems, for HRA is to develop realizable measures for management purposes. These measures can be utilized in acquisition, allocation, development, conservation or retention, and reward or compensation decisions.

It is difficult, though, to think of humans as resources or assets because they are not legally owned by the organization and because of the societal constraints and taboos put on the concept of dollarizing them. It is very difficult, even sometimes impossible, to quantify the experience in the cost of human capital where human capital means, in addition to experience, knowledge and skills. Assuming productivity as a function of work experience, then investment in humans can be calculated in three ways: (a) as an acquisition cost, (b) a replacement cost, or (c) as an economic value cost to the organization.

Acquisition cost is calculated from historical or original transactions to acquire the resource or the asset. Replacement cost is calculated by estimating the total outlays to replace the asset. An economic value cost is imputed by approximating the present discounted value of a human. In essence, the three ways try to calculate what the asset cost, what it would now cost, and what its value is.

HRA applies methods of accounting to the management of personnel. It may be defined as the reporting and calculation of value and cost of humans as resources of an organization. It includes accounting for investment in humans, then economic value and replacement cost. HRA measurement models can be divided into two main groupings: (a) value models, both nonmonetary and monetary, and (b) cost models. Nonmonetary Human Resource Value Measurement Models can be used in three different situations: (a) decision situations that do not need monetary measures, such as lay-off decisions, (b) proxies for monetary measures, such as employees ranking; and (c) leading-indicator situations to forecast monetary measures. These nonmonetary models provide the behavioral and organizational variables which, although they are usually unquantifiable, nevertheless compose a system that oversees the changes in the conditions of the human resources of the organization. The Monetary Human Resource Measurement Models try to calculate, in money terms, the value of humans to an organization. These models are beneficial if management wants to base decisions concerning aquisition, training, and development of human assets on a value-cost calculation. Human Resource Value Measurement Models can be applied in service organizations. Human Resource Cost Measurement Models have face validity, and there may be no way to calculate their validity empirically. They are applied in organizations such as (a) a manufacturing company, (b) a CPA firm, (c) an insurance company, and (d) a bank. The civilian and military

sectors are researched in order to find what kinds of models or methodologies they use for their personnel costing.

I am an economist by training, taught economics courses in the areas of Macro- and Micro-Economics, International Trade, Public Finance, Economic Development, Mathematical Economics, and Money and Banking. I headed a Department of Economics and directed the development and implementation of a new emphasis, Management Science, for the department. I researched and simulated lifetime incomes for government employees in an oil-producing country and studied the impacts of government distributive policies on those streams of income. With this in mind and the need of the USAF for someone with such background to quantify the work experience in the cost of human capital, I was chosen on the 1985 USAF-UES Summer Faculty Research Program to do this job.

II. OBJECTIVES

The objectives of this 1985 summer research effort are:

1. To survey the literature for what has been done on the subject of quantifying work experience in the cost of human capital.

2. To identify the models, approaches, or methodologies, if any, that have been used to put a price (cost) on human experience.

Sections III, IV, and V form the bulk of the report and contain the models, approaches, techniques, and the military personnel costing procedures and methodologies that have been identified in the literature to realize the above-mentioned objectives of this research.

III. LITERATURE FINDINGS

The literature search shows that there are three kinds of HRA models that depend on different human capital measurement foundations. These models are either Historical Cost, or Replacement Cost, or Future Expected Economic Value Costs in terms of present values or discounted cash flow model.

The different HRA models that are found in the literature deal with such variables as the organization's investment in on-the-job training (OJT), personnel replacement costs, or net realizable value of a human, with little or no mention of empirical data.

Historical (Outlays) Cost Model

These costs refer to the acquisition costs of personnel by the organization. They can be derived from transactions data. The Historical Model stresses the investment in human assets. It would account for the investment in human assets as the unexpired part of the costs for recruiting, hiring, training, and developing personnel for the organization. This model has some strong advantages; namely, acquisition cost is consistent with the current accounting methods for other long-term assets, and the model is simple, inexpensive, and feasible to install within a reasonable time span.

Figures 1 through 3, Appendix A, represent three different versions of the Historical (outlays) Cost Model that appeared in the literature. Very minimal differences are shown among them. The Historical Cost Model does not qualify to quantify the work experience in the cost of human capital, because it shows one part of the human's cost, that is, the previous expenditures on the individual.

Replacement Cost Model

These are costs to replace the organization's existing personnel, if they need to be replaced. They show what it would cost the organization to recruit, hire, train, and develop personnel to their present level of performance and familiarity with the organization and its functions. In the Historical Cost Model, original or historical costs are stressed, while in this model, the Replacement Cost Model, current costs are of greater relevance and provide better information for the management than historical costs, in that they are more current, realistic, and market oriented. Professor Teel (1983) says that if you find that replacement costs, after using the model, amount only to a few weeks pay, then it would not be cost effective to engage in reducing turnover of personnel in the organization. But if they exceed one-third the average annual salary for a job, where turnover is high, then the organization might increase its productivity by identifying the cause of personnel turnover and working on alleviating it. Since human capital can be expensive, there is a great need to assess the cost that would have to be incurred to replace humans if their employment is abruptly terminated.

Figures 4 through 7 are four different versions of the Replacement Cost Model. Two of them (Figures 5 and 6) do not mention anything about separation costs (discharge costs), and one (Figure 7) mentions something about the vacancy costs. Except for this distinctive difference, they are almost the same. This model makes a better candidate for quantifying the work experience in the cost of human capital, because these costs are not previous costs, instead, they are current costs.

Present Discounted Value or Discounted Cash Flow Model

This model shows the concept of economic value of humans; i.e., the present value of that part of the organization's future benefits that are attributable to humans. This model is more sophisticated than the other models in measuring human asset value. If it is possible to predict the future benefits individuals will generate, then, by discounting them, a human asset value will be determined. According to this model, a typical earnings profile first increases with age because of the ability of the individual to learn and thus increase his/her productivity. As the individual matures, productivity may decrease due to the technological obsolescence and health deterioration, expressed by a decline in annual earnings. The earnings profile terminates at retirement or upon death if that happens earlier. The economic value of a person at age t is the present discounted value of his remaining future earnings from employment. This value for a discrete income stream is:

$$V_t = \sum_{t}^{T} \frac{I}{(1+d)^{T-t}}$$

where V_t = Human capital value of an individual t years old.

I = Individual's estimated annual earnings up to termination time; i.e., I = Revenues - Costs.

d = Discount rate.

T = Termination rate (retirement or death whichever comes first).

This model, Discounted Cash Flow Model, is the best conceptual model of all the other models. If resources can be said to be economic assets and we acquire them, then the future benefits and costs for these assets are what we are interested in, and not the past expenditures or the present ones. The major disadvantage of this model is its subjectivity due to the heavy emphasis on predictions.

Figure 3, Appendix A, is an example of a Discounted Cash Flow Model or a Present Discounted Value Model. This model, or a similar version, is a good candidate for quantifying the work experience in the cost of human capital because it imputes the future benefits and costs of an individual and not his/her past or current outlays.

IV. CIVILIAN COSTING - APPROACHES AND TECHNIQUES

The civilian sector uses three approaches: the Economic Approach, which is similar to the Present Discounted Value or Discounted Cash Flow Model; the Accounting Approach, which is similar to the Historical Cost or Outlays Model; and the Alternative Investment Approach, or the Opportunity Cost idea. This model is broader in scope than the other two. To ascribe costs for these approaches, three techniques are used, namely the Key Man Insurance Technique, the Causal-Intervening Variable Technique, and the Investment Quantification Technique.

Tables 1 and 2, Appendix B, show the summary of civilian personnel costing, and a summary of differential characteristics of each approach.

Approaches

The Economic Approach. This approach deals with the present discounted value of an asset's future revenues. It says that an individual's value to an organization should be measured as the present discounted value of his/her future services, minus the costs incurred by the organization for acquiring, developing, maintaining, and utilizing those services over the working years. This approach is similar to the present discounted value or discounted cash flow model.

The Accounting Approach. This approach deals with the historical cost of an asset adjusted for depreciation. It assesses dollar costs of actions taken by the organization in behalf and as a direct result of personnel. It interprets the present value of an asset as the total of the organization's outlay which can be directly traced to it.

This approach places directly a dollar cost on human assets and is based on historical data. According to its simple form, no trials are attempted to calculate cost consequences of personnel deeds or individual productivity. According to its sophisticated form, it takes into consideration the previous effort of the individual in behalf of the organization. It avoids value notation and intermediate variables, and favors using personnel factors that can be directly expressed in dollars. This approach is similar to the historical cost model.

The Alternative Investment Approach. This approach deals with the value of an asset that could be realized if it had been invested for another purpose. It resorts, as the economic approach does, to indirect methods for assigning dollar costs to human assets. It is the potential value which is lost by not applying the asset to the most profitable alternative use foregone because of its present usage. This approach uses the same three interpretations of human asset monetary worth and its measures, namely: (a) current value of an asset in terms of the expenditure costs which were spent to acquire the asset and bring it to its current state, (b) current value of an asset in terms of the replacement costs to replace it in case of its loss, (c) current value of an asset in terms of profits that are accruing to the organization because of it. This approach, like the economic one, can be utilized to assess previous outlays of resources and to guide their future outlays. This approach is not the replacement cost model. Instead, it encompasses the previous and the future expenditures of an asset.

Techniques

The Key Man Insurance Technique. This technique, which was developed by the insurance industry, calculates the present discounted value of earnings lost because of the asset's loss, the replacement cost, and the profit lost because of the resource managerial efforts loss. It may be applied within any of the three basic approaches to personnel costing. It is designed to quantify the worth of an individual to an organization if his services were to be lost. The details of this technique and how it works are found within the economic approach. This technique works best when the products of an individual's efforts can be quantified.

The Causal-Intervening Variable Technique. This technique calculates variables such as attitudes, motivation, loyalties, goals, and performance. It may be applied within any of the three basic approaches to personnel costing. It associates a quantitative value estimate with personnel and provides information to guide the creation of organizational policy to maximize the value of personnel to the organization. It is suitable for prediction and control more than historical documentation. Examples of causal variables are goal emphasis, reward system, and work facilitation; examples of intervening variables are perception of organizational and personal goals, motivation, and decision making. Its distinctive drawback, though, is that the quantification of such variables is extremely more difficult and complex than just their identification.

The Investment Quantification Technique. This technique calculates all the outlays incurred to acquire the asset and bring it to its best operational level, such as recruiting and acquisition, formal training, familiarization, OJT, experience, and resource development. It deals directly with dollar cost for human resources. It may be applied within any of the basic three approaches to personnel costing.

V. MILITARY COSTING

Military costing practices, currently in use, are nothing more than different versions of the accounting approach to personnel costing in the civilian sector. Economic value of humans are being avoided altogether. Costs which can be ascribed to acquisition, training, and sustenance of military personnel are taken into consideration most of the time. Military costing is usually conducted along two lines of thought: (a) the personnel costing and (b) the billet (job) and system costing. There are five basic cost aggregates within these two lines of thought: (a) acquisition costs, (b) training costs, (c) sustenance costs, (d) separation costs, and (e) life cycle costs. Acquisition costs amount to adding all outlays necessary to recruit and induct, and training costs boil down to summing all expenditures incurred to change the person from the induction state to the performance state. Sustenance costs comprise those costs which maintain the individual in his/her present state of capacity. Separation costs have to do with the person in separation from the service, such as administrative costs and post retirement benefits. Life cycle costs are those costs that have to do with the person's costs throughout his/her tenure. The civilian sector, industry in particular, registers outlays on an individual basis, while the military sector does it on the basis of averages. The major problems of the military personnel costing are in the assessment and calculation of OJT costs, medical benefit costs, retirement benefit costs, and billet (job) and life cycle costing. The problem with OJT costs is that they either are too simplistic or are too dependent upon survey data rather than actuarial data. The problem with medical benefit costs is the lack of centralized accounting systems, lack of enough detail in medical training program cost files, lack of suitable cost breakdown by individual funding authorities, lack of definite management and funding agencies, and lack of amortization programs. The problem with retirement benefit costs is that the way they are calculated

is very gross--either on the basis of the current year's retirement budget divided by the retirees during that year, or the pension multiplied by life expectancy, adjusted for inflation. The military sector has no comprehensive personnel costs associated with a billet, and an accurate life cycle costing for personnel seems to demand a set of cost parameter estimates, the applicability of each being closely defined, that is not available. The most problematic cause which restricts military personnel costing to the assessment of gross averages is the lack of a good way to apportion costs to individuals.

There are three types of problems that face the Air Force in its personnel costing: (a) cost calculation, (b) standardization, and (c) implementation. The most important problem of cost calculation is the number of personnel costing requirements denoted as necessary. The lack of general cost term definitions is a second problem. A third problem is the need for better accuracy and a higher degree of computational inclusiveness in the calculation of indirect cost. The prediction of service life and the progression and utilization of personnel through their individual careers is a fourth problem. The lack of an accepted way to classify personnel according to whether they make a direct or indirect support to weapon systems and the lack of standardization are two additional problems of cost calculation.

The most demanding problem of standardization is the need for more specificity and compatibility in cost estimates. The lack of uniform definitions for the different costing terminologies is a second problem. A third problem is the collection and formatting of personnel cost data. The need for clear guidelines to be used by cost analysts when they want to make decisions concerning cost allocation is another problem. The last category of problems is that of implementation; the major one has to do with operational and policy considerations. Part of the resolution of the personnel

costing problems lies in the availability of data and how they are appplied. Are they going to be applied to handle engineering design trade-offs, system support trade-offs, or budgeting/planning issues? The best technique or methodology for the Air Force to use in its personnel costing would be the one that gets the best data to support it. Little, other than the Accounting Approach and Investment Qualification Technique, is found in the civilian sector which can be used by the Air Force personnel cost analyst. The inadequacies of the other approaches and techniques for military personnel costing stem from their dependencies on subjective analysis and many assumptions concerning human behavior and productivity. Table 3, in Appendix B, gives a comparison between the Air Force and Civilian Personnel Costing. Appendix C is a Replacement Cost Model suggested by military personnel to solve the problem of quantification of work experience in the Cost of Human Capital. This model is a good model except it does not include all the ingredients to calculate the individual's worth. It seems that a lot of research should be done before an acceptable complete and correct set of cost elements is included in a cost model. Previous studies have looked at personnel costs without giving enough thought about how costs were reached and why.

VI. RECOMMENDATIONS

It is recommended that all of the models, approaches, and techniques that have been identified through the literature search be looked at carefully to select one of them, or a composite model, to quantify the work experience in the cost of humans.

Another recommendation is the serious consideration of the present Discounted Cash Flow Model as a tool to impute the human's worth.

A third recommendation is the usage of more than one model, from those identified, to calculate the cost of human experience for comparison purposes.

I recommend that human's worth be calculated in the selected AFSCs as a follow-on research. The reliability of a chosen model to calculate the value in dollars of a human is of tremendous benefit for the Air Force, or any other organization for that matter. This is especially important for management and budgeting purposes. Follow-on work on the research could be in the form of identifying specific AFSCs, collecting the necessary data, and calculating the worth of an individual in each one of them.

Core References

Books

Cascio, W.F. (1982). Costing human resources: The financial impact of behavior in organizations. Van Nostrand Reinhold Co.

Flamholtz, E. (1974). Human resource accounting. Encino, CA: Dickenson.

Journals

Brummet, R.L., Flamholtz, E.G., & Pyle, W.C. (1968, April). Human resource measurement - A challenge for accountants. The Accounting Review, 43(2), 217-224.

Brummet, R.L., Pyle, W.C., & Flamholtz, E.G. (1969, July-August). Human resource accounting in industry. Personnel Administration, pp. 34-46.

Flamholtz, E.G., & Geis, G. (1984). Development and implementation of a replacement cost model for measuring human capital: A field study. Center for Human Resource Management, Institute of Industrial Relations, UCLA, Personnel Review, 13(2), 25-35.

Flamholtz, E.G., & Kaumeyer, R.A., Jr. (1980). Human resource replacement cost information and personnel decisions. A field study. Human Resource Planning, pp. 111-17.

Flamholtz, E.G., Geis, G.T., & Perle, R.J. (1984, N-D). A Markovian model for the valuation of human assets acquired by an organizational purchase. tabs. Interfaces, 14, 11-15.

Oliver, J., & Flamholtz, E. Human resource replacement cost numbers, cognitive information processing, and personnel decisions: A laboratory experiment. Journal of Business Finance and Accounting, 5(2), 137-57.

Roser, S.R. (1983, S-O). A practical approach to the use of human resource accounting. tab. Managerial Planning, 32, 35-9.

Savich, R.S., & Ehrenreich, K.B. (1976, Spring). Cost/Benefit analysis of human resource accounting alternatives. Human Resource Management, pp. 7-18.

Teel, K.S. Recruitment. (1983, December). Personnel Journal, pp. 956-60.

Wright, R. (1970, April). Managing man as a capital asset. Personnel Journal, pp. 290-98.

Military

Baran, H.A. (1977). USAF military personnel costing: Problems and approaches (AFHRL-TR-77-39, AD-A047 761). Wright-Patterson AFB, Ohio: Advanced Systems Division, Air Force Human Resources Laboratory.

Fleming, K.H. et al. (1985). A methodology for estimating the full cost of replacing trained Air Force personnel. Colorado Springs, USAFA, Department of Economics.

Rand

Beltramo, M.N. (1974). Considering the cost of DoD personnel: A look at some issues requiring further analysis (P-5166). Santa Monica, CA 90406: The Rand Corporation.

Oisher, G.H. (1982). Military systems cost analysis (A summary lecture for the AFSC cost analysis course) (RM-2975-PR). Santa Monica, CA: The Rand Corporation (for the USAF).

McCullough, J.D. (1965). Cost-effectiveness: Estimating systems costs (P-3229). Bethesda, MD: The Rand Corporation (for a Symposium on Cost-Effectiveness Analysis sponsored by the Washington Operations Research Council on 14-16 June 1965).

Related References

Billet (Job) Costs

Goldfarb, R.S., & Mangum, S.L. (1983). Estimation of on-the-job training costs for satellite communications ground station equipment repairers (MOS 26Y) (Task Order #MDA903-82-C-0383). Washington, D.C. The George Washington University, Economics Department.

Haber, Sheldon et al. (1983). A conceptual framework for estimating life cycle manpower costs by MOS (Contract No. MDA903-82-C-0383). Washington, D.C.: The George Washington University, Economics Department.

Koehler, E.A. (1981). Life cycle Navy officer billet costs - FY81 (Report No. NPRDC TR-81-12). San Diego, CA 95152: Navy Personnel Research and Development Center.

Koehler, E.A. (1980). Navy reserve billet costs - FY1980: An interim report (AD A132286). Alexandria, VA 22304-6145: Defense Technical Information Center.

Rixon, N. (1973). The cost impact of a longer career for the USAF line officer force: A steady state approach (AD 760111). Springfield, VA 22151: National Technical Information Service.

Spencer, L.M., Jr. (1984, July). How to calculate the costs and benefits of an HRD program. Training, pp. 40-51.

Separation or Discharge Costs

Stephen, R.A., Carrol, H.E., & Brown, N. (1972). Comparison of Navy and Air Force administrative and disciplinary discharges (AD 752 500). Springfield, VA 22151: National Technical Information Service.

Manpower Problems

Marsel, A.P. (1975). An imputation method for estimating civilian opportunities available to military enlisted men (R-1565-ARPA). Santa Monica, CA 90406: The Rand Corporation (for Defense Advanced Research Projects Agency).

Norrblom, E.M. (1976). The return to military and civilian training. (R-1900-ARPA). Santa Monica, CA 90406: The Rand Corporation (for Defense Advanced Research Projects Agency).

Miscellaneous

Biswas, B.D., & Hestwood, T.M. (1975). Projecting base payroll costs. Compensation Review.

Gay, R.M., & Nelson, G.R. (1974). Cost and efficiency in military specialty training (P-5160). Santa Monica, CA 90406: The Rand Corporation (for 8th Annual Department of Defense Cost Research Symposium at Airlie House, VA).

Holdsworth, D.R., & Rinehart, S.C. (1982). Unit replacement system analysis (URSA1)(AD-A131292). Alexandria, VA 22304-6145: Defense Technical Information Center.

Hoskins, J.A. (1974). Modified TOPCAP objective force structure model (AFHRL-TR-74-64, AD-A004 760). Lackland AFB, TX: Manpower and Personnel Systems Division, Air Force Human Resources Laboratory.

Massey, H.G., Novick, D., & Peterson, R.E. (1972). Cost measurement: Tools, and methodology for cost effectiveness analysis (P-4762). Santa Monica, CA: The Rand Corporation.

OJT Costs

Eisele, C.R., Bell, T.R., & Laidlaw, C.D. (1979). Cost Analysis of Air Force on-the-job training: Development and demonstration of a methodology (AFHRL-TR-78-88, AD-A069 791). Lowry AFB, CO: Technical Training Division, Air Force Human Resources Laboratory.

Samers, B.N., Dunham, A.D., & Nordhauser, F. (1974). Evaluation of methodology for estimating the cost of Air Force on-the-job training (AFHRL-TR-74-73, AD-A005 298). Lackland AFB, TX: Manpower and Personnel Systems Division, Air Force Human Resources Laboratory.

Samers, B.N., Dunham, A.D., & Nordhauser, F. (1974). The development of a methodology for estimating the cost of Air Force on-the-job training (AFHRL-TR-74-34, AD-785 141). Lackland AFB, TX: Manpower and Personnel Systems Division, Air Force Human Resources Laboratory.

Retention Costs

Bendick, G.L., & Jones, D.J. (1981). An examination of dual track career management: Current pilot attitudes and cost analysis (AD-A111371). Alexandria, VA 22304-6145: Defense Technical Information Center.

Gotz, G.A., & McCall, J.J. (1980). Estimating military personnel retention rates: Theory and statistical method (R-2541-AF). Santa Monica CA 90406: The Rand Corporation (for USAF).

McCracken, A.P. (1984). Cost of officer retention versus replacement (AD-A146297). Alexandria, VA 22304-6145: Defense Technical Information Center.

Saving, T.R., & Stone, B.M. (1985). Retention of Air Force enlisted personnel: An empirical examination (AFHRL-TP-85-6). RRC, Inc., Bryan, Texas (for AFHRL, AFSC, USAF, Brooks AFB, TX. Contract No. F33615-80-C-0021).

Snedeker, M.J. (1983). A model for determining the cost of giving or withholding a desired assignment from a rated officer with six to eleven years service (AD-A134393). Alexandria, VA 22304-6145: Defense Technical Information.

Systems Costs

Crosetto, C.F. (1968). D6-53570 aircraft operations and maintenance cost model (AD 845551). Alexandria, VA 22304-6145: Defense Technical Information Center.

Kincade, C.G. (1973). A cost effectiveness approach for aircrew training with laser guided tactical weapons (AD916531). Alexandria, VA 22304-6145: Defense Technical Information Center.

Turnover Costs

Atchison, T.J., & Lefferts, E.A. The prediction of turnover using Herzberg's job satisfaction technique. Personnel Psychology, 25, 53-64.

Berry, G.A., Weaver, C.N., Watson, T.W., & Finstuen, K. (1982). Bibliography of military and non-military personnel turnover literature (AD A122895). Alexandria, VA 22304-6145: Defense Technical Information Center.

Flamholtz, E.G. (1983). Personnel turnover cost and management in naval operations (AD A128765). Alexandria, VA 22304-6145: Defense Technical Information Center.

Flanigan, J.M., & Little, L.J.R. (1980). A model of aircraft maintenance officer turnover (AD-A087089). Alexandria, VA 22304-6145: Defense Technical Information Center.

Hom, P.W., Katerberg, R., Jr., & Hulin, C.L. (1979). Comparative examination of three approaches to the prediction of turnover. Journal of Applied Psychology, 64(3), 280-90.

Appendix A

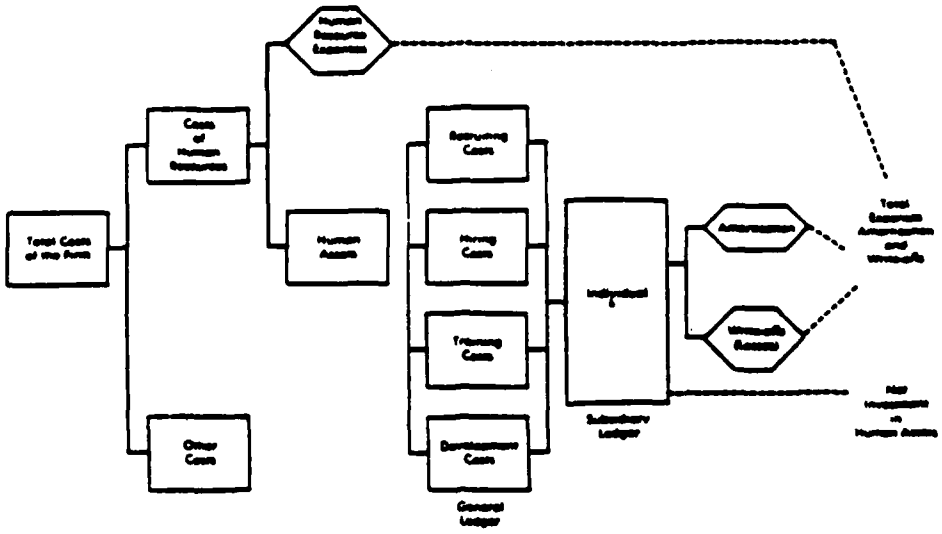

Human Resource Accounting System
Input Variables for an Historical
Cost Model

1. RECRUITING:
   - ADVERTISING
   - AGENCY FEES
   - INTERVIEWER TRAVEL:
     - Transportation
     - Meals
     - Lodgings
     - Salary/Time + Payroll Costs
   - CANDIDATE TRAVEL:
     - Transportation
     - Meals
     - Lodging
     - Expenses
   - COMMUNICATIONS COST:
     - Letters
     - Telephones
     - Telegrams

2. HIRING:
   - RELOCATION COSTS
   - MEDICAL TESTS
   - OVERHEAD COSTS
     - Establishing Records
     - Employment Briefings
     - Pay While in Processing

3. TRAINING:
   - (1) PRE-JOB FORMAL TRAINING
     - (New Employees)
       - Instructor's Time
       - Employee's Pay + Payroll Costs
       - Training Aids
     - FAMILIARIZATION
       - (New Employees)
       - Employee's Pay + Payroll Costs
     - SPECIAL TRAINING
   - (2) ON-THE-JOB TRAINING
     - Instructor's Time
     - Employee's Pay

4. DEVELOPMENT:
   - REIMBURSED EDUCATION EXPENSES
     - Tuition
     - Books
     - Travel
   - COMPANY SEMINARS
     - Instructor's Pay
     - Employee's Pay + Payroll Costs
   - Books, Supplies & Equipment
     - Transportation
     - Meals
     - Lodging
     - Other
   - SELF-STUDY ON CO. TIME
   - PROFESSIONAL ASSOCIATION DUES
   - PROFESSIONAL PUBLICATION SUBSCRIPTIONS
   - COMPANY SPECIAL PROJECTS
   - PUBLICATION EXPENSES
   - TECHNICAL DEVELOPMENT

Figure 1. Human Resource Historical Cost Model

Source: Savich, R.S., & Ehrenreich, K.B. (1976, Spring). Cost/Benefit analysis of human resources accounting alternatives. Human Resource Management, p. 9.

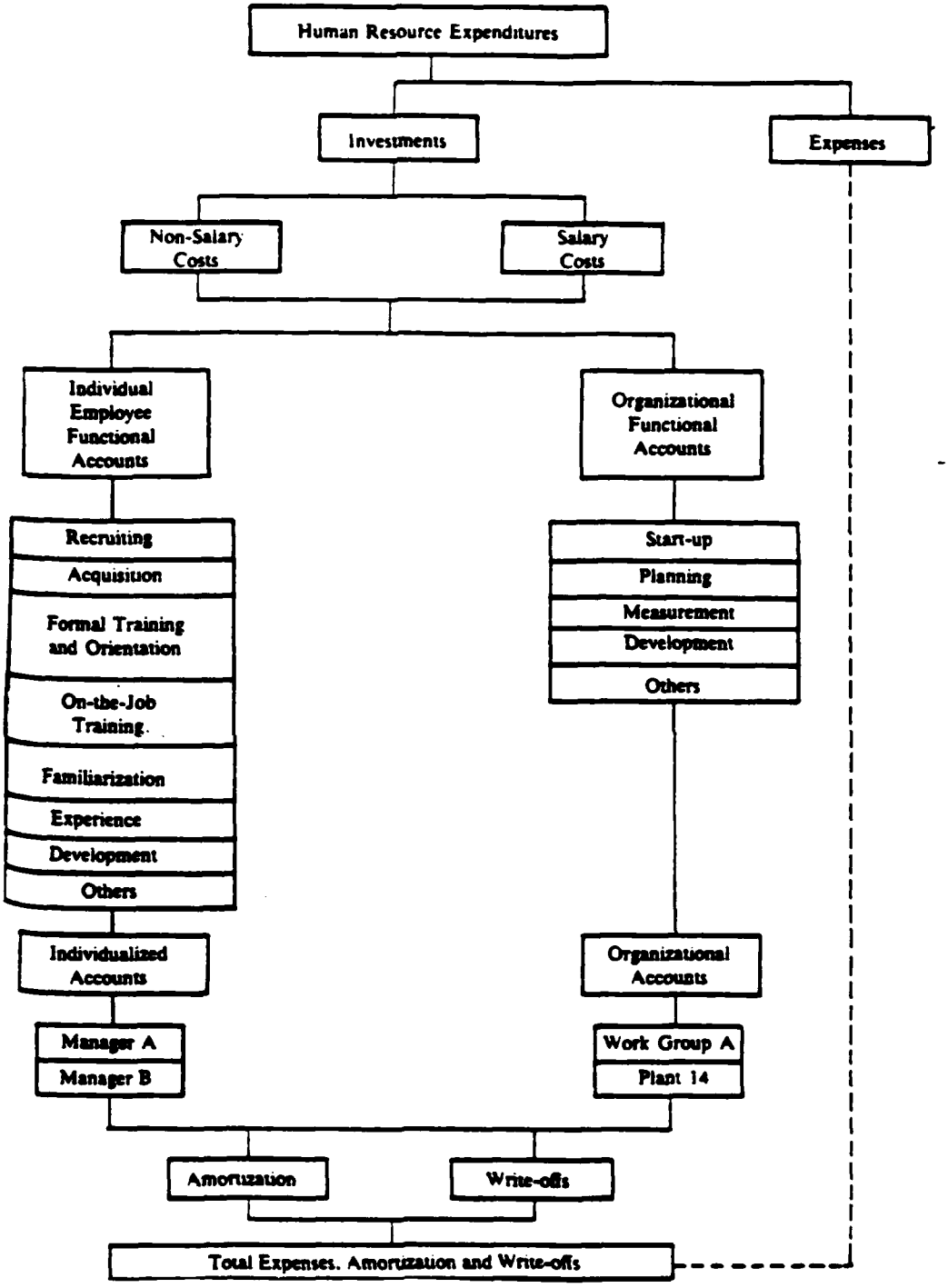

Figure 2. Model of an Outlay Cost Measurement System

Source: Brummet, R.L., Pyle, W.C., & Flamholtz, E.G.. (1969, July-August). Human resources accounting in industry. Personnel Administration, p. 41.

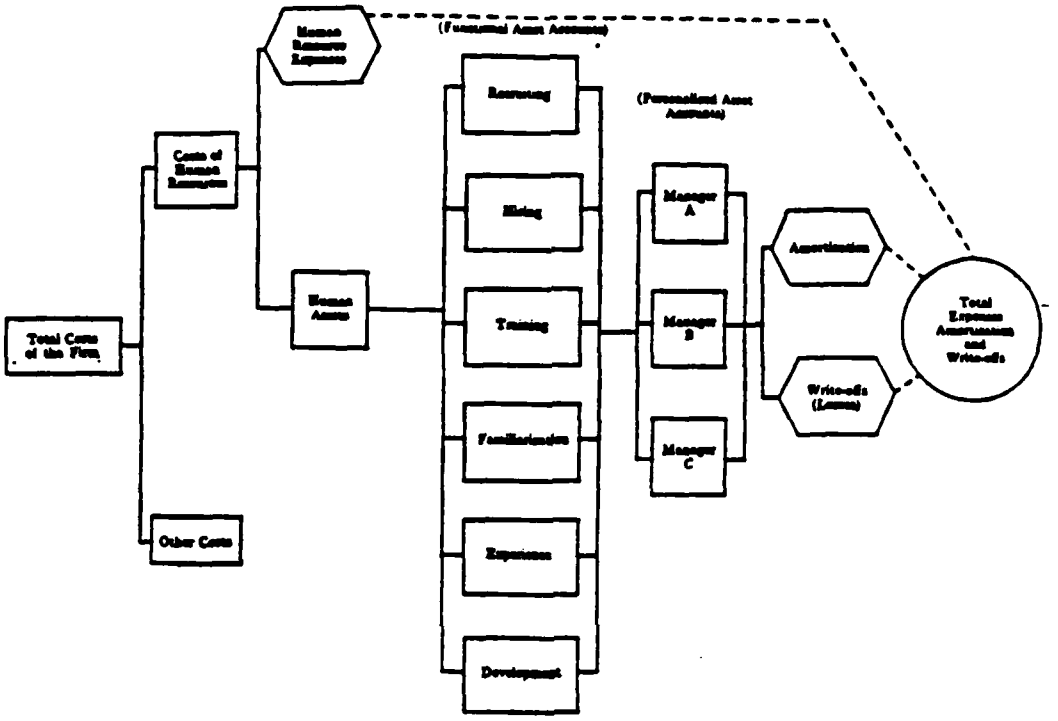

Figure 3. Generalized Model of Human Resources Accounting System for Investments in Managers

Source: Brummet, R.L., Flamholtz, E.G., & Pyle, W.C. (1968, April). Human resource measurement - A challenge for accounts. The Accounting Review, 43(2), 222.

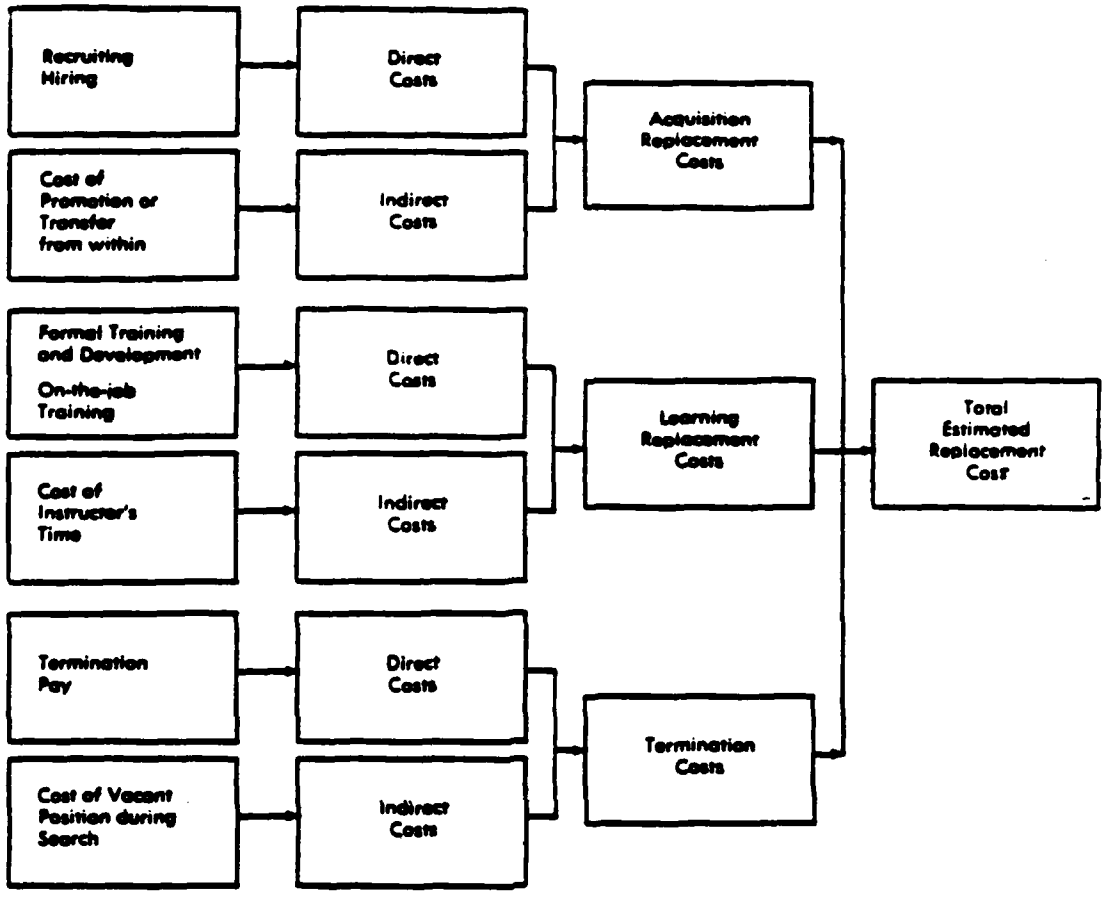

ACQUISITION COSTS: Same as cost basis, i.e., advertising, agency fees, travel, communications, relocation, medical and overhead costs, but using current replacement costs to rehire and restart the total organization.

LEARNING COSTS: Replacement Cost would be an estimate of bringing new employees to the current level of competence.

TERMINATION COSTS: Any termination pay plus estimated cost revenues during time period position is being refilled.

Figure 4. Flamholtz Model Human Resource Replacement Cost

Source: Savich, R.S., & Ehrenreich, K.B. (1976, Spring). Cost/Benefit analysis of human resource accounting alternatives. Human Resource Management, pp. 12-13.

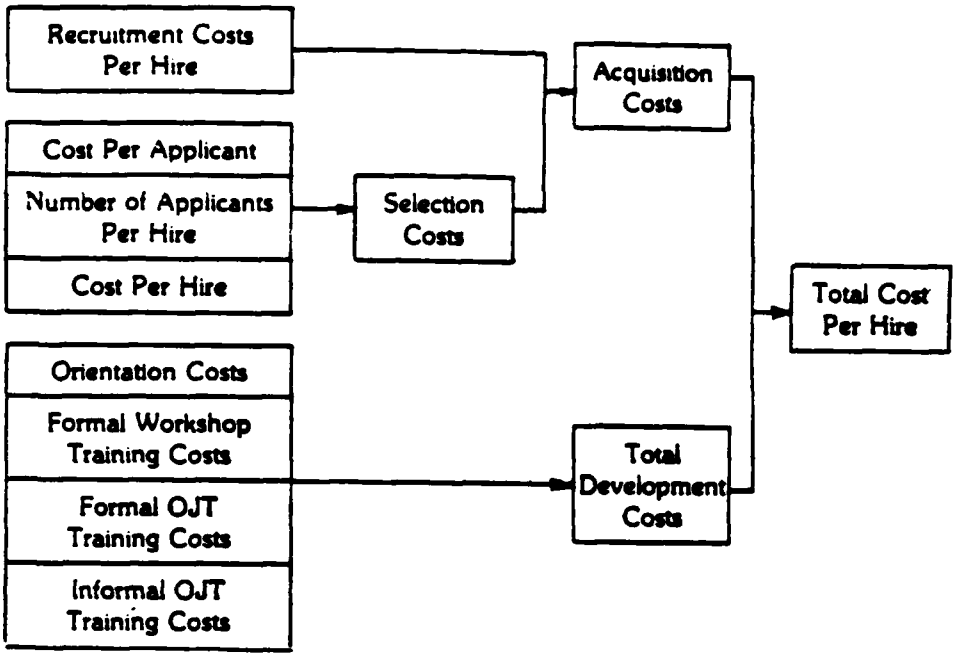

Figure 5. Model for Calculation of Cost Per Hire

Source: Flamholtz, E.G., & Kanmeyer, R.A., Jr. (1980). Human resource replacement cost information and personnel decisions: A field study. Human Resource Planning, p. 113.

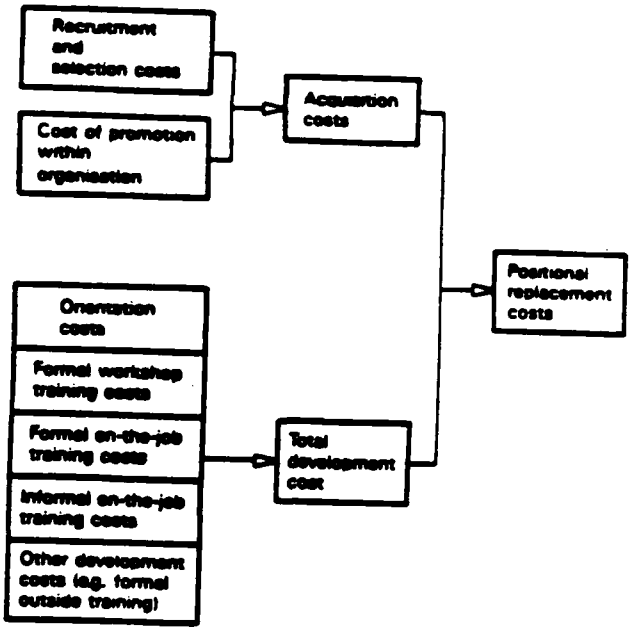

Figure 6. Model for Calculations of Positional Replacement Cost

Source: Flamholtz, E.G., & Geis, G. (1984). The development and implementation of a replacement cost model for measuring human capital: A field study. Personnel Review, 13(2), 27.

Separation Costs

Reduced productivity before departure
Time lost discussing departure
Terminee's time in exit interview
Exit interviewer's time
Compilation of exit interview information
Administrative paperwork
Lower morale among peers

Vacancy Costs

Lost production sales during vacancy
Overtime pay to others

Acquisition Costs

Advertising
Brochures
Employment agency fees
College recruiting
Application processing
Applicant travel
Reference checks
Interviewing
Medical exam
Psychological exam
Moving and relocation
Accounting and payroll entries
Human resources department overhead

Training Costs

New hire orientation
  Employee's time
  Trainer's time
Formal job training
  Employee's time
  Trainer's time
On-the-job training
  Supervisor's time
  Non-supervisory helper's time
Substandard performance of new employee
Extra work for others to offset substandard performance
Higher error rate for new employee

Figure 7. Employee Replacement Cost Elements

Source: Teel, K.S. (1983, December). Recruitment. Personnel Journal, p. 956.

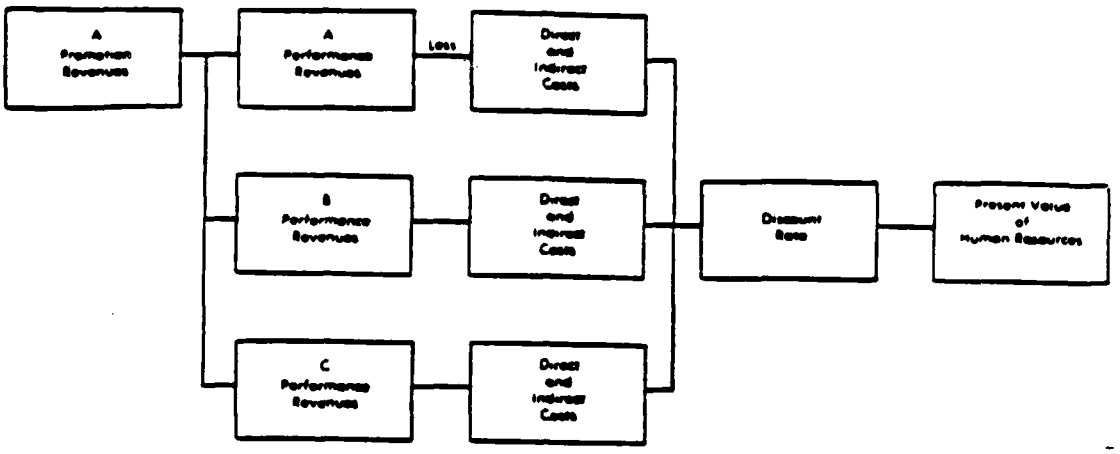

Human Resource Accounting System Input Variables for Discontinued Cash Flow Model

Revenues

Promotion—Consists of contracts obtained due to direct influence of personnel involved.

Performance—Consists of billable time spent working directly on projects.

Expenditures

All costs listed under both historical and replacement cost models.

Future salary costs—includes all direct as well as indirect costs of compensating personnel.

Figure 8. Human Resource Discounted Cash Flow Model

Source: Savich, R.S. & Ehrenreich, R.S. (1976, Spring). Cost/Benefit analysis of human resources accounting alternatives. Human Resource Management, p. 16.

APPENDIX B

Table B1. Summary of Civilian Personnel Costing

Basic Approaches to Personnel Costing

Economic Approach – establishes net value of difference between investment and returns.

Primary Use: to analyze value rather than cost of personnel in terms of a comparison of investment to returns.

Accounting Approach – establishes gross value in terms of investment cost

Primary Use: to assess dollar cost of organizational actions in behalf of the individual

Alternative Investment Approach – establishes net value in terms of comparative yield on investment

Primary Use: to assess the yield of an investment in personnel in terms of a comparison with alternatives

Basic Techniques for Ascribing Cost or Value
(Useable in any approach listed)

Key Man Insurance Technique – appraises net value in terms of loss to organization if individual were to be removed.

Primary Use: when organizational product can be tied to the efforts of an individual

Causal-Intervening Variable Technique – appraises the internal state and health of the organization attributable to the individual in terms of variables which link it to the presence of the individual

Primary Use: when organizational product cannot be tied to the efforts of an individual

Investment Quantification Technique – appraises the gross value of an individual in terms of the acquisition, transformation, and sustenance costs expended on his behalf

Primary Use: when organizational product cannot be tied to the efforts of an individual and/or the individual's contribution to the organizational effort cannot be directly quantified in terms of cost compatible variables.

Source: Baran, H.A. (1977). USAF military personnel costing: Problems and approaches (AFHRL-TR-77-39). Wright-Patterson AFB, Ohio: Advanced Systems Division.

Table B2. Summary of Differential Features of the Methodology

	Accounting Approach	Economic Approach	Alternative Investment Approach
Investment Quantification Technique	Quantifies recorded investment expenditures. Does not consider returns or alternatives. No requirements for projections of personnel productivity, behavior, or career progression. Very objective.	Quantifies net worth by balancing investment expenditure with dollar notation of returns. Requires productivity and career projections, and means to translate investment benefit into dollar notation. Subjective and difficult to validate, depending upon product of personnel.	Quantifies difference between investments either in terms of expenditure or net worth. See Accounting Approach and Economic Approach cells of this row for features of each choice. Requires detailed knowledge of investment alternative.
Key Man Insurance Technique (Almost a limited subset of the investment quantification technique.)	Similar to above cell but, addresses the quantification of recorded investment expenditures for an individual rather than a personnel type or group. Requires record keeping on an individual basis.	Similar to above cell but, addresses the quantification of the net worth of an individual rather than a personnel type or group. Requires record keeping on an individual basis.	Similar to above cell but, addresses the quantification of differences between investments in individuals rather than personnel types or groups. Requires record keeping on an individual basis.
Causal Intervening Variable Technique	Similar to above cells. Uses additional variables, requiring subjective measurement, which are difficult to link to investment cost; e.g., personal adaptability. Usually applied to managerial personnel. Very subjective and difficult to validate.	Similar to above cells, but includes subjectively measured variables related to group dynamics and individual behavior. Attempts to tie net worth to attributes other than direct productivity; e.g., leadership qualities. Very subjective and difficult to validate.	Similar to above cells but, is much more subjective and difficult to validate because it employs additional variables requiring subjective measurement concerning both the actual and alternative investment.

Note. — Difficulty of implementation increases from left to right and top to bottom of matrix.

Source: Ibid.

Table B3. Comparison Table of Air Force and Civilian Personnel Costing

Civilian Personnel Costing	Air Force Personnel Costing
Often entails the concept of value in addition to cost.	Restricted to objective dollar cost notation.
Often predicated upon an analysis of human behavior and individual personality traits.	Restricted to trend analysis of group behavior; e.g., reenlistment rate or average tenure.
Often employs the concept of net as opposed to gross cost, involving the measurement of returns as a counterbalance on investment.	Restricted to gross cost estimation without regard to realized or potential return on investment.
Type of Approach employed: (a) Economic, (b) Accounting, (c) Alternative Investment	Type of Approach employed: Accounting
Type of Techniques employed: (a) "Key Man" Insurance, (b) Causal-Intervening Variable, (c) Investment Quantification	Type of Techniques employed: Investment Quantification
Often can objectively quantify the benefits to the organization stemming from individual personnel.	Restricted to subjective or at best quasi-objective quantification of benefits to the Service from individual action affecting pipeline flow of personnel; e.g., reenlistment rate.
Often maintains a central costing activity which promotes commonality in: cost term definitions, cost element aggregation, and pertinent data collection.	Existence of central costing activity of restricted authority and responsibility, serving in the role of an assimilator rather than a coordinator of costing activities operating elsewhere.
Often can objectively trace expenditures to individual personnel on the basis of individual cost records from date of acquisition.	Restricted to the use of cost records compiled on the basis of gross expenditures which can only be traced to individual personnel on the basis of cost apportionment by average. An exception is sustenance cost.

Source: Ibid.

Appendix C

Colonel Fleming's Methodology for:
Estimating the Full Cost of Replacing Trained AFP

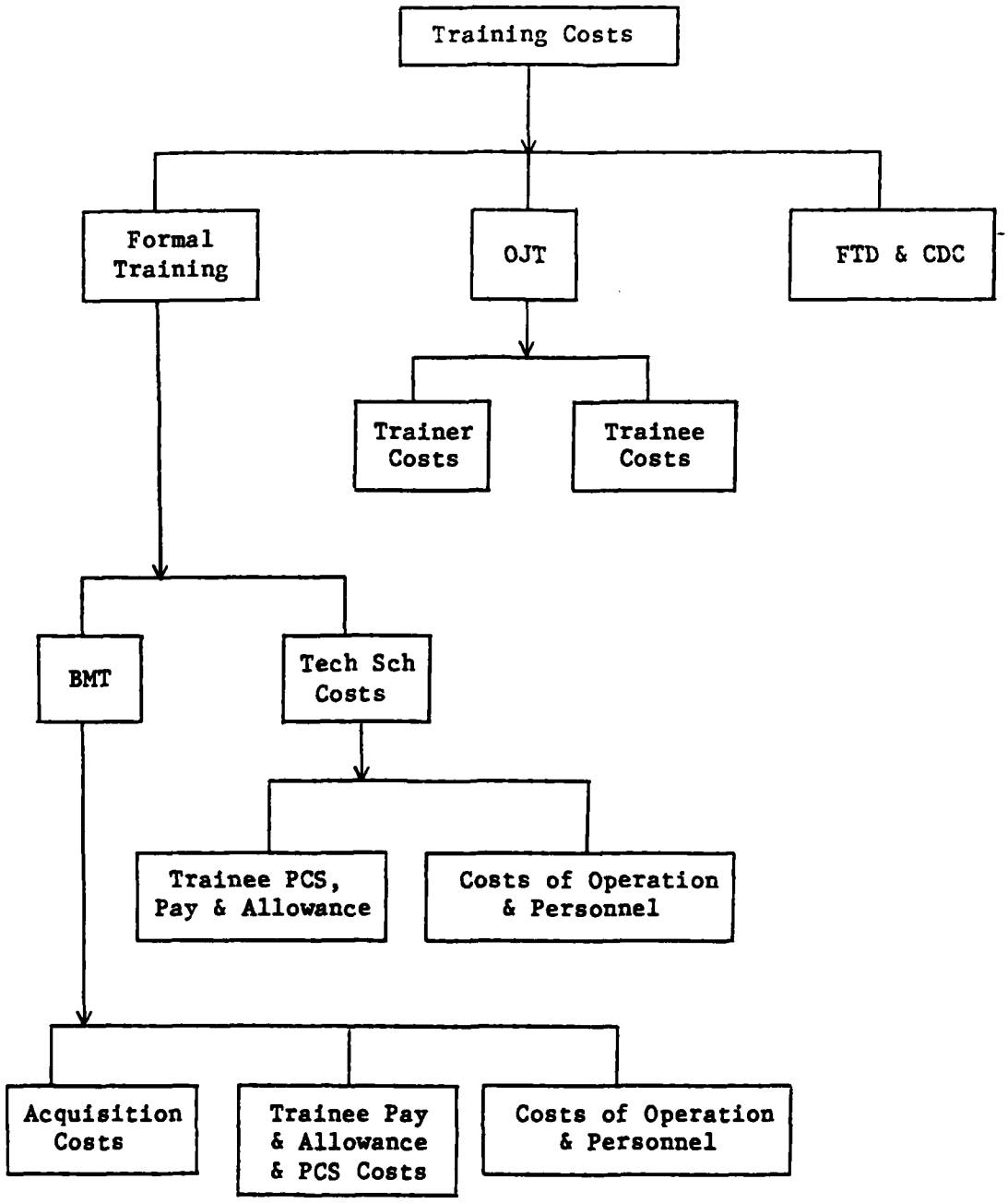

Graphical Representation

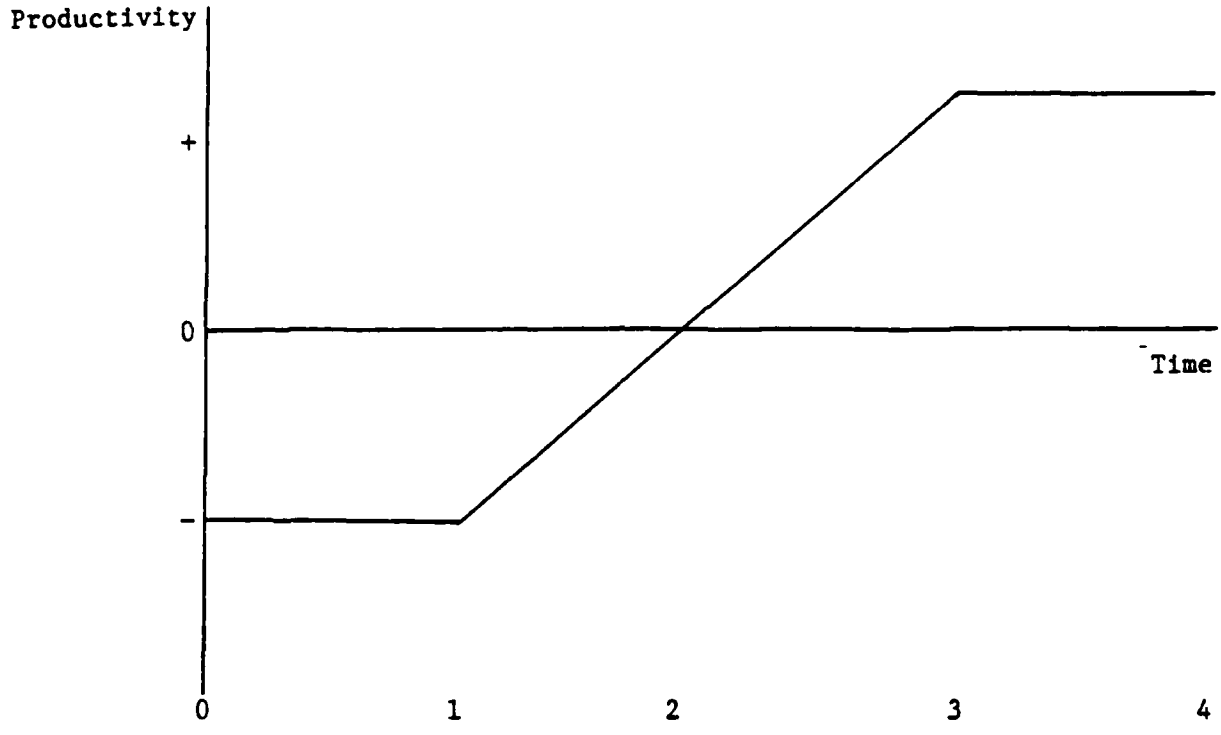

At time 1:

Pure costs = Training + Entitlements. This is due to negative productivity.

Between 1 & 3:

OJT costs; at first we have negative productivity, and then positive productivity. OJT brings individual to a fully productive stage. The individual at that stage does not need supervision and can analyze and complete all chores of the job on his/her own.

Between 3 & 4:

This is the pay-back period for the organization which incurred costs for the earlier training of the individual.

Mathematical Representation

Looking at the graphical representation:

Cost 12 = [Entitlements at actual pay grade for time 12]

This is a weighted average of an enlistee's progression in rank; 12 is the total number of months.

$$+ \sum_{i=1}^{12} \left[1 - \frac{(12)_i}{12}\right] (\% \text{ of trainer's time})[\text{trainer's salary}].$$

This is the opportunity cost of a trainer for OJT.

$$- \sum_{i=1}^{12} \left[\frac{(12)_i}{12}\right] (\text{Salary of E5}).$$

This is the productivity of the enlistee.

Replacement costs with steady attrition rate = Training cost + Entitlement costs + OJT costs

(1 + % Extra Attrition) + (Extra Attrition) (Salary of E5) (12 + Sch Time).

The last term represents an opportunity cost in terms of foregone productivity happening from mistakenly considering the enlistees who have already separated.

1985 USAF-UES SUMMER FACULTY RESEARCH PROGRAM/

GRADUATE STUDENT SUMMER SUPPORT PROGRAM

Sponsored by the

AIR FORCE OFFICE OF SCIENTIFIC RESEARCH

Conducted by the

UNIVERSAL ENERGY SYSTEMS, INC.

FINAL REPORT

THE EFFECTS OF RAPHE STIMULATION AND IONTOPHORESIS OF SEROTONERGIC AGENTS ON GRANULE CELL ACTIVITY IN RAT LATERAL CEREBELLAR CORTEX.

Prepared by:	Dr. Deborah Armstrong Christopher McNair Scott Bischoff
Academic Rank:	Assistant Professor Graduate Student Medical Student
Department and University:	Division of Life Sciences University of Texas at San Antonio University of Texas Health Science Center at Houston
Research Location:	USAF School of Aerospace Medicine, Clinical Sciences Division, Psychiatry Branch, Brooks AFB, Texas 78235
USAF:	Dr. David Terrian
Date:	August 12, 1985
Contact No:	F49620-85-0013

THE EFFECTS OF RAPHE STIMULATION AND IONTOPHORESIS OF SEROTONERGIC AGENTS ON GRANULE CELL ACTIVITY IN RAT LATERAL CEREBELLAR CORTEX.

by

Deborah L. Armstrong, Ph.D
Christopher McNair
Scott Biscoff

ABSTRACT

Stimulation of the dorsal raphe resulted in modulation of granule cell spontaneous activity. This provides support for the proposal that serotonin functions as a transmitter in the granular layer of the cerebellar cortex, however, the diversity of the observed responses does not permit a precise determination of the nature of the activated synapses. Of the eleven cells that responded consistently, six displayed decreased spontaneous activity, three were excited by the stimulation, and four cells displayed a biphasic response of initial excitation followed by inhibition. The iontophoretic application of serotonin decreased the spontaneous activity of the majority of cells tested and this effect could not be blocked by methysergide. Several cells were excited by serotonin application and this effect could be blocked by methysergide.

Acknowledgement

The authors' would like to thank the USAF School of Aerospace Medicine and Universal Energy Systems, Inc. for providing the opportunity to spend a summer working on this very stimulating research project. Special thanks to Dr. David Terrian for keeping us all on the right track.

I. INTRODUCTION

Based on evidence from anatomical, physiological, and biochemical studies serotonergic efferents of the brain stem raphe nuclei contribute to the mossy fiber system innervation of the cerebellar glomeruli. The anatomical mapping includes fluorescent histochemistry (4,13) and autoradiography following intracisternal injection of ^{3}H-serotonin (7). In both cases labeling was identified within structures resembling the large mossy fiber rosette terminal (25). Additional orthograde transport studies (6,8,12) ,use of retrogradely transported horseradish peroxidase (8,21) and immunocytochemistry (5) have verified the existance of 5-HT fibers within the cerebellum, however, the innervation is complex. Chan-Palay (8) describes three distinct systems: mossy fibers, fine axons that ascend to the molecular layer and bifurcate in manner resembling parallel fibers, and finally, a diffuse axonal system that innervates both the deep cerebellar nuclei and the cerebellar cortex.

Physiolgical studies to determine the functional significance of these serotonergic fibers are scarce and concentrate on Purkinji cell responses to raphe stimulation or iontophoresis of serotonergic agents (7,21-24). However, they do demonstrate that serotonergic mechanisms probably play a role in modulating cerebellar cortical activity. Obviously, a more thorough investigation of serotonergic transmission in the granular layer is needed.

The results of recent uptake studies utilizing an

isolated glomerular preparation have shown that a high affinity uptake system for serotonin does exist in this region (26). These studies are part of an ongoing project to identify cerebellar glomeruli neurotransmitter systems and their interactions with one another. The positive results of these experiments have provided a solid base on which to begin an investigation of the physiological responses of cerebellar granule cells to serotonergic stimulation.

II. OBJECTIVES

The primary objective of this summer's research period was to determine the response of granule cells to raphe stimulation. Since the dorsal raphe is such a well defined cluster of serotonergic cells in the rat we elected to begin with this particular nucleus. It is also one of four raphe nuclei that anatomical studies have shown to project to the cerebellar cortex. An initial sampling of recording electrode placements in the lateral hemisphere foli was planned to determine whether or not specific regions were more likely to contain responsive cells. To strengthen the proposal that responses were indeed mediated via activation of serotonergic synapses a second group of experiments was planned in which recordings made with multibarrel electrodes would enable the iontophoretic application of serotonergic receptor antagonists during stimulation evoked responses. These experiments would aid in determining the functional role of serotonin in information processing at the level of the cerebellar glomerular synapse.

III. GRANULE CELL RESPONSE TO DORSAL RAPHE STIMULATION

The majority of experiments examining serotonin's influence on cerebellar activity have dealt with Purkinji or subcortical cell responses to raphe stimulation. Utilizing extracellular recording techniques, Strahlendorf et al (22) have reported that stimulation of the raphe centralis superior or inferior produces initial bursting of fastigial and Purkinji cells followed by reduced spontaneous activity lasting up to 1600 msec. When stimulation of the sensorimotor cortex or radial nerve was applied during this period of raphe conditioning evoked spike activity was suppressed to an even greater extent than spontaneous activity, leading to the suggestion that serotonin modulates the ratio of spontaneous activity (noise) to evoked activity (specific responses to afferent signals) (24). Since very little information is known about the possible role of serotonin in the modulation of granule cell activity our initial experiments were planned to simply investigate the direct affect of raphe stimulation on granule cells.

METHODS

Adult Sprague-Dawley rats from Holztman suppliers were used. Animals were anesthetized with urethane (1.5 mg/kg body weight) injected intraperitoneally and supplemented as needed. Rectal temperature was continuously monitored and body temperature maintained at 37±0.5 C° by means of a heating pad equipped with a negative feedback circuit. After placement in

a stereotaxic headholder and exposure of the skull surface the occipital bone was removed to expose the lateral aspects of the vermis and one cerebellar hemisphere. After removal of the overlying dura matter a 1% solution of agar in physiological saline was placed on the cortical surface to prevent drying and reduce surface noise. An additional hole was made in the skull for positioning of the stimulating electrode, coordinates: A -6.5, L +1.0, V 6.5-7.0, into the dorsal raphe (14). Extracellular recordings were made with glass capillary electrodes drawn and broken to a tip diameter of 5-10 μm (1 to 5 Megohm impedances), filled with 3 M NaCl saturated with fast green for later verification of electrode tip placement. Unit activity and field potentials were amplified by a high input impedance preamplifier and audio amplifier, displayed on a Tektronix storage oscilloscope for photography, and then fed into a window discriminator (20) for signal sorting. Data was stored on magnetic tape for further analysis or relayed to a chart recorder for on line observations. The recording electrode microdrives were tilted to fascilitate electrode penetration into the crowns of the cerebellar folia. Concentric bipolar stimulating electrodes (Rhodes Medical Instrumets, Inc.) were used to apply single rectangular pulses(60 Hz), 0.5 msec in duration and ranging from 0-500 nA intensity, using a WPI Programmable stimulator.

RESULTS

The response to dorsal raphe stimulation was not as robust as we had anticipated. Out of the 87 cells sampled in

the granule layer only 11 responded consistantly to stimulation. Six of these cells displayed decreased spontaneous activity, three were excited by the stimulation and four cells displayed a biphasic response of initial excitation followed by a long period of suppressed activity. The location of these cells in the intermediate to far lateral anterior lateral hemisphere corresponded to areas expected to have significant innervation by serotonergic fibers (5) although they were not concentrated in any one folia or defined region.

Figure 1 illustrates the response of a cell whose spontaneous activity was suppressed by raphe stimulation. The high frequency, low amplitude action potentials of this cell found at a depth of 560 μm below the surface suggest that it is indeed a granule cell(9). With increasing stimulus intensities the degree of supression increases to a maximum duration of 230 msec.

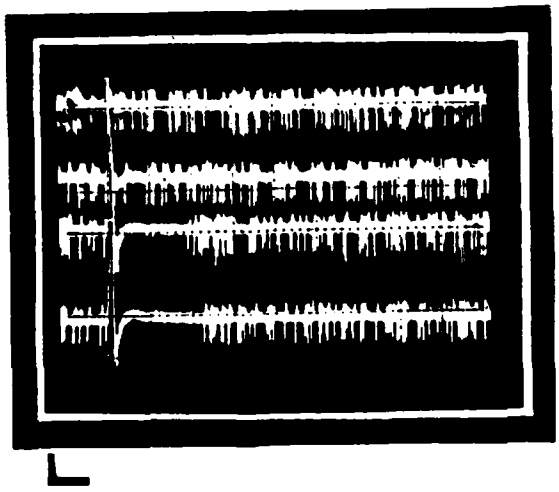

Fig. 1. Response of granule cell to single pulse stimulation of the dorsal raphe. Each trace formed by three beam sweeps. Stimulus indicated by artifact to the left of each trace. From top to bottom traces indicate: control baseline, 20, 30, and 50μA stimulus intensity. Scale markers denote 100msec and 1mv.

Figure 2 illustrates the biphasic type response that was observed in four cells. This type of response resembles that of Purkije cells as described by Strahlendorf et al (22). The average latency for onset of the stimulatory phase was 25 msec. followed by a longer (200-250 msec) inhibition. The pure excitatory response that was observed in three cells had a much shorter latency (10-15 msec) as illustrated in Figure 3. It is interesting to note that this effect was apparent in granular layer regions displaying lower spontaneous activity. It is possible that this response was masked at other sites by ongoing background stimulation.

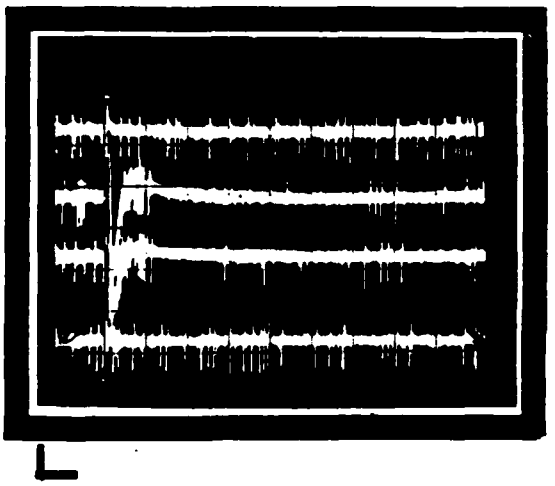

Fig 2. Example of granule cell responding to dorsal raphe stimulation with initial bursting activity followed by a long period of suppressed activity. Top and bottom traces are control baseline sweeps. Second and third middle traces display response to 20 and 30 μA stimulus intensity. Scale markers denote 50 msec and 1mV.

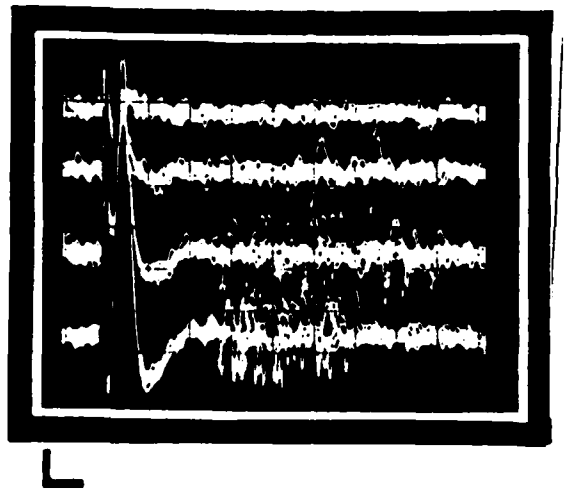

Figure 3. Example of granule layer cell activated by dorsal raphe stimulation. Each trace formed by five beam sweeps. From top to bottom the traces indicate: control baseline, 30, 40, and 60 μA stimulus intensity. Scale markers denote 5msec and 1mV.

The small number of cells encountered in the granular layer that responded to our stimulation was disappointing. However, the highest number of responsive cells were identified during the latter part of the research period following some procedural modifications. We now believe that our original stimulating arrangement may have been causing some damage to the raphe neurons, thus lessening the probability of producing normal stimulus responses. Because of time limitations we proceeded with the iontophoretic studies alone rather than combined with stimulation effects.

IV. IONTOPHORESIS OF SEROTONERGIC AGENTS

At best one could say that the literature on neuronal responses to local application of serotonergic compounds is

M) and receptor antagonists including cyproheptadine HCl (14.6 mM), methysergide maleate (0.01 M) M). The pH of all chemicals used were adjusted as needed and each solution was filtered (Millipore Corp., 0.22 um). The chemicals were electrophoretically applied to neurons by calibrated DC currents using a Neurophore BH-2 microiontophoresis system (Medical Systems Corp.). Control procedures for assessing microiontophoretic effects were carried out. A retaining current of 5 nA was utilized to prevent the spontaneous diffusion of active ions from the capillary barrels. To study the interaction between chemicals one was applied continuously while the other was applied at regular intervals.

RESULTS

A total of 33 cells were tested with serotonergic agents and glutamate. Five of these cells did not display a reliable response to glutamate and are excluded from this discussion. Of the remaining 28, the majority, nineteen, were inhibited by 5-HT. An example of this response is illustrated in Figure 4. The reduction in activity is significant and endures beyond the period of drug application. At higher doses ($\geq$ 50 nAmps) several cells oscillated in activity before returning to a normal baseline. Application of methysergide using current levels that did not directly affect cell activity had no or very little affect on this supression of activity. There are several reports in the literature of 5-HT receptor antagonists having minimal affect on serotonin induced inhibition (1,15,16).

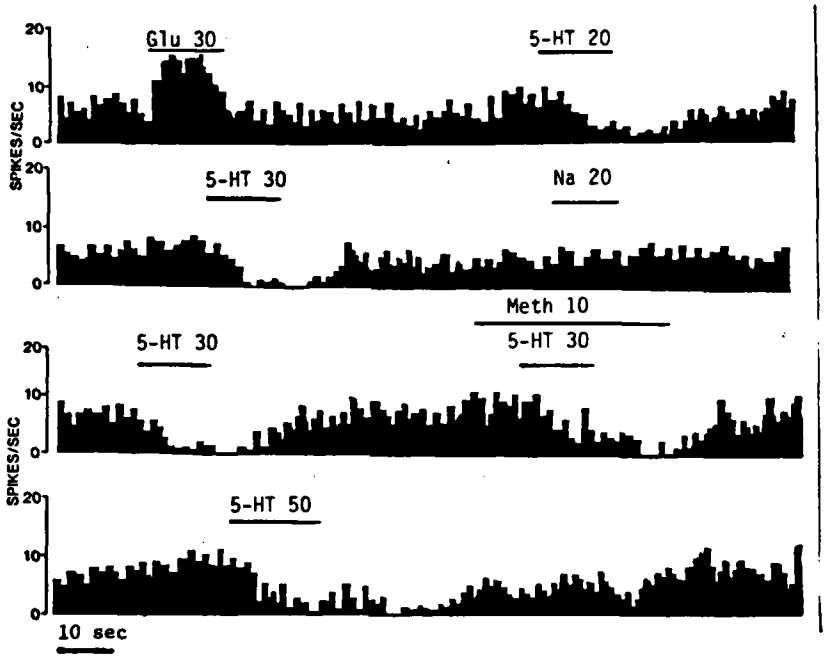

Figure 4. Reduction of granule cell activity in response to pulses of serotonin (5-HT). Rows are from continuous strip chart record of activity (spikes/sec) of single cell. Bars indicate duration and intensity (nAmps) of current application. Application of 5-HT receptor antagonist methysergide (Meth) did not block inhibitory effect. Glu indicates glutamate.

Of the nine cells that were not inhibited by 5-HT, seven displayed increased activity and two were not affected by any level of 5-HT ejection current. Figure 5 illustrates this excitatory response and as can be seen the effect could be blocked by methysergide. The excitatory response differed from that produced by glutamate in that it was not as immediate in onset and offset, however, the excitation never display the long duration that characterized the inhibitory responses.

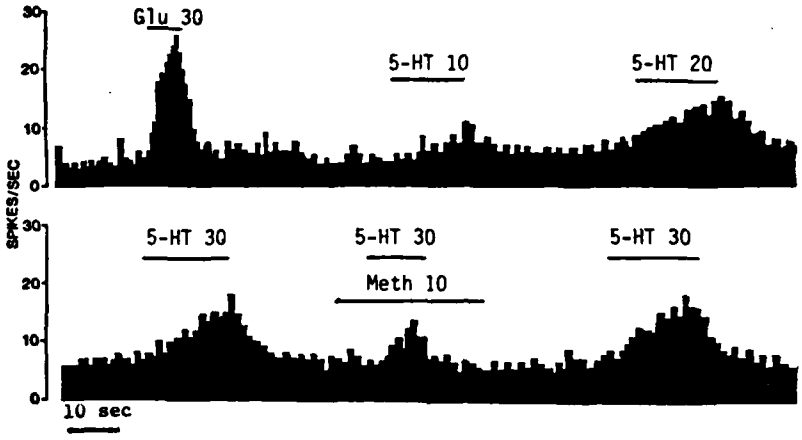

Figure 5. Example of increased activity of granule cell in response to serotonin application. This effect could be partially blocked by ejection of methysergide (Meth).

RECOMMENDATIONS

Despite the limited number of cells that responded to stimulation the results are very exciting in terms of providing a frame work for deliniating distinct serotonergic pathways based on the type of response illicited in granule cells. The prolonged inhibitory response indicates a type of humoral modulation that could be mediated by the fine serotonergic fibers that do not appear to make definite synaptic contacts with target cells within the granular and molecular layers. The fact that some granule cells did respond with short latency bursts supports the idea of serotonergic mossy fiber innervation. At the present time we are concentrating on integrating the stimulation and iontophoretic techniques as we had originally planned.

REFERENCES

1. Aghjanian, G. K. and R. Y. Wang. Physiology and Pharmacology of central serotonergic neurons. In: Psychopharmacology: A Generation of Progress. M. A. Lipton, A. DiMascio and K. F. Killam (eds.) Raven Press, New York, 1978.

2. Aghajanian, G.K. and C.P. Vandermaelen. Intracellular recordings from serotonergic dorsal raphe neurons: pacemaker potentials and the effect of LSD. Brain Res. 238: 463-469,1982.

3. Aghajanian, G.K. and J.M. Lakoski. Hyperpolrization of serotonergic neurons by serotonin and LSD: studies in brain slices showing increased K+ conductance. Brain Res. 305: 181-185, 1984.

4. Anden, N. E., K. Fuxe and U. Ungerstedt. Monoamine pathways to the cerebellum and cerebral cortex. Experientia 23: 838-839, 1967.

5. Bishop, G. A., R. H. Ho and J. S. King. Localization of serotonin immunoreactivity in the deep cerebellar nuclei of the opossum. Neurosci. Abstr. 10: 750, 1984.

6. Bobillier, P., S.Seguin, F. Petitjean, D. Salvert, M. Touret and M. Jouvet. The raphe nuclei of the cat brainstem: A topographical atlas of their efferent projections as revealed by autoradiography. Brain Res. 113: 449-486, 1976.

7. Bloom, F. E., B. J. Hoffer, G. R. Siggins, J. L. Barker and R. A. Nicoll. Effects of serotonin on central neurons: microiontophoretic application. Fed. Proc. 31: 97-106,1976.

8. Chan-Palay, V. Cerebellar Dentate Nucleus: Organization, Cytology and Transmitters. Berlin: Springer-Verlag, 1977.

9. Eccles, J. C., M. Ito and J. Szentagothai. The Cerebellum as a Neuronal Machine. Springer-Verlag, New york, 1967.

10. Eccles, J. C., K. Sasaki, and P. Strata. The potential fields generated in the cerebellar cortex by a mossy fiber volly. Exp. Brain Res. 3: 58-80, 1967.

11. Eccles, J. C., K. Sasaki and P. Strata. A comparison of the inhibitory actions of Golgi cells and of basket cells. Exp. Brain Res. 3; 81-94, 1967.

12. Halaris, A. E., B. E. Jones and R. Moore. Axonal transport in serotonin neurons of the midbrain raphe. Brain Res. 66: 555-574, 1976.

13. Hokfelt, T. and K. Fuxe. Cerebellar monoamine nerve terminals, a new type of afferent fibers to the cortex cerebelli. Exp. Brain Res. 9: 63-73, 1969.

14. Konig, J. R. F. and R. A. Klippel. The Rat Brain: A Stereotaxic Atlas of the Forebrain and Lower Parts of the Brain Stem. Baltimore: Williams and Wilkins, 1963.

15. McCall, R. B. and G. K. Aghajanian. Serotonergic facilitation of facial motoneuron excitation. Brain Res. 169: 11-27, 1967.

16. McCall, R.B. Serotonergic excitation of sympathetic preganglionic neurons: a microiontophoretic study. Brain Res. 289: 121-127, 1983.

17. Park, M.R., J.A. Gonzales-Vegas and S.K. [illegible]tai. Serotonergic excitation from dorsal raphe stimulation recorded intracellularly from rat caudate-putamen. Brain Research 243: 49-58, 1982.

18. Peroutka, S. J., R. M. Lebovitz and S. H. Snyder. Two distinct central serotonin receptors with different physiological functions. Science 212: 827-829,1981.

19. Peroutka, S. J. and S. H. Snyder. Multiple serotonin receptors: differential binding of (^{3}H)5-hydroxytryptamine, (^{3}H)Lysergic Acid Diethylamide and (^{3}H)Spiroperidol. Mol. Pharmacol 16: 687-699, 1979.

20. Peterson, R. C., A. D. Simpson, M. J. Wayner and H. Yagi. A window discriminator for sorting electrical signals. Physiol. Behav. 4: 865-867, 1969.

21. Shinnar, S., R. J. Maciewicz and R. J. Shofer. A raphe projection to cat cerebellar cortex. Brain Res. 97: 139-143, 1973.

22. Strahlendorf, J. C., H. K. Srahlendorf and C. D. Barnes. Modulation of cerebellar neuronal activity by raphe stimulation. Brain Res. 169: 565-569, 1979.

23. Strahlendorf, J. C. and G. D. Hubbard. Serotonergic interactions with rat cerebellar purkinje cells. Brain Res. Bull. 11: 265-269, 1983.

24. Strahlendorf J. C., H. K. Strahlendorf and C. D. Barnes. Comparative aspects of raphe-induced modulation of evoked and spontaneous cerebellar unit activity. In: The Role of Peptides and Amino Acids as Neurotransmitters, pgs. 217-225.

Alan Liss, New York, 1981.

25. Szentagothai, J. Glomerular synapses, complex synaptic arrangements, and their operational significance. The Neurosciences. 427-443, 1970.

26. Terrian, D.M., W.I. Butcher, P.H. Wu and D.L. Armstrong. Isolation of glomeruli from areas of bovine cerebellum and comparison of ^{3} serotonin uptake. Brain Res. Bull. 14: 469, 1985.

1985 USAF-UES SUMMER FACULTY RESEARCH PROGRAM/
GRADUATE STUDENT SUMMER SUPPORT PROGRAM

Sponsored by the
AIR FORCE OFFICE OF SCIENTIFIC RESEARCH
Conducted by the
UNIVERSAL ENERGY SYSTEMS, INC.
FINAL REPORT

TEMPERATURE DEPENDENCE OF ION-MOLECULE ASSOCIATION REACTIONS: HALIDE ION ADDITION REACTIONS

Prepared by:	Lucia M. Babcock
Academic Rank:	Assistant Professor of Chemistry
Department and University:	Department of Chemistry Louisiana State University, Baton Rouge, LA
Research Location:	Air Force Geophysics Laboratory/LID Hanscom AFB, MA
USAF Research	John F. Paulson
Date:	25 September 1985
Contract No:	F49620-85-C-0013

TEMPERATURE DEPENDENCE OF ION-MOLECULE ASSOCIATION REACTIONS: HALIDE ION ADDITION REACTIONS

by

Lucia M. Babcock

ABSTRACT

We have found increasing evidence that halide ion addition to the boron trihaldies proceeds via both radiative and collisional stabilization pathways. This is, to our knowledge, the first observation of such a phenomenon. In our studies this summer at Air Force Geophysics Laboratory, we have continued our examination of these interesting association reactions by looking at the temperature dependence of the additions over the range 200K to 400K using a temperature variable Selected Ion Flow Tube. Our studies provide further evidence for both the radiative and collisional stabilization mechanisms, and also reveal the dependence upon temperature of several ion-molecule association reactions. The temperature dependence found agrees well with a simple model of ion-molecule association, and we are in the process of analyzing the data further. In addition, we have examined a series of halide ion addition reactions using several different neutral molecules in an attempt to identify other systems which might exhibit radiative stabilization channels, and to characterize the properties which lead to such behavior. Finally, we have studied the temperature dependence of some bimolecular reactions of the boron trihalides in order to establish some of their chemical properties and energetics.

ACKNOWLEDGMENTS

I would like to thank the people at Air Force Geophysics Laboratory/LID, Hanscom AFB for their support and hospitality during my stay. In particular, John Paulson, Fred Dale, Michael Henchman, and Al Viggiano deserve special thanks for their technical assistance as well as their friendship. The support of the Air Force Systems Command and the Air Force Office of Scientific Research through the Summer Faculty Research Program is gratefully acknowledged, as is the very competent administration of the program by Universal Energy Systems, Inc. Finally, a great deal of credit for the magnitude and quality of the research carried out go to Charles R. Herd and Paula S. Ruhr, two of my graduate students. Their long hours and professional attitudes made our accomplishments possible.

I. INTRODUCTION:

Our research group has always been interested in the gas phase ion-molecule chemistry of negative ions.[1-6] A most interesting examination of the addition of the halide ions F^- and Cl^- to the boron trihalides BF_3 and BCl_3 using a variety of different buffer gases to collisionally stabilize the addition product presented compelling evidence for the presence of a radiative channel for stabilization.[1] These reactions imply a radiative process which occurs on a time scale which is at least comparable to the rate of collisional stabilization under flowing afterglow conditions.

Our work at Air Force Geophysics Laboratory (AFGL) this past summer represents the continuation of a collaboration which began as a result of our mutual interest in the general area of ion-molecule association reactions. Dr. John Paulson's group at AFGL has long been involved in using a temperature variable Selected Ion Flow Tube (SIFT) to examine the temperature dependence of ion-molecule reactions in general, with a particular interest in association reactions.[7,8] Because of this common interest, we thought it mutually beneficial to examine the temperature dependence of these unique boron trihalide systems using the temperature variable SIFT at AFGL.

II. OBJECTIVES OF THE RESEARCH EFFORT:

The boron trihalides are Lewis acids and can add anions to form tetrahedral borate anions as shown below:

These reactions are exoergic, and, as a result, the complex is initially formed in an excited state. This excess energy resulting from the formation of the boron halide ion bond must be removed for stabilization of the BX_4^- product. In a previous examination of the addition of fluoride ion to BF_3 and of chloride ion to BCl_3 and BF_3, we found strong evidence for the

existence of both radiative and collisional stabilization of the product anion.[1] The mechanism is as shown:

$$BX_3 + X^- \rightleftharpoons (BX_4^-)^*$$

$$(BX_4^-)^* \begin{cases} \longrightarrow BX_4^- \\ \longrightarrow BX_4^- + h\nu. \end{cases}$$

The expression for the observed rate constant is:

$$k_{obs} = \frac{k_a k_s(M) + k_a k_r}{k_d + k_s(M) + k_r}$$

These halide addition reactions appear to be unique in that they exhibit BOTH radiative and collisional stabilization of the excited $(BX_4^-)^*$ under the conditions found in typical flowing afterglow experiments (i.e. 0.2 to 2.5 torr). This implies a radiative process which occurs on a time scale at least comparable to the collision rate multiplied by the collisional stabilization efficiency factor. To our knowledge, these boron trihalide reactions are the first reported in which such a phenomenon occurs.

Our research efforts at AFGL this past summer were directed toward the examination of these interesting addition reactions as a function of temperature, and also toward the identification of other association reactions which show similar behavior. Through these studies, it was our hope to gain more complete understanding of both the collisional and radiative processes themselves and also to begin to characterize systems in which radiative stabilization can compete effectively with collisional stabilization in the pressure range 0.2 to 5.0 torr. Throughout these studies involving an investigation of radiative stabilization in ion-molecule association reactions, we have had as a continuing aim the study of the temperature dependence of gas phase ion-molecule addition reactions as well. Though theory

AD-A166 176 UNITED STATES AIR FORCE SUMMER FACULTY RESEARCH PROGRAM 03/13
1985 TECHNICAL RE (U)UUNIVERSAL ENERGY SYSTEMS INC
DAYTON OH R C DARRAH ET AL. DEC 85 AFOSR-TR-86-0139
UNCLASSIFIED F49620-85-C-0013 F/G 5/9 NL

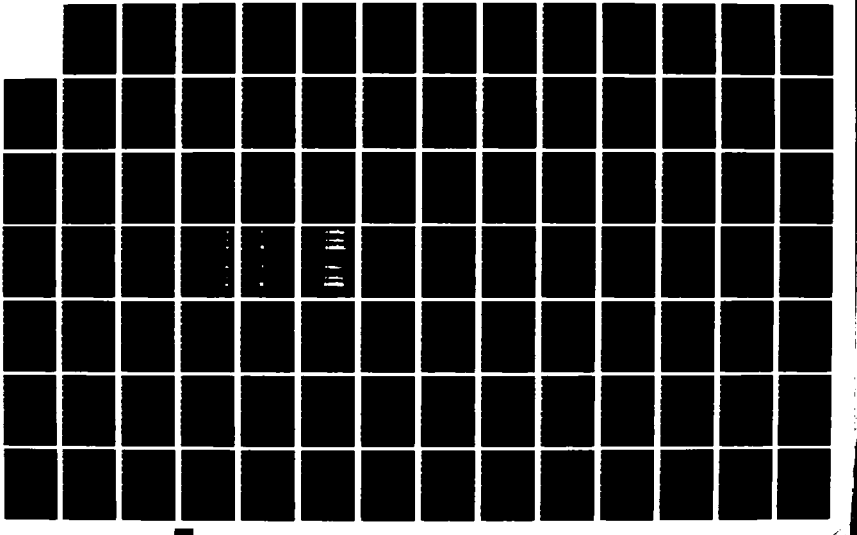

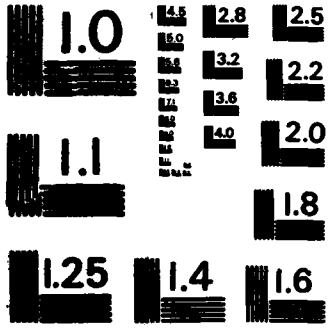

MICROCOPY RESOLUTION TEST CHART
NATIONAL BUREAU OF STANDARDS-1963-A

predicts the general negative temperature dependence seen in this class of reaction,[9-11] the exact temperature dependence is difficult to predict. Experimentally, the temperature dependence of collisionally stabilized ion-molecule association reactions is seen to be fairly complex and to vary from system to system.[12] It is important both for experimental and theoretical reasons, then, to learn as much as possible about the effect temperature has upon these reactions.

Finally, in the course of our examination of the addition of halide ions to the boron trihalides BF_3 and BCl_3, we found evidence for some interesting bimolecular reactions. The latter part of our stay at AFGL was therefore devoted to looking at some bimolecular reactions of the neutral boron trihalides with polyatomic anions; the temperature dependence of these reactions was also examined.

III. RESULTS:

All of our studies were carried out using the temperature variable Selected Ion Flow Tube (SIFT) at AFGL. The technique is described briefly in Section IV. The systems examined fall into two general classes: addition reactions, and bimolecular reactions. In the first category, we looked at the addition of F^-, Cl^-, and Br^- to BF_3, BCl_3, SF_4, and SiF_4, as well as the addition of Cl^- to Cl_2. In the second category, we examined the reactions between BCl_4^- and SF_4, BF_3, SiF_4, and SF_6; between BCl_3 and F^- (a bimolecular reaction in contrast to the other reactions of boron trihalides with halide anions); and between BCl_3 and BF_4^-, SF_5^-, and OH^-. All reactions were studied in helium buffer gas over a temperature range 200K to 400K and a pressure range 0.2 to 0.8 torr. The results of our studies for each system are presented below.

Halide Ion Addition to BF_3 and to BCl_3

We examined the reactions of BF_3 with F^-, Cl^-, and Br^-, and of BCl_3 with Cl^- and Br^- over the temperature and pressure ranges mentioned above. In all cases the only primary product observed

is that resulting from addition of the halide ion: the boron tetrahalide, BX_4^-. The observed rate coefficients for all of these reactions increases as pressure increases at a given temperature. In addition, the observed rate coefficient increases as temperature decreases. This general type of behavior is indicative of association reactions which are occuring in a pressure and temperature regime where collisional stabilization efficiency is less than unity. That is, it takes more than a single collision with the inert buffer gas (in this case helium) to remove enough energy from the initially excited product ion to convert it into stable product. Both the pressure and temperature dependence of the reactions producing BF_4^-, BCl_4^-, BF_3Cl^-, and BCl_3Br^- are consistent with the general mechanism given previously in which both radiative and collisional stabilization are occurring. In the case of Br^- addition to BF_3, we think that the radiative process may be much less important. This is reasonable since one would expect this bond strength to be small and since the observed rates are quite slow as well. Figures 1 and 2 show the variation of k_{obs} with temperature and pressure for some of these association reactions.

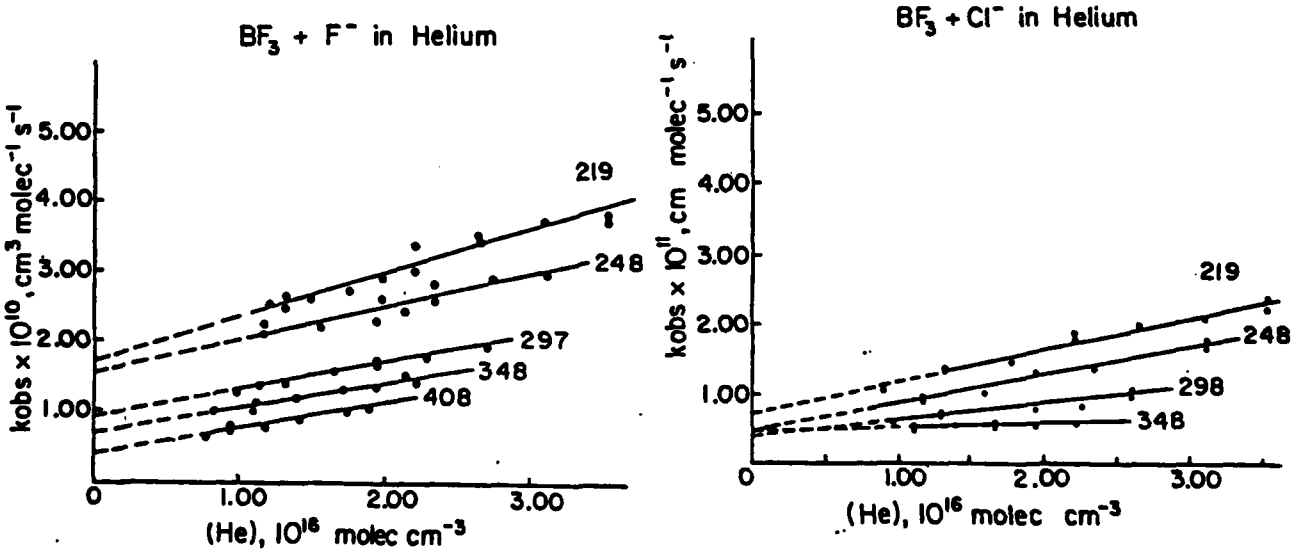

Figure 1. Temperature and Pressure Dependence for Addition of F^- and of Cl^- to BF_3.

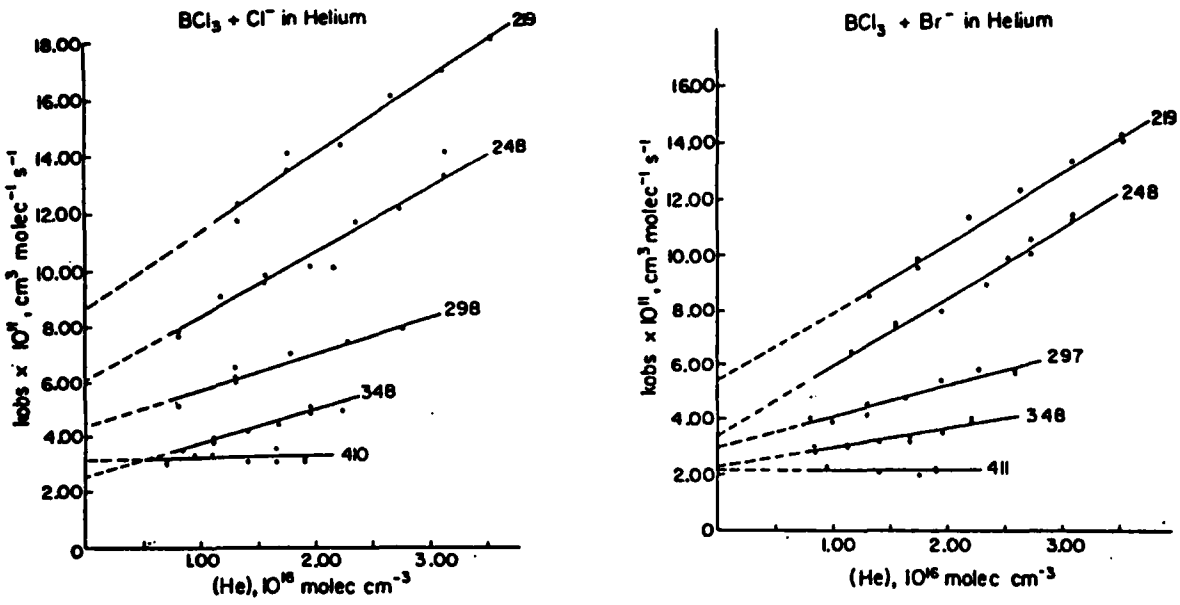

Figure 2. Temperature and Pressure Dependence of Addition of Cl^- and of Br^- to BCl_3.

Recalling that the expression for the observed rate coefficient, k_{obs}, is:

$$k_{obs} = \frac{k_a k_s (M) + k_a k_r}{k_d + k_s (M) + k_r}$$

it is clear that the temperature dependence of k_{obs} without complications from the pressure dependence can be obtained by looking at the observed rate coefficient as a function of temperature at constant (M). We have done this, and a typical set of data are shown below in Figure 3.

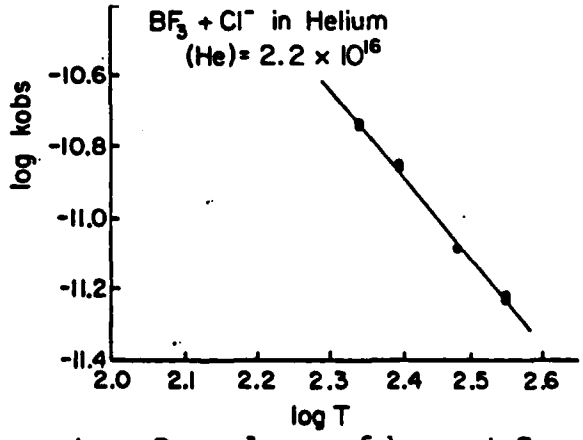

Figure 3. Temperature Dependence of k_{obs} at Constant (He) for the Addition of Cl^- to BF_3.

The functional dependence upon temperature of these association reactions is of the correct magnitude predicted by simple theory.

We are in the process of a detailed interpretation of our results, and plan to compare them to theoretical predictions. The preliminary examination carried out thus far strongly supports our original mechanism in which radiative stabilization as well as collisional stabilization plays an important role in the production of the stable boron tetrahalides.

Halide Ion Addition to Silicon Tetrafluoride

We are interested in identifying other systems which undergo radiative as well as collisional stabilization in ion-molecule association reactions examined under flowing afterglow or SIFT conditions. Candidates for such behavior appear to be systems in which the associating ion is a halide ion and the bond formed in the addition reaction is quite favorable energetically. In addition, it seems reasonable to expect that systems in which the excited complex has several internal degrees of freedom are good candidates for radiative association since the lifetime of such complexes will be longer. For these reasons, we decided to look at the addition of halide ions to silicon tetrafluoride, SiF_4.

Fluoride ion, F^-, chloride ion, Cl^-, and bromide ion, Br^- all add to SiF_4 to form the pentacoordinate anion of general formula SiF_4X^-. All reactions were studied over a pressure range 0.2 to 0.8 torr and a temperature range of 200K to 400K.

In the case of fluoride addition, the reaction is given below:

$$SiF_4 + F^- \longrightarrow SiF_5^-$$

For all temperatures studied in the range mentioned above (408K, 348K, 298K, 248K, and 219K), the observed rate coefficient did not vary with pressure over the range 0.2 to 0.8 torr. However, the rate coefficient did vary with temperature, increasing from about 0.9×10^{-9} at 408K to about $1.4 \times 10^{-9} cm^3 molec^{-1} s^{-1}$ at 248K and 219K. The value at the lower temperatures appears to be

approaching a constant value which is close to the collision (Langevin) rate for these reactants. Therefore, we think that we are close to the saturation limit even at the high temperatures, and that the rate coefficient is thus not very sensitive to pressure. Over our limited pressure range, we cannot observe any dependence upon pressure within experimental error. The temperature dependence, however, indicates that we reach the saturation limit only at the lower temperatures. This behavior is consistent with an association reaction which is occurring in the "nearly saturated" regime of the rate coefficient vs. pressure curve. We are in the process of analyzing the data in more detail to determine whether a radiative component is present and to assess the temperature dependence of this addition reaction.

The addition of Cl^- to SiF_4 produces the single primary product SiF_4Cl^-. The observed rate coefficient is clearly pressure dependent over the range 0.2 to 0.8 torr for the five temperatures between 200K and 400K examined. Even at the lowest temperature studied, 219K, we do not see evidence for saturation of the rate coefficient. The general behavior of this system with temperature and pressure is similar to that observed for the addition of halide ions to the boron trihalides; it is possible that both radiative and collisional stazbilization are playing roles in the addition of chloride ion to silicon tetrafluoride. A more detailed analysis of our data will help to determine this.

The addition of bromide ion to silicon tetrafluoride is quite slow. Under our experimental conditions, we were able to measure rate coefficients only at the two lowest temperatures, 219K and 248K. For all cases where a rate coefficient was measured, the value of k_{obs} was in the range 5×10^{-12} to $1.7 \times 10^{-11} cm^3 molec^{-1} s^{-1}$. There is an increase in the observed rate coefficient as pressure is increased, and the observed rate coefficient also increases as temperature is decreased. Both of these are consistent with ion-molecule association. The only product observed is SiF_4Br^-. As in the case of the addition of Br^- to BF_3, the rates are very small, and the bond formed is most

likely quite weak. It is possible that radiative stzbilization does not play an important role in the formation of the stable SiF_4Br^- product. Again, we are in the process of analyzing our data more fully, and hope to determine the mechanism by which this addition reaction occurs.

Halide Ion Addition to Sulfur Tetrafluoride

The addition of halide ions to sulfur tetrafluoride to produce the corresponding sulfur pentahalide anions also appears to be a class of reaction in which radiative stabilization might occur. The strengths of the bonds formed are generallly favorable energetically, and several vibrational degrees of freedom are available to the excited complex making a long-lived state probable. Therefore, we examined the addition of F^-, Cl^-, and Br^- to SF_4 over the temperature and pressure ranges mentioned above.

Fluoride ion adds to SF_4 to produce the sulfur pentafluoride anion, SF_5^-. At temperatures of 408K, 348K, 298K, and 248K, the observed rate coefficient increases as pressure increases indicating that the association reaction rate has not yet reached the saturated collision limit. At the lowest temperature studied, 219K, the observed rate coefficient is independent of pressure and has a value of 1.3×10^{-9} $cm^3molec^{-1}s^{-1}$. Clearly we are approaching the collision limit for association in this system. Again it is difficult to tell from a preliminary analysis of the data whether or not radiative stabilization is playing an important role in this reaction.

The addition of chloride ion to sulfur tetrafluoride produces only the single primary product SF_4Cl^- as shown below:

$$SF_4 + Cl^- \longrightarrow SF_4Cl^-.$$

This reaction was examined only at three temperature: 219K, 248K, and 298K; the pressure range was 0.2 to 0.8 torr. At the two lower temperatures, additional products which we have tentatively assigned as secondary products appear. There are two products in

addition to SiF_4Cl^- at 248K, and three in addition to the primary product at 219K. We are in the process of assigning these products. The behavior of the observed rate coefficient with temperature and pressure is characteristic of the previous ion-molecule addition reactions which have been discu ed. An increase in pressure results in a larger value for k_{obs}, nd k_{obs} is also seen to increase as temperature decreases. The general behavior is, once again, similar to that observed for the boron trihalide cases where we have compelling evidence for radiative association as well as collisional association. Further analysis of our results will help determine whether or not this is the case for the chloride ion addition to sulfur tetrafluoride.

As the last in the series of halide ion additions to SF_4, we looked at the addition of bromide ion. The pressure dependence of k_{obs} over the range 0.2 to 0.8 torr was measured at each of three temperatures: 220K, 248K, and 296K. The behavior of the observed rate coefficient is qualitatively the same as that of Cl^- addition to this neutral; that is, the rate coefficient increases with increasing buffer gas concentration, and shows a negative temperature dependence. We do not see any evidence for approach to the saturation limit in this system. A preliminary examination of the data indicate that they are not inconsistent with a radiative association channel in addition to the collisional one. Further reduction of our data for this and all of the halide ion additon reactions of SF_4 should begin to shed light on the mechanism which is operating in these systems.

Chloride Ion Addition to Cl_2

Finally in our series of association reactions, we chose to look at the addion of chloride ion, Cl^- to diatomic chlorine:

$$Cl^- + Cl_2 \longrightarrow Cl_3^-.$$

This reaction is of interest because we have studied it previously in a flowing afterglow at ambient temperatures[2], and have also carried out some quasi-classical mechanical trajectory

calculations[3,4] on this system. The bond strength for the formation of the new bond is quite energetically favored as in the cases mentioned above, but the number of degrees of freedom available to the excited complex is considerably smaller. The flowing afterglow studies[2] show that the three-body association rate is small, and that the reaction proceeds without any radiative component in the pressure range 0.2 to 5.0 torr at room temperature. For these reasons, we wanted to examine the temperature dependence of Cl^- addition to Cl_2 to contrast it to systems where we have strong evidence for radiative as well as collisional stabilization.

Because the reaction is so slow, we were able to make measurements at only the extreme conditions of low temperature (219K, 248K, and 298K) and high pressure (0.7 and 0.8 torr) accessible in our SIFT apparatus. The rate coefficients obtained under these conditions are on the order of $5x10^{-13}cm^3molec^{-1}s^{-1}$, and are therefore not very reliable since they represent the lower limit on bimolecular rate coefficients which can be measured in our apparatus. However, the general behavior observed is consistent with an association in which collisional stabilization predominates under our conditions of temperature and pressure. As expected, k_{obs} shows a negative temperature dependence and a positive pressure dependence. As in the flowing afterglow study, the reaction seems to be occurring under low pressure conditions; that is, the rate of unimolecular decomposition of the excited Cl_3^- is much greater than the rate of stabilization via collision with the helium buffer gas.

Bimolecular Reactions Involving the Boron Trihalides

In an effort to gain some insight into the energetics of the reactions of the boron trihalides BF_3 and BCl_3, and also to begin an examination of some of the mechanisms which could result in some of the interesting secondary products which we observed in our halide ion addition studies, we undertook the study of the following bimolecular reactions as a function of both temperature and pressure:

$$BCl_4^- + SF_4 \qquad (1)$$

$$BCl_4^- + BF_3 \qquad (2)$$

$$BCl_4^- + SiF_4 \qquad (3)$$

$$BCl_4^- + SF_6 \qquad (4)$$

$$F^- + BCl_3 \qquad (5)$$

$$BF_4^- + BCl_3 \qquad (6)$$

$$SF_5^- + BCl_3 \qquad (7)$$

$$OH^- + BCl_3. \qquad (8)$$

Reactions (1) through (4) do not proceed to any appreciable extent under our experimental conditions. An analysis of the energetics of the reactants will allow us to make some conclusions about the energetics of chloride addition to BCl_3; the chloride affinity of this neutral has not been reported as yet.

The reaction of F^- with BCl_3 does not produce the addition product as in the other halide ion studies presented above, but rather undergoes the following bimolecular reaction:

$$BCl_3 + F^- \longrightarrow Cl^- + BCl_2F.$$

The secondary product BCl_4^- is produced, presumably in a three-body association of the neutral BCl_3 with the primary product, Cl^-. This reaction is both pressure and temperature independent over the range 0.2 to 0.8 torr and 220K to 353K as one expects for a bimolecular reaction. The average rate coefficient measured for this process is $1.4 \times 10^{-9} cm^3 molec^{-1} s^{-1}$; the reaction is obviously proceeding at the collision limit.

The reaction of BF_4^- with neutral boron trichloride produces BCl_3F^- as the only primary product, with BCl_4^- as a secondary product. Again the reaction is independent of temperature and pressure over the range mentioned above, and the average value of the bimolecular rate coefficient is 6.2×10^{-10} $cm^3molec^{-1}s^{-1}$ which is approximately half of the Langevin rate. We propose the following sequence of bimolecular reactions for the production of the primary and secondary ions formed:

$$BCl_3 + BF_4^- \longrightarrow BCl_3F^- + BF_3$$

$$BCl_3F^- + BCl_3 \longrightarrow BCl_4^- + BCl_2F.$$

The reaction of boron trichloride with the sulfur pentafluoride anion, reaction (7) above, is analogous to that for the reaction of BCl_3 with BF_4^-. The primary ion produced is BCl_3F^-, and the boron tetrachloride anion is produced in a secondary reaction. As in the case above, the first step is fluoride transfer to the neutral BCl_3. The product ion BCl_3F^- then participates in a bimolecular reaction with BCl_3 to produce BCl_4^-. This reaction is independent of temperature and pressure as expected, and also has a rate coefficient which is approximately half of the Langevin rate.

The final bimolecular reaction which we examined was the reaction of the hydroxide ion, OH^-, with BCl_3 at room temperature. As in the reaction of BCl_3 with F^-, the primary product formed is Cl^- in a bimolecular ligand exchange process, and this product reacts further with the neutral boron trichloride to produce BCl_4^- in a termolecular addition reaction:

$$BCl_3 + OH^- \longrightarrow Cl^- + BCl_2OH$$

$$BCl_3 + Cl^- \longrightarrow BCl_4^-.$$

At room temperature, the reaction rate coefficient shows no dependence upon pressure; but, of course, the amount of BCl_4^-

produced in the termolecular secondary reaction increases as pressure is increased. The average rate coefficient for the bimolecular ligand exchange process is 1.4×10^{-9} $cm^3 molec^{-1} s^{-1}$, again essentially the collision limit.

IV. EXPERIMENTAL TECHNIQUE:

All of the studies presented above were performed using the temperature variable flow tube (SIFT) at AFGL. A schematic of the apparatus is show below in Figure 4.

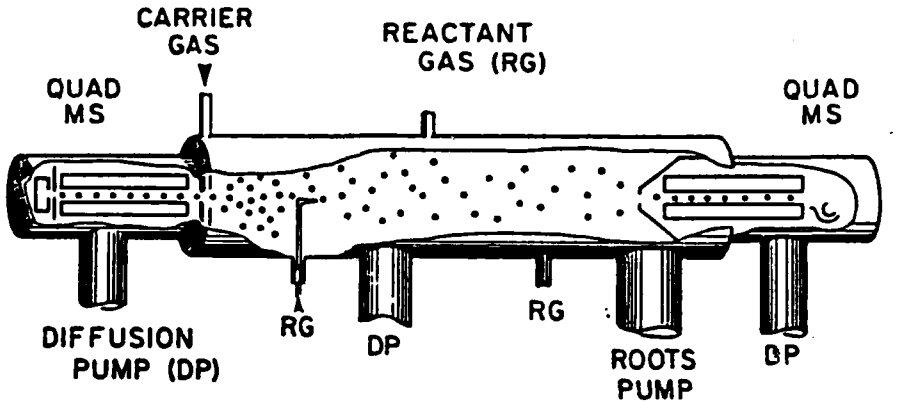

Figure 4. Schematic representation of the Selected Ion Flow Tube (SIFT) used in our experiments.

The SIFT technique is a method for studying gas phase ion-molecule reactions in a fast flow reactor under thermal conditions. Thermalization of the reactant ions and neutrals is brought about by collision with the large excess of inert buffer gas (helium in our case) which constantly flows through the reaction chamber; the helium makes up over 95% of the gases in the SIFT. Ions are initially produced in a high pressure ionization source (left side of the schematic), and the desired reactant ion is "sifted" out of the mixture by the first quadrupole mass filter. This selection of reactant ion is a powerful technique for isolating the single reactant ion which is to be studied, and also allows for the removal of most of the neutral gas(es) which are used to generate the reactant ion

before entrance into the reaction chamber. This is a significant advantage over the situation encountered in the conventional flowing afterglow apparatus where reactant ions are produced in the reaction tube itself, and one must deal with the complications which may occur due to production of more than one ion and/or the presence of the unreacted neutral used to produce the reactant ion. The ion which has been selected by the first quadrupole is then injected into the flow tube itself; the inert helium carrier gas also enters the tube at this point. The neutral reactant gas is added downstream of the injection point, and from there to the detection chamber, the ion-molecule reactions take place. At the downstream end of the reaction chamber, a fraction of the reacting mixture is sampled through a small orifice; the rest of the gases are pumped away by a high speed Roots pump. The gases which have passed through the sampling orifice then enter a second quadrupole mass filter where both the remaining reactant ion and any product ions are quantitatively analyzed. Rate information is obtained from the decay curve of the reactant ion as a function of added neutral reactant gas.

Temperature variation and control is achieved by circulating heated or cooled fluids through coils surrounding the reaction segment of the flow tube. The tube is jacketed in a vacuum chamber which is evacuated to prevent heat exchange to the atmosphere. Temperature is monitored by means of platinum resistance thermometers which are located along the reactor. Pressure in the reaction chamber is monitored using a capacitance manometer, and changes in pressure are brought about by varying the flow of the helium carrier gas and/or throttling the valve leading to the Roots pump.

As mentioned above, ions are produced via ionization of appropriate neutrals in the high pressure ion source. For our studies, F^- was produced from ionization of SF_6, Cl^- from CCl_4, and Br^- from CH_3Br. The reactant ions BCl_4^-, BF_4^-, and SF_5^- used in the bimolecular studies were produced via electron impact on BCl_3, BF_3, and SF_6 respectively.

V. RECOMMENDATIONS:

The interesting phenomenon whereby both radiative and collisional stabilization occur in ion-molecule association reactions certainly deserves more study. The detailed analysis of the work we did this past summer at AFGL should begin to address questions such as: (1) is formation of a strong bond in the association process a necessary criterion for observing this phenomenon? (2) can we see the same behavior in systems with very few degrees of freedom available to the excited complex? and (3) do the other halide ion addition reactions we have examined have both radiative and collisional pathways? Furthermore, we plan to complement our experimental data with calculations of the temperature dependence which various theories predict for ion-molecule association reactions. Through this examination, we hope to gain insight into the ion-molecule association process in general, and, in particular, into those processes occurring in our reactions particular. Finally, with the analysis of our data, we should be able to begin to characterize those systems in which radiative stabilization can compete with collisional stabilization under flow tube conditions. With this information, a systematic search for systems displaying this behavior can be made.

Finally, in addition to the limited pressure range experiments which can be carried out in flowing afterglow and SIFT experiments, it would be very informative to examine these reactions under both lower and higher pressure conditions. We are currently involved in a collaborative effort with Prof. T.B. McMahon (University of Waterloo) to study these reactions under very low pressure conditions in ion cyclotron resonance (ICR) experiments.

REFERENCES

1. Babcock, L.M. and G.E. Streit, "Third-Body Effects in Termolecular Reactions: Halide Ion Addition to BF_3 and BCl_3," J. Phys. Chem., Vol. 88, 1984, p. 5025.
2. Babcock, L.M. and G.E. Streit, "Ion-Molecule Reactions of Cl_2 with Cl^- and F^-," J. Chem. Phys., Vol. 76, 1982, p. 2407.
3. Babcock, L.M. and D.L. Thompson, "Dynamics of Association and Decay. A Model Study of $Cl_2 + Cl^- \rightleftharpoons Cl_3^{-*}$ Using Quasiclassical Trajectories," J. Chem. Phys., Vol. 78, 1983, p. 2394.
4. Babcock, L.M. and D.L. Thompson, "Dynamics of Ion-Induced-Dipole Capture: Effects of Mass and Collision Energy," J. Chem. Phys., Vol. 79, 1983, p. 4193.
5. Babcock, L.M. and G.E. Streit, "Electron Attachment to SF_4," J. Phys. Chem., Vol. 86, 1982, p. 1240.
6. Babcock, L.M. and G.E. Streit, "Negative Ion-Molecule Reactions of SF_4," J.Chem. Phys., Vol. 75, 1981, p. 3864.
7. Hierl, P.M. and J.F. Paulson, "Translational Energy Dependence of Cross Sections for Reactions of OH^- with CO_2 and SO_2," J. Chem.Phys., Vol. 80, 1984, p. 4890.
8. Viggiano, A.A. and J.F. Paulson, "Temperature Dependence of Associative Detachment Reactions," J. Chem. Phys., Vol. 79, 1983, p. 2241.
9. Clary, D.C. "Rates of Chemical Reactions Dominated by Long-Range Intermolecular Forces," Mol. Phys., Vol. 53, 1984, p. 3.
10. Bates, D.R. "Ion-Molecule Association," J. Phys. B: Atom. Molec. Phys., Vol. 12, 1979, p. 4135.
11. Herbst, E. "A Statistical Theory of Three-Body Ion-Molecule Reactions," J. Chem. Phys., Vol. 70, 1979, p. 2201.
12. Ferguson, E.E. "Constraints on the Temperature Variation of Three-Body Ion-Neutral Association Reaction Rate Constants," Chem. Phys. Lett., Vol. 101, 1983, p. 141.

1985 USAF-UES SUMMER FACULTY RESEARCH PROGRAM/

GRADUATE STUDENT SUMMER SUPPORT PROGRAM

Sponsored by the

AIR FORCE OFFICE OF SCIENTIFIC RESEARCH

Conducted by the

UNIVERSAL ENERGY SYSTEMS, INC.

FINAL REPORT

ACTIVE CONTROL OF FLEXIBLE STRUCTURES

Prepared by:	Francesco L. Bacchialoni
Academic Rank:	Associate Professor
Department and University:	Electrical Engineering University of Lowell, Lowell, Massachusetts
Research Location:	Air Force Geophysics Laboratorry, Aerospace Systems Division, Systems Integration Branch
USAF Research:	Jack R. Griffin
Date:	1 October 1985
Contract No:	F49620-85-C-0013

ACTIVE CONTROL OF FLEXIBLE STRUCTURES

by

Francesco L. Bacchialoni

ABSTRACT

Contol of flexible structures requires as a prerequisite modelling of the structures, and this problem is considered first. Mechanically flexible systems require in theory an infinite number of elasic modes to describe their behavior, but in practice they are usually modelled by large finite-dimensional systems. In this report, a cantilever beam has been modelled using a state variable technique. Two analytical models have been set-up from the equations of the same cantilever beam, one using 4 points (and 8 states), the other using 8 points (16 states). In both cases initial conditions corresponding to the beam lowest mode have been applied, in order to have a predictable state trajectory. Unfortunately, the results are different from what expected and deemed not satisfactory. Limited time of the project prevented a thorough debugging of the situation.

ACKNOWLEDGEMENT

The author would like to thank the Air Force Office of Scientific Research and Universal Energy Systems, Inc. for providing him with the opportunity to spend a very worthwhile and interesting summer at the Air Force Geophysics Laboratory, Hanscom AFB, Massachusetts. He would like to acknowledge the laboratory, in particular the Development and Verification Branch of the Aerospace Engineering Division for its hospitality and excellent working conditions. Finally, he would like to thank Mr. Jack Grffin for accepting this area of investigation and for his guidance and collaboration.

I. INTRODUCTION

The Air Force Geophysics Laboratory and in particular its Aerospace System Division requires investigation of controllers for space systems including experiments and support hardware. The research effort described in this report is a natural continuation and outgrowth of previous research conducted on control systems for space related electromechanical systems such as free-flying shuttle launched spacecraft, and Get-Away-Special experiments. In addition, AFOSR has ongoing requirement for research on control aspects of flexible systems.

Professor Bacchialoni has been involved in control systems, classical and modern, for more than 25 years, at MIT Lincoln Lab., teaching at the University of Lowell, and at AFGL in three Summer Faculty Research Programs. Lately, he spent a sabbatical year at AFGL, working on a GAS controller, and on a paper related to the topic of control systems with resonant load. His expertise and availability matched the requirements of the research objective of interest to AFGL.

II. OBJECTIVES OF THE RESEARCH EFFORT

Preliminary goals of this research effort consisted in obtaining a good understanding of the problems found in the active control of flexible structures, and to have some practical means to analyze relatively simple systems. This work has been considered as a beginning effort in this field, which is extremely wide and open to abstract and applied

research. Continuation of effort will eventually be needed for practical results.

The approach to this effort consisted in:

1. Modelling of flexible structures.
2. Preliminary tests of discrete models.
3. Tentative control strategies, time permitting.
4. Plan for continuation of effort.

III. MODELS

The first task of the control engineer consists in constructing a mathematical model of the system in consideration. The model construction is extremely important and critical since the following work of analysis and synthesis is done on the model and not on the physical hardware. The model must include a sufficiently detailed description of the system without exceeding what is really necessary[1,2,3,4].

Another task of the engineer is to decide about sensors and actuators to be used and their location on the system being studied.

Finally, the engineer has to establish the control law that the active controller is going to implement[1,2].

Mechanical systems always include elements which are flexible: when the subsystem to be controlled has more than a certain amount of flexibility, the usual modelling involving rigid body motions is no longer satisfactory, and distributed-parameter models must be utilized to better

approximate the properties of the physical elements. As examples of the latter group one can consider some microwave antennas, optical telescopes, airplane wings, thin structures for space applications, etc. In this last category there are flexible beams attached to space vehicles, as for example structures designed to support solar cells, where the mechanical flexibility appears prominently as a result of minimization of the structural masses [6,7,8].

In particular, large space structures tend to have low frequency, lightly damped bending modes, closely spaced in frequency. Almost invariably, the structure has to pointed, and the motion is determined by a controller. Very likely the controller bandwidth will include some of the low frequency modes of the structure, thus making active control of these modes unavoidable.

The systems considered in this report include mechanical subsystems where the spatial distribution is an important feature. For these systems, this distributed nature can be described by partial differential equations. Active control of these systems means application of control forces aiming to bring the system to a desired state.

In theory, mechanically flexible systems require an infinite number of elastic modes to completely describe their behavior. In practice, they are usually modelled by large finite-dimension systems. To what extent the model approximates the physical hardwareby using finite dimensions involves an engineering judgement between the conflicting

factors of maintaining the better model (distributed-parameter) and of being able to obtain engineering results, such as location of sensors and actuators, and control laws.

A lumped-parameter system is modelled by the relationship of its state vector $\underline{x(t)}$, its control vector $\underline{u(t)}$, and its output vector $\underline{y(t)}$. These vectors have a finite number of components, and there is one independent variable, time. In the case of linear, time-invariant systems, the usual model has the form:

$$\underline{\dot{x}(t)} = [A]\,\underline{x(t)} + [B]\,\underline{u(t)}$$

$$\underline{y(t)} = [C]\,\underline{x(t)} + [D]\,\underline{u(t)}$$

A distributed-parameter system can similarly be described by the relationship between its state, control and output vectors. Here the independent variables are time and one or more spatial coordinates. There are many subtle difficulties that result from this modelling, and at this point it is not clear where it is advantageous to abandon the detailed analysis of this model, constructed in the most general fashion.

A practical method for modelling distributed-parameter systems consists in approximating the infinite-dimensional system by a finite-dimensional, lumped-parameter model. A relative simple method is modal analysis, which consists in finding the eigenfunctions (modes) and eigenvalues of the distributed-parameter model and then assume that only the first few lower modes are to be considered. This procedure

constructs a finite-dimensional model which approximates the original system, and which can be analyzed by the usual state-variable techniques. The main disadvantage of this technique is that a good engineering judgement is needed to establish the number of the significant modes. In models of complicated systems it may be very difficult to select the modes to be included in the model from the set of all the modes of the physical subsystem.

IV. TYPICAL EXAMPLE

In order to have some concrete results, let us consider the problem of a flexible cantilever beam[5], driven by a torque applied to the built-in end. Only small displacements will be considered. Fig. 1 shows this beam. It is assumed that flexural stiffness, mass per unit length and viscous friction per unit length are constant versus position on the beam and time.

If we consider only the transverse deflections, for small amplitudes the equation of motion is[2]:

$$EI \frac{\partial^4 y(x,t)}{\partial x^4} + \rho \frac{\partial^2 y(x,t)}{\partial t^2} + \beta \frac{\partial y(x,t)}{\partial t} = 0 \qquad (1)$$

where:

x = horizontal distance from left end of beam

t = time

y(x,t) = transverse deflection of beam

EI = flexural stiffness

ρ = mass per unit length of beam

β = viscous friction per unit length of beam

The bending moment is:

$$M(x,t) = EI \frac{\partial^2 y(x,t)}{\partial x^2} \tag{2}$$

and the shear force is given by:

$$S(x,t) = \frac{\partial}{\partial x} M(x,t) \tag{3}$$

Equation 1) is subject to both boundary and initial conditions. It may be converted into a set of ordinary differential equations by using finite differences to represent derivatives. The distance along the beam is broken into N segments of equal length Δx. To simplify notation, use subscripts $0,.....N$ to identify the variables at each length increment. Many different approximation formulas for the derivatives of a variable exist. Here we assume:

$$\left.\frac{\partial y}{\partial x}\right|_n = \frac{y_{n+1} - y_n}{\Delta x} \tag{4}$$

$$\left.\frac{\partial^2 y}{\partial x^2}\right|_n = \frac{y_{n+1} - 2y_n + y_{n-1}}{(\Delta x)^2} \tag{5}$$

$$\left.\frac{\partial^4 y}{\partial x^4}\right|_n = \frac{y_{n+2} - 4y_{n+1} + 6y_n - 4y_{n-1} + y_{n-2}}{(\Delta x)^4} \tag{6}$$

Applying the above, we get:

$$M_n = EI \frac{y_{n+1} - 2y_n + y_{n-1}}{(\Delta x)^2} \tag{7}$$

$$S = \frac{M_{n+1} - M_n}{\Delta x} \tag{8}$$

From 1):

$$M_{n+1} - 2M_n + M_{n-1} + \rho(\Delta x)^2 \left.\frac{d^2y}{dt^2}\right|_n + \beta(\Delta x)^2 \left.\frac{dy}{dt}\right|_n = 0 \qquad (9)$$

Before writing the complete set of difference equations for the N cells, the boundary conditions must be considered. Our cantilever beam has a free end at the right-hand extremity of the beam. This means zero shear and moment at beam end.

Let $M_{N+1} = M_N = 0$. From 9) we get:

for $n = N$:

$$M_{N-1} + \rho(\Delta x)^2 \left.\frac{d^2y}{dt^2}\right|_N + \beta(\Delta x)^2 \left.\frac{dy}{dt}\right|_N = 0 \qquad (10)$$

and for $n = N - 1$:

$$-2M_{N-1} + M_{N-2} + \rho(\Delta x)^2 \left.\frac{d^2y}{dt^2}\right|_{N-1} + \beta(\Delta x)^2 \left.\frac{dy}{dt}\right|_{N-1} = 0 \qquad (11)$$

proceeding along we get from 9):

$$\left.\frac{d^2y}{dt^2}\right|_n = \frac{1}{(\Delta x)^2\rho}(-M_{n+1} + 2M_n - M_{n-1}) - \frac{\beta}{\rho}\left.\frac{dy}{dt}\right|_n \qquad (12)$$

applicable until the left hand boundary is reached. Here, for $n = 0$, we assume:

$$M_c = T(t) \qquad \text{applied torque} \qquad (13)$$

and:

$$M_{-1} = y_{-1} = y_0 = 0 \qquad (14)$$

We can represent these equations by means of a Signal Flow Graph, which can help in writing the state equation of the discretized system. An example with N = 4 follows, with

its Signal Flow Graph in Fig. 2, where the following symbols have been adopted:

$$A = \frac{EI}{(\Delta x)^2} \qquad B = \frac{1}{(\Delta x)^2 \rho}$$

Notice that in our example the beam has been assumed of uniform mechanical construction, and notice also that viscous damping has been introduced into this model. While the damping of the usual materials is very low (almost negligible), local damping may be produced by independent feedback subsystems, and its effects may be investigated. With this configuration it is assumed to have uniform damping along the length of the beam, appearing concentrated at the points of the discrete model.

The state equation derived from the Signal Flow Graph model of figure 2 is:

$$\dot{\underline{x}}(t) = \begin{bmatrix} 0 & 0 & 0 & 0 & 1 & 0 & 0 & 0 \\ 0 & 0 & 0 & 0 & 0 & 1 & 0 & 0 \\ 0 & 0 & 0 & 0 & 0 & 0 & 1 & 0 \\ 0 & 0 & 0 & 0 & 0 & 0 & 0 & 1 \\ -6C & 4C & -C & 0 & -\beta/\rho & 0 & 0 & 0 \\ 4C & -6C & 4C & -C & 0 & -\beta/\rho & 0 & 0 \\ -C & 4C & -5C & 2C & 0 & 0 & -\beta/\rho & 0 \\ 0 & -C & 2C & -C & 0 & 0 & 0 & -\beta/\rho \end{bmatrix} \underline{x}(t) + \begin{bmatrix} 1 \\ 0 \\ 0 \\ 0 \\ 0 \\ 0 \\ 0 \\ 0 \end{bmatrix} u(t) \qquad (15)$$

where $C = AB = \dfrac{EI}{(\Delta x)^4 \rho}$

The beam here considered has the following

characteristics:

length = 2 meters

width = 20 mm

heigth = 2 mm

mass/unit length ρ = $108 \cdot 10^{-3}$ Kg/m (Aluminum)

Moment of Inertia I = $13.333 \cdot 10^{-12}$ m^4

Modulus of Elasticity E = $60 \cdot 10^{9}$ newtons/m^2

V. RESULTS

The state variable model was tested by inserting precalculated initial conditions corresponding to the lowest mode of the beam, and zero input. In addition, the damping was initially set to zero. It was expected that the beam oscillated at the lowest natural frequency.

The numerical result, instead, showed unexpected values of displacements and velocities, and a roughly periodic motion, with a period considerably longer than the theoretical one. The model was modified, by insertion of moderate damping, but the result were similar to the ones obtained without damping, and equally disappointing. The model was further modified, with the assumption of 8 sections on the beam (16 states). Zero damping was initially used, and moderate damping afterwards, again with results different from the expected ones!

Clearly, something is wrong. The state variable computer program has been used previously with excellent results, the

numerical values adopted for our model have been repeatedly checked, and no error has been discovered. The conclusion, at this point, is that more time is needed in order to obtain reasonable results.

VI. RECOMMENDATIONS

The whole model construction procedure should be reviewed and analyzed again. The reason why the present model does not work is well hidden, and finding it is beyond the time limit of this project, which was started pehaps too optimistically! But more work on the same general line of thought should finally give positive results.

After modelling is satisfactory, the problem of finding suitable control laws for different problems can be faced and hopefully solved.

REFERENCES

1. Athans M., "Toward a Practical Theory of Distributed Parameter Systems", (Correspondence), IEEE Transactions on Automatic Control, April 1970, pp. 245-247.

2. Takahashi Y., Rabins M.J., Auslander D.M., Control and Dynamic Systems, Reading, MA, Addison-Wesley, 1970.

3. Aziz A.K., Wingate J.W., Balas M.J., editors, Control Theory of Systems Governed by Partial Differential Equations, New York, Academic Press, 1977.

4. Ray W.H., Lainiotis,D.G., editors, Distributed Parameter Systems Identification, Estimation and Control, New York, Marcel Dekker, 1978.

5. Howe R.M., Haneman V.S., "Solution of Partial Differential Equations Using Electronic Differential Analyzer", Proceedings of the I.R.E., October 1953, pp. 1497-1508.

6. Balas M.J., "Feedback Control of Flexible Systems", IEEE Transactions on Automatic Control, August 1978, pp. 673-679.

7. Balas M.J., "Trends in Large Space Structure Control

Theory: Fondest Hopes, Wildest Dreams", IEEE Transactions on Automatic Control, June 1982, pp. 522-535.

8. Sridhar M.J., Auburn J.N., Lorell K.R., "Identification Experiment for Control of Flexible Structures", IEEE Control Systems Magazine, May 1985, pp. 29-35.

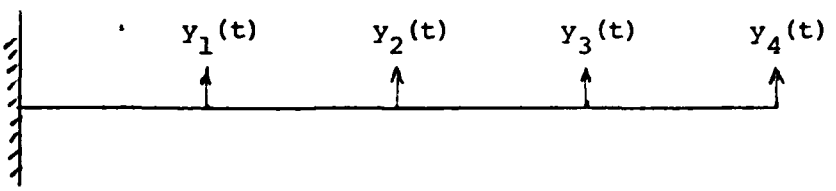

FIGURE 1: CANTILEVER BEAM

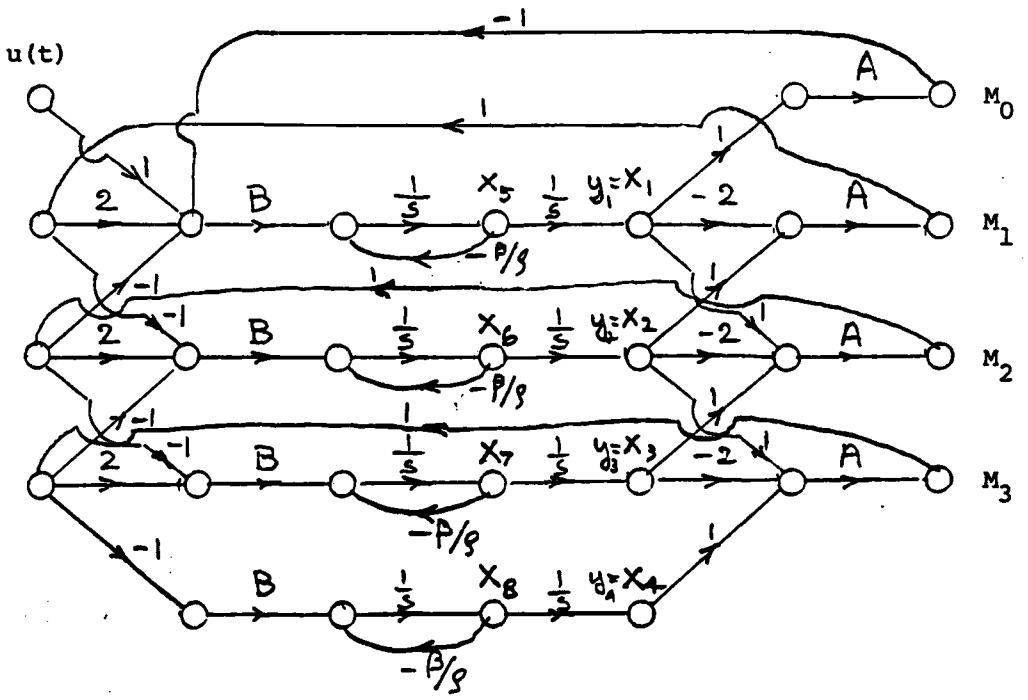

FIGURE 2: SIGNAL FLOW GRAPH MODEL OF CANTILEVER BEAM

1985 USAF-UES SUMMER FACULTY RESEARCH PROGRAM

GRADUATE STUDENT RESEARCH PROGRAM

Sponsored by the

AIR FORCE OFFICE OF SCIENTIFIC RESEARCH

Conducted by the

UNIVERSAL ENERGY SYSTEMS, INC.

FINAL REPORT

GAS EXCHANGE IN THE RABBIT USING HIGH FREQUENCY VENTILATION IN HIGH ALTITUDE

Prepared by	:	Dr.Mukul R. Banerjee and Yolman Salinas
Academic Rank	:	Professor and Medical Student
Department and University	:	Department of Physiology Meharry Medical College
Research Location	:	Crew Technology Division Brookes Air Force Base
USAF Research	:	Dr. Neel B. Ackerman, Jr.
Date	:	August 16, 1985
Contract No.	:	F49620-85-C-0013

GAS EXCHANGE IN THE RABBIT USING HIGH FREQUENCY VENTILATION IN HIGH ALTITUDE

by

Mukul R. Banerjee
and Yolman Salinas

ABSTRACT

The efficiency of a high frequency flow interruption technique in maintaining an adequate gas exchange in the rabbit was tested, first at ground level and then in a hypobaric chamber at 8,000 feet simulated altitude. This was immediately followed by retesting under ground level conditions. Four adult New Zealand White male rabbits were used. The anesthesized and intubated rabbits, injected with a muscle relaxant, were ventilated at 1,5, and 7 Hz with a minute ventilation of 1,2,3 liters per minute respectively. Data were collected for approximately one hour at each frequency. The parameters recorded were : systemic arterial pH, pCO2, HCO3, PO2, blood pressure, heart rate, proximal air way pressure, inspired and expired flow rates, inspired and expired volume, con centration of O2 and CO2 in mixed expired air. The high-frequency ventilation technique utilized did not adversely affect the arterial PCO2 of rabbits at high altitude. Also, the arterial-alveolar PO2 ratio showed an improvement at high altitude with high-frequency ventilation. We conclude that high-frequency ventilation maintained an adequate pulmonary gas exchange in rabbits at high altitude.

ACKNOWLEDGEMENTS

The author would like to thank the Air Force Systems Command, the Air Force Office of Scientific Research and the Universal Energy Systems, Inc. for providing him with a Research Fellowship which made this work possible.

The author would also like to express his appreciation for the generous support and guidance of Dr. Neel B. Ackerman, Jr..

Thanks are due to Mr. Yolman Salinas, medical student of Meharry Medical College for providing valuable assistance throughout this project.

The active cooperation of the personnel in Crew Technology Division is gratefully acknowledged with particular reference to TSgt Ernest Roy for his technical help.

I. INTRODUCTION :

It has recently been demonstrated that an adequate gas exchange in the lungs can be maintained by high frequency ventilation with tidal volumes close to the dead space volumes(4,5,6,7). This technique appears to minimize the injury to the lung tissue associated with conventional mechanical ventilation. High frequency ventilation falls into three somewhat arbitrary categories : high frequency positive pressure ventilation, high frequency jet ventilation or high frequency flow interruption, and high frequency oscillatory ventilation. Of these three techniques, high frequency oscillatory ventjlation has gained widespread attention(2). However, this technique does not appear to be superior to other techniques(1). Fletcher et al(3), have described a high frequency flow interruption technique which prevents an admixture of inspired and expired gases. It allows collection of expired gas for an accurate measurement of volume and gas composition.

Last year under a similar summer faculty research program we developed and modified Fletcher's high frequency ventilation technique. The technique was satisfactory in ventilating a mechanical lung model. By introducing a compliant chamber in the inspiratory line we were able to eliminate the initial pressure spike developed in the inspiratory line during the expiratory phase of the breathing cycle. The inspiratory flow waveform became essentially frequency independent. As the performance of the HFV system in hypobaric conditions is not known, the follow-up work included an evaluation

of the performance of the technique in live animals both at ground level and at high altitude.

II OBJECTIVES

The main objective in this work is to evaluate the efficiency of the high frequency flow interruption technique in maintaining an adequate pulmonary gas exchange in rabbits under hypobaric conditions. A simulated altitude of 8,000 feet was chosen because it is the common cabin pressure in most military aircrafts. We would also like to compare the performance of the technique on the same animal both at ground level and at high altitude with the mean proximal airway pressure not exceeding 10 cmH20.

III. METHODOLOGY

Four New Zealand White male rabbits weighing between 3.3 to 3.7 kg were used. The animals were fasted overnight. The ventral neck and groin areas of the animal were shaved following Ketamine anesthesia [50 mg/kg, i.m.]. Prior to the insertion of a cuffed endotracheal tube, 4 mm i.d., the rabbit was injected intravenously with sodium pentobarbital, 15 mg/kg into the lateral vein of the ear. The dose was progressively increased, as needed, to abolish the foot-pinch reflex. An angio-catheter of an appropriate size was inserted into the right femoral artery and positioned percutaneously for the collection of blood sample and the measurement of blood pressure. Blood gas was analyzed immediately following collection by the use of a Corning Model 158 pH/Blood Gas Analyzer. Blood pressure was measured by the use of a Gould P23ID pressure transducer connected to the arterial line and filled with Lactated Ringer's solution.

The high frequency ventilation technique used is illustrated below in block diagrams:

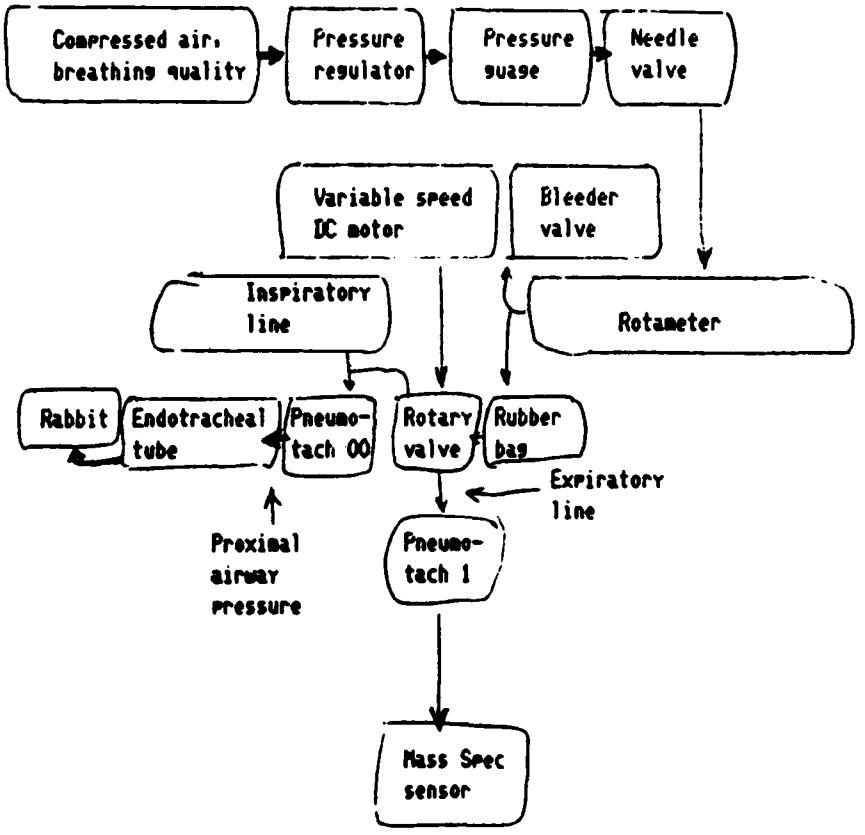

Compressed air of breathing quality was provided to the system being controlled by the pressure regulator and monitored by the pressure guage. Air flow rates were set by the needle valve being approximated by the rotameter. The bleeder valve regulated the airway pressure developed in the system. The rubber bag prevented the initial rise in inspiratory pressure during the expiratory phase of the breathing cycle.

The opening in the rotary valve to the endotracheal tube alternated between inspiratory and expiratory lumes with an I/E duration of 1. The inspiratory flow was determined by using a Fleisch pneumotachograph #00 and a Validyne MP 45-1 differential pressure transducer system. Expiratory flow was determined by using a Fleisch pneumotachograph #1 and a Validyne MP 45-14 differential pressure transducer system. The response of the pneumotachographs was linear and identical upto a flow rate of 5 liters per minute. Above this flow rate, the response of the pneumotachograph #00 was non-linear. The inspiratory and expiratory volumes were determined by the electrical integration of the flow signals. Close agreement was obtained with the volumes recorded simultaneously by a spirometer connected at the end of the expiratory tubing upto a frequency of 10 Hz.

The sensor of the Mass Spectrometer (Perkin Elmer 1100 Medical Gas Analyzer) was placed inside the expiratory tubing, approximately two feet away from the expiratory port of the rotary valve. The site was suitable for the measurement of the concentration of oxygen and carbon dioxide in the mixed expired air.

Airway pressure, inspiratory and expiratory flow rates and volumes, blood pressure, expired concentrations of oxygen and carbon dioxide were continuously recorded by the use of an eight-channel strip-chart recorder (Gould 2800S).

The blood gas status of the anesthetized and intubated rabbit was determined before connecting the endotracheal tube to the high-frequency ventilator. With the rabbit connected to the ventilator, spontaneous respiratory movements were abolished by the injection of pancuronium bromide, 0.2 mg/kg.

The ventilator was initially set for a breathing frequency of 1 Hz and an air flow rate of 1 liter per minute. Arterial blood samples, 0.5 ml each, were collected after 20 minute ventilation at this setting followed by another collection after an interval of 10 minutes. Following the collection of blood samples each time, the arterial line was flushed with 5 ml Lactated Ringer's Inj. USP (Abbott Laboratories). Ventilator settings were then changed to 5 Hz and 2 liters per minute. Blood samples were collected after 10 and 20 minutes. Next, ventilator settings were changed to 7 Hz and 3 liters per minute. Blood collection was made using the same schedule as before. The rabbit was then exposed to a simulated altitude of 8,000 feet in an altitude chamber. After 20 minute exposure to the hypobaric condition, blood samples were collected using the schedule mentioned earlier. The ventilator settings were subsequently changed to 5 Hz and 2 liters per minute and finally to 1 Hz and 1 liter per minute. After returning to the ground level, blood gas measurements were again made using a similar schedule with the sequence being 1 Hz and 1 liter per minute, 5 Hz and 2 liters per minute and 7 Hz and 3 liters per minute.

IV. RESULTS

Typical tracings of the different physiological parameters recorded at frequencies of 1, 5 and 7 Hz are shown in Figures 1, 2 and 3 respectively (see appendix B). It is evident that the inspiratory and expiratory flows were independent of each other with respect to time. Also, the inspiratory and expiratory minute volumes were similar. Thus, there was no leak allowing gas to pass directly from the inspiratory line to the expiratory line of the ventilator. Introducing a compliant rubber bag between the needle valve and the rotary valve made the airway pressure smooth, without any sharp changes, particularly at low frequency.

Figures 4 and 5 show the changes in air flow rates at high altitude due to air density (see appendix B). Ventilator settings were adjusted after ascending to 8,000 feet and also after descending from 8,000 feet, so that ventilatory flow rates were identical with those at ground level before any collection of data.

The data collected on different physiological parameters are sumarized in Tables 1-3 (see appendix B). Carbon dioxide output and oxygen uptake were calculated from their respective concentrations in inspired and expired air and the minute volume. Respiratory exchange ratio was calculated by dividing carbon dioxide output by oxygen uptake. Alveolar oxygen tension was calculated by using the alveolar gas equation, taking into account the barometric pressure at the ground level on different days and at 8,000 feet.

The data were analyzed by repeated measures of analysis of variance. The results of the analysis are shown below with their individual probability factors. A dash indicates P> .05.

TABLE 4. Results of the analysis of variance.

	BF/ALT Interaction	Breathing Frequency	Altitude Level
pH	.3502-	.3764-	.0473
PCO2	.8051-	.1809-	.6959-
HCO3	.4696-	.0073	.0101
PO2	.1872-	.0678-	.0001
Paw	.0445	.0001-	.0016-
BP	.2008-	.2524-	.9126-
HR	.0554-	.1256-	.0016
VCO2	.0101	.0040-	.0001-
VO2	.0001	.1967-	.0001-
R	.0014	.0075-	.0007-
PAO2	.1655-	.0345	.0001
a/A	.5100-	.1322-	.0014

pH, PCO2, HCO3, PO2 — are of arterial blood, Paw — proximal mean airway pressure, BP — mean systemic arterial blood pressure, VCO2 — carbon dioxide output, VO2 — oxygen uptake, R — respiratory exchange ratio, PAO2 — alveolar PO2, a/A — ratio of arterial over alveolar PO2.

Physiological responses showing interaction between breathing frequency and altitude level were plotted in figures 6-9 (see appendix B). In figure 6, it is seen that the mean airway pressure was lower at high altitude. This can be explained by the low density of air requiring less driving pressure for the same ventilatory flow rates, particularly at high frequency. Figures 7 and 8 show that both carbon dioxide output and oxygen intake by the rabbit were greater at high altitudes which decreased with some overshoot upon return to ground. This probably does not represent a change in metabolic rate by the animal but a change in the body gas stores. Figure 9 (see appendix B) is a reflection of previous two diagrams. It shows that at 1 Hz , the respiratory exchange ratio increased at high altitude which increased even further upon return to ground level. These values at the end of the thirty minute time period were

greater than the initial values at the ground level.

Duncan's multiple range test was utilized to test the individual means when the altitude level - breathing frequency interaction was not significant below the 0.05 level.

Arterial pH at high altitude was significantly higher than the pH upon return to the ground level. Similarly, arterial pH initially at ground level was significantly more alkaline than the pH upon return to the ground level from 8,000 feet. This is a reflection of a similar change in arterial blood bicarbonate. Blood PCO2 was not influenced significantly by the altitude level. The rabbit was able to maintain its arterial PCO2 uninfluenced by either the altitude level or the frequency of breathing, tested in this project.

Arterial PO2, on the otherhand, was sigficantly lower at high altitude than at ground level. This is due to the lower barometric pressure at 8,000 feet. Alveolar PO2, calculated by alveolar gas equation using appropriate barometric pressure showed a similar change. The ratio between arterial PO2 over alveolar PO2 was, in fact, significantly improved at high altitude. The improved response continued for thirty minutes even after return to the ground level.

While the mean arterial blood pressure was uninfluenced by either the level of altitude or the breathing frequency, the heart rate was significantly higher at ground level than at high altitude. Pre-altitude values were not restored wilthin thirty minutes of return to the ground level.

V. CONCLUSIONS AND RECOMMENDATIONS.

The results show that the high-frequency flow interruption technique utilized in this project with a breathing frequency as high as 7 Hz did not adversely affect the arterial PCO2 of rabbits at a simulated altitude of 8,000 feet. Also, the arterial-alveolar PO2 ratio showed an improvement at high altitude with high-frequency ventilation.

However, complete data were obtained on four rabbits only during this summer period. Thus, the results and their analysis are good for suggesting trends only. We were, in fact, surprised to see statistical significance among data even with such a small number of animals.

For greater reliability of the results obtained, the experiment obviously needs to be repeated with a larger number of animals. The experiment should be extended with breathing frequencies greater than seven times the normal breathing rate of the animal tested here. Also, the performance of the high-frequency ventilation technique on pulmonary gas exchange at altitude greater than 8,000 feet needs to be evaluated.

REFERENCES

1. Ackerman, N.B. and R.A. DeLemos. High Frequency Ventilation. in Current Problems in Pediatrics, ed. L. Barness. Year Book Medical Publishers, 1984, pp 259-293.

2. Chang, H.K. Mechanisms of Gas Transport during Ventilation by High-Frequency Oscillation. J. Appl. Physiol.: Respirat. Environ. Exercise Physol., 56: 553-563, 1984.

3. Fletcher, P.R., M.A. Epstein and R.A. Epstein. A New Ventilator for Physiologic Studies during High-Frequency Ventilation.. Resp. Physiol., 47: 21-38, 1982.

4. Gillespie, D.J. High-Frequency Ventilation. A New Concept in Mechanical Ventilation. Mayo Clin. Proc., 58: 187-196, 1983.

5. Kamm, R.D., A.S. Slutsky and J.M. Drazen. High-Frequency Ventilation. CRC Rev. Biomed. Engg., 9: 347-379, 1983.

6. Quan, S.F., J.C. Calkins, T.J. Conahan and C.K. Waterson. High-Frequency Ventilation—a Promising New Method of Ventilation. Heart and Lung, 12: 152-155, 1983.

7. Slutsky, A.S., R. Brown, J. Lehr, T. Rossing and J.M. Drazen. High-Frequency Ventilation : a Promising New Approach to Mechanical Ventilation. Med. Instr., 15: 229-233, 1981.

APPENDIX B

TABLE 1. Mean values and standard deviations of data recorded at a frequency of 1 Hz.

	GROUND		ALTITUDE		BACK TO GROUND	
pH	7.45	.08	7.44	.03	7.41	.05
PCO2	31.73	7.70	30.15	1.28	29.98	3.41
HCO3	21.30	2.05	20.43	.55	19.00	1.33
PO2	88.88	7.65	82.00	7.02	124.33	6.03
Paw	3.60	.46	3.80	.28	4.15	.44
BP	102.25	11.33	116.00	19.25	114.00	17.04
HR	281.25	28.39	235.00	10.00	232.50	15.00
VCO2	11.17	.75	14.93	1.98	10.90	2.00
VO2	14.93	1.64	17.38	1.94	11.38	1.19
R	.75	.05	.86	.05	.96	.11
PAO2	103.74	11.84	73.34	1.56	114.65	5.68
a/A	.86	.09	1.12	.08	1.09	.05

---

pH, PCO2, HCO3, PO2 — are of arterial blood, Paw — proximal mean airway pressure, BP — mean systemic arterial blood pressure, VCO2 — carbon dioxide output, VO2 — oxygen uptake, R — respiratory exchange ratio, PAO2 — alveolar PO2, a/A — ratio of arterial over alveolar PO2.

TABLE 2. Mean values and standard deviations of data recorded at a frequency of 5 Hz.

	GROUND		ALTITUDE		BACK TO GROUND	
pH	7.46	.04	7.35	.06	7.43	.04
PCO2	32.08	1.82	33.53	1.79	32.55	2.57
HCO3	22.68	1.07	18.68	2.03	21.30	.68
PO2	90.30	7.83	121.88	8.80	73.65	1.16
Paw	4.25	.50	4.50	.42	4.05	.25
BP	113.00	19.97	115.00	21.69	112.00	17.96
HR	270.00	00.00	210.00	24.49	230.00	20.00
VCO2	12.00	1.12	10.12	.81	16.52	1.27
VO2	13.60	1.72	9.55	.57	19.65	1.79
R	.89	.03	1.06	.09	.84	.04
PAO2	110.08	3.18	114.60	.03	69.80	4.21
a/A	.82	3.09	1.06	.04	1.06	.06

TABLE 3. Mean values and standard deviations of data recorded at a frequency of 7 Hz.

	GROUND		ALTITUDE		BACK TO GROUND	
pH	7.46	.05	7.45	.03	7.38	.04
PCO2	32.08	2.94	29.18	2.25	32.23	1.85
HCO3	22.68	1.37	20.38	1.04	19.23	.98
PO2	90.30	4.75	79.20	6.27	123.30	10.10
Paw	4.25	.50	5.68	.22	6.40	.40
BP	113.00	15.78	116.50	19.82	118.00	26.15
HR	270.00	17.32	255.00	17.32	220.00	17.32
VCO2	12.00	.49	19.67	.53	11.79	1.09
VO2	13.60	1.79	22.74	.90	9.60	.00
R	.89	.13	.87	.05	1.23	.12
PAO2	110.08	4.79	74.86	.14	120.10	1.22
a/A	.82	.07	1.06	.06	1.03	.07

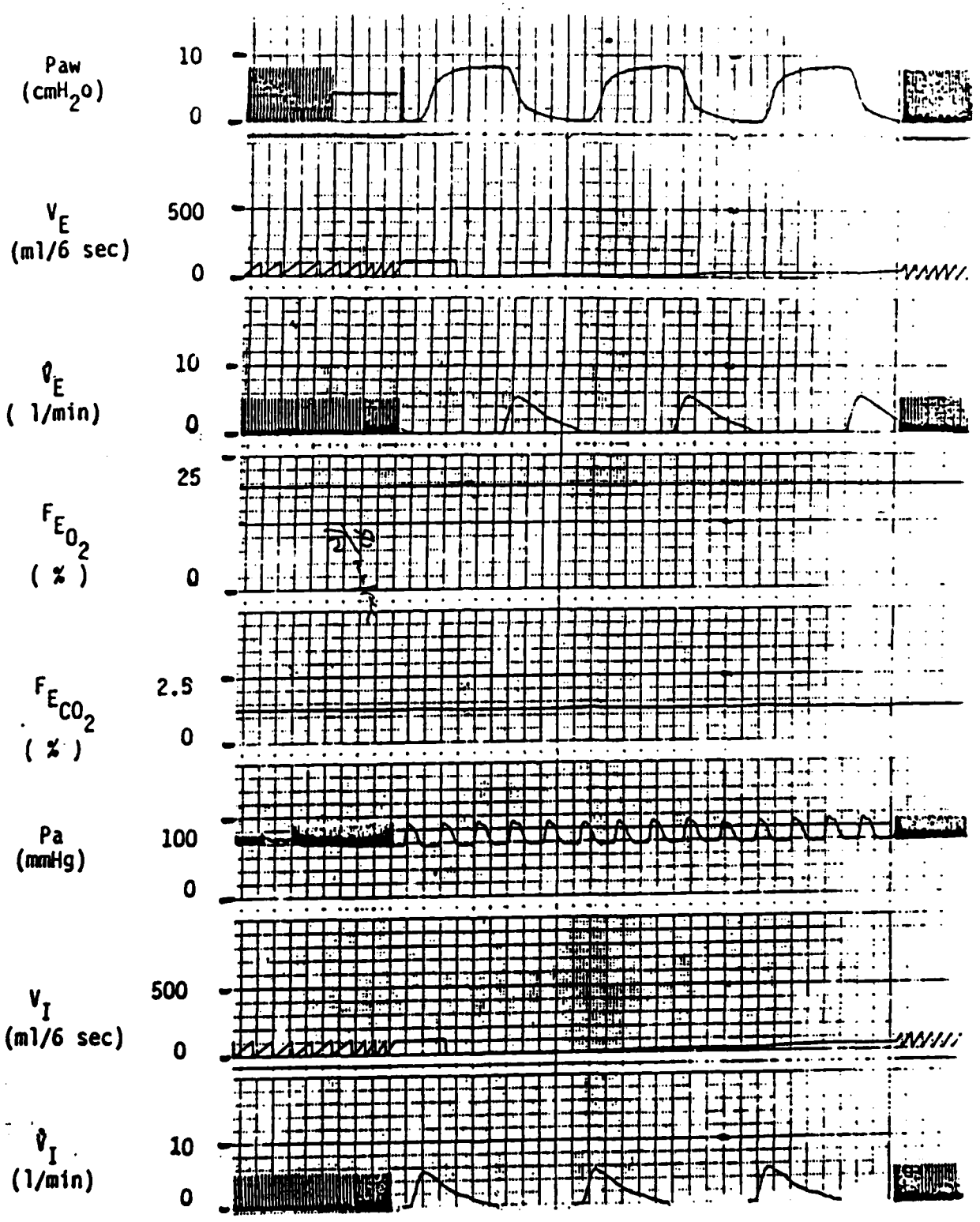

Figure 1. Airway pressure (Paw), expiratory volume (V_E), expiratory flow ($\dot{V}_E$), concentration of oxygen in expired air ($F_{E_{O_2}}$), concentration of carbon dioxide in expired air ($F_{E_{CO_2}}$), arterial pressure (Pa), inspiratory volume (V_I), and inspiratory flow ($\dot{V}_I$) recorded at 1 Hz. Paper speed is 50 mm/second.

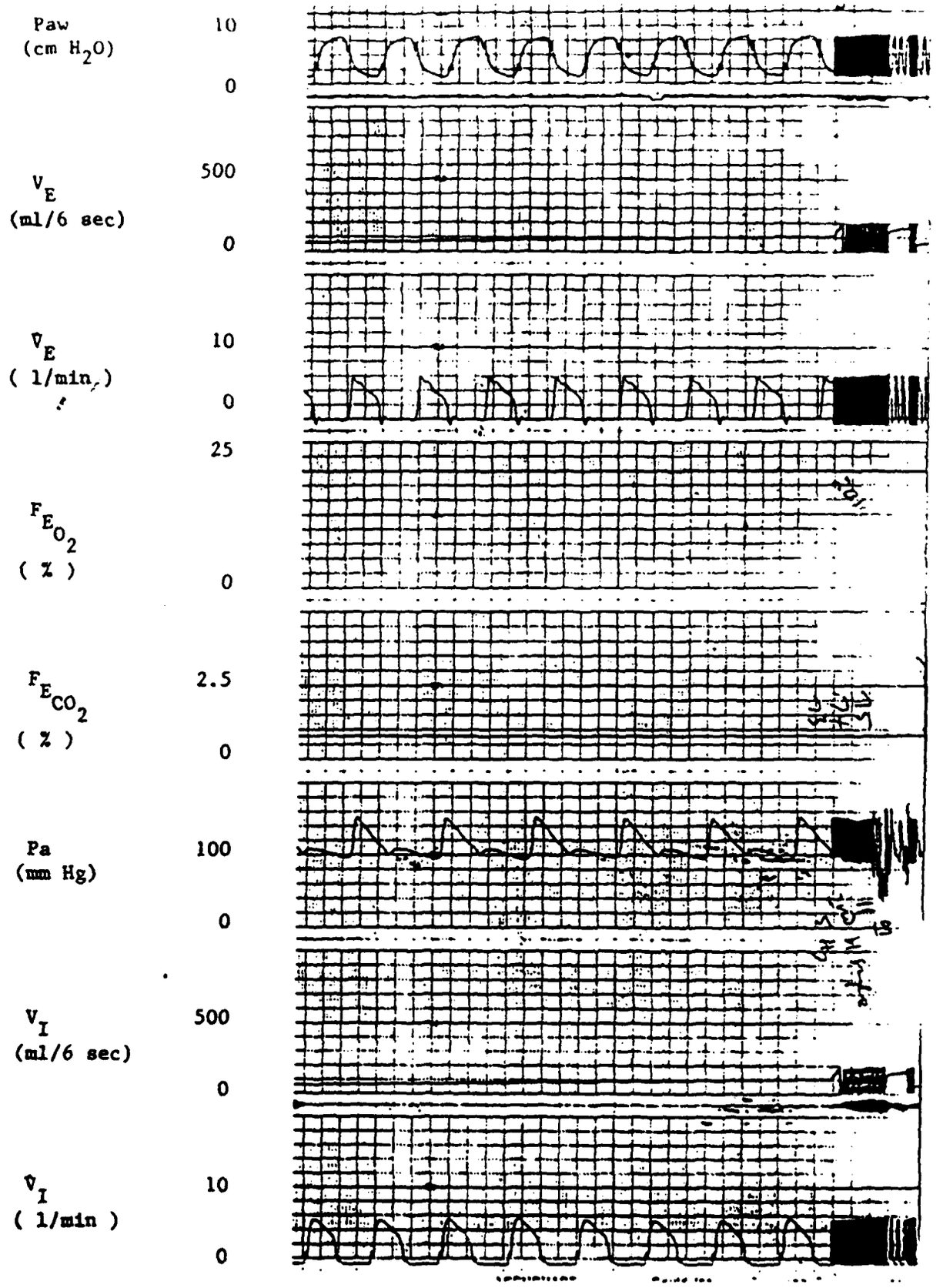

Figure 2. Data recorded at 5 Hz.
Paper speed is 100 mm/sec.

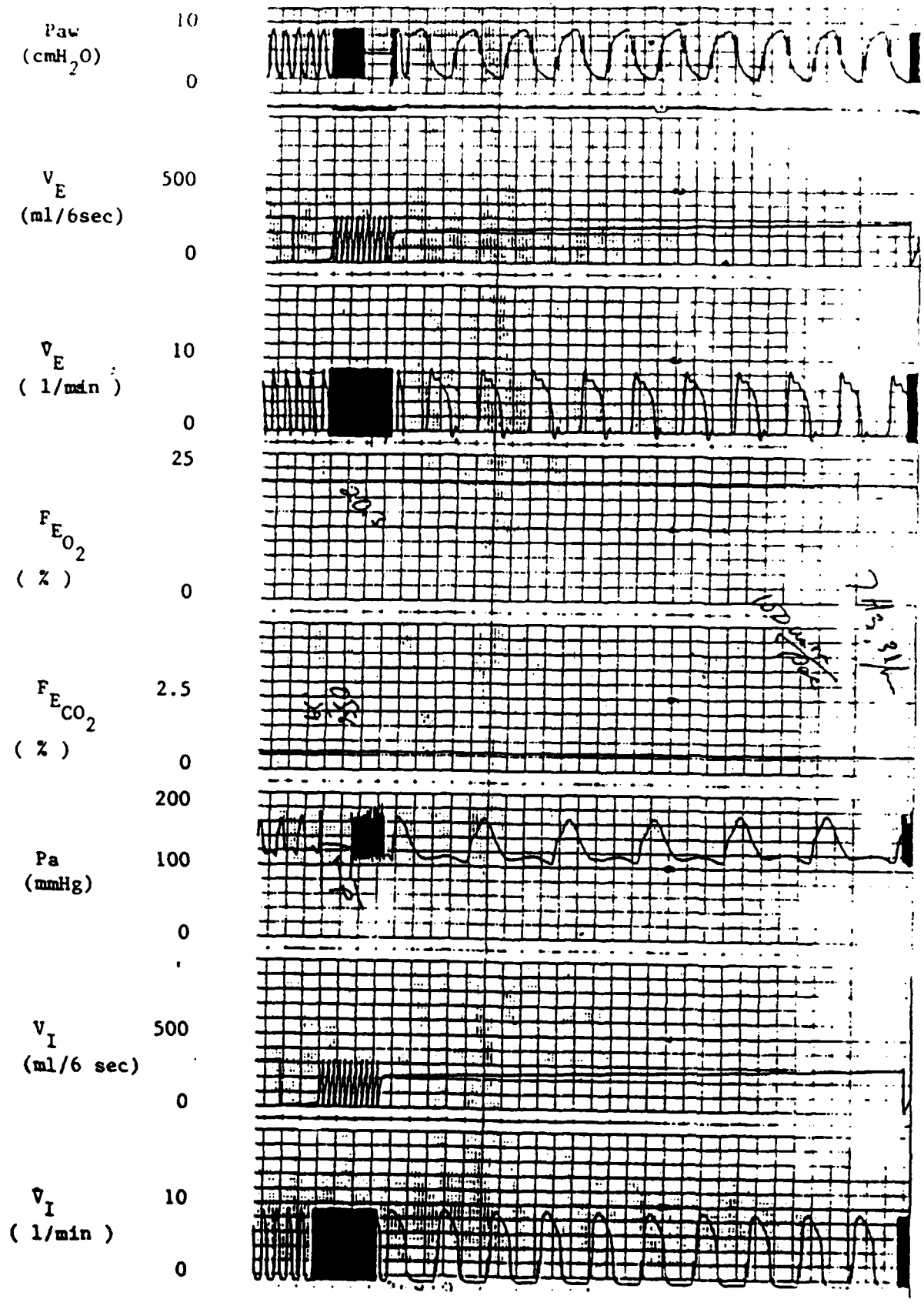

Figure 3. Data recorded at 7 Hz.
Paper speed is 100 mm/sec.

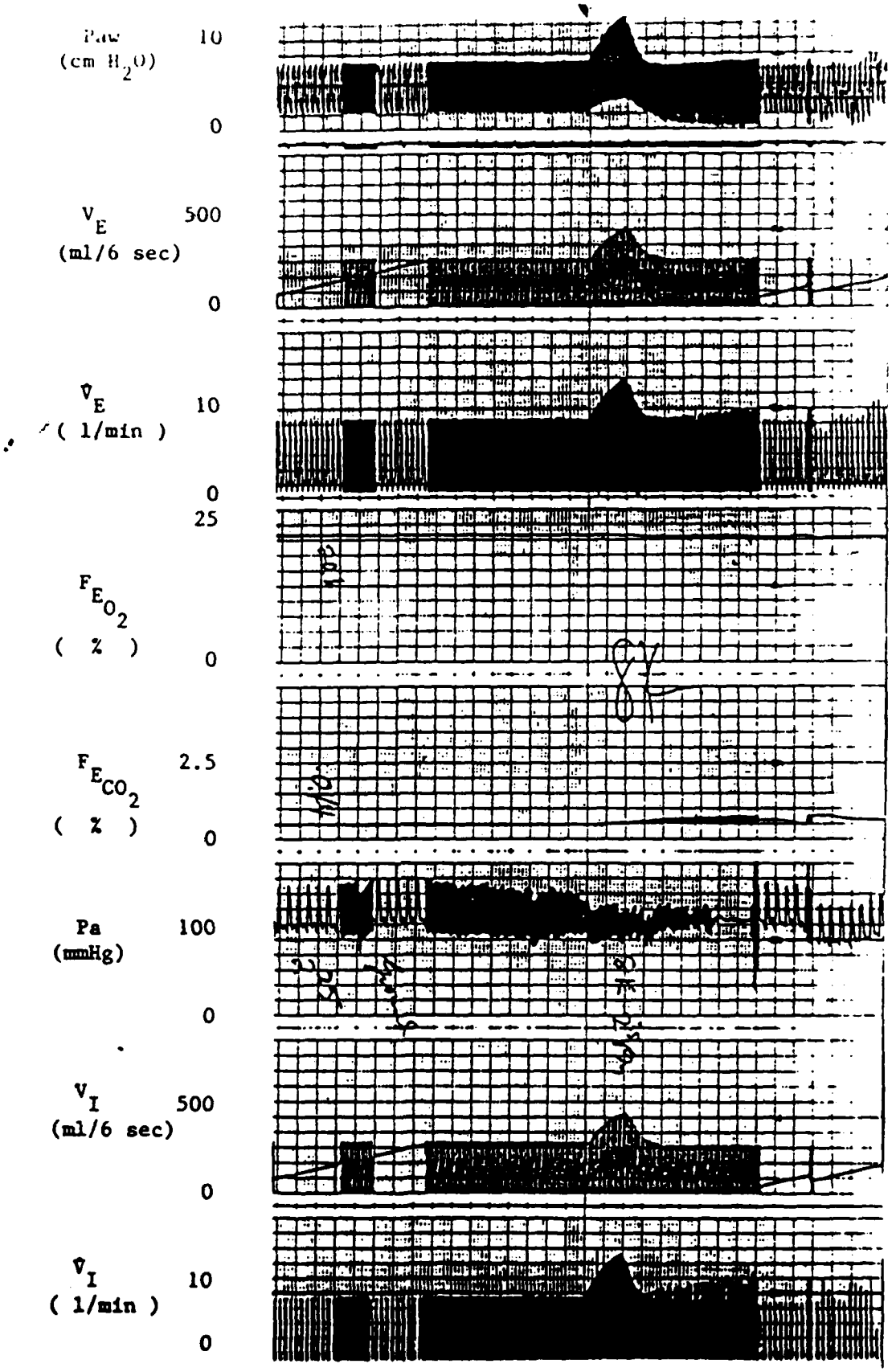

Figure 4. Change in airflow rate during ascent to 8,000 feet. Arrow indicates start of ascent. Data recorded at 7 Hz.

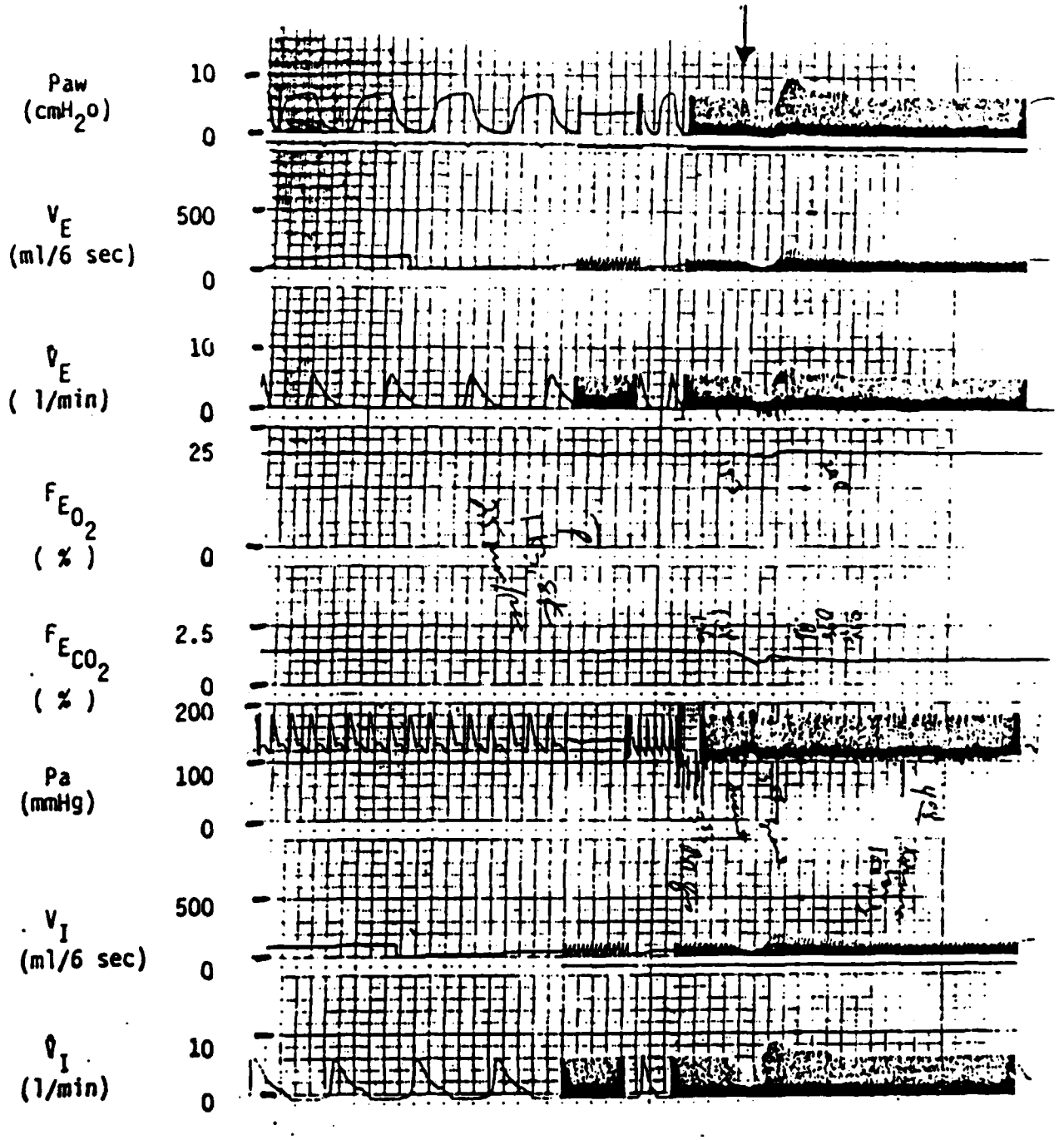

Figure 5. Change in airflow rate during descent back to ground. Arrow indicates start of descent. Data recorded at 1 Hz.

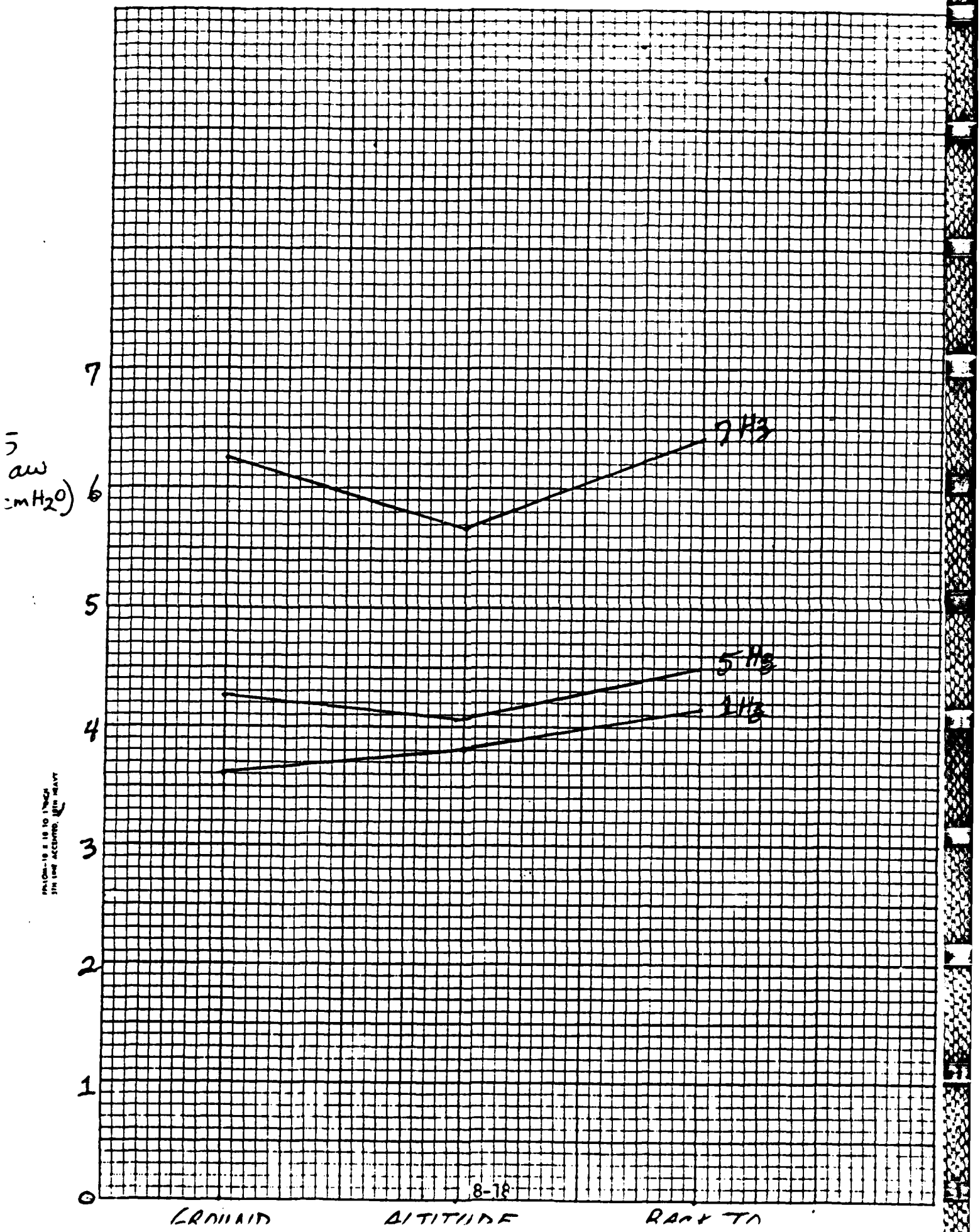
7
6
5
4
3
2
1
0
2 Hz
5 Hz
2 Hz
8-18

Figure 7

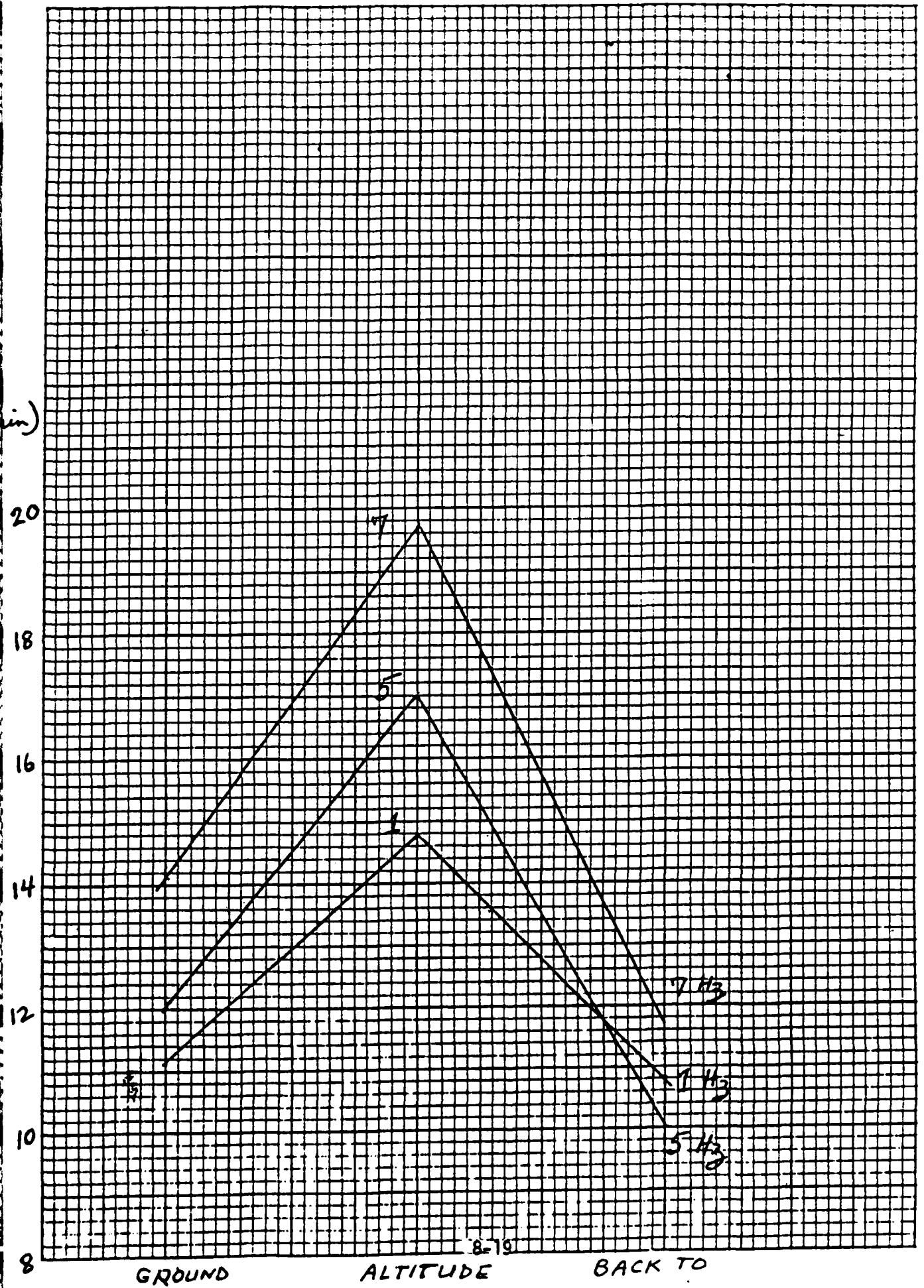
in)
20
18
16
14
12
10
8
7
5
1
7 Hz
1 Hz
5 Hz
8-19
GROUND
ALTITUDE
BACK TO

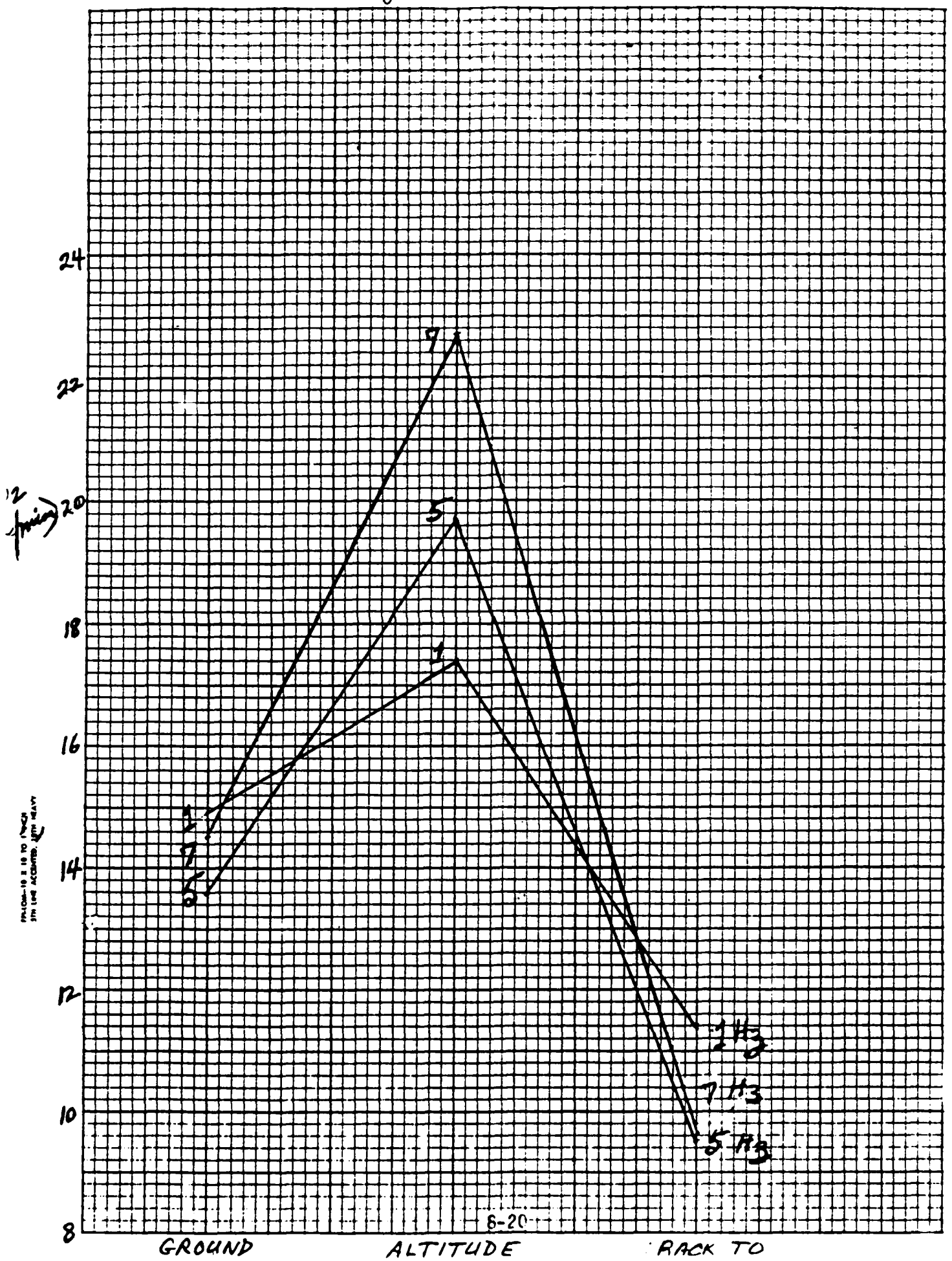
24
22
20
18
16
14
12
10
8
9
5
1
7
5
1 H3
7 H3
5 H3
GROUND
ALTITUDE
RACK TO

Figure 1

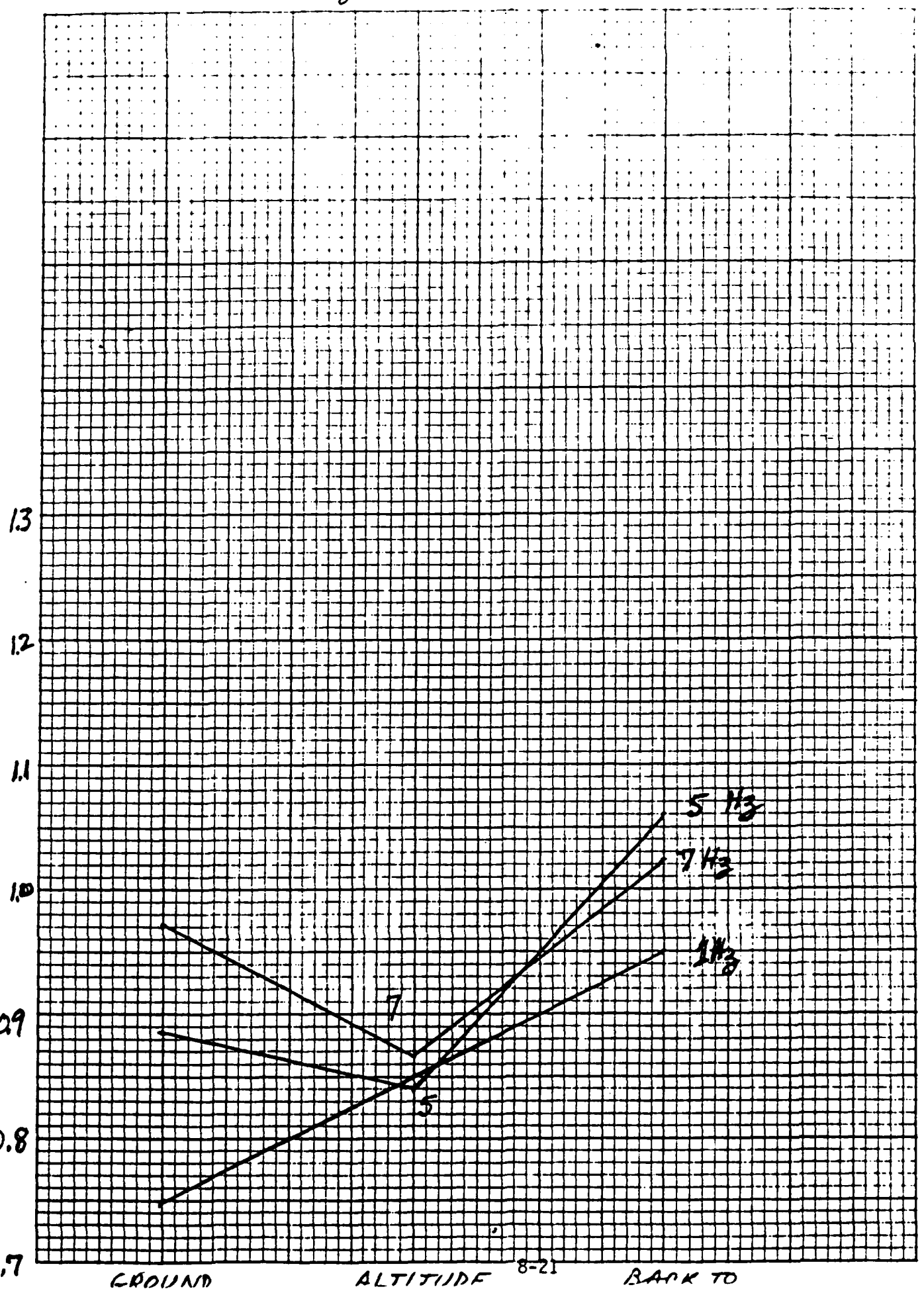

1985 USAF-UES SUMMER FACULTY RESEARCH PROGRAM/

GRADUATE STUDENT SUMMER SUPPORT PROGRAM

Sponsored by the

AIR FORCE OFFICE OF SCIENTIFIC RESEARCH

Conducted by the

UNIVERSAL ENERGY SYSTEMS, INC.

FINAL REPORT

COMPUTER AUTOMATED, TEST MIRROR REGISTRATION SYSTEM FOR THE RING LASER GYRO

Prepared by:	Dr. Rex Berney and	John Taranto
Academic Rank:	Associate Professor	Graduate Student
Department and University:	Physics Department University of Dayton	
Research Location:	Air Force Wright Avionics Laboratories Ring Laser Gyro Laboratory	
USAF Research Contact:	Dr. Kent Stowell	

Date: 13-AUG-85

Contract No.: F49620-85-C-0013

COMPUTER AUTOMATED, TEST MIRROR REGISTRATION SYSTEM FOR THE RING LASER GYRO

by

Rex Berney

and

John Taranto

ABSTRACT

The goal of the project was to develop an automatic optical element positioner for the ring laser gyro experiment. Various schemes for using a CCD line scan camera for precision positioning of optical elements were investigated. It was found that one micron precision repositioning of an optical element could be achieved using scattered laser light and appropriate optics. An interface for the CCD line scan camera to the LSI-11/23 computer was designed and built, and the controlling software, both FORTRAN and MACRO code, was written.

ACKNOWLEDGEMENTS

The authors would like to express their appreciation to the Ring Laser Gyro Laboratory at the Air Force Wright Avionics Laboratories, the Air Force Systems Command, and the Air Force Office of Scientific Research for providing the opportunity to engage in this research project and to interact with the Air Force scientists at the Wright-Patterson Air Force Base. The authors would also like to express their appreciation to Dr. Kent Stowell, Jim Grote, and Samual Adams for their assistance and hospitality during this ten week program.

I. Introduction

The ring laser gyro has become an important part of inertial guidance systems with both military and commercial applications. Traditional mechanical inertial guidance systems have many moving parts, are quite heavy, need significant electrical power, and require frequent maintenance. On the other hand, the ring laser gyro has no moving parts, requires little electrical power, is quite compact, and requires no maintenance.[1]

In addition to navigational systems, the ring laser gyro can be used to study basic physical phenomena. Proposed studies include an optical test of metric gravitation theories from general relativity.[2]

In a two-mode ring laser system, small amounts of the two circulating laser beams are mixed. The resulting beat frequency is linearly proportional to the rotation rate of the ring laser in the inertial reference frame. For small rotation rates this beat frequency will go to zero, which is called mode locking (see Figure 1). This non-linear behavior is due to mirror imperfections causing backscattering of waves from one mode into the other mode. Current concern for improved mirror surfacing techniques and the mode locking behavior associated with the ring laser gyro allows the gyro system to be used for analyzing mirror

surface quality in relation to the precision of the ring laser gyro.

If the gyro system is to be used to analyze mirror surface quality, a system for precision placement of the test mirror element is necessary. This will allow the mirror to be removed from the system for further surface treatment and then to be precisely repositioned in the ring laser system for further analysis. With this concept in mind the Ring Laser Gyro Lab purchased a Fairchild line scan camera and subsystem and a DRV11-J parallel interface board. Our project was to utilize these components and develop a test mirror registration system for the ring laser gyro experiment. This project was partitioned into four parts: optical development, computer interfacing, software, and system integration. These four areas will be discussed in detail in sections III through VI.

The nature of this project allowed us to utilize our skills in computer interfacing and optical design. Dr. Berney has been involved with computer interfacing for several years with the NSF Chautauqua Program and has also had computer interfacing and optical design experience as an advanced lab instructor at the University of Dayton. John Taranto has experience in optical design and computer interfacing through his undergraduate degree at the University of Dayton.

II. OBJECTIVES

The goals and objectives initially established for this program were unaltered during the course of the program. The goals and objectives were to investigate several schemes for accurate registration of the test optical mirror associated with the ring laser gyro experiment in the Avioncs Laboratory at Wright-Patterson Air Force Base. This was to involve computer interfacing to a linear array charge coupled device (CCD) camera and developing programs and proceedures for using the CCD camera for an alignment instrument of the test mirrors.

III. OPTICAL DEVELOPMENT

The optical development required the familiarization of the line scan camera and its limitations. The Fairchild 1500C line scan camera has a 2048 element linear array CCD (charge coupled device). Each element, known as a pixel, is a square 13 microns on edge and the pixels are 13 microns on center. Therefore, the area of the detector array is 2.66 cm by 13 microns.

The CCD is illuminated with light and each pixel builds up some amount of charge proportional to the incident light intensity. The charges of the CCD are sequentially read out by the Fairchild 1320 CCD camera control unit. The

resulting line scan is transferred to the pixel locator accessory.

The pixel locator takes the analog voltage of each pixel and compares it with an adjustable DC reference voltage. The pixel locator records the number of times the pixel voltage crosses the DC reference voltage and the pixel number associated with these transitions. The pixel locator also records whether the transition was from high to low or from low to high; this is known as the transition polarity. This information is stored in FIFO (First In First Out) memory in the pixel locator. The polarity is stored as a TTL high if the transition is from low to high and as a TTL low if the transition is from high to low. Two adjacent pixels must be above the reference voltage in order for a high to low transition to be recorded. Single pixel transitions are counted and their location are recorded and their polarity is stored as a TTL high. This last statement contradicts the operating instructions for the pixel locator, but is the way the pixel locator operated in the laboratory[3].

The important considerations are: 1.) The pixel locator is a binary device. It can only return information relative to a reference intensity. This means trying to map features of an optical element would be difficult. 2.) The CCD array pixels are spaced on 13 micron centers. Thus, a

magnification of ten of the test mirror elements is needed to achieve one micron resolution. Resolution better than one micron is not necessary because of the mechanical limits of the stages. 3.) The final system should be under computer control. The repositioning of an optical element should only require replacing the element in the holder and running a computer program to achieve the precise repositioning.

There seems to be little or no literature on the use of a CCD line scan camera and computer interface for precision registration of optical elements. The robotics, computer, and engineering literature is concerned more with pattern recognition than with positioning.

The test mirror elements we are using have cylindrical symmetry, requiring a mark of some sort on the elements edge or surface. We tried a scribed line on the edge, a line on the surface, and a dot on the surface. For illumination we tried existing light, a bright white light source, and laser light. The three requirements listed above could only be met with laser illumination and the scribed dot.

Only laser light, focused to a line, scattering off the scribed dot gave us a signal which could be recognized from the computer in a repeatable fashion. The limiting factor was the pixel locator. The scribed dot illuminated in this fashion gives a signal above any background signal.

The final optical design is shown in Figure 2. The focal lengths and sizes of the required lenses are given in the Recommendations section. The laser, positive cylindrical lens, and spherical concave lens make a sharply focused line about 1.2 cm long. The light collecting optics, and the two spherical convex lenses give a magnification of about ten. When a scribed dot passes through the laser line, enough light is scattered to make a signal at the CCD array well above the background light signal. The signal out of the pixel locator is then a single sharp peak about three or four pixels wide.

IV. Computer Interfacing

The entire ring laser gyro experiment will be controlled by an LSI-11/23 based computer from Cambridge Digital. The operating system is the RSX-11M multiuser system. The interfacing of the computer to the line scan camera is through a DRV11-J interfacing board built by Digital Equipment Corporation.

The DRV11-J has four word size (sixteen bit) bi-directional ports. The pixel locator requires three binary signals to control the camera operation and has twenty-four binary data lines. This forced us to use three of the ports since each individual port cannot be part input and part output.

The four ports on the DRV11-J are labeled A, B, C and D. We used port A as an input port for the twelve address lines from the pixel locator and for four other pixel locator output lines. Port B is also an input port and has the eight binary lines representing the number of transitions in one scan of the camera. The three control lines required by the camera are connected to port C of the DRV11-J. Thus, ports A and B must be input ports and port C must be an output port. Table 1 shows the connection of the DRV11-J connector J1 (it has both ports A and B) and J2 (it has ports C and D) to the pixel locator connector J3. The numbers in the various columns represent the pin numbers for the connection of J1 or J2 to J3. For example, port A bit 0 of the DRV11-J is to be connected to address line 0 of the pixel locator. This is done by connecting pin 37 of J1 to pin 21 of J3 (see Table 1.)

The connectors on the DRV11-J (J1 and J2) are fifty pin headers and the pixel locator connector is a female DB-50 plug. Our interface cable has a DB-50 male connector on one end and socket headers of 50 pins (for J1) and 20 pins (for J2) on the other end. The ribbon cable has fifty wires and is approximately 20 feet long.

V. Software

The FORTRAN software must control the DRV11-J interface board which in turn will control the pixel locator control lines. The flow of information between the computer and camera via the pixel locator is determined by the state of three binary lines: READ*, RUN*, and CMCO (the * indicates an active low signal.) These three signals are input into the pixel locator to control the camera operation. Port C bits 0, 1, and 2 of the DRV11-J are used to control the pixel locator.

Figure 3 shows the key features of the camera operation by the three control lines. In general, the RUN* line was not used for our application. This line was be held in the high state throughout the data collection since we did not want continually updated data. We used the CMCO line (also called the "snapshot" control line) to acquire a set of data from a single line scan of the camera. The CMCO line is normally held low, which causes the pixel locator to take a set of data when it is raised to the high state. This is shown as point 1 in the timing diagram of Figure 3.

The information available from the pixel locator after the CMCO line has been pulsed consists of the number of transitions (up to 255), and the pixel locations of the transitions (only the first 40 transitions). The eight binary lines from the pixel locator containing the number of transitions data are connected to the lowest eight lines of

port B on the DRV11-J board. This information is accessed by the computer at point 2 in Figure 3.

Once the number of transitions is known, the pixel locations and polarity can be read in from the pixel locator through port A. This information is stored in a 40 element FIFO (First In First Out) memory. The FIFO memory data operates as shown by points 3 through 9 in Figure 3. The first pixel location and polarity are available after the CMCO line has been pulsed. The second pixel location and polarity is available after the normally high READ* line has been pulsed low. This new piece of data is read at point 5 in Figure 3. The READ* pulse followed by the data input is repeated until all of the transition locations have been input to the computer.

If the number of transitions is greater than 40 the FULL* line will become active (it goes low) and FIFO stores no further data. This FULL* line is available at port A, but we have not used this line in any of our software. It has not been used since there should be no more than a couple of transitions for any one scan of the camera.

The actual FORTRAN code for controlling the camera and inputting the data consists of a call to a subroutine which is itself made up of other FORTRAN and MACRO subroutines. This subroutine may then be called any time new data is required from the camera.

Appendix A contains a listing with annotation of a sample main program (QTEST2), the camera setup subroutine (QSETUP), the main subroutine (QCAM) and its subroutines (QTNUM, QOC, QDATA, and QDLY), and a data analysis subroutine (QWID).

QTEST2 first calls QSETUP to set ports A and B of the DRV11-J as input ports, and sets port C as an output port. QTEST2 then calls the key subroutine QCAM. QCAM calls the port C controlling subroutine, QOC, three times. Before each call a number, NCAM, is defined by determining how each of the three lines READ*, RUN*, and CMCO needs to be set. Bit 0 controls CMCO, bit 1 controls RUN*, bit 2 controls READ*. Thus, defining NCAM=0 and calling QOC will result in all three control lines being low . By defining NCAM to be first 6, then 7, and then 6 again, with calls to QOC between each definition, causes a low to high and high to low pulse on the CMCO line while holding READ* and RUN* high. This forces the pixel locator to take data from one camera scan. The inclusion of QDLY between calls to QOC assures a long enough delay so that the CMCO pulse will not be missed by the pixel locator.

QCAM then calls QTNUM which returns the number of transitions in the variable ITNUM. QDATA is then called ITNUM times and receives the pixel transition locations and their corresponding polarities (0 = dark to light, 1 = light to dark.) The polarity is at port A (bit 13) and the pixel

location is at port A (bits 0 to 11). QDATA returns two variables IPIX (the pixel location) and IPOLE (the polarity) each time it is called. When QDATA returns to QCAM these two variables become part of two arrays, IPIXDT and IPOLDT, which eventually contain the entire data set of pixel locations and polarities. Between each call to QDATA the READ* line must be pulsed to move out the successive data values from the FIFO memory. After all the data has been returned from the pixel locator QCAM returns to the main program with the arrays IPIXDT and IPOLDT containing all of the pixel locator data. If the pixel locations are not an increasing set of numbers, QCAM automatically takes another set of data.

QTEST2 then calls QWID. This subroutine takes the data from the arrays IPIXDT and IPOLDT and calculates a two dimensional array DATAPX. The contents of this array is filled with the center values of the bright peaks and the width of the peaks. Finally, QTEST2 prints the data for the camera scan to the CRT.

The two subroutines QCAM and QWID will form the data collection part of an automatic optical positioning system. The other major subroutine, which still needs to be written, is the stepper-motor controller. The building of the stepper-motor controller should be done shortly.

VI. System Integration

As discussed in section III, the optical system and camera are capable of one micron resolution. Sections IV and V presented the interfacing and software development required for transferring the camera data into the main computer. There are several hardware items which must be built or bought before the project can be completed.

The major items still to be built are the actual mountings for the camera and optics on the ring laser gyro table. These mounts should be finished by late August, 1985. The electronics for the stepper-motor interface is almost complete and should also be in the system by late August. The items which need to be purchased are the lenses, and laser for imaging the scribed spot on the line scan camera.

Once the hardware is in place and the computer operating system has been regenerated to recognize the DRV11-J interface, the development of the automatic registration scheme for the mirror elements will consist of developing the FORTRAN code and testing the precision of the system.

VII. Recommendations

There are three recommendations:

1. The optics needed for the system are listed below along with specific part numbers from the Melles Griot catalog. Other manufactures can certainly be used.

a.) A plano-cylindrical lens of focal length 30 cm. Melles Griot # 01 LCP 019.

b.) A plano-concave spherical lens of focal length -40 cm. Melles Griot # 01 LPK 013.

c.) A plano-convex spherical lens of focal length 100-cm. Melles Griot # 01 LPX 187.

d.) A plano-convex spherical lens of focal length 0.16 cm. Melles Griot # 01 LPX 413.

2.) A HeNe cylindrical laser head and power supply. For example, a 2 mW laser and power supply from the Ealing Optics Catalog # 25-0837 and # 25-0894.

3.) The use of an area scan camera may be more appropriate for the registration problem. The advantage is that the camera "sees" in two dimensions. The disadvantage is the larger pixel size (18 microns, and 30 microns on center horizontally and vertically). We only briefly used the area scan camera because the power supply was not delivered until the end of our ten week program. This system should be investigated more thoroughly.

References

1. W. W. Chow, J. Gea-Banacloche, and L. M. Pedrotti, "The ring laser gyro," Reviews of Modern Physics, January 1985, 57 (1), pp. 61-104.

2. Misner,C.W.,K.S. Thorne, and J.A. Wheeler, Gravitation, San Fransisco, Freeman, 1973.

3. Fairchild, Operating Instructions for the Pixel Locator Accessory for Fairchild Line Scan Camera Subsystems,1981.

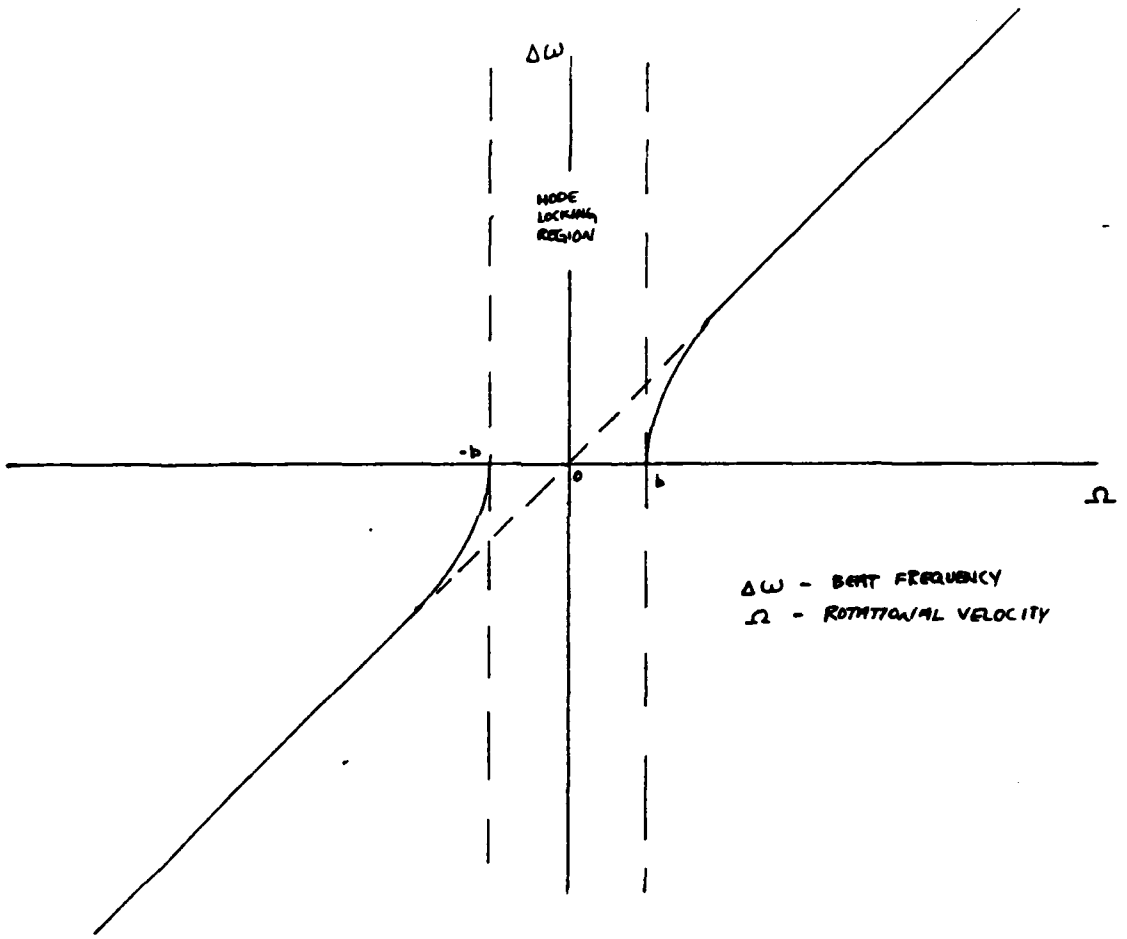
Δω
MODE LOCKING REGION
-b
0
b
Ω
Δω - BEAT FREQUENCY
Ω - ROTATIONAL VELOCITY

FIGURE 1

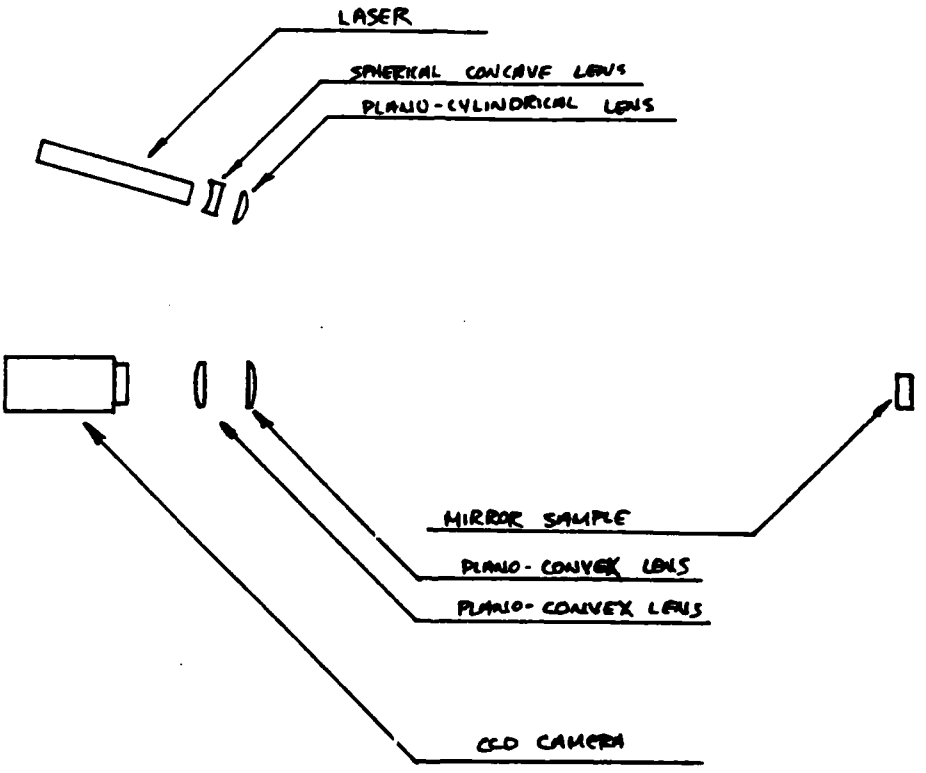
LASER
SPHERICAL CONCAVE LENS
PLANO-CYLINDRICAL LENS
MIRROR SAMPLE
PLANO-CONVEX LENS
PLANO-CONVEX LENS
CCD CAMERA

FIGURE 2

PROGRAM TIMING DIAGRAM FOR RECEIVING DATA FROM PIXEL LOCATOR

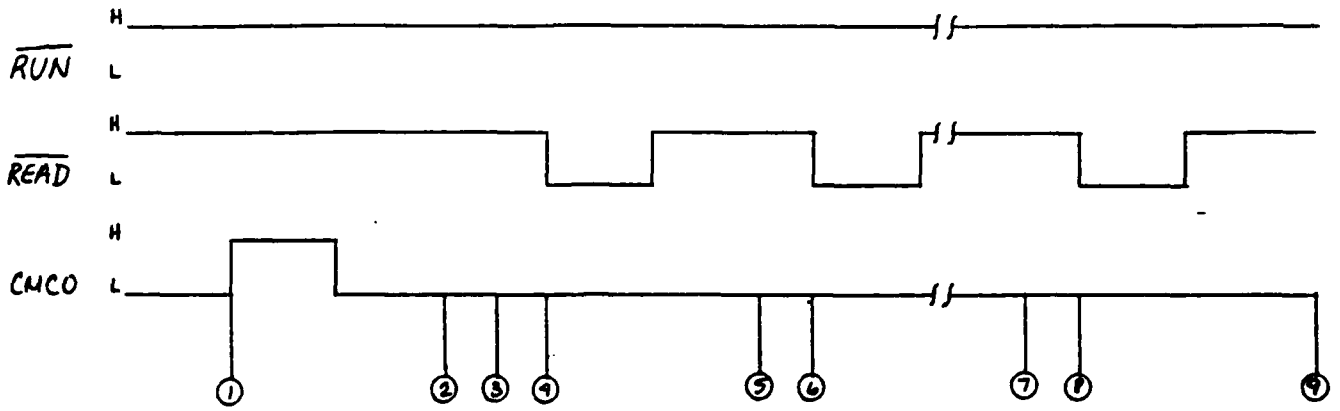

1	SNAPSHOT TAKEN AND TRANSITION LOCATIONS STORED IN FIFO WITH FIRST WORD IN FIFO OUT
2	INPUT NUMBER OF TRANSITIONS, N, FROM PIXEL LOCATOR
3	READ IN FIRST WORD
4	SECOND WORD INTO FIFO OUT
5	READ IN SECOND WORD
6	THIRD WORD INTO FIFO OUT
7	READ N-1 WORD
8	N^{th} WORD INTO FIFO OUT
9	READ IN N^{th} WORD

FIGURE 3

DRV11-J		J1	J3	Pixel locator
GROUND		17	18	GROUND
Port A	I/O 15	45	6	FULL*
"	14	46	5	BR
"	13	43	4	DR
"	12	49	2	POLE
"	11	48	32	Add 11
"	10	44	31	" 10
"	9	50	30	" 9
"	8	47	29	" 8
"	7	41	28	" 7
"	6	36	27	" 6
"	5	42	26	" 5
"	4	35	25	" 4
"	3	40	24	" 3
"	2	38	23	" 2
"	1	39	22	" 1
"	0	37	21	" 0
Port B	I/O 15	6	NC	
"	14	5	NC	
"	13	8	NC	
"	12	2	NC	
"	11	3	NC	
"	10	7	NC	
"	9	1	NC	
"	8	4	NC	
"	7	10	45	Data 7 (# of Transitions)
"	6	15	44	" 6
"	5	9	43	" 5
"	4	16	42	" 4
"	3	11	41	" 3
"	2	13	40	" 2
"	1	12	39	" 1
"	0	14	38	" 0
		J2	J3	
Port C	I/O 2	13	1	READ*
"	1	12	8	RUN*
"	0	14	7	CMCO

* = active low

TABLE 1

APPENDIX A

The following is an annotated listing of the four FORTRAN and four MACRO programs used for controlling the line scan camera, data transfer to the computer, and data analysis.

```
C       MAIN PROGRAM:  QTEST2.FOR
C       MAIN SUBPROGRAM:  QCAM.FOR,QSETUP.MAC
C
C
C       DELAY FOR CAMERA SCAN IS SET IN SUBROUTINE QCAM AT
C       A VALUE NUMDLY=100.  NUMDLY IN THIS MAIN PROGRAM IS
C       SET AT A VALUE 32000 TO ALLOW ONE TO VIEW THE DATA
C       ON A CRT.
C
C       MAIN PROGRAM=>CALLS SUBPROGRAM QSETUP.
C              CALLS QCAM AND PRINTS OUT THE NUMBER OF TRANSITIONS
C              AND THE TRANSITION PIXEL LOCATIONS AND THE TRANSITION
C              POLARITY(0=DARK TO LIGHT,1=LIGHT TO DARK)
C              IT ALSO PRINTS OUT THE NUMBER OF PEAKS, 2 OR MORE PIXELS
C              WIDE,THE CENTER OF THE PEAKS AND THEIR WIDTH.
C
C       DESCRIPTIONS OF SUBPROGRAMS AND VARIABLES:
C
C              QSETUP.MAC=>SETS PORTS A AND B AS INPUT PORTS AND
C                     SETS PORT C AS OUTPUT PORT.
C              QCAM.FOR=>PULSES THE CMCO LINE OF THE CAMERA
C                     SUBSYSTEM,USING SUBROUTINE QOC;  WHICH 'TAKES A
C                     PICTURE',I.E.,SCANS CAMERA'S CCD ONCE.  QCAM RECEIVES
C                     THE NUMBER OF PIXEL TRANSITIONS, THE PIXEL NUMBERS
C                     (LOCATIONS) ON THE CCD, AND THEIR CORRESPONDING
C                     POLARITY(0=DARK TO LIGHT, 1=LIGHT TO DARK)
C                     AND STORES THE LOCATIONS AND POLARITIES IN TWO ARRAYS,
C                     IPIXDT AND IPOLDT RESPECTIVELY.
C              QTNUM.MAC=>IS USED, BY QCAM.FOR, TO RECEIVE THE NUMBER OF
C                     PIXEL TRANSITIONS.
C              QOC.MAC=>SENDS AN OCTAL NUMBER OUT TO PORT C, WHICH CONTROLS
C                     THE RUN, READ, AND CMCO LINES.  THIS SUBPROGRAM IS
C                     USED BY SUBPROGRAM QCAM.
C              QDLY.FOR=> IS USED IN SUBPROGRAM QCAM TO SETUP A DELAY
C                     TO ASSURE ENOUGH TIME FOR TRANSFER OF DATA THROUGH
C                     THE DATA BUS LINE.  IT IS ALSO USED IN THE MAIN
C                     PROGRAM TO ALLOW ONE TO VIEW THE DATA ON A CRT.
C              QDATA.MAC=>USED BY SUBPROGRAM QCAM TO RECEIVE THE PIXEL
C                     TRANSITION LOCATIONS AND THEIR CORRESPONDING
C                     POLARITY.
C              QWID.FOR=>CALLED BY SUBPROGRAM QCAM TO DETERMINE THE NUMBER
C                     OF PEAKS, THE CENTER OF THE PEAKS AND THE WIDTH OF THE
C                     PEAKS.
C       VARIABLES:
C              NUMDLY:  DELAY NUMBER, USED BY SUBROUTINE QDLY.
C              NUMPK:  NUMBER OF PEAKS.
C              NCAM:  OCTAL NUMBER SENT OUT TO PORT C, BY SUBPROGRAM
C                     QOC, TO SET THE RUN, READ, AND CMCO LINES.
C              ITNUM:  NUMBER OF TRANSITIONS IN ONE SCAN RETURNED BY
C                     SUBPROGRAM QTNUM.
C              IPIX:  TRANSITION LOCATIONS, RETURNED BY SUBPROGRAM
C                     QDATA.
```

```
C
C             IPOLE:  TRANSITION POLARITY(0=DARK TO LIGHT,1=LIGHT TO DARK),
C                     RETURNED BY SUBPROGRAM QDATA.
C             IPIXDT:  ARRAY SETUP IN SUBPROGRAM QCAM, COMPOSED OF THE
C                      TRANSITION LOCATIONS, IPIX.
C             IPOLDT:  ARRAY SETUP IN SUBROGRAM QCAM, COMPOSED OF THE
C                      TRANSITION POLARITIES, IPOLE.
C             DATAPX:  2-DIMENTIONAL ARRAY OF PEAK CENTERS,DATAPX(*,1), AND
C                      ASSOCIATED PEAK WIDTHS,DATAPX(*,2).
C
C
      DIMENSION IPIXDT(40),IPOLDT(40)
      DIMENSION DATAPX(20,2)
      EXTERNAL QDATA,QSETUP,QTNUM,QWID
      COMMON NUMDLY,IPIXDT,IPOLDT,DATAPX,NUMPK
      COMMON /CAMPAR/ NCAM
      COMMON /TRNSUM/ ITNUM
      COMMON /PIXDAT/ IPIX,IPOLE
      CALL QSETUP                    !SETUP OUTPUT PORT C,INPUT PORTS A&B
20    CALL QCAM                      !RECEIVE DATA FROM CAMERA SYSTEM
      CALL QWID
      DO 70 I=1,30                   !CLEAR SCREEN
      WRITE(5,80)
70    CONTINUE
      WRITE(5,200)ITNUM              !WRITE NUMBER OF TRANSITIONS
      WRITE(5,300)
      DO 10 I=1,ITNUM                !WRITE TRANS. NUMBER,LOCATION AND POL.
      WRITE(5,100) I,IPIXDT(I),IPOLDT(I)
10    CONTINUE
      IF(NUMPK .LT. 1) GOTO 45       !WRITES PEAK DATA IF THERE IS 1 OR
      WRITE(5,400)                   !MORE PEAKS.
      DO 40 J=1,NUMPK
      WRITE(5,500) DATAPX(J,1),DATAPX(J,2)
40    CONTINUE
45    WRITE(5,50)                    !MANUAL DELAY
      ACCEPT 60,LL
      GOTO 20                        !GET NEW DATA
50    FORMAT(' HIT ENTER TO CONTINUE')
60    FORMAT(I5)
80    FORMAT(' ')
100   FORMAT(10X,I3,3X,I6,3X,I6)
200   FORMAT(' NUMBER OF TRANSITIONS:',I4)
300   FORMAT(15X,' TRANLOC',1X,' POLARITY')
400   FORMAT(13X,' MID PT',8X,' WIDTH')
500   FORMAT(10X,F8.2,7X,F8.2)
      STOP
      END
```

```
      SUBROUTINE QCAM
C
C     SUBRPROGRAM QCAM.FOR
C           CALLED FROM ANY PROGRAM AND RETURNS THE NUMBER
C           OF TRANSITIONS(ITNUM), THE ARRAY OF TRANSITION
C           LOCATIONS(IPIXDT), AND THE ARRAY OF TRANSITION
C           POLARITIES(IPOLDT).
C
      DIMENSION IPIXDT(40),IPOLDT(40)
      COMMON NUMDLY,IPIXDT,IPOLDT
      COMMON /CAMPAR/ NCAM
      COMMON /TRNSUM/ ITNUM
      COMMON /PIXDAT/ IPIX,IPOLE
      NUMDLY=100                    !SET DELAY LONG ENOUGH TO  ALLOW
C                                   !TRANSMITION THROUGH DATA BUS.
C     PULSE CMCO=>L-H-L
C
40    NCAM=6
      CALL QOC
      CALL QDLY
      NCAM=7
      CALL QOC
      CALL QDLY
      NCAM=6
      CALL QOC
      CALL QDLY
C
C     RECEIVE NUM OF PIXEL TRANSITIONS, ITNUM. THEN RECEIVE THE
C     LOCATIONS, IPIX, OF THE TRANSITIONS.
C
      CALL QTNUM
C     ***     LIMITED TO 40 WORDS BY FIFO   ***
      IF (ITNUM .GE. 40) ITNUM=40
      DO 10 I=1,ITNUM
      CALL QDLY
      CALL QDATA
      IPIXDT(I)=IPIX                !SETUP ARRAY OF TRANSITION LOCATIONS
      IPOLDT(I)=IPOLE               !SETUP ARRAY OF TRANSITION POLARITIES
C
C     PULSE READ LINE FOR NEW DATA FROM FIFO
C
      NCAM=2
      CALL QOC
      CALL QDLY
      NCAM=6
      CALL QOC
      CALL QDLY
10    CONTINUE
20    CONTINUE
C
C     CHECK TO SEE IF THE DATA IS OK. (ALL INCREASING NUMBERS
C     IN IPIXDT ARRAY.)
```

```
C
      IF (ITNUM .LE. 1) GOTO 50
      IDUM=IPIXDT(1)
      DO 30 I=2,ITNUM
      IF (IPIXDT(I) .LE. IDUM) GOTO 40
      IDUM=IPIXDT(I)
30    CONTINUE
50    CONTINUE
      RETURN
      END



C     SUBROUTINE QDLY.FOR
C
C     SUBROUTINE FOR VARIABLE DELAY DURATION
C
C     NUMDLY PASSED FROM OTHER ROUTINES.
C           NUMDLY MINIMA=1
C           NUMDLY MAXIMA=32000 (ABOUT 2 SEC.)
C
C
      SUBROUTINE QDLY
      COMMON NUMDLY
      DO 10 I=1,32000
      IF(I .EQ. NUMDLY) GOTO 100
10    CONTINUE
100   RETURN
      END



      SUBROUTINE QWID
      DIMENSION IPIXDT(40),IPOLDT(40)
      DIMENSION DATAPX(20,2)
      COMMON /TRNSUM/ ITNUM
      COMMON NUMDLY,IPIXDT,IPOLDT,DATAPX,NUMPK
      NUMPK=0                          !SET PEAK COUNTER TO ZERO
      DO 20 K=1,ITNUM-1
      IF (IPOLDT(K) .EQ. 0) GOTO 20    !CHECK FOR POLARITY CHANGES OF
      IF (IPOLDT(K+1) .EQ. 1) GOTO 20 !1 TO 0.(DARK->LIGHT->DARK)
      NUMPK=NUMPK+1                    !INCREMENT PEAK COUNTER
C
C     SETUP ARRAY OF PEAK MIDPOINTS AND WIDTHS.
C
      DATAPX(NUMPK,2)=FLOAT(IPIXDT(K+1)-IPIXDT(K))
      DATAPX(NUMPK,1)=DATAPX(NUMPK,2)/2.0+FLOAT(IPIXDT(K))
20    CONTINUE
      RETURN
      END
```

```
        ;       QSETUP.MAC => DRV11-J PORT SETUP ROUTINE
        ;       SET UP PORTS A & B FOR INPUT
        ;       AND PORT C FOR OUTPUT
        ;       FORTRAN CALL IS OF THE FORM:
        ;       CALL QSETUP
        .TITLE  QSETUP.MAC
        .PSECT
        CSRA    =164160
        CSRB    =164164
        CSRC    =164170
QSETUP::
        CLR     @#CSRA          ; SET UP PORT A FOR INPUT
        CLR     @#CSRB          ; SET UP PORT B FOR INPUT
        MOV     #400,@#CSRC     ; SETUP PORT C FOR OUTPUT
        RTS     PC              ; RETURN
        .END
```

```
        ;       SUBROUTINE QOC=> MOVES OCTAL NUMBER, NCAM,
        ;       OUT TO PORT C.
        ;
        ;       NCAM=7 => CMCO=1,RUN=1,READ=1
        ;       NCAM=6 => CMCO=0,RUN=1,READ=1
        ;       NCAM=2 => CMCO=0,RUN=1,READ=0
        ;
        ;       CALLED FROM SUBROUTINE QCAM
        ;       CALL OF FORM: CALL QOC
        ;
        ;
        .TITLE  QOC.MAC
        .PSECT  CAMPAR,RW,D,GBL,REL,OVR
NCAM:   .BLKW   1
        .PSECT
        DBRC    =164172                 ; DATA BUFFER REGISTER C LOCATION
QOC::   MOV     @#NCAM,@#DBRC           ; MOVE NCAM OUT TO PORT C
        RTS     PC                      ; RETURN
        .EVEN
        .END
```

```
        ;       SUBROUTINE QTNUM=> RETREIVES NUMBER OF TRANSITIONS
        ;       FROM LINE SCAN CAMERA.
        ;
        ;       CALL FROM SUBROUTINE QCAM
        ;       CALL OF FORM:  CALL QTNUM
        ;
        .TITLE  QTNUM.MAC
        .PSECT  TRNSUM,RW,D,GBL,REL,OVR
ITNUM:  .BLKW   1
        .PSECT
        DBRB    =164166         ; DATA BUFFER REGISTER LOCATION
QTNUM:: MOV     @#DBRB,R0       ; 16 BIT WORD FROM PORT B TO R0
        BIC     #177400,R0      ; LOG AND TO MASK TOP 8 BITS
                                ; NUMBER TRANS IS LOWER 8 BITS
        MOV     R0,@#ITNUM      ; NUMBER OF TRANS INTO ITNUM
        RTS     PC              ; RETURN
        .EVEN
        .END
```

```
        ;SUBPROGRAM:  QDATA.MAC
        ;
        ;SUBROUTINE TO RETREIVE PIXEL LOCATION DATA FROM
        ;LINESCAN CAMERA SUBSYS FIFO MEMERY
        ;
        ;CALL FROM QCAM.FOR:  CALL OF FORM=> CALL QDATA
        ;
        .TITLE  QDATA.MAC
        .PSECT  PIXDAT,RW,D,GBL,REL,OVR
IPIX:   .BLKW   1
IPOLE:  .BLKW   1
        .PSECT
        DBRA    =164162         ;DATA BUFFER REGISTER A LOCATION
        ;
QDATA:: MOV     @#DBRA,R0       ;MOVE WORD AT DBRA INTO R0
        ;
        ;CHECK POLARITY OF TRANSITION BY CHECKING BIT 13 OF PORT A
        ;SET IPOLE=1 IF LIGHT TO DARK TRANSITION AND IPOLE=0 IF
        ;DARK TO LIGHT TRANSITION.
        ;
        MOV     #1,@#IPOLE
        BIT     R0,#010000
        BNE     OVER
        MOV     #0,@#IPOLE
OVER:   BIC     #170000,R0      ;MASK OUT THE TOP 4 BITS FROM PORT A
        MOV     R0,@#IPIX       ;MOVE BOTTOM 12 BITS TO IPIX(TRANS LOCATION)
        RTS     PC              ;RETURN
        .EVEN
        .END
```

1985 USAF-UES SUMMER FACULTY RESEARCH PROGRAM/

GRADUATE STUDENT SUMMER SUPPORT PROGRAM

Sponsored by the

AIR FORCE OFFICE OF SCIENTIFIC RESEARCH

Conducted by the

UNIVERSAL ENERGY SYSTEMS, INC.

FINAL REPORT

^{27}Al Spin Lattice Relaxation Measurements in Alkylammonium-Chloroaluminate Room-temperature Electrolytes

Prepared by:	Richard D. Bertrand
Academic Rank:	Professor of Chemistry
Department:	Department of Chemistry
University:	University of Colorado at Colorado Springs
Research Location:	Frank J. Seiler Research Laboratory
USAF Research:	Dr. John Wilkes
Date:	September 3, 1985
Contract No.:	F49620-85-C-0013

^{27}Al Spin Lattice Relaxation Measurements in Alkylammonium-Chloroaluminate Room-temperature Electrolytes

by

Richard D. Bertrand

ABSTRACT

Spin lattice relaxation times (T_1) were measured at several temperatures for alkylammonium-chloraluminate room-temperature melts. Most of the measurements were made for the 1-methyl-3-ethylimidazolium-/aluminum chloride system with a 0.60 apparent mole fraction of $AlCl_3$. The observation of a relatively slow relaxation for ^{27}Al in $AlCl_4^-$ and fast relaxation for a melt containing a 1:1 mixture of $AlCl_4^-$ and $Al_2Cl_7^-$ are consistent with rapid exchange of ^{27}Al in $AlCl_4^-$ with $Al_2Cl_7^-$. The results indicate an exchange lifetime for $AlCl_4^-$ less then or equal to the relatation time for ^{27}Al in $Al_2Cl_7^-$ of about 200 μs.

I. INTRODUCTION: The author's professional background includes 20 years experience in the applications of Nuclear Magnetic Resonance (NMR) spectroscopy to problems in chemistry. This experience has included the measurement of the values and signs of spin-spin coupling constants in transition metal complexes of phosphorus donors, study of aromatic-solvent induced chemical shifts, study of ^{13}C-^{13}C spin-spin coupling in small ring molecules, and examination of the mechanisms of ^{13}C spin lattice relaxation. This background proved valuable to the people of the Frank J. Seiler Research Laboratory for in discussions with Dr. Wilkes at the Seiler Laboratory it was noted that Seiler personnel could not reproduce the work of Matsumoto and Ichikawa[1] which involved measurement of ^{27}Al spin lattice relaxation times in room temperature molten salts. Indeed, it appeared they were unable to measure this parameter for the aluminum chloride system of interest. Since the author is quite experienced at NMR spectroscopy, and spin lattice relaxation time measurements in particular, it was decided to propose examination of this problem. In addition, study of the nature of materials dissolved in the molten salts was proposed. It was suggested that examination of compounds known to form complexes with chloride might prove to be instructive.

II. OBJECTIVES OF THE RESEARCH EFFORT: The electrochemistry group at the Frank J. Seiler Research Laboratory has for some time been studying the chemical and physical properties of room temperature chloro-aluminate molten salts of alkyl ammonium halides. As the ratio of aluminum chloride to alkyl ammonium halide increases, changes in the

composition of the aluminum halide anions present in the mixture occur. The result is the formation of oligomeric aluminum species such as $Al_2Cl_7^-$. It is of interest to understand the dynamic nature of these aluminum species, that is, the processes involved and their relative rates for the exchange of aluminum among the possible species. The approach originally proposed involved measurement of the ^{27}Al spin-lattice relaxation times (T_1) using the Freeman-Hill pulse technique since earlier workers at the Seiler Laboratory were unsuccessful in using the inversion recovery technique.

Matsumoto and Ichikawa[1] obtained nonlinear logarithmic magnetization relaxation curves for ^{27}Al at non-stoichiometric compositions for the n-butylpyridinium chloride/aluminum chloride melts. These authors state that the curvature in these plots is due to non-single exponential decay of the ^{27}Al magnetization. Linear logarithmic decay curves were obtained for stoichiometric mixtures. These results were explained by using a model of the chemical and spin dynamics that assumed (i) each aluminum in the separate species present under non-stoichiometric conditions has a distinct relaxation time and (ii) the Bloch equations hold for the T_1 of each species. Exchange of ^{27}Al between the assumed two species present in the non-stoichiometric melts (these include $AlCl_3$ and $Al_2Cl_7^-$ for melts with an apparent mole fraction aluminum chloride between 0.5 and 0.66, and $Al_2Cl_7^-$ and $Al_3Cl_{10}^-$ for melts with apparent mole fraction aluminum chloride between 0.66 and 0.75) provides a path for ^{27}Al nuclear relaxation. Solution of the two differential equations produced by these assumptions led the

authors to a three parameter equation allowing solution for the relaxation time for the two exchanging species and the fraction of equilibrium magnetization due to one of the two species. Independent measurements gave the authors the ratio of the equilibrium magnetizations for the two species, and thus the mole fraction of each aluminum species present. These authors concluded that exchange between the aluminum species of the non-stoichiometric melts was slow and comparable to the relaxation rates for the species containing ^{27}Al.

In addition to the project mentioned above, it was also originally proposed to examine the spin-spin relaxation times (T_2) of ^{27}Al in these melts as well as the nature of materials dissolved in these liquids. The T_2 study might shed additional light on the nature of the exchange processes involving aluminum in its various forms. Study of the NMR spectra of the metal nuclei of soluble metal salts, such as platinum chloride, might give information as to the nature of the species formed in the molten salt solution. It was proposed to examine the effect changing the aluminum chloride composition would have on the nature of the dissolved metal ion. Since platinum has a rich chloride chemistry and ^{195}Pt is very amenable to study by NMR, it was proposed to examine the chemistry of platinum chloride in these melts.

III. EXPERIMENTAL PROCEDURE AND RESULTS. Room temperature molten salts were made from aluminum chloride sublimed in high vacuum and 1-methyl-3-ethylimidazolium chloride or n-butylpyridinium chloride prepared by Seiler Laboratory personnel.

All NMR measurements were carried out on a JEOL FX 90 Q spectro-

meter operating at 2.1 Tesla. The spectrometer was equipped with pulse programmer and sample temperature controller. Samples were contained in either 5 mm OD or 10 mm OD thin-walled NMR tubes and were prepared in an inert atmosphere dry box. The software package used for spectrometer control was supplied by JEOL as version FAFT 72. It was discovered after attempts were made to measure T_1's of ^{13}C for known compounds that the software supplied as the inversion recovery T_1 program was actually a single pulse data acquisition program. This program was replaced with the inversion recovery program supplied with the older version FAFT 70 software. Use of this program successfully reproduced the literature value of the ^{13}C T_1 for air saturated benzene. When applied to measurement of the T_1 of ^{27}Al in a room temperature molten salt, it was found impossible to invert the magnetization of the ^{27}Al nucleus. Further examination of the pulse program revealed inclusion of an additional time period between application of the π pulse and the $\pi/2$ pulse which could not be reduced below 1 ms. Rewriting the sequence to eliminate this time interval resulted in successful T_1 determinations for ^{27}Al.

Data reduction to obtain T_1 was accomplished using a nonlinear least squares program[2] modified by the author. A two parameter fit to the equation

$$\ln \frac{M_0 - M_t}{2 M_0} = \frac{-t}{T_1} + B \qquad (1)$$

and a three parameter fit to the equation

$$M_t = A + B \exp(-t/T_1) \qquad (2)$$

were carried out. Here, A, B and T_1 are the fitting parameters, $-M_0$ and M_t are magnetizations at infinite time and time t, respectively.

The proposal to measure T_1 using the Freeman-Hill method was made before the reasons for earlier failures to measure T_1 of ^{27}Al were understood. Since T_1's could be measured using the inversion recovery method, the Freeman-Hill method was not pursued.

Table 1 presents the results of ^{27}Al T_1 measurements for the alkyl ammonium chloride mixtures with aluminum chloride as a function of apparent mole fraction aluminum chloride and temperature. In some cases, several measurements were made at the same temperature on different samples of the same composition or on the same sample at different times in an attempt to discover aging effects.

At the end of the contract time, an examination began of the NMR spectrum of lead(II) chloride dissolved in a room temperature melt of the 1-methyl-3-ethylimidazolium chloride/aluminum chloride system with a 0.30 apparent mole fraction of $AlCl_3$. The ^{207}Pb NMR signal for a saturated aqueous solution of lead(II) nitrate in a 10 mm OD sample tube could readily be observed in a few minutes. A homogeneous solution was prepared of lead(II) chloride in the melt with a mole ratio of chloride to lead chloride of 0.5, but the ^{207}Pb NMR signal was not observed. The chemical shift range for lead is extremely large, and insufficient time remained to make a complete search for this signal. Lead was chosen for initial investigation instead of platinum because it is inexpensive and its chemistry in these melts is of interest at the Seiler Laboratory.

Because of the time involved in carrying out the spin-lattice relaxation studies, it was not possible to examine the spin-spin relaxation times.

Table 1. ^{27}Al spin lattice relaxation times (in μs, except where indicated) as a function of temperature for the 1-methyl-3-ethylimidazolium chloride/aluminum chloride system (except where indicated) having an apparent mole fraction aluminum chloride of 0.60 (except where indicated). Results are given for fits to Equation (1) and Equation (2). Uncertainties are standard deviations.

Temp. (°C)	T_1 (μs, Eqn. 1)	T_1 (μs, Eqn. 2)	Note
0	87	93	
	97 ± 5	83 ± 2	in freezer 2 days
	77 ± 2	103 ± 2	run 2 of above sample
	90 ± 1	105 ± 7	
15	130 ± 1	146 ± 2	
	113 ± 1	139 ± 6	heated from 0°
	112 ± 3	119 ± 3	run 2 of above sample
	96 ± 6	154 ± 2	downward curvature for plot of Equation (1)
	122 ± 2	156 ±5	
20	147 ± 2	180 ± 6	
	106 ± 8	173 ± 3	downward curvature for plot of Equation (1)
	113 ± 9	138 ± 3	
	113 ± 9	176 ± 2	downward curvature for plot of Equation (1)

Table 1. Continued

25	177 ± 2	195 ± 4	
	153 ± 2	177 ± 3	
	170 ± 1	199 ± 10	heated from 15°
	177 ± 1	190 ± 4	
	194 ± 1	195 ± 1	
	--	179 ± 1	these three results
	--	174 ± 3	showed upward curvature
	--	200 ± 3	in plot of Equation (1)
30	181 ± 3	222 ± 4	
	162 ± 5	222 ± 5	slight downward curvature in plot of Equation (1)
	--	220 ± 5	showed upward curvature for plot of Equation (1)
34	--	239 ± 6	showed upward curvature for plot of Equation (1)
	226 ± 2	235 ± 2	
35	--	246 ± 7	showed upward curvature for plot of Equation (1)
	222 ± 2	250 ± 3	
	168 ± 3	212 ± 5	
	136 ± 1	150 ± 3	
55	52.4 ± .2 ms	51 ± 10 ms	apparent mole fraction $AlCl_3$ = 0.50

Table 1. Continued

25	15 ± 1 ms	12.6 ± .6 ms	1-methyl-3-ethylimidazolium bromide melt, apparent mole fraction $AlCl_3$ = 0.40
	91 ± 3	119 ± 1	remaining results are for n-
35	124 ± 1	141 ± 3	butylpyridinium chloride melt
	143 ± 6	177 ± 16	apparent mole fraction $AlCl_3$ =
	115 ± 4	152 ± 6	0.60.
	136 ± 1	150 ± 3	π and $\pi/2$ pulse times misset
			to 0.7 of correct value
65	263 ± 3	307 ± 4	

III. DISCUSSION: The results obtained in this study did not agree with the work of Matsumoto and Ichikawa[1]. In all but a few instances, the logarithmic magnetization recovery curves for ^{27}Al were linear. Since in most cases, the measurement of the magnetization was carried out to 90% recovery, it is not likely a long-time curvature was missed. In a few cases, upwardly curving logarithmic magnetization curves were observed, but these observations were not reproducible. When data from these nonlinear logarithmic decay curves were reduced using a three parameter exponential fitting program, the calculated T_1's agreed with those obtained for the same or different samples when linear logarithmic decay curves were obtained. One reason for using a three parameter exponential fit to obtain T_1 is that experimental imperfections such as misset pulse lengths and pulse droop show up in the non-T_1 parameters, giving accurate T_1's. Indeed, when the pulse lengths were purposely misset to 0.7 of their correct values, linear logarithmic decay curves were obtained with a T_1 in agreement with that measured using correct pulse settings and a three parameter exponential fit. It may be argued that, although a non-linear logarithmic magnetization decay curve may be due to non-single exponential decay, it may also result from other factors associated with the experimental technique.

Work of Wilkes, Frye and Reynolds[3] indicate a relativly slow exchange between $AlCL_4^-$ and $Al_2Cl_7^-$ for melts of 1-methyl-3-ethylimidazolium chloride having 0.60 mole fraction $AlCl_3$. At the temperatures

involved here, the exchange lifetime is 2-3 ms. The T1 for $^{27}AlCl_4^-$ in a 0.50 mole fraction $AlCl_3$ melt is in the neighborhood of 50 ms, whereas the T_1 for ^{27}Al in the 0.60 mole fraction $AlCl_3$ melt is around 0.2 ms. Since the relaxation time for $AlCl_4^-$ is larger than its exchange lifetime, the contribution of $^{27}AlCl_4^-$ to the overall ^{27}Al relaxation time cannot be any less than the exchange lifetime. Yet, in the presence of $Al_2Cl_7^-$ the ^{27}Al relaxation time is less than the exchange lifetime, and no contribution to ^{27}Al relaxation due to slow aluminum exchange can be found. It should be emphasized that in this study, linear logarithmic magnetization curves were obtained over a time span covering nearly complete recovery of the magnetization to its equilibrium value. It seems likely that the exchange lifetime for $^{27}AlCl_4^-$ is less than or equal to 0.2 ms and not the several ms reported earlier[3]. Should this be the case, the results of this study for the ^{27}Al relaxation time in the acidic melt can be explained by an exchange of $^{27}AlCl_4^-$ which is faster than the relaxation of $^{27}AlCl_4^-$ and which is at least as fast as the relaxation of ^{27}Al in $Al_2Cl_7^-$.

IV. RECOMMENDATIONS: Additional experimental work is necessary to sort out some of the conflicting results described above. It is possible that the exchange lifetime in these melts is extremely sensitive to the composition of the melt. Investigation of the spin-lattice relaxation behavior of ^{27}Al in these mixtures for melts of differing composition which are carefully prepared is in order. Some of this experimental work should be carried out using a higher field spectrometer so as to resolve the resonances due to the individual

chloroaluminate species. Perhaps examination the spin-spin relxation behavior of these melts would be revealing. In homogeneous liquids, to a first approximation, T_1 should equal T_2, but if ^{27}Al motion is not isotropic, this may not be so. T_2 measurements thus may give information on the nature of aluminum exchange processes in these mixtures.

ACKNOWLEDGMENTS

I would like to thank a number of people at the Frank J. Seiler Research Laboratory for their assistance in helping me carry out this work. John Wilkes encouraged me to apply to the Summer Faculty Research Progam in order to carry out this project. His assistance in introducing me to the details of laboratory procedures and his helpful comments on the nature of the experimental results are greatly appreciated. Towner Scheffler and Lloyd Pflug were very helpful in teaching me the operation of the NMR spectrometer. Jack Fannin's help was invaluable in debugging the least-squares routine used in the data reduction for this project. His comments about the meaning of the measurements are much appreciated. Jeff Boon's help by preparing the compounds used in these studies saved me much time and is greatly appreciated. Helpful discussions with Chet Dymek are also appreciated. Sponsorship of this work by the Air Force Systems Command, Air Force Office of Scientific Research, is greatfully acknowledged.

LITERATURE CITED

1. Matsumoto, T., Ichikawa, K., "Determination of the Aluminum-27 Spin Lattice Relaxation Time and the Relative Number of Each Chloroaluminate Species in the Molten 1-n-Butylpyridinium Chloride-/$AlCl_3$ System," J. Am. Chem. Soc., **1984**, vol. 106, pp 4316-4320.
2. Schreiner, W, Kramer, M, Krischer, S, and Langsam, Y, "Nonlinear Least-Squares Fitting," PC Tech Journal, **1985**, vol 3, p. 170-190.

3. Wilkes, J. S., Frye, J. S., and Reynolds, G. F., "^{27}Al and ^{13}C NMR Studies of Aluminum Chloride-Dialkylimidazolium Chloride Molten Salts," Inorg. Chem., **1984**, vol. 22, p. 3870-3872.

1985 USAF-UES SUMMER FACULTY RESEARCH PROGRAM/

GRADUATE STUDENT SUMMER SUPPORT PROGRAM

Sponsored by the

AIR FORCE OFFICE OF SCIENTIFIC RESEARCH

Conducted by the

UNIVERSAL ENERGY SYSTEMS, INC.

FINAL REPORT

NATURAL LANGUAGE UNDERSTANDING USING RESIDENTIAL GRAMMAR AND ITS USE IN AUTOMATIC PROGRAMMING

Prepared by: Dr. Christian C. Wagner
Academic Rank: Assistant Professor
Department and University: School of Engineering and Computer Science, Oakland University, Rochester, MI 48063

Prepared by: Dr. Peter J. Binkert
Academic Rank: Associate Professor
Department and University: Department of Linguistics, Oakland University, Rochester, MI 48063

Prepared by: Ms. Kathleen A. Malin
Academic Rank: MS Candidate in Linguistics
Department and University: Department of Linguistics, Oakland University, Rochester, MI 48063

Prepared by: Ms. Frances M. Vallely
Academic Rank: MS Candidate in Computer Science
Department and University: School of Engineering and Computer Science, Oakland University, Rochester, MI 48063

Prepared by: Mr. Thomas L. Schnesk
Academic Rank: MS Candidate in Computer Science
Department and University: School of Engineering and Computer Science, Oakland University, Rochester, MI 48063

Research Location: Air Force Human Resources Laboratory, Training Systems Division, Lowry Air Force Base, CO 80230-5000

USAF Research: Hugh L. Burns, Major, USAF

Date: August 28, 1985

Contract No: F49620-85-C-0013

AD-A166 176 UNITED STATES AIR FORCE SUMMER FACULTY RESEARCH PROGRAM 04/13
1985 TECHNICAL RE (U)UNIVERSAL ENERGY SYSTEMS INC
DAYTON OH R C DARRAH ET AL. DEC 85 AFOSR-TR-86-0139
UNCLASSIFIED F49620-85-C-0013 F/G 5/9 NL

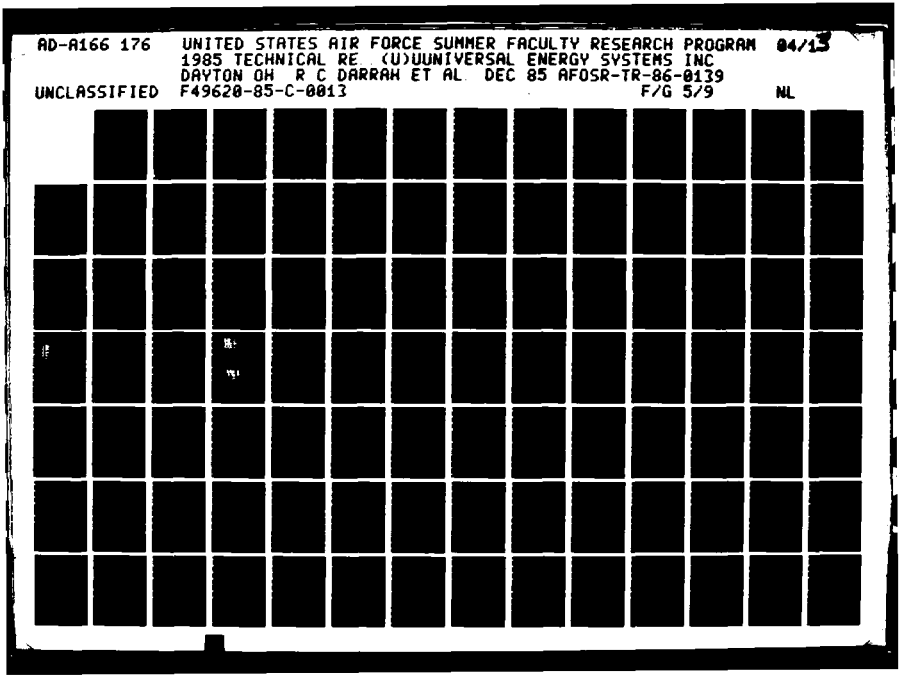

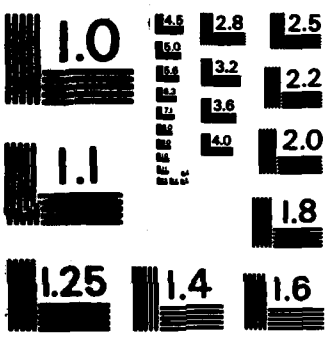

MICROCOPY RESOLUTION TEST CHART
NATIONAL BUREAU OF STANDARDS-1963-A

NATURAL LANGUAGE UNDERSTANDING USING RESIDENTIAL GRAMMAR AND ITS USE IN AUTOMATIC PROGRAMMING

by

Dr. Peter J. Binkert
Dr. Christian C. Wagner

Mr. Thomas L. Schnese
Ms. Frances M. Vallely
Ms. Kathleen A. Malin

The research outlined here focuses on the development of a methodology for the creation of a natural language interface. It includes a set of software tools and procedures based on a non-transformational theory of language called Residential Grammar (RG; Binkert, 1983, 1984, 1985). The development of the natural language tools began with two parallel efforts. The computer science team worked on the implementation of the LISP version of the RG syntactic parser of English, while the linguistic team concentrated on the development of a first set of semantic features out of which the case relations of language could be defined. Once completed, the natural language understanding tool could be integrated into a computer's operating system to act as an interface between a computer system and a computer user. This would reduce the confusion caused by the various command languages on different computer systems.

ACKNOWLEDGEMENTS

The entire research team would like to thank the Air Force Systems Command, Air Force Office of Scientific Research and the Human Resources Laboratory, Training Systems Division for a most exciting summer of research away from the ordinary cares of academic life. Major Hugh Burns and Colonel Crow should be especially commended for providing us with an environment of people, computers, and resources well-suited to our needs and they did so with a concern and courtesy that we all appreciated.

Although it may seem like a long list, we felt so welcomed by the people at the Air Force Human Resources Laboratory that we wish to thank a number of other people for the help they have given us:

Captain Massey, Captain Griffith, Master Sergeant Cruz

Dr. Martha Polson

Ms. Betty Slye

Mr. Rodney Darrah, Ms. Sue Espy

Dr. Roger Pennell, Dr. Joe Yasutake, Mr. Joe Gordon, Mr. Alan Marshall

I. INTRODUCTION

In the summer of 1985, the Air Force Human Resources Laboratory (AFHRL), Training Systems Division, served as the host for a research project funded by the Air Force Office of Scientific Research through the Summer Faculty Research Program / Graduate Student Summer Support Program. The research was conducted by two faculty members and three graduate students from Oakland University, Rochester, MI. The central problem addressed by this research team was the understanding of natural language by computer. The goal of the research was to begin the development of a set of software tools for natural language understanding that could be applied to arbitrary software settings, thus, eliminating much of the redundant research now being carried on in natural language processing.

To the degree that natural language understanding tools could be built, a wide variety of Air Force and Human Resources Laboratory goals could be advanced. For example, a natural language understanding tool could be integrated into a computer's operating system to act as an interface between a computer system and a computer user. This could greatly reduce the confusion caused by the widely differing command languages on different computer systems like the VAX, the IBM and the Cyber systems available at AFHRL. Another place

in which a natural language tool could be of great service is in the many training activities of the Air Force. At the AFHRL, the tools would allow a more human-like communication between student and automated tutor as in the Rule-Kit expert system developed for them by General Dynamics. A natural language interface would allow responses to a wider range of arbitrary requests from the user of the expert system. As these few examples illustrate, once the natural language tools are developed, projects within the AFHRL need no longer create their own natural language systems but, instead, need only use the expanding set of tools.

The research team from Oakland was an interdisciplinary group consisting of three members from the field of computer science and two from linguistics. Dr. Christian Wagner, an assistant professor of engineering and computer science at Oakland University, has been an active researcher in artificial intelligence for twelve years and worked on externally funded research in applying AI to medical diagnosis and treatment as well as decision making in education. With colleagues at Oakland University he has co-chaired major artificial intelligence conferences, developed graduate and undergraduate courses in AI, and run professional development seminars on robotics and advanced automation. Recent research interests have included the

problems of automatic programming and the control of computer and robotic systems through natural language systems with hardware based semantics. Working with Dr. Wagner were two masters degree candidates in computer science, Frances Vallely and Thomas Schnesk. Ms. Vallely has extensive experience in LISP and training in artificial intelligence with an MS in mathematics. She is a university faculty member in computer science and mathematics at Lawrence Institute of Technology and The University of Michigan - Dearborn. With a BS in computer science, Mr. Schnesk has worked as a systems analyst for General Motors. During the last year he has served as a graduate teaching assistant at Oakland University, and faculty member in computer science at The University of Michigan - Flint campus.

Dr. Peter Binkert is an associate professor in linguistics at Oakland University. His theory of Residential Grammar, RG, (Binkert, 1983, 1984, 1985) is the basis for the syntactic parsing tool; the feature-based style of analysis begun in RG is also the basis for the first part of the semantic feature system, those defining cases. His vast knowledge of syntactic theory and extensive research experience were an absolute necessity for the project's progress. Kathleen Malin, a graduate student with an MS in linguistics, has been working with the theory of Residential

Grammar for the past year. Together with Dr. Binkert, she has been involved in the creation of a semantic feature system as well as in the perfection of a case feature system.

II. OBJECTIVES

The stated objectives for the summer research at Lowry Air Force Base were as follows:

1) Case Feature System - A major effort in the linguistic side of the research was the elaboration and clarification of a set of linguistic features out of which the case relations across human languages can be constructed. The use of features for the definition of case relations was to parallel the syntactic feature matrix of Residential Grammar.

2) Semantic Feature System - A central idea behind the planned research in machine understanding of language was that the semantic features for an artificially intelligent system must be grounded in reality. Two different methods for such grounding were attempted: grounding in the universals across human languages and grounding in the physical capabilities of a computer system. This effort

involved expertise in both linguistics and computer science as well as extensive exploration of semantic relationships.

3) LISP Implementation of RG Parser - Because LISP is (a) the language of choice for artificial intelligence in the United States, (b) is definable in the DOD language Ada (Reeker, 1985), and (c) is an easy language in which to implement feature-based systems, a major effort of the research was to translate an existing RG parser written in the language PL-1 into the language LISP.

4) LISP Implementation and Testing of Semantic Feature System - As the semantic feature system for defining cases was completed, it was to be implemented in LISP and integrated with the LISP version of the RG parser.

5) Design and Implementation of Natural Language Front End to an Automatic Programming Systems - The ultimate goal of this phase of the research was to connect the natural language understanding tool (including the syntactic and semantic components) to an automatic programming system.

As the research progressed, modification of the original objectives was required due to resource and time constraints. First, it was discovered that the current LISP capabilities at the Human Resources Laboratory were not

adequate, specifically, no supported and viable version of a LISP processor was available on their VAX computer system. The power of a VAX is generally required for natural language processing because of the large size of dictionary and encyclopedic entries for the words and concepts of the language. Contact was made with DECUS (the DEC users group) to see if a free version of LISP were available for VMS4.0 on the VAX. Unfortunately, it was not. The development of the computer systems, therefore, had to remain bound on the IBM-PC microcomputers for the duration of the project at Lowry.

As translation of the parser from PL-1 into LISP progressed, an unanticipated new objective arose, namely, the redesign of parts of the parser. As the graduate students worked to translate the parser, it became evident that changes had to be made to the parser to more clearly reflect the framework of the syntactic theory. For example, the format of the dictionary entries was modified to allow for the link between semantically related nouns, noun forms, verbs, verb forms, etc. Where words such as "think," "thinker" and "thought" were originally treated as three separate lexical entries, the revised dictionary now lists them all under "think," as subforms of one entry. In addition, the syntactic categories were slightly revised to not only

account for the change in the dictionary entries, but also to more accurately represent links between similar grammatical forms. For example, words indicating temporal and positional location such as "here," "there," "now" and "then" were previously classified only as nouns with the added feature of either +LOCATIVE OF TIME or +LOCATIVE OF PLACE. It became apparent that parsing could be facilitated if new quantifier categories were added to account for these concepts.

III. APPROACHES AND RESULTS

The development of the natural language tools began with two parallel efforts: one by the computer science team to work on the implementation of the LISP version of the syntactic parser of English, the second by the linguistic team to work on the definition of a first set of semantic features out of which the case relations of language could be defined. The results of these efforts are summarized below, by objective.

1) Case Feature System - The approach taken in the definition of a case feature system parallels the successful approach taken in the development of the feature system for the RG syntactic model: a search was made for a set of

semantic features out of which case relations could be defined. As the search proceeded, the two criteria constantly applied to the possible feature systems were the ability to explain case differences across natural languages and the expressibility of the features in terms of the hardware capabilities of computer and robotic systems.

Although not considered by the research team to be in its final form, a set of very promising semantic features has been specified out of which the case relations across natural languages can be defined. Even more, the proposed feature system seems to capture the generalizations of Fillmore's (1966, 1967, 1977) and Gruber's (1965, 1976) case theories and Schank's (1975, 1977) conceptual dependency theory without containing some of the inherent redundancy.

The current feature system provides a complete specification of the case or thematic relation played by every argument (noun phrase) in association with every predicate in the sentence. It provides a means for associating the syntactic components of the sentence such as "subject" and "object" with thematic roles such as "agent" and "patient." The system utilizes twelve binary features which are highly transportable across natural languages and across other conceptual models (e.g., case grammar and conceptual

dependency theory). The theory states that each case relation is an abbreviation for a group of semantic features, just as each syntactic category is represented by an abbreviation of syntactic features. For each semantic entry, all features are specified with one of three possible values: "+", "-", or "+/-". At the current time the twelve semantic features are divided into six primary features and six secondary features. Brief and informal definitions of the features, based on precise and technical specifications, are provided below:

PRIMARY SEMANTIC FEATURES:

POSITIONAL: + having a primary focus on location, orientation, or movement in space or time
- not having a primary focus on location, orientation, or movement in space or time

DISJUNCTIVE: + emphasizing separation
- separation not emphasized

CONJUNCTIVE: + emphasizing union or association
- union or association not emphasized

EXTENSIONAL: + emphasizing the extent of space
- extent of space not emphasized

PROXIMAL: + involving contact
- non involving contact

FIRST ORDER: + involving relationships relative to a point, line or surface
- involving relationships relative to area or volume

SECONDARY SEMANTIC FEATURES:

TEMPORAL: + focusing on time
- focusing on place

Relating to the x, y, z axes:

VERTICAL: + a positive value on the z axis
- a negative value on the z axis

HORIZONTAL: + a positive value on the x axis
- a negative value on the x axis

FRONTAL: + a positive value on the y axis
- a negative value on the y axis

INTERVAL: + involving a medial position
- not involving a medial position

INTENSIVE: + involving a range from average to maximal
- involving a range from minimal to average

Given the existing case feature system, a classification scheme for verbs and prepositions is being created for the efficient storage of large numbers of syntactic and semantic features through simple inheritance networks.

The case feature system proposes that case relations like GOAL, EXPERIENCER, SOURCE, AGENT, et cetera, are actually labels for constellations of semantic features. The commonality in GOAL and EXPERIENCER is the feature [+CONJUNCTIVE] which denotes association or union; the

commonality in SOURCE and AGENT is [+DISJUNCTIVE], which denotes dissociation or separation. Therefore, the fact that the same thematic marker (preposition, postposition, grammatical case, etc.) is used for a variety of thematic relations can be attributed to the presence in those relations of the same feature. The loss of descriptive adequacy in theories of case grammar is shared by other related theories and semantic systems; the common features associated with thematic relations are not expressible, and it becomes a complete accident that the same marker is used across relations.

In addition to the loss of descriptive adequacy, there is a loss of explanatory adequacy in other theoretical frameworks. Thematic relations like SOURCE and GOAL cannot be related in any direct way to the concepts which form semantic networks or to the concepts which underlie other semantic constructs, e.g., the primitives in conceptual dependency theory (Schank 1975, 1977). In short, there is little transportability between the systems, so that the valuable insights of each cannot be gathered into one framework.

For example, it is clear that thematic relations like SOURCE and GOAL from case theory are associated with primitives like EXPEL and INGEST from conceptual dependency theory. But

the two theories are constructed in such a way that this association cannot be specified. Yet, the grammatical facts of natural language, in particular, the distribution of thematic markers, clearly indicate that there must be a connection between thematic relations and semantic fields in general. The same feature which shows up in relations like SOURCE and AGENT ([+DISJUNCTIVE], e.g., "from") should form part of the definition of words like "aversion," "deprive," "need," and so on; and, that feature should also show up in the definition of a primitive like EXPEL if a theory contains such a primitive. Similarly, the same feature that shows up in relations like GOAL and EXPERIENCER ([+CONJUNCTIVE], e.g., "to") should form part of the definition of words like "inclination," "supply," "abundance," and the like and show up in a proposed primitive like INGEST. This feature-based approach to thematic relations provides an explanation for why the same groupings of markers occur repeatedly in natural languages.

The feature system has been challenged through native speaker intuition and comparison to other languages, specifically Japanese. It appears, at this time, that the case feature system proposed here has an advantage over other case grammars. Since the system asserts that the [-POSITIONAL] relations are based on the [+POSITIONAL] ones,

at least the framework for [-POSITIONAL] is given by the existing one for [+POSITIONAL]. As a result, any number of nonpositional thematic relations can and have been posited. The case feature system can explain why the same grammatical case, preposition or postposition ("from" in examples a-g below) embraces both positional and nonpositional relations in examples such as the following:

a. He ran from his office.

b. He is back from Europe.

c. Keep this away from the children.

d. She can't tell red from orange.

e. He can't find any relief from pain.

f. They will be here an hour from now.

g. We got a note from the dean.

It explains why a class like "separative notions" should remain intact diachronically and dialectally.

In addition to the above linguistic support for the case feature system, given a perceptual apparatus (human or machine), the feature definitions can be made very precise. The feature [+/-POSITIONAL] (an intentional renaming of +/-

CONCRETE to emphasize the hardware grounding of the feature) divides semantic concepts into two sets: those that are abstract ([-POSITIONAL]) and those that are concrete ([+POSITIONAL]). This opposition can be precisely defined in terms of the physical capacities of real computing systems. At Oakland University, our Automatix Vision system can compute the area of any object in its visual field with a call to the system function TOTAL_AREA. If, in the computer's memory, a concept has been associated with a non-zero area, it must be concrete ([+POSITIONAL]), i.e., the computer has seen one or been informed that it is possible to see one. If no such association exists, the concept must be abstract ([-POSITIONAL]). By relating as many of the features as possible to the physical capacities of the system in this way, we can begin to attribute real understanding to the computer system, in particular, understanding that makes possible independent verification of natural language statements it receives. Though the entire system has yet to be completed, the case features will be applied to all syntactic categories in hopes of producing a comprehensive semantic description of any given language. The case feature system must be integrated into the larger semantic model and semantic net.

2) Semantic Feature System - Outside of the semantic features defining case relations, little explicit or

extended work was possible on semantic features. We discovered, however, the existing semantic features do, in fact, provide an explanation for the multiple senses and wide range of associations typically given to verbal expressions. It provides a means for specifying higher cognitive concepts such as comparison and quantification. For example, given the verb pair "enter/exit," an adequate semantic mapping of the pair would include the following information:

a. They are motion verbs.

b. 1. "enter" indicates motion forward;
   2. "exit" indicates motion away.

c. They indicate contact with the location.

d. They require three dimensions.

e. The dimension of the location varies.

f. They are related to the prepositions "into/out of" respectively.

g. They mean "go into/go out of."

The RG case feature system represents these relations as follows:

a. [xDISJUNCTIVE, -xCONJUNCTIVE] (Where -x implies the opposite value of x and x may be +/-)

b. 1. "enter" is [-DISJUNCTIVE, +CONJUNCTIVE]
   2. "exit" is [+DISJUNCTIVE, -CONJUNCTIVE]

c. [+PROXIMAL]

d. [-FIRST ORDER]

e. [-EXTENSIONAL]

f. "into/out of" have the same features

g. go is [xDISJUNCTIVE, -xCONJUNCTIVE]

In order for a semantic parser to be utilized in a natural language processor, there must be a theory of semantics as its underlying base. The notion of semantic nets became the model for the base.

A semantic net is a graphical method used for the representation of knowledge. A net consists of nodes representing objects, concepts, or events, and links between the nodes, representing their interrelations. One key feature of the semantic net representation is that important associations can be made explicitly and succinctly: relevant facts about an object or concept can be inferred from the nodes to which they are directly linked, without a search through a large database.

The theoretical aspects of the semantic theory for parsing natural language are in the final stages of formalization. Unfortunately, due to time restrictions, we were unable to complete the implementation of a semantic feature system that would adequately represent the scope of human perceptions within the framework of semantic nets.

3) LISP Implementation of RG Parser - One of the primary objectives of the research to be carried out at Lowry AFB was to translate the existing RG syntactic parser into LISP. Initially the RG parser was implemented using PL/I on the MULTICS system at Oakland University.

The motivation for selecting LISP, as the language of choice over the PL/I version was several fold. LISP is generally acknowledged as the standard U.S. language for work done in the realm of artificial intelligence. A LISP representation facilitates the introduction of semantic features. Also, variations on LISP written in ADA are currently under consideration.

Initially the focus of the work on the parser was viewed as a straight forward task of translation from PL/I into LISP. As the translation process proceeded, however, several problems arose. It became clear that the implementation of the original parser was not conducive to a simple translation into a transportable LISP system. The PL/I parser used character strings and non-portable system calls to the MULTICS mainframe system extensively. Indexing, rather than recursion, was used throughout for the purpose of searching forward and backward over a given sentence. The PL/I routines were excessively large and used deeply nested if-then constructions. Finally, the theoretical basis for

the parser, the RG model, had taken on several important improvements and modifications since the original parser was written. Because of these and other design considerations, an alternate format and some extensive redesign of the system became necessary to take full advantage of LISP as well as the theory of Residential Grammar.

The first step in the design of the LISP system was an investigation into an appropriate global data structure for the representation of the required graphemic, syntactic and semantic knowledge required. As with most LISP systems, the choice of data structures was essentially a semantic network. The net centered on five major node types: word nodes, concept nodes, syntactic nodes, semantic nodes, and functional nodes. Word nodes represented the graphemic input that the system could receive. Each word node was hooked to one or more concept nodes that contained all information relative to the word. The concept node pointed to the various syntactic types of the concept which, in turn, were connected to the various semantic meanings for the given syntactic type. Finally, the semantic meaning was hooked to a functional node which specified the precise function call and argument list required to perform any action.

This data structure required the creation and implementation of numerous constructor and selector functions. Once these

were complete, a dictionary of several hundred concepts was prepared. These concepts contained virtually all of the functions words of the language and enough of the content words to provide an adequate test of the system software.

As the LISP parser evolved, the use and control of these data structures was managed in a way different than the original PL/I parser, specifically, an augmented transition network (ATN) system was created and various, separate ATNs were created to handle the problems of word disambiguation and functional analysis. The following is a graphical representation of an existing ATN designed for the purpose of disambiguating verbs:

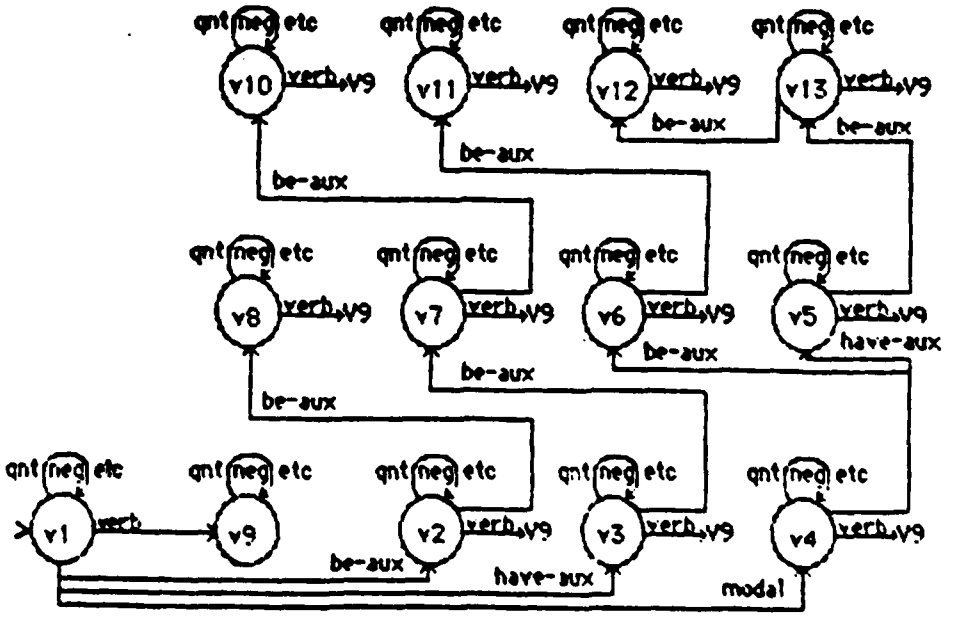

The many, small ATNs that were created each performed specific tiny tasks. The decisions made by the ATNs were only those decisions that were certain so that no backup and no unnecessary searching was performed. The ATN formalism provided a means for specifying the logic of parsing in a manner that more closely reflected the role of the syntactic categories of RG theory. The modularity of the independent ATNs also helped to clarify the grammatical disambiguation process and enhance the possibilities for alteration or expansion of the disambiguation process at a later time if it becomes necessary. Although extensive testing has not been completeed, we feel that the benefits of the change from the PL/I design to the ATN design in LISP will be quite notable. This change in objective has required substantially more time than anticipated since the control flow of the PL/I program was no longer very useful in the translation process.

The balance of the effort involving the LISP parser was centered on the implementation of routines to handle the functional analysis process.

4) LISP Implementation and Testing of Case and Semantic Feature System - This is the one objective that could not be realized during the summer research. The primary reason for this was the greater than expected time committment required

for the translation of the PL/I parser into LISP. Although the objective was not met, a great deal was learned about the problem that will make the eventual solution more correct and rapid. First, the ATN system for manipulating the syntactic parsing provides a straightforward formalism for the statement of the case relationship and semantic processing we will require. Second, the delay will provide us with greater time to study the proposed semantic feature system before attempting to implement them. There is a degree of uncertainty, at this time, as to the correctness of the specific features chosen for case analysis since there is no underlying model yet developed that will predict what these features should be (as there was a specific tree model that predicted the twelve syntactic features of the original parsing system).

5) Design and Implementation of Natural Language Front End to an Automatic Programming Systems - Research efforts for the design and implementation of a natural language front end to an automatic programming system had to begin, obviously, with the development of an automatic programming system itself. The design chosen centered on the concept that a computer's understanding must be grounded in the primitive processes that it can perform.

The design and implementation of the automatic programming system (AUTOP) is still in its formative stages; however, many of its characteristics have been defined. The overall model of the system design process will be based on the PSL/PSA system developed by Teichroew (1978). This system has been widely used in industry and government and seems to have the expressive power to describe an information processing environment. The focus of AUTOP will be to develop a running computer system in a top down fashion that eventually connects to primitive functions of which the underlying computer system is capable. This development will be based on an interactive dialog between the user and the program environment concerning, initially, the five major aspects of a computing system: input, storage, processing, output, and control.

During this short summer session, only a few of the AUTOP components were designed and tested. This allowed a small automatic programming system to be written and tested in a short amount of time. More interestingly, however, the components developed during the ten weeks now act as new primitives available to the AUTOP user in the creation of other new system. For example, in the creation of the program AUTOP, a set of menu driving functions were created (i.e., functions for the construction of data structures required by a menu and routines for the use of these

structures to display a menu, get a selection, and take the designated action). These menu routines are used by AUTOP to perform its functions. In addition, however, these menu routines are now available for AUTOP to use, itself, as it helps another user create a new system. Indeed, in typical computer science style, it might be possible to specify the AUTOP program itself using the AUTOP system. As the AUTOP system expands, the set of "basic primitives" that become the foundation for other systems expands in size and complexity.

At the current time, the basic primitives are divided into two classes: selector and constructor functions. As their names imply, constructor functions enable the user to define and build the basic data structures required and the selector functions query the data structures. The overall goal of an automatic programming system is to define these two basic primitive classes for the user's data and connect them together into a comprehensive working system whereby the user can interactively interface with a computer and design a functional problem solving tool.

The implemented parts of the main system provide control over initial start up (access) of the system and, then, allow eight possible activities. These activities center on the definition of the computing task required by the

user. They are as follows:

1. Create a new system
2. Work on an existing system
3. List existing systems
4. Save a system to a disk
5. Load a system from a disk
6. Run an existing system
7. List data in an existing system
8. Terminate the programming session

These eight options are developed and accessed by the constructor and selector functions that are recursively linked.

Since the main system is divided into separate activities that, in turn, will need to be subdivided, it was only logical that one of the first constructor functions required was that of a menu builder. Menu listing and selecting functions logically followed. These functions can, then, be accessed by the user to develop and build menus as necessary for his individual programming needs while accessing the system, thus utilizing the recursive features of the system. To date in the project, development includes the ability to control and limit access to the system, create a subsystem and establish security for that subsystem, list all

subsystems and save subsystems to a disk for later access.

Work is continuing in the area of describing and building the actual data structures required for the subsystems. The development of data structures is heading in the form of menu and form type input. Eventually, it is the goal of the team to incorporate the natural language tools described earlier into the automatic programming system.

IV. RECOMMENDATIONS AND FUTURE RESEARCH

Our comments on the summer research center on two different areas: the success and future directions of the research performed over the summer and an evaluation of the summer faculty research program and the graduate summer program as well.

Overall, the research effort over the summer was quite successful. Major sections of the RG parser have been implemented in LISP using the ATN formalisms, a tentative set of semantic features for defining case relations is complete, the ATN formalism is ready for the implementation of the case relation data, and the automatic programming system which can eventually be connected to the natural language understanding system has been started.

The current research will continue on several fronts. The natural language understanding tools being developed will be extended to: (1)implement the semantic feature system and extend the semantic framework beyond features associated primarily with verbs to features of other categories; (2)construct semantic nets from the new features; and (3)connect the features and nets to the hardware and software capabilities of existing computer systems. The parsing system will also be examined from another angle, to see if it would be possible for the syntactic parsing program to build the actual RG tree structures as an outcome of parsing the sentences. This would guarantee the correctness of the parser, demonstrate the strengths of the RG theory, and provide a visual demonstration of the same theory. Finally, the automatic programming system will be refined and expanded, possibly as part of a doctoral dissertation, to allow for the creation of simple computer systems under computer control.

The extension to the semantic features for our system will begin with the primitive perceptual, motor, and reasoning capabilities of a network of hardware and software available at Oakland University. This network will serve as a useful target at which our initial investigations of higher level semantic concepts will be aimed, but should in no way be viewed as a limiting or final choice. On this network, we

have an AUTOVISION II system from Automatix, Inc., a PUMA robotic manipulator from Unimation, and a MACLISP programming environment from Honeywell. These hardware and software resources provide us with approximately 45 visual parameters for sensing visual data about an object in a computer's field of view, ten manipulator parameters for sensing position of the arm and controlling its operation, and hundreds of MACLISP functions for sensory, reasoning and control functions.

The reexamination of the parsing method has been suggested by the staff because of the non-obvious way in which the RG model is currently implemented. As a series of separate ATNs, the present LISP parser more clearly isolates the syntactic features of RG. However, a much more concise description of RG is possible now that the ATN formalism has been implemented. Once the co-occurence restrictions of the various parts of speech are specified, the tree structure defining the functional structure of a sentence can be specified. Therefore, if possible, we hope to examine a method of parsing by the merging of RG trees.

The automatic programming system will continue to expand in the five areas described earlier: input, storage, process, output, and control. Essentially, the varieties of inputs

are relatively limited, i.e., a menu input, a form input, a prompt-response input, an analog input, and maybe a few others. The storage types are similarly limited to a small set of primitive types and then a construction mechanism for building arrays and structures from them. As all of the five areas are examined, it becomes clear that recursive nets of inputs within inputs, outputs within outputs, etc. combined with the constraints of the type from PSL/PSA can adequately describe a system. The key is that the bottom of these hierarchies must be in the physical capacities of the software/hardware system on which the program is being developed.

In essence, the purpose of our future research is to develop a system whose understanding is built upon a particular set of hardware capabilities so that it can comprehend not only concrete relationships but also abstract ones. There is a continuous thread from the RG syntactic features that specify grammatical relations to the semantic features that specify case relations to the semantic relations that specify higher cognitive concepts. This entire progression is grounded in the sensory, motor and reasoning capacities of a hardware system.

As for the USAF program and the UES contractors, we have only praise. The members of the Air Force at Lowry were

exceptionally open and helpful in getting us set up and giving us a place to work, supplies, and people to work with. From Colonel Crow and Major Burns to the enlisted personnel, from other university faculty at the HRL to civilian employees, the courtesy and concern for our work was refreshing and appreciated. The contractors from UES were flexible, friendly and demonstrated an efficiency that we at a university greatly envied. The possibilities for integrating our research into the programs of the USAF are much greater as we have made many contacts with members of the military and artificial intelligence researchers here in the University of Colorado. We all feel that the program offered by the Air Force for summer faculty and graduate student research is outstanding and are very glad that we were given the opportunity to participate.

REFERENCES

Binkert, P.J. (1983). Syntactic features in nontransformational grammar. In A. Chukerman, M. Marks & J. Richardson (Eds.), CLS 19, Papers from the nineteenth regional meeting, Ann Arbor, MI: Edwards Brothers.

Binkert, P.J. (1984). Generative grammar without transformations, New York: Mouton Publishers.

Binkert, P.J. (1985). Categorial versus feature-based parsing. To appear in Proceedings of the third annual conference on intelligence systems and machines, Oakland University, Rochester, MI.

Fillmore, C. (1966). Toward a modern theory of case. In D. Reibel and S. Schane (Eds.), Modern studies in English. Englewood Cliffs, NJ: Prentice-Hall.

Fillmore, C. (1967). The case for case. In E. Bach and R. Harms (Eds.), Universals in Linguistic Theory. New York: Holt, Rinehart and Winston.

Fillmore, C. (1977). The case for case reopened. In P. Cole and J. Sadock (Eds.), Syntax and semantics, vol. 8. New York: Academic Press.

Gruber, J. (1965). Studies in lexical relations. Doctoral dissertation, MIT. Bloomington: Indiana University Linguistics Club.

Gruber, J. (1976). Lexical structures in syntax and semantics. New York: North-Holland.

Schank, R.C. (1975). Conceptual information processing. New York: American Elsevier.

Schank, R.C. & Abelson, R.P. (1977). Scripts, plans, goals, and understanding. Hillsdale, N.J.: Lawrence Eribaum.

Teichroew, E. (1978). PSL/PSA. ISDOS Project, Department of Industrial and Operations Engineering, The University of Michigan, Ann Arbor, MI.

1985 USAF-UES SUMMER FACULTY RESEARCH PROGRAM/

GRADUATE STUDENT SUMMER SUPPORT PROGRAM

Sponsored by the

AIR FORCE OFFICE OF SCIENTIFIC RESEARCH

Conducted by the

UNIVERSAL ENERGY SYSTEMS, INC.

FINAL REPORT

SPEECH EFFECTS OF HIGH SUSTAINED ACCELERATION: A PRELIMINARY STUDY

Prepared by:	Z.S. Bond
Academic Rank:	Associate Professor
Department:	Department of Linguistics
University:	Ohio University
Research Location:	Biological Acoustics Branch
	Biodynamics and Bioengineering Division
	Aerospace Medical Research Laboratory
USAF Research:	Thomas J. Moore
	Timothy R. Anderson

Date:	12 August, 1985
Contract:	F49620-85-C-0013

SPEECH EFFECTS OF HIGH SUSTAINED ACCELERATION: A PRELIMINARY STUDY

by

Z.S. Bond

ABSTRACT

The acoustic-phonetic structure of speech produced under adverse circumstances such as high noise levels, vibration, and stress, has received little investigation. The purpose of this study was to provide some preliminary data concerning speech produced under high sustained acceleration. Acoustical measurements were made of a set of words as spoken by two subjects at 1G and 6Gz. Words produced under acceleration were different from words produced at 1G in both durational and spectral characteristics.

ACKNOWLEDGEMENTS

This work was sponsored by the Air Force Office of Scientific Research/AFSC, United States Air Force, under Contract F49620-85-C-0013.

I appreciate the assistance of all the people at AMRL/BB who made my summer pleasant and profitable. I particularly want to acknowledge the help of Tom Moore and Tim Anderson.

I. Introduction: If automatic speech recognition systems are ever to be usefully employed in aircraft cockpits, these systems will have to be able to recognize not only speech produced under good speaking conditions but also speech produced in many types of adverse circumstances, for example, noise, stress, vibration, and so forth. Acceleration is one of the adverse circumstances for speech production needing investigation.

Accelerations are classified according to the direction in which they act on the human body by a three-axis (x, y, z) coordinate system. Headwards acceleration tends to displace body tissue footward; the resultant force is termed positive G or Gz. This is the type of acceleration experienced in aircraft emerging from a dive, for example. High sustained acceleration is defined by Burton, Leverett, and Michaelson (1974) as exposure to acceleration forces of 6G or greater for periods in excess of 15 seconds.

The physiological effects of exposure to high sustained acceleration have been investigated quite extensively (Sharp and Ernsting, 1978, provide a review). Of these effects, two seem to be particularly relevant to speech: changes in respiration and limits to muscle control. According to Gillies (1965), positive acceleration produces "little respiratory

embarrassment, at least at levels compatible with consciousness... The first [symptom] ... is a slight difficulty with inspiration as the thorax has to be lifted against a greater gravitational force, and for the same reason the expiratory phase becomes more rapid" (p. 618). Respiratory symptoms would be expected to be present at 5 or 6 Gz.

The increase in weight under acceleration has effects on mobility involving large muscles at even relatively low levels. It is impossible to raise from the sitting position at 3Gz, for example. However, fine control movements can be performed with little or no loss of accuracy at accelerations of at least 8Gz (Sharp and Ernsting, 1978).

In order to maintain vision and even consciousness at higher accelerations, some anti-G straining maneuvers are necessary. These involve pulling the head down, tensing the skeletal and abdominal muscles as far as possible, and increasing intrathoracic pressure by forcibly exhaling against a partially or completely closed glottis (Burton, et al., 1974). Since these straining maneuvers undoubtedly have an effect on vocal tract configuration, they may also have some effect on speech quality.

II. Objectives: This investigation examined speech samples of two speakers, produced in normal circumstances and at high sustained acceleration, to obtain preliminary information

about the effects of acceleration on the acoustic-phonetic structure of speech. These data are of some interest in themselves, in that they provide information about human speech production under adverse circumstances and thus aid in understanding human speech production in general. The data may also have practical value in testing automatic speech recognition systems.

III. Method: The speakers were both male, volunteer members of the Acceleration Hazardous Duty Panel. The subjects were permitted to participate in the experiment only upon the approval of an attending medical officer.

The speaking style of the two men sounded quite different at first hearing. The first speaker, identified as #7900011, spoke more rapidly and at a higher perceived pitch than the second speaker. The second speaker, #790002, had a pronounced tendency to laryngealize the final portions of the last syllable of words, producing some of these with extremely low vocal fold vibration rates. For example, he ended one token of the word two at a fundamental frequency of 40 Hz.

Materials. The recordings of speech under acceleration were produced using the centrifuge at Wright-Patterson Air Force Base, Ohio, as a part of a speech data base for the development and evaluation of automatic speech recognition

systems for use in military aircraft (Anderson and Moore, 1984; Anderson, Moore and McKinley, 1985).

The recordings were made using a TEAC Tascam 44 4-channel tape recorder and a M-101 noise-canceling military microphone, rather than a laboratory microphone. The speakers were wearing oxygen masks which undoubtedly contribute some distortion to the speech signal. Since the microphone is located in the oxygen mask, the recordings contain the sounds of breathing which sometimes overlap the onset of words and create difficulties in locating their beginings, particularly of words with initial fricatives; finally, sometimes the speech signal itself is noisy.

Each speaker recorded five tokens of each item from a list of Air Force vocabulary words while sitting in the gondola of the accelerator. Then, each speaker recorded several tokens of each word in random order while being accelerated at 6Gz. The number of tokens recorded at 6Gz was determined by the physical state of the subject. A subject was allowed to reach 6Gz for 4½ minutes per day only if he had no significant objective or subjective evidence of fatigue. Consequently, the number of tokens of each word recorded at 6Gz varies from word to word and from subject to subject.

From these recordings, five words were selected for analysis. The words varied in length from one to four

syllables and contained a number of different vowels and consonants. However, the recorded vocabulary did not permit a detailed analysis of a large portion of English segments. The words selected for analysis were: two, seven, zero, frequency, and the letter sequence CCIP, pronounced as /sisiaipi/.

Measurements. Each token of each word was digitized at 16KHz using a 6.4 KHz anti-aliasing filter and 16 bit resolution; each token was stored on disk. Recording and analysis was performed by SPIRE (Zue and Cyphers, 1985) on the Symbolics 3670. Fig. 1 is a display created by SPIRE of the word two, as produced by speaker 790002 at 6Gz. The SPIRE display shows a wide-band spectrogram, formants, the wave-form, and the LPC spectrum. One period is marked on the wave-form.

Segment boundaries were located from a wide-band spectrogram display and a wave-form display, using the segmentation criteria suggested by Peterson and Lehiste (1960) as far as possible. At times, however, segmentation of the test words was difficult or indeterminate because the segment boundaries themselves are indistinct or because of the recording quality and the occasional presence of noise.

Measurements were made of the first three formants of all identifiable vowels, the duration of each word, the duration

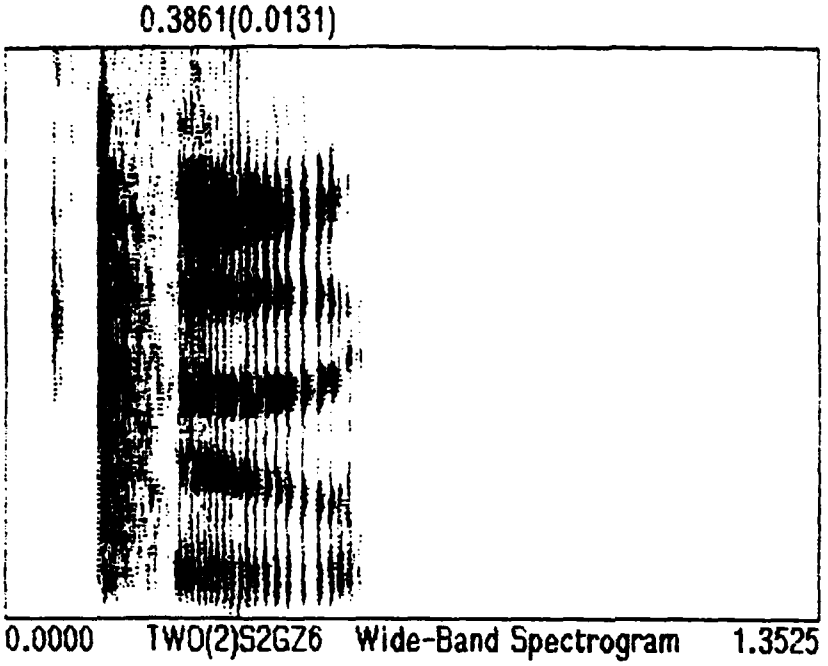

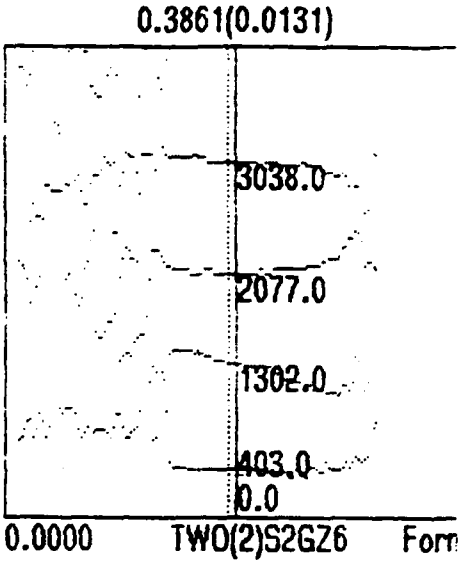

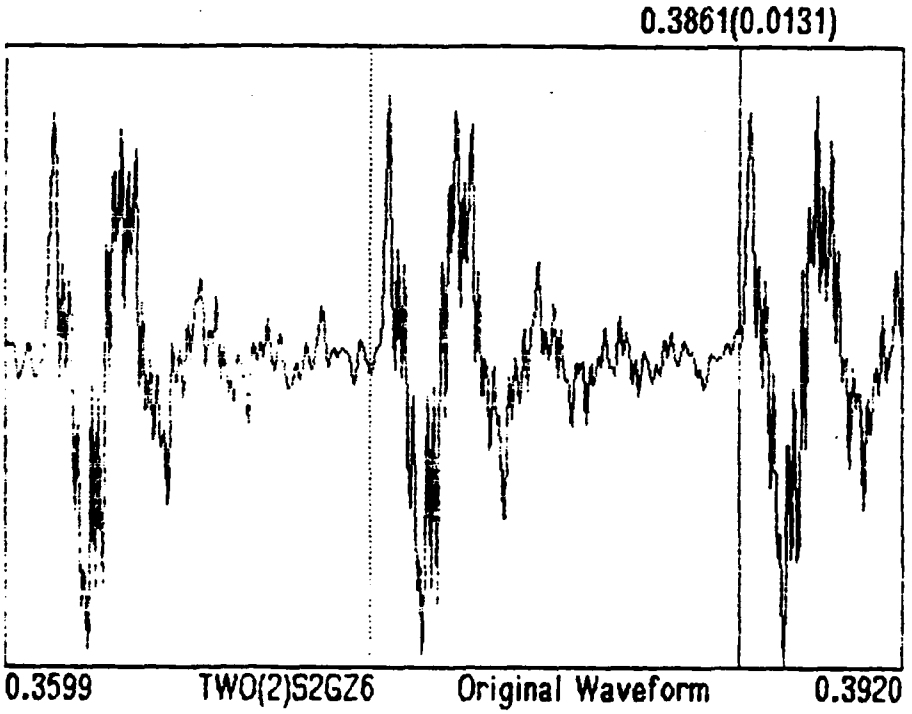

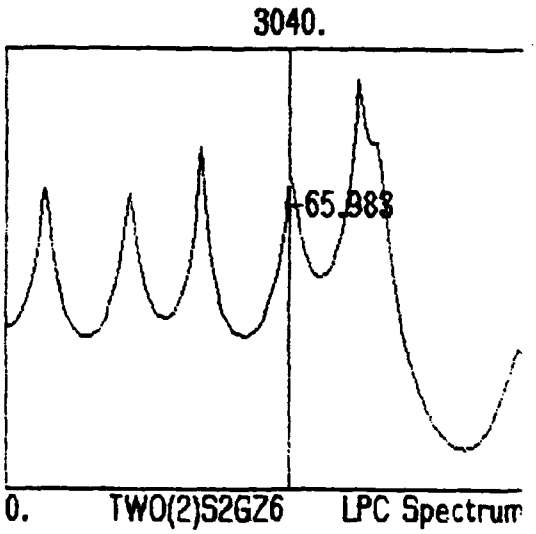

Fig. 1. SPIRE display of the word <u>two</u>, at $6G_z$

of each vowel with a clearly defined boundary, the duration of all intervocalic obstruents, the fundamental frequency, and amplitude within low and high frequency bands at the mid-point of each syllable. In addition, LPC spectrum slices were obtained of stressed vowels.

IV. Results. While speaking under acceleration at 6Gz, both speakers sounded perfectly intelligible and even natural, though other portions of the recording suggested that they were experiencing considerable physical stress and practicing anti-G straining maneuvers to maintain vision. It is not clear whether speech produced under acceleration could be identified as such without other information. However, measurable differences between speech produced at 1G and at 6Gz could be found for both speakers.

Vowel and diphthong formants. Although the vowel space of the two speakers is different, acceleration appears to affect the vowel formants in essentially the same way for both. For speaker 7900011, the second formant of /i/ is lowered and the first formant of /u/ is raised. There is some tendency for the second formant of /ɛ/ to be lowered as well. The first formant of all three vowels is higher in speech produced under acceleration. This speaker begins the vowel /u/ with a very fronted but rounded glide. As a consequence, the formant values of the vowel remain elevated for most of its duration.

The change in the formant pattern under acceleration of speaker 790002 is very similar. For him also, the second formant is lower for /i/ and /ɛ/, higher for /u/. The first formant is somewhat raised for the two front vowels, but not for the back vowel /u/.

The value of the third formant does not appear to be systematically affected by sustained acceleration for either speaker.

Acceleration affects the formant patterns of diphthongs of both speakers in a similar way, lowering the second formant and raising the first formant of both components of /ai/. Fig. 2 shows a SPIRE display for the word CCIP, as produced by speaker 790002 at 1G and at 6Gz. The cursor in the spectrogram and the formant display indicates the lowest value reached by F2 in the diphthong. For /oʊ/, the first formant of both components is somewhat higher and the second formant somewhat lower. As is the case for the monophthongal vowels, the value of the third formant of diphthongs does not appear to be shifted systematically in speech produced under acceleration.

The changes in the formant patterns of vowels for both speakers suggest that the effects of acceleration are to compact the vowel space by shifting the formants of vowels towards a centralized position. In articulatory terms, this formant shift would imply reduced displacement of the

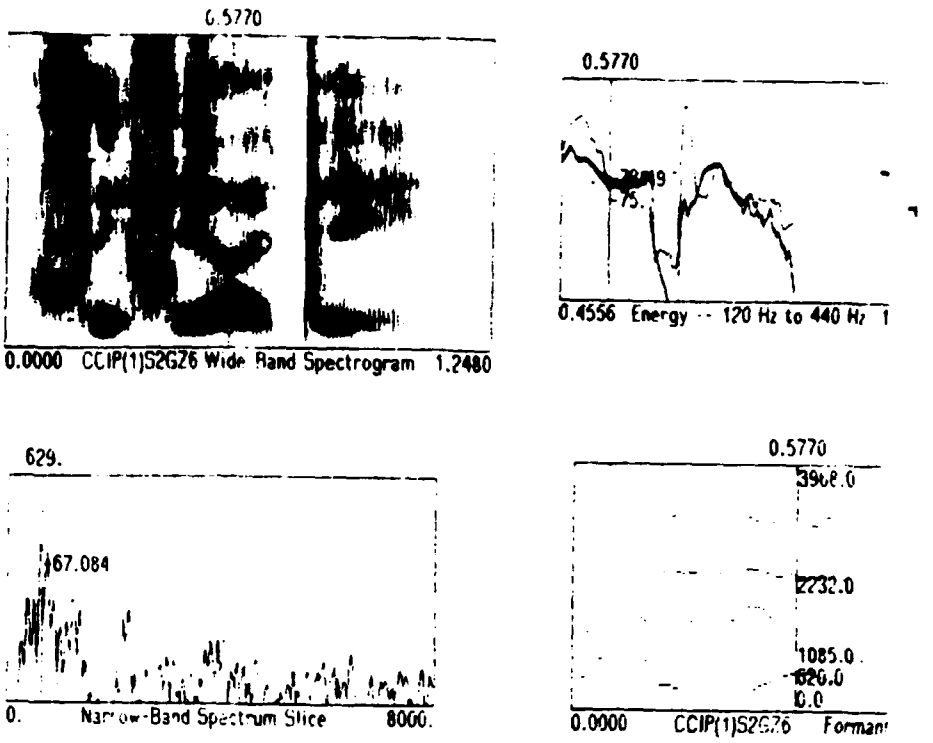

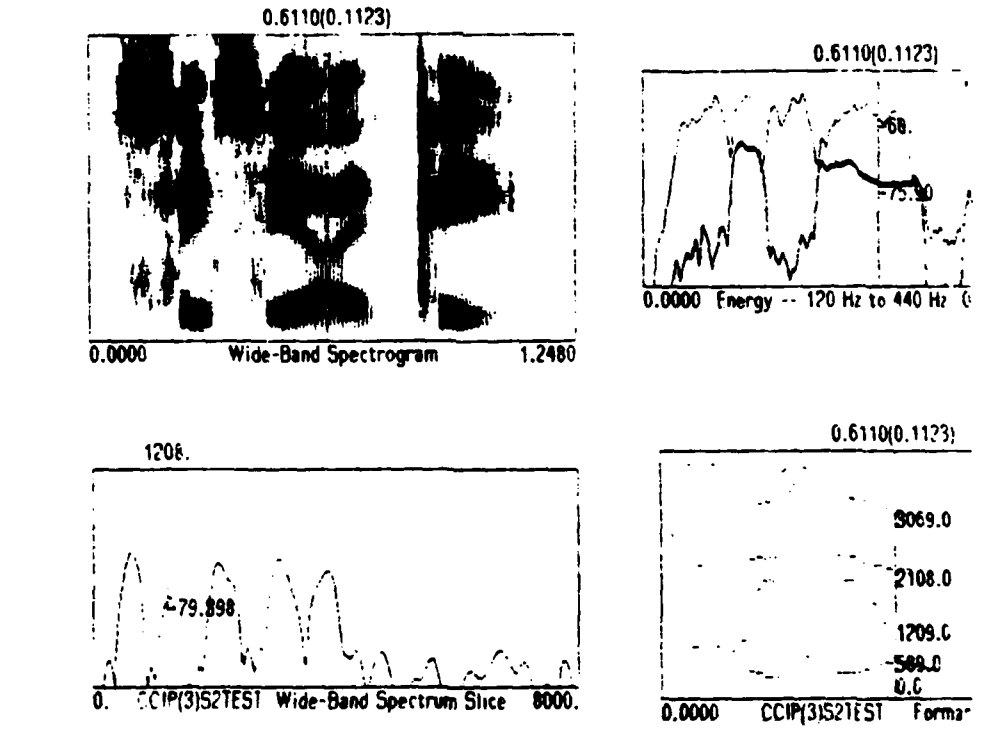

Fig. 2. SPIRE display of the word CCIP at 6 G_z and 1G

articulators. The effect is most clearly present for the second formant which is traditionally associated with tongue advancement.

Fundamental frequency. F0 means and ranges were determined, as measured in all syllables receiving primary stress and in unstressed syllables of two- syllable words under the two acceleration conditions. The F0 range of speaker 790002, who uses some very low vocal fold vibration rates word-finally, is greater than that of speaker 7900011. Under acceleration, the mean fundamental frequency value for both speakers is raised and the fundamental frequency range is increased in stressed syllables. For speaker 7900011, the F0 mean and range in unstressed syllables remain unaffected by acceleration; for speaker 790002, the range decreases somewhat and, correspondingly, the mean increases. The differences in the mean and the range, however, are relatively modest.

Word duration. The two speakers differ in the durations of words they habitually employ and the effects of acceleration on the duration of words are also different for them. Speaker 7900011 speakes relatively rapidly so that his productions of the test words are almost invariably shorter than the other speaker's. The ranges of his productions are very limited, indicating little variabiliy in word duration. Four of the five test words have a slightly higher mean

duration under acceleration; the range of durations does not appear to be affected.

In contrast, speaker 790002 uses greater absolute durations for all words than speaker 7900011 and the range of his utterances is quite extensive. The effects of acceleration on word duration are variable. For three test words, CCIP, frequency, and two, the mean word duration increases under acceleration; for the remaining two words, the mean duration decreases. For two words, zero and frequency, the range increase under acceleration; for the remaining words, the range decreases.

Segment duration. Of the consonants, only the duration of intervocalic obstruents could be measured with adequate accuracy. The measured consonants were the fricatives, /s/ in the words frequency and CCIP and /v/ in seven, and the stops /p/ in CCIP and /k/ in frequency. Both speakers showed slight but very systematic differences in the duration of all these consonants; under acceleration, the mean duration of each consonant decreased slightly. For example, the /s/ in CCIP had a mean duration of 112 msec. at 1G, 86 msec. at 6Gz for speaker 7900011. The comperable values for /s/ in frequency are 120 msec. vs. 105 msec. The same relationships are present for speaker 790002. The /s/ in CCIP has a mean duration of 133 msec at 1G, 114 msec. at 6Gz. The /s/ in frequency measured 162 msec. vs. 112 msec.

The vowels which could be segmented for unambiguous duration measurements were /u/ in two, /ɛ/ in seven, final /i/ in frequency, and first and final /i/ in CCIP. Acceleration had different effects on vowel durations for the two speakers. For speaker 7900011, the mean duration of each vowel invariably increased, from as little as 14 msec. increase for the first vowel in CCIP, to as much as 37 msec. for the final vowel in the same word. For speaker 790002, on the other hand, the effect of acceleration was variable; the average duration of two vowels, /i/ in frequency and /ɛ/ in seven, decreased under acceleration, by 6 msec. and 20 msec., respectively. The duration of the remaining vowels increased, from 14 msec. for the first vowel in CCIP to 90 msec. in two.

It would seem that the changes in word duration associated with acceleration are primarily a function of vowel duration, varying from speaker to speaker. The effects of accelerartion on consonants, though quite small, are similar for both speakers.

Amplitude. There was no appreciable difference between the 1G and 6Gz speaking condition in measures of relative amplitude within the selected high-frequency and low-frequency bands. Examination of LPC spectrum slices for a selection of words produced at 1G and 6Gz showed considerable variability but no detectable trends. It is possible that acceleration has no effect on the relative level of high vs. low frequencies.

It is equally possible, however, that the two frequency bands examined were ill-chosen, particularly with respect to the recording conditions. A detailed examination of what is sometimes called 'spectral tilt' is clearly indicated.

V. Conclusion. Even though speech produced under acceleration does not sound unintelligible or distorted, it does exhibit some specific acoustic-phonetic changes when compared with speech produced under less adverse conditions. The speech of the two speakers examined in this study was affected differently by acceleration.

The formant pattern was affected in the same way for both speakers. The second formant tended to be lower for the front vowels /i, ɛ/ and higher for the back vowel /u/. The first formant was higher for most vowels. The formants of diphthongs were also shifted in the same way for both speakers.

The effects of acceleration on word duration were different for the two speakers. One speaker produced almost all words under acceleration at a greater mean duration; for the other speaker, some words increased in duration, others did not. Mean vowel duration followed the same pattern as word duration, increasing for almost all vowels for one speaker, not for the second. Consonants were invariably shorter in words produced under acceleration for both.

Fundamental frequency increased in stressed syllables for both speakers. But, even though a concomitant increase in the higher frequency components of the speech spectrum would be expected (i.e. a difference in spectral tilt), it was not observed.

These are small but measurable and relatively systematic differences between speech produced under acceleration and speech produced in a more favorable environment. It is possible to speculate about the changes in speech production which are responsible for these differences.

The changes in word duration may result from changes in the pattern of respiration. Under high acceleration, the rate of exhalation increases. Since speech is produced with a slow, gradual and very controled exhalation, it is possible that speakers are attempting to control their exhalation rate and in the process, sometimes are overcompensating. Respiration patterns, however, provide no explanation for the differential effects of acceleration on consonant vs. vowel duration. That vowels might become longer while a speaker is trying to control exhalation is reasonable. That consonants become shorter needs an articulatory explanation.

The consistent formant changes observed under acceleration depend on changes in the articulatory pattern. It seems unlikely that impaired mobility of the articulators

is responsible, since fine motor control is unimpaired at accelerations higher than 6Gz. Rather, the changes in articulation may very well be associated with the straining anti-G maneuvers practiced by the speakers. These maneuvers would tend to increase pharyngeal tension and lead to lessened mobility of the articulators, particularly of the tongue.

Finally, the increase in F0 might be associated with increased laryngeal tension, again a result of the straining maneuvers practiced to counteract the effects of acceleration. The increased laryngeal tension should lead not only to increased F0 but to an increase in the higher-frequency components of the glottal spectrum. This increase was not observed, though better observational techniques may reveal it.

VI. Recommendations. Further research dealing with the effects of acceleration on speech should explore three areas: different acceleration levels, other speakers, and a more extensive sample of English segments.

It would be valuable to investigate acceleration levels between 1G and 6Gz, to determine whether minimal effects on speech would be detectable at lower accelerations. Lower acceleration levels would also help in separating the effects of acceleration from the effects of the anti-G straining maneuvers.

Since the two speakers responded differently,the variability of speaker response to acceleration needs to be investigated.

The generalizations which can be made on the basis of the analyzed words is limited. A selection of words which would provide a more detailed inventory of English consonants and particularly vowels would be valuable.

References

Anderson, T.R. and Moore, T.J. (1984). "Characterizing requirements of speech I/O for military cockpit environments." Proceedings of Speech Tech '84, New York: Media Dimensions, 77-80.

Anderson, T.R., Moore, T.J., and McKinley, R.L. (1985). "Issues in the development and use of a speech recognition data base for military cockpit environments." Proceedings of Speech Tech, '85, New York: Media Dimensions, 172-176.

Burton, R.R., Leverett, S.D., and Michaelson, E.D. (1974). "Man at high sustained +Gz acceleration: a review." Aerospace Medicine, 45, 1115-1136.

Davis, J.R., Ratino, D.A., Van Patten, R.E., Repperger, D.W., and Frazier, J.W. (1984). "Performance and physiological effects of multiple, sequential, +Gx acceleration exposures (space plane boost profiles). Aerospace Medical Research Laboratory Technical Report AFAMRL-TR-84-012.

Gillies, J.A. (1965). A Textbook of Aviation Physiology. Oxford: Pergamon Press.

Peterson, G.E. and Lehiste, I. (1960). "Duration of Syllable Nuclei in English." Journal of the Acoustical Society of America, 32, 693-703.

Sharp, G.R. and Ernsting, J. (1978). "The effects of long duration acceleration." In Aviation Medicine, V. I, Physiology and Human Factors, G. Dhenin and J. Ernsting (eds.), London: Tri-Med Books.

Zue, V.W. and Cyphers, D.S. (1985). "The MIT SPIRE system." Proceedings of Speech Tech '85, New York: Media Dimensions, 277-279.

1985 USAF-UES SUMMER FACULTY RESEARCH PROGRAM

Sponsored by the

AIR FORCE OFFICE OF SCIENTIFIC RESEARCH

Conducted by the

UNIVERSAL ENERGY SYSTEMS, INC.

FINAL REPORT

AUTOMATIC DETERMINATION OF OBJECT ORIENTATION IN 2-D IMAGES

Prepared by:	Dr. Kevin W Bowyer
Academic Rank:	Assistant Professor
Department and	Computer Science and Engineering
University:	University of South Florida
Research Location:	Directorate of Computer Sciences, Applied Mathematics Lab (KRB), Eglin AFB
USAF Research:	Mr. Al Smith
Date:	July 26, 1985
Contract No:	F49620-85-C-0013

AUTOMATIC DETERMINATION OF OBJECT ORIENTATION IN 2-D IMAGES

by

Kevin W. Bowyer

ABSTRACT

This report deals with the problem of determining the orientation of 3-D objects from their appearance in images. The proposed method for solving this problem combines techniques of image enhancement, edge detection, hidden surface projection, and optimization. The immediate application of the method is in demonstrating the feasibility of a more automated Graphic Attitude Determining System (GADS). However, the techniques involved should also have important applications in computer vision and robotics.

ACKNOWLEDGEMENTS

I would like to express appreciation to the people in the Air Force Systems Command and the Air Force Office of Scientific Research who are responsible for this innovative program. I would also like to thank Dr. Robert Braswell, chief of the Directorate of Computer Sciences, for his encouragement and his help in arranging this fellowship.

Ralph Duncan and Bill Clements provided a great deal of assistance and were especially generous of their time during the pre-summer visit. Al Smith provided a regular technical input and guidance during the summer research period. Thanks also to George Weekly, for taking time to review and comment on earlier drafts of this report. And thanks to Calvin George and all the people in the systems group for welcoming me into their working area.

I. INTRODUCTION

The GADS (Graphic Attitude Determining System) is used at Eglin Air Force Base for the purpose of verifying the compatibility of stores to aircraft. The current version of GADS was developed in the late 1970's and has been in regular use for over five years.

The primary inputs to GADS are a 3-D model of the store involved and a series of images showing the store during separation. The GADS operator is able to bring an image up on the display and then use a custom-designed joystick and other controls to rotate a projection of the store model on the display. The operator visually fits the model projection to the store as it appears in the images of separation. This fitting step is the most time-consuming and labor-intensive aspect of the current GADS. The output from processing a sequence of images is a time history of the position and attitude of a store during separation from the aircraft.

The motivations for considering the development of a revised GADS are, in order of importance:

1) faster processing of data,
2) less operator-intensive processing, and
3) increased accuracy in the output.

II. OBJECTIVES OF THE RESEARCH EFFORT

The objective of this research effort is to identify the important issues in developing a more highly automated version of GADS, and to propose a possible method of operation for such a system.

The central problem in developing a more highly automated GADS is how to automate the fitting of a 2-D projection of the store model to the store as it appears in an image. Therefore this report concentrates on the algorithms necessary rather than on the hardware which might support such a system.

III. PROPOSED ALGORITHM FOR DETERMINATION OF OBJECT ORIENTATION

A diagram of the proposed operation of a more automated GADS appears in Figure 1. The proposed algorithm iteratively generates a sequence of estimates of the parameters of orientation. At each step in the sequence, the store model is used to calculate a theoretical 2-D projection of the store, and the store outline obtained from the projection is compared to that obtained from the real image in order to generate the next set of parameter estimates.

The processing steps in Figure 1 are numbered so that they may be easily related to following discussion.

1.A. Digitizing images. This is the simplest of the

subproblems, and primarily involves selecting hardware for the best available combination of price, speed, and compatibility with the computer system to be used.

1.B. Image enhancement. Image enhancement is not a necessary step, and in fact is not done in the current GADS. However, it has the potential to improve the accuracy of further processing at a relatively small cost in processing time. Image enhancement would be performed only once for each image, and would not be a part of the iterative algorithm.

The related techniques of "histogram equalization" and "histogram specification" are used to improve the contrast of images and highlight features which might otherwise be obscured. Histogram equalization is less powerful, but also requires less specific knowledge about the image. Both techniques operate by analyzing the frequency histogram of pixel intensities:

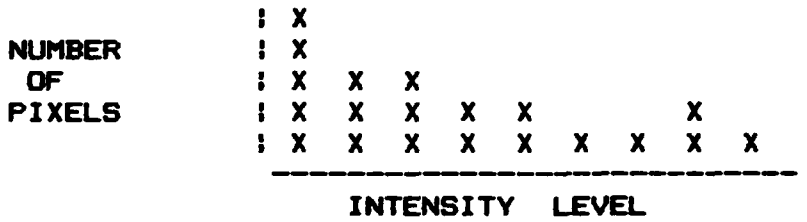

If this histogram is already "flat" (has the same number of pixels at each intensity level), then histogram equalization will have no effect. However, histograms of real-world images tend to have distinct peaks and valleys. This is especially true when the object of interest in the image is obscured by

poor lighting. In this case the pixel intensities of the object of interest are too near those of the background for the object of interest to be easily distinguished. Histogram equalization will expand the separation between these pixel intensities. (Expanding the separation of pixel intensities in one area of the histogram naturally implies compressing the separation between pixel intensities in the other areas.) There are many examples of histogram equalization resulting in dramatic improvement in the quality of images [1,2].

Histogram equalization proceeds by obtaining the cumulative distribution function of pixel density from the raw histogram. The vertical axis of the cumulative distribution function is quantized into as many levels as are available for pixel intensity. The pixels in the image are re-mapped into (potentially) new intensity values by looking up the original value on the horizontal axis and finding its translation on the vertical axis.

Histogram equalization cannot be guaranteed to modify the image in a useful way. As a pathological case, consider a histogram which has two peaks, corresponding to an image with a large shadowy area and a small bright area. If the object of interest in the image is located in the bright area, then equalization will make it even more obscured than in the original image.

Histogram specification achieves better image enhancement than histogram equalization by incorporating knowledge of the range of intensity levels in the object of interest. The shape of the re-mapped histogram is specified to increase separation around exactly these levels. In the case of GADS, the data for histogram specification could come from the average intensity in a small area around a pixel known to be in the store. On the first image of a sequence, this pixel might be selected by the operator; afterward it could be estimated from previous images.

1.C. Edge detection. Edge detection algorithms have been widely studied [1,3,4], and there are several edge detection algorithms which might be appropriate for use in GADS. However, the different edge detection algorithms vary greatly in processing time. A factor of 10 might occur between a simplified Roberts "cross operator" and a "LaPlacian" operator. (Edge detection operators are discussed in [2] and [5].)

1.D. Object isolation. An edge detection algorithm applied to an image produces edges related to all the objects in the image (clouds, underbody of plane, etc). For later processing steps, it is important to have an image in which all edges are due to the store. Thus a "cleaning" step must be applied after edge detection to remove extraneous edges.

Good heuristics are known for removing isolated edges which arise because of noise in the image [2,3]. In addition, it will

be necessary to incorporate some application-specific heuristics to remove edges which arise due to real objects. The basis of these heuristics could be having the operator select a point in the interior of the store, and/or indicate a rectangle enclosing the store. (Any information entered by the operator should only be needed for the first image of a series, since the system should be able to make its own prediction for successive images.) From this information, all edges outside the basic area of interest could automatically be deleted. Then any remaining isolated edges outside the outline of the store could be deleted.

2.A. Calculate initial parameter estimates. Initial estimates for the parameters of orientation must somehow be obtained from the operator, at least for the first image in a sequence.

2.B. Calculate 2-D projection, with hidden surface removal. The objective of this step is to use the estimates of the parameters of orientation to calculate a theoretical 2-D edge outline which can be compared to the edges in the real image.

The mathematics for projecting a point on a 3-D object onto a 2-D image are well understood. The transformation matrix for arbitrary rotation, translation, scaling, and central projection is described by, among others, Giloi [5].

Hidden surface algorithms have historically been viewed as computationally expensive. In addition, most algorithms have

approximated the surface of an object with a fixed number of polygons. The problem with this is that the approximation may not be as accurate as desired, or if the polygons are made small enough to guarantee accuracy processing becomes even more expensive. Recent advances promise slightly improved computational times, and accuracy limited primarily by the fineness of the 2-D image matrix for which the projection is calculated. A good general overview of hidden surface algorithms appears in [5]. Further references which seem especially relevant to GADS are [6] and [7].

Stores in the current GADS are modelled as a construction of two types of primitive pieces: 1) truncated cones (for the body) and 2) extra pieces (fins) defined by points and edges between points. A "truncated cone" is defined by the radii at two points along an axis which runs from top to bottom through the center of the store. Since this model has proven accurate and easy to use, there seems to be little reason to make major changes. This form of definition can in fact be used to advantage in constructing a simple and efficient hidden surface algorithm.

One addition to the model which might prove useful is the ability to define a color for each piece of the model.

Sketch of the recommended algorithm for 2-D projection:

Begin with the truncated cone at one end of the store. Pick

some number of points spaced at equal intervals around the circles defining the top and bottom of the cone. (For instance, 36 points at 10 degree spacing.) Take the first two points on each circle. These four points define a trapezoid which approximates the surface of a portion of the store (Figure 2).

Calculate the projection of the four model surface points onto the 2-D image plane. The four projected points either lie in some area of at most four contiguous pixels, or they lie in some larger area (Figure 3). The two cases are treated differently.

If the points span a four-pixel area or smaller, then the distance from the trapezoid to the image plane is compared to the current "z-buffer" value for each of the (up to four) pixels. ("Z-buffer" is a term used in the literature for a running record of the smallest 'model surface to image plane' distance.) If the new value is less than the current z-buffer value, then this piece of the model surface lies closer to the image plane than any piece previously examined. In this case, the current z-buffer value should be replaced with the new value. In addition, if the object's color is being modeled, then the color buffer entries for each of the (up to four) pixels should also be updated.

If the four projected points span a greater than four pixel area, then the approximation to the model surface is not precise enough and needs to be refined. This is done by slicing the

original truncated cone in half and picking points on the (now) three circles which are spaced half as far apart as the original points. In this way, the original approximation to a portion of the store surface is replaced by four separate and more precise approximations. Each of these more precise approximations is examined in the same way, with some being further refined and some being used immediately to update the image matrix.

This basic algorithm proceeds around the entire surface of the model, with a few extra refinements to increase speed. In this way, the precision of the approximation (and so the amount of computation) is automatically adjusted to reflect the resolution of the image matrix and the projection of the store.

The results of the 2-D projection/hidden surface step are 1) an image matrix in which the pixel values reflect the distance from the store surface to the image plane, and also optionally 2) an image matrix in which the pixel values represent the color of the store surface.

2.C. Edge detection on the projected 2-D image. The silhouette edge of the store is easily found; it is simply the outer perimeter of the projected pixels. Edges which lie inside the silhouette and arise from the structure of the store (fins, bolts, etc) can be found by edge detection applied to the matrix of distance values. Edges which lie inside the silhouette and arise due to the coloring of the store's surface can be found by

edge detection on the color-value matrix. Some combination of these two should be chosen to correspond as closely as possible to the edges found in the real image.

3.A. Locate corresponding edge points in the images. We now have one set of edges obtained from the real image and a second set of edges from the projection. We want to use the differences between the two sets of edges in some way to improve the estimates of the parameters. However, the two sets of edges are likely to be different in many details and will only accidentally contain the same number of pixels. Therefore it would be very difficult to make a pixel-by-pixel comparison.

One way to proceed is to select a small number (6 to 20) of pixels that summarize distinctive features which appear in both sets of edges. The selection of these points is necessarily heuristic and a sequence of several strategies may be needed. The heuristics should be designed to select a group of pixels which uniquely describe the parameters of orientation. The individual points should also be selected in a way that minimizes the possibility of selecting a noise pixel.

Each set of edges can be reduced to a group of chain codes which allow quick and easy processing to search for specific features along the edge. A "chain code" is created by selecting a starting point along the edge and then recording the movements necessary to move along the edge [2,3]. The chain codes for the

edges can be processed to look for the following features:

a) "corner points" are pixels where the slope of the chain code changes drastically and there is a relatively constant slope for several pixels on either side.

b) "curve points" are pixels where the slope of a curved edge reaches a minimum.

A search for points based on these criteria could result is as many as a dozen points selected from a set of edges, most coming from the rear of the store near the fins (Figure 4).

Selected points from the two sets of images now need to paired together as "corresponding" points. The pairing might be done by starting at an obviously corresponding point (for example, the tip point) and proceeding around the edges to locate points which are in the same area and have similar surrounding edge shape. If fewer than eight pairs of edge points are found, then a backup selection heuristic may be needed. This heuristic might select a number of points at equally spaced intervals along smooth edges. At the end of this step, we have reduced the edges derived from the real and projected images to a set of about a dozen corresponding points in the two images.

3.B. Calculate new parameter estimates based on comparison of corresponding points in the two images. The 2-D coordinates of pixels in the projected image translate to known 3-D coordinates on the surface of the model. The 2-D coordinates of pixels in the real image correspond to unknown points on the surface of

the actual store. We now use the "corresponding" points to ask the question: what parameters of orientation make the known points on the surface of the model best correspond to the coordinates of the pixels in the real image?

The method of "damped least squares" has been shown to be especially useful in this type of problem [9]. This method has shown good convergence and refinements can be made to reject bad data points which may occasionally creep in.

3.C. Test for convergence of estimates. The parameter estimates resulting from the "damped least squares" solution in the previous step should be better than the original estimates. A new projected image can be calculated using the new parameter estimates, and new edges found on the new projected image, and new points selected from these new edges. These points can then be used in another damped least squares solution, and so on. This process can be repeated until the parameter estimates reach a desired level of accuracy.

IV. RECOMMENDATIONS

Elements of the proposed algorithm should be implemented and tested on a selection of images processed by the current GADS. The results should indicate the feasibility of a "fully automated" system. Tests to check the feasibility of the major steps in the proposed algorithm are described below.

Image enhancement methods should be implemented and tested on a selection of images of different quality. A comparison of edges detected on the unenhanced, histogram equalized, and histogram specified versions of an image should indicate whether image enhancement is worthwhile to include in a revised GADS.

A selection of several different edge detection algorithms should be implemented and tested on the set of sample images. The algorithms which produce suitable results should be ranked according to their relative execution speed and potential suitability for implementation on an array processor.

A collection of heuristics should be developed which allow the edges arising from the store to be isolated from the other edges in an image. These heuristics should be implemented and tested on the same set of sample images.

The "fitting procedure" which consists of hidden surface projection, landmark point selection, and least squares optimization should be implemented and tested. The parameter estimates resulting from this fitting procedure should be compared with those obtained using the current GADS.

The relative execution speed of the various processing steps should be determined, and any bottlenecks identified. Slower steps should be investigated for possible re-organization that

would speed them up. Possibilities for "parallel" or "vector" implementation should be identified.

The results of the recommended tests should provide a rational basis for the specification of requirements for a revised GADS.

Several further considerations, in the area of quality control, might also be mentioned. It is important that the system provide feedback which allows an operator to assess the reliability of the results. At a minimum, an automated GADS should be able to provide:

a) record of real image,

b) record of detected edges overlaid on real image,

c) record of edges found in the projected image,

d) record of projected edges overlaid on real image edges,

e) history of changes in parameter estimates.

The complete "manual" capabilities of the current GADS should be a subset of any new system. No automated system will work perfectly on all data, and bugs may arise even after long use of the system. There is no reason not to provide any new system with a manual backup method which is known to work.

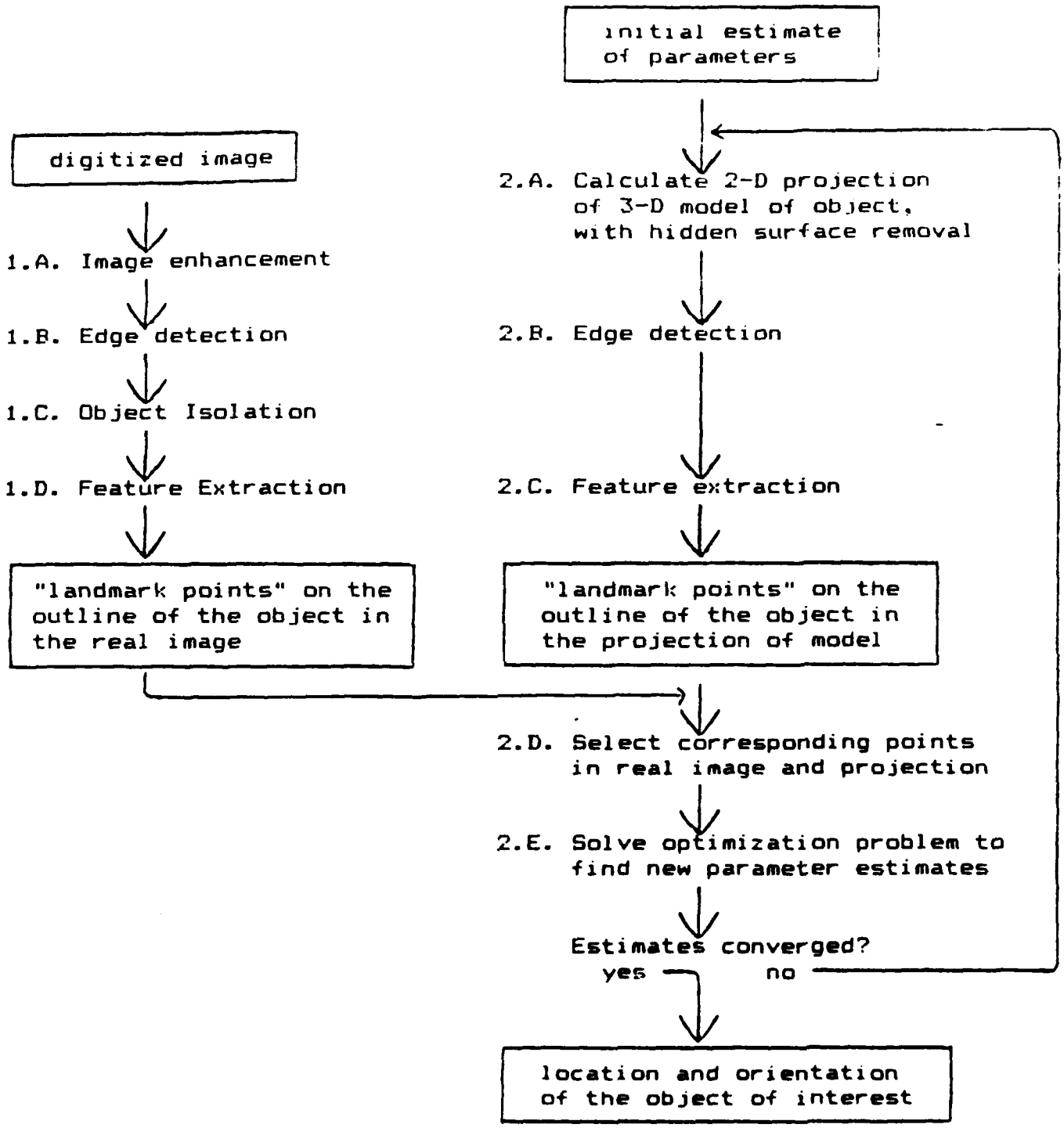

Figure 1. Diagram of Algorithm to Find Location and Orientation

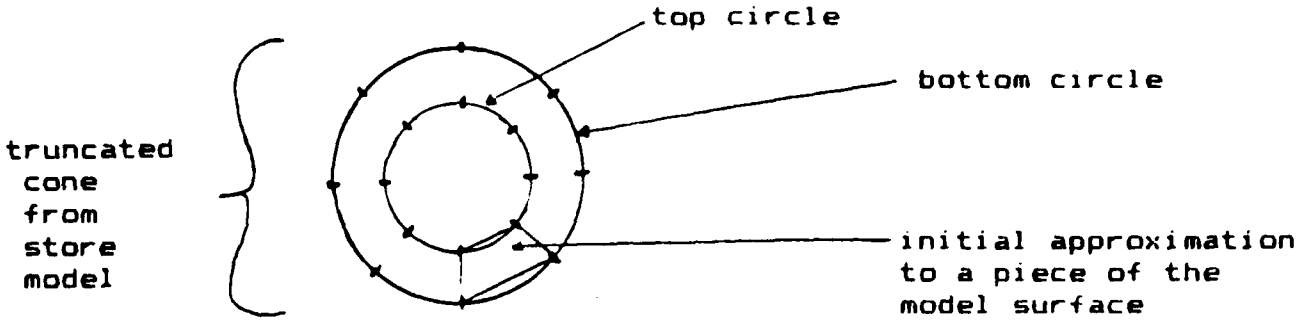

Figure 2. Trapezoid Approximation to a Piece of Truncated Cone Model.

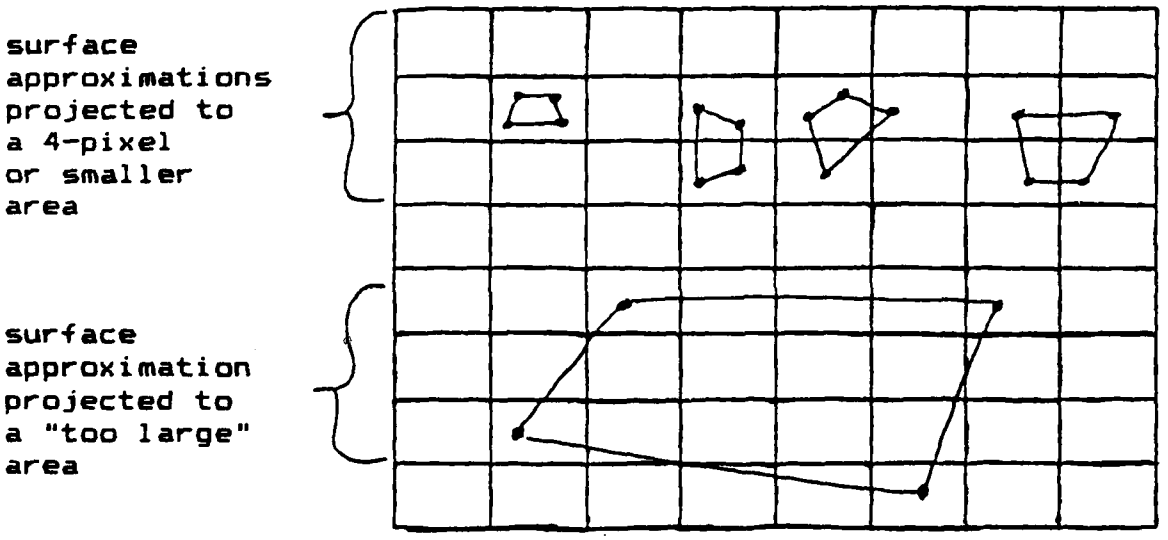

Figure 3. Possible Projections of Corners of Trapezoid Approximation.

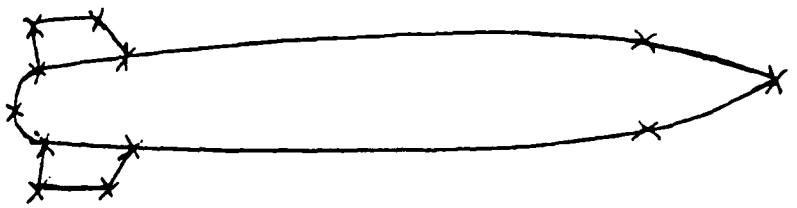

Figure 4. Possible Detected Feature Points on the Store Silhouette.

1985 USAF-UES SUMMER FACULTY RESEARCH PROGRAM/
GRADUATE STUDENT SUMMER SUPPORT PROGRAM

Sponsored by the
AIR FORCE OFFICE OF SCENTIFIC RESEARCH
Conducted by the
UNIVERSAL ENERGY SYSTEMS, INC.

FINAL REPORT

Simulation of Jet Injection Using RAVEN

Prepared by: Eugene F. Brown

Academic Rank: Professor

Department and University: Mechanical Engineering Department, Virginia Polytechnic University

Research Location: Weapons Laboratory, Laser Device Division, Fluid Mechanics Branch, Computational Fluids Team.

USAF Research: Dr. N. L. Rapagnani

Date: 23 August 1985

Contract No: F49620-85-C-0013

ABSTRACT

The transverse injection of a sonic jet into a transonic free-stream flow was calculated using a three-dimensional Navier-Stokes computer program called RAVEN. Satisfactory results were obtained including the prediction of the bow shock, the separation shock, and the expected amount of penetration. Additional work is proposed including the addition of turbulence modelling and the calculation of a supersonic, reattaching, back-step flow.

I. INTRODUCTION: This summer I was assigned to the Fluid Mechanics Branch (ARDE) of the Air Force Weapons Laboratory (AFWL). ARDE had the responsibility for calculations experiments which were bring carried out for the Oxygen-Iodine Laser Branch (ARDA) in support of the COIL project. It was felt that my experience with developing and running large scale computer codes and particularly my experience with transonic internal flows would permit me to make an effective contribution to this project.

II. OBJECTIVES OF THE RESEARCH EFFORT: The objective of the work in which I was involved was to determine the extent of mixing between a nitrogen freestream and a transverse jet of helium. This simulates the injection of iodine into an oxygen freestream in a energy transfer laser. For these calculations the RAVEN code (1) was to be used. It was my responsibility to carry out these calculations. I was also involved in an advisory capacity in planning the experiments. During the planning of these experiments, my suggestions on contouring the wind tunnel nozzle and methods of measurement were solicited. Ultimately the results of my calculations will be compared with the results of the experiments to obtain a knowledge of the trajectory and configuration of the jet as well as the nature and extent of the mixing which takes place.

III. FAMILARIZATION WITH RAVEN: The experiments being supported by ARDA involve the transverse injection of a laminar sonic jet into a laminar transonic freestream. Although this is a three-dimensional problem, it is not a particularly complicated case from the standpoint of the full capabilities of RAVEN (which includes chemical kinetics and laser pumping calculations in addition to the capabilities exercised here). It does pose a formidable problem from the standpoint of an uninitiated user, however. For this reason I began by running several simplified cases one of which appeared as test cases in the users manual for the program. The first of these was a 15° wedge nozzle run in a two-dimensional mode with laminar, Mach 2 inlet flow. Typical results from these calcualtions are shown in Figure 1 where the velocity vectors in the nozzle are plotted. The existence of the surprisingly thick boundary layer

is due to the fact that the calculation is laminar rather than turbulent. Although it is not particularly clearly shown in the velocity vector plots, the pressure contours such as those shown in Figure 2 clearly show an unexpected oblique shock which spans the nozzle. I was expecting the flow to be shock-free. This experience illustrates the importance of carefully considering the inlet conditions if expected results are to be obtained. In this case I expected that the calculations would simulate a radially expanding supersonic flow. The boundary conditions compatible with this situation are a constant value of velocity along the arc of a circle centered at the apex of the nozzle; however, the velocity input to the calculations was constant along a vertical line perpendicular to the centerplane of the nozzle.

The second case I ran was the two-dimensional equivalent of the three-dimensional injection problem. This was a useful test case since results could be obtained quite quickly (in comparison with the three-dimensional case), and I could therefore learn in an inexpensive way how to configure the input for a two species (nitrogen and helium) injection problem. I felt I needed some experience doing this, since none of the cases in the users manual described a two-species problem. Figure 3 shows the velocity vector plot after 500 iterations. The results are as expected with the jet penetration at the downstream plane being approximately four injection diameters.

This brings up the whole question of the proper setting of the downstream boundary conditions. In the calculations shown here, extrapolation-type boundary conditions have been imposed which, due to the recirculating nature of the flow on the downstream boundary, are clearly inappropriate. In order to set the downstream boundary conditions properly it would be necessary to increase the size of the computational region in the downstream direction so as to entirely contain the zone of recirculating flow. The flow at the downstream boundary would then be directed out of the computational zone, and therefore extrapolation boundary conditions could be legitimately used. The failure to properly set the downstream boundary conditions was evident in later calculations where the results appeared to be becoming unstable at 800 iterations.

IV. RAVEN SIMULATION: Having gained sufficient experience at this point, three-dimensional injection calculations were begun. In these calculations (just as in the two-dimensional case) the Mach number of the freestream was set equal to 1.4 and the injected jet was assumed to be sonic. The static pressure of the (nitrogen) freestream was assumed to be 10 torr and the static pressure of the (helium) injected jet was assumed to be 100 torr. The total temperature of both the nitrogen and helium flows was assumed to be equal to 300K. The 6mm-diameter helium jet was simulated by a 6 mm square, the center which was located 9 mm downstream from the entrance of the computational volume. In order to minimize the number of grid points required in the simulation, attention was given to selecting the smallest computational volume possible. Further reduction in the number of computational points was achieved by taking advantage of the plane of symmetry of the problem. Accordingly a computational volume nominally 8 x 6 x 2 cm positioned in the plane symmetry of the flow was used in the calculations. The mesh spacing used was one-half of the injection jet diameter. This gave a grid of 4,704 (28 x 21 x 8) nodes.

V. RESULTS OF CALCULATION: The first calculations were carried out with a reduced value of the jet velocity. In these calculations the jet velocity was set equal to the velocity of the freestream, namely, 41,800 cm/s. The results of these calculations are shown in Figure 4 and contain the velocity vectors predicted in the flow field at the 140th iteration. Compared with the two-dimensional calculations, the region of recirculating flow downstream of the jet is sharply reduced. In fact in these calculations it is not even in evidence. It must be kept in mind, however, that these calculations are not fully converged nor may the mesh size be sufficently fine to pick up the small zone of recirculating flow which would be expected to appear downstream of the jet.

When the calculations were carried out to 1040 iterations and examined, the results were disappointing. The calculations clearly had not converged. Even more disturbing was the fact that the jet penetrated into the freestream much farther than should be expected. I felt that this unusual result might be due to beginning the calculations too close to the location where the jet was injected. This makes it impossible to

capture the bow shock and therefore results in a situation where unrealistic inlet flow conditions are prescribed upstream of the jet.

Accordingly, the calculations were regrided so that the injection location lay 5½ diameters downstream of the plane where the calculations were begun. In addition these new calculations were run with a ratio of jet static pressure to freestream static pressure of 5 rather than 10. This was done because, in preliminary experimental tests using the higher static pressure ratio, the jet was found to block the test section.

The results of the new calculations were very satisfying. I experienced convergence at approximately 600 iterations. I confirmed this by running the calculations for an additional 400 iterations and observed no change in the results. Figure 5 contains the velocity vectors in the center plane at 840 iterations. The penetration is 4 diameters at 6 diameters downstream of the jet. This was about what I expected. The density contours are shown in Figure 6. They show the expected compression immediately ahead of the jet, as well as the bowshock. Figure 7 shows the helium contours (again in the center plane). Large concentration gradients are shown on the windward side of the jet associated with the rapid mixing which takes place there and a much more gradual decrease in helium concentration on the leeward side of the jet. Of interest is the "wrinkle" shown in the "1" concentration contour. I believe that this is due to the so-called "separation shock" which results from the impingement of the supersonic freestream on the zone of separated flow produced by the injection of the jet.

VI <u>RECOMMENDATIONS</u>: These calculations should be regarded as only a first step in the actual verification of RAVEN code. Clearly a definitive statement on the quality of the results must await the collection of data from the injection experiments which are currently underway. Nevertheless it is possible to speculate on the source of the inevitable discrepancies which will arise between these predictions and the data which we are awaiting and to make recommendations for overcoming these difficulties.

I am confident that one of the difficulties we will face is the rather coarse mesh which was used in the calculations. The scale of the interaction between the freestream and the jet is perhaps an order of magnitude less than the scale of the mesh used in the calculations. To resolve the complex shock wave boundary layer interaction phenomena which is occurring here, I suggest that the calculations be run with an expanding grid which clusters points along the wall which contains the jet.

It also concerns me that the calculations are currently being run with a value of viscosity which approximately 100 times the actual value. This was done in order to achieve a suitably low value of the cell Reynolds numbers. This avoids computational instabilities. Attention should be given to examining the true limits of cell Reynolds number for such calculations (perhaps using the two-dimensional counterpart of this problem) in order to run the calculations with a value of the viscosity as close to the actual value as possible.

In order to obtain reasonable results, it may well be necessary to introduce some sort of a turbulence model to account for the unsteadiness which is known to exist in such problems even at the low Reynolds numbers present in laser devices. To account for this I recommend that the k-epsilon turbulence model be investigated to determine if improved agreement with the experiment is produced. Other turbulence models should be investigated as well.

Another interesting case related to the performance of laser devices is that of calculating the flow over a rearward facing step. There is some excellent data available from the 1980/81 Stanford Conference on Complex Turbulent Flows (2) for just such a case. An important extension of the present work to further validate RAVEN would be to attempt to calculate such a configuration. I recommend that this be carried out.

It is my hope that AFOSR will be able to support this research through their Research Initiation Grant Program. Because of a prior commitment I, myself, will be unable to participate in the work directly; however, I have briefed my colleague, Dr. Hal L. Moses, on my summer's work. In fact, he has already visited me and my Air Force colleagues here at Kirt-

land and is very eager to continue the work which I have begun. He is currently interviewing prospective Graduate Assistants to help him with this work.

I hope that arrangements to continue this work can be made promptly. Clearly it is in the best interests of everyone concerned to see that this work is continued without unnecessary delay.

ACKNOWLEDGEMENTS

I am very grateful to the Air Force Systems Command, Air Force Office of Scientific Research, for selecting me for their Summer Faculty Research Program. I am particularly grateful to Major Gerald A. Hasen and Dr. N. L. Rapagnani for suggesting this project. I am particularly grateful to Captain Martin J. Trout and Dr. R. R. Mikatarian with whom I worked on a daily basis and without whose help in running RAVEN and interpreting its results I would have been able to accomplish a small fraction of the work reported here.

REFERENCES

1. Hendricks, W.L. et al., "RAVEN: A Computer Code for the Solution to the Time-Dependent, Three-Dimensional Navier-Stokes Equations with Non-Equilibrium Chemistry, Laser Gain, and Turbulence, Vol I and II, AFWL-TR-138, Vol I and II, April 1983.

2. Kline, S. J., B. J. Cantwell, and G. M. Lilley, 1980-81 AFOSA, HTTM, Stanford Conference on Complex Turbulent Shear Flows, Vol. I, 1981, pp 479-481.

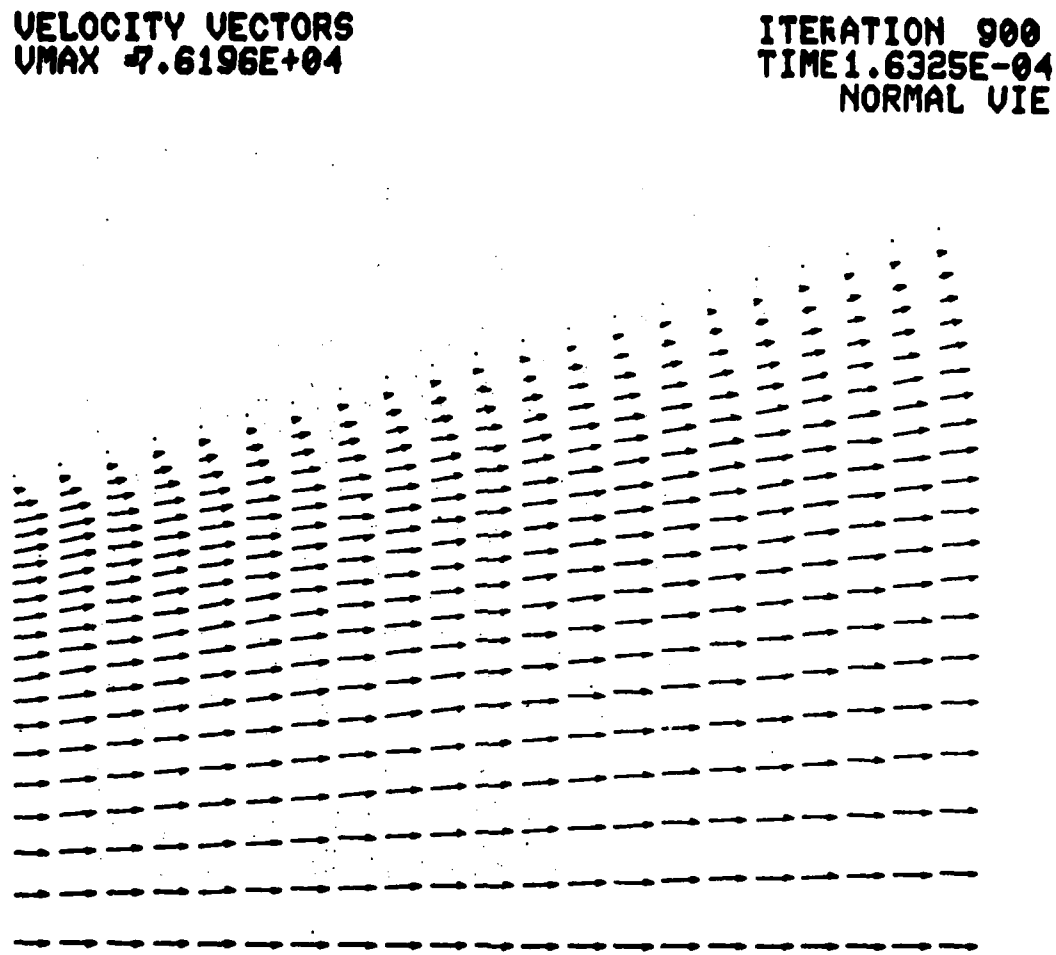

Fig. 1. Velocity Vectors, 15- Degree Wedge

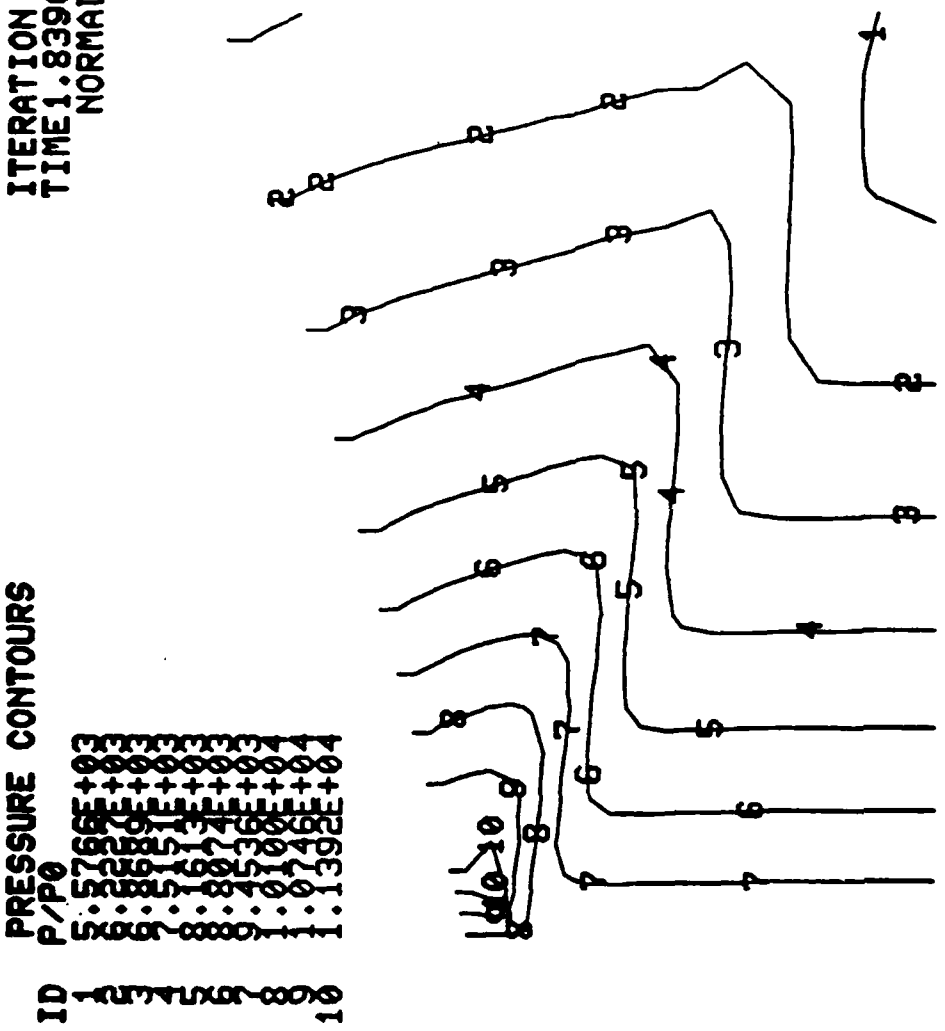

Fig. 2. Pressure Contours, 15-Degree Wedge

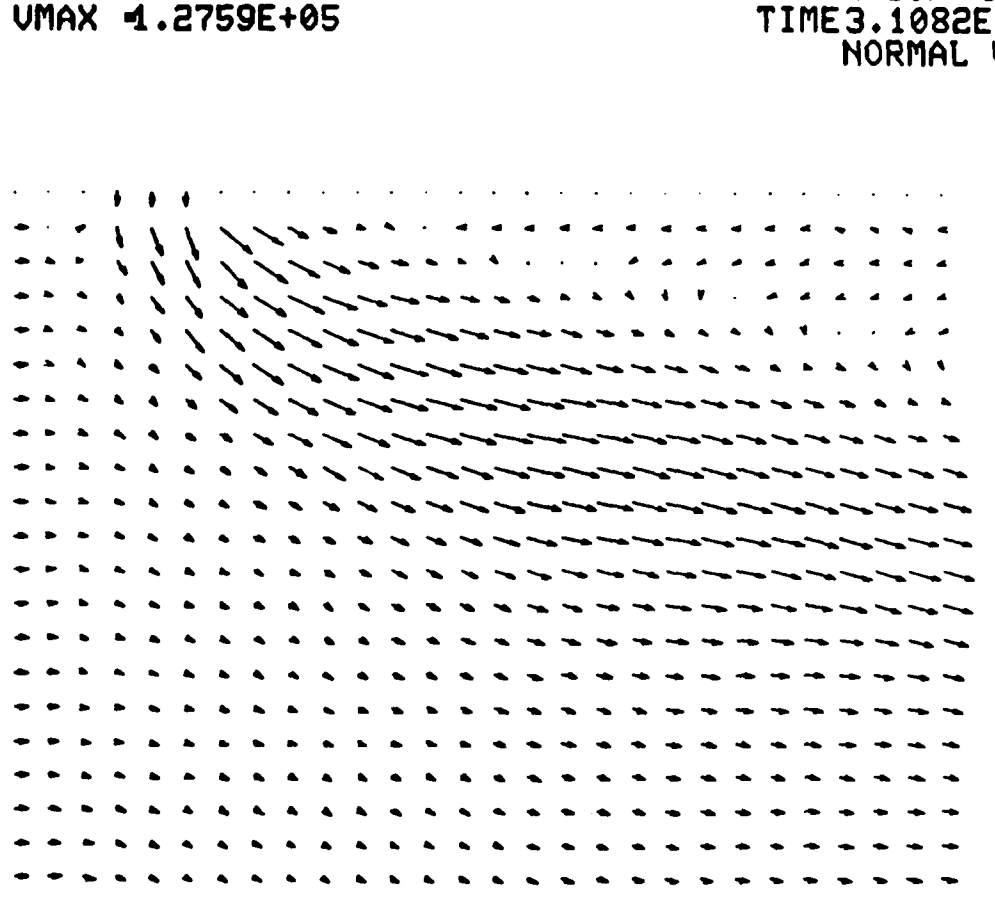

Fig. 3. Velocity Vectors, 2-D Injection

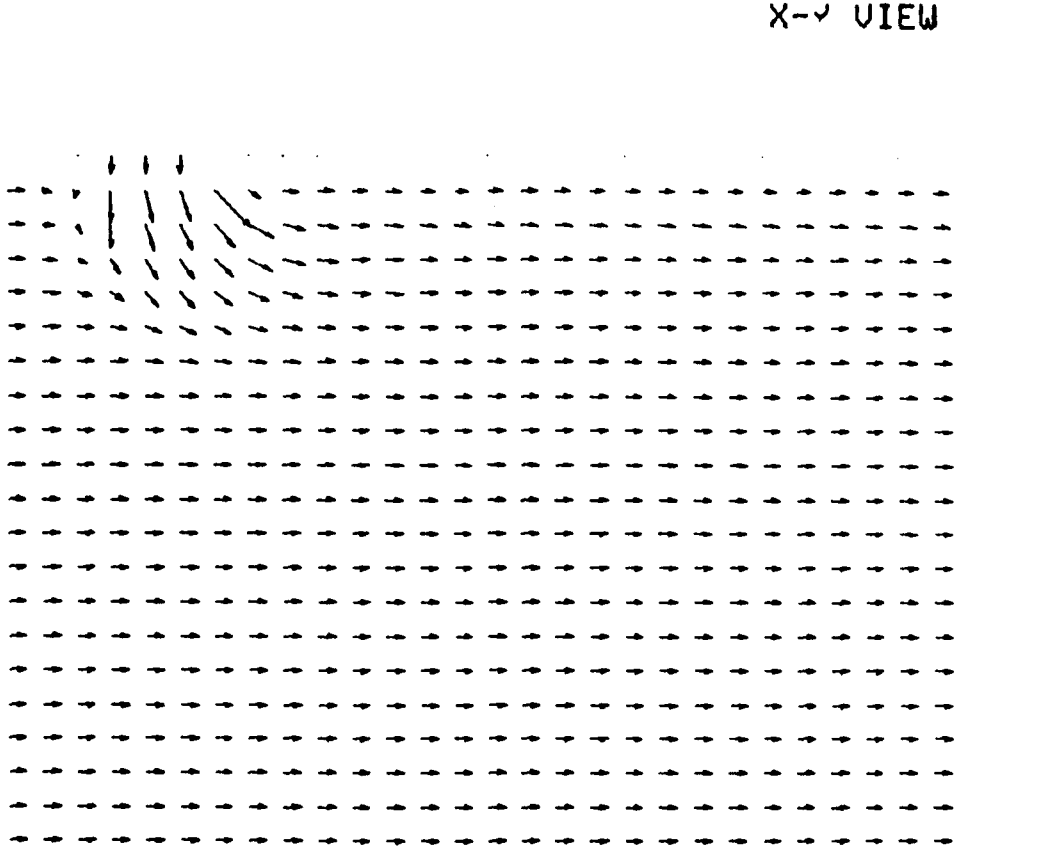

Fig. 4. Velocity Vectors, 3-D Injection, Original Calculation

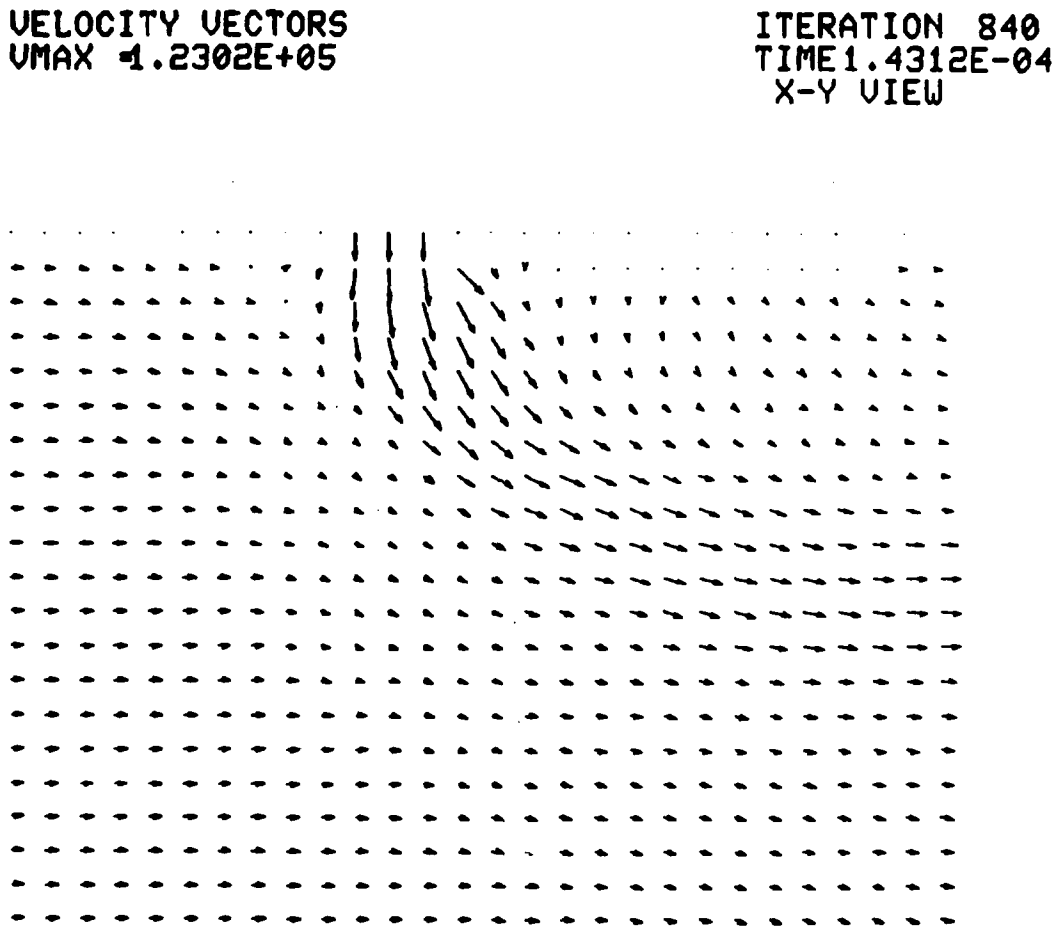

Fig. 5. Velocity Vectors, 3-D Injection, New Calculations

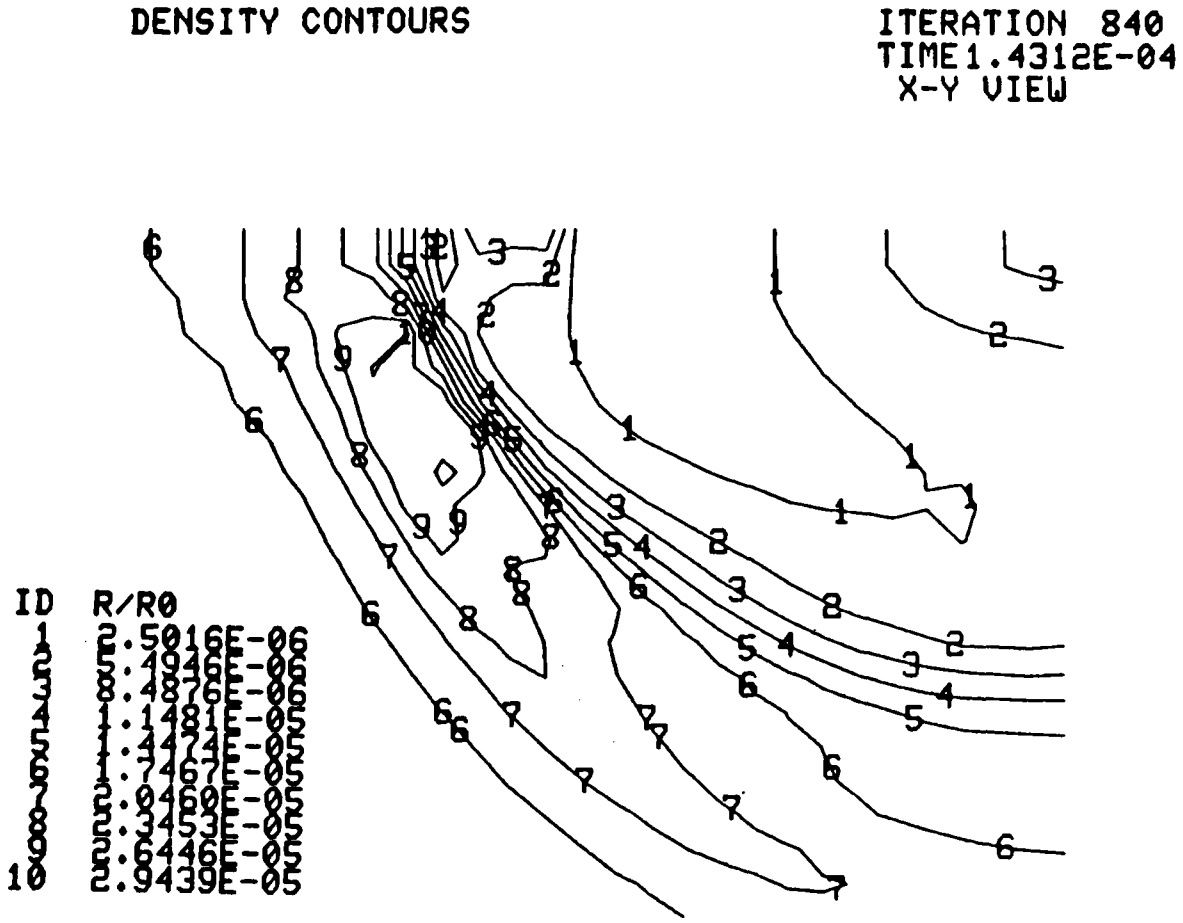

Fig. 6. Density Contours, 3-D Injection

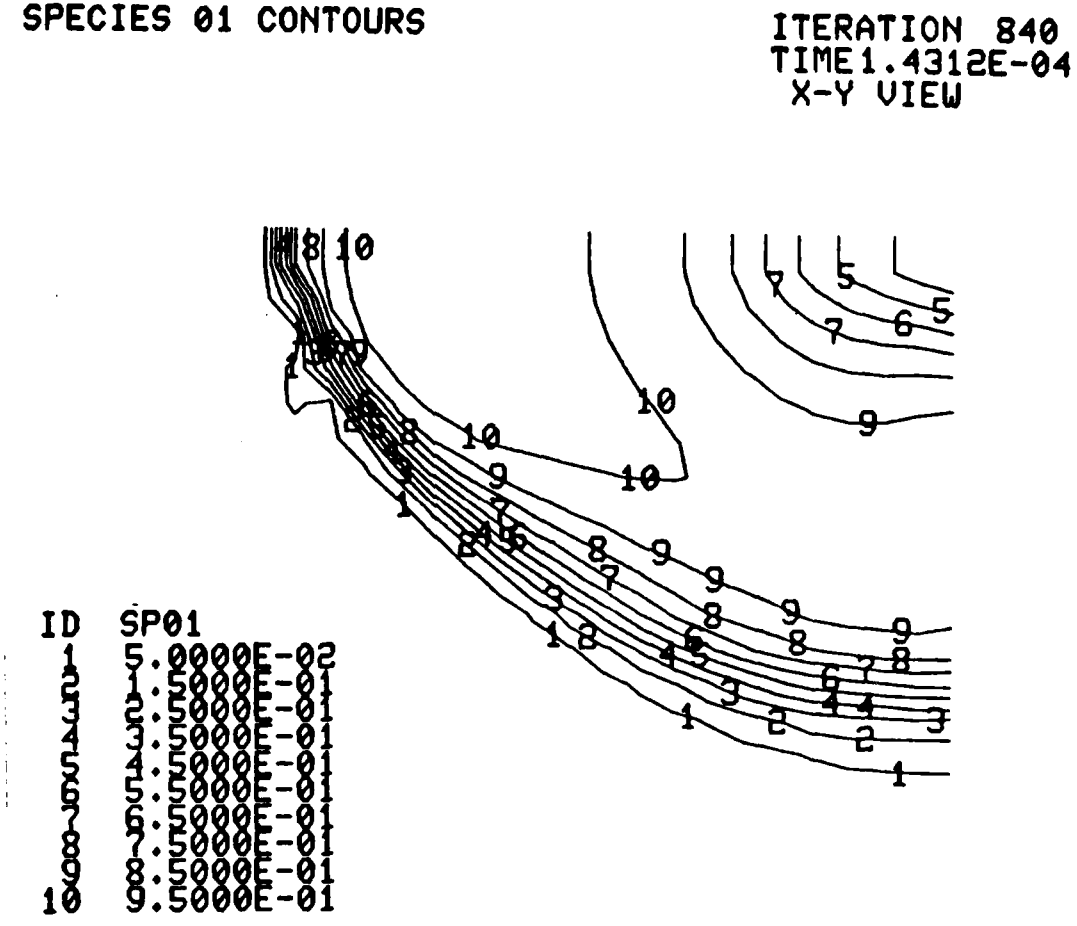

Fig. 7. Helium Concentration Contours, 3-D Injection

1985 USAF-UES SUMMER FACULTY RESEARCH PROGRAM/

GRADUATE STUDENT SUMMER SUPPORT PROGRAM

Sponsored by the

AIR FORCE OFFICE OF SCIENTIFIC RESEARCH

Conducted by the

UNIVERSAL ENERGY SYSTEMS, INC.

FINAL REPORT

THE IMPACT OF COGNITIVE STYLES AND SUBJECT MATTER ON INSTRUCTIONAL DESIGN

Prepared by:	Linda J. Buehner, Ed.D.
Academic Rank:	Assistant Professor
Department and University:	Department of Education, Wittenberg University
Research Location:	Air Force Human Resources Laboratory, Logistics and Human Factors Division, Ground Operations Branch
USAF Research:	Mr. Bertram W. Cream
Date:	15 August 1985
Contract No:	F49620-85-C-0013

THE IMPACT OF COGNITIVE STYLES AND SUBJECT MATTER ON INSTRUCTIONAL DESIGN

by

Linda J. Buehner, Ed.D.

ABSTRACT

Basic research in neuropsychology, learning theory, memory, and cognitive psychology have contributed to knowledge concerning human learning. This research has been applied to the identification of cognitive styles, defined as an individual's unique method of processing information. Research into ways to apply this knowledge through computer-based instruction, the increased use of microcomputers, and the introduction of artificial intelligence techniques into training has permitted more effective use of computer-based instruction in training applications. Instructional designers, however, are not currently provided with adequate techniques for the development of individualized instruction. Research also acknowledges the importance of taking into account the nature of the training subject matter content. Guidelines concerning information presentation in computer-based instruction should be provided for instructional designers to allow for the individual cognitive style of the trainee and for differences in subject matter content. This paper reviews current research in neuropsychology, cognitive style, and instructional design. It will provide a framework for further research in the most effective mode of information presentation, considering the interaction of cognitive style and training subject matter.

ACKNOWLEDGMENTS

The author would like to thank the Air Force Systems Command and the Air Force Office of Scientific Research for making possible a rewarding Summer Faculty Research Fellowship at the Air Force Human Resources Laboratory, Logistics and Human Factors Division, Ground Operations Branch, Wright-Patterson Air Force Base, Ohio. I would like to express my sincere appreciation to the Laboratory, particularly to the Branch, for providing a stimulating working environment. All members of the Branch willingly provided enormous professional and personal support, which has been greatly appreciated. Special thank go to Mr. Bertram Cream for his insightful guidance throughout the project, Mr. Lawrence Finegold for many helpful discussions and editorial comments, Dr. Lawrence Reed, Mr. Michael Young, and Dr. Michael Venturino for helpful discussion, Ms. Rosemarie Preidis for sharing her knowledge about the Air Force, and Mrs. Katherine Paris for administrative support.

Introduction

Basic research in the areas of learning theory, memory, neuropsychology (hemisphericity), and cognitive psychology (information processing) have all made significant contributions to our knowledge about how human learning occurs. This knowledge has been applied to the identification of cognitive styles. Cognitive styles include the unique patterns an individual utilizes in processing information. Research into ways to apply this knowledge, including methodological development in the use of computer-based instruction, the advent of more powerful and inexpensive microcomputers, and the introduction of artificial intelligence techniques into training, has permitted more effective and cost-efficient use of computer-based instruction in a wide variety of training applications.

Instructional designers, however, are not currently provided with adequate tools and techniques for the development of instructional programs tailored to the individual needs of the trainee (learner). In many of the current training programs, it is assumed that all trainees process and store information in the same manner. It is the responsibility of the trainee to match their learning to the format of the instruction. Recent research demonstrates that trainees process information differently (e.g., Messick, 1966; Kogan, 1971). For example, some individuals best retain information presented graphically and holistically, while others best process information serially (with verbal presentation). Some researchers (e.g., Moore & Nawrocki, 1979) also acknowledge the importance of taking into account the nature of the subject matter or task characteristics when planning instruction. This knowledge can facilitate retention and eventual transfer of training to the job situation.

Currently, designers of computer-based instruction are not provided adequate guidelines for the development of programs which both meet individual cognitive style characteristics of trainees and allow for differences in the subject matter content. The problem lies both in the

current lack of adequate, detailed knowledge of certain critical aspects of cognitive style and the manner in which to structure and present training material. If the elements of subject matter content and cognitive style are consistently considered when planning instruction, it is proposed that training effectiveness and efficiency can be enhanced. With the development of guidelines for instructional designers, computer-based instruction shows promise in its capacity to allow for flexibility in instruction to meet individual needs.

The objective of this paper is to review current research in the areas of neuropsychology, cognitive psychology, and instructional design and to then develop proposed guidelines for the design of computer-based instruction which will provide a framework for further research. This paper first approaches this objective through a review of current research in neuropsychology and cognitive psychology. The neuropsychological research addresses the functions of the left and right hemispheres of the brain in human information processing. Research in cognitive psychology builds on the knowledge of hemispheric processing through the study of cognitive styles. The paper then combines this knowledge with research in instructional design and the nature of subject matter. This review then serves as a basis for combining the critical aspects of cognitive style and subject matter content into a proposed identification of concerns relevant to the design of computer-based instruction.

Current Research in Neuropsychology

Research into the organization and functioning of the human brain has resulted in the identification of two hemispheres having some separate but cooperatively-shared responsiblities in the processing of information (e.g., Luria, 1973; Ornstein, 1977; Kinsbourne, 1978; Hart, 1983; Hermann, 1981). Kinsbourne (1978) and others discuss the basic factors of cerebral lateralization. The left hemisphere is primarily responsible for logical/deductive/analytic thought, verbal/alphanumeric functioning, and language development. The right hemisphere's role relates to

holistic (global) thought, inductive reasoning, synthesis of information, and the processing of visual/spatial information. While the left hemisphere responds to symbolic/verbal input, the right processes non-verbal (non-phonetic) input, as in tonal/musical information. The left hemisphere processes the names of individuals, while the right is associated with facial recognition and retention (e.g., Rubenzer, 1979). In tasks involving planning and mathematical calculation, the left hemisphere has primary processing responsibility. The right hemisphere emphasizes the processing of visual/spatial relationships (Hermann, 1981) and alternately aids in such tasks as driving a car (involving the synthesis of much information) and geometry (Frances and Sperry, 1977). The asymmetrical responsibilities of the human brain appear to be task-dependent to a degree (Schwartz et. al., 1976). Although each hemisphere accepts primary responsibility for certain functions, these responsibilites may be shared for some tasks. These functions appear to be located, as described, in approximately 98% of all right-handed persons and 75% of all left-handed persons (Wittrock, 1980).

The two hemispheres process information resulting from sensory input. Sensory input to the left side of the body (hand, eye, ear, etc.) is processed in the right hemisphere (e.g., Wittrock, 1980) and input to the right side of the body is processed in the left hemisphere. Studies such as Sperry's (1968) support this processing notion. Sperry displayed the word "keycase" to a number of subjects. The word "key" was displayed to the left visual field (implying right-hemisphere processing) and "case" to the right visual field (implying left-hemisphere processing). After viewing these words, the subjects were shown a list of words and asked to identify the word they were shown. The subjects identified "case" as the word shown earlier. Additionally, the subjects were asked to feel inside a bag for the object representing the word they had initially seen. In this case, the subjects identified the key. Through this research, Sperry supports the concept of contralateral processing, defined as the processing which is carried out in the opposite hemisphere from the sensory input.

Taylor (1978), in research on reading comprehension, supports the notion that visual/spatial processing is the responsibility of the right hemisphere. In this research, it was demonstrated that iconic presentations (e.g., diagrams, charts, pictures) of verbal information (alphanumeric, auditory) facilities comprehension, and the processing of this information is a function of the right hemisphere. Kimura (1973) also relates kinesthetics to the right hemisphere due to the pronounced preference for the left hand to be used for the reading of braille. In perceiving relationships, the right hemisphere is capable of simultaneously processing information (Rubenzer, 1979). If presented with several variables, the right hemisphere can process these variables best simultaneously rather than sequentially.

In verbal processing tasks, Kimura (1961) identified the left-right dichotomy and later (Kimura, 1967) conducted research in cerebral asymmetry in dichotic listening. This research indicated that melodic patterns are best processed through the left ear (right hemisphere) and words/digits are best processed through the right ear (left hemisphere). Additional research on aspects of right-hemisphere processing was conducted with left-right hemisphere-damaged patients (Faglioni, Spinnler & Vignolo, 1960). The results indicated that right hemisphere-damaged subjects performed poorly on meaningless sound tests and left hemisphere-damaged subjects performed poorly on meaningful sound tests. The experiments conclude that the recognition of non-verbal and perceptually complex auditory patterns are processed mainly in the right hemisphere.

Some research (Wittrock, 1980) indicates that the processing of music is different for trained musicians than for casual listeners. It is postulated that trained musicians process music through the left hemisphere. Trained musicians analyze the sounds and elements of music in much the same way as an individual deductively processes a word or sentence. With casual musical listeners, however, the emphasis in processing is on the global elements of music and primary processing occurs in the right hemisphere. Zenhausern (1978) also supports the

notion that input to the right hemisphere is holistic, but acknowledges that, at times, it may be analytic in its processing. The importance of these "global" elements in processing is also supported by Kolers and Roediger (1984). In discussing the proceduralist perspective of information processing, the secondary features (e.g., configuration of words, prosodic cues, etc.) are an important addition to primary features (e.g., symbology, etc.) for effective information processing. The results of these studies suggest initially preferred processing modes, but shared responsibilities (e.g., skill and complexity) increase. As these skills encourage shared hemispheric processing, however, both holistic (secondary) and analytic aspects are important.

Although each hemisphere appears to have varying responsibilities, it is simplistic to assume a dichotomous relationship (e.g., Luria, 1973; Hermann, 1981; Schwartz et. al, 1976). The interaction of both hemispheres is, instead, viewed as a complementary relationship. Hemispheric processing is a continuum in which dominance is distributed. The utilization of both hemispheres for certain tasks has been demonstrated, but differential aptitudes in functions may lead to the emphasis of one hemisphere over another in individual processing (e.g., Dumas & Morgan, 1975). It is postulated that approximately 68% of the general population are left-hemisphere dominant and 23% are right-hemisphere dominant, with approximately 9% of mixed dominance (e.g., Hart, 1982). Although emphasizing the cooperation of both hemispheres for effective information processing (e.g., Rubenzer, 1979; Reynolds & Torrance, 1981), the evidence of cerebral dominance is growing and it appears that this dominance and lateralization of functioning develops quite early in life (Kinsbourne, 1975), during infancy and preschool years.

In research to support this notion, Bracht (1970) cites evidence that the emphasis on verbal input results in superior performance for subjects with low spatial ability and spatial input proves more successful for subjects with low verbal ability. Cohen & Freeman (1978) have found that left-handed individuals (though to be right-hemisphere dominant) are

poorer readers than right-handed individuals (thought to be mostly left-hemisphere dominant). In addition, left-handed subjects rely more heavily on the visual analysis of text and demonstrate more difficulty than right-handed subjects when the text is visually distorted.

Read (1981), in research with subjects having had unilateral temporal lobectomy, studied the use of visual imagery in the processing of information. The results of the research suggest that imagery can be utilized by both hemispheres, but its use may be task-dependent. Read found that individuals with right-hemisphere damage could still use imagery when solving a deductive reasoning task (thought to be a left-hemisphere task). Individuals with left-hemisphere damage could not, and had difficulty solving the deductive reasoning task. He suggests the possibility of two types of imagery, alphanumeric/symbolic imagery and perceptual, which relates to the more global/spatial elements of imagery. If the left-hemisphere damaged subjects were also left-hemisphere dominant, then this damage could, indeed, prevent the use of imagery since they may not systematically use much imagery in thought processing. Likewise, damage to the "dominant" hemisphere will create difficulty in solving deductive reasoning tasks, regardless of the use of imagery (alphanumeric or perceptual). The right-hemisphere damaged subject, on the other hand, may utilize much imagery in solving all problems, and damage to the right hemisphere still enables the use of alphanumeric imagery. Pellegrino & Kail (1982) identify research procedures to begin to identify spatial aptitude with tasks.

Results of the neuropsychology research to date imply a lateralization of functions in the two hemispheres, with the right hemisphere predominantly responsible for spatial, holistic, inductive processing and the left hemisphere predominantly responsible for analytic, sequential, verbal processing. However, cooperation between both hemispheres, for the most effective processing of information, is emphasized in research. There is evidence to suggest that although information is processed with both hemispheres, individuals tend to process information differently. These differences may indicate a

AD-A166 176 UNITED STATES AIR FORCE SUMMER FACULTY RESEARCH PROGRAM 85/13
1985 TECHNICAL RE (U)UNIVERSAL ENERGY SYSTEMS INC
DAYTON OH R C DARRAH ET AL DEC 85 AFOSR-TR-86-0139
UNCLASSIFIED F49620-85-C-0013 F/G 5/9 NL

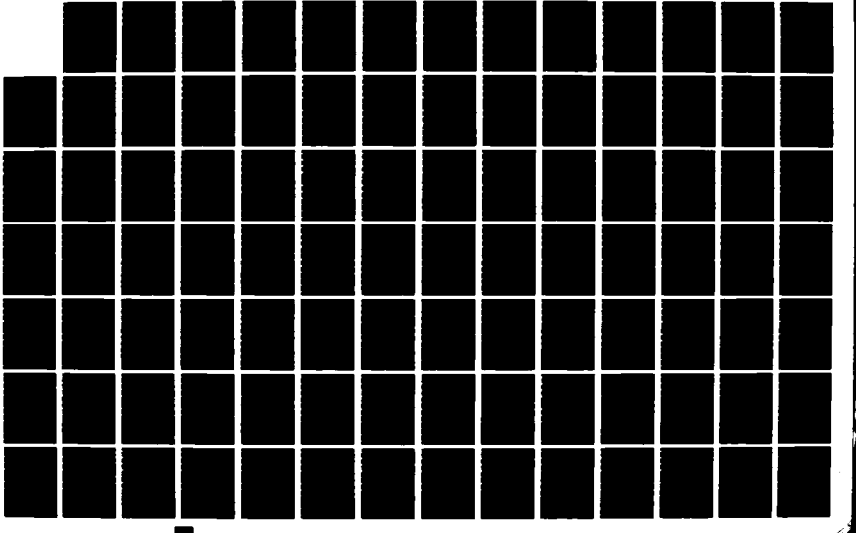

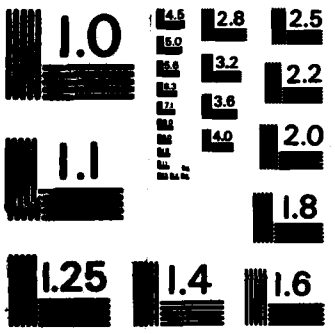

MICROCOPY RESOLUTION TEST CHART
NATIONAL BUREAU OF STANDARDS-1963-A

dominance of one hemisphere over the other. Therefore, although processing capability is drawn from both hemispheres, individuals tend to emsphasize the capability of one hemisphere as a "starting" place for information processing and this emphasis varies among people. This brief review of current research in neuropsychology indicates some agreement on the characteristics of left- and right-hemispheric processing. These identified characteristics appear to relate to the dominant processing mode of individuals and are listed in Table 1. For example, if an individual is identified as "left-hemisphere dominant," the individual may display many of the identified characteristics of left-hemisphere dominance (see Table 1). Current research is only beginning to relate the characteristics within each processing mode to each other. Much of this study is conducted in the area of cognitive psychology. The review of cognitive psychology research attempts to combine neuropsychological research with additional research in cognitive styles.

Current Research in Cognitive Psychology

Emerging from neuropsychology research into the realm of cognitive psychology is the notion of cognitive style. Cognitive style, initially termed by Allport (1937), has been described as an individual's typical mode of thinking, problem-solving, perceiving, and remembering (Schwen, Bedner & Hodson, 1979). Ausburn & Ausburn (1978) refer to cognitive style as the psychological dimensions that represent consistencies in an individual's method of acquiring and processing information. Cognitive style is thought to include all processes used in information processing: perception; thought; memory; imagery; and problem-solving. These individual differences in cognitive styles appear to be related to hemispheric dominance (Wittrock, 1980) and differences in modes of processing information (Ausburn & Ausburn, 1978). These differences are not related to <u>which</u> hemisphere is utilized, only to the <u>degree</u> in which one is used over another.

Messick (1966) identified nine dimensions of cognitive style. Kogan (1971) and Lowenfeld (1970) each added an additional dimension. Many

reviews of the research conducted on these eleven styles (described in Table 2) have been written (e.g., Ragan et. al., 1979; Ausburn & Ausburn, 1978; Wittrock, 1980). In addition to these dimensions, Kolb (1976) identifies two styles, each with two categories. The first style includes concrete experience and abstract conceptualization. This aspect of style depicts the continuum of thinking in terms of abstraction. The second category includes active experimentation and reflective observation. This style relates to the continuum of learner interaction with the environment. Therefore, Kolb continues to identify the continuum with a dichotomous relationship at each end.

Pask & Scott (1972) divide cognitive styles into serialistic and holistic processors. Serialists view the world in a progressive, developmental, sequential pattern. Holists, on the other hand, relate to more global perspectives of situations. Serving as a basis for conversation theory (Pask, 1984), this serialist versus holist dichotomy has been used to define learner characteristics for the design of instruction.

Each of these perspectives of cognitive styles indicate a bi-polar relationship (Witkin et. al, 1977), with the two extremes of each relationship defined. Current research in cognitive processing emphasizes the dichotomous, hierarchical functioning of the left and right hemispheres. It is imperative to continue to emphasize that in individuals, the range represents a continuum within the dichotomy, and an individual's style represents an emphasis toward one end of the dichotomous factor. It is proposed that this dichotomy of cognitive style may also have a relationship to the dominance characteristics of left- and right-hemispheric processing. Many of the characteristics of left-/right-hemisphere processing appear to also relate to cognitive style dimensions. A proposed attempt to combine the research in neuropsychology and cognitive psychology is presented in Figure 1. As an individual progresses up the "thinking skills" hierarchy, thinking processes become more abstract, complex, and integrated (proposed by both left and right hemisphere). Characteristics of left- and

right-hemispheric processing dominance are listed on the appropriate side of the triangular diagram in Figure 1. As a result of study into the characteristics of each cognitive style dimension, the dichotomies of style have been matched to the characteristics of the two hemispheric processing patterns. The dimensions of conceptualization and learning behavior are proposed as both hierarchical and lateral characteristics. Other dimensions of styles are proposed as lateral characteristics with hierarchical blending toward complementary as "higher- order" thinking occurs.

One aspect of this dichotomy, verbal versus visual (spatial) processing, has been extensively considered. Lohman (1979) reviewed evidence of the division between verbal and visual/spatial processing. Verbal processing is defined as the recognition/retention of alphanumeric symbology, as in the reading of text. Visual (spatial) processing includes the pictorial, graphic representations, including pictures. Kozlowski & Bryan (1977), in their study on spatial orientation and individual differences, acknowledge that individuals process spatial information differently and with varying degrees of success. Levin et. al. (1974) also support learning style differences for words and pictures. The results of their study indicate that the use of imagery in reading with subjects who are strong "picture learners" enhances reading achievement. Imagery does not, however, help the subjects categorized as "weak" picture learners. In another study on spatial information processing, Cooper (1982) reports that analytic processors have decreased reaction time for the recognition of more complex spatial information, while holistic processors do not. Holistic processors recognize global features of spatially-presented materials, but when it becomes necessary to note fine details or features, analytic processors perform more adeptly. Holistic processors generally have difficulty noting details, while analytic processors have strengths in recognizing details but have difficulty with global information. In a second study, Cooper presented spatial information to alternate visual fields (left-right) to determine hemispheric processing. Results of the study indicate the same patterned response as in his earlier study and led him to conclude that holistic/

analytic cognitive processing style has no relationship to hemispheric processing, which would not support the serialist/holist division as depicted in Figure 1. Cooper's conclusion does not, however, take into consideration the research on individual preference (strength) in cognitive style. If, indeed, individual learners have preference of style, then it would be difficult for them to modify this preference. Therefore, the patterned response would remain constant and Cooper could have attained these results for this reason, as an individual may respond most effectively in the dominant mode. Analytic processors (left-hemisphere dominant) would continue to "operate" in a dominant modality, and, if presented information contralateral to that mode, processing may still be affected.

In a second study relating cognitive styles to reading comprehension, Pitts & Thompson (1984) found a relationship between inferential comprehension and the style dimension of field-independence/field-dependence. Inferential comprehension relates to an individual's ability to progress beyond factual knowledge to infer underlying concepts in the reading. It was found that field-independent students perform better in inferential comprehension. Inferential comprehension analyzes factual information to systematically structure understanding. The results of this research support the nature of field-independence as analytic byistic demonstrating the strength of field-independent individuals in inferential comprehension. Wittrock (1980) relates both the reflective and analytic style dimensions with left-hemisphere dominance, and impulsive, global styles with right-hemispheric dominance. Ausburn & Ausburn (1978) also reference evidence to demonstrate relationships between various style dimensions, as discussed. In addition, Zelnicker & Jeffrey's (1976) research findings support a relationship to reflective-impulsive styles with left-/right-hemispheric processing strategies. Impulsive style is related to global (right) processing and reflective styles to analytic (left) processing.

Through the research on cognitive style, some general characteristics can emerge (e.g., Ausburn & Ausburn, 1978). A first general character-

istic of cognitive style that appears to surface from research is that an individuals's cognitive style remains stable over time and across tasks (e.g., Garger & Guild, 1984). This style preference develops early and remains somewhat unchanged. The degree of dominance may change, but the dominance itself appears to be stable over time. Secondly, although there seems to be only a minimal relationship of style to general overall ability (e.g., Satterly, 1976), there does appear to be relationships between various style dimensions as was earlier discussed and depicted in Figure 1. Relationships between impulsivity, holistic processing, and inductive reasoning, for example, are identified as relating to each other and to right-hemispheric processing (e.g., Ausburn & Ausburn, 1978). Thirdly, there is evidence to suggest the relationship of cognitive style to learning tasks (e.g., Bryan, 1977; Levin et. al., 1974). When a task requires a transformation in processing which is incompatible with a learner's style, the learner may not perform the task successfully. It is, therefore, postulated that when classroom learning is affected by style, the instructional designer should consider cognitive styles as a factor when planning instruction. Since styles are resistant to long-term change and appear stable over time, it may be difficult to adjust an individual's style to meet a generalized instructional format. Many times, however, this may be what instructional designers expect to occur. Often, training programs may be designed without consideration of cognitive style and learners may be expected to adjust to the style of the instruction. If a mismatch does occur, it could be interpreted that the learner is not successful in the assigned task. This can then be viewed as a learner-based problem. However, if this situation is instead addressed as an instructional-based rather than learner-based problem, modifications can be made to the instruction to meet the individual needs of the learner. If the modifications are appropriate to the cognitive style of the learner, then perhaps greater success could be achieved and training enhanced. Viewing this situation as an instructional-based problem allows instructional designers the freedom and creativity to design interactive learner programs to <u>individualize</u> instruction.

Cognitive Styles and Instruction

Accepting the postulate that relating cognitive styles to effective learning is an instructional rather than learner-based problem, it becomes important to devise a manner in which instructional modification can be successfully accomplished. A look at current research in this area can begin to clarify the notion of the modification of instruction to meet the individual needs of the learner.

Glaser (1976) proposes a "psychology of instruction." The goal of this as a discipline is to provide the linkage between the psychological knowledge of learning and the educational applications of this knowledge. Considerations in developing this linkage include both the research on cognitive styles and an analysis of the tasks to be learned. Miller (1980) also emphasizes the importance of knowledge of the learner and the interaction of this knowledge with instructional design concerns. According to Miller, the instructional designer's role is to devise conditions in the learner's external environment to support the internal cognitive processes.

Federico & Landis (1984) support the importance of the design of instruction to consider cognitive style dimensions in order to aid individuals in learning information more readily and retaining/retrieving information more effectively. Others (e.g., Birkey & Moon, 1984; Grasha, 1984) stress the importance of matching instructional mode and cognitive style. Grasha (1984) cautions, however, that a consistent match may create a non-motivational attitude in learners, not encouraging accommodation to variety. As has been emphasized, however, the most effective learning occurs with cooperative processing of both hemispheres. This would then imply the use of a variety of instructional methods to promote optimum utilization of integrative ("whole brain") processing.

A question arises as to the most appropriate matching of individual cognitive style and the requirements (subject matter) of the task for the

most effective model of instructional presentation. Classification systems attempting to address these issues have been somewhat vague in demonstrating the interactions of style and subject matter (Ausburn & Ausburn, 1978). An initial attempt at developing such a classification (Ausburn, Ausburn & Ragan, 1980) is laudible, but could be expande and specified. This listing identifies tasks and the cognitive style r lated to each task. If, however, many cognitive styles are related, it may be reasonable to assume that most styles would be involved (to varying degrees) in every task. The differences may instead occur in the mode of the presentation of information taking into consideration style and task.

Wittrock (1979) supports the utilization of current research on process-oriented individual differences in the design of instruction. He discusses several dimensions of cognitive style (analytic-global, field-independent/field-dependent, and serialistic-holistic) and the implications of these styles in aptitude-treatment interactions. Wittrock considers the aptitudes (styles) of an individual and the ways in which these aptitudes interact with, or are affected by, the treatments. The treatments, in this case, are instructional programs. In addition, in her principles of instructional design Baggett (1983) emphasizes the design of individualized instruction based upon knowledge about cognitive styles.

Through the research on cognitive style and the initial support of the interaction of style and instruction, several general principles seem to emerge. These proposed principles refer to the presentation of computer- based instruction.

1. Individuals vary in the way in which they most effectively process/retain information.

2. It is postulated that the cognitive style of an individual differs in relation to hemispheric dominance in information processing.

3. Although individuals may have preferred styles, it is proposed that the best learning occurs when a learner processes information utilizing both hemispheres.

4. It is suggested that the design of instruction should consider cognitive styles of individual learners, emphasizing the notion of "whole-brain" processing.

5. Given the research in cognitive styles, it is proposed that instruction should consistently include:

a. Opportunities for an individual to adjust aspects of the instructional environment (e.g., order of presentation, perspective taken, questions asked/answered, etc.)

b. A combination of verbal information (text, auditory input) and spatial information (graphics, pictures, graphs, etc.) which are closely related to one another.

c. The advanced organization of the training program through an initial overview of the training, opportunities for review, and reinforcement.

d. Opportunities for the learner to apply the new information to a variety of learning situations in order to enhance retention and transfer.

6. It is suggested that both the instruction and the testing should be consistent with the learner's cognitive style. For example, if the training program itself provides both visual and verbal information, then the testing should provide for both visual and verbal information as well. Little research has been done in this area. In a study conducted by Moore (1978) on the effectiveness of graphics for computer-based instruction, the mode of testing was not consistent with the mode of instruction. In this study, a written

textual test was given after all treatments, including the graphics treatment condition, and the use of graphics was not supported. Moore et. al. (1978) identified the difference between the instructional mode and the test mode as a problem with this study. Therefore, if an individual learned the information graphically, it may be most useful to test retention in the same format (graphically) unless transfer to verbal format was consistently reinforced.

Although these proposed general principles have not been consistently developed and researched, some research has been conducted on various dimensions of cognitive style and the interactions of style with instruction. Bush et. al. (1965) conducted a study which included five - presentation conditions including text (two conditions), graphics, listening, and the use of audio-visual materials (film, etc.). The results of the study indicated that indivudals with high reading comprehension performed better under the verbal (text) conditions. Likewise, lower readers utilized the characteristics of graphics, films, and other spatially-oriented materials to enhance instructional performance. Although these results may not be surprising, it may support the need for systematic integration of graphics in instruction. These results relate to Cohen & Freeman's (1978) study of readers discussed earlier, which indicates the possibility that left-hemisphere dominant individuals, in general, are better readers and the use of visual/spatial information can enhance comprehension for poorer readers (thought to right-hemisphere dominant).

In additional research on imagery, Ausburn (1976) studied visual and haptic cognitive styles and each group's use of imagery. Visual learners performed better than haptic learners on visual imagery tasks. Both groups performed better under multiple (simultaneous) imagery con . . ons over the linear (sequential) presentation. This supports the relevance of style to performance and can also give some initial evidence to suggest that content may have a preferred mode of presentation. Other studies (Rigney & Lutz, 1974; Hauch & Verstagen, 1983) support the use of imagery in instruction to enhance learning.

Another aspect of cognitive styles and the display of information was conducted by Geiselman & Samet (1982). In the study with military personnel, it was discovered that performance was enhanced when subjects were permitted to organize/format information to meet their individual style for information input. Subjects preferred to spatially arrange information individually and performance increased with the ability to do so.

Some instructional techniques can be especially useful for adapting to various cognitive style dimensions. A proposed listing of possible instructional strageties matched to cognitive style is found in Table 3. This chart individually identifies cognitive style dimensions with some proposed techniques that may enhance instructional effectiveness. Much of the current computer-based instruction is dichotomous (visual-verbal) in the nature of information presentation. When considering this presentation mode along with the research reviewing the interaction of cognitive styles and instructional design, it may be possible to begin to specifically identify some effective presentation formats for visual-verbal information. Some postulated general guidelines arising from research in the presentation of verbal-spatial information are:

1. When both verbal and spatial information are presented in synchrony, it may be advantageous (due to contralateral hemispheric processing of the visual field) to place visual information to the left of verbal (Wickens, 1984b). With visual information to the left of the visual field, it may more effectively be processed by the right hemisphere.

2. Proper spacing of information appears to be important for adequate information processing. For example, Hathaway (1984) found that textual material is read more easily when double-spaced than when single-/triple- spaced.

3. More imaginative, rather than traditional, use of media to supplement text can be effective (Jamison et. al., 1974). Creative uses of graphics, films, etc. appear to enhance training performance.

4. When verbal (text or auditory input) and visual (spatial) information are both presented, the most effective mode of presentation appears to be to present both visual and verbal information in synchrony, or to present the visual before the verbal (Baggett & Ehrenfencht, 1983).

5. When visual information is presented, it appears that it is most effective to locate the critical visual information in the center of the visual field (Neumann, 1984). Neumann notes that this position may vary in size depending upon the perceptual grouping pattern of an individual. It may be possible that this also relates to cognitive style.

6. The use of visual in addition to verbal information seems to result in less time to complete tasks and in higher retention, both short-term (King, 1975) and long-term (Baggett & Ehrenfeucht, 1983).

7. Wickens (1983) supports the notion that verbal-visual information should be presented in such a manner as to increase processing and decrease the opportunity for resource competition.

(NOTE: Additional specific guidelines for developing visual displays can be found in Smith [1979] and Dansereau et. al., [1975]).

Increased use of auditory input in computer-based instruction could expand the presentation model for individualized instruction in the near future, but verbal/visual modes appear to be the two most predominant at this time.

Research Concerns

Research in the areas of cognitive styles and instructional design is still in its infancy. Future research could focus on the following concerns:

1. Is there a correlation among the dimensions of cognitive style as depicted in Figure 1?

2. Do these cognitive styles affect all learning situations? To what degree?

3. Can instructional strategies (such as those listed in Table 3) be utilized to enhance complementary processing of information with both hemispheres? Are there certain strategies appropriate for a given cognitive style dimension?

It is possible to look at the progression of instruction in a similar hierarchical format to that in Figure 1. Various dimensions of cognitive style can be related to steps in the instructional design of a lesson. Likewise, instructional strategies can be related to both the lesson and the style dimensions. Figure 2 displays a proposed hierarchical flow of instruction, strategies, and cognitive style. Additional research concerns relating to Figure 2 are:

1. Does the interaction of the lesson design, cognitive style, and instructional strategies progress as depicted in Figure 2?

2. Can a taxonomy or a listing of instructional guidelines be developed to enhance the effectiveness of training programs through increased success in learning?

These research concerns begin to identify some of the crucial elements in the interaction of cognitive style and instructional design. As research continues to identify the relationships of the various dimensions of cognitive style, more specific trainee characteristics can emerge. From these trainee characteristic descriptions, guidelines for the most effective presentation of information in training programs can be developed. Some considerations in the proposed development of such guidelines will be identified.

The Development of Instructional Guidelines

If there are proposed correlations among style dimensions and it is possible for instructional strategies to be matched to style and subject matter (task requirements), it would be helpful to instructional designers to have guidelines aiding in the development of instructional programs. Reviewing information on learner cognitive style and mode of presentation are only two areas to consider. What many researchers considering aptitude- treatment interactions are missing is the manner in which these two areas interact with the content subject matter. Staver's (1984) study suggests the worth of looking at the most appropriate format based on the type of information presented. As Ausburn (1976) concluded, subject matter content does have a preferred mode of presentation and Trafton (1984) recognizes that mathematic instruction is more effective when knowledge about the instructional mode best utilized for content is emphasized. Wickens (1984) discusses the potential that certain operations (e.g., computational and problem-solving) can be trained utilizing either spatial or verbal code, and this decision may be task-dependent.

Taxonomies developed to explain aspects of the learning process have been developed and have gained widespread acceptance (e.g., Bloom, 1956; Gagne, 1964). Some taxonomies have begun to deal with higher-order thinking skills (e.g., Stuart & Burns, 1984). Additionally, some taxonomies for use by instructional designers have been developed to combine task and content (Merrill & Boutwell, 1973). Moore & Nawrocki (1978) have slightly adapted the Merrill & Boutwell taxonomy for initial research on graphics in computer- assisted instruction. This taxonomy appears more narrowed in format and applicability.

A taxonomy that could be useful to instruction designers would combine dimensions of cognitive style, subject matter content, and the most effective form of information presentation. The support of the development of such a taxonomy or set of guidelines is supported by the researchers in this area (Moore & Nawrocki, 1978; Glaser, 1976; Grasha, 1984).

After reviewing literature on taxonomy development for human performance (e.g., Fleishman, 1967; Wheaton, 1968; Miller, 1971; Fleishman, 1975), an attempt to develop such a taxonomy can be undertaken. The proposed instructional guideline instrument in Table 4, designed for computer-based instruction, could serve as a basis for further research in this area. The table lists cognitive style dimensions and provides an initial classification system for subject matter. These classification areas are defined as follows:

Knowledge. This content includes factual background information necessary for an individual's general and specific knowledge about a particular topic. This information may be necessary for performance of a specific task and can include areas such as mathematics, history, procedures, descriptions, etc.

Skills. Skill subject matter content contains information involving the carrying out of an action. This includes the "hands-on" information necessary for performing an act and may rely on subject matter gained from knowledge content. Skill can include such tasks as operating a radar system, repairing a portion of a plane, flying a plane, ordering munitions, etc.

Attitudes. Attitude content involves the subject matter relating to the acceptance/understanding of information. This may include attitudes toward mathematics, handling weapons, interpersonal communication, etc.

Decision Making. Subject matter in this category involves a combination of two or more areas. Tasks include mission planning, mission implementation, etc.

It is important to note that these are not discrete categories. They are instead intended to serve as an initial system to begin research in this area. Future work should delineate and define the content in a more detailed, specified manner. Located at the junction points of cognitive

style and subject matter content are an initial listing of instructional strategies to encourage integrative processing while also meeting individual needs of learners.

Relevance to Air Force Training and Follow-on Research

Up to this point, discussion has focused on current research issues relevant to general instructional design concerns. In the area of military training, this information can be especially useful.

Current military training follows many design procedures, one of which is the Instructional Systems Design. Instructional Systems Design approaches instruction in a behavioral (sequential, programmed) manner and identifies steps for the development and evaluation of training programs. This model includes the following steps:

1. Analysis of system requirements
2. Definition of education/training requirements
3. Development of objectives and testing
4. Planning/validating of instruction
5. Instructional implementation and evaluation.

The considerations of cognitive style dimensions and subject matter content can be applied at each step in the Instructional Systems Design process. Initial guidelines such as those proposed in Table 4 can be useful at each step in the planning, implementation, and evaluation of instruction. Cognitive style and subject matter content considerations can influence the initial system analysis (Step 1 in the Instructional Systems Design process) as well as the planning, implementation, and evaluation of instruction. Miller (1980) recognizes that Instructional Systems Design with its behavioral emphasis does not reflect current research in cognitive psychology. Consideration of style dimensions can, however, be easily integrated into this process. In reviewing the information in Table 4, evidence of overlap in instructional strategies is evident. But an awareness of the purpose of each of these strategies

in the context of the content and the cognitive style dimension in each category may be crucial to effective training programs.

A significant trend in the military is the increased use of computer-based individual training. In many of these individual training programs the learner must adapt to the format of the instruction. The exciting potential of computer-based instruction can create individualized instruction, designed to be modifiable to meet the needs of all learners in a variety of learner settings and situations. The increased use of computer-based instruction in military training can allow for the use of the knowledge of cognitive styles to enhance training and, hopefully, the long-term effectiveness of training. If enhanced learning occurs through cooperative hemispheric processing, the individualized computer-based instruction can also enhance this cooperation through the use of a variety of combinations of text, graphics, and eventually sound. Recent reviews of computer-based instruction (e.g., Montague & Wulfeck, 1984) support the potential development of individualized instruction, through applying theories of information processing and learning styles to program development.

In most training programs, emphasis is placed on training efficiently, effectively, and in a cost-effective manner. If training programs are designed with an awareness of cognitive style characteristics, it is proposed that overall training should take less time and result in enhanced comprehension. Likewise, if hierarchical structure throughout training enhances higher-order thought and cooperative hemispheric functioning, then this may also result in long-term retention and transfer of information. Over time, this can affect length of training, effectiveness of training, and cost.

Current research development in the area of artificial intelligence can also serve as a tool in enhancing military training. Through progress in artificial intelligence techniques, computer-based instruction can begin to become more adaptive to individualize

instruction. Using artificial intelligence as a tool, computer-based instruction can begin to pre-assess trainee cognitive styles and design instruction to enhance both the strengths and weaknesses of trainees. Some dimensions of cognitive style have been addressed in the development of authoring systems utlizing artificial intelligence (e.g., Gable & Page, 1980; the CASTE system; Pangaro, 1984).

This paper raises several important issues relevant for follow-on research in the area of cognitive styles and instructional design. The interaction of cognitive styles and subject matter with instructional design procedures creates the possibility of improved training through the development of guidelines for instructional designers. A major research issue which can be addressed that may lead to the development of such guidelines is:

> The retention of instructional information modified in presentation format matched to cognitive style and subject matter content.

This issue can be addressed through basic research designed to test the proposed table of guidelines matched to style and subject matter variables (Table 4).

It can be possible through further research to design military training to meet the individual characteristics of the learner. One important learner characteristic is that of cognitive style. The goal of this method of instructional design is not to develop instructional programs geared solely to the dominant style of the trainee, but to <u>enhance</u> the individual's potential for higher-level cooperative processing which can, in turn, result in more effective learning through the use of increasingly effective training technology.

REFERENCES

1. Allport, G.W. (1937). Personality, a psychological interpretation. New York, NY: Holt and Company.
2. Ausburn, F.B., Ausburn, F.D. & Ragan, T.J. (February, 1980). Task analysis schema based on cognitive style and supplantational instructional design with application to an Air Force training course (Technical Report No. AFHRL-TR-79-59). Brooks Air Force Base, TX: Air Force Human Resources Laboratory.
3. Ausburn, F.B. (1976). Multiple versus linear imagery in presentation of comparative visual location task to visual & haptic college students. DAI, 37, 100A. (University Microfilms No. 76-15794).
4. Ausburn, L.J. & Ausburn, F.B. (1978). Cognitive styles: implications for instructional design. Educational Communication and Technology Journal (formerly AV Communication Review), 26 (4), 337-354.
5. Baggett, P. (January, 1983). Four principles for designing instructions (Technical Report No. 121-ONR). Boulder, CO: Institute of Cognitive Science.
6. Baggett, P. & Ehrenfeucht, A. (Spring, 1983). Encoding and retaining information in the visuals and verbals of an educational movie. Educational Communication and Technology Journal, 31 (1), 23-32.
7. Beck, J. & Shaw, W.A. (1959). An analysis of some important problems in learning and teaching (Memorandum EP-1). University of Pennsylvania.
8. Birkey, C. & Moon, J. (1984). Future directions for adult education and adult educators. Journal of Teacher Education, 35 (3), 25-29.
9. Bracht, G.H. (1970). Experimental factors related to aptitude-treatmert interactions. Review of Educational Research, 40, 627-645.
10. Britt, D.H. (1971). An improved method for instructional development: learner types. Audiovisual Instruction, 16 (4), 14-15.
11. Bush, W.J., Gregg, D.K., Smith, E.A. & McBride, C.B. (December, 1965). Some interactions between individual differences and modes of instruction (Report No. AMRL-TR-65-228). Dayton, OH: Wright-Patterson Air Force Base, Aerospace Medical Research Laboratories.

12. Cohen, G. & Freeman, R. (1978). Individual differences in reading strategies in relation to cerebral asymmetry. In Requin, J.: Attention and Performance VII. Hillsdale, NJ: Lawrence Erlbaum Associates, Publishers, 411-426.

13. Cohen, B.D., Brent, S. & Silverman, A.J. (1973). Field independence and lateralization of function in the human brain. Archives of General Psychiatry, 28, 165-167.

14. Cooper, L.A. (1982). Strategies for visual comparison and representation: individual differences. In Sternberg, R.J. Advances in the Psychology of Human Intelligence: Volume I. Hillsdale, NJ: Lawrence Erlbaum Associates, Publishers, 77-124.

15. Cronbach, L.J. & Snow, R.E. (1981). Aptitudes and instructional methods. New York, NY: Irvington Publishers, Inc.

16. Cronbach, L.J. & Snow, R.E. (1977). Aptitudes and instructional methods: a handbook for research on interactions. New York, NY: Irvington Publishers, Inc.

17. Danscreau, D.F., Long, G.L., McDonald, B.A., Actkinson, T.R., Collins, K.W., Evans, S.H., Ellis, A.M. & Williams, S. (June, 1975). Learning strategy training program: visual imagery for effective learning (Technical Report No. AFHRL-TR-75-47). Brooks Air Force Base, TX: Air Force Human Resources Laboratory.

18. Department of the Air Force. (May 25, 1979). Instructional System Development. Air Force Manual 50-2. Washington D.C.: U.S. Government Printing Office.

19. Drewitt, R. & Sonnenberg, J. (December, 1982). Final report: contract with the Institute for Curriculum and Instruction (Technical Report No. 2310). Gunter Air Force Station, AL: Air Force Logistics Management Center.

20. Dumas, R. & Morgan, A. (1975). EEG asymmetry as a function of occupation, task, and task difficulty. Neuropsychologia, 13, 219-228.

21. Faglioni, P., Spinnler, H. & Vignolo, L.A. (1969). Contrasting behavior of right and left hemisphere-damaged patients on a discriminative and a semantic task of auditory recognition. Presentation of European Brain and Behavior Society, Marseille, France, 366-389.

22. Federico, P.A., Landis, D.B. (1984). Cognitive styles, abilities, and aptitudes: are they dependent or independent? Contemporary Educational Psychology, 9 (2), 146-161.

23. Fischhoff, B. & Bar-Hillel, M. (December, 1980). Focusing techniques as aids to inference (Technical Report No. PTR-1091-80-6). Eugene, OR: Decision Research.

24. Fleishman, E.A. & Quaintance, M.D. (1984). Taxonomies of human performance: the description of human tasks. Orlando, FL: Academic Press, Inc.

25. Fleishman, E.A. (1975). Toward a taxonomy of human performance. American Psychologist, 30, 1127-1149.

26. Fleishman, E.A. (1967). Performance-assessment based on an empirically derived task taxonomy. Human Factors, 9 (4), 349-366.

27. Franco, L. & Sperry, R.W. (1977). Hemispheric lateralization for cognitive processing of geometry. Neuropsychologia, 15, 107, 114.

28. Gable, A. & Page, C.V. (1980). The use of artificial intelligence techniques in computer-assisted instruction: an overview. International Journal of Man-Machine Studies, 12, 259-282.

29. Garger, S. & Guild, P. (1984). Learning styles: the crucial differences. Curriculum Review, 23 (1), 9-12.

30. Geiselman, R.E. & Samet, M.G. (1982). Personalized versus fixed formats for computer-displayed intelligence messages. IEEE Transactions on Systems, Man, and Cybernetics, SMC-12 (4), 490-495.

31. Glaser, R. (1976). Components of a psychology of instruction: toward a science of design. Review of Educational Research, 46 (1), 1-24.

32. Goebel, L.G. (February, 1962). Some references related to Air Force activities in programmed learning (Technical Report No. 4951). Washington D.C.: Office of Aerospace Research.

33. Grady, Michael P. Teaching and Brain Research. New York, NY: Longman, Inc., 1984.

34. Grasha, A.F. (1984). Learning styles: the journey from Greenwich Observatory to the college classroom. Improving College and University Teaching, 32 (1), 46-53.

35. Hart, L.A. (1983). Human Brain and Human Learning. New York, NY: Longman, Inc.

36. Hathaway, M.D. (1984). Variables of computer screen display and how they affect learning. Educational Technology, 7-11.

37. Hauck, D & Verstegen, M. (1983). New concepts in aircrew training using computer-generated imagery. Proceeding of the Interservice/ Industry Training Equipment Conference (5th), Volume 1 (Report No. AD-A-142-774). Washington D.C.: American Defense Preparedness Association.

38. Herman, N. (1981). The creative brain. Training and Development Journal, 10-16.

39. Jamison, D., Suppes, P. & Wells, S. (1974). The effectiveness of alternative instructional media: a survey. Review of educational research, 44, 1-61.

40. Kearsley, G. (1985). Automation in training and education. Human Factors, 27 (1), 61-74.

41. Kimura, D. (March, 1973). The assymetry of the human brain. Recent Progress in Perception, 246-254.

42. Kimura, D. (1967). Functional asymmetry of the brain in dichotic listening. Cortex, 3, 163-178.

43. Kimura, D. (1961). Cerebral dominance and the perception of verbal stimuli. Canadian Journal of Psychology, 15, 166-177.

44. King, W.A. (1975). A comparison of three combinations of text and graphics for concept learning (Report No. NPRDC TR 76-16). San Diego, CA: Navy Personnel Research and Development Center.

45. Kinsbourne, M. & Hicks, R. (1978). Functional cerebral space. In J. Requin (ed.), Attention and Performance VII. Hillsdale, NJ: Lawrence Earlbaum Associates, Publishers, 345-362.

46. Kinsbourne, M. (1978). The asymmetrical function of the brain. New York, NY: Cambridge University Press.

47. Kinsbourne, M. (1975). The ontogeny of cerebral dominance. In Aaronson, D & Reiber, R. (eds.). Developmental psycholinguistics and communication disorders. New York, NY: New York Academy of Sciences.

48. Kogan, N. (1971). In G.S. Lesser (ed.). Educational implications of cognitive styles. Psychology and educational practice. Glenview, IL: Scott Foresman & Co., 242-292.

49. Kolb, D. (1976). The learning style inventory. Boston, MA: McBer and Company.

50. Kolers, P.A. & Roediger, H.L. (1984). Procedures of Mind. Journal of Verbal Learning and Verbal Behavior, 23 (4), 425-429.

51. Kozlowski, L.T. & Bryant, K.J. (1977). Sense of direction, spatial orientation, and cognitive maps. Journal of Experimental Psychology: Human Perception and Performance, 3, 590-598.

52. Levin, J.R., Divine-Hawkins, P., Kerst, S.M. & Guttman, J. (1974). Individual differences in learning from pictures and words: the development and application of an instrument. Journal of Educational Psychology, 66, 296-303.

53. Lohman, D.F. (October, 1979). Spatial ability: a review an reanalysis of th correlational literature (Technical Report No. 8). ONR, 458: Personnel and Training Research Program, Psychological Services Division.

54. Lowenfeld, V. & Brittain, W.L. (1970). Creative and mental growth (5th edition). New York, NY: Macmillan.

55. Luria, A. (1973). The working brain: an introduction to neuropsychology. New York, NY: Basic Books, Chapter 1.

56. Merrill, M.D. & Boutwell, R.C. (1973). Instructional development: methodology and research. Review of Research in Education, 1, 95-131, F.E. Peacock Publishers, Inc. (eds.), Itasca, IL.

57. Messick, S. (1966). The criterion problem in the evaluation of instruction: assessing possible, not just intended outcomes. Princeton, NJ: Educational Testing Service.

58. Miller, G.G. (1980). The relevance of cognitive psychology to instructional technology. Proceeding of the 2nd Interservice/ Industry Training Equipment Conference (Report No. AD-A107437). Alexandria, VA: Defense Technical Information Center.

59. Miller, R.B. (March, 1971). Development of a taxonomy of human performance: design of a systems task vocabulary (Technical Report No. 11). Washington D.C.: American Institute for Research

60. Montague, W.E. & Wulfeck, II, W.H. (1984). Computer-based instruction: will it improve instructional quality? (Report No. NPRDC 84-54). Washington D.C.: Chief of Naval Operations.

61. Moore, M.V., Nawrocki, L.H. & Simutis, Z.M. (1979). The instructional effectiveness of three levels of graphics displays for computer-assisted instruction (Technical Paper No. 359). Washington, D.C.: U.S. Army Research Institute for the Behavioral and Social Sciences.

62. Moore, M.V. & Nawrocki, L.H. (1978). The educational effectiveness of graphic displays for computer assisted instruction (Technical Paper No. 332). Alexandria, VA: U.S. Army Research Institute for the Behavioral and Social Sciences.

63. Neumann, O. (1984). Automatic processing: a review of recent findings and a plea for an old theory. In Prinz, W. and Sanders, A.F. (eds.). Cognition and Motor Processes. Berlin, Germany: Springer-Verlag.

64. Norman, D.A. (August, 1980). Errors in human performance (Technical Report 8004). University of California, San Diego, CA: Center for Human Information Processing.

65. Ornstein, R.E. (1977). The psychology of consciousness (2nd ed.). New York, NY: Harcourt Brace Jovanovich.

66. Pask, G. (1984). Review of conversation theory and a protologic (protolanguage), lp. ECTJ, 32 (1), 3-40.

67. Pask, G. & Scott, B.C.E. (1972). Learning strategies and individual competence. International Journal of Man-Machine Studies, 4, 217-53.

68. Pellegrino, J.W. & Kail, Jr., R. (1982). Process analyses of spatial aptitude. In Sternberg, R.J. (ed.). Advances in the Psychology of Human Intelligence. Hillsdale, NJ: Lawrence Erlbaum Associates, Publishers, 311-365.

69. Pellegrino, J.W. & Glaser, R. (1979) Cognitive components and correlates in the analysis of individual differences. Intelligence, 3, 187-214.

70. Pitts, M.M. & Thompson, B. (1984). Cognitive styles as mediating variables in inferential comprehension. Reading Research Quarterly, 19 (4), 426-435.

71. Ragan, T.J., et. al. (1979). Cognitive styles: a review of the literature (Report No. AFHRL-TR-78-90I). Brooks Air Force Base, TX: Air Force Human Resources Laboratory.

72. Read, D. (1981). Solving deductive-reasoning problems after unilateral temporal lobectomy. Brain & Language, 12, 116-127.

73. Reynolds, C. & Torrance E.P. (1981). Perceived changes in styles of learning and thinking (hemisphericity) through direct and indirect training. The Journal of Creative Behavior, 12 (4), 247-252.

74. Rigney, J.W. & Lutz, K.A. (October, 1974). CAI and imagery: interactive computer graphics for teaching about invisible processes (Technical Report No. 74). Arlington, VA: Office of Naval Research.

75. Robinson, E.R.N. & Knirk, F.G. (1984). Interfacing learning strategies and instructional strategies in computer training programs. Chapter 6 in Muckler, F.A. (ed.). Human Factors Review. Santa Monica, CA: Human Factors Society, Inc., 109-238.

76. Rubenzer, R. (1979). The role of the right hemisphere in learning and creativity implications for enhancing problem solving ability. The Gifted Child Quarterly, 23 (1), 78-101.

77. Samples, B. (1975). Educating for both sides of the human mind. The Science Teacher, 42 (1), 21-23.

78. Santostefano, S.G. (1969). Cognitive controls versus cognitive styles: diagnosing and treating cognitive disabilities in children. Seminars in Psychiatry, 1, 291-317.

79. Satterly, D.J. (1976). Cognitive style, spatial ability, and school achievement. Journal of Educational Psychology, 68 (1), 36-42.

80. Schwartz, G., Davidson, R. & Pugash, E. (1976). Voluntary control of patterns of EEG parietal asymmetry: cognitive concomitants. Psycho-physiology, 13 (6), 498-504.

81. Schwen, T.M., Bedner, A.K. & Hodson, K. (1979). Cognitive styles: boon or bane? Viewpoint in Teaching and Learning, 55, 49-63.

82. Smith, S. (December, 1979). Requirements, definition, and design guidelines for the man-machine interface in C^3 system acquisition (Technical Report No. MTR-3888). Bedford, MA: The MITRE Corporation.

83. Sperry, R.W. (1968). Hemisphere deconnection and unity in conscious awareness. American Psychologist, 23, 723-733.

84. Staver, J.R. (1984). Effects of method and format on subjects' responses to a control of variables reasoning problem. Journal of Research in Science Teaching, 21 (5), 517-526.

85. Stewart, W.J. (1984). Brain-congruent instruction: does the computer make it feasible? Educational Technology, 24 (5), 28-30.

86. Stuart, J.A. & Burns, R.W. (1984). The think process: a proposed instructional objectives classification scheme. Educational Technology, 24 (7), 21-26.

87. Taylor, R. (February, 1978). Computers and hemispheric functioning. Presented at seminar, Teacher's College, Columbia University, New York, NY.

88. Trafton, P.R. (1984). Toward more effective, efficient instruction in mathematics. Elementary School Journal, 84 (5), 514-528.

89. Van Rossum, E.J. & Schenk, S. (1984). The relationship between learning conception, study strategy, and learning outcome. British Journal of Educational Psychology, 54 (pt. 1), 73-83.

90. Weaton, G.R. (December, 1968). Development of a taxonomy of human performance: a review of classificatory systems relating to tasks and performance (Technical Report No. 1). Washington D.C.: American Institutes for Research.

91. Wickens, C.D. (1984b). The multiple resources model of human performance: implications for display design. AGARD/NATO Proceedings, Williamsburg, VA: 17-1 - 17-7.

92. Wickens, C.D. (1984). Processing resources in attention. In Parasuraman, R. & Davies, D.R. (eds.). Varieties of Attention, New York, NY: Academic Press.

93. Wickens, C.D., Sandry, D.L. & Vidulich, M. (1983). Compatibility and resource competition between modalities of input, central processing, and output. Human Factors, 25 (2), 227-248.

94. Wittrock, M.C. (1979). The cognitive movement in instruction. Educational Research, 8 (2).

95. Wittrock, M.C. (1980). Education and the cognitive processes of the brain. In Cognitive Processes of the Brain, 61-102.

96. Witkin, H.A., Moore, C.A., Goodenough, D.R., & Cox, P.W. (1977). Field dependent and field independent cognitive styles and their educational implications. Review of Educational Research, 47, 1-64.

97. Zelniker, T. & Jeffrey, W.E. (1978). Attention and cognitive style in children. In Hale, G. & Lewis, M. (eds.). Attention and Development of Attentional Skills, New York, NY: Plenum Press.

98. Zenhausern, R. (1978). Imagery, cerebral dominance, and style of thinking: a unified field model. Bulletin of the Psychonomil Society, 12 (5), 381-384.

Left hemisphere	Right hemisphere
analytic	global/holistic
deductive	inductive
verbal	spatial
difficulty synthesizing	synthesis
less prone to distraction	more prone to distraction
introvert	extrovert
can resist influence of others	can be influenced by others
narrow attention deployment	more broad attention deployment
uses phonetic cues in language interpretation	uses non-phonetic cues in language interpretation
maximizes differences between things	minimizes differences in things (merge)
language processing strengths	kinesthetic processing strengths
	sensitive to needs of others

Characteristics of Left-/Right-Hemisphere Dominance

Table 1.

1. Field-independence vs. Field-dependence (Witkin, 1965)
Manner is which an individual perceives oneself in space. Field-independent individuals perceive analytically and can easily separate "figure" from "ground." Field-dependent individuals perceive globally and have difficulty organizing/separating simple from more complex figures.

2. Reflective vs. Impulsive (Kagan, 1965)
The speed and manner in which hypotheses are selected and processed. Reflective individuals delay a long period of time before acknowledging a solution. Impulsive individuals select the first solution and are many times incorrect as a result.

3. Sharpening vs. Leveling (Holzman, 1952; Klein and Schlesinger, 1951)
Consistent individual variations in memory assimilation (in the identification and integration of impressions. Sharpening reflects a tendency to maximize perceived differences and is less prone to confusion of similar stimuli. Leveling individuals minimize perceived differences and merge past memory.

4. Breadth of Categorizing (Petigrew, 1958; Kogan, 1971)
The degree to which an individual will include items within categories. Individuals with narrow categorization styles are resistant to the inclusion of many items in a single category. Individuals with a broad style demonstrate a willingness to include many items within one category.

5. Scanning (Messick, 1970)
Individual differences in attention deployment which produce variations in vividness of experience and range of awareness. Discussed in terms of narrow or broad deployment of attention.

Table 2.

Fifteen Cognitive Styles

6. Tolerance for Unrealistic Experiences (Klein & Schlesinger, 1951)
Individual differences resulting from research in apparent movement which include the willingness to accept perceptions which vary from experience. A less tolerant individual style is more binding to reality and has a more restricted range of illusionary movement. A more tolerant style allows for a broader range.

7. Cognitive Complexity-Simplicity (Kelly, 1955)
Individual differences in the tendency to interpret the world in a complex, multi-dimensional way. This includes the number of dimensions and individual forms in judgements or the number of discriminations within constructs. Current research reviews the continuum of abstractness/ concreteness.

8. Conceptualizing Styles (Messick & Kogan, 1963)
This dimension is concerned with an individual's preferred approach to the categorization of similarities/differences among stimuli. This includes two aspects: equivalence range (very similar to breadth of categorization) and conceptual differentiation (differentiation-compartmentalization). Differentiation is the number of groups to which more than a single item are assigned. Differentiation correlates with verbal knowledge and vocabulary level (synthesis of information). Compartmentalization indicates the number of single items not placed in any categorical group. Compartmentalization correlates negatively with creativity and demonstrates difficulty in generating alternate conceptual schemes.

9. Constricted vs. Flexible Control (Gardner et. al., 1959)
This cognitive style represents an indiviudal's vulnerability to cognitive and environmental distraction. A constricted style represents retention of incidental stimulation and a flexible style indicates failure of retention. Kogan (1971) questions this interpretation of terminology. For these purposes, the terms will be reversed.

10. Distractibility (Santostefano, 1969)

The degree to which an individual reacts to contradictory cues. This is an "outgrowth" of constricted vs. flexible control which has been related to (but different from) field-dependence/field-independence. This style implies a range of individual proneness to distraction. This aspect of cognitive style has not been researched as thoroughly as others.

11. Visual vs. Haptic (Lowenfeld, 1970)

The degree to which an individual relies on visual or kinesthetic cues for information processing. The visual individual uses visual imagery, holistic processing, and the integration/synthesis of component parts. The haptic individual uses "bodily" perceptions, and is kinesthetically-oriented. An "indefinite" individual combines the use of both.

12. Cautiousness vs. Risk-taking (Kogan, 1971)

This aspect of style relates to an individual's willingness to take risks in decision-making situations. Although, at times, this dimension is task specific, there are some individuals who consistently perform at either cautious or risk-taking levels. Other individuals tend to react according to task.

13. Concrete vs. Abstract Conceptualizaton (Kolb, 1976)

This cognitive style dimension relates to the degree of abstractness an individual utilizes in conceptualizing information. A concrete conceptualizer uses concrete experiences and an abstract conceptualizer utilizes abstractions to conceptualize information.

14. Active Experimentation vs. Reflective Observation (Kolb, 1976)

This aspect of cognitive style refers to the degree of involvement preferred by an individual when learning a concept. Active experimentation refers to active "hands-on" experiences in learning as opposed to more reflective, "thought-oriented" style.

15. Serialist vs. Holist (Pask & Scott, 1972)

The style indicating the manner in which an individual prefers to input information. A serialist follows a deductive, analytical approach with a preferred presentration sequence organized in a step-by-step, developmental format. The holist prefers to view the more global elements of information initially, then supports these elements with sequential detailing.

Style characteristics and thinking skills

Characteristics
- analytic processing
- deductive reasoning
- verbal orientation
- difficulty synthesizing
- introvert
- can resist influence of others
- maximizes differences
- less prone to distraction
- uses phonetic cues

NOTE: As one moves up (↑) the hierarchy, the division/strengths of left and right hemispheres become less pronounced and more integrated processing occurs.

Characteristics
- global/holistic processing
- inductive reasoning
- visual/spatial orientation
- synthesizer
- extrovert
- sensitive to needs of others
- merges differences
- combines items in categories
- uses non-phonetic auditory cues

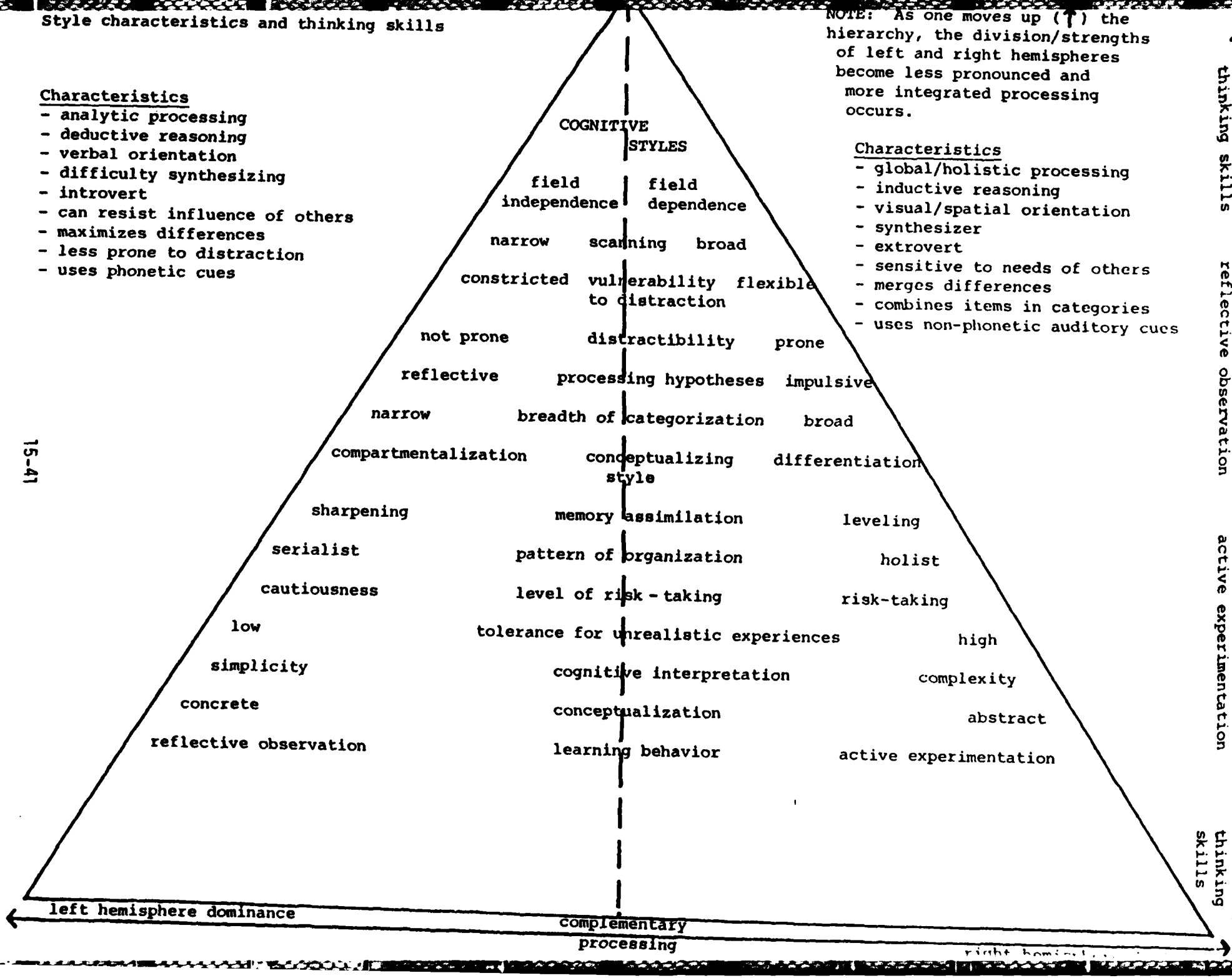

1.	Field-Independence - use advanced organizer to define advanced relationships - use of highlighting - review to synthesize information	Field-Dependence - use of advanced organizer - use of highlighting - review to direct synthesis of information
2.	Reflective - adjust the pacing on instruction - highlight points of emphasis during instruction	Impulsive - adjust the pacing of instruction to "slow down" for effective performance - highlight points of emphasis during instruction
3.	Sharpening - demonstrate relationships through use of a "web" - use mnemonics to combine characteristics - utilize all levels of questioning to force combination of training components	Leveling - highlight differences - use mnemonics to direct combinations - use variety of questioning techniques to focus and direct attention
4.	Narrow Categorization - use "webs" to structure information - use of advanced organizers to provide overview of training - use frequent review and reinforcement to combine training components	Broad Categorization - use webbing to structure information - use of advanced organizers to focus attention on important aspects of training program - use highlighting to direct attention

Table 3.

Cognitive Styles and Possible Instructional Modifications

5. Narrow Scanning

- spread spacing on page and use highlighting
- use graphic symbols as keys to direct attention
- display information at different times to clearly direct attention

Broad Scanning

- focus attention with use of highlighting
- use graphic symbols as keys to focus attention
- display information at different times to clearly direct attention

6. Low Tolerance for Unrealistic Experiences

- use realistic examples (visual and verbal)
- use a variety of examples for application of concepts
- use actual materials whenever possible

High Tolerance for Unrealistic Experiences

- use realistic examples (visual and verbal
- use a variety of examples for application of concepts
- utilize color and graphics in training program to enhance interest

7. Cognitive Simplicity

- use of highlighting to narrow field of vision
- use of outline/mapping to organize information
- arrange information well-spaced on screen (minimize "clutter")

Cognitive Complexity

- provide graphic organizer (cognitive map) to organize training for trainee
- utilize realistic examples to apply training to variety of situations
- use mnemonics to combine and classify information

8. Compartmentalization

- use of webbing/mapping
- choose experiences forcing the combination of categorization
- use variety of questioning techniques and feedback to encourage the identification of interrelationships among training components

Differentiation

- use of webbing/mapping
- use of highlighting to classify appropriate information
- provide realistic examples demonstrating application of training information

9. Constricted

- use highlighting to emphasize
- use of different size lettering, etc., to stress organization of information
- progressively include additional information

Flexible

- use highlighting to narrow focus of attention to important training components
- utilize graphics and color to provide interest and examples of information presented
- provide frequent opportunities to trainee to review/reinforce information presented

10. Distractibility

(not prone)

- arrange information on screen for best retention of most possible amount of information
- allow trainee flexibility to determine amount of feedback and review
- use graphics and color to vary presentation mode

(prone)

- limit amount of information displayed at a given time
- use highlighting to limit attention direction
- provide frequent feedback and reinforcement
- provide frequent review of colors and graphics

11. Visual

- use color and graphics to reinforce ideas
- provide realistic experiences to provide trainee opportunity to apply training
- provide outline for organization of training

Haptic

- use color and graphics to reinforce concepts
- provide experiences for trainee to work with equipment, etc. that training program is teaching ("hands-on")
- provide realistic examples to assist trainee in applying information presented

12. Cautiousness

- use directed learning experiences
- provide experiences for aided generalizations
- provide experiences which sequentially become more complex

Risk-Taking

- use directed learning experiences to control amount of information and direct attention
- use highlighting to focus attention on appropriate information
- provide experiences which sequentially become more complex

13. Concrete Conceptualization

- begin with concrete experience and move toward abstract
- use mnemonics to combine and categorize training content
- use webbing to show relationships among training components

Abstract Conceptualization

- begin with concrete experiences, allowing flexibility for holistic processing
- provide realistic experiences to apply knowledge gained through training
- provide opportunities for frequent review and reinforcement

14. Active Experimentation

- provide experiences for trainee to apply information to realistic situations
- give realistic examples throughout training program
- provide frequent review and reinforcement to apply knowledge

Reflective Observation

- allow flexibility for trainee to review information presented
- allow flexibility for pacing and review of information presentation
- provide realistic examples of applications of information presented

15. Serialist

- provide learning experiences in sequential manner
- gradually induce holistic processing
- use questioning to force both sequential and holistic processing

Holist

- introduce information holistically
- force sequential development of concepts within a holistic framework
- use of questioning to force both sequential and holistic processing

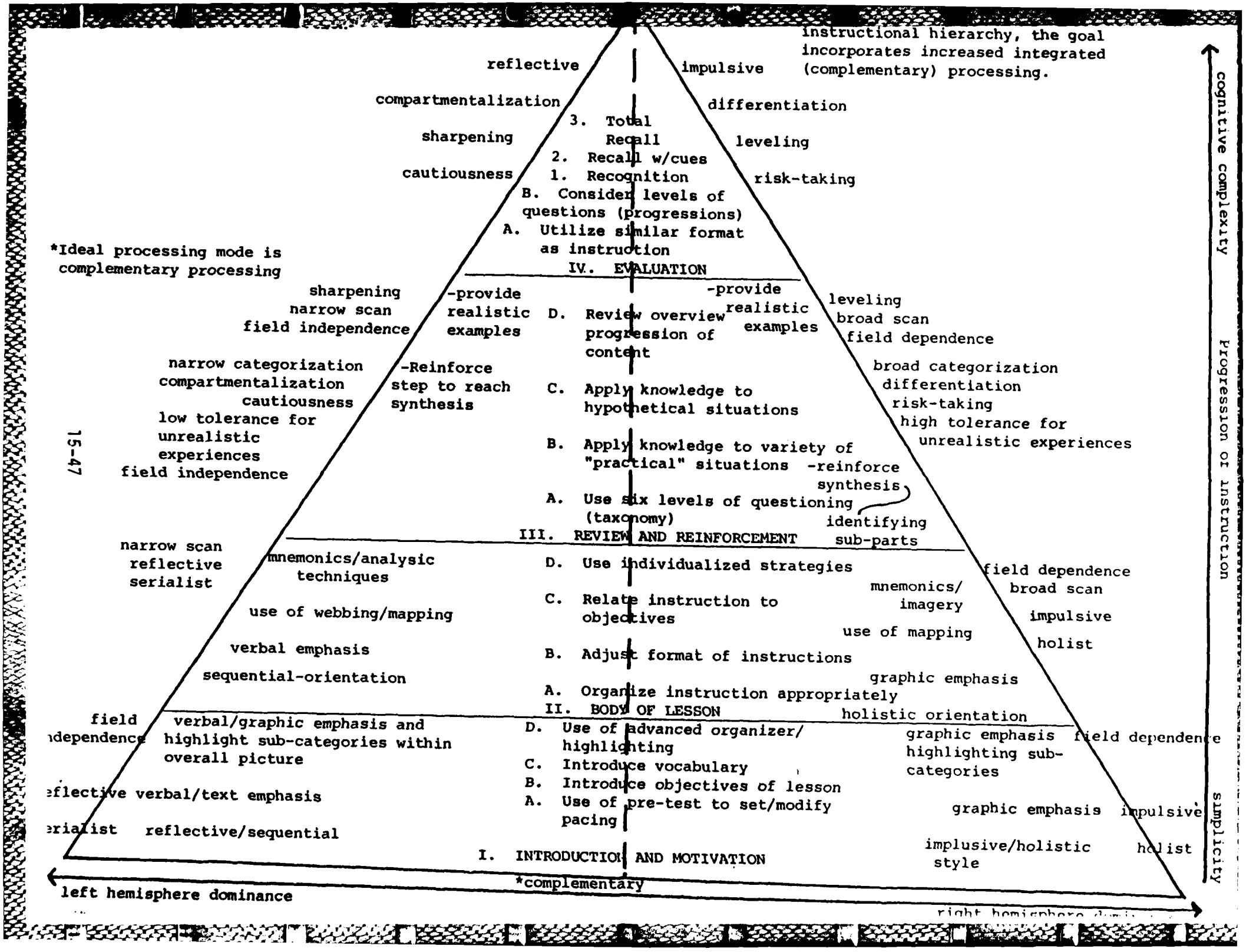
instructional hierarchy, the goal incorporates increased integrated (complementary) processing.
reflective
impulsive
compartmentalization
differentiation
sharpening
leveling
cautiousness
risk-taking
3. Total Recall
2. Recall w/cues
1. Recognition
B. Consider levels of questions (progressions)
A. Utilize similar format as instruction
IV. EVALUATION
*Ideal processing mode is complementary processing
sharpening
narrow scan
field independence
-provide realistic examples
D. Review overview progression of content
-provide realistic examples
leveling
broad scan
field dependence
narrow categorization
compartmentalization
cautiousness
low tolerance for unrealistic experiences
field independence
-Reinforce step to reach synthesis
C. Apply knowledge to hypothetical situations
broad categorization
differentiation
risk-taking
high tolerance for unrealistic experiences
B. Apply knowledge to variety of "practical" situations
-reinforce synthesis
A. Use six levels of questioning (taxonomy)
identifying sub-parts
III. REVIEW AND REINFORCEMENT
narrow scan
reflective
serialist
mnemonics/analysic techniques
D. Use individualized strategies
field dependence
broad scan
impulsive
holist
mnemonics/ imagery
use of webbing/mapping
C. Relate instruction to objectives
use of mapping
verbal emphasis
B. Adjust format of instructions
sequential-orientation
graphic emphasis
A. Organize instruction appropriately
II. BODY OF LESSON
holistic orientation
field independence
verbal/graphic emphasis and highlight sub-categories within overall picture
D. Use of advanced organizer/ highlighting
graphic emphasis highlighting sub-categories
field dependence
C. Introduce vocabulary
B. Introduce objectives of lesson
reflective verbal/text emphasis
A. Use of pre-test to set/modify pacing
graphic emphasis
impulsive
serialist
reflective/sequential
implusive/holistic style
holist
I. INTRODUCTION AND MOTIVATION
*complementary
left hemisphere dominance
right hemisphere
cognitive complexity
Progression of instruction
simplicity
15-47

	DECISION MAKING	ATTITUDES	SKILLS	KNOWLEDGE
-goal statements -simultaneous overall picture w/highlighting -realistic experience	-provide both cognitive & emotional reasoning/ support -provide experiences which allow for several viewpoints	-provide paper-based/material-based info to demonstrate part/whole -color-coding -numbering steps /items	-agenda/advanced organizer -building block approach w/ frequent review -text & graphics w/highlighting -adjust text size	field independence field dependence
-pre-test to determine mismatches -examples to show results of actions -controlled pacing	-allow "thought-time" -interactive format -encourage alternate viewpoints as options	-exploration time in addition to sequential development -pre-test	-use branching to direct learning -adjust pacing through pre-test	reflective impulsive
-mnemonics -use of questioning to direct attention to important components	-allow time for sharing thoughts -provide experiences in which many opinions are expressed	-icons/mnemonics as memory aides -diagrams in addition to actual materials	-webbing to show relationships -highlight to show component parts -advance organizer	sharpening leveling
-highlighting -provide applied structured situations to direct categorization appropriately	-demonstrate results of opinions (small-/large-scale) -discuss similarities/differences among varying opinions	-flow charts -discussion of similarities/ differences through observation -color-coding	-advanced organizer -highlighting -webbing -mnemonics	narrow categorization broad categorization
-use of both text /graphics simultaneously -use of highlighting to stress application of info	-highlighting to focus/re-focus attention -provide experience to review opinions & structure thoughts	-concentrate on one aspect at a time/provide materials in addition to equipment -structure w/ frequent review /reinforcement	-use of text & graphics display simultaneously or graphics first -provide overview & frequent review of info	narrow scan broad scan

Table 4.
Training Strategies for Identified Cognitive Styles and Subject Content

	DECISION MAKING	ATTITUDES	SKILLS	KNOWLEDGE
-realistic display -demonstrate results of choices made by trainee	-provide realistic examples & experiences -provide examples from several viewpoints	-use actual materials during training or closely simulated materials -use of text & graphics w/ materials	-relate knowledge to practical examples/then move to more abstract -use of both text & high resolution graphics	<u>low</u> tolerance for unrealistic experiences <u>high</u>
-freedom to arrange display format individually -demonstrate results of choices made	-provide examples demonstrating varying viewpoints -use "webbing" technique to demonstrate interrelationships	-provide examples for application purposes -provide frequent review/reinforcement	-apply knowledge to variety of situations -relate to knowledge base of individual experience	compartmentalization comceptualizing differentiation
-provide structured experiences, providing larger amount of decision making as trainee progresses	-provide variety of examples and discuss pro/cons -use of multi-level questioning techniques	-mnemonics/icons as memory aides -allow flexibility in pacing/review	-use of mnemonics -use of icons for memory techniques and categorization	constructed control flexible control
-small steps & demonstrate results of choices -structure initial choices w/ narrow options moving to wider range	-use of visual aids to demonstrate results of various choices -decision-making activities to demonstrate	-exploration time -flexibility to adjust work environment -demonstrate results of actions	-progress developmentally to higher-level thinking -provide practical examples/ applications of knowledge	cautiousness risk-taking
-text & graphics simultaneously -highlighting to emphasize salient features necessary for decision making	-use of visual aides to direct thoughts -use of highlighting to emphasize likeness & differences	-provide actual/ realistic experiences -direct attention through mnemonics/icons as memory aides	-use highlighting to focus attention appropriately -use of graphics closely related to text & presented simultaneously	<u>not prone</u> distractibility <u>prone</u>

	DECISION MAKING	ATTITUDES	SKILLS	KNOWLEDGE
-permit individual formatting of info -allow freedom to explore/demonstrate results	-provide opportunities for both sequential & holistic thought -use multi-level questioning for flexibility	-show both overall picture & parts -allow freedom to explore materials while also providing some directed structure	-adjust sequence of presentation -provide frequent examples of larger picture-webbing -combine text & graphics	serialist holist
-provide realistic experiences through text & graphics moving to simulations, etc. -provide examples to demonstrate results of choices	-provide realistic experiences to demonstrate varying viewpoints -provide simulations, "hands-on" experiences	-provide trainee w/text/graphics simultaneously -provide actual materials, film, etc. of materials	-use of text & graphics -provide application experiences for trainees	visual haptic
-movement from concrete examples relevant to trainee to variety of situations -demonstrate results of choices made by trainee	-movement from trainees point of reference to vary viewpoints -provide realistic applications	-movement from concrete to abstract w/application to variety of situations -begin from trainee's concrete experience level	-use pre-test to determine knowledge base of trainee -begin w/concrete experiences/text/graphics	concrete conceptualization abstract
-movement from experience direct relevant to trainee's experiences to move varied situations -flexibility of "think time" w/ sequential development to shorten time required	-provide simulations, role-playing, etc. -allow "thought-time" for processing of info	-allow directed exploration -provide feedback & adjust structure to individual progress	-begin w/freedom to explore by acknowledging knowledge base -questioning techniques which direct ideas & provide think time	active experimentation reflective observation

1985 USAF-UES SUMMER FACULTY RESEARCH PROGRAM

Sponsored by the

AIR FORCE OFFICE OF SCIENTIFIC RESEARCH

Conducted by the

UNIVERSAL ENERGY SYSTEMS, INC.

FINAL REPORT

POLYNOMIAL FEEDBACK CONTROL FOR ROBOTIC MANIPULATORS

Prepared by:	Dr. Connie K. Carrington
Academic Rank:	Assistant Professor
Department and University:	Mechanical Engineering Department, University of South Carolina
Research Location:	AFWAL/FIGCA, Wright-Patterson AFB
USAF Research Focal Point:	Capt. Kristin Farry
Date:	September 19, 1985
Contract No.:	F49620-85-C-00

POLYNOMIAL FEEDBACK CONTROL FOR ROBOTIC MANIPULATORS

by

Dr. Connie K. Carrington

ABSTRACT

New nonlinear feedback control laws using redundant kinematic parameters are developed for nonlinear dynamical systems. The use of Euler parameters instead of angles replaces the transcendental nonlinearities with polynomials in the equations of motion, permitting the systematic development of polynomial feedback control laws. This control method is successfully applied to spacecraft attitude maneuvers using conjugate angular momenta as feedback variables, and gains that are power series in time are found in closed-form. To apply this method to robotic manipulators, a new derivation from optimal control theory is found for the costate equations, in which the position-dependent inertia matrix does not need to be inverted. Polynomial control laws with time-dependent gains can then be determined in closed-form. The method is applied to the equations of motion for a two-link manipulator.

ACKNOWLEDGEMENTS

The author would like to thank the Flight Dynamics and Materials Laboratories at Wright-Patterson AFB and the Air Force Office of Scientific Research for a most rewarding summer of study and research. The lectures, briefings, and daily interaction with the members of the Control Analysis group was intellectually stimulating and truly a pleasure. Bernie Grooms provided much assistance with TEX and other computer software at the Flight Dynamics Lab. The author would also like to acknowledge the support and direction of Captain Kristin Farry. Her collection of current robotics literature and our daily discussions provided the base for a productive summer of research.

I. INTRODUCTION: The development of new feedback control laws for robotic manipulators was investigated during the ten week Summer Faculty Research Program. This study was an extension to robotics of the author's Ph.D. dissertation in spacecraft attitude control. The dissertation research included the investigation of suboptimal nonlinear feedback laws for spacecraft pointing that would be easily implemented in on-board, real-time computation. Large-angle, rapid-rotation spacecraft maneuvers were studied, using Euler parameter kinematics and angular velocities or generalized angular momenta as feedback variables. The same variables were used this summer to parameterize the motion of a two-link robotic manipulator, and polynomial feedback control laws using these variables were developed. The USAF research program in robotics is funding and reviewing the development of new control laws for improving the accuracy and speed of robotic manipulators, and hence there is interest in the development of new control laws.

There are several advantages that nonlinear feedback control laws have over feedforward control schemes, such as computed-torque control. The computation of control signals from polynomial feedback laws involves just a few multiplications of feedback signals by a set of stored gains, requiring little processing time or memory. Furthermore, these control laws are extremely smooth, providing continuous trajectories unlike those that may be found with gain scheduling or piecewise-continuous controls.

Polynomial feedback laws are readily developed when the state equations are in polynomial form. This is accomplished with dynamical systems by using the Euler parameters or quaternions for kinematic variables, which removes the transcendental nonlinearities present in angle formulations. Since the Euler parameters are once redundant, the computational singularities that occur with angles are also avoided, so that clearly defined control laws are provided for all points in the work space.

II. OBJECTIVES OF THE RESEARCH EFFORT: The summer research was directed at parameterizing a two-link manipulator in terms of Euler parameters and developing polynomial feedback laws using optimal control theory. Since the author was unfamiliar with robot dynamics and current control schemes, the first goal was to survey the literature in this field. A representative example for a two-link manipulator was selected from Paul[1], which was then rewritten using Euler parameters. The classical development of costate equations from optimal control theory requires the equations of motion in state-space form. Unfortunately, the full nonlinear equations governing the motion cannot be put into state-space form without inverting the state-dependent inertia matrix, producing ungainly constraint equations for the optimal control problem. A better approach is to rederive the optimal control formulation using the original equations of motion, without matrix inversion. This derivation

produces costate equations that can then be solved by assuming a polynomial form for the costates. Coefficients of like powers in the states are collected, producing sets of equations that may then be solved for the gains.

The derivations above used the Euler parameters and link angular velocities as feedback variables. An alternate set of feedback states include the Euler parameters and the conjugate angular momenta derived by Morton[2] for spacecraft attitude dynamics. Polynomial feedback laws for spacecraft control using these variables were investigated, and simulations of several maneuvers were executed. The success of these control laws for spacecraft maneuvers suggest that the conjugate angular momenta may be suitable for robotic control laws.

III. SPACECRAFT ATTITUDE CONTROL:

Polynomial feedback control using the Euler parameters and the conjugate angular momenta is investigated for a simple dynamical system representing rigid-body spacecraft attitude control. The kinematic dependence of the inertia matrix that occurs in manipulator dynamics is not present in this system, although gyroscopic nonlinearities similar to those in robotics do appear. Hence a study of rigid-body orientation using these new variables will illuminate some of the advantages or problems that occur with polynomial feedback laws.

A. Equations of motion.

The attitude control problem for a rigid spacecraft is governed by a set of kinematic equations defining orientation of the body with respect to an inertial frame, and a set of dynamic equations representing rotational motion. The orientation of a body-fixed reference frame $\{\hat{\underline{b}}\}$ to an inertial frame $\{\hat{\underline{n}}\}$ is given by the projection

$$\{\hat{\underline{b}}\} = [C]\{\hat{\underline{n}}\} \tag{1}$$

where [C] is the direction cosine matrix. Instead of three Euler angles, the four Euler parameters[3,4] will be used to parameterize the elements of [C]. The Euler parameters are defined as

$$\begin{aligned} \beta_0 &= \cos(\Phi/2) \\ \beta_i &= l_i \sin(\Phi/2) \qquad i = 1,2,3 \end{aligned} \tag{2}$$

where l_i are components of a unit vector along the principal axis of rotation when rotating from $\{\hat{\underline{n}}\}$ to $\{\hat{\underline{b}}\}$, and Φ is the rotation angle for that reorientation.

Rotational motion is governed by Euler's equations, which are generally written in terms of the angular velocity components ω_i. Consistant with the development of Hamilton's canonical equations[5], Euler's equations are reformulated in terms of generalized angular momenta p_i that are conjugate to the Euler parameters. They are defined from the rotational kinetic energy T as follows

$$p_i = \frac{\partial T}{\partial \dot{\beta}_i} \qquad i = 0,1,2,3 \tag{3}$$

The equations governing the time derivatives of the Euler parameters are also reformulated in terms of the generalized

angular momenta, producing the following eight equations of motion[2]

$$\{\dot{\underline{p}}\} = -\frac{1}{4}[Q(p)][I^{-1}]_4[Q(p)]^T\{\underline{\beta}\} + 2[Q(\beta)]\{\underline{u}\}_4$$
$$\{\dot{\underline{\beta}}\} = \frac{1}{4}[Q(\beta)][I^{-1}]_4[Q(\beta)]^T\{\underline{p}\} \tag{4}$$

where $[Q(\beta)]$ and $[I^{-1}]_4$ are 4x4 matrices defined as follows

$$[Q(\beta)] = \begin{bmatrix} \beta_0 & -\beta_1 & -\beta_2 & -\beta_3 \\ \beta_1 & \beta_0 & -\beta_3 & \beta_2 \\ \beta_2 & \beta_3 & \beta_0 & -\beta_1 \\ \beta_3 & -\beta_2 & \beta_1 & \beta_0 \end{bmatrix} \tag{5}$$

and

$$[I^{-1}]_4 = \text{diag}\ \{0,\ 1/I_1,\ 1/I_2,\ 1/I_3\} \tag{6}$$

I_1, I_2, and I_3 are the spacecraft moments of inertia in a body-fixed, principal-axis reference frame. The nonzero elements of $\{\underline{u}\}_4$ are the control torques about the principal axes

$$\{\underline{u}\}_4 = \{0,\ u_1,\ u_2,\ u_3\}^T \tag{7}$$

B. Optimal Control Problem.

The state equations are cubic polynomials, so that polynomial feedback control laws may be developed using an optimal control formulation.[6,7] No linear terms are present in Eqs. (4), however, and there are fewer control variables than states, so that the algebraic gain equations are in many instances degenerate. In these cases no solution can be found for constant gains.[8] However, time-dependent gains may be found using the cubic state equations in Eqs. (4). The tracking problem can be formulated using a performance index that minimizes the difference between the state and

the target, and a final state penalty can be posed. The costates are written as polynomials in the states $\underline{x}$, and the gain equations are defined from the costate equations by equating coefficients of powers in $\underline{x}$. The differential equations defining the gains are simple, so that closed-form solutions may be found by integration. The terminal boundary conditions for the costates, which are determined by the performance index, specify constants of integration in the expressions for the gains. A single-axis rotation example will illustrate the technique.

For single-axis maneuvers about the first principal axis, Eqs. (4) reduce to the following equations

$$\begin{aligned}
\dot{x}_1 &= 4\bar{I}(x_1x_2x_4 - x_2^2x_3) - 2x_4u \\
\dot{x}_2 &= 4\bar{I}(x_1x_2x_3 - x_1^2x_4) + 2x_3u \\
\dot{x}_3 &= 4\bar{I}(x_1x^2{}_4 - x_2x_3x_4) \\
\dot{x}_4 &= 4\bar{I}(x_2x^2{}_3 - x_1x_3x_4)
\end{aligned} \tag{8}$$

where $\underline{x} = \{p_0\ p_1\ \beta_0\ \beta_1\}^T$ and u is the control torque to be determined. For the following performance index

$$J = \frac{1}{2}\underline{z}^T(t_f)H\underline{z}(t_f) + \frac{1}{2}\int_{t_0}^{t_f}\{\underline{z}^TQ\underline{z} + u^2\}dt \tag{9}$$

where $\underline{z}(t) = \underline{x}(t) - \underline{r}(t_f)$ and $\underline{r}(t_f)$ is the desired final state, the control is

$$u = 2(x_4\lambda_1 - x_3\lambda_2). \tag{10}$$

λ_1 and λ_2 are the costates corresponding to the conjugate angular momenta p_0 and p_1, and λ_3 and λ_4 correspond to Euler parameters β_0 and β_1.

The terminal boundary conditions on the costates are determined by the performance index in Eq. (9)

$$\underline{\lambda}(t_f) = H\underline{z}(t_f) \tag{11}$$

By assuming the coestates are polynomials in the states,

$$\lambda_1(t) = s_i(t) + k_{ij}(t)x_j + d_{ijk}(t)x_j x_k + \ldots \tag{12}$$

substituting this expansion into the costate equations, and then equating coefficients of like powers of x, we obtain sets of differential equations for the gains.

For this example, the weighting matrices Q and H are

$$\begin{aligned} Q &= \text{diag}\{\, q_1 \; q_2 \; q_3 \; q_4\} \\ H &= \text{diag}\{\, h_1 \; h_2 \; h_3 \; h_4\} \end{aligned} \tag{13}$$

The *zeroth-order* equations are

$$\dot{s}_i = q_i r_i(t_f) \tag{14}$$

with boundary conditions

$$\underline{s}(t_f) = -H\underline{r}(t_f) \tag{15}$$

producing the following solution

$$s_i(t) = -q_i r_i(t_f)(t_f - t) - h_i r_i(t_f) \tag{16}$$

The linear equations are

$$\begin{aligned} \dot{k}_{ii} &= -q_i && i=1,2 \\ \dot{k}_{33} &= -q_3 + 4s_2^{\,2} \\ \dot{k}_{44} &= -q_4 + 4s_1^{\,2} \\ \dot{k}_{ij} &= 0 && i \neq j \end{aligned} \tag{17}$$

with boundary conditions

$$K(t_f) = H \tag{18}$$

and the quadratic equations are

$$
\begin{aligned}
\dot{d}_{114} &= s_2/2I \\
\dot{d}_{123} &= -s_2/4I \\
\dot{d}_{124} &= -s_1/4I \\
\dot{d}_{134} &= -4k_{11}s_2+s_4/4I \\
\dot{d}_{144} &= 4k_{11}s_1-s_3/4I \\
\dot{d}_{213} &= -s_2/4I \\
\dot{d}_{214} &= -s_1/4I \\
\dot{d}_{233} &= s_1/2I \\
\dot{d}_{233} &= 4k_{22}s_2-s_4/4I \\
\dot{d}_{234} &= -4k_{22}s_1+s_3/4I
\end{aligned}
\tag{19}
$$

and $\dot{d}_{ijk} = 0$ where not otherwise specified. The terminal boundary conditions for these equations are $d_{ijk}(t_f) = 0$, and the solutions contain linear through cubic powers in time. Similar polynomials in time are found for higher order gains.

C. Numerical Example.

A rapid large-angle, spin-down maneuver was simulated with I=1.00 kg m^2 and t_f=20 sec. The boundary conditions for the maneuver are listed in Table 1, and the performance indices in Table 2. The performance index weights were

$$H = Q = \text{diag}\{0.1\ 0.1\ 0.1\ 0.1\} \tag{20}$$

The conjugate angular momenta and Euler parameters are plotted in Figs. 1 and 2. Fig. 3 contains the maneuver angle and control torque histories.

Table 1

SINGLE-AXIS BOUNDARY CONDITIONS

State	Initial State	Final State
ϕ(rad)	$-\pi/3$	$\pi/3$
ω(rad/sec)	1.000	0.000
β_0	0.866	0.866
β_1	-0.500	0.500
p_0(kg m^2 rad/sec)	1.000	0.000
p_1(kg m^2 rad/sec)	1.732	0.000

Table 2

SINGLE AXIS PERFORMANCE INDICES

POLYNOMIAL FEEDBACK CONTROL

λ	Performance Index
$s_i + k_{ij}x_j$	3.13
$s_i + k_{ij}x_i + d_{ijk}x_jx_k$	0.49

Note that $\lambda_i = s_i + k_{ij}x_j$ only controls angular momentum, and the addition of quadratic terms are required for attitude control. Since the control influence matrix contains the Euler parameters, $\lambda_i = s_i + k_{ij}x_j + d_{ijk}x_jx_k$ produces in cubic control terms in the state equations. This cubic feedback law provides a significant reduction in the performance index by reducing the Euler parameter errors, even though larger angular momentum values are incurred.

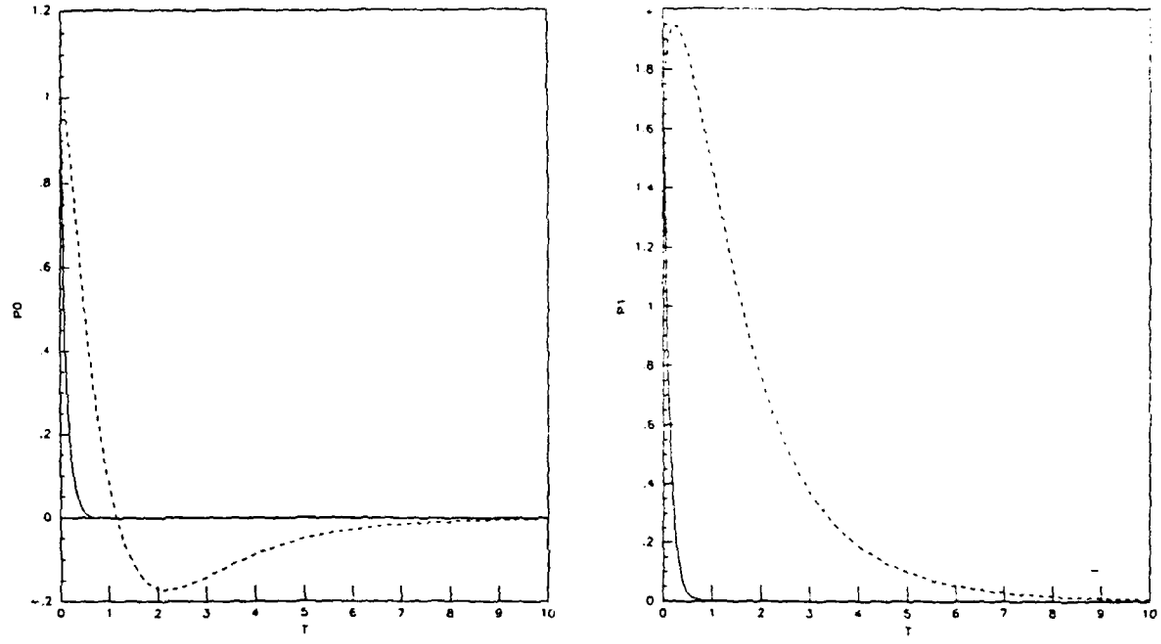

Fig. 1 Single-Axis Conjugate Angular Momenta

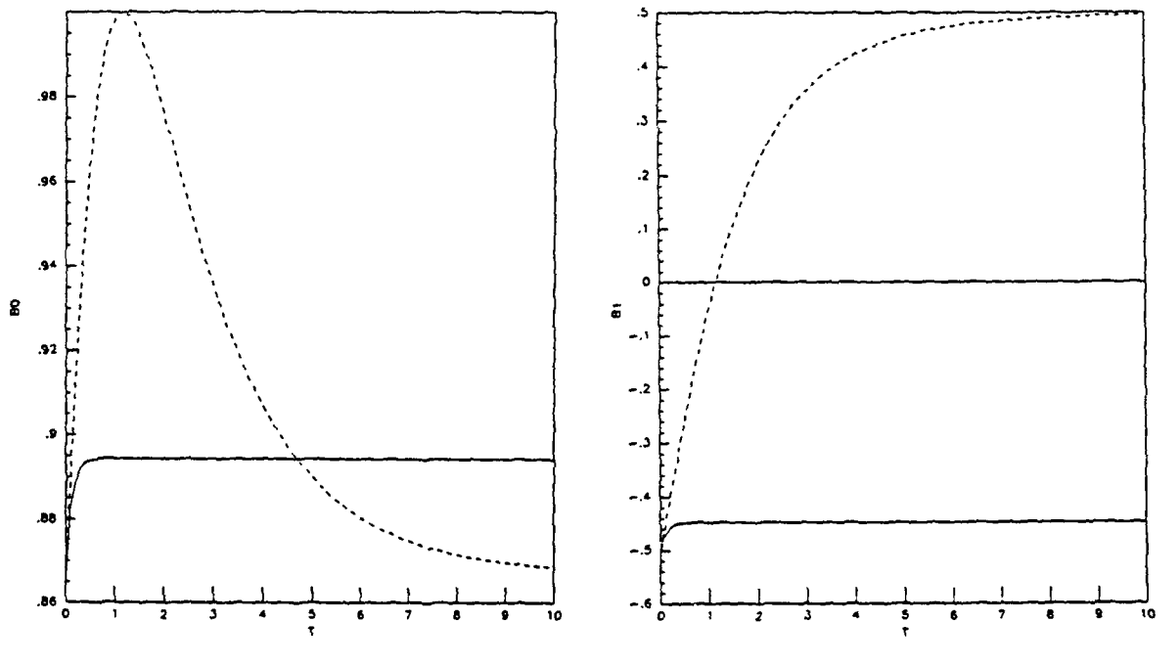

Fig. 2 Single-Axis Euler Parameters

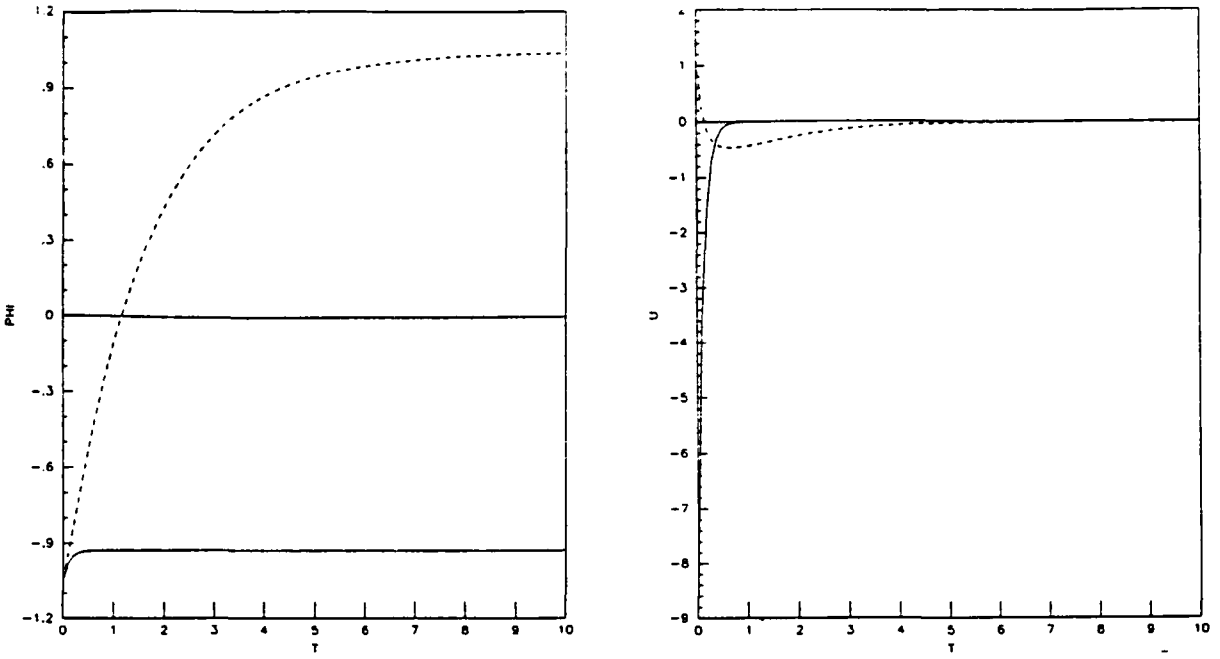

Fig. 3 Single-Axis Maneuver Angle and Control Torque

The solid lines in Figs. 1 through 3 correspond to $\lambda_i = s_i + k_{ij}x_j$, and the dashed lines correspond to $\lambda_i = s_i + k_{ij}x_j + d_{ijk}x_j x_k$.

IV. TWO-LINK MANIPULATOR CONTROL:

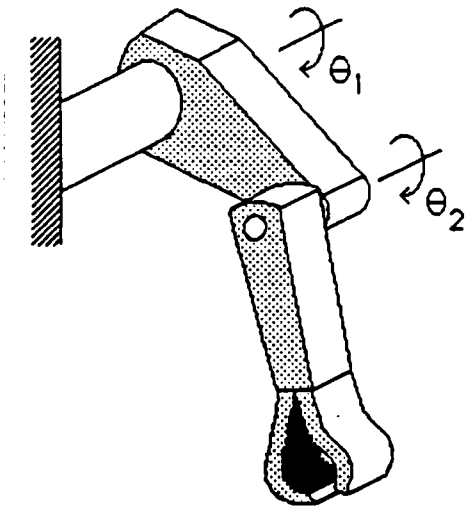

Fig. 4 Two-Link Planar Manipulator

A two-link, two-joint planar manipulator is shown in Fig. 4. The equations of motion derived by Paul[1] may be rewritten in the form presented by Golla et.al.[9] as

$$M\ddot{\underline{\theta}} = \underline{N}(\underline{\theta},\dot{\underline{\theta}}) + \underline{D}(\underline{\theta}) + \underline{u} \tag{21}$$

where $\underline{\theta} = \{\theta_1, \theta_2\}^T$ is the position vector of the two links, and $\underline{u} = \{u_1, u_2\}^T$ is the control torque vector to be applied to the joints. The inertia matrix is

$$M = M^O + M^C \cos\theta_2 \tag{22}$$

where

$$M^O = \begin{bmatrix} (m_1+m_2)d_1^2+m_2d_2^2 & m_2d_2^2 \\ m_2d_2^2 & m_2d_2^2 \end{bmatrix} \tag{23}$$

and

$$M^C = \begin{bmatrix} 2m_2d_1d_2 & m_2d_1d_2 \\ m_2d_1d_2 & 0 \end{bmatrix} \tag{24}$$

The gyroscopic terms that produce Coriolis and centripetal forces are

$$\underline{N}(\underline{\theta},\dot{\underline{\theta}}) = \begin{bmatrix} m_2d_1d_2\dot{\theta}_2^2 + 2m_2d_1d_2\dot{\theta}_1\dot{\theta}_2 \\ m_2d_1d_2\dot{\theta}_1^2 + 2m_2d_1d_2\dot{\theta}_1\dot{\theta}_2 \end{bmatrix} \sin\theta_2 \tag{25}$$

and the gravity terms are

$$\underline{D}(\underline{\theta}) = g\begin{bmatrix} (m_1+m_2)d_1\sin\theta_1+m_2d_2\sin(\theta_1+\theta_2) \\ m_2d_2\sin(\theta_1+\theta_2) \end{bmatrix} \tag{26}$$

A. Euler Parameter Kinematics.

The equations of motion in Eqs. (21) may be rewritten in terms of the Euler parameters β_{01}, β_{31}, β_{02}, β_{32}, the first two parameters corresponding to joint 1 and the second two corresponding to joint 2. Note that rotation for each

joint is about the z-axis, producing a nonzero β_3. The four Euler parameters for the two-link manipulator are

$$\begin{aligned} \beta_{01} &= \cos(\theta_1/2) \\ \beta_{31} &= \sin(\theta_1/2) \\ \beta_{02} &= \cos(\theta_2/2) \\ \beta_{32} &= \sin(\theta_2/2) \end{aligned} \tag{27}$$

and the equations relating their time rate of change to the link angular velocities ω_1 and ω_2 are

$$\begin{aligned} \dot{\beta}_{01} &= -\tfrac{1}{2}\beta_{31}\omega_1 \\ \dot{\beta}_{31} &= \tfrac{1}{2}\beta_{01}\omega_1 \\ \dot{\beta}_{02} &= -\tfrac{1}{2}\beta_{32}\omega_2 \\ \dot{\beta}_{32} &= \tfrac{1}{2}\beta_{02}\omega_2 \end{aligned} \tag{28}$$

The equations of motion may then be written as

$$M\dot{\underline{\omega}} = \underline{N}(\underline{\beta},\underline{\omega}) + \underline{D}(\underline{\beta}) + \underline{u} \tag{29}$$

where

$$\cos\theta_2 = \beta_{02}^2 - \beta_{32}^2 \tag{30}$$

is substituted into Eq. (22), and

$$\begin{aligned} \sin\theta_1 &= 2\beta_{01}\beta_{31} \\ \sin\theta_2 &= 2\beta_{02}\beta_{32} \\ \sin(\theta_1+\theta_2) &= 2\beta_{01}\beta_{31}(\beta_{02}^2-\beta_{32}^2)+2\beta_{02}\beta_{32}(\beta_{01}^2-\beta_{31}^2) \end{aligned} \tag{31}$$

are substituted into Eqs.(25) and (26). Note that the state equations, Eqs.(28) and (29), are polynomials in the states $\underline{\beta}$ and $\underline{\omega}$.

B. Optimal Control Problem.

The tracking problem of driving the states $\underline{\beta}$ and $\underline{\omega}$ to specified positions and velocities may be posed as minimizing a performance index of the form

$$J = \frac{1}{2}\underline{z}^T(t_f)H\underline{z}(t_f) + \frac{1}{2}\int_{t_0}^{t_f}\{\underline{z}^T Q\underline{z} + \underline{u}^T\underline{u}\}dt \tag{32}$$

The vector $\underline{z} = \underline{x}-\underline{r}(t_f)$, where $\underline{r}(t_f)$ is the target state. This functional is minimized subject to the state equations, which are usually written in state-space form. Since the coefficient matrix M in Eq. (29) is a function of the states, inversion of this inertia matrix produces a polynomial form that is difficult to use. Hence a rederivation of the variations in J using the state equations as they appear in Eqs. (28) and (29) produce the-following necessary conditions for optimality from Pontryagin's principle[10]

$$Q^T\underline{x} + \underline{\lambda}^T\left[\frac{\partial N}{\partial \underline{x}} + \frac{\partial D}{\partial \underline{x}} - \frac{\partial M}{\partial \underline{x}}\dot{\underline{x}}\right] + \dot{M}^T\underline{\lambda} + M^T\dot{\underline{\lambda}} = 0 \tag{33}$$

$$u_1 = -\lambda_1 \qquad u_2 = -\lambda_2 \tag{34}$$

By defining the state vector as

$$\underline{x} = \{\omega_1\ \omega_2\ \beta_{01}\ \beta_{31}\ \beta_{02}\ \beta_{32}\}^T \tag{35}$$

and assuming

$$\lambda_i = s_i + k_{ij}x_j + d_{ijk}x_jx_k + \ldots. \tag{36}$$

as before, then the costate equations in Eq. (33) are polynomials in the states. The only difficulty occurs in the term

$$\underline{\lambda}^T\frac{\partial M}{\partial \underline{x}}\dot{\underline{x}} \tag{37}$$

since $\dot{\underline{x}}$ cannot be directly substituted from Eq. (29) for states x_1 and x_2. However, a polynomial form for $\dot{\underline{x}}$ can be found by inverting the inertia matrix M using a Neumann series, where

$$M = M^o[I+P] \tag{38}$$

$$P = [M^o]^{-1}M^c(x_5^2 - x_6^2) \tag{39}$$

and $$M^{-1} = [I-P+P^2-P^3+....][M^o]^{-1} \tag{40}$$

so that

$$M^{-1} = [M^o]^{-1} - [M^o]^{-1}M^c[M^o]^{-1}(x_5^2 - x_6^2) + ... \tag{41}$$

This matrix is then postmultiplied by the right-hand-side of Eq. (29) and substituted for $\dot{\underline{x}}$ in Eq. (33). The costate equations are then purely polynomials in $\underline{x}$, so that coefficients of like powers of $\underline{x}$ may be collected to produce equations for the gains s_i, k_{ij}, and d_{ijk}.

The zeroth-order equations are

$$[M^o]\begin{Bmatrix}\dot{s}_1\\ \\ \dot{s}_2\end{Bmatrix} = \begin{Bmatrix}q_1r_1(t_f)\\ \\ q_2r_2(t_f)\end{Bmatrix} \tag{42}$$

$$\dot{s}_i \quad q_ir_i(t_f) \qquad i = 3, 4, 5, 6$$

These equations are easily solved in closed-form since $[M^o]$ is a constant matrix whose inverse is well-defined. The constants of integration are determined by the terminal boundary conditions specified in Eq. (15).

The linear equations are similar, requiring the inverse of M^o for k_{1j} and k_{2j}, and may also be solved in closed-form by substituting the solutions to Eqs. (42) into the nonhomogeneous terms of these differential equations. The constants of integration are determined by the boundary conditions in Eq. (18).

V. CONCLUSIONS:

In the previous two sections, suboptimal polynomial feedback laws were developed for nonlinear dynamical systems. The kinematics was parameterized in terms of the Euler parameters, so that polynomial nonlinearities replace transcendental terms in the state equations. The control laws produced from this formulation were simulated for rigid-body spacecraft attitude maneuvers, and were found to satisfactorily control both position and angular velocity using quadratic expansions for the costates.

The development of polynomial control laws for robotic manipulators must accomodate a position-dependent inertia matrix. A new form for the costate equations was derived from optimal control theory, so that inversion of the inertia matrix is unnecessary. Equations for zeroth-order, linear, and quadratic gains could then be derived and solved in closed-form, subject to terminal boundary conditions specified by the performance index.

The control laws produced by this method have time-dependent gains that are easily-programmed power expansions in t. Hence, this control formulation requires little memory or processing time, and yet accomodates many of the nonlinearities present in robotic manipulators or spacecraft attitude control.

VI. RECOMMENDATIONS:

The simulation results for spacecraft attitude maneuvers demonstrated that polynomial feedback laws can

effectively control position and velocity without linearization of the system dynamics. The analysis for a two-link manipulator using the same kinematic parameters demonstrates that this control method can also be applied to robotic manipulators. Future research would include computer simulations for the two-link model, similar to those demonstrated for spacecraft maneuvers. The quadratic gain equations would be derived, and all the gain equations solved in closed-form. A computer simulation code would then be written to demonstrate these control laws. If the two-link manipulator can be effectively controlled by these new laws, then the state equations for a six-link manipulator could be attempted.

The control laws developed here minimize a performance index that penalizes the errors between actual angle and target angle values for each joint of the manipulator. A better performance index would penalize end-effector position and velocity errors, rather than prescibing a priori the target states for each joint. A study of this second class of performance indices, which are task-oriented, could be applied to two- or three-link manipulators using Euler parameter kinematics and nonlinear feedback control laws.

REFERENCES

1. Paul, Richard P., Robot Manipulators: Mathematics, Programming, and Control, MIT Press, Cambridge, MA, 1983.
2. Morton, Harold S., Jr., "A Formulation of Rigid-Body Rotational Dynamics Based on Generalized Angular Momentum Variables Corresponding to the Euler Parameters," AIAA/AAS Astrodynamics Conference, Seattle, WA, Aug. 1984, Paper No. 84-2023.
3. Whittaker, E.T., A Treatise on the Analytical Dynamics of Particles and Rigid Bodies, Dover Publications, New York, 1944.
4. Kane, T.R., Likins, P.W., and Levinson, D.A., Spacecraft Dynamics, McGraw-Hill Book Co., New York, 1983.
5. Meirovitch, Leonard, Methods of Analytical Dynamics, McGraw-Hill Book Co., 1970.
6. Carrington, C.K. and Junkins, J.L., "Nonlinear Feedback Control of Spacecraft Slew Maneuvers," J. of Astronautical Sciences, Vol. 32, No.1, Jan-Mar. 1984, pp. 24-45.
7. Carrington, C.K. and Junkins, J.L., "Optimal Nonlinear Feedback Control for Spacecraft Attitude Maneuvers", to appear in J. of Guidance, Control, and Dynamics, (AIAA Paper No. 83-2230-CP, Gatlinburg, Tenn.)
8. Carrington, C.K., "Optimal Nonlinear Feedback Control of Spacecraft Attitude Maneuvers," Ph.D. Dissertation, VPI&SU, Dec. 1983.

9. Golla, David F., Garg, Subash C., and Hughes, Peter C., "Linear State-Feedback Control of Manipulators," from Robot Motion: Planning and Control, Brady, Michael, et.al., MIT Press, 1983.

10. Kirk, Donald E., Optimal Control Theory, Prentice-Hall, Inc., 1970.

1985 USAF-UES SUMMER FACULTY RESEARCH PROGRAM/
GRADUATE STUDENT SUMMER SUPPORT PROGRAM

Sponsored by the
AIR FORCE OFFICE OF SCIENTIFIC RESEARCH

Conducted by the

UNIVERSAL ENERGY SYSTEMS, INC.

FINAL REPORT

MODIFICATION AND EVALUATION OF HEAT TRANSFER CALCULATIONS USING THE AFWAL PNS CODE

Prepared by:	R. R. Chamberlain
Academic Rank:	Assistant Professor
Department and University:	Aerospace Engineering The University of Alabama
Research Location:	Flight Dynamics Laboratory Aeromechanics Division High Speed Aero Performance Branch Aerodynamic Heating Group
USAF Research:	Mr. Richard D. Neumann
Date:	9 September 1985
Contract No:	F49620-85-C-0013

MODIFICATION AND EVALUATION OF HEAT TRANSFER CALCULATIONS USING THE AFWL PNS CODE

by

R. R. Chamberlain

ABSTRACT

This report describes the computational study which was performed using the AFWAL PNS code. The main features of interest are the calculations of heat transfer rates and skin friction coefficients. It is found that there are cases for which the PNS code does not predict results which are consistent with classical analytical analyses. This study indicates that the lack of correlation is associated with such a rapid and apparently nonphysical boundary layer growth that classical analysis is no longer valid. Recommendations for further study on the question of the boundary layer thickness and its relationship to the calculation of flow field gradients are put forth and discussed.

ACKNOWLEDGMENTS

I wish to express my sincere appreciation to Mr. Richard D. Neumann and Mr. Jerold L. Patterson of AFWAL/FIMG for their technical assistance as well as for their help in making my summer faculty research experience both enjoyable and successful. I am also grateful for the sponsorship of the Air Force Systems Command and the Air Force Office of Scientific Research, without whose support this study would not have been possible.

I. INTRODUCTION

My particular research interest is in the area of computational fluid dynamics. I have a strong educational and research background in classical fluid mechanics, gas dynamics and numerical analysis. My previous experience has been with the development of original numerical algorithms for complex flow calculations, but I have also been involved with existing fluid dynamics codes. I am able to quickly feel comfortable with large and unfamiliar computer programs, and this particular ability helped me to a great extent during the Summer Faculty Research Program.

The United States Air Force has recently initiated an intensive research effort in hypersonic flow with applications to reentry vehicles and high altitude missile systems. The physics of the fluid behavior in this flight regime is quite unlike that which is normally encountered at lower speeds. In particular, aerodynamic heating now becomes an important design consideration since the flow velocity is great enough that the fluid temperature near the vehicle becomes very high. This causes the body to heat up and, if left unchecked, could also lead to mission failure for an improperly designed vehicle. It is thus of great interest to be able to accurately predict aerodynamic heating rates so that proper design input variables are known.

One of the tremendous difficulties encountered in hypersonic flow research is the reproduction of actual high altitude flight conditions in the laboratory. Over the years, there has been a realization that flight test and laboratory data alone are not enough to design and analyze a new system. The supercomputer has proven itself to be an invaluable design aid, and there is no exception for hypersonic flow applications. The Parabolized Navier-Stokes (PNS) code, developed at NASA Ames and at AFWAL, is one of the foremost state-of-the-art computer codes for predicting supersonic and hypersonic flow fields. I worked with this code at AFWAL, running various test cases and checking the results, in order to verify its accuracy and improve its performance and efficiency. Since I have always had a strong interest in the

computational aspects of hypersonic flow, it was indeed fortunate to have been associated with the Aerodynamic Heating Group. This final report documents the work which was performed during the period 20 May to 26 July 1985.

II. OBJECTIVES OF THE RESEARCH EFFORT

The research effort concentrated primarily on the use and modification of the PNS code which has already been successfully applied to a wide range of problems of current interest (e.g., the X24-C). During some previous tests, however, it was observed that several problems arose when the code was applied to very high Mach number, low Reynolds number flows, especially when the flow was laminar. The flow solutions for certain simple geometries in the hypersonic Mach number range were not consistent with the results expected from classical theory. Specifically, the heat transfer rates predicted were too large and did not follow the classical trend. It was thus originally believed that some error existed in the PNS code. The error was thought to be simply a programming mistake, or it may have had a more fundamental origin, such as the incorrect treatment of the boundary conditions. The original objectives were thus to change the key features of the heat transfer calculations and the implementation of the wall boundary conditions and then to observe what solution changes were brought about. During the course of this research, however, it was determined that no single, simple error could account for the unexpected behavior of some of the solutions. Furthermore, it also appeared that the first order boundary treatment at the solid surface was sufficient for practical purposes. The anomalous behavior at high Mach number remained, however, and the research objectives were thus modified to carry out a more detailed study of this behavior. It was decided to determine what additional physical conditions were associated with the calculation of the unexpected heat transfer rates so that the actual problem itself could be more fully defined.

III. OUTLINE OF THE RESEARCH EFFORT

Much interest and attention have recently been given to the solution of the PNS equations because of the relative ease with which they may be handled as compared to the full Navier-Stokes equations. The essential difference is that the parabolized set of equations is no longer elliptic in the streamwise direction, and hence the solution may be obtained by marching downstream from an initial plane of data. In most cases, this results in an order of magnitude savings in computational effort.

The algorithm of present interest is embodied in the AFWAL/NASA merged PNS code, as described by Kaul and Chaussee (Ref. 1). Their formulation allows the calculation of hypersonic flow fields about blunted cones and cylinders, as well as complex configurations such as the X24-C. The PNS code is also capable of providing force and moment data, as well as surface pressures, skin friction and heat transfer rates. In a total design effort, all of this information would be required. For the present, however, we shall restrict our attention to the accurate estimation of skin friction and heat transfer.

A series of test runs for the PNS code have been designed and run on the AFWAL Cray 1S supercomputing system. The simple configuration of a sphere/cylinder was chosen since classical boundary layer and heat transfer solutions for the case of a cylinder are well known. In fact, for the purely axisymmetric flow which is considered here, the equations for the cylinder are identical to those for the classical flat plate.

In order to demonstrate the difficulty in calculating heat transfer rates at high Mach numbers, we define the parameter $\frac{St\sqrt{Re_{\infty x}}}{\sqrt{p/p_\infty}}$, where St is the Stanton number given by $St = \frac{k(\frac{\partial T}{\partial n})_w}{\rho_\infty u_\infty c_p(T_w - T_0)}$. This quantity is used as the primary heat transfer parameter since it is predicted by classical theory to be constant. Figure 1 illustrates the problem which is observed at Mach 24 for the simple case of a sphere/cylinder. For

high Reynolds numbers (above 1×10^6 /ft), the axial profiles of heat transfer vs. x appear to approach the classical value for a flat plate. For the relatively low Reynolds number of $Re = 5 \times 10^4$ /ft, however, the solution departs significantly from the flat plate value. This observation contradicts the expected trend which is demonstrated by classical theory.

Two approaches to resolve this problem are identified and implemented. The first is to modify the calculation of the normal temperature gradient which is used to calculate $\dot{Q}$ at the body surface. The second is to increase the order of accuracy of the surface boundary conditions. Both of these approaches could potentially lead to better heat transfer calculations since they deal directly with the accuracy of the flow variables at the body surface.

Calculation of Surface Normal Flow Field Gradients

Previously, a streamline oriented coordinate system was used near the body to approximate $\frac{\partial T}{\partial n}$ and $\frac{\partial V}{\partial n}$, but this could be inaccurate at high Mach numbers where large gradients are encountered. The new calculation involves the use of body geometry rather than streamline geometry for computing the normal direction and hence the normal gradient. For consistency, the calculation of skin friction is similarly modified, and these changes to the PNS code take place in the subroutine BLVAR. In addition, since it was found to be necessary to expand and clarify the output of surface variables, the entire subroutine is rewritten.

The rate at which heat is transferred to or from a body follows the Fourier law of heat conduction, which is expressed as

$$\dot{Q} = - k \nabla T \cdot \hat{n} \qquad (1)$$

The cartesian components of ΔT in an arbitrary curvilinear coordinate system take the form

$$T_x = T_\xi \xi_x + T_\eta \eta_x + T_\zeta \zeta_x \quad (2a)$$

$$T_y = T_\xi \xi_y + T_\eta \eta_y + T_\zeta \zeta_y \quad (2b)$$

$$T_z = T_\xi \xi_z + T_\eta \eta_z + T_\zeta \zeta_z \quad (2c)$$

Since the PNS code uses only an axis-normal grid system, the quantities ξ_y and ξ_z are zero. Furthermore, it is consistent with the PNS approximation to drop the heat flux terms which contain partial derivatives with respect to the streamwise coordinate ξ. Therefore, Equations 2a-2c involve only T_η and T_ζ, as well as the metrics of the transformation, which are defined as

$$\eta_x = -J(y_\xi z_\zeta - y_\zeta z_\xi)$$

$$\eta_y = J(x_\xi z_\zeta - x_\zeta z_\xi)$$

$$\eta_z = -J(x_\xi y_\zeta - x_\zeta y_\xi)$$

$$\zeta_x = J(y_\xi z_\eta - y_\eta z_\xi)$$

$$\zeta_y = -J(x_\xi z_\eta - x_\eta z_\xi)$$

$$\zeta_z = J(x_\xi y_\eta - x_\eta y_\xi)$$

The Jacobian J in this case reduces to

$$J = [x_\xi (y_\eta z_\zeta - y_\zeta z_\eta)]^{-1}$$

We now define a unit normal vector n as

$$\hat{n} = \frac{\zeta_x \hat{i} + \zeta_y \hat{j} + \zeta_z \hat{k}}{\sqrt{\zeta_x^2 + \zeta_y^2 + \zeta_z^2}} \tag{3}$$

The heat flux at the body thus becomes

$$\dot{Q} = \frac{-k(T_x \zeta_x + T_y \zeta_y + T_z \zeta_z)}{\sqrt{\zeta_x^2 + \zeta_y^2 + \zeta_z^2}}$$

where T_x, T_y and T_z are given by Equations 2a-2c. This calculation of $\dot{Q}$ is considered to be improved as compared to the previous approximation due to the fact that it uses the local body geometry rather than local streamline directions as a reference for computing $\nabla T \cdot \hat{n}$.

We now consider the calculation of skin friction, both in the streamwise and the circumferential directions. The axial component of shear stress is denoted by τ_{xz} and from the full Navier-Stokes equations is defined by

$$\tau_{xz} = \mu(\xi_z u_\xi + \eta_z u_\eta + \zeta_z u_\zeta + \xi_x w_\xi + \eta_x w_\eta + \zeta_x w_\zeta) \tag{4}$$

Dropping the streamwise partial derivatives and taking account of the grid system and the wall boundary conditions ($u = v = w = 0$), we may express τ_{xz} as

$$\tau_{xz} = \mu(\zeta_z u_\xi + \zeta_x w_\zeta) \tag{5}$$

In a similar fashion, the circumferential component of shear stress is given by

$$\tau_{yz} = \mu(\zeta_z v_\zeta + \zeta_y w_\zeta) \tag{6}$$

These two quantities are now used to compute the axial and circumferential skin friction coefficients, respectively.

Second Order Wall Boundary Conditions

As described by Schiff and Steger (Ref. 2), the viscous wall boundary conditions are both implicit and first order. Using the notation of Reference 1, these boundary conditions for constant wall temperature are expressed in matrix form as

$$\bar{a}\,\Delta\tilde{q}_1 + b\,\Delta\tilde{q}_2 = f \tag{7}$$

where

$$\bar{a} = \begin{bmatrix} 1 & 0 & 0 & 0 & 0 \\ 0 & 1 & 0 & 0 & 0 \\ 0 & 0 & 1 & 0 & 0 \\ 0 & 0 & 0 & 1 & 0 \\ \dfrac{-\gamma(\gamma-1)T_\infty}{T_w} & 0 & 0 & 0 & 1 \end{bmatrix}$$

$$\bar{b} = \begin{bmatrix} -\left(\dfrac{J_2}{J_1}\right)^{j+1} & 0 & 0 & 0 & 0 \\ 0 & 0 & 0 & 0 & 0 \\ 0 & 0 & 0 & 0 & 0 \\ 0 & 0 & 0 & 0 & 0 \\ 0 & 0 & 0 & 0 & 0 \end{bmatrix}$$

$$f = \begin{bmatrix} \dfrac{(J_1^j - J_1^{j+1})\tilde{e}_1^j - (J_2^j - J_2^{j+1})\tilde{e}_2^j}{J_1^{j+1}} \\ 0 \\ 0 \\ 0 \\ 0 \end{bmatrix}$$

This form, although only first order, is very convenient since it fits directly into the block tridiagonal structure of the finite difference equations.

We now consider an alternative form given in matrix notation as

$$\bar{a}\,\Delta\tilde{q}_1 + \bar{b}\,\Delta\tilde{q}_2 + \bar{c}\,\Delta\tilde{q}_3 = f \qquad (8)$$

where we now define

$$\bar{a} = \begin{bmatrix} -3 & 0 & 0 & 0 & 0 \\ 0 & 1 & 0 & 0 & 0 \\ 0 & 0 & 1 & 0 & 0 \\ 0 & 0 & 0 & 1 & 0 \\ \dfrac{-\gamma(\gamma-1)T_\infty}{T_w} & 0 & 0 & 0 & 1 \end{bmatrix}$$

$$\bar{b} = \begin{bmatrix} \frac{4J_2^{j+1}}{J_1^{j+1}} & 0 & 0 & 0 & 0 \\ 0 & 0 & 0 & 0 & 0 \\ 0 & 0 & 0 & 0 & 0 \\ 0 & 0 & 0 & 0 & 0 \\ 0 & 0 & 0 & 0 & 0 \end{bmatrix}$$

$$\bar{c} = \begin{bmatrix} \frac{-J_3^{j+1}}{J_1^{j+1}} & 0 & 0 & 0 & 0 \\ 0 & 0 & 0 & 0 & 0 \\ 0 & 0 & 0 & 0 & 0 \\ 0 & 0 & 0 & 0 & 0 \\ 0 & 0 & 0 & 0 & 0 \end{bmatrix}$$

$$f = \begin{bmatrix} 3\left(\frac{J_1^{j+1} - J_1^{j}}{J_1^{j+1}}\right)\tilde{e}_1 - 4\left(\frac{J_2^{j+1} - J_2^{j}}{J_1^{j+1}}\right)\tilde{e}_2^{j} + \left(\frac{J_3^{j+1} - J_3^{j}}{J_1^{j+1}}\right)\tilde{e}_3^{j} \\ 0 \\ 0 \\ 0 \\ 0 \end{bmatrix}$$

This formulation implements the constant wall temperature boundary condition as a second order, one-sided difference. However, the matrix structure of the equations is no longer tridiagonal unless the unknown

quantity $\Delta\tilde{q}_1$ is eliminated from the system. When this is done, the second order implementation becomes

$$(A\bar{b} - \bar{a}B)\Delta\tilde{q}_2 + (A\bar{c} - \bar{a}C)\Delta\tilde{q}_3 = Af - \bar{a}f \qquad (9)$$

Where A, B, C and F are defined from the governing finite difference equations at the first interior mesh point, and $\bar{a}$, $\bar{b}$, $\bar{c}$ and f are given as above. It should be noted that the overall system is reduced in order by one since now the quantity $\Delta\tilde{q}_1$ has been eliminated. Its values are easily recovered from Eq. (8) after the block tridiagonal inversion step.

IV. RESULTS

The revised normal gradient calculation seems to have had little effect on the overall result for heat transfer. Although the present formulation is more consistent with the programming pattern of the PNS code, it has not influenced the results to the extent desired. The fundamental reason for this is still unknown. However, this finding does confirm that the results are not as sensitive to the flow field gradient calculations as was first believed. This suggests that a more thorough investigation of the problem illustrated in Fig. 1 is needed.

The reaction of the PNS code to the implementation of second order wall conditions was dramatic but inconclusive. Very soon after the marching process started from the initial plane of data, an instability developed and the solution soon diverged. The second order, one-sided difference formulation for wall boundary conditions is often unstable since it degrades the diagonal dominance of the matrix system. For this reason it is usually not employed, although it has been known to be successful in the numerical solution of elliptic equations.

The present version of the PNS code (PNSTST1) contains the input parameter IOBC which is set to 1 for first order wall conditions and to 2 for second order. The use of IOBC = 1 is recommended.

V. ALTERNATIVE APPROACHES

Although accomplished, the original research goals did not improve the performance of the PNS code for the case of the Mach 24 sphere/cylinder. It was thus decided to investigate more carefully the results that were being obtained using the above modifications.

Figure 2 shows the thermal boundary layer profile plotted against the similarity coordinate $\frac{y}{x}\sqrt{Re_{\infty x}}$ for a Mach 20 test case. The PNS result is compared against the classical flat plate solution for a wall to free stream temperature ratio of 6. This figure clearly shows that the thermal boundary layer predicted by the PNS code is much thicker than expected. The same trend is also observed at lower Mach numbers, and thus it appears that the problem for sphere/cylinders is not entirely confined to very high Mach number, low Reynolds number flows.

Since it is desired to find the conditions under which the PNS code will reproduce the classical results for skin friction and heat transfer, it is now clear that we must try to thin the boundary layer. One approach is to vary the Reynolds number, realizing that to some degree this parameter controls the boundary layer thickness. Figure 3 shows how changing the Reynolds number by two orders of magnitude affects the temperature profiles between the body and the shock. The higher Reynolds number profile is thinner, as expected, but not nearly to the extent that is desired. Thus, changing the Reynolds number alone is not sufficient for our purposes.

The real significance of Fig. 3, however, is that it reveals what a substantial portion ($\sim$65%) of the distance between the body and the shock is taken up by the boundary layer. In fact, the boundary layer is so thick that it far exceeds the body radius, which in this case is 0.5 inches. This fact may offer a potential clue to the heat transfer situation since it is apparent that the fundamental premise of boundary layer theory, namely that $\delta/r << 1$, is being violated. Based upon this observation, we would expect that as δ/r becomes smaller than 1, the boundary layer approximation would be better satisfied, and the heat transfer would then reduce to the classical solution. In order to test

this hypothesis, a body whose radius varies with x, such as a cone, is considered. Figure 4 shows the resulting relationship between δ/r and the cone half angle for the Mach 24 case. In Fig. 5, the corresponding heat transfer parameter is plotted vs. x for four sphere/cones with different half angles and is compared to the result for the sphere/cylinder at $M_\infty = 24$. These figures clearly demonstrate that as δ/r becomes smaller (i.e., as the cone half angle increases as shown in Fig. 4), the classical solution is recovered. The incorrect heat transfer predictions for the case of the cylinder are thus seen to be symptoms of a boundary layer which is too thick, and any proposed solution to the current problems must address this issue.

VI. RECOMMENDATIONS

One of the dangers of comparing the hypersonic PNS results to classical boundary layer theory is the obvious mismatch in the test conditions. For example, classical theory assumes that the flow solution outside of the boundary is known a priori, whereas the PNS code computes the boundary layer and the shock layer solutions simultaneously. Therefore, in order to fully validate the PNS results for the case of the sphere/cylinder, it will be necessary to perform a boundary layer calculation alone using the PNS algorithm. It is recommended that the PNS code itself be used for this test with special care taken to exclude the shock layer calculation as well as to initialize the code with an appropriate boundary layer starting solution.

A preliminary calculation of this sort is summarized in Fig. 6. The shock layer calculation has been removed, and the starting solution is just a free stream profile. The fact that the PNS solution does not identically reproduce the classical result under these conditions demonstrates the need for a careful test of the way in which the PNS code handles the boundary layer. This is necessary in order to determine the appropriateness of the Beam and Warming algorithm (Ref. 3) as well as of the mesh system being used. To the knowledge of this author, this

algorithm has not been applied to boundary layer flows on cylinders or flat plates. A numerical experiment of this sort is thus warranted in order to confirm that we can indeed expect to reproduce classical solutions accurately.

Another point which should be investigated is the use of simple stretched grids in regions of large flow gradients (e.g., near the body). Although this is standard practice, it may be possible to reduce the size of these gradients somewhat by considering alternative transformations. A reduction in the magnitude of the flow gradients would increase the accuracy of heat transfer calculations since small errors would no longer tend to be amplifed. It is thus recommended that standard boundary layer transformations be considered. This would help reduce the steepness of the flow gradients and would also maintain a constant boundary layer thickness in terms of the natural boundary layer coordinate. As we have already seen, the extremely rapid growth of the boundary layer for the case of the sphere/cylinder is related to the lack of correlation between the classical heat transfer results and the PNS predictions. It is believed that following this suggestion would begin to alleviate some of the problems observed in previous calculations.

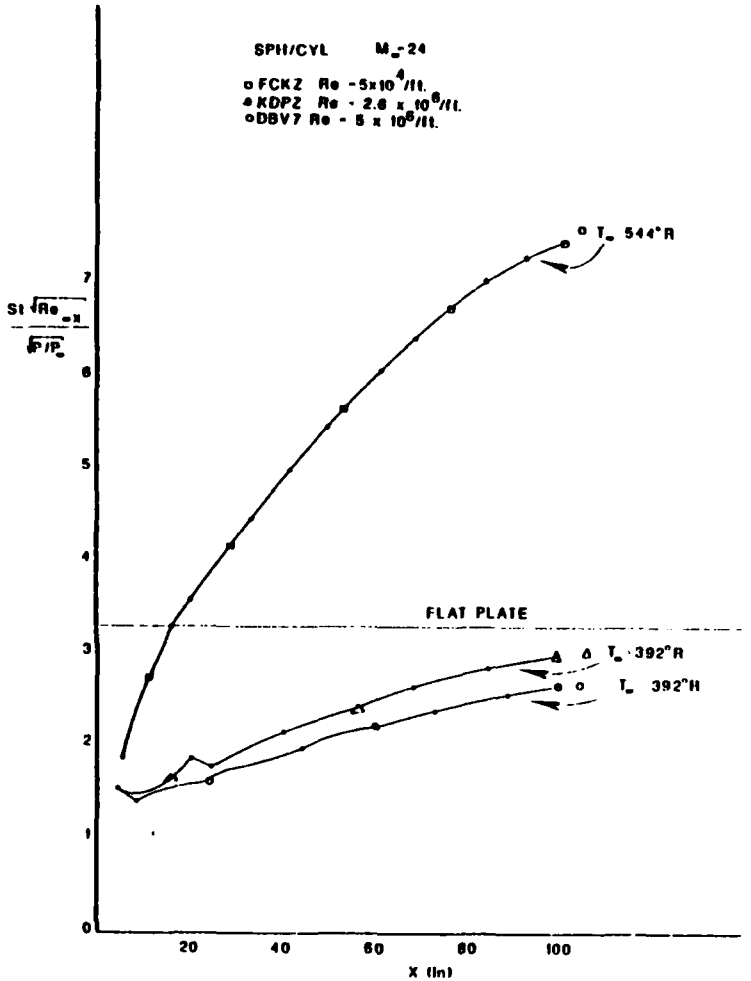

Figure 1. Heat transfer parameter $\frac{St\sqrt{Re_{\infty x}}}{\sqrt{P/P_\infty}}$ vs. x on a sphere/cylinder at M_∞=24 for three Reynolds numbers.

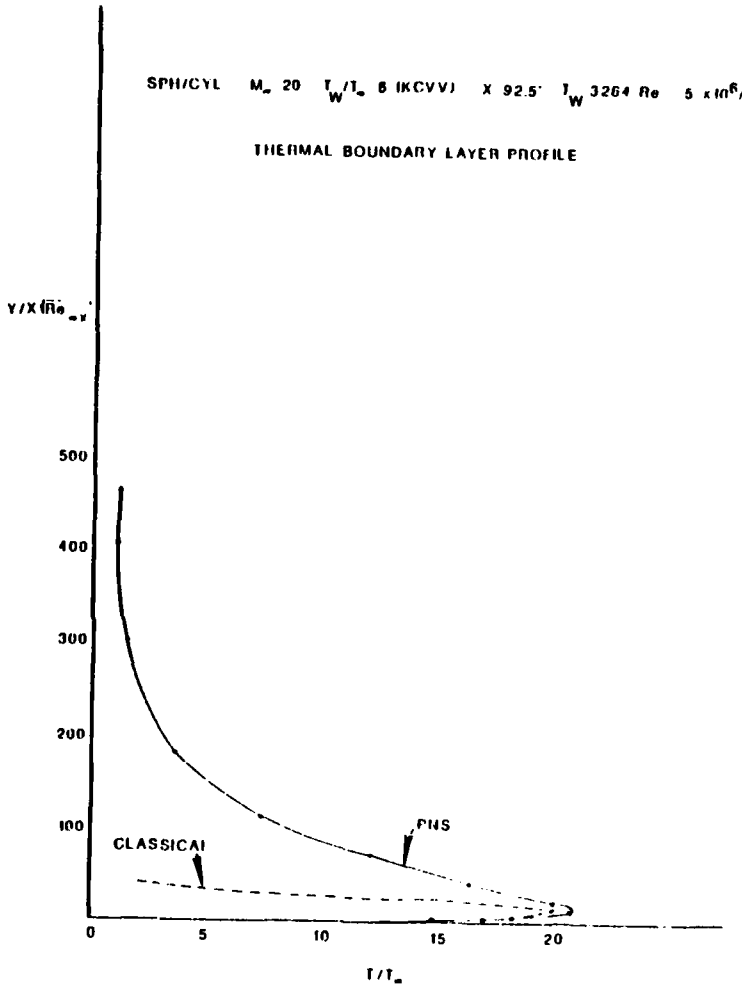

Figure 2. Comparison of the PNS thermal boundary layer profile for a sphere/cylinder with the classical flat plate solution for M_∞=20 and Re=5x10^6/ft.

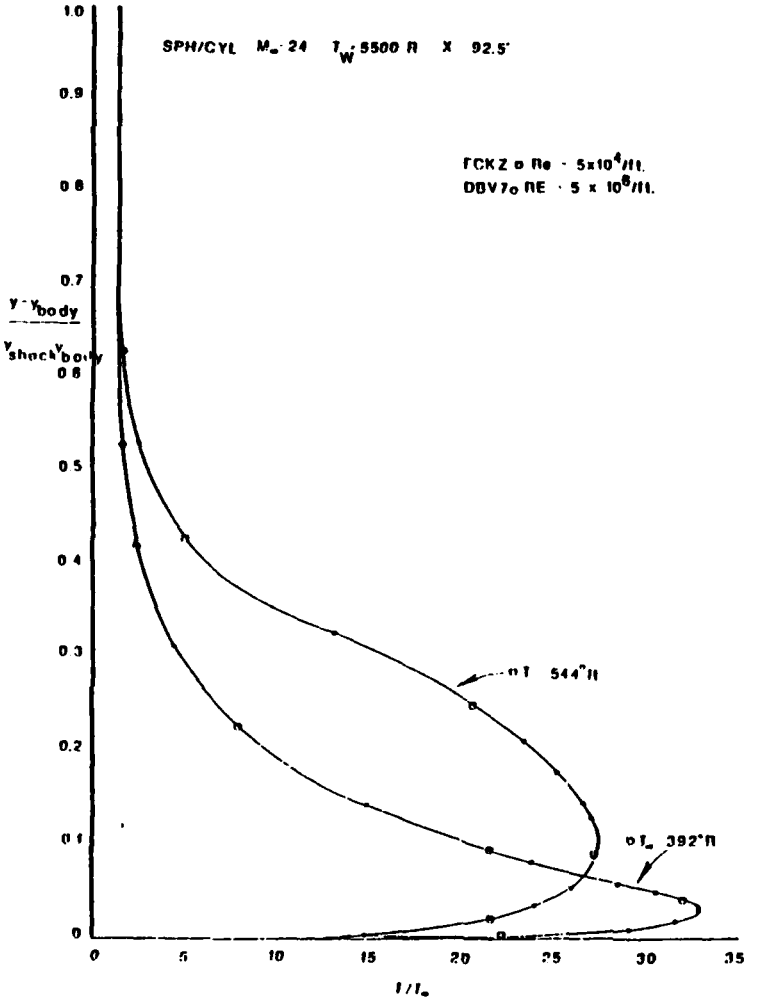

Figure 3. Thermal boundary layer and shock layer profiles on a sphere/cylinder at M_∞=24 for two Reynolds numbers. Note that the solution for Re=5x10^6/ft has a thinner profile but also a steeper surface gradient.

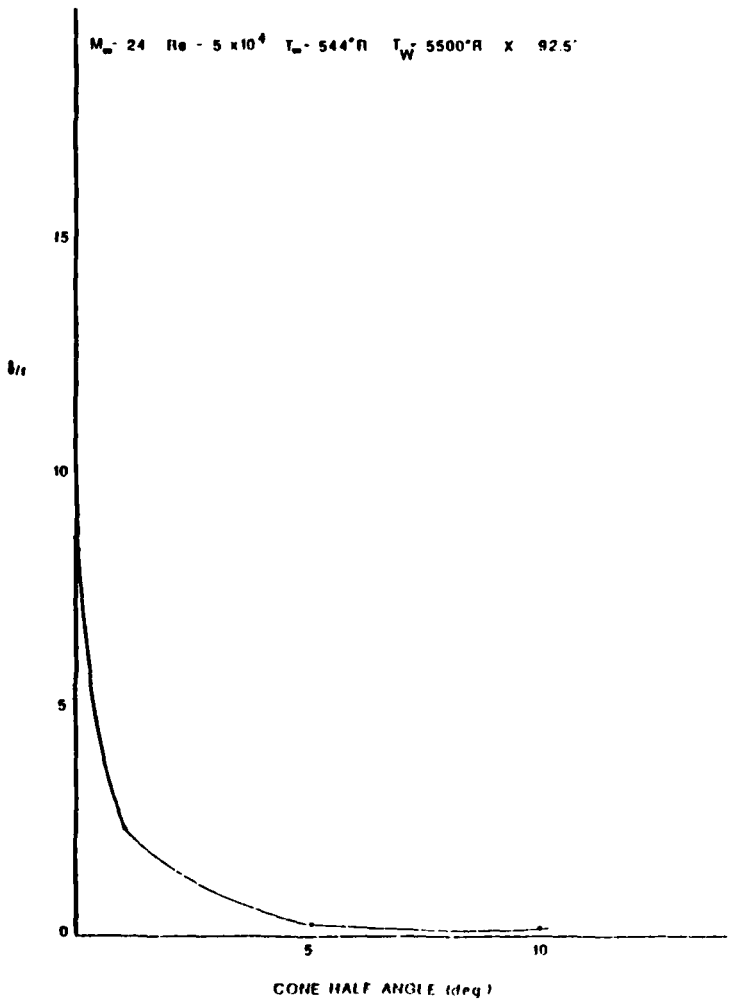

Figure 4. Plot of δ/r vs. cone half angle on a sphere/cone at M_∞ = 24 and Re=5x10^4/ft.

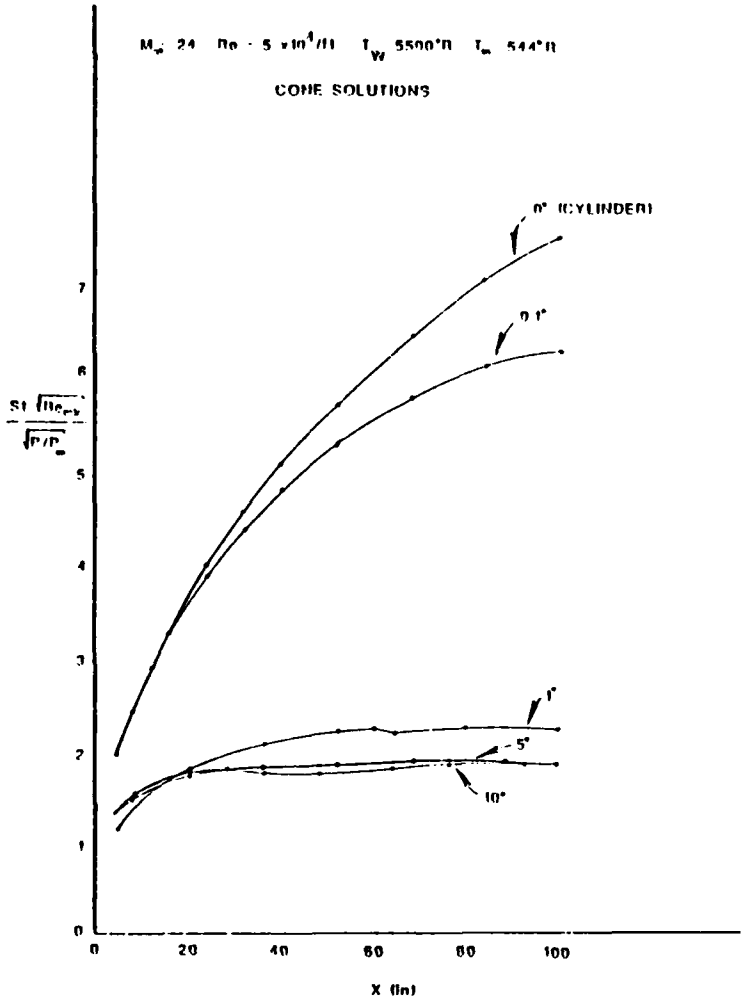

Figure 5. Demonstration of the effect of varying the cone angle on the heat transfer. As the cone angle decreases toward 0^o, the heat transfer begins to depart from the expected trend. M_∞=24 and Re=5x10^4/ft.

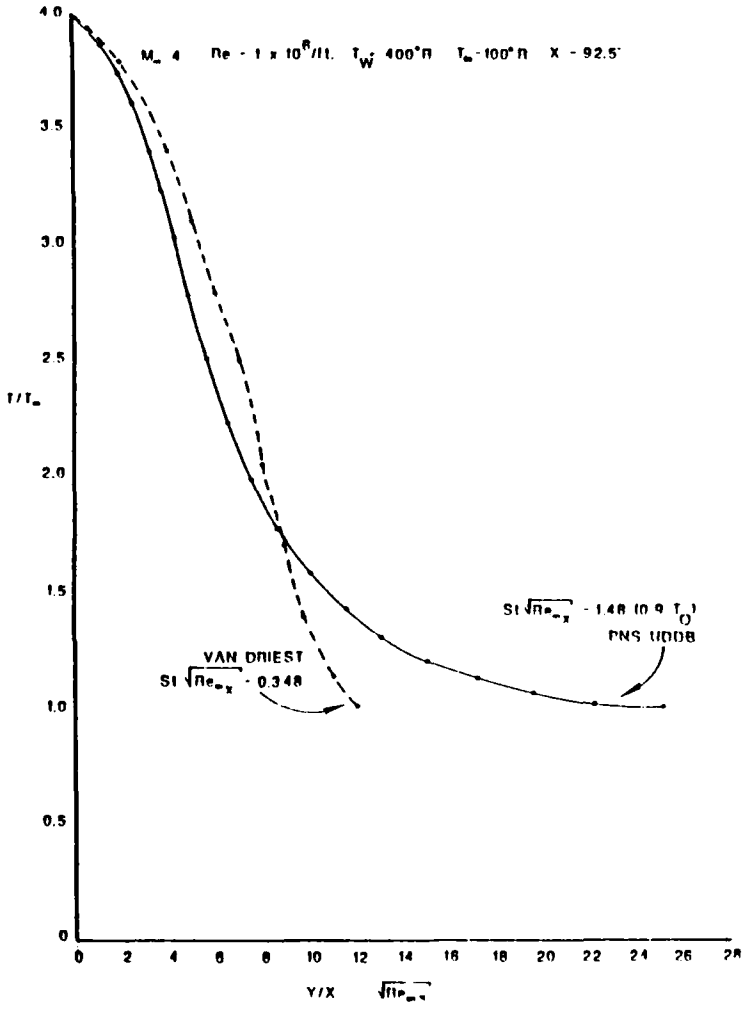

Figure 6. Preliminary results of the boundary layer experiment for the PNS code. The temperature ratio T/T_∞ on a sphere/cylinder is plotted vs. the similarity parameter $\frac{y}{x}\sqrt{Re_{\infty x}}$ and compared to the flat plate result with M_∞=4, T_W/T_∞=4 and Re=1x10^6/ft.

REFERENCES

1. Kaul, U.K. and Chaussee, D.S., AFWAL Parabolized Navier-Stokes Code: 1983 AFWAL/NASA Merged Baseline Version, AFWAL-TR-83-3118, May 1984.

2. Schiff, L.B. and Steger, J.L., "Numerical Simulation of Steady Supersonic Viscous Flow," AIAA paper 79-0130, January 1979.

3. Beam, R. and Warming, R.G., "An Implicit Factored Scheme for the Compressible Navier-Stokes Equations," AIAA Journal, Vol. 16, pp. 393-402, April 1978.

1985 USAF-UES SUMMER FACULTY RESEARCH PROGRAM
GRADUATE STUDENT SUMMER SUPPORT PROGRAM

Sponsored by the

AIR FORCE OFFICE OF SCIENTIFIC RESEARCH

Conducted by the

UNIVERSAL ENERGY SYSTEMS, INC.

FINAL REPORT

OPTICAL AND X-RAY TOPOGRAPHIC CHARACTERIZATION OF UNDOPED SIMI-INSULATING GaAs

Prepared by:	Jharna Chaudhuri
Academic Rank:	Assistant Professor
Departant and University:	Mechanical Engineering Department Wichita State University
Research Location:	AFWAL/AADR, Electronic Research Branch, Avionics Laboratory
USAF Research:	Dave Look
Date:	September 15, 1985
Contract No:	F49620-85-C-0013

OPTICAL AND X-RAY TOPOGRAPHIC CHARACTERIZATION OF UNDOPED SEMI-INSULATING GaAs

by

Jharna Chaudhuri
Assistant Professor

ABSTRACT

Distribution of EL2 concentration, variation in local strain and composition, as well as dislocation pattern in undoped semi-insulating GaAs were characterized by using different techniques. The GaAs single crystals were grown by liquid encapsulated Czochralski method. The concentration of deep donor EL2 was measured by optical absorption method. A comparison of EL2 concentration in crystals grown under low pressure and high pressure was made, which showed that the crystals grown under low pressure have less EL2 concentration.

X-ray rocking curve analysis was performed to measure dislocation densities as well as non-uniform strains arising from local lattice distortions. An attempt was also made to determine the local variation in composition in the wafer. This x-ray rocking curve analysis study is at a preliminary stage at present and needs further detailed investigation.

ACKNOWLEDGEMENTS

I would like to thank Dr. Philip Stover, Mr. Eugene R. Nichols and the rest of the staff of AFWAL/AADR for their help during the course of this study. In particular, I am grateful to Dr. Dave Look for his continuous support and guidance during this period.

In addition, I would like to thank Dr. Wade W. Adams, Dr. P Galen Lenhert and Mr. Joseph O'Brian at AFWAL/ MLBP for letting me use the four cycle diffrachometer and also helping me to set up the samples. I thank Ms. Katherine Thomas, the secretary of Mechanical Engineering Department at Wichita State University for typing the final report. Lastly, I would like to thank Dr. James Ho, Professor of the Physics Department at Wichita State University for introducing this program to me.

This work was supported by AFOSR through the 1985 USAF-UES Summer Faculty Research Program

I. INTRODUCTION

Undoped semi-insulating GaAs is currently being used in the development of a number of high performance electronic devices. These include low and high power field effect transistors, monolithic microwave integrated circuits, high speed digital integrated circuits and high speed charged coupled devices. The high resistivity of this material is due to an electrical compensation resulting in the Fermi level being pinned to a midgap donor deep level labeled EL2.

It has been reported that the spatial variation of EL2 concentration results in the corresponding variation in electrical properties.[1] There is a striking similarity between the distribution of EL2 and dislocation pattern in the material.[2,3,4]

II. OBJECTIVES OF THE RESEARCH EFFORT

The aims of the present project are the following:

1. To determine the distribution of EL2 concentration in undoped semi-insulating GiaAs wafers, grown under different conditions.
2. To investigate a possible correlation between EL2 defects and dislocations.
3. To measure residual strains which arises due to a possible stoichiometric variation in the material.

III. EXPERIMENTAL TECHNIQUES

Undoped semi-insulating (001) GaAs single crystals grown both by the high pressure LEC (liquid Encapsulated Czochralski) method and, the low pressure LEC method were used in the present study. Slices of about .06, cm thick and either 7.6 cm (3in) in diameter or 5.1 cm (2 in) in diameter were cut perpendicular to the growth direction from the seed end, middle portion, and tail end of the crystals.

Optical Absorption Method

The EL2 concentrations at different positions in the wafer were determined

by the photo-absorption method.[2] The absorption coefficient of EL2 level at wavelength λ_1, $\alpha_1(\lambda_1)$ is expressed in the following equation (Appendix A).

$$\alpha_1 = -\frac{1}{x} \ln \left[\frac{-(1-R_1)^2 + \sqrt{1-R_1^4 + 4\gamma^2 R_1^2}}{2\gamma_1 R_1^2} \right] \quad (1)$$

where $$\gamma = \left(\frac{P_1}{P_2}\right) \frac{\lambda_1}{\lambda_2} \frac{(1-R_2)^2}{1-R_2^2} \quad (2)$$

X = thickness of the wafer.

P_1 and R_1 are the power transmitted through the wafer and reflection coefficient at λ_1 respectively.

P_2 and R_2 are the power transmitted and reflect on coefficient at λ_2, the wavelength at which the absorption coefficient α_2 due to EL2 is zero respectively.

$\lambda_1 = 1.1\ \mu$

$\lambda_2 = 1.8\ \mu$

The EL2 concentration is then obtained by using the following equation

$$N = \frac{\alpha_1}{\sigma}$$

where σ = cross-section = 8.5×10^{-17}

Figure 1 shows the experimental set up used for the optical obsorption measurement with the component types and manufacturers specified in Table 1. The set up consists of a tungsten halide light source with a silicon filter, a monochromator having variable entrance and exit slits and an adjustable achromatic lens, an external chopper, a sample holder with X-Y microscopic translation stage, and a detector. The exit slit of the monochromator was set at 2mm and thus the bandwidth of light used is.05 μm. The monochromatic light of $.25mm^2$ was focused on the sample which was moved along the <110> direction and each time the transmitted power through the wafer was detected.

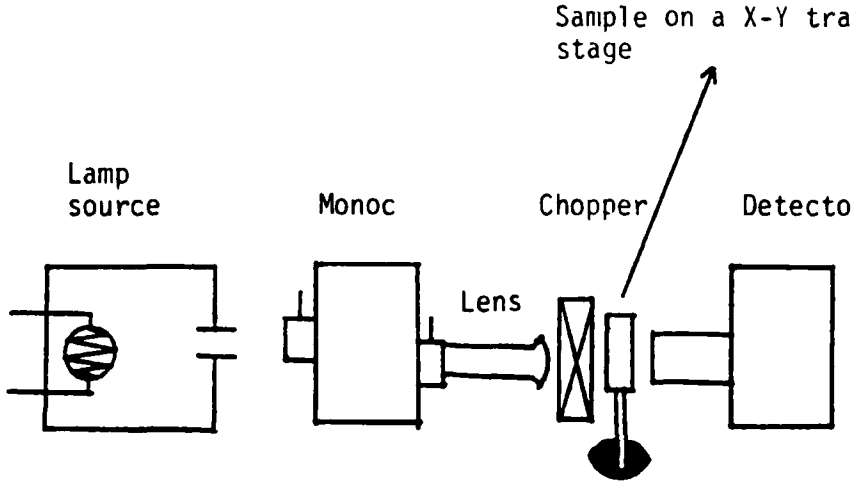

Figure 1. Schematic diagram of experimental set-up for Photon Absorption distribution measurement

Table I. Equipment identification for the various items shown in Figure 1. (Abbreviations: B & L = Bausch and Lomb, L. P. C = Laser Precision Corporation.)

Designation	Mfg. Type and Model No.
Lamp Source	B & L[1] Tungsten Halide Source (33 - 86 - 39 - 01)
Monochromator	B & L High - Intensity Moroc, 1.4 - 3.2 μm Grading (Housing: 33 - 86 - 25, Grading: 33 - 86 - 78)
Lens	B & L Achromatic Condenser Lens (33 0 86 - 53)
Detector	L. P. C[2]. Pyroelectric Radiometer

1. Bausch and Lomb, 820 Linden Ave., Rochester, N.Y. 14625

2. Precision Corp., 1231 Hart St., Utica, N. Y. 13502

In order to insure that the intensity(photons/cm^2sec) of the incident light is the same at the two different wavelengths, a normalization procedure was followed. The incident power P_1at λ_1 was detected with the entrance slit opened to 6mm, the maximum width. Then the required incident power P_2 expressed at

$$P_2 = \frac{P_1\lambda_1}{\lambda_2} \quad \text{at wavelength } \lambda_2 \qquad (3)$$

was obtained by adjusting the entrance slit to 2.5 mm, in this case.

X-Ray Rocking Curve Analysis Method

An automated four cycle diffractometer[6] was used for this experiment. The GaAs wafer together with a microscopic translation stage was mounted on the camera. The spot size was reduced to 500μ by using collimators and slit systems both on incident and diffracted beams. The wafer was then rotated (rocked) through its entire reflection, and the intensity versus angular rotation, the rocking curve, was recorded by using a computer.

Any hKℓ reflection in a perfect crystal reflects x-ray intensity at the Bragg position over an angular range of few seconds known as the rocking curve. The rocking curve is a sensitive measure of the lattice misalignment induced by the deformation. The local misorientation in the lattice due to the presence of dislocations broadens the rocking curve. The total width at half the intensity of the maximum of the rocking curve, known as the half-width, β , is a sensitive indicator of dislocation density. The half-width β of the rocking curve obtained from different positions on the wafer was calculated.

If there is a nonuniform strain distribution in the wafer, the rocking curve peak from different parts of the crystal will be at different parts 2θ angular positions. From the shift of the rocking curve one can measure the variation of lattice parameter by using the following expression (Bragg condition).

$$\Delta d = \frac{\lambda}{2\,(\sin\theta_1 - \sin\theta_2} \qquad (4)$$

where λ = wavelength of Cu K_1 radiation

= 1.540562 Å

$2\theta_2$= rocking curve peak position for no strain or average strain

$2\theta_1$ = rocking curve peak from a particular position of the crystal

The quantity, $\frac{Ad}{d} = \varepsilon$ is then the strain component. The lattice parameter at different positions in the wafer was calculated from the 2θ value of the rocking curve peak. Since 004 reflection was used, the calculated $\varepsilon = \frac{\Delta d}{d}$ is the normal strain along the 001 axis, in this case

IV . EXPERIMENTAL RESULTS AND DISCUSSION

Figures 2 and 3 show the variation of EL2 concentration with position in the wafer. The average EL2 concentrations in each wafer examined are listed in Table 2. In general the linear profile of EL2 concentration across the crystals is W shaped, having lowest concentration in the ring region (i.e. in the region between the center and edge). This result is in agreement with the result obtained before.[2] The EL2 concentrations in crystals grown under low pressure are less in general than those in the crystals grown under high pressure. Among the crystals grown with the high pressure LEC method, the crystals grown under the low-gradient growth condition have a lower EL2 concentration.

The halfwidth β of the x-ray rocking curves corresponding to the positions in the crystal are given in figure 4. The β values for the middle part of crystal R103 are higher than those from the tail end, indicating presence of less dislocations in the tail end. No comments will be made about the variation of dislocation density across a particular wafer until further detailed study.

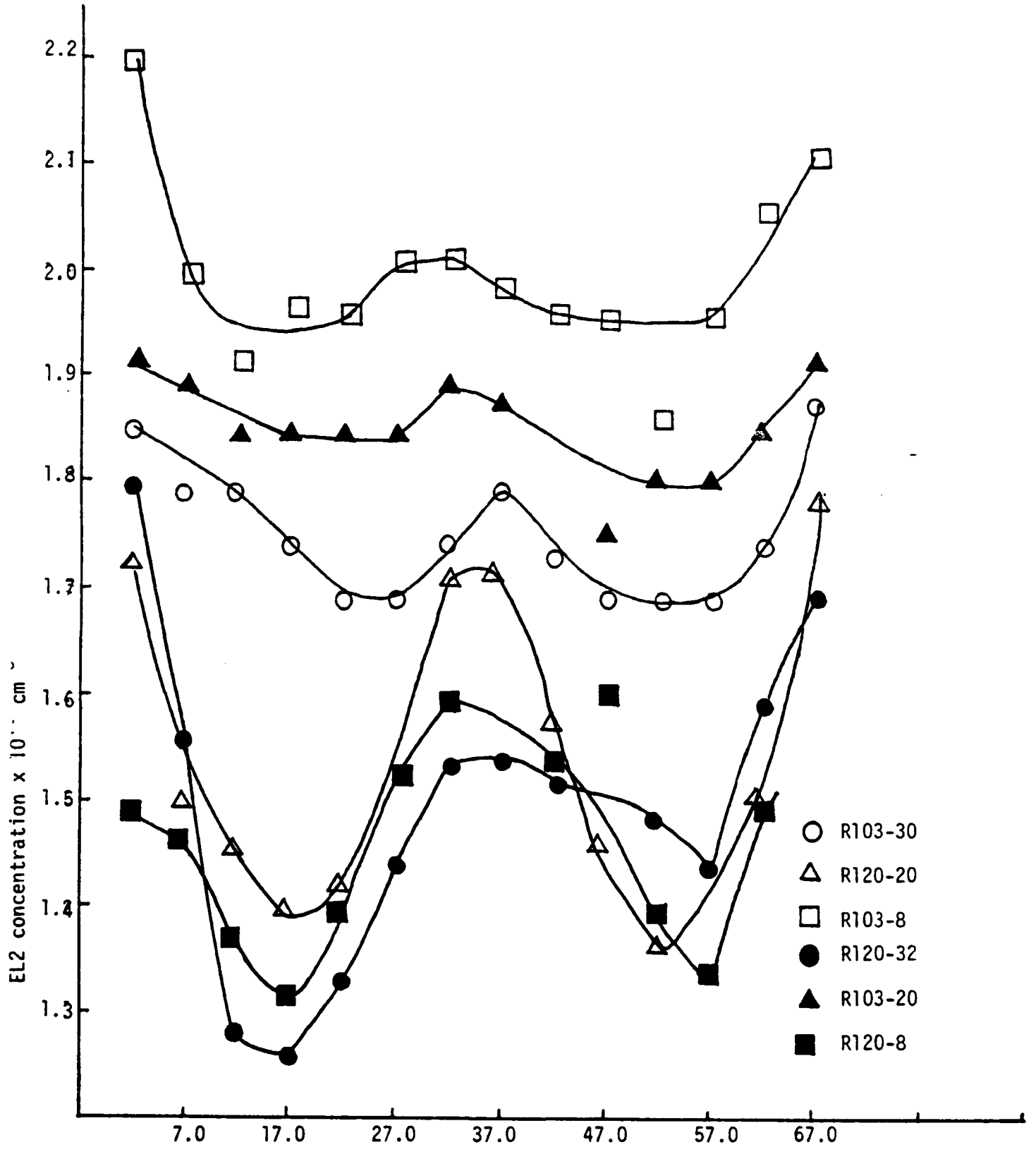

Figure 2 . Variation of EL2 concentration with the distance across the crystal along <110> (7.0 mm refer to the distance from one edge of the crystal)

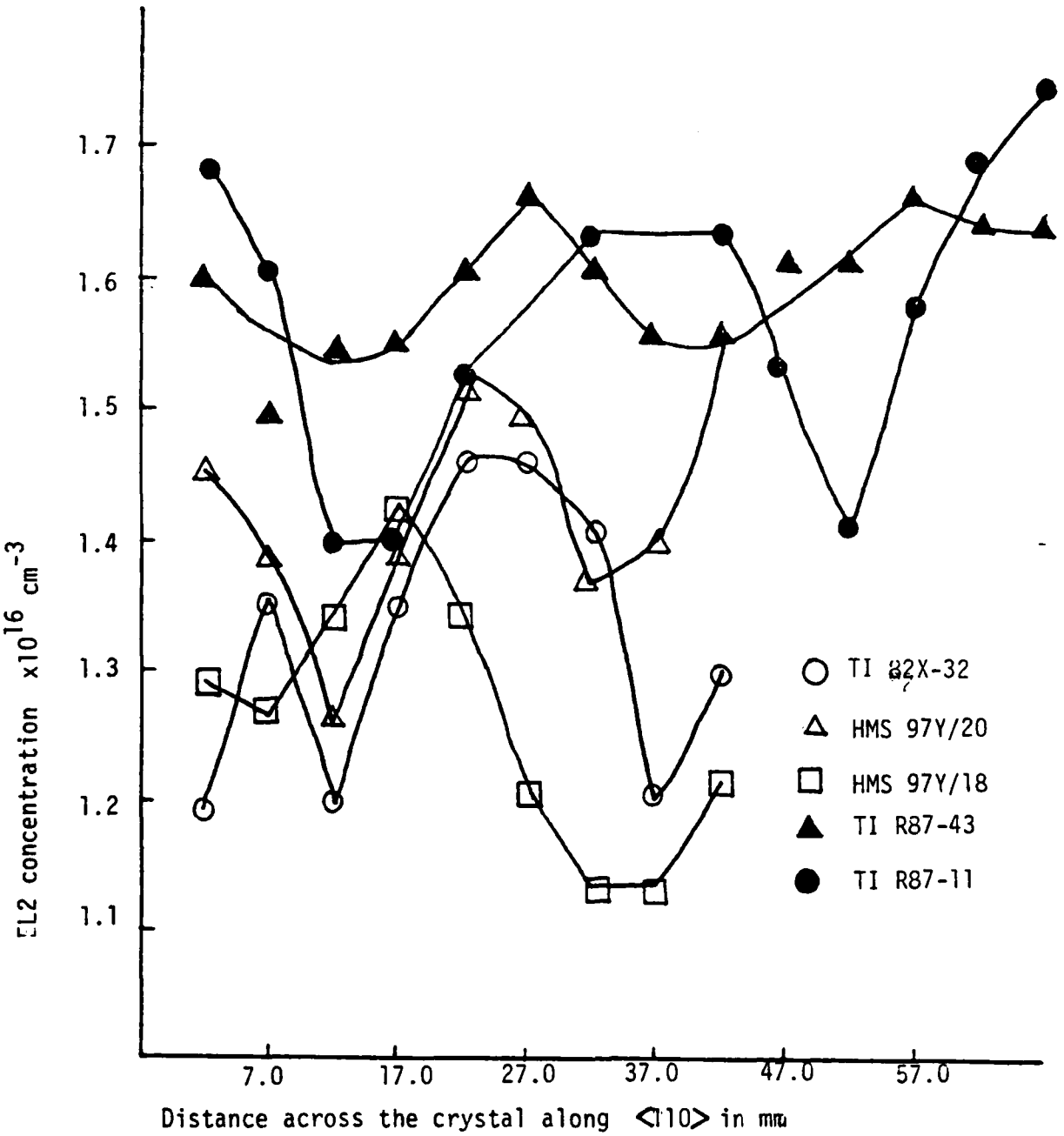

Figure 3 . Variation of EL2 concentration with the distance across the crystal along <110> (7.0 mm refer to the distance from one edge of the crystal)

Table II. Average EL2 Concentrations in Different Samples.

Sample No.	Average EL2 Concentrations $X10^{16}$. CM^{-3}
R 103-8	2.00
2 103	1.77
R 103-30	1.79
R 120-8	1.48
R 120-20	1.55
R 120-32	1.50
82x-32	1.32
97Y/20	1.42
97Y/18	1.26
R-87-43	1.59
2-87-11	1.58

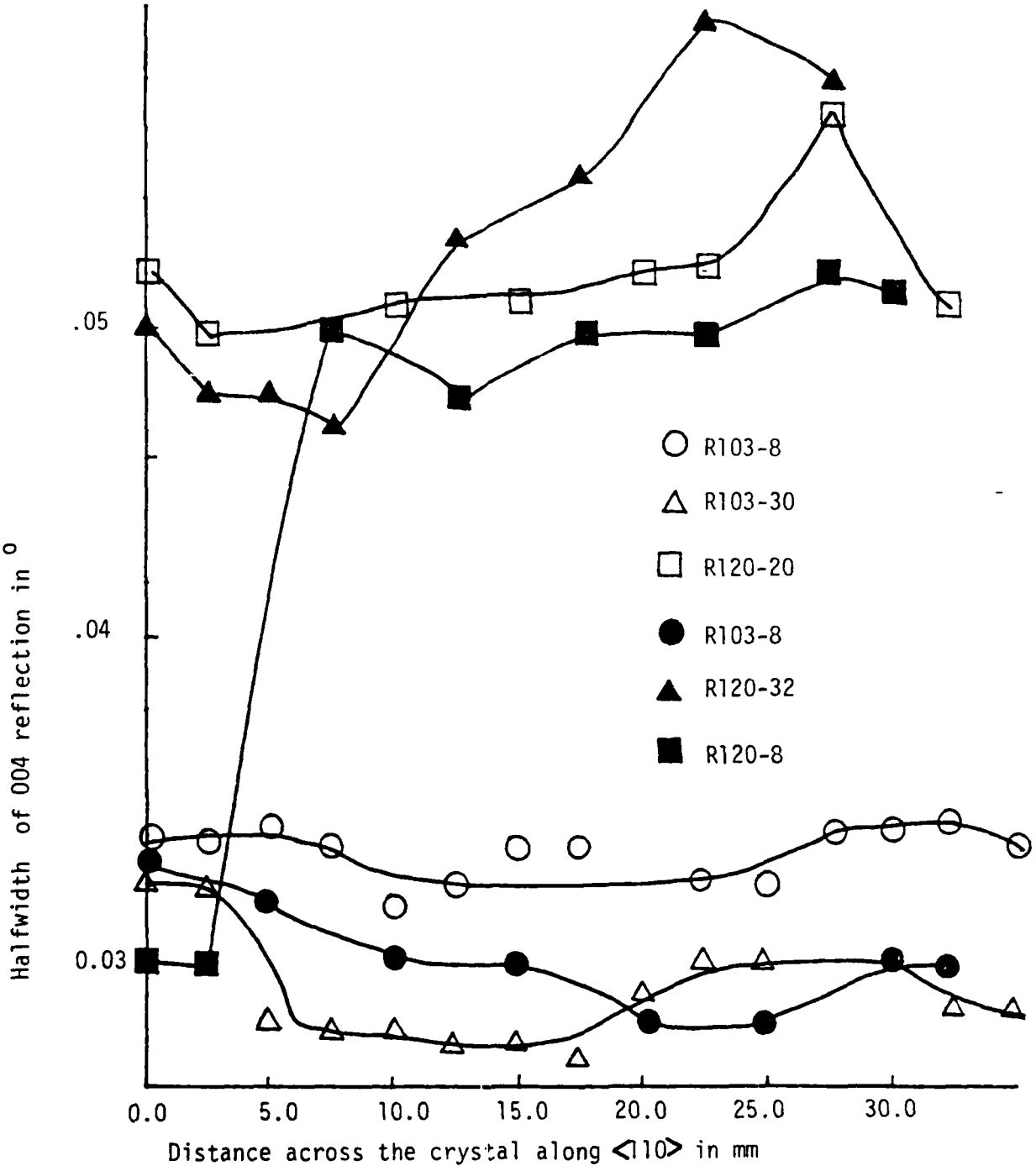

Figure 4 . Distribution of dislocation densities with the position in the crystal along <110>(0.0 mm refer to the center position)

AD-A166 176 UNITED STATES AIR FORCE SUMMER FACULTY RESEARCH PROGRAM 06/13
1985 TECHNICAL RE (U)UNIVERSAL ENERGY SYSTEMS INC
DAYTON OH R C DARRAH ET AL DEC 85 AFOSR-TR-86-0139
UNCLASSIFIED F49620-85-C-0013 F/G 5/9 NL

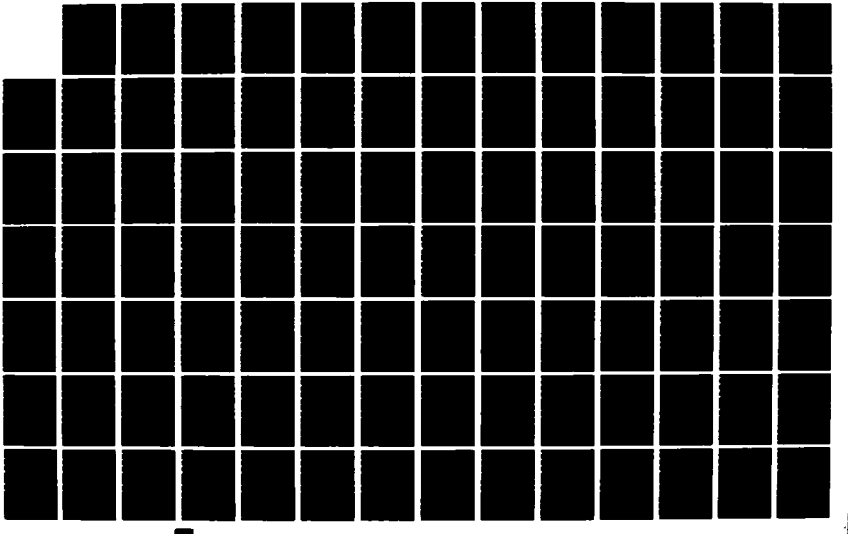

MICROCOPY RESOLUTION TEST CHART
NATIONAL BUREAU OF STANDARDS-1963-A

The local variations of normal strain (i.e. along (001) direction) in wafers are shown in Figure 5. The results indicate that the strain changes from a state of tensile strain to a state of compressive strain from the center to the edge of the crystal. The amount of strain at each position as shown are merely qualitative at this moment.

Figure 6 shows the variation of Aresenic concentration in the crystals. The composition of As is calculated by using the following equation[5]

$$x = \frac{vd\ No - 4\ As}{4Ga} \qquad (9)$$

where

x is the fraction of Ga atom in the non-stoichiometric compound Ga_xAs.

v is the volume of the unit cell which is calculated from measured lattice parameter. At the stoichiometric composition (i.e. 50 Ga - 50 As) Lattice parameter 5.65321 ± 0.00003 A° at 25°c.[5]

N_o = Avogadro's Number = $6,024 \times 10^{23}$

d = density = 5.3169 gm/cm^3.

The average values of Arsenic concentration in each wafer are shown in Table 3. The arsenic concentration is higher and close to 50% in the crystals grown under low thermal gradient, and it decreases from the middle part to the tail end of the crystal. It is important to notice that a small local variation in composition produces a large strain in the crystal. (Figures 5 and 6).

V. SUGGESTION FOR FUTURE WORK

Many of the results obtained in the present project need a further detailed study in order to assist in growing more homogeneous GaAs crystals.

Quantitative mapping of EL2 concentration across the wafer will be continued in the Air Force Laboratory. A complete automation of the experimental set up is in progress.

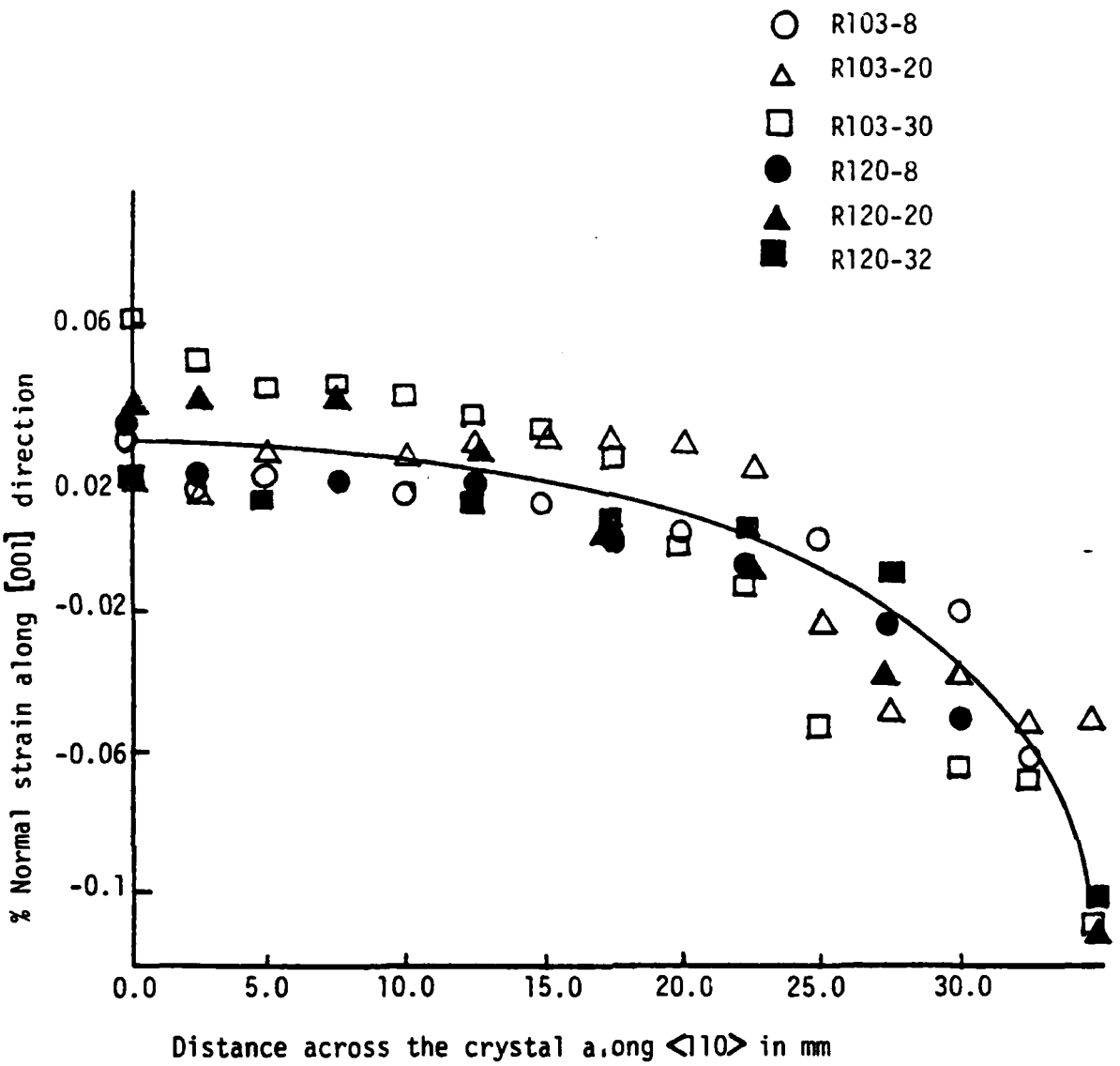

Figure 5 . Variation of %normal strain along 001 with the distance in the crystal across <110> direction (0.0 mm refer to the center position)

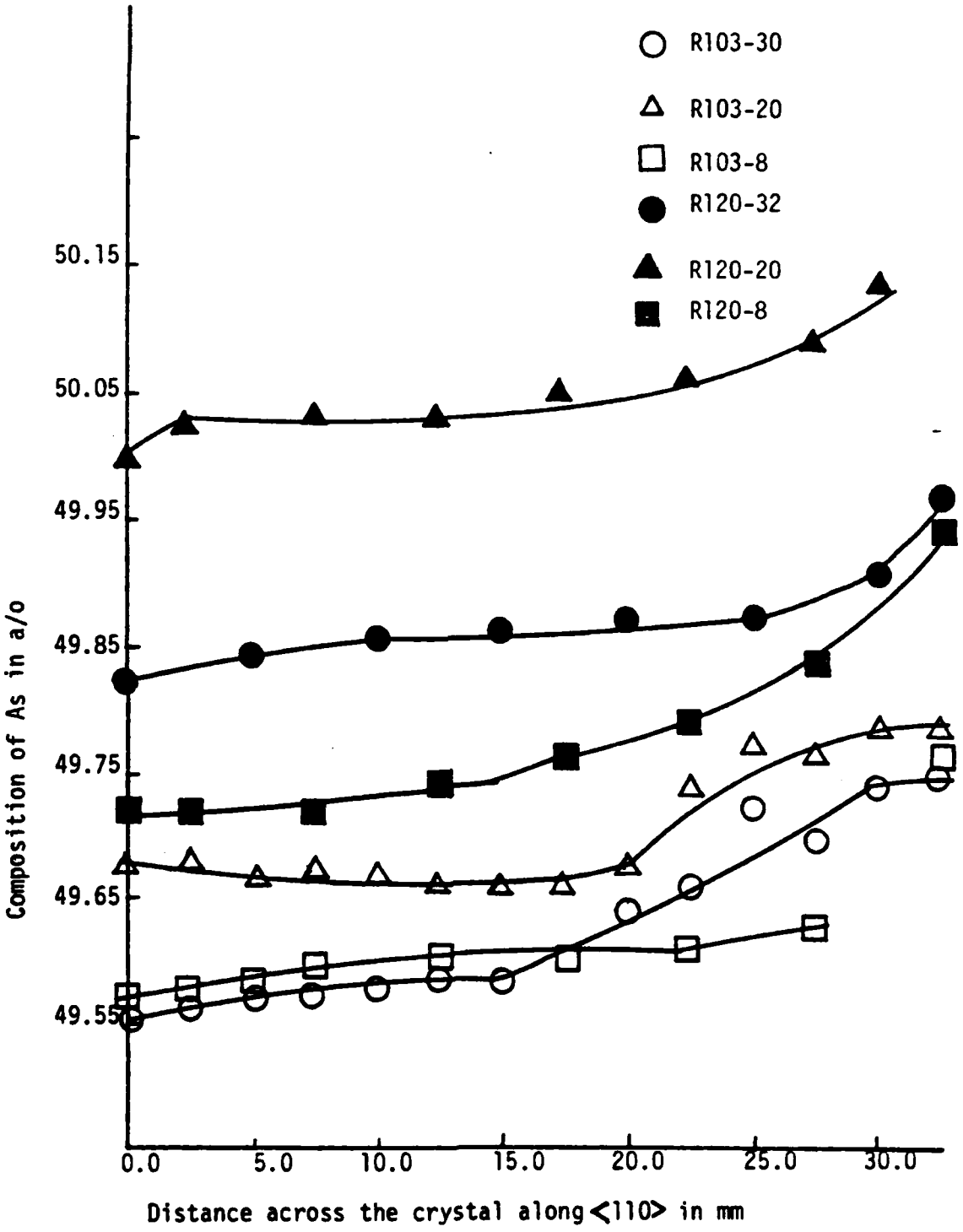

Figure 6 . Variation of composition with the position in the crystal along <110> (0.0 mm refer to the center position)

Table III. Average Composition of Arsenic in Each Crystal.

Crystal No.	Ave. Composition of Arsenic in %
R103-8	49.873
R103-20	49.703
R103-30	49.640
R120-8	50.058
R120-20	49.776
R120-32	49.612

It is suggested that the rocking curve analysis of the crystals should be continued to measure the dislocation density, local strain and composition across the crystal more precisely. It is also suggested to use x-ray transmission topographic technique and Berg-Barett x-ray reflection topographic technique[ ] to image distribution of dislocations or dislocations related defects in the crystals. The advantages of these techniques are that these are highly sensitive techniques to reveal structural or compositional inhomogeneties non-destructively.

VI. CONCLUSION

Undoped semi-insulating GaAs, which is to be used for the production of GaAs integrated circuits, were characterised by the optical absorption and x-ray rocking curve analysis techniques. Liquid Encapsulated Czochralski method, which is the most popular method at present, was used to grow single crystals of GaAs. Variations of EL2 concentration across the diameter of each wafer is of W shaped, with lowest EL2 concentration in the ring region. The concentration of EL2 was found to be less in the crystals grown under low pressure than in the crystals grown under high pressure. Among the crystals grown under high pressure, crystals grown under low thermal gradiant have lower EL2 concentration, especially in the ring region.

X-ray rocking curve analysis showed a variation of dislocation density as well as local strain and composition in the wafer. X-ray rocking curve analysis study is at a preliminary stage at present. No comment will be made on the variation of dislocation density without further detailed study. Measurement of local composition in the crystals definitely indicates a variation in the lateral as well as vertical direction, which also needs a more precise determinati

APPENDIX A

The transmission coefficient[7] is defined as the ratio of transmitted to incident power I/I_o. If the specimen has a thickness x, an absorption coefficient α, and a reflectivity R, the overall transmission is given by

$$T = \frac{(1-R)^2 \exp(-\alpha x)}{1-R^2 \exp(-2\alpha x)} \qquad (1A)$$

Thus

$$\frac{T_1}{T_2} = \frac{(1-R_1)^2 e^{-\alpha_1 x}}{(1-R_2)^2 e^{-\alpha_2 x}} \cdot \frac{1-R_2^2 e^{-2\alpha_2 x}}{1-R_1^2 e^{-2\alpha_1 x}}$$

Where T_1 = transmission coefficient at wavelength λ_1

T_2 = transmission coefficient at wavelength λ_2

R_2 = reflection coefficient at λ_1 = .3046

R_2 = reflection coefficient at λ_2 = .2921

α_1 = absorption coefficient at λ_1

α_2 = absorption coefficient at λ_2

Let $\alpha_2 = 0$

Then

$$\frac{T_1}{T_2} = \left[\frac{(1-R_1)^2 \quad e^{-\alpha_1 x}}{1-R_1^2 \quad e^{-2\alpha_1 x}}\right] \qquad \left[\frac{1-R_2^2}{(1-R_2)^2}\right]$$

Or $$\alpha_1 x = -\ell n \left[\frac{-(1-R_1)^2 + \sqrt{(1-R_1)^4 + 4y^2 R_1^2}}{2y R_1^2}\right]$$

Where $$y = \frac{T_1}{T_2} \cdot \frac{(1-R_2^2)}{1-R_2^2} = \frac{P_1 \lambda_1}{P_2 \lambda_2} \cdot \frac{(1-R_2)^2}{1-R_2^2}$$

P_1 = Power transmitted through the wafer of λ_1

P_2 = Power transmitted through the wafer at λ_2

REFERENCES

1. Holmes D. E., Elliot, K. R., Chen, R. I., and Kirkpatrick, C. G. (1982). In Semi-Insulating III-V Materials Evian P.19, (S. Makram-Ebeid and B. Tuck eds.); Shiva Publishing, Nantwich, U.K.

2. Martin G. M., Jacob, G., Galtzene, A. and Schwab, C., In proceedings of the 11th International Conference on Defects and Radiation - Effects in Semi-Conductors, Oiso, Tokyo.

3. Holmes, D. E., Chen, R. I., Elliott, K. R., and Kirkpatrick, C. G., (1983). Appl. Phys. Letter, 43, 305; Holmes D. E. and Chen, R. I.,(1984). J. Appl. Phys., 55, 3588.

4. Stirland, D. J., Grant I, Brozel, M. R., and Ware R. M. Proc. 3rd Oxford Conf. Microscopy of Semidonductor Materials, Inst. Phys. Conf. Ser. (to be published.); Brozel, M. R., Grant, I., Ware R. M. and Stirland, D.J., (1983). Appl. Phys. Lett., 42, 610; Skolink, M. S., Brazel, M. R., Grant, I., Stirland, D. J. and Ware, R. M., 1983, Electronic Materials Conference.

5. M. E. Straumanis and C. D. Kim; Acta Cryst. (1965), 19, 256.

6. Leonid V. Azaraff; Elements of X-ray crystallography McGraw-Hill Book Co.

7. Jacques I. Pankave; Optical Processes in Semiconductors, Dover Publications, Inc. (1971).

8. B. K. Tanner; X-Ray Diffraction Topography, Pergamon Press, 1976.

1985 USAF-UES SUMMER FACULTY RESEARCH PROGRAM/
GRADUATE STUDENT SUMMER SUPPORT PROGRAM

Sponsored by the
AIR FORCE OFFICE OF SCIENTIFIC RESEARCH
Conducted by the
UNIVERSAL ENERGY SYSTEMS, INC.

FINAL REPORT

VISUALIZATION OF JET FLAMES

Prepared by:	Lea D. Chen
Academic Rank	Assistant Professor
Department and University:	Department of Mechanical Engineering The University of Iowa Iowa City, Iowa
Research Location:	Fuels Branch Fuels and Lubrication Division Aero Propulsion Laboratory Wright Aeronautical Laboratories WPAFB, Ohio
USAF Research:	W. M. Roquemore
Date:	August 20, 1985
Contract No:	F49620-85-C-0013

Report Approval: W. M. Roquemore

Effort Focal Point Signature
W. M. Roquemore
AFWAL/POSF
WPAFB, OH 45433
Telephone: (513) 255-6813

Visualization of Jet Flames

by

Lea D. Chen

ABSTRACT

Two different techniques of flow visualization were used to study structures of hydrocarbon jet diffusion flames. It was concluded that a chemically reactive scheme[1], which forms $TiO_{2(s)}$ in flows, provides the best visualization of fluid motion of jet diffusion flames, and caution should be exercised in interpreting images of axisymmetric jet flames using refractive index methods such as schlieren and shadowgraph visualization. In the near burner region, four distinct flow structures can be identified: flame zone, large outer vortices, smaller inner vortices, and potential core. It was found that Reynolds number is not sufficient in characterizing vortex structures of jet flames, instead, local strain rates seem to be more proper to use. It is recommended that continual efforts are needed to perfect the 2-D visualization method for high temperature environments and quantitative measurements. It is also recommended that other means for 2-D temperature measurements and 3-D flow visualization deserve research efforts.

ACKNOWLEDGMENTS

The sponsorship of the Air Force Systems Command, Air Force Office of Scientific Research through 1985 SFRP is acknowleged. The author is in debts to the superb technical support from Fuels Branch of Aero Propulsion Laboratory, Wright Aeronautical Laboratories. The author wishes to express special thanks to Dr. W. M. Roquemore of APL for many stimulating discussions and support throughout this research.

I. INTRODUCTION

L. D. Chen received his Ph.D. (1981) and M.S. (1979) degrees in mechanical engineering from Pennsylvania State University, and a B.S. degree in mechanical engineering (1974) from National Taiwan University. He was graduate assistant of Department of Mechanical Engineering at Penn State from 1977 to 1980. During the period of 1980 to 1982, he was on a joint appointment from the same department and Applied Research Laboratory of Penn State, holding rank of research assistant, research associate, and assistant professor. Since August 1982, he has been with Department of Mechanical Engineering and Division of Energy Engineering at The University of Iowa, holding rank of assistant professor.

L. D. Chen has been conducting experimental and theoretical research in combustion since 1977. He conducted studies on ignition and combustion of liquids under high pressure conditions, particle-laden turbulent jets, evaporating and combusting sprays, reacting gas jets in liquid metals, slurry spray flames, and turbulent jet diffusion flames. His research work has resulted in eleven journal articles and thirteen conference papers. He has directed three M. S. theses, and one Ph.D. dissertation (at its final stage) at The University of Iowa.

L. D. Chen's background in combustion and strong interests in hydrocarbon turbulent jet diffusion flames has brought him to conduct research at APL (Aero Propulsion Laboratory, Wright Aeronautical Laboratories, WPAFB, Ohio). During his tenure of 1985 UES-USAF SFRP, he utilized a newly developed technique for combustion diagnostics in studying the structure of jet diffusion flames. The diagnostic technique utilizing 2-D laser sheet-lighting techniques was developed by W. M. Roquemore at APL, e. g. see Ref. [1], for studying combustion processes.

II. OBJECTIVES OF THE RESEARCH EFFORT

The objectives of the research are to compare different techniques of flow visualization, and to study the structure of hydrocarbon jet diffusion flames.

III. EXPERIMENTAL METHODS

Introduction. Flow visualization has long been employed in experimental study of fluid mechanics and heat transfer phenomena. Two widely used methods are those utilizing scattered light from small particles, and those utilizing the variation in refractive index, commonly known as schlieren (density gradient) and shadowgraph (second derivative of density gradient). LSM (light scattering method) generally requires foreign materials to be seeded in the flow and RIM (refractive index method) is applicable only when noticeable variations in density are observed. Detailed reviews of these methods can be found in Merzkirch [2].

There have been several 2-D flow visualization techniques for qualitative and quantitative measurements. For example, large vortical structures were observed in diffusion flames stabilized by a bluff body [1], Lorenz/Mie scattering [3] and Rayleigh scattering [4] were used for concentration measurements of axisymmetric jets, and streak photography was employed to obtain velocity vectors of a water-tunnel flow [5].

The method which was described in [1] and utilized in the present study, differs from previous LSM in how particles are introduced to flow. Particles were formed in the flow, at a reaction interface where $TiCl_{4(g)}$ and $H_2O_{(g)}$ react to form $TiO_{2(s)}$, as opposed to preformed particles in previous LSM studies, e.g. see [3,5,6]. Reactive systems have been used in flow visualization, e.g. see [7,8,9]; however, a scheme which can easily be implemented to combusting flows was first introduced by Roquemore, et. al. [1]. It should be noted that the reaction of $TiCl_{4(g)}$ and $H_2O_{(g)}$ occurs under isothermal conditions, and yields submicron particles [1]. This is particularly important since energy will not be added to, or taken from the combustion system under study, and submicron particles will respond to flow variations almost instantaneously.

This report describes the apparatus for 2-D LSM, and RIM (schlieren and shadowgraph) flow visualization, and a summary of structures of hydrocarbon jet diffusion flames as viewed from these techniques. Specific recommendations for future considerations are also included.

Apparatus. A Nd:Yag laser (Quanta Ray Model DCR-24) was used to provide laser light for

2-D LSM and RIM (schlieren and shadowgraph) visualization. The optical arrangement is shown in Fig. 1. The pulse ouput (10 ns duration) of 532 nm beam from a Nd:Yag laser was splitted into two beams through a beam splitter (BS). One of the two beams was used as a pump beam for a dye laser having two dye cells (DC1 and DC2) which gives a 631 nm beam output. The dye laser has a more uniform (spatially) beam than that directly from the output of a Nd:Yag laser.

The optics for 2-D sheet lighting consists of a telescope (T), a cylindrical lenz (L1), and a mirror (M), using the 532 nm beam from a Nd:Yag laser. Schlieren/shadowgraph visualization utilizes the 631 nm beam in conjunction with a condensing lenz (L2) and two schlieren mirrors (SM1 and SM2). When the photographically made knife edge (KE) was removed from the arrangement, shadowgraph visualization was made. The advantage of using the above-mentioned arrangement is that simultaneous visualization can be taken for 2-D LSM and RIM. This was accomplished by synchronizing a still camera for 2-D LSM and a Nd:Yag laser, meanwhile the short duration of the laser pulse (10 ns) served as a shutter of a second camera which was used to record RIM images.

The test arrangement is illustrated in Fig. 2. A fuel nozzle was located at the center of a coaxial jet assembly which was mounted in a small vertical combustion tunnel at APL as described in [1]. The annular jet has a divergent section and a flow straightner, which consists of a honeycomb and fine mesh screens, to provide low velocity and low turbulence surrounding air for the fuel jet[1]. The fuel nozzle was designed to be interchangeable with different geometries. A contracted nozzle (inside diameter of 10 mm) following the contour specifications of ASME and two tube nozzles (inside diameter of 11 and 22.5 mm) having a length of 450 mm were used in the experiments.

IV. RESULTS AND DISCUSSIONS

A systematic research was conducted to study structures of jet diffusion flames fueled with hydrocarbons. Two methods of flow visualization, 2-D LSM and RIM, were compared. Effects due to burner exit conditions were examined using burners of different diameters (10, 11, and 22.5 mm) and different geomerties (contracted nozzle and long tube), and interections between combustion and fluid flow were examined by comparing cold and combusting jets under same

burner exit conditions. Two different fuels were also studied to explore effects resulting from different fuel properties, and to assess the validity of using Re in characterizing combusting jets. Test conditions include propane jet flames with exit velocities in the range of 0.01 to 3.8 m/s for 22.5 mm burner (tube), 0.2 to 9.9 m/s for 11 mm burner (tube), and 0.06 to 13.5 m/s for 10 mm burner (nozzle), and ethylene jet flames with exit velocities of 0.01 to 3.6 m/s for 22.5 mm burner (tube) and 0.07 to 16.9 m/s for 10 mm burner (nozzle). Annular air jet was maintained at a velocity of 0.15 m/s.

A totle of more than 1300 still photographs and more than 60000 ft. of high speed cinegraph were taken. There exists a wealth of information concerning structures of jet flames and it would exceed the scope of this report, should detailed discussions be covered. A brief summary of the findingns is provided here, detailed discussions on the comparison of LSM and RIM visualization are being prepared[10], and those on structures of jet diffusion flames will appear in [11].

LSM and RIM usually yielded qualitatively similar visualization; however, caution should be exercised when RIM is employed for axisymmetric flows. This is due to the fact that line-of-sight image is projected for RIM visualization which represents a spatially averaged picture. Some misleading images were obtained. Most noticeable ones are those for jet flames issuing from a burner of 22.5 mm, in which cell structures were observed in the entire flowfield without the presence of a potential core. This is due to strong density variations in the shear layer surrounding a potential core and viewed through a spatially averaged manner.

In the near burner region, the structure of a jet flame can be divided into four regions: flame zone, outer shear layer, inner shear layer, and optential core. It is noted that as many as eight regions may be identified, however, these four regions have most distinct structures. Flame zone is the luminous reaction zone where chemical reactions take place and outside the flame zone there exists a outer shear layer where large vortical structures are generally observed. As for the inner shear layer, where smaller vortical structures are present when exit velocity of fuel jet exceeds certain values, it separates flame zone from potential core. Negatively buoyant wakes were also observed with propane fuel, under the conditions of low burner exit velocities and 22.5 mm burner.

From observations, burer exit Reynolds number is not sufficient to characterize structures of jet flames. Instead, structures seem to be related with local strain rates, for examples, inner vortical structures appear to be moving either inward or outward, depending on the direction of velocity gradient, or the sign of strain rate ($\partial u/\partial r$). It appears that vortical structures and vortex dynamics may play an important role in turbulent flows, and understanding of the instability of free shear layers may shed some lights to the nature of turbulence. It was also found that a certain frequency around 13 to 15 Hz could be observed from strobing the Nd:Yag laser. This frequency can not be explained by the Kelvin/Helmholz linear instability theory and more work is needed to quantify this observation.

V. RECOMMENDATIONS

It is concluded that 2-D LSM is a powerful tool in studying combustion processes. The use of an isothermal reactive scheme to form submicron particles in the flow appears to provide most detailed informations among the techniques examined. There are still rooms to perfect the technique, however. Specific recommendations, which are limited to improving the 2-D visualization technique, are summarized in the following:

1. It was found that surface reflectivity of $TiO_{2(s)}$ deteriorates at high temperatures. This creates problems in flow visualization at high temperatures. Different reactive systems need to be examined and particles having better reflectivities at high temperatures need to be identified.

2. Quantitative informations on the mixing process can be obtained from 2-D LSM visualization in conjunction with image analysis. This involves digitizing flow images to obtain concentration levels (intensity of scattered light). Calibration of background light intensity and quantifying optical properties at different temperatures are needed. In addition, particles with more stable surface reflectivity over a wide range of temperatures are desired for this purpose.

3. Techniques of obtaining 2-D temperature measurements will be of great importance to combustion diagnostics. In addition, 2-D velocity measurements also appear of importance to quantify transport processes in a combustion environment.

4. Simultaneous visualization of reaction zones, e.g. laser induced fluorescence of OH^-, and structures of jet flames will provide information concerning the characteristics of combustion processes.

5. 3-D visualization using holographic techniques deserves research efforts. This is in view of three dimensional motions observed in turbulent flames.

REFERENCES

1. Roquemore, W. M., Tankin, R. S., Chui, H. H., and Lottes, S. A., "The Role of Vortex Shedding in a Bluff-Body Combustor", Proc. ASME 1985 Winter Annual Meeting, New Orleans, Dec. 1985.

2. Merzkirch, W., Flow Visualization, Academic Press, 1974.

3. Long, M. B., Chu, B. T., and Cheng, R. K., AIAA J 19:1151-1157 (1981).

4. Escoda, M. C. and Long, M. B., AIAA J. 21:81-84 (1983).

5. Utami, T. and Ueno, T., Expt. Fluids 2:25-32 (1984).

6. Hussain, A. K. M. F. and Clark, A. R., J. Fluid Mech. 104:263-294 (1981).

7. Denbigh, K. G., Dombrowski, N., Kisiel, A. J., and Place, E. R., Chem. Eng. Sci. 17:573 (1962).

8. Sherikar, S. V. and Chevray, R., in Turbulent Shear Flows 3 (L. J. Bradury, F. Durst, B. E. Launder, F. W. Schmidt, and J. H. Whitelaw, ed.), 1981, pp. 124-131.

9. Breidenthal, R. E., J. Fluid Mech. 109:1-24 (1981).

10. Roquemore, W. M. and Chen, L-D., "Visualization of Jet Flames" (in preperation for Comb. Flame).

11. Chen, L-D., Roquemore, W. M., Trump, D. D., and Goss, L. P., "Structures of Jet Flames" (in preperation for 21st Symposium (International) on Combustion).

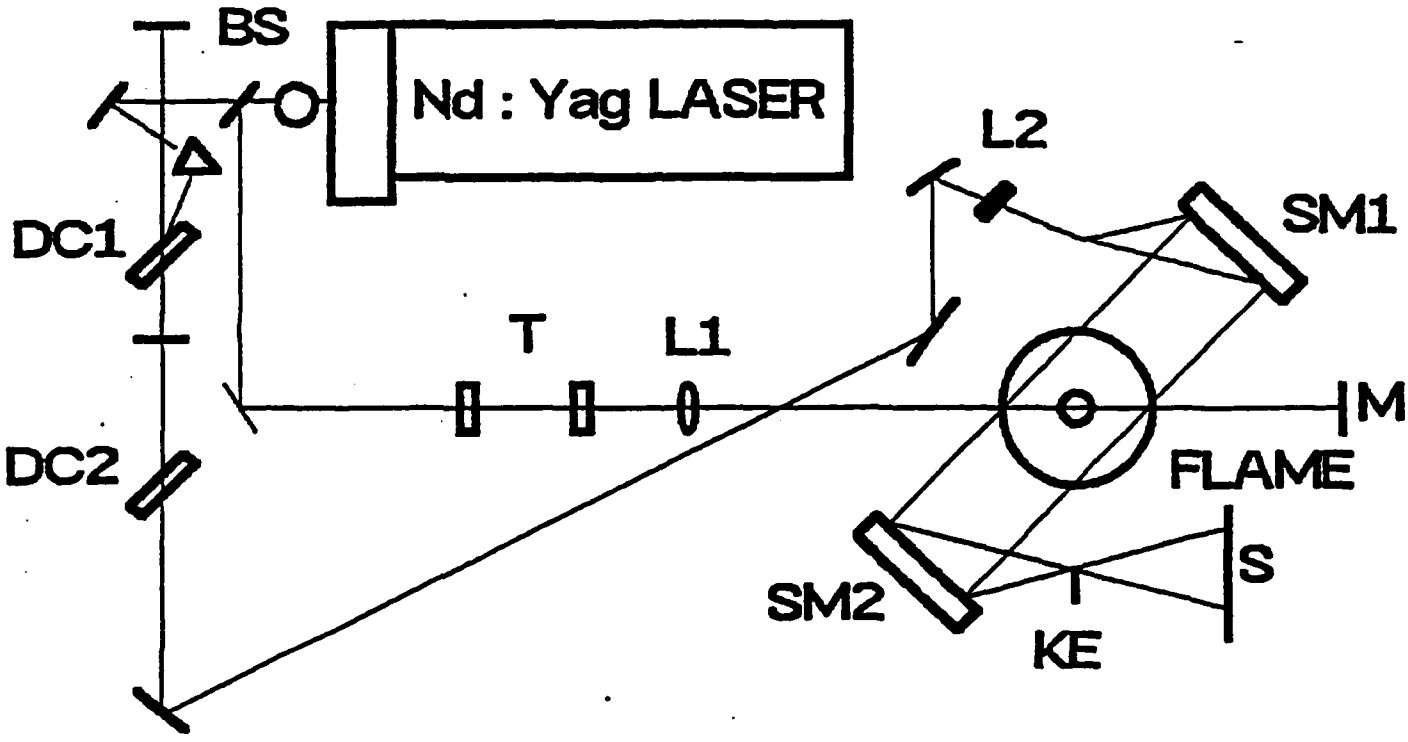

Figure 1. Optical arrangement of LSM and RIM visualization.

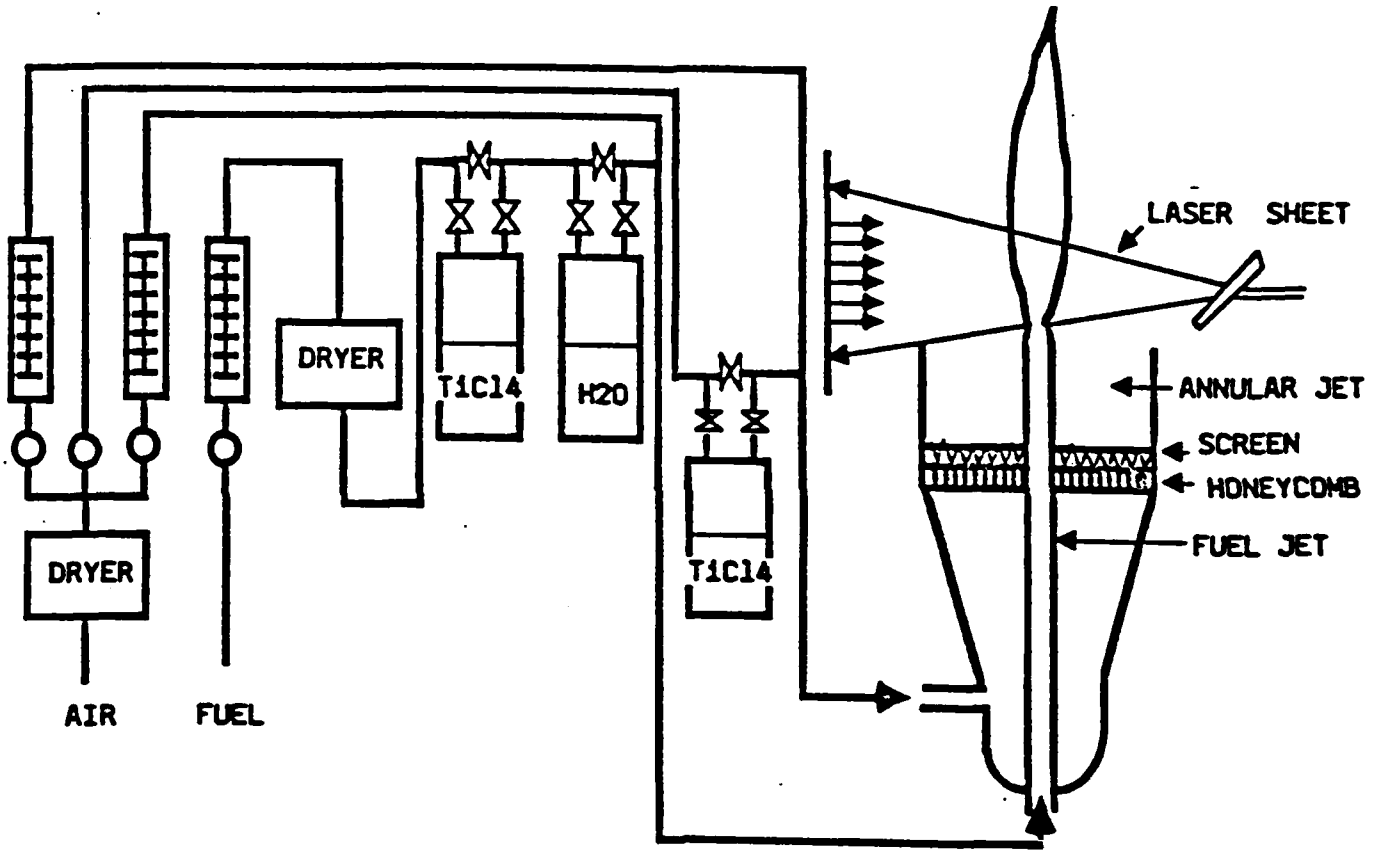

Figure 2. Schematic diagram of burner design and gas supply.

1985 USAF-UES SUMMER FACULTY RESEARCH PROGRAM/

GRADUATE STUDENT SUMMER SUPPORT PROGRAM

Sponsored by the

AIR FORCE OFFICE OF SCIENTIFIC RESEARCH

Conducted by the

UNIVERSAL ENERGY SYSTEMS, INC.

FINAL REPORT

SPLINES AND THE FOURIER TRANSFORM

Prepared by: David B. Choate

Academic Rank: Assistant Professor

Department and University: Math/Computer Science

Xavier University of New Orleans

Research Location: RF Transmission Laboratory, DC division,

DCC branch, DCCD section

USAF Research: John Patti

Date: August 7, 1985

Contract No: F49620-85-C-0013

SPLINES AND THE FOURIER TRANSFORM

by

David B. Choate

ABSTRACT

Given a sampled-data system we develop a technique using cubic splines to estimate the main lobe of its Fourier Transform. A formula for an arbitrary entry of a Hadamard matrix of any dimension is also given.

ACKNOWLEDGEMENTS

I am indebted to the Air Force Systems Command, the Air Force Office of Scientific Research and the RF Transmission Laboratory for permitting me to participate in the Summer Faculty Program. Particular thanks are due to John Patti, my Effort Focal Point, who inspired the investigation of splines in connection with the Fourier Transform and whose helpful criticisms brought me more than once back to the right path. I also wish to thank Richard Smith for posing the problem described in Section III.

I. INTRODUCTION: David Choate has a Ph.D in mathematics from the University of Southwestern Louisiana. He has done research in algebra, number theory and number theoretic transforms, the last of which is used in signal processing.

II. OBJECTIVES OF THE RESEARCH EFFORT:

Goal 1. Find a formula for an arbitrary entry of a Hadamard matrix of any dimension.

Goal 2. Find the Fourier Transform of a spline through a sampled-data system.

Goal 3. Find the curve through the sampled-data system whose Fourier Transform is the spline through its discrete spectrum.

Note: All the following results, unless otherwise indicated, are the author's— at least in so far as a literature search of the the lab's technical library can determine. The name Patti refers to John Patti, my Effort Focal Point, and Smith refers to Richard Smith a colleague of John's. Scott Fuller is a Co-op student.

III. a. The approach taken in establishing the formula given in Goal 1 made use of mathematical induction and some elementary results in tensor analysis. The derivation is lengthy, so we do not include it.

b. Theorem 3.1 (Choate, Smith) Let L be a non-negative integer. Set $2^L = N$. Then a formula for an arbitrary entry of a $2^L x 2^L$ Hadamard matrix under the Walsh or sequency ordering is given by

$$h(k,n) = (-1)^{\sum_{i=0}^{L-1} r_i n_i} \qquad k,n = 0, \ldots, N-1 \text{ where } (k)_{10} = (k_{L-1} \cdots k_0)_2$$

and $(n)_{10} = (n_{L-1}n_{L-2} \cdots n_0)_2$ (base 2) and

$$r_0 = k_{L-1},\ r_1 = k_{L-1} + k_{L-2},\ \cdots,\ r_{L-1} = k_1 + k_0$$

Algorithm 3.2 How to find h(i,j) the element in the ith row and jth column of a $2^L x 2^L$ Hadamard matrix under the Walsh or sequency ordering.

Enter L,i and j where $1 \leq i \leq 2^L$ and $1 \leq j \leq 2^L$. (i and j must be positive integers; L is a non-negative integer.)

Set $k = i - 1$ and $n = j - 1$.

$k(\text{mod}2) = k_0$

$(k - k_0)/2 = q_0$

$q_0(\text{mod}2) = k_1$

$(q_0 - k_1)/2 = q_1$

$q_1(\text{mod}2) = k_2$

$\vdots$

$(q_{L-3} - k_{L-2})/2 = q_{L-2}$

$q_{L-2}(\text{mod}2) = k_{L-1}$.

Also,

$n(\text{mod}2) = n_0$

$(n - n_0)/2 = p_0$

$p_0(\text{mod}2) = n_1$

$\vdots$

$(p_{L-3} - n_{L-2})/2 = p_{L-2}$

$p_{L-2}(\text{mod}2) = n_{L-1}$.

Form $r_0 = k_{L-1}$, $r_1 = k_{L-1} + k_{L-2}$, $\cdots$, $r_{L-1} = k_1 + k_0$

If $\sum_{i=0}^{L-1} r_i n_i \pmod 2 = 0$, then write $h(i,j,) = +1$.

If $\sum_{i=0}^{L-1} r_i n_i \pmod 2 = 1$, then write $h(i,j,) = -1$.

IV. a. We now give an algorithm for a cubic spline, its first three derivatives and its Finite Fourier Transform. The approach taken in making this Transformation is through integration by parts, which can be accomplished since the third derivative of a cubic spline is a constant on each of its subintervals.

b. Algorithm 4.1 (Ahlberg, Patti, Choate) How to find the Periodic Spline, $S_\Delta(t)$, passing through N points, its first three derivatives and its Finite Fourier Transform.

Enter time sample: $t_0 < t_1 < \ldots < t_N$ where $\Delta = t_i - t_{i-1}$ is fixed for $1 \leq i \leq N$.

Set $P = t_N - t_0$.

Enter the prescribed set of ordinants: $x_0, x_1, \cdots, x_N$.

Set $\delta = 3^{1/2} - 2$. (4.1.1)

$$A^{-1}_{i,j} = \frac{\delta^{N-|j-i|} + \delta^{|j-i|}}{(2+\delta)(1-\delta^N)} \quad \text{for } 0 \leq i,j \leq N \qquad (4.1.2)$$

$$M_i = (18/\Delta^2)\left[\sum_{j=0}^{N} A^{-1}_{i,j} \cdot (x_j)\right] + (6\Delta^2)x_i \ , \qquad (4.1.3)$$

where $0 \leq i \leq N$.

When t is confined to $[\, t_{j-1}, t_j]$, $S_\Delta(t)$ is equal to (4.1.4)

$$\left[M_{j-1}(t_j - t)^3\right]/(6\Delta) + M_j(t - t_{j-1})^3/(6\Delta) +$$

$$\left[x_{j-1} + (M_{j-1}\Delta^2)/6\right]\left[(t_j - t)/\Delta\right] + \left[x_j - (M_j\Delta^2)/6\right]\left[(t - t_{j-1})/\Delta\right]$$

Also $S'_\Delta(t) = -M_{j-1}(t_j - t)^2/(2\Delta) + \left[M_j(t - t_{j-1})^2\right]/(2\Delta)$ (4.1.5)

$$+ (x_j - x_{j-1})/\Delta + \left[(M_j - M_{j-1})\cdot\Delta\right]/6 .$$

and $S''_\Delta(t) = M_{j-1}\left[(t_j - t)/\Delta\right] + M_j\left[(t - t_{j-1})/\Delta\right]$ (4.1.6)

Differentiating again we get $S'''_\Delta(t) = (M_j - M_{j-1})/\Delta$ (4.1.7)

$$\int_{t_{j-1}}^{t_j} S_\Delta(t)\,\cos wt\,dt \qquad (4.1.8)$$

$$= (1/w)\left[S_\Delta(t_j)\sin wt_j - S_\Delta(t_{j-1})\sin wt_{j-1}\right]$$

$$+ (1/w^2)\left[S'_\Delta(t_j)\cos wt_j - S'_\Delta(t_{j-1})\cos wt_{j-1}\right]$$

$$- (1/w^3)\left[S''_\Delta(t_j)\sin wt_j - S''_\Delta(t_{j-1})\sin wt_{j-1}\right]$$

$$- (1/w^4)\left[S'''_\Delta(t_{j-1})\cos wt_j - S'''_\Delta(t_{j-1})\cos wt_{j-1}\right]$$

So $\int_{-P/2}^{+P/2} S_\Delta(t)\,\cos wt\,dt = \sum_{j=1}^{N}\int_{t_{j-1}}^{t_j} S_\Delta(t)\,\cos wt\,dt$ (4.1.9)

Similarly,

$$\int_{t_{j-1}}^{t_j} S_\Delta(t)\sin wt\,dt \quad = \qquad (4.1.10)$$

$$\left[M_{j-1}(t_j - t)^3\right]/(6\Delta) + \left[M_j(t - t_{j-1})^3\right]/(6\Delta) + \left[x_{j-1} + (M_{j-1}\Delta^2)/6\right]\cdot[(t_j - t)$$

$$+ \left[x_j - (M_j\Delta^2)/6\right](t - t_{j-1})/\Delta \quad .$$

$$S'_\Delta(t) = -M_{j-1}(t_j - t)^2/2 + M_j(t - t_{j-1})^2/2 \qquad (4.1.5)$$

$$+ (x_j - x_{j-1})/\Delta + \left[(M_j - M_{j-1})/6\right]\cdot\Delta$$

$$S''_\Delta(t) = M_{j-1}\cdot(t_j - t)/\Delta + M_j\cdot(t - t_{j-1})/\Delta \qquad (4.1.6)$$

$$S'''_\Delta(t) = (M_j - M_{j-1})/\Delta \qquad (4.1.7)$$

$$\int_{t_{j-1}}^{t_j} S_\Delta(t)\ \text{coswt}\,dt \qquad (4.1.8)$$

$$= (1/w)\left[S_\Delta(t_j)\cdot\text{sinwt}_j - S_\Delta(t_{j-1})\cdot\text{sinwt}_{j-1}\right]$$

$$+ (1/w^2)\left[S'_\Delta(t_j)\ \text{coswt}_j - S'_\Delta(t_{j-1})\ \text{coswt}_{j-1}\right]$$

$$- (1/w^3)\left[S''_\Delta(t_j)\ \text{sinwt}_j - S''_\Delta(t_{j-1})\ \text{sinwt}_{j-1}\right]$$

$$-(1/w^4)\left[S'''_\Delta(t_{j-1})\ \text{coswt}_j - S'''_\Delta(t_{j-1})\ \text{coswt}_{j-1}\right]$$

$$\int_{-P/2}^{+P/2} S_\Delta(t)\ \text{coswt}\,dt = \sum_{j=1}^{N}\int_{t_{j-1}}^{t_j} S_\Delta(t)\ \text{coswt}\,dt \qquad (4.1.9)$$

$$\int_{t_{j-1}}^{t_j} S_\Delta(t)\ \text{sinwt}\,dt = \qquad (4.1.10)$$

$$= (-1/w)\left[S_\Delta(t_j)\cos wt_j - S_\Delta(t_{j-1})\cos wt_{j-1}\right]$$

$$(+1/w^2)\left[S'_\Delta(t_j)\sin wt_j - S'_\Delta(t_{j-1})\sin wt_{j-1}\right]$$

$$(+1/w^3)\left[S''_\Delta(t_j)\cos wt_j - S''_\Delta(t_{j-1})\cos wt_{j-1}\right]$$

$$(-1/w^4)\left[S'''_\Delta(t_{j-1})\sin wt_j - S'''_\Delta(t_{j-1})\sin wt_{j-1}\right] .$$

$$\text{So} \int_{-P/2}^{+P/2} S_\Delta(t)\sin wt\, dt = \sum_{j=1}^{N} \int_{t_{j-1}}^{t_j} S_\Delta(t)\sin wt\, dt \qquad (4.1.11)$$

Notation: Set $F(x(t)) = X(w)$ be the Fourier Transform of $x(t)$ or its Finite Fourier Transform. And j, not originally an index, is $\sqrt{-1}$.

$$F(S_\Delta(t)) = \int_{-P/2}^{+P/2} S_\Delta(t)\cos wt\, dt + j\int_{-P/2}^{+P/2} S_\Delta(t)\sin wt\, dt \qquad (4.1.12)$$

Remark 1. Equation 4.1.2 requires only $(N+1)(N+2)/2$ computations since $A_{i,j} = A_{j,i}$.

Remark 2. For large N $A_{i,j} \approx \delta^{|j-i|}/(2+\delta)$ and can be replaced by this value at the cost of an error given by

$(\delta^{N-|j-i|} + \delta^{|j-i|})/(2+\delta)(1-\delta^N)$. This error, of course, decreases for a large sampled-data system.

Remark 3. The spline on a sampled-data system exists [1, p.16] and is unique [1, p.18].

4.2 Convergence

Theorem 4.2.1 (Alhberg) If $x(t)$ is a signal with a continuous fourth derivative passing through $(t_0, x_0), \ldots, (t_N, x_N)$, $\Delta = t_j - t_{j-1}$ fixed for $j = 1, \ldots, N$, then

$$|x(t) - S_\Delta(t)| < K\Delta^4 \quad .$$

This leads to a simple result.

Theorem 4.2.2 (Choate) If $x(t)$ is a signal with a continuous fourth derivative passing through $(t_0, x_0), \ldots, (t_N, x_N)$, $\Delta = t_j - t_{j-1}$ fixed, then $F(S_\Delta(t)) \rightarrow F(x(t))$ as $\Delta \rightarrow 0$.

Proof.

$$|F(x(t)) - F(S_\Delta(t))|$$

$$= \left| \int_{-P/2}^{+P/2} x(t) - S(t) \; e^{jwt} \, dt \right|$$

$$\leq \int_{-P/2}^{+P/2} |x(t) - S_\Delta(t)| \, |e^{jwt}| \, dt$$

$$K\Delta^4 \int_{-P/2}^{+P/2} 1 \, dt = K\Delta^4 P \quad .$$

From this the result follows.

Remark 4. How fast the Fourier Transforms of a signal and the spline through a data sample will converge seems difficult to determine however. since the constant K depends on the δ constant in the definition of uniform continuity, whose existence is demonstrated by contradiction. Moreover, the more practical problem before us is to determine to the best accuracy the main lobe of the Fourier Transform given a fixed Δ while the convergence above depends on a shrinking one. And, as has been mentioned, the Fourier Transform of a spline will converge to the Fourier Transform of the signal but at an unknown rate.

V. a. To overcome this difficulty we appeal to a celebrated theorem of Holladay [1, p.3] with which much of the present day theory of splines began.

Theorem 5.1 (Holladay) Let $a = t_0 < t_1 < \ldots < t_N = b$ and let a set of real ordinants $\{x_i\}$, $i = 0, \ldots, N$, be prescribed. Then of all functions $x(t)$ having a continuous second derivative on $[a,b]$ and such that $x(t_i) = x_i$ $(i = 0, \ldots, N)$, the spline function, $S_\Delta(t)$, with $S''_\Delta(a) = S''_\Delta(b) = 0$, minimizes the integral

$$\int_a^b |x''(t)|^2 \, dt \, .$$

The proof is not difficult. Holladay's Theorem is often called the minimum curvature property. And since the curvature of the spline is the least possible, it should be the best approximation to a curve through a given set of points. Since we wish the best approximation of the main lobe of the Fourier Transform of a signal, one method is clearly to apply the Fast Fourier Transform to the sampled-data system and then put a nonperiodic spline through the discrete frequency spectrum.

But it is possible to approach all calculations in the time domain after we prove the following sequence of theorems.

b. Theorem 5.2 (Choate) Let $x(t)$ be a curve whose Fourier Transform, $F(x(t)) = X(w)$, exists. Then the curvature of $X(w)$ is given by

$$2\pi \int_{-\infty}^{+\infty} t^4 [x(t)]^2 \, dt$$

PROOF. Since $F(x(t))$ exists, we know by [1, p.16] that $F(t^2x(t)) = X''(w)$. Setting $h(t) = t^2x(t)$, we have $H(w) = F(h(t)) = X''(w)$. Now set $z(t) = \left[t^2x(t)\right]\cdot\left[t^2x(t)\right] = h(t)\cdot h(t)$. By convolution $Z(w) = (1/(2\pi))\int_{-\infty}^{+\infty} H(\alpha)H(w-\alpha)\,d\alpha$.

So $Z(0) = (1/2\pi)\int_{-\infty}^{+\infty} H(\alpha)H(-\alpha)\,d\alpha$

$= (1/2\pi)\int_{-\infty}^{+\infty} |H(\alpha)|^2\,d\alpha$ since $H(\alpha)$ and $H(-\alpha)$ are

complex conjugates.

Therefore

$$(2\pi)\int_{-\infty}^{+\infty} t^4\left[x(t)\right]^2\,dt = (2\pi)\,F\left\{t^4\left[x(t)\right]^2\right\}\Big|_{w=0}$$

$$= (2\pi)\,Z(0) = \int_{-\infty}^{+\infty} |H(\alpha)|^2\,d\alpha$$

$$= \int_{-\infty}^{+\infty} |X''(w)|^2\,dw\,,$$ which is the curvature of $X(w)$ on $(-\infty, +\infty)$.

Comment 1. The nth moment of $x(t)$ is defined to be $\int_{-\infty}^{+\infty} t^n x(t)\,dt$, $n = 0, 1, 2, \ldots$, [2, p.16]. So clearly the fourth moment of $\left[x(t)\right]^2$ times 2π is the curvature of $X(w)$.

Comment 2. Define $X^2(w)$ as $F\left\{\left[x(t)\right]^2\right\}$. Then the curvature of $X(w)$ is $(2\pi)\int_{-\infty}^{+\infty} t^4\left[x(t)\right]^2\,dt = (2\pi)\,\frac{d^4\left[X^2(0)\right]}{dw}$ by [2, p.16].

But observe that $X^2(0) = \int_{-\infty}^{+\infty}\left[x(t)\right]^2 e^{-j\cdot 0\cdot t}\,dt = \int_{-\infty}^{+\infty}\left[x(t)\right]^2\,dt$,

the total energy delievered by the source [2, p.28] So 2π

times the fourth derivative (wrt w) of the total energy delievered by the source is the curvature of X(w) .

Example 5.3 Define $x_i(t) = \begin{cases} \left[(x_i)(t_i)^2\right]/t^2 & \text{for } t_i \le t \le t_{i+1} \\ 0 \text{ elsewhere} \end{cases}$

for $0 \le i \le N-1$. Once again $t_0 = a$ and $t_N = b$. Let $x(t) = \sum_{i=0}^{N-1} x_i(t)$. Clearly $x(t_i) = x_i$ for $0 \le i \le N-1$. Observe that $x(t)$ may have $N - 1$ discontinuities. Squaring the above equation and multiplying by t^4 we get

$$z(t) = t^4\left[x(t)\right]^2 = \begin{cases} x_i^2 t_i^4 & \text{for } t_i \le t \le t_{i+1} \\ 0 & \text{elsewhere} \end{cases} \text{ . So}$$

$$2\pi \cdot Z(0) = (2\pi)\int_{-\infty}^{+\infty} t^4\left[x(t)\right]^2 dt$$

$$= (2\pi)\int_a^b t^4\left[x(t)\right]^2 dt$$

$$= (2\pi)\left\{\sum_{i=0}^{N-1}\int_{t_i}^{t_{i+1}} t^4\left[x(t)\right]^2 dt\right\}$$

$$= (2\pi)\left\{\sum_{i=0}^{N-1}\int_{t_i}^{t_{i+1}} (x_i)^2(t_i)^4\, dt\right\}$$

$$= (2\pi)\left\{\sum_{i=0}^{N-1} (x_i)^2(t_i)^4(t_{i+1} - t_i)\right\}$$

$$= (2\pi\Delta)\cdot\left\{\sum_{i=0}^{N-1} (x_i)^2(t_i)^4\right\}, \text{ the curvature of X(w). Note that}$$

this value decreases when the time coordinants are less than one or close together.

Example 5.4 For example we set $b_i = \dfrac{2\ln\{(x_{i+1}/x_i)(t_{i+1}/t_i)^2\}}{(t_i - t_{i+1})}$

and insist that the ordinants x_i be all positive or all negative. (For a finite sampled-data system this can always be contrived by a translation.) Let $A_i = (x_i)(t_i)^2 \exp(b_i t_i)/2$.

Then $x_i(t) = \begin{cases} \left[\sqrt{A_i}\ \exp(-b_i t)/2\right]/t^2 & t_i \le t < t_{i+1} \\ 0 \text{ elsewhere} . \end{cases}$

passes through (t_i, x_i) and agrees with $x_{i+1}(t)$ at t_{i+1}. So $x(t) = \sum_{i=0}^{N-1} x_i(t)$ is certainly continuous--and passes through the data sample.

Now $t^4 \left[x_i(t)\right]^2 = \begin{cases} A_i \exp(-b_i t) & t_i \le t < t_{i+1} \\ 0 \text{ elsewhere} . \end{cases}$

This implies

$$2\pi\ Z(0) = 2\pi \int_{-\infty}^{+\infty} t^4 \left[x(t)\right]^2 dt$$

$$= 2\pi \sum_{i=0}^{N-1} \int_{t_i}^{t_{i+1}} A_i \exp(b_i t)\, dt$$

$$= 2\pi \sum_{i=0}^{N-1} A_i \left\{ \left[\exp(-b_i t_i) - \exp(-b_i t_{i+1})\right] / b_i \right\}$$

, the curvature of X(w), which is small for unequal intervals of time which grow in size.

The next theorem will give us some idea of what a spline function must look like when it is also the Fourier Transform of a continuous time signal.

Theorem 5.5 (Choate) Let $F(w) = B(w)e^{j\Psi(w)}$ be a Fourier Transform of some continuous time signal $f(t)$. We further require that $F'(0) \neq 0$. Among all such functions whose derivatives have the same amplitude, the one which minimizes $\int_{-\infty}^{+\infty} |F''(w)|^2 \, dw$ is of the form $F(w) = B(w)$.

PROOF. Let $F'(w) = A(w)e^{j\phi(w)}$. Then

$$|F''(w)|^2 = \left|\frac{dF'}{dw}\right| = \left(\frac{dA}{dw}\right)^2 + A^2\left(\frac{d\phi}{dw}\right)^2 .$$

So among all functions whose first derivative has amplitude $A(w)$, the one which minimizes $\int_{-\infty}^{+\infty} |F''(w)|^2 \, dw$ has $\phi'(w) = 0$, or $\phi(w)$ is a constant, say k. So in other words $F'(w) = A(w)\cos k + jA(w)\sin k$. But since $F(w)$ is the Fourier Transform of some $f(t)$, $F'(w)$ is the Fourier Transform of $-jtf(t)$ [2, p.16]. This means $A(0)\cos k + jA(0)\sin k = F'(0)$ is real [p.17, 2], or $A(0)\sin k = 0$. So either $A(0) = 0$ in which case $F'(0) = 0$ contrary to hypothesis or $\sin k = 0$, which implies $k = n\pi$ where n is an integer. This would mean that $F'(w) = A(w)\cos k = A(w)\cos n\pi = A(w) = A(w) + j\cdot 0$.

But $F'(w) = \left[B'(w) + jB(w)\Psi'(w)\right] e^{j\Psi(w)}$

$$= \left[B'(w)\cos\Psi(w) - B(w)\Psi'(w)\sin\Psi(w)\right] + j\left[B(w)\Psi'(w)\cos\Psi(w) + B'(w)\sin\Psi(w)\right]$$

Equating imaginary parts we obtain

$$0 = B(w)\Psi'(w)\cos\Psi(w) + B'(w)\sin\Psi(w).$$

If $\sin\Psi(w) \equiv 0$, then $\Psi(w) = n\pi$ and the conclusion $F(w) = B(w)$ follows.

If $\sin\Psi(w) \not\equiv 0$, then

$$B(w)\Psi'(w)\cot\Psi(w) + B'(w) = 0 , \quad \text{or}$$

$$\frac{-dB}{B} = (\cot\Psi)\, d\Psi , \text{ which implies}$$

$$c = -\ln|\sin\Psi| + \ln|B| = \ln|\sin\Psi \cdot B| , \quad \text{or}$$

$$c' = B(w)\sin\Psi .$$

Thus $F(w) = B(w)e^{j\Psi(w)}$

$$= B(w)\cos\Psi(w) + jc' .$$

But again $F(0)$ is real, which implies $c' = 0$, or $F(w) = B(w)$, a real valued function.

Another result of this ilk which we only state is

Theorem 5.6 (Choate) Let $\Delta : -B = w_0 < w_1 < \ldots < w_N = +B$ and a set of real numbers be given. Let $A(w)$ be a real valued, differentiable function in $C^2[-B,+B]$ passing through (w_i, y_i), $i = 0, \ldots, N$, and with $A''(-B) = A''(+B) = 0$. Further assume that $\Psi(w)$ is a real valued differentiable function. Set $F(w) = A'(w)e^{j\Psi(w)}$. Then

$$\int_{-B}^{+B} |F'(w)|^2\, dw \quad \text{is minimal when } A(w) = S_\Delta(w) \text{ and } \Psi(w) = 0.$$

(i.e. $F(w) = S'(w)$)

Let $\Delta : -B = w_0 < \ldots < w_N = +B$ be a mesh of equal subintervals (i.e. $\Delta = w_i - w_{i-1}$ is fixed for $i = 1, \ldots, N$) in the frequency domain. Let $\{y_i\}$ be a prescribed set of spectral ordinants. By Theorem 5.5 and Holladay's Theorem the spline, $S_\Delta(w)$, passing through the discrete Fourier Spectrum $\{(w_0,y_0), \ldots, (w_N,y_N)\}$, is real valued (with trivial exceptions). So for band-limited signals

$$s(t) = (1/2\pi)\int_{-B}^{+B} S_\Delta(w)e^{jwt}\,dw$$

$$= (1/2\pi)\int_{-B}^{+B} S_\Delta(w)\cos wt\,dw + (j/2\pi)\int_{-B}^{+B} S_\Delta(w)\sin wt\,dw .$$

If we insist that the continuous signal $s(t)$ be real valued, then we have:

$s(t) = (1/2\pi)\int_{-B}^{+B} S_\Delta(w)\cos wt\,dw$, an integral which can be evaluated by parts as in 4.1.8 and 4.1.9 . So we obtain in a similar manner:

$$\text{So } s(t) = \sum_{j=1}^{N}\int_{w_{j-1}}^{w_j} S_\Delta(w)\cos wt\,dw \qquad (5.7)$$

$$= \sum_{j=1}^{N}\Big\{(1/t)\left[S_\Delta(w_j)\sin(tw_j) - S_\Delta(w_{j-1})\sin(tw_{j-1})\right]$$

$$+ (1/t^2)\left[S'_\Delta(w_j)\cos(tw_j) - S'_\Delta(w_{j-1})\cos(tw_{j-1})\right]$$

$$- (1/t^3)\left[S''_\Delta(w_j)\sin(tw_j) - S''_\Delta(w_{j-1})\sin(tw_{j-1})\right]$$

$$- (1/t^4)\left[S'''_\Delta(w_{j-1})\cos(tw_j) - S'''_\Delta(w_{j-1})\cos(tw_{j-1})\right]\Big\},$$

If we require that s(t) pass through the sampled-data system (t_0,x_0) , ... , (t_N,x_N) , then we get a matrix with N + 1 equations, namely,

$$x_i = \sum_{j=1}^{N}\Big\{(1/t_i)\Big[S_\Delta(w_j)\sin(t_iw_j) - S_\Delta(w_{j-1})\sin(t_iw_{j-1})\Big] \quad (5.8)$$

$$+ (1/t_i^2)\Big[S'_\Delta(w_j)\cos(t_iw_j) - S'_\Delta(w_{j-1})\cos(t_iw_{j-1})\Big]$$

$$- (1/t_i^3)\Big[S''_\Delta(w_j)\sin(t_iw_j) - S''_\Delta(w_{j-1})\sin(t_iw_{j-1})\Big]$$

$$- (1/t_i^4)\Big[S'''_\Delta(w_{j-1})\cos(t_iw_j) - S'''_\Delta(w_{j-1})\cos(t_iw_{j-1})\Big]\Big\},$$

i = 0, ... , N , and N + 1 unknowns, namely, the M_i's (4.1.3). [Recall that S_Δ , S'_Δ , S''_Δ , and S'''_Δ are all in terms of the M_i's. (See 4.1.4, 4.1.5, 4.1.6 and 4.1.7.) and that the w_j's are known.]

The solution to this matrix (5.8) must exist since $S_\Delta(w)$ exists [1, p.16]. Therefore $S_\Delta(w)$, the spline through the Discrete Fourier Spectrum, can be determined without leaving the time domain.

VI.a. The algorithms described in sections III and IV have both been put on computer by Scott Fuller and John Patti. It is possible, of course, to use a machine to solve the matrix (5.8) given in section V, but I would prefer, before doing so, to determine whether the calculations involved can be simplified.

b. A spline through a discrete Fourier Spectrum is the best possible estimate of the true spectrum (Holladay 5.1). In section V we developed a way to determine the real valued curve through a given data sample whose Fourier Transform is a spline through the discrete Fourier Spectrum. The determination of this time curve may be done strictly in terms of time by 5.8. Moreover the curvature of the spectral spline itself can be computed in terms of time alone by 5.2. In any follow-on work I would hope to simplify the computations involved in finding the solution to 5.8 by way of 5.2. In addition, I would investigate whether windows and filters would simplify the computations.

c. The number of multiplications and additions in 5.8 is large. I would suggest that an algorithm not be written to implement this theorem before theoretical attempts to simplify are exhausted.

REFERENCES

1. Ahlberg, J.H., Nilson, E.N., Walsh, J.L., The Theory of Splines and Their Applications, New York, New York, Academic Press, Inc., 1967.

2. Papoulis, A., The Fourier Integral and It's Applications, New York, New York, McGraw-Hill Book Company, Inc., 1962

1985 USAF-UES SUMMER FACULTY RESEARCH PROGRAM/

GRADUATE STUDENT SUMMER SUPPORT PROGRAM

Sponsored by the

AIR FORCE OFFICE OF SCIENTIFIC RESEARCH

Conducted by the

UNIVERSAL ENERGY SYSTEMS, INC.

FINAL REPORT

PROTECTION FROM NONNUCLEAR WEAPONS : A PROBABILISTIC APPROACH

Prepared by:	Karen C. Chou
Academic Rank:	Assistant Professor
Department and University:	Department of Civil Engineering Syracuse University
Research Location:	HQ AFESC/RDCS Tyndall AFB Panama City, Florida
USAF Research:	Mr. Jack Hayes
Date:	July 1985
Contractor No.	F49620-85-C-0013

Atch 1

PROTECTION FROM NONNUCLEAR WEAPONS : A PROBABILISTIC APPROACH

by

Karen C. Chou

ABSTRACT

It is well known that uncertainty exists in all aspects of structural design. The randomness can have significant effect on the reliability of design. The design specification for structures protected from nonnuclear weapons is studied here using a probabilistic approach. A stochastic process called Markov chain is suggested for modelling the detonation locations relative to a target during a sequence of attacks. The model will enable an engineer to evaluate the probability that the target being completely destroyed, severely damaged, lightly damaged, etc. This information will allow one to specify a more realistic design load factor to achieve the desired reliability level for the structure.

ACKNOWLEDGEMENTS

The author would like to express her appreciation to the Research Engineering and Services Laboratory Engineering Division, ~~Research Directorate~~, U.S. Air Force Engineering and Services Center, Tyndall AFB, Florida for the hospitality during her stay as a Summer Fellow. Special thanks are due to Mr. Hank Marien, Capt. Paul Rosengren and Dr. Paul Thompson for their assistances and fruitful discussions.

Appreciation is also extended to the Air Force System Command, Air Force Office of Scientific Research for sponsoring the program and providing such a unique opportunity.

SECTION 1
INTRODUCTION

The author is an assistant professor of civil engineering at Syracuse University. She received her B.S. in civil engineering with a second major in mathematics from Tufts University; her M.S. and Ph.D. in structural engineering from Northwestern University. Prior to her Ph.D. study, the author has worked at Harza Engineering Co. where she used finite element method extensively to analyse structures related to hydropower plants. Her research interest has primarily been focused on the probabilistic study of engineering related areas, with special emphases on structural reliability. Published articles include structural system reliability on ductile framed structures; structural member reliability including material nonlinearity; wind speed probability distribution and wind power simulations for wind energy conversion sites. Currently, the author serves on two technical committees, ASCE Structural Division's Committee on the Safety of Buildings and ACI Committee 348 Structural Safety.

The author performed the attached study at the Air Base Survivability Branch, Research Engineering Division of U.S. Air Force Engineering and Services Center, Tyndall AFB. One of the Branch's objectives is to develop design specifications for Air Force shelters to withstand various nonnuclear weapons attack. Safety of personnel, integrity of shelters, construction constraints, and cost effectiveness are among the areas of concern in the specifications. The philosophy of structural reliability used in buildings, in the author's opinion, can be applied here to gain a better understanding of the shelter's response under the uncertain environment. This information will enable the Air Force to specify more realistic design criteria.

SECTION 2
OBJECTIVES

A structure is considered safe for as long as the resisting capability exceeds the loads acting upon it. Whenever the above relationship does not hold during the structure's lifetime, the structure will fail. Due to the randomness in both load and resistance and economic feasibility, it is impossible to have an absolutely safe design. The amount of risk (level of probability of failure) one has to accept depends on the consequence of failure and many other factors. Thus it is essential to treat the randomness of the parameters involved in a systematic manner so that a meaningful evaluation of structural reliability can be obtained. There is no exception to the types and functions U.S. Air Force facilities are designed for if one wishes to sustain a desirable reliability level.

It is difficult to predict the types and magnitudes of load that a structure will experience in its design lifetime. The resistance of the structure is also uncertain. One may say that if one designed the worst possible case, the structure should be adequately protected. The question then would be, "How does one evaluate conservatism?", or "Is this concept really economically feasible?", that is, "Is this structure unreasonably over-designed?". The anwer to these questions is not always obvious.

Studies and full scale testings have been done on shelter response. Unfortunately few, if any, have treated the stochastic nature of the problem in a systematic manner. The objective of this study is to suggest areas pertinent to protective design from nonnuclear weapons which require study in their uncertain nature. In particular, the probability that a target being hit during a sequence of attacks, is studied in detail. A stochastic model is developed to characterize the detonation locations.

In Section 3, an outline on potential areas for stochastic study is discucssed. Section 4 presents the formulation of stochastic modelling of detonation locations. Finally, Section 5 presents some discussion and suggestions.

SECTION 3

OUTLINE OF POTENTIAL AREAS FOR STOCHASTIC STUDY

The interest in applying probabilistic and statistical concepts to structural safety has grown tremendously over the past decade. Most of the emphases have been on buildings (e.g. Peir & Cornell, 1973; Ditlevsen, 1978; Ang & Ma, 1979; Ellingwood et al., 1980; Harris, Corotis and Bova, 1981; Wen, 1981; Moses, 1982; ANSI, 1982; Winterstein & Cornell, 1984; Chou, Corotis & Karr, 1985) and less extensively on other structures such as bridges (Tang, 1969), nuclear power plants (Christian, Borgeson & Tringale, 1978; Fardis, Cornell & Meyers, 1979; ASCE, 1981), offshore structures (Moses, 1979; Bea, 1980; Angelides, Veneziano & Sunder, 1981) and others. However, reliability study in structures designed to protect from nonnuclear weapons is very limited. Potential areas which require consideration for stochastic study are presented herein.

An engineer needs to understand the behavior of loads and resisting capacities in order to design a safe, cost effective structure. Since these two parameters are, in general, not known with certainty, a study on their stochastic characteristics is necessary. In the area of random loads, the force or pressure exerted on a structure depends primarily on the weapons (types of weapons). Uncertainty arises from the type of weapon used during any attack (different weapons have different accuracy and destructive capability) or sequence of attacks. An equivalent force or pressure magnitude experienced by a structure should be related to the location where an explosive device detonates. The frequency of attacks in a fixed duration also has an influence on the survivability of the structure.

In the area of resistance, studies should be focused on both the material strength and structural response. Due to the quality of workmanship, equipments, and environmental effects, the material strength may vary. This variation may or may not have significant effects on the resisting capability depending on what the members or structures are designed for (e.g., shear, bending). Many basic

building materials have been studied by various researchers. Results are available in technical journals. They are also summarized in a National Bureau of Standards special publication (Ellingwood et al., 1980). Statistical study on other materials (including different specified strength) pertinent to Air Force construction needs should be performed to supplement the current information.

Structural member reliability is usually simple to analyze and it is what the current codes are based on (ACI, 1977; AISC, 1978, 1983; ANSI, 1982). However, a system consisting of integrated members would definitely behave differently. Numerous researches have been done on the reliability of a structural system (Stevenson & Moses, 1970; Ditlevsen, 1978, Ang & Ma, 1979; Kam, Corotis & Rossow, 1983; Lin & Corotis, 1985). The studies are primarily on ductile frame structures where failure occurs whenever a plastic mechanism is formed. These are generally more applicable to building type structures. Since some of the Air Force facilities where shapes and functions are significantly different from the regular building type, separate reliability study must be performed to gain more realistic understanding of the safety of the structure being designed.

Finally, the design must also be cost effective. This objective can usually be fulfilled by optimization. Due to the uncertainty existing in some parameters (i.e., load magnitudes, material properties, etc.) and various levels of reliability, optimization alogorithm has to incorporate these uncertainties (Frangopol, 1984). In addition, in any design, there exists some criteria which are difficult to quantify with the regular set theory and are unable to be incorporated into the optimization alogorithm. These criteria, such as esthetic, functionals, failure consequences, are usually described verbally. With the introduction of fuzzy set theory by Professor Zadeh of University of California, Berkeley in 1965 (Zadeh, 1965), it is possible to quantify the verbal parameters. Thus these parameters can be added to the objective function to obtain a better optimal design.

SECTION 4

STOCHASTIC MODELLING OF DETONATION LOCATIONS

Among the areas discussed in Section 3, one specific area, the probability that a target being hit during a sequence of attacks, will be discussed in greater detail in this section. The survivability of a structure depends on the relative magnitudes between load and resistance. The load magnitude (applied on a target) depends on where the detonation occurs relative to the target. For instance, if a structure is well situated such that the probability of being hit "right-on" or close enough to cause damages is quite small, then the design would be different from the one which may have high probability of having severe damages. In other words, the survivability of the former structure is much higher than the latter one. Due to the accuracy of weapon, human judgement, environmental effects and other factors, where the explosive device lands is highly randomized within certain limits. If one is interested in the uncertainty of load magnitudes, it would be more feasible to study the stochastic behavior of detonation location relative to a target. The reason is that there is a unique relationship between the detonation location and the load (force or pressure) experienced by the target according to weapon types. Once the model of detonation location is established, the pressure-weapon type relationship can be implemented to evaluate the damage level.

If attacks occur infrequently, i.e., the duration between any two attacks is relatively long, and the attacks are independent, i.e., there is no relationship among attacks; then the modelling would be quite simple. However, this type of attacks does not occur often. And if it does occur, the type of weapon used would likely be very accurate or carefully guided by other equipments and/or the magnitude of the explosion is very large. The protective design scheme under this situation would take on a different philosophy. In this study, the interest is in the situation where a sequence

of attacks occurs. The weapon is not assumed to be highly sophisticated so that it usually requires several attempts before the target is completely destroyed. Although technology has gone to the level where weapons can be designed with such accuracy that the target can be destroyed with one shot, in small scale warfare these sophisticated weapons may not be used.

In developing the detonation location (location where an explosive device lands) model, the target is assumed to be fixed in space. During a sequence of attacks, it is quite clear that the detonation locations are related to a certain degree with each other in the sequence. An attacker would, quite naturally, try to adjust his position and the weapon's position after each shooting to achieve his goal of hitting the target. Thus each detonation location depends on previous detonation locations. To model such a sequence is very complicated. Also, the mathematics involved is usually prohibitively complicated for any numerical evaluation. However, it is adequate to assume that the next detonation location depends strongly only on the current one and weakly on any previous ones. And if the assumption of "weak dependence" is further approximated by independence and the attacks are considered as discrete steps, then the detonation location can be modelled by a Markov chain (Benjamin and Cornell, 1970). In this case, the detonation location in any attack only depends on the immediate preceding location and independent of all previous ones.

A detonation location for any attack can be described by the following parameters:

1. Radius of attack R which is the distance between the center of the target and the attack location. The value of R is defined between zero and infinity ($0<R<\infty$);
2. Line of action with length r_a whose value depends on the type of weapons;
3. Orientation angle B is the angle between the radius of attack and a reference line. The value of B is defined between 0 and 2π radian ($0<B<2\pi$). The angle is positive

when measured counterclockwise from the reference line; and

4. Angle of attack Θ is the angle between the radius of attack and the line of action. The value of Θ is defined between $-\pi/2$ and $\pi/2$ radians ($-\pi/2 < \Theta < \pi/2$). The angle is positive when measured counterclockwise from the radius of attack.

A typical detonation location is shown in Fig. 1. In defining the range of values for the above parameters, some judgement was made. The length of line of action r_a is assumed to be constant for a given weapon type. Since there is more control on the weapon's firing projectile, any variation in that regard is assumed to be small. The angle of attack Θ is defined only between $-\pi/2$ and $\pi/2$ radians because during any normal attack, it is highly unlikely that one would aim the weapon at a direction completely opposite from the target.

For a given attack, say the i-th one, the detonation location is given by one of the sixteen possible outcomes shown in Fig. 2. For illustration purpose, assume the detonation location is given by location 1 in Fig. 2a. Since the firing is off-target (the detonation location is off to the left and short of the target), the attacker would tend to move towards the target and to his right. In addition, he may also rotate the weapon (horizontally) clockwise from its current direction so that the combination of all these movements would yield at a position where the line of action is aligned with the radius of attacks (i.e., $\Theta_{i+1} = 0$) and the radius of attack $R_{i+1} = r_a$). The outcome of (i+1)-th attack can still take on any one of the sixteen possible relative locations as shown in Fig. 2. In general, the new location will likely be more desirable than the i-th one. The (i+2)-th attempt will be adjusted according to the outcome of the (i+1)-th attack. The sequence of such attacks theoretically can continue on indefinitely.

In order to fully describe the model mathematically, it is necessary to know the initial state probability q_i (1), and the

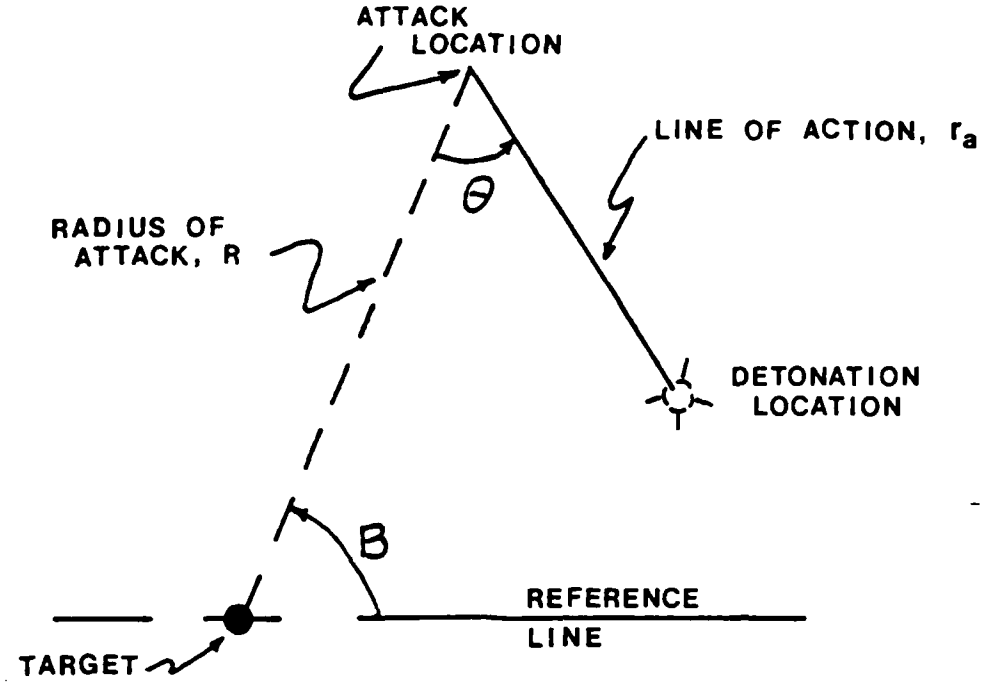

Figure 1. Typical Detonation Location

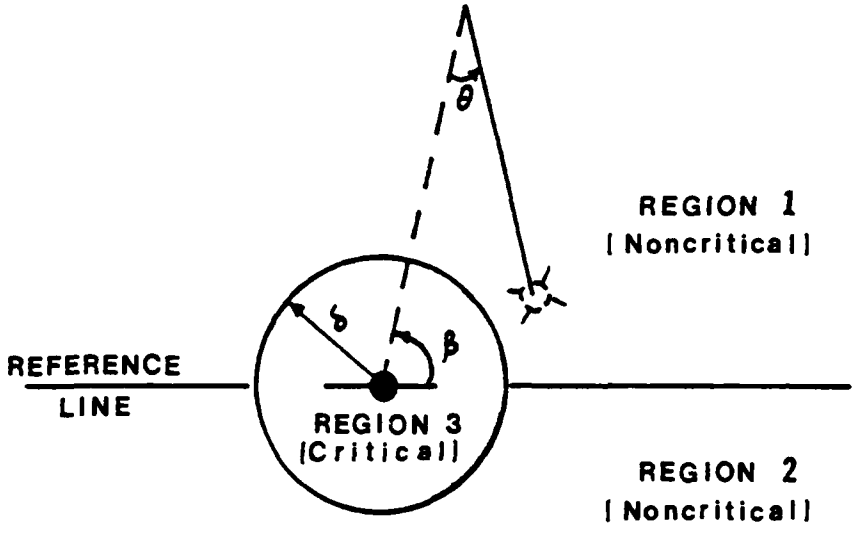

Figure 3. Typical Critical and Noncritical Regions of Detonation Locations

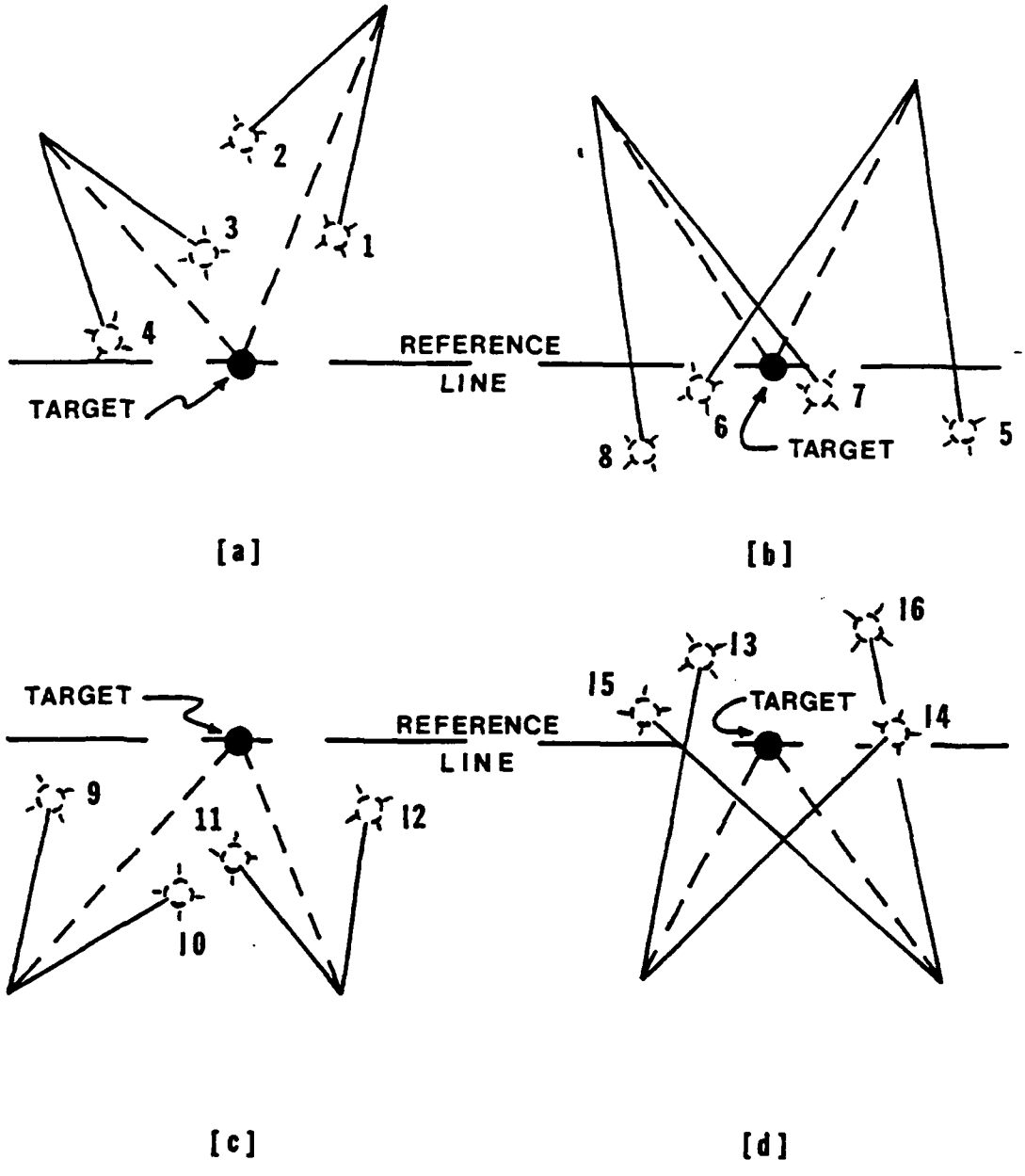

Figure 2. Typical Detonation Locations

transition probability $p_{ij}(n)$. It is clear from prior discussion that the future detonation location depends on the current one, and-such location can be described geometrically by the radius of attack R, orientation angle B, angle of attack Θ and by the line of action r_a. The initial state probability $q_i(1)$ is the probability that the detonation location being in region i in the first attempt. And, the transition probaiblity $p_{ij}(n)$ is simply the conditional probability that the detonation location will be in state j at the n-th attempt given it is in state i at the (n-1)-th attempt. Furthermore, the new radius of attack R is independent of the angles B and Θ. Thus the transition probability can be given by the product of two condition probability functions,

$$\begin{aligned} &P[R_n,\ B_n,\ \Theta_n \mid R_{n-1},\ B_{n-1},\ \Theta_{n-1}] \\ =&P[R_n \mid R_{n-1},\ B_{n-1},\ \Theta_{n-1}]\ P[B_n,\ \Theta_n \mid R_{n-1},\ B_{n-1},\ \Theta_{n-1}] \end{aligned} \qquad (1)$$

Since all the random parameters are continuous, it is more convenient to establish the probability density functions (pdf) first, then derive the probability distribution. Equation 1 can be rewritten for the continuous case as

$$\begin{aligned} &f_{R_n, B_n, \Theta_n \mid R_{n-1}, B_{n-1}, \Theta_{n-1}}(r_n, \beta_n, \theta_n, r_{n-1}, \beta_{n-1}, \theta_{n-1}) \\ =&f_{R_n,\ R_{n-1}, B_{n-1}, \Theta_{n-1}}(r_n, r_{n-1}, \beta_{n-1}, \theta_{n-1}) \\ &* F_{B_n, \Theta_n \mid R_{n-1}, B_{n-1}, \Theta_{n-1}}(\beta_n, \theta_n, r_{n-1}, \beta_{n-1}, \theta_{n-1}) \end{aligned} \qquad (2)$$

Equation 2 can fully represent the probability that the detonation location is at (r_n, β_n, θ_n) given that it was at $(r_{n-1}, \beta_{n-1}, \theta_{n-1})$ in the preceding attempt.

To further simplify the Markov model, the continuous space which contains the detonation locations is discretized into three regions as shown in Fig. 3. In this study, region 3 (circular

section centered on target with radius δ) is assumed to be a critical region within which the target will be completely destroyed (no longer functional) upon detonation. Regions 1 and 2 are assumed to be noncritical. This, however, does not imply that any detonation occurring in regions 1 and 2 will have no effect on the integrity of the structure. It only implies that at least portion of the structure remains functional upon detonation. The boundaries of these regions can be derived by geometry as function of R, B, Θ, r_a, and δ.

After the conditional pdf (Eqn. 2) is established and the regions in which detonation may occur are identified, the transition probability $p_{ij}(n)$ is simply the integration of the joint conditional pdf given by Eqn. 2 over the regions of (n-1)-th and n-th steps. Each transition probability $p_{ij}(n)$ represents the i-th row, j-th column entry of the transition probability matrix Π (n) which is used to compute the marginal (unconditional) probability for detonation location being in any region.

Besides the transition proabilities, it is also necessary to evaluate the initial state probability $q_i(1)$, which is the (unconditional) probability that the detonation location being in region i in the first attempt. This information is necessary because subsequent states may depend on the initial state. The initial state probability $q_i(1)$ is simply the probability that the detonation location is at (r_1,β_1,θ_1) which is the joint probability distribution of R_1, B_1 and Θ_1,

$$q_i(1) = \int_{\text{region } i} f_{R_1, B_1, \Theta_1}(r_1,\beta_1,\theta_1)\, dr_1\, d\beta_1\, d\theta_1 \qquad (3)$$

Similar to the transition probability matrix, $q_i(1)$ for i = 1, 2 and 3 forms the initial state probability vector $\underline{q}(1)$.

With the information on both the transition probability matrix and the initial state probability vector, one can, theoretically, evaluate the unconditional or marginal probability that the detonation location falls in any region in any attempt. For example, the probability for the detonation location being in region i in the n-th attempt is given by

$$q_i(n) = \sum_{j=1}^{3} q_j(1) p_{ji}^{(n-1)}(1) \qquad (4)$$

in which $P_{ji}^{(n-1)}(1)$ = the transition probability from state j to state i in (n-1) steps (attempts) starting from the first step (attempt).

Another information of interest given by the model is the number of attempts necessary until the detonation location falls in a particular region for a given marginal probability value. A question in this aspect could be, "When will the target be hit?". This question can be translated in a stochastic sense as "In which attempt will the process first enter state 3?".

SECTION 5

DISCUSSIONS AND RECOMMENDATIONS

Protective design from nonuclear weapons is examined in a very fundamental level and from a different perspective. A stochastic process called Markov chain is suggested for modelling the variations of detonation locations during a sequence of attacks. These variations can be due to weapon accuracy, human judgement, environmental effects and others. The concept of developing the model is presented in this report. The proposed model is also flexible enough that an user can define the size of critical region (region 3) to reflect the level of damage with which an engineer is concerned. The transition probability and initial state probability can be evaluated without any restriction as to the types of conditional pdf (Eqn. 2), parameters R (radius of attack), B (orientation angle) and Θ (angle of attack) can have. Therefore, it allows an user to change the pdf for the variables R, B and Θ for each situation. In summary, the proposed model is a generic stochastic model that permits the users to supply their own probability distribution models for the parameters, R, B and Θ to evaluate the probability that a target will have a certain damage level due to a sequence of attacks. However, the formulation as presented is primarily based on logical probabilistic reasoning. Verification with actual data or simulated data is required before this model can be adopted. It is recommended to have follow up study to verify the model discussed here with simulated data. Refinements and revisions should be made during the subseuqnet study to finalize the model.

A few suggested areas for probabilistic studies are also presented. Some of the areas can be studied indepently, e.g., resistance statistics; while others can incorporate the finding of the stochastic model proposed here, e.g., structural reliability. It is expected that the outcome of this model will lead to more realistic design specifications for protective design from nonnuclear weapons.

REFERENCES

1. "ACI Standard 318-77 Building Code Requirements for Reinforced Concrete", American Concrete Institute, Detroit, MI, 1977.
2. "AISC Specification for the Design, Fabrication and Erection of Structural Steel for Buildings", American Institute of Steel Construction, Chicago, IL, Nov., 1978.
3. (Proposed) "Load and Resistance Factor Design Specification for Structural Steel Building", Trial Document, American Institute of Steel Construction, Chicago, IL, Sept., 1, 1983.
4. Ang, A. H-S, and H-F Ma, "On the Reliability Analysis of Framed Structures", Proc. of the Specialty Conf. on Probabilistic Mechanics and Structural Reliability, ASCE, Tucson, Jan. 1979.
5. Angelides, D.C., D. Veneziano and S.S. Sunder, "Random Sea and Reliability of Offshore Foundations", Journal of Engineering Mechanic Division, ASCE, No. EM1, Feb., 1981, pp. 131-148.
6. "ANSI-A58.1 Building Code Requirements for Minimum Design Loads for Buildings and Other Structures", American National Standards Institute, New York, NY, 1982.
7. ASCE Special Publication, "Structural Analysis and Design of Nuclear Plant Facilities", American Society of Civil Engineers, New York, NY, 1981, 553pp.
8. Bea, R.G., "Reliability Considerations in Offshore Platform Criteria", Journal of Structural Division, ASCE, No. ST9, Sept., 1980, p. 1835-1854.
9. Benjamin, J.R. and C. A. Cornell, Probability, Statistics, and Decision for Civil Engineers, McGraw-Hill, New York, NY, 1970.
10. Chou, K.C., R.B. Corotis and A.F. Karr, "Nonlinear Response to Sustained Load Processes", Journal of Structural Engineering, ASCE, January, 1985, pp. 142-157.
11. Christian, J.T., R.W. Borjeson and P.T. Tringale, "Probabilistic Evaluation of OBE for Nuclear Plants", Journal of Geotechncial Division, ASCE, No. GT7, July, 1978, pp. 907-920.

12. Ditlevsen, O., "Narrow Reliability Bounds for Structural Systems", Report No. 145, The Danish Center for Applied Math. and Mechanics, The Technical University of Denmark, October, 1978.

13. Ellingwood, B.R., T.V. Galambos, J.G. MacGregor and C.A. Cornell, "Development of a Probability Based Load Criterion for American National Standard A58 Building Code Requirements for Minimum Design Loads for Buildings and Other Structures", Special Publication No. 577, National Bureau of Standards, Washington, D.C., June, 1980.

14. Fardis, M.N., C.A. Cornell and J.E. Meyers, "Accident and Seismic Containment Reliability", Journal of Structural Division, ASCE, No. ST1, Jan., 1979, pp. 67-84.

15. Frangopol, D.M., "A Reliability-Based Optimization Technique for Automatic Plastic Design", Computer Methods in Applied Mechanic and Engineering, 1984 (in press).

16. Harris, M.E., R.B. Corotis and C.J. Bova, "Area-Dependent Processes for structural Live Loads", Journal of Structural Division, ASCE, No. ST5, May, 1981, pp. 857-872.

17. Kam, T.Y., R.B. Corotis and E.C. Rossow, "Reliability of Nonlinear Framed Structure", Journal of Structural Engineering, ASCE, No. 7 July, 1983, pp. 1585-1601.

18. Lin, T.S. and R.B. Corotis, "Reliability of Ductile Systems with Random Strengths", Journal of Structural Engineering, ASCE, No. 6, June, 1985, pp. 1306-1325.

19. Moses, F., "Strategies for Implementing Reliability in Offshore Design Codes", Proc. of the Specialty Conf. on Probabilistic Mechanics and Structural Reliability, ASCE, Tucson, Jan., 1979.

20. Moses, F., "System Reliability Developments in Structural Engineering", Structural Safety, Vol. 1, Elsevier Scientific Publishing Co., Amsterdam, 1982, pp. 3-13.

21. Peir, J-C, and C.A. Cornell, "Spatial and Temporal Variability of Live Loads", Journal of Structural Division, ASCE, No. ST5, May, 1973, pp. 903-920.

22. Stevenson, J. and F. Moses, "Reliability Analysis of Fram Structure", Journal of Structural Division, ASCE, No. ST11, Nov., 1970, pp. 2409-2427.

23. Tang, C.C., "Life Expectancy of Highway Bridges to Vehicle Loads", Journal of Engineering Mechanic Divison, ASCE, No. EM6, Dec., 1969, pp. 1417.

24. Wen, Y-K, "Stochastic Dependencies in Load Combination", Third International Conferene on Structural Safety and Reliability (ICOSSAR 81), Trondheim, Norway, June 23-25, 1981.

25. Winterstein, S.R. and C.A. Cornell, "Energy Fluctuation Scale and Diffusion Models", Journal fo Engineering Mechanics, ASCE, Feb., 1984, pp. 125-142.

26. Zadeh, L., "Fuzzy Sets", Information and Control, Vol. 8, 1965, pp. 338-353.

1985 USAF-UES SUMMER FACULTY RESEARCH PROGRAM/
GRADUATE STUDENT SUMMER SUPPORT PROGRAM

Sponsored by the
AIR FORCE OFFICE OF SCIENTIFIC RESEARCH
Conducted by the
UNIVERSAL ENERGY SYSTEMS, INC.
FINAL REPORT

FLUID RECIRCULATION, DEPLOYMENT AND RETRACTION OF THE EXPANDABLE RADIATOR

Prepared by:	Louis C. Chow
Academic Rank:	Associate Professor
Department and University:	Mechanical Engineering Dept. Washington State University
Research Location:	Aero-Propulsion Laboratory, Aerospace Power Division, Power Technology Branch, Nuclear/Thermal Technology Group
USAF Research:	Dr. J. E. Beam
Date:	Sept. 30, 1985
Contract No:	F49620-85-C-0013

FLUID RECIRCULATION, DEPLOYMENT AND RETRACTION OF THE EXPANDABLE RADIATOR

by

Louis C. Chow

ABSTRACT

The focus of the present work is on the fluid recirculation, deployment and retraction of an expandable, megawatt pulse power radiator. Three methods of rolling up the radiator are explored. The bag can be collapsed flat and rolled up like a drum. The bag can be folded up like a paper lantern in 3 ways. The bag can also be rolled up internally or externally lengthwise on its circumference like a sock. Four mechanisms for condensate return are described. The condensate can be moved to the base of the radiator by a wiper. It can be pumped out of the radiator through liquid return channels. A rotating bag can provide the required body force for liquid return. The liquid can also be moved to the base of the radiator by simply requiring the bag to roll in completely. Other miscellaneous items such as flow unsteadiness are also considered. Finally, for follow-on research, two tasks are recommended.

I. INTRODUCTION:

Future space missions require peak electric power in the megawatt range. Based on mission and orbital cycles envisioned, there can be systems that will generate waste heat in the form of pulses with a peak to average ratio of 10^4 or more [1]. Conventional radiators are sized to reject peak powers, and "turned down" to reject off peak loads. Such conventional radiators are capable of near constant load thermal control over a range of nominally 10/1 peak to average heat loads. For high power, weight constrained applications with very high peak to average ratios, conventional radiator designs are of limited applicability.

Utilization of expendables for cooling imposes a fundamental limit on operation time. There is also a severe mass penalty associated with periodic testing. Koenig [2] and later Elliott [3] have suggested the use of a rotating balloon radiator concept to provide ultralightweight, large radiator surfaces. Since late 1983, a "collectible" expendable concept, also known as the expandable pulse power radiator has been investigated at the Air Force Aero Propulsion Laboratory. A description of the expandable pulse power radiator was given in [4]. Basically, in the "collectible" expendable concept, utilization of a coolant through flash evaporation is assumed as the technique to cool a high power density device. However, unlike the expendable coolant concept, the coolant vapor is collected in an expandable, variable surface area thin metallic or plastic radiator. The vapor is condensed within the radiator during an interpulse period, and the condensate is pumped back or brought back by other means to the coolant reservoir to be recycled.

In [4], it was identified that for very high peak to average heat loads, a low surface to volume inflatable bag or bellow radiator is a promising design by virtue of its large energy storage characteristic. The structure of the radiator is made of a low-density, thin flexible material that can be collapsed and stored in a compact form and can be expanded readily when high peak power heat loads are imposed. The bag

or bellow structure has a characteristically large volume to mass ratio. Hence, it can take in a large amount of vapor during the pulse period and reject waste heat through condensation and radiation during the interpulse period. This design results in a lightweight radiator which is very compact in the stowed position and can be protected easily from micrometeoroid damages except when in use.

In [4], two of the several important areas identified for further investigation are:

1. Flow through a pierced membrane into a vacuum environment, and,
2. Fluid recirculation schemes for various deployment and retraction mechanisms.

The first problem has been addressed under a different task and will be reported elsewhere. The second problem is the focus of the present study.

II. OBJECTIVE OF THE RESEARCH EFFORT:

The main objective of the present work was to investigate the different possible mechanisms for the deployment and retraction of the expandable radiator. The approach is to investigate all the possible methods to deploy and retract the radiator bag and all the liquid recirculation schemes. The merits and potential problems of each configuration will be discussed. The discussions will be based on one hypothetical duty cycle.

III. RESPONSE OF THE RADIATOR TO A DUTY CYCLE:

A typical power demand profile could include short periods of high power draw interspersed with much longer periods when power is needed only at

a low level. For a more detailed discussion of the power profile, the reader is referred to [1,4]. The following illustrative case is considered. An orbit altitude of 1000 km is assumed. This corresponds to an orbital period of 6300 seconds. It is assumed that high power is needed during about 1/6 of the orbital period or 1000 seconds. During these 1000 seconds, termed the "ground station" flyover period, a high peak power draw is needed for 5 seconds, followed by a low power level period of 95 seconds, and again followed by another 5-second draw of high peak power, and so on. Thus, during the flyover period, there will be a total of 10 pulses. The waste heat generation profile is similar to the power profile. For the rest of the orbital period, the power demand is very low. The expandable radiator can make use of this period, known as the rest period, to reject most of the waste heat generated and stored in the radiator.

The lumped model of a cylindrical bag described in [4] is used here. The input to the model is given in Table 1. The length of the 3-m diameter radiator versus time is shown in Figure 1. The maximum length of the radiator is 19.9 m, occurring at the end of the last pulse during the flyover period. It can be seen that, while the radiator retracts somewhat during the periods between pulses, most of the heat rejection occurs during the rest period. This long rest period is essential to the operation of the present expandable radiator. At the end of one orbital period, the length of the radiator is less than 0.04 m.

Some of the pertinent features of the above illustrative case are:

1. During the burst period, the radiator extends by about 2.6 m in a 5-second period, or at a rate of about 0.5 m/s. If the area of the vapor inlet is 1/4 of the radiator cross-sectional area, then the velocity of the vapor entering the radiator is about 2 m/s. Two points should be considered here. First, will the sudden inflow of vapor at about 2 m/s cause any instability to the radiator? Second, will the radiator over-expand and start an oscillatory behavior?

Table 1. Input to Dynamic Response Calculations

Temperature of radiator	373 K
Heat sink temperature	250 K
Emissivity of bag material	0.7
Peak load	$5MW_t$
Pulse duration	5 seconds
Period between pulses	95 seconds
Number of pulses	10
Diameter of the cylindrical bag	3 m
Orbital Period	6300 seconds
Flyover period	1000 seconds
Rest period	5300 seconds
Orbital altitude	1000 km

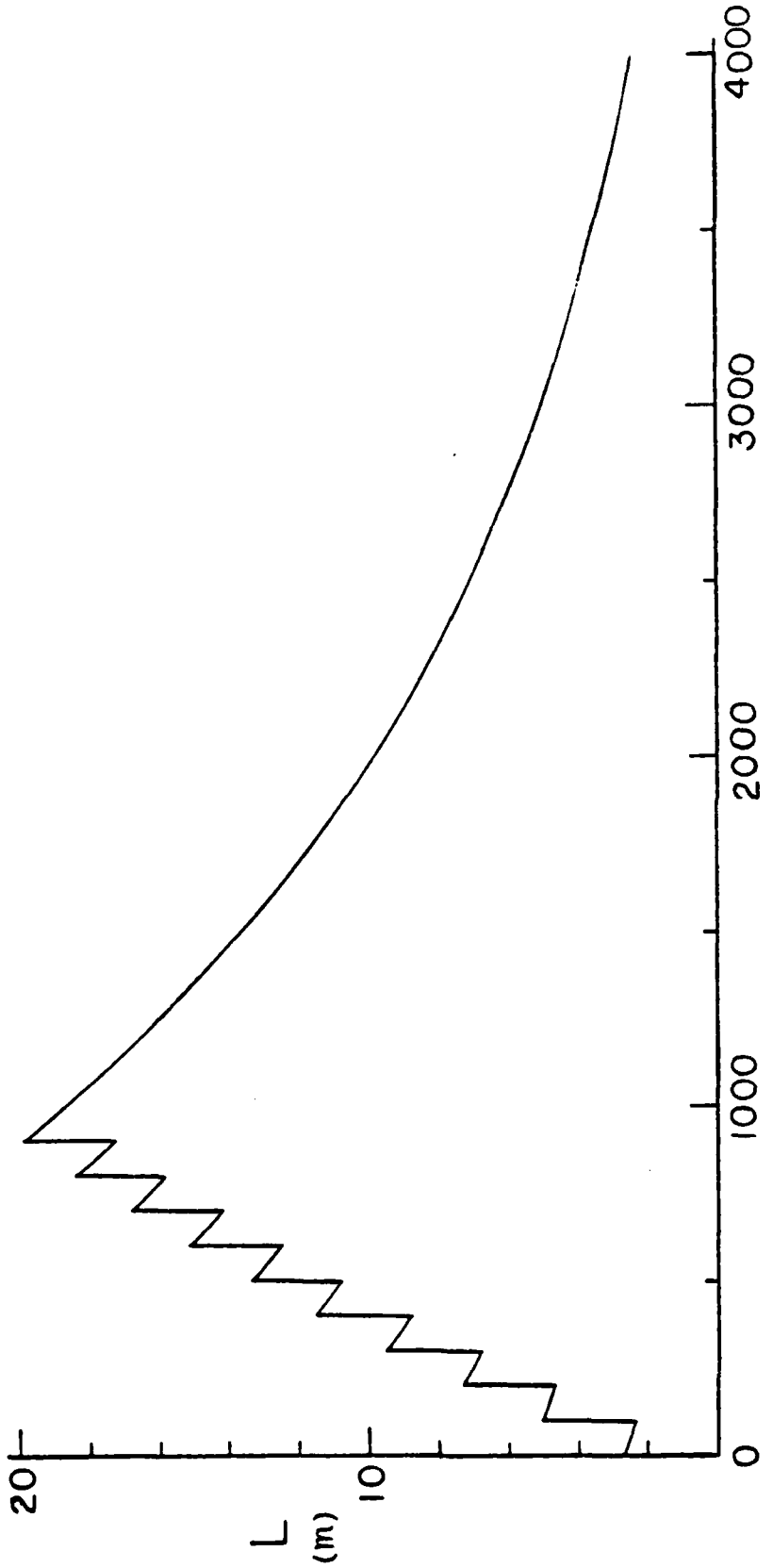

FIG. 1

2. The mass of the coolant needed to remove 5 MW_t of waste heat for 50 seconds through flash evaporation is about 111 kg. The volume of the coolant, if all condensed, is only 0.116 m^3. The volume of the radiator at the maximum length is about 141 m^3.
3. If the condensate return occurs during the entire orbital period, the average mass flow rate is only about 0.0176 kg/s. This means that the velocity of the liquid return can be very slow, resulting in very low pumping requirements.

IV. ROLL IN AND OUT OF RADIATOR BAG:

1. Drum Type - (see Figure 2) The radiator can be collapsed flat lengthwise and roll onto a drum. The roll drum has an electric motor for roll in and roll out. The electric motor is controlled by a pressure sensor located inside the radiator. It should be noted that the diameter of the drum when fully rolled in needs not be large. If L_m is the maximum length of the radiator and b is the thickness of the collapsed flat bag, then the diameter of the drum is approximately given by $(4bL_m/\pi)^{1/2}$. For example, if L_m=30 m and b=1 cm, then the diameter of the drum is about 0.6m.

2. Paper Lantern Type - (see Figures 3, 4 and 5) There are three methods to deploy and retract the radiator. The first method relies on a large helical tension spring made of spring steel attached to the cylindrical surface of the bag. During deployment, the internal pressure of the incoming vapor can extend the spring and push the bag outward. As the vapor condenses, the spring will pull the end of the bag towards the spacecraft. The key element in this first method is the design of a large helical spring (3 m in diameter) with a constant restoring force. The second method of retracting the bag is to use tethers to pull the end of the radiator toward the spacecraft. There can be 4, 8 or 12 tethers running lengthwise along the radiator. The tethers are fixed in the appropriate

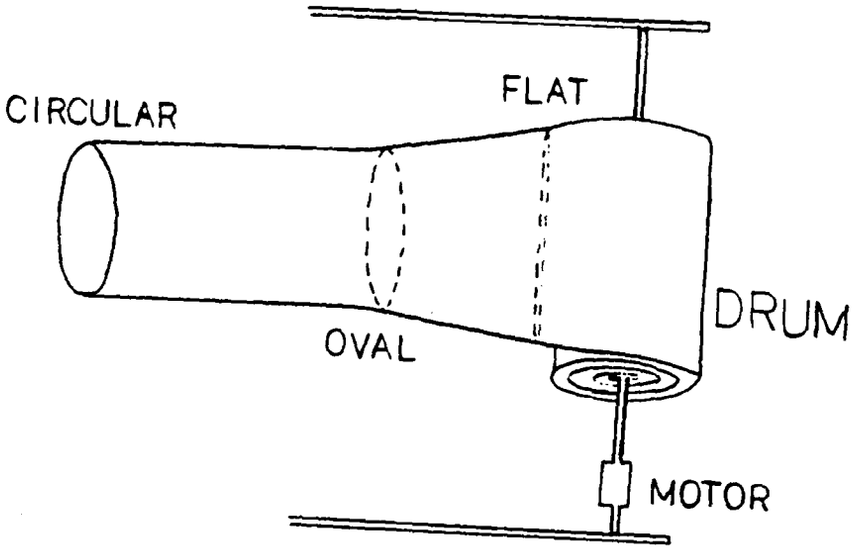

FIG. 2

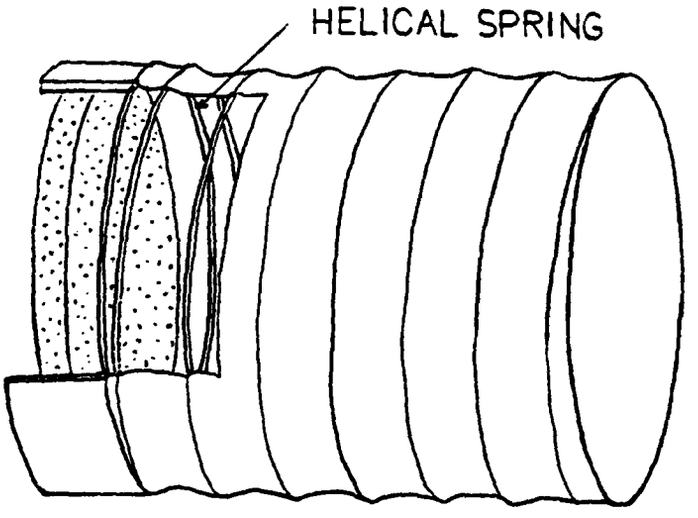

FIG. 3

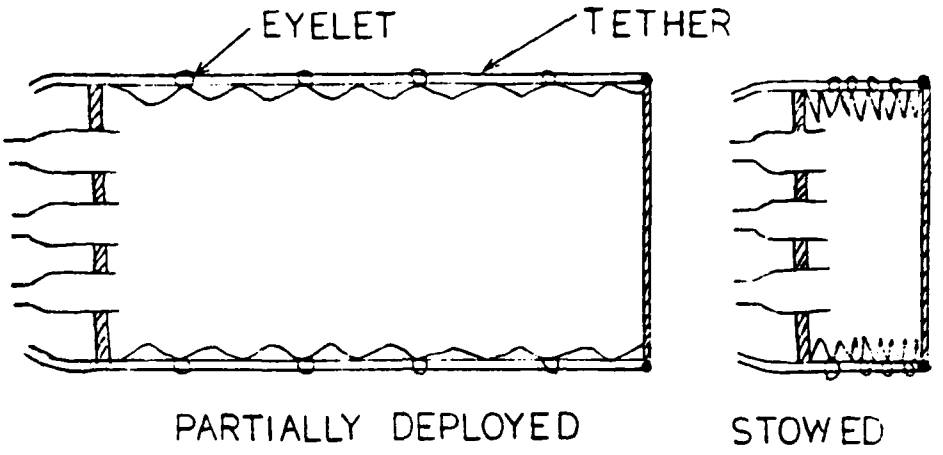
EYELET
TETHER
PARTIALLY DEPLOYED
STOWED

FIG. 4

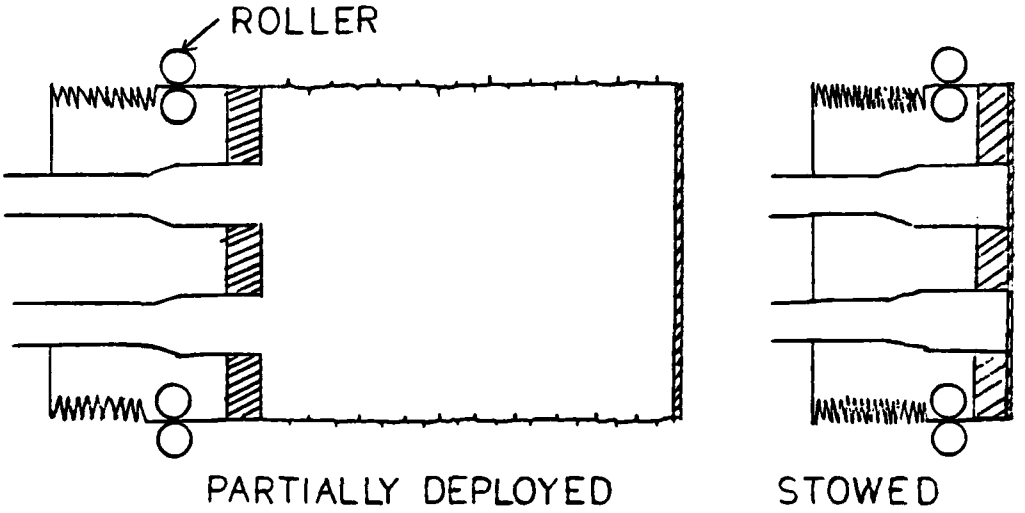
ROLLER
PARTIALLY DEPLOYED
STOWED

FIG. 5

locations by the eyelets. The roll in of the tethers can be pneumatically controlled based on the internal pressure of the radiator. It is possible to put some kind of a weak spring structure so that the collapse of the bag will be spread out more or less uniformly along the bag. The roll out of the radiator can be simply done by the internal pressure. The third method of retracting the bag is to use rollers. These rollers can also be pneumatically controlled. However, the manner in which the bag is collapsed is different compared to the second method. In the second method, the collapse can occur anywhere along the radiator whereas, in the third method, the collapse will only occur at the base of the radiator.

3. Sock Type - (see Figure 6) The bag can be rolled up lengthwise on its circumference just like a sock. The roll up can be done externally (see Figure 6) or internally. The external rollup requires the bag material to be slightly stretchable, whereas the internal rollup can cause some wrinkles on the bag material. Several pairs of rollers located around the circumference of the bag will be needed to roll up the bag.

V. CONDENSATE RETURN MECHANISMS:

The key element of the present "collectible" expendable concept is to capture and condense the vapor and return the condensate to the coolant reservoir to be reused. There are several ways for the condensate return:

1. Wiper - (see Figure 7) The vapor condenses on the inside surface of the bag. Except when the condensate layer is thick, the liquid tends to stick on the wall due to surface tension. The wiper is mechanically controlled by using a tether. The tether runs from the base of the bag to the far end of the bag and back after going around

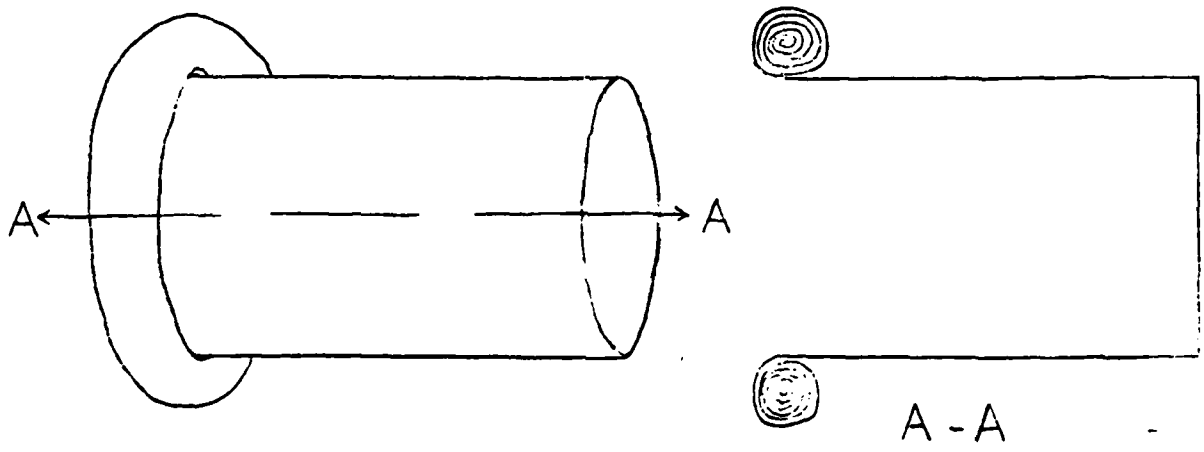

FIG. 6

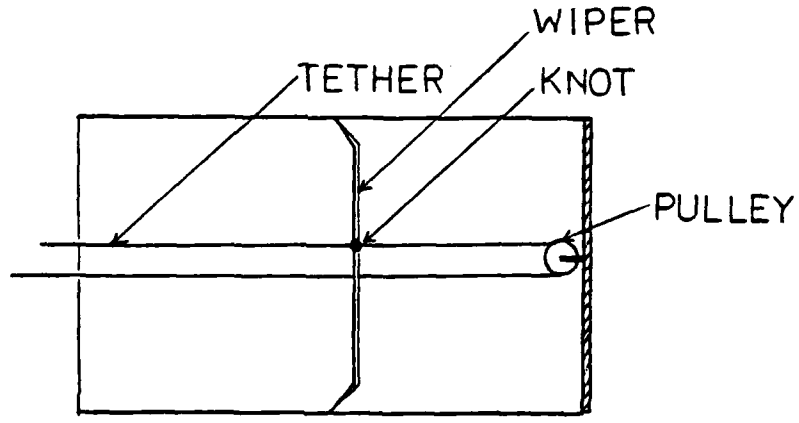

FIG. 7

a pulley. The wiper should have several holes large enough so that the vapor can flow freely as the wiper moves in and out. Also, the edge of the wiper should be designed such that the wiper can sweep the condensate layer only if the wiper is being pulled in towards the base of the radiator. The condensate accumulated at the base of the radiator can be removed by an aspiration pump or a positive displacement pump with a dry guard switch which allows the pump to function only if the tube leading to the pump is primed.

2. Liquid Channel - The bag has small holes or slits on its wall so that the condensate can flow through the holes or slits to the liquid return channels. The bag material should also have a capillary structure to lead the condensate to the holes or slits. The liquid return channels can be made of rigid tubes or collapsible tubes and they can run lengthwise on the wall or spiral around the bag. The choice depends on how the bag is rolled up. For example, the collapsible tubes should be used if the drum type bag rollup is used (see Figure 2). However, if the paper lantern type with tether is used (see Figure 4), one can use eight rigid tubes and have them spiral around the bag wall in a helical manner (see Figure 8). In this case, the tubes should be 45 degrees out of phase. The tubes can also act as weak springs to achieve more uniform foldings as the tethers are pulled in. In any of the above choices, the liquid channels can be located inside or outside the bag wall. Finally, at the base of the radiator, all the liquid return channels can be connected to an aspiration pump or a positive dispacement pump for liquid removal.

3. Rotating Bag - (see Figure 9) This requires a bag that has a slight taper. The key idea is to use the component of the centrifugal acceleration along the bag wall to provide the necessary body force for the liquid return. This concept is very similar to the rotating heat pipe [5]. It can be shown that in order to provide sufficient body force for the liquid return, the bag needs only to rotate at a

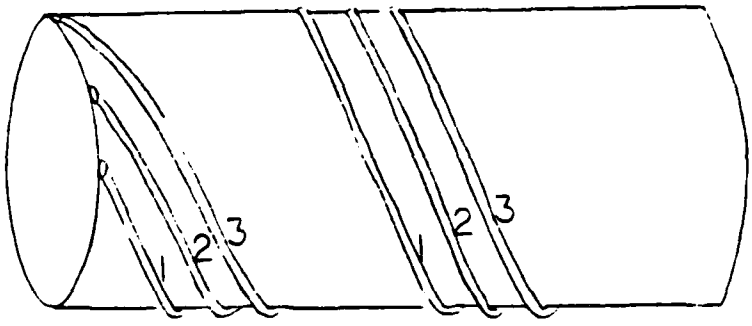

ONLY 3 OF 8 TUBES SHOWN

FIG. 8

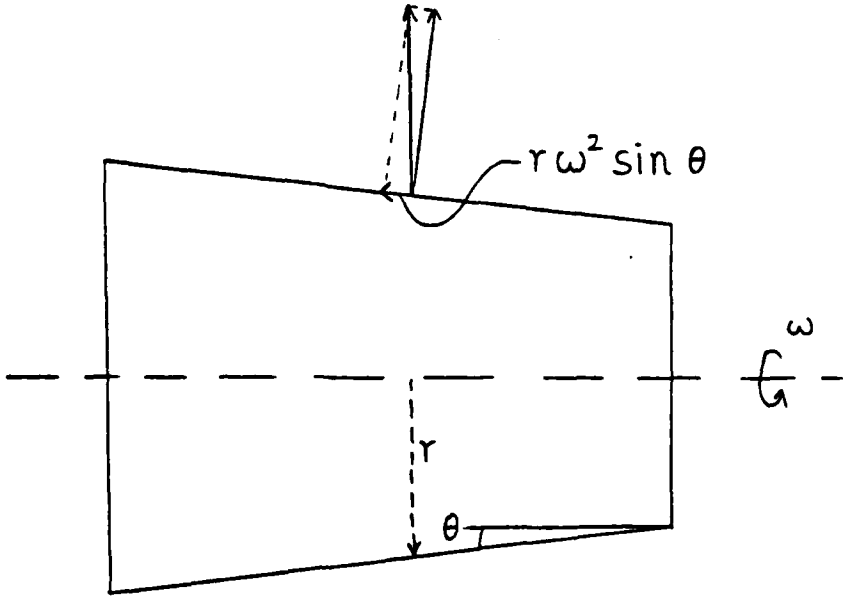

FIG. 9

few rpm (see Appendix A).

4. This fourth method merely requires the bag to be rolled in almost completely after it has reached its maximum length. It is shown in Appendix B that for a radiator with an initial length of 20 m, the average thickness of the condensate film is less than 1 cm even after the radiator has retracted to a length of 1 m. A pump can be used to remove the condensate at this point. By requiring the bag to roll in eliminates the complications of the previous three liquid recirculation schemes. It should be noted that the near complete roll in of a bag is not a stringent requirement. If additional vapor is generated before the bag is rolled in, the vapor can simply directed to a second bag.

VI. MISCELLANEOUS CONSIDERATIONS:

1. Flow Unsteadiness - As described in Section III, during the burst mode, the vapor enters the bag with a velocity of 2 m/s. The sudden inflow of vapor may cause an acoustic pressure disturbance of the order of 400 N/m^2. It is not likely that this low acoustic pressure disturbance will trigger any type of instabilities of the radiator. However, the bulk movement of the radiator caused by the inflow of vapor may cause the radiator to overexpand and oscillate.

2. Condensation Instabilities - The condensation process inside the radiator is very quiet and slow because it is heat transfer limited. No waterhammer events are expected to occur. The types of condensation instabilities such as those occurred in the capillary pumped loop or complete condensation of a vapor inside a tube are not applicable here [6].

3. Kelvin-Helmholtz Instabilities - The condensate first forms on the wall of the radiator and will remain there. This is because the

Weber number (based on the film thickness and the interfacial velocity) is much less than unity. The liquid-vapor interface should be stable except when a wiper is used for condensate removal. In this case, the liquid on the wall may be sheared away if the wiper is not kept at a very low velocity.

4. Liquid Return Channels - At the slits where the condensate enters the liquid return channels, it may be desirable to put a wick material at the slits so that only the liquid, but not the vapor can enter the liquid return channels. If the pressure inside the liquid return channels is less than about 1000 N/m^2 lower than the pressure of the vapor inside the radiator, the vapor cannot break the liquid-vapor interfaces at the wick and enter the channels. The liquid return channels can be self-primed because they have a smaller effective radius of curvature than the radiator.

VII. RECOMMENDATIONS:

Based on the findings of the present efforts, the following tasks are recommended:

1. To select the most promising radiator configuration and to perform the design work on the deployment and retraction of the radiator and the fluid recirculation scheme. It is possible that this task may require some simple heat transfer and fluid flow experiments to be performed.

2. To interact with the structural design experts and to jointly build a prototype radiator. The essential elements needed to be considered are material selection and structural stabilities during deployment and retraction of the radiator.

ACKNOWLEDGEMENTS

The author would like to thank the Air Force Office of Scientific Research and the Universal Energy Systems, Inc. for providing him with the opportunity to spend a very worthwhile and interesting summer at the Air Force Aero Propulsion Laboratory. Many of the ideas described here are based on discussions with many individuals, namely, Dr. J.E. Beam, Dr. E.T. Mahefkey, Mr. R. Ponnappan, Mr. J.H. Ambrose and Mr. D.E. Tilton. Their contributions are sincerely appreciated.

REFERENCES

1. Mahefkey, E.T., "Military Spacecraft Thermal Management: The Evolving Requirements and Challenges," AIAA Progress in Astronautics and Aeronautics, Vol. 86, edited by P.E. Bauer and H.E. Collicott, 1983.

2. Prenger, F.C., and J.A. Sullivan, "Conceptual Designs for 100-Megawatt Space Radiators," Proceedings of a Symposium, Advanced Compact Reactors Systems, National Academy of Sciences, Washington, D.C., November 15-17, 1982.

3. Elliott, D.G., "External Flow Radiators for Reduced Space Powerplant Temperature," 1st Symposium on Space Nuclear Power Systems, University of New Mexico, Albuquerque, New Mexico, January 11-13, 1984.

4. Chow, L.C., E.T. Mahefkey, and J.E. Yokajty, "Low Temperature Expandable Megawatt Pulse Power Radiator," AIAA 20th Thermophysics Conference, Williamsburg, Virginia, June 19-21, 1985, AIAA Paper No. 85-1078.

5. Gray, V.H., "The Rotating Heat Pipe: A Wickless Hollow Shaft for

Transporting High Heat Fluxes," ASME Paper No. 69-HT-19, 1969.

6. Bhatt, B.C., and G.L. Wedekind, "Transient and Frequency Response Characteristics of Two Phase Condensing Flows: With and Without Compressibility," Journal of Heat Transfer, Vol. 102, pp. 495-500, 1980.

Appendix A

Consider a rotating bag with a taper angle of θ (see Figure 9), the component of the acceleration along the wall of the radiator is $r\omega^2 \sin\theta$ We will assume the radiator has an initial length of L_o and the length is decreasing as the vapor condenses inside the radiator. Let x be measured from the far end of the radiator. We will choose r(x) such that the film thickness δ is only a function of x. This quasi-steady situation is obtained if the condensate is removed as fast as the condensation rate at a given x location. *If* δ is small compared to the radius of the radiator, it can be shown that, for small θ , the condensate mass flow rate at a given x location is given by:

$$\dot{m} = \frac{2\pi\rho r^2 \omega^2 \sin\theta\ \delta^3}{3\nu} \qquad (A-1)$$

This is also equal to

$$\dot{m} = \frac{q_{rad}\, A}{h_{fg}} \qquad (A-2)$$

where A(x) is the area of the exposed radiator from x=0 to x. A rough estimate will show that to provide sufficient body force for the liquid return, the bag needs only to rotate at a few rpm.

Appendix B

From the lumped model of [4], it can be shown that the length of the radiator is given by

$$L = C e^{-\beta t} - \frac{D}{4} \qquad (B-1)$$

where

$$\beta = \frac{4 \varepsilon \sigma (T^4 - T_s^4)}{D \rho_v h_{fg}} \qquad (B-2)$$

If the initial length of the radiator is L_o, then

$$L = (L_o + \frac{D}{4}) e^{-\beta t} - \frac{D}{4} \qquad (B-3)$$

The volume of the condensate is given by

$$VOL = (L_o - L) \frac{\pi D^2}{4} \frac{\nu_f}{\nu_g} \qquad (B-4)$$

and the average film thickness δ is given by

$$\delta = \frac{D}{4} \frac{\nu_f}{\nu_g} \left(\frac{L_o}{L} - 1 \right)$$

If L_o= 20 m, D= 3 m, and for the same situation as listed in Table 1, L, V and are plotted versus t in Figure B-1.

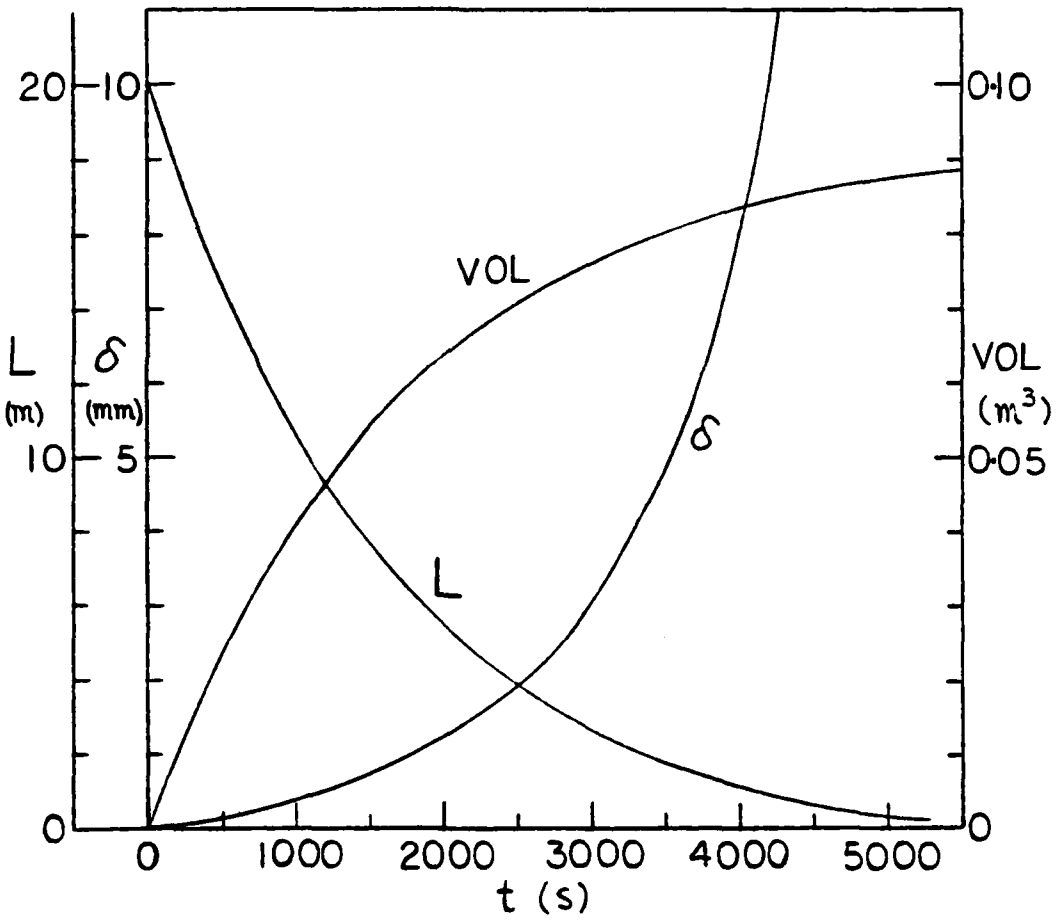
20
10
0·10
VOL
L
(m)
δ
(mm)
VOL
(m³)
10
5
0·05
L
δ
0
0
0
1000
2000
3000
4000
5000
t (s)

FIG. B1

1985 USAF-UES SUMMER FACULTY RESEARCH PROGRAM/

GRADUATE STUDENT SUMMER SUPPORT PROGRAM

Sponsored by the

AIR FORCE OFFICE OF SCIENTIFIC RESEARCH

Conducted by the

UNIVERSAL ENERGY SYSTEMS, INC.

FINAL REPORT

APPLICATIONS OF INTERNAL REFLECTION SPECTROSCOPY TO THE CHARACTERIZATION OF THERMOSET POLYMERS

Prepared by:	Derald Chriss
Academic Rank:	Assistant Professor
Department and	Department of Chemistry
University:	Southern University
Research Location:	Wright-Patterson AFB, Materials Laboratory, Polymer Branch, Properties Group
USAF Research:	Dr. Ivan J. Goldfarb
Date:	August 26, 1985
Contract No:	F49620-85-C-0013

Applications of Internal Reflection Spectroscopy to the Characterization of Thermoset Polymers

by

Derald Chriss

ABSTRACT

Internal reflection spectroscopy has been explored as an additional means of characterizing thermoset polymers. The results indicate that internal reflection spectroscopy (also known as attenuated total reflection (ATR)), is an important means of analysis. ATR is especially critical when the thermoset polymers are highly absorbing thin films, or when they are obtained in rigid and bulky forms (cases where ordinary transmission spectra are not useful).

Specimens obtained and analyzed were an acetylene terminated sulfone (ATS), a meta-acetylene terminated bisphenol A (MATB), polybisthiazole (PBT), and a thermoset polyimide LARC-TPI). Samples were in the form of thin films, powders, fibers and rigid bars. Spectra obtained via ATR, show close resemblance to transmission spectra, which allows for a comparative study. Finally, the results indicate that ATR enables one to incorporate IR as an additional characterizing method.

I. Introduction

Analysis via infrared spectroscopy has been proven as a very valuable tool, for not only chemists, but other scientist as well. In a number of instances, infrared analysis represents one of the quickest and simplest means of identifying major functional groups present within a sample. In addition, a vast number of infrared spectra have been compiled for quick comparison.[1,2]

Characterization of compounds involves analysis by as many different techniques as possible. Infrared analysis, plays an important role in characterization, when suitable samples can be obtained. Suitable samples are described as those which could be obtained in the form of thin films, those which may be dissolved in a suitable solvent, or those which could be ground into very small particles, from which mulls or transparent discs could be prepared. However, samples obtained in this laboratory often do not lend themselves to these conventional forms of infrared analysis. In addition, it is not possible to analyze these samples in their natural states via these conventional infrared techniques.

The materials obtained in this laboratory, are usually thick and bulky and are, for the most part, very rigid. These

polymer samples do not readily lend themselves to one of the conventional IR techniques stated above. However, infrared analysis of these polymeric materials is now possible on site, due to the acquisition of internal reflection spectroscopic (or attenuated total reflection (ATR)) capabilities. ATR spectra can be conveniently obtained via an accessory attachment provided by most infrared spectrometer manufacturers.[3]

Considering my past experiences in spectroscopic analysis and characterization studies, it was decided that I should be a good candidate to implement and illustrate the usefulness of ATR as an aid in the characterization of the polymeric materials obtained at this research location. The major thrust of this project involves the use of ATR in the analysis of a rigid class of thermoset polymers which have been completely cured and postcured. In addition, samples in the form of thin films were obtained and ATR as well as transmission spectra were obtained for comparison purposes. For illustrative purposes, samples of powders, fibers, thin films, and rigid bars were obtained, from other researchers, for analysis.

Specifically, the thermoset samples studied are acetylene terminated oligomers. They are being considered by the Air Force for use in high temperature adhesives and composites.

II. Objectives of the Research Effort

The major objective of this research effort was to implement and illustrate the usefulness of internal reflection spectroscopy as it applies to the characterization of thermoset polymers. Internal reflection spectroscopy represents the means by which a specific class of acetylene terminated thermoset polymers may be analyzed via infrared spectroscopy. It is also an objective to show that ATR allows for the spectroscopic analysis of powders, fibers and other (rigid) samples, all in their natural states.

The first phase involved the set up of the ATR attachment. This included analysis of a series of test samples which could be readily compared to the literature. The second phase involved the analysis of the acetylene terminated oligomers and the various other types of materials obtained on site. Included in this phase was the preparation of samples, particularly the surfaces. Also specific techniques were used for powders and fiber samples. The third phase involved the actual analysis.

The future applications of this project will include the ability to follow the different states of cure of the resins via ATR. Time did not allow for this phase to be accomplished.

III. Experimental

Curing Procedure for Acetylene Terminated Sulfone (ATS)

Specimens prepared consisted of 4-20mL bars, 4-40mL bars and 8-20mL dogbone samples. The sample was placed in a vacuum oven (13.5g in an aluminum pan) and degassed at 100°C for one hour. The sample of ATS was then poured into pre-cleaned silicon rubber molds, and held for an additional hour at 100°C. Oven temperature was then increased to 140°C and this temperature was held for 10 hours. Samples were then allowed to cool to room temperature before postcure. The postcure procedure consisted of heating the specimens to 250°C and holding this temperature for 4 hours, then allowing cooling to room temperature. (The ATS was obtained from Gulf)

Curing Procedure for Meta-Acetylene Terminated Bisphenol A (MATB)

Specimens prepared were the same as for ATS. The weighed sample (13.0g) was placed in a vacuum oven and degassed at 80°C for 1 hour, poured into silicon rubber molds and held at 80°C for an additional hour. The temperature was then increased to 140°C and this temperature held for 15 hours. The temperature was then increased to 170°C and held for five hours. Samples were then allowed to cool to room temperature before postcure. Postcure consisted of heating to 250°C for four hours then

cooling to room temperature. (The MATB was obtained from Fluorochem Inc.)

Surface Preparations

For samples obtained in the form of thin films, the only preparation was to cut the films to the dimensions of the reflecting crystal (50mm by 9mm). Films studied were LARC-TPI a polyimide (Mitsui Toatsu Chemicals Inc.), and Polybisthiazole (PBT), obtained from Celanese.

For bar samples, the specimens were cut to the crystal dimensions and then subjected to a three stage grinding and polishing sequence. The sequence consisted of grinding one surface with Carbimet 180 grit abrasive discs followed by additional grinding with Carbimet 400 grit abrasive discs. Polishing of the surfaces was accomplished by using 0.3 micron alumina oxide (Buehler) and buffing with a felt pad. The samples of this form were ATS and MATB.

Powdered samples (fine) were simply prepared by dipping the reflecting crystal in the powder. In the case of a powdered sample which is not finely ground, briquettes should be made (using 5,000 to 8,000 psi of pressure).

Fiber samples were obtained but the procedure used did not allow good ATR spectra to be obtained.

IV. Results and Discussion

All spectra were obtained via a Beckman FT 1100 FTIR system. The ATR accessory used was a Barnes Model 300 (continuously variable) along with a 50mm by 9mm by 3mm parallelopiped KRS5 crystal as the internal reflecting element. The resolution setting was 4 cm^{-1} for each spectrum. Table 1 shows the respective angles of incidence used in each case. As can be seen from the spectra obtained (Figures 1 thru 7), bands above 2000 cm^{-1} are not shown (a characteristic of ATR). Another characteristic of ATR is the broadening of bands at the longer wavelengths[3]. There may also be slight shifting of bands at the longer wavelengths.

Figures 1 and 2 illustrate an important advantage of ATR. Figure 1 shows that LARC-TPI is a strongly absorbing medium and therefore transmission spectra do not yield useful information, whereas the ATR spectrum (Fig. 2), allows one to gather useful information for analysis. Of particular interest is the imide band at 1375 cm^{-1}. Using ATR, it is possible to follow the degree to which imidization has occured in both the film and powdered samples (Fig. 3). Fig. 3 also illustrates the ease with which powdered samples may be analyzed via ATR.

Figures 4 and 5 illustrate the close resemblances of ATR and transmission spectra. Both spectra were of a PBT film.

Table I: Spectral Acquisition Information

Name	Form	Type Spectrum	Angle of Incidence
LARC-TPI	Film	Transmission	--
LARC-TPI	Film	ATR	47°
LARC-TPI	Powder	ATR	49°
PBT	Film	Transmission	--
PBT	Film	ATR	49°
ATS	Bar	ATR	51°
MATB	Bar	ATR	49°

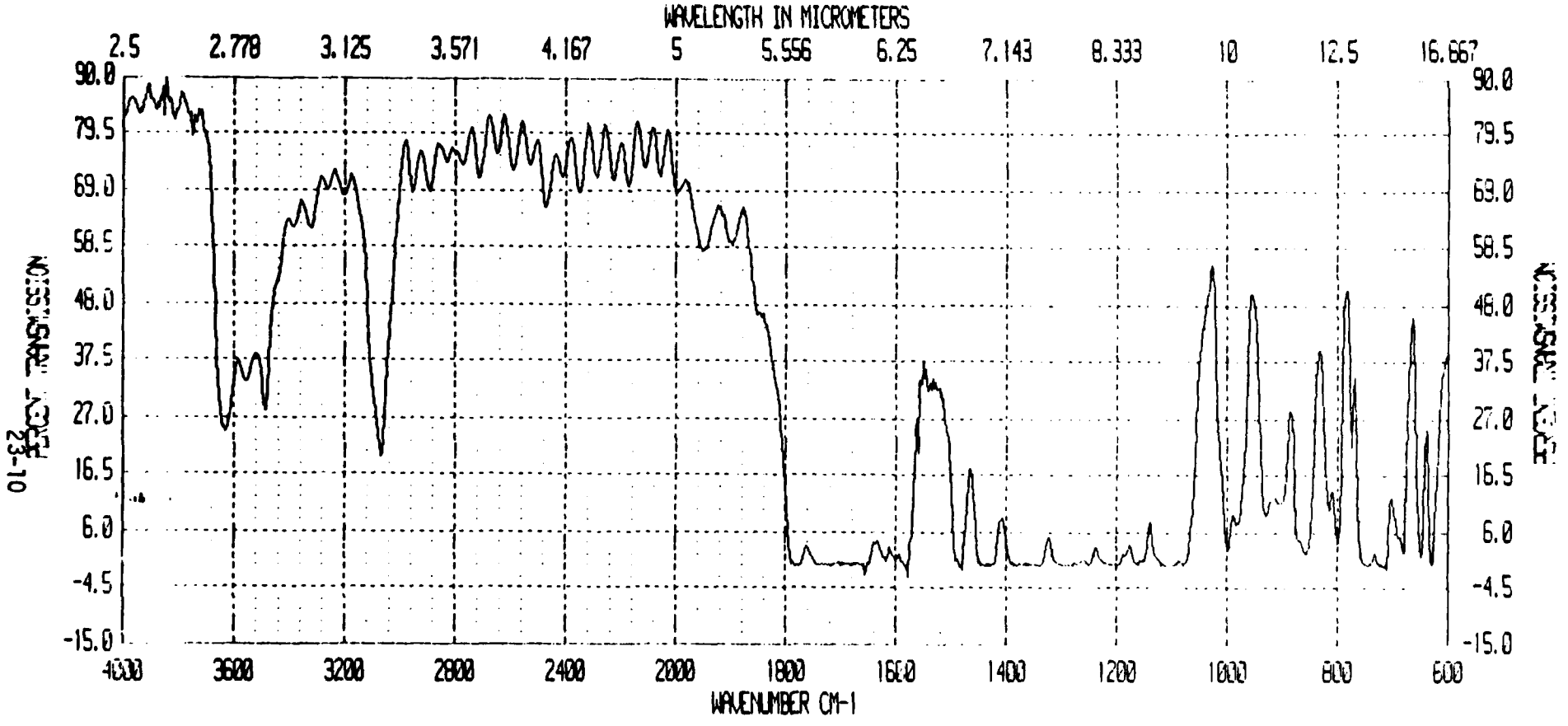

Figure 1: Transmission Spectrum of LARC-TPI Film

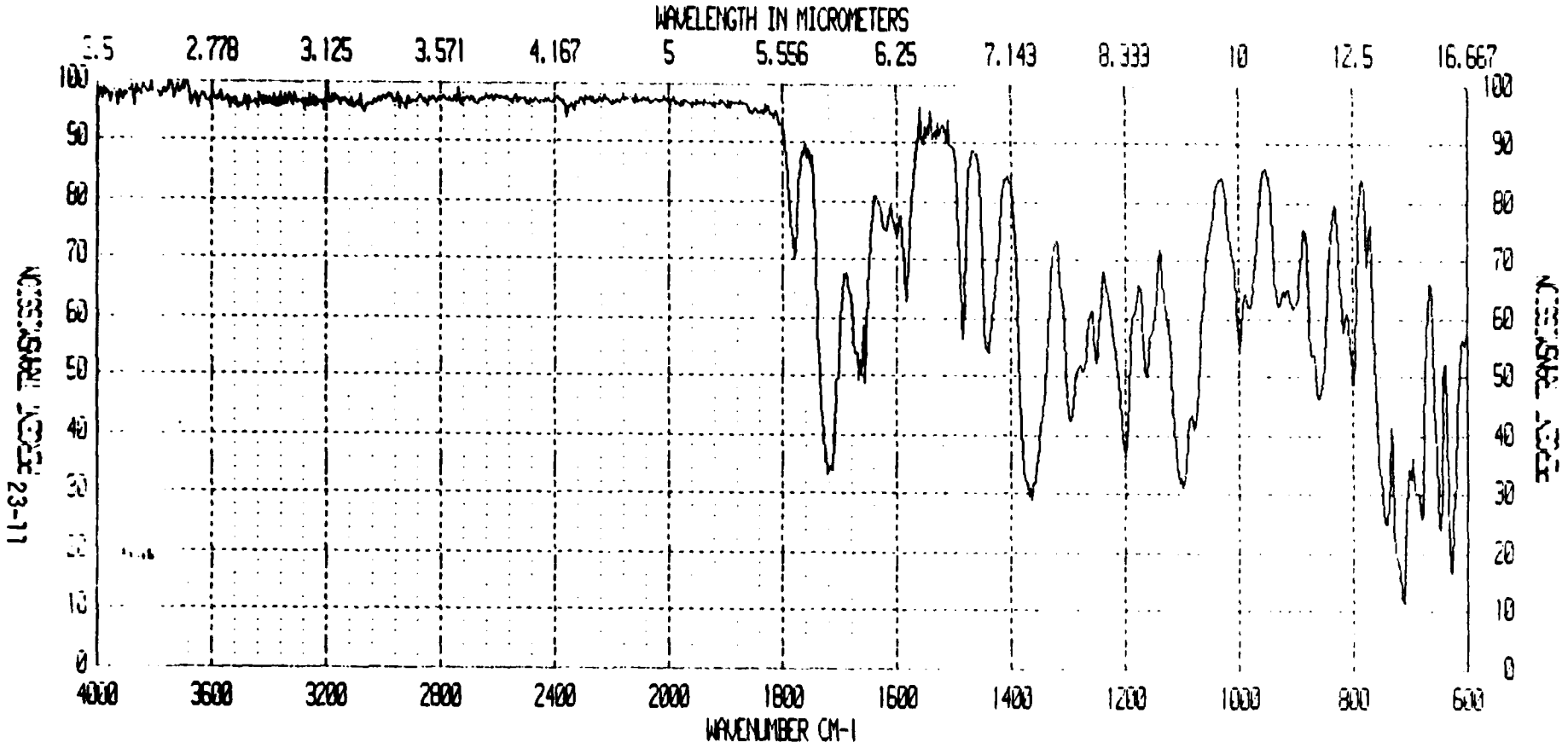

Figure 2: ATR Spectrum of LARC-TPI Film

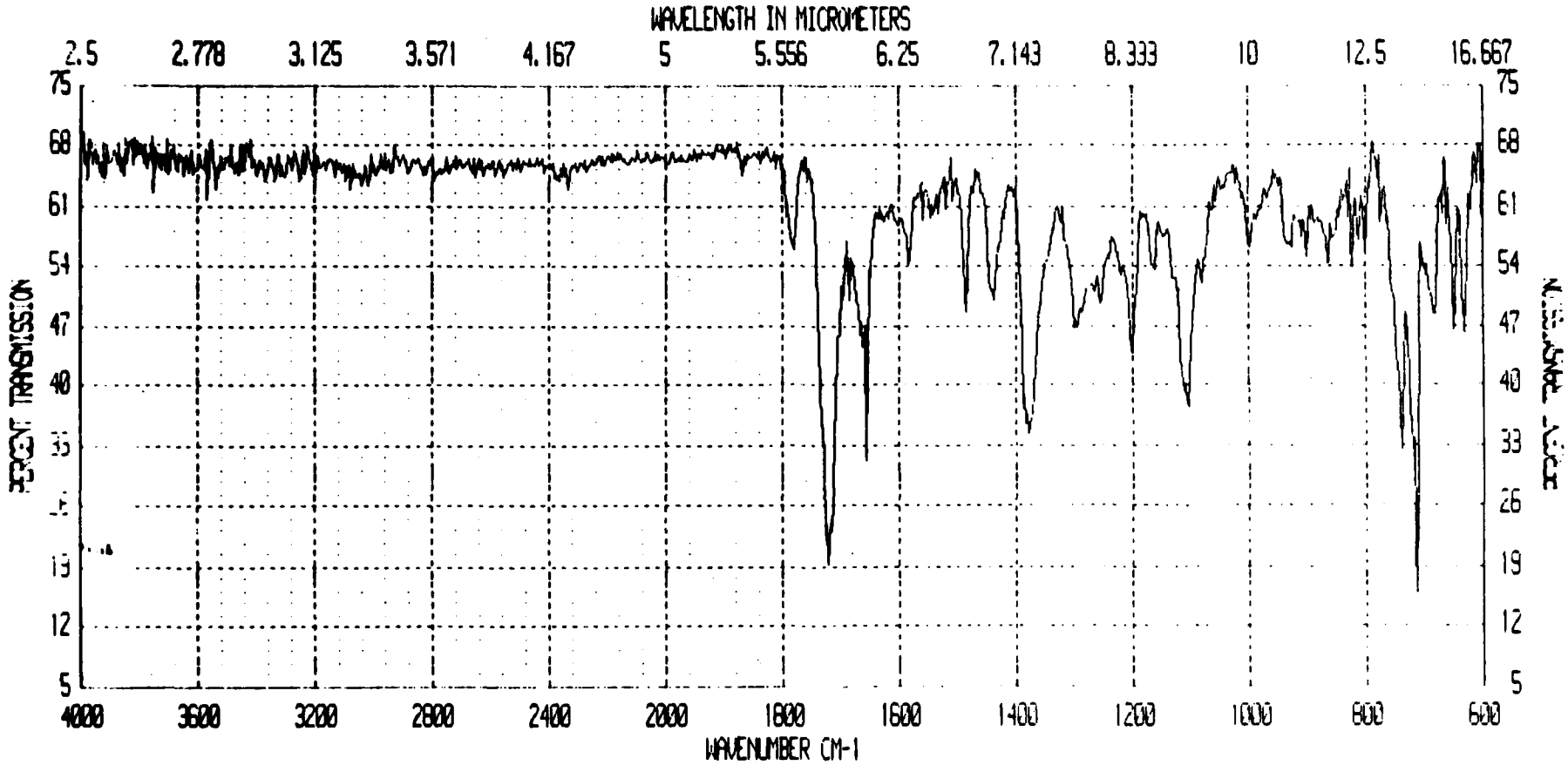

Figure 3: ATR Spectrum of LARC-TPI Powder

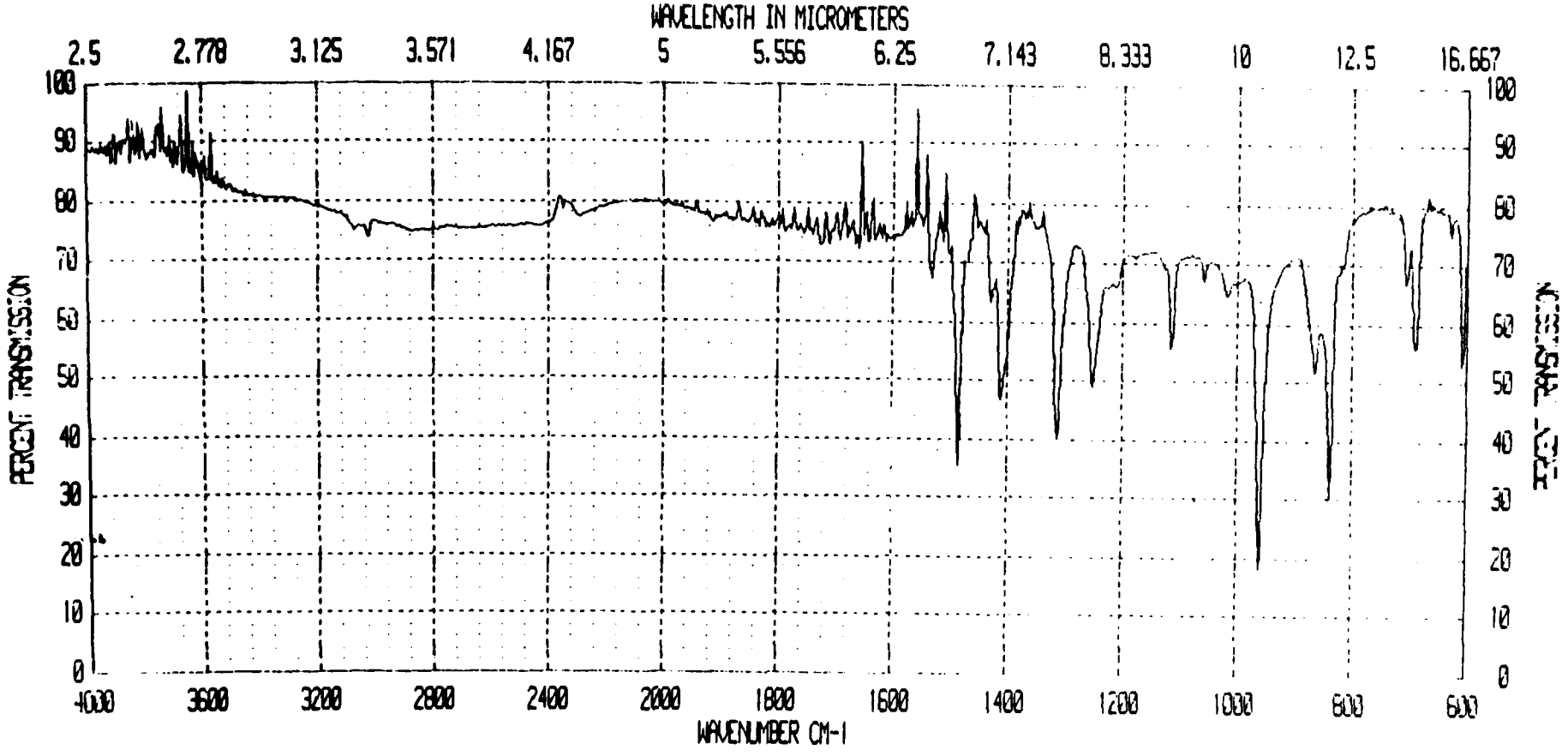

Figure 4: Transmission Spectrum of PBT

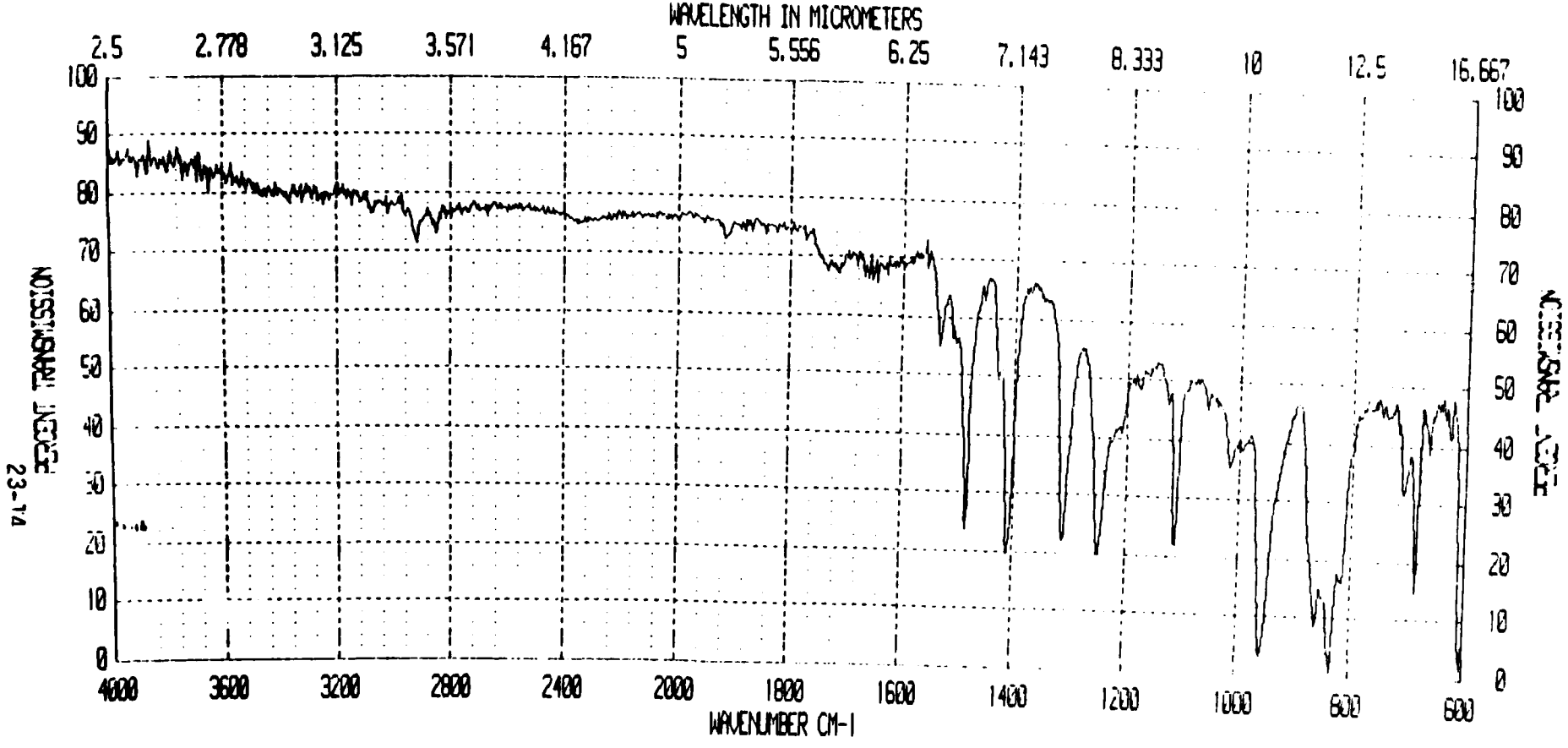

Figure 5: ATR Spectrum of PBT

The bands at about 1535(w) and 1490(s) cm^{-1} are characteristic of a thiazole system. These spectra particularly illustrate the similarities of ATR and transmission spectra in the IR fingerprint region.

The ATR spectra of ATS (Fig. 6), clearly reveals bands at 1146 and 1103 cm^{-1} which are attributed to the SO_2 stretching frequencies of sulfones. Other distinguishable bands and their assignments are at 1573cm^{-1}(ring stretching), 1229 cm^{-1} (phenol C-O-C stretch), 830 cm^{-1} (S-O-C stretch) and at 555 cm^{-1} (SO_2 scissoring). In addition, the band at 697 cm^{-1} is attributed to the C-H bending for monosubstituted terminal acetylenes, is also revealed.

Revealed in the ATR spectrum of MATB (Fig. 7), are the ring and stretching frequencies at 1503 and 1214 cm^{-1} respectively and the C-H bending frequency of monosubstituted terminal acetylenes at 692 cm^{-1} . Also distinguishable is the sharp band at 1167 cm^{-1} which is attributed to $C(CH_3)_2$ stretching.

V. Conclusions

It is hoped that these results illustrate the usefulness of internal reflection spectroscopy as it applies to the characterization of thermoset polymers. However, one must be cautious in making band assignments due to the slight differences obser-

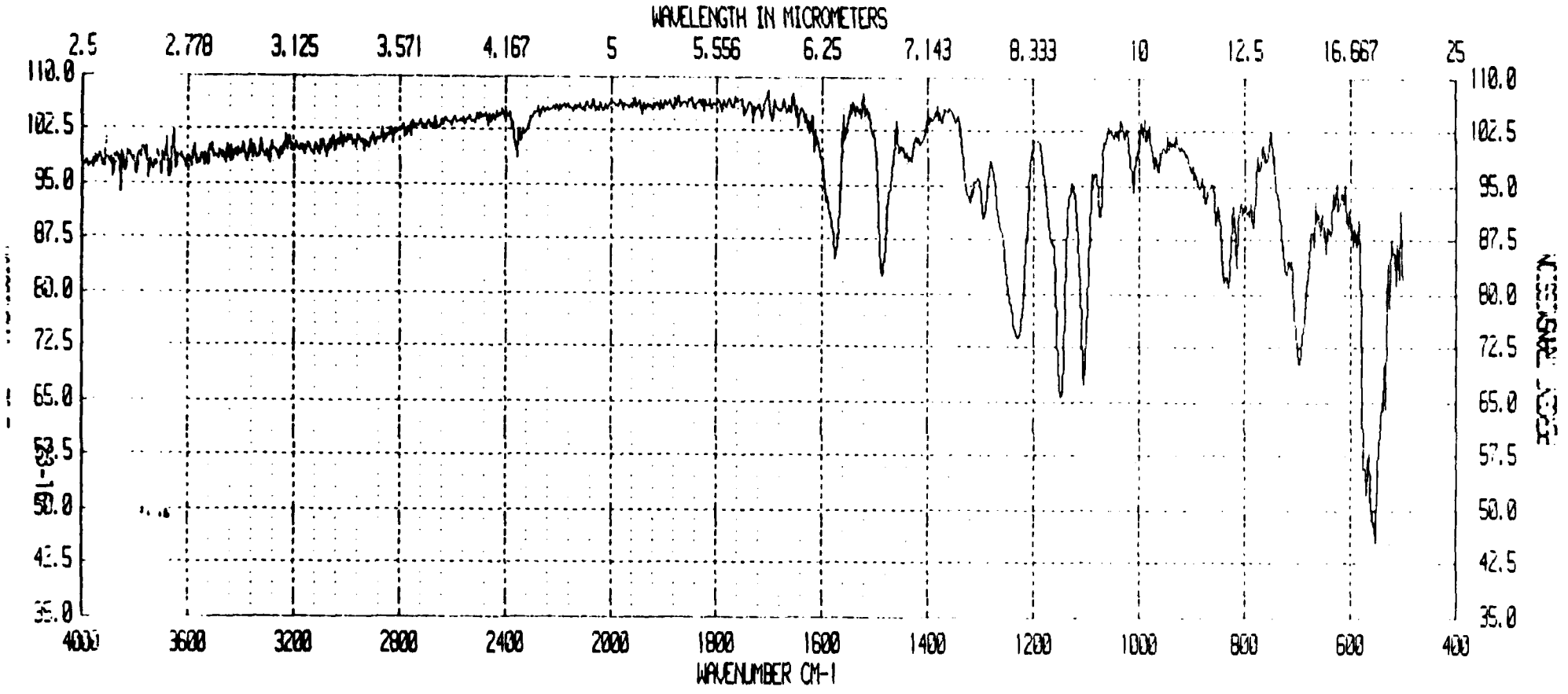

Figure 6: ATR Spectrum of ATS

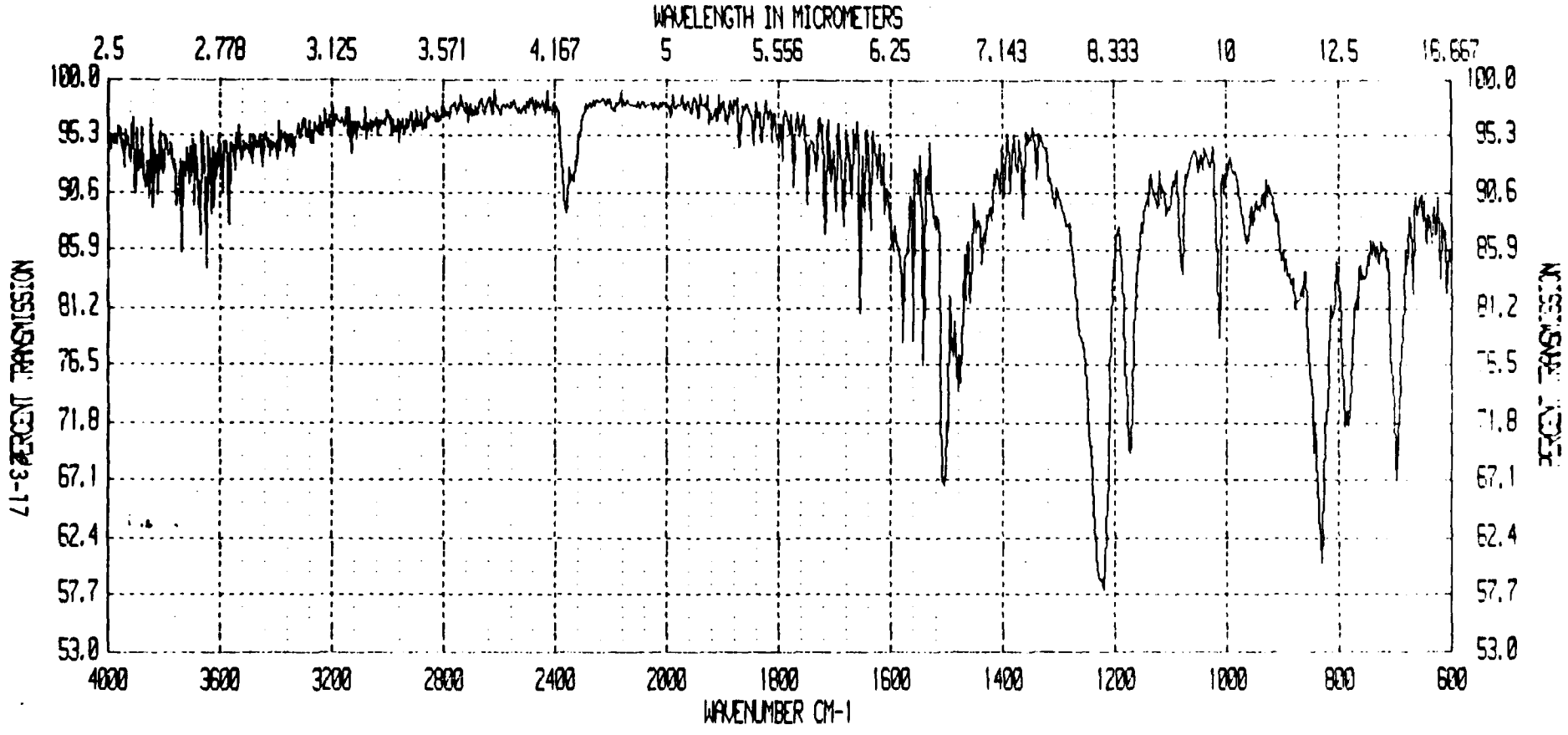

Figure 7: ATR Spectrum of MATB

ved using ATR. Presently, numerous researchers are using ATR for analysis and hopefully in the near future, vast libraries of ATR spectra will be compiled and become available for comparison.

VI. Recommendations

It is recommended that top priority be assigned to the preparation of fibers to be analyzed via ATR. Careful and tight wrapping of the fiber around the reflecting crystal should be sufficient. It is important that good contact between the crystal and the fiber surface be maintained over as much of the crystal surface as possible. Any powders which are used (which are not finely ground) should be thoroughly ground before being used. This is to prevent possible scratching of the crystal's surfaces.

In order to follow the curing of a polymer, it will be necessary to obtain samples which have undergone various curing stages. The spectra of these different specimens should have distinct characteristics in the infrared region. This would allow for the comparison between the different stages of the curing and the final cured product. One of the distinct differences, which should be observed, should be the presence of monomer units as well as the higher weight oligomers during the initial stages of cure. This may also show up in terms of bands

AD-A166 176 UNITED STATES AIR FORCE SUMMER FACULTY RESEARCH PROGRAM 87/13
1985 TECHNICAL RE (U)UUNIVERSAL ENERGY SYSTEMS INC
DAYTON OH R C DARRAH ET AL. DEC 85 AFOSR-TR-86-0139
UNCLASSIFIED F49620-85-C-0013 F/G 5/9 NL

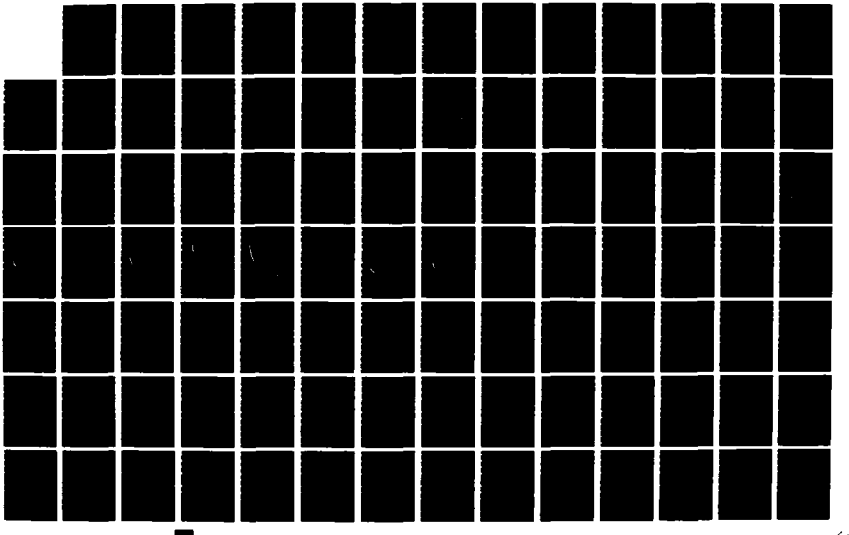

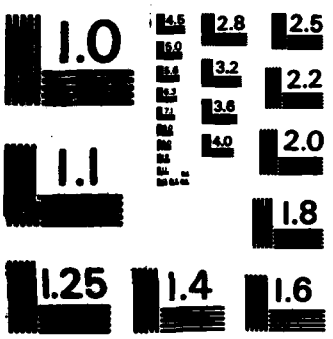

MICROCOPY RESOLUTION TEST CHART
NATIONAL BUREAU OF STANDARDS - 1963 - A

(hopefully sharp), which may be shifted or bands which may increase or decrease or both. However this will have to be determined by future analysis.

Acknowledgments

Sincere appreciation is expressed to the Air Force Office of Scientific Research and the Air Force Systems Command for sponsoring this work. In addition the author wishes to thank Dr. Ivan J. Goldfarb and all the other employees of the Polymer Branch of the Materials Laboratory at Wright-Patterson Air Force Base, for their valuable assistance in this project.

References

1. Sadtler Standard Infrared Prism Spectra, 1972
2. Pouchert, C.J., The Aldrich Library of Infrared Spectra, 2nd Ed, Aldrich Chemical Co., (1975)
3. Harrick, N.J., Internal Reflection Spectroscopy, Harrick Scientific Corp., Ossining, NY, (1979)
4. Henniker, J.C., Infrared Spectra of Industrial Polymers, Academic Press, New York, (1967), p.89

1985 USAF-UES SUMMER FACULTY RESEARCH PROGRAM/

GRADUATE STUDENT SUMMER SUPPORT PROGRAM

Sponsored by the

AIR FORCE OFFICE OF SCIENTIFIC RESEARCH

Conducted by the

UNIVERSAL ENERGY SYSTEMS, INC.

FINAL REPORT

APPLICATIONS OF FIBER OPTICS AT LOW TEMPERATURES

Prepared by:	David Y. Chung
Academic Rank:	Professor
Department and	Department of Physics and Astronomy
University:	Howard University
Research Location:	Rome Air Development Center, Solid State Sciences Division Electro-Optical Device Technology Branch, Hanscom AFB, MA
USAF Researh:	Dr Richard Payne
Date:	August 4, 1985
Contract No:	F49620-85-C-0013

APPLICATIONS OF FIBER OPTICS AT LOW TEMPERATURE

by

David Y. Chung

Abstract

With the advancement of fiber optic technology, many interesting applications are possible at low temperatures. A systematic testing of different fibers for use at helium temperature (4.2°K) were performed. The advantages of using fiber are many fold compared with the conventional optics. It allows experiments to be performed without an optical dewar. Small sample holders can be made to fit into a conventional helium container and also in the case of using the superconducting magnet for high field magnetooptical work.

What we have demonstrated in this report is that the usefulness of the fibers at low temperatures and its potential for wide applications are not much different from room temperature counterpart. Except there are unusual advantages of using fibers which will be discussed in detail in the report.

Acknowledgements

The author would like to thank Drs. Andrew C. Yang and Richard Payne for suggesting this area of research and for their collaboration and coordinations, and Dr Richard A. Soref and Charles W. Tsacoyeanes for their many helpful discussions and encouragement.

He would also like to thank the Air Force Systems Command, the Air Force Office of Scientific Research and the Universal Energy Systems for providing him with the excellent opportunity to spend a productive and interesting summer at the Rome Air Development Center, Hanscom AFB, MA.

Finally, he would also like to acknowledge the technical support from SSgt Stephen Spaziani, Dr Herbert Lipson, and Lionel Bouthillette.

I. INTRODUCTION:

The use of optical techniques in measurements offers many advantages over conventional transduction techniques. These include immunity to electromagnetic interference, high sensitivity, lack of mechanical moving parts and a compact format. Optical transducers may be utilized in many ways, involving the modulation by an external influence of the phase, frequency, intensity or polarization of a light wave. Phase modulation, detected interferometrically is one extremely sensitive means of measurement[1].

The new possibilities offered by optical fibers stimulated research toward optical sources and detectors compatible in size and reliability, with low power consumption. Semiconductor LED and solid state detectors (photodiodes) appeared the most promising devices. With the advancement on producing low loss fiber at longer wavelength, (e.g. at 1.55μm with less than 0.2 db/km loss) very large bandwidths can be obtained. Material dispersion is an ultimate limiting factor for the information carrying capacity of optical fibers. These two features - very low loss, very low dispersion - disclosed exciting new possibilities for large distance, high bit rate transmission with optical fibers.

With all the advantages and fast progress in fiber optical technology, very little work has been devoted to its applications for low temperatures. It is the purpose of this work to try to bridge the gap so that the use of fibers can be applied to many masterial testing and device applications to low temperatures. With many years of experience in low temperature research of mine and the capability in fiber optic research of RADC, it would be most appropriate to develop and combine the two disciplines together here. In the following, after some

brief discription of the objective of the objective of this research we are going to give the low temperature set up in Ch. III and fiber optical measurements in Ch. IV. A summary of results will be given in Ch. V and recommendations for further research in Ch. VI.

II. OBJECTIVES:

The main objectives for this summer research are: (1) to evaluate and perform the actual testings on the use of different types of fibers down to liquid helium temperatures (i.e. 4.2°K), (2) to apply the fiber optical technology to low temperature measurements such as sensors and device testing. Due to many advantages of measurements at low temperatures, such as low noise and sensitive detectors at long wavelength, compact and stable environment, the development along this line might result in very useful devices, such as very fast detectors (up to 500MHz) using superconducting bolometers, etc.[2].

III. LOW TEMPERATURE ARRANGEMENT:

We divide this chapter into two parts: (a) Dewar and vacuum system and (b) Temperature measurements.

a. Dewar and Vacuum System:

A variable temperature dewar (made by Janis) was used for our experiment. This particular dewar has an optical window, but we did not use the window; we only used the dewar as a means to reach low temperatures. In fact any liquid helium dewar could serve the purpose. The low temperature system is shown in Figure 1. A diffusion pump was used for pumping the nitrogen jacket to assure good vacuum each time before the outside dewar is filled with liquid nitrogen. Also the helium transfer tube (not shown) needs pumping to make sure smooth

transfer of liquid helium into the dewar occurs.

It normally takes about one hour for the whole system to cool down to liquid nitrogen temperature (77°K). During that time optical measurement could easily be carried out as a function of temperature, as it slowly cools down the inside dewar where the optical fiber and thermocouple thermometer are located. After double checking the optical system to make sure they are in good working order, liquid helium is then transferred into the inside dewar from a helium storage tank. This normally takes about 20 to 30 minutes, and 2 to 3 liters of liquid helium was used in the process. After the optical measurements were made at helium temperature (4.2°K) we can also raise the temperature of the fiber sample by lifting the fiber - thermocouple assembly from the liquid heliuum bath slightly. With this operation some measurements can be made between 4.2° to 77°K. However, the temperature stability in this range is not that good. But we can compare with the measurements made when we purposely slow down the liquid helium transfer process (as the temperature slowly drifted downwards).

b. Temperature Measurements:

There are many ways one can measure the temperatures[3] down to 4.2°K. Due to the preliminary nature of this project, we are not trying to set up for measuring the temperature with great accuracy. Therefore we decided to use the thermocouple junctions as proper thermometers. Two kinds of T.C. wires were used: (1) Alumel - Chromel (Omega Eng. Inc.) and (2) Copper - Constantan pairs. (1) is useful all the way down to 4.2°K but (2) is only useful to about 77°K. A calibration curve of thermal emf vs. temperature is given in Figure 2. With one reference junction at 0°C, one can easily read off the temperature of the

other junction which is attached to the fiber coil in the low temperature dewar. It turns out the optical power and associated change in the fiber due to temperature change are not large, therefore the T.C. did give us adequate temperature readings. For a more sensitive measurement of optical output in an interferometric arrangement, a better temperature control and more accurate temperature measurements are required. In summary, the present low temperature system is adequate for our optical measurements and testing purpose.

IV. OPTICAL MEASUREMENTS:

There are many different ways one can test optically how a fiber works at low temperatures. The methods we choose depend on what kinds of associated electrical equipment are available to us. In this chapter we will describe the (a) intensity, (b) polarization, and (c) interferometric measurements separately. The results of each will be discussed in the next chapter V.

The configuration we choose for the fiber to be tested is in the form of a coil. About 20 turns were wound around a nylon rod (1/2" diameter) and then a masking tape was used to secure the fiber coil on the outside. One of the thermocouple junctions was also mounted near the fiber coil for temperature measurements. One of the reasons for choosing this coil configuration is that it has been used by others for many stress and magnetic sensors (at room temperature)[1].

a. Intensity method:

To measure the optical loss due to temperature variation down to 4.2°K, we can easily monitor the intensity output from the fiber being tested by a photodetector as the fiber temperature changes. This method was reported by a recent article[4]. A related work applied to

spectroscopic work using fiber bundle was reported in Ref. 5.

b. Polarization method:

The optical set up is very similar to that of (a) except with a linear polarizer (LP) and an analyzer (LA) were used at the input and output respectively (see Figure 3). In this arrangement, one can easily measure the polarization change of a single mode fiber due to the temperature change. This method can also be used in the future for the measurement of polarization preserving fiber which is known to be a useful temperature sensor at room temperature and above[6].

c. Interferometric methods:

One of the most sensitive methods to measure the phase changes in the fiber due to external influence is by comparing the path difference between two optical paths. The more commonly used configuration is the Mach-Zahnder interferometer. The optical layout is shown in Fig. 4. The He-Ne laser light is coupled into the fiber by a microscopic lens; this fiber is part of the 2 x 2 coupler. One branch of the coupler is connected to a "reference" arm then onto a second 2 x 2 coupler to a photodetector. The other arm of the first coupler is connected to the sensor coil (in the low temperature dewar) and then to the second coupler as shown in Fig. 4. The "reference" arm can be a fiber coil (of the same type and similar length) a Pockels cell or a Bragg cell[7]. When a Pockels cell is used, the phase of 'Ref' can be changed to compensate the sensor branch for a small phase detection of the output, thereby an accurate change in polarization state of the fiber can be monitored as a function of temperature. The Bragg cell can be used for optical hetrodyne detection. The Bragg cell used was a 12 MHz acousto-optical cell. With this arrangement the photodetector at the output is

a fast photo-diode. After going through an IF amplifier (for 12MHz, or a wide-band rf amplifier) one can display the output on an oscilloscope. One can also modulate the A/O cell for phase detection. The optical alignment of Bragg cell is very tricky (see ref. 7). However, due to the instability problem observed at the output we could not obtain any useful results due to the temperature change in the sensor branch. Some improvements are needed before this powerful method can be used for the sensor applications at low temperature. The associated problems and some recommendations will be given in chapter VI.

With the present arrangement, one can easily extend the mesurements to other wavelength. This can be achieved by replacing the He-Ne laser by a laser diode (or other longer wavelength laser such as CO_2 laser) and the photo-detector to match the wavelength of interest. For longer wavelength, there is a distinct advantage here, namely the most sensitive detectors are operated at liquid helium temperatures. However, special fiber has to be used for these longer wavelength measurements. In addition, some sensitive superconducting bolometers are also available for high-frequency modulation detection as demonstrated recently in ref. 2 and 8.

V. SUMMARY OF RESULTS:

The purpose of this project is to test different kinds of optical fibers to liquid helium temperature and evaluate their optical performance and mechanical durability. In the following we will briefly summarize the results on the few fibers we used by different methods. Further suggestions and recommendations on future work will be given in Chapter

VI.

a. Intensity measurements:

Both single and multimode fibers have been tested at nitrogen and helium temperatures, and optical power monitored as the fiber sample cooled. In general, the light intensity drops slightly (approximately 20%) as one would expect. The types of fibers tested in this project are listed in table I. We conclude that all the fibers listed here are usable down to liquid helium temperature (4.2°K). For some fiber the plastic jacket can also survive the low temperature environment as long as the cooling rate is slow. The results of this testing is in general agree with recent work by Tzngelsrath et al (ref. 4) except in some cases, small peculiar variation with temperature were observed.

b. Polarization measurements:

For a single mode fiber, we do expect the polarization to change in the fiber coil as a function of temperature (or other parameters). However, due to the crude set up we have and the inability to rotate and provide accurate angular readings of the polarizer and analyzer used, the small changes in angles can not be measured with any certainty. Although we did see a trend of change due to the cooling down of temperatures of the fibers. This can easily be improved in future work. The use of polarization preserving fiber for low temperature sensor is very promising. (As it has been demostrated for room and higher temperature measurements recently).

c. Interferometric measurements:

We did some preliminary experiment with L.P. and L.A. in the set up as shown in Figure 4. Some systemetric variations in polarization were observed as a function of temperatures. However, due to the high

sensitivity of the interferometric arrangement, the instability problems are very serious which effects the reliability of our data. Using a Pockels cell or Bragg cell and an A.C. lock-in detection scheme would eliminate some of the problems. But a stable laser source and temperature control on the 'ref' arm are to be improved to say the least.

VI. RECOMMENDATIONS

The use of fiber optics at low temperatures has proven to be possible and beneficial with this project. There are many directions one can go from here, depending on what kind of problems one has to solve and which applications one can utilize the low temperature environment. We briefly give the recommendations here:

a. The simplicity in dewar design (without an optical window) and space saving for optical path with fiber optics, make it possible to extend most optical spectroscopy work in UV, visible and IR to low temperatures.

b. Different kinds of sensors can be made for low temperature use, e.g. stress, magnetic field, electric field, and temperatures.

c. Polarization measurements of the fiber can be improved by using proper components, such as polarizing beam splitter, quarter wave plates and Wollaston prism, etc. This is an important problem because for any kind of sensor applciations, one needs to deal with the polarization state of the fiber precisely especially in the polarization preserving fiber.

d. With the proper interferometric set up, one can utilize the extremely high sensitivity of the optical phase measurements for low temperatures. The use of Bragg or Pockels cell and A.C. detections scheme

should improve the stability of the system. A stable laser source is also necessary for high precision work. We wish to continue this work by requesting a mini-grant for Howard University.

e. There are many low temperature devices such as sensitive long wavelength detectors, e.g. $Cd_xHg_{1-x}Te$ can be easily utilized with proper fibers. Also, the electronics and microelectronics using superconducting junctions can also be applied for fast optical detections[8]. Much work along this direction can be worked out. We believe this is a very fruitful area for the Air Force to explore for the future device applications.

Table 1. List of Fibers Used for Testing

	Mode	Core diameter	Type
1)	Single mode	8.7μm	Corguide optical waveguide
2)	Single mode	4μm	EMT-20990 A
3)	Multimode	~ 50μm	ITT 821129-402
4)	Multimode (concentric core)	inner core: 50μm outer core: 25-30μm cladding: 18μm	Gallileo No. 3

REFERENCES

1. Giallorenzi, T.G., Bucaro, J.A., Dandridge, A., Sigel, G.H., Jr., Cole, J.H., Rashleigh, S.C., and Priest, R.G., "Optical Fiber Sensor Technology," IEEE J. Quantum Electronics, QE-18, pp. 626-65 (1982).

2. Enomoto, Y., Suzuki, M., and Murakami, T., "Highly Sensitive Optical Detector Using Superconductivity Materials (BPB)" Jap. J. of Appl. Phys., 23, pp. L333-335 (1984).

3. See for example - White, G.K., "Experimental Techniques in Low Temperature Physics", Cambridge University Press (1957).

4. Tanglesrath, A., Larson, D.R., Phelan, R.J., and Franzen, D.L., "Attenuation of Multimode Fibers Cooled to Liquid Helium Temperatures", Proc. SPIE, no. 500, pp. 124-130 (1984).

5. Heiman, D. "Fiber Optics for Low Temperature Spectroscopy", Rev. of Sci. Instrum. 56 684 (1985).

6. Corbe, M., Kersay, A.D., Liu, K., and Jackson, D.A., "Remote Temperature Sensing Using Polarization Preserving Fiber", Electronic Lett., 20, pp. 67-69 (1984).

7. Soref, R.A., "Voltage-Controlled Optical/RF Phase Shifter" to be published in IEEE J. of Light Technology. (1985)

8. See for example - Proceedings of International Conferences on Magnetism IEEE MAG, (1985).

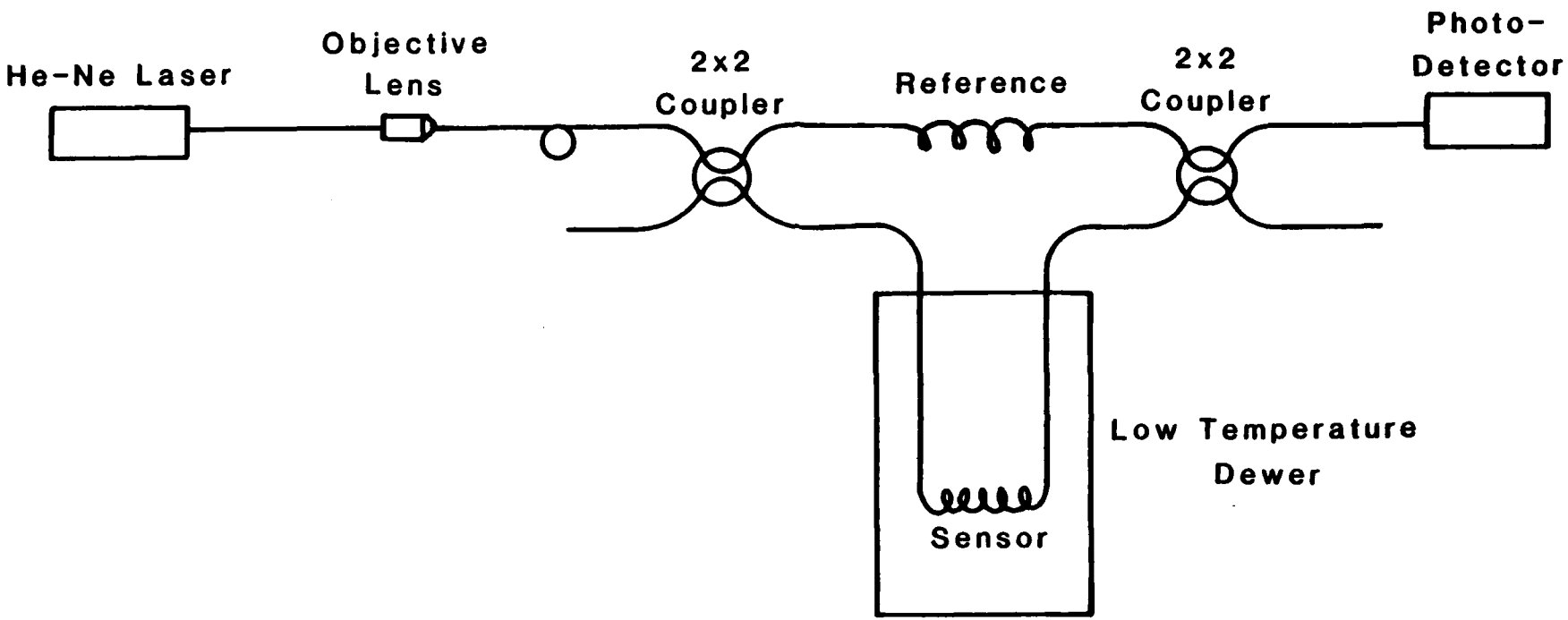

24-15

Interferometric Arrangement For Fiber Optics Sensor

FIGURE 4

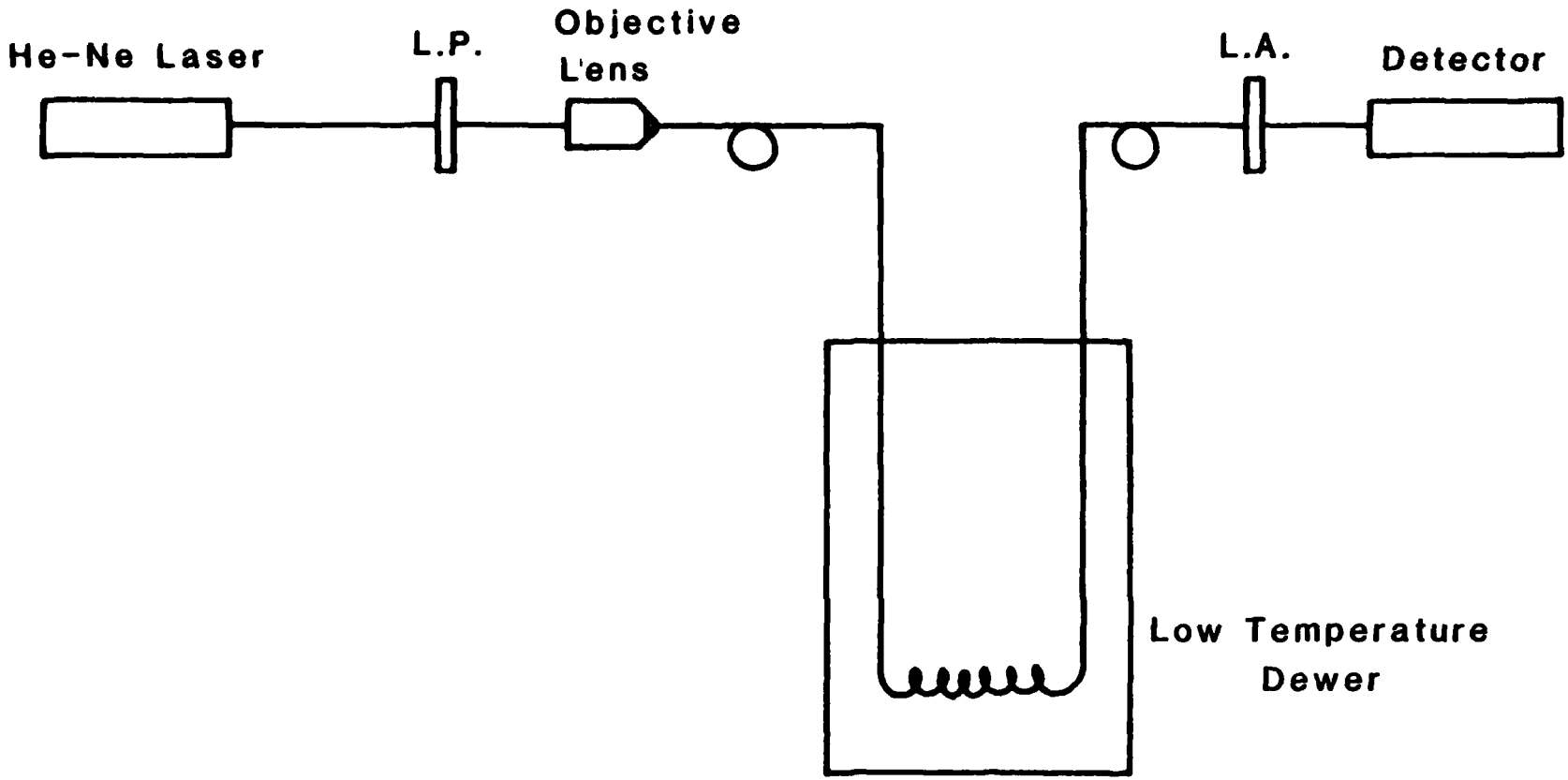

24-16

Polarization Measurements Of Fibers At Low Temperature

FIGURE 3

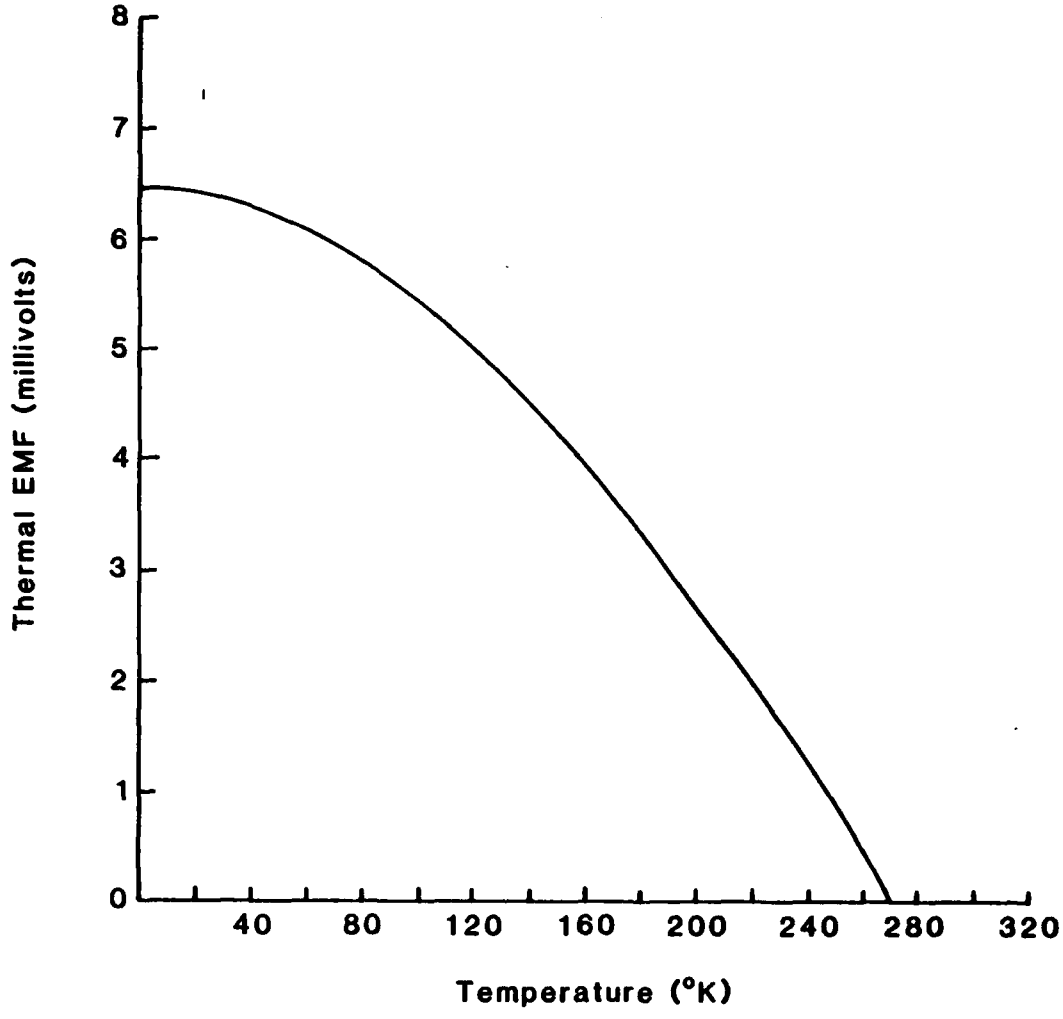

Thermal EMF Of Type K(Ni-Cr vs Ni-Al)
Thermocouple Junctions

FIGURE 2

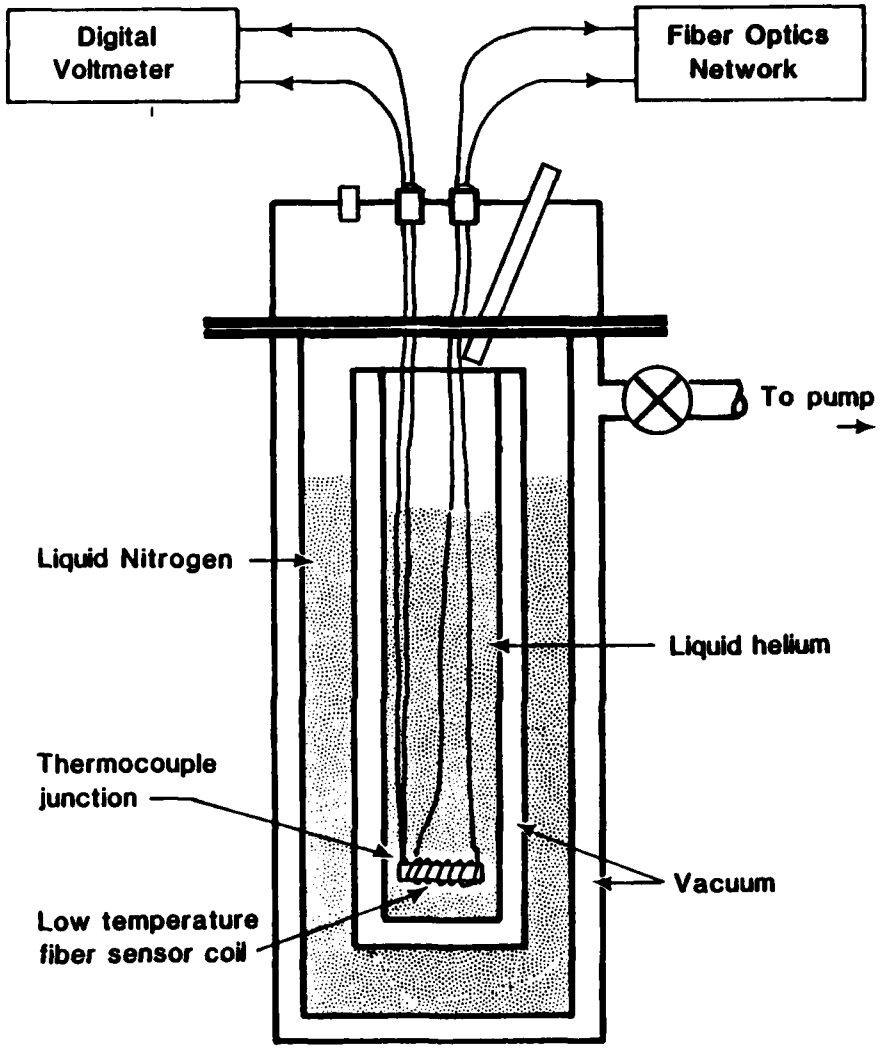

Low temperature dewar and sample arrangement.

FIGURE 1

1985 USAF-UES SUMMER FACULTY RESEARCH PROGRAM/

GRADUATE STUDENT SUMMER SUPPORT PROGRAM

Sponsored by the

AIR FORCE OFFICE OF SCIENTIFIC RESEARCH

Conducted by the

UNIVERSAL ENERGY SYSTEMS, INC.

FINAL REPORT

EVALUATION OF SELECTED PARAMETERS WHICH AFFECT K_d WHEN MEASURED USING HPLC INSTRUMENTATION

Prepared by:	Gale J. Clark
Academic Rank:	Professor of Chemistry
Department and	Department of Chemistry and Physics
University:	Middle Tennessee State University
Research Location:	Headquarters Air Force Engineering Services Center, Engineering Research Directorate, Environics Division, Tyndall Air Force Base, Florida
USAF Research:	Capt. Richard Ashworth
Date:	15 August 1985
Contract No:	F49620-85-C-0013

EVALUATION OF SELECTED PARAMETERS WHICH AFFECT K_d WHEN MEASURED USING HPLC INSTRUMENTATION

by

Gale J. Clark

ABSTRACT

The sorption coefficient for naphthalene onto a sample of soil was measured using the column technique for the purpose of evaluating potential effects that the experimental methodology and instrumentation might have on the value obtained. The data was examined for possible effects due to changes in flow velocity, influent concentration, and method of development. The reproducibility of the data from different columns packed with the same soil was also studied. It was found that the apparently common practice of simply switching the pump inlet from one reservior to another in order to change the solution being passed through the column ultimately gave a sorption coefficient which was actually a composite reflecting sorption within the pumping system as well as on the soil. Evaluation of other effects were hindered by this phenomena. The major recommendation derived from this study was to redesign the experimental system so as to eliminate the sorption due to the system and then reevaluate the other parameters.

ACKNOWLEDGEMENTS

The author thanks the Air Force Systems Command, Air Force Office of Scientific Research, and Headquarters Air Force Engineering Services Center, Engineering Research Directorate, Environics Division, Tyndall Air Force Base, Florida for providing the opportunity and the financial support provided for this research. I would also like to thank my sponsor, Capt. Richard Ashworth, for suggesting the problem, his persistence in securing the material necessary to do the project, and his encouragement throughout the summer. Finally, I would like to thank the entire group in the Environics Division at Tyndall Air Force Base for their support and assistance in this effort.

SECTION I

INTRODUCTION

One area of interest to the Environics Division at Tyndall Air Force Base is the movement of pollutants in groundwater systems. To develop engineering models for this movement it is necessary to obtain the sorption coefficients for the potential pollutants on the soil. These values traditionally have been measured using a batch equilibration procedure; however, recently several workers have reported studies based on a column technique using instrumentation designed for high performance liquid chromatography (HPLC). The workers in the Environics Division who were interested in using this column technique are nonchemists and felt that it was desirable that a chemist familiar with chromatographic techniques evaluate this newer method for measuring soil sorption characteristics.

As an analytical chemist, I have studied the application of HPLC in the analysis of various systems for organic compounds. Also, I have measured the distribution ratios of some organochlorine pesticides in liquid-liquid extraction systems. These studies have given me some knowledge of the factors which could be expected to affect the measurement of adsorption coefficients on soil even though I had no experience with soils prior to this summer. The methods used to determine adsorption coefficients is also quite different to that used in the usual determinations with HPLC. Nevertheless, the instrumentation is the same. Apparently the interests of the laboratory and my background are reasonably well-matched.

SECTION II

OBJECTIVES OF THE RESEARCH EFFORT

The major objective of this research effort was to evaluate the column technique for determining sorption coefficients of organic compounds onto soils. It was intended to examine the effects of as many of the following experimental factors as a 10-week time period would allow: (a) the effect of flow velocity on sorption data, (b) the ability to reproduce sorption data from column to column, (c) the effect of development technique on sorption data, (d) the effect of particle size and uniformity on sorption data, (e) the effect of column dimensions on sorption data, and (f) the effect of influent concentration on sorption data.

SECTION III

BACKGROUND

The movement of pollutants in groundwater systems is a problem of increasing concern in many areas of the country. Since groundwater contamination has been detected on or near several U.S. Air Force Bases, the Air Force is included with those conducting research into this problem.

When a compound in solution is allowed to equilibrate with a solid surface, a portion of the material may besorbed onto the surface. For a given set of equilibrium conditions, the ratio ofthe solute concentration on the solid to the solute concentration in solution is defined as the sorption coefficient K_d. Since this is one of the principal parameters used to predict the way potential pollutants move in groundwater systems, it is necessary to have a large number of reliable K_d values.

The method most widely used to measure sorption coefficients is a batch equilibration procedure. The literature related to this technique has been reviewed recently by Ainsworth and co-workers (1). In this procedure solutions having varying concentrations of the compound of interest are shaken with several different portions of the solid material for about 24 hours. Samples of the solution are then analyzed. Any decrease in concentration is assumed to be due to sorption. The concentration of solute on the solid can then be calculated. The slope of a plot of solid phase concentration vs liquid phase concentration is equal to K_d. This procedure is well established but requires a large amount of time. There are also

concerns about the validity of these data obtained under static conditions when used to predict behavior in dynamic underground systems.

In the last few years, several workers, including Goerlitz (2), Rao and co-workers (3,4), and Schwarzenbach and Westall (5), have used a column technique for measuring soil sorption coefficients. In these studies, the soil is packed into a column. Solutions of the solute are then pumped through the soil column using standard HPLC equipment until the concentration of solute passing from the column is equal to the input concentration. The concentration of the effluent is usually determined by collecting small samples over the course of the experiment and analyzing them using either liquid scintillation counting or gas chromatography. Goerlitz, however, analyzed the column effluent with detectors commonly found on commercial HPLC instrumentation. The detector signal was recorded on a strip chart recorder continuously through the experiment, thus, greatly simplifying the procedure. Regardless of the method for analyzing the effluent concentration, a plot of concentration/initial concentration (C/C_{init}) vs pore volumes (P) of effluent is then used to determine K_d. Three methods of calculating K_d are commonly used. One is based on measuring the number of pore volumes required for the effluent concentration to reach one-half the initial concentration compared to a nonretained solute. This ratio is known as the retardation factor (R). When linear isotherms can be assumed K_d is calculated using the equation:

$$R = 1 + (p/\Theta)K_d \qquad (1)$$

where p is the bulk density and Θ is the porosity. In the second

method, the retardation factor is determined by measuring the area in front of the curve compared to the area in front of a similar curve for a nonretained substance. The value for K_d is then calculated using Equation 1 (see Reference 4). The third method of calculating K_d is to determine an effective dispersion coefficient for the column using a nonretained substance and then use this value to solve the differential equation describing solute transport (see Reference 2).

From the foregoing discussion, the column technique of determining sorption coefficients is seen to be a form of frontal analysis chromatography. Unfortunately for this application, modern commercial HPLC instrumentation is optimized for elution chromatography, and the validity of obtaining frontal analysis curves with this instrumentation, while seemingly very similar, has not been extensively documented in the literature.

Schwarzenbach and Westall (5) reported some shifts in the position of the frontal analysis curves when sorption coefficients for mono-, di-, and trichlorobenzene were measured at a linear flow velocity (u) of 8.7×10^{-4} cm/s compared to 1.0×10^{-2} cm/s. This was thought to be caused by kinetic limitations in reaching equilibrium. These workers found little effect on the shape of the curves when the influent concentration was reduced by 50 percent indicating that the concentrations were within the linear portion of the isotherm.

Rao and Davidson (3) used a constant linear flow velocity in their studies of pesticide sorption; however, Rao (4) has noted a flow velocity effect in other work. Piwoni (6) has also noted an effect of linear flow velocity, but none of the latter reports have reached the

literature. Rao and Davidson (3) also found a change in the curves obtained when the influent concentration was changed from 50 ug/mL to 5000 ug/mL for 2,4-D amine or from 5 to 50 ug/mL for atrazine. More extensive reports of the effects of changes in the various operational parameters have not appeared in the literature.

SECTION IV

EXPERIMENTAL MATERIALS AND METHODS

A. REAGENTS

All chemicals used in this study were A.C.S. reagent grade materials obtained from commercial suppliers and used as received. All aqueous solutions were prepared with high purity distilled-deionized water obtained from a Milli-Q water system. Solutions which were to be passed through the liquid chromatograph were filtered through 0.2 um filters.

B. APPARATUS

The liquid chromatograph used in this study consisted of a single Perkin Elmer Series 10 pump module, a LC-85B Ultraviolet (UV) detector equipped with autocontrol, and a LC-25 Differential Refractive Index (RI) detector connected in series with the UV detector. The pump module was modified to provide additional pulse dampening by inserting a loop of stainless steel tubing (0.2 mm i.d. x 3 m) between the internal filter and the injector inlet. The signal from the UV detector was recorded on a Perkin Elmer LCI-100 computing integrator operated in the recorder mode and the signal from the RI detector was recorded on a strip chart recorder. The actual pumping rate of the pump was computed for each run after measuring the time required to collect an accurately determined volume of effluent. A Micromeritics Flowsorb Model 2300 instrument was used to obtain the BET surface area of the soil.

C. SOIL COLUMNS

The soil used in this study was a sample from Lowry Air Force Base which had been obtained by the Tyndall Air Force Base Environics Division Laboratory for some other studies and was known to have a low organic carbon content. The soil sample was screened through a series of standard screens by the Tyndall Air Force Base Soils Laboratory. Soil columns were packed with a portion of the 100/200 mesh fraction of the soil into a stainless steel column (0.46 cm i.d. x 15 cm). The first column was packed by applying a partial vacuum to the column and pouring the dry soil into the top while continuously tapping the outside of the column with a small rubber-tipped mallet. The second and third columns were prepared in a similar fashion except that after adding a small portion of soil, the column bed was compacted using a metal rod which was just small enough to go into the column. Additional soil was then added and the compacting was repeated until the column was filled.

The total organic carbon content of the soil fraction was determined by dichromate oxidation using the procedure described by Walkley and Black (7). The BET surface area of the soil was measured using the procedure described in the operating mannual for the instrument (8).

D. PROCEDURE

Initially the pump reservoir was filled with 0.01 M $CaCl_2$ solution and the system was flushed with this solution. The soil column was then connected to the pump module leaving the discharge end of the column open. Approximately 25 mL of 0.01 M $CaCl_2$ solution was pumped through the column at a flow rate of about 0.1 mL/min. Without

interupting the flow, the discharge end of the column was connected to the detectors and the system was allowed to equilibrate until a stable baseline was obtained.

Some pulse displacement curves were obtained by simply injecting 20 uL of either 0.1 M $CaCl_2$ solution or 30 mg/L aqueous naphthalene solution using the standard HPLC injector. The frontal analysis curves were obtained by very quickly removing the pump inlet line from the 0.01 M $CaCl_2$ solution and transferring it to a second reservoir containing aqueous 0.015 M $CaCl_2$ and the organic compound being investigated. The test solution was passed through the column until the traces from both detectors reached plateaus and then the mobile phase was changed back to the 0.01 M $CaCl_2$ solution. This solution was passed through the column until the detector signal returned to the initial baseline level. The volume of the system was obtained by a similar technique with the column removed from the system.

The bulk density of the soil packing was obtained by weighing the empty column then weighing again after it was packed. The weight of soil was obtained by difference and then divided by the volume of the column, which was calculated from its dimensions, to give the bulk density. The particle density was measured by displacement of water and used to calculate the volume of the soil particles. This in turn was used to calculate the porosity and pore volume.

The data from the frontal analysis curves was replotted with C/C_{init} as the y-axis and pore volumes as the x-axis. To do this, the total volume of mobile phase displaced through the column at a number of points during the run was corrected for system volume and divided

by the pore volume of the column. The detector signal at each of these points was also measured and divided by the signal level reached on the plateau of the curve. The curves for $CaCl_2$ were plotted from the data recorded on the RI detector while the curves for the organic compound were obtained from the UV detector. For the compounds used in this study no interference by $CaCl_2$ was detected in the UV detector and no interference by the organic compound was found in the RI detector.

The plotting just described was accomplished with a digital plotter which calculated a cubic-spline fit for the data and integrated the area in front of the curves. The retardation factor was calculated from the ratio of the area in front of the $CaCl_2$ curve to the area in front of the curve for the compound of interest. Values for K_d were then calculated using Equation 1.

The data obtained without a column was plotted in the manner described except that it was offset to the right on the plot by one pore volume. This was to generate a curve which should be identical to that of a nonretained substance and was used to judge any artifacts of the HPLC instrumentation which might appear in the curves.

SECTION V

RESULTS AND CONCLUSIONS

The results of the various soil characterization studies are summarized in Table 1. Table 2 summarizes the data describing the columns prepared in this study. Figure 1 shows a typical plot of C/C_{init} vs. pore volumes and Table 3 summarizes all the values of K_d obtained in these studies.

Figure 2 shows that the effect of flow rate on the nonretained $CaCl_2$ solution is minimal. The curves in Figure 3 for naphthalene show that flow rate has an obvious effect when reduced to a very low value. Since this flow rate is at the lower limit of the design range of the pump, it would be desirable to repeat this experiment. Unfortunately, the curve at 0.011 mL/min could not be repeated on the same column since column one plugged near the end of the desorption. In the past, changes such as those observed in Figure 3 have been attributed to a failure to reach equilibrium at the faster flow rates. If the present observations are found to be reproducible, the same explanation is probably also valid in this situation.

In the context of this report, studies involving changes in flow rate imply changes in linear flow velocity since the same column is being used. Linear flow velocities are a function of not only flow rate but also the cross sectional area and porosity of the column and are actually the factor which partially determines whether equilibrium is achieved. Before any additional attention is given to effects of flow velocity, there are other factors to consider.

SECTION V

RESULTS AND CONCLUSIONS

The results of the various soil characterization studies are summarized in Table 1. Table 2 summarizes the data describing the columns prepared in this study. Figure 1 shows a typical plot of C/C_{init} vs. pore volumes and Table 3 summarizes all the values of K_d obtained in these studies.

Figure 2 shows that the effect of flow rate on the nonretained $CaCl_2$ solution is minimal. The curves in Figure 3 for naphthalene show that flow rate has an obvious effect when reduced to a very low value. Since this flow rate is at the lower limit of the design range of the pump, it would be desirable to repeat this experiment. Unfortunately, the curve at 0.011 mL/min could not be repeated on the same column since column one plugged near the end of the desorption. In the past, changes such as those observed in Figure 3 have been attributed to a failure to reach equilibrium at the faster flow rates. If the present observations are found to be reproducible, the same explanation is probably also valid in this situation.

In the context of this report, studies involving changes in flow rate imply changes in linear flow velocity since the same column is being used. Linear flow velocities are a function of not only flow rate but also the cross sectional area and porosity of the column and are actually the factor which partially determines whether equilibrium is achieved. Before any additional attention is given to effects of flow velocity, however, there are other factors to be considered.

TABLE 1. SOIL CHARACTERISTICS

Particle Size Distribution

Screen Size (U. S. Standard Mesh)	Percent Passed
10	100.00
20	99.94
40	89.65
60	74.22
80	63.58
100	57.05
200	32.39

Total Organic Carbon of 100/200 Mesh Fraction : 0.10 percent

Surface Area : 19.2 m^2/g

Moisture Content : 2.7 percent

TABLE 2. SOIL COLUMN DATA

	Column 1	Column 2	Column 3
Wt. Packing (Dry)	3.1798 g	3.1889 g	3.5945 g
Dimensions	0.46 x 15 cm	0.46 x 15 cm	0.46 x 15 cm
Total Volume	2.49 mL	2.49 mL	2.49 mL
Bulk Density	1.28 g/mL	1.28 g/mL	1.44 g/mL
Particle Density	2.52 g/mL	2.52 g/mL	2.52 g/mL
Porosity	0.49	0.49	0.43
Pore Volume	1.23 mL	1.23 mL	1.06 mL

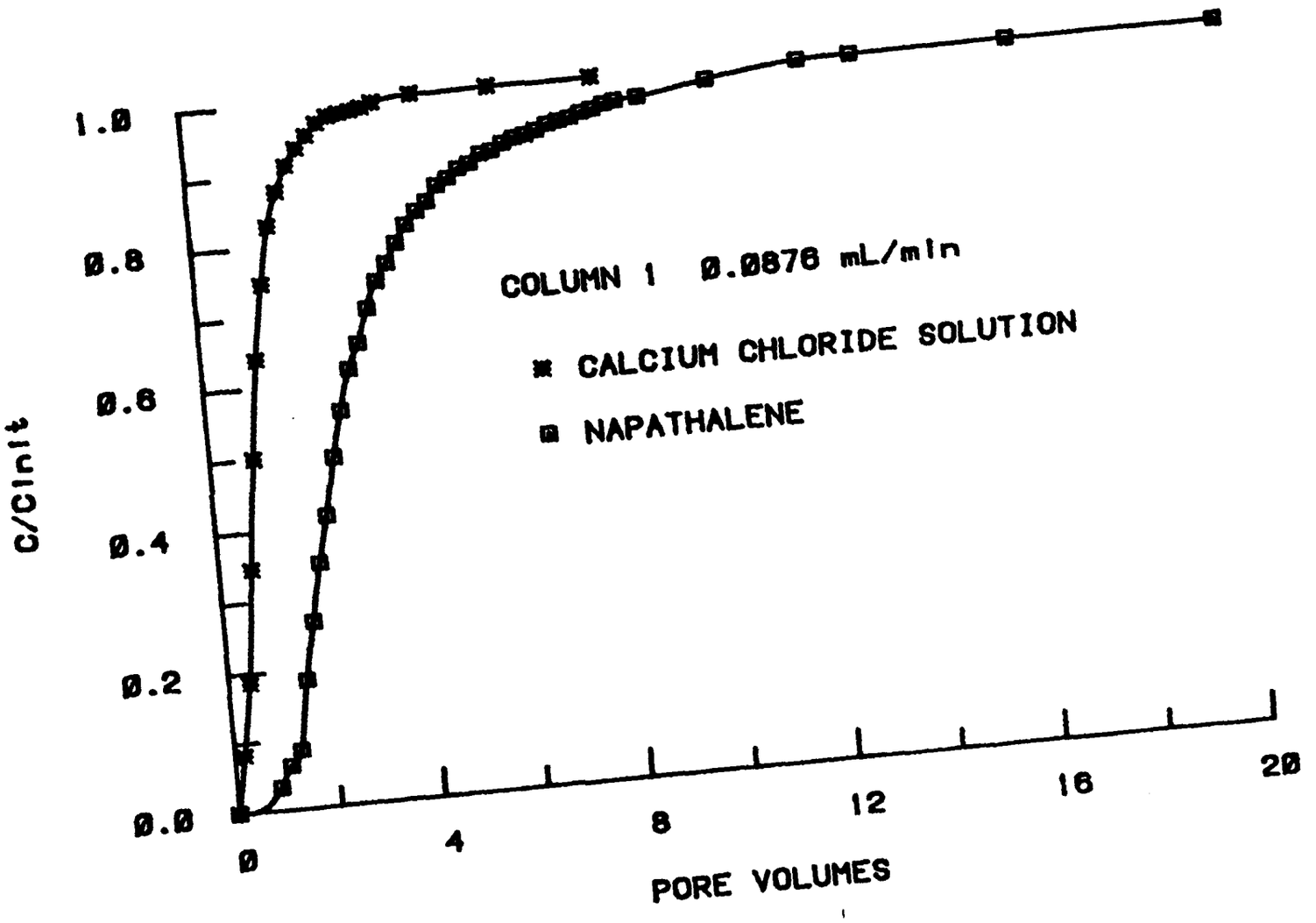

Figure 1. Typical Frontal Analysis Curves

TABLE 3. SORPTION COEFFICIENTS FOR NAPHTHALENE

Column 1 Referenced to Calcium Chloride

Run	Flow Rate (mL/min)	Initial Concentration (mg/L)	K_d (mL/g)
1	0.185	30	0.62
2	0.0876	30	0.80
3	0.011	30	2.52

Column 3 Referenced to Calcium Chloride

Run	Flow Rate (mL/min)	Initial Concentration (mg/L)	K_d (mL/g)
1	0.0876	30	0.56
2	0.0862	30	0.57
3	0.0862	3	0.51

Column 1 Referenced to Naphthalene Without Column

Run	Flow Rate (mL/min)	Initial Concentration (mg/L)	K_d (mL/g)
1	0.185	30	0.41
2	0.0876	30	0.32
3	0.011	30	0.21

Column 2 plugged before any sorption coefficients could be obtained.

Runs 2 and 3 on Column 3 were made with a back pressure of about 2600 psig compared to about 400 in Run 1.

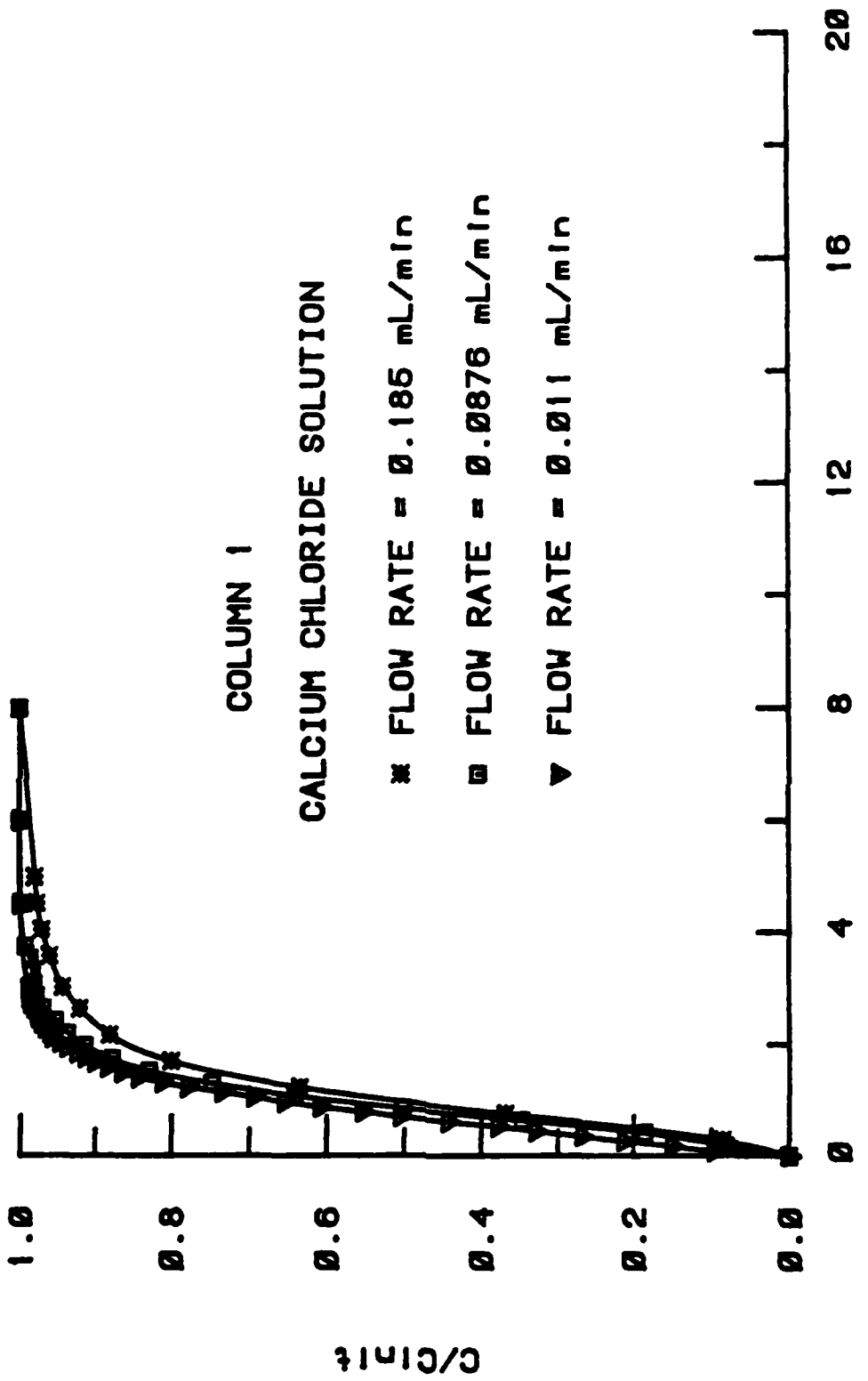

Figure 2. Frontal Analysis Curves for Calcium Chloride at Varying Flow Rates

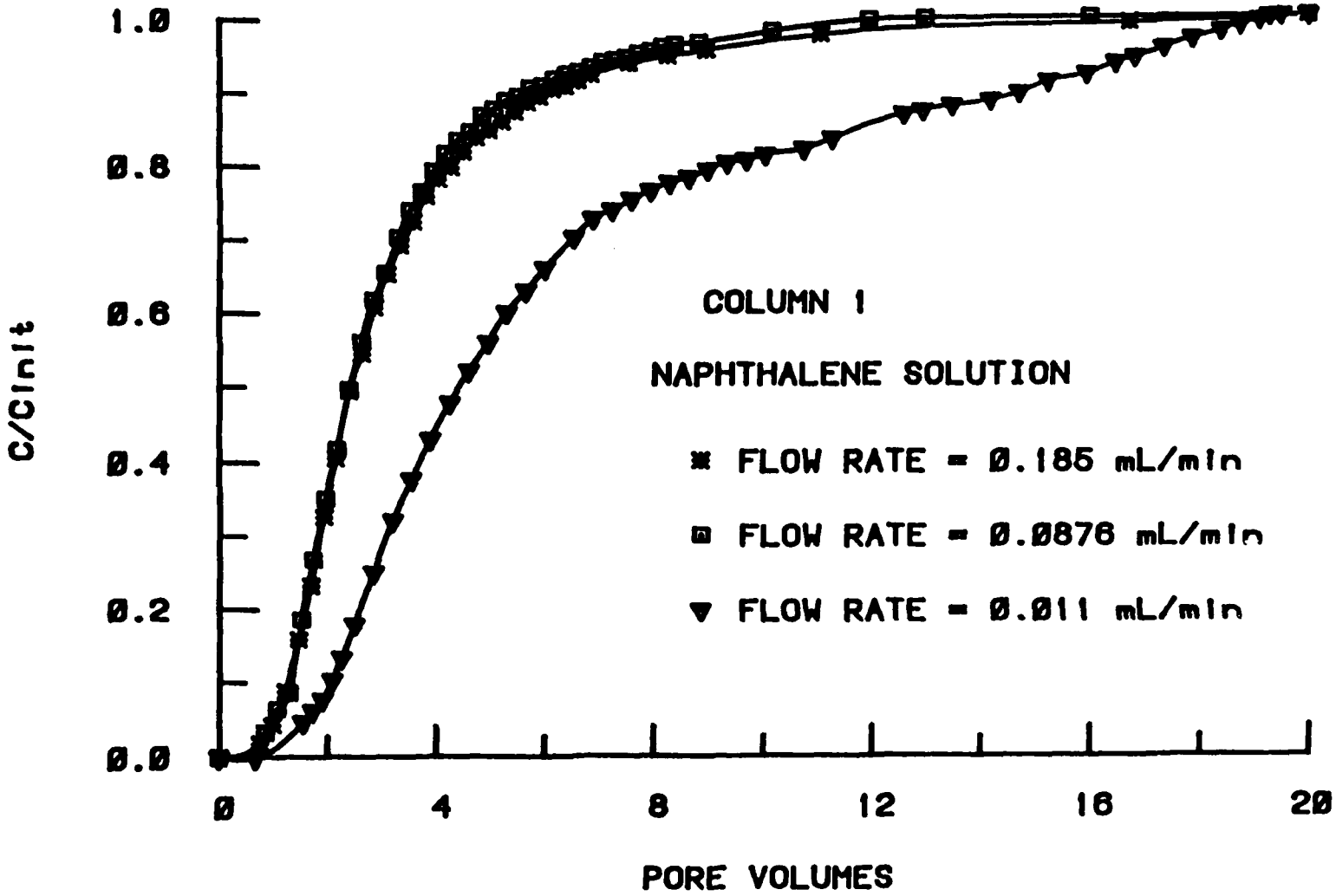

Figure 3. Frontal Analysis Curves for Naphthalene at Varying Flow Rates

Figure 4 shows a set of curves from column 3 plotted on the same graph with a set of curves from column 1 obtained at the same flow rate and approximately the same concentration. There is a significant change in the position of the curves; however, when the K_d values are calculated, a shift in the $CaCl_2$ curve more than compensates for the shift in the naphthalene curve since the K_d calculated from column 3 decreases compared to column 1.

During the latter stages of the first run with column 3 the back pressure increased from about 400 psig to about 2600 psig and a small disturbance in the curve was observed. A second run was performed using the conditions of the first run. The results of those two runs are shown in Figure 5. Small shifts in both the $CaCl_2$ curve and the naphthalene curve are evident. When the sorption coefficients are compared there is no significant difference.

In a third experiment with column 3, the initial concentration of the naphthalene was reduced from about 30 mg/L to about 3 mg/L. The curves from that experiment are shown in Figure 6 plotted along with the data from run 2. Only negligable changes are observed.

One of the early problems in this work was to determine the volume of the system. This was necessary to correct the total volume of effluent for the volume of the pump and the connecting lines. It was thought that the system volume could be measured by simply measuring the volume required for the solute of interest to reach one-half of its influent concentration in an experiment without a column. When this was done using the $CaCl_2$ solution and the value applied to a set of data, curves such as those already presented were obtained. The difference between the system volume and the volume required for

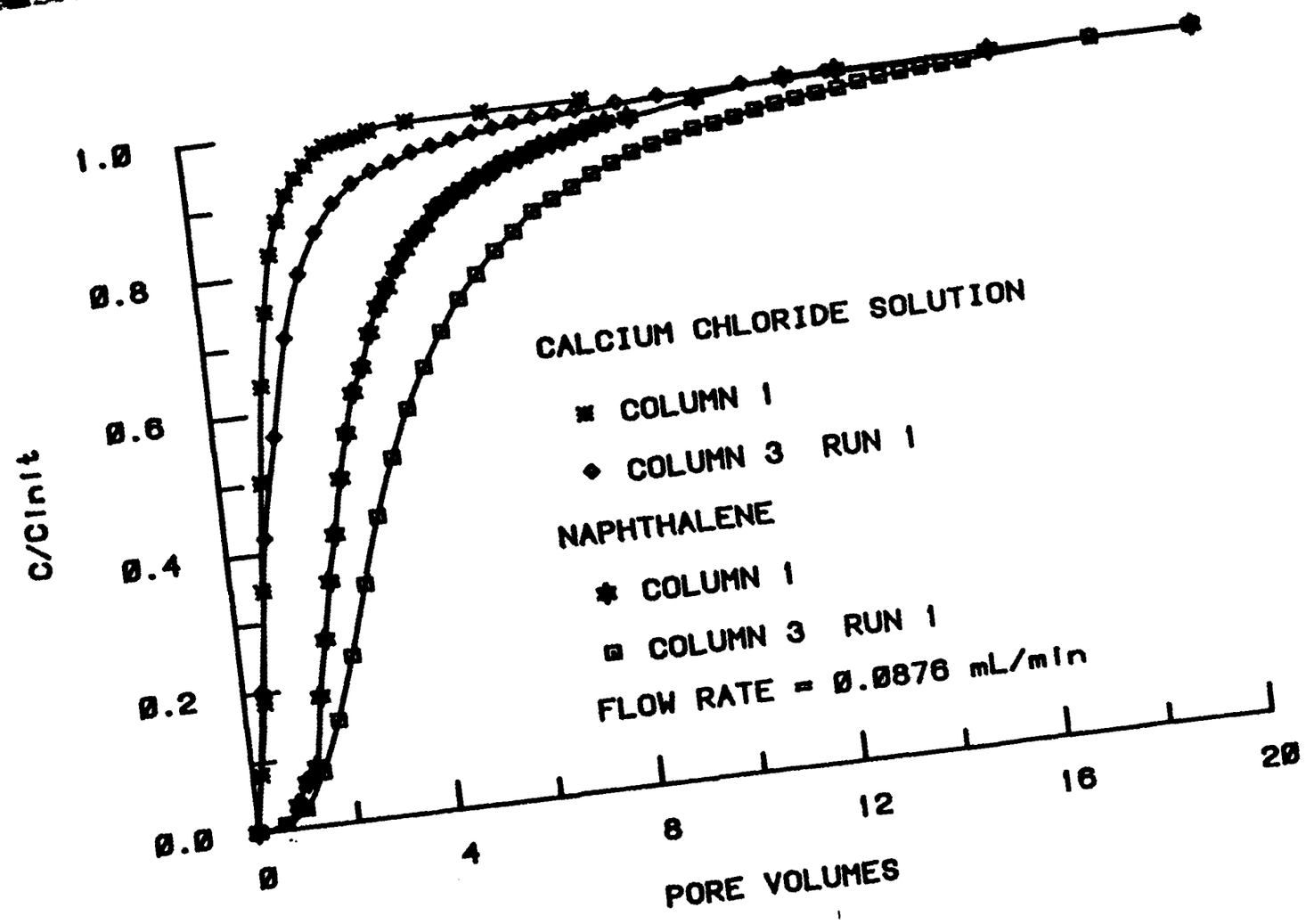

Figure 4. Frontal Analysis Curves From Two Columns

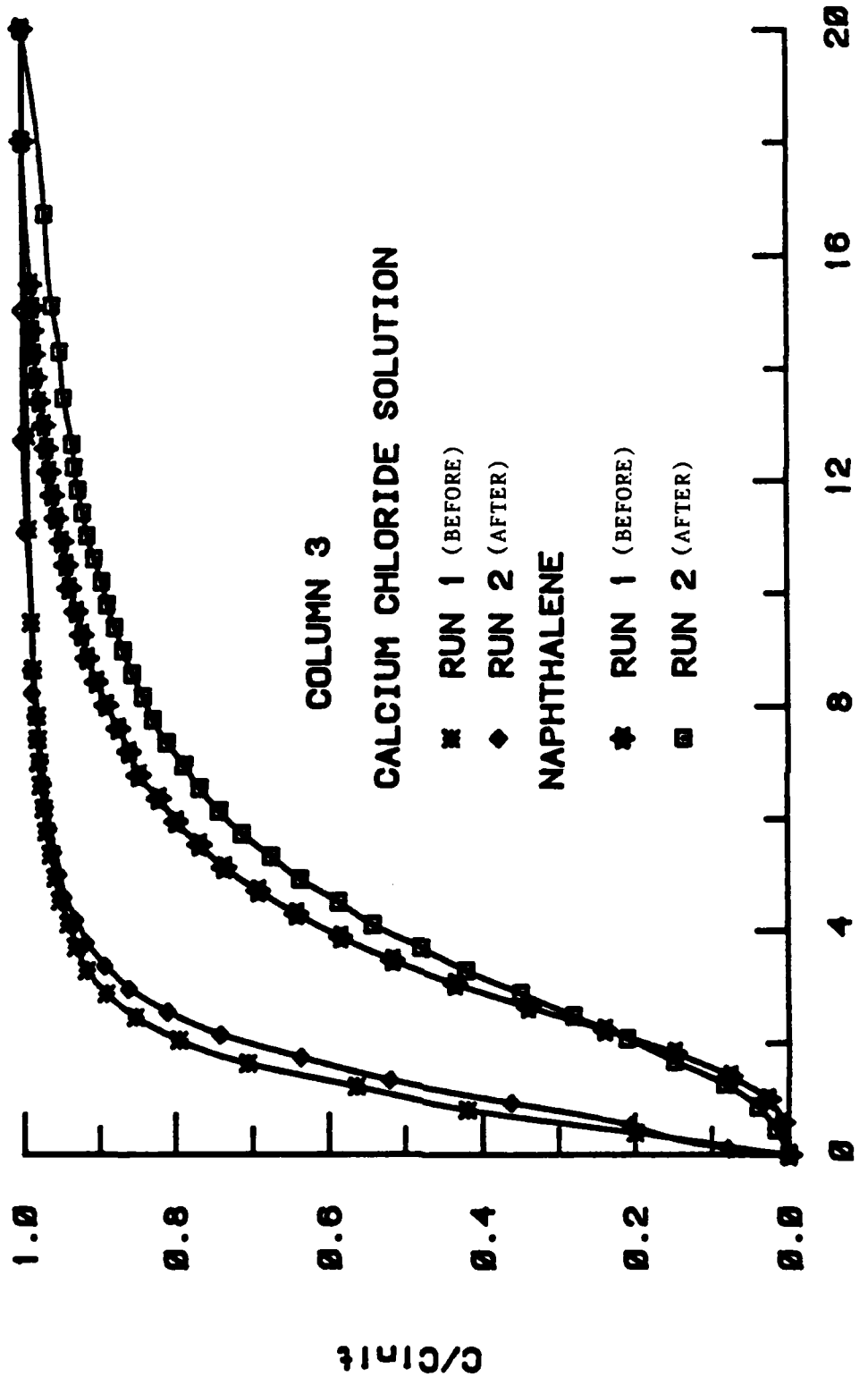

Figure 5. Frontal Analysis Curves Before and After Pressure Increase

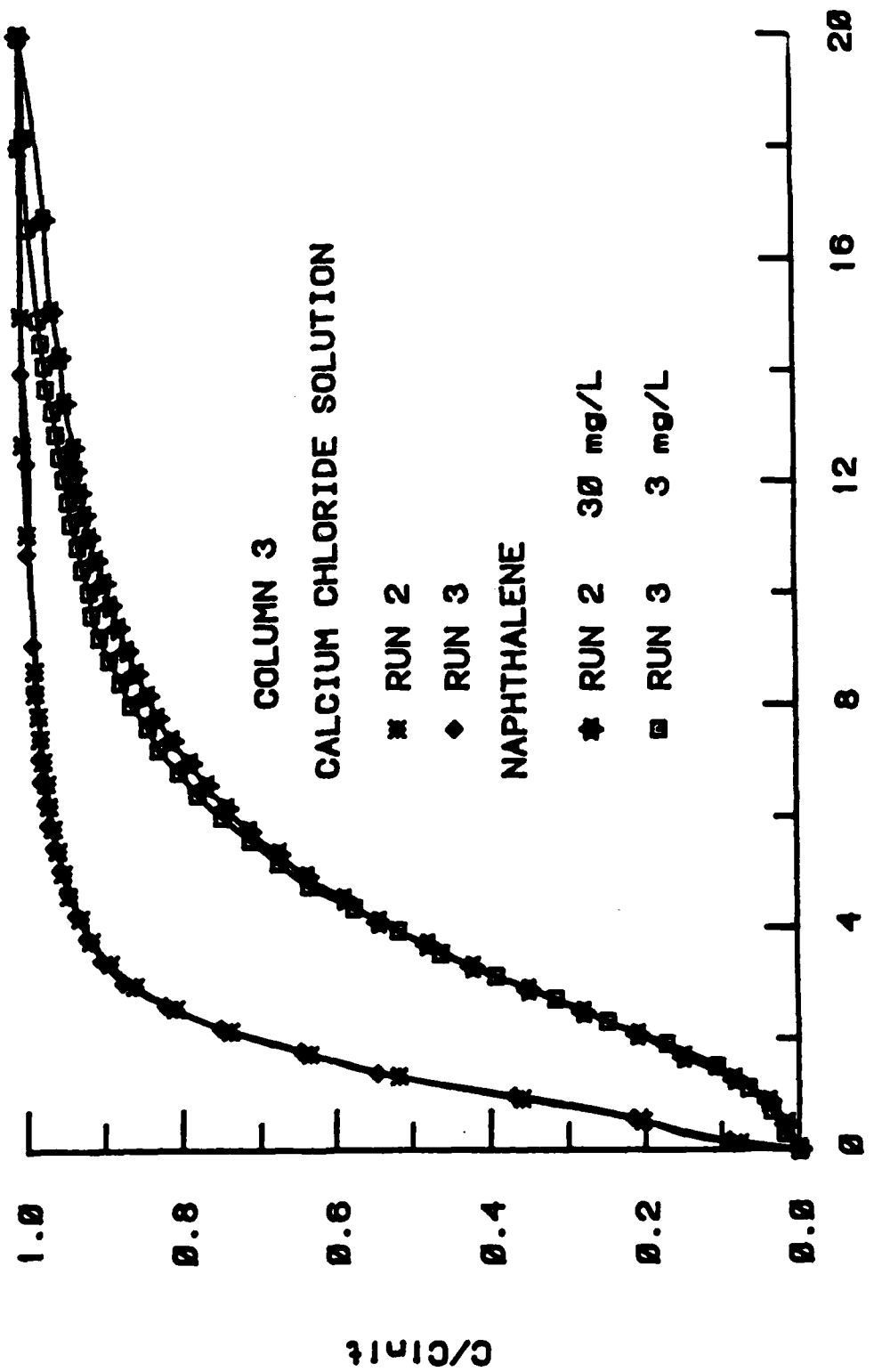

Figure 6. Frontal Analysis Curves at Two Concentrations

the $CaCl_2$ to reach one-half of its influent concentration with a column in the system was within experimental error of the pore volume determined as described earlier. This could be expected if the system was not causing any distortions in the data. A plot of data taken with and without a column is shown in Figure 7.

It would be expected that without a column the data obtained using the UV detector with naphthalene would differ from the $CaCl_2$ data obtained with the RI detector by only the volume of the tubing between the two. As seen in Figure 8, this was not observed. The curves for naphthalene are shifted to the right compared to the $CaCl_2$ even though the UV detector is between the pump and the RI detector. Flow rate is also seen to have a much greater effect on the naphthalene curves than on those for $CaCl_2$. These results were quite confusing initially, but, it is now thought that the naphthalene is sorbing to a measurable degree in the HPLC equipment. Additional evidence for this explanation of the data was provided when a solution of $Ca(NO_3)_2$, which absorbs ultraviolet radiation around 300 nm, was passed through the system. The plots obtained in this experiment are shown in Figure 9 and exibit the characteristics which were expected with the naphthalene.

Since there is evidence that the system retards the movement of the naphthalene, the validity of the K_d values obtained in this study is questionable. Retardation factors and the corresponding values for K_d can be calculated by using the ratio of the area in front of a curve for naphthalene without a column to the corresponding area with a column present. These values are included in Table 3 for column 1.

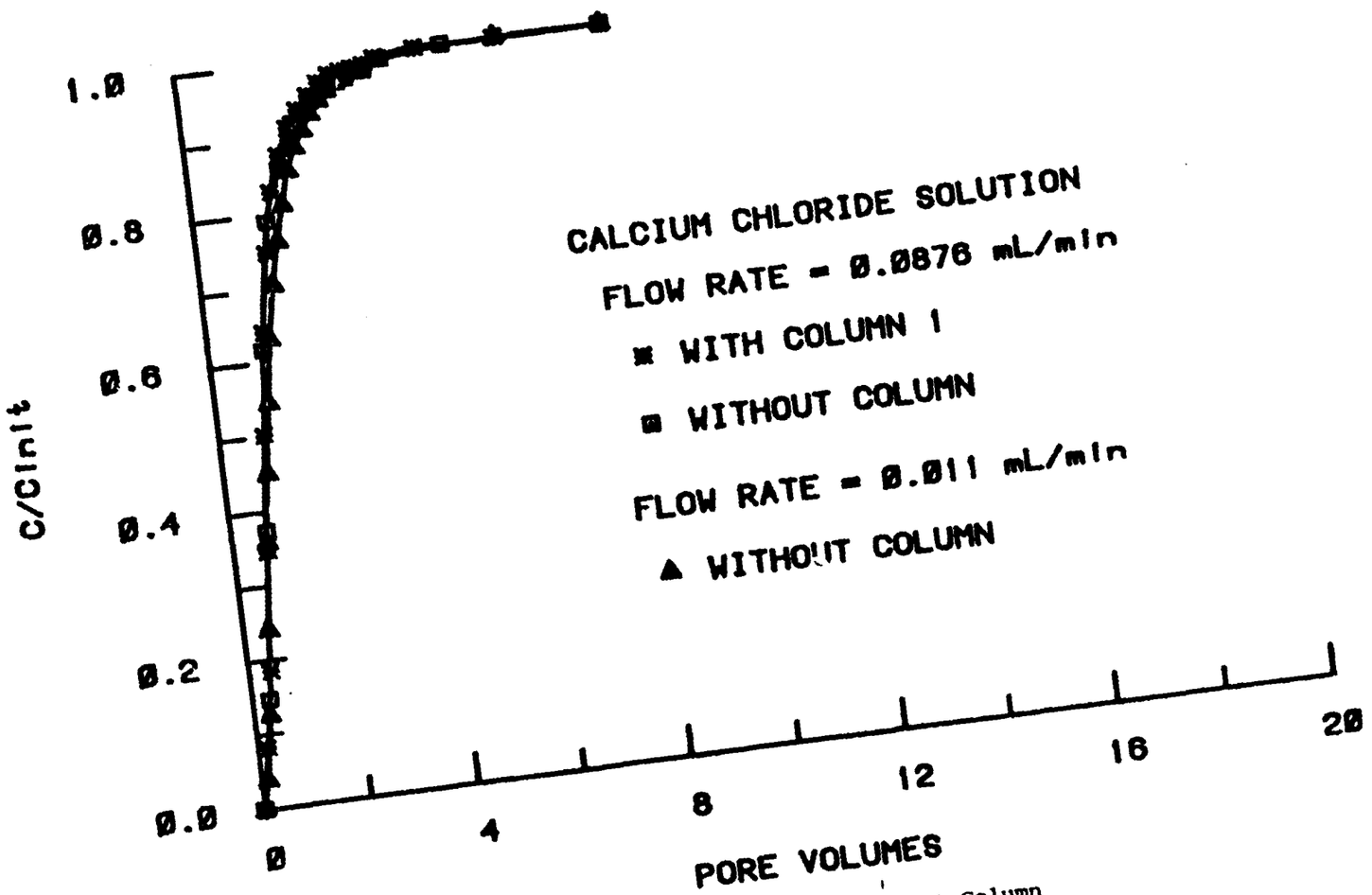

Figure 7. Frontal Analysis Curves of Calcium Chloride With and Without Column

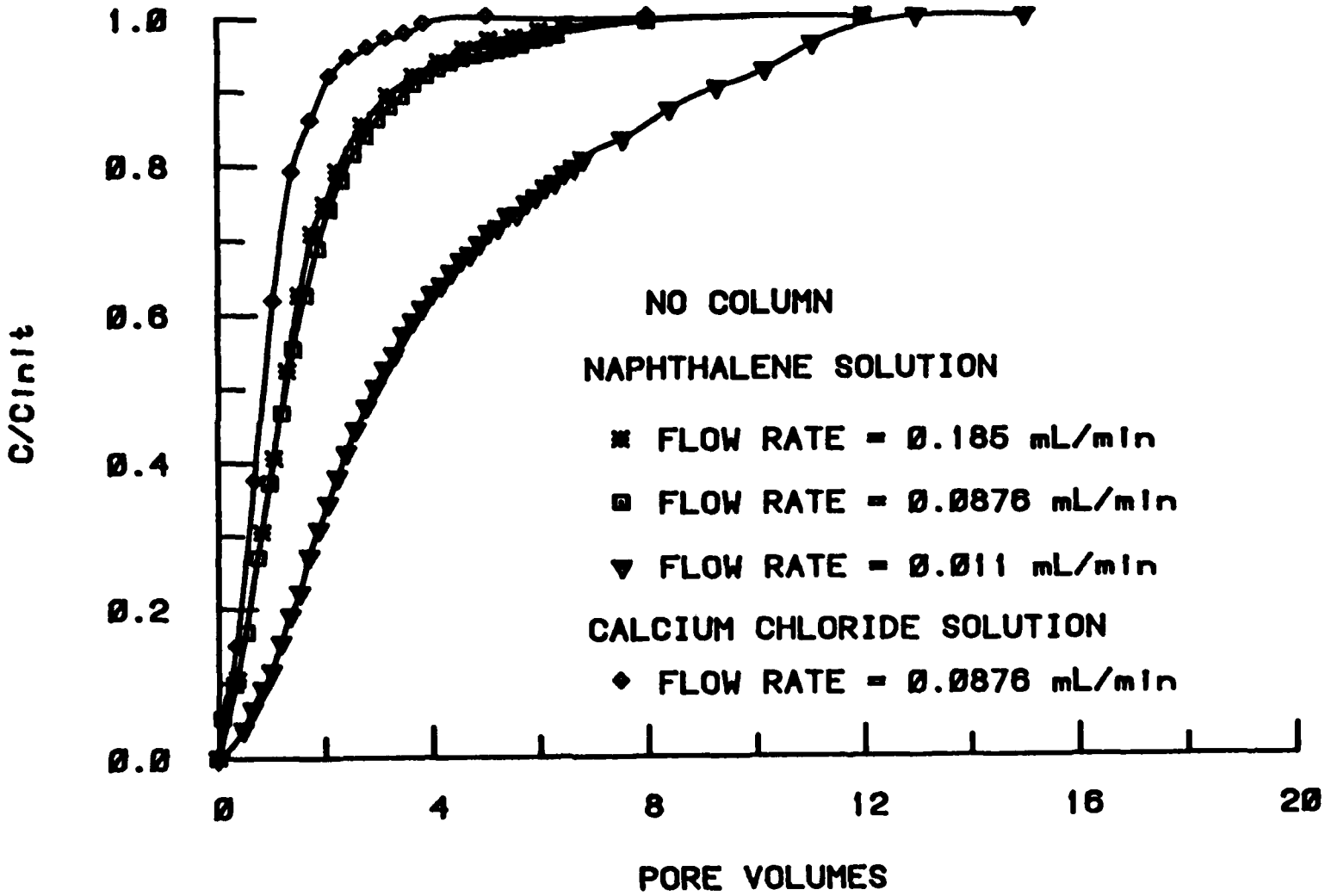

Figure 8. Frontal Analysis Curves of Naphthalene Without Column

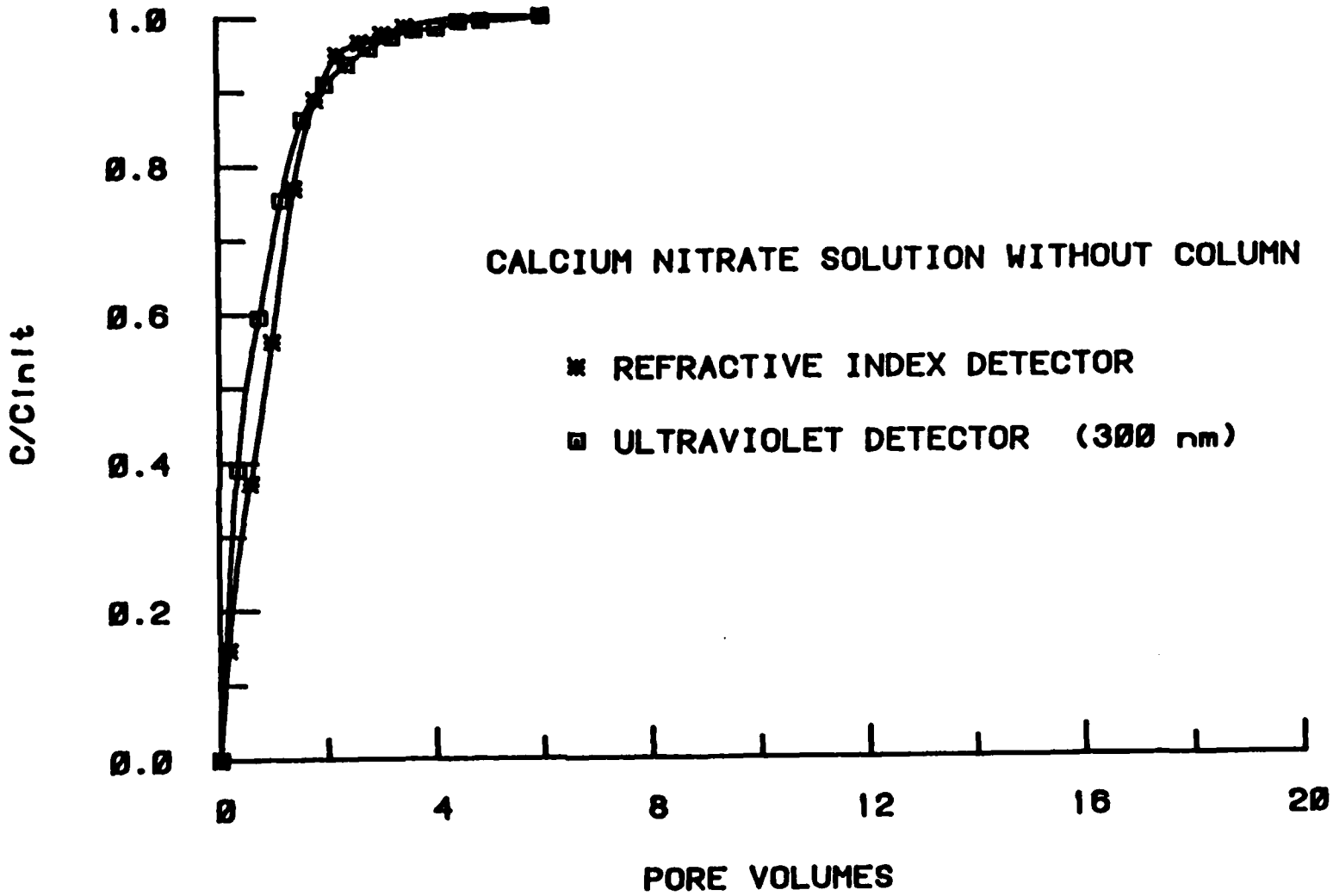

Figure 9. Frontal Analysis Curves of Calcium Chloride with Two Detectors

The change with flow rate is opposite to that described previously in this discussion and is of a lesser magnitude. This latter approach should be considered unreliable until it is verified by additional studies. A better solution to this problem would be to redesign the system in a way that would avoid the problem entirely.

The data from a small number of pulse displacement experiments are summarized in Table 4. The values of K_d obtained by this development technique are generally lower than those obtained by frontal analysis. Because of time limitations in a 10-week program, the pulse displacement studies were of too limited a scope to be of much value for other comparisons at this point eventhough they appear to be in fair agreement with the values obtained by frontal analysis and referenced to naphthalene without a column.

The conclusions presented in this report should be considered tentative since they are based on a limited number of replications of the experiments and because of the effects the system itself may have on the data. Flow rate probably effects the value of K_d but the extent of the effect is uncertain. The maximum flow velocities consistent with the system reaching equilibrium need to be established. The values obtained from one column to another are not as reproducible as is desirable and this will have to be improved before the column technique can be applied widely. Concentration does not seem to be a factor in determining the K_d but a greater number of experiments are needed to verify this.

The effects of particle size and uniformity and column dimensions could not be addressed in this study because of time limitations.

TABLE 4. SORPTION COEFFICIENTS DETERMINED BY PULSE DISPLACEMENT

Compound	Flow Rate (mL/min)	K_d(mL/g)
Trichloroethylene	0.2	0.054
	0.2	0.057
Naphthalene	1.5	0.28
	1.5	0.34
	1.0	0.31
	0.5	0.31

SECTION VI

RECOMMENDATIONS

The information presented in this report indicates that a much better understanding of the effects of the various operational parameters is required before the column technique for determining sorption coefficients merits widespread use. Specifically it is recommended that:

1. The system should be redesigned to eliminate the potential effect of sorption by the system on the values of K_d.
2. The effects of flow rate on sorption coefficients should be re-examined using values below 0.1 mL/min or, if different size columns are used, below the linear flow velocity which this flow rate represents in the current study.
3. Additional columns should be prepared and evaluated until a technique is found to give reproducible column characteristics.
4. Additional evidence for the absence of a concentration effect should be obtained by evaluating a larger number of compounds over a wider range of concentrations.
5. The original objectives of this study, which could not be addressed due to time limitations, should be extensively investigated.

LITERATURE CITED

1. Ainsworth, C. C., R. A. Griffin, I. G. Krapac, and W. R. Roy, "Use of Batch Adsorption Procedures for Designing Earthen Liners for Landfills," Land Disposal of Hazardous Waste, Proceedings of the Tenth Annual Research Symposium at Ft. Mitchell, Ky., April 3-5, 1984, Municipal Enviornmental Research Laboratory, Office of Research and Development, U. S. Environmental Protection Agency, Cincinnati, Ohio, EPA-600/9-84-007, April 1984, pp 154-161.

2. Goerlitz, D. F., "A Column Technique for Determining Sorption of Organic Solutes of the Lithological Structure of Aquifers," Bull. Environ. Contam. Toxicol. 32, pp 37-44 (1984).

3. Rao, P. S. C. and J. M. Dividson, "Adsorption and Movement of Selected Pesticides at High Concentrations in Soils," Water Resources 13, pp 375-380 (1979).

4. Nkedi-Kizza, P., P. S. C. Rao, and A. G. Hornsby, "The Influence of Organic Co-solvents on Leaching of Hydrophobic Organic Chemicals Through Soils," Env. Sci. and Tech. In Review; Personal Communication, 1985.

5. Schwarzenbach, Rene P. and John Westall, "Transport of Nonpolar Organic Compounds from Surface Water to Groundwater. Laboratory Sorption Studies," Env. Sci. and Tech. 15, pp 1360-1367 (1981).

6. Piwoni, Marv, Mini-Conference on Soil Sorption Phenomena, Tyndall Air Force Base FL, June 1985.

7. Allison, L. E., "Organic Carbon" in Methods of Soil Analysis; Part 2. Chemical and Microbiological Properties, C. A. Black et al. (eds), Am. Soc. of Agronomy (1965).

8. Instruction Manual for Flowsorb Model 2300, P/N: 230/42801/00, Micromeritics, 5680 Goshen Springs Rd., Norcross, Ga. 30093, 14 March 1984.

1985 USAF-UES SUMMER FACULTY RESEARCH PROGRAM/

GRADUATE STUDENT SUMMER SUPPORT PROGRAM

Sponsored by the

AIR FORCE OFFICE OF SCIENTIFIC RESEARCH

Conducted by the

UNIVERSAL ENERGY SYSTEMS, INC.

FINAL REPORT

DIPOLE MOMENT OF InP IN THE MELT

Prepared by:	David R. Cochran
Academic Rank:	Assistant Professor
Department and	Electrical and Computer Engineering Department
University:	Clemson University
Research Location:	Rome Air Development Center
	Hanscom AFB
	Solid State Sciences Division
	Electromagnetic Materials Technology Branch
	Electronic Materials Section
USAF Research:	James Singletery, Captain, USAF
Date:	23 July 1985
Contract No:	F49620-85-C-0013

DIPOLE MOMENT OF InP IN THE MELT

by

David R. Cochran

ABSTRACT

The properties of devices are strongly dependent on the quality of the material in which they are fabricated. The properties of these materials, in turn, are directly related to their nature in the molten state and the conditions on the melt from which they are pulled. The basis of this project was the examination of one of the properties of liquid InP, namely, its dipole moment. The determination of this property is expected to yield information for modeling the growth of InP. The experimental design involved the measurement of the static dielectric constant using a form of the heterodyne beat method. The analysis model was the Debye model for polarization of a molecule, having a permanent dipole moment, in a dilute solution of the molecule in a non-polar solvent.

ACKNOWLEDGEMENTS

This research was performed in collaboration with James Singletery, Captain, USAF, and assisted by the Electronic Materials Section of the Solid State Sciences Division of Rome Air Development Center, Hanscom AFB, MA. The research was sponsored by the Air Force Office of Scientific Research/AFSC, United State Air Force, under Contract F49620-85-C-0013.

1. INTRODUCTION

Dr. David R. Cochran is an Assistant Professor of Electrical and Computer Engineering at Clemson University. He is a member of the IEEE professional societies on Electron Devices and Quantum Electronics, and he is also a member of the National and South Carolina Society of Professional Engineers. He is a registered professional engineer in the state of South Carolina.

The teaching and research interests of Dr. Cochran include semiconductor device reliability, solid state electronics, quantum electronics, fiber optics and fiber optic sensors. As an investigator, Dr. Cochran has recently completed contracts on subharmonic signal generation and the development of methods and procedures for comparing electronic component technology. He also developed courses in the area of electro-optics. His research has included material depth profiling utilizing Auger spectroscopy, and the analysis of the effect of nonparabolicity on the surface statistics of narrow-gap zincblende semiconductors. As a Research Scientist at Vought Corporation, Dr. Cochran was responsible for the oxide reduction of thin films of VO_2 to V_2O_3 and the subsequent measurement of the quality of the V_2O_3 films.

The Electronic Materials Section, ESM, of Rome Air Development Center, RADC, at Hanscom AFB, MA is involved in the investigation of indium phosphide, InP, for use in electronic and opto-electronic devices. InP is a III-V material whose material properties are

similar to the narrow-gap zincblende semiconductor that Dr. Cochran has previously investigated. For use in devices, the InP substrates need to be semi-insulating and as defect free as possible. A major area of research at ESM is the fabrication of defect free substrates. This requires investigation of InP in its molten form. The project now under study is the investigation of the dipole moment of an InP molecule in the liquid state. This project would be appropriate for any investigator in the area of solid state physics, chemistry or electrical engineering, or the areas involved with magnetohydrodynamics.

II. OBJECTIVES

The goal of this research effort was the measurement of the dipole moment of InP in its molten state. The successful completion of this project was expected to provide additional information on the properties of InP in the melt at temperatures near the melting point. This data may aid in the determination of the condition of the InP just prior to crystallization. Studies on the viscosity of InP in the liquid state [1] have indicated that InP forms clusters prior to crystallization. The data on the dipole moment may also indicate the usefulness of applying an electric field during growth from the melt to obtain defect-free material. Investigations have shown that an applied magnetic field provides a non-random temperature distribution in the melt [2-6]. Here it is assumed that the uniform conditions of the melt provides uniformity in the pulled crystal, hence, less defects.

III. BACKGROUND

The demands of an expanding technology require the development of novel electronic devices utilizing standard silicon technology, or the use of variations of the standard device configurations based on new materials such as GaAs and InP. The basic properties of these new materials indicate that they are a faster medium than silicon. In addition, the emergence of lightwave technology has accelerated the investigation of these material technologies beginning with the development of optical systems based on GaAs. However, with the optimal transmission characteristics of lightwave systems located at wavelengths longer than GaAs sources and Si detectors, device technology has moved towards systems based on InP.

Today silicon is a mature technology. The fabrication of semi-insulating silicon substrates for a myriad of device applications is well developed. Such substrates in the GaAs and InP technologies have not yet reached a stable foundation for device applications. As part of their mission directives, ESM is charged with the investigation of the fabrication of InP both from the melt and in epitaxial form. To this end, the investigation of defect free substrates is a major part of the research conducted at the RADC facilities at Hanscom AFB, MA.

In order to advance the state-of-the-art in the growth of epitaxial layers, defect free semi-insulating substrates of InP are required. These substrates are fabricated from their liquid form,

which necessitates the investigation of the properties of InP in its molten form to understand and subsequently control the process by which InP crystalizes. One property of InP in the liquid state is the dipole moment of an InP molecule.

B. Dipole Moment

The dipole moment of a molecule can be determined in several different fashions. Most of these methods measure the dielectric constant of the medium, in this case, liquid InP. The dielectric constant is considered by examining the polarization resulting from the application of an electric field. The polarization is defined in terms of a polarization vector which has units of dipole moment per unit volume. This polarization vector is due both to permanent dipole moments and induced dipole moments.

In a material, an applied electric field will act on the medium to induce a polarization on a molecule. Since each molecule is polarized, the molecules as a whole forming the medium will act on individual molecules. Consider a small cavity in a dielectric medium between two plates in which an electric field is applied. The force involved can be divided into three components: 1) the force due to the charge density on the plates which is due to the externally applied field, 2) the force due to the polarization outside the cavity, and 3) the force due to the material inside the cavity. Neglecting the force inside the cavity, one can obtain the Clausis-Mosotti equation: [7-10]

$$\frac{\varepsilon-1}{\varepsilon+2}\frac{M}{\rho} = \frac{4\pi}{3}N\alpha \qquad (1)$$

where ε is the dielectric constant, M is the molecular weight, ρ is the density of the dielectric medium, N is Avogadro's number, and α is the polarizability of the molecule. The polarizability is an indication of the molecules tendency to form an induced dipole upon application of an electric field.

In the above case, permanent dipoles were not considered. To incorporate these dipoles into the system, consider the cavity to have a permanent dipole moment, μ, with the molecule regarded as a rigid system of charges. The potential energy of a molecule due to an applied electric field, E, at an angle Θ to the moment is

$$u = -\mu E \cos\Theta. \qquad (2)$$

Since the orientations of all the permanent dipole moments are not at the angle Θ but are distributed, the Maxwell-Boltzman distribution law can be used to find an average moment of one molecule. This average moment, $\bar{m}$, in the classical Debye theory is given by [8,9]

$$\bar{m} = \frac{\mu}{3}L(\mu E/3kT) \qquad (3)$$

where L(x) is the langevin function defined by [8,9]

$$L(x) = \coth x - \frac{1}{x} . \qquad (4)$$

For $\mu E/3kT \ll 1$, the average moment becomes

$$\bar{m} = \frac{\mu^2}{3kT}E . \qquad (5)$$

The relationship between the dielectric constant and the permanent dipole moment including the induced moment becomes in the Debye

form [7-10]

$$\frac{\varepsilon-1}{\varepsilon+2}\frac{M}{\rho} = \frac{4\pi}{3}N\left(\alpha + \frac{\mu^2}{3kT}\right). \quad (6)$$

The Debye equation is strictly valid for dilute gases, but may be applied to dilute solutions of liquids.

The theory of dielectric constant has been examined in variations of the Debye model by Onsager, Kirkwood, Frohlich and many others [7-25]. These further studies expand the model in various ways such as considering ellipsoidal rather than spherical molecules, considering the problem using a statistical-mechanical approach, and formulating general expressions to include the interactions or correlations of dipole moments.

As stated earlier, the Debye model is applicable for dilute gases. For a dilute amount of solute in a solvent, the Debye model can also be applied since the small amount of solute lends itself to little interaction of the solute molecules. The solvent should be a non-polar fluid insuring no permanent dipole moment in the solvent. It is the permanent dipole moment of the solute that is measured using the expression [10]

$$\frac{\varepsilon-1}{\varepsilon+2}\,\frac{f_1M_1+f_2M_2}{\rho} = f_1R_1 + f_2R_2 \quad (7)$$

with

$$R_1 = \frac{4\pi\alpha_1}{3}N \quad (8)$$

$$R_2 = \frac{4\pi}{3}N\left(\alpha_2 + \frac{\mu_2^2}{3kT}\right) \quad (9)$$

$$f_1 = \frac{n_1}{n_1+n_2} \quad (10)$$

$$f_2 = \frac{n_2}{n_1 + n_2} \qquad (11)$$

where the subscripts 1, 2 refer to solvent and solute, respectively, n_i are the number of molecules per unit volume, ε is the dielectric constant of the solution, and ρ is the density of the solution. This expression can yield μ_2 by making measurements of ε for small values of f_2 as a function of temperature. This data extrapolated to k_1, equal to zero will yield μ_2.

A molecule can have a permanent dipole moment only if it does not have inversion symmetry. As a first experimental attempt to determine the dipole moment of InP by measuring the static dielectric constant of a solution, In will be taken as the solvent with small amounts of InP dissolved in it. Difficulties may arise since In is a metal.

IV. EXPERIMENTAL METHODS

The experimental methods for the determination of the dipole moment can be divided into two categories: those that use static dielectric constant measurements, and those that do not involve the measurement of the static dielectric constants.

A. Non Static Measurements

The Stark effect can be used in microwave spectroscopy to measure the permanent electric dipole moment. This is based upon the shift in the energy levels that occurs upon application of an electric field to a molecular system. The absorption line of the molecule is examined. Since an application of an electric field changes the energy states, a change in the frequency of absorption

occurs which is directly related to μ^2.

Microwave absorption can also be used by measuring the real and imaginary parts of the complex dielectric function in terms of a dielectric relaxation time. The ratio of the imaginary part to the real part of the dielectric function is called the loss tangent, tan δ, and is given by [8,9]

$$\tan\delta = \frac{\varepsilon''}{\varepsilon'} = \frac{(\varepsilon'+2)}{\varepsilon'} \frac{4\pi N c \mu^2}{27 k T} \frac{\omega\tau}{1+\omega^2\tau^2} \qquad (12)$$

with

$$\mathcal{E} = \varepsilon' + i\varepsilon'' \qquad (13)$$

where c is the speed of light, k is Boltzmann's constant, T is the temperature in degrees Kelvin, τ is the dielectric relaxation time, and ω the frequency. Measuring the loss tangent, through index of refraction and absorption measurements, at two frequencies allows the determination of τ which when applied to one of the measured loss tangents produces the dipole moment, μ.

Another method that utilizes the energy of a molecule in an applied field is the molecular beam method. In this method, a collimated beam of molecules generated from a heated source travels through a series of electric fields created by fixed plates. The transition occurring in the energy states is related to a frequency whose measurement in a known electric field yields the dipole moment if the moment of inertia of the molecule is known.

These are but a few of the techniques available for examining

the dipole moment without measuring the static dielectric constant [7-9, 26-33].

B. Static Measurements

The measurement of the dipole moment from the static dielectric constant usually involves the determination an unknown capacitance. This unknown capacitance is the capacitance of a cell whose dielectric is a molecular compound under study in liquid or gaseous form. These cells have a variety of different forms [8,9]. Three of the different ways this capacitance can be found are the capacitance bridge method, the resonance method and the heterodyne beat method [8,9].

The heterodyne method was chosen for this project. Two signal generators are employed; one with a fixed reference frequency, f_o, and one with a variable frequency dependent upon the capacitance of the cell. The capacitance that forms the variable frequency generator consists of the cell, C_o, in series with a parallel combination of a fixed capacitance, C_1, and a variable capacitance. Initially, the cell is filled with air as its dielectric, and the variable capacitance is adjusted to C_2 so that the frequency from the cell arrangement has frequency, f_o. This is accomplished by mixing the two signals from the generators and then filtering to examine the difference signal. The variable generator is adjusted to f_o by changing the variable capacitor until the difference signal is zero. After adjusting for the air-filled cell, the cell is

filled with the solution, thus changing its capacitance. This results in a change of the variable frequency from f_o, noted by a non-zero difference frequency. The variable capacitor, C_2, is then changed by an amount ΔC_2 to re-establish the frequency, f_o. The change ΔC_2 is related to the change in the cell capacitance, ΔC, by [30]

$$\Delta C = \frac{-\Delta C_2 C_o}{(C_1+C_2)^2 + \Delta C_2 (C_o + C_1 + C_2)} \qquad (14)$$

Since the dimensions of the cell are not changed, the dielectric constant, ε, of the solution is given by

$$\varepsilon = \frac{C_o + \Delta C}{C_o} \qquad (15)$$

with the result

$$\varepsilon - 1 = \frac{\Delta C}{C_o} = \frac{-\Delta C_2}{(C_1+C_2)^2 + \Delta C_2 (C_o + C_1 + C_2)} \qquad (16)$$

The fixed frequency, f_o, is set to 1 kHz making the measured dielectric constant the static dielectric constant for all practical purposes. Making the capacitance measurements for a range of concentrations of InP in a solvent as a function of temperature will produce the dipole moment using equations (7-11) and (16).

The measurement cell consists of a modification to the normal crucible configuration used to grow InP from the melt. This arrangement consists of polycrystalline indium phosphide covered by a B_2O_3 cap to contain the phoshorous in the melt. The B_2O_3 cap is liquid at the measurement temperatures but it does not mix with the In solution. The pulling shaft is modified to hold an electrode

plate and a plate is attached to the bottom of the crucible in this design. The effective capacitances of the crucible and the B_2O_3 cap will be taken into account in the calibration procedures. If more exact measurements of the cell design are required, special ampoules for the In-InP solution can be fabricated. Some of the properties of InP in the melt such as resistivity, design, and viscosity have been measured [34-38]. This data will be applied where needed.

V. LIMITATIONS

A. State of the Project

At the present, the experimental set-up is still in construction. This is due to the procurement system which, beginning with the identification of the minor electronic parts necessary, it has taken six weeks to obtain these parts. Any work that is not completed in the ten week period will probably be completed by Captain Singletery.

B. Aspects of the Research Approach

Indium is taken as the solvent since an indium molecular system has inversion symmetry, hence no permanent dipole moment. For the usual measurement of a dipole moment, compounds like benzene are taken as the solvents; however, at the melting point of the InP these compounds are in their gaseous state. Indium is a metal. With no InP added to the indium solution, the capacitance of the cell should be the series capacitance of the B_2O_3 cap and the crucible.

It is felt that the small amounts of InP added will give the indium solution sufficient capacitance to alter the frequency of the variable generator to provide a measureable dielectric constant. Experimentation will determine this point. If the metallic properties of In make this procedure unuseable, then In_2Te_3 can be used as the solvent. In its liquid form, In_2Te_3 is a semiconductor which should provide a capacitance for the cell. Unfortunately, it should also be a polar compound. A recent method using polar solvents in a limiting fashion has been reported [18]. However, this method requires the measurement of more parameters.

It has been reported that III-V compounds are metallic in the liquid state though they are semiconductors as solids [39-42]. For a metal, the dielectric function is considered in terms of a potential screening function [43-47]. Its physical significance is somewhat different than that for a dielectric at low frequencies. Thus, this experimentation should yield more information on the nature of InP in the liquid state. Should the measurement of the dipole moment of InP in the designed system be unattainable, a more elaborate means can be devised.

VI. RECOMMENDATIONS

A. Implementation of Results

Since the dipole moment is related to bonding, this data should be examined in conjunction with the data on viscosity, density, and resistivity to model the state of InP in the melt.

Given the approximate magnitude of the dipole moment, the feasibility of using an applied electric field interacting with the dipole moment to control the melt conditions during crystal growth should also be investigated.

B. Suggestions for Follow-on Research

Investigations of the utilization of applied electric fields in the growth of epitaxial layers and substrates of other materials have been made [48-51]. As a direct follow-on to the research on dipole moments, the effects of an electric field on the growth of InP from the melt based on phenomenological properties other than the dipole moment should also be examined. The data base on liquid properties of InP should be verified and expanded. In addition, numerical simulations of the growth of InP should be performed for applied magnetic fields, for applied electric fields and currents, and for applied magnetic and electric fields to examine the various effects on the thermodynamics of the InP melt.

C. Suggestions for Related Research

There are various other aspects related to the fabrication of device quality InP-based materials. For growth of epitaxial layers, the substrates must be processed through a surface preparation step, using different cleaning solutions. Not all "recipes" yield the same quality surface. A useful project would therefore entail the surface analysis of the substrates using techniques such as Auger spectroscopy, scanning electron microscopy, energy dispersive

x-ray analysis, etc. for different types of cleansing procedures.

Once a substrate is prepared, an epitaxial layer of a ternary or quaternary lattice matched to the InP substrate is grown. The relationship between lattice matching, the quality of device material, stress, and the optical and electronic properties of the epitaxial layer should be further examined.

Many of the InP materials will be used in optical systems as sources, detectors, or modulators. The data on the optical properties of the InP family of materials should be expanded for a wider range of light energies and doping characteristics then presently available. In addition, the nonlinear optical properties of InP should be given further investigation.

REFERENCES

1. Glazov, V.M., "Structural Analysis by the Cluster Model of Indium Phosphide in the Pre-crystallization Period," Russian J. of Physical Chemistry, 1977, Vol. 51 (10), pp. 1492-1493.
2. Miheleic, M. and Wingerath, K., "Numerical Simulations of the Czochralski Bulk Flow in an Axial Magnetic Field: Effects on the Flow and Temperature Oscillations in the Melt," J. of Crystal Growth, 1985, Vol. 71, pp. 163-168.
3. Hirata, H. and Inque, N., "Study of Thermal Symmetry in Czochralski Silicon Melt under a Vertical Magnetic Field," Jap. J. of Applied Physics, 1984, Vol. 23, pp. L527-L530.
4. Kuroda, E., Kozuka, H. and Takano, Y., "The Effect of Temperature Oscillations of the Growth Interface on Crystal Perfection," J. of Crystal Growth, 1984, Vol. 68, pp. 613-623.
5. Oreper, G.M. and Szekely, J., "The Effect of an Externally Imposed Magnetic Field on Buoyancy Driven Flow in a Rectangular Cavity," J. of Crystal Growth, 1983, Vol. 64, pp. 505-510.
6. Langlois, W.E. and Lee, K., "Czochralski Crystal Growth in an Axial Magnetic Field: Effects of Joule Heating," J. of Crystal Growth, 1983, Vol. 62, pp. 481-486.
7. Bottcher, C.J.F., Theory of Electric Polarization, Volume I, Amsterdam, Elsevier Scientific Publishing Company, 1973.
8. Hill, N.E., Vaughan, W.E., Price, A.H., Davies, M., Dielectric Properties and Molecular Behavior, London, Van Nostrand Reinhold Company, 1969.

9. Smith, J.W., Electric Dipole Moments, London, Butterworth Scientific Publications, 1955.

10. Van Vleck, J.H., The Theory of Electric and Magnetic Susceptibilities, Oxford University Press, 1932.

11. Felderhof, B.U., "Electrohydrodynamic Effects in Dielectric Relaxation," Molecular Physics, 1984, Vol. 51 (3), pp. 813-824.

12. Omini, M., "A Theory of Electric Polarization in Liquids. I Nonpolar Liquids," Physica, 1976, Vol. 83A, pp. 431-453.

13. Omini, M., "A Theory of Electric Polarization in Liquids. II Polar Liquids," Physica, 1976, Vol. 84A, pp. 129-142.

14. Omini, M. "A Theory of Electric Polarization in Liquids. III Dielectric Relaxation," Physica, 1976, Vol. 84A, pp. 492-506.

15. Omini, M. "A Theory of Electric Polarization in Liquids. IV Discussion of the Approximations," Physica, 1977, Vol. 88A, pp. 478-496.

16. Anderson, J.E. and Ullmen, R., "Molecular Relaxation in a Fluctuating Environment," J. of Chemical Physics, 1967, Vol. 47 (6), pp. 2178-2184.

17. Gurikov, Yu. V., "The Orientation Van Der Waals Interactions in Polar Liquids," Russian J. of Physical Chemistry, 1983, Vol. 57 (2), pp. 263-264.

18. Malecki, J, Nowak, J., and Balanicka, S., J. of Physical Chemistry, 1984, Vol. 88, p. 4148-4152.

19. Bossis, G., "Real Dipolar Moment Associated with an Ellipsoidal Polar Molecule and the Static Dielectric Constant of Mixtures of Polar and Non-Polar Liquids," Molecular Physics, 1982, Vol. 47 (6), pp. 1317-1332.

20. Brot, C., "Anisometric Molecules in Dense Fluids IV. The Static Permittivity of Solutions and Neat Liquids of Ellipsoidal Polar Molecules: Extension of the Onsager Model," Molecular Physics, 1983, Vol. 45 (3), pp. 543-552.

21. Neumann, M., Steinhauses, O., and Pawley, G.S., "Consistent Calculation of the Static and Frequency-Dependent Dielectric Constant in Computer Simulations," Molecular Physics, 1984, Vol. 52 (1), pp. 97-113.

22. Banyai, L. and Gartner, PO., "Clausius-Mosotti Limit of the Quantum Theory of the Electronic Dielectric Constant," Physical Review B, 1984, Vol. 29 (2), pp. 728-734.

23. Adams, D.J., "Computer Simulation Study of Polar Liquids: Static and Dynamic Properties," Proc. of Royal Society of London A, 1984, Vol. 394, pp. 137-160.

24. Stiles, P.J. and Hubbard, J.B., "Polarization Diffusion and Dielectric Friction in Polar Liquids," 1984, Chemical Physics, Vol. 84, pp. 431-439.

25. Bordewijk, P., "On the Separation of Long-Range and Short-Range Dipole Correlations in Polar Fluids," 1978, Chemical Physics, Vol. 33, pp. 451-464.

26. Bottcher, C.J.F. and Bordewijk, P., Theory of Electric Polarization, Volume II, Amsterdam, Elsevier Scientific Publishing Company, 1978.

27. Davies, M., ed., Dielectric and Related Molecular Processes, Volume I, London, The Chemical Society Burlington House, 1972.

28. Davies, M., ed., Dielectric and Related Molecular Processes, Volume II, London, The Chemical Society Burlington House, 1975.

29. McClellan, A.L., Tables of Experimental Dipole Moments, San Francisco, W.H. Freeman and Company, 1963.

30. Zahn, C.T., "The Electric Moment of Gaseous Molecules of Halogen Hydrides," Physical Review 1924, Vol. 24, pp. 400-417.

31. Whiffen, D.H., Thompson, H.W., "Measurements on the Absorption of Microwaves. I.", Transactions of Faraday Society, 1946, Vol. 42A, pp. 114-122.

32. Whiffen, D.H., and Thompson, H.W., "Measurements on the Absorption of Microwaves. II.," Transactions of Faraday Society, 1946, Vol. 42A, pp. 122-129.

33. Sack, R.A., "On the Frequency Dependene of the Dielectric Constant in Dipolar Solids", Transactions of Faraday Society, 1946, Vol. 42A, pp. 61-66.

34. Glazov, V.M., Davlerov, K., Nashel'skii, A. Ya., Mamedov, M.M., "Thermal Expansion and Volume Change on Melting of Indium Phosphide," Russian Journal of Physical Chemistry, 1977, Vol. 51 (10), pp. 2558-2562.

35. Glazov, V.M., Nashel'skii, A. Ya., Rzaev, R.F., and Mamedov, M.M., "Investigation of Electrical Properties of Indium Phosphide at High Temperatures Including Liquid Range," Soviet Physics of Semiconductors, 1976, Vol. 10 (5), p. 498-501.

36. Glazov, V.M. and Kiseler, A.I., "Solubility and Interaction of Donor and Acceptor Doping Elements in Indium Phosphide," Russian Journal of Physical Chemistry, 1977, Vol. 51 (8), pp. 1148-1150.

37. Glazov, V.M., Dovletov, K., Nashel'skii, A. Ya., and Mamedov, M.M., "Changes of Short-Range-Order Structure in Fused InP on Heating" Translation from Izvestiya Akademii Nauk SSSR, Neorganicheskie Materialy, 1977, Vol. 13 (1), pp. 34-37.

38. Regel, A.R. and Glazov, V.M., "Structure Defects in Molten Semiconductors (Review)," Soviet Physics of Semiconductors, 1983, Vol. 17 (10), pp. 1105-1116.

39. Glazov, V.M., Chizhenskaya, S.M. Glagoleva, N.N., Liquid Semiconductors, New York, Plenum Press, 1969.

40. Cutler, M., Liquid Semiconductors, New York, Academic Press, 1977.

41. Allgaier, R.S., "Interpretation of Transport Measurements in Electronically Conducting Liquids," Physical Review, 1969, Vol. 185 (1), pp. 227-244.

42. Allgaier, R.S., "Interpretation of Transport Measurements in Electronically Conducting Liquids. II Hall Mobility," Physical Review B, 1970, Vol. 2 (6), p. 2257-2259.

43. Shimaji, M., Liquid Metals, New York, Academic Press, 1977.

44. March, N.H., Liquid Metals, Oxford, Pergamon Press, 1968.

45. Ziman, Z.M., Principles of the Theory of Solids, Cambridge University Press, 1972.

46. Ziman, Z.M., ed., The Physics of Metals .I Electrons, Cambridge University Press, 1969.

47. Sturm, K., "Core Polarization in Dielectric Response of Simple Metals," Solid State Communication, 1983, Vol. 48 (1), pp. 29-32.

48. Wargo, M.J., and Witt, A.F., "Numerical Modelling of Electirc Current Induced Growth Layers Generated During Czochralski Pulling," J. of Crystal Growth, 1984, Vol. 66, pp. 541-546.

49. Yang, X.F., Huang, L., and Gatos, H.C., "Selective Epitaxial Growth of GaAs by Liquid Phase Electroepitaxy," J. of Electrochemical Society, 1982, Vol. 129 (1), pp. 194-197.

50. Jastrzebski, L., Imamura, Y., and Gatos, H.C., "Thickness Uniformity of GaAs Layers Grown by Electroepitaxy," J. of Electrochemical Society, 1978, Vol. 125 (7), pp. 1140-1146.

51. Kumagawa, M., Witt, A.F., Lichtensteiger, M., and Gatos, H.C., "Current-Controlled Growth and Dopant Modulation in Liquid Phase Epitaxy," J. of Electrochemical Society, 1973, Vol. 120 (4), pp. 583-584.

1985 USAF-UES SUMMER FACULTY RESEARCH PROGRAM/
GRADUATE STUDENT SUMMER SUPPORT PROGRAM

Sponsored by the

AIR FORCE OFFICE OF SCIENTIFIC RESEARCH

Conducted by the

UNIVERSAL ENERGY SYSTEMS, INC.

FINAL REPORT

LASER RAMAN LABORATORY RESEARCH

Prepared by:	Alvin D. Compaan
Academic Rank:	Professor
Department and University:	Department of Physics Kansas State University
Research Location:	Avionics Lab, AFWAL/AADR Wright-Patterson AFB, OH 45433
USAF Research:	Dr. Dietrich Langer
Date:	August 7, 1985
Contract No:	F49620-85-C-0013

LASER RAMAN LABORATORY RESEARCH

By

Alvin D. Compaan

USAF-UES Summer Faculty Fellow

ABSTRACT

The activities described in this report cover four principal areas: 1) assisting and advising in the setting up of a laser Raman laboratory which had just been moved from another building, 2) pulsed laser annealing of ion-implanted GaAs with an excimer laser, 3) Raman studies on these heavily doped samples, and 4) evaluating possible directions for upgrading the Raman lab. The setting up of the Raman lab involved precision optical alignment of a spectrometer and several lasers and repair of several instruments which were found to be functioning well below specifications. After successful instrumentation intregation in the new lab, Raman data were acquired on a wide range of samples prepared by molecular beam epitaxy, conventional growth, or ion implantation followed by thermal or pulsed excimer-laser anneal. This laser anneal was performed in the author's lab at Kansas State University. Options for upgrading of the Raman laboratory in AFWAL/AADR with multichannel detection capability are also briefly discussed.

I. INTRODUCTION—Scientific Background and Laboratory Interests

My scientific background has centered around the use of lasers to study solids since my Ph.D. work at the University of Chicago (1971). This work was in the field of quantum optics and pulsed laser interactions with insulating crystals. Beginning with my post doctoral work at New York University (1971-73), I have worked in the field of Raman scattering in semiconductors. Since 1980 I have also been active in studies of pulsed laser annealing in semiconductors using pulsed Raman techniques for transient temperature analysis.

My background in laser Raman scattering in semiconductors and in pulsed laser annealing led to my interest in the summer faculty appointment at the AFWAL/AADR Avionics Lab. The need here for an experienced scientist in Raman scattering nicely matched my interest in obtaining better understanding of materials problems associated with electronic devices. Thus, the summer appointment has been mutually beneficial.

II. OBJECTIVES OF THE RESEARCH EFFORT

My research objectives while participating in the USAF-UES Summer Faculty Research Program were the following:

1. To become familiar with fundamental materials problems related to the technology of III-V semiconductor devices and problems of current concern in avionics.
2. To assist in calibrations and alignment of the instruments (esp. lasers and spectrometers) in the new Raman laboratory in Bldg. 620 and to provide advice to other personnel working in this lab.
3. To evaluate the needs and potential advantages of upgrading some of the instruments in the Raman lab for multispectral detection capability.
4. To begin studies of XeCl excimer-laser-annealed, ion-implanted GaAs and GaAlAs.

A further objective developed early on in the summer project. This was to interact strongly with Lt. Chris Leak and provide him sufficient

guidance and training that he could pursue further state-of-the-art Raman studies as independently as possible.

III. ALIGNMENT, CALIBRATION, AND REPAIRS IN THE RAMAN LABORATORY

When I arrived for my summer faculty appointment on May 20, I found that essentially all of the instruments for the Raman lab had been moved over to the new lab in building 620. However, some services (electricity for the lasers, and cooling water) were not yet available. This slowed down our work by several days. Nevertheless, Chris Leak and I began working on the design of the laser focussing and collection optics. This was followed with work on the spectrometer, photomultiplier, photon counting electronics, and lasers as services became available. In the course of this work I found a variety of systems which were either malfunctioning or poorly functioning and optical systems which could be improved significantly by redesigning the layout. The following is a summary of the repairs and improvements which were made with the assistance of Lt. Leak since the laboratory was moved from building 450.

A. Resolution of Cooling Water Problems. Since the Raman lab was the first to try out the recirculating water system for laser cooling we ended up "debugging" the system. (This word may almost be taken literally—the water quality became frightfully dirty and still remains, in my opinion below the standards needed for long-term laser cooling.) The water pressure was alternately too high and too low for several weeks as new systems were added. The situation appears now to have stabilized acceptably with the addition of pressure gauges on input and output lines and a pressure regulator on the input. Unfortunately one expensive laser was damaged before the problems were resolved.

B. Laser Start-Ups. A total of four lasers have been restarted in the Raman lab after the move to building 620—small Spectra Physics Argon, large Spectra Physics Krypton, and two small Coherent Krypton lasers (one of Don Reynolds and one of Bill Theis). In the process I demonstrated to Chris Leak how to "rock" the rear reflector mounts of the Spectral Physics and the Coherent lasers to find the lasing condition. Leak and I also changed the transformer taps in the power

supply of the Coherent laser of Theis to compensate for the high pressure condition of the tube as we found it. I also demonstrated the mirror replacement procedure and Brewster window cleaning. With my pump-out kit sent from Kansas State University we successfully lowered the Kr pressure in the Theis laser from 145mT to the manufacturer's recommended 100mT. This should improve the output power on the red lines (6471, 6764Å).

C. Spex Spectrometer Alignment and Calibration. The wavelength calibration and tracking accuracy of the Spex 1401 were throughly checked. In addition, the spectral response of the Spex + detection system was determined by using a standard (black body) light source (2800K color temperature). This was done with the "new" old PM tube in place (see below). Since much of our Raman work later in the summer involved polarization dependent measurements, we determined the ratio of spectrometer system efficiencies for both horizontal and vertical input polarizations. The response to 2800K black body source is shown in Fig. 1. In the process of making these calibration measurements, I discovered that the detected polarization ratio is quite different for very narrow slits (<20μm) than for the wider slits (~50-500μm) normally used for Raman spectra. I believe this may be due to scattering from the edges of the slits which apparently enhances the throughput for vertically polarized light.

D. Photomultiplier and Electronics Repairs.

—Problems with the PAR discriminator were identified and traced to a shorted chip which has now been replaced.

—The PM tube which had been used for the past several months (years?) was found to have very low sensitivity. One of the two old RCA 31034A tubes was found to be OK (the other is bad). It's sensitivity is better by a factor of nearly 100!

—Upon installation of the "new" tube a complete pulse height distribution from the PM amplifiers was plotted (using the PAR discriminator in the "window" mode). The discriminator threshold could then be set at the optimum location (simultaneously minimizing the dark count and maximizing the photon signal). Settings: Gain "X 0.3."

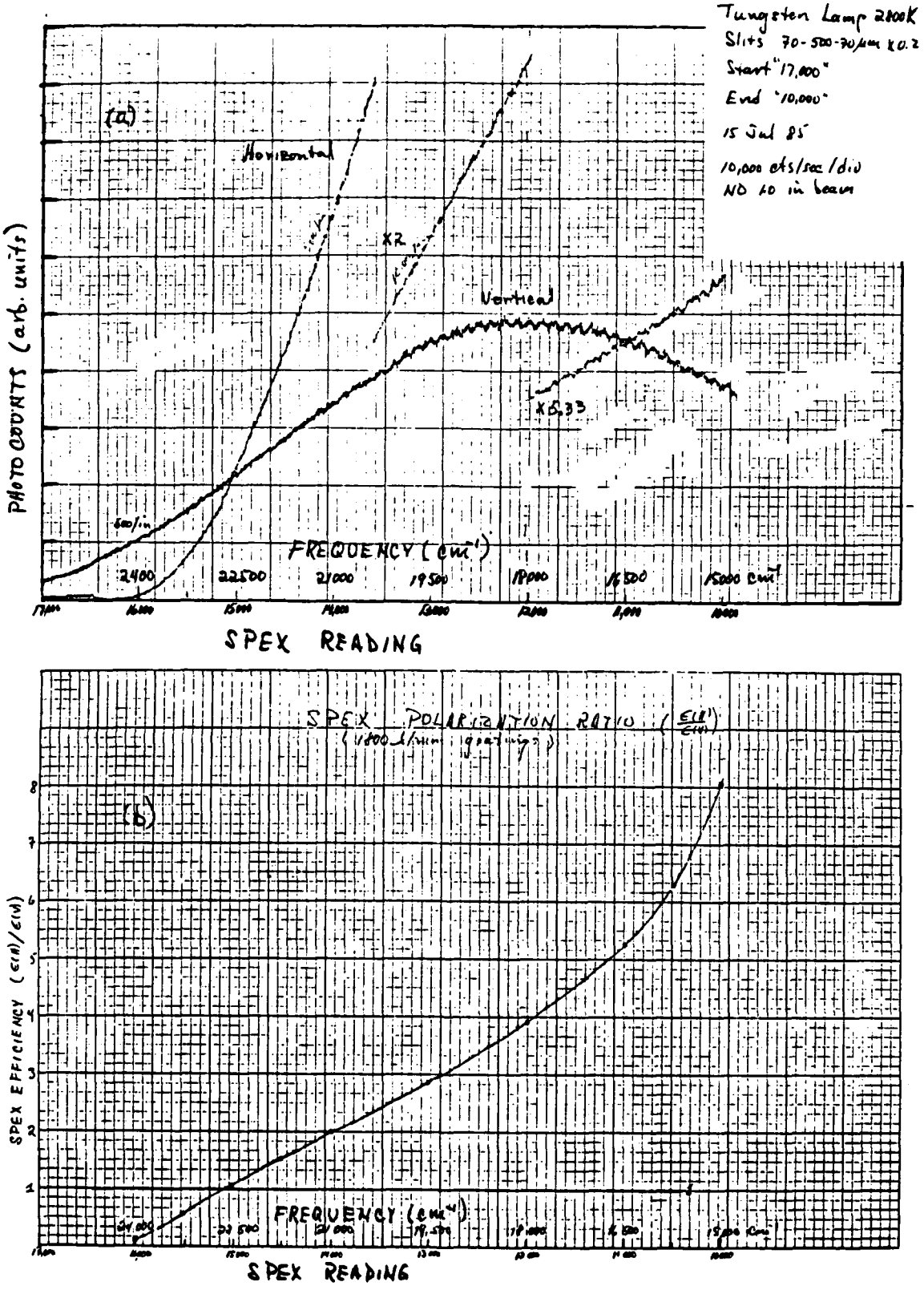

Figure 1. a) Detected signal (photocounts/sec) as a function of frequency for both horizontal and vertical polarizations. Light source was a ~2800K black body (tungsten) lamp, b) Ratio of efficiencies, horizontal to vertical as a function of frequency.

Threshold 2.0, PM voltage 1600V. The plot of count rate vs. threshold setting for a window of 1mVX0.3 is given in Fig. 2.

NOTE: A slight problem still remains with the numerical display of the top counter. The third digit from the right has the 2^2 bit burned out. However the analog output is OK.

—Adjustments were made on the interconnecting cables between counters and the discriminator. Both counters now read the same (except for the problem mentioned above).

—60 cycle hum on the X-Y plotter was greatly reduced by plugging it in to the same outlet strip as the discriminator, PM voltage supply, and counters.

E. Photomultiplier Housing and Lens Assembly.

—The LN_2 vapor-cooled housing had been installed without the floating lens assembly. After checking that the floating lens plus the lens in the insulated window gave a reasonable slit image at the location of the RCA photocathode, we installed the adjustable (floating) lens assembly. This enhanced the signal noticeably.

—There have been some difficulties with the LN_2 control for the PM housing. The valve was replaced and a chip and transitor replaced in the control unit. The valve "chattering" has now stopped. Temperature control is excellent.

—The exit slit of the Spex 1401 was discovered to have a 13μm reading error. That is, the slit reached its minimum width of ~4μm when the micrometer read 17μm. Thus Chris Leak and I reset the zero on this micrometer to read correctly.

F. Laser Focussing Lenses and Filtering.

—The system was set up to focus to a line image. A combination of weak focussing with a 50cm focal length spherical lens at 27cm from the sample and a 10cm focal length cylindrical lens at 78cm from the sample give a good line image on the sample. This line images to a ~1cm height on the entrance slit of the Spec 1401.

—After some searching we located a collection of narrow band ("spike") interference filters which work reasonable well. Their pass bands are not centered on Ar or Kr laser lines so they generally require

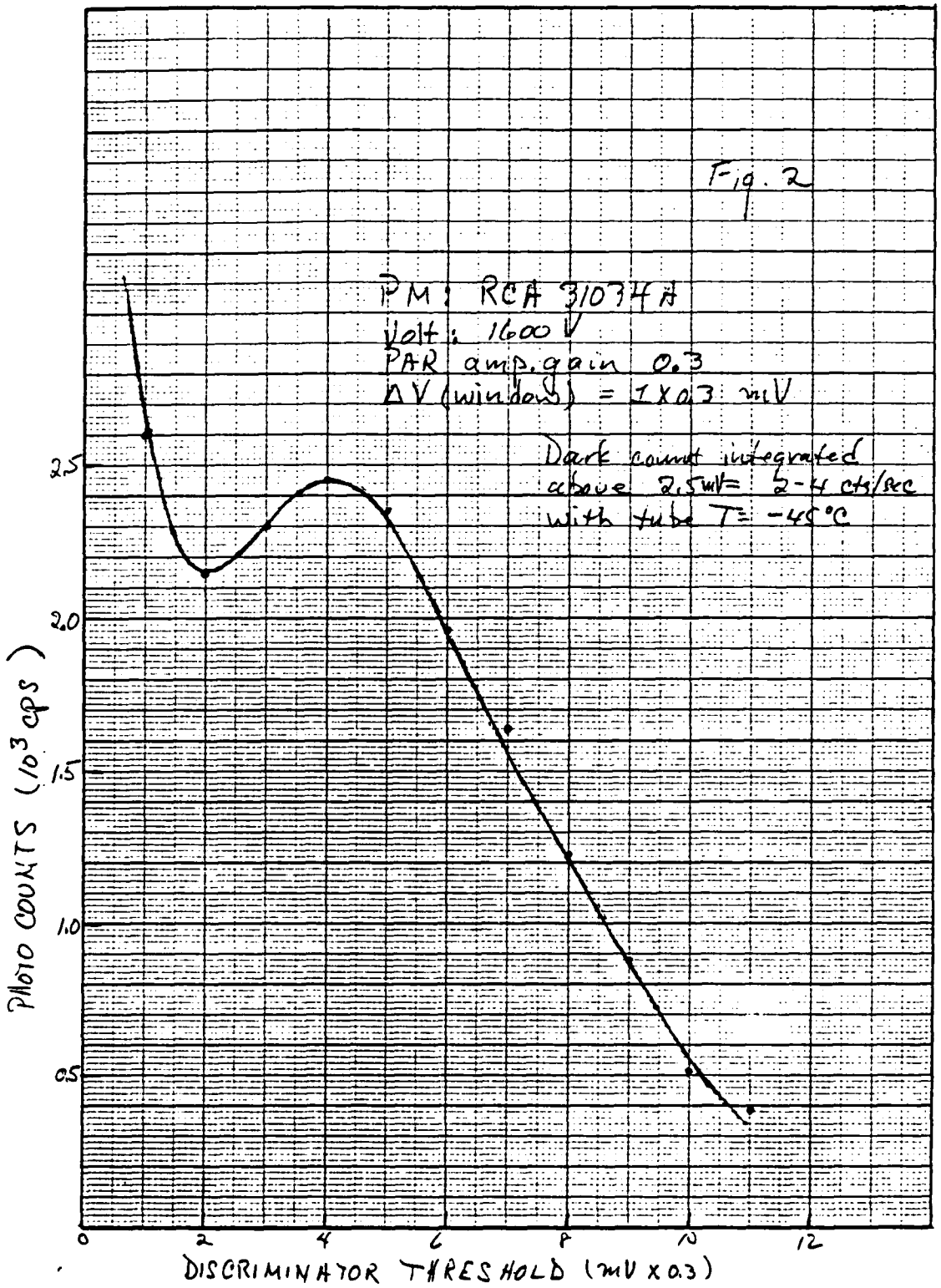

Figure 2. Count rate from a white light source as a function of threshold setting with PAR discriminator in "window" mode. Photomultipler voltage 1600V, gain "X0.3," window width 1.0mV.

a considerable rotation to shift the pass band appropriately. This reduces the throughput in some cases to ~30-35%. The purpose of these "spike" filters is to suppress plasma emission (non-lasing) lines from the laser output. I recommend acquiring several such filters centered on the commonly used laser lines. These are available at modest cost from thin film coating houses such as Melles Griot, Corion, Baird-Atomic, CVI, etc.

—Another solution to the problem of laser plasma lines is to filter with a prism. I recommend acquiring a Pellin-Broca (90° constant deviation) prism for use in rejecting the laser plasma emission lines. We are trying to locate an optical house which manufactures this type of prism.

As a temporary and rather clumsy alternative we set up a 60° prism (borrowed from Don Reynolds) to disperse the laser light. It is important that this be done in a horizontal plane if a vertical line focus is used on the sample. The plasma lines are thus horizontally separated and hence not imaged through the entrance slit of the spectrometer. A sketch of the optical layout is given in Fig. 3.

G. Collection Optics.

—I discovered that the lens most recently used for collection of scattered light had severe spherical aberrations (being a single-element f/2 lens). We are now using a 75mm focal length f/2 compound lens (coated) which works well in combination with a 300mm lens to focus the collimated beam into the entrance slit of the SPEX.

—We are presently looking for a faster collection lens f/1 to f/1.4 to further improve the collection speed.

8. Polarizers and Polarization Rotators.

—We have determined the transmission characteristics of three "Polaroid"-type film polarizers. All three have different efficiencies. The best (a new one) has been mounted on a "Molectron" rotatable mount. Its transmission characteristics are shown in Fig. 4.

—A Fresnel Rhomb-type polarization rotator has been mounted in the laser beam to provide the flexibility of changing the input polarization at the sample. Normally horizontal polarization is chosen at the sample

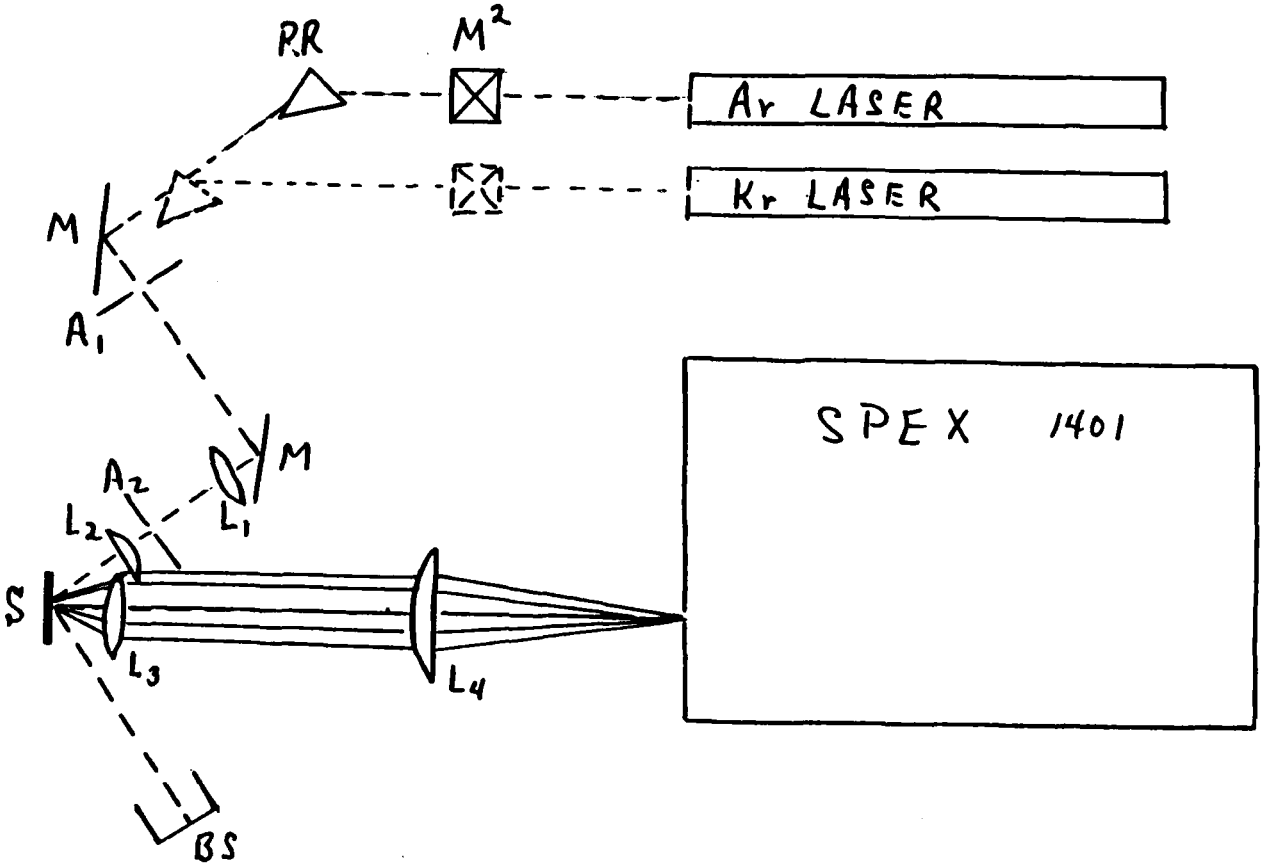

Figure 3. Optical path for laser and scattered light. M^2 is a two mirror combination used to raise the beam height, PR=prism, M=mirror, A_1,A_2=apertures, S=sample, P=Polaroid-type polarizer and lenses L_1 (f=50cm), L_2 (f=10cm, cylindical), L_3 (f=75cm, f/2), L_4 (f=30cm).

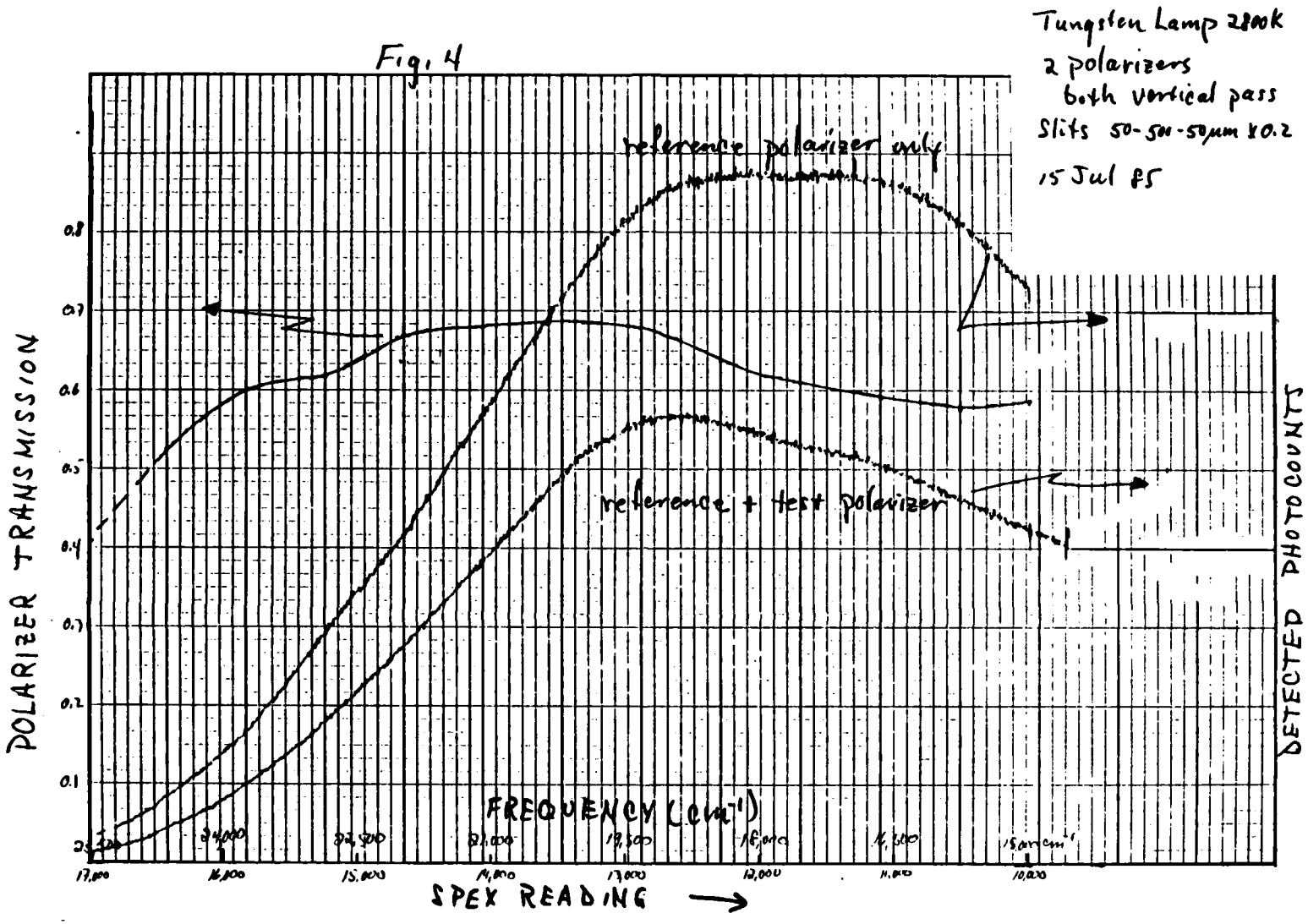

Figure 4. Detected signal for 1 "reference" polarizer and for "reference" plus polarizer chosen for all Raman work with both polarizers vertical. Polarizer transmission is the ratio and is shown by the smooth solid curve.

to maximize coupling of light into the vertically mounted sample. This also maximizes transmission through the prism.

—It is my understanding that a polarization "scrambler" has been ordered. This would be useful to avoid some of the difficulties relating to the polarization-dependent response of the spectrometer.

9. Room Darkening Difficulties. Because the Raman lab shares space with the Fourier transform infrared lab our need for a darkened room hinders the IR work. A room-separating, opaque curtain is an absolute necessity. Theis and Hoelscher have been very generous in adapting to a "lights-out" situation but this should not be necessary. I understand that a curtain has been ordered but as of this writing it remains ephemeral.

IV. EXCIMER LASER ANNEALING OF ION-IMPLANTED GaAs

The XeCl excimer laser in my laboratory at Kansas State University was used to prepare several types of implanted GaAs samples by pulsed laser annealing. This was accomplished during a return trip to KSU from June 10-14, 1985. The samples included several implanted with ^{29}Si with doses from $1X10^{13}$ to $1X10^{15}/cm^2$, others with Te or Mg ions. Some samples were "as-implanted," some capped with Si_3N_4 but otherwise unannealed, some oven-annealed to 850C° while capped. The XeCl laser annealing was done in air at room temperature with natural surfaces and with capped surfaces (i.e., the laser beam penetrated the transparent cap). Typical laser fluences were $0.3J/cm^2$ and $0.6J/cm^2$. The threshold for epitaxial regrowth via the melt phase was first determined to be $\sim 0.2J/cm^2$ by using a series of anneal spots of varying energy and checking by Raman scattering for epitaxial regrowth. This check relies on the Raman polarization selection rules.[1]

The 1/4 x 1/4 inch samples were then annealed by rastering the sample with translation stages to give overlapping spots over a total area ~0.1 in. by 0.25in.

V. RAMAN STUDIES OF LASER-ANNEALED SAMPLES

These samples have been extensively investigated by Raman scattering. We have made a comparison among several samples implanted with ^{29}Si to doses of $2x10^{14}/cm^2$ and $1x10^{13}/cm^2$. For both doses we find that

the samples which were annealed with the Si_3N_4 caps in place show much greater carrier activation than the uncapped samples. Thus the presence of the cap apparently enhances the anneal effectiveness possibly by inhibiting As loss during the melt phase regrowth. We are, however, concerned that there may be some Si or possibly N incorporation from the cap. This effect of capping is present even though at $0.6J/cm^2$ the cap is almost entirely blown off the surface after the annealing raster pattern is completed. Examples of Raman spectra are shown in Fig. 5. Note that with increasing carrier activation the line labeled L^- grows relative to the line labeled LO. This is a well-known behavior which is due to LO (longitudinal optical) phonon screening by the free carrier plasma.[2,3,4] From these spectra we can estimate that the free carrier-density is somewhat greater for $0.6J/cm^2$ than $0.3J/cm^2$ (capped sample) and much greater than for the uncapped sample. Later work on a sister sample annealed at $0.3J/cm^2$ indicated clearly on L^+ plasmon-phonon coupled mode at $\Delta\bar{\nu}\sim 850cm^{-1}$. This is characteristic of a carrier density of $\sim 8x10^{18}/cm^3$.

In order to verify these results and to determine the sign of the charge carriers, Hall effect measurements were made. The results indicated carrier concentrations of $1.7x10^{19}/cm^3$ and $1.4x10^{19}/cm^2$ for $0.3J/cm^2$ and $0.6J/cm^2$ respectively, <u>assuming</u> the carries are limited to a $0.1\mu m$ thick suface layer. Carrier type was negative. The results are summarized in Table 1. The mobility appears to be consistent with that expected (due to ionized impurity scattering) at these carrier concentrations. These concentrations are higher than have been obtained previously for Si-doped GaAs and suggest that further work along these lines may yield encouraging results for producing heavily doped n-type GaAs layers. Some emphasis should be given to the role of and need for the Si_3N_4 cap. Perhaps a proximity cap of quartz or a pressurized ambient might also be effective.

An additional asymmetric peak occurs in the $0.6J/cm^2$ sample spectrum at $\sim 385cm^{-1}$. This position is very close to that observed in high resolution infrared absorption for the Si vibrational local mode in the GaAs lattice.[6] However, the peak is very broad and asymmetric. This is

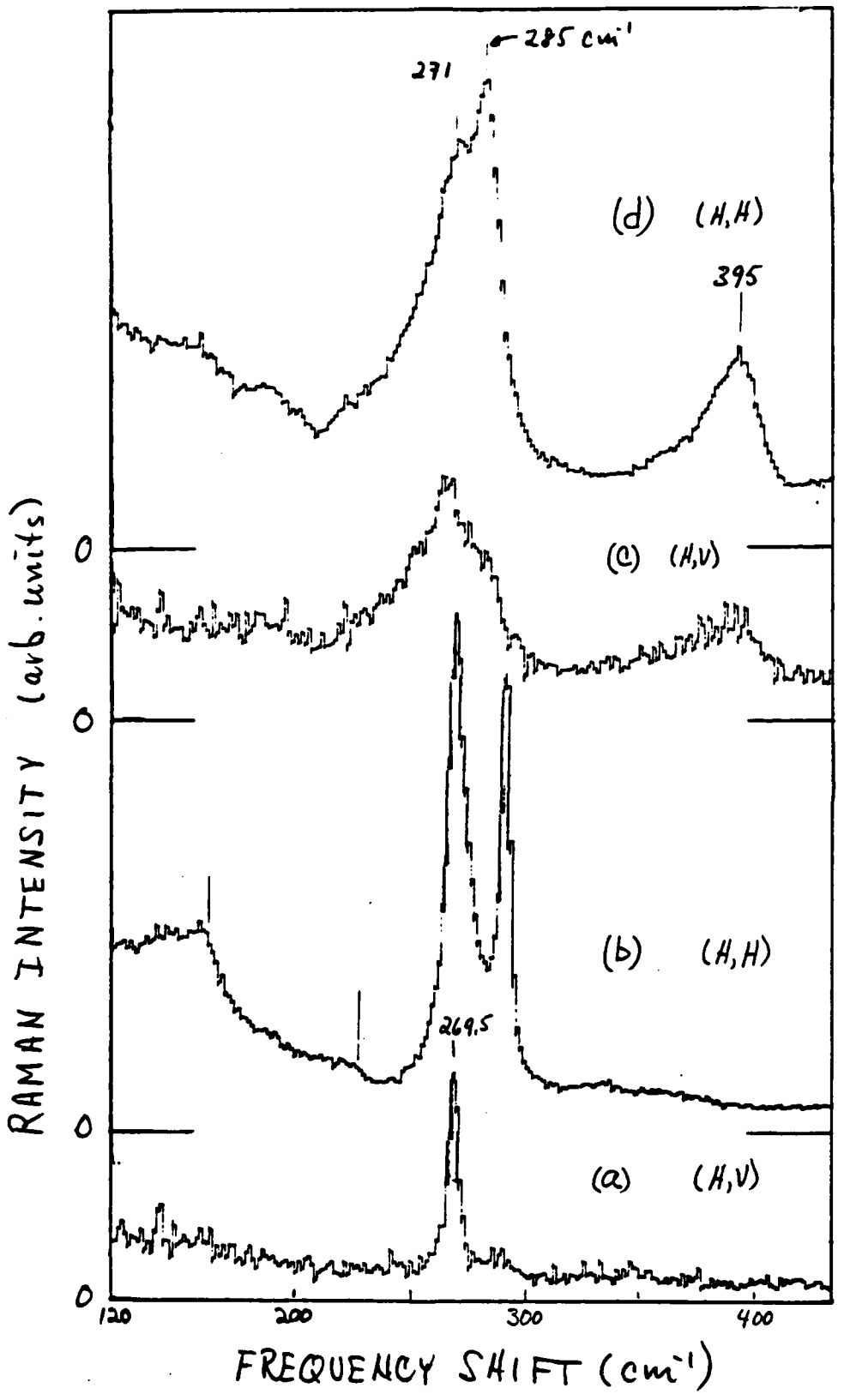

Figure 5. Composite Raman spectra of Si_3N_4 capped GaAs (100 surface) implanted with Si ($3x10^{14}/cm^2$ at 100keV) and XeCl excimer laser annealed (λ=308μm) for two different anneal fluences $0.2J/cm^2$-traces (a) & (b), and $0.5J/cm^2$-traces (c) & (d). Raman source λ=514.5nm, 400mW. Incident, E_i, and scattered, E_s, polarizations are indicated in the notation (E_i, E_s) where H|| [011] and V|| [0$\bar{1}$1].

similar to the behavior of the intrinsic phonon modes, LO & L^-, which is a result of phonon-plasmon interactions.[3,5] We tentatively ascribe this peak to a Si local mode broadened by interaction with the plasma. Some asymmetry may also arise from a distribution of local mode frequencies from various normal modes and different sublattice sites of the Si atoms.

Other samples which had moderate or high carrier concentrations before laser annealing appear to show (from the Raman spectra) a reduction in carrier concentrations after XeCl annealing. All of these samples were annealed capless.

Much of our interpretation of the above results have relied on published Raman studies of several other groups on heavily doped GaAs.[3-5] However, we also checked some of the published results and extended the available data by our own studies on bulk GaAs (Zn-doped ~$3x10^{18}/cm^3$, and Si-doped ~$3x10^{19}/cm^3$). Thus we were able to check the polarization selection rules for the "L^-" and "LO" peaks for both heavy p-type and heavy n-type doping. We find that the normal polarization selection rules[1] are violated in the heavily doped samples. The behavior is similar but not identical to that reported in refs. 3, 4, & 5.

In summary, these preliminary experiments have suggested two interesting results. 1) The first is that pulsed excimer laser annealing may be capable of producing n-type carrier concentrations with reasonable mobilities from ion-implanted Si in GaAs. An essential ingredient appears to be the prevention of changes in surface stoichiometry, e.g., through the use of Si_3N_4 cap during annealing. Other "capping" techniques should also be tried. 2) The second result is that significant changes are seen in the Raman spectra at very high dopant densities. It appears likely that these can be correlated with the carrier density and dopant substitutionality (via vibrational local modes) so that Raman scattering may become a useful nondestructive probe of these properties.

A firm theoretical understanding of the origins of these changes in the Raman peaks is not yet complete. Thus the behavior of the Raman

scattering at high carrier and impurity densities remains an important subject for further research.

VI. OPTIONS FOR INSTRUMENTATION UPGRADES-MULTISPECTRAL DETECTION

The photomultiplier with its photon counting sensitivity is nicely suited to the needs of the double or triple spectrometers necessary for Raman scattering in semiconductors. Being a single element system, however, limits its data acquisition speed. Recently two types of multispectral detectors have become commercially available. The following is a brief synopsis of their characteristics with some notes on their applicability for this Raman lab and the typical studies done in it.

Discussion of multi-element detectors for Raman scattering must begin with the recognition that fully exploiting their capabilities is not possible with the typical double spectrometer. This is a consequence of the fact that the intermediate slit must be opened at least half as wide as the dectector array in the typical additive dispersion instrument. This problem has been solved by the design of a triple spectrometer which employs a subtractive dispersion spectrometer as a prefilter. The third stage utilizes a three-grating turret to provide adjustable dispersion before the multi-element arrays. The most flexible system appears to be the SPEX "Triplemate." Instruments SA also markets a similar system.

Multi-element detector arrays fall into two main classes: 1) analog detectors using a vidicon, reticon, or charge-coupled device arrays (CCD), and 2) photoemitters using microchannel plates for amplification and a spatially sensitive anode. We shall briefly describe the detector types and then compare advantages and disadvantages.

A. Analog Detectors. The various types of analog detector arrays have been described in detail by Chang[7] and will only be briefly summarized here.

Vidicons use an image intensifier stage with typically 20kV acceleration potential from the photocathode to a two-dimensional silicon diode array. Readout is accomplished by scanning an electron beam across the back side of the array to recharge diodes discharged by

the photo-electrons. Each charge increment is sensed as a voltage pulse which must be digitized. The vidicon is necessarily rather bulky and is not easly cooled with thermo-electric (Peltier) coolers. The PAR OMA-II system integrates vidicon detectors and computer analysis in one complete package.

CCD's and reticons are completely solid state devices and therefore much smaller and easily cooled with Peltier-effect coolers. CCD's have two dimensional capability while the reticon is a one dimensional array with individual elements typically 2 to 5 mm high and 25μm wide. Each employs microchannel plates for amplification after the photocathode. CCD arrays are not commerically available, to this author's knowledge, apparently because of reliability and sensitivity problems. Reticon-based systems are available from Princeton Applied Research, Tracor Northern and Princeton Instruments.

B. Photon Counting Arrays. Within the last two years, ITT (Electro Optical Products Division) and Hamamatsu have developed and marketed commercially photomultiplier tubes employing two or three stages of microchannel plates for photoelectron amplification and a resistive anode plate as a position sensitive detector with two dimensional spatial encryption. The x-y position sensing requires analog (pulse height) information but the event record is actually single photon counting. Thus these systems have many of the behavior characteristics of photomultiplier tubes although they are noticeably smaller due to the use of microchannel plates rather than many dynode stages.

C. Advantages/Disadvantages. All of the multi-element detector systems are expensive compared with traditional PM tubes and preamp-amplifier-discriminator systems. Prices range typically from $40-100 K including the front-end computer.

Of these systems the photon-counting array is probably the easiest to use since it operates rather like a PM tube. However, the digitizing of x & y locations requires at least 10μsec. Thus, this detector is best used in combination with CW lasers. It is especially attractive for Raman scattering from thin layers or surfaces where signal levels are very low. Detected photocounts are of course linear in incident

photons except for dead time effects at high counting rates. Tsang[8] has recently described the advantages of the ITT system for thin film studies.

Analog arrays have the distinct advantage of responding proportionately to 1 to 10^3 or more photons whether they arrive in 1psec or 1ser. Thus their forte lies in conjunction with pulsed laser systems. Their chief disadvantage, in the view of this author, is the analog to digital conversion and linearity problems in the detector. Single photon detection sensitivity is achieved but a large background must always be subtracted away and the detectors suffer from "lag" especially when cooled. Many detectors require "prefogging" by flashing an LED near the photocathode prior to the spectral acquisition. My experience at Kansas State University with an intensified vidicon (PAR OMA-II) showed a change of slope (detected signal vs. photon fluence) with increasing photon fluence. These features make the analog multi-element arrays complicated to use.

Finally, with both types of detector one must be aware of possible limitations due to element size (typically 25μm) and array size (typically 1/2 or 1 inch). Because of these it is most valuable to use a spectrometer with variable dispersion for a variety of situations.

VII. RECOMMENDATIONS:

A. Raman Laboratory Equipment. The lasers and spectrometer are now operating near optimum. Most of the following improvements were discussed in the body of this report (section IV) and action has been taken to obtain these items. There are: 1) a fast collecting lens with f-number ~1 and focal length 75-90mm, 2) a polarization scrambler, 3) a new photomultiplier tube (RCA 31034A), 4) a Pellin-Broca prism , 5) several laser line "spike" filters.

The interfacing of the new Zenith 100 microcomputer for data acquisition and spectrometer stepper motor control is underway. This desperately needs to be expedited. The installation of a room-darkening curtain is also badly needed.

Over the longer range, I think the technology of multichannel photon counting detection and compatible triple spectrometers is now adequately

developed that a major upgrade should be considered within the next couple of years. Such a system would not only speed data acquisition but facilitate, e.g., Raman studies on thin epilayers and single quantum well structures.

B. Excimer Laser Annealing Potential. The Raman and Hall effect studies on the XeCl laser-annealed GaAs suggest interesting potential for fabrication of very heavily doped material. The evidence as yet is necessarily sketchy, however the following statements appear justified by the preliminary work this summer:

1) The presence of a Si_3N_4 cap enhances carrier activation from Si implantations. However more work is needed to verify that Si and/or N from the cap is not incorporated during laser annealing.
2) One should try other techniques of "capping" to prevent As loss without the extra processing step needed for the Si_3N_4 cap. These might include a quartz cover slip or a high pressure inert gas ambient.
3) Raman scattering is a flexible tool to use for nondestructive evaluation of free carrier densities and composition in laser-processed or MBE-grown GaAs and GaAlAs. It has the advantage of high spatial resolution (to ~1μm if necessary).
4) In addition to studies of "capping" variations, I believe that below-melt-threshold annealing with a pulsed excimer laser holds considerable promise for improving carrier activation in ion-implanted material. A mini-grant proposal is being prepared for follow-up work along this direction.

VIII. ACKNOWLEDGEMENTS

The author is grateful for fellowship support of the Air Force Systems Command, Air Force Office of Scientific Research and to the many scientists associated with the Avionics Labortory (AFWAL/AADR) at Wright-Patterson AFB for their hospitality and assistance. Among these I should especially like to thank P. Stover, E. Nichols, D. Langer, A. Ezis, D. Look, D. Reynolds & P. Yu for innumerable acts of assistance and advice. For cheerfully accepting frequent room "black-outs" to allow Raman scattering to proceed—B. Theis & J. Hoelscher. Finally,

the invaluable collaboration of C. Leak in the Raman Laboratory is deeply appreciated.

REFERENCES

1. Cardona, M., in Light Scattering in Solids II, Topics in Applied Physics, 50 (Springer-Verlag, Berlin, 1980).
2. Reviews of electronic raman scattering from free carrriers are given by M.V. Klein, in Light Scattering in Solids I (Topics in Applied Physics, 8) p. 47, and by A. Pinczuk, G. Abstreiter and M. Cardona, in Light Scattering in Solids IV (Topics in Applied Physics 54) M. Cardona, ed. (Springer-Verlag, Belin, 1983) p. 10.
3. Olega, D., & M. Cardona, Phys. Rev. B24, 7217 (1981); D. Olego & M. Cardona, Sol. St. Commun. 32, 375 (1979).
4. Dornhaus, R., R.L. Farrow & R.K. Chang, Sol. St. Commun. 35, 123 (1980).
5. Nicholas, R.J., & H.J. Stolz, Sol. St. Electron, 25, 55 (1981).
6. Theis, W.M., & W.G. Spitzer, J. Appl. Phys. 56, 890 (1984).
7. Chang, R., in Light Scattering in Solids II (Topics in Appl. Phys. 50) (Springer-Verlag, Berlin, 1980) p
8. Tsang, J.C., in Dynamics on Surfaces, Ed. by B. Pullman, et al., (D. Reidel, 1984) p. 379.

AD-A166 176 UNITED STATES AIR FORCE SUMMER FACULTY RESEARCH PROGRAM 88/13
1985 TECHNICAL RE (U)UNIVERSAL ENERGY SYSTEMS INC
DAYTON OH R C DARRAH ET AL DEC 85 AFOSR-TR-86-0139
UNCLASSIFIED F49620-85-C-0013 F/G 5/9 NL

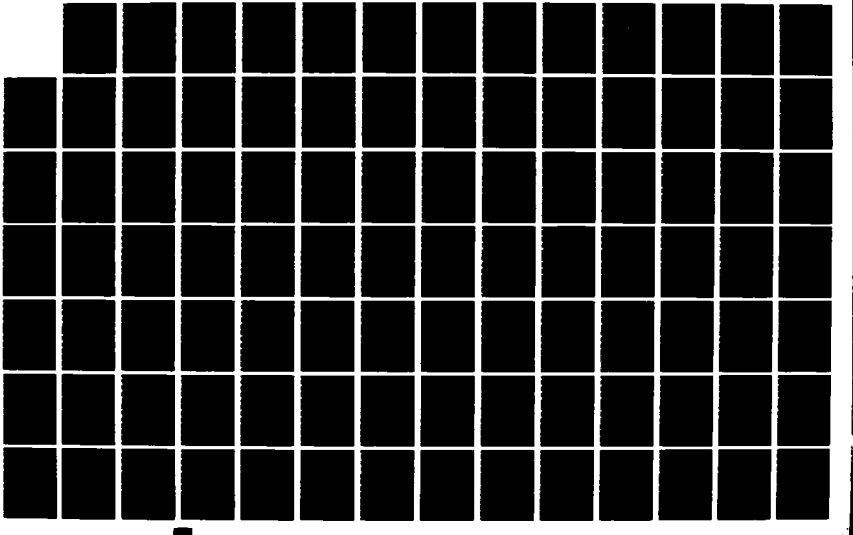

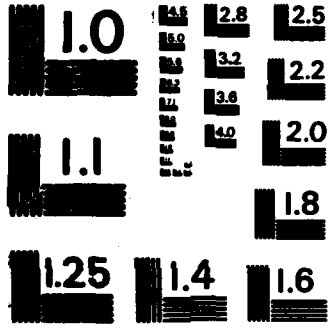

MICROCOPY RESOLUTION TEST CHART
NATIONAL BUREAU OF STANDARDS-1963-A

1985 USAF-UES SUMMER FACULTY RESEARCH PROGRAM/

GRADUATE STUDENT SUMMER SUPPORT PROGRAM

Sponsored by the

AIR FORCE OFFICE OF SCIENTIFIC RESEARCH

Conducted by the

UNIVERSAL ENERGY SYSTEMS, INC.

FINAL REPORT

AERONAUTICAL DECISION-MAKING

FOR AIR FORCE PILOTS

Prepared by:	Thomas J. Connolly, Ed.D.
Academic Rank:	Professor
Department and University:	Aeronautical Science Department Embry-Riddle Aeronautical University
Research Location:	Human Resources Laboratory; Operations Training Division; Operational Unit Training Branch
USAF Research	Elizabeth L. Martin, PhD
Date:	9 Aug 1985
Contract No:	F49620-85-C-0013

AERONAUTICAL DECISION-MAKING

FOR AIR FORCE PILOTS

by

Thomas J. Connolly, Ed.D

ABSTRACT

One of the most critical aspects of flying is manifested in the capability of the pilot to make decisions which reflect his overall understanding of the flight situation. At the present time, training in the cognitive processes required for good aeronautical decision-making is haphazard at best. This study represents an effort to investigate techniques and methodologies for teaching effective decision-making strategies to pilots. Since at least a part of human judgement is based upon bias factors (costs and payoffs) or tendencies to use information not related to safety in choosing courses of action, the implication can be inferred, that if properly developed, this factor of motivation would tend to halt the use of information not directly related to safety and to direct the pilot's decision towared the use of rational processes. A concept model, based on this aspect of judgment, was developed as a part of the study which offers a methodology by which a systematic training program can be conceptualized, designed, and implemented. In addition, a prototype training manual, which includes a student handout on "Pilot Decisional Attribute Questionnaire" (PDAQ) for "Aeronautical Decision-Making" has been developed and optimized.

ACKNOWLEDGEMENTS

This study was completed under a Summer Faculty Fellowhip sponsored by the Air Force Systems Command, Air Force Office of Scientific Research and was conducted at the Air Force Human Resources Laboratory: Operations Training Division. The training manual developed as a part of the study is based on an FAA report "Pilot Judgment Training & Evaluation, Volumes I-II" (DOT/FAA/CT-85-56), Embry-Riddle Aeronautical University, June 1982. Additionally, information provided by R.S. Jensen, Ohio State University and A. Diehl, FAA Program Scientist, proved invaulable in the completion of the study.

Numerous other individuals and organizations provided vital contributions. Among these were; Capt Steve Fessler and Capt Mark Fantasia, US Air Force, Dr E. Martin and Dr W. Nelson, AFHRL, the General Aviation Manufacturers Association (GAMA), the Canadian Air Transportation Administration, and the Australian Department of Aviation.

I. INTRODUCTION

One of the most critical aspects of flying is manifested in the capability of the pilot to make decisions which reflect his overall understanding of the flight situation. The speed, decisiveness, and quality of these decisions are of vital importance and are frequently made in a high stress environment. While pilot training design has made progress during recent years, significant gaps exist both in design methodology and existing programs with respect to systematic training of higher level skills. Training in aeronautical decision-making is currently haphazard at best. However, a review of the training and training research literature reveals a growing interest in the development and implementation of guidelines and materials for this kind of training for pilots.

Exceptional ability at aircraft control is of little or no value if the pilot does not know where and when he should maneuver his aircraft. In addition, a detailed and comprehensive knowledge of all aspects of the aeronautical sciences is wasted on the pilot who fails to recognize and understand his own limitations or is unable to relate his own affective needs to the operation of the aircraft. Individual differences, particulary exagerated under varying degrees of stress, dictate that all pilots in general, and military pilots specifically, must possess exceptional capabilities in critical decision making.

As an active participant in all aspects of flight training since 1963, I have acquired both the interest and the skills required to investigate the challenging new concept in training. This experience includes the design and day-to-day management of both civilian and military pilot training programs, along with a background of innovative research into this subject - most significant as the "Curriculum/Syllabus Specialist" in the 1979 Embry-Riddle response to the FAA Phase II solicitation for the development of pilot judgment materials.

II. OBJECTIVE

1. Develop a model for designing an "Aeronautical Decision-Making" course in the AF-UPT program.

2. Develop a training manual on "Aeronautical Decision-Making" for use in the Air Force UPT programs.

Effort.

This was an effort designed to investigate techniques and methodologies for Training pilots in aeronautical decision-making in a military air training environment. The effort, then, was largely investigative in nature in order to analyze the problem, viz., how to define and teach effective decision making using cognitive processess for optimum utilization under realistic military training situations.

III. APPROACH

1. Current technology in the development and utilization of cognitive processes in decision-making was researched.

2. Current syllabi, instructor guides, tests, and instructional practices were reviewed and analyzed and current UPT Instructor pilots and Flight standards pilots were interviewed.

3. Training techniques and instructional methodologies to improve training were investigated and applied to the problem of improving pilot judgment.

IV. RESULTS

1. In 1976 the Federal Aviation Administration (FAA) became interested in formalizing research into the question of "Judgment Training" and they initiated a multi-phased program at that time. One year later two researchers,

Jensen and Benel, from the Aviation Research Laboratory at the University of Illinois, issued a report which represented Phase I of this FAA project. The authors found "many studies related to pilot judgment in a peripheral way, but only one which directly related" (Thorpe, Martin, Edwards and Eddowes, 1976). The Phase I report, then, really represents the first attempt to define the process of pilot judgment, describe its nature, and identify possible means for improvement.

Jensen expanded his definition in 1982 to include a continuum from perceptual responses to cognitive decisions. He stated that these two aspects of judgment may be considered as two ends of the continuum based on cognitive complexity and decision time. Perceptual judgments, which occur at one end of the continuum, are less complex, frequently involving as little as only one piece of fairly accurate information, and from which responses are determined with highly learned motor behavior. The responses are usually quite simple and immediate.

At the other end of the continuum are the cognitive judgments. These are complex in that they usually involve a large number of relevant pieces of highly probabilistic information. They usually require a choice from among several alternatives, and they are frequently affected by emotions, values and social pressures. In addition, they normally permit some deliberation before a control response is required. Considering these factors, Jensen proposed the following definition of cognitive judgment in flying airplanes:

(a) "The ability to search for and establish the relevance of all available information regarding a situation, to specify alternative courses of action, and to determine expected outcomes from each alternative.

(b) The motivation to choose and authoritatively execute a suitable course of action within the time frame permitted by the situation, where: (1) "Suitable" is an alternative consistent with societal norms; (2) "Action" includes no action, some action, or action to seek more information."

The second part of the definition is of particular interest in that it refers to motivational tendencies. The emphasis being on the directional aspects of motivation rather than on intensity. At least a part of a pilot's judgment is based upon bias factors (costs and payoffs) or tendencies to use information not related to safety in choosing courses of action. The implication is that if properly developed, this factor of motivation would tend to halt the use of information not directly related to safety and to direct the pilot's decision toward the use of rational processes.

Others, such as Dr Fritz H. Brecke, a member of the technical staff of Logicon, Inc, have identified what they believe are a number of limitations with the Jensen definition and conseequently have redefined it:

1. "It is a mode of cognitive operation which is delimited by strictly deterministic modes on the one side, and by intuition on the other, where the borderline between judgment and intuition is less sharp than that between the deterministic mode of operation and judgment.

2. It occurs under conditions of uncertainty.

3. It is applicable to any type of cognitive task, regardless of its taxonomic classification."

As pointed out by Brecke himself, this definition adds little, if anything, in the way of explaining why people arrive at different qualities of decisions when presented with identical situations under conditions of uncertainty. Consequently he also attempts to identify those factors or variables which appear to control a person's ability to exercise judgment. The factors are:

1. "The difficulty of the judgment task. How many factors must be considered and how accurate and factual is the data;

2. The availability of relevant cognitive strategies. As defined by Gagne' and Briggs (1974). This means the capability "to manage the processes of attending, learning, remembering, and thinking;

3. The level of stress, both external and internal to the problem;

4. The individual's coping mechanisms for dealing with stress."

Factors number three and four are of particular interest to us here. In his discussion of stress "internal to the problem" he is interested in stress which results from the task itself where as "external" stress is a term used to identify that stress which is generated as a result of the "background problem" or the individual's motivation. In other words, we see again the acknowledgement of the importance of the affective factors much the same as Jensen was focusing on in the second part of his definition. They appear to agree that regardless of how the pilot actually goes about making a good decision it is critical that he learn to identify and ignore the consideration of non-rational data, i.e., job security, prestige, peer pressure, financial gain, recognition, etc. If he can do this, then the possibility of his applicaton of "good judgment" to the flight problem has been dramatically enhanced.

A great deal of literature has been published, at the theoretical level, on the difficulty of the decision-making task itself. There is, however, a paucity of information dealing specifically in training for improvement in critical decision-making as applied to flight training. As pointed out by Crosby (1977), pre-training appears to be sound and economical but there simply has not been sufficient research for a complete understanding of the process. Development of a technique/methodology would, no doubt, provide the pilot with improved skills in decision-making. It would also give him training in the ordering of events in accordance with their priorities.

In 1979, the FAA launched Phase II of their judgment training project which led to the development of the first training materials for civil aviation pilots in the United States and a number of foreign countries. A unit of instruction was also designed for the 34th Tactical Airlift Instructor School and there are active projects with a number of major air carriers to include aeronautical training courses.

The value of the Phase II project is that it identifies a strategy for isolating the stress factors and then training the pilot to deal with them specifically. This concept may be easier to understand if the three factors - task difficulty, stress (internal), and motivation (background) were arranged as the three axes of an orthogonal system of coordinates, or as three vectors originating from the same point. Decision-making or judgment itself is then simply defined as the resultant vector.

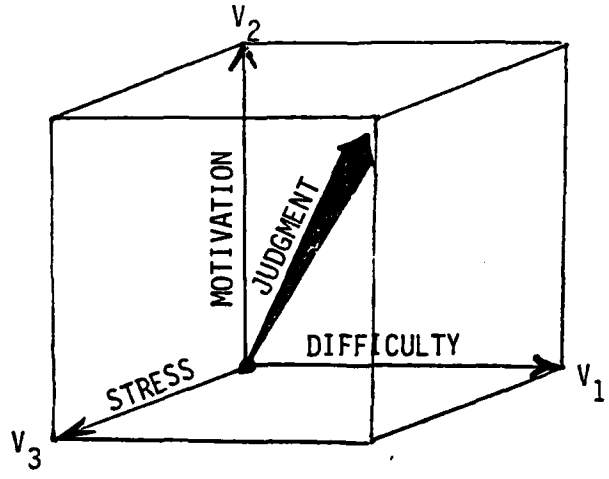

Figure 1. MST Model: Good judgment as a function of motivation, stress, and difficulty.

2. The first part of Jensen's definition deals with V_1 (Task Difficulty) on the MST Model and it is accurate to note that the traditional training programs actually appear to do a remarkably effective job of addressing the problem of task difficulty. The flight student is processed through a very well organized and effective training program which provides him with the tools necessary to rapidly analyze large amount of probabilistic data, determine the relevancy of the data to various courses of action, discriminate between those courses of action and determine possible outcomes. In-flight training itself is characterized by an emphasis on this type of behavior. The problem is that V_R (Judgment) is affected in both direction and intensity by the magnitude of V_2 (Motivation) and V_3 (Stress) and at this time there is no indication in any of the course material reviewed of a formal program for teaching the student pilot the cognitive skills necessary to control these two affective vectors.

Interviews with flight instructors and flight standard pilots both revealed an empirical acknowledgement of the presence and importance of internal and external stress. Indeed every instructor interviewed stated a firm belief in the importance of "thinking under pressure." It was commonly refer to it as "airmanship" or "head work" in the cockpit, and all the instructors claim to be teaching and evaluating their students in this very important aspect of flying. Curiously enough, none of those interviewed could recall a specific example of a planned lesson objective for judgment training or of any attempt to formalize this all-important training.

Graduates of the present system can be characterized as reasonably competent airmen, well-indoctrinated in applicable procedures and rules where decision-making abilities under real life stress are relatively unknown. The current system may best be characterized as a variation of the old apprentice/master system. Under this system, the pilot upon completing his basic training, is assigned to a "master" or even a number of "masters." These "high-time" pilots are there to guide the new pilot when faced with problems requiring judgment. Should the "apprentice" pilot be called upon to make a decision, he must act on the basis of skills developed prior to flight training. If he is lucky, everything works out and he grows and develops as a pilot.

Considered in this light, it would seem that training in the perceptual-motor type judgment tasks is probably effective in as much as a set of rules or procedures normally serve to simplify the task but also serve to reduce or remove stress as it is related to the flight problems (internal) and minimize the affect of personal motivation (external) as it relates to non-safety or non-rational considerations.

The only examples of training in the cognitive judgment tasks which this study was able to identify exist in the form of feedback, such as accident scenarious in the various safety magazines where the pilot's action are discussed post-facto. The decisions were categorized as good or bad on the basis of the outcome and nowhere was there any comment about the process leading up to the decision.

Given the above, the next logical question is: "If judgment training is so important, then why is it not included in the average aircrew training curriculum?" There are two possible reasons. First of all, it is easier to train overt, observable behaviour. The second reason is probably related to the idea that each accident requires another rule or prodecure. The idea is that errors due to bad judgment can somehow be reduced by regulation and proceduralization.

If the concept model presented earlier is applied to the current UPT program, conclusions concerning the validity of training methods can be established and new strategies can be defined specifically aimed at the development of good judgment performance under various degrees of conflict and/or cognitive dissonance (as defined by Festinger).

3. The MST model developed as part of this study offers a methodology by which a systematic training program can be conceptualized, designed, and implemented.

First of all, judgment training must enable the trainee to distinguish the flight problem from the background problem. As indicated earlier, background problems may include such things as medical emergencies and business trips. However, they can be considerably more subtle than that. One technique for sorting backgound problems with a high degree of negative potential, into recognizable families is to classify them according to the common human defense mechanisms or hazardous thought profiles as they relate to unsafe flight activity. Impulsive behaviour or execessive machismo, brought about by peer group pressure, are good exampies.

The advantage in using the hazardous-thought profile approach is that when given a behavioral objective such as "the student will identify the background problem or hazardous thought pattern correctly in x out of y cases," it should not be too difficult to design appropriate instruction. Such instruction would generate in the student an awareness of how the background problem may bias or interfere with his judgment in solving the flight problem. Secondly, by learning the goals and principles of coping, the student can learn to control stress as it relates to the flight problem itself.

The three-pronged MST model allows for a systematic design of materials and scenarios which are carefully focused on the two here-to-fore neglected areas of concern.

The F-15 situational emergency training (SET) program is one example of an attempt to address this training need. Another is the F-14 syllabus developed by Vega, Incorporated. The F-14 program provides for an easily identifiable progression as the student advances through the various levels of cognitive skill learning, with each level being introduced and tested prior to attempting the move to the next higher level. One problem with both of these innovative programs is that they too ignore the very critical aspects of internal and external stress. There is no doubt the student is challanged to perform under stressful situations which continue to build in intensity, but nowhere does there appear to be any formal conscious effort to teach methods and techniques for coping with and reducing the effect of V_2 and V_3, thereby resulting in improved decision-making.

The MST model suggests a building block strategy or course of instruction. The pilots should first be trained in the classroom in the general principles of stress control and hazardous thought profiles identification. Once they are able to identify the principles and demonstrate an understanding of how these principles relate to the flight situation, they would proceed to the simulator environment where a variety of exercises would be presented which would permit the opportunity to apply the newly acquired knowledge, and then, of course, the skill should be transferred to the airplane or in-flight environment itself.

Based on the information acquired during this study, a prototype training manual for "Aeronautical Decision-Making" has been developed and optimized. This manual is directed at the first two levels of learning and is intended for use in the classroom environment. (Appendix I)

V. RECOMMENDATIONS

1. The complete "Aeronautical Decision-Making" course should be developed, tested, and then implemented as a part of the UPT program during the fall of 1986.

a. A validation study of the manual should be conducted. This study could be conducted in a formal civilian flight training environment which would provide the advantage of non-interference with the Air Force UPT program and would, at the same time, produce results that would be generalized to the UPT environment.

b. A simulator-based unit of instruction should be constructed and validated to develop the "skill to apply" level of learning. This could be accomplished in conjunction with the validation study indicated above. Using a series of LOFT-type scenarios, the student would be offered the opportunity to apply his newly acquired knowledge in a controlled environment with maximum positive reinforcement.

c. During the summer of 1986 the course should be revised as needed and the in-flight phase developed. In conjunction with this final stage of development, the required coordination with ATC at Randolph AFB, TX should be accomplished.

REFERENCES

Brecke, F., Instructional Design for Aircrew Judgment Training. Unpublished paper, Logicon, Inc., San Diego, CA, 1983

Fishbein M., and Ajzen, I., Belief, Attitude, Intention and Behavior: An Introduction to Theory and Research. Reading, MA: Addison - Wesley, 1975.
Gagne, R.M., and Briggs, L.J., Principles of Instructional Design. New York: Holt, Rinehart, and Winston, Inc., 1974

Gibson, J.H., Optimized Flight Crew Training: A Step Toward Safer Operations. Fort Worth, TX: American Airlines, Flight Training Academy, 1969

Goldstein, I.L., Training: Program Development and Evaluation. Belmont, CA: Wadsworth, 1974.

Jarvis, I., and Mann, L., Decision Making: A Psychological Analysis of Conflict, Choice, and Commitment. New York: Fre Press, 1977.

Jensen, R.S., and Benel, R.A., Judgment Evaluation and Instruction in Civil Pilot Training. Report No. FAA-RD-78-24 by Aviation Research Laboratory, University of Illinois, December 1977.

Jemen, R.S., Pilot Judgment: Training and Evaluation. Proceedings of the 11th NTEC-Industry Converence, Nov 1978, pp 71-83.

Kogan, N., and Wallach, M., Risk Taking: A Study of Cognition and Personality. New York: Holt, Rinehart, and Winston, 1964.

Shealey, J.E., Risk-Taking in Skilled Task Performance. Proceedings of the Eighteenth Annual Meeting of the Human Factors Society. Santa Monica, CA: Human Factors Society, 1974.

Slovic, P., Analyzing the Expert Judge: A Descriptive Study of Stockbroker's Decision Processes. Journal of Applied Psychology, 1969, 53, 255-263.

Taylor, R.N., and Dunnette, M.D., Influence of Dogmatism, Risk-Taking Propensity, and Intelligence on Decision-Making Strategies for a Sample of Industrial Managers. Journal of Applied Psychology, 1974, 59, 420-423.

Thorpe, J.A., Martin, E.L., Edwards, B.J., and Eddowes, E.E., Situational Emergency Training: F-15 Emergency Procedures Training Program. Williams Air Force Base, AZ, Technical Report No. AFHRL-TR-76-47 (1), June 1976.

APPENDIX A

Prototype Training

Manual

AERONAUTICAL DECISION MAKING

FOR AIR FORCE PILOTS

CONTENTS

Chapter 1. Pilot Decisional Attribute Questionnaire (PDAQ). 2
Questionnaire. 2
Scoring of PDAQ. 7

Chapter 2. Introduction to Aeronautical Decision Making 10
Background 10
Definition 13
Pilot Responsibility 15
Relationship of Judgment to Training 16
"Pilot Error". 16
Attitudes in Aeronautical Decision Making. 17
Interpreting Your PDAQ Results 17
The Poor Judgment Chain. 18
Two Principles of the Poor Judgment Chain. 19
Breaking the Poor Judgment Chain 19

Chapter 3. Identification Practice of Hazardous Attitudes 21
Better Decision Making Through Practice. 21

Chapter 4. Antidotes for Hazardous Thoughts 32
The Five Antidotes 32
Antidote Identification Exercise 33
Recognizing and Replacing Hazardous Thoughts Exercise. . .35

Chapter 5. Influences and Resolution of Stress. 46
Defining Stress. 46
The Effects of Stress. 47
Stress Questionnaire for Self Assessment 48
Time and Stress. 50
Stress and Performance 51
Coping with Stress 53
"Improving My External Environment" Exercise 53
"Coping with Job Stress" Exercise. 54
Job Stress Profile 55
Coping with Stress while Flying. 57

PREFACE

This is a prototype Decision Making manual developed at the Air Force Human Resources Laboratory, Williams AFB, AZ in an effort to improve military aviation safety. This manual is intended to be used by Air Force student pilots as part of their regular training program. A specific plan for implementation and validation has been proposed and if this program proves successful, similar advanced training materials may be developed for both Simulator and In-Flight use.

The manual was prepared under the technical direction of:

Elizabeth L. Martin, Phd
AFHRL/OT
Williams AFB. AZ 85240-6457

Richard S. Jensen, PhD
Department of Aviation
Ohio State University
PO BOX 3022
Columbus, OH 43210

Alan Edward Diehl, PhD
Program Scientist - Human Performance
Federal Aviation Administration
ATTN: AAM-540
800 Independence Av, SW
Washington, DC 20591

ACKNOWLEDGEMENTS

This Training Manual is based on a number of efforts, all of which grew out of the FAA report "Pilot Judgment Training and Evaluation, Volumes I - III" (DOT/FAA/CT-82-56), Embry-Riddle Aeronautical University, June 1982. Among these efforts was material provided as a result of research conducted at Ohio State University by Dr R. S. Jensen and Dr J. Adrian. Their information proved invaluable and represents the heart of the manual. Additionally, the Chapter on Stress was taken from a "Judgment Training Manual for Australian Pilots, developed by Dr Adrian Ashman as part of a project funded by the Australian Department of Aviation and conducted at the University of Newcastle.

Numerous other individuals and organizations provided vital contributions. Among these were; Capt Steve Fessler and Capt Mark Fantasia, both of the US Air Force, Dr W. Nelson, AFHRL, the General Aviation Manufacturers Association (GAMA), and the Canadian Air Transportation Administration.

Research sponsored by the Air Force Office of Scientific Research/AFSC, United States Air Force, under Contract F49620-85-C-0013. The United States Government is authorized to reproduce and distribute reprints for governmental purposes notwithstanding any copyright notation hereon.

Chapter 1

PILOT DECISIONAL ATTRIBUTE QUESTIONNAIRE (PDAQ)

Over the years each of us develops strategies to deal with life and the people around us to best accomplish our goals. Some of these strategies become deeply engrained in us and we call them personality traits. These traits are fairly well established by the time we are six years old and are very difficult to change thereafter. Other strategies, that are less deeply engrained, are called attitudes and can be changed quite easily, especially under pressure from several sources at the same time. We are constantly bombarded with attempts to change our attitudes by teachers, theologians, all forms of advertising, parents, peers, and superiors. Attitudes can be subdivided into various attributes that are known to affect pilot decision making.

The following is a questionnaire designed to assist you in determining your attributes as a pilot decision maker. Please answer all of the questions as honestly as you can. Your honest responses to these questions will greatly improve your performance in the remainder of this unit of instruction. There are no right or wrong answers and you will not show the results to anyone. The questionnaire is offered for the sole purpose of helping you to determine your decisional attributes as an Air Force pilot. Following the questionnaire, you will be shown how to score and interpret the results. The remainder of the book is a guide to assist you in your AERONAUTICAL DECISION MAKING.

Instructions

1. Read each of the situations and five alternatives. As you read, try to place yourself in an airplane under the given circumstances.

2. Choose your most likely thought pattern in response to the situation and place a "1" in the space provided next to that alternative.

3. Continue by placing a "2" beside your next most probable thought pattern and then "3", "4", "5", in order of your next to least likely thought patterns.

4. Complete all ten situations and be certain to fill in every blank.

Remember - This questionnaire has no correct answers and is intended for your information only. Some (or all) of the alternatives given may not represent the way you would think at all. However, for this questionnaire you should assign a rank to all of them.

Situation 1

Nearing the end of a long flight, your destination airport is reporting 800 and 1/2, fog and haze. You have just heard another aircraft miss the

approach (ILS minimums are 200 and 1/2). You decide to attempt the ILS approach. Why did you make this attempt?

_____ a.Ceiling and visibility estimates are often not accurate.
_____ b.You are a better pilot than the one who just missed the approach.
_____ c.You might as well try, you can't change the weather.
_____ d.You are tired and just want to land now.
_____ e.You've always been able to complete approaches under these circumstances.

Situation 2

You are scheduled to ferry an aircraft with no deicing equipment through an area in which "light to moderate rime or mixed icing in clouds, and precipitation above the freezing level," has been forecast. You decide to make the trip thinking...

_____a. You believe that you can adjust your altitudes enroute to avoid ice accumulation
_____b. You've been in this situation lots of times and nothing has ever happened to you.
_____c. You must get home in two hours and can't wait.
_____d. You do not let an icing forecast stop you; they're usually overly cautious anyway.
_____e. There's nothing you can do about atmospheric conditions anyway.

Situation 3

You get to the airport for a schedule cross-country flight. A fellow pilot whose girlfriend lives at your destination, is scheduled as your co-pilot. The airplane you had scheduled has been grounded for avionics repairs. You are offered an airplane as a substitute that has an HSI and radios which you have never used. You take off on your flight with no additional briefing on the equipment unfamiliar to you. Why?

_____a. If the equipment is so difficult to operate, you would not have been "offered" the plane as a substitute.
_____b. You are in a hurry to make the scheduled arrival.
_____c. Equipment checkouts often are not needed.
_____d. You do not want to admit to your co-pilot that you are not familiar with the equipment.
_____e. You probably won't need to use the fancy equipment anyway.

Situation 4

You arrive at your destination airport on a Quick Turn Around Cross-Country Flight. Your prior calculation before departing had determined that you should have enough fuel to complete the trip with the required

reserve. However, the winds on the trip over were greater than anticipated and you are not sure of the exact fuel burn in your aircraft. You decide to head for home without refueling because:

_____a. You can't waste time staying overnight because you and your co-pilot have to be at work in the morning.
_____b. The required fuel reserves are overly conservative.
_____c. The wind will probably die down for the return trip.
_____d. You don't want to admit to your lack of planning in front of anyone else.
_____e. It's not your fault the airport services are usually so slow; you will just have to try to make it home.

Situation 5

You have been cleared for the approach on an IFR practice flight with a safety pilot on board. At the outer marker, ATC informs you of a low-level wind shear alert reported for your intended runway. Why do you continue the approach?

_____a. You just have to show the safety pilot that you can make this approach inspite of the wind.
_____b. It has been a perfect approach so far; nothing is likely to go wrong.
_____c. Those alerts are for other, less experienced pilots.
_____d. You need two more approaches to be current and want to get this one completed.
_____e. The tower cleared you for the approach, so it must be ok.

Situation 6

You are about to fly the T-37 on a cross-country flight, during taxi you notice a vibration. You go ahead and take-off without checking further. Why?

_____a. You have to be at your destination by five and you're running late already; you can have it checked there.
_____b. You've noticed that vibration before and nothing has ever come of it.
_____c. You don't want your co-pilot to think you can't handle the aircraft, so you just disregard the vibration.
_____d. Requirements for two perfectly smooth running engines are overly conservative.
_____e. Maintenance just checked this plane yesterday; they would have caught any real problem.

Situation 7

You are enroute in instrument meterological conditions and are receiving conflicting information from your two nav receivers. You continue on your route of flight and shortly discover that the radios are so bad that you can

not get a definite fix on your location. You figure ATC will soon suggest that you are off course and ask you to correct it. You are thinking...

_____a. Try to figure out where you are so ATC won't find out first that you didn't know.
_____b. You will continue to navigate on your newer, more expensive receiver; the manufacturer must have made sure that it works.
_____c. You will get yourself out of this jam, you always do.
_____d. If ATC calls, you can be non-committial, if they knew all, they would only make things worse.
_____e. Quickly tell ATC that you are lost and wait impatiently for their response.

Situation 8

As you turn final on an IFR approach, ATC calls and asks you how much fuel is on board. You know that you only have two minutes until you reach the approach point, and wonder why they have inquired as to your fuel status. You are also aware of severe thunderstorm activity nearby, but there are no such problems where you are presently flying. You assume you may be told to "hold" and think...

_____a. Your fuel is fine but you want to get down quickly, before the storm hits!
_____b. You are in line with the runway now and believe that you can land, even in any crosswind that might come up.
_____c. You will have to do this approach; the weather probably won't get any better.
_____d. You are not going to let ATC have you holding in possibly severe weather; it's not their neck.
_____e. The pilot who landed before me did okay; what could possibly happen?

Situation 9

You are on an IFR flight of only fifty miles. Your airplane develops a malfunctioning turn coordinator. You are a relatively low-time instrument pilot. The visibility is continually worsening and nearing approach minimums at your destination. You make this trip thinking...

_____a. You've never had a need to use the turn coordinator.
_____b. You have passed your instrument flight test and believe that can handle this weather.
_____c. Why worry about it; ATC will get you out anyway.
_____d. You had better keep going before things get worse and you have to turn around.
_____e. Back up systems are not needed for such a short trip.

Situation 10

You are established on cruise above 10,000 feet. You notice you forgot to disconnect the "gold key", and do not do it now. Why not?

_____a. Disconnecting it at this point might look like you are afraid; you don't want to alarm your co-pilot.
_____b. Regulations are unnecessary for enroute operations.
_____c. You haven't been hurt yet by leaving it connected.
_____d. What's the use; if it's your time, it's just your time.
_____e. You've got to get the airplane under control; there's no time for it.

Scoring Key
(Remove this page from manual)

Scoring Instructions

From your PDAQ answers, write in the table below your rank for each alternative shown. Sum the ranking scores for each scale and enter at the bottom. These totals should then be marked on the PDAQ profile on the next page.

Situation	Scale I	Scale II	Scale III	Scale IV	Scale V	Total
1	a_____	d_____	e_____	b_____	c_____	15
2	d_____	c_____	b_____	a_____	e_____	15
3	c_____	b_____	e_____	d_____	a_____	15
4	b_____	a_____	c_____	d_____	e_____	15
5	c_____	d_____	b_____	a_____	e_____	15
6	d_____	a_____	b_____	c_____	e_____	15
7	d_____	e_____	c_____	a_____	b_____	15
8	d_____	a_____	e_____	b_____	c_____	15
9	e_____	d_____	a_____	b_____	c_____	15
10	b_____	e_____	c_____	a_____	d_____	15
Total	_____	_____	_____	_____	_____	150

The sum of your scores across must be 15 for each situation. If it is not, go back and make sure that you transferred the scores correctly and check your addition. The grand total should be 150.

(This page intentionally left blank).

PDAQ PROFILE

Total Raw Scores (from Scoring Key):

Place an "X" below at the point that corresponds to your total score for each scale. You have completed your Pilot Decisional Attribute Profile. Chapter 2 will explain the scales and their significance to your decision making as an Air Force pilot.

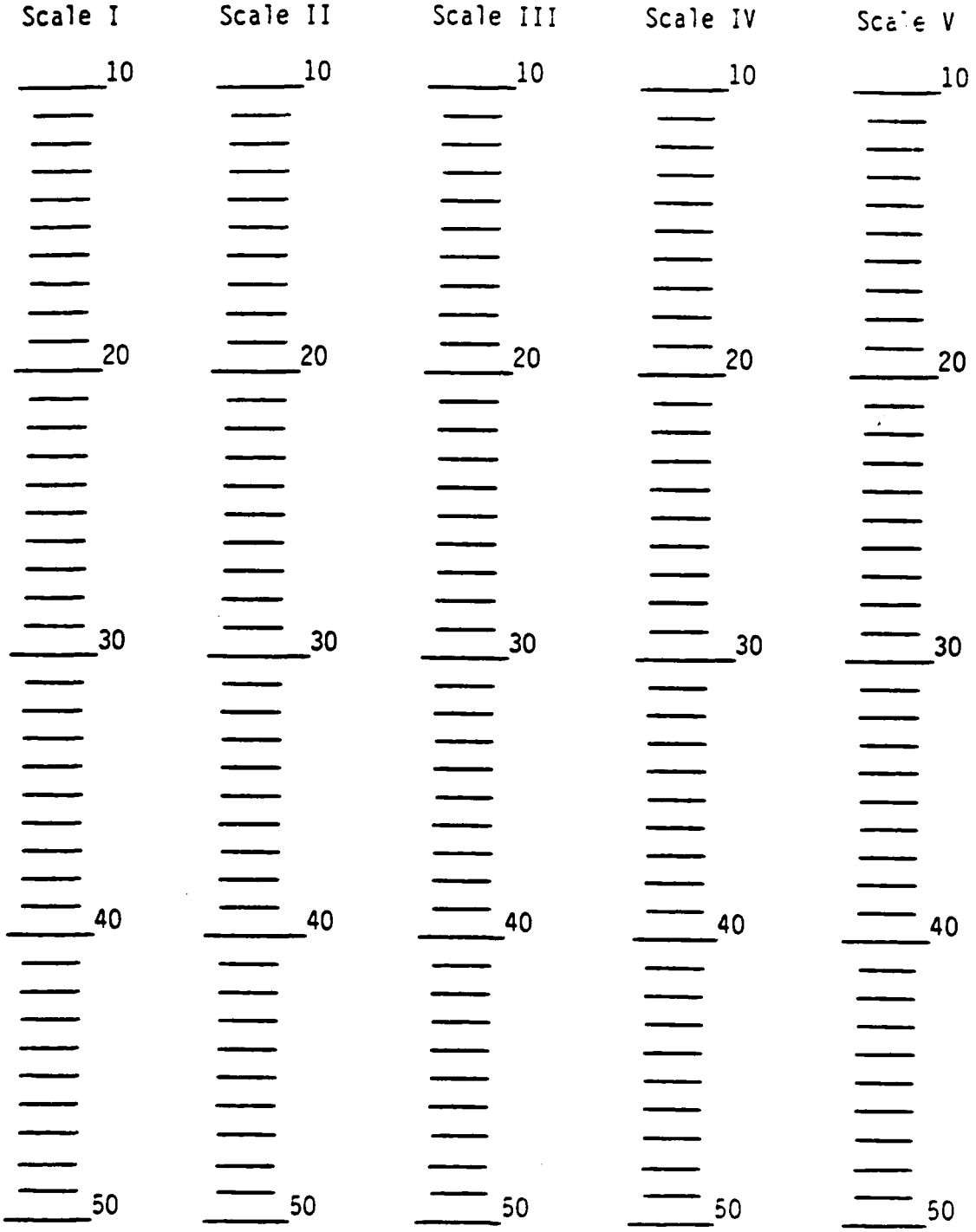

Chapter 2

INTRODUCTION TO AERONAUTICAL DECISION MAKING

There are two types of pilot judgment and both play a part in many accidents. The first, called perceptual judgment, refers to the sensation, perception and decision making processes involved in fairly simple situations requiring rapid control movements. Examples are distance, clearance, speed, closure rate, and altitude judgments.

Perceptual judgments are highly influenced by expectancies. If one expects to see something a certain way and he does see something close to what he expects, but not the same, he will probably report and act as though he saw what he expected. Therefore, his actions or inactions in the perceptual area would be based on a false assumption. Although perceptual judgment is important to aviation safety, it receives a great deal of attention in conventional flight training and is not considered further in this manual.

The second type of pilot judgment is cognitive judgment. Cognitive-judgment, the topic of this manual, refers to the thinking process that the pilot goes through in making a decision involving probabilistic information and several alternatives. It includes both the ability to think clearly, throughly, and quickly and the motivation to decide using criteria set by societal norms. In multi-person flight crews good judgment also includes the effective use of the other members of the crew in the decision process.

One can make a long list of a pilot's failures in cognitive judgment some of which might cause failures in perceptual judgment. These include:

1. Failure to use a checklist.
2. Failure to use a standard approach procedure.
3. Failure to lower flaps.
4. Failure to maintain required airspeed for no-flap approach.
5. Failure to set reference speed bug accurately.
6. Demonstration of touch-and-go landings of various types with minimal experience in aircraft.
7. Failure to properly assess the atttention requirements for control of high performance aircraft in traffic pattern.

Now the question becomes what might cause these failures in cognitive judgment? The reasons go beyond experience, training, and testing as they are conducted today.

Background

From the beginning of aviation history, pilots have been expected to exercise a considerable amount of judgment in the overall task of flying an airplane. The Wright brothers owe a great deal of their success to the fact that they exercised good aeronautical judgment at a time when many of their colleagues were killing themselves by considering flight to be nothing more than a thrill or adventure. They 1) knew and 2) respected the risks involved.

These are the two keys to good aeronautical decision making. Both of these ideas will be presented to you in several different ways throughout this manual.

In recent years, increasing demands in our society for safety, dependability, economy, effectiveness, and reduced energy consumption have increased the complexity of flying operations magnifying the pressures for good pilot judgment. Furthermore, technological advances that have eased much of the pilot's burden for precise aircraft control have not greatly eased the pilot's decision-making workload. In fact, these advances have changed the role of the pilot from one of controller to one of manager and decision maker. This new emphasis has created new demands for cockpit management and decision making.

If it were merely a matter of learning flying skills, pilot training would be a trivial task for most people. Unfortunately, because actual flying conditions are never quite the same as those used to develop aviation regulations, procedures, and performance limitations, the safety of each flight also depends upon significant amount of evaluation and interpretation of existing conditions by the pilot.

For example, the conditions used to develop flight performance values for a particular type of airplane are usually ideal, including clean airplane surfaces, a new engine, and a company test pilot. In actual conditions the pilot must compare the book values obtained in ideal conditions with those in which he finds himself. The actual conditions may include a dirty airplane, a slightly used engine, and a less than perfect pilot. He must then evaluate many other conditions such as gross weight, center of gravity, wind, temperature, humidity, altitude, etc, for comparison with those found in the book to determine his expected flight performance. Finally, he must check the present and forecast weather, the terrain, and expected traffic density and compare them with an estimate of his own capability before determining whether or not his planned flight will be safe. Examples such as these requiring decisions with less than perfect information can be found in all areas of flight activity.

Furthermore, every decision that the pilot makes is colored by physiological, psychological, and social pressures that are very difficult to weigh properly on the spot. For example, just as persons watching a sporting event may "see" an infraction or foul differently depending upon their vantage points and which team they support, a pilot may be influenced to view the weather outlook or his own abilities differently depending upon the importance he assigns to a given flight. Some pilots may be susceptible to social pressures that result in less than perfect judgment. Potential sources of social pressure include peer reaction, fear of failure, and censure from superiors.

The Pilot Judgment Problem. An analysis of accident statistics by categories of pilot behavior activities reveals the serious nature of the judgment problem. Most analyses of aviation accident statistics have found that 80 to 85 percent can be assigned broadly to "pilot error" and the

mainder to mechanical malfunctions. To determine why pilots are making cident-causing errors it is useful to classify pilot activities into three tegories as follows:

1. Procedural Activities - the management of the powerplant, fuel, vehicle configuration, autopilot, displays, navigation, and communication.

2. Perceptual Motor Activities - vehicle control, judgment of distance, speed, altitude, and clearance, hazard detection, and geographic orientation.

3. Decisional Activities - including the self-assessment of skill, knowledge, physical, and psychological capabilities, the assessment of aircraft and ground system capabilities, hazard assessment, navigation planning, and flight priority adjustment.

To determine the relative importance of each of these activities in Civil iation accidents, statistics from the National Transportation Safety Board tomated Aircraft Accident and Incident Information System from 1970 through 74 were classified into the three behavioral categories given above. Then e total number of both fatal and non-fatal accidents during the five-year iod were determined for each of these behavioral categories. The results these analyses are shown below.

	FATAL	NON-FATAL
Procedural	264 (4.6%)	2230 (8.6%)
Perceptual-Motor	2496 (43.8%)	14561 (56.3%)
Decisional	2940 (51.6%)	9087 (35.1%)

Examinations of these data provide valuable indications of possible knesses in current programs and they reveal an important distinction. A ority of the non-fatal pilot-caused accidents (56.3%) were the result of lty perceptual-motor behavior. The most significant factors here ("failure maintain flying speed" and "misjudgment of distance, speed, altitude, or arance") are called perceptual judgment. These are highly learned ceptions and control movements that must be made quickly, in some cases tinuously.

On the other hand, a majority of the fatal pilot-caused accidents (51.6 cent) are the results of faulty decisional behavior, called cognitive gment. The most significant factors in this area are "continued VFR into wn adverse weather" and "inadequate preflight planning or preparation." nitive judgment describes the decisional activities involved in choosing a rse of action from among several alternatives. Obviously, cognitive gment is similar to perceptual judgment in that both involve making ices. However, there is a basic difference. The second, refers to isions for which set procedures have not always been established or may e been forgotten.

Flight instructors use various terms referring to this cognitive judgment as "headwork," "thinking ahead," and "staying ahead of the aircraft." In

a more general sense pilots sometimes refer to it as professionalism or commandability. Usually, more time is available to evaluate the situation, a large number of possible courses of action must be considered, and there is a greater degree of uncertainty concerning the existing situation and possible outcomes. For these reasons, cognitive judgements have been the source of greater misunderstanding in pilot training and evaluation. The remainder of this manual deals with cognitive judgment.

Lest you be led to believe that such decisions are made by one group of pilots only, an examination of airline accidents reveals that some of the worst disasters were the result of similar failures, e.g., Air Florida Boeing 737 at Washington National Airport, Eastern L1011 in the Florida Everglades, and KLM 747 at Ternerife. The unfortunate fact is that very little is being done to improve pilot decision making, perhaps because of an attitude in the aviation community that nothing can be done about it. This is one attempt to change that attitude.

Definition

Pilot judgment refers to a process that the pilot goes through in formulating a decision. As shown in Figure 1, there are various ways in which this intellectual process can be influenced through training. Going from the judgment process to the decision involves many other situational factors that may influence the final decision as well. These factors affect the decision from the standpoint of pilot motivation. (See Figure 1)

As indicated above, there is an important distinction that must be made between knowledge and motivation in aeronautical decision making. This distinction is shown in the following definition:

Aeronautical Decision Making is:

1. The ability to search for and establish the relevance of all available information regarding a flying situation, to specify alternative courses of action, and to determine expected outcomes from each alternative.

2. The motivation to choose and authoritatively execute a suitable course of action within the time frame permitted by the situation:

   where:

   a. "Suitable" is an alternative consistent with societal norms.

   b. "Action" includes no action, some action, or action to seek more information.

The first part of the definition refers to intellectual abilities. It depends upon the pilot's capabilities to sense, store, retrieve, and integrate information. It is purely rational and could be stated mathematically. If it were possible to separate this part of human judgment from the second part

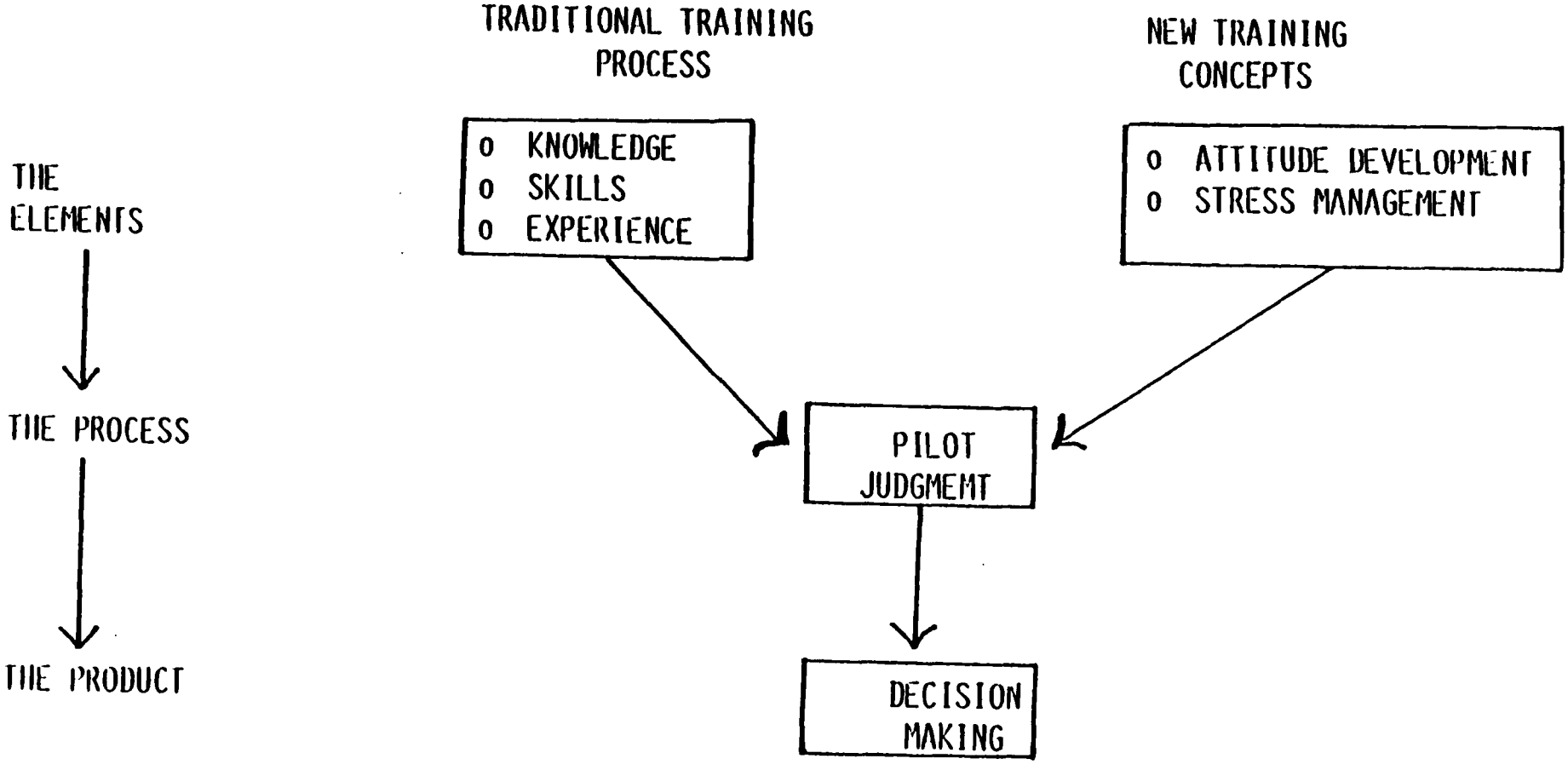
TRADITIONAL TRAINING PROCESS
NEW TRAINING CONCEPTS
o KNOWLEDGE
o SKILLS
o EXPERIENCE
o ATTITUDE DEVELOPMENT
o STRESS MANAGEMENT
THE ELEMENTS
THE PROCESS
THE PRODUCT
PILOT JUDGMEMT
DECISION MAKING

Figure 1.

(which it is not), we would solve problems in much the same way as a computer. This is not to say that our decisions would be error free. Probabilistic information is used and the performance is dependent upon the amount, type, and accuracy of information stored as well as inherent and learned capabilities to process information.

The second part of the definition is where the decision takes place and indicates that it can be affected by motivations and attitudes. It says that a part of pilot judgment is base upon tendencies to use less than purely safety information in choosing courses of action. There is a tendency in all pilots to consider non-safety factors, such as job demands, convenience, monetary gain, self-esteem, adventure, committment, etc, before taking action. However, if properly developed, this part of pilot judgment would tend to reduce the use of information not directly related to the safety of the flight and to direct the pilot's decision toward the use of more rational processes.

Pilot Responsibility

When the Air Force designates a pilot, it is granting that pilot the privilege to use public airspace and air navigation facilities. In accepting this privilege, the pilot is expected to adhere to the rules without engaging in any activities which might infringe on the rights and safety of others. At all times it's the pilot's responsiblity to operate an aircraft safely, legally, and carefully.

The pilot in command always has direct responsiblity for the operation of his aircraft, a responsiblity not shared with anyone else - not with controllers, passengers, or flight instructors. Awesome as these responsibilities are, they're not spelled out in detail in any official document. When designated, a pilot is expected to use his "good judgment" to understand and interpret the rules in individual situations and in the most responsible manner.

The rules are not designed to guarantee your safety as a pilot even if you follow them to the letter. They are made to permit you, the pilot, who has acquired the bast possible skill at a given level, to operate your aircraft with as much freedom as safety will allow. "Minimums" are provided for approaches as well as for maneuvers in specific airplanes. The assumption in establishing these minimums is that the pilot is properly qualified to fly the maneuver.

To illustrate and to demonstrate that judgment is needed in aircarrier operations as well, the FAA permits a fully loaded 727 to land on Runway 36 at National Airport with a 10 knot tailwind. This maneuver is possible with perfect pilot technique. However, the air carriers do not take advantage of this privilage except under the most ideal circumstances with the best pilots. This is pilot judgment on the part of the aircarriers. Anyone who may be less than a perfect pilot should not exercise the full privileges offered by FAA regulations. This places a heavy responsibility on the pilot to determine how far from the perfect pilot he is and to set his margin for error accordingly. We can see, then, why the exercise of good judgment is so crucial to flying safely.

Relationship of Judgment to Training

Two types of judgment training are needed. The first is intellectual. It must show the cues to look for to recognize a deteriorating situation such as "getting behind" the aircraft close to the ground. It should teach the need for standard approach patterns and the consequences of not following them. It should drill on the use of a checklist in single-pilot high performance aircraft in particular and show why a checklist is important in all types of aircraft. This training should emphasize the need for placing one's complete attention on the airplane in terminal and pattern operations and ways to insure that this is done.

The second judgment training area is motivational and considers the need for strict pilot discipline. This type of judgment training should be aimed at motivating the pilot to be cautious and safety conscious. All flying is in part driven by the "background problem" which includes factors such as financial gain, ego building, flight-time building, social and peer pressure, adventure, and pressures from superiors or job duty. In motivational judgment training the pilot must be taught to recognize the force behind these background issues and to subordinate these when they begin to cause one to take unnecessary risks.

Strict discipline and attention to aircraft control can be learned over time but are far more effectively learned through deliberate judgment training. Students who have never seen their instructors compromise the checklist or traffic pattern will not so easily do so themselves.

Furthermore, to be effective such training must demonstrate the consequences of not following such procedures. It should show what can happen when an abnormal traffic pattern is used and how difficult it is to recover from such a pattern. It should demonstrate the effect of slow-speed flight near the ground with no flaps. It should include discipline in this area. Each of these ideas could be taught in a flight simulator or an interactive computer simulating the particular aircraft dynamics. Many of these ideas could also be taught in a ground school. The days of luck and experience as effective teachers of these concepts are gone. We must use more modern techniques that are tailored to the more complex, less forgiving aircraft that we fly.

"Pilot error"

The use of the term "pilot error" to describe an accident cause is an oversimplification that implies that the pilot intended to do what he did causing the accident. Pilots intend to fly safely. Nevertheless, they do make decisional errors. Usually, their skill or luck is sufficient to get them out of situations resulting from poor judgment (a term for the general concept of decisional errors). The goal of this book is to teach you, the Air Force pilot, techniques to avoid situations that require luck or skill greater than you may possess. Good judgment means avoiding situations that require superior skill to overcome.

Attitudes in Aeronautical Decision Making

In aviation we begin to develop attitudes about flying when we first think about it. These attitudes develop as we discuss flying with other pilots. They are reinforced or changed by our flight instructors and our flying experiences. Sometimes attitudes developed in other areas of our lives carry over to influence our flying attitudes. These influences can be very healthy and assist us in our approach to flying. Other attitudes may be harmful to safe flight. Attitudes are important in aviation because they influence our decision making.

How a pilot handles his or her responsibilities as "pilot-in-command" depends to a large degree upon ingrained attitudes - toward safety, toward him or herself, and toward flying. Attitudes are learned; we are not born with them. Good attitudes can be developed - again through training - into a positive mental framework that encourages and produces good pilot judgment. On the other hand, bad pilot habits created by previously learned poor attitudes can be changed through training into good attitudes. How you can develop positive attitudes toward flying is the primary subject of this judgment training program.

Five Hazardous Attitudes. Certain attitudes or hazardous thought patterns in pilots are often associated with aviation accidents when they are present in the extreme. The following is a list of five of these hazardous attitudes:

1. "Anti-authority" - This attitude is found in pilots who resent any external control over their actions. It is a tendency to disregard rules and procedures.

2. "Impulsivity" - This attitude is found in pilots who act quickly, usually in the manner that first comes to mind.

3. "Invulnerability" - This attitude is found in pilots who act as though nothing bad can happen to them.

4. "Macho" - This attitude is found in pilots who continually try to prove themselves better than others. They tend to act overconfident and attempt difficult tasks for the admiration it gains them.

5. "Resignation" - This attitude is found in pilots who feel that they have little or no control over their circumstances. They are resigned to let things be as they are. They may deny that the situation is as it appears. They are likely to fail to take charge of the situation. They may also let other people or committments influence their decision making.

Interpreting Your Pilot Decisional Attribute Questionnaire

The following table is a summary of the concepts discussed above and shows you how your decisional attributes discovered in Chapter 1 fit in. You should refer to your profile in Chapter 1. The peaks in the curve indicate possible

hazardous attributes in your decision making that should receive attention. The next chapter will show you how to deal with these attributes.

Profile	High Scale	Attribute	Explanation
	I	Anti-Authority	"The Regs are for someone else."
	II	Impulsivity	"I must act now - there's no time."
	III	Invulnerability	"It won't happen to me."
	IV	Macho	"I'll show you. I can do it."
	V	Resignation	"What's the use?" "It's not as bad as they say." "They're counting on me."

The Poor Judgment Chain

Accident data suggests that most mishaps result from a series of poor pilot decisions which may be called the "poor judgment chain." One erroneous decision increases the probability of another and as the poor judgment chain grows, the probability of a safe flight decreases. Therefore, the student is instructed that the chain must be broken as soon as possible, beginning with the pilot's recognition that a poor judgment has been made. Consider the following example:

A non-instrument rated pilot, with limited experience flying in adverse weather, wanted to arrive at his destination by a certain time, and he was already 30 minutes late. In spite of his weather inexperience, he decided to fly through an area of possible thunderstorms to reach this area just before dark. Arriving in the thunderstorm area, he encountered lightning, turbulence, and heavy clouds. Night was approaching, and the thick cloud cover made it very dark. In the darkness and turbulence, the pilot became spatially disoriented because he failed to trust his instruments.

This pilot made several errors in judgment. First, he let his desire to arrive at his destination on time override his concern for a safe flight. Then he overestimated his flying abilities and decided to use a route that took him through a potential area of thunderstorm activity. Next, the pilot pressed on into obviously deteriorating conditions instead of changing course or landing prior to his destination.

The disastrous results, however, need not have been a foregone conclusion. The pilot could have broken the PJ Chain at any time, but he did not. Good judgment would have meant flying around the adverse weather and accepting the fact that he might be late. Once in the bad weather, good

judgment could have led the pilot to decide to avoid flying into clouds and turbulence. Finally before becoming disoriented in the dark, the pilot could have used good judgment to calm himself and rely on his instruments.

Two Principles of the PJ Chain

The first principle of the PJ Chain is that one poor judgment increases the probability that another will follow. Decisions are based on information that the pilot has about himself, the aircraft, and the environment. He or she is less likely to make a poor decision if this informaton is accurate. Thus, one poor decision increases the availability of false information which may then negatively influence decisions that follow.

The second principle of the PJ Chain is that as the PJ Chain grows, the alternatives for safe flight decrease. If a pilot selects a bad alternative, the options available to select better alternatives may be lost. For example, if a pilot makes a poor decision and flies into hazardous weather, the alternative to circumnavigate the weather is probably lost.

Breaking the PJ Chain

Because pilot judgment is a mental process, pilots can be trained - or even retrained if necessary - to use good judgment in the first place or to reduce the influence of the hazardous decisional attributes mentioned above. Breaking a PJ Chain in itself is an act of good pilot judgment. There are five steps that you can use to do so. (Note: While reading the following explanations for each step, refer to Figure 1 to understand better how the five steps work together to break a poor judgment chain.)

1. Recognize PJ: Get Feedback - Recognize that you may have made a poor decision and admit your error. If error recognition does not occur, your ability to prevent another poor decision is reduced. To recognize a poor decision, you must receive feedback.

   Feedback is received from two sources: your senses which give you an awareness of the situation or an observer. In training your best feedback comes from an outside observer, such as your flight instructor. Then, as training progresses, you learn to provide your own feedback. This is sometimes difficult because many people are hesitant to admit an error in judgment. Yet, as indicated above, safe flight requires these types of decisions.

2. Check for Stress - A high degree of stress and anxiety can reduce a pilot's ability to exercise good judgment. Later we will show you how to recognize your own stress and anxiety levels and reduce them.

3. Engage in Problem Resolving - Problem resolving is the necessary activity of correcting all hazardous situations that have resulted from the poor judgment. You will be learning more about pilot problem resolving activities later in this manual.

4. Search for Other PJ's - Remember that poor judgments tend to occur in chains. If one poor judgment is recognized, be absolutely certain that it is the only one currently affecting the operation of the aircraft.

5. Review Original PJ Give Self Feedback - After a PJ Chain has been broken, review the original poor decision, usually best done as soon as possible after landing. Critically examine what it was and how you came to make it. This review provides feedback you need to avoid beginning a similar poor judgment chain in the future.

Chapter 3

IDENTIFICATION PRACTICE OF HAZARDOUS ATTITUDES

Better Decision Making through Practice

This chapter is designed to help you identify and understand the five hazardous attitudes and to see how they can influence your reaction to situations requiring judgment. As you recall, the five hazardous attitudes are:

I	ANTI-AUTHORITY	"The Regs are for someone else."
II	IMPULSIVITY	"I must act now - there's no time."
III	INVULNERABILITY	"It won't happen to me."
IV	MACHO	"I'll show you. I can do it."
V	RESIGNATION	"What's the use?"

Refer back to Chapter 2 and review the explanations of the hazardous attitudes. Once you have refreshed your memory with the definitions, continue with this exercise.

Below you will find another series of true flying situations. At the end of each situation, you will be asked to select an alternative which best illustrates the reactions of a pilot who has a particular hazardous attitude. After you select what you feel is the best alternative, look immediately at the appropriate response list for the proper response. This page will tell you if your answer is correct or incorrect. If you answered correctly, go on to the next situation. If you answered incorrectly, you will be told why. Then go back to the situation and select another alternative.

KEEP SELECTING ALTERNATIVES UNTIL YOU SELECT THE CORRECT ONE. Do not be concerned if you select a wrong alternative. You will learn something from the feedback given to you. The lessons are deliberately repetitious and thus, get easier as you go along.

THE ANTI-AUTHORITY HAZARDOUS ATTITUDE

From the five choices following each situation, pick the ONE choice that is the best example of an Anti-authority hazardous attitude. Check your answers on the next page before continuing. REMEMBER - if you did not choose the correct answer, select another until you choose the correct one.

Situation 1:

You approach the VOR and the controller asks if you intend to make a full VOR procedure or would accept a right turn of more than 90 degrees to the final approach course. You state that you will make the turn directly onto final at 2,000 feet though this will press you to get established on the approach. Which of the following alternatives best illustrates the ANTI-AUTHORITY reaction?

a. It wasn't your idea to make the approach like this.

b. No controller is going to influence your flying.

c. You don't need the full approach, you know you are a good instrument pilot.

d. You are in a hurry and don't wish to bother with the full approach.

e. You know the controllers will be impressed with this approach.

A GOOD JUDGMENT THOUGHT ... "Make as much time available on an approach as possible, you may need it."

Situation 2:

You are advised of the current destination weather: "ceiling 400 feet, visibility two miles ... "The published minimum descent altitude is 400 feet above ground level. From your communications with radar, it is apparent you are experiencing some course problems due to malfunctioning directional gyro and indeed you are. In spite of this you elect to "make a pass at it." Which of the following alternatives best illustrates the ANTI-AUTHORITY reaction?

a. You know you can make the approach, you've been in worse situations and have come through.

b. Minimums are quire conservative and you know you can dip down just enough to get in.

c. You don't like to fly with malfunctioning equipment and want to land immediately.

d. Wait 'till the guys hear this one!

e. It's not your fault the DG isn't working, so you might as well try it.

A GOOD JUDGMENT THOUGHT ... "Stay on the ground if you find yourself with an airplane inadequate for the task at hand - expecially under instrument conditions."

RESPONSE LIST 1

THE ANTI-AUTHORITY HAZARDOUS ATTITUDE

Situation 1:

Alternative a: By assuming someone else has responsibility for your approach, you exhibit a "what's the use?" attitude. Go back to Situation 1 and select another alternative.

Alternative b: Correct. "The Regs are for someone else" attitude assumes controllers are interfering with your business. You are thinking in an anti-authority manner. Go on to Situation 2.

Alternative c: Here you are taking the "it won't happen to me" stand. You think of yourself as invulnerable. Go back to Situation 1 and select another alternative.

Alternative d: This is the hazardous thought of impulsivity: "I must act now - there's no time." Go back to Situation 1 and select another alternative.

Alternative e: Whenever your wish to impress someone influences your decision, this is the macho attitude; "I'll show you. I can do it." Go back to Situation 1 and select another alternative.

Situation 2:

Alternative a: Invulnerability emphasizes "it won't happen to me." Go back to Situation 2 and select another alternative.

Alternative b: Absolutely! This is the anti-authority attitude where the rules are for someone else. Go on to Situation 3.

Alternative c. Decisions made in haste characterize the impulsivity hazardous thought pattern, "I must act now - there's no time." Go back to Situation 2 and select another alternative.

Alternative d. No. This kind of thinking typifies the macho attitude. Go back to Situation 2 and select another alternative.

Alternative e. This kind of response suggests an attitude of resignation - "What's the use?" You have no control over the events. Go back to Situation 2 and select another alternative.

THE IMPULSIVITY HAZARDOUS ATTITUDE

From the five choices following each situation, pick the ONE choice that is the best example of an Impulsivity Hazardous attitude. Check your answers on the next page before continuing. REMEMBER - if you did not choose the correct answer, select another until you choose the correct one.

Situation 1:

At 10,000 feet on an IFR flight above a thin layer, you became aware of a slight change in the "feel" of your engine. Three minutes later a small vibration began and you detected an odd, hot smell in the cockpit. Which of the following alternatives best illustrates the IMPULSIVITY reaction?

a. Nothing will happen, the engine was just over-hauled.

b. You figure there isn't anything you can do, it is the mechanics' fault.

c. You don't want to tell ATC, they might try to tell you what to do.

d. There are no flames yet and you can handle the situation.

e. You immediately chop the power, push the nose over and call ATC.

A GOOD JUDMENT THOUGHT ... "Haste makes waste."

Situation 2:

As you enter the pattern you normally lower the flaps. The tower suddenly changes the active runway. Distracted, you forget to use the before-landing checklist. On short final you find yourself dangerously low with a high sink rate. Glancing back, you realize that you forgot to extend the flaps. Which of the following alternatives best illustrates the IMPULSIVITY reaction?

a. You feel that nothing is going to happen because you've made intentional no-flap landings before.

b. You laugh and think, "Boy, this low approach will impress people on the ground."

c. You think that using a checklist is a stupid requirement.

d. You immediately grab the flap handle and add full flaps.

e. You think, "It's all up to whether I get an updraft or downdraft now."

RESPONSE LIST 2

THE IMPULSIVITY HAZARDOUS ATTITUDE

Situation 1:

Alternative a: No. This is the "It won't happen to me" attitude of being invulnerable. Go back to Situation 1 and select another alternative.

Alternative b: Putting the responsibility on someone else shows the attribute of resignation. Go back to Situation 1 and select another alternative.

Alternative c: Resenting the authority of someone else or thinking anti-authority hazardous thought pattern. Go back to Situation 1 and select another alternative.

Alternative d: No. This is showing the macho attitude of "I can do it." Go back to Situation 1 and select another alternative.

Alternative e: Absolutely! "I must act now - there's no time" is the thought behind this alternative. Go on the Situation 2.

Situation 2:

Alternative a: Feeling that nothing bad can happen suggests the invulnerability hazardous thought pattern, "It won't happen to me." Go back to Situation 1 and select another alternative.

Alternative b: When you are thinking about impressing people on the ground, watch out for the macho hazardous thought, "I can do it" Go back to Situation 1 and select another alternative.

Alternative c: Thinking that checklists are stupid suggests that you feel the aircraft designers, the government, and your instructor - all of whom urge the use of checklists - are wrong. This suggests a "Don't tell me" reaction which is the anti-authority hazardous thought. Go back to Situation 1 and select another alternative.

Alternative d: Right! Immediately adding full flaps without thinking is an example of the impulsivity hazardous thougnt, "Do something quickly." Unfortunately, in this situation, full flaps will probably only increase the sink rate. Go on to Situation 2.

Alternative e: If you are convinced that it's up to the wind, this implies the hazardous thought of resignation, "What's the use." Go back to Situation 1 and select another alternative.

THE INVULNERABILITY HAZARDOUS ATTITUDE

From the five choices following each situation, pick the ONE choice that is the best example of an Invulnerability Hazardous attitude. Check your answers on the next page before continuing. REMEMBER - if you did not choose the correct answer, select another until you choose the correct one.

Situation 1:

You are enroute to your destination which is in a Group I TCA, actually only five miles inside the TCA. Your destination is reporting MVFR, so you elect to cancel your IFR flight plan and skirt in under the lower limit of the TCA and request a special VFR landing. Which of the following alternatives best illustrates the INVULNERABILITY reaction?

a. There is really nothing ATC could do to help in this situation anyway.

b. You do this all the time, no problem.

c. TCA's are just another control device put on pilots.

d. This is the first idea that comes to mind, you go for it.

e. This is the way the good pilots do it.

A GOOD JUDGMENT THOUGHT ... "Accept all the help you can get."

Situation 2:

You've made this approach at least one hundred times, many times down to minimums. The early morning ground fog these summer mornings presents even a more challenging picture. As you reach the MDA, you peer through the muck, straining to see that familiar scene. Just as the "TO/FROM" indicator flips, you catch a glimpse of what you know must be the end of the runway. You go for it. Which of the following alternatives best illustrates the INVULNERABILITY reaction?

a. You've made this approach so many times, you could do it with your eyes shut.

b. You know the minimums can be fudged, just a bit.

c. There's really nothing to this, all's well that ends well.

d. Land it now, there's no time to waste.

e. I hope luck is with me now, it's out of my control.

A GOOD JUDGMENT THOUGHT ... "Make sure that the runway is in the eye of the beholder."

RESPONSE LIST 3

THE INVULNERABILITY HAZARDOUS ATTITUDE

Situation 1:

Alternative a: This is an attitude of resignation - "What's the use?" Nobody can help me anyway. Go back to Situation 1 and select another alternative.

Alternative b: You're right! Invulnerability hazardous thoughts include "It won't happen to me." Go on to Situation 2.

Alternative c: No. "Regs are for someone else" is the anti-authority attitude. Go back to Situation 1 and select another alternative.

Alternative d: The need to "act now" is shown here. This is the impulsivity hazardous thought pattern. Go back to Situation 1 and select another alternative.

Alternative e: Identifying with the thought "I can do it" is the macho attitude. Go back to Situation 1 and select another alternative.

Situation 2:

Alternative a: No. This is the macho attitude. Go back to Situation 2 and select another alternative.

Alternative b: Thinking "the Regs are for someone else" is the hazardous thought of anti-authority. Go back to Situation 2 and select another alternative.

Alternative c: Correct. "It won't happen to me" is the attitude of being invulnerable. Go on to the next hazardous attitude.

Alternative d: No. "I must act now - there's no time" is the hazardous attitude of impulsivity. Go back to Situation 2 and select another alternative.

Alternative e: "Figuring the situation is out of your control is thinking in the resignation hazardous attitude mode. Go back to Situation 2 and select another alternative.

THE MACHO HAZARDOUS ATTITUDE

From the five choices following each situation, pick the ONE choice that is the best example of a Macho Hazardous attitude. Check your answers on the next page before continuing. REMEMBER - if you did not choose the correct answer, select another until you choose the correct one.

Situation 1:

On a trip to the east coast, you stop at an enroute Air Force Base for fuel. After refueling, the density altitude prior to your departure is reported as 10,500 feet. You are already slightly heavy when you depart. At the rate you are climbing, you will just barely clear the minimum crossing altitude at the next intersection on your route of flight. Which of the following aternatives best illustrates the MACHO reaction?

a. There is really nothing you can do about it; it is up to ATC to make sure you clear.

b. The MCA's have plenty of leeway for clearance. So what if you're a little low.

c. Don't worry, you're a good pilot and will make it.

d. When you see that you cannot climb enough you immediately inform ATC of your situation without determining your intentions.

e. Mountain flying isn't any different and you've never run into any problems before. Nothing will happen.

A GOOD JUDGMENT THOUGHT ... "Understand and use your aircraft performance charts."

Situation 2:

On an IFR flight plan you emerge from a cloud to find yourself within three-hundred feet of a helicopter. Which of the following alternatives best illustrates the MACHO reaction?

a. You're not too concerned, everthing will be alright.

b. You should fly a little closer, just to show him ...

c. It's not your responsibility to keep separated.

d. You quickly turn away and dive, to avoid a collision.

e. With events like this, why should you ever follow the rules.

A GOOD JUDGMENT THOUGHT ... "Fly defensively."

RESPONSE LIST 4

THE MACHO HAZARDOUS ATTITUDE

Situation 1:

Alternative a: Assuming someone else is responsible for you is the resignation hazardous attitude. Go back to Situation 1 and select another alternative.

Alternative b: "The Regs are for someone else" and not necessarily for you is thinking in the anti-authority mode. Go back to Situation 1 and select another alternative.

Alternative c: Right! Thinking "I'll show you. I can do it" is the macho hazardous attitude. Go on to Situation 2.

Alternative d: Acting before thinking is exercising the impulsivity hazardous attitude. Go back to Situation 1 and select another alternative.

Alternative e: Saying nothing will happen to you is acting invulnerable. Go back to Situation 1 and select another alternative.

Situation 2:

Alternative a: No. This is the attitude that you have never had problems before and it would never happen to you. Go back to Situation 2 and select another alternative.

Alternative b: That's it. Macho hazardous thought include "I'll show you." Go on to the next hazardous attitude.

Alternative c: Taking for granted that you are not in control is the hazardous attitude of resignation. Go back to Situation 2 and select another alternative.

Alternative d: This is acting on impulse; "I must act now, there's no time." Go back to Situation 2 and select another alternative.

Alternative e: An attitude that the rules do not have to be followed shows the anti-authority hazardous thought pattern. Go back to Situation 2 and select another alternative.

THE RESIGNATION HAZARDOUS ATTITUDE

From the five choices following each situation, pick the ONE choice that is the best example of a Resignation Hazardous attitude. Check your answers on the next page before continuing. REMEMBER - if you did not choose the correct answer, select another until you choose the correct one.

Situation 1:

You are pilot in command of an IFR flight in IMC. You have just encountered embedded thunderstorms on your route of flight. Which of the following alternatives best illustrates the RESIGNATION reaction?

a. What's a little storm? You always come through these situations.

b. Quick, turn around to get out of it.

c. Though your instructor taught you to slow down in turbulence, you're going to bore right through this as fast as possible. What did he know?

d. It's ATC's responsibility to keep you out of the weather.

e. You can handle this like a pro.

A GOOD JUDGMENT THOUGHT ... "If caught in a storm, follow procdures."

Situation 2:

You have just run your two wing fuel tanks dry. It is apparant that the fuel guage is not indicating properly. You are in and out of clouds on your IFR flight plan at night. Which of the following alternatives best illustrates the RESIGNATION reaction?

a. You can really show them now!

b. You can still make your destination; those reserve requirements are just formalities.

c. Well, that's the way things go. There's nothing you can do.

d. You've been in tight spots before and everything always works out.

e. You must land now, there is no time.

A GOOD JUDGMENT THOUGHT ... "Cross check your fuel consumption."

RESPONSE LIST 5

THE RESIGNATION HAZARDOUS ATTITUDE

Situation 1:

Alternative a: Assuming nothing will happen to you is the attitude of invulnerability. Go back to Situation 1 and select another alternative.

Alternative b: No. This is acting on impulse. Go back to Situation 1 and select another alternative.

Alternative c: Going against an authority figure is the anti-authority attitude. Go back to Situation 1 and select another alternative.

Alternative d: Correct! This is the hazardous attitude of resignation. The acceptance of the fact that the situation is not in your control and you cannot change things typifies this attitude. Go on to Situation 2.

Alternative e: "I can do it" is the macho attitude. Go back to Situation 1 and select another alternative.

Situation 2:

Alternative a: No. "I'll show them" is thinking in the macho hazardous attitude pattern. Go back to Situation 2 and select another alternative.

Alternative b: "The Reg's are for someone else" is the hazardous attitude of anti-authority. Go back to Situation 2 and select another alternative.

Alternative c: Yes. This idea of not being able to control the situation is the hazardous attitude of resignation. Go on to the next exercise.

Alternative d: The invulnerability hazardous attitude involves not believing that it could happen to you. Go back to Situation 2 and select another alternative.

Alternative e: No. This is the attitude of impulsivity. "I must act now, there's no time." Go back to Situation 2 and select another alternative.

Chapter 4

ANTIDOTES FOR HAZARDOUS THOUGHTS

After having completed the previous section carefully, you now should be able to identify the five major hazardous thoughts which contribute to poor pilot judgment. Moreover, by considering your own actions and reactions to difficult or stressful situations you will be more aware of and alert to them in your own thinking. This is an important first step in eliminating them from your judgments. This chapter is designed to teach you a way to counteract hazardous thoughts so that they do not affect your actions.

Since you cannot think about two things at once, one way to keep from thinking a hazardous thought is to think another thought. By telling yourself something different from the hazardous thought, you are "taking an antidote" to counteract the hazardous thought. You remove a hazardous thought by substituting the antidote. Thus, if you discover yourself thinking, "It-won't happen to me", mentally tell yourself, "That is a hazardous thought." Recognize a hazardous thought, and then say its antidote yourself.

To do this, you must MEMORIZE THE ANTIDOTES for each of the hazardous thoughts. Learn them so well that they will automatically come to mind when you need them.

ANTIDOTE RECALL

Do not start this lesson until you have learned the antidotes thoroughly. Practice them now as you would a checklist. Without referring to the text, write the antidote to each hazardous thought below. Check your statements with those on the next page, and if you are correct, continue. If not, study the antidotes until you can write them word-for-word from memory.

Hazardous Thought	Antidote
ANTI-AUTHORITY: "Don't tell me what to do!"	"Follow the rules. They are usually right."
IMPULSIVITY: "Do something - quickly!"	"Not so fast. Think first."
INVULNERABILITY "It won't happen to me."	"It could happen to me. Be careful."
MACHO "I can do it."	"Taking chances is foolish."
RESIGNATION: "What's the use?"	"I'm not helpless. I can make a difference."

ANTIDOTE IDENTIFICATION

Each of the following situations contains a description of what is happening in a flight situation and what the pilot is thinking. Correctly apply the hazardous thought antidotes.

Instructions:

1. In Situation 1, review the thinking and actions of the pilot, then look for signs of hazardous thoughts. When you recognize one, write its name and its antidote.

2. After completing Situation 1, review the answers. Do not proceed with the other situations until you have done so. Your responses should closely match the hazardous thought responses identified in the key. (Note: Different people may see the same situation slightly differently, so your answers may not be identical to the key. However, your answers should agree with the key for at least three of the hazardous thoughts, and you should have written, word-for-word, the correct antidote.)

3. If you do not do well on situation 1, study your answers to discover what misunderstandings you have about the hazardous thoughts and their antidotes. If necessary, return to earlier chapters in this manual to clear up any confusion before going on to the next situation. This is very important - you will learn more from this exercise if you are clear about the material covered up to this point, than if you simply read through the exercise without working carefully through it.

4. Continue with the remaining situations in the same manner. Follow the instructions at the end of the situation key to guide you to the completion of this section.

Situation 1:

A relatively new 2LT, assigned as an instructor to ATC, has gained approval to take one of the Squadron's T-37 aircraft on a cross-country over the weekend. He plans the trip to a midwest Air Force Base not far from his home town of about 1,000 people. In the air, the pilot thinks, "It's great to be up here without a student to worry about or another instructor criticizing everything I do. The do-it-by-the-book attitude of the Training Command takes all the fun out of flying."

As he approaches his destination, he decides to make a pass over his home town and land at the small municipal airport. He thinks, "It won't be dangerous at all...the airport is well maintained and everone will get quite a charge out of it. I'll just extend the ETA on my VFR flight plan so I won't get in trouble and the Air Force will never know."

"If anyone should happen to check on me or find out I landed at an unauthorized airport, I'll just tell them it was a precautionary landing. O.K., I'll do it. The plan is foolproof."

The 2LT makes a hard landing and nearly runs off the runway before he gets the aircraft stopped. However, he is very proud of himself and he thinks, "Right on! You're a natural for being a great pilot."

As he taxis to the ramp area, a county sheriff's car drives up with the lights going. Surprised that a sheriff's deputy would pay any attention to his landing here, he starts cursing this unpleasant turn of events. "I just know this cop is going to foul up my whole day. Why don't they stick to catching real criminals and leave people like me alone to have some harmless fun? If it weren't for my bad luck, this cop wouldn't have come along and this would have been a great afternoon."

Do not proceed with Situation 2 until you have reviewed the answer key to this situation on page 43.

Situation 2:

A student and instructor are returning from a VFR dual cross-country, and they decide to "buzz" a group of sun bathers. The instructor is an experienced pilot and has related stories of doing this kind of thing many times before. In fact, he often brags that someday he will be a member of the "Thunderbirds," and then everybody will be able to see his talents on display.

The student obviously gets a charge out of it. However, as a low-time pilot, he wonders if they are not pushing their luck. He is not worried about an accident, however, because he is convinced that his instructor is a great pilot who can handle anything that might happen.

As they are "buzzing" the beach, both are interested in watching for the reactions of the sunbathers on the ground. They descend lower than usual on the third pass. When they try to climb out, the plane does not make it over the power transmission lines. They catch a line, sparks fly, and the wing sustains minor damage. The student yells, "We're going to crash, we're going to crash!"

The IP is shaken, but he maintains control of the airplane and tells his student, "Calm down and let's fly this thing back to the Base, or we're going to be in big trouble over this. I told you I could handle anything in this airplane."

As they head for the Base, the airplane continues to fly without difficulty. They have a good laugh over the incident, telling one another that it is another great adventure in their flying careers. The IP says "We'll report this as a bird strike and I think I can arrange things with mainenance so it stays that way. You know, if the power company had any sense, they would bury all those power lines. If they would do that, pilots like us would have an easier time of flying safely."

Do not proceed with situation 3 until you have reviewed the answer key to this situation on page 43.

Situation 3:

A 2LT is authorized a cross-country to a civilian airport with a part-time tower. His approval specified that he must arrive while the tower is in operation and the Airport Traffic Area is in effect. There is a NOTAM on the runway lights but he is in a hurry and neglects to check.

As things would have it, he arrives late and is faced with a night landing and no runway lights. He thinks, "I didn't consider the possibility of arriving this late. I should have checked the NOTAMS." Then he becomes angry with the airport management, thinking, "They could work out something with these lights, either leave them on at night, or install a pilot controlled system. Who are they to control how late I land? I'll see the manager tomorrow and tell him a thing or two about how to run an airport."

Determined to land, he declares, "I'm landing here tonight, lights or no lights. I'll just have to rely on myself and show them how a top-notch Air Force pilot can do whatever needs doing." He chooses the runway which parallels the highway adjacent to the airport and uses the street lights as reference. Unsure of his height above the runway, he flares too quickly and begins to float. He immediately forces the airplane onto the runway rather than going around or extending his landing.

After landing hard, the aircraft swerves off the runway and into a fence. He is unhurt, but the airplane is substatioally damaged. To himself, he says, "If the lights were on, this would not have happened."

A few minutes later some people arrive to see what has happened. He starts telling them how the accident is the fault of the airport management. Someone asks him why he decided to land without airport lights. "There should be more rules about how to run an airport and less about how to fly airplanes."

Check your answers to this section with the appropriate key on page 44.

RECOGNIZING AND REPLACING HAZARDOUS THOUGHTS

You have now learned the meaning of the five hazardous thoughts and the antidotes to substitute for them. But, for judgment training to benefit you, the mental process of recognizing a hazardous thought, substituting the correct antidote, and then supplying good judgment thoughts must become automatic.

The following exercise, provides additional practice in recognizing potential hazardous thoughts in various flight situations, recalling the correct antidote, and thinking of good pilot judgment for the same situation.

Instructions

1. Read each situation and the description of the pilot's thinking.

2. In the blanks beneath each situation, fill in the hazardous thought and antidote, and a brief description of good pilot judgment for the same situation. (You do not need to write complete sentences.)

3. Ask your instructor to review your answers when you have completed the first five situations.

Situation 1:

Pushing in the fuel quantity test switch fails to return the fuel quantity indicator needle to zero, indicating that the fuel gauging system is not operating properly. Everything else appears to be normal and so you elect to continue the take-off! Your "co-pilot" feels strongly that you should discontinue the flight and return to Base. You become upset and inform him that you have seen this kind of thing before and it always turns out to be a faulty instrument.

Hazardous Thought:

Antidote:

Good Judgment:

Situation 2:

You have been cleared for a night visual approach into an airport surrounded by a very confusing pattern of lights. You are not sure if this is the airport. Nothing looks familiar, but it has been over a year since you were last here. You decide not to say anything and to go ahead and land, thinking, "This has to be it, lets land and get this flight over with."

Hazardous Thought:

Antidote:

Good Judgment

Situation 3:

You are assigned to take a visiting "VIP" on a T-37 orientation flight. You neglect to ensure that he has the "Parachute Arming Lanyard Anchor" properly secured. Rather than pointing it out now, you go ahead and take off. You know that, as a good pilot, you could handle any emergency long enough to get him buckled up properly.

Hazardous Thought:

Antidote:

Good Judgment:

Situation 4:

Landing at an unfamiliar airport for fuel, you give instructions to the line crew and run inside the terminal to go to the washroom. Returning to the aircraft, you are in a hurry and do not check the position of the fuel filler cap. You feel that the responsibility for ensuring that the fuel filler caps are positioned properly is not yours anyway.

Hazardous Thought:

Antidote:

Good Judgment

Situation 5:

You are assigned to a local night solo flight. After take-off you fly into a low-hanging cloud layer which you hadn't noticed before. You think that you'll be out of the clouds soon because the sky looked clear from the ground. Besides, you have flown through light cloud before in the daylight.

Hazardous Thought:

Antidote:

Good Judgment:

Situation 6:

You are on a cross-country flight with three other T-37's and are scheduled for a night launch to return home. After a very light lunch, the other pilots, all of whom are having a beer, invite you to join them for an afternoon on the beach. They have a cooler of beer and food already packed. They remind you that you have flown the route many times and that the weather conditions look to remain excellent. They begin to mock you for not drinking with them. You decide to join them, thinking that just one beer will not have a bad effect on you.

Hazardous Thought:

Antidote:

Good Judgment:

Situation 7:

The tower advises you to land on a runway other than the one your prefer. You see other airplanes using the runway of your choice and wonder why you have been denied permission. Since the recommended runway is on the far side of the airport, you radio the tower and ask for a reconsideration. You feel that if other pilots can land their aiplanes on the other runway, so can you.

Hazardous Thought:

Antidote:

Good Judgment

Situation 8:

Because of strong headwinds on a cross-country flight, you land at an auxillary airfield to refuel only to learn they are out of fuel. The Operations Officer suggests that you backtrack 50 miles to an airfield that has fuel. You continue the flight because your own instructor approved your flight plan with knowledge of the weather conditions.

Hazardous Thought:

Antidote:

Good Judgment:

Situation 9:

The weather forecast calls for drizzling rain across the ranges. En route, you notice ice accumulating on the wings. You are not sure what to do because you have never encountered this problem before. Because the airplane is still flying well, you are tempted to do nothing. Your co-pilot suggests you might radio for information. You radio for information but decide to ignore the advice since the airplane is continuing to fly well and the ice buildup doesn't seem to be getting worse.

Hazardous Thought:

Antidote:

Good Judgment:

Situation 10:

It is a bleak winter's morning. The temperature is below zero and you are not looking forward to the flight north. Visibility is just over three miles. It snowed earlier in the day. The ceiling is 1,100 feet. Earlier the airplane was cleared of what remained of the slushy snow, but take-off has been delayed for 15 minutes because of an advancing low cloud. Sleety conditions appear to be returning from the south, there are already flakes dropping on the screen, and you wonder if you will be able to take-off. You feel there is no use getting the ice removed, it is only going to form again.

Hazardous Thought:

Antidote:

Good Judgment:

Situation 11:

On final approach at night, you fly into patches of ground fog which severely limits visibility. Your altitude is 150 feet, and you debate whether you can level off at the correct height and land properly or whether you should abort the approach. You feel that the situation presents a challenge and you give your mind completely over to making the landing.

Hazardous Thought:

Antidote:

Good Judgment:

Situation 12:

The weather briefer advises you of possible hazardous weather conditions at your destination. En route, you encounter a brief thunderstorm and increasingly poor visibility. Although you have plenty of fuel to return to your departure point, you have a hunch that the weather will improve before you reach your destination. You think that the weather people are always complicating your flights, and sometimes, such as now, it is best to ignore them.

Hazardous Thought:

Antidote:

Good Judgment:

Situation 13:

Ideally, you would like to arrive early for an important date. If you stick to your flight plan, you will just make it, assuming there are no delays. Another alternative would be to take a route over the mountains, which will get you there much earlier. If you choose the latter, it means you mignt encounter a little low-hanging cloud near the peaks, while good weather prevails over the planned route. You tell yourself that there is no sense sticking to the planned route because, "There's nothing else to do to be sure to make it early."

Hazardous Thought:

Antidote:

Good Judgment:

Although you have had some practice at recognizing dangerous thought patterns, and applying the antidotes, this is not really the end of your learning about the five hazardous thought. When you were learning your checklists, you most likely practiced them when you had time. Treat the hazardous thoughts and the antidotes in the same way. Practice them so that they become familiar only by making them a part of you. Will you automatically apply them when the antidote is needed most?

Turn to the next section, or collect the Stress package from your instructor.

Answer key to Situations

Situation 1

Hazardous Thought: "It's great to be up here without an instructor criticizing everything I do. His do-it-by-the-book attitude takes all the fun out of flying."

Antidote: Anti-authority - "Follow the rules. They are usually right."

Hazardous Thought: "I'll land at an unauthorized airport".

Antidote: Impulsivity - "Not so fast. Think first."

Hazardous Thought: "The plan is foolproof."

Antidote: Invulnerability - "It could happen to me."

Hazardous Thought: "Right on! You're a natural for being a great pilot."

Antidote: Macho - "Taking chances is foolish."

Hazardous Thought: "If it weren't for my bad luck, this cop wouldn't have come along and this would have been a great afternoon."

Antidote: Resignation - I'm not helpless. I can make a difference.

Situation 2

Hazardous Thought: In fact, he often brags that someday he will be a member of the Thunderbirds and then everybody will be able to see his talents on display.

Antidote: Macho "Taking chances is foolish."

Hazardous Thought: He is convinced that his IP is a great pilot who can handle anything that might happen.

Antidote: Invulnerability - "It could happen to me."

Hazardous Thought: The student panics and yells, "We're going to crash, we're going to crash!"

Antidote: Impulsivity - "Not so fast. Think first."

Hazardous Thought: "Calm down and let's fly this thing back to the Base or we're going to be in big trouble over this. I told you I could handle anything in this airplane."

Antidote: Macho - "Taking chances is foolish."

Hazardous Thought: ...telling one another that it is another great adventure in their flying careers.

Antidote: Invulnerability - "It could happen to me."

Hazardous Thought: "If they would do that, pilots like us would have an easier time of flying safely."

Antidote: Resignation - "I'm not helpless. I can make a difference."

Situation 3

Hazardous Thought: "They could leave the lights on at night. Who are they to control how late I can land?"

Antidote: Anti-authority - "Follow the rules - they are usually right."

Hazardous Thought: I'll just have to rely on myself and show them how a top-notch Air Force pilot can do whatever needs doing."

Antidote: Macho - "Taking chances is foolish."

Hazardous Thought: He immediately forces the airplane onto the runway rather than going around or extending his landing.

Antidote: Impulsivity - "Not so fast. Think first."

Hazardous Thought: To himself, Bill says, "If the lights were on, this would not have happened."

Antidote: Resignation - "I'm not helpless. I can make a difference."

Hazardous Thought: Bill starts telling them how the accident is the fault of the local airport management.

Antidote: Resignation - "I'm not helpless. I can make a difference."

Hazardous Thought: "Look, I'm an experienced pilot. Having no lights is not a serious problem."

Antidote: Macho - "Taking chances is foolish."

Hazardous Thought: "There should be more rules about how to run an airport and less about how to fly airplanes."

Antidote: Anti-authority - "Follow the rules. They are usually right."

Chapter 5

INFLUENCES AND RESOLUTION OF STRESS

Flying or not, one of the most fundamental issues when dealing with safety is how we deal with stress. Stress in its various forms has a large number of causes and consequences. In this section, we examine stress as it affects our lives in general and our flying performance. Suggestions are tnen made to enable us to deal with stress more effectively.

Simply recognizing the involvement of stress does not necessarily solve our problems. We must try to understand stress and how to cope with it. The growing interest in stress reflects the widespread awareness that stress is related to many physical and mental disorders, and to a large number of home and work-related accidents.

DEFINING STRESS

Stress is the term we use to describe the body's nonspecific response to demands placed upon it, whether these demands are pleasant or unpleasant. This description is important because the body reacts in the same way to any change. The change can be physical or emotional, painful or pleasant, or even life threatening. The change for you could be an unexpected windsheer encountered on landing, recognizing low oleo pressure during your pre-flight check, travelling on vacation, losing your wallet, or cutting your finger. Our bodies will respond to these and all other demands in three stages: First, there will be an alarm reaction; then resistance; and finally, exhaustion (if the stress continues). This three-stage response is part of our primitive biological coping mechanism which would have prepared our ancestors for fight or flight.

Alarm Reaction. In the alarm stage, the body recognizes the stressor, and prepares for fight or flight by activating a part of the brain (called the hypothalamus) which stimulates the pituitary gland to release hormones. These hormones trigger the adrenal glands to pour out adrenaline. Adrenaline increases heartbeat and rate of breathing, raises blood sugar level, increases perspiration, dilates the pupils, and slows digestion. The process results in a huge burst of energy, greater muscular strength, and better hearing and vision. You may have experienced several alarm reactions during your flying, for example, a sudden buffeting on low final. You may recall the effects of your body's alarm reaction.

Resistance. In the resistance stage, the body repairs any damage caused by the stress and may adapt to some stresses such as extreme cold, hard physical labor, or worries. Fortunately, most physical and emotional stressors are of brief duration and our bodies cope with the physiological demands of the stress. During our lifetime we go through the first two stages many times. We need these response mechanisms to react to the many demands and threats of daily living.

However, if the stress continues (for example, if you were caught on a VFR flight in instrument conditions, or realize that you may not reach your destination because of a fuel shortage), the body will remain in a constant state of readiness for fight or flight. It will be unable to keep up with the demands, leading to the final stage of exhaustion.

Exhaustion. Exhaustion generally affects only specific parts of the body and is temporary. For instance, marathon runners experience in their muscles and cardiovasuclar system severe stress which leads to exhaustion, but after a good rest they are back to normal and look forward to the next race. If exhaustion continues without relief over an extended period, there is risk of one of the diseases of stress (such as high blood pressure, arterio-sclerosis, migraine headaches, gastrointestinal disorder, rheumatiod arthritis, or asthma). The body may even give up, resulting in death.

ALL STRESS IS NOT BAD

Life without stress would be pretty dull. In reasonable doses, stress adds excitement to life. It is impossible to live without experiencing some degree of stress. Even when we are asleep our bodies are functioning, providing us with dreams which produce some stress.

Some situations can prompt bad stressors, causing damage or distress. Other types of stress are pleasurable, such as the exhilaration as we accelerate down the runway on take-off. Further, what may be stressful for one person may not be stressful for another.

THE EFFECTS OF STRESS

It is very easy to dismiss the effect of stress if we consider that it is having little impact upon our day-to-day functioning. However, the cumulative effect of persistent high levels of stress may lead to irritability, short temper, and low frustration tolerance in the short term. In the long term, continued stress may lead to changes in the nervous system and the body organs, including reduction of white cells and suppression of the immune system, creating conditions for disease.

Self-Observable Signs of Stress

1. General irritability, hyperexcitation, or depression.
2. Pounding of the heart, an indicator of high blood pressure.
3. Dryness of the throat and mouth.
4. Impulsive behaviour, emotional instability.
5. The overpowering urge to cry or run and hide.
6. Inability to concentrate, flight of thoughts and general disorientation.
7. Feelings of unreality, weakness or dizziness.
8. Predilection to become fatigued, and loss of the sense of fun in life.
9. "Floating anxiety" (We are afraid although we do not know exactly what we are afraid of).

10. Emotional tension and alertness, feeling of being "keyed up".
11. Trembling, nervous ticks.
12. Tendency to be easily startled by small sounds.
13. High-pitched, nervous laughter.
14. Stuttering and other speech difficulties.
15. Grinding of the teeth.
16. Insomnia.
17. Hyperactivity (A tendency to move about without any reason, an inability to just physically relax).
18. Sweating.
19. The frequent need to urinate.
20. Diarrhea, indigestion, queasiness in the stomach, and sometimes vomiting.
21. Migraine headaches.
22. Premenstrual tension or missed menstrual cycles.
23. Pain in the neck or lower back.
24. Loss of, or excessive appetite.
25. Increased smoking.
26. Increased use of legally prescribed drugs, such as tranquilizers or amphetamines.
27. Alcohol and drug addiction.
28. Nightmares.
29. Accident proneness.

How much Stress is in Your Life?

Put a tick in the "Happened" column if you have recently experienced the event described, then go back and count the number of ticks. Total your score.

Item No.	Happened ( )	Life Event
1.	_____	Death of spouse
2.	_____	Divorce
3.	_____	Marital Separation
4.	_____	Jail Term
5.	_____	Death of close family member
6.	_____	Personal injury or illness
7.	_____	Marriage
8.	_____	Lost your job
9.	_____	Marital reconciliation
10.	_____	Retirement
11.	_____	Change in health of family member
12.	_____	Pregnancy
13.	_____	Sex difficulties

14.	_____	Gain of new family member
15.	_____	Business readjustment
16.	_____	Change in financial state
17.	_____	Death of close friend
18.	_____	Change to different line of work
19.	_____	Change in number of arguments with spouse or partner
20.	_____	Mortgage or loan over $10,000
21.	_____	Foreclosure of mortgage or loan
22.	_____	Change in responsibilities at work
23.	_____	Son or daughter leaving home
24.	_____	Trouble with in-laws or partner's family
25.	_____	Outstanding personal achievement
26.	_____	Spouse or partner begins or stops work
27.	_____	You begin or end work
28.	_____	Change in living conditions
29.	_____	Revision of personal habits
30.	_____	Trouble with boss or instructor
31.	_____	Change in work hours or conditions
32.	_____	Change in residence
33.	_____	Change in school or teaching institution
34.	_____	Change in recreational activities
35.	_____	Change in church activities
36.	_____	Change in social activities
37.	_____	Mortgage or loan less than $10,000
38.	_____	Change in sleeping habits
39.	_____	Change in number of family social events
40.	_____	Change in eating habits
41.	_____	Vacation
42.	_____	Christmas
43.	_____	Minor violations of the law

Total number of ticks for 12 months: _____

The more change you have, the more likely you will suffer a decline in health. Of those who scored over 20 ticks, mostly in the top half of the table, 80 percent have a chance of a serious health change. With about 20 ticks distributed over the table, about 50 percent get sick in the near future. With less than half, but not more than a quarter, about 30 percent get sick in the near future.

TIME AND STRESS

The urgency of time drives most of us. Demands exceed the time available and overloading means that stress response is dangerously aroused. Irritability, impaired judgment, hypertension, headaches, and indigestion are frequent early signs of distress and potential illness. This is of crucial concern in the field of aviation in which safety checks play a major role.

Chronic Overload: Do you:

Rush your speech?
Hurry or complete other people's speech?
Hurry when you eat?
Hate to wait in line?
Never seem to catch up?
Schedule more activities than you have time available?
Detest "wasting" time?
Drive too fast most of the time?
Often try to do several things at once?
Become impatient if others are too slow?
Have little time for relaxation, intimacy, or enjoying your environment?

Most of us go back and forth between such hurried behavior and a more relaxed schedule, but if you answered "yes" to most of the above, you may be suffering from chronic overload.

Overcommitment and Self-Imposed Obligations. A very natural behavior for many people is their inability to say "no" to requests. The consequence is frequently a great deal of stress generated by the subsequent awareness that the commitment cannot be met. Overcommitment also occurs when overzealous people obligate themselves when they know at the time that the likelihood of completing the task is remote.

Modern life imposes on our limited store of time powerful pressures to behave as though we were capable of doing several things at once. Much of our life stress comes from self-imposed obligations. Does yours?

STRESS AND FLYING

In flying, we must consider three classes of stressors; physical, physiological, and psychological.

Physical stressors include conditions associated with the environment such as temperature and humidity extremes, noise, vibration, and lack of oxygen, often encountered in flight.

Physiological stressors include fatigue, lack of physical fitness, sleep loss, missed meals (which have led to a low blood sugar level), discomfort associated with a full bladder or bowel, and disease.

Psychological stressors are the social or emotional factors related to life stressors which we dealt with earlier, or they may be precipitated by mental workload such as analysing an aircraft problem in flight, or navigation.

When you need to consider only one thing at a time to reach a decision, you generally will have no difficulty making a decision. In flight, however, you will frequently have to deal with many situations simultaneously. Some times decisions are based on incomplete information within a short time period.

For example, in a cross-country flight you may realize that you are much lower on fuel than you expected. The clouds ahead appear to be building, and there is considerable interference on the radio. You are off course and you can't seem to find a familiar ground reference point. On top of this you failed to take a comfort stop before the flight and you now have a full bladder. The cabin heater is not functioning properly, and you are now starting to encounter turbulence. You now have many things on your mind. You begin to worry about arriving at your destination on time. You begin to worry about a forced landing and damaging the aircraft.

Your palms are now beginning to become sweaty and your heart is starting to pound. You feel a growing tension, and your thinking is becoming confused and unfocused. You may give too much attention the the "what if" questions which should be ignored.

You are reaching, or have already reached the overload state. It is inevitable that you will begin to make poor judgments that will result in a series of bad decisions. These might include pressing on into bad weather, or overflying good landing areas until you are almost out of fuel.

There can be plenty of stress to cope with in the flying environment itself without adding to them the burden of your life stressors. On the other hand, your life stressors may be sufficiently great already. That one poor (initial) judgment can lead to a dangerous compounding of stress-creating conditions. Stress effects are cumulative. They will eventually build to a point where the burden is intolerable unless you know how to cope.

STRESS AND PERFORMANCE

Let us review our major conclusions. Stress has a cumulative effect. Some degree of stress can be of assistance in some situations; and stressors which persist over a long period can severely affect our performance and health. So stress would seem to have a positive effect on performance when it is low, performance will peak at an optimum level of stress, then decline as stress increases further.

Furthermore, complex or unfamiliar tasks require a higher level of performance than simple or overlearned tasks. Complex and unfamiliar tasks also are adversely affected by increasing levels of stress.

In flying, accidents often occur when the task requirements exceed pilot capabilities, especially when stressors such as fatigue and emotional complications are involved.

COPING WITH STRESS

Up to this point, we have focused upon what stress is, and how it can affect us. Now we turn our attention to how we might best cope with stress.

By learning the goals and principles of coping, you can use stress constructively to promote good health, self-development, and flight safety.

As stated previously, stress is the product of an entire lifestyle. It is not just the product of an occasional crisis. Consequently, each person must learn to monitor personal internal arousal levels and find ways to relieve stress. Health can be protected by using constructive coping response to balance stress. For example, you can simply take a five-minute break and relax.

Total Body Approach: The Wellness Concept. The total body approach takes account of six aspects of well-being:

1. Physiological
2. Nutritional
3. Environmental
4. Emotional
5. Spiritual
6. Lifestyle values.

What you do in one of these areas supports, enhances, and capitalizes on actions in other areas.

For instance, poor eating habits may increase your stress level, leading to weight problems and lack of vitality. This lack of energy may slow down productivity and lead to increased pressure at home and at work to get things done. The pressure can lower your self-esteem or defensive behaviors, thus throwing your entire lifestyle out of balance and increasing your stress to unhealthy levels.

Behaviors consistent with good health and low stress are:

1. Minimizing or stopping activities detrimental to your health, such as smoking or drinking to excess.

2. Increasing health-producing behavior, such as relaxing at regular intervals.

3. Using self-regulation and self-control information, such as appropriate time management and thought stopping (deliberately stopping yourself from thinking negatively).

4. Being trained in health promotion strategies and technologies. These would include simple techniques as "time out" (a five-minute shut down when you recognize that stress is increasing - you can do this quite effectively in your workplace, or taking the phone off the hook if you need to solve one problem at a time), to more involved techniques which require formal training such as self-hypnosis and biofeedback.

5. Accepting responsibility for your own health, such as developing a stress reduction program.

Coping Responses

People who get along well in life can respond to any given situation with appropriate behavior. Coping behaviors include a variety of responses:

1. Emoti al - humor, anger, sadness, excitement;
2. Pers al habits - eating, smoking, s . physical activity, drinking;
3. Unconscious habits - nail biting, sighing, finger drumming;
4. Absorption in job, family, hobby.

Flexibility and a creative range of coping behaviours enable people to handle considerable stress. A limited coping repertoire may be harmful. For instance, if eating or drinking is the primary coping response to stress, obesity or alcoholism is likely to present its own problems. It is a bad idea to use "addictive" solutions to handle life stressors. Other potentially destructive responses include violence, procrastination, drug abuse, overwork, poor sleeping habits (sleep disorder), compulsive spending sprees, total withdrawal, and caustic remarks. They make a problem worse or initiate a new one rather than solve anything.

Complete the following guide for stress reduction.

IMPROVING MY EXTERNAL ENVIRONMENT

1. One way I can reduce unnecessary noise and irritations around me is to:

2. The amount of sleep I need each day in order to be maximally alert and able to cope with stress is:

3. I presently get that amount of sleep or rest.

Yes _____ No _____

4. (For those who answered No to #3):
A way I could rearrange my schedule in order to get enough sleep is:

5. Some changes or crises I foresee over the next year are:

6. Ways I can deal with these stresses are:

COPING WITH JOB STRESS

1. Identify kinds of stress you experience.

When does it occur?
How frequently?
Who or what is involved?
Any bad habits involved?

2. Prioritize which job stresses bother you most. Choose one to work on first.

3. Review coping methods you've tried with what success/failure?

4. Consider possible solutions.

Which can be implemented with most ease?

Who can help with implementaton?

JOB STRESS PROFILE

1. Some sources of job stress for me are:

2. Clues that reveal to myself and others that job stress is an important stress factor in my life:

3. How I now cope with job stress:

4. Some ideas or new ways to cope with job stress I want to try:

5. One step I will take the next working day to reduce job stress for me:

25 Ways of Combating Job Stress

Here are some ways that have been suggested to cope with job stress. Which can be applied in flying? Begin with the easier and simpler ones first to build your confidence before you embark on a more ambitious program of changes.

1. Start off your day with breakfast.

2. Occasionally chnge your routine by meeting a friend or co-worker for breakfast - allow enough time to really enjoy it.

3. Avoid drinking coffee or soft drinks all day; drink water or fruit juice instead.

4. Organize your work - set priorities.

5. Write it down, don't overburden your memory.

6. Don't try to be perfect, doing everything right at all times.

7. Don't try to do two, three or more things at once.

8. Consider occasionally coming in earlier or staying later instead of taking your work home with you every night.

9. Reduce the noise level if possible.

10. Restrict telephone calls by having them held or close the door when you are extra busy or need to concentrate.

11. Consider planning to use uninterrupted blocks of time.

12. Create a pleasant work environment in your immediate surroundings.

13. Speak up about petty annoyances while respecting the other's feelings.

14. Develop co-worker support networks. Can peak workloads be shared?

15. Don't take your job with you on breaks.

16. Take a lunch break away from work.

17. Occasionally go out to lunch with a co-worker or friend.

18. Take a ten or twenty-minute meditation break during lunch hour, or a yoga or exercise break.

19. Optimize your health with good nutrition, exercise, sleep and rest.

20. Monitor your work, rest, recreation balance. Are changes needed?

21. Develop with co-workers your own brand of happy hour or celebrate birthdays or other events as a break in the routine.

The following require more effort but will have long-term pay-offs.

22. Develop a wider variety of sources of gratification in your life, family, friends, hobbies, interests. Plan occasional special weekends or mini-vacations.

23. Consider changing your job or having your job responsibilities changed to better meet your interests and skills.

24. Be assertive, learn how to express differences, make requests and say "no" constructively. Consider taking a course in assertive training.

25. Don't overlook the emotional resources available to you that are close at hand - co-workers, supervisor, spouse, friends. This suggestion needs to be underscored for the male sex, who are programmed by society to avoid discussing or acknowledging feelings and problems but pay for it in stress disease.

COPING WITH STRESS WHILE FLYING

1. Identify the kinds of stress you experience.

   When does it occur?
   How frequently?
   Under what conditions does it occur?
   Are any bad habits involved (Refer to the 5 hazardous thoughts)?

2. Prioritize which stress concern you most.

   Choose one to work on first.

3. Review coping methods you've tried with what success/failure?

4. Consider possible solutions:

   Which can be implemented with most ease?

   Who can help with implementation?

From the 25 ways of combating stress, listed above, write those you can use to advantage (perhaps in an adapted form).

Making Go/No Go Decisions Before a Flight

It is part of good safety procedures that you give your aircraft a thorough preflight inspection, yet most pilots forget that as they are in control of a machine, they are well advised to give themselves an equally thorough preflight inspection. The I'M SAFE CHECKLIST is one way of doing this. You'll find the I'M SAFE CHECKLIST on the next page, but here are some specific suggestions.

1. Before you make a flight, limit your intake of liquids, especially caffeine - it acts as a diuretic. Drinking coffee has become a regular part of our working lives, but it has some serious short term and long term effects. Too much caffeine can cause headaches, irritability, sleeplessness and heart problems. Six cups of instant (or four cups of percolated) coffee a day is considered by health authorities to be TOO MUCH.

2. Never fly when you are angry or emotionally upset.

3. Never get into a situation where you must get to your destination at all cost.

4. YOU ALONE are pilot-in-command and YOU ALONE make the GO or NO GO DECISION.

Cockpit Stress Management

Avoid situations that distract you from flying the aircraft. If you feel tension mounting, here are some things you can do:

Loosen your collar;

Stretch your arms and legs;

Open air vents;

Don't hesitate to ask controllers to help, for instance, to speak more slowly or to give you a position fix (this is of extreme importance if you are not sure of your position);

Don't hesitate to declare an emergency when necessary or let other people know about your situation. Don't delay until it is too late!

Spend a few minutes with your instructor and jot down some other suggestions for reducing tension or anxiety while in flight.

The point is - reduce your workload to reduce stress levels - provide youself with the proper environment in which to make sound judgments. If an emergency does occur, be calm - think for a moment, weigh the alternatives, then act. Remember that fear and panic are your greatest enemies during an inflight emergency.

Your greatest tool for combating fear and panic is to familiarize youself thoroughly with your aircraft, its systems, and emergency procedures, along with the navigation/communications frequencies along your route of flight. Above all, maintain proficiency in your aircraft, for proficiency builds confidence. Know and respect your own personal limits. Give yourself plenty of leeway of an "out" when needed. Always have a "plan" and an "alternate plan" - leave yourself an out! Plan stops to allow adequate time for rest, for meals, and to stretch your legs.

Another situation that may generate stress involves letting little mistakes bother you until they build into a "big thing." If you make a mistake which you detect and correct, the most sensible thing to do is to forget about it and return your entire attention to flying. Don't keep thinking, "Why did I do it?", "How could I have been so stupid?", "Where did I go wrong?", What happens if I do it again?", If you do this, your mental energies and attention will be distracted form the job of flying. Wait until after you land, then "debrief" and analyze past actions.

ARE YOU FIT TO FLY?

THE "I'M SAFE" CHECKLIST

I LLNESS	Do I have any symptoms?
M EDICATION	Have I been taking prescription or over-the-counter drugs?
S TRESS	Am I under psychological pressure from the job? Am I under physical stress? Am I worried about financial matters, health problems, or family discord?
A LCOHOL	Have I been drinking or using non-prescribed drugs within eight hours? Within 24 hours?
F ATIGUE	Am I tired and not adequately rested?
E ATING	Am I adequately nourished?

1985 USAF-UES SUMMER FACULTY RESEARCH PROGRAM/

GRADUATE STUDENT SUMMER SUPPORT PROGRAM

Sponsored by the

AIR FORCE OFFICE OF SCIENTIFIC RESEARCH

Conducted by the

UNIVERSAL ENERGY SYSTEMS, INC.

FINAL REPORT

FEASIBILITY STUDY ON THE LOGISTICS OPERATIONAL ASSESSMENT MODEL

Prepared by:	Hobert H. Corley, Jr.
Academic Rank:	Teacher
Department and:	Mathematics
School:	Coalton High School
Research Location:	Air Force Human Resources Laboratory/ Logistics and Human Factors Division Logistics Systems Branch
USAF Research:	Major Joseph F. Nerad, Jr.
Date:	August 19, 1985
Contract No:	49620-85-C-0013

FEASIBILITY STUDY ON THE LOGISTICS OPERATIONS ASSESSMENT MODEL

By

Robert H. Corley, Jr.

ABSTRACT

The purpose of this project was to determine if it is feasible to integrate logistics models with combat operational models. This project also determines the requirements for the integration of logistics model modules into a combat operational model. This report describes the benefit of developing this new model and states some of the problems expected in integrating these models. This report also gives a list of models that can be used for this integration.

ACKNOWLEDGEMENTS

Research sponsored by the Air Force Office of Scientific Research/AFSC, United States Air Force, under Contract F49620-85-C-0013. The United States Government is authorized to reproduce and distribute reprints for governmental purposes not withstanding any copyright notation hereon.

I would like to thank the Air Force Systems Command, Air Force Office of Scientific Research, and the Human Resources Laboratory/Logistics & Human Factors Division Logistics Systems Branch (HRL/LRL) for selecting me as a summer fellow at Wright Patterson AFB. I would like to thank Major Joseph Nerad for his guidance and help on the Logistics Operational Assessment Model project and all the menbers of LRL for their help and information. I would also like to thank UES for conducting the Summer Faculty Research Program and providing all the information about Dayton that made my stay in Dayton enjoyable.

Grateful acknowledgement is extended to XMCO INC. for information about converting codes.

I. INTRODUCTION

This project was in the USAF Human Resources area, which deals with making computers and software more adaptable to the user's needs. This particular project involved integrating simulation models to make the simulations more realistic and more useful to USAF personnel.

As a teacher, this author is very interested in making the products of computer science easier to use and more valuable to the user. The ease of use and adaptability of a program is important to the user, particularly if that user is not specifically trained in computer science.

Along with M. S. degrees in both Mathematics and Computer Science, this author has experience in designing a variety of display and information systems. Specific background experiences which contributed to success in this project include information systems design and communication with customers at Computer Sciences-Technicolor Associates, design of Command, Control, and Display systems at Vitro Laboratories, and design of alphanumeric displays at Singer-Link.

This project provided an excellent opportunity to apply past experiences and education to a specific problem in a pleasant working environment. The UES Summer Faculty Research Program is a valuable and enjoyable experience.

II. OBJECTIVES OF THE RESEARCH EFFORT

The objectives of this research effort were to determine the feasiblity of integrating logistics and combat operational models and to determine the requirements for the integration. This report gives a list of models that could be integrated to produce the Logistics Operational Assessment Model.

III. OBSERVATIONS

According to members of the Logistics and Human Factors Division Logistics Systems Branch, there are some problems with the present logistics models and combat operational models. One way of solving these problems would be to integrate some logistics models with some combat operational models.

There are several problems associated with logistics models. It takes a long time to set up data files. In fact, these models still use a card format to input data. The data used for determining failure rates are based on peace time conditions. In general, none of these models deal with fabrication of parts; and these models do not simulate cannibalization in the same way as maintenance crews cannibalize parts in the field.

There are also several problems associated with combat operational models. One of the biggest problems associated

with certain combat operational models is that they are not realistic. For example, if a bomb explodes on a runway in some models, the runway always becomes inoperable. In real life, the extent of the damage may vary greatly. In some models, needed parts and aircraft appear with no waiting period. In real life, the part may be in the shop being repaired or on order from the depot. Therefore, some logistics modeling is needed to make the combat operational models more realistic.

After reviewing the literature and interviewing several people, three readily available logistics models were selected. They are Theater Simulation of Airbase Resources (TSAR), Logistics Composite Model (LCOM), and Dynamic Multi-Echelon (Dyna-METRIC). A description of each follows.

TSAR is a theaterwide logistics model whose fuction is to examine the effects of interdependent resources upon the sortie capabilities of single- or multi-base structures. It is also labor intensive. This model is modular in design since it has over a hundred subroutines. It is not hardware dependent, is written in FORTRAN, and requires 1000K of memory. One of TSAR's assets is that it provides measures of input on sortie generation resulting from resource replenishment between losses and outside the theater. Limitations of TSAR are (1) It does not generate battle damage data; and (2) It does not provide the level of detailed analysis the LCOM does in describing, particularly manpower usage. Limitation (1) can be overcome because TSAR

is designed to accept and analyze battle damage impact.

LCOM is a logistics model whose function is to analyze the support requirements of weapon systems and to assess the impact of support resource shortages on the operational status of the weapon. This model is designed to simulate one airbase, but can simulate more than one base. It runs on the Honeywell 600/6000, CDC 6600/7600, and ITEL AS/5 (IBM 360/370) and is written in SIMSCRIPT. LCOM requires 800K of core. A major drawback to using this model is that it is written in SIMSCRIPT. The structure of SIMSCRIPT makes it difficult to rewrite LCOM in another language in order to integrate it with combat operational models.

The Dyna-METRIC model is used to simulate the dynamic wartime behavior of repairable item stocks and to determine either the optimal stockage for supporting a specified sortie rate or the maximum sortie rate attainable with a given stockage. This model can handle a variety of single-base and multi-base configurations such as in-house repair facilities and central integrated repair facilities. It is modular in design since it has many subroutines. This model is written in FORTRAN and RATFOR and runs on an IBM 4331/370 and H6060. It requires 192K words of core. Dyna-METRIC's limitations are (1) Repair procedures are unconstrained and stationary except when repair capabilities are explicity stated; (2) Forecast sortie rates do not directly reflect flight-line resources and the daily employment plan; (3) Component failure rates vary only with flying intensity; (4) Aircraft

within each base are assumed to be nearly interchangable and fully mission capable; and (5) All echelons component repair processes are identical.

Through literature and interviews, two combat operational models were researched. These models, TSAR using inputs from Airbase Damage Assessment (TSARINA) and Tactical Warfare Model (TACWAR), are discussed below.

TSARINA generates damage by simulating an enemy attack on an airbase. This model interfaces with TSAR. It is not machine dependent and is written in FORTRAN. TSARINA needs 485K of core memory. A drawback to using TSARINA is that its results are not necessarily realistic. For example, if a bomb explodes on a runway, the runway always becomes inoperable. In real life this not always the case.

TACWAR is a combat operational model designed to evaluate the relative effectiveness of opposing combat forces employing conventional, nuclear, and chemical weapons which can be delivered by ground and air means. It has modular design and a model control element. It is written in FORTRAN and runs on the Honeywell 6080 and VAX 11/780. It needs between 60K and 180K of storage to run. It operates on a theaterwide level. Some limitations of TACWAR are (1) Logistics aspects are very aggregated; (2) Forward edge of battle area (FEBA) movement and attrition are determined by force ratios and lookup tables, so individual conventional weapons systems and their performances are not explicitly modeled; (3) Break through situations are represented by a

modification to movement rates; and (4) command, control, communication, intelligence, and electronics warfare are not played. Limitation (1) above can be overcome by integrating TACWAR with a logistics model. Limitation (4) can be partially overcome by integration with an intelligence model. Correcting limitations (2) and (3) would require rewriting present code.

Component models of the Logistics Operational Assessment Model should be modular in design. The most effective integration of models may involve selecting complimentary portions of models rather than entire models. With models which are modular in design, the portions are more easily isolated from the entire model and integrated into another model.

The Logistic Operational Assessment Model needs about 1000K of core memory to run. This means the model can run a mini computer such as VAX 11/780. This model could even run on an AT&T Unix computer. The AT&T Unix computer comes with 0.5 megabytes of memory, a 10 megabyte harddisk, and the ability to access 2 megabytes of RAM and 2.1 megabytes of vitual memory.

IV. PROBLEMS

A variety of problems can arise when two or more programs are integrated. For example, variables may be named differently in each program. The code may not match. The programs may execute at different rates. Most models will

have to be changed from a card format to a format that will interact with the user.

Specifically, in developing the Logistics Operational Assessment Model, much of the code must be rewritten even if all the models integrated use the same language. Of the models reviewed in this study, only TSAR and TSARINA can be used together as written. All the other models have different variable names, codes, and/or execution rates. Integration of TSAR and TSARINA does not provide the realism desired.

V. CONCLUSION

This project gives the Air Force a chance to correct some limitations that exist in the current models. It also provides an opportunity to improve the method of data entry and to update existing data files. This project is feasible, as logistic and combat operational models with modular design already exist.

One method of creating the Logistics Operational Assessment Model is to integrate TACWAR with TSAR and the part of Dyna-METRIC that simulates the movement of parts through the repair facilities. This irtegrated model could run on a mimi-computer such as the VAX 11/780 and would provide sufficient realism. To perform this task one would need the following types of personnel: a primary investigator for six months at a cost of $28,000; a data manager for eighteen months at a cost of $46,000; a technical writer for eighteen months at a cost of $31,200; a senior computer

scientist for eighteen months at a cost of $65,520; and three computer scientists for eighteen months at a cost of $159,120. The computer time for developmenting and testing the model using this method would cost about $430,500. The total cost of for developing this model using this method is about $761,220. (See Tables V.1 and V.3.)

The second method of creating the Logistics Operational Assessment Model is to perform the same integration as in the first method but to rewrite everything into PASCAL. The Logisics Operational Assessment Model then could run on the new AT&T Unix microcomputer with 1.5 megabytes of RAM memory and a 10 megabyte hard disk. The AT&T Unix comes with 0.5 megabytes of RAM memory and a 10 megabyte harddisk as well as the capability of accessing 2.1 megabytes of virtual memory at a cost of $5600. The AT&T Unix with a 20 megabyte hard disk costs $6200. Each additional 0.5 megabyte of RAM costs $1000. A printer for the AT&T Unix costs about $750. The PASCAL compiler costs about $250. To perform this task, the following types of personnel are needed: a primary investigator for 6 months at the cost of $28,000; a technical writer for 2 years at the cost of $41,600; a data manager for 2 years at the cost of $62,400; a senior computer scientist for 2 years at the cost of $87,360; and three computer scientists for two years at the cost of $212,160. The total cost of developing the Logistics Operational Assessment Model using method two is about $440,120. (See Tables V.2 and V.3.)

PERSONNEL FOR FIRST METHOD

Title	Number	Time	Cost
Primary Investigator	1	6 months	$28,000
Technical Writer	1	18 months	$31,200
Data Manager	1	18 months	$46,000
Senior Computer Scientist	1	18 months	$65,520
Computer Scientist	3	18 months	$159,120
Total			$329,840

Table V.1. Personnel, time and costs for first method of integration

PERSONNEL FOR SECOND METHOD

Title	Number	Time	Cost
Primary Investigator	1	6 months	$28,000
Technical Writer	1	24 months	$41,600
Data Manager	1	24 months	$62,400
Senior Computer Scientist	1	24 months	$87,360
Computer Scientist	3	24 months	$212,160
Total			$431,520

Table V.2. Personnel, time and costs for second method of integration

DEVELOPMENT COST

Requirement	First Method	Second Method
Personnel	$329,840	$431,520
Computer Time	$430,500	N/A
VAX 11/780	Available	N/A
AT&T Unix*	N/A	$5,600
Extra RAM	N/A	$2,000
Printer	N/A	$750
PASCAL Compiler	N/A	$250
Total	$760,340	$440,120

*Includes a 10 megabyte harddisk and 0.5 megabytes of RAM.

Table V.3. Summary of development costs for both methods.

VI. RECOMMENDATIONS

I recommend the second method for developing the Logistics Operational Model. In this method one integrates TACWAR, TSAR, and Dyna-METRIC and translates those portions of the models that were integrated into PASCAL so the Logistics Operational Assessment Model will run on the AT&T Unix. One benefit of using a microcomputer to run the Logistics Operational Assessment Model is that one will not tie up a multi-user computer such as VAX 11/780 to run this model. It also costs less to develop and use the model on microcomputers, as charges for computer time do not occur.

GLOSSARY

Abbreviation	Meaning
Dyna-METRIC	Dynamic Multi-Echelon
FMC	Fully Mission Capable
FEBA	Forward Edge of Battle Area
LCOM	Logistics Composite Model
TACWAR	Tactical Warfare Model
TSAR	Theater Simulation of Airborne Resources
TSARINA	TSAR using inputs from Airbase Damage Assessment

REFERENCES

1. Sacks, Jonathan, "AT&T Escalates the Micro War," Popular Computing, McGraw-Hill, pp. 62-67, 146-147, June, 1985.

2. Selected Logistics Models and Techniques, HQ AFSC/AL, DCS Acquisition Logistics, Andrews AFB, DC.

3. Asiala, Carl F. amd Loy, Susan L., ARDR Logistics and Maintenance Resource Quantification Subtask-1 Computer Simulation and Math Models, Universal Energy Systems, Inc., February, 1983.

4. Asiala, Carl F. and Loy, Susan L., Summary Report Subtask-2 Computer Simulation and Math Models Interface Analysis, Universal Energy Systems, Inc., May, 1983.

5. Pyles, Raymond, The Dyna-METRIC Readiness Assessment Model Motivation, Capabilities, and Use, Santa Monica, CA., The Rand Corporation, October, 1982.

6. Emerson, Donald, USAFE Airbase Operations in a Wartime Enviroment, Santa Monica, CA., The Rand Corporation, October, 1982.

7. Emerson, Donald, TSARINIA--User's Guide to a Computer Model for Damage Assessment of Complex Airbase Targets, Santa Monica, CA., The Rand Corporation, July, 1980.

8. Emerson, Donald E., An Introduction to the TSAR Simulation Program Model Features and Logic, Santa Monica, CA., The Rand Corporation, February, 1982.

9. Institute for Defense Analysis Tactical Warfare (TACWAR) Model Program Maintenance Manual Part I, Command and Control Technical Center, Cameron Station, Alexandria, Va., September, 1977.

10. Institute for Defense Analysis Tactical Warfare (TACWAR) Model Program Maintenance Manual Part II, Command and Control Technical Center, Cameron Station, Alexandria, Va., September, 1977.

11. Institute for Defense Analysis Tactical Warfare (TACWAR) Model Program Maintenance Manual Part III, Command and Control Technical Center, Cameron Station, Alexandria, Va., September, 1977.

12. Catalog of Wargaming and Military Simulation Models, Studies, Analysis, and Gaming Agency, Organization of the Joint Chiefs of Staff, May, 1982.

1985 USAF-UES SUMMER FACULTY RESEARCH PROGRAM/

GRADUATE STUDENT SUMMER SUPPORT PROGRAM

Sponsored by the

AIR FORCE OFFICE OF SCIENTIFIC RESEARCH

Conducted by the

UNIVERSAL ENERGY SYSTEMS, INC.

FINAL REPORT

Photo-Hall Study of Doped and Undoped Semi-Insulating GaAs

Prepared by:	Dr. Billy Covington
Academic Rank:	Assistant Professor
Department and University:	Department of Physics Sam Houston State University
Research Location:	Air Force Wright Aeronautical Laboratories Materials Laboratory, Electromagentic Materials Division, Laser and Optical Materials Branch
USAF Research Colleague:	Dr. W. C. Mitchel
Date:	July 26, 1985
Contract No:	F49620-85-C-0013

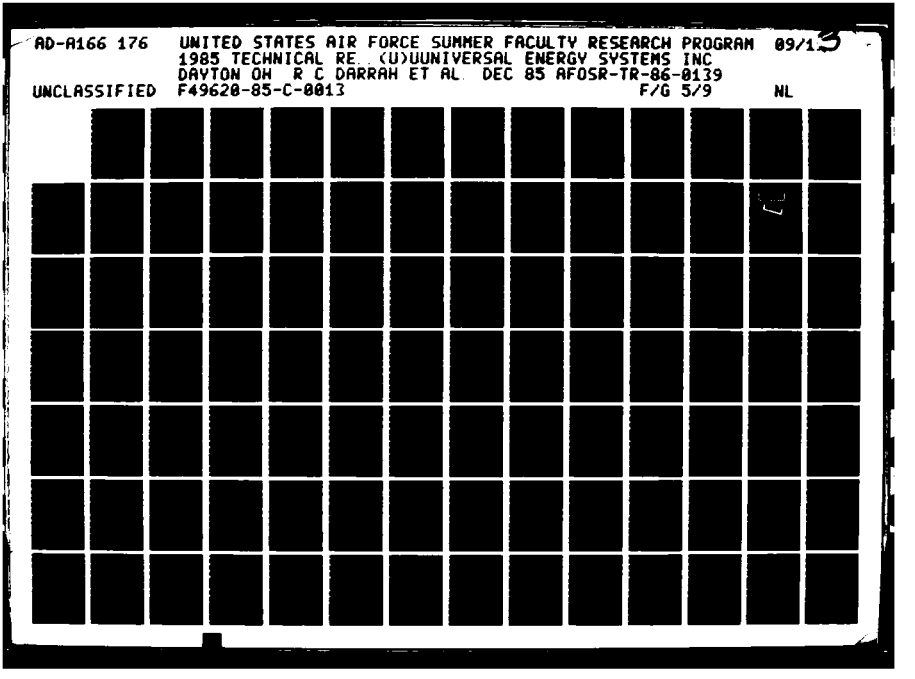
AD-A166 176 UNITED STATES AIR FORCE SUMMER FACULTY RESEARCH PROGRAM 09/13
1985 TECHNICAL RE (U)UNIVERSAL ENERGY SYSTEMS INC
DAYTON OH R C DARRAH ET AL DEC 85 AFOSR-TR-86-0139
UNCLASSIFIED F49620-85-C-0013 F/G 5/9 NL

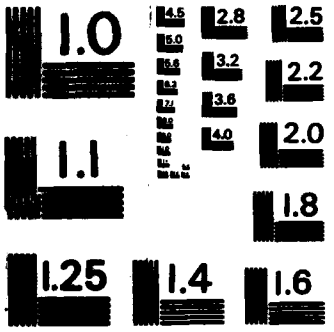

MICROCOPY RESOLUTION TEST CHART
NATIONAL BUREAU OF STANDARDS - 1963 - A

Photo-Hall Study of Doped and Undoped Semi-Insulating GaAs

by

Billy C. Covington

Abstract

We present the results of a photo-Hall study of semi-insulating undoped gallium arsenide and antimony doped gallium arsenide. The carrier concentration, resistivity, and mobility values are presented as a function of sample temperature and wavelength of light illuminating the sample. The resistance as a function of the length of time of illumination at a particular wavelength and temperature is also presented. The photo quenching of the photoconductivity by inducing the metastable state of the deep donor defect EL2 is reported as well as the effect of annealing on the recovery of the photoconductivity. Conclusions are made as to the effect the wavelength of the illuminating light has on sample resistivity and recommendations are made for additional research.

Acknowledgement

The author would like to express his appreciation to the Air Force Systems Command, the Air Force Office of Scientific Research, and to Universal Energy Systems, Inc. for providing the opportunity to do research at the Air Force Wright Aeronautical Laboratories, Materials Laboratory, Wright-Patterson AFB, Ohio. He wishes to thank the Materials Laboratory staff for their support and in particular to thank Dr. W. C. Mitchel for his guidance and assistance with this project.

I. Introduction

The development of high quality semiconducting material for the fabrication of infrared detectors and electronic devices for use in missile, satellite, and aircraft imaging systems is a research area of continuing importance. One semiconducting material which is currently being extensively investigated is gallium arsenide (GaAs). A particular area of GaAs research which has recently received considerable attention is the investigation of the structure of the EL2 defect center in semi-insulating (resistivity $10^7 \Omega$-cm) GaAs.[1] The EL2 defect is a deep donor which is responsible (through some type of compensation mechanism) for the semi-insulating properties of undoped GaAs. Semi-insulating undoped GaAs is gaining great technological importance because of its use in fabricating very high speed integrated circuits. For this reason it is important that the nature of the EL2 defect be understood.

The EL2 defect produces very unusual optical and electrical properties in GaAs.[2-10] The photo response is greatly altered by photons having energies in the range of 1 to 1.25 eV. Samples which have large ($10^{16} cm^{-3}$) concentrations of EL2 exhibit a strong optical quenching of the photoconductivity when illuminated with these photons. The photoconductivity remains quenched until the sample is heated to a temperature of approximately 140K. Subsequent cooling to 77K restores the photoconductivity.

It has been proposed by Levinson[11] that EL2 is composed of a shallow donor defect together with a deep donor defect. When both defects are positively charged, the transition to an unstable configura-

tion occurs because of the strong Coulombic repulsion. The system returns to equilibrium when an electron is captured by the deep level thus generating a Coulombic attraction between the deep and shallow levels.

Recently, Jimenez[2] et. al. proposed a model in agreement with Levinson's theory. The propsoed model involves the deep EL2 donor level capturing a shallow defect X thus forming the complex EL2-X. It is suggested that this process is possible because of the ionization of EL2 by photons ranging in energy from approximately 1 to 1.25 eV. The reaction rate for defect capture by EL2 is faster than the rate of capture of an electron from the valence band by the ionized EL2 thus making the EL2-X formation possible.

Not all researchers[3,8,12,13] are in agreement with the above model but most agree that EL2 is associated with the As_{Ga} antisite defect. Much of the disagreement centers around whether EL2 is due to an isolated As antisite or to an antisite complex.

The author became involved with the research reported herein after a conversation with Dr. W. C. Mitchel of the Air Force Materials Laboratory. The author had previously been studying the optical and electrical properties of radiation damaged silicon and germanium and had just recently begun to investigate GaAs. Dr. Mitchel suggested the project because such a small amount of photo-Hall research has been done on undoped semi-insulating GaAs. The photo-Hall data collected during this research project should correlate well with the infrared absorption and electron paramagnetic resonance data that will be collected as part of another research project the author is conducting.

II. Objective

The primary objective of this research was to observe by the photo-Hall technique the EL2 and any associated defect centers in semi-insulating GaAs. Originally we had planned to only investigate undoped semi-insulating GaAs, but since time permitted the decision was made to include an antimony doped sample of GaAs.

The ultimate goal of the research was to obtain carrier concentration, resistivity, and mobility data that could be associated directly with the EL2 defect. This type of data in conjunction with existing - infrared absorption, electron spin resonance, Hall, photoluminescence, deep level transient spectroscopy, and magnetic circular dichroism data should aid in the determination of the EL2 structure.

III. Experimental Techniques

In the initial stages of the research, rectangular shaped samples measuring 7 x 7 x 0.5 mm were used. It was later determined that a cross shaped sample provided a somewhat less noisy voltage and current reading. Subsequently, cross shaped samples of approximately the same overall dimensions as the rectangular samples were used for the remainder of the study.

The experimental procedure consisted of using an indium-tin alloy solder to attach copper wires to each of the four points of the cross shaped samples or to each of the four corners of the rectangular samples. After attachment of the wires, a sample would be mounted on a copper block but shielded electrically from the block by a sheet of BeO. A silicon diode thermometer was in direct contact with the BeO.

The copper block was then attached to the cold finger of a liquid helium dewar. A gold plated mirror was mounted on the cold finger at an angle of 45° to the plane of the sample.

Once the tail section of the dewar containing the sample was in position between the poles of the electromagnetic, it was possible to direct light through the single glass window of the tail section onto the gold mirror and thus onto the sample. An aperture located directly in front of the sample allowed only the center portion of the sample to be illuminated.

The light source was a high pressure Xenon lamp. The light from the lamp was passed through a Bausch and Lomb monochrometer which was operated in the spectral range 0.7 to 1.6μ. Visible and higher frequency light was blocked from the sample by a filtering system.

The electrical connections made to the sample and the procedure of obtaining voltage, current, and magnetic field data follow the typical guarded Van der Pauw procedure.

Typically, data were collected after cooling the sample to 77K in the dark and then illuminating the sample with a particular wavelength of light. The sample would then be warmed to approximately 140K where additional data were taken. The procedure would then be repeated with a different wavelength illuminating the sample. The collected data were converted into carrier concentration, resistivity, and mobility values by a computer program.

IV. Results

Part (1) Rectangular Rockwell Sample

The first sample investigated was a rectangular shaped

semi-insulating undoped sample grown by the liquid encapsulated Czochralski (LEC) method by Rockwell International. Preliminary tests indicated this sample contained more of the oxygen related [illegible] defect then the EL2 defect. The carrier concentration, resistivity, and mobility for various sample conditions are presented in Table I. The values presented are the average of several data values.

Table 1.

Carrier Concentration, Resistivity, and Mobility Data for Rockwell Sample

Illumination	T(K)	cc(cm^{-3})	R(Ω-cm)	μ_H (cm^2/Vs)
In Dark	295	1.31×10^5	9.72×10^7	4879
In Dark	78	U.M.	U.M.	U.M.
Room Light	295	1.43×10^5	8.09×10^7	5417
1.15 μ	78	5.75×10^7	4.71×1.5	1737
1.01 μ	295	1.45×10^7	1.32×10^6	6343
1.01 μ	78	1.13×10^{10}	7.68×10^2	7259
.95 μ	78	2.69×10^{10}	2.74×10^2	8473
.90 μ	78	3.54×10^{10}	2.11×10^2	8359

U.M. = unmeasureable

It is evident from the resistivity data that the sample is very sensitive to temperature and wavelength of light illuminating it. As expected, the resistivity decreases as the illuminating wavelength approaches the band edge at approximately 0.82μ.

Part (2) Rectangular Cominco Sample

The next sample investigated was a rectangular shaped undoped semi-insulating sample grown by the LEC method by Cominco, Inc. Preliminary tests indicated this sample had a larger concentration of EL2 then EL0. The carrier concentration, resistivity, and mobility for various sample conditions are presented in Table 2. The values presented are the average of several data values.

Table 2.

Carrier Concentration, Resistivity, and Mobility Data for Cominco Sample

Illumination	T(K)	cc(cm^{-3})	R(Ω-cm)	μ_H (cm^2/Vs)
In Dark	295	4.30×10^5	2.93×10^7	4965
In Dark	78	U.M.	U.M.	U.M.
Room Light	295	4.46×10^5	2.51×10^7	5596
1.37μ	78	3.75×10^7	6.85×10^5	2432
1.12μ	78	1.00×10^8	1.81×10^5	3433
1.03μ	78	1.87×10^9	1.46×10^4	2273
.95μ	78	5.06×10^9	3.61×10^3	3425
.88μ	78	1.27×10^{10}	2.05×10^3	2404
.82μ	78	7.34×10^8	1.51×10^4	5633
.81μ	78	1.59×10^9	1.71×10^4	2398

U.M. = unmeasureable

As with the Rockwell sample, the resistivity decreases as the band edge is approached by the illuminating light.

In an attempt to photoquench the photoconductivity, the sample was illuminated with 1.08μ light for two hours. At the end of two hours, the sample was illumianted with .81μ light and the data obtained were compared with data taken before the 1.08μ illumination. In Table 3 the values obtained are presented. All data were obtained at 78K.

Table 3.

Time Dependent Data for Cominco Sample

Illumination	Time (mins.)	cc(cm^{-3})	R(Ω-cm)	μ_H (cm^2/Vs)
.81μ	-	1.59×10^9	1.71×10^4	2398
1.08μ	start	3.87×10^9	3.71×10^3	4348
"	20	1.30×10^8	1.71×10^5	2800
"	48	9.59×10^7	4.39×10^5	1482
"	52	5.63×10^8	6.79×10^5	-
"	120	1.91×10^{10}	6.81×10^5	-
.81μ	-	6.44×10^8	4.19×10^3	-

Even though there is some scatter in the data and some of the mobility values were not calculated, the trend present in the data is in agreement with previously reported results,[1] i.e., the resistivity of the sample continually increased during the entire two hour illumination

with 1.08μ light. What is not in agreement is that the resistivity upon being illuminated with .81μ light after the 1.08μ illumination is not larger which signifies an enhanced photoconductivity rather than a quenched photoconductivity. The following part (3) will give additional information about this type of behavior.

Part (3) Cross Shaped Cominco Sample

As was previously discussed, the decision was made to use a cross shaped sample in order to reduce some of the noise generated by the rectangular sample configuration. The carrier concentration, resistivity, and mobility for various sample conditions are presented in Table 4. The values presented are the average of several data values.

Table 4.

Carrier Concentration, Resistivity, and Mobility

for Cross Shaped Cominco Sample

Illumination	T(K)	cc(cm^{-3})	R(Ω-cm)	μ_H (cm^2/Vs)
In Dark	295	1.31×10^5	9.72×10^7	4879
In Dark	78	U.M.	U.M.	U.M.
Room Light	295	4.00×10^5	2.88×10^7	5435
.95μ	78	2.42×10^{10}	1.42×10^2	18,375
.90μ	78	5.20×10^{10}	7.73×10^1	15,530

U.M. = unmeasureable

Time dependent data for the sample are given in Table 5. The sample was first illuminated with .90μ light for 1 hour and 5 minutes and then illuminated with 1.08μ light for 1 hour and 7 minutes before once again illuminating with .90μ light. All data were obtained at 78K.

Table 5.

Time Dependent Data for Cross Shaped Cominco Samples

Illumination	Time (mins)	cc(cm^{-3})	R(Ω-cm)	μ_H(cm^2/Vs)
.90μ	start	2.53×10^{10}	1.24×10^{2}	19,910
"	13	5.20×10^{10}	7.73×10^{1}	15,530
"	31	9.04×10^{10}	3.54×10^{1}	19,530
"	55	1.33×10^{11}	2.56×10^{1}	18,390
"	65	1.40×10^{11}	2.38×10^{1}	18,770
1.08μ	15	2.21×10^{8}	4.45×10^{4}	6,357
"	67	2.58×10^{8}	7.12×10^{4}	3,403
.90μ	-	1.95×10^{11}	2.18×10^{1}	14,720

As with the data in Table 3, the resistivity increases during the time of illumination with the 1.08μ light, but again upon switching back to the 0.90μ light the resistivity is lower than the previous 0.90μ value. It should be noted that a significant decrease in the value of the mobility has taken place. It does appear from this data that the

photoconductivity has not been quenched by the 1.08μ light. In fact, if anything it appears there has again been an enchancement in the photoconductivity. This type of behavior has been previously reported,[6] but only for samples grown by the horizontal Bridgman method.

In order to determine what affect a prolonged illumination at one particular wavelength would have on the sample, it was illuminated with a 0.95μ light for 4 hours and 30 minutes. During this time the carrier concentration changed from 5.75×10^9 to $7.02 \times 10^9 cm^{-3}$, the resistivity changed from 6.42×10^2 to $5.33 \times 10^2 \Omega$-cm, and the mobility changed from 16,900 to 16,670 cm^2/Vs. No indication of a quenched photoconductivity is evidenced by these data.

With the assumption that the sample needed to be illuminated with 1.08μ light for a longer period of time to produce the metastable state of EL2, the sample was illuminated for 2 hours and 35 minutes. Only the voltage and current were monitored during this time so only resistance data could be calculated. The initial resistance value with 0.95μ illumination was $2.27 \times 10^2 \Omega$. After 1.08μ illumination, this value changed to $2.48 \times 10^3 \Omega$ under 0.95μ illumination. This amount of change in the resistance is indicative of a quenching of the photoconductivity. The change in the resistance by a factor of approximately eleven is in reasonable agreement with changes reported in the photoconductivity and photo-current by other researchers.[9,2]

In an attempt to recover the photoconductivity, the sample was heated to a temperature of 155K and then cooled to 78K. The resistance value prior to heating was $1.13 \times 10^3 \Omega$ with .95μ illumination. After the heat treatment, the resistance value was $8.43 \times 10^2 \Omega$ with .95μ illumination.

Even though the resistance of the sample is less than the value prior to annealing, the change is so small as to be within the probable error for the data. Several additional heat treatments were attempted on this sample but all produced ambiguous results.

Part (4) Antimony Doped Sample

In order to determine the affect that doping would have on the carrier concentration, resistivity, and mobility values, the decision was made to investigate a sample doped with antimony. The sample was grown by the LEC method by Westinghouse Corporation.

The data values obtained for the sample are given in Table 6.

Table 6.

Carrier Concentration, Resistivity, and Mobility

for GaAs:Sb

Illumination	T(K)	cc(cm^{-3})	R(Ω-cm)	μ_H (cm^2/Vs)
In Dark	295	8.44×10^8	1.32×10^4	5587
Room Light	295	8.50×10^8	1.32×10^4	5585
1.08μ	78	6.37×10^8	7.62×10^3	12860
1.01μ	295	9.83×10^8	1.13×10^4	5624
.95μ	295	1.02×10^9	1.08×10^4	5650
.95μ	78	7.37×10^{10}	5.77×10^1	14690

Comparison of these values with the values presented in Tables 1, 2, and 4 indicate the expected result that carrier concentration is significantly increased and resistivity decreased for the doped sample.

The time dependent data for the sample are given in Table 7. All data were obtained at 78K.

Table 7.

Time Dependent Data for GaAs:Sb

Illumination	Time (mins)	cc(cm^{-3})	R(Ω-cm)	μ_H (cm^2/Vs)
.95μ	start	7.37×10^{10}	5.77×10^{1}	14,690
"	56	8.81×10^{10}	5.74×10^{1}	12,490
"	107	8.48×10^{10}	5.72×10^{1}	12,870
1.08μ	start	5.42×10^{7}	6.77×10^{4}	17,010
"	12	5.33×10^{7}	6.88×10^{4}	17,040
.95μ	stop	8.79×10^{10}	1.31×10^{2}	5,418

As is indicated by the data in Table 7, the amount of change in carrier concentration and resistivity with time is not nearly so great for the doped sample as for the undoped samples. The resistivity data do show an increase after illumination with 1.08μ light, but the change is too small to be statistically significant. We are doubtful that the last mobility value at .95μ is a valid number.

V. Conclusions

The following conclusions have been made concerning the effects of temperature and wavelength of illuminating light on the resistivity and thus the photoconductivity for semi-insulating undoped and alloyed GaAs.

(1) For undoped semi-insulating GaAs at 78K, illumination with light in the spectral range .81 to .95μ produces a continuing decrease in the resistivity for illumination times of approximately of one hour. Illumination with 1.8μ light produces a continuing increase in the resistivity for illumination times in excess of two hours.

(2) A two hours illumination with 1.8μ light does produce a photoquenching of the photoconductivity. The photoconductivity is not unmistakably recovered after an anneal to 155K and subsequent cooling to 78K.

(3) For antimony doped GaAs at 78K, illumination with .95μ light for times in excess of 100 minutes has little or no effect on the resistivity of the sample. Illumination with 1.08μ light produces a slowly increasing resistivity. No sign of a quenched photoconductivity was observed.

VI. Recommendations

We feel that the quality of the data can be improved as well as additional useful data can be obtained by doing the following:

(1) A more intense lamp should be used to induce the change from EL2 to the metastable state. This would reduce the data

collecting time as well as insuring saturation of the metastable state. We suggest using a high intensity tungsten lamp.

(2) Along the lines of suggestion (1), it might be worthwhile to try using a Nd:Yag laser (1.06μ) to induce the change to the metastable state. This should certainly insure saturation of the metastable state.

(3) Data should be collected as a function of wavelength and temperature. The values for the resistivity, carrier concentration, and mobility at a particular wavelength and in the temperature range 77 to 300K provide additional useful information such as activation energies for EL2, EL0, and any other defects present.

(4) Additional samples grown by various techniques should be studied. In particular, comparison of samples rich in EL0 and samples rich in EL2 should provide interesting and useful data.

(5) In addition to the photo-Hall study, an EPR and IR absorption study should be made of the same sample material. Correlation of the data from all three studies should provide valuable information about the structure of EL2 as well as information about other defects and impurities in GaAs. Studying the shallow acceptors by IR absorption would be particularly useful because it would provide information about the compensation process which occurs when EL2 converts to the metastable state.

References

1. Makram-Ebeid, S., P. Langlade, and G. M. Martin, "Nature of EL2: the Main Native Midgap Electron Trap in VPE and Bulk GaAs," Semi-Insulating III-V Materials, Kah-nee-ta, pg 184, Ed. D. C. Look and J. S. Blakemore, Shiva Publ.

2. Jimenez, J., P. Hernandez, and J. A. de Saja, "Optical Quenching of the Near-intrinsic Photocurrent in Semi-insulating Bulk GaAs," J. Appl. Phys. 57 (12), 5290 (1985).

3. Hofmann, D. M., B. K. Meyer, F. Lohse, and H. M. Spaeth, "Optically Detected Electron-Nuclear Double Resonance of As-Antisite Defects in GaAs," Phys. Rev. Lett, 53 (12), 1187 (1984).

4. Martin, G. M., "Optical Assessment of the Main Electron Trap in Bulk Semi-insulating GaAs," Appl. Phys. Lett. 39 (9), 747 (1981).

5. Taniguchi, M., T. Ikoma, "Spectral Distributions of Photo Quenching Rate and Multimetastable States for Midgap Electron Traps (EL2 Family) in GaAs," Appl. Phys. Lett. 45 (1), 69 (1984).

6. Jimenez, J., M. A. Gonzalez, P. Hernandez, and J. A. de Saja, "Optically Enhanced Defect Reactions in Semiconducting Bulk GaAs," J. Appl. Phys. 57 (4), 1152 (1985).

7. Samuelson, L., P. Omling, E. R. Weber, and H. G. Grimmeiss, "Optical Properties of EL2 in GaAs," Semi-Insulating III-V Materials, Kah-nee-ta, pg. 268, Ed. D. C. Look and J. S. Blakemore, Shiva Publ.

8. Meyer, B. K., J. M. Spaeth, and M. Scheffler, "Optical Properties of As-Antisite and EL2 Defects in GaAs," Phys. Rev. Lett., 52 (10) 851 (1984).

9. Vincent, G., D. Bois, and A. Chantre, "Photoelectric Memory Effect in GaAs," J. Appl. Phys. 53 (5), 3643 (1982).

10. Taniguchi, M., Y. Mochizuki, and T. Ikoma, "Photoquenching Effect at the Midgap Electron Traps (EL2 Family) in Different GaAs Crystals," Semi-Insulating III-V Materials, Kah-nee-ta, pg. 231, Ed. D. C. Look and J. S. Blakemore, Shiva Publ.

11. Levinson, Mark, "Charge-state-controlled Structural Relaxation of the EL2 Center in GaAs," PHys. Rev. B, 28 (6), 3660 (1983).

12. Meyer, B. K. and J. M. Spaeth, "As_{Ga} Antisities and Their Relation to EL2 Defects in GaAs," J. Phys. C: Solid State Phys., 18, L99 (1985).

13. Deiri, M., K. P. Homewood, and B. C. Cavenett, "Identification of EL2 in GaAs as the As_{Ga} Antisite Centre", J. Phys. C: Solid State Phys., 17, L627 (1984).

1985 USAF-UES SUMMER FACULTY RESEARCH PROGRAM/

GRADUATE STUDENT SUMMER SUPPORT PROGRAM

Sponsored by the

AIR FORCE OFFICE OF SCIENTIFIC RESEARCH

Conducted by the

UNIVERSAL ENERGY SYSTEMS, INC.

FINAL REPORT

SPIN FORMED MIRRORS

Prepared by:	Dennis J. Cravens
Academic Rank:	Department Chairman
Department and	Math and Science
University:	Vernon Regional Junior College
Research Location:	A.F. Rocket Propulsion Laboratory
	Liquid Propulsion
	Advanced Concepts
USAF Research	Gerald Naujokas
Date:	August 15, 1985
Contract No:	F49620-85-C-0013

SPIN FORMED MIRRORS

by

Dennis Cravens

ABSTRACT

The equipotential surface of a rotating fluid in a gravitational field assumes a parabolic contour. By catalytic polymerization of a fluid styrene and polyester resin mixture it is possible to generate a solid paraboloid. The focal length to diameter ratios accessable by this method can be much less than one and are primarily limited by only rotational velocities. A 1.05 m 1.2 f/d on-axis paraboloid and a 3.0 m 0.8 f/d on-axis paraboloid were prepared. Experimental methods for the on-axis paraboloids and a 3.0 m f/d #0.18 collector are described. Applications of the method for mold production of solar concentrators by thermosetting aluminized mylar are discussed.

ACKNOWLEDGEMENTS

The author wishes to thank the Air Force Systems Command and the Air Force Office of Scientific Research for their role as sponsors of this research program which was administered by Universal Energy Systems.

The author especially wishes to express appreciation to the Advanced Concepts Branch of the Rocket Propulsion Lab. The atmosphere of concern for innovative methods this group displays will undoubtedly have a long lasting effect on future research of this author.

I. Introduction

The low weight and packaged volumes of inflatables make them extremely attractive for use as collectors and concentrators in space environments. Typical applications of such systems include centimeter wavelength antennas, solar concentrators and collectors for E-M radiation detection. These inflatables have drastically reduced deployment costs compared to traditional segmented mechanical systems. Inflatables can be deployed in space without manual assistance. They are not effected by launch vibrations and shocks. They have low manufacture cost per given apeture. Most importantly they have the outstanding ability to fit into a small volume of arbitary shape at an extremely low weight to apeture ratio.

Due to these unique characteristics the Rocket Propulsion Laboratory is investigating the use of inflatables for its efforts in developing a solar powered rocket. In this application an inflatable paraboloid is utilized as a solar concentrator for heating a working material such as hydrogen. This requires production of parabolic surfaces with small focal length to diameter ratios with reduced slope errors.

The research involved in this report evolved from a suggestion by the summer faculty researcher to study the quality of an inflatable that was initially thermoset to a parabolic shape. Such a device is expected to have a reduced

obligatory pressure as well as reduced inherent strain. To this end the investigation centers on the production of a suitable mold and calculations of these expected surfaces.

The unique approach taken by this report is the rapid fabrication of parabolic molds by use of rotational methods. This method allows production of very large parabolic sections with focal length to diameter ratios of less than one. In addition it is possible to produce off-axis parabolic contours which would be extremely difficult to generate at the required sizes by traditional approaches.

II. Objectives

The preliminary objectives were concerned primarily with analytical issues and experimental designs. After the on-site visit it was decided that the theoretical framework was sufficiently sound to focus most of the summer effort on the experimental procedures. The following objectives were outlined:

a) Report on analytical development of spin formed and inflatable/rigidized concepts for solar concentrators.

b) Analyze the concentrator's merit based on size, weight and light gathering efficiency.

c) Develop mathematical models incorporating weight, solar flux, pointing accuracy and optical figure to determine space concentrator performance.

d) Define and conduct experiments producing on and

off-axis paraboloidal mirrors by spin forming.

e) Define methods of building plaster molds out of the plastic mirrors. Build molds if possible.

f) Demonstrate surface accuracy of these molds.

g) Other topics will also be studied as time permits.

III. Analytical Developments and Merits

A free flowing surface of a liquid rotating with uniform angular velocity assumes the form of a paraboloid. This approach was attempted in the 1870's by R.C. Carrington and the 1900's by R.W. Wood[1]. These attempts used mercury as a reflective fluid. This early work suffered from vibrations from supports and drives and is currently being reinvestigated utilizing air bearings by Boren[2]. It is possible to select materials that can be solidified after they assume the paraboloid shape. Such approaches have been taken by Archibold[3] and Leighton[4,5]. Recently Roger Angel at the University of Arizona is attempting to use this method to rough form an eight meter glass blank while it is molten.[6]

As can be seen in figure 1 the equipotential surface of a liquid in a rotating dish is governed by

$$\frac{dz}{dr} = \frac{mr\omega^2}{mg} \qquad 1$$

where m is the specific gravity of the liquid, z the vertical coordinant component, g is the gravitational constant and ω is the angular velocity. Integration gives

$$z = \omega^2 r^2/2g \qquad 2$$

with the integration constant chosen so that z=0 at the

FIGURE 1 Formation of Paraboloid

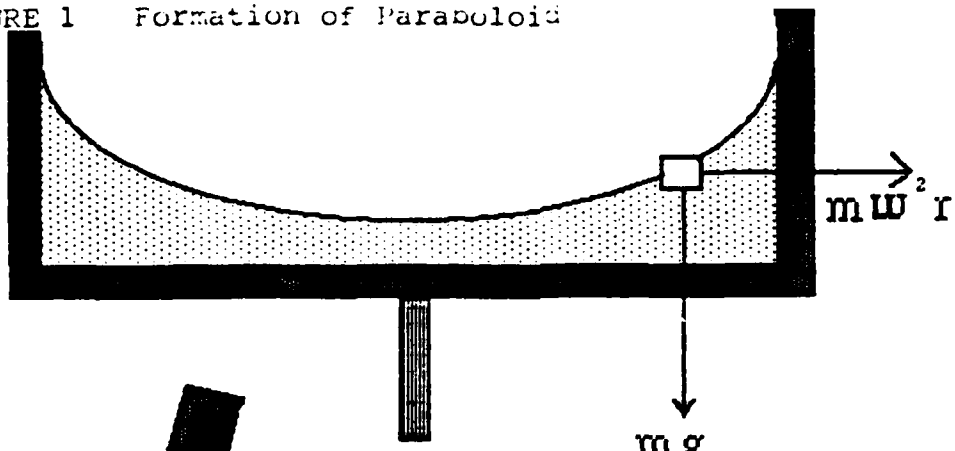

FIGURE 2 Tilted Axis

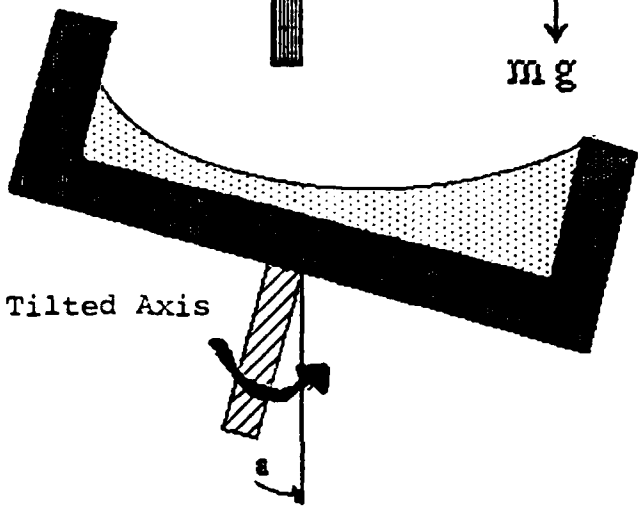

FIGURE 3 Measured Depth vs. Theoretical Parabola

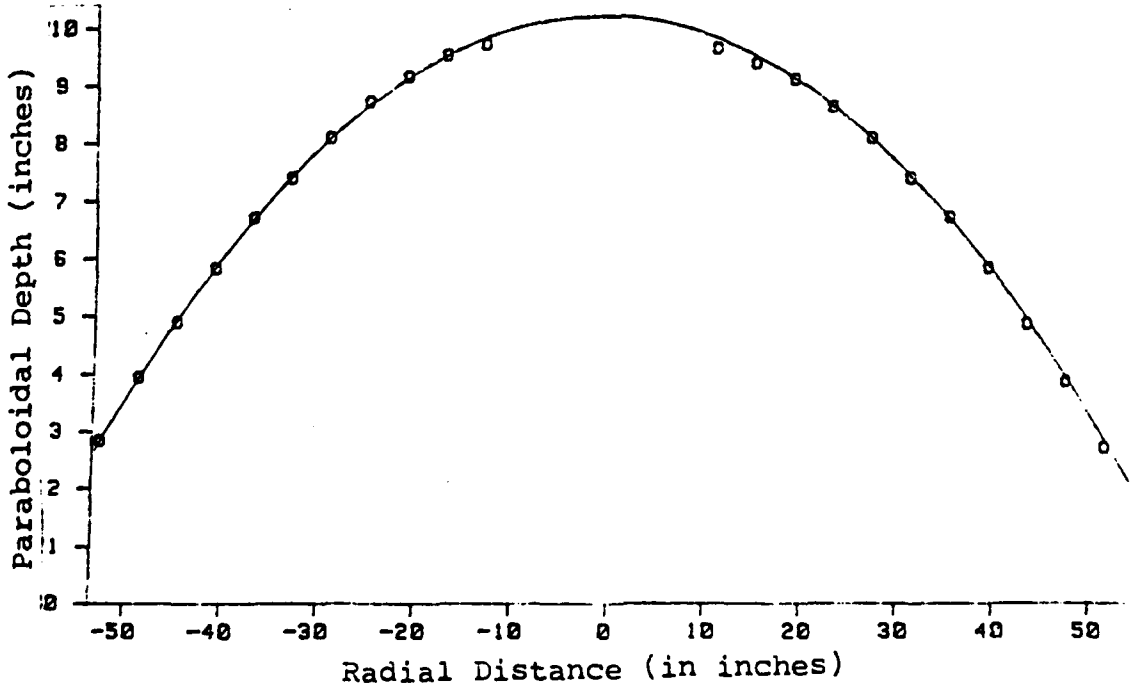

center of rotation. This is a paraboloid with a focal length of

$$f = g/2\omega^2 \qquad 3$$

i.e. $$\omega = \sqrt{g/2f} \qquad 4$$

A similar approach (figure 2) can be used to predict deviations of the surface due to misalignment of the vertical direction and rotational axis. Here

$$\frac{dz}{dr} = \frac{m\omega^2 r \cos\alpha}{ma - m\omega^2 r \sin\alpha} \qquad 5$$

with α the misalignment angle. This can be shown by power series expansion to give

$$z = \frac{\cos\alpha \; r^2\omega^2}{2g} - \frac{\cos\alpha \; \sin\alpha \; \omega^4 r^3}{3g} - (-1)^n \frac{\cos\alpha \; \sin\alpha^{n-1} \; \omega^{2n} r^{n+1}}{(n+1)g^n} \ldots \qquad 6$$

which is seen to converge if $\omega^2/g<1$. It can also be seen that the distortions become larger at increasing apeture sizes.

In the regions near the outer edge the surface departs from paraboloid. This is caused by the finite surface tension of the liquid and the contact angle of the fluid and vessel. In principle the container's profile can be made so that the contact angle of the fluid approaches the desired surface. In practice, however, the vessel possesses vertical sides. The surface at the edge obeys

$$\frac{dv}{ds} = \frac{m\,gz}{c} \qquad 7$$

where v is the unit vector tangent to the surface, s is the line element of the curve and c is the surface tension. At

regions other than at the wall we obtain with x being the distance from the wall

$$\frac{d^2z}{dx^2} = \frac{m\,gz}{c} \qquad 8$$

so that

$$z = A\,\exp\left\{-(mg/c)^{1/2}\,x\right\} \qquad 9$$

The deviation of the surface near the wall is now seen as decaying exponentially as the distance from the wall increases. The constant A can be shown to be set by the contact angle θ and $\tau = \sqrt{mg/c}$ as

$$A = \frac{-\tan\theta}{\tau \exp(-\tau x)} \qquad 10$$

with typical values of m = 1g/cc and c = 20 dyne/cc the edge effect will be significant only within a few centimeters of the wall ($\Delta z < 6 \times 10^{-5}$ cm).

IV. Optical Performance

The system efficiency for this application is measured by the ratio of energy delivered to target to the incident solar energy. The performance of a thruster will be linked to the flux levels at the target. The main factors appear to be the solar irradiance profile, the surface slope error, the specular spreading and pointing errors. The two additonal factors of the clear vapor retention membrane quality and window quality will not be treated here.

Exact solution of such performance utilizing extensive analytical work will not be suitable until exact engineering features are determined. It is, however, possible to

approximate a general system which can be utilized to guide initial choices of specific systems. Considering concentrator performance the factors above should be taken into account simultaneously. Due to the impracticability of doing this for the general system, the Gaussian beam method was chosen as an approximation which should give values to within 90% of the extensive analysis. This method (by Aparisi)[7] uses an effective reflective beam profile with a flux intensity distribution being a normal distribution function. The intercept factor ϕ is defined as the quantity of radiant energy passing through a circular section located at the focal plane with a radius r and is normalized by the total energy passing through the focal plane. The expression for ϕ is

$$\phi = 1 - \exp\left\{ - \frac{r^2}{2\sigma^2} \right\} \qquad 11$$

Experimental verification of the approximation can be found in the references (Tepyakov[8], Grilikhes[9]). The factor σ is the effective standard deviation of the Gaussian.

The effective deviation is approximated by the combined effects of the contributing deviations:

σ_{sun} - the solar irradiance profile

σ_{sur} - surface slope error

σ_p - pointing errors

and σ_{spec} - specular spreading of mirror

by the formula

$$\sigma = \sqrt{\sigma_{sun}^2 + (2\sigma)_{sur}^2 + \sigma_p^2 + \sigma_{spec}^2} \qquad 12$$

The value best suited for σ_{sun} from earth orbits appears to be 2 to 2.86 m rads (even with a solar half angle of 4.65).[7] Typical σ_{spec} for aluminize films is from 2 mrads[10] down to possibly 1 mrad[11] for special cases. The pointing deviation is for small (<3 mrad) rapid errors about a fixed spot, such as natural mechanical vibrations with a Gaussian distribution. Larger errors can be treated as displacements of the entire focal spot.

This approximation method normally results with slightly conservative figures as to the tightness of the spot diameter. The results, however, should be adequate for initial fabrication stages when only general RMS values of surface errors are known and when contributions from the clear vapor retainment covers are unknown.

V. Experimental Factors and Methods

a. Rotation -- The most critical factor in successful generation of the surfaces is the production of a constant angular velocity over the polymerization times. The Rucker centrifuge located at the Rocket Propulsion Laboratory - Edwards AFB proved to supply the required stability. The centrifuge rotor assembly weighs approximately 50,000 pounds which furnishes a large amount of rotational inertia. The centrifuge is located in a large circular pit of 46 feet in diameter and has a table top area of 20 feet in diameter. This area is capable of supporting loads of 30,000 pounds and can operate up to 80 rpm's with unbalanced loads of 4,000

pounds. These factors made it nearly ideal for this application.

As can be seen in equation 6 the rotational axis must align with the local gravitational field. To verify this alignment a 5 inch pool of mercury was placed near the rotational axis of the centrifuge. This served as an artifical horizon. A laser was aimed so that the beam reflected upward from the pool to a reference spot located 10.25 m from the axis. The mercury pool was then replaced by a first surface mirror which was adjusted to reflect the beam to the same spot previously recorded. This assured the normal of the mirror's surface was vertical compared to the artifical horizon.

The centrifuge was rotated slowly by hand and any deviation of the beam from the reference spot was noted. The extreme deflection of the beam spot was 2.3 cm and occurred after the rotor arm was rotated to 30° W of North. Using the fact that the tangent of the tilt half angle is related to the deflection magnitude it was determined that the RPL centrifuge was off alignment by not more than 1.1 mrad in a tilt direction 30° west of north.

The angular velocity was found not to drift by more than 0.02 rpm in extended runs of up to 6 hours at 17.64 rpm. The drift was found to be a general trend of increasing velocity during the course of the day. It is likely that this is a result of the viscosity decreases due to the

temperature rise of the hydraulic drive fluid. The velocity is more stable towards the end of extended runs where the experiment is most sensitive to variations.

b. Containment -- The best results are obtained from containment vessels which have bottoms with C_∞ symmetry about their rotational axes. Departures from this symmetry can introduce waves resulting from non-zero angular acceleration and misalignment of the rotational axis. In addition it is benefical to have the polymerization taking place in a media of constant thickness. Constant thickness minimizes any surface defects resulting from mold shrinkage (change in volume during polymerization). These factors were supplied by first roughing in the parabolic shape by hand carving a polyurethane foam used as a filler. This was then covered by 4 layers of plaster which was cast by the rotational method. A commerical dry wall mix was employed. The mixture ratio that proved best suited was at least 11 quarts of water per 25 pounds of dry wall.

It is mandatory that the mixture has a viscosity sufficiently low as to be "self-leveling". Trial and error showed that the best surfaces were made when the mixture was 1) well blended 2) strained through a wire mesh to remove any lumps 3) low viscosity 4) allowed to have a long setting time and 5) applied as multiple layers of material. Acrylic binders or paints can be introduced to decrease the porosity of the surface. The purpose of the plaster is to form a

uniform container bottom of approximately parabolic shape. This reduces the volume of required plastic resins, decreases surface waves and imparts a uniform thickness to future layers for uniform curing rates.

The container must also be fitted with a lid to avoid distortions due to air currents and particle contamination. A plastic film was initially used but it was found that vapor would condense on the plastic and drip to the surface. The method adopted was to first cover the container with paper which would absorb the condensation and then a plastic film for a tight gas seal. The container was flushed with nitrogen before the procedure and a slow nitrogen flow was allowed to furnish a positive gas pressure. Nitrogen was selected to avoid radical interaction at the surface which results when oxygen is available to the styrene radicals.

c. Resin materials -- The original experimental design was to use pure styrene monomer for the plastic resin. However, due to the excessive summer temperature at Edwards all locally available styrene was found to be heavily inhibited with TBC to prevent auto polmerization and thermal runaway. Since the styrene was already purchased the decision was made to copolymerize the styrene with a polyester casting material. Styrene is typically added to such materials at concentrations of up to 30% to impart extra hardness to the finished product. The mixture chosen here was a 25% styrene (Arco monomeric styrene with > 750 ppm TBC) and a 75%

polyester casting material (Hapol 1300-1E).

The plastic mixture should be allowed to set to assure uniformity. If it is not mixed well there will be small indentations on the surface due to evaporation of unpolymerized styrene droplets at the surface. The mixture should also be degassed by vacuum to avoid bubbles. The experimental method employed here was to mix the components and allow to set overnight in a depressurized vessel.

The catalyst should be added at the last possible minute so that the viscosity will be low enough to assure a equipotential surface before poylmerization begins. Care must be shown to avoid bubble formation during mixing of catalyst. A 9% methyethyl ketone peroxide (MEKP-9) catalyst solution was added. The catalyst volume should be 1% to 2% of the total resin volume. This percentage is variable but the goal is a resulting mixture which will have a setting time of 3 to 5 hours. The exact values depend on the age of materials and temperatures. Values for a given resin lot were found by trial and error on small 100 ml sized samples.

d. Angular accelerations -- The fluid was introduced to the container while it was stationary and samples taken. The rotational speed was initially increased at 4 rpm's per minute. The angular velocity was taken to a value 10% greater than the desired velocity. This allows the fluid to wet the entire surface and make contact with the container walls, and also allows fluid movement less effected by surface tension

effects. After 3 minutes the speed was reduced to the preselected value given by equation 4.

The rotation is held constant for an additional 1 hour past the time that the samples indicate the resin is no longer fluid. The deacceleration was done slowly to avoid introducing stresses into the uncured material. This was kept to less than 4 rpm's per minute.

VI. Surface Quality

The initial experimental approach was to use styrene or polyester resin for the final surface. This was used successfully in the production of the smaller 1 m trial collector. However, this approach was not successful in the larger 3 m trials. Five attempts with varying ratios of styrene and polyester were made. These resulted in the plastic either buckling or cracking a day after its formation. In the mixtures containing more than 30% styrene the cracking of the plastic was more prevalent near the outer edges.

This cracking is thought to be caused by reactionary forces of internal strains due to rotation and the strains due to "mold shrinkage". The strains due to release of the rotational forces may be controlled by extending the rotational period to include a lengthened curing time and by increasing thickness of resin pour. The thicker resin pours will, however, exacerbate the internal strains caused by the shrinkage. To combate this it is expected that epoxy resins

systems should be tried, as well as longer setting times. Epoxy resins should also decrease the vapor difficulties that arose from the use of styrene with the large surface areas.

The plaster mixes proved to give the most consistant surfaces. Such plaster paraboloids could be dried and used directly for drape molding or creep formation of mylar films. The results of a 3 meter f/d 0.8 paraboloid formed at 13.65 rpm's is depicted in figure 3. The measurements were taken by placing a 2 inch aluminum angle beam across the surface and measuring the distance from the beam to the paraboloids surface with a machinists square. The RMS error of the surface to the best fit paraboloid was 0.05 in. This is of the order of the expected errors inherent in the measuring process due to beam sag and surface softness. For future measurements a thin reflective tape will be attached to the surface and laser ray tracing methods will be employed. This should give both a sensitive reliable method to gauge the surface and also a realistic model of what can be expected from thermosetting thin films to the surface.

VII. Additional Topics

In addition to the work in producing models that might be used to thermoset paraboloidal films the following ideas were briefly studied during the summer research program by the author as variations on existing methods.

a. Moldless thermosetting of films -- The molds and

films to be used by the solar project are normally measured by ray tracing of their surfaces with a laser while experiencing a pressure differential between the front and back surfaces. It may be possible to use an active system of correcting the surface by monitoring the surface contour with an optical laser and locally heating any distortion with a infrared source. This heating would cause "creeping" of the pressurized film as it yields to the pressure differential. Once the surface has yielded to the correct surface contour the local heating would terminate. Such a method would retain the advantages of thermosetting the film but avoid mold production problems.

b. Production of acoustical ground effects by lasers -- It may be possible to generate infrasonic, ultrasonic, and sonic waves in an atmosphere by laser thermal blooming. By locally seeding the atmosphere with SF_6 the absorption cross section drastically increases for the 10.6 micron CO_2 laser bond. An airborne or space based laser can be directed to the seeded area. The atmosphere can then be used to produce acoustical waves by modulating the laser beam.

c. Direct use of ionizing radiation for electric power production -- It may be possible to utilize beta emission from a low level radioactive source to produce electrical current. The method would be similar to thermionic generators. Instead of heating the cathode to simulate an electron flow the cathode would consist of a beta emitter.

The beta emission would be used as an electron flow. To minimize the lose of energy as heat, the resonating circuit would be tuned to a period approximating the average time between disintegrations. Such "radionic" devices could be designed (with proper isotope selections) with high power to weight ratios and low external radiation. It is hoped that a prototype of such a device can be made during future grants.

VIII. Recommendations

It is suggested that the investigation of the rotational method be continued to produce the 3 meter off-axis paraboloid at RPL. In addition, the thermosetting of aluminized mylar to such concave models should be attempted and the resulting concentrators be tested by optical means. During learning of techniques it is suggested that the thermosetting be attempted on small plaster molds before trying the 3 meter sizes.

Studies in non-traditional long-lived high-output beta energy converters should be investigated and a small proof of concept prototype be constructed. This should include library research in non-traditional theories that may lead to new and useful power and propulsion methods (such as nuclear predictions made by the 5-D Dynamic Theory).

References

1. Wood, R.W., "The Mercury Paraboloid as a Reflecting Telescope," Astrophysical Journal, vol. 29, 1909, pp. 164-178.
2. Borra, Ermanno F., "The Liquid-Mirror Telescope as a Viable Astronomical Tool," J. Royal Astronomical Soc. of Canada, vol. 76, August 1982, pp. 245-256.
3. Archibald, Paul B., "A Method for Manufacturing Parabolic Mirrors," J. of Solar Energy, vol 1, April 1957, pp. 2-3.
4. Leighton, R.B., "Notes on Spincast Plastic Parabolic Mirrors," Cal. Tech in house publication.
5. Neugebauer, G. and Robert B. Leighton, "The Infrared Sky," Scientific American, August 1968, pp. 185-194.
6. Mammana, Dennis L., "The Incredible Spinning Oven," Sky and Telescope, July 1985, pp. 7-8.
7. Wen, L., L. Huang, P.Poon, W. Carley, "Comparative Study of Solar Optics for Paraboloidal Concentrators," J. of Solar Energy Engineering, vol. 102, November 1980, pp. 305-315.
8. Teplyakov, D.I., "Concentration Ratio of Paraboloidal Solar Concentrators Deduced from Geometric Optics," Geliotekhnika, vol. 7, no. 6, 1971, pp. 10-25.
9. Grilikhes, V.A., "Experimental Investigations of the Distribution of Irradiance in the Near Focal Region of a Parabolic Concentrator," Geliotekhnika, vol. 4, 1968, pp. 31-36.
10. Pettit, R.B. and E.P. Roth, "Solar Mirror Materials: Their Properties and uses in Solar Concentrating Collectors," Solar Materials Science, vol. 5, 1980, pp.171-197.
11. Pettit, R.B., private communication, 20 June 1985.

FIGURE 1 Formation of Paraboloid

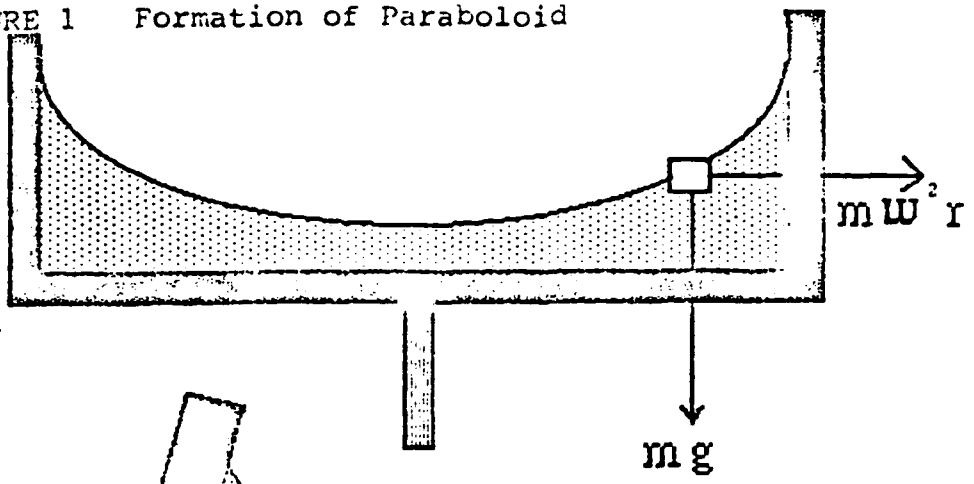

FIGURE 2 Tilted Axis

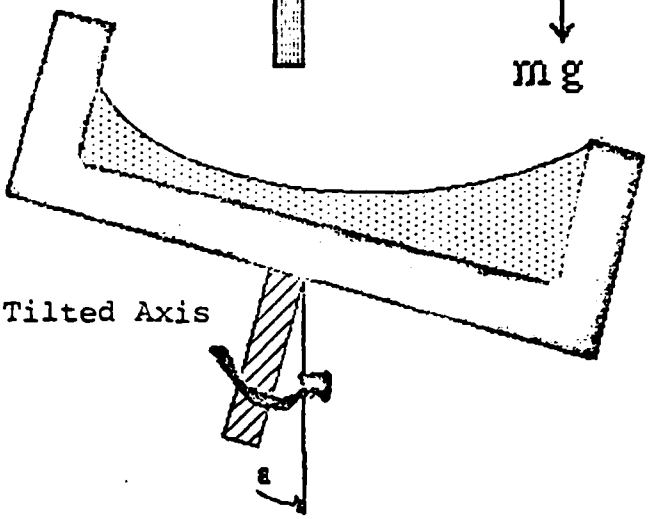

FIGURE 3 Measured Depth vs. Theoretical Parabola

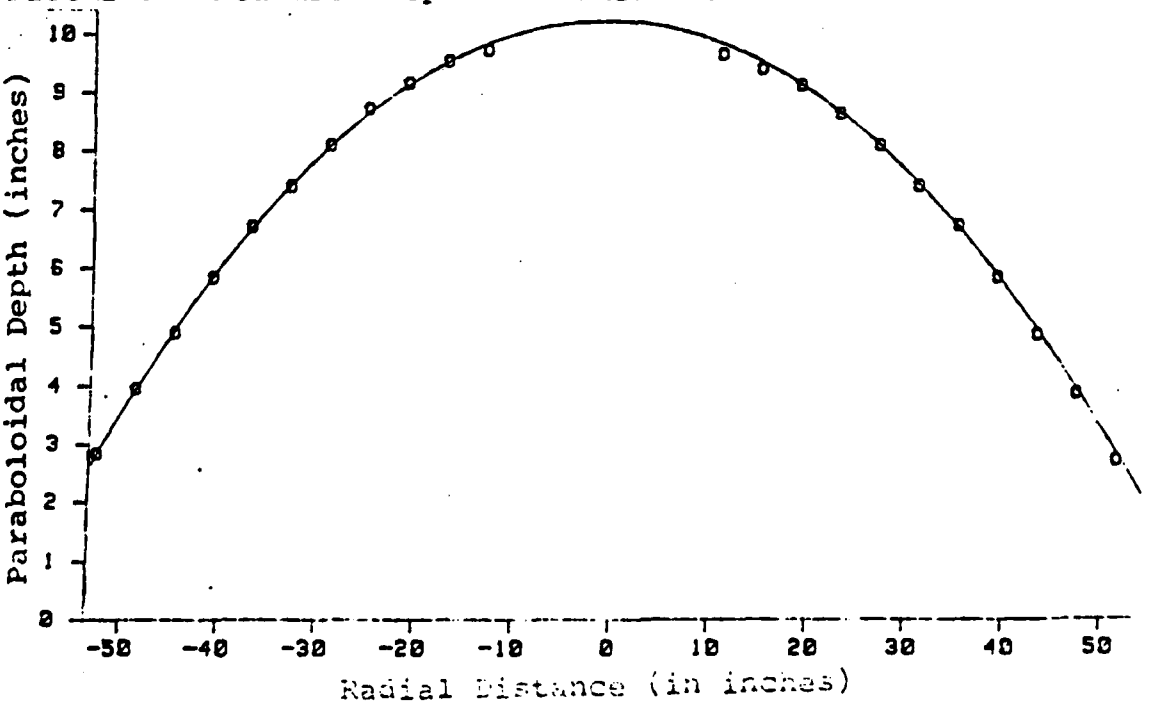

1985 USAF-UES SUMMER FACULTY PROGRAM/

GRADUATE STUDENT SUMMER SUPPORT PROGRAM

Sponsored by the

AIR FORCE OFFICE OF SCIENTIFIC RESEARCH

Conducted by the

UNIVERSAL ENERGY SYSTEMS, INC.

FINAL REPORT

HIGH-TEMPERATURE ACROSS-PLY TESTING OF C/C COMPOSITES

Prepared by:	Parviz Dadras
Academic Rank:	Associate Professor
Department and	Mechanical Systems Engineering
University:	Wright State University
Research Location:	AFWAL Material Laboratory
	Wright-Patterson AFB, Ohio 45433
USAF Research	Dr. J.M. Whitney
Date:	August 14, 1985
Contract No:	F49620-85-C-0013

HIGH-TEMPERATURE ACROSS-PLY TESTING OF C/C COMPOSITES

by

Parviz Dadras

ABSTRACT

Across-ply tensile testing of c/c composites at elevated temperatures is considered. Alternative methods for testing at temperatures up to 4000°F are suggested. These methods are based on graphite-graphite and graphite metal joining procedures, as well as other relevant processes for graphite coating. In particular, liquid-solid phase joining (brazing), and joining from suspensions are proposed.

Two alternative designs for mechanical gripping are also suggested.

I. Introduction

Carbon/carbon composites have a good potential for high temperature applications beyond the useful range of superalloys. Successful utilization of these composites requires the development of testing methods for the complete characterization of mechanical and physical properties. In particular, property determination at temperatures equal to, and even beyond the expected service temperature is mandatory. In view of the anisotropic nature of these composites a variety of experiments such as in-plane tension and compression, interlaminar shear, across-ply tension, flexure, and short-beam shear tests have to be performed. At present, the most complete testing facility for c/c materials is at the Southern Research Institute (SoRI) with few other centers such as P&WA/GPD having only limited capabilities. High-temperature testing to 4000°F (2204°C) under most loading conditions is now possible at SoRI and data on in-plane tension and compression, interlaminar and short beam shear tests at 2000°F (1093°C) and 3000°F (1649°C) are available [1].

In contrast to other testing methods, high-temperature across-ply testing is not possible at present. The room temperature test (Fig. 1) is in accordance with ASTM-C297 which is for tension test of flat sandwich constructions in flatwise plane. For this test to be possible, the strength of the adhesive bond between the specimen and the pull rods must be greater than the across-ply strength of the composite. Since adhesives for temperatures higher than 1000°F (538°C) are not available, the limitation of this method for high temperature testing is evident.

The specimen geometry, which is usually a small disk with a diameter less than one inch and a thickness equal to the thickness of the composite sheet, renders mechanical gripping with difficulty. Another method for across-ply tensile testing is by diametral compression of composite disks [2]. The elasticity solution of this problem [3] indicates large stress gradients and substantial deviations from axial loading conditions. As such this method is not considered suitable for mechanical property determination.

II. Objectives of The Research Effort:

The objective of this project is to develop testing methods for across-ply tensile testing at temperatures up to 4000°F (2204°C).

III. Significance:

The importance of carbon/carbon composites for engine and rocket applications has been demonstrated. For design and utilization of these composites it is necessary that complete material data for modes of loading be made available.

The significance of across-ply tensile testing becomes evident when one considers some common strength values for 2-D c/c composites. While the in-plane tensile and compressive strengths are usually higher than 20 ksi(138 MPa) and the interlaminar shear strength is more than 2 ksi (13.8 MPa), the across-ply tensile strength is limited to only 360 psi (2.5 MPa). The transverse tensile strength of 3-D isotropic c/c composites determined in the same manner as across-ply tensile strength is also very small and limited to 400 psi (2.7 MPa). It is imparative that these low strength values must be considered in the design of c/c composite

components. Also, experimental techniques for their evaluation under service conditions need to be developed.

The mechanical properties of c/c composites are relatively temperature-insensitive. Their elastic moduli decrease with temperature in the usual manner. Their strength, however, may decrease or increase with temperature, depending on fabrication methods and processing conditions. For example, compared with room temperature values, the in-plane tensile strength at 2000°F (1093°C) for two sets of composite specimens from two different manufacturers showed an increase of 18% for one set and a decrease of 16% for the other set of specimens. The variations of across-ply tensile properties with temperature are not known. It is likely that this property will be most affected by coating conditions and the environmental reactions at higher temperatures.

IV. Recommendation:

a. Nonfusion Joining

In this method graphite pull rods will be connected to the c/c composite specimens by nonfusion joining. In this respect, solid-phase joining (diffusion welding) and liquid-solid-phase joining (brazing) are two alternatives.

Diffusion welding of graphite to itself without a diffusion aid is not possible [4]. By using refractory metal foils inserted between two graphite blocks diffusion welds of sufficient strength (2 to 7 ksi) have been produced [4]. However, this requires very high temperatures (>2300°C) and pressures (~1420 Psi) for the diffusion annealing treatment. A variation on this approach, which is in fact a brazing

process, involves coating the refractory metal foil with an appropriate metallic film (<0.001 inch thick) so that an eutectic composition at lower temperatures will be produced, resulting in a higher diffusion rate from the liquid phase at the eutectic temperature. As an example of this method, copper-coated titanium foils have been used to join graphite to different refractory metals at temperatures in the neighboorhood of Ti-Cu eutectic temperature (885°C) and under low pressure (<100 Psi).

The coated foil approach is a convenient and relatively easy method and is proposed as an alternative in this project. The joint produced by the copper-coated titanium foil cannot be employed at temperatures approaching 885°C, as the exhaustion of copper by diffusion into graphite is not possible (nearly zero diffusion in the C-Cu system [5]) and the copper-rich eutectic compsition will persist throughout. Higher temperature joints can be produced by substituting titanium with zirconium (Zr-Cu eutectic temperature = 965°C [6]) or niobium (Nb-Cu eutectic temperature ≃ 1100°C [7]). For testing applications at T < 1000°C copper-coated titanium, zirconium, and niobium foils will be employed in this project.

For temperatures higher than 900°C the ternary brazing alloy systems developed at the Oak Ridge National Laboratories [8-10] will be employed. In Table (1) some of these systems are given. Only one alloy system (Ti-Zr-Ta) is planned for use in this project. This alloy is suitable for T < 1600°C, in regard to the Ti-C eutectic temperature which is 1650 ± 7°C [11] and the expected strength of TiC at 1600°C (compressive yield strength at 1600°C is ~4.5 ksi [12]).

In general, graphite-graphite bonding depends on carbide formation. Therefore, strong carbide formers such as Ti, Zr, and Nb are likely choices for use as filler metals in brazing systems. Moreover, it has been demonstrated [9] that alloys rich in these elements wet graphite readily. In view of these evidences it is proposed that an alloy system consisting of 22 wt.%Nb-Zr be evaluated for testing applications at T>1600°C. Based on the eutectic temperatures for Zr-C (1835 ± 20°C [11]) and Nb-C (2353 ± 10 [11]), an approximate brazing temperature of 1740-2000°C can be used. The brazing process will be followed by diffusion annealing at 1700°C, during which time the concentration of Nb in the undepleted filler alloy is expected to rise. This is due to the fact that the diffusivity of carbon for the growth of Zr-C is much greater than that for Nb-C [13]. It is to be appreciated that the diffusion of carbon, and not of the refractory specie, controls the carbide growth [14,15]. As a result, the melting point of the undepleted filler alloy (attempts will be made to make this very small) will increase beyond the original minimum temperature of 1740°C. In this fashion the upper limit for the applicability of this joint, set by the eutectic temperature of Zr-C (1835 ± 20°C) can be extended to about 1800°C (3272°F). A similar procedure with a filler alloy of 10 wt.% Mo-Nb is also possible. This alloy can be rolled at room temperature [7] and has a melting point of about 2400°C [7]. The expected brazing temperature for this alloy (2200-2450°C), however, is higher than the 4000°F (2204°C) target temperature. Because of this, as well as higher incurred costs, the use of this alloy is proposed on an optional basis.

In selecting alloy systems for the suggested testing applications thermal expansion compatibility between the alloys, the carbides, and the graphite is not of major concern. This is due to the fact that the proposed test temperatures for different alloy systems are usually within 200°C of the brazing temperatures and testing is performed in situ without cooling to room temperature.

In conducting the proposed joining method, it is important that the diffusion zone does not penetrate too deep into the specimen. This can be prevented by controlling the diffusion time and temperature before the actual tensile loading of the specimen. An approximate measure of the penetration depth will be obtained by metallographic examination of the longitudinal sections of the tested specimens.

b. Mechanical Gripping

For testing of c/c composite sheets with a thickness $\geq \frac{1}{4}$ inch (6.4mm) the feasibility of mechanical gripping will be exmained. Two alternative designs are proposed (Fig. 2). A state of true axial loading is not produced in these cases and only approximate values for the across-ply tensile strength are expected. The extent of approximations and the reliability of the results will be evaluated experimentally at room temperature and by an elasticity solution for the preferred alternative, should the experimental findings warrant this.

The proposed specimen geometries for alternatives (a) and (b) are shown in Fig. 2, and the details for the pull rods are depicted in Fig. 3. At least four specimens will be tested by each method at room temperature. Also, four standard room-temperature tests (Fig. 1) will be

conducted on the same material and under the same testing conditons. To eliminate the possibility of machining-induced damage to the specimens, a second set of tests will be performed using electrodischarge machined specimens. The experimental results will then be studied and the potential for further work will be examined.

If the continuation of this task is decided, an elasticity solution for the selected method (amongst the alternatives (a) and (b)) will be found and the required toolings for high temeprature testing will be fabricated. In Fig. (3) proposed toolings for high temperature testing are shown. Obviously, only one set of tooling for the selected method will be manufactured.

A three-dimensional elasticity solution applicable to alternative (a) already exists [16]. This solution is for an isotropic cylinder which is stretched by shear forces distributed uniformly over two strips of the side surface. A limiting case of this problem when the length of the loading strips vanishes, viz. the problem of extension of a cylinder by shear forces acting in opposite directions over two circumferences, is also of interest for the solution of this problem. According to the latter solution for an isotropic material with Poisson's ratio $\upsilon = 0.25$ and the specimen dimensions shown in Fig. (4) a distribution of normal stresses (Fig. 4b) will prevail as a result of loading. Because of the anisotropy of the c/c composite specimens and the greater in-plane strength relative to across-ply strength, a shallower stress gradient (shown as dotted line in Fig. 4b) is expected. Also, due to the Poisson's ratio differences (for c/c composites υ is -0.15 to 1.2,

depending on orientation and temperature) other variations will also come into effect.

c. Other Joining Methods

Graphite-graphite joining by other processes, mostly developed for graphite coating, is also possible. For example, in one such process [17] a suspension consisting of a solution of polystyrene in an organic solvent (such as benzene) and suspended refractory metal powders is applied to the contact areas between the specimen and the pull rods. During heating in vacuum the volatile components of the suspension are removed, some of the organic substances are converted into spongy carbon, and joining promoted by carbide formation is ensued.

The application of an yttria adhesive which is used for coating of graphite crucibles for uranium melting operations in nuclear fuel fabrication is another alternative. The coating process [18] is under U.S. Patent 4087573, May 2, 1978, assigned to U.S. Department of Energy. For joining purposes the following procedure is proposed.

A suspension of Y_2O_3 in a dilute acid (nitric or hydrochloric) is prepared and after a short curing time in air, the resulting paste is applied in between the contacting surfaces while maintaining a low compressive force to insure uniform spread and alignment. The paste will harden spontaneously in a short time into a rigid porous mass. On heating to above 1000°C the porous mass decomposes to the original oxide which remains firmly bound to the surfaces as a tough oxide layer. Yttria (Y_2O_3) is known as a very stable oxide. However, the strength of the spongy yttria layer (melting point = 2410°C) is not known. Also, the

nature of its bound with graphite and the bound strength have not been determined. A remote possibility of affecting the specimen properties during the application of the paste or the decomposition of the porous mass also exists. In spite of these uncertainties, it is proposed that the applicability of this process, as well as the process based on coating from a suspension of refractory metal powder to be investigated. The important factors favoring these processes are their potential for use in a wide range of temperatures and the convenience of their use.

Other coating processes such as chemical vapor deposition, plasma are spraying, and liquid metal infiltration are also potential methods for graphite-graphite joining. In these cases, the coated surfaces (specimen and pull rod end surfaces), while in contact under compressive laoding, have to be subjected to a diffusion/conversion step to promote solid state diffusion and carbide formation. The formation of a strong adherent joint, however, is not guaranteed. Furthermore, most of these processes are of equal and perhaps greater difficulty than those already proposed. As such, these methods will not be investigated in this project.

d. Experimental Procedure

The across-ply tension tests are performed on a 25kn screw-driven Instron equipped with load cell and recorder. A vacuum furnace capable of producing 4000°F (2204°C) and maintaining a vacuum of at least 10^{-4} torr during the test will be used. Such a furnace can be obtained from Centorr, Brew, or VFS, manufactured to the customer's specifications. W5% Re-W26% Re thermocouples which are for measuring temperatures up to

4200°F, and extension grade wire type cx, all supplied by Omega Engineering, will be used for temperture measurement.

The loading assembly (Fig. 5) consists of graphite rods with 304 stainless steel extension links and provision for application of small compressive loads in addition to the usual tensile loading. The compression capability is necessary for most of the proposed joining methods except for the mechanical gripping option. The proposed water cooling scheme and the use of 304 stainless steel extension links, in spite of the very high temperatures, are justified as the required height of the heated zone is not expected to exceed 2 inches (50.8mm) for most cases and substantially lower temperatures will prevail at the top and bottom regions of the furnace. In the final design of the loading assembly the proper selection of the graphite rod in regard to the anisotropy of mechanical and physical properties is very important. For pyrolytie graphite, for example, a trade-off between tensile strength and thermal conductivity will become a concern, as higher values for both of these properties are associated with the same orientation.

Alignment of the loading assembly is of utmost importance in the conduct of the proposed tests. The use of a universal joint and a pin connection at the two ends of the load assembly provides for self-alignment. Nevertheless, necesary precautions will be taken to insure alignment in tension as well as in compression loading.

The required brazing alloys can be obtained commercially on special order basis (Teledyne Wah Chang and KBI). However, Mr. W.T. O'Hara (MLLM) has agreed to arrange for their production and processing at the

Experimental Metal Processing Laboratories, AFWAL, Wright-Patterson AFB, OH 45433. Yttrium oxide powder (99.9% pure) is relatively inexpensive and is commerically available (Aran Isles Chem. Inc.). Copper plating of titanium and zirconium foils will be done by electroplating. Because of the high electrochemical potential of these metals in aquous solutions and their high reactivity in air at room temperatiure (existence of protective oxide coatings), a pretreatment such as anodic etching or acid pickling [19,20] will be necesasry prior to the electroplating operation.

Acknowledgments

The sponsorship of the Air Force Systems Command, Air Force Office of Scientific Research, and the Material Laboratory, AFWAL, Wright-Patterson AFB is gratefully acknowledged.

REFERENCES

1. Schmid, T.E., "Oxidation Resistant Carbon/Carbon Composites for Turbine Engine Aft Sections," AFWAL-TR-82-4159, 1982, Materials Laboratory, AFWAL, Wright-Patterson AFB, Ohio 45433.
2. Mao, T.H., and M.J. Owen, "Through-The-Thickness Tensile Strength of Fiber-Reinforced Plastics," in Composite Materials: Testing and Design, (Sixth Conference), ASTM STP 787, 1981, Philadelphia, Pa., pp 5-18.
3. Okubo, H., "The Stress Distribution in an Aeolotropic Circular Disk Compressed Diametrically," J. Mathematics and Physics, Vol. 31, Part 1, 1952, pp. 75-83.
4. Pattee, H.E., R.M. Evans, and R.E. Monroe, "Joining Ceramics and Graphite to Other Materials," NASA SP-5052, NASA, Washington, D.C., 1968.
5. Hausner, H.H., and M.G. Bowman, editors, Fundamentals of Refractory Compounds, Plenum Press, New YOrk, 1968, p. 217.
6. Hansen, M., Constitution of Binary Alloys, McGraw-Hill, 1958.
7. Prokoshkin, D.A., and E.V. Vasil'eva, Alloys of Niobium, Israel Program for Scientific Translations, Jerusalem, 1965.
8. Donnelly, R.G., and G.M. Slaughter, "Weldability Evaluation of Advanced Refractory Alloys," Welding Journal, Vol. 45, No. 6, 1966, Res. Suppl., pp. 250-s to 257s.
9. Fox, C.W., and G.M. Slaughter, "Brazing of Ceramics," Welding Journal, Vol. 43, No. 7, 1964, pp. 591-597.
10. Canonico, D.A., N.C. Cole, and G.M. Slaughter, "Direct Brazing of Ceramics, Graphite and Refractory Metals," Welding Journal, Vol. 56, No. 8, 1977, pp. 31-38.

11. Rudy, E., "Compendium of Phase Diagram," AFML-TR-65-2, Part V, 1969, Air Force Materials Laboratory, Wright-Patterson AFB, Ohio, 45433.

12. Hollon, G.E., "Carbides as High-Temperature Structural Materials," in High Temeprature Technology, Proceedings Third Int. Symp. on High Temperature Technology, Stanford Research Institute, California, 1967, pp. 257-264.

13. Wallace, T.C., "Diffusion and Chemical Kinetics Related to Problems in High-Temperature Chemistry of Refractory Carbides," in Fundamentals of Refractory Compounds, H.H. Hausner and M.G. Bowman, editors, Plenum Press, N.Y., 1968, pp. 133-154.

14. Krikorian, N.H., T.C. Wallace, R. Krohn, and M.G. Bowman, "The Formation of Carbide Surfaces on Tantalum and Tantalum-Tungsten Alloys," ibid., pp 421-432.

15. Brizes, W.F., Westinghouse Astronuclear Laboratory Report, WANL-TR-205, March 1967.

16. Laur'e, A.I., Three-Dimensional Problems of the Theory of Elasticity," Interscience Publishers, N.Y., 1964.

17. Samsonov, G.V., and A.P. Epik, "Coatings on Graphite," in Coatings of High-Temperature Materials, H.H. Hausner, eed., Plenum Press, N.Y., 1966, pp. 87-111.

18. Torrey, S., ed., Adhesive Technology, Developments Since 1977, Chem. Tech. Review No. 148, Noyes Data Corp., Park Ridge, N.J., 1980, pp 471-472.

19. Lowenheim, F.A., ed., Modern Electroplating, 3rd. Ed., John Wiley & Sons, Inc., N.Y., 1974.

20. Berkowitz, J.B., and N.H. Emerson, Plating Methods, NASA SP-5114, 1972, NASA, Washington, D.C.

TABLE 1

Ternary alloys for brazing graphite and refractory metals [10]

ALLOYS	APPROXIMATE BRAZING TEMPERATURE, °C	REFRACTORY	GRAPHITE
Ti-V-Cr	1550-1650	X	X
Ti-Zr-Ta	1650-2100	X	X
Ti-Zr-Ge	1300-1600	X	X
Ti-Zr-Nb	1600-1700	X	X
Ti-Zr-Cr	1250-1450	X	
Ti-Zr-B	1400-1600	X	

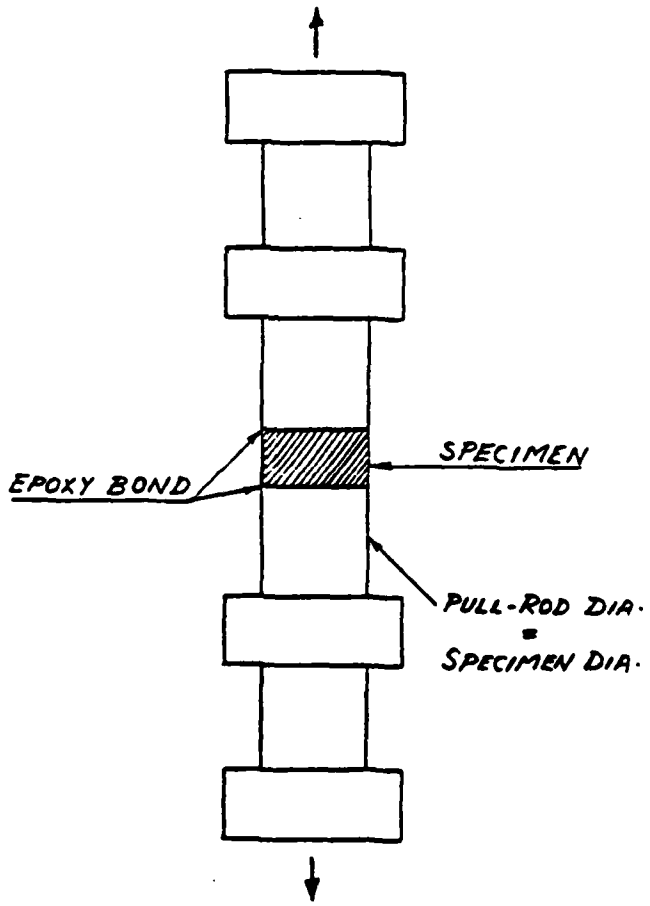

Fig. 1. Room-temperature across-ply tensile test.

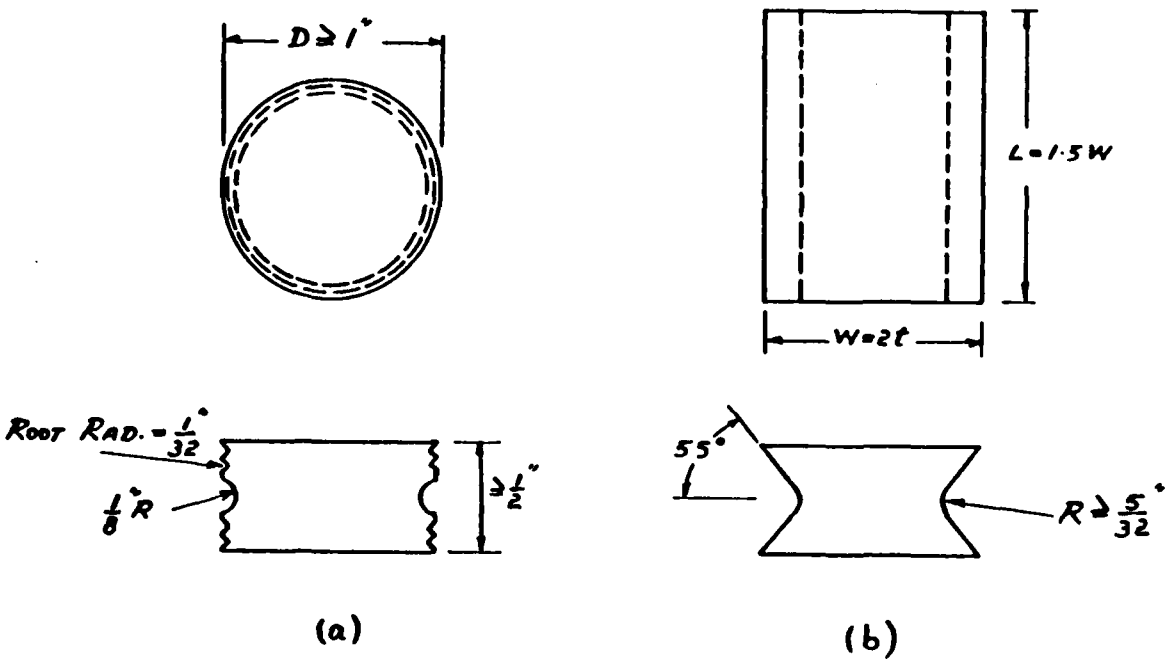

Fig. 2 Mechanical gripping, specimen geometries

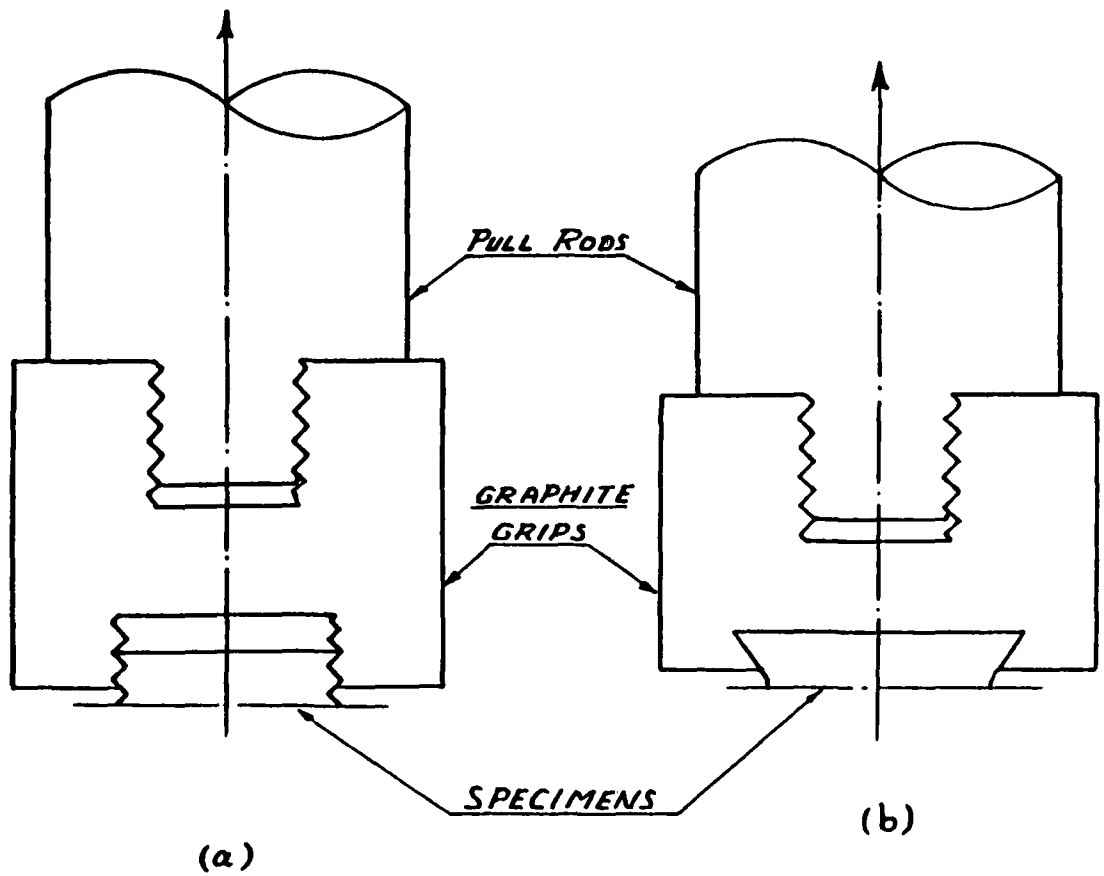

Fig. 3 Mechanical grips. The upper grips are only shown.

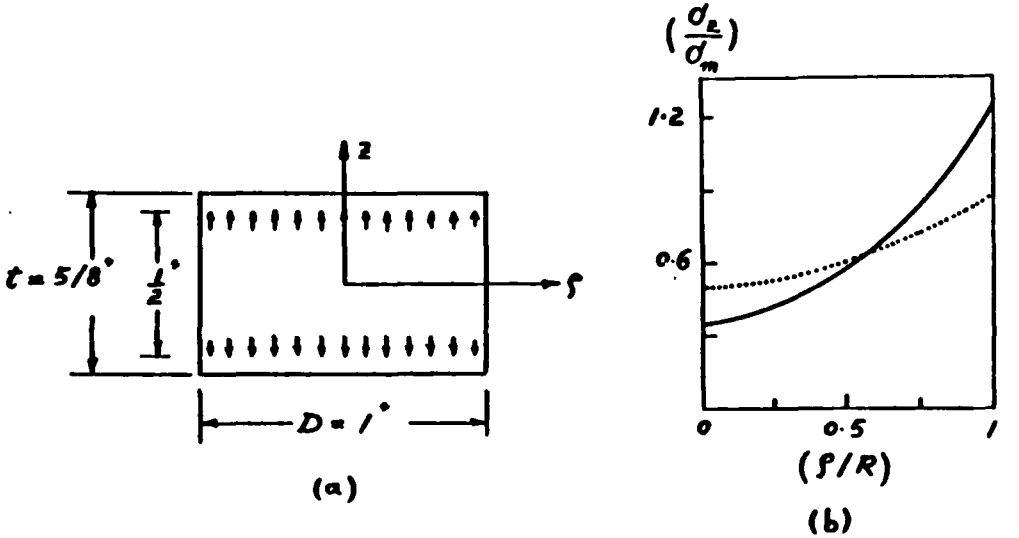

Fig. 4 (a) Mode of loading, and (b) distribution of normal stress σ_z, σ_m is the average normal stress and R = D/2.

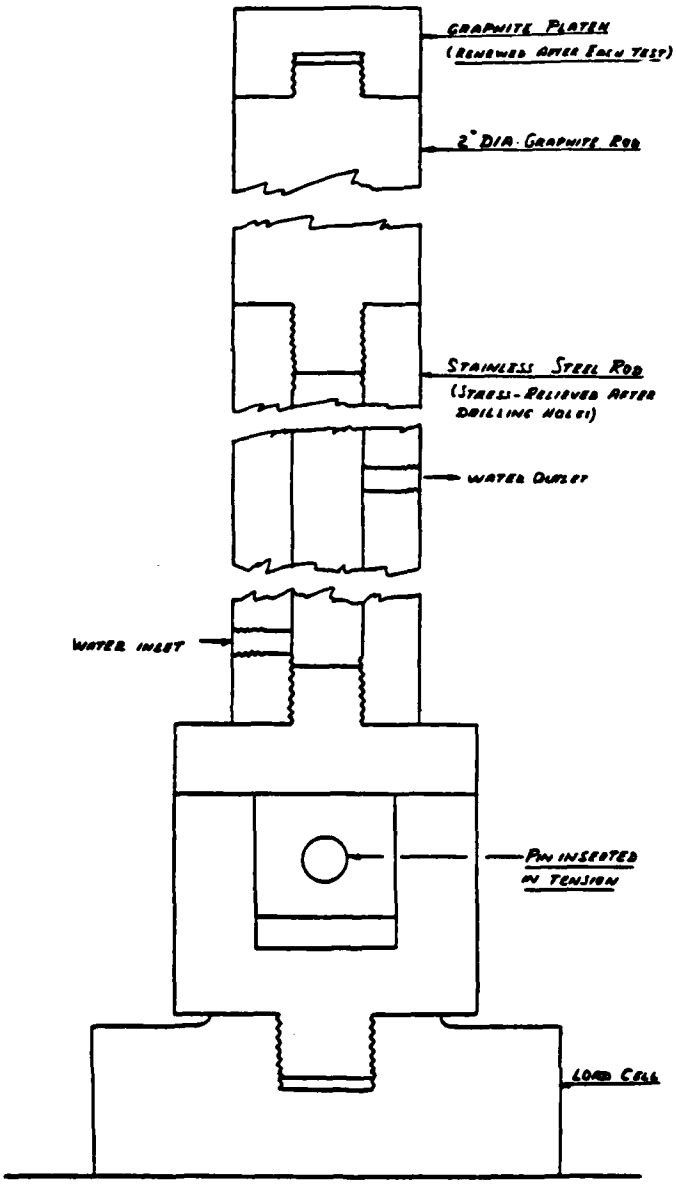

Fig. 5 Preliminary Design for the lower pull rod. The upper pull rod is similar. A universal joint will be installed in the upper pull rod for tension loading.

1985 USAF - UES SUMMER FACULTY RESEARCH PROGRAM/

GRADUATE STUDENT SUMMER SUPPORT PROGRAM

Sponsored by the

AIR FORCE OFFICE OF SCIENTIFIC RESEARCH

Conducted by the

UNIVERSAL ENERGY SYSTEMS, INC.

FINAL REPORT

STATISTICAL DESCRIPTIONS OF SHAPE IN $\mathbb{R}^2$ AND $\mathbb{R}^3$

Prepared by:	Charles B. Davis
Academic Rank:	Assistant Professor
Department and	Department of Mathematics
University:	University of Toledo
Research Location:	Modelling and Analysis Branch (BBM)
	Biodynamics and Bioengineering Division
	Aerospace Medical Research Laboratories (AMRL)
	Wright-Patterson Air Force Base
USAF Research Contact:	Ints Kaleps

Date:	September 1, 1985
Contract No:	F49620 - 85 - C - 0013

STATISTICAL DESCRIPTIONS OF SHAPE IN $\mathbb{R}^2$ AND $\mathbb{R}^3$

by

Charles B. Davis

ABSTRACT

Criteria for statistically useful characterizations of shape are identified, with particular reference to the use of biostereometric data. The Fourier Descriptors of Zahn and Roskies seem to be good candidates in $\mathbb{R}^2$, although two modes of sensitivity to digitization are demonstrated which could limit their usefulness as shape characterization statistics for comparative purposes across a population. Procedures for extending the Fourier Descriptor representations to curves and bands in $\mathbb{R}^3$ are presented, and recommendations concerning empirical studies of the usefulness of the procedures with real data sets are given.

I. INTRODUCTION

The Modelling and Analysis Branch, Biodynamics and Bioengineering Division, Aerospace Medical Research Laboratories (AMRL/BBM) has long been interested in quantitative descriptions and summaries of measurements of the human body. It has acquired unusually detailed data bases of such measurements and has developed unique modelling capabilities based on these measurements for use in simulations such as those of the response of aircrew to the forces of flight and of ejection. To date, the major use of the data has been in obtaining "typical" inertial and dynamical properties of human bodies and body segments for use in such simulations, with little attention paid to the statistical characterization of the kind of "typicality" involved. (The exception to this has been reference to and use of Department of Transportation 5th, 50th, and 95th percentile anthropomorphic manikins, without, however, much concern for the meaning of the stated percentiles or of the relation of the population from which these percentiles are obtained to populations of interest to the Air Force. Indeed, the whole aspect of defining such percentiles appropriately for various applications would itself make an interesting study in ergonomics.)

Data similar to that currently available or soon to be acquired by BBM, if obtained from an appropriately chosen sample from a population of interest, could potentially enable one to similarly characterize the variability of many important physical characteristics. In many cases, though, the characteristic desired has not yet been quantized, so only the most rudimentary of the standard statistical descriptions of the sample or of the population would apply. For example, in describing the part of the human face with which a respirator should make contact, standard statistical descriptions (means, standard deviations, correlations, etc.) can be made of the overall height and width, but not to the rather more complex idea of the <u>shape</u> of the contact region. One would like to develop procedures for quantizing such characteristics in a way which would allow for meaningful comparisions across samples or populations.

Surprisingly, there seems to be little advice in the statistical literature on such questions. Most statistical methods assume that one knows what measurements ought to be made (although well-established techniques exist for extracting subsets or combinations of such measurements which are "optimal" in some sense for some purpose). Further, virtually all standard methods insist that the <u>same</u> measurements be available on all subjects, a criterion which is nearly meaningless in the absence of a specified quantization procedure, especially with regard to the kinds of data which can be expected to be available on human body shapes.

II. OBJECTIVES OF THE RESEARCH EFFORT

The focus of this research effort, therefore, has been to investigate and develop "statistically useful" shape characterization statistics. A statistically useful shape characterization statistic (SCS) in this context will have these properties: (1) it will be of low dimension relative to the data that it summarizes; (2) it will be invariant under translations, rotations, and changes of scale; (3) it will be insensitive to variations in the location or number of data points on the objects measured; (4) objects whose SCS's are close (as numbers or vectors) should be similar in meaningful ways; and (5) standard statistical methods (such as averages, percentiles, principle component analyses, etc.) should be meaningful when applied to SCS's.

Such SCS's should be easiest to develop for two-dimensional ($\mathbb{R}^2$) objects, of course. For BBM applications, it would be also desirable to derive SCS's for surfaces in $\mathbb{R}^3$. An intermediate and rather more tractable problem is to derive SCS's for bands in $\mathbb{R}^3$, such as the contact region for the respirator mentioned previously.

Although the data available or to become available do not represent a random sample from an appropriate population, it can be used to test and refine the techniqes to be developed and to study their properties and limitations. Ideally such studies would address both the usefulness of the SCS's and their sensitivity to the nature of the available data. Carrying out these studies would, of course, involve developing the necessary computer software.

III. THE BIOSTEREOMETRIC DATA SETS

Although SCS's identified and studied are usable quite generally without regard to the origin of the data involved, the data previously mentioned as being available or to become available was obtained by the biostereometric technique, which presents some constraints. It will therefore be useful to describe this briefly.

In the biostereometric procedure, a subject (a person's body or head, in these data sets) is photographed simultaneously from opposite directions by pairs of cameras; the stereo photographs include measurement references, and a pattern is projected on the subject to enhance apparent surface texture. Subsequently, an optical device similar in function to a range-finder is used by a technician to read off three-dimensional coordinates of points on the surface of the subject. In the "body" data set, these were taken along sections of constant height, approximately two centimeters apart, approximately equally spaced with respect to distance across the photograph. In the "head" data set, the resolution should be about four times finer.

One result of this procedure is that data points are spaced somewhat randomly and quite non-uniformly over the surface of the subject, with data points much scarcer on the sides of the subject not facing the cameras than on those facing the cameras; as will be seen later. Another result is that different numbers of data points are available for different subjects measured, with the number being dependent on the size of the subject and on the technician. Furthermore, no precise relationship exists between the positions of measurements obtained on different subjects. (This is not quite true; the coordinates of a relatively small collection of points defined anatomically and labelled on each subject were recorded. However, these will not be useful for producing SCS's; see the discussion of landmarks below.)

A final point is that these measurements are made with limited precision (i.e., with rounding), and with potential for random error. One would like a good SCS to focus its attention on differences between the objects being measured, ignoring as much as possible differences induced by the measurement process.

IV. LANDMARKS OR NOT?

Two general types of approaches to shape characterization were identified early: those using standard "landmarks" (probably identified by a human analyst), and those based only on data such as that mechanically produced by the biostereometric process.

An intriguing version of the former would involve using a monotone transformations of the coordinate axes to fit identified landmarks to some prototype (perhaps a particular realization of the 50^{th} percentile manikin, for body data), and then use the parameters of the fitted transformation as the SCS. Carrying out such an approach would involve identifying a sufficiently rich family of monotone transformations of $\mathbb{R}^2$ and $\mathbb{R}^3$, along with appropriate fitting algorithms.

Such approaches were not pursued, however, in favor of more general and flexible approaches requiring less human analyst intervention and accomodating arbitrary amounts of data per subject. None-the-less, as will be seen, human analyst intervention (or very sophisticated programming!) will be necessary for many important applications. For example, describing the contact band for the respirator in terms of biostereometric data, which will be a rather non-trivial task with the intervention of a human analyst, becomes a very complicated pattern recognition problem when one contemplates complete automation. In fact, in this case it seems that either man or machine will be much less capable than a well-trained interaction; see the

recommendations for further work on the respirator problem below.

V. FOURIER DESCRIPTORS OF CURVES IN $\mathbb{R}^2$

In $\mathbb{R}^2$ the boundary of a simply connected object (a one-piece object without holes) is a simple closed curve. If this curve can be parameterized in polar coordinates $(\theta, r(\theta))$, $0 \leq \theta \leq 2\pi$, where the distance, $r(\theta)$, from some "center" point is a single-valued function of the polar angle θ, then a Fourier expansion of the function $r(\theta)$ is clearly appropriate and useful. Typically, with a reasonably smooth curve, a small number of Fourier coefficients will allow one to reproduce the original curve quite closely, and these coefficients can serve as the desired SCS's.

These Fourier coefficients do not satisfy all the desiderata given above for SCS's, of course. For one thing, the coefficients will be multiplied by any scale factor applied to the object itself, so that a scale-free shape representation would need to be based on some standardization; this is easily accomplished. Also, the phase angles for the terms of the Fourier expansion will be dependent on the orientation of the object with respect to the angle $\theta = 0$. This will not be true of the amplitudes, of course, and linear combinations of phase angles can be derived which will be invariant with respect to origin.

The biggest problems are with respect to the need for an origin for the polar coordinate representation. This approach is simply unavailable when one cannot find a suitable origin with respect to which a single-valued $r(\theta)$ can be found. When it is possible to find such an origin, there will generally be infinitely many possible suitable origins, and the function $r(\theta)$ (and consequently the resulting SCS's) will vary with the choice of origin. A possible resolution is to insist that the origin be the center of mass of the object or of its boundary (not necessarily the same!); this will suffice so long as it produces a univalent $r(\theta)$. Otherwise, the need to choose a center in a manner which is consistent from one object in the population to the next remains unanswered.

An elegant solution to these difficulties was presented by Zahn and Roskies in 1972 [1]. They suggest normalizing the total length of the curve to 2π, and then representing either the direction (angle of the tangent) or the curvature of the curve as a function of elapsed arclength. The latter is, of course, the derivative of the former, which makes it unavailable when the direction function is not differentiable. In practice one will usually represent a boundary curve by a polygonal curve connecting a finite sequence of points. Since a polygonal curve has 0 curvature everywhere except

at the vertices, where curvature is undefined, they decided to develop the former representation.

So long as the boundary does not intersect itself, as one proceeds from a starting point on the curve in a counterclockwise direction around the curve and back to that point, the tangent angle will change by a total of 2π (- 2π when proceeding in a clockwise direction, as do Zahn and Roskies). In order to produce a periodic function, then, one uses the tangent angle minus (plus) the elapsed arclength.

The Fourier expansion of this as a function of arclength can then be obtained, and various functions of the coefficients used as SCS's; these are called Fourier Descriptors (FD's). These meet many of the desiderata for SCS's easily: they are location- and scale-invariant, and rotation-invariant as well if one removes the initial angle, so long as a consistent starting point is employed; they can be defined for any simple closed curve, without need for defining a "center", with computation being reasonably straightforward for polygonal curves; and typically small numbers of coefficients suffice to give reasonable reproductions of the original object. The phase angles (but not the amplitudes) do depend on the choice of starting point, although again invariant linear combinations of phase angles can be derived. A slight drawback to this approach is that reconstructions of a boundary based on a finite number of coefficients need not, in general, produce closed curves. (Strackee and Nagelkerke [2] give a modification of the Zahn and Roskies FD's designed to close the reconstructed curve by altering the first few (usually two) coefficients. Even in their examples, however, their procedure produces noticeable distortions of the basic dimensions of the reconstructed object. We prefer simply allocating 1/N of the discrepancy to each of N (equally spaced) points in a reconstruction. This strategy will not affect the originally computed FD's themselves, which is desirable here since our emphasis is on comparing FD's from different objects in the population.)

We give below a generalization of the Zahn-Roskie development. This generalization removes the restriction that the boundary curve not be self-intersecting. In fact, we allow for the total angle change to be quite arbitrary, not restricted to multiples of 2π. This is unnecessary in $\mathbb{R}^2$, of course, but will be useful when extending this technology to bands in $\mathbb{R}^3$. Let

L	be the total length of the curve;
$0 \leq l \leq L$	be the elapsed arclength in this parametrization;
$\theta(l)$	be the accumulated change in direction angle at l;
$\delta_0 = \theta(0)$	be the initial direction;

$\phi(l) = \theta(l) - \delta_0$ be the direction angle with initial direction removed.

Then $\phi(0) = 0$, and $\phi(L) = C(2\pi)$; C will be 1 in the case of a simple non-intersecting closed curve travelled in a counterclockwise direction. L will contain all the size information about the curve; we reparametrize by letting

$0 \leq t = \frac{2\pi l}{L} \leq 2\pi$, or

$l = \frac{Lt}{2\pi}$. Then

$\phi^*(t) = \phi(\frac{Lt}{2\pi}) - Ct$, so that

$\phi^*(0) = \phi^*(2\pi) = 0$.

ϕ^* is now extended periodically, and is amenable to the Fourier expansion

$$\phi^*(t) = \mu_0 + \sum_{k=1}^{\infty} (a_k \cos kt + b_k \sin kt)$$

$$= \mu_0 + \sum_{k=1}^{\infty} A_k \cos (kt - \alpha_k).$$

In reconstructing the curve, using only N terms (pairs of coefficients, really) of the Fourier expansion, we have

$$x(l) = x(0) + \int_0^l \cos \theta(\lambda)\, d\lambda \quad \text{and} \quad (l) = y(0) + \int_0^l \sin \theta(\lambda)\, d\lambda \text{ , where}$$

$$\theta(\lambda) \approx \delta_0 + C\frac{2\pi\lambda}{L} + \mu_0 + \sum_{k=1}^{N} A_k \cos (kt - \alpha_k).$$

We usually perform this reconstruction by taking very short increments $\Delta\lambda$, multiplying by the appropriate function of θ evaluated at the midpoint of the arclength interval, or perhaps averaged at the endpoints.

VI. COMPUTING FD's FOR POLYGONAL CURVES

Consider a polygonal curve formed by m vertices $V_1, \ldots, V_m$, with V_0 being identified with V_m. Let

Δl_i be the distance from V_{i-1} to V_i and

$\Delta\phi_i$ be the change in direction angle at V_i.

$l_i = \sum_{k=1}^{i} \Delta l_k$ is the distance from V_0 to V_i, and

$\phi(l) = \sum_{k=1}^{i} \Delta\phi_k$ for $\sum_{k=1}^{i} \Delta l_k \leq l \leq \sum_{k=1}^{i+1} \Delta l_i$, with $\phi(l) = 0$ elsewhere.

Substituting these and previously given relationships into the usual formulas for computing Fourier coefficients,

$$\mu_0 = \frac{1}{2\pi}\int_0^{2\pi} \phi^*(t)\,dt, \qquad a_n = \frac{1}{\pi}\int_0^{2\pi} \phi^*(t)\cos nt\,dt, \text{ and}$$

$$b_n = \frac{1}{\pi}\int_0^{2\pi} \phi^*(t)\sin nt\,dt,$$

gives eventually the following simple computational formulas:

$$\mu_0 = C\pi - \frac{1}{L}\sum_{i=1}^{m} \Delta\phi_i\, l_i, \qquad a_n = -\frac{1}{n\pi}\sum_{i=1}^{m} \Delta\phi_i \sin\frac{2\pi n l_i}{L}, \text{ and}$$

$$b_n = \frac{1}{n\pi}\sum_{i=1}^{m} \Delta\phi_i \cos\frac{2\pi n l_i}{L}.$$

(We observe that there is no need for V_0 and V_m to be the same, in the above formulation, since the introduction of the C ensures that the resulting function will be periodic! In this case, the computational formulas given here hold.)

As a practical matter, we would point out that if one assumes that C = 1 with a simple closed curve, then one should take care that $-\pi < \Delta\phi_i < \pi$ at each vertex! An angle of $\pm\pi$ will be ambiguous, of course; for example, for the polygonal curve shown in Figure 1 one will get different values for all coefficients and for C depending on the value of $\Delta\phi_3$. Should one permit such retracings, FD's for arbitrarily complicated curves can be computed; however, exploring these will remove us from our agenda here.

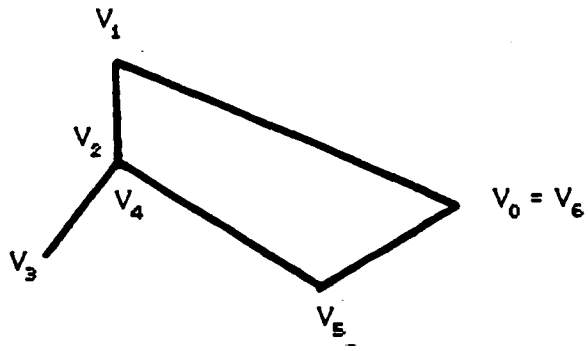

Figure 1. Values of C and of all FD coefficients will vary depending on the choice of π or $-\pi$ for $\Delta\phi_3$.

VII. EXAMPLES AND PICTURES

No discussion of Fourier descriptors of shape would be complete without some figures illustrating the rapidity with which successive FD reconstructions approximate the original object. Figure 2 presents an easily recognizable object with a k-fold

radial symmetry; it can be shown that therefore the FD amplitudes A_i will be 0 unless i is a multiple of k. As is typical, the reconstructions approach the original quickly away from the points. Figure 3 presents a digitized boundary of a handwritten "4", after Zahn and Roskies [1]. In spite of the angularity of the original object, recognizable reconstructions emerge with only 8 to 10 FD pairs. Note that the noise induced by the digitizing process begins to show up after 20 FD pairs are used in the reconstruction. Figure 4 presents the same data, with the same FD's, but using our procedure for closing the reconstructed curve.

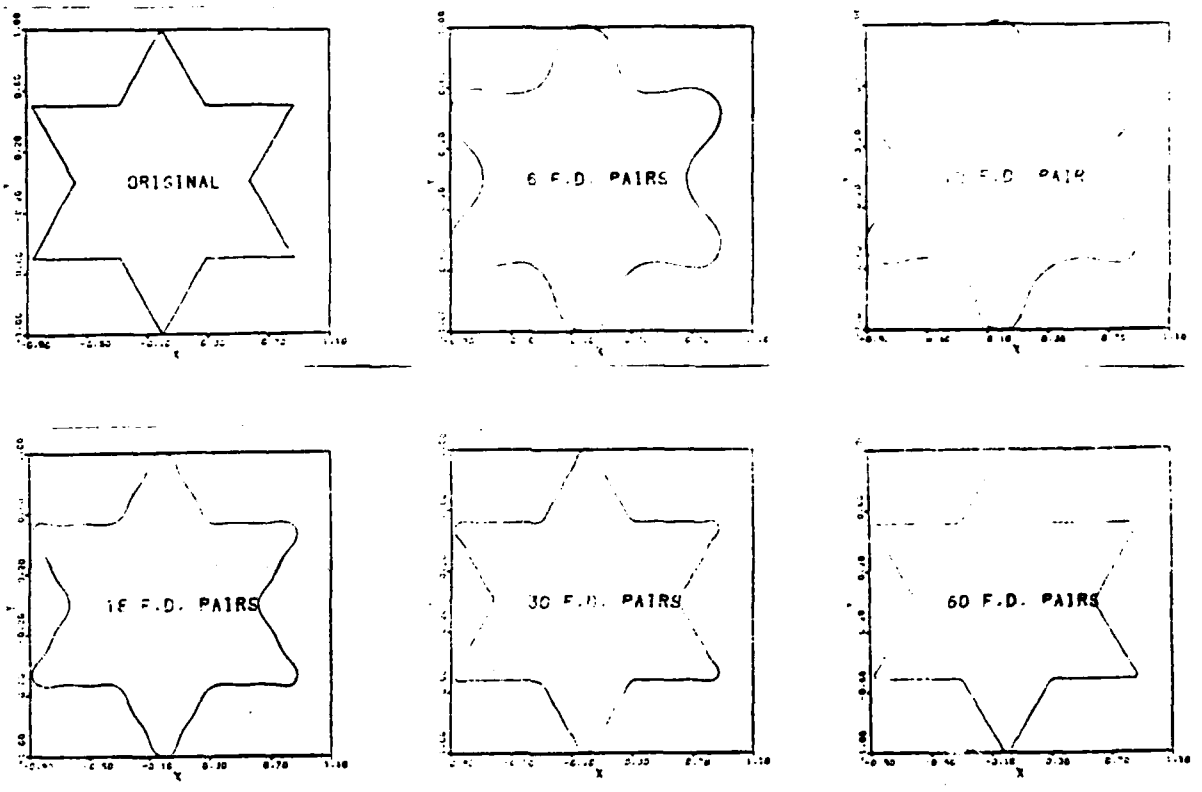

Figure 2. Reconstruction of a symmetric object using various numbers of FD coefficient pairs. A_i will be 0 here unless i is a multiple of 6.

It will be useful to examine the FD coefficients for Figure 2 a bit more closely. With a starting point at one of the interior points, each phase angle is $\frac{\pi}{2}$. Amplitudes for frequency (or harmonic) 6m are $\frac{1}{m}$ for m odd and $\frac{1}{3m}$ for m even, quite contradicting the assertion of Pavlidis [3] that only $\frac{N}{2}$ distinct descriptors are

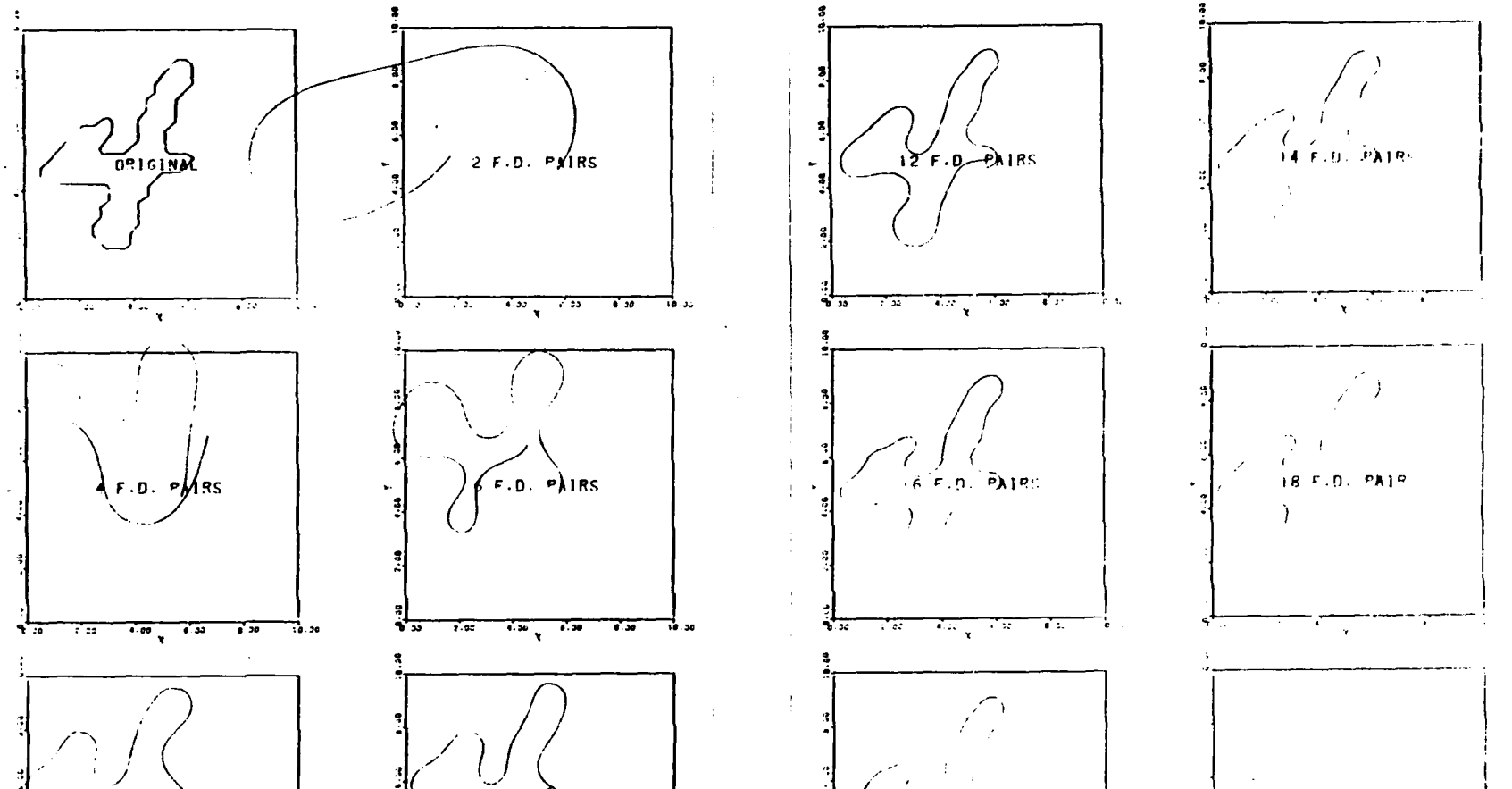

Figure 3. Boundary of a handprinted "4", after Zahn and Roskies, with reconstructions using various numbers of FD coefficient pairs.

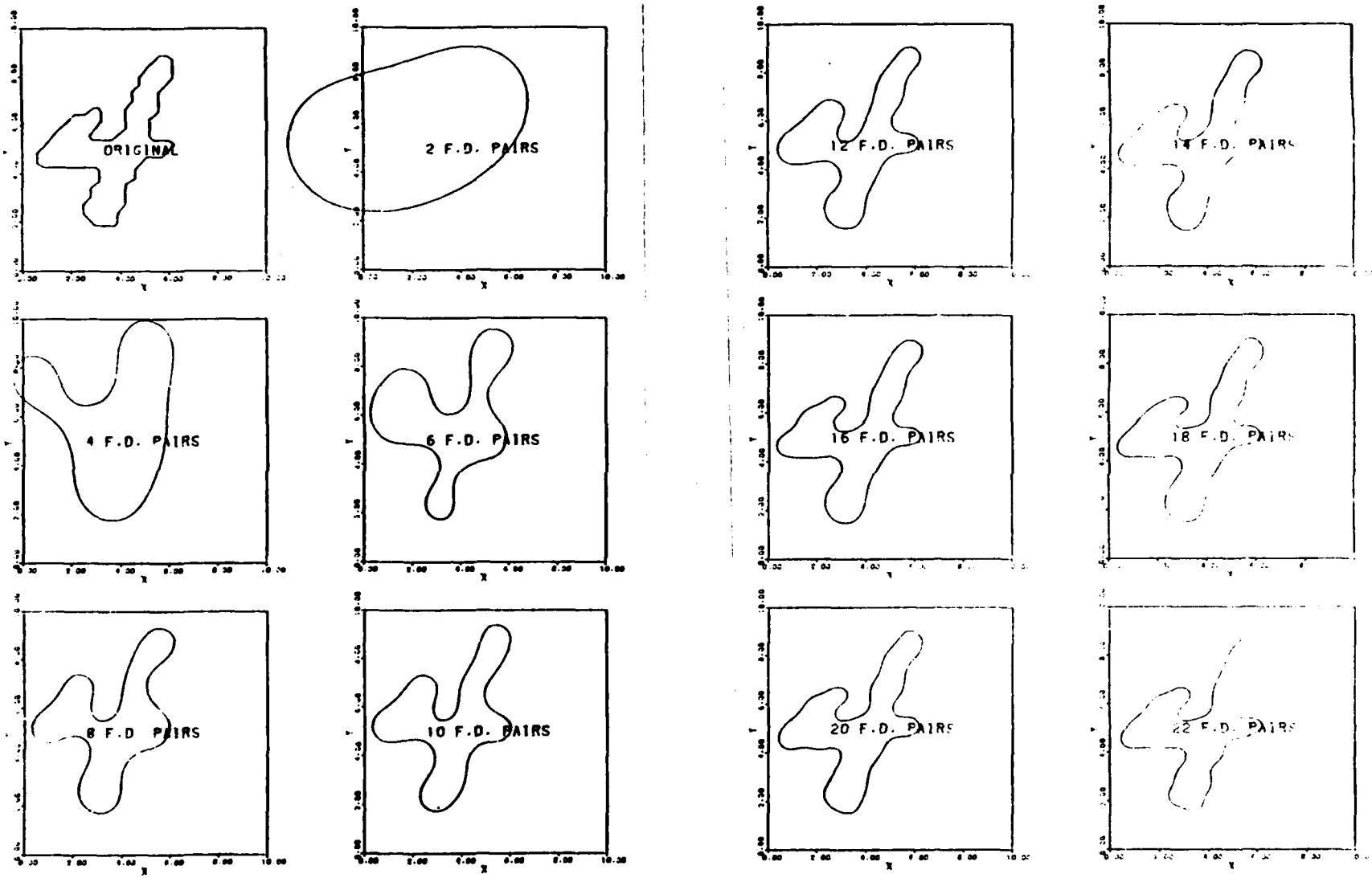

Figure 4. The same data and FD's as in Figure 3, but using our simple method of closing the reconstructed curve.

produced for a polygon with N vertices. (See below for more on this "Nyquist frequency" fallacy.) Similarly, his assertion that this technique "cannot distinguish between, say, a square and an equilateral triangle, given only by their vertices" is nonsense.

For further discussion and more examples, see Bennett and MacDonald [4]. These authors give as a rule of thumb the statement that between 3P and 4P harmonics are needed to achieve a reasonable amount of boundary detail, where P is the number of sharp bends in the boundary. They also report other studies, consistent with this rule, which state that between 15 and 20 harmonics are optimum for the problem of automated character recognition. Of course, these statements give little advice on the numbers of FD pairs to be needed to describe the range of variability within a class or a population.

VIII. SENSITIVITY OF FD's TO DIGITIZATION

In the examples of the previous section we observe that a fairly small number of FD pairs suffices to give reasonably recognizable reconstructions of reasonably smooth curves, but that does not necessarily mean that this small number will be adequate for quantizing variation in shape of a given population of similar objects. We also observe, in Figure 3, that after about the first 20 FD pairs, the reconstructions seem to begin to resemble the digitized version of the object more than the original (presumably smooth) object itself. This raises the question of just what effect the digitization process has on the FD's, and when FD pairs for higher harmonics should be regarded as resulting from the digitization process rather than from the object being measured.

In order to get some feeling for the magnitude of this effect, an experiment was conducted. We started with actual biostereometric data from a head section represented by 29 points. These were interpolated by hand and eye to produce a data set with 371 points, which was then smoothed using least-squares smoothing splines to produce a very smooth head section represented by 2000 points. The FD spectrum of this was computed, and amplitudes for frequencies above 20 were adjusted to fall off exponentially to .0001, up to harmonic 100. A closed reconstruction with 2000 points based on this FD spectrum was then created using our closing procedure; this was the object analyzed. The object is shown in Figure 5, and its FD spectrum (without digitization) is given in Figure 6. (Note: ears would be on the top and bottom in this view, but the cameras were on the sides, so the ears were lost in the biostereometric

procedure!)

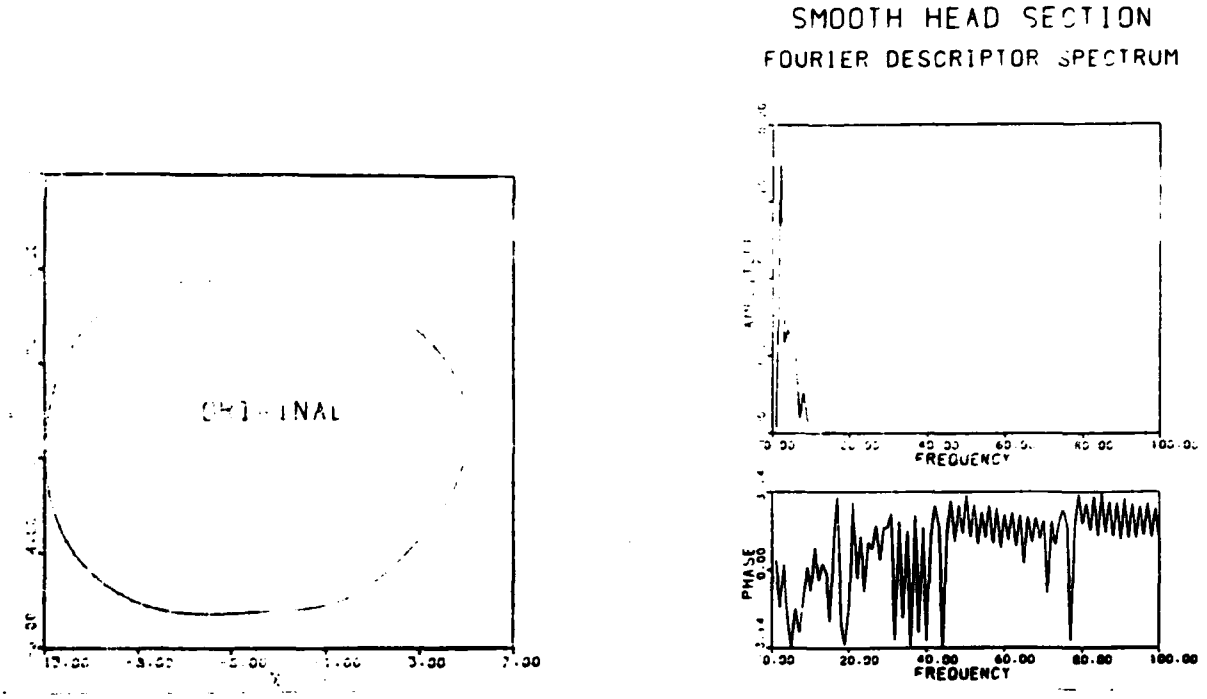

Figure 5 (left). An ultra-smooth head section, based originally on biostereometric data.

Figure 6 (right). The Fourier Descriptor (FD) spectrum for the object in Figure 5.

Two aspects of the digitization process were considered separately. One is the effect introduced by representing a continuous curve by a finite number of points; we chose 200, 100, and 50 points equally spaced about the perimeter of the object. The other is the angularity induced by rounding the data. The object's size is about 14 by 18 centimeters; we rounded successively to .001, .01, and .1 centimeters. For each combination of number of points and rounding unit the FD spectrum was computed, along with the transfer function relating it to the original FD spectrum given in Figure 6. Figure 7 shows these transfer functions, giving the log(gain) and frequency shift at each frequency. With 200 points and rounding to .001 cm., little damage is done, at least to the amplitude spectrum, as the log(gain) stays around 0. The irregularity

after the $20^{th.}$ harmonic or so probably simply reflects the low level of the original spectrum there. With rounding to .01 and .1 cm., however, substantial increases in the high frequency (roughly $16^{th.}$ harmonic and up) amplitudes are found. This is disturbing, since these displacements are of the order of only one part per hundred or per thousand, an order of magnitude easily surpassed by measurement error! The .01 rounding unit amplitudes increase to around .002 at a frequency of 40 or so, and the .1 rounding unit amplitudes increase to around .015 a bit sooner. The 100 point representations show the same rounding effect, of about the same magnitude. In addition, where rounding does not produce a noticeable gain (the .001 version), a broad peak centered at frequency 100 begins to be visible. With the 50 point representations the broad peaks at frequencies 50 and 100 predominate, at least where they are not obscured by the rounding effects. This peak at 50 appears to begin at frequency 30 or so; perhaps the misguided avoidance of frequencies above the so-called "Nyquist frequency" of $\frac{N}{2}$ is in fact desirable, although for reasons rather different from those implied by the use of that term. (The Nyquist frequency, above which harmonics are aliased with and therefore indistinguishable from lower frequencies, is valid when continuous functions are sampled at N equally spaced points, with the Fourier spectrum being computed from the resulting discrete sequence. This does not apply in this situation, of course, since we compute our FD coefficients as integrals over the whole curve. See, e.g., Koopmans [5] for more on this matter.) We observe also that the two effects are not additive (at least on this logarithmic scale), in the sense that the observed FD amplitude spectrum at a particular frequency seems to reflect the effect predominant at that frequency.

Apparently, then, the digitization process can readily induce noise, at least above some frequency. If one anticipates that 15 to 20 FD pairs will be needed to give a reasonably accurate rendering of a contour, then one should plan on using at least 40 roughly equally spaced points in the polygonal curve approximation. (The alternative of attempting to filter the effect of the finite number of points by applying the inverse of the transfer function observed here is intriguing, and perhaps possible; however, as "representing by a finite number of points" is not a linear filter, they validity and usefulness of this inverse filter are not guaranteed, and should be studied more carefully.) Likewise, when data are rounded, FD pairs of amplitudes comparable with that of the noise induced by rounding should be ignored. The level at which this occurs increases as the rounding is more gross, but is alarmingly high for rounding units such as the .1 above which would be inconsequential for most statistical

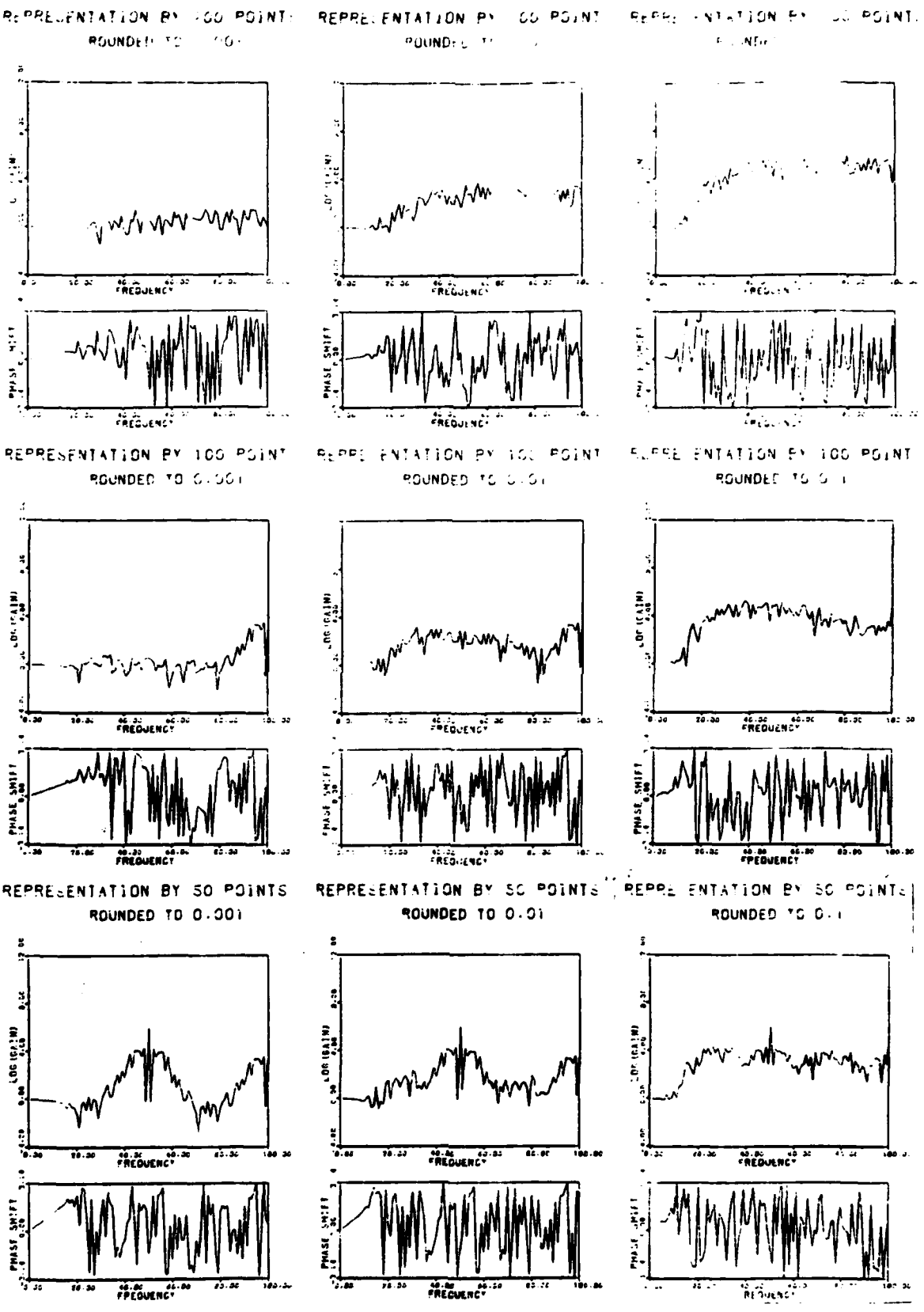

Figure 7. Digitization-induced transfer functions.

purposes.

The effect which random errors in measurement might have on the FD spectrum has not been investigated, although we would guess that it would be similar in nature to the effect of rounding.

IX. EXTENSION TO CURVES AND BANDS IN $\mathbb{R}^3$

Extending the FD technology to simple closed curves in $\mathbb{R}^3$ is simple in principle, in that the parameterization by arclength remains the same, and the angle of the tangent at any point simply becomes a two-dimensional vector. One simply computes FD's for each component of the angle vector and decides on some number of coefficients to use as the SCS. Actually, since the components of the angle vector are likely to be "correlated", it seems likely that a more parsimonious SCS could be obtained by using the FD's for one angle component along with the transfer function relating the FD's of the second angle component to the first.

There are choices to be made in deciding just what those two angle components should be. Two possibilities are described in this section.

One may decide to choose a reference plane and project the curve onto that plane, treating the angle in that projection as the first angle component and the angle made by the tangent vector with that plane as the second component. Such an approach seems quite suitable for applications such as the respirator contact band where the curve has a reasonably well-defined natural plane to project upon.

Few changes need be made in the previously given algorithm to carry out this scheme, aside from carrying out the transformations necessary to compute the projections and angles involved. The major change will come in the reconstruction phase. If coordinates in the plane are labelled x and y, with z being perpendicular to the plane, and θ is the angle in the plane and τ the angle between the tangent to the curve and the plane, the reconstruction formulas will look like these:

$$x(1) = x(0) + \int_0^1 \cos\theta(\lambda)\cos\tau(\lambda)\,d\lambda; \quad y(1) = y(0) + \int_0^1 \sin\theta(\lambda)\cos\tau(\lambda)\,d\lambda; \text{ and}$$

$$z(1) = z(0) + \int_0^1 \sin\tau(\lambda)\,d\lambda.$$

This resembles the familiar transformation from spherical to rectangular coordinates, of course.

This approach requires the existence of a natural plane for the projection, which will be consistently defined from one object in the population to the next. For

curves for which this approach will be appropriate, we would expect that the moment of inertia about one of the eigenvectors of the inertial tensor for the curve will be rather greater than those for the other two eigenvectors, so that a plane perpendicular to that eigenvector will be a good candidate for the projection plane. One should, of course, be careful to use the center of mass and inertial tensor of the curve itself, not just of the set of vertices, to minimize the variation in the choice of reference plane from object to object due to arbitrary placement of vertices on the object, as variation in this choice will alter the angle components and therefore alter the FD's derived from them.

In order to extend this development to bands in $\mathbb{R}^3$, one can in some fashion identify a tangent vector to the band at each point of a curve to which the band is to be attached. (In the case of a polygonal curve, it will suffice to identify such a tangent at each vertex.) The angles made by these tangent vectors with the reference plane will then provide the third angle component for which FD's and possibly transfer functions will be computed to serve as SCS's. Satisfactory methods of identifying such tangent vectors with biostereometric data, as for the respirator problem, have not yet been worked out; see the recommendations below.

So long as the curve in $\mathbb{R}^3$ is reasonably flat, variations in the orientation of the reference plane will be minor, resulting in minor variations in the resulting FD's. Otherwise, it will be desirable to employ an approach based strictly on local features of the curve, much as the FD's in $\mathbb{R}^2$ are designed to avoid a need for reference to the curve's center.

Such a parameterization may be accomplished in the manner described here. First, approximate the curve desired by a polygonal curve, pick a starting vertex, and record the direction of the initial edge (two angle components). Also, record the direction of the second edge (in any fashion, although only one degree of freedom exists). Then, at each vertex record the angle between adjacent edges in the plane defined by those edges as the first angle component. For the second angle component, take a plane perpendicular to the edge joining V_{i-1} and V_i, and project the preceding and succeeding edges onto it, taking the angle between them as the change in angle at V_i. The sum of these angle changes will be quite arbitrary, of course, not constrained to multiples of 2π as in $\mathbb{R}^2$ or the previous approach to curves and bands in $\mathbb{R}^3$. For bands, perhaps at each vertex the angle made by an appropriate tangent to the band with the plane defined by the adjacent edges will be useful. Again, reasonable ways of obtaining this tangent from biostereometric data have yet to be developed.

This latter approach is available for quite general curves and bands in $\mathbb{R}^3$, even perhaps for Mobius strips, with suitable care. It is not clear which approach will be better for the respirator problem; this will need to be determined empirically, after the problems of obtaining appropriate values for tangent angles noted above have been solved.

X. RECOMMENDATIONS I: TESTING FD's AS SCS's

The techniques involved in producing FD's of curves in $\mathbb{R}^2$ and curves and bands in $\mathbb{R}^3$ have been worked out and appropriate software prepared, for the most part. Details yet to be worked out include reconstruction formulas for the second, general method for curves and bands in $\mathbb{R}^3$ and procedures for specifying the appropriate tangents at vertices (or along edges) for attaching bands to curves in $\mathbb{R}^3$, especially when dealing with biostereometric data.

The most important thing lacking at this point is a trial on a suitable scale of the statistical usefulness of the FD technique, for the purposes discussed in the introduction.

An ideal oportunity to finish developing these techniques and carry out such a trial is presented by BBM's current acquisition of the FAA biostereometric data on heads, whose linear resolution is about four times better than that of the whole body data previously available. Since the motivation for the development of the band FD technology is the problem of fitting full-face respirators to the range of face shapes to be encountered, carrying out such a trial with this "object" with this data set will be definitely of interest to AMRL/BBM.

A major and previously unaddressed problem must be solved in order to carry out this study; that is the problem of extracting data points describing the band which the respirator ought to fit from the biostereometric data with enough facility to make such data available for a reasonably large sample. Given the computing resources and personnel available at BBM, one can imagine the development of rather sophisticated interactive computer graphics for this purpose (among others). Extracting the appropriate data from a biostereometric description "by hand" is extremely difficult and time-consuming, and creating a program which could automatically recognize where the respirator should fit seems much more difficult. Therefore, it seems that developing the man-machine interaction to carry out this task would be quite worthwhile in itself. An added benefit to be derived from developing this capability

would be the resulting ability to display the goodness of fit of reconstructions in $\mathbb{R}^3$, an ability simply absent at the present. Such pictures are important to understanding how the technique works, as we demonstrated in section VII by our examples.

Of course, simpler experiments can be designed to test the statistical usefulness of FD's. For example, in $\mathbb{R}^2$, one can collect a large data set of, say, handprinted "4"'s (to continue with the example in section VII) including several examples from each of many subjects, and study the usefulness of the FD's as classification statistics for determining authorship. Another example might be a rather more modest study of head (perhaps forehead) shapes using the band FD technologies on the FAA head data.

Regardless of the particular studies chosen, it will be necessary to carry out empirical studies such as these to determine the degree of usefulness of FD's as SCS's; it is difficult to conceive of theoretical analyses or of simulation studies which would adequately assess this.

XI. RECOMMENDATIONS II: FD's OF SURFACES IN $\mathbb{R}^3$

A rather more challenging extension to the FD SCS technology presented here would be to develop analogous procedures for surfaces (perhaps of solid objects) in $\mathbb{R}^3$, such as heads. Procedures applicable for completely general surfaces would be elusive, we feel; however, for objects or surfaces which would admit to a representation in spherical coordinates of the form $r = r(\theta,\phi)$, θ representing "longitude", ϕ representing "latitude", and r a single-valued function, it would seem possible.

To begin such a study, one would identify an appropriate collection of basis functions for the spherical harmonics necessary, and develop appropriate coefficient fitting techniques and inversion procedures, along with graphical and/or other techniques for ascertaining the adequacy of a reconstruction made using a small set of non-zero coefficients. Coefficient fitting will undoubtedly involve integration over the surface of the object. In $\mathbb{R}^2$, when the surface was a polygonal curve, this integration could be reduced to a summation over the vertices. In $\mathbb{R}^3$, if the surface is represented by points placed arbitrarily on the surface, developing analogous summation procedures will involve deciding on appropriate piecewise planar approximations connecting the vertices; this may well be computationally intensive as well as nontrivial due to possible ambiguities in decisions. If this is successful, integrations may be replaced by summations over vertices, and the process of ascertaining the usefulness of the resulting FD's as SCS's begun. Alternately, other

ways of integrating, perhaps approximately, using the available data could be developed.

This scheme could be undertaken for surfaces representable by a univalent function $z = z(x,y)$ in rectangular coordinates, of course, although it is difficult to imagine surfaces of interest which would be so described which would really have periodic representations.

ACKNOWLEDGMENTS

The support and assistance of Ints Kaleps, AMRL/BBM, and Bob Beecher, University of Dayton Research Institute are gratefully appreciated, as is the sponsorship of the Air Force Systems Command, the Air Force Office of Scientific Research, and the Aerospace Medical Research Laboratories, Wright-Patterson Air Force Base.

REFERENCES

1. Zahn, C. T. and R. Z. Roskies, "Fourier Descriptors for Plane Closed Curves", IEEE Transactions on Computers, C-21, 1972, 269-281.
2. Strackee, J. and N. J. D. Nagelkerke, "On Closing the Fourier Descriptor Presentation", IEEE Transactions on Pattern Analysis and Machine Intelligence, PAMI-5, 1983, 660-661.
3. Pavlidis, T., "Algorithms for Shape Analysis of Contours and Waveforms", IEEE Transactions on Pattern Analysis and Machine Intelligence, PAMI-2, 1980, 301-312.
4. Bennett, J. R. and J. S. MacDonald, "On the Measurement of Curvature in a Quantized Environment", IEEE Transactions on Computers, C-24, 1975, 803-820.
5. Koopmans, L. H., The Spectral Analysis of Time Series, New York, Academic Press, 1974, chapter 3.

1985 USAF-UES SUMMER FACULTY RESEARCH PROGRAM/

GRADUATE STUDENT SUMMER SUPPORT PROGRAM

Sponsored by the

AIR FORCE OFFICE OF SCIENTIFIC RESEARCH

Conducted by the

UNIVERSAL ENERGY SYSTEMS, INC.

FINAL REPORT

An Assessment of the Development of a DNA Probe for Mycoplasma hominis and Ureaplasma urealyticum.

Prepared by:	Vito G. DelVecchio, Ph.D.
Academic Rank:	Professor of Biology
Department and	Biology Department
University:	University of Scranton Scranton, Pennsylvania 18510
Research Location:	United States Air Force School of Aerospace Medicine Epidemiology Division Laboratory Services Branch Microbiology Section Brooks AFB TX 78235-5301
USAF Research	Vee E. Davison, Ph.D.
Date:	August 5, 1985
Contract No:	F49620-85-C-0013

AN ASSESSMENT OF THE DEVELOPMENT OF A DNA PROBE FOR MYCOPLASMA HOMINIS AND UREAPLASMA UREALYTICUM

by

Vito G. DelVecchio, Ph.D.

ABSTRACT

A rapid and simple test for the presence of Mycoplasma in clinical specimens would be of immense value in the diagnosis of conditions in which these organisms may be the etiological agents. The commercially available Mycoplasma TC Kit was found to be of no use in the testing of clinical specimens. An initial investigation into the development of a DNA probe for M. hominis and U. urealyticum was undertaken. Cultural conditions, efficient DNA isolation techniques, and exact protocols for agarose gel electrophoresis were established for these organisms. The initial data indicate that additional work is warranted and that a DNA probe can successfully be developed. Preliminary investigations suggest that M. hominis and U. urealyticum both possess plasmid DNA molecules. If confirmed by further investigation, these studies will demonstrate the first plasmid found in U. urealyticum.

Acknowledgments

I wish to acknowledge the support of the Air Force System Command, Air Force Office of Scientific Research and the help offered by the staff of Universal Energy Systems.

My deepest appreciation and gratitude are extended to all of the people at the Epidemiology Division, School of Aerospace Medicine, Brooks Air Force Base. Special thanks must be given to Mr Clifford Miller, Jr., whose constant help made much of the project's accomplishments possible, and to Mr Robert Ball and Master Sergeant Joe Mokry, whose support reached many areas of this project. Special thanks is also given to Mr Robert Tatsch and the staff of the Radiation Sciences Division.

The confidence extended by Dr Louis Blouse served as a source of inspiration by constantly bringing to mind the importance of the objectives of the project. Lastly, the rewards and enjoyment that I derived from this project would not have been possible without the permeating influence and help of Dr Vee Davison. Her constant support, encouragement, and intellectual stimulation was always there when most needed.

I. Introduction

Mycoplasma hominis and *Ureaplasma urealyticum* belong to the class *Mollicutes* (soft-skin since they lack cell walls) and as such represent the smallest known free-living organisms. These organisms are further characterized as members of the family *Mycoplasmataceae* because their genomic DNA is of small size (5×10^8 daltons) and low G + C content.

M. hominis and *U. urealyticum* were once thought to be commensal inhabitants of the urogenital tract of humans. They have been increasingly implicated as being associated with or as the etiological agents of a variety of urogenital conditions such as urethritis, prostatitis, epididymitis, Reiter's syndrome, Bartholin's abscess, vaginitis, cervicitis, salpingitis, acute pyelonephitis, nongonococcal urethritis, and pelvic inflammatory disease (Mardh, 1983; Taylor-Robinson, 1979 and 1983). These organisms have been suspected of causing infertility, fetal wastage, and reproductive failures (Cassell, 1983; Swenson, 1979; Kundsin, 1981). *Mycoplasmas* have been found in placenta and membranes of spontaneously aborted fetuses (Embree, 1980). Although these fetuses appear normal, *Mycoplasma* have been isolated from lesions in their lungs (Romano, 1971; Quinn, 1983) and in the liver, heart, lungs, brain, and viscera (Taylor-Robinson). They may also play a casual role in congenital malfunctions of infants for histological examination of brain tissue and internal organs display profound circulative disorders and degenerative changes indicative of the pathological process.

Currently there is no method of direct examination for the presence of these organisms in clinical specimens. Assessment of clinical samples is accomplished by the isolation and identification of these species on two different highly complex culture media. This present system has many disadvantages such as preparation of two different media which contain several ingredients which must be sterilized by filtration and which are relatively expensive. Media preparation is time-consuming and entails a considerable investment of effort. These media are easily contaminated by normal microbial flora, and cell debris present in clinical specimens can cause the formation of artifacts and consequent false positives (Clyde, 1983). This diagnostic procedure has extremely low sensitivity and at times as much as a 30% margin of error (Tully, 1983). The slow growth rate of these organisms demands long incubation periods and this greatly prolongs the interval between receipt and assessment of the clinical sample.

The Microbiology Section of the Epidemiology Division of the School of Aerospace Medicine at Brooks Air Force Base is particularly concerned with Mycoplasma infection of the urogenital tract. Special attention is directed at pregnant women in the last two months of pregnancy since these microorganisms can affect the pregnancy as well as the fetus itself. Therefore, the most sensitive means of diagnosis is of great use in screening and testing for Mycoplasma infection.

My research interests have been in the area of utilization of a variety of immunochemical and/or electrophoretic techniques in the investigation of various proteins, nucleic acids, enzymes, and viruses.

My work on the nucleic acid content of the virus particles of Agaricus bisporus, the cloning of DNA to the virus particles genomic RNA into E. coli, and the development of a biotinylated diagnostic probe contributed to my assignment to the Virology Function of the Microbiology Section.

II. Objectives of the Research Effort:

To assess the feasibility of the Mycoplasma TC Kit, which is marketed by Gen-Probe, San Diego CA 92123, for the direct examination of clinical specimens for the presence of Mycoplasma.

If the Mycoplasma TC Kit cannot be used to detect Mycoplasma in clinical specimens, then the possibility of developing a DNA probe for the presence of the Mycoplasma will be investigated and the development of such a probe will be initiated.

To test for the presence of plasmid DNA molecules in M. hominis and U. urealyticum. These data are needed because the presence of plasmid DNA could interfere with restriction endonuclease digests. The presence of plasmids may also be associated with the pathogenicity of an organism.

III. a. Approach to Assess the Mycoplasma TC Kit for the Direct Examination of Clinical Specimens for the Presence of Mycoplasma.

The initial objective of this project was to assess the feasibility of the kit for detecting Mycoplasma titers of clinical specimens. Although this kit was devised for testing of Mycoplasma contamination of

tissue cultures, the technical information suppl ed by the manufacturer did not preclude its use for the examination of clinical specimens. This kit utilizes a DNA probe which contains regions which are homologous to the rRNA of Mycoplasma and Acholeplasma, moderately homologous to bacterial rRNA, and nonhomologous to mammalian cellular and mitochondrial rRNA. This kit is based upon the DNA probe being able to hybridize with homologous rRNA of Mycoplasma and Acholeplasma and to form stable double stranded hybrids.

The methodology indicated by Gen-Probe was followed. Briefly, designated amounts of microbial cultures were centrifuged at 15000 x g for 10 minutes, the cellular pellet was suspended in 100 ul of 0.15 M NaCl, and then placed in a WestChem Mini Betavial. One hundred ul of ^{3}H-DNA probe solution was added and the mixture was incubated in a 72^{o}C water bath for one hour. Care was taken to insure that the vials were totally submerged in the water bath. After hybridization a solution of hydroxyapatite was added, and the vials were incubated at 72^{o}C for 5 minutes. This adsorbs any hybridized probe which was then collected by centrifugation at 2000 rpm for one minute. The pellet was then washed to remove residual unbound DNA, centrifuged at 2000 rpm or one minute, collected, and mixed with 5 ml of WestChem Cytoscint Fluid. The amount of ^{3}H-DNA which hybridized with the rRNA of different organisms was ascertained by recording the beta emission on an LKB RackBeta Liquid Scintillation Counter equipped with an Apple 2C computer.

The following experimental design was carried out to test the suitability of the Mycoplasma TC Kit for the assessment of clinical samples. Examples of microorganisms which are commensal to the human urogenital tract were chosen along with M. hominis and U. urealyticum. The example of a gram negative organism used was E. coli (ATCC 25922). Staphlyococcus epidermidis (ATCC 12228) which is Gram positive, and Candida albicans (ATCC 14053) were grown to log phase in BHI broth. One part of the above cultures was diluted to 300 parts and 1 ml of this dilution was used in the Gen-Probe test. M. hominis (ATCC 14027) and (Brooks AFB clinical specimen) U. urealyticum were grown in Arginine and Urea Broth, respectively, for five days and 2 mls of the undiluted culture was utilized in the Mycoplasma TC Kit.

Positive and negative controls, which were purchased from the manufacturer, were also included in the testing procedure. The positive control consisted of Mycoplasma rRNA and was used to test the performance of the assay. The negative control was made up of rRNA which contained no Mycoplasma nucleic acid and allowed the determination of nonspecific background.

III. b. Results of the assessment of the Mycoplasma TC Kit.

The following data were typical of CPM obtained for the organisms included in the study.

	CPM	% Hybridization*
Positive Control	1822.0	8.7%
Negative Control	65.5	0.3%
S. epidermidis	571.8	2.7%
C. albicans	43.0	0.2%
E. coli	814.5	3.9%
M. hominis	385.3	1.8%
U. urealyticum	121.8	0.6%
Standard Probe*	2098.0	-

*Standard Probe -- cpm elicited by a solution of 10 ul of ^{3}H-DNA probe in 5 ml of Cytoscint Fluid.

*% Hybridization -- (Actual cpm/Total counts) x 100.

The total count is the cpm one would expect if 100% hybridization was obtained. This is equal to the Standard Probe cpm x 10.

As can be seen from the above, the Mycoplasma TC Kit cannot be used in testing clinical specimens for other microorganisms which also inhabit the urogenital tract, such as S. epidermidis and E. coli; these contain ribosomes in which the rRNA contains nucleotide sequences which can hybridize with the ^{3}H-DNA probe used in the Mycoplasma TC Kit. It must be kept in mind that these cultures, along with the C. albicans, are diluted 1 to 300 prior to testing. The DNA probe is more specific for M. hominis than it is for U. urealyticum. In conclusion, a more specific DNA probe is needed to test for the presence of Mycoplasma and Ureaplasma in clinical specimens.

IV. a. Approach Taken to Investigate the Possibilities of Developing a DNA Probe for the Presence of Mycoplasma.

The development of DNA probes which are specific for M. hominis and U. urealyticum will allow a highly sensitive, rapid, and direct means for examining clinical specimens. These DNA-probes will compliment with genomic DNA segments which are unique to each of these species and thus will cross react with normal microbiological flora. The test will detect picogram quantities of Mycoplasma DNA in clinical samples. Once developed, the diagnostic procedure will be simple, rapid, involve no culture media and has the possibility of being automated so that a minimum of workhours will be needed to assess a large number of samples. Since the DNA-probes will be cloned into a plasmid of E. coli, an unlimited supply of the probe will be available. These probes will be tagged with biotin

and thus can be detected with an avidin-signal complex. This eliminates the need for a radioactive label and as such results in a "cleaner" and safety laboratory procedure.

Methodology. The following approach as used to assess the feasibility of development of a DNA probe for M. hominis and U. urealyticum:

Define growth and cultural conditions needed to provide adequate quantities of Mycoplasma to isolate and purify genomic DNA for the development of a DNA probe.

Determine the best method of isolation and purification of genomic DNA from Mycoplasma and Ureaplasma -- as well as genomic DNA from E. coli, C. albicans, and S. epidermidis.

IV. b. Results. Mycoplasma have a characteristic slow growth rate in laboratory cultures. This problem is circumvented by the use of large inocula to initiate growth and the utilization of large quantities of Arginine Mycoplasma broth for the growth of M. hominis or Urea broth for U. urealyticum. After many trials and errors, it was determined that adequate amounts of Mycoplasma could be obtained if 750 ml of media is inoculated with 250 ml of inoculum. Cultures should be harvested after a minimum of seven days growth. All cultures were monitored daily for pH changes as indicated by phenol red since the accumulation of end products can result in loss of viable cells. These conditions of growth were con-

firmed after consultation with Dr J. G. Tully, Mycoplasma Section, National Institutes of Allergy and Infectious Diseases, National Institutes of Health.

Genomic DNA was isolated from E. coli, C. albicans, and S. epidermidis by the methods outlined by Rodriquez (1983). Mycoplasma DNA was isolated by the methods of Taylor (1983), Cerone-McLernon (1980), and Christiansen (1981). Early attempts at DNA purification utilized cells grown in 100 or 250 ml cultures for at least seven days. Although small pellets of cells were obtained from these cultures, no DNA was isolated. This could have been due to the small size of the cell harvest or the simultaneous degredation of DNA through the liberation of DNase early in the extraction procedure. The simultaneous liberation for DNA and DNAse can degrade DNA. This DNA hydrolysis could be stopped by the inclusion of Proteinase K in the lytic buffer. Proteinase K will digest DNAse and thus prevent destruction of the genomic DNA. The DNA purification method of Gross-Bellard (1973) addressed this problem and, therefore, was used to isolate DNA from the Mycoplasma. DNA was isolated from Mycoplasma and Ureaplasma and a single band was seen upon agarose gel electrophoresis.

V. a. Approach Utilized to Determine the Presence of Plasmids in M. hominis and U. urealyticum.

Initial attempts at isolation of plasmid DNA will be carried out using the protocol of Gross-Bellard (1973). Since this method is extremely gentle and does not differentiate between genomic and plasmid DNA, any

extrachromosomal DNA molecules should be visualized upon agarose gel electrophoresis. Preferential isolation of plasmid DNA molecules will also be carried out by the method of Rodriguez (1983).

V. b. Results of Search for Presence of Plasmid DNA.

Both M. hominis and U. urealyticum contained plasmid DNA molecules. The extrachromosomal DNA molecules were visualized on agarose gels using the isolation technique of Gross-Bellard (1973). The plasmid molecules were found in a high concentration relative to the genomic DNA which suggests that many molecules are most likely present in an individual cell. This report represents the first time a plasmid has been documented in Ureaplasma urealyticum.

VI. a. Recommendation.

The Mycoplasma TC Kit is of no value in the assessment of clinical specimens for the DNA probe of this kit hybridized with nucleic acids from a wide variety of microorganisms. Many of these microorganisms are normal inhabitants of the urogenital system of humans. The kit is of use for testing of tissue cultures for one knows by visual observations if microorganisms, other than Mycoplasma, are present; therefore, when testing tissue cultures one can be reasonably certain that only Mycoplasma are the subject of the Mycoplasma TC Kit.

The best possible approach for testing of clinical specimens would be a DNA probe which would be specific for Mycoplasma nucleic acids. Before this can be accomplished, one must determine optimum conditions for growth of the Mycoplasma to obtain working quantities of DNA. As was pointed out previously, extremely small quantities of DNA were obtained using standard methods. After consultation with Dr J. G. Tully and by experience it has been determined that the following measures should be taken to insure adequate quantities of Mycoplasma cells:

- At least two liters of Mycoplasma cultures should be used for a DNA isolation.

- The two-liter culture should consist of eight 250 ml cultures.

- A large (one to four) inoculum should be used.

- Growth should be closely monitored to insure log phase growth.

- M. hominis should be grown in the SP-4 medium of Tully. This medium uses fetal calf serum in place of horse serum. This should result in increased growth for it has been reported that antibodies in horse serum can greatly inhibit the growth of Mycoplasma. Thallium acetate is replaced with penicillin since thallium may also inhibit the growth of Mycoplasma.

- Fetal calf serum will be used to prepare the Urea broth which is utilized in growing U. urealyticum.

These conditions should result in a greater amount of growth and working quantities of DNA.

The method of Gross-Bellard should be used for the isolation of DNA from Mycoplasma since the protocol guards against the digestion of DNA early in the extraction procedure. Another improvement in this technique may be decreasing the time periods of dialysis. Although the tubing is treated to prevent absorption of DNA, a decrease in the length of time of dialysis may result in greater yields. All glassware should be siliconized to prevent the absorption of DNA.

The DNA plasmids should also be isolated by method which will specifically select for these molecules. Such methods are outlined in Rodriguez (1983).

VI. b. Suggestions for Follow-on Research. The following protocol will result in the development of a DNA probe.

The genomic DNA of M. hominis and U. urealyticum will be digested with the restriction endonucleases BamHI and PstI. The endonucleases recognize guanine-plus-cytosine-rich sequences and generate a small number of fragments (Razin, 1983). Each of these endonucleases cleave the plasmid pBR 322 at a recognition site. BamHI will disrupt the circular plasmid within the gene responsible for tetracycline resistance whereas the site for PstI is located in the gene which confers ampicillin resis-

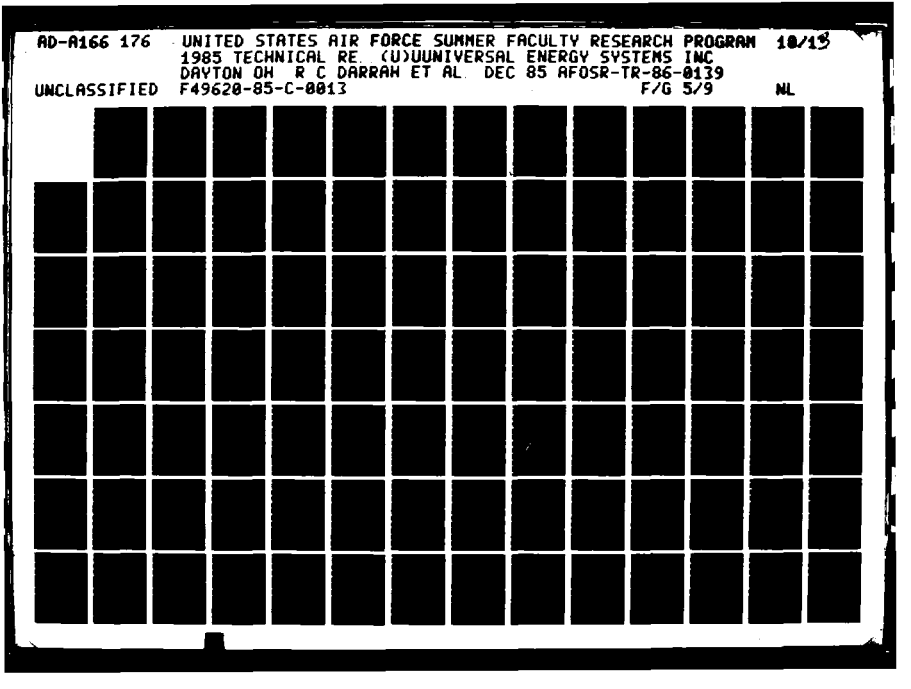
AD-A166 176 UNITED STATES AIR FORCE SUMMER FACULTY RESEARCH PROGRAM 10/13
1985 TECHNICAL RE (U)UNIVERSAL ENERGY SYSTEMS INC
DAYTON OH R C DARRAH ET AL DEC 85 AFOSR-TR-86-0139
UNCLASSIFIED F49620-85-C-0013 F/G 5/9 NL

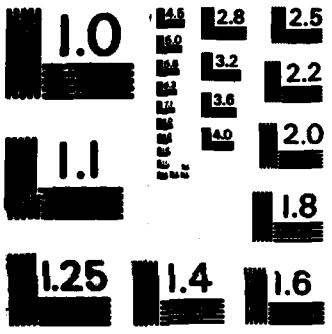

MICROCOPY RESOLUTION TEST CHART
NATIONAL BUREAU OF STANDARDS - 1963 - A

tance. Therefore, these restriction endonucleases and the E. coli pBR 322 plasmid offer an ideal cloning system for these specialized mycoplasmal gene probes.

The restriction endonuclease-generated DNA fragments will be electrophoresed on an analytical Hoefer Minnie Submarine Agarose Gel Unit or a preparative BRL H-4 submerged unit. Selected low molecular weight DNA fragments will be liberated from low-melting-temperature agarose gels according to the method of Libby (1985) or the fragments will be separated on BRL Prep Gel and dissociated from the agarose on a Konte Electrodialysis Unit. The eluted DNA fragments will be biotinylated using the procedure of Langer (1981) which exploits the nick-translation properties of DNA polymerase I.

The specificity of the biotinylated DNA fragments (potential DNA-probes) for either M. hominis or U. urealyticum will be determined by Southern blotting (Southern, 1975). A complete spectrum of other Mycoplasma species, as well as other microorganisms, will also be included in this specificity evaluation. The presence of biotinylated fragments which have hybridized with complimentary DNA strands on the nitrocellulose paper will be visualized using avidin-alkaline phosphate polymers as outlined by Leary (1983).

Once a gene sequence has been determined to have sufficient specificity to serve as a DNA probe it will be cloned into E. coli. DNA fragments which have been generated by either BamHI or PstI will be combined with pBR 322 plasmid which has been made linear with either of these

endonucleases. Since the pBR 322 vector and the restriction fragments will have identical cohesive ends (as generated by either BamHI or PstI) recombinant DNA molecules will be formed. The DNA backbone will be reformed using the enzyme T4 DNA ligase (Dugaiczyk, 1975; Sgaramella, 1970; Sugino, 1977). Alkaline phosphatase will be employed to prevent vector recircularization (Perbal, 1984).

Recombinant DNA will be introduced into competent E. coli cells by the method of Maniatis (1982). Transformed cells will be detected by replica plates of colonies grown on media with or without ampicillin or tetracycline depending on the restriction endonuclease used in the cloning protocol. Transformed E. coli can be further tested for the presence of specific DNA sequences by the colony hybridization method of Yang (1984) and of Leary (1983).

E. coli will yield an unlimited supply of DNA-probes. Biotinylation and isolation of the DNA-probes will be accomplished as needed or to build up a large stock. The dot hybridization procedure of Leary (1983) will be carried out on a BRL HybriDot manifold. This technique will allow the rapid and highly specific detection of M. hominis and U. urealyticum in clinical specimens.

The plasmid DNA molecules will be subjected to restriction endonuclease mapping with subsequent sequencing of the plasmids. Listing of strains of Mycoplasma for antibiotic sensitivity which may correlate with

the presence or absence of plasmid will also be undertaken. Mapping of plasmid genes will then be accomplished via transformation of competent Mycoplasma cells.

VI. c. Any Other Suggestions Having Bearing on the Research You Will Accomplish. A DNA probe which is specific for M. hominis and U. urealyticum (and various types thereof) will greatly facilitate the examination of clinical specimens. Probes which will hybridize with genus, species, and genotypes will be developed. Along with this immediate benefit, the DNA probe will also impact upon broader areas of science and research.

The known serovars of M. hominis will be defined by the use of restriction endonuclease and DNA probes developed to these different Mycoplasma types. Investigations of the reactivity (and crossreactivity) of the various DNA probes with the different types of Mycoplasma will contribute greatly to the general field of Mycoplasma systematics. These same techniques will also be applied to investigate the possibility of the existence of different genotypes of U. urealyticum. Isolates of these organisms form different locales of infection or commensalism will also be characterized by these techniques.

Since it has been suggested that certain types of M. hominis and U. urealyticum may be commensal whereas other types are possibly disease producing, the high resolution offered by a DNA probe for different serovars and genotypes will lead to a more complete definition of

pathogenicity of these organisms. The DNA probe will also clarify the "grey" area between commensal, opportunistic, and virulent types of Mycoplasma.

These probes can also be used to locate individual Mycoplasma cells in tissues of the body and from tissue cultures. Biotinylated DNA probes have been utilized in this respect with great success. Such in situ hybridization and visualization will clarify the interplay of Mycoplasma with their host cells. Since there is such an intimate relationship between Mycoplasma and mammalian cell plasma membrane, the possibility of the two cells sharing nucleic acids or the chance that the nucleic acid components share homolgous sequences will be studied. The answer to these questions will have significance in many areas of mycoplasmology and possibly broaden our general knowledge of microbiology.

The presence of plasmids in these organisms may be associated with pathogenic characteristics and antibiotic resistance properties. The plasmids nucleic acid sequence and antibiotic resistance genes will be of great aid in determining the function of these extrachromosomal DNA molecules on these organisms. A probe for these plasmids can easily be developed. Such a probe will enable one to determine if plasmid DNA molecules are involved in the category of Mycoplasma within host cells.

REFERENCES

Cassell, G. H., J. B. Younger, M. B. Brown, et al. Microbiologic study of infertile women at the time of diagnostic laparoscopy: association of Ureaplasma urealyticum with a defined subpopulation. New Eng. J. Med. 1983. 308:502-505.

Cerone-McLernon, A.M., and G. Furness. The preparation of transforming DNA from Mycoplasma hominis strain Sprott tet^r and quantitative studies of the factors affecting the genetic transformation of Mycoplasma salivarium strain S9 tet^r to tetracycline resistance. Can. J. Microbiol. 1980. 26:1147-1152.

Christiansen, C., F.T. Black, and E.A. Freindt. Hybridization experiments with DNA from Ureaplasma urealyticum serovars I to VIII. Int. J. of Syst. Bacteriol. 1981. 31:259-262.

Clyde, W.A., et al. Laboratory diagnosis of chlamydial and mycoplasmal infection. In Balows, A., W. J. Hausler (eds.) Diagnostic procedures for bacterial, mycotic and parasitic infections. American Public Health Association, Washington, D.C., p. 511-528.

Dugaiczyk, A., Boyer, H.W. and Goodman, H.M. Ligation of EcoRI endonuclease-generated DNA fragments into linear and circular structures. J. Mol. Biol. 1975. 96:171-184.

Embree, J.E., et al. Placental infection with Mycoplasma hominis and Ureaplasma urealyticum. Obstet. Gynecol. 1980. 56:475-481.

Gross-Bellard, M., Oudet, P. and Chambon, P. Isolation of high molecular weight DNA from mammalian cells. Eur. J. Biochem. 1973. 36:32-38.

Kundsin, R.B., et al. Ureaplasma urealyticum incriminated in prenatal morbidity and mortality. Science.1981.213:474-476.

Langer, P.R., A.A. Waldrop, and D.C. Ward. Enzymatic synthesis of biotin-labeled polynucliotides: novel nucleic acid affinity probes. Proc. Natl. Acad. Sci. 1982. 79:4381-4385.

Leary, J.J., D.J. Brigati, and D.C. Ward. Rapid and sensitive colorimetric method for visualizing biotin-labeled DNA probes hybridized to DNA or RNA immobilized on nitrocellulose: Bio-blots. Proc. Natl. Acad. Sci. 1983. 80:4045-4049.

Libby, L.S., J.H. Fisher, and C. Scoggin. A method of isolating nick-translated DNA by subsequent separation on low-melting-temperature agarose. Anal. Biochem. 1985.146:23-27.

Maniatis, T., E.F. Fritsch, and J. Sambrook. Molecular Cloning: A laboratory Manual. Cold Spring Harbor Laboratory. 1982. p. 249-253.

Mardh, Per-Anders. Mycoplasma PID: A review of natural and experimental infections. The Yale Journal of Biology and Medicine. 1983. 56: 529-539.

Perbal, B.V. A practicle guide to molecular cloning. John Weley and Sons, Inc. 1984, p. 259-263.

Quinn, P.A., et al. Serological evidence of U. urealytecum infection in neonatal respiratory disease. The Yale Journal of Biology and Medicine. 1983. 53:565-572.

Razin,S., R. Harasowa, and M. F. Barile. Cleavage patterns of the mycoplasma chromosome, obtained by using restriction endonucleases, as indicators of genetic relatedness among strains. Int. J. Syst. Bacteriol. 1983. 33: 201-206.

Rodriguez, R.L., R.C. Tait. Recombinant DNA Techniques. 1983. Addison-Wesley Pub. Co., Reading Mass. 45-46, 162-163, 167-168.

Romano, N. et al. T-strain of mycoplasma in bronchopenunonic levage of an aborted fetus. New Eng. J. Med. 1971. 285: 950-952.

Sgaramella V., van de Sande J.H., Khorana, H.G. Studies on polynucleotides. C. A novel joining reaction catalyzed by the T4-polynucleotide ligase. Proc Natl Acad Sci USA. 1970. 67:1468-1475.

Southern, E.M. Detection of specific sequences among DNA fragments separated by gel electrophoresis. J. Mol. Biol. 1975. 98: 503-517.

Sugino, A., Goodman, H.M., Heyneker H.L., Shine I, Boyer H.B., Cozzarelli N. Interaction of bacteriophage T4 RNA and DNA ligases in joining of duplex DNA at base-paired ends. J. Biol Chem. 1977. 252:3987-3994.

Swenson, C.E., A. Toth, W.M. O'Leary. U. urealyticum and human infertility: The effect of antibiotic therapy on semen quality. Fertil. Steril. 1979. 31: 660-665.

Taylor, M.A., M.A. McIntosh, J. Robbins and K. Wise. Cloned genomic DNA sequences from Mycoplasma hyorhinis encoding antigens expressed in Escherichia coli. Proc. Natl. Acad. Sci. 1983. 80: 4154-4158.

Taylor-Robinson, D. The role of mycoplasma in non-gonococcal urethritis. The Yale Journal of Biology and Medicine. 1983. 56: 537-543.

Taylor-Robinson, D., W.M. McCormack. Mycoplasma in human genito-urinary infections. In Tully, J.G. and R.B. Whitcomb (eds.) The Mycoplasma. 1979. 2: 308-366.

Tully, J.G., et al. Evaluation of Culture media for the recovery of Mycoplasma hominis from the human urogenital tract. Sex. Trans. Dis. 1983. 10: 256-60.

Yang, H. L. DNA dependent diagnosis using nonradioactive colony hybridization. 84th Annual Meeting, American Society for Microbiology, St. Louis, Missouri, Abstract, 1984, p. 240.

1985 USAF UES SUMMER FACULTY RESEARCH PROGRAM/
GRADUATE STUDENT SUMMER SUPPORT PROGRAM

Sponsored by the

AIR FORCE OFFICE OF SCIENTIFIC RESEARCH

Conducted by

UNIVERSAL ENERGY SYSTEMS, INC.

FINAL REPORT

EFFECTS OF NUCLEAR RADIATION ON THE OPTICAL CHARACTERISTICS OF LASER COMPONENTS

Prepared by:	Dr. Hermann J. Donnert
Academic Rank:	Professor
Department and University	Department of Nuclear Engineering Kansas State University
Research Location:	Frank J. Seiler Research Laboratory Directorate of Lasers and Aerospace Mechanics
USAF Research:	Dr. Albert J. Alexander, Major, USAF
Date:	16 August 1985
Contract No.:	F49620-85-C-0013

EFFECTS OF NUCLEAR RADIATION ON THE OPTICAL CHARACTERISTICS OF LASER COMPONENTS

by

Dr. Hermann J. Donnert

ABSTRACT

In view of requirements stemming from projects under the auspices of the Strategic Defense Initiative, work has been initiated to explore the effects of nuclear radiation on the optical characteristics of laser components. Pre-irradiation tests have been conducted and samples have also been exposed to the fast-neutron environment in the beam stop of the Los Alamos Meson Physics Facility and to energetic electrons in the beam of EG&G's LINAC. Computer codes for analysis of experimental data have been developed, tested, and used to obtain preliminary results. Further experiments of relevance are in various stages of planning.

ACKNOWLEDGEMENTS

The author acknowledges most gratefully the financial support provided by the Air Force Systems Command, the Air Force Office of Scientific Research, the Frank J. Seiler Research Laboratory, and Universal Energy Systems, Inc..

The author is gratefully indebted to many individuals who have contributed to the project and deserve praise for their helpful contributions: Lt Col J. Pletcher, Jr., Lt Col K. Siegenthaler, Major T. Deaton, Major S. Czyzak, and Mr. F. Kibler of FJSRL; Dr. L. Rosen, Dr. J. Bradbury, Dr. R.D. Brown, Dr. N.S.P. King, Dr. W. Hughes, Dr. S. Foltyn, Dr. M. Moore, Dr. F.B. Harrison, Dr. W.W. Wadt, and Mr. B. Guffy of LANL; Dr. R. Hamil and Dr. P. Brannon of SNL; Dr. L. Hocker, Dr. P. Zagarino, Dr. S. Iverson, Dr. S. Lutz, Mr. S. Jones, Mr. R. Sturges, and Mr. Paul Nash of EG&G; Dr. W. Kunzler and Dr. W. Wasson of AFWL. Very special thanks for help over and beyond the call of duty in facilitating the effort and making the author's life easy to to Mr. B. Hatfield for fabrication of necessary equipment items and to Ms. L. Kelly for untiring secretarial support.

The author expresses thankful tribute to his graduate students, Mr. M. Ferrel, Mr. G. Scronce, and Mr. K. Stroh of Kansas State University of their excellent summer work at FJSRL. Their work has been a vital part of the overall effort.

Last, but not least, the author expresses his sincerest gratitude to one of his former doctoral students, Major A. Alexander of FJSRL. His unwaivering support and encouragement will always be remembered.

I. INTRODUCTION:

Determination of nuclear-radiation effects on the optical characteristics of laser components, such as mirrors and windows, has recently become a matter of vital interest with the scope of several projects under the auspices of the Strategic Defense Initiative (SDI). Such knowledge, at least of a phenomenological nature, is of utmost and urgent importance for the design of laser systems for anti-missile defense applications. In the long run, basic understanding of response kinetics and the concomitant ability to formulate theoretical models will be essential to harden these systems and reduce their vulnerability to hostile actions.

Based on the common knowledge of solid-state physics, energy deposition from absorption of nuclear radiation changes the microstructure of the crystal lattice and the distribution of the eletrons and holes in quantum - mechanically available energy states; to complicate matters, inevitable impurities and dislocation defects are generally of profound importance. Such changes impact a variety of physical properties of the solid material, such as electrical conductivity and optical absorbance. Thus, the essential question to be answered is not whether germane effects will actually occur, but as to what their magnitude and the associated practical significance for the military systems design might be.

Except for efforts by the author and his graduate students at FJSRL[1,2,3,4,5,6] and by researchers at Sandia National Laboratory (SNL)[7,8], virtually no significant research to explore this vital problem area has been reported. Published observations of nuclear-irradiation effects on the performance of fiber optics[9], although in themselves certainly interesting, are of exceedingly limited value in addressing the laser-component problem because the vagaries in solid-state behavior and the lack of a sound theoretical understanding preclude any quantiatively credible scientific inference. Also, some very preliminary and limited information for dielectric coatings relating to cosmic radiation encountered by space

vehicles, having been published lately[10], is of very little relevance for SDI system applications. Simply speaking, the state-of-the-art is on square one.

To conduct the investigation reported here requires diversified expertise in several scientific disciplines: radiation physics and nuclear radiation effects, solid-state physics, plasma physics, laser physics, and optics. All these necessary ingredients are within the author's repertoire of extensive research experience.

II. OBJECTIVES OF THE RESEARCH EFFORT:

The objectives of the research effort is the exploration of nuclear-irradiation effects on the laser-damage threshold of laser components to be used in military applications of laser systems with strong emphasis on problems relevent to the Strategic Defense Initiative (SDI). Short-range goals are directed toward satisfying some immediate high-priority SDI requirements in a timely manner. Long range goals entail the development of theoretical models and basic understanding of the relationship between observed macrophenomena (refelectivity, absorbance, etc.) and microphenomena at the atomic and electronic scale of solid-state physics.

III. NEUTRON-IRRADIATION EFFECTS.

Mirrors (multiple dielectric coatings of ZrO_2 and SiO_2 on Si substrate) designed for optimum reflectivity at the I-laser wavelength $\lambda = 1.315$ μm, were exposed to fast neutrons in the beam stop of the Los Alamos Meson Physics Facility (LAMPF). The pristine-sample reflectivity $R_o = 0.99 \pm 0.01$ was reduced to $R = 0.71 \pm 0.08$ for samples subjected to a fast-neutron fluence[11] of about 1.5×10^{22} neutrons/m^2. Further samples will be exposed to lesser fluence levels after the current modification project of the LAMPF beam-stop facility is completed. Detailed results are documented in a report by Ferrel.[12]

IV. EFFECTS OF ELECTRON-BEAM IRRADIATION:

Mirrors (multiple dielectric coatings of Al_2O_3 and SiO_2 on fused silica substrate) designed for optimum reflectivity at the KrF-laser wavelength λ = 248 nm as well as metal-coated mirrors (200 nm Al layer on fused-silica substrate and layers of 90 nm Cu plus 200 nm Ag on fused-silica substrate) were irradiated with intense energetic-electron pulses in the beam of the electron LINAC operated by EG&G Energy Measurements, Inc. The coatings were subjected under the following nominal conditions:[13] (a) pulse duration τ = 20 ns, dose rate D = 2.5 krad/ns, dose D = 50 krad; (b) pulse duration τ = 20 ns, dose rate D = 3.5 krad/ns, dose D = 70 krad; and (c) pulse duration τ = 45 ns, dose rate D = 2.8 krad/ns, dose D = 126 krad. Reflectivity of the samples was observed in a time interval of about 1.2 μ s during and immediately following the electron-beam pulse. Reflectivity and absorption of the samples were also measured two weeks after irradiation. Comparison of the results with values for the pristine samples reveals that the effects are very small. Additional irradiations are planned to study the optical characteristics of these mirrors under conditions of electron-beam pulses in the pulse duration range from about 100 ns to 1 μ s. It should be noted that these electron irradiations give, at least qualitatively, an indication of gamma-radiation damage effects that might be anticipated. Detailed results are documented in reports by G.W. Scronce[14] and K.A. Stroh.[15]

V. PROJECT COORDINATION AND PLANNING OF CONTINUED COOPERATIVE EFFORTS:

Current and planned future experiments in the planning stages are being closely coordinated with SDI projects at LANL and SNL. Cooperative work relationships have been established which will be highly beneficial to all parties involved. Many details of this topic are classified.

VI. RECOMMENDATIONS.

In veiw of the critical importance for certain SDI projects, study of effects of nuclear radiation on the optical characteristics of laser components should be continued with vigor. The scope should be expanded with consideration for the vital needs as they evolve from SDI projects. Initial support for continuation of this SFRP and GSSSP work will be sought through the 1985-86 minigrant program with further funding to be sought from AFOSR and LANL.

REFERENCES

1. M.A. Ferrel, FJSRL and KSU, private communication.
2. G.W. Scronce, FJSRL and KSU, private communication.
3. K.A. Stroh, FJSRL and KSU, private communication.
4. M.A. Ferrel, Final Report, 1984 USAF-SCEEE GSSSP.
5. H.J. Donnert, Final Report, 1984 USAF-SCEEE SFRP.
6. H.J. Donnert, M.A. Ferrel, and K.D. Zook, "Effects of Neutron Irradiation on the Optical Properties of laser Mirrors," Proceedings of Topical Meeting on High-Power-Laser Optical Components, DARPA, October 1984.
7. P.J. Brannon and R.A. Hamil, SNL, private communication.
8. P.J. Brannon and R.W. Morris, "Nuclear Radiation Induced Absorption in Optical Materials," SNL Report SAND84-2437, 1985.
9. D. Boucher, ed., "Optical Fibers in Adverse Environments," SPIE Report, Volume 404, 1983.
10. L.B. Fogdall, S.S. Cannaday, and T.M. Donovan, "Radiation Stability of Dielectric Coatings for HF Laser Optics," Proceedings of the High Power Lser Optical Components Meeting, 19-20 November 1981, Report AFWAL-TR-84-4152, 1984.
11. R.D. Brown, LANL, private communication.
12. M.A. Ferrel, Final Report, 1985 USAF-UES GSSSP.
13. P.A. Zagarino, EG&G, private communication.
14. G.W. Scronce, Final Report, 1985 USAF-UES GSSSP.
15. K.A. Stroh, Final Report, 1985 USAF-UES GSSSP.

1985 USAF-UES SUMMER FACULTY RESEARCH PROGRAM

Sponsored by the

AIR FORCE OFFICE OF SCIENTIFIC RESEARCH

Conducted by the

UNIVERSAL ENERGY SYSTEMS, INC.

FINAL REPORT

Energetic Materials via Alkoxyfluorinations of Alkenes with Xenon Difluoride

Prepared by: Dr. Melvin Druelinger

Academic Rank: Professor of Chemistry

Department and University: Chemistry Department
University of Southern Colorado

Research Location: Air Force Rocket Propulsion Laboratory
Liquid Rocket Division, Chemistry and Materials Branch
Basic Chemical Research Section, Edwards AFB, CA

USAF Research: Dr. Robert Chapman

Date: September 16, 1985

Contract No: F49620-85-C-0013

Energetic Materials via Alkoxyfluorinations of Alkenes with Xenon Difluoride

by

Dr. Melvin Druelinger

ABSTRACT

Xenon difluoride (XeF_2), is a novel and selective fluorinating agent for organics. The selectivity can be altered by the judicious selection of reaction conditions. Alkoxyfluorinations occur when XeF_2 is added to alkenes in the presence of simple alcohols and acid catalysts. Interest in the synthesis of novel fluorinated energetic materials to serve as binders and plasticizers made this reaction a good candidate for further study.

The system investigated used the energetic alcohol 2-fluoro-2, 2-dinitroethanol and alkenes chosen from a mechanistic viewpoint (norbornene and indene). The desired products incorporate fluorine and the energetically useful fluorodinitroethyl group. Studies included variations in temperature, solvent and catalyst type and concentration. Five isomeric alkoxyfluorination products were formed with norbornene. Less than one equivalent of boron trifluoride etherate favored simple difluoride addition products. Data suggest an ionic pathway. Solvent incorporation interferes with the desired reaction in acetonitrile. Indene is readily polymerized under the reaction conditions except in the presence of simple (nonenergetic) alcohols. It did not undergo the desired reaction. Because of the small scale used and the complex mixtures formed, structure indentification was achieved primarily by gas chromatography and mass spectra.

Several recommendations regarding the continuation of this study are made.

ACKNOWLEDGMENTS

The author would like to thank the Air Force Systems Command, the Air Force Office of Scientific Research and Universal Energy Systems for providing an opportunity to spend a rewarding summer conducting research at the Air Force Rocket Propulsion Laboratory, Edwards Air Force Base, CA.

The author is grateful to Dr. Robert Chapman for suggesting the project. His multifaceted professional and personal support contributed significantly to the success of the project. Dr. Ricardo Silva and Mr. Stuart Dimock, also summer participants, provided helpful technical discussions and contributed greatly in making the summer a pleasant one professionally and personally. The author would like to thank the personnel in the Chemistry and Materials Branch of the Liquid Rocket Division for their hospitality and assistance. Their professional demeanor and the congenial atmosphere they created were greatly appreciated. I would like to additionally single out the support given by 1st Lt. John Andreshak (NMR and GC), Mr. Roy Wurzbach (MS), Mr. W. Robbs (GC Trapping), Mr. J. Nakamura (administrative) and Mr. W. Roe (administrative).

Finally special thanks are due to Mrs. Lucy Aldaz (USC) for typing the manuscript.

I. INTRODUCTION:

An active research program that explores the preparation and properties of energetic materials that either are, or may be, used for solid rocket propellants, explosive fills and related purposes is maintained by the Basic Chemistry Section, Chemistry and Materials Branch of the Liquid Rocket Division, Rocket Propulsion Laboratory at Edwards AFB. One of the more important goals of this program is to design and prepare new classes of energetic materials that either have a greater energy content and/or superior stability (particularly thermal) than those currently in use. Another important goal is to develop energetic materials that could replace nonenergetic binders, plasticizers, oxidizers and crosslinking agents currently used.

The incorporation of energetic binder/plasticizer ingredients into solid propellant and explosive formulations offers an excellent approach for increasing the energy output during combustion and detonation processes, respectively. Currently, nonenergetic materials are in wide use. While the formulated ingredients perform the required functions, they are dead weight when compared to the energy output of the fuel/oxidizer or explosive materials used in solid propellants and munition charges. These nonenergetic components add weight and consume space in propellant/munition cavities, while contributing no significant energy enhancement to performance results.

The substitution of energetic materials that perform these functions (binder/plasticizer) could add significant energy contributions to combustion and detonation processes resulting in higher specific impulse during propellant combustion and more efficient blast effects in explosives detonation. These increased performance characteristics would offer increased range or payload opportunities in strategic missiles, longer standoff ranges in tactical missiles and higher yield detonation processes in munitions applications. Energetic binder/plasticizer development has suffered, however, from a lack of efficient high yield synthesis procedures. Such methods are required to produce materials possessing acceptable energetic thermal and hydrolytic stability properties.

It is well known that the introduction of one or more nitro groups will drastically increase the energy content of a molecule. The addition of a fluoro substituent usually lends a degree of thermal stability and increases the initial density of a molecule. With these concepts in mind, obvious target molecules would contain polyfunctionality involving nitro and/or fluoro groups.

The research reported herein is then part of an ongoing Air Force interest in the synthesis of novel fluorinated energetic materials. These and related investigations may lead to new or novel compounds or improved routes to known structures of interest in this field.

It has been observed previously that the novel fluorinating agent xenon difluoride (XeF_2) can selectively fluorinate organic compounds and that selectivity can be altered and enhanced by the judicious selection of reaction conditions resulting in a change in mechanistic pathway.[1] The solid XeF_2 is also a safe and easily handled fluorination agent.[2] Furthermore, recent results show that alkoxyfluorinations occur when XeF_2 is added to alkenes in the presence of simple alcohols and acid catalysts.[3] In the absence of alcohols, difluorinations result.

$$>C=C< + XeF_2 + ROH \xrightarrow{BF_3\ (HF)} F-\overset{|}{\underset{|}{C}}-\overset{|}{\underset{|}{C}}-OR \qquad (1)$$

This research project was intended to further explore and exploit these findings, specifically as related to the synthesis of energetic materials using XeF_2, an energetic alcohol (2-fluoro-2,2-dinitroethanol) and selected alkenes. The products resulting from the anticipated alkoxyfluorination of the pi bond would have the energetically useful fluorodinitroethyl group incorporated as well as an additional fluorine atom. Such a system would meet the desired structural requirements outlined earlier. The study was designed to probe the reaction from both a mechanistic and synthetic viewpoint.

The author has conducted research with XeF_2[1,4] and has worked with energetic materials including fluoropolynitroalkyl compounds.[5] His training as a physical organic chemist and experience as a synthetic chemist make him well-qualified for an investigation such as this combining mechanistic studies, synthesis and structure elucidation.

II. OBJECTIVES OF THE RESEARCH EFFORT:

This research was designed, as noted above, to explore, extend and exploit the recent findings that alkoxyfluorinations occur when Xenon Difluoride is added to alkenes in the presence of simple alcohols and acid catalysts.[3] Specifically, our interest was to ascertain whether energetic alcohols behave similarly and give rise to energetic alkoxyfluorinated products. This included a study of the scope of the reaction, including reaction conditions such as solvents, temperature, catalyst concentration and type. Ultimately our goal was to elucidate the mechanism of this addition reaction on model compounds so we could utilize it to design and synthesize energetic materials of interest.

The energetic alcohol chosen was 2-fluoro-2,2-dinitroethanol (FDNEOH). The products resulting from the anticipated vicinal alkoxyfluorination of alkenes would have the energetically useful fluorodinitroethyl group incorporated as well as an additional fluorine atom. The two alkenes chosen for study were norbornene and indene.

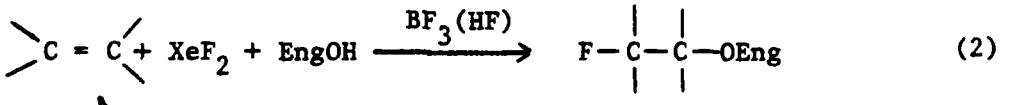

(2)

Alkenes: 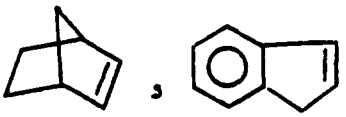 Alcohol: $CF(NO_2)_2CH_2OH$

The questions to be answered in this study are a) does the reaction work in these systems? b) What is the generality of the reaction c) What is the mechanism? d) What are the products? and e) What is their stereochemistry?

III. APPROACH:

As noted above, the focus of this study was on the addition of the energetic alcohol 2-fluoro-2,2-dinitroethanol and Xenon difluoride to the alkenes norbornene and indene in the presence of boron trifluoride (BF_3). The alkene systems were chosen as key substrates to explore from both a mechanistic and synthetic viewpoint. First, the norbornene system is well known to be an excellent mechanistic probe. Product elucidation should provide valuable insight into the pathway-radical or ionic. The stereochemistry of the products in this system provides important mechanistic information. Initial efforts involved the use Lewis acid catalysis (BF_3)

in line with work in simpler systems.[3] The focus was centered on a detailed study of reaction products as a function of reaction conditions (solvent temperature, catalyst concentration) in an effort to better understand and control this type of reaction. The second target substrate, indene, was selected as a representative arylalkene and because extensive work on alkoxyfluorinations has already been done with simple alcohols and indene[3] and this would be logical extension of the series. Techniques used include those standard to organic product isolation, purification and structure elucidation. Specifically, in this study, they included gas chromatography for (analysis and isolation), NMR spectroscopy and mass spectroscopy (for structure determination). Reactions were run on a very small scale due to possible hazards.

IV. THE NORBORNENE SYSTEM: BACKGROUND, RESULTS AND DISCUSSION:

Shortly after its discovery in 1962, xenon difluoride (XeF_2) was found to react with alkenes to give vicinal difluorides.[6] Perhaps the most extensively and carefully studied alkene is norbornene due to its role as mechanistic and stereo-chemical probe. Both Shackelford[7] and Zupan[8] have shown that Lewis acid catalysts and XeF_2 lead to a rich and varied chemistry dependent on temperature and catalyst.

Using hydrogen fluoride as a catalyst and methylene chloride as solvent, Zupan[8a] found seven products, including six isomeric difluoronorbornanes (2,3-, 2,5-, and 2,7-). There was no clear dominance. He later studied several catalyst systems and temperature effects with similar results. Mechanistically, a cationic intermediate was favored. The multiplicity of products and their distribution was explained via Wagner-Meerwein rearrangements. In the case of the 2,3-adducts, a free radical intermediate was proposed.

Shackelford's careful studies[7] with boron trifluoride etherate as catalyst clearly showed a preference for the 2-exo-5-exo(5) and 2-endo-5-exo(4) difluoronorbornane isomers. He also showed that the 2-exo-7-anti isomer (3) rearranges to the 2,5- system and that cationic intermediates explain this selectivity.

Subsequent work by Hildreth[1,4] led to a clear preference for the 2,3-difluoro isomers (2,6) in the photochemically initiated reaction. Novel solvent incorporation was found with acetonitrile. These results were clearly shown to arise from a mechanistic change to radical intermediates.

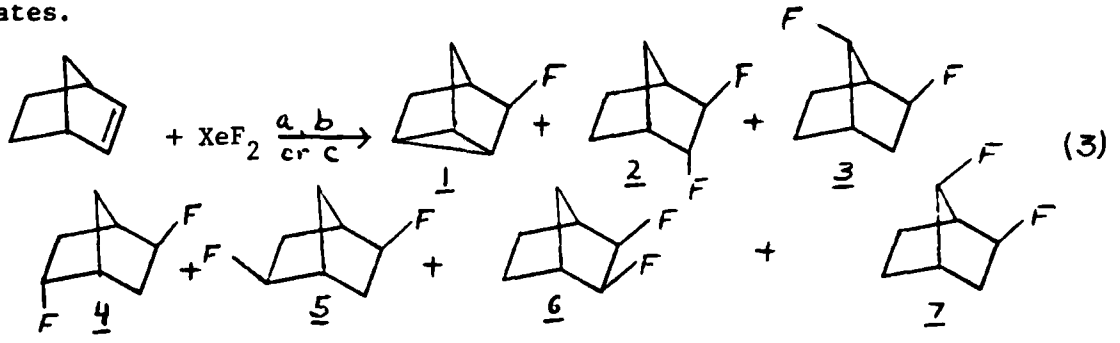

(3)

a. HF b. $BF_3 \cdot Et_2O$ c. hν

In anticipation of the competitive formation of difluoronorbornanes in the alkoxyfluorination reactions, several reactions were run using literature conditions[7,8] in order to prepare authentic difluonorbornanes. It was thought that this would make it unnecessary to isolate thse compounds by the tedious and time-consuming process of gas chromatographic trapping in the alkoxyfluorination reactions. By comparing gas chromatographic retention times and mass spectral fragmentation patterns the identifications could be readily made. The reactions selected were norbornene and xenon difluoride under the following conditions 1) BF_3, 24 hr, -39° 2) no catalyst, 60 min, 25° and 3) HF(g), 60 min, 25°. These conditions have been reported by Shackelford and Zupan. Unfortunately our results did not parallel those reported very well. In the first case, four products were formed as expected, but the percentages differed significantly from those reported by Shackelford, making the identification somewhat tenuous. The 2,5-isomers(4,5) dominate the 2,7-isomers (3,7) with essentially no 2,3-isomers(2,6) or fluoronortricyclane(1) produced. The Zupan conditions also produced four isomers in substantial quantities. The first three are the same as those in the Shackelford reaction. The fourth is different (shorter retention time), perhaps the exo-2,3-isomer(6) as opposed to the exo, syn -2,7-isomer(3). The product distributions in the latter two cases were somewhat similar implying that little or no HF(g) was actually introduced in the last case. Supporting this supposition was the observation that no dark blue coloration was observed.[8] Considerable experimentation was done using

several GC columns and temperature conditions to find optimal separation conditions. The identities of these products are based then on gas chromatographic patterns and retention times and on mass spectral comparisons from literature values and from data in Shackelford's research notebook.

The alkoxyfluorination of norbornene using methanol as a reactant has been demonstrated by Shackelford.[3b] He used both boron trifluoride and hydrogen fluoride (generated in situ) as catalysts. The only difluoronorbornanes produced were the 2,3-(2,6)isomers along with fluoronortricyclane(1). Three 2,3-isomers of methoxyfluorination were produced along with only one 2,7-methyoxyfluoro adduct and no 2,5-adducts. Once again, this work was repeated to produce authentic componds for gas chromatographic and mass spectral comparisons. The latter were studied in an attempt to facilitate the stereo-chemical assignments in the energetic alcohol addition reaction. The results of this study are in basic agreement with those reported earlier.[3b]

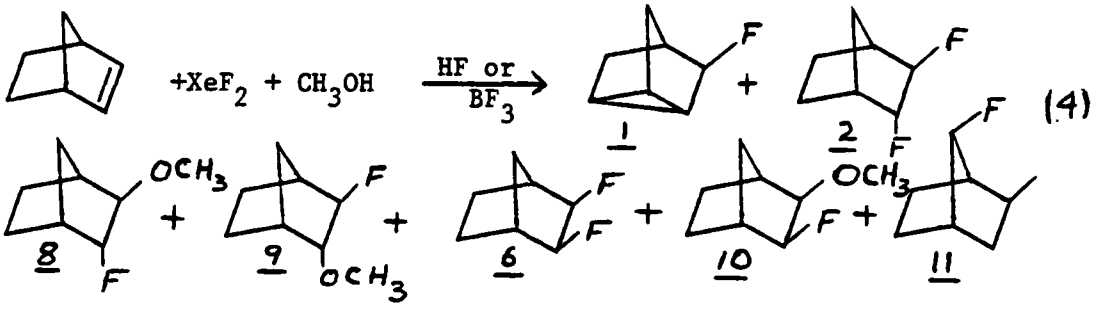

(4)

While the product mixture is complicated, it is much less so than theoretically possible. Over forty different mono- and disubstituted products could be formed. There are a number of unidentified peaks, but they are very minor. Shellhamer and Shackelford[3] have proposed a mechanism to explain the stereo-chemical and orientational effects they observed in their studies. This involves the formation, in methanol, of an unstable reactive species, methoxyxenon fluoride (CH_3O-XeF,12). They speculate that hydrogen fluoride generated *in situ* complexes with this intermediate to form an O-protonated species 13 which leads to addition resulting from an apparent "F^+" electrophile. This suggestion explains the regiospecificity in the HF-catalyzed reaction. In the presence of BF_3, the intermediate 12 is complexed to form 14. Addition to the alkene from this species occurs via an apparent "RO^+" electrophile which explains the regiospecificity in the boron trifluoride catalyzed reaction.

Our attempts to directly observe the intermediate 12 will be discussed later.

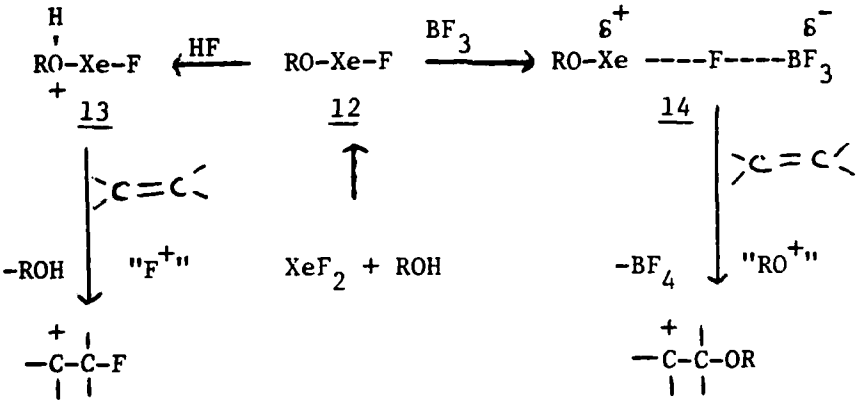

Scheme I

The alkoxyfluorination of norbornene with the energetic alcohol 2-fluoro-2,2-dinitroethanol (FDNEOH) was carried out in three solvents (methylene chloride, acetonitrile and neat FDNEOH) at temperatures ranging from -78°C to 0°C and with 0-1 equivalents of boron trifluoride etherate. The results are summarized in Table I. The desired alkoxyfluorination did occur although to widely varying degrees. The major experiments are briefly discussed below.

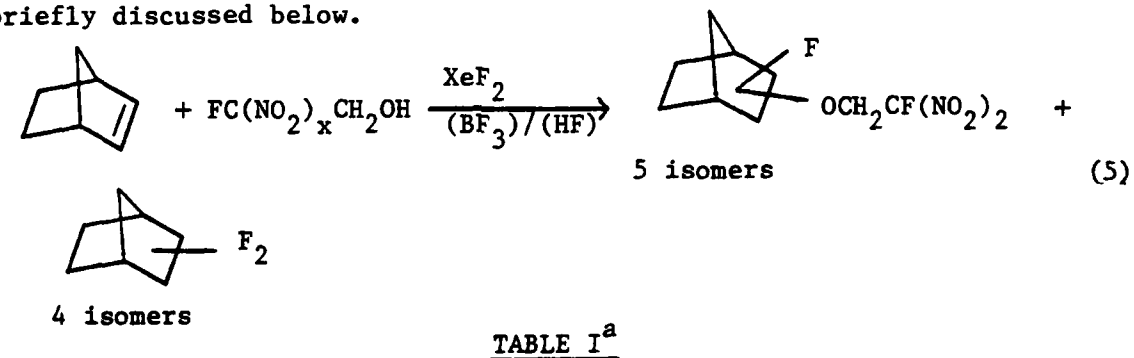

(5)

TABLE I[a]

Product Distribution and Conditions
of Norbornene-FDNEOH Alkoxyfluorination Reaction

RUN	Solvent	T	BF_3(eq)	RO/F	F_2	Comments
1	CH_2Cl_2	- 78,-5	1	82	18	
2	CH_2Cl_2	- 78,-5	0	23	55	b
3	CH_3CN	- 31,RT	1	Small	--	c
4	CH_2Cl_2	- 78,-5	0.2	15	85	
5	FDNEOH	0,RT	0	56	--	d

a. Data taken from capillary GC-MS, uncorrected

b. 18% FDNEOH, 82% products; of the products, 22% is fluoronortricyclane

c. Solvent adduct is almost exclusive product

d. 44% FDNEOH

The difluoronorbornane isomers formed were primarily the 2,5- (5,3) and the 2,7-(7) compounds in that order. The ratio of 2,5- isomers is about 2. Only in run 2 was the fluoronortricyclane significant, which accounts in part for the apparent discrepancy with run 4.

These data suggest that the desired energetic alkoxyfluorinated adducts are favored using one equivalent of $BF_3 \cdot Et_2O$. Lesser amounts favor the difluoro isomers. In the absence of BF_3, HF (in situ generated) takes over and fluoronortricyclane production becomes significant, as noted in earlier work in the absence of alcohols. The reaction in neat fluorodinitroethanol (solvent and reactant, HF generated in situ) gave a relatively low product yield, but it was largely uncontaminated by difluoronorbornanes. The alkoxyfluorinated product distribution was similar to that in the other cases.

Extensive gas chromatographic analyses using a variety of temperature programs and column substrates gave at best three peaks for the alkoxyfluorinated adducts (one at worst). The three peak pattern in order of increasing retention time, had relative values, depending on reaction conditions, in the ranges 2-40%, 50-80%, and 9-11%. The use of capillary GC-MS proved to be the key to this study, especially because of the greater resolving power, the complex reaction mixtures and the small quantities of products dealt with. The middle peak, using capillary GC-MS, was actually composed of three peaks leading to a total of five energetic alkoxyfluorinated adducts. Unfortunately, because the data was gathered very late in the project due to machine availability and because the model compound mass spectral patterns were not sufficiently helpful, neither the stereochemical nor isomeric identities of these energetic alkoxyfluorinated adducts have yet been definitively determined. For similar reasons, the adducts have not been isolated, although an attempt was made. Four of the peaks (one unresolved, double) were trapped, but system failure did not lead to either sufficient purity nor quantity.

Work in this line will contine.

In all cases, the isomeric adducts were identified as isomers by their mass spectral "parent" peaks at 246 (M-20). The most probable identities at this point, subject to further data analysis and interpretation, for the three major peaks in order of retention time are the exo-2-fluoro-endo-5-alkoxy(15), exo-2-alkoxy-exo-5-fluoro(16) and exo-2-alkoxy-syn-7-fluoro(17) isomers. The identities of the other two isomers are even less certain. Based on the methoxyfluorinations,

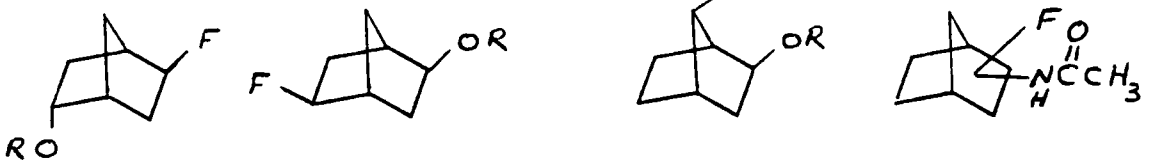

15 16 17 18

the 2,3-isomers must be serious candidates although their formation would seem to be probably from radical intermediates. This is at odds with current data arguing for a cationic mechanism.

Perhaps the most novel finding in this system is that in acetonitrile, an even more complex mixture results and that the major product is a fluoroacetamido(18) product formed by solvent incorporation. The isomeric identity is uncertain. Only a small amount of alkoxyfluorination occurs and virtually no difluoronorbornanes are formed. This type of product was obtained from radical intermediates in a photochemical reaction,[1] but could also result from a cationic intermediate. The latter is favored at this time. The identification is based on mass spectral data which rules out a cyanomethyl adduct. The product results from trapping the fluoronorbonylcation with the solvent at the nitrogen terminus followed by aqueous hydrolysis.

In summary, the energetic alkoxyfluorination has been shown to occur in the norbornene-FDNEOH system. Five isomers are produced. Boron trifluoride promotes their formation in methylene chloride. In neat FDNEOH, in situ HF suffices. Acetonitrile is an unsatisfactory solvent due to solvent incorporation. The data are consistent with a cationic intermediate,(see also the formal summary section at the end of this paper).

V. THE INDENE SYSTEM: BACKGROUND, RESULTS, AND DISCUSSION:

Arylalkenes have been the subject of several XeF_2 studies. In 1977 Zupan studied the fluorination of indene and obtained 70:30 trans-cis mixture of difluoroindanes.[9] More recently Shellhamer and coworkers have used indene as a key substrate in their alkoxyfluorination studies with methanol[9,36] and with other alcohols[11]. Because of its structure type, relative simplicity, potential mechanistic value, accessibility and the work already done in this system, we chose to study indene as our second model compound. This work is intended to be part of a larger investigation on alkoxyfluorinations in collaboration with Professor D. Shellhamer, Point Loma College.

Initial efforts followed the literature procedures of Zupan[9] to produce authentic reference compounds for the difluoroadducts. We obtained these products in a 70:30 mixture of the trans: cis isomers, 1,2-difluoroindanes. These were clearly the major isomers and this was in excellent agreement with those of Zupan. Having authentic samples in hand greatly aided the identification process in later reactions. As with all compounds studied, extensive gas chromatographic work was done to establish optimal analytical conditions.

Shellhamer's fluoroalkoxylation with indene and methanol was repeated.[10,3b] The HF catalyzed reaction (<u>in situ</u> generated) was more reproducible than the BF_3catalyzed reaction. These reactions confirmed that the difluorination is competitive with the methoxyfluorination, but the latter predominates. The products are valuable models for stereochemical assignments based on their mass spectral patterns since the structures have been determined.

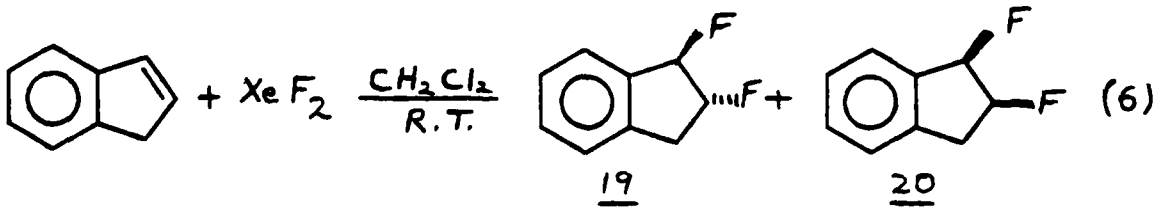

19 20 (6)

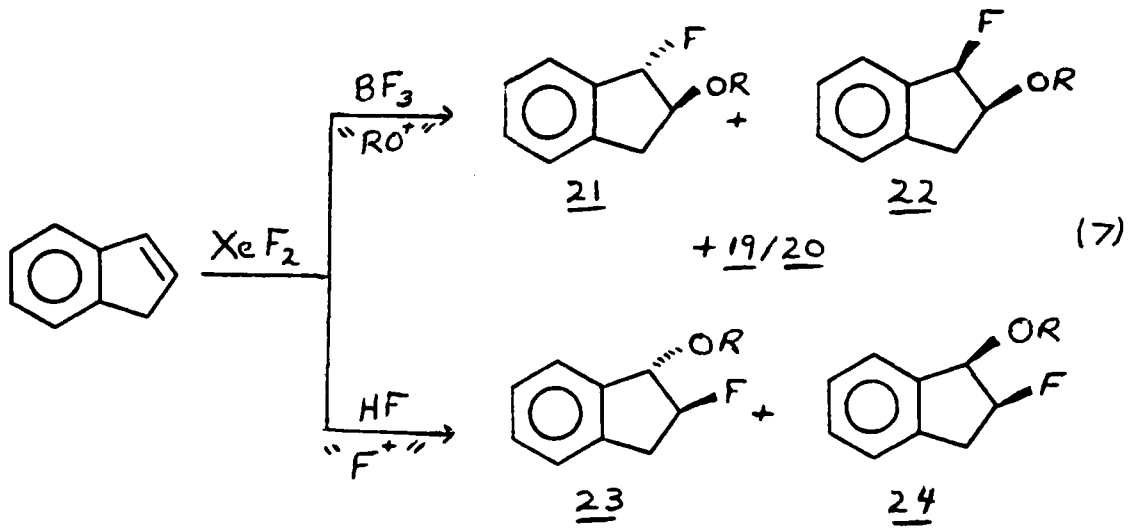

(7)

Armed with these successes, attention was turned to the energetic fluoroalkoxlation with FDNEOH. Shellhamer used the methanol as both solvent and reactant. This is impractical with the energetic alcohols because of their expense. We elected then to use methylene chloride and room temperature (Zupan conditions). Reactions were run both in the presence of boron trifluoride and in its absence (HF generated in situ) with an equivalent of the energetic alcohol (FDNEOH). The reactions were interesting in that colors (blue and red respectively) were generated when the reactants were mixed. This suggests a charge transfer, pi-complex or radical ion type intermediate. Gas chromatographic analysis revealed, in both cases, the complete loss of indene but no product formation, not even the difluoroindanes (capillary GC-MS later revealed traces of these compounds). There were no long retention time peaks well beyond the times expected for adducts based on work in the norbornene system. There was no evidence of the desired alkoxyfluorination adducts in methylene chloride.

These surprising and disappointing results are explained based on a series of NMR studies in acetonitrile, methylene chloride and methanol. In the initial experiment, the purity of XeF_2 was examined by xenon-129 NMR in acetonitrile. The alcohol was added with no change. The addition of indene to the NMR tube afforded an immediate white precipitate; no BF_3 had been added. This suggested polymerization to polyindene. It was then confirmed using carbon-13, fluorine-19 and proton NMR that indene is rapidly polymerized by either XeF_2 or BF_3 alone in either methylene

chloride or acetonitrile. Using capillary GC-MS, very small quantities of indene and the 1,2-difluoroindanes were detected showing that while the polymerization is rapid and rather complete, it is not total. There was no indication however by NMR or GC of any energetic alkoxyfluorinated products. The FDNEOH itself did not polymerize indene.

The original experiments with XeF_2 and indene in methylene chloride were repeated in the NMR spectrometer. Polymerization was readily observed and the polymer is soluble. This explains the low product yields and why the reaction wasn't observed earlier. Studies repeating literature experiments confirmed that published reports were not aware of this major problem.

Another very revealing set of experiments in deuterated methanol showed that polymerization does not occur in that solvent with either XeF_2 or BF_3. This is in sharp contrast to the results in acetonitrile and methylene chloride. Remarkably then, methanol prevents polymerization. This suggests that the neat energetic alcohol may give the desired alkoxyfluorination adducts. Unfortunately, time did not permit evaluation of this possibility.

As a final note on the indene system, a novel result (solvent incorporation) was detected by capillary GC-MS in the acetonitrile solvent reaction. Three long retention time peaks were identified as solvent adducts, 1,2-fluoroacetamide products. This was verified using deuterated solvent. The "parent" peak was 176 (196-HF) for each one along with an m/e peak at 46 (CD_3CO^+). The position location and stereochemistry are unknown at this time, and they are minor products compared to the polymer. As with norbornene then, acetonitrile is an unsuitable solvent.

We presently favor cationic intermediates in these reactions based on the solvent incorporation, the apparent isomeric orientation and the fact that the reaction proceeds in the dark.

In a final series of experiments, an attempt was made to detect the proposed reactive alkoxyxenon fluoride intermediate FDNEO-Xe-F. Xenon difluoride and fluorodinitroethanol were mixed at -30° in deuterated methylene chloride. The NMR spectrum of the following nuclei were examined at 10° intervals to $25^\circ C$, xenon-129, fluorine-19, carbon-13 and

proton. Unfortunately, no spectrum attributable to any reactive intermediate was detected.

VI. SUMMARY:

Energetic alkoxyfluorinated adducts are produced by the addition of xenon difluoride and 2-fluoro-2,2-dinitroethanol to norbornene. One equivalent facilitates the reaction relative to simple difluorination of the pi bond. The reaction occurs in a solvent or with the neat alcohol. Acetonitrile is an unsuitable solvent because of solvent incorporation leading to fluoroacetamido adducts. Isomeric and stereochemical assignments are not yet firm due to instrumentation problems and difficulties in isolating pure materials. The latter is due to the small scale reactions and the resulting complex mixtures. A cationic mechanism is favored.

Similar adducts were not obtained with indene because this material readily polymerizes under most conditions examined. Solvent adducts were obtained in acetonitrile. Methanol prevents or inhibits this polymerization suggesting neat alcohol as reactant and solvent may lead to the desired products. An ionic pathway is also favored in this case.

Attempts to detect an alkoxyxenon fluoride intermediate by low temperature NMR failed.

VII. RECOMMENDATIONS:

These results show that the desired reaction does occur with norbornene and points the way for suitable conditions for it to occur with indene. They strongly support the need for additional research in this area and demonstrate its potential. Time constraints and instrumentation difficulties coupled with small scale reaction and complex mixtures combined to prevent the realization of a number of project goals. Therefore the primary recommendation is that this study be continued.

The most important specific recommendation is that the products be isolated so that the structure determination and stereochemistry can be determined by NMR and MS. This can be facilitated by operating on a larger scale, especially since reaction parameters have been determined for the norbornene reaction. Isolation may then be accomplished by gas chromatography, flash chromatography, medium pressure chromatography

and/or preparative thick layer chromatography.

Specific reactions to be run include the use of the neat energetic alcohol with and without boron trifluoride in both the norbornene and indene systems - especially the latter.

To extend the knowledge gained in this work to other materials of interest, other energetic alcohols should be investigated including 2,2-dinitropropanol and trinitroethanol. The alcohols should be added to energetic alkenes such as fluorodinitroethyl vinyl ether. The products would be of considerable interest as potential energetic plasticizers.

As our work indicates, solvents play an important role. In addition to using neat alcohol, other solvents of interest would be ether, THF and SO_2. More work with temperature effects would also be useful.

The key role of the catalyst should be investigated further, varying both the catalyst concentration and type. In particular the use of Nafion-H could be especially interesting. Other catalysts of interest include trifluoroacetic acid, HF-pyridine and other Lewis Acid catalysts.

The mechanistic details need to be better understood. In addition to structure indentification, the use of photochemical initiation (favoring radicals) and radical traps (such as nitroso compounds, nitrones and 1,3-dinitrobenzene) are highly suggested.

Finally, this reaction sequence involving energetic alkoxyfluorinations should be extended to other pi-bonded systems including imines (C=N), acetylenes (C≡C) and conjugated dienes (C=C-C=C).

In collaboration with Professor D. Shellhamer and co-workers at Point Loma College and Dr. Robert Chapman and Major Scott Shackelford of the Rocket Propulsion Laboratory at Edwards Air Force Base, this work will be published as part of a study of alkoxyfluorinations of alkenes using a variety of alcohols of varying electronegativity.

These proposals for further investigation will be developed and expanded in a Mini-Grant proposal to follow this report.

REFERENCES

1. R. A. Hildreth, M. L. Druelinger and S. A. Shackelford, "Xenon Difluoride Fluorination. IV. Photochemically Initiated Xenon Difluoride Fluorination of Norbornene," Tetrahedron Letters, 1982, 23, 1059 and earlier papers in this series.

2. S. A. Shackelford, R. R. McGuire and J. L. Pflug, "Xenon Difluoride fluorination. I. Aliphatic Alkenes Fluorinated by a Convenient Benchtop Procedure", Tetrahedron Letters, 1977, 363.

3. a. D. F. Shellhamer, et al., "Evidence for the Existence of Methyl Hypofluorite: Methanolysis of Xenon Difluoride," Tetrahedron Letters, 1982, 23, 2157.
   b. D. F. Shellhamer, et al., "The Regioselective Chemistry of Methoxyxenon Fluoride", Journal of Organic Chemistry, 1985, accepted for publication.

4. R.A. Hildreth, M.L. Druelinger, L.P. Davis and N.M. Ely, "Mechanism and Stereochemistry of Photochemically Initiated Reaction of Xenon Difluoride with Norbornene," 180th National Meeting of the American Chemical Society, Las Vegas, 24-29 August, 1980.

5. a. R.A. Hildreth, R.L. Wallace, M.L. Druelinger and B.A. Loving, "New Energetic Plasticizers: Synthesis, Characterization and Potential Applications," Proceedings of the 1978 Joint Air Force Systems Command - Naval Materials Command Science and Engineering Symposium, 1978, Vol. IV (Basic Research), Air Force Office of Scientific Research, 968-978.
   b. M. Druelinger, "Synthesis and Characterization of Novel Polynitroaliphatic Materials," 1977 USAF-ASEE Summer Faculty Research Program Research Reports, Vol I, 1977, Technical report 78-0348 (report No. 16), Government Acession No. ADA051624 (14 pages).

6. T-C Shieh, N.C. Yang and C.L. Chernick, J. Am. Chem. Soc., 1964, 86, 5022.

7. a. S.A. Shackelford, "Xenon Difluoride Fluorination. II. Selective Synthesis of the Novel 2-exo-5-endo and 2-exo-5-exo- difluoronorbornane Isomers," Tetrahedron Letters, 1977, 4265.
   b. S.A. Shackelford, "Xenon Difluoride Fluorination. 3. Mechanism and Selectivity of Boron Trifluoride Etherate Catalysis in the Norbornene Model," J. Org. Chem., 1979, 44, 3485.

8. a. M. Zupan, A. Gregorcic and A. Pollak, "Fluorination of Bicyclic Olefins," J. Org. Chem., 1977, 42, 1562.
   b. A. Gregorcic and M. Zupan, "Fluorination with Xenon Difluoride. XXII. The Role of Catalyst and Temperature on the Fluorination

of Norbornene and Norbornadiene," Bulletin of the Chemical Society of Japan, 1980, 53, 1085.

9. M. Zupan and A. Pollak,"Fluorination with Xenon Difluoride. Stereochemistry of Fluorine Addition to Phenyl Substituted Olefins," J. Org. Chem., 1977, 42, 1559.

10. D.F. Shellhamer, et al., "Evidence for the Existence of Methyl Hypofluorite: Methanolysis of Xenon Difluoride," Tetrahedron Letters, 1982, 23, 2157.

11. D.F. Shellhamer, et al., unpublished work.

1985 USAF-UES SUMMER FACULTY RESEARCH PROGRAM

Sponsored by the

AIR FORCE OFFICE OF SCIENTIFIC RESEARCH

Conducted by

UNIVERSAL ENERGY SYSTEMS, INC.

FINAL REPORT

METAL ALKOXIDE SYNTHESIS OF HIGH TEMPERATURE MATRICES

Prepared By: Dr. Charles H. Drummond III

Academic Rank: Associate Professor

Department and University: Department of Ceramic Engineering, The Ohio State University

Research Location: AFWAL/MLLM, Wright-Patterson AFB, OH

USAF Research: K. S. Mazdiyasni

Date: September 20, 1985

Contract No: F49620-85-C-0013

METAL ALKOXIDE SYNTHESIS OF HIGH TEMPERATURE MATRICES

by

Charles H. Drummond III

ABSTRACT

A number of investigations involving metal alkoxide derived high temperature matrix compositions were conducted. Metal alkoxide syntheses of hafnium, zirconium, niobium, and yttrium were completed. A study of particle morphology and properties of acid, neutral and base hydrolysized alkoxides was initiated. High temperature compositions in the Nb_2O_5-ZrO_2 system were studied. Crystallization studies of zirconia and cordierite nucleated amorphous cordierite powders were initiated. An investigation of ZrO_2 toughening amorphous silica was also begun.

ACKNOWLEDGEMENTS

The author would like to acknowledge the support of the Air Force Systems Command, the Air Force Office of Scientific Research, and Universal Energy Systems, Inc. which made possible the research conducted at the Air Force Wright Aeronautical Laboratory (AFWAL). The collaboration and guidance of Mr. K. S. Mazdiyasni were extremely helpful and beneficial. The assistance of personnel in the Materials Processing Group made for a rewarding and enjoyable summer. Thanks also to Lou Henrich for preparation of this paper.

I. INTRODUCTION:

During the 1984 summer I participated in this same program in the Materials Processing and High Temperature Branch Laboratory of the Air Force Wright Aeronautical Laboratories. I conducted work on SiC reinforced glass-ceramic composites. This work resulted in a paper and presentation with K. S. Mazdiyasni at the 9th Annual Conference on Composites in January 1985 at Cocoa Beach, FL. A follow-on research grant also continued the work at Ohio State and has supported a graduate student who will be finishing a Master's thesis this December and also making a presentation at the 10th Annual Conference on Composites in 1986. Thus, there is a strong interest in the area of composite synthesis. A desire to continue and broaden the investigations in this area of research was the motivation to work this summer at Wright-Patterson AFB. As an Associate Professor of Ceramic Engineering at The Ohio State University, with interest in glass and glass-ceramics, I have a background which complements the interest in developing high temperature composites which continues at the Materials Laboratory at Wright-Patterson AFB.

II. RESEARCH OBJECTIVES:

The following research objectives were outlined in the pre-summer proposal:

1) Synthesis and fabrication of moderately high temperature (1200-1500°C) matrix compositions and composites.
2) Synthesis of high temperature (1600-2000°C) matrix compositions.
3) Familiarization with metal alkoxide synthesis.

The initial objectives were further defined in the course of the summer's work to include:

4) Crystallization studies.

5) Matrix toughening with a second phase, such as zirconia.

III. RESULTS

The work completed or in progress for each of the objectives is described below.

1) Synthesis and Fabrication of Moderately High Temperature Matrix Compositions and Composites

A graduate student at The Ohio State University is in the process of completing a Master's thesis in this area. Work last summer, 1984, is summarized in a report (1), "SiC Reinforced Glass-Ceramic Composites," and was subsequently presented (2) with K. S. Mazdiyasni ("SiC/Zirconia-Cordierite Glass-Ceramic Composites") at the 9th Annual Conference on Composites at Cocoa Beach, FL in January, 1985. In this work, low expansion, alkali-free, zirconia-nucleated, and high zirconia cordierite glass-ceramic composites reinforced with NICALON$^{(R)}$ SiC fibers were prepared. The matrix was synthesized from metal alkoxides and vacuum hot-pressed to theoretical density. The composites were vacuum hot-pressed with approximately 40-50 vol.% fiber content. Partially stabilized zirconia was found to be present in both the zirconia-nucleated and high zirconia compositions. The latter also had a significant amount of zirconia in addition to the high cordierite phase.

Phase identification by x-ray of the matrix and composite compositions as well as DTA and TGA studies were conducted.

The graduate student work supported by a Research Initiation Program award from the USAF is continuing the study by examining zirconia-cordierite compositions with 15 and 30 mol.% zirconia. Matrix and composite samples have been prepared. Characterization of these samples by x-ray, DTA, TGA, chemical analysis, and microscopy, in addition to strength measurements is being completed. With these results and those of last summer a range of zirconia concentrations from 2 - 30 mol.% zirconia will have been investigated. A number of important issues are being addressed. The role of partially stabilized zirconia in these materials and the possible enhancement by transformation toughening and its effect on the mechanical properties of glass and glass-ceramics, in general, are being studied. Also the conditions for the formation of zircon and its effect on the matrix are being examined. These results will be from the basis of the student's Master's thesis to be completed in December, 1985 and reported at the 10th Annual Conference on Composites in January, 1986.

2) Synthesis of High Temperature Matrix Composition

Originally it was intended to synthesize a number of compositions of high temperature oxides of aluminum, hafnium, zirconium, yttrium, and niobium and various combinations of these oxides. This would have been a large undertaking. A limited number of compositions were synthesized during this summer's work.

The metal alkoxide synthesis of the individual alkoxides will be summarized in the next section. I wish here to briefly describe the fabrication of the matrix compositions and the compositions prepared. One of the advantages of the metal alkoxide synthesis is that homogeneous compositions of two or more oxides can easily be prepared by the mutual solution of the individual metal alkoxides in varying amounts followed by hydrolysis, drying, and calcination to form fine-grained amorphous oxide powders. These powders can then be vacuum hot-pressed to form a dense, pore-free matrix or the powder may be used for isothermal time-temperature studies.

Measured amounts of the individual metal alkoxides to give the desired composition are refluxed to form a homogeneous solution. The solution is then slowly added to a neutral, acidic or basic aqueous solution to form a sol. This is followed by neutralization with the addition of NH_4OH to a pH of 8.5 to form a viscous hydroxide slurry. Rotovapping and drying converts this to a somewhat agglomerated powder which is then ground and calcined at 500°C to form a fine-grained, oxide powder of the desired composition.

The following nominal compositions were synthesized: $Nb_2O_5 \cdot ZrO_2$ and $8Nb_2O_5 \cdot ZrO_2$. The ZrO_2-Nb_2O_5 phase diagrams are shown in Figure 1. A eutectic at 1435°C is the lowest liquid formation temperature with Nb_2O_5 melting at 1500°C and zirconia at close to 2800°C. This is a high temperature system, and there have been no reported studies of compositions synthesized from metal alkoxides.

One sample was hot-pressed to a temperature greater than 1435°C and was extruded from the die. Another sample was hot-pressed to 1300°C and a portion of this sample was subsequently heat-treated at 1000°C in air for 30 minutes. Both samples were x-rayed. βNb_2O_5 and $Zr_8Nb_2O_{21}$ were identified, which would be expected from the phase diagrams. The as-hot-pressed sample was black due to reduction of ZrO_2 to ZrO_{2-x}. This is attributed to the high rate of diffusion of oxygen in these materials. Subsequent heat treatment resulted in oxidation and changing the color to white. Because of this high oxygen mobility in these materials it is generally believed than that any material which exhibits this behavior is unsuitable for the presently commercially available NICALON(R) SiC reinforced composites. The oxidation of the NICALON(R) SiC fibers results in a deterioration in strength of the fibers. This process may be unavoidable in materials with high oxygen diffusion rates.

The multiplicity of phases at the ZrO_2 rich end of the phase diagram and the attainment of a higher temperature matrix (> 1640°C) suggested it would be desirable to synthesize an $8Nb_2O_5 \cdot ZrO_2$ composition. A very dense sample was hot-pressed. The sample was black and was cut for four-point strength measurement and heat treatment. The heat treatment was at 1000°C packed in Zyttrite(R) powder to slow down the oxygen diffusion. The heat treated sample was white but when polished exhibited cracks and was not suitable for strength measurement. Most likely stresses generated during heat-treatment caused the cracking. Both samples x-rayed as $ZrO_2 \cdot nNb_2O_5$, the same pattern as hydroxide derived material. The as-hot-pressed sample had a strength of 15.6 ksi, not a remarkable value.

More work in this system is desirable since it is a high temperature material. These compositions may have interesting electrical properties, and composites should be fabricated to determine if indeed the SiC fibers are degraded at the aforementioned processing conditions to achieve a theoretically dense matrix.

3) Familiarization with Metal Alkoxide Synthesis

Metal alkoxides of Zr, Nb, Hf, and Y were prepared. The Zr, Hf, and Nb were synthesized from the chlorides as follows:

$$ZrCl_4 + 4C_3H_7OH + 4NH_3 \xrightarrow[5°C]{C_6H_{14}} Zr(OC_3H_7)_4 + 4NH_4Cl \quad (1)$$

$$NbCl_5 + 5C_3H_7OH + 5NH_3 \xrightarrow[5°C]{C_6H_{14}} Nb(OC_3H_7)_5 + 5NH_4Cl \quad (2)$$

$$HfCl_4 + 4C_3H_7OH + 4NH_3 \xrightarrow[5°C]{C_6H_{14}} Hf(OC_3H_7)_4 + 4NH_4Cl \quad (3)$$

The metal chloride is added to dry isopropyl alcohol and dry hexane as a solvent. The flask is chilled to 5°C in an ice bath. Anhydrous NH_3 is bubbled until the reaction is completed. The NH_4Cl is filtered. The solvated alkoxide is stored for further study. The oxide concentration maybe determined by thermogravimetric analysis.

The yttrium isopropoxide was synthesized from the metal shavings as follows:

$$Y + 3C_3H_7OH \xrightarrow[HgCl_2]{82°} Y(OC_3H_7)_3 + \frac{3}{2}H_2 + Hg + HCl \quad (4)$$

The metal is added to dry isopropyl with $HgCl_2$ as a catalyst. The material is refluxed and the composition determined as previously described.

At least six syntheses were completed and the necessary experience in metal alkoxide synthesis was obtained in the course of this summer's work.

4) Crystallization Studies

Two studies are in progress. As a result of last summer's work regarding the crystallization of cordierite-zirconia matrices in which x-ray identification of hot-pressed and isothermal studies gave different results, and in an attempt to lower the crystallization temperature, the following experiment was devised. Metal alkoxide derived pure cordierite ($2MgO \cdot 2Al_2O_3 \cdot 5SiO_2$) and cordierite with 2% zirconia amorphous oxides powders were prepared.

The experiment is still in progress. The minimum temperature for the crysatllization of high cordierite will be determined in each case. Then amorphous oxide powders with 3-5% crystallized cordierite will be hot-pressed to see if a lowering of the crystallization temperature can be obtained.

The second study involves the study of the characteristics of alkoxide derived oxides of Zr, Hf, Nb, and Y from acid, neutral, and base hydrolysis. The degree of fluctuation of the gel and particle

size, surface area, and microstructure of the oxide powders will be investigated. No such study has been reported on these materials and characterization of powders obtained by different hydrolysis conditions may lead to controlled and improved microstructure of oxides of these materials.

5) Matrix Toughening with a Second Phase

One of the possible desirable effects of adding ZrO_2 to cordierite compositions in addition to serving as a nucleating agent is the possibility that tetragonal zirconia particles may form. When these particles transform to the monoclinic phase with the application of a stress, additional strength and toughening is observed. A simple system in which to investigate this effect is amorphous SiO_2 with zirconia. A 95% SiO_2-5 mol.% ZrO_2 amorphous powder was prepared by refluxing zirconium isopropoxide with tetraethoxysilane, and hydrolyzing, neutralizing, drying, and grinding. A sample hot pressed at 600°C for 15 min. was completely amorphous with minimal densification. A sample hot-pressed at 1000°C gave amorphous SiO_2 and predominately metastable tetragonal zirconia. This study is still in progress.

IV. RECOMMENDATIONS

A large number of high temperature matrix materials are possible incorporating Hf, Y, Zr, and/or Nb and needs to be investigated. The advantages of alkoxide derived oxides of these materials include high purity, fine-grain, and homogeneous powders. In the synthesis of high temperature materials, these powders can be fabricated at much lower

temperatures from several hundred to perhaps even 1000°C lower. These particular materials have extremely high melting temperatures and are very promising as high temperature matrices for fiber reinforced ceramic composites.

A study to see if these materials can be used as the matrix for SiC or other fibers, whiskers or powders to form a high temperature composite would hold great promise. In particular, the question of high oxygen diffusion and its possible effects would seem to be critical and should be addressed.

Another area which warrants further study is the control of particle morphology by alteration of the processing steps including hydrolysis and calcining. Careful control of the process to produce fine-grained uniform homogeneous powders can result in improved materials.

The nucleation studies, if a significant reduction in crystallization temperature can be obtained, would lead to a whole host of possible investigations.

Finally, the possibility of increased fracture toughness in glasses and glass-ceramics by the introduction of small particles of tetragonal zirconia is currently an active area of research. The advantages of metal alkoxides need to be explored as a way for forming these materials.

These topics will be further explained in a proposal for a research initiative grant which will follow shortly.

REFERENCES

1. Drummond, III, C. H., "SiC Reinforced Glass-Ceramic Composites," USAF-SCEEE Summer Faculty Research Report, September 1984.

2. Drummond, III, C. H. and Mazdiyasni, K. S., "SiC Zirconia-Cordierite Glass-Ceramic Composites," 9th Annual Conference on Composites Proceedings, Cocoa Beach, FL, January 25, 1985, in press.

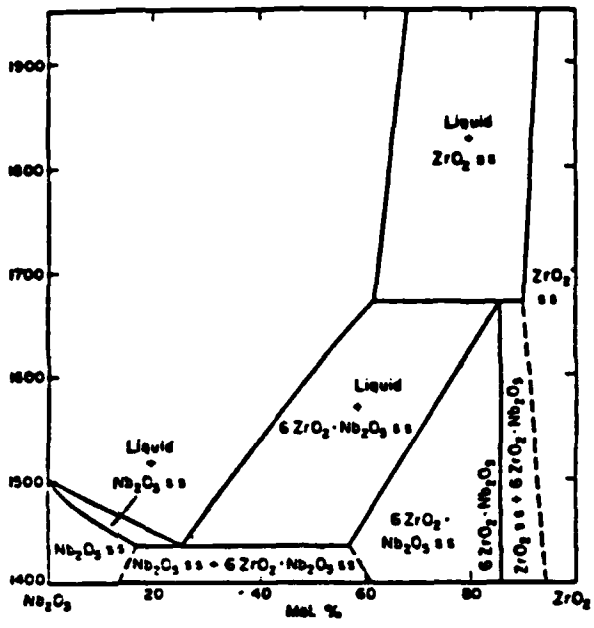

FIG. 373.—System ZrO_2–Nb_2O_5. ss = solid solution.

R. S. Roth and L. W. Coughanour, *J. Research, Natl. Bur. Standards*, 55 [4] 212 (1955); RP2621.

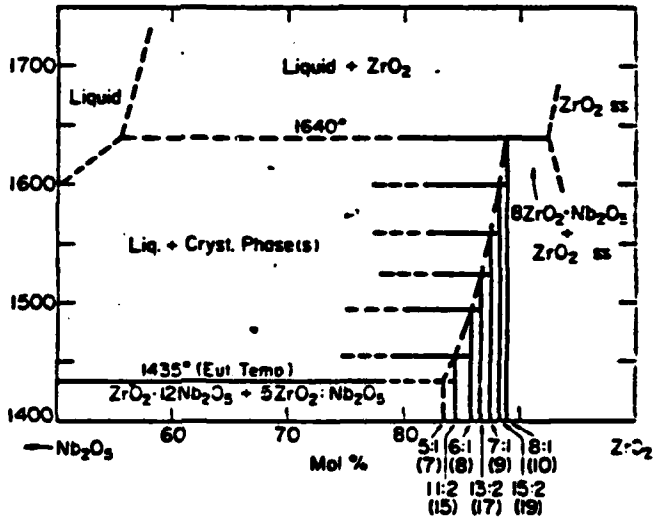

FIG. 4457.—System Nb_2O_5–ZrO_2, proposed ZrO_2-rich portion as modified by the compilers to conform with "Note Added in Proof." Numbers with colons indicate mole ratios of ZrO_2 to Nb_2O_5 of the proposed phases; numbers in parentheses indicate the multiplicity of the *b* axis of the proposed phases.

R. S. Roth, J. L. Waring, W. S. Brower, and H. S. Parker, *Nat. Bur. Stand. (U.S.), Spec. Publ.*, 1972, No. 364.

Figure 1. Nb_2O_5-ZrO_{12} Phase Diagrams.

1985 USAF-UES SUMMER FACULTY RESEARCH PROGRAM/

GRADUATE STUDENT SUMMER SUPPORT PROGRAM

Sponsored by the

AIR FORCE OFFICE OF SCIENTIFIC RESEARCH

Conducted by the

UNIVERSAL ENERGY SYSTEMS, INC.

FINAL REPORT

Computer Modeling of GaAs and AlAs-GaAs Solar Cells

Prepared by:	Dr. Leroy E. Eimers
Academic Rank:	Associate Professor of Physics and Mathematics
Department and University:	Department of Science and Mathematics Cedarville College
Research Location:	Air Force Wright Aeronautical Laboratories/ Aero Propulsion Laboratory/ Energy Conversion Branch/ Solar Energy Conversion
USAF Research	W. Patrick Rahilly
Date:	1 September 1985
Contract No:	F49620-85-C-0013

Computer Modeling of GaAs and AlAs-GaAs Solar Cells

by

Dr. Leroy E. Eimers

ABSTRACT

A computer simulation of the graded-bandgap $Al_xGa_{1-x}As$ solar cell is developed based on a modified finite element numerical method proposed by Gummel and modified by Lamorte. The method consists of dividing the solar cell into finite sections within which those constants which would vary due to the changing composition of the material are considered fixed. The transport equations can then be solved within each section and the solutions matched at the boundary by the appropriate boundary conditions. The model employs relationships for the electrical constants of an AlAs-GaAs alloy given by a number of sources in the literature. The resulting simulation, written in BASIC, runs on IBM-compatible microcomputers.

ACKNOWLEDGMENTS

The author would like to express his appreciation to the Air Force Systems Command, Air Force Office of Scientific Research for its sponsorship of the Summer Faculty Research Program, which made this work possible. Also appreciated is the hospitality and atmosphere of the Air Force Wright Aeronautical Laboratories, Aeropropulsion Laboratory, and in particular Joseph Wise and the Solar Energy Conversion Group of the Aero Space Power Division. It was especially gratifying to work with W. Patrick Rahilly, who was more than generous with his time, suggestions and encouragement in working out problems encountered in the research. The author would also like to acknowledge several helpful telephone conversations with Michael Lamorte and the assistance of Lt. Robert Morris.

I. INTRODUCTION:

The author is a theoretical physicist, having received his B.S. degree with a major in mathematics and a major in physics from Hobart College in Geneva, N. Y., and his M.S. and Ph.D. degrees in theoretical physics from Syracuse University. For two years he was an assistant editor of the Physical Review. Since that time he has been teaching physics and mathematics on the undergraduate level. During this period he has developed an interest and proficiency in the use of microcomputers and have taught courses in programming and computer science.

It was therefore natural that he would be interested in the project that was proposed for his summer faculty research program of developing a computer model of a graded bandgap semiconductor, since this crossed the boundaries of several of his interests, including use of the computer and of differential equations, which he teaches regularly, and of solid state physics of solar cells.

II. OBJECTIVES OF THE RESEARCH EFFORT:

The initial objectives of the project included the following: To study several methods of computer modeling of solar cells as they have been implemented by various investigators. To compare these methods with the method utilized by Lamorte [1,2] for modeling silicon-based solar cells. If the compari-

son should so indicate, to implement Lamorte's method for the case of aluminum arsenide gallium arsenide alloy solar cells. Finally, if sufficient time were available, to utilize the model for the study of the resistance of graded-bandgap solar cells to degradation by radiation damage. During the course of the investigation it was found that this final goal was too ambitious for the ten-week period of time available. (One additional subgoal that was added in the course of the study was the writing of a utility program that became necessary as the size of the modeling program grew, a program to list the variables used in a program written in Zenith's ZBASIC and to catalog all occurences by line number.)

III. BACKGROUND:

The theoretical modeling of carrier transport in an aluminum arsenide-gallium arsenide multiple bandgap and graded bandgap solar cell is a subject that has received much attention in recent research. Concomitant with this there has been much effort devoted to the develpment of computer modeling of solar cells, both silicon-based and III-V based. Unfortunately, most of the methods (see for example, Southerland and Hauser, pp. 43ff.) involve long and complicated iterative procedures that require extensive computer time as well as considerable core memory. For these reasons, they are not suitable for a small "personal computer" such as the Zenith 100. One method

that does not involve these disadvantages to as great an extent as many others is the method first suggested by Gummel [3] and further developed in a series of reports by M. F. Lamorte [see for example, 1, 2]. These reports present a method for quasi-linearization of the transport equations that appeared to offer the possibility of implementation on the Zenith-100 microcomputer.

The method employs a one-dimensional model (although it has also been adapted to two-dimensional situations). This method employs a closed-form solution that is applied to every meshpoint. We start with the transport equations in the form given by Van Roosbroeck (see for example, [2], p. 3; or [4], p. 73)

$$
\begin{aligned}
\vec{J}_n &= n q \mu \vec{E} + q D_n \vec{\nabla} n \\
\vec{J}_p &= p q \mu \vec{E} - q D_n \vec{\nabla} p \\
\frac{\partial n}{\partial t} - \frac{\vec{\nabla} \cdot \vec{J}_n}{q} &= G_n - U_n \\
\frac{\partial p}{\partial t} + \frac{\vec{\nabla} \cdot \vec{J}_p}{q} &= G_p - U_p \\
\vec{\nabla} \cdot \vec{E} &= \frac{q}{\epsilon} (p - n + N_D - N_A)
\end{aligned}
\qquad (1)
$$

These equations constitute a system of coupled partial differential equations that describe the carrier densities, current densities and electric field in a semiconductor as functions of time and position. For solar cels, the steady state condition is assumed, causing the partial time derivatives of p and n to vanish. We assume further that the semi-

conductor is divided into small slabs and that within any slab the dependent variables experience only small changes in value from point to point of the mesh. The transport equations may then be combined, employing the additional assumption that the internal electric field has negligible gradient, to give us the electron continuity equation in the p-type region:

$$\int_0^{\lambda_c} \alpha N_0 \exp\left(-\int_0^x \alpha\, dx'\right) d\lambda + D_n \frac{d^2 n_p}{dx^2} + \mu_n E_p \frac{dn_p}{dx} - \frac{n_p - n_{p0}}{\tau_n} = 0 \qquad (2)$$

This equation is a second order linear differential equation and can be solved, in principle, to give us solutions (in the jth slab) of the form

$$n_{pj} = B_{1j} e^{\omega_{1j} x} + B_{2j} e^{\omega_{2j} x} + B_{3j}(x) \qquad (3)$$

where B_{1j} and B_{2j} are constants of integration, and

$$\omega_{(1,2)j} = -\frac{\mu_{nj} E_{pj}}{2 D_{nj}} \pm \sqrt{\left(\frac{\mu_{nj} E_{pj}}{2 D_{nj}}\right)^2 + L_{nj}^{-2}} \qquad (4)$$

are the effective electron diffusion lengths with and against the electric field, and the particular solution is

$$B_{3j}(x) = \frac{1}{\omega_{2j} - \omega_{1j}} \left[G_{1j}(x) e^{\omega_{1j} x} + G_{2j}(x) e^{\omega_{2j} x} \right]$$

$$G_{(1,2)j} = \pm \frac{1}{D_{nj}} \int_0^x \exp(-\omega_{(1,2)j} x') \int_0^{\lambda_c} \alpha_j N_{0j} \exp\left(-\int_0^{x'} \alpha_j\, dx''\right) d\lambda\, dx' \qquad (5)$$

(See also a similar treatment by Fahrenbruch and Bube [4] using slightly different notation.) In practice, the integral term is extremely complicated and must be integrated numerically. This

is especially true in graded-bandgap solar cells where the absorption coefficient is a function of the composition of the material used and will vary from point to point (or in our linearized approximation, slab to slab) as the composition varies.

Since we have assumed that the semiconductor cell is divided up into (not necessarily equal) slabs of equal-depth boundaries, the solution will differ from slab to slab. To find a global solution, it is necessary to match up the solutions at the boundaries of the slabs.

The boundary conditions consist of the requirement that the electron density and the current density be equal at the boundary of adjacent slabs. (The electron density equality requirement must be modified if there is a discontinuity in the bandgap energy at the interface of the two slabs.) If there are N sections, then there are 2N constants of integration to be determined. The continuity of the carrier density and of the current give us two conditions at the boundary of consecutive slabs, resulting in 2N-2 conditions for 2N unknown constants. The final two conditions come from the surface, where the current density for the minority carrier is determined by the recombination velocity, and from the boundary of the space-charge (depletion) region, where the excess minority carrier density is determined by the intrinsic carrier density and the voltage across the junction. This results in a system of N

equations in N unknowns, which is well determined.

The system of equations can be solved by inversion of the matrix of coefficients, but this is an expensive process in terms of time and effort. An alternative is to solve the matrix by the method of Gaussian elimination. This is especially attractive because for any row of the matrix, the entries arise from the boundary conditions between successive slabs only and are therefore mostly zeros. This means that the matrix can be compressed and stored in the computer in a very compact form [(2N x 4) rather than (2N x 2N)]. Once the constants have been computed, we can use them to construct an approximate solution for the minority carrier density. This is a single iteration. Successive iterations then use the previous approximation to solve for the electric fields within the solar cell for the next iteration. This process is repeated until the desired degree of accuracy is achieved.

The final package of software that does the modeling incorporates the results of several articles that deal with graded-bandgap solar cells. The simplicity of the method (although it involves extensive preparatory work to provide data for application to any new composition of semiconductor) makes it feasible for use on a microcomputer.

As mentioned above, our goal is ultimately to apply the model to an investigation of the resistance to degrading of a graded-bandgap solar cell under exposure to radiation.

IV. DESCRIPTION OF THE PROGRAM:

The first section of the program is initialization. The user must select such things as the amount of screen display desired. Then he is given the choice of either computing a photon absorption profile for a new spatial distribution of relative concentrations for the alloy, or of using one that has been previously computed and stored in a file. If the choice is made to develop a new grading profile and corresponding photon absorption profile, the parameters determining the depth and degree of grading are input, as well as the number of mesh-points desired. If the choice is to use the result of previous calculation, this information is obtained from data in a file that must be specified by the user.

In order to maximize the flexibility of the program, it was decided that, as much as possible, submodels describing the electrical and optical constants for aluminum arsenide gallium arsenide alloys of different compositions should be placed in the program as defined funtions (a feature of BASIC). Thus they can be easily changed as improved experimental data is obtained. The first portion of the program is thus given to the definition of these functions, which include calculation of the bandgap, effective masses of electrons and holes, dielectric constant, electron and hole mobilities, diffusion lengths, and lifetimes as functions of position (and hence composition),

all based on the work of Sutherland and Hauser [6]. Following this are several functions for the calculation of the values of constants used in Lamorte's method such as mobility ratio and effective diffusion length in the presence of an electric field.

Following the defined functions is the section for computing the photon profile,mentioned above. If the choice was made to develop a new grading profile and corresponding photon absorption profile, the program then essentially performs a numerical integration of the term

$$\Delta N_j = \int_0^{\lambda_c} \alpha_j N_{oj} \exp\left(-\int_0^{x'} \alpha_j \, dx''\right) d\lambda \qquad (6)$$

which occurs several places in the calculation. This is done by computing the absorption constant (using a model developed by Hutchby and Fudurich [5]) for the slab for each wavelength in the AMO spectrum. (A graph of the output from this section of the program showing the absorption constant as a funtion of the wavelength and the composition of the alloy is given in Fig. 1.) Then from the number of photons in that wavelength interval incident on the slab, the number of photons absorbed is computed, as well as the number that pass through without absorption to be incident on the next section. Those absorbed in a given slab are summed up over the entire spectrum (or any subportion chosen). This process is repeated for each separate section of the solar cell until the desired depth is reached.

The information on the composition profile, number of mesh-points, total incident photons and photon absorption is then stored in a file for future use as well as its immediate use in subsequent portions of the program.

Next the main portion of the program computes the electron density distribution function, based on the theoretical procedure discussed briefly above. For each section, the molar concentration of AlAs at that depth is calculated from the concentration profile and the corresponding values for constants such as carrier density, mobilities, and diffusivity. Then the components of the electric field are computed including a photoelectric term, an impurity term, a resistance term and a bandgap narrowing term. The "drift" terms are then computed from this data, and the generation term (Eq. 5, the particular solution to the nonhomogeneous differential equation for the section) due to photon absorption is calculated for the current slab.

The generation term (Eq. 5) presented particular difficulty in calculation. The method finally arrived at was the following: The assumption was made that the absorption constant, which is a function both of wavelength and composition of material, could be replaced by an "effective" absorption constant for each section of semiconductor considered. This was computed from the number of incident photons (above the cutoff frequency) and the number of photons absorbed in the section by

treating them as though they were due to a monochromatic source. With this assumption, we can make the approximation:

$$B_{3j}(y_{oj}) = \frac{1}{\omega_{3j}-\omega_{1j}} \cdot \frac{\bar{\alpha}_j N_{oj} e^{-\bar{\alpha}_j x}}{D_{nj}} \left(\frac{-1}{\omega_{1j}+\bar{\alpha}} + \frac{1}{\omega_{3j}+\alpha} \right) \qquad (7)$$

The model seems to be quite stable and rapidly convergent to its final result. A sample current-voltage curve from the output for a one-micron thick layer of p-type gallium arsenide is given in Fig. 2. Linearly graded cells of aluminum-arsenide gallium-arsenide alloy produce similar curves with higher cutoff voltages.

V. RECOMMENDATIONS:

Several features were not incorporated into the model because of lack of time. First (and simplest), these would include the incorporation of an antireflection coating using realistic numerical data. The current model assumes a perfect coating with zero reflection.

A second feature lacking is the n-type layer and its contribution, which is absent in the current model. Although the majority of the contribution to the current of the solar cell arises from the top layer (the p-type layer in this p-on-n solar cell), the second layer cannot be totally ignored without raising a question as to the reliability of the conclusions drawn from the model.

A third feature requiring attention is the execution speed of the program. Many constants are recalculated that could be calculated once and stored for subsequent interations. This would be fairly simple, the main requirement being a sufficient period of time to do so.

A fourth item which should be addressed is the fact that, although the gradient of the electric field was assumed to be negligible in the process of linearizing the equations to put them into a form amenable for solution within each slab, the electric field may not have a small gradient. A less-rigorous assumption which would cover a larger number of cases would be to assume that the gradient of the electric field was not necessarily zero, but was a constant over the slab. In this case there would be an additional term under the radical in the computation of the effective drift velocities in the presence of an electric field. This would make the model more realistic and should be investigated.

Anyone wishing to obtain a copy of the program of the simulation (which will run on most IBM compatible computers) and/or a copy of the variable-listing program (which currently runs only in ZBASIC but can be easily modified to other versions of BASIC) should contact the author at the Department of Science and Mathematics, Cedarville College, Cedarville, OH 45335, or Joseph Wise, TAM, Solar Energy Conversion, AFWAL/POOC-2, W-PAFB, OH 45433 for further information.

References

1. Lamorte, M. F., Comprehensive Solar Cell Computer Modeling. Quarterly Progress Report No. 1. June 1984. (JPL No. 9950-924, JPL Contract No. 956741, RTI Project No. 415U-2850). Available from National Technical Information Service, U. S. Department of Commerce, Springfield, Virginia.

2. Lamorte, M. F., Comprehensive Solar Cell Computer Modeling. Quarterly Progress Report No. 2. September 1984. (DOE/JPL/956741-84/02, DE84017384) Available from National Technical Information Service, U. S. Department of Commerce, Springfield, Virginia.

3. Gummel, H. K., "A Self-Consistent Iterative Scheme for One-Dimensional Steady-State Transistor Calculations", IEEE Trans. Electron Devices, ED-11, 455-465, 1964

4. Fahrenbruch, A. L. and Bube, R. H., Fundamentals of Solar Cells. New York, Academic Press, 1985.

5. Hutchby, J. A. and Fudurich, R. L., "Theoretical analysis of $Al_xGa_{1-x}As$-GaAs graded band-gap solar cell", Journal of Applied Physics, 47, pp. 3140-3151, 1976.

6. Sutherland, J. E. and Hauser, J. R., A theoretical study of heterojunction and graded band gap type solar cells. Annual Report on NASA Grant No. NSG 1116, April 1977.

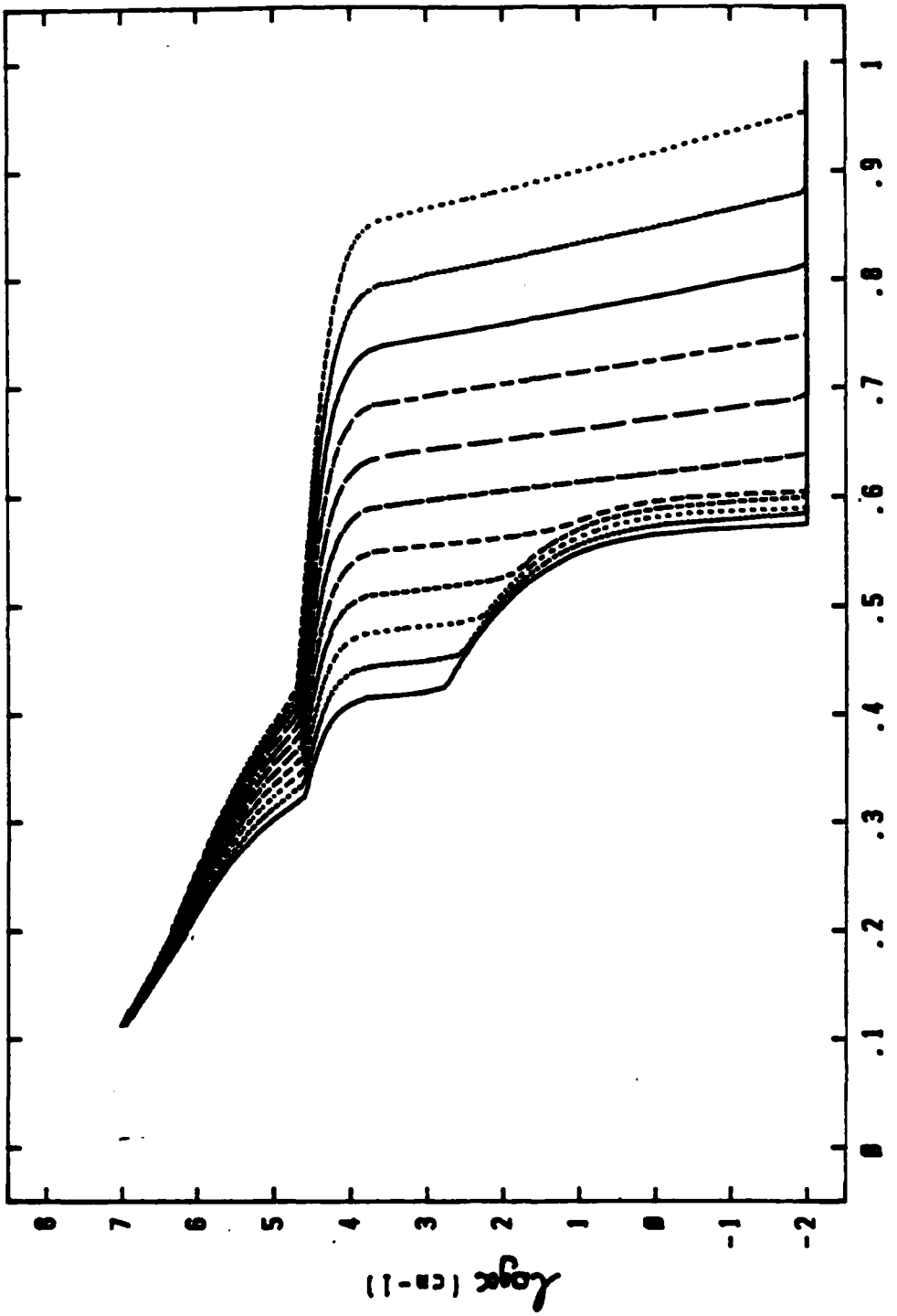

Figure 1. Plot of Log of absorption constant as function of wavelength for different compositions of $Al_xGa_{1-x}As$. Solid line on left: x=1; dotted line on right: x=0.

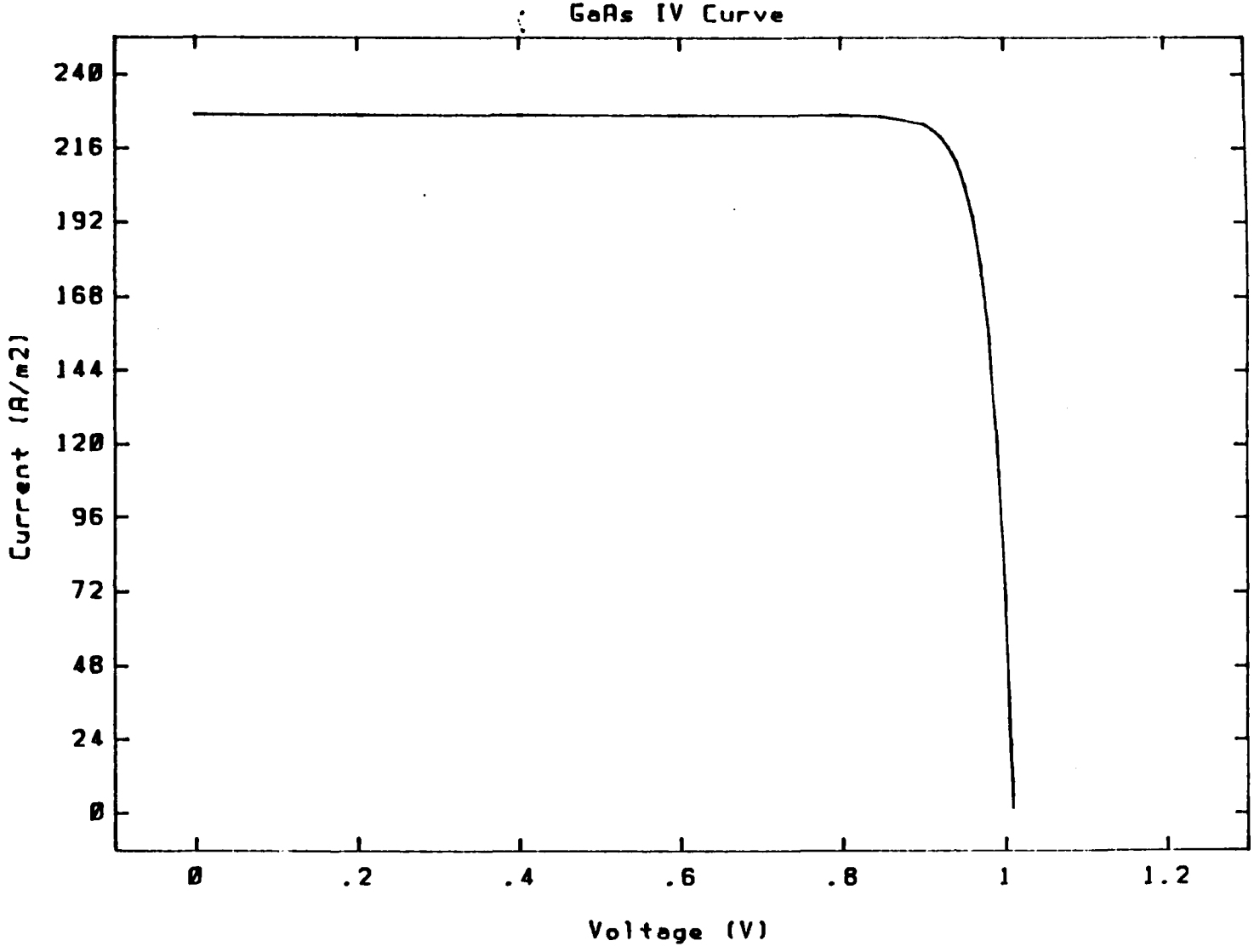

Figure 2. Typical IV Curve for GaAs

1985 UASF-UES SUMMER FACULTY RESEARCH PROGRAM/
GRADUATE STUDENT SUMMER SUPPORT PROGRAM

Sponsored by the

AIR FORCE OFFICE OF SCIENTIFIC RESEARCH

Conducted by the

UNIVERSAL ENERGY SYSTEMS, INC.

FINAL REPORT

Prepared by:	Dr. Hudson B. Eldridge
Academic Rank:	Assistant Professor
Department and	Physics Department
University:	University of Central Arkansas
Research Location:	Air Force Weapons Laboratory
	Advanced Weapons Office
	Applied Technology Division
	Weapons Technology Branch
USAF Research:	Capt. Rex Kiziah
Date:	July 27, 1985
Contract No:	F49620-85-C-0013

ANALYZING GAMMA RAY AND NEUTRON EMISSION SPECTRA

by

Hudson B. Eldridge

ABSTRACT

A method is presented for transferring data files from the fixed disk of an ND-6700 to a VAX computer using a Z-100 microcomputer to emulate a terminal for the ND-6700. Software developed for the Z-100 is discussed which permits a degree of analysis, printouts, and/or graphical displays of the spectral data. The analysis functions include rebinning the data, converting channel number to energy, correcting for solid angle and incident flux, and/or unfolding recoil proton spectra to determine the incident neutron spectra. Graphical displays may be either a point plot or a histogram and the user is prompted for legend and coordinate axis labels.

A method is also discussed for determining experimentally the response function for the detectors used in accumulating these spectra. Some preliminary data from these experiments are presented.

ACKNOWLEDGEMENTS

This Research was sponsored by the Air Force Office of Scientific Research/AFOSR, United States Air Force, under contract F49620-85-C-0013 and accomplished at the Air Force Weapons Laboratory, AW, AWY, AWYW at Kirtland AFB, New Mexico. At that facility, special thanks is extended to Capt. Rex Kiziah who suggested the project and offered advice and encouragement throughout it's execution.

nuclear structure studies. This work is quite similar to my thesis problem at UCLA. The particular problem being investigated in the section where I was assigned was to determine the spectral character of the emissions from various materials bombarded with beams of neutral Hydrogen atoms. It was felt that I would be able to assist with the analysis of the considerable amount of raw spectral data obtained thus far.

Some of the detectors used in these investigations are relatively new and the response of the detectors is not as well known as would be required for the type of analysis desired for the acquired data. Because of my past experience and current interest, it was felt that I could perform the measurement of detector response functions in addition to assisting with the data analysis.

II. OBJECTIVES OF THE RESEARCH EFFORT:

One technique being investigated at the Air Force Weapons Laboratory in response to the President's Strategic Defense Initiative to neutralize offensive missiles after they were launched is the use of neutral particle beams. The possibility of using the spectral characteristics of the resultant emissions when the beam impended the target is also being investigated as a means of controlling the neutral beam weapon. Toward this end, a research program is under way to determine the spectral characteristics of various materials, the type likely to be used in missile construction, as seen by detectors suitable for that type of environment. Data had been taken for several materials using high energy electrons and protons but there remained the job

of completing a detailed analysis of the resultant neutron and gamma spectra as to energy and flux. Two separate but related projects were discussed by my effort focal point and myself as to how I could best serve the effort during my SFRP appointment. One was to measure the detector response functions for the BGO scintillation type detectors and the second was to assist in the software development for the spectral analysis.

Since a degree of analysis could be accomplished without the detector response functions we chose to apply the first part of my effort here to the development of software. The latter part, which could also be continued back at the University of Central Arkansas, would consist of the response function measurements.

III. SCHEME TO TRANSFER FILES FROM A ND 6700 TO A Z 100:

Considerable data consisting of the Gamma and Neutron emission spectra from various materials bombarded with high energy protons or electrons had been accumulated with a ND 6700 data acquisition system and several types of detectors. The ND 6700 system, being primarily a data acquisition system, did not provide sufficient memory to support the software necessary to perform a suitable analysis of the data. At the present time adequate software is available on a VAX computer system, so a practical method was required to somehow transfer this data from the permanent storage of the ND 6700 to a storage medium acceptable to the VAX system. To this end, I was given the task of writing the above spectra from the ND 6700 to a magnetic tape in a format suitable for the VAX system.

The suitable analysis software mentioned above was installed on a VAX at the Los Alamos National Laboratory and had been previously used by one of the investigators of this project who was now at Kirtland; however, a VAX system was available at Kirtland AFB and software was available to support a data link from the ND 6700 to the VAX at Kirtland. The first approach was then to install a telephone line fron the building that housed the ND 6700 to the building that housed the VAX at Kirtland. With the support software installed in it's respective machine and the machines connected by a telephone line, files of data could be transferred between the machines. The software existing on the VAX at Los Alamos could then be installed in the local VAX and the analysis performed thereby or the files could be written to magnetic tape by the local VAX and be transported to the VAX at Los Alamos and the analysis be carried out there. This approach was followed until it appeared that installation problems with the telephone line would delay the project to such a degree that it was felt an alternate method should be investigated if a means of data transfer was to be operational by the time my appointment terminated.

The next means of accomplishing the above data transfer which was investigated was to write the data files from the ND 6700 to a Zenith Z 100 microcomputer, from there write the files to a floppy disk, hand carry the floppy disks to a nearby building where an operational telephone line was installed to the local VAX, and there, using a second Z 100, transfer the data files to the local VAX. The files could then be available for either of the means of analysis discussed above. It is this scheme of data transfer that

will be described in this report; but first, a quick overview of the method will be given.

First the data in the ND 6700 is in a format that does not lend itself to easy manipulation external to that device. A FORTRAN program was consequently written for the ND 6700 which converted the ND formatted numbers into more universal ASCII format and the spectrum so formatted was then written onto the fixed disk of the ND 6700. The program ZSTEM was then used, in the Z 100, to have the Z 100 emulate a terminal of the ND 6700 and the converted data file was read to the fixed disk of the Z 100. This file could then be copied to a floppy disk by the Z 100 and/or be analyzed with any software that could be supported by the Z 100. With this possibility of a degree of analysis on the more easily accessible Z 100, a program was written in BASIC for the Z 100 to provide graphical displays, graphical plots, rebinning of the data, and/or printouts of regions of interest of the original or rebinned data. This program has been described and a BASIC source listing given [1] although the program resides within the Z 100 in the complied form as CMAST.

A word of caution is in order regarding the hardware link of the Z 100 to the ND 6700. The aforementioned hardware is only a RS 232 cable from channel 2 of the SCP board of the ND 6700 to the J2 input of the Z 100 and only pins 1,2,3, and 7 should be connected between the devices. If any additional pins are connected, quite eratic behavior was found to result. This phenomenon was not investigated in the interest of expediency but would in and of itself provide an additional interesting project.

The general features of this program, CMAST, resident in the Z-100 Micro-computer that will do limited analysis and furnish hard copy of pulse height spectra accumulated with a ND 6700 analyzer system will now be outlined. It is assumed that the spectra to be analyzed reside on the hard disk of the ND 6700 in the same numerical form in which they were accumulated. The Z-100 then emulates a remote terminal for the ND-6700, reads the selected spectra onto its own hard disk, performs minor conversions on the data, and then furnishes a print-out and/or a graph of the data.

Two types of graphical displays, selectable by the user, are available. The first type of display allows the user to select any 512 channels of the spectrum and display them on either a logarithmic or linear plot in the same manner as the pulse height analyzer would, i.e. the abscissa is channel number and the ordinate is a dot whose distance from the abscissa is proportional to the number of pulse-heights recieved in that channel. The second type of display permits the user to rebin a selectable region of the data, i.e. integrate over a selectable number of channels, and then obtain a printout of the binned data and/or a histogram type plot of the rebinned data. The ordinate and abscissa can be modified (linearly) so as to display more meaningful results such as counts per unit flux per energy per unit solid angle as a function of energy. The third type of analysis that may be done is to unfold a recoil proton spectrum to obtain the incident neutron spectrum. Either type permits a dump of the resultant graph to the printer.

ray or neutron spectra that were incident upon a scintillation type detector. Of critical importance in this unfolding process is the response function of the detector. There are two ways that this response function may be determined: calculate it from first principles taking into account all the possible processes resulting from the interaction of the incident radiation with the detector or experimentally measure the response of the detector in a geometry similiar to it's anticipated use for a sufficient number of monoenergetic sources to empirically arrive at an expression for the response function. If the last method is employed the response function so obtained will be strictly valid only for that detector in that geometry.

This experimental approach to the determination of response functions for BGO (bismuth germanate) has been applied successfully by Moss and co-workers at the Los Alamos National Laboratory [2] for gamma rays and by Hausser and co-workers at Chalk River Nuclear Laboratories for neutrons [3] using a 762mm diameter by 762mm length cylindrical detector. Since the size and/or geometrical arrangement used in prior work is different from those of interest to the Air Force Weapons Laboratory, published data are not strictly applicable; however, it is felt that those methods could be used to obtain the required response functions.

In pursuing the above methods we have accumulated pulse height spectra from four calibrated gamma sources irradiating a 1" X 1" BGO detector using pulse processing electronics used in the Weapons Laboratory Experiments. Although these spectra are of a preliminary nature and served primarily to acquaint myself with

VI. RECOMMENDATIONS:

The software developed during this project and discussed earlier is now being used for transfer of data files and preliminary analyses. The source BASIC programs are provided so changes may be made if differing analysis formats are required.

With regard to the response function measurements, it is recommended that pulse height spectra be accumulated from an integral line BGO crystal photomultiplier tube combination irradiated with individual calibrated gamma sources of sufficient intensity to reproduce the geometry of the Weapons Laboratory experiments. The dynode output from the photomultiplier base should be shaped and amplified using the identical electronics equipment as was used in the original experiments so as to make the resultant response functions applicable to detectors of interest to the Weapons Laboratory. At first one should measure spectra from Mn54, Cr51, Hg203, Cs137, Sn113, Be7, Sr85, and Zn65 because of their relatively simple gamma spectra and then a spectrum should be obtained from a PuBe neutron source (for the 4439 Kev gamma ray). When a sufficient number of spectra have been accumulated from the calibrated sources, a simultaneous least squares type fit of these data to find the best values for the 17 parameters in Moss' empirical formula for the response function could be performed. It is anticipated that a considerable amount of computer time on a system comparable to the VAX would be expended in exploring the quality, sensitivity, and uniqueness of the fit. Consequently it is proposed to measure at the University of Central Arkansas the response of a particuliar detector for a number of calibrated gamma ray sources using similiar pulse

Figures 1 and 2 are plots of a typical spectrum printed with the first option where 512 channels of the spectrum are shown in each figure for a spectrum of 1024 channels total. A graphical plot of the same spectrum which would be generated using option 2 or 3 is shown in Figure 3, while a plot for a different spectrum obtained using option 5 is shown in Figure 4. The user is prompted for legend input and the various factors for energy, solid angle, and flux conversions and in the option 2 or 3 case the data was rebinned with 16 of the original channels per channel in the rebinned spectrum, while the option 5 case was rebinned with 32 of the original channels per channel in the rebinned spectrum. These graphs were dumped from memory to the printer using commercially available software.

IV. COPYING FILES FROM THE Z 100 FIXED DISK TO THE VAX:

At this point a number of spectra should exist as files on the fixed disk of the Z 100. To provide portability as well as backup storage, these files should, in general, be copied onto the Z 100 51/4 inch floppy disks. This proceedure has been described in detail in reference 1 and will not be repeated here. With the data files copied to floppy disks and these floppy disks transported to the building where the Z 100 is located that has the operational line connecting it to the VAX system, the files may be transferred to the VAX. Again, for details, the reader is directed to reference 1..pa

V. RESPONSE FUNCTION MEASUREMENT

It is of interest to the Air Force Weapons Laboratory to be able to unfold pulse height spectra and thereby obtain the gamma

calculated spectra using Moss' formula and his parameters. Figure 5 shows a measured spectrum from a Mn54 source and Figure 6 shows a spectrum calculated for Mn54 using Moss' formula with his 17 parameters. Exact agreement is not expected since Moss' detector was a different size and used in different geometry; however, the differences are in the proper direction. Since Moss' parameters are for a much larger crystal i.e. 3" x 3", the formula predicts a smaller Compton contribution to the spectra than is measured by this smaller detector i.e. 1" x 1".

REFERENCES

1. Eldridge, H.B., "A Method For Transferring Data Files From a Nuclear Data, Inc. Data Acquisition System to a VAX Computer", Air Force Weapons Laboratory Technical Report, (To be published).

2. Moss, C.E., E.J. Dowdy, A.E. Evans, M.E. Hamm, Lucas, M.C., and E.R. Shunk, "Unfolding Bismuth-Germanate Pulse-Height Distributions to Determine Gamma-Ray Flux Spectra and Dose Rates", Nuclear Instruments and Methods in Physics Research, 219 (1984) 558-564.

3. Hausser, O., M.A. Lone, T.K. Alexander, S.A. Kushneriuk, and J. Gascon, "The Prompt Response of Bismuth Germanate and NaI(Tl) Scintillation Detectors to Fast Neutrons", Nuclear Instruments and Methods, 213 (1983) 301-309.

handeling electronics as was used in the Weapons Laboratory experiments and from these data evaluate the 17 parameters in Moss' expression for that detector.

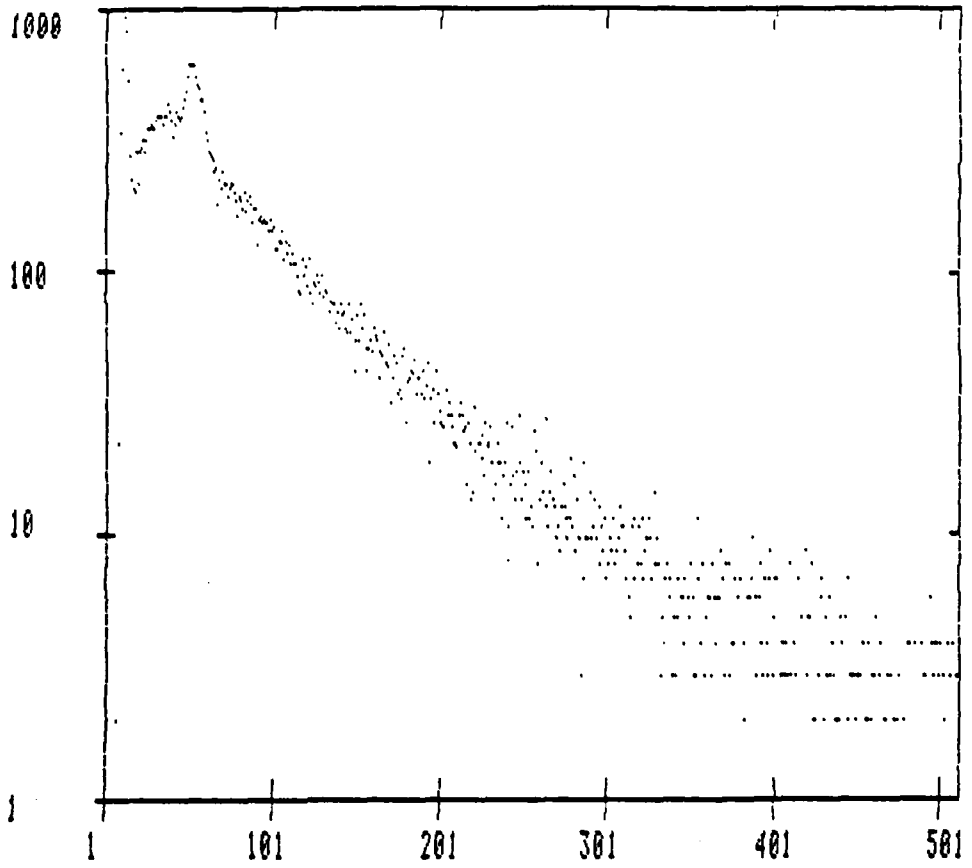

Figure 1

First 512 channels of a 1024 channel spectrum plotted using option 1 of the program CMAST

I. INTRODUCTION:

My PhD thesis at the University of California at Los Angeles consisted of the experimental measurement of the angular and energy dependence of polarized proton scattering from Oxygen in the 50 MeV region. Prior to starting my thesis work, I assisted with the construction and the modifications of the UCLA cyclotron so as to incorporate strong focussing. I also devoted a considerable amount of effort to the development of the negative Hydrogen ion source for that machine as well as the extraction and consequent external beam line development of the polarized proton beam.

Prior to my experimental work in Nuclear Physics, I had survived a long history of data processing experiences starting with the ORACLE at Oak Ridge National Laboratory and ending up with the IBM 7090 at the same location but at a much later time. At the time of my application for this program, I maintain an active interest in a number facets of the computer industry including logic circuit design, software development, educational applications, and cybernetics. I personally own and utilize extensively a medium sized popular brand microcomputer.

This assignment has provided me an opportunity to apply my Nuclear Physics experience to a timely problem as well as allow me to assist in the data analysis, making extensive use of state of the art computing and data acquisition equipment. The Air Force Weapons Laboratory, my assigned research location for the SFRP, is conducting research related to neutral particle beam weapons where negative Hydrogen ions will be accelerated in a fashion somewhat as was done with earlier particle accelerators for the purpose of

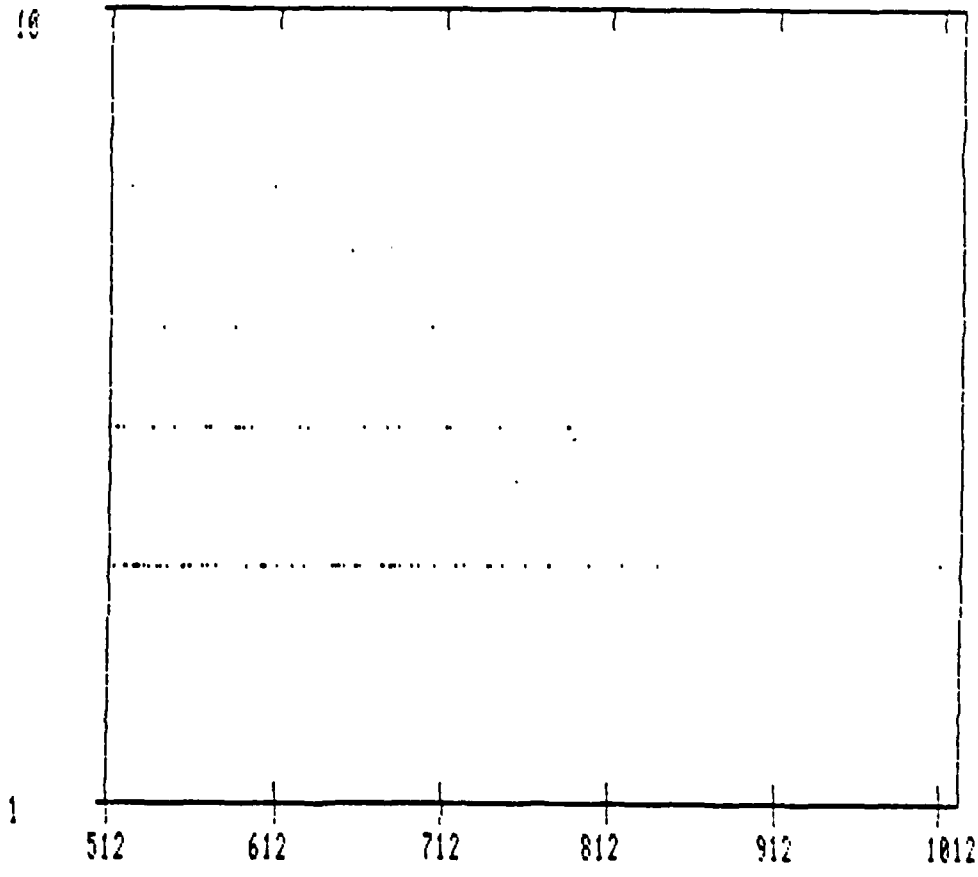

Figure 2

Second 512 channels of a 1024 channel spectrum plotted using option 1 of the program CMAST

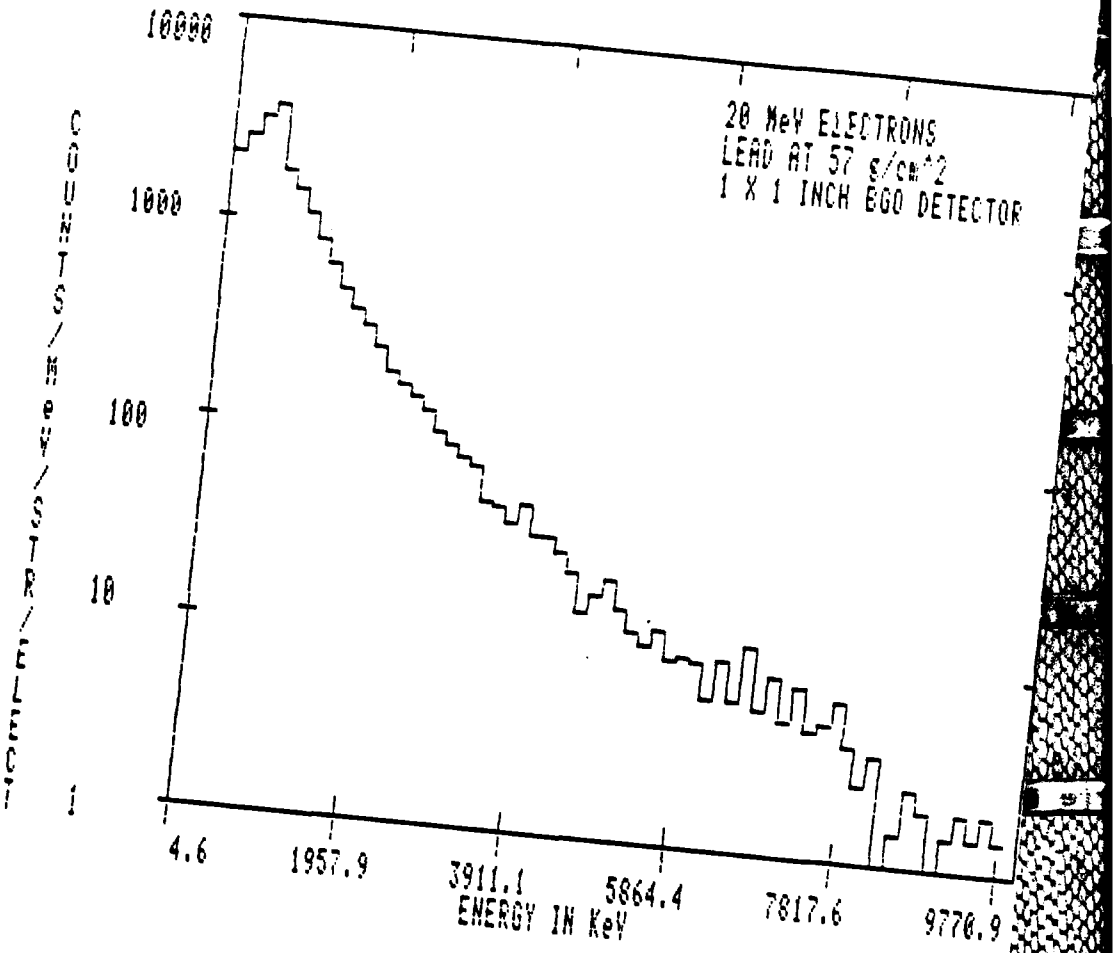

Figure 3

1024 channel spectrum (Fig. 1 and Fig. 2) plotted using option 3 of the program CMAST, rebinned with 16 channels per bin, and abscissa converted to energy.

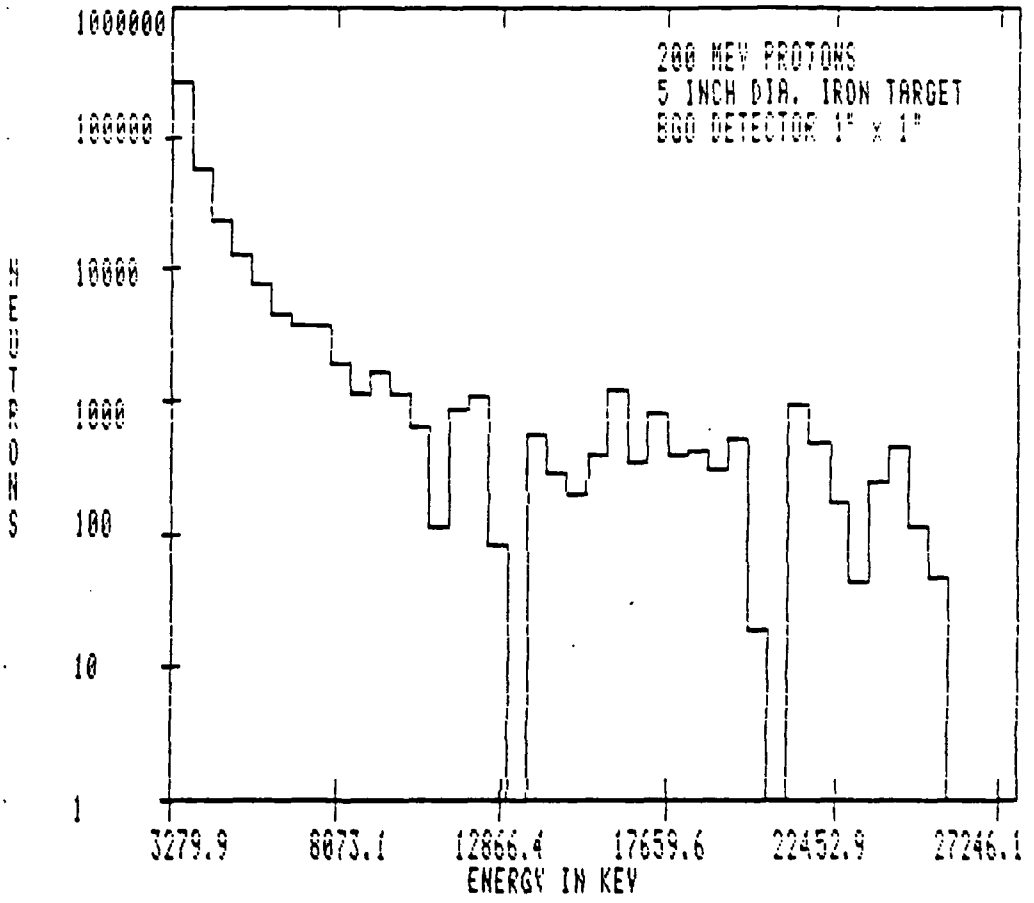

Figure 4

Plot of part of a 4096 channel spectrum rebinned with 32 channels per bin and plotted using option 5 of the program CMAST

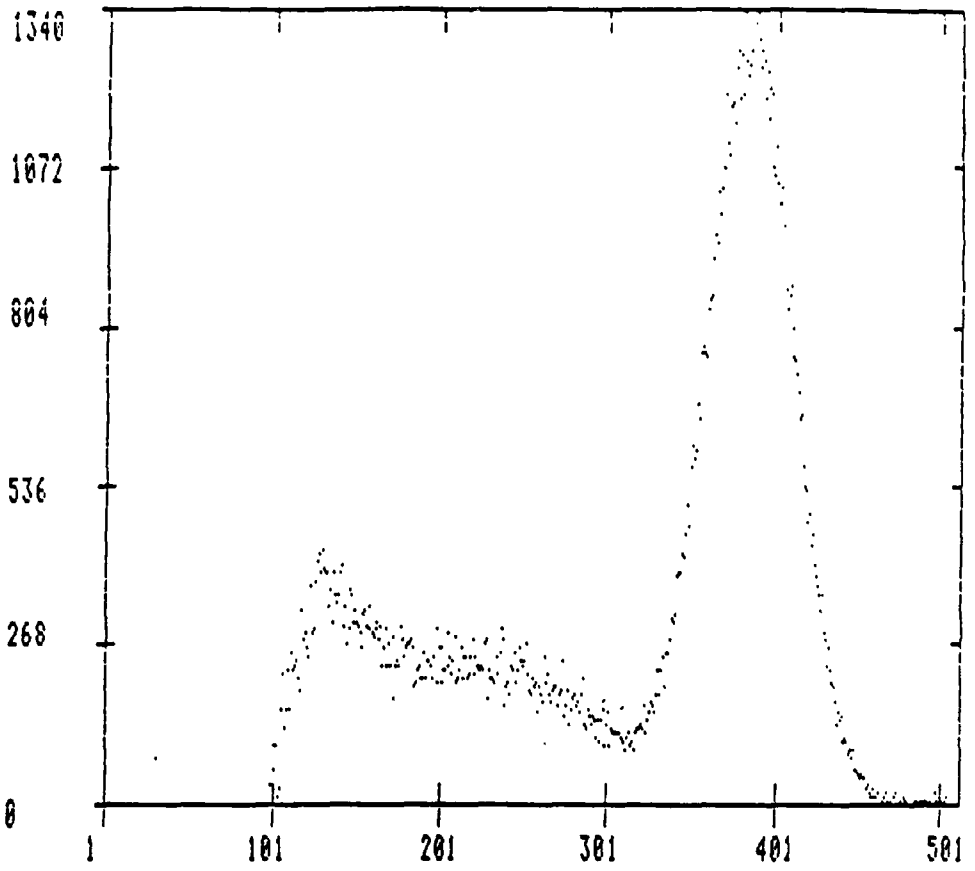

Figure 5
Measured Response of a 1" x 1" BGO Scintillator to a Mn^{54} Source

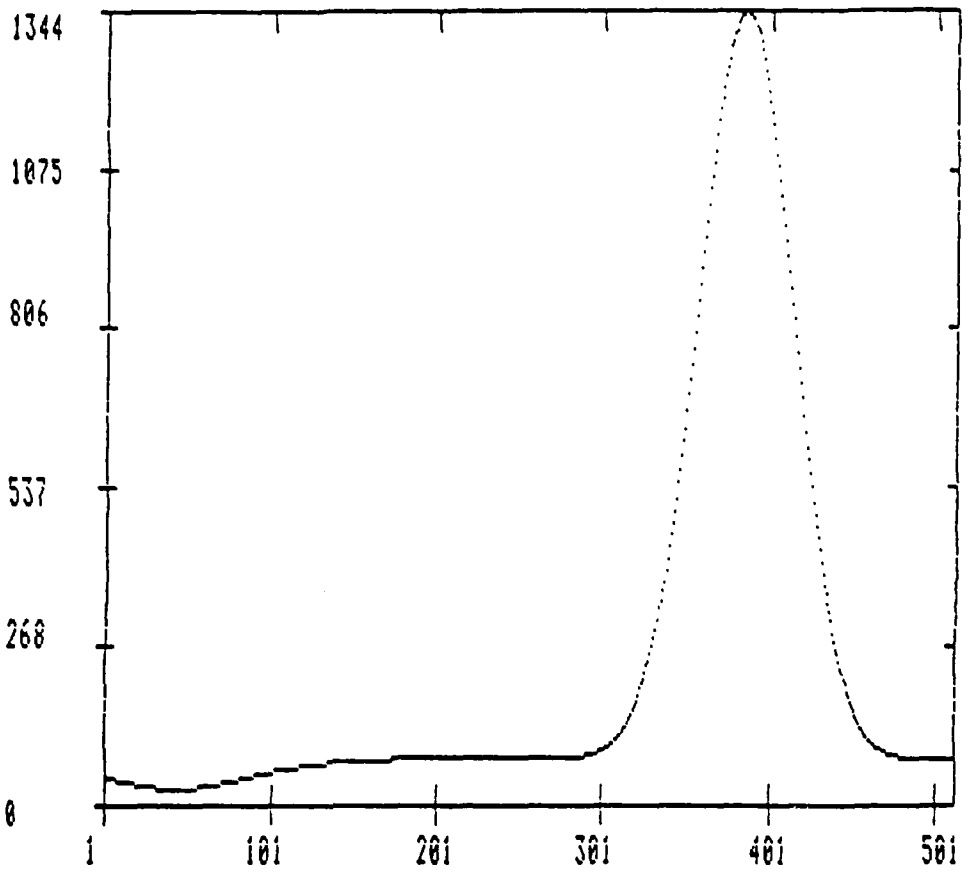

Figure 6

Calculated Response of a 3" x 3" BGO Scintillator to a 835 kev gamma using Moss' Formula

1985 USAF-UES SUMMER FACULTY RESEARCH PROGRAM/

GRADUATE STUDENT SUMMER SUPPORT PROGRAM

Sponsored by the

AIR FORCE OFFICE OF SCIENTIFIC RESEARCH

Conducted by the

UNIVERSAL ENERGY SYSTEMS, IN.

FINAL REPORT

GEOPHYSICAL PERTURBING FORCES ON THE FRANK J. SEILER LARGE PASSIVE RESONANT RING LASER GYRO

Prepared by:	Dr. Harry W. Emrick
Academic Rank:	Associate Professor
Department and University:	Department of Engineering (EG) Colorado School of Mines Golden, Colorado 80401
Research Location:	Frank J. Seiler Research Laboratory (FJSRL/NHG) USAF Academy Colorado Springs, Colorado 80840-6528
USAF Research:	Major Gerald L. Shaw, Project Director
Date:	16 August 1985
Contract No.:	F49620-85-C-0013

GEOPHYSICAL PERTURBING FORCES ON THE FRANK J. SEILER LARGE PASSIVE RESONANT RING LASER GYRO

by

Dr. Harry W. Emrick

ABSTRACT

Commencing with participation in a Laser Gyro Program Review and culminating with a paper presentation to an International Conference on Earth Rotation, the summer research program at FJSRL was both a challenge to explore the diverse capabilities of ring laser technology and an opportunity to renew and update my geodetic and geophysical knowledge as applied to this project and other on-going scientific activities. The USAF Academy site offers unique opportunities to the scientific community heretofore untapped.

I. INTRODUCTION:

The variety of both academic and research interests in my background provided a foundation upon which to build a mutually satisfying summer research program with FJSRL with the potential for follow-on activities at CSM for both the short and long term. My academic research has usually been in the applications of geodesy to surveying, photogrammetry, cartography, gravity, engineering and space programs. The particular parameter of interest to me personally is local/regional gravity and its effect on the Large Passive Resonant Ring Laser Gyro (LPPRLG). My long term goal is to initiate both an academic program and modernized surveying and engineering practices to include the available technologies. This summer internship could provide some potential for enhancing these personal goals by providing funds for travel and equipment purchase and graduate student support for which CSM has support problems for the next year. There seems to be a recurring interest in funding of geodetic-geodynamic type activities during the next several years and my purpose is to obtain some of these funds, providing that I can find a mechanism to establsih a program at CSM of a cooperative nature with the other universities in the state with competent faculty but no formal academic program in geodesy. Much of my time at FJSRL was spent in a review of the literature. I am also writing legislation for the establishment of state funding for a Colorado "Surveying and Mapping Coordinator" which should provide some more leverage to hire PhD types into the area with Geodesy background and interests. Legislation takes about three years for new programs to be sorted out and run through the hoops, no matter how viable they may appear. Jefferson county, where I am county surveyor, has an excellent chance for some NOAA/NGS funding as a Model County for the national Multipurpose Cadastre/Land Information System program, which can bring more attention and activity to the region. It is hoped that between the various federal agencies in Colorado, including the Air Force Academy's Geography personnel and FJSRL's scientists, some type of movement in this basic earth information field should be forthcoming. There is a need for advanced studies in these areas in the Rocky Mountain region where so much is now constrained in the applications of engineering due

to a lack of knowledge of the elements of measurements on the earth's surface and subsequent movements of the earth's crust.

II. OBJECTIVES OF THE RESEARCH EFFORT:

a. Advise on alignment and other engineering aspects of the LPRRLG system.

b. Predict the geophysical effects and noise level on the system.

c. Recommend procedures for determining more accurately the geodetic parameters involved.

d. Design follow-on research considering both the hardware and software.

(Three other areas were identified in early March - digital control, small lasers and data analysis; however, they were either too far removed from my experience and expertise or not ready for analysis, or both.)

III. ALIGNMENT:

a. The suggested approaches to alignment or azimuth uncertainties all require more direct access from outside the building to the Iso-Pad than is now available. Some of the possibilities for investigation are: 1) use a light source with a beam splitter, target mirrors and target grids, a la Wirtanen and Mertz, AFGL[1]; 2) Koester prisms, a la Douglas D. Berkner, Martin Marietta, Denver[2]; 3) diodes and target a la Emrick, CSM; 4) 30 m $\pm$ Michelson Interferometer a la Bender, CU/JILA; 5) other techniques unfamiliar to this author such as an advanced gyro system colocated on the Iso-Pad, etc.

b. Some impetus was given to the solution to this problem with the planned establishment of 80+ GPS monumented points throughout AFA and adjoining Farrish Memorial encampment. These monuments, in conjunction with gravity surveys and inertial positioning could establish a more refined gravity field in the local area for use in a better local vertical determination. The bedrock-to-pad optical alignment sensors require approval at higher levels, since major construction and equipment purchases will be required. These ideas are recorded in my interim reports to UES and the future planning teams should take the alignment problem into consideration.

IV. GEOPHYSICAL EFFECTS:

a. Extensive USAFA Library research (Appendix B) as well as the FJSRL funded participation in the National American Geophysical Union meeting in Baltimore have assisted greatly in the compilation of the various geophysical effects from very short periods to very long periods. The many excellent papers presented and the opportunity for personal interaction provided the reference frame for most of my thoughts on earth rotation.

b. The results of this part of the effort are summarized in Figures 6 and 7 in Appendix A.

V. PRECISE GEODETIC PARAMETERS:

a. Reviewing my own work and the interim developments of others, I have suggested the following: 1) tie the Iso-Pad to bedrock; 2) measure Δx, Δy, Δz, Δaz to establish variations during the experiments; 3) compare with another geophysical observatory in the vicinity but offsite during the experiments; 4) obtain absolute positional/azimuth information to a greater detail with more extensive instrumentation; 5) tie in with suggested CSM and existing NOAA/NGS and NASA networks.

b. The Academy will be placing over 80 geodetic monuments for doppler satellite positioning with GPS receivers. This event alone partially accomplishes 1-4 above and 5 is dependent upon DMA's data policy and future FJSRL coordination with them.

VI. FOLLOW-ON RESEARCH:

a. My recommendation/proposal will be to provide funding for faculty travel to technical meetings, graduate student and faculty follow-on consulting with FJSRL-LPRRLG to update on new events/technology which supersede the present status/plan. The graduate student would study specific aspects of the effort such as instrumentation, computer models and simulations and the alignment situation.

b. The results thus far are: 1) requesting $20,000 follow-on from UES as per VI a) and VII b); 2) for higher levels of funding I am

contacting AFGL to establish the complete geophysical/geodynamics observatory as previously mentioned.

VII. RECOMMENDATIONS:

a. My recommendations are included above and in the paper which follows as Appendix A.

b. My follow-on grant request will be to continue participation in the LPRRLG project with one day per month visits for September-April (8 days @ $450/day), three professional/technical meetings ($2500), two weeks full time during the summer of 1986 ($4500), plus the remainder for Dr. Tom Dobecki, CSM earthquake seismologist, and his graduate student, Mr. Schneider.

c. My other suggestion is for AFOSR to provide suppor so that FJSRL/NHG can establish a true and excellent geophysical/geodynamics observatory at AFA which is so near to the transplanted heart of the U.S. Space Program.

VIII. ACKNOWLEDGEMENTS:

I wish to acknowledge all of the agencies and individuals who have made this summer a productive and enjoyable one. They are: the United States Air Force Systems Command (AFSC), the Air Force Office of Scientific Research (AFOSR), the Frank J. Seiler Research Laboratory (FJSRL), Lt Colonels Pletcher and Siegenthaler, Majors Rotge' and Shaw and Mr. Simmons. They were all very helpful and understanding.

REFERENCES

1. Wirtanen, T.A., and Mertz, M., "Design of a Unique Azimuth Monitoring Device," AIAA Paper No. 80-1754, Danvers, MA, 11-13 Aug 80.
2. Berkner, D.D., "Koester Prism Analysis," DARPA, DOD, Arlington, VA, Report MCR-81, Martin Marietta Aerospace, Denver, CO, Dec 81.

IX. APPENDIX A: Measuring Earth Rate Perturbations with a Large Passive Ring Laser Gyro

The Frank J. Seiler Research Laboratory (FJSRL), where this experiment is housed, was dedicated in 1963 in honor of the U.S. Air Force pioneer of in-house research laboratories, Colonel Frank J. Seiler (1907-1962).

The isolation test pad (Iso-Pad) (Figure 1) was designed and constructed in the late 1960's in order to provide a stable platform for the testing of various inertial systems components. This stable platform was constructed on a base of crushed granite aggregate. The Iso-Pad weighs almost 200,000 kilograms. There are four pairs of pneumatic isolators (Figure 2) for low frequency isolation (DC to 0.1 HZ) in response to the on-line commands from a high-quality, two-axis tiltmeter for a maintained position relative to the local vertical of $\pm$0.001 arc sec. The edges of the pad are maintained within $\pm$0.2 micrometers of their desired height with respect to floor level. The high frequency (0.1 to 20 Hz) isolation is accomplished with two horizontal and four vertical seismometers connected in a real time microprocessor controlled feedback loop. The vibrators effectively isolate the system to 10^{-8} G. Recommenations include a continuously monitoring tidal gravimeter during the experiments.

The Large Passive Resonant Ring Laser Gyro (LPRRLG) now under construction at FJSRL takes advantage of what is known as the Sagnac Effect (Figure 3). Optical rotation sensing dates back to the early 1900's. Sagnac[1] and others experimented with an interferometer device to measure the dispersion property of various types of glass. Sagnac rotated his device and noted the difference between the predicted and the experimental results from a known sample. Rotation of the device (with regard to the fixed stars) between the clockwise (cw) and counter clockwise (ccw) beams produces an effective difference in path length. This is detected by the measured fringe shifts, and is called the Sagnac Effect.

Referring to Figure 3, we see that the cw beam completes a round-trip in a time (τ_{cw}). During this time interval the beamsplitter has rotated to position B. Conversely, during a round-trip

time for the ccw beam (τ_{ccw}) the beamsplitter has moved only to position A. The difference in round-trip time ($\delta\tau$) is given by ($\tau_{cw} - \tau_{ccw}$). We have that

$$\tau_{cw} = \frac{2\pi R + \Delta S''}{C} = \frac{\Delta S''}{\Omega R} \tag{1}$$

and

$$\tau_{ccw} = \frac{2\pi R - \Delta S'}{C} = \frac{\Delta S'}{\Omega R} \tag{2}$$

$$\delta\tau = \frac{4\pi R^2 \Omega}{C^2 - (\Omega R)^2} = \frac{4A}{C^2} \Omega \tag{3}$$

The fringe (phase) shift is given by

$$\Delta z = \frac{c}{\lambda} \delta\tau = \frac{4A}{\lambda C} \Omega \tag{4}$$

where: A now represents the enclosed area of the loop, and λ is the wavelength of the (optical) radiation. The Δz thus observed was found to be independent of path shape, center of rotation, and also of the co-moving refractive medium for the beam path.

The measurement of the fringe shift (fringe position) is a DC analog measurement (basically a light intensity measurement). A different approach was suggested by Rosenthal[2] in 1962, which utilizes a laser source and resonant ring cavity. Such a ring laser device was first constructed by Macek and Davis[3] in 1963 (Figure 4). The non-rotating ring possesses a resonant mode such that there are $q = l_o/\lambda_o$ wavelengths around the ring. This mode however is degenerate in that there will be both a cw and a ccw beam with q wavelengths. However, for $\Omega \neq 0$ the degeneracy is removed. The difference in transit time corresponds to effective path length changes for the cw and ccw beams.

Therefore, in order to maintain resonance: $\delta\lambda = \frac{\delta l}{q} = \frac{\delta l}{(l_o/\lambda_o)}$

and: $\frac{\delta\lambda}{\lambda_o} = -\frac{\delta\gamma}{\gamma_o} = \frac{\delta l}{l_o} = \frac{C\delta t}{l_o}$;

in order to complete this operation for both beams:

$$\frac{\delta\gamma'}{\gamma_o} = \frac{C\tau}{\ell_o} \; ; \; \frac{\delta\gamma''}{\gamma_o} = \frac{C\tau''}{\ell_o} \; ;$$

therefore: $$\Delta f = \Delta\gamma = \frac{\gamma_o}{\ell_o} C \Delta\tau = \frac{\gamma_o}{\ell_o} \frac{4A}{C} \Omega \; ;$$

and: $$\Delta f = \frac{4A\Omega}{\ell_o \lambda_o} \qquad (5)$$

Detection in the passive ring gyro is accomplished by heterodyning (Figure 5) the two counter-rotating beams and thus observing the beat frequency, Δf.

The LPRRLG system has the theoretical potential for measuring changes in effective rotating rates of a few parts in 10^{-10} of earth rate for averaging times of a few seconds.[4] The present capability is 10^{-6} earth rate for averaging times on the order of a day.

The Iso-Pad is well instrumented, albeit isolated from the local terra firma. We are recommending that a complete set of instrumentation be installed nearby to monitor geophysical amd atmospheric effects during the experiments. Additionally, it is recommended that two or three interferometers be installed at 45^o angles extending into the bedrock. Various azimuth monitoring techniques are also being studied.

The LPRRLG on the Iso-Pad will also provide for an ideal location for comparing other inertial frame measuring techniques.

The various geophysical effects (Figures 6 and 7) can be explored once the initial tests are completed. It is hoped that the FJSRL site will become a true geophysical observatory and as such will be visited frequently by the state-of-the-art instrumentation with capabilities for: satellite laser ranging, real time satellite interferometry, inertial positioning systems, moving base gradiometers, absolute gravimeters, etc.

The Colorado School of Mines has an operational geophysical observatory at Bergen Park, not far from Denver, Colorado, and is planning another observatory on recently donated land in South Park, Colorado, which is less populated.

These three locations as well as others could be joined for simultaneous observations and scientific comparisons.

Additonally, a regional gravity program has been established by the "Mines" geophysics department for inclusion in the NASA Geodynamics Programs such as the Geopotential Research Mission (GRM) and the ongoing Crustal Dynamics Project with the regional ground truth being furnished by CSM and the subsequent improvement of geodetic parameters positively influencing the LPRRLG program.

"This research is sponsored by the Air Force Office of Scientific Research/AFSC, United States Air Force, under contract F49620-85-C-0013. The United States Government is authorized to reproduce and distribute reprints for governmental purposes notwithstanding any copyright notation hereon."

REFERENCES

1. Post, E.J., "Sagnac Effect," Reviews of Modern Physics, Vol. 39, No. 2, 1967.
2. Rosenthal, A.H., "Regenerative Circulatory Multiple-Beam Interferometry on the Study of Light Propogation Effects," Journal of the Optical Society of America, Vol. 52, No. 10, Oct 1962.
3. Macek, W.M. and Davis, D.T.M., Jr., "Rotation Rate Sensing with Traveling-Wave Ring Lasers," Applied Physics Letters, Vol. 2, No. 3, 1 Feb 1963.
4. Shaw, G.L., and Simmons, B.J., "A 58 m^2 Passive Resonant Ring Laseer Gyroscope," Proc. SPIE, No. 78, p. 117, 1984.

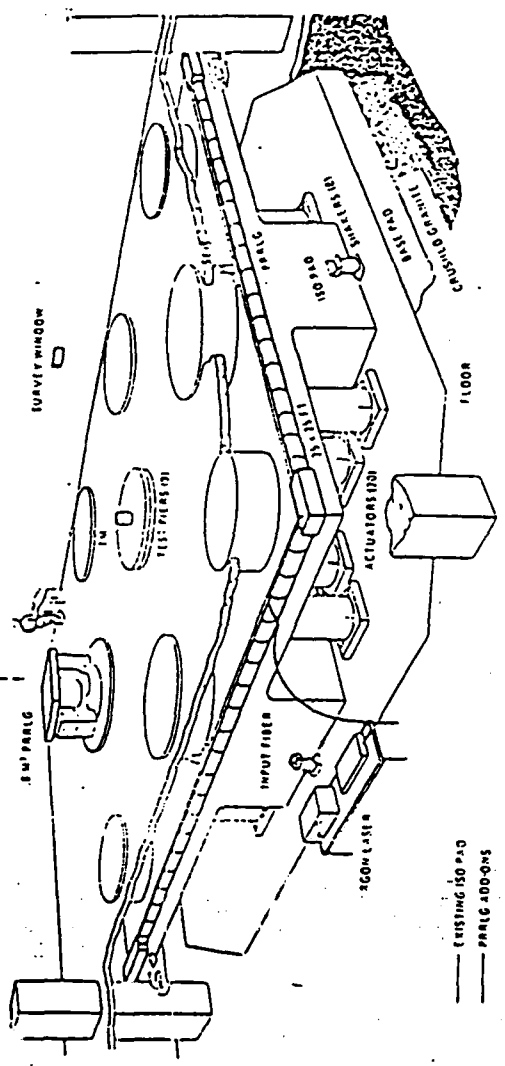
SURVEY WINDOW
FLOOR
ACTUATORS
INPUT FIBER
EXISTING ISO PAD
PARLG ADD-ONS

FIGURE 1

FIGURE 2

PNEUMATIC ISOLATORS (DC-0.1 HZ)
- 4 OUTSIDE PAIRS VARY TO TILTMETER COMMANDS
- INNER TANKS MAINTAIN HEIGHT TO ± 0.2 MICROMETER

SHAKERS (0.1 - 20 Hz)
- AVERAGE 2 HORIZONTAL OR 4 VERTICAL SEISMOMETERS FOR TANSLATION DIFFERENCE
- MATCHED PAIRS OF SEISMOMETERS FOR ANGLE

Figure 3

SAGNAC EFFECT

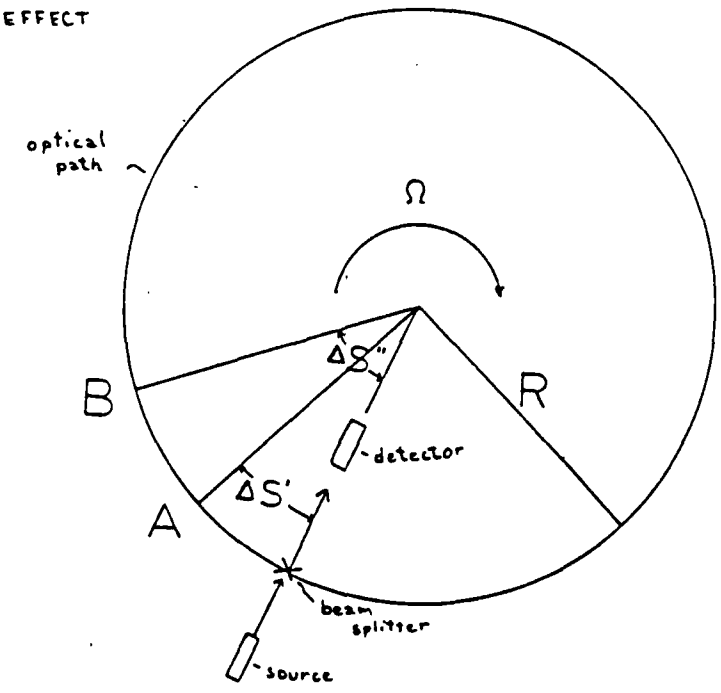

AD-A166 176 UNITED STATES AIR FORCE SUMMER FACULTY RESEARCH PROGRAM 11/13
1985 TECHNICAL RE (U)UNIVERSAL ENERGY SYSTEMS INC
DAYTON OH R C DARRAH ET AL DEC 85 AFOSR-TR-86-0139
UNCLASSIFIED F49620-85-C-0013 F/G 5/9 NL

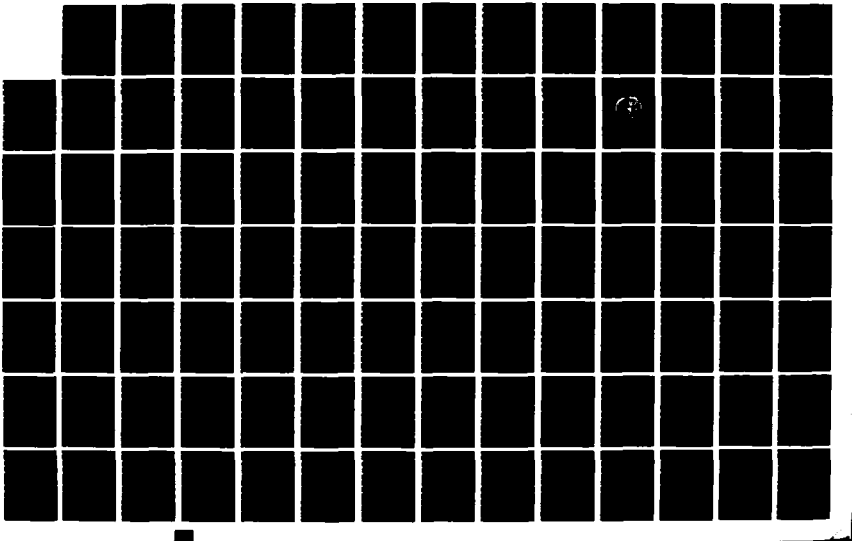

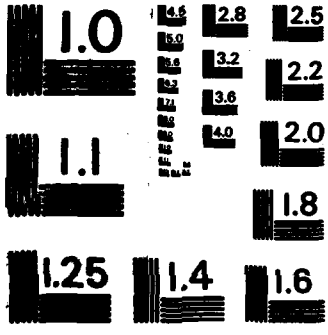

MICROCOPY RESOLUTION TEST CHART
NATIONAL BUREAU OF STANDARDS - 1963 - A

Figure 4

MACEK and DAVIS RING LASER GYRO

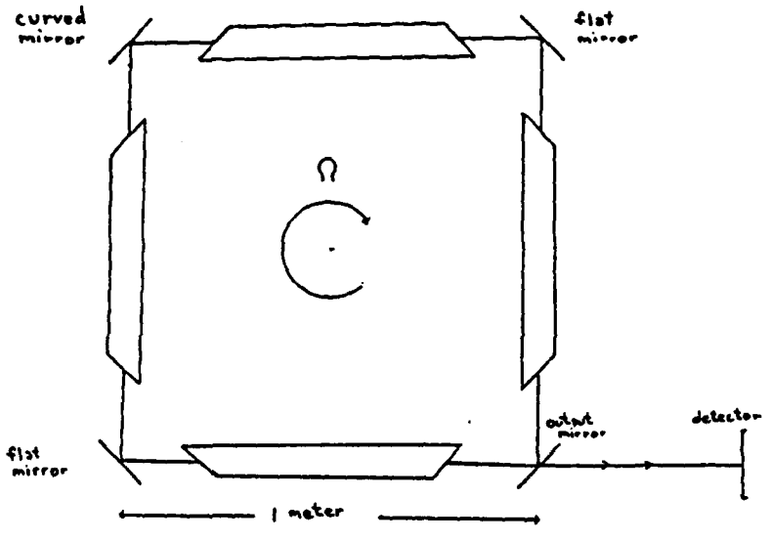

FIGURE 5

BASIC RING LASER

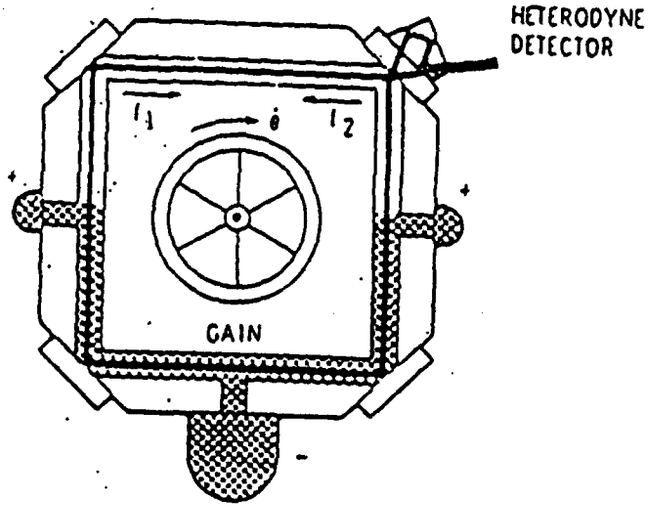

Figure 6

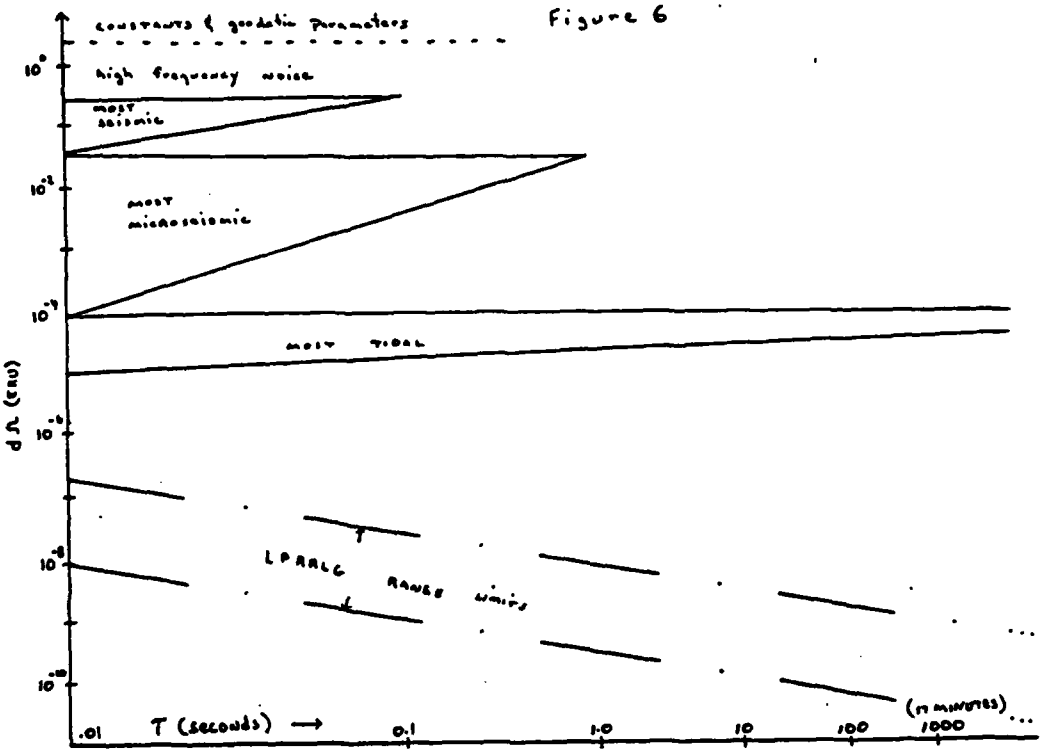

Figure 7

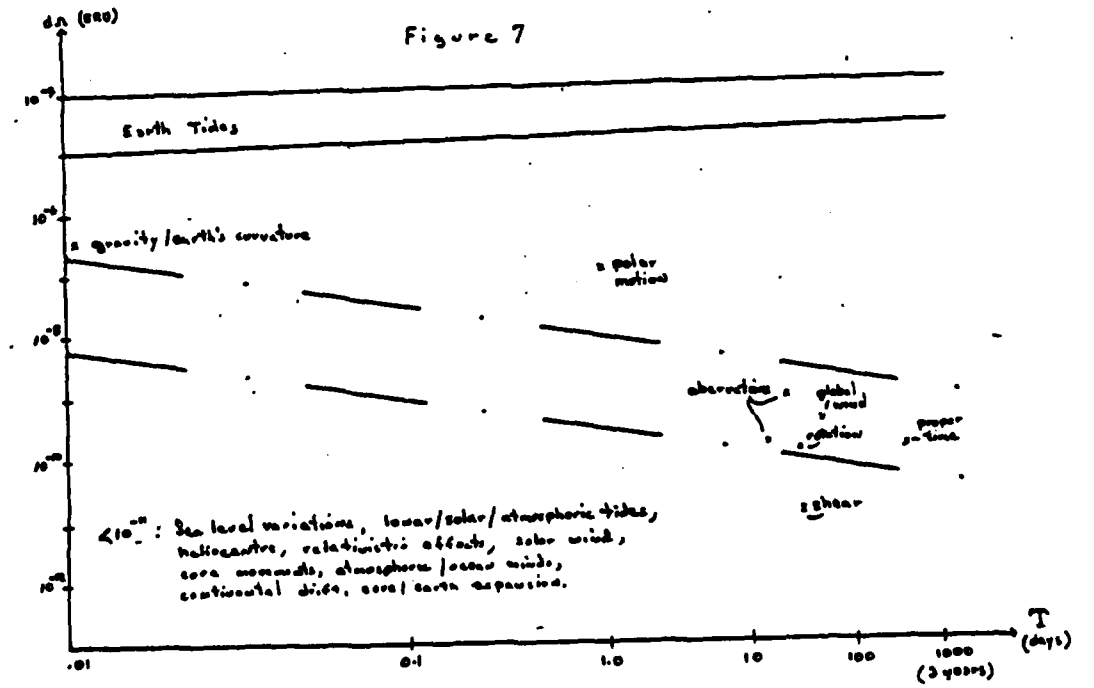

X. APPENDIX B: Library Research

The following section is an alphabetical by author listing of the primary references concerning the geophysical effects as may be detected by the LPRRLG and are the basis for Figures 6 and 7 in Appendix A.

Jon Berger and Judah Levine, "The Spectrum of Earth Strain From 10^{-8} to 10^{2} HZ," Journal of Geophysical Research, American Geophysical Union, 2000 Florida Avenue, NW, Washington DC, 10 Mar 74, Vol. 79, No. 8, pp. 1210-1214.

This reference was mentioned during a visit to Dr. Peter Bender at JILA on the University of Colorado campus and provided an initial basis for the continuing review of the literature on this topic. Four frequency bands of the power spectrum of the earth strain fluctuations were compared over 10 decades at three sites separated by a minimum of 1200 kms. Band one was greater than 0.5 Hz and above 60 Hz the system noise in one strain meter began to dominate the earth noise. Band two was divided into two subbands, 10^{-4} to 2.5×10^{-2} and 2.5×10^{-2} to 0.5 Hz of which the former is for typical seismic activity and the latter registers microseismic events. The tidal band was from 10^{-5} to 10^{-4} Hz and secular terms are in the less than 10^{-5} Hz band. The sites are Poorman Mine in Boulder, CO; Pina Flats, CA; and Queensbury Tunnel, Yorkshire, England.

John J. Degnan, "Advanced Satellite Laser Ranging Systems," Transactions, American Geophysical Union, 1985 Baltimore, MD, national meeting, Instrument Electro-Optics Branch, NASA/Goddard Space Flight Center, Greenbelt, MD. To be published.

In this paper, he presented his claim for sub-arc-sec pointing accuracy and 250 fsec streak camera resolution.

M-K Fujimoto, S. Aoki, K. Nakajima, T. Fukushima, S. Matsuzaka, "General Relativistic Framework for the study of Astronomical/Geodetic Reference Coordinates," Proceedings of Symposium No. 5: Geodetic Applications of Radio Interferometry, NOAA Technical Report No. 95 NGS 24, Rockville, MD, 1982, pp. 26-35.

This paper deals mainly with the various coordinate systems/reference frames. On the last page of this paper, comparisons of tidal potential effects and gravitational effects to the relativistic effects are made and the former are 1 and 2 orders of magnitude less respectively than the determinations of the observational and positional measurements. This shows the needs of even more precise positioning before additional effects can be given credibility.

J.C. Harrison, Earth Tides, A Hutchinson Ross Benchmark Book, Van Nostrand Reinhold Company, New York, 1985, pp. 5-47 272/289-291, 400-409.

This reference book, edited by Professor Harrison, contains a series of prominent articles. The first one is from 1950 but still is very current according to the editor. It is "On Earth Tides" by Eiichi Nishimura. He covers earth rigidity with observations which we find difficult to duplicate in precision today in our studies in California. He links strain to tilt (1 nonoradian of tilt is produced by 1 nonstrain (10^{-9})). Using sensitive tiltmeters ($\pm$ 0.02/mm) he finds as much as 0.01 change in deflection of the verticaldue to tidal effects. He also finds that the effects vary with time and location. The second article is "Tidal Forces" by Julius Bartels in which he generates and explains a model. The third article, which I considered important, is "Detailed Gravity-tide Spectrum Between one and four Cycles per Day" by R.J. Warburton and J.M. Goodkind. Anomolous results were achieved but it is unknown if they are location or time variants. The last article was by Judah Levine, whose article, "Strain-tide Spectroscopy" includes a mention of his 30 meter long laser strainmeter. This type of instrumentation was suggested by the Boulder group at JILA for use at FJSRL-LPRRLG for torsion type determinations. He also shows some analysis and discusses other instrumentation such as a cyrogenic gravimeter. Lovine could possibly assist in the torsion/rotation instrumentation for the Iso-Pad if this is in the plans for the future.

Charles A. Lundquist and Henry D. Friedman, "Scientific Horizons from Satellite Tracking," Research in Space Science, Smithsonian Institution Astrophysical Observatory, Cambridge, MA, 30 Dec 66, SAO Special Report No. 236, pp. 177-185.

In Chapters 7 and 8, the periods due to body tidal effects causing secular earth rate deceleration and an energy budget are shown in Tables 5, 6, and 7 respectively. The length of day varies from 0.14 x cos (reduced latitude) for a period of 18.5 years to 0.33 x cos (reduced latitude) for a period of 13.66 days (plus 0.14 x cos (reduced latitude) for a period of 13.63 days). Table 6 shows secular deceleration of -0.1×10^{-11} for variations in sea level; 21.0×10^{-11} for lunar tide; 6.2×10^{-11} for solar tides; -1.6×10^{-11} for atmospheric tide; 1.2×10^{-11} for both short and long period core effects; $<10^{-5}$ for angular momentum from solar wind; $<10^{-12}$ for angular momentum from atmospheres and $< 10^{-13}$ from oceans; $< 7 \times 10^{-13}$ for continental unrest; $< 3 \times 10^{-12}$ for thermal expansion and $<3.1 \times 10^{-12}$ for growth of the core. The energy budget ranges from -4.4×10^{26} ergs per year for the tidal friction to 1×10^{28} ergs per year for solar radiation.

A.J. Rudman, R. Ziegler and R.F. Blackely, "Fortran Program for Generation of Earth Tide Gravity Values," Geophysical Computer Programs, 4, Department of Natural Resources, Bloomington, IN, 1977, Occasional Paper 22, p. 1.

In addition to the computer program in this document, a comparison of theoretical and observed values is given for tidal gravity readings; however, today an order of improvement in gravity readings is possible which may provide problems with some of these programs.

K.P. Schwarz, "A Comparison of Models in Inertial Surveying," Proceedings of the Second International Symposium on Inertial Technology for Surveying and Geodesy, Division of Surveying Engineering, University of Calgary, Calgary, Alberta, Canada T2N 1N4, 1981, pp. 61 and 68.

This paper relates to the uncertainties in the Litton type of Inertial Positioning System due to geophysical, astronomical and

timing effects. For these purposes the relativistic effects are on the order of 10^{-7} of the estimated positional accuracy at the time of the report.

C.F. Yoder, J.G. Williams, and M.E. Parke, "Tidal Variations of Earth Rotation," Journal of Geophysical Research, American Geophysical Union, 2000 Florida Avenue, Washington DC, 10 Feb 81, Vol. 86, No. 62, pp. 881-891.

In this paper they have rederived the major tidal effects for all terms greater than 0.002 milliseconds (1mm). These formulae would also need to be reevaluated in terms of the general improvements in accuracy in the last three years.

NOTE: Abstracts of the above references will be left on file in FJSRL/NHG.

Additional references and papers were valuable in the determination of the state-of-the-art for the consideration of the geophysical and relativistic effects in scientific experimentation potentially related to the LPRRLG studies. The relevant results and authors are listed below:

VLBI has been able to determine UT1 with a precision of 0.1 millisec of time from a single hour of observations each day. This is from a draft of a paper by Dr. W.E. Carter of NOAA, NOA, C&GS, NGS, "Daily UT1 Determinations from IRIS VLBI Observations," submitted to Nature. He also has a paper submitted to Science wherein he states the comparison of pole position by VLBI and SLR in agreement to 2 millisec of arc (about 6 cm at one earth radius).

Water Vapor Interferometry (WVI) can provide for $1:10^{14}$ in resolving the ambiguity caused by the atmosphere in GPS etc. measurements and by using the proper Kalman Filter an accuracy of position can be obtained to less than 0.6 cm. A hydrogen maser is used as reported by T.A. Herring of MIT/SAO, Cambridge, MA. This was in a Q&A session at the 1985 AGU meeting. During the same session, W.E. Clark, NGS, reported accuracies of 3 mm using the WVI techniques.

A general reference book on Geophysics and Solid Earth Geophysics as well as reference books on Geodesy, Physical Geodesy and Satellite

Geodesy could provide the bulk of background information required as an entre to Geodynamics, Gradiometry and other interdisciplinary programs which are now utilizing observational geophysics and geodesy. To my knowledge, there does not now exist a single reference handbook for solid earth geophysive/geodesy as exists in most fields of engineering.

1985 USAF-UES SUMMER FACULTY RESEARCH PROGRAM

FINAL REPORT

QUASIPARTICLES AND THE TRANSITION TO TURBULENCE

Prepared by:	Dr. John E. Erdei
Academic Rank:	Assistant Professor
Department and University:	Department of Physics University of Dayton
Research Location:	Aero-Propulsion Laboratory Wright-Patterson Air Force Base
USAF Research:	Dr. W. M. Roquemore
Date:	9/4/85
Contract No.	F49620-85-C-0013

ABSTRACT

A suggestion has been made that some of the observed properties of fluid flows can be explained on the basis of particle, or quantum mechanical principles. The possibility of such a description has been considered by searching for a mathematical basis for this suggestion. By using a treatment of the convective instability as a guide, it is believed that an order parameter description is a foundation upon which to build. This paper discusses the relevant features of the formation of Benard convection cells, and how one might extend the ideas to shear flows.

ACKNOWLEDGEMENT

I would like to thank the Air Force Systems Command and the Air Force Office of Scientific Research for their sponsorship of my research. I would also like to acknowledge the Aero-Propulsion laboratory at The Wright-Patterson Air Force Base, and especially Dr. W. M. Roquemore for providing facilities and support for my research this summer. My stay at the base has provided the avenue for many fruitful discussions regarding the properties of various flow configurations.

I would also like to thank Dr. L. D. Chen and Dr. R. Piccirelli for their help and interest in developing a long term collaboration in this area. Little progress would have been made without their help.

I. INTRODUCTION

The Aero-Propulsion Laboratory at Wright-Patterson Air Force Base has had an experimental and computational involvement in the area of turbulence for a number of years. The work of this laboratory has resulted in some rather dramatic demonstrations of the complexity of various flow configurations through visualization techniques. However, along with the complexities of the detailed motion, certain macroscopic features appear to be universal in character, as seen, for example, in the formation of large vorticies in shear flows. Out of the enormous number of possible realizations allowed by the billions of degrees of freedom, only certain bulk characterisics are observed. These observations have led to the suggestion that a situation similar to that seen in quantum systems is occuring. Although classical predictions allow for a continuous set of energy states for the hydrogen atom, nature selects out preferred states, the quantum states, which govern the true characteristics of the atom. An alternate point of view is that these bulk features are fundamental "particles" in the flow in the same sense that photons and phonons are

fundamental "particles" (or quasiparticles) in electromagnetic radiation and lattice vibrations.

It was with these ideas in mind that the summer research was initiated. The situation is fairly complex, however, since these concepts require a formal basis in order to become useful as a predictive tool. The search for such a formalism occupied the bulk of the funding period.

The flow visualization experiments provide some important clues in how to approach the problem. First, the observations clearly demonstrate the cooperative motion of macroscopic portions of the fluid. Second, there is a transition which can be associated with the onset of the cooperative motion, similar to the transition observed in equilibrium phase transitions. Also, from a computational point of view, it is desirable to be able to retain the classical features of the flow. The natural framework would appear to be given in the area of critical phenomena[1]. In modern theories, an equilibrium phase transition is characterized by a change of state of the system, and is described by a wave function like field called an order parameter. Over the last decade, the

treatment of this area has become quite sophisticated, and in fact has been extended to non-equilibrium situations.

In non-equilibrium studies, it had been observed for a number of years that certain systems exhibit peculiar behavior under the right conditions[2]. Since the early observations, a rich variety of characteristics have been studied, such as limit cycles, dissipative structures, etc[3]. Theoretically, these characteristics appear as preferred solutions to the equation of motion of the system under study. In fact, it has been pointed out that these solutions act as the "elementary particles" for the system under study[4], and the study of their formation, evolution, and interactions has become an area of intense interest. The situation is similar to the existence of localized wave packets representing the elementary particles of quantum mechanics. And, analogous to the way in which superposition of wavelike properties can be replaced by particles which dominate macrosopic scales, these preferred solutions in non-equilibrium classical systems are dominant on macroscopic scales.

II. OBJECTIVES

We feel that there are two key elements of this formalism. First, mathematics have been developed which allow a link between the equations of motion for the system under study and an order parameter formalism[5]. As stated earlier, order parameter theories are efficient in describing macroscopic features of the theory. In fact, order parameters have been referred to as macroscopic wave functions. Secondly, an order parameter theory is usually phrased in terms of a Landau-Ginzburg free energy, and as a result, a constraint exists on the possible observable configurations. The preferred arrangement is the one that minimizes the free energy. In the study of the cellular structure produced by the convective instability (to be discussed in the next section), energy minimization predicts the shape of the cells, or the so-called dissapitive structures. These structures can act as the "quasiparticles" for the system, and the order parameters are associated with the probability density for finding these quasiparticles in the system.

Thus, it would seem that a workable model for the quantum interpretation can be housed in the framework of

non-equilibrium phase transitions. The summer objective was to determine the amount of influence the area has had in fluid menchanics, and specifically on the types of flow configurations of interest to the Aero-Propulsion Laboratory. We have found that the development of Benard convection cells may be very much in line with our interests. The rest of this report is devoted to a discussion of the important features of the Benard problem and how we may use them to our advantage.

III. ORDER PARAMETERS AND THE CONVECTIVE INSTABILITY

The convective instability can be observed in a well known arrangement in which an horizontal layer of fluid is heated from below so that there is a vertical temperature gradient. For low temperature gradients, heat is transferred to the upper surface by conduction, but as the gradient is increased, a marked change in behavior occurs at a specific critical temperature gradient. At the critical value, the fluid initiates a cooperative motion, which is characterized by the formation of Benard convection cells. The patterns formed by these cells can be very complex (see figure 1).

For our purpose, a major step was taken when it was realized that the transition to cellular structure could be viewed as a phase transition far from thermal equilibrium, and that the powers of modern critical phenomena could be brought to bear[5]. Specifically, Landau's concept of an order parameter could be used in the description of the transition. To see the general ideas of the procedure, we give a brief description of the treatment of the convective instability. The equations governing the mechanics are the equations of heat transport and the Navier-Stokes equation,

$$\frac{\partial u_i}{\partial t} = u_j \frac{\partial u_i}{\partial x_j} - \frac{1}{\rho_0}\frac{\partial p}{\partial x_i} + \left(1 + \frac{\delta\rho}{\rho_0}\right) g_i + \nu \nabla^2 u_i + F_i^{(u)}(\underline{x},t) \quad (1)$$

$$\frac{\partial T}{\partial t} = -u_j \frac{\partial T}{\partial x_j} + \kappa \nabla^2 T + F^{(T)}(\underline{x},t) \quad (2)$$

$$\frac{\partial u_i}{\partial x_i} = 0 \quad (3)$$

where ρ_0 is the mean density of the fluid,
$\delta\rho$ is the deviation from the mean density due to thermal expansion,
g_i are the components of the gravitational field,
ν is the kinematic viscosity,
$F^{(u)}, F^{(T)}$ are the fluctuating forces,
u_i are the components of the velocity field,
T is the temperature of the fluid.

By using appropriately defined quantities, these equations can be non-dimensionalized.

We then seek "neutral solutions", $u_K^N(x)$, which are solutions at the threshold of the instability which neither decay nor grow, ie, they are time independent. These solutions are valid at the critical temperature gradient, and can be found in the literature[7,8]. Next, a more general solution away from the instability is determined by taking a linear conbination of the neutral solutions,

$$u(\underset{\sim}{x}) = \sum_K A_K u_K^N(\underset{\sim}{x}) \tag{4}$$

where the K denotes a finite bandwidth, and expanding the quantites in the equation by a standard perterbative technique. The iteration procedure produces in a natural way an "existence condition" for the expansion coefficents in order that the iteration be consistent. We do not reproduce the mathematics, but for completeness display the general form of the result,

$$\frac{\partial A_K}{\partial t} = L A_K + N_K([A_K]) + F_K \tag{5}$$

where L is a linear operator, and N_K contains all non-linear terms. The important feature of this equation is that it is in the form of a Langevin equation for a variable A_K, and it can be shown that such an equation can be used to derive an associated Fokker-Plank equation:

$$\frac{\partial f}{\partial t} = -\iint dx\,dy \sum_K \left\{ \frac{\delta}{\delta A_K} \left[L A_K + N_K(\{A_K\}) + c.c. \right] f \right.$$
$$\left. + Q \iint dx\,dy \sum_K \frac{\delta^2}{\delta A_K \delta A_K^*} f \right. \qquad (6)$$

where f is the probability distribution function for the problem. But stationary solutions of the equation are related to a thermodynamic free energy through the relation

$$f \propto \exp\left(-\frac{\mathcal{F}}{Q}\right) \qquad (7)$$

where $\mathcal{F}$ is a free energy for the system. For the convective instability,

$$\mathcal{F} = \iint dx\,dy \left\{ \sum_K A_K^* \left(\frac{\partial}{\partial x_{(K)}} - \frac{i}{\sqrt{2}\,\pi} \frac{\partial^2}{\partial y_{(K)}^2} \right)^2 A_K \right.$$
$$\left. + \sum_K \alpha |A_K|^2 - \tfrac{1}{2} \sum_{KK'} \beta_{KK'} |A_K|^2 |A_{K'}|^2 \right\} \qquad (8)$$

where α is a Rayleigh number number dependent quantity which can be positive or negative, and the $\beta_{KK'}$ are constants. Thus, we are led to Landua's concept of macroscopic wave functions; the A_K are the order parameters for the system, and the free energy description is in one-to-one correspondence with the free energies used to treat equilibrium critical phenonema. Very simply, for gradients below the critical gradient, $\alpha < 0$, minimizing the free energy yields the result that the minimum in energy is produced when there are no "quasi-particles" in the system, while above the critical gradient $\alpha > 0$, the energy is minimized by the production of these particles, which are the result of a cooperation by the fluid in bulk. Plus, the geometric arrangement of the cooperative motion is specified by the configurations of the A_K which minimize $\tilde{\mathcal{F}}$. This calculation supports the cellular features of figure 1.

IV. THE EXTENSION TO SHEAR LAYERS

The formalism described in the previous section provides a mathematical basis for the description of ordered states in a fluid system, namely the onset of

Benard convection. These ordered states, through the use of an order parameter, describe macroscopic properties of the system which can be treated as entities in their own right. As a result, a foundation exists for the theoretical treatment of the "quasiparticle" description of the configuration. However, the instability described above is missing a key ingredient which is of great importance to experimental work at the APL; a more interesting class of flows involves a shear layer. But although shear layers are of great importance as an area of study, some of the observed characteristics of real shear flows present technical difficulties which must be treated. For example, in a splitter plate, the width of the turbulent region grows as a function of distance from the trailing edge. Also, there is a mean flow which convects vorticies downstream. As a result, structures which form evolve as a function of space and time, producing a very dynamic situation. No such complication exists in the onset of convection.

In order that progress can be made, we suggest a foundation upon which to build a description of a shear layer and the transition to turbulence. If there is a critical parameter, it is probably related to the Reynolds number, but due to the increasing width of the region of

shear, this number is not constant, but is a function of position, increasing downstream. The convective instability can be studied at fixed temperature gradient (ie, fixed Rayleigh number), so that convection cells do not evolve in time.

This changing Reynolds number allows one to see a full range of transition phenomena in one experiment, from the onset of the first instability (or, alternatively, from the appearance of the first quasiparticles) which we associate with the formation of specific types of large scale structures, all the way to the production of many "particles" in the turbulent regeme. The production and destruction of many of these interacting particles may be associated with chaotic behavior. The same set of transitions can be seen with the convective instability if the temperature gradient is continually increased.

V. RECOMMENDATIONS

If the above picture is adopted, then there is a way in which one may begin a complete study of shear layer systems. One would need an arrangement where the dynamical elements can be controlled, thereby isolating specific transition phenomena. Just such a situation

arises when the fluid is held in a vertical column and an horizontal temperature gradient is imposed. Here, the formation of large structures is driven by shear rather than simply bouyancy, but the basics are similar to that of the horizontal layer. And, once again, the critical properties can be controlled experimentally. The theoretical treatment of this arrangement with emphasis on order parameter properties will form the basis of a porposal to AFOSR through the Mini-Grant Program. If successful, the procedure will provide support for the concept of particle type behavior for more complicated shear flows. A further advantage of this configuration is that the system can be set up in a laboratory and studied experimentally in conjunction with the theoretical work carried out in the Mini-Grant Program.

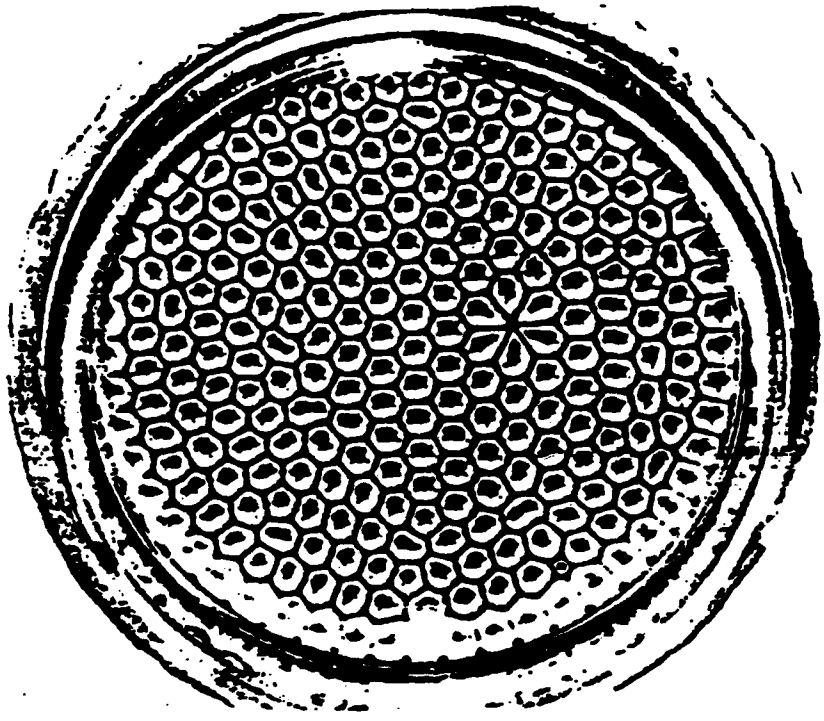

FIGURE 1. The cellular pattern of convection cells for the convective instability.

REFERENCES

1. Amit, D., Field Theory, the Renormalization Group, and Critical Phenomena (McGraw-Hill, Inc., 1978).

2. Fermi, E., Collected Works, Vol. 2 (University of Chicago Press, 1965).

3. See, for example, Supp. Prog. Theo. Phys., 64, (1978).

4. Zabusky, N., Physics Today, 36 (July, 1984).

5. Haken, H., Rev. Mod. Phys., 47, No. 1, 67 (1975).

6. Lugt, H., Amer. Sci., 73, 162 (1985).

7. Newell, A., and Whitehead, J., J. Fluid Mech., 38, part 2, 279 (1969).

8. Schluter, A., Lortz, D., and Busse, F., J. Fluid Mech., 23, part 1, 129 (1965).

1985 USAF-UES SUMMER FACULTY RESEARCH PROGRAM/
GRADUATE STUDENT SUMMER SUPPORT PROGRAM

Sponsored by the
AIR FORCE OFFICE OF SCIENTIFIC RESEARCH
Conducted by the
UNIVERSAL ENERGY SYSTEMS, INC.
FINAL REPORT

STATISTICAL BIASES IN IRLV MEASUREMENTS OF TURBULENT FLOWS

Prepared by:	Dah-Nien Fan
Academic Rank:	Professor
Department and	Mechanical Engineering
University:	Howard University
Research Location:	Aero-Optic Instrumentation Group
	Experimental Engineering Branch (AFWAL/FIMN)
	Aeromechanics Division
	Flight Dynamics Laboratory
USAF Research Colleague:	Dr. George L. Seibert
Date:	August 5, 1985
Contract No:	F49620-85-C-0013

STATISTICAL BIASES IN IRLV MEASUREMENTS OF TURBULENT FLOWS

by

Dah-Nein Fan

ABSTRACT

Biases in individual realization laser velocimeter (IRLV) measurements of turbulent flows have been topics of intense research since the first bias was reported by McLaughlin and Tiederman in 1973. A review of available literature on the subject reveals (i) the existence of 14 different sources of statistical biases in IRLV, (ii) 10 schemes proposed for bias corrections of IRLV raw data, and (iii) the critical need of a comprehensive theory capable of predicting the joint effects of a multitude of bias sources in a realistic experimental IRLV setup. This report advocates a major thrust toward constructing a theoretical yet realistic bias model of an entire IRLV system. Such a theory when completed should not only lay to rest the decade-old confusion and controversy in interpreting IRLV data, but also remove the last remaining major obstacle in the development of IRLV system as an independent tool for flow diagnostics. Taking a first step in this direction, this report describes some of the important components in a general statistical model suitable for analyzing IRLV biases. Results from a few elementary models are also described in some detail.

"This document was prepared under the sponsorship of the Air Force. Neither the US Government nor any person acting on behalf of the US Government assumes any liability resulting from the use of the information contained in this document or warrants that such use will be free from privately owned rights."

ACKNOWLEDGMENTS

The author wishes to express his appreciation to Dr. George L. Seibert, Technical Manager of the Aero-Optic Instrumentation Group, AFWAL/FIMN, for suggesting the research and reviewing this report. Thanks are also due to Messrs Charles H. O'Heren, Dean C. Miller, Clifford B. Weissman, members of the Aero-Optic Group for their assistance.

The sponsorship of the Air Force Systems Command, Air Force of Scientific Research USAF, and the administrative support of the Universal Energy Systems, Inc. are hereby gratefully acknowledged.

I. INTRODUCTION

An individual realization laser velocimeter (IRLV) is a laser Doppler velocimeter (LDV) with optical arrangements in the dual-beam model [1]. Laser Doppler velocimetry, a nonintrusive technique for flow measurements, has seen intense development and made great strides since its debut a little over two decades ago [2]. In the meantime the IRLV has evolved as the most versatile among various LDV systems, e.g. the reference-beam and the two-spot, for flow diagnostics. It is estimated [3] that about 80-90 percent of all fluid flow measurements, attempted by means of LDV, can be satisfactorily carried out by IRLV. (Reference-beam anemometers are advantageous at high particle concentrations.)

Rather than sensing directly the fluid velocity, what an IRLV actually measures is the velocity of, or the Doppler frequency of the light scattered by a set of particles naturally present or artificially seeded in the conveying fluid. While traversing by chance the measuring volume of an IRLV, a particle for its velocity to be recorded as a valid data point, must scatter light within a preset range of intensity and cross enough interference fringes. It is not difficult to see that IRLV measures the true velocity of the conveying fluid if the scattering particles are "frozen" (as far as their motions are concerned) in the fluid and the flow is steady. However the situation is quite different if the flow to be diagnosed is a fluctuating or turbulent one.

In a turbulent flow the statistics of the velocities of IRLV sampled particles renders, in general, a biased description of the random motion of the conveying fluid. The ultimate goal of IRLV diagnostics of a turbulent flow is the determination of its velocity probability density function (PDF) from which the mean velocity, the Reynolds' stress, energy spectrum and higher-order moments of velocity can be deduced. Specifically, the complication is that the velocity histogram constructed from IRLV measurements is that of the recorded set of particles, which after normalization is not necessarily equal to the PDF of the underlying turbulent flow. As a matter of fact, significant bias can exist

even in the absence of particle lag when light-scattering particles are of submicron sizes. A bias occurs whenever the chance of a particle making a measurement is dependent upon its velocity. Potential sources of bias permeate an IRLV system. They can be at the measuring volume due to particle arrival statistics and optical arrangements, at the photomultiplier, in the detection/validation electronics, and even in the data-handling algorithms.

The list of IRLV statistical biases reported in literature over the years is a long one. The earliest known bias is the so-called individual realization bias [4]. It arises because a larger than average mass of fluid, and hence a larger than average number of scattering particles, passes through the measuring volume during periods when the velocity is faster than the mean. By the same token a smaller mass of fluid and a smaller number of scattering particles pass through the measuring volume during periods when the velocity is smaller than the mean. In addition to the individual realization bias, nine biases were documented in [5]. They are

comparator tolerance bias
clock accuracy bias
incomplete signal bias
particle acceleration bias
negative velocity bias/directional ambiguity
frequency cut-off bias
particle lag bias
particle distribution bias
multiple particle bias

However, the list above is still incomplete. The possibility of compressibility bias [6] in high-speed turbulent flows must be added. In [7] the dependence of statistical flow quantities on the averaging mode (data-handling algorithm) was noted. It should be mentioned in this connection the biasing effects of a sample-and-hold processor on

IRLV measurements was investigated recently in detail [8]. The less obvious photodetector bias due to the dependence of Doppler signal amplitude and visibility at the output from the photomultiplier on particle velocity was observed in [9]. In [10] the Bragg cell bias, or multiple measurements bias was reported. Sources of biases are numerous indeed.

To gain a crude idea on the relative importance of various biases the following figures are taken from Table 7 in [5]. The percentages quoted are valid strictly for the specific set of parameter values investigated in [5].

Individual realization bias	1 - 13%
Comparator tolerance bias	0.5 - 13%
Incomplete signal bias	0.4 - 15%
Particle acceleration bias	0.1 - 0.7%
Clock accuracy bias	0.1%
Negative velocity bias	0.4%
Frequency cut-off bias	any value depending on the cut-off frequency setting

That the Bragg-cell bias can compensate to a large degree the individual realization bias was reported in [10]. The compressibility bias is likely of the order of the square of the turbulence Mach number which, according to [25], has a value no more than 0.2 even in strong shear layer with main stream Mach numbers up to 5. The particle-lag bias of particles with diameters less than about 0.2 μm [3, p.350] is insignificant even in high speed flows. In [26] 2-8 percent lower mean velocities near the wall in the turbulent boundary layer were attributed to effects of artificial seeding or concentration gradient. Magnitude of photomultiplier bias like the frequency cut-off bias can vary geatly, e.g. $\pm$50%, depending on the discrimination-level setting [9].

Now the host of biasing factors interacts nonlinearly. The nonlinearity and the multitude of biasing factors mentioned earlier have confounded attempts to mitigate biases in IRLV turbulence measurements. To be sure some biases can be significantly reduced through frequency

shifting, the use of submicron seeding particles, the selection of proper trigger-threshold and comparator-tolerance settings, operating IRLV at low seeding concentrations so multi-particle events are rare, and decreasing the size of the measuring volume. Refer to [11] for a more detailed discussion. Nevertheless eliminations here can never be complete.

Thus if physical significance is to be attached to IRLV measurements of a turbulent flow field, it is apparent that a correct means of handling or processing the potentially biased experimental data must be provided to compensate the combined net biasing effect existing in a particular IRLV experiment. Accepting the hypothesis of ergodicity, statistical quantities of turbulence can be derived from time intergrals or time averaging. For IRLV measurements with mean date rates greater or of the order of the highest frequency contributing to the turbulence spectum, the mean velocity of a turbulent flow field can be well approximated, say, by a trapezoidal algorithm to the turbulent velocity versus time curve. Hence both velocity and time measurements are needed [12]. For sparsely seeded flows the state is a confusing, if not controversial, one. Bias-correction algorithms and recommendations for IRLV data processing abound, garnished with their respective proponents and detractors. Algorithms reported in literature include

the reciprocal of speed weighting [4] (Its application requires three-dimensional velocity data.)

the harmonic average [4] (An approximation to the previous scheme requires only the predominant velocity component.)

the residence - time weighting [6, 7] (This requires the simultaneous measurements of a velocity component as well as the time duration of the Doppler signal. The derivation given in [6] without considering the mass of particle-conveying fluid swept into the measuring volume, is ques tionable. From [7] it can be seen that qualitatively the idea behind this scheme is similar to the first one.)

the particle-interarrival-time weighting (Its implementation requires measurements of time elapsed between successive velocity recordings [13] in addition to the velocity com ponent itself; in [14] the weighting factor is taken to be the separation time between a high quality (thus recorded) burst and the next detectable low-quality burst.)

the combined velocity and Bragg-cell biases correction [10]

random sampling of recorded data [15]

constant time-window ensemble-averaged algorithm [16]

the arithmetic ensembled average (This time honored simple scheme was recently advocated implicitly in [17]).

equal-time sampling (In [18] the first-data point in each time interval is sampled; in [19] instead the velocity closest to the middle of the window is considered to represent the fluid velocity at this time interval.)

To account for biases in IRLV data from turbulent velocity measurements, an experimentalist today is facing no less uncertainties than his/her predecessors did a decade ago. This is unfortunately so in spite of the euphoria of the late seventies [20] that problems in signal processing and data analysis (thus bias correction) seemed to be well understood and methods then existing were adequate. To indicate how far the pendulum has swung in the opposite direction, the following quotes appear to summarize the prevailing mode of despair.

". . . No theory can adequately predict these statistics as many uncontrollable and unmeasurable variables in the system can influence the statistics to an important degree. Therefore unless the rather specialized and rare conditions of many measurements per flow correlation times are obtained, one should not use any of the previously proposed "corrections." . . ." [17].

". . . It is necessary to apply a number of different techniques to the same raw data before one can ascertain

the flow velocity. . . . The main difficulty is in deciding which bias correction to adopt. . . ." [19].

It is important that one must not lose sight of the significant amount of ground work having been laid over the years in delineating various aspects of IRLV operation, which can lead to statistical biases. The culprit of the current depressing state of affair seems to be the lack of a comprehensive statistical theory which bases its bias-correction predictions on the system analysis of a realistic statistical model of an entire IRLV experimental setup. Because of the number of different time scales and parameters involved, such a theory is necessarily complex and is by no means trivial to construct. Its importance can never be overestimated if IRLV is to realize its full potential as an indepenent diagnostic tool for flow configuration where no other techniques can provide benchmark measurements for comparison.

IRLV statistical biases including particle lag in laser velocimetry have been major concerns to the Aero-Optic Instrumentation Group (AFWAL/FIMN). The work reported herein is the first theoretical investigation of biases undertaken within the Group. Previously, the Group relied on experimental verification of known flows to determine system bias (if any) and then an analysis of the proposed experimental set-up to estimate if bias would be a problem.

II. OBJECTIVES OF THE RESEARCH EFFORT

The objectives of the research effort are

to review available literature on statistical biases in IRLV measurements of turbulent flows,

to assess the need of bias-correction algorithms, if at all, in interpreting IRLV raw data,

to identify areas where additional research in IRLV statistical biases can be most beneficial, and

time permitting, to initiate preliminary research on a critical area identified above for possible follow-on work through the mini-grant program.

All the above research objectives have been successfully accomplished to a great degree, considering the total effort is restricted to a period of ten weeks.

III. PRELIMINARIES TO SYSTEM ANALYSIS OF IRLV BIASES

3.1 Rationale

Reasons for undertaking a system approach to IRLV bias analysis are that

- the nonlinear couplings among the 14 bias sources render compensation schemes generated by analysis of single bias sources inadequate, if not useless.
- the dependence of bias compensation on relevant physical parameters can come about only through a system analysis and system analysis will predict quantitatively the net compensation to IRLV raw data under a given experimental setup.

3.2 Premises

The approach is statistical/stochastic. The following assumptions are made in the IRLV bias model.

- Scattering particles are sufficiently small so particle lag bias is not considered.
- The IRLV system is ideal. Thus optics are perfect and there are no noises present.
- The turbulence is stationary.
- The specific particle number (number of particles per unit fluid mass) is a constant.
- The size distribution of particles is specified, e.g. size PDF as a function of equivalent aerodynamic/optical radius.
- Particle arrival statistics at a measuring volume is Poisson [21].

3.3 Measuring Volume

The measuring volume of a particle is defined to be the volume enclosed by a surface where the particle will first scatter light of sufficient intensity to trigger the detection electronics. Thus the

measuring volume is a function of laser power, optical arrangements, particle size, photomultiplier and amplifier settings, and threshold level [12, 22].

3.4 System Model

The probabilistic model can be considered to be a cascade system in terms of conditional PDF's [17]. The apparent particle-velocity PDF, $P_a(\vec{v})$ is thus expressed as

$$P_a(\vec{v}) = \int_0^\infty Q_4\{Q_3,Q_2,Q_1,P\}Q_3\{Q_2,Q_1,P\}Q_2\{Q_1,P\}Q_1\{P\}P(\rho,\vec{v})d\rho \qquad (1)$$

where $P(\rho,\vec{v})$ is PDF of density ρ and velocity $\vec{v}$ of the turbulent flow at a point common to all measuring volumes, $Q_1\{P\}$ is conditional probability of a particle arriving at its measuring volume when the fluid there has density ρ and velocity $\vec{v}$, $Q_2\{Q_1,P\}$ is the conditional probability of the particle triggering the IRLV counters, $Q_3\{Q_2, Q_1,P\}$ is the conditional probability of the particle having triggered the counters for recording a measurement, and $Q_4\{Q_3,Q_2,Q_1,P\}$ is the conditional probability accounting for distortion (or compensation) in PDF due to data-handling algorithms.

If the product of conditional probabilities is independent of ρ and $\vec{v}$, then $P_a(\vec{v})$ is identical to the turbulent velocity PDF, $P(\vec{v})$. The IRLV is then unbiased. Otherwise it is said to be statistically biased. An ideally compensated system would have Q_4 proportional to the reciprocal of $Q_3Q_2Q_1$ if the later does not vanish. It should be noted that information on the turbulent flow is last in domains where a conditional probability vanishes. This is easily seen in the case of incompressible flow where $P(\vec{v})$ is obtainable as $(Q_4Q_3Q_2Q_1)^{-1}P_a(\vec{v})$ (except for a possible normalization factor) only if the product $Q_4Q_3Q_2Q_1$ does become zero.

Now each Q_i, i=1,2,...,4, is associated with some of the IRLV biases discussed in I. The associations are summarized as follows:

Q_1 - Individual-realization bias, finite measuring-volume effect, dead-time effect, and compressibility bias.

Q_2 - Photomultiplier bias.

Q_3 - Incomplete-signal bias, comparator-tolerance bias, clock-accuracy bias, particle-acceleration bias, multiple-particle bias, photomultiplier bias, Bragg-cell bias, frequency cut-off bias, and finite measuring-volume effect.

Q_4 - Data-handling algorithm (e.g. the use of any bias-correcting scheme mentioned in I.), data-editing bias (e.g. the elimination of measurements outside, say, $\pm 3\sigma$), and compensator algorithm, if any.

Some of the above mentioned biases or effects have been quantified in literature, but a number of them are at present only qualitatively described and need more research.

3.5 Three-Dimensional Considerations

It is essential that three-dimensional effects be fully considered in any system model. Turbulence is inherently three-dimensional. Moreover, it was reported [23] that one-dimensional analysis tends to overestimate possible bias errors, for example, due to correlations between velocity and particle concentration.

3.6 A Necessary Condition

A necessary condition for any system model of IRLV statistical biases to be valid is that in the limit when the time interval between successive measurements tends to zero uniformly throughout a sufficiently long measuring period, all biasing effects vanish (without introducing spurious Q_4).

IV. SOME ELEMENTARY STATISTICAL BIAS MODELS

4.1 Omnipotent Processor

An omnipotent processor is a hypothetical processor capable of measuring every and all particles arriving separately or simultaneously at the measuring volume, and recording each particle's velocity once.

Consider an IRLV system with an omnipotent processor enabled for a time interval τ with $Q_2=1=Q_3=Q_4$, so only Q_1 is to be investigated.

According to the Poisson distribution the conditional probability (when the fluid at the measuring volume has density ρ and velocity $\vec{v}$) of k particles arriving at the volume during the sampling time τ is [21]

$$q_k = \frac{(\beta A_1 \rho V \tau)^k}{k!} \exp(-\beta A_1 \rho V \tau) \tag{2}$$

where β is the specific particle number (per unit mass of fluid), and A_1 is the maximum cross sectional area of the measuring volume in the direction perpendicular to the velocity $\vec{v}$. Thus A_1 is a function of the direction of $\vec{v}$ as well as the particle size. The expected number of data points of $(\vec{v}, \rho)$ is therefore

$$\sum_{k=1}^{\infty} k q_k = \beta A_1 \rho v \tau \tag{3}$$

For a given particle size or monodisperse particles, equation (1) gives

$$P_a(\vec{v}) = A_1 V \tau \int_0^{\infty} \beta \rho P(\rho, \vec{v}) d\rho / \alpha \tag{4}$$

where the normalization factor α, a constant, is given by

$$\alpha/\tau = \int_{\infty} A_1 v \int_0^{\infty} \beta \rho P(\rho, \vec{v}) d\rho d\vec{v} \tag{5}$$

($d\vec{v}$ is a differential volume element in the velocity space.)

A few important points should be noted in equations (4) and (5). First the total measurement time τ does not appear in $P_a(\vec{v})$. However; τ must be long enough to record a sufficiently large number of data points so statistical fluctuations in the mean quantities of interest are within desired error bounds.

Second, $P_a(\vec{v})$ can be determined from the velocity histogram of IRLV measurements. The central task of bias compensation is to recover the turbulent velocity PDF

$$P(\vec{v}) = \int_0^\infty P(\rho,\vec{v})d\rho \tag{6}$$

from equations (4). Compressibility and paricle-distribution biases manifest themselves in the integral in equation (4). Finite measuring-volume effect is reflected in A_1.

If the seeding is uniform and the flow is incompressible, then one has

$$P_a(\vec{v}) = A_1 V P(\vec{v}) / \int_{-\infty}^{\infty} A_1 V P(\vec{v})d\vec{v} \tag{7}$$

So $P(\vec{v})$ is proportional to $(A_1 V)^{-1} P_a(\vec{v})$ if v is nonzero. Equation (7) quantifies the individual-realization bias [4] provided A_1 is determined for every measuring volume (particle size) and for every direction in an IRLV setup.

4.2 Single Measurement in a Constant Time Interval

A somewhat more realistic situation is to modify the omnipotent processor in 4·1 such that it can only register one data point per sampling time τ. The conditional probability of <u>at least</u> one particle arriving at the measuring volume is

$$1 - \exp(-\beta A_1 \rho V \tau)$$

Again take $Q_2 = 1 = Q_3$; but Q_4 is such that each cycle that records a measurement is assigned the weight = 1 and a cycle without measurement is given the weight = 0. When a sufficiently large number of measurements has been made, the measured apparent PDF is

$$P_a(\vec{v}) = \int_0^\infty [1-\exp(-\beta A_1 \rho V \tau)]P(\rho,\vec{v})d\rho/d\alpha \tag{8}$$

where the normalization constant α now is equal to

$$\int_{-\infty}^{\infty}\int_0^\infty [1-\exp(-\beta A_1 \rho v \tau)]P(\rho,\vec{v})d\rho d\vec{v}$$

In the limit $\beta A_1 \rho v \tau << 1$ only single-particle arrivals contribute to measurements. Then equation (8) is equivalent to equation (4). The incompressible case was studied in [24].

It was argued in [18] that $P_a(\vec{v})$ vanishes if the speed of the particle is less than the ratio of the length of the (one-dimensional) measuring volume to the sampling time τ. This is questionable because there is a finite probability of finding a particle in the measuring volume when the processor is enabled; namely not all particles recorded are necessarily swept into the measuring volume during the time period 1. This is especially so when fringe shift is used.

It is apparent that the conditional probability used in this section does not include the effects of multiple-particle bias. An attempt was made in [18] to incorporate the multiple-particle bias in the theoretical one-dimensional analysis. It was shown that the multiple-particle bias leads to further overestimate in the mean velocity and underestimate of the turbulence intensity.

4.3 The Sample-and-Hold Processor

The sample-and hold processor is a D/A device wherein the results of the last successful measurement is held until the next successful measurement. This data-handling scheme weights a measurement by the interarrival time to the next successful measurement. In [8] the particle-sampling statistics was investigated when both individual-realization bias and the time-between-measurements weighting were present.

The analysis in this case is quite involved. Because of page limitations it will not be described here.

4.4 A Detector with a Dead Time

If a detector with a dead time T measures the velocity of a particle, say at the time t=0, it is again able to measure <u>another</u> particle after a time interval T has elapsed. The conditional probability that a particle is accepted at t=0, given the velocity $\vec{v}$, is the probability that a particle arrives at the measuring volume at t=o and that no particles have been accepted in the time interval $-T<t<0$.

The analysis of the present case is also given in [8] and will not be described here.

V. RECOMMENDATIONS

Two data-handling recommendations and one research recommendation are presented to the Aero-Optic Group, AFWAL/FIMN based upon information reviewed in this study.

5.1 Data-Handling Recommendatons

It is recommended that if the time between successive data points in IRLV measurements of turbulent flows is much less than the turbulent flow correlation time, then the time-averaged algorithm of [12] should be adopted in determining statistical quantities. Specific steps to implement the algorithm are as follows

Experimental-data set of the form {(ti,Ui),i=1,2,...,N} is required, where t_i is the time of the i-th measurement and U_i is the i-th measurements of a velocity component.

The mean-velocity component u is calculated by

$$\bar{u} = \frac{1}{T}\sum_{i=2}^{N} U_i \Delta t_i \qquad (9)$$

where $T=t_n-t_1$, and $\Delta t_i=t_i-t_{i-1}$

(or by a trapezoidal approximation

$$\bar{u} = \frac{1}{2T}\sum_{i=2}^{N} (u_i+u_{i-1})\Delta t_i \qquad (10)$$

for better accuracy.)

The mean-square fluctuating-velocity component $\overline{u'^2}$ is calcu lated by

$$\bar{u'^2} = \frac{1}{T}\sum_{i=2}^{N} u_i'^2 \Delta t_i \qquad (11)$$

where $u_i' = u_i - \bar{u}$

The autocorrelation function $R_{uu}(\tau)$ is calculated by

$$R_{uu}(\tau) = \frac{1}{t_m - t_1} \sum_{i=2}^{M} u_i' u_i'(t_i+\tau)\Delta t_i, \quad \tau > \frac{T}{N-1} \tag{12}$$

where $t_{N-1} < t_M + \tau < t_N$ and $U_i'(t_i + \tau)$ is the linearly interpolated value of the velocity component at $t=t_i + \tau$, i.e.,

$$u'(t_i + \tau) = Uj' + (t_i + \tau - tj)\ \Delta Uj / \Delta tj \tag{13}$$

where $t_{j-1} < t_i + \tau < tj$, and $Uj = Uj - Uj-1$.

It is further recommended that in all other instances the ensemble (arithmetic) - averaged algorithm of [27], for example, should be adopted in determining statistical quantities until new information indicates otherwise. Specific steps to implement the algorithm are as follows.

Experimental-data set of the form $\{(u_i),\ i=1,2,\ldots,N\}$ is required ($N \approx 800$ is recommended).

The mean-velocity component $\bar{u}$ is estimated by

$$\bar{u} = \frac{1}{N} \sum_{i=1}^{N} u_i \tag{14}$$

The mean-square fluctuating-velocity component $\overline{u'^2}$ is estimated

$$\overline{u'^2} = \frac{1}{N} \sum_{i=1}^{N} (u_i - \bar{u})^2 \tag{15}$$

The estimated standard deviation σ_e is

$$\sigma_e = (\overline{u'^2})^{1/2} \quad , \text{ if } N >> 1 \tag{16}$$

The raw experimental-data set is statistically edited by applying the Chauenet's criterion, i.e., for the 95% confidence

level all data which lies outside $\pm 2\sigma$ from the mean is rejected. The edited-data set is now

$$\left\{(u_i),\ -2\sigma_e \le u_i - \bar{u} \le 2\sigma_e,\ i = 1,2,\cdots,M,\ M \le N\right\}$$

Final values of $\bar{u}$, $\overline{u'^2}$ and σ_e are estimated by repeating once previous steps with the edited-data set.

The population means u and σ are given by

$$u = \bar{u} \pm 2\sigma_e/\sqrt{M} \tag{17}$$

$$\sigma = \sigma_e \pm \sqrt{2}\sigma_e/\sqrt{M} \tag{18}$$

for the 95% confidence level. Thus if the sample standard deviation σ_e is to differ from the population standard deviation by no more than 5%, the value of M must be no less than 780.

5.2 A Research Recommendation

It is recommended that research toward the final goal of predicting the combined effects of statistical biases in an IRLV experimental set-up be initiated using the systems approach described herein this report as a new departure.

Need: There exists no rational theory which adequately predicts the net compensation required to interpret IRLV measurements of turbulence in the presence of a multitude of statistical biases. The need of such a theory is critical.

Significance: The proposed research, if successful, will remove the last remaining obstacle in the development if IRLV system as an independent tool for flow diagnostics, so experimentalists will have a theoretically-based method to reduce biased IRLV measurements of turbulent flows.

Rationale for Using Systems Approach: Please refer to Section 3.1 in this report for rationale.

Approach: The proposed research can be divided into three major phases in sequence.

(1) System Modeling - The goal of the first phase is to establish the governing relation or equation between the probability density function (PDF) of IRLV measured velocity (Input to the system) to PDF of the turbulent flow (Output). Tasks in this phase include (a) assessing the relative importance of the 14 or so sources of statistical biases surveyed earlier in this report, (b) deriving a quantitative relation for each source or a combination of sources characterizing its (their) biasing effects to be used in the system model (At present these relations are either nonexistent or too restrictive and in need of generalization.), (c) establishing a system model for analyzing biases consistent with IRLV-system operations, (d) deducing the governing input-output PDF equation and the nondimensional parameter appeared therein.

(2) System Analysis - The two goals of the second phase are (a) to investigate mathematically consequences and adequacy of the system model for IRLV biases, and revise/refine the system model, if needed and (b) to propose a practical scheme for bias correction based on theoretical predictions of the system model. Tasks in this phase include (a) investigating general mathematical properties of the PDF input-output equation derived in Phase (1), (b) studying in detail consequences of the PDF equation in the limit of high IRLV data rates and in slowly decaying isotropic turbulence, (c) from insights gained in (a) and (b), refining or modifying the system model if desirable, and (d) to establish a practical scheme for bias compensation of IRLV measurements of turbulence, in particular to identify the set of flow quantities to be measured, e.g. velocity, interarrival time, residence time, density, ..., etc., in order to implement the bias correction.

(3) Experimental Verificaton and System Synthesis - In this phase the bias-compensation scheme established in phase D(2) is to be mechanized for on-line IRLV-data processing or for off-line stored-data

reduction by computers. At this point dedicated IRLV experiments measuring the required set of quantities will be suggested for verification of the bias-correction computer code derived from the system bias model.

Scope of Work Proposed for Mini Grant: It is proposed that the tasks described in phase (1) System Modeling above constitute the scope of work of a possible mini-grant award. Because of the magnitude and complexity of the proposed research, substantial additional funds will be needed to carry out the subsequent tasks of phases (2) and (3). It is felt that with the mini-grant as the seed money, the chance of obtaining support for continuing research on bias compensation of IRLV measurements of turbulent flows will be greatly enhanced.

REFERENCES

1. F. Durst, A. Melling, and J. H. Whitelaw, Principles and Practice of Laser-Doppler Anemometry, New York, Academic Press, 1976, p. 9.
2. Y. Yeh, and H. Z. Cummins, "Localized Fluid Flow Measurements with an He-Ne Laser Spectrometer," Applied Physics Letters, Vol. 4, No. 10, May 1964, pp. 176-178.
3. Ref. 1, p. 318.
4. D. K. McLaughlin, and W. G. Tiederman, "Biasing Correction for Individual Realization of Laser Anemometer Measurements in Turbulent Flows," The Physics of Fluids, Vol. 16, No. 12, December 1973, pp. 2082-2088.
5. R. D. Flack, and H. D. Thompson, "The LDV's Potential in Understanding Tubulent Sturcture," Proc. Minnesota Symposium on Laser Anemometry, Bloomington, Minnesota, October 1975, pp. 1-67.
6. W. K. George, Jr., "Limitations to Measuring Accuracy Inherent in the Laser Doppler Signal," The Accuracy of Flow Measurements by Laser Doppler Methods, Skovlunde, Denmark, 1976, pp. 20-63.
7. J. M. Owen, and R. H. Rogers, "Velocity Biasing in Laser Doppler Anemometers, "The Accuracy of Flow Measurements by Laser Doppler Methods, Skovlunde, Denmark, 1976, pp. 89-114.
8. R. V. Edwards and A. S. Jenson, "Particle-Sampling Statistics in Laser Anemometers: Sample-and-Hold Systems and Saturable Systems," J. Fluid Mech., Vol. 133, 1983, pp. 397-341.
9. D. F. G. Durao and J. H. Whitelaw, "Relationship Between Velocity and Signal Quality in Laser Doppler Anemometry," J. Phys. E: Sci. Instrum., Vol 12, 1979, pp. 47-50.
10. J. F. Meyers and J. I. Clemmons, Jr., "Processing Laser Velocimeter High-Speed Burst Counter Data," Laser Velocimetry and Particle Sizing, Edited by H. D. Thompson and W. H. Stevenson, Hemisphere Publishing Corporation, Washington, 1979, pp. 300-313.
11. T. C. Roesler, W. H. Stevenson, and H. D. Thompson, "Investigation of Bias Errors in Laser-Doppler Velocimeter Measurements," Tech-

nical Report AFWAL-TR-80-2105 (AD A 097040), December 1980, 78 pages.

12. P. E. Dimotakis, "Single Scattering Particle Laser Doppler Measurements of Turbulence," Applications of Non-Intrusive Instrumentation in Fluid Flow Research, AGARD-CP-193, 1976, paper 10.
13. D. O. Barnett and H. T. Bentley, III, "Statistical Bias of Individual Realization Laser Velocimeter," Proc. the Second International Workshop on Laser Velocimetry, Vol I, Engineering Experiment Station Bulletin No. 144, Purdue University, 1974, pp. 428-442.
14. W. Hoesel and W. Rodi, "New Biasing Elimination Method for Laser-Doppler Velocimeter," Rev. Sci. Instrum., Vol. 48, No. 7, July 1977, pp. 910-919.
15. D. F. G. Durao and J. H. Whitelaw, "The Influence of Sampling Procedures on Velocity Bias in Turbulent Flows," The Accuracy of Flow Measurements by Laser Doppler Methods, Skovlunde, Denmark, 1976, pp. 138-149.
16. F. Durst, F. Ernst, and M. Founti, "A New Counter Signal Processor for True Time-Averaged Fluid Velocity Measurements," Proc. Second International Symposium on Applications of Laser Anemometry to Fluid Mechanics, Lisbon, Portugal, 1984, paper 4.4.
17. R. V. Edwards and J. F. Meyers, "An Overview of Particle Sampling Bias," Proc. Second International Symposium on Applications of Laser Anemometry to Fluid Mechanics, Lisbon, Portugal, 1984, paper 2·1.
18. R. V. Edwards, "A New Look at Particle Statistics in Laser Anemometer Measurements," J. Fluid Mechanics, Vol. 105, 1981, pp. 317-325.
19. M. Biffin, T. C. Claypole, H. P. Evans, S. Narayanan, and N. Syred, "The Influence of Particle Arrival Rate," Proc. Second International Symposium on Applications of Laser Anemometry to Fluid Mechanics, Lisbon, Portugal, 1984, paper 2·5.

20. W. H. Stevenson, "A Historical Review of Laser Velocimetry," Laser Velocimetry and Particle Sizing, Edited by H. D. Thompson and W. H. Stevenson, Hemisphere Publishing Corporation, Washington, 1979, pp. 1-12.

21. W. Feller, An Introduction to Probability Theory and Its Applications, Vol I, John Wiley and Sons, Inc., New York, 1968, p. 156.

22. M. C. Whiffen, J. C. Lau, and D. M. Smith, "Design of LV Experiments for Turbulence Measurements," Laser Velocimetry and Particle Sizing, Edited by H. D. Thompson and W. H. Stevenson, Hemisphere Publishing Corporation, Washington, 1979, pp. 197-207.

23 J. O. Asalor and J. H. Whitelaw, "The Influence of Combustion-Induced Particle Concentration Variations in Laser-Doppler Methods, Skovlunde, Denmark, 1976, pp. 115-137.

24. R. V. Edwards, "How Real Are Particle Bias Errors?" Laser Velocimetry and Particle Sizing, Edited by H. D. Thompson and W. H. Stevenson, Hemisphere Publishing Corporation, Washington, 1979, pp. 79-85.

25. J. O. Hinze, Turbulence, McGraw-Hill Book Co., New York, 1975, p. 310.

26. D. A. Johnson, W. D. Bachalo, and D. Modarress, "Laser Velocimeter Supersonic and Transonic Wind Tunnel Studies," Proc. Minnesota Symposium on Laser Anemometry, Bloomington, Minnesota, October 1975, pp. 68-82.

27. W. J. Yanta, "Turbulence Measurements with a Laser Doppler Velocimeter," NOLTR 73-94, May 1973, 77 pages.

1985 USAF-UES SUMMER FACULTY RESEARCH PROGRAM

Sponsored by the

AIR FORCE OFFICE OF SCIENTIFIC RESEARCH

Conducted by the

UNIVERSAL ENERGY SYSTEMS, INC.

FINAL REPORT

ANALYTICAL METHODS FOR THE DETERMINATION OF CHOLESTEROL AND CHOLESTEROL ESTERS IN SALIVARY FLUIDS

MACK FELTON, JR., Ph.D.

PROFESSOR OF BIOLOGY

DEPARTMENT OF BIOLOGY

SOUTHERN UNIVERSITY-NEW ORLEANS

USAF SCHOOL OF AEROSPACE MEDICINE,

BROOKS AIR FORCE BASE, TEXAS 78235-5301

DR. HARVEY A. SCHWERTNER

AUGUST 23, 1985

F49620-85-C-0013

ANALYTICAL METHODS FOR THE DETERMINATION OF CHOLESTEROL AND CHOLESTEROL ESTERS IN SALIVARY FLUIDS

Abstract

Gas-liquid chromatography is the analytical method recommended for quantitating cholesterol and cholesterol esters in salivary fluids. This selected method has the sensitivity for studying the effects of diurnal variation and the effects of salivary flow rates on cholesterol concentrations. Development of a non-invasive method for predicting coronary disease in Air Force flying personnel is desirable. The patient population that comes to the Aeromedical Consultation Service at Brooks Air Force Base for evaluation is unique. These air crewmen differ from civilian populations in that they are much younger and are mostly asymptomatic for heart disease. An attempt was made to express concentrations of cholesterol and cholesterol esters on a creatinine and sodium basis. An exhaustive literature search strongly supports the selection of gas-liquid chromatography as the method to continue this investigation, but does not support use of the parameters, creatinine and sodium. Other biochemical parameters will be considered for correlation with cholesterol and cholesterol esters concentrations. Establishment of a relationship between cholesterol and cholesterol esters concentrations in human blood serum and saliva would facilitate the development of the non-invasive method for securing biological fluids from patients. Improved experimental design should play a large role in bringing the goal and purpose of this investigation to fruition.

INTRODUCTION

The purpose for this study was to develop a non-invasive method for predicting CAD in relatively young, asymptomatic air crew members. Various gas-chromatographic methods for analyzing cholesterol and cholesterol esters in salivary fluids will be evaluated. In addition, we will identify possible effects of diurnal variation and the effects of salivary flow rates on cholesterol concentrations. An interesting aspect of this investigation is that the Air Force personnel that are referred to the Aeromedical Consultation Service at Brooks Air Force Base for medical examinations differ markedly from civilian populations. They are usually younger than the civilian population and are mostly asymptomatic for heart disease. We are especially interested in the detection of early stages of coronary artery disease since it would allow preventative measures to be taken before severe disease takes place.

The analytical method selected for quantitating cholesterol and cholesterol esters in salivary fluids was gas-liquid chromatography. This technique was selected because of its high sensitivity and accuracy (Metcalfe, 1971) (Ferrel, 1977) (Derks, 1985)[12,6,5]. Gas-liquid chromatography has the capacity to measure substances in the micro and nanogram concentration range.

Biological parameters utilized in diagnostic tests for patient evaluation were correlated to cholesterol and cholesterol esters. There was no documented evidence in the literature that would allow expressing cholesterol and cholesterol esters on a creatinine or sodium basis (Chiou et al, 1977) (Chiou and Pu, 1979) (Golland and Mookerjee,

1978)[3,4,7]. Some of the other biological parameters can be examined to determine if a relationship to concentrations of cholesterol and cholesterol esters exist.

Future investigations planned will include attempts to correlate the concentrations of cholesterol and cholesterol esters in blood serum to the concentrations of cholesterol and cholesterol esters in saliva. The need to establish the quantitative relations between serum and saliva is essential to achieve the goal and purpose of this project. However, there can be qualitative benefits from these endeavors that could lessen the number of times that invasive methods must be used.

The Summer Faculty Fellow, Mack Felton, Jr., had the pleasure of participating in the Summer Research Program in the summer of 1982, here at Brooks Air Force Base School of Aerospace Medicine. Dr Raymond G. Troxler was the Brooks Air Force Base colleague that shared the research problem in the summer of 1982. The research interest of the summer of 1982 involved a study designed to predict coronary heart disease. Although, the problem was not totally solved, there was evidence that the project had serious merit. The conclusion was that the problem might be approached, statistically utilizing prescribed formulas along with computer assistance.

Mack Felton, Jr. and Dr Harvey A. Schwertner, became acquainted during the summer of 1982. There were several informal discussions about lipid research which was the common thread in the Clinical Pathology Branch at Brooks Air Force Base. The principals agreed they would like to collaborate on research related to lipid analyses. Dr. Schwertner graciously accepted Mack Felton, Jr. as a Summer Research Fellow to work in his laboratory this summer, 1985.

At the master's and doctoral level, Mack Felton, Jr., had formal course work in endocrinology, neurophysiology, biochemistry, radiation chemistry, isotope methodology and activation analysis. However, the greatest concentration of course work was in the field of microbiology.

OBJECTIVE OF THE RESEARCH EFFORT

The goal of this summer's research program was to develop analytical methods for quantitating cholesterol and cholesterol esters in salivary fluids. The effects of diurnal variation and the effects of salivary flow rates on cholesterol concentrations were also to be studied.

The purpose of the study is to develop a non-invasive method for predicting coronary heart disease in Air Force flying personnel who are referred to the Aeromedical Consultation Service for medical evaluation to remain on flight status.

The patient population differs from the civilian population in that they are much younger and are largely asymptomatic for heart disease. The methods to be developed will eventually be used to predict coronary artery disease at relatively early stages. Such methods have not been developed because patients with premature heart disease are not readily available for such studies.

At the beginning of this study the following objectives were established to achieve the goal and complete purpose of this study:

1. To review the literature for previous studies of lipids in salivary fluids and for methods of analyzing lipids in physiological fluids.

2. To develop an analytical procedure for quantitating cholesterol and cholesterol esters in salivary fluids.

3. To determine within-day and between day coefficients of variation of the analytical method.
4. To determine diurnal variation of cholesterol and cholesterol esters in salivary fluids.
5. To determine the effects of salivary flow rates on cholesterol and cholesterol esters concentrations. To determine if results can be expressed on a creatinine and sodium basis.

MATERIALS AND METHODS

Sample Collection

Ten healthy individuals will be recruited to participate in this study. Five adult males and five adult females will be asked to provide saliva samples. Sex, age, body weight, body height and body surface area will be recorded. Unstimulated samples will be collected at 8 A.M., 1:30 P.M. and 8 P.M. into screw-capped glass vials for seven consecutive days. All volunteers will be required to rinse their mouths with deionized water before providing the saliva samples. A five minute rest period will ensue, then 10-15 ml. of saliva will be collected. Designated individuals will provide 8 A.M. samples with fasting after their evening meal. Other individuals will be asked to provide blood specimen with their saliva samples on given days for comparative work. After the first week of daily sample taking, some volunteers will be asked to follow the routine one day of each week for nine weeks. Blood samples will be frozen and analyzed later.

Ten ml of an individual saliva sample will be immediately treated with buffered (pH 7.0) EDTA and filtered through a 0.45 Mm HA Millipore filter. The filtrate will be dialyzed exhaustively against distilled

water and lyophilized (Slomiany et al, 1982)[16]. The lyophilized sample will be extracted twice, each time 24 hours with chloroform: methanol (2:1, v/v) and filtered through a grade-F sintered glass funnel to retain any insoluble protein residue. The lipids contained in the filtrate are dried, dissolved in a volume of chloroform then processed by thin-layer chromotography.

Thin layer chromatography will be performed on the 10x10 cm HP-KF plates (Whatman). The individual neutral lipids, visualized on thin-layer plates with a fluorescent spray, will be identified by comparison with chromatograms of authentic standards, after marking their perimeters, the spots will be scraped and recovered from the gel by elution with chloroform: methanol. Following removal of solvent total cholesterol and cholesterol esters will be determined by the method of Blomhoff (1973)[2].

Total Cholesterol Determination

To 16x125 mm test tubes, 4.7 ml of 95% ethanol and 0.3 ml of 33% KOH in aqueous solution will be added to 2.0 ml of previously described and processed saliva. After thorough mixing for about 15 seconds on a Vortex mixer hydrolysis will be performed for fifteen minutes at 55°C in a water bath. After briefly cooling, 5 ml of distilled water and 10 ml of hexane (n-hexane pure, Merck Co., Rahway, New Jersey) will be added. The solution will be mixed for thirty (30) seconds on a Vortex and allowed to stand until complete separation of the two phases occur, usually ten minutes. From the upper phase 5.0 ml will be removed and evaporated under a stream of nitrogen. To the dry residue, 200 µl of 100 mg/100 ml of 5α-cholestane (Sigma Chem. Corp., St. Louis, Mo.) in chloroform will be added.

Free Cholesterol Determination

In a 16x125 mm test tube used for free cholesterol estimation 9.0 ml of 95% ethanol and 3.0 ml diethyl ether will be added to 2.0 ml of previously described and processed saliva. After mixing for approximately fifteen (15) seconds on a Vortex mixer the solution will be allowed to stand for 5.0 minutes and then centrifuged at 2000 r.p.m. for 10 minutes. After decanting the solvent phase this will be evaporated to dryness with nitrogen in a water bath at 55°C. To the dry residue 200 µl of 100 mg/100 ml or 50 mg/100 ml 5α-cholestane in chloroform will be added. A second extraction with 7.0 ml of 95% ethanol and 3.0 ml of diethyl ether will be performed.

0.1 ml of a mixture of N_1O-bis (trimethylsily trifluoroacetamide and pyridine (1:2 by volume) will be mixed with all saliva samples prepared either for total cholesterol or free cholesterol determinations. The samples will be prepared in Teflon lined screw cap tubes and left overnight at room temperature.

The volume of sample injected into the gas chromatograph from each sample to be analyzed will be 1.0 µl. A model 3700 gas chromatograph (Varian, Palo Alto CA) equipped with both a flame ionization detector or an electron capture detector will be used for the analyses.

RESULTS

The major result of this investigation has been the selection of a specific gas-liquid chromatographic technique that will be employed in the analyses of blood serum and saliva for the quantitation of cholesterol and cholesterol esters. The designated procedure is a combina-

tion of the technique reported by Blomhoff (1973)[2] and modifications of that technique employed by Slomiany et al (1982)[16] for the evaluation of lipid content.

The objectives numbered one and two for this investigation (see Objectives of the Research Effort) have been accomplished. Continued work should facilitate the determination of the remaining objectives. A review of the literature reveals that samples of blood and plasma have been analyzed for lipid content, specifically for cholesterol and cholesterol esters, utilizing gas-liquid chromatographic analytical methods (Blomhoff, 1973) (Ferrell, 1977) (Derks, 1985)[3,6,5]. The literature also contains more than adequate documentation of the capability of the gas-liquid chromatographic assay for analyzing salivary secretions for the presence of cholesterol and cholesterol esters (Slomiany, et al, 1980)(Slomiany et al, 1982)(Slomiany et al, 1983)[17,16,13].

The literature does not contain valid documentation that gas-liquid chromatographic analysis can be used to determine the cited objectives numbered (three (3), four (4) and five (5) in this study. However, continued investigation should determine the validity of these objectives. At this point of the investigation there is no certainty about expressing concentrations of cholesterol and cholesterol esters on a creatinine or sodium basis. However, it must be stated that continued pursuit of this experimental approach should lead to the use of other biochemical parameters that might correlate well with analyses of cholesterol and cholesterol esters.

Experimentally, a desired objective would be the demonstration of a direct relation between the concentrations of cholesterol and cholesterol esters in serum, and the concentrations of cholesterol and cholesterol esters in salivary secretions collected from donors. Proof of this relationship would enable the development of a calibrated standard curve procedure to be used routinely in the clinical laboratory as a non-invasive method for determining the quantities of cholesterol and cholesterol esters in the body fluids of patients.

DISCUSSION

The use of gas-liquid chromatography to analyze lipids was first reported in the literature in 1952 (James, 1952)(Metcalfe, 1971)[10,12]. Gas-liquid chromatography is used routinely in the clinical laboratory and has become a very important tool in biomedical research. The technique allows for the acquisition of accurate qualitative and quantitative data because of the highly sensitive detectors employed in the instrumentation. This high sensitivity facilitates the quantitation of lipids such as cholesterol and cholesterol esters in small volume as small as ten (10) to fifty (50) µl (Ferrel, 1977)[6].

The determination of a non-invasive method for predicting coronary heart disease in Air Force flying personnel is highly desirable. Development of a non-invasive procedure would find considerable use and application in the routine or in civilian clinical laboratories. The goal of this research program was to develop analytical methods for quantitating cholesterol and cholesterol esters in salivary fluids. The analytical method employing gas-liquid chromatography has been sufficiently documented as a technique that will measure cholesterol and cholesterol esters in the 10^{-6} to 10^{-9} gram range (Metcalfe, 1971)[12,6].

The purpose of this study was to develop a non-invasive method for predicting coronary artery disease (CAD) in Air Force flying personnel. The gas-liquid chromatographic method selected has the sensitivity required for assaying biological fluids such as blood serum and salivary fluids. Blomhoff (1973)[2] reported recovery studies of known serum samples. The recovered free cholesterol samples were quantitated at the 25, 49, 101, 160 and 174 µg level. The recovered total cholesterol samples were quantitated at the 101, 245, 518, 210, 299 and 376 µg level. Recovery and quantitation of such small amounts of cholesterol is indicative of the high sensitivity of the detectors utilized in gas-liquid chromatography. Hence, this strongly suggests that this assay technique can facilitate the development of the non-invasive method for predicting coronary heart disease.

Slomiany et al (1983)[13] recorded the concentrations of cholesterol in both parotid and submandibular saliva. In an investigation of the association of lipids with proteins and glycoproteins in human saliva, parotid saliva was found to contain 0.58±0.13 mg of cholesterol/100 ml of saliva. Analysis for cholesterol esters revealed 0.96±0.20 mg of cholesterol esters/100 ml of saliva in parotid fluid and in submandibular saliva 0.89±0.20 mg of cholesterol esters/100 ml of saliva. In another study of the lipid composition of human submandibular gland secretion from light and heavy calculus formers, Slomiany et al (1980)[17] provided the following information: light calculus formers cholesterol was assayed at 4.38±1.44 mg/100 mg of lipids and cholesterol esters were assayed at 1.02±0.08 mg/100 mg of lipids; heavy calculus formers' cholesterol was assayed at 2.25±0.86 mg/100 mg of lipids and cholesterol esters were assayed at 2.92±0.21 mg/100 mg of lipids.

lipids; heavy calculus formers' cholesterol was assayec at 2.25±0.86 mg/100 mg of lipids and cholesterol esters were assayec at 2.92±0.21 mg/100 mg of lipids.

The data cited above again demonstrates the ease with which small quantities of cholesterol and cholesterol esters can be evaluated in blood sera or saliva. Perhaps continued pursuit and experimental design are the prevailing factors that limit the achievement of a non-invasive method for predicting coronary heart disease.

In attempting to carry out the goal and purpose of this investigation five objectives were established. The first two objectives were accomplished, the remaining three were not. There was not sufficient evidence in the literature to suggest that any other investigators had obtained data that would confirm the achievement of these three objectives.

There was no evidence in the literature that would allow for the determination of within-day and between-day coefficients of variation. There was no confirmation of the determination of diurnal variation of cholesterol and cholesterol esters in salivary fluids. There was not sufficient evidence to determine the effects of salivary flow rates on choelsterol and cholesterol esters concentrations. There was not sufficient evidence to determine whether concentrations of cholesterol and cholesterol esters could be expressed on a creatinine or sodium basis (Chiou et al, 1977)(Chiou et al, 1979)[3,4].

Goll and Mookerjee (1978)[7] studied the correlation of biochemical parameters in serum and saliva in azotemic patients and patients of chronic hemodialysis. They reported that in patients who had received chronic hemodialysis treatments, concentrations of creatinine and uric

acid correlated well with those in simultaneously drawn unstimulated whole saliva, both before and after dialysis. The reported values for creatinine (n=11, n=the number of samples) was 4.52±0.69 mg/100 ml in blood serum and 0.979±0.18 mg/100 ml in saliva. Their data was treated by multiple regression analysis. The linear regression of the correlation for predialysis serum versus saliva was expressed as $y = 0.141x + 0.459$. The linear regression for post dialysis of creatinine for blood serum versus saliva was expressed as $y = 0.132x + 0.214$. The correlation coefficients for both predialysis and postdialysis sera and saliva was highly significant at less than the two and one-half percent level ($p<0.025$). These investigators found no significant correlation between the serum and saliva parameters such as glucose, electrolytes, lactic dehydrogenase, total protein, albumin, calcium, inorganic phosphate, total bilirubin, alkaline phosphatase, serum glutamic oxaloacetic transaminase and blood urea nitrogen. All of Goll and Mookerjee's data was analyzed by an automated sequential multiple analyzer, either an SMA6, or an SMA12.

A non-invasive method for predicting coronary heart disease would become closer to reality if a significant relationship was determined to exist between the concentrations of cholesterol and cholesterol esters in blood serum versus the concentration of cholesterol and cholesterol esters in human saliva. However, if the non-invasive method for determining coronary heart disease is not imminent, progress in terms of qualitative benefits would go a long way toward relieving the physical stress and mental anguish associated with invasive methods for securing biological fluids from patients.

CONCLUSIONS

Gas-liquid chromatography is an excellent analytical method for quantitating cholesterol and cholesterol esters in salivary fluids. Continued pursuit of this investigation utilizing gas-liquid chromatography as an analytical procedure might provide information on the effects of diurnal variation and salivary flow rates on cholesterol concentrations. Gas-liquid chromatography is an analytical method that is well suited for developing a non-invasive method for predicting coronary disease in Air Force flying personnel. The choice of gas-liquid chromatography is sound because of the highly sensitive and precise measurements of samples provided by this analytical technique. Gas-liquid chromatography has the capacity to measure accurately at the microgram (10^{-6}g) and nanogram (10^{-9}g) levels. Experimental design could facilitate the expression of cholesterol and cholesterol esters concentrations on a creatinine or sodium basis. If not, then other biochemical parameters routinely determined in the clinical laboratory may be applicable in relation to cholesterol and cholesterol esters concentrations. If, after a prolonged and thorough investigation employing the suggested analytical method is unsuccessful in its quantitative aspect, there could still be sufficient benefits derived of a qualitative nature. Should the planned research provide for a decrease in the required blood samples taken from patients to be replaced with saliva samples to be used in the analyses of biochemical tests, the use of gas-liquid chromatography as an analytical instrument should be deemed a success. There would be a marked reduction in the trauma long associated with invasive techniques.

RECOMMENDATIONS

The goal, purpose and objectives established for this summer's research program are very worthwhile and when completely accomplished will provide long term benefits. During this summer's endeavors gas-liquid chromatography was designated as the analytical method for achieving the desired goal, purpose and objectives. Based on the insights gained over the period of this summer and the existing evidence in the literature the following recommendations are tendered for consideration:

1. The methodology employing use of gas-liquid chromatography to analyze and quantitate cholesterol and cholesterol esters in salivary fluid should receive the highest priority possible from the Air Force Office of Research.
2. Development of a non-invasive method for predicting coronary heart disease in Air Force flying personnel lies within the capability of existing methodologies such as gas-liquid chromatography. Continued pursuit and experimental design may be the only existing hinderances. All necessary support should be enhanced; solving this problem is imperative.
3. Early information sharing between Summer Faculty Fellows and research sponsors would increase the amount of work accomplished. Understandably, this is a part of the nature of the pre-summer visit. However, early contact could make a difference in productivity.
4. This particular recommendation has nothing to do with the specifics of summer's research. Perhaps it is more in the nature

which participating summer faculty come. When all the summer's research final reports are compiled in final form, please consider forwarding one or two copies to the office of the president or chancellor and to the libraries of the respective campuses of each of the summer research fellows. I would expect this gesture to produce a great deal of positive feedback.

ACKNOWLEDGEMENTS

I am pleased to express my appreciation to the Air Force Systems Command, the Air Force Office of Scientific Research, and the Brooks Air Force Base School of Aerospace Medicine for providing me an opportunity to participate in the Summer Faculty Research Program.

I would like to thank Dr. Harvey A. Schwertner for his generosity in sharing his research interests with me. I must express my gratitude to Dr. Bryce Hartman, Mr. Lloyd Foster and Mr. Rodney C. Darrah and his staff at Universal Energy Systems, Incorporated, for facilitating my participation in this summer's Faculty Research Program.

I would like to extend my sincere appreciation to all the personnel of the Clinical Pathology Branch whose services rendered made my stay within the Branch very comfortable and cordial.

REFERENCES

1. Aono, M., Murtry, V.L.N., Witas, H., Slomiany, A. and Slomiany, "Lipids of submandibular saliva in cysticfibrosis," IRCS Medical Science 10, 1982, p. 159.

2. Blomhoff, J.P., "Serum cholesterol determination by gas-liquid chromatography," Clinica Chimica Acta 43, 1973, pp. 257-265.

9. Jacobsohn, Gert M. and Montiel, Rafael J. "Cholesterol content of human parotid saliva," Lipids 4(5), 1968, pp. 380-383.

10. James A.T. and Martin, A.J.P., "Gas-liquid partition chromatography: the separation and micro-estimation of volatile fatty acids from formic acid to dodecanoic acid," Biochemical Journal 50, 1952, pp. 679-690.

11. Mandel, I.D. and Eisenstein, A., "Lipids in human salivary secretions and salivary calculus," Archs. Oral Biol. 14, 1969, pp. 231-233.

12. Metcalfe, L.D., "Lipid analysis by gas chromatography," Recent Advances in Gas Chromatography, edited by Irving I. Domsk and John A. Perry, 1971, pp. 267-285.

13. Slomiany, B.L., Witas, H., Murty, V.L.N., Slomiany, A. and Mandel, I.D., "Association of lipids with proteins and glycoproteins in human saliva," Journal of Dental Research 62(1), 1983, pp. 24-27.

14. Slomiany, B.L., Zdebska, E., Murty, V.L.N., Slomiany, A., Petropoulou, K., and Mandel, I.D., "Lipid commposition of human labial salivary gland secretions," Archs. Oral Biol. 28(8), 1983, pp. 711-714.

3. Chiou, S.L., Hsu, F.H., Westenfelder, Christof, and Kurtzman, Neil A., "Correlation of creatinine levels in saliva and plasma in normal subjects and renal patients," Research Communications in Cnemical Pathology and Pharmacology 16(3), 1977, pp. 549-556.

4. Chiou, W.L. and Pu, Frances S., "Creatinine VIII: Saliva levels of endogenous "true" creatinine in normal subjects," Clin. Pharmacol. Ther. 25(6), 1979, pp. 777-782.

5. Derks, Henks J.G.M., vanHeiningen, Alida, and Koedam, Hans C., "Gas-chromatographic determination of cholesterol in serum: candidate reference method," Clin. Chem. 31(5), 1985, pp. 691-694.

6. Ferrell, William J., "Gas-liquid chromatography as a method for analysis of serum cholesterol," CRC Critical Reviews in Clinical Laboratory Sciences 8(3), 1977, pp. 259-276.

7. Goll, Robert D. and Mookerjee, Basab K., "Correlation of biochemical parameters in serum and saliva in chronic azotemic patients and patients on chronic hemodialysis," Journal of Dialysis 2(4), 1978, pp. 399-414.

8. Haeffner, E.W. and Hoffman, C.J.K., "Direct quantitation of free cholesterol in total serum extracts by computer assisted gas-liquid chromatography," Journal of Chromatography 228, 1982, pp. 268-272.

15. Slomiany, B.L., Aono, M., Murty, V.L.N., Slomiany, A., Levin, M.J., and Tabok, L.A., "Lipid composition of submandibular saliva fromnormal and cystic fibrosis individuals," Journal of Dental Research 61(10), 1982, pp. 1163-1166.

16. Slomiany, B.L., Murty, V.L.N., Aono, M., Slomiany, A., and Mandel, I.D., "Lipid composition of human parotid and submandibular saliva from caries-resistant and caries susceptible adults," Archs. Oral Biol. 27, 1982, 803-808.

17. Slomiany, B.L., Slomiany, A. and Mandel, I.D., "Lipid compmosition of human submandibular gland secretion from light and heavy calculus formers," Archs. Oral Biol. 25, 1980, pp. 749-751.

18. Wang, Stephen T. and Peter, Frank, "Gas-liquid chromatographic determination of fatty acid compmosition of cholesterol esters in human serum using silica sep-pak cartridges," Journal of Chromatography 276, 1983, pp. 249-256.

1985 USAF-UES SUMMER FACULTY RESEARCH PROGRAM/

GRADUATE STUDENT SUMMER SUPPORT PROGRAM

Sponsored by the

AIR FORCE OFFICE OF SCIENTIFIC RESEARCH

Conducted by the

UNIVERSAL ENERGY SYSTEMS, INC.

FINAL REPORT

Personality Correlates of Pilot Performance

Prepared by: Edna Fiedler, Ph.D. and Christine Cato

Academic Rank: Associate Professor

Department and University: Department of Psychology, St. Mary's University

Research Location: AFHRL/MOAA

USAF Research: Dr Jeffrey Kantor

Date: Aug 9, 1985

Contract No: F49620-85-C-0013

Personality Correlates in Pilot Performance

by

Edna Fiedler, Ph.D. and Christine Cato

ABSTRACT

This paper reports on literature reviews of both the typical pilot personality profile, as well as the personality correlates of flight training outcome and flight safety. Next, the analyses of two different studies are reported. The first study found that combat ready fighter pilots from eight NATO countries scored similarly on the personality factors of conscientiousness and experimenting (Cattell's 16PF). The second study reports on the effectiveness of the Pilot Personality Inventory (PPI) in predicting Undergraduate Pilot Training (UPT) outcome. Similar to previous findings in this area, it was found that the PPI was not able to reliably predict UPT outcome across different samples of pilots. The next section of this paper presents the general conclusions from both the literature reviews and the results of the above studies. Finally, the most promising future approaches for studying (1) the use of a personality measure to predict pilot performance, and (2) future research possibilities with the Defense Mechanism Test, which is currently being used by several European countries, are discussed.

ACKNOWLEDGEMENTS

We wish to extend our appreciation to the Air Force Systems Command, the Air Force Office of Scientific Research, and Universal Energy Systems, Inc., for granting us the opportunity to spend this summer in an intellectually demanding job with the Air Force Human Resources Laboratory at Brooks AFB, Texas.

The Human Resources Laboratory, through the Manpower Acquisition Branch provided us with a stimulating work atmosphere. Especially kind thanks go to the following individuals.

Dr Jeffrey Kantor's organization of the task, and patience was critical in making this summer such a productive one. His excellent and thorough feedback at critical points in the research effort were essential in ensuring the quality of the final product.

Major John Quebe not only shared his office, but also his considerable knowledge and understanding of the world of pilots and the Air Force mission.

Dr David Hunter's knowledge of the area often increased our understanding while guiding us to further research.

Dr Malcolm Ree's sustained interest and statistical comments regarding the analyses were invaluable in contributing both to our knowledge and to the final report.

Miss Sandy Stringfellow, who, worked diligently with much good humor to complete the typing in a timely manner.

PERSONALITY CORRELATES TO PILOT PERFORMANCE

I. INTRODUCTION

The appropriate selection and classification of rated officers is essential to the mission of the USAF. The Force Acquisition Branch (MOAA) of the Human Resources Laboratory (HRL) is developing an improved pilot selection system using a computerized Basic Attribute Test (BAT), which assesses a range of (1) information processing skills and (2) personality attributes. Preliminary data has been collected and are now being evaluated to identify the significant predictors of flying performance. Once the integrated pilot selection system is implemented, Air Training Command projects a minimum savings of $2,000,000 a year. This will enable instructor pilots to spend more time working with students who will graduate. One part of this data bank, personality attributes, had not yet been analyzed. Personality factors are an elusive area of psychology, cutting across many subdisciplines. However, the use of a clinically based assessment instrument necessitated the use of clinical psychologists as consultants. At the same time, the research and development setting of HRL required the necessary research background needed to analyze results and design future studies.

The senior author, Edna Fiedler, a licensed psychologist and Mental Health Service Provider, received her doctorate in Social/Personality, as well as having done post doctoral training in clinical psychology. She has both the clinical and social/personality research skills required to analyze

the personality test results. Currently, as Chair of the Psychology Department, she oversees both the Industrial/Organizational and Clinical graduate programs and teaches courses in personality at both the undergraduate and graduate levels. With these qualifications and experience in mind and the need of the USAF for someone with such a background, she was chosen by the USAF-UES Summer Faculty Program to analyze the personality data.

The second author, Christine Cato, received her bachelors degree in Psychology with a minor in Management, and is currently working on her masters degree in Industrial Psychology. Her training thus far has given her the necessary skills to work under supervision in this area.

II. OBJECTIVES OF THE RESEARCH EFFORT

The preliminary objectives for the 1985 summer research effort were:

Goal 1. Complete initial psychometric evaluations of the Pilot Personality Inventory (PPI). The PPI is part of the USAF pilot selection and classification research program which has as its objective identifying those people with an excellent chance of completing training and of becoming hightly successful operational pilots.

GOAL 2. Compare the 16PF personality profiles of the pilots of eight NATO countries for pattern coefficents. This analysis is part of an international effort to assess similarities and differences among pilots cross-culturally.

GOAL 3. Complete analysis of the Autobiographical Inventory (ABI) begun by Bernd Willkomm of the Flugmedizinisches Institut der Luftwaffe. The ABI was initially given in the Federal Republic of Germany and was then given here in the United States. The ABI scores were compared to flight screening program (FSP) outcome.

GOAL 4. Alternatives to the Defense Mechanism Test (DMT), currently being used in Norway, Denmark, and Great Britain for screening pilots, will be discussed as to their feasibility in screening USAF pilots.

GOAL 5. Suggest research possiblities focusing on the psychological issues relevant to the selection of astronauts for long duration space flights.

Due to the complexities arising in the analyses of the pilot personality factors, Goal 5 was dropped and a new objective was added:

GOAL 6. Based on a literature review and current ongoing research efforts, present a research proposal to revise the personality inventory or develop an alternative so as to increase its usefulness in predicting pilot performance.

Sections III, IV and V form the bulk of the report and contain the approaches taken to meet the above listed objectives and the results of these approaches.

III. PERSONALITY CORRELATES OF PILOT PERFORMANCE

INTRODUCTION

The military has a vested need in determining what makes personnel more effective in combat. One military group receiving considerable attention because of the high costs of training and importance in battle has been aviators. An historical overview of the role of personality testing and pilot performance from the 1940's to the mid 1970's is available to the interested reader through several literature reviews (Ellis and Conrad, 1948; Hunter, 1985; North and Griffin, 1977; Rossander, 1980; Sells, 1956; and Youngling, Levine, Mocharnuk, and Weston, 1977).

The present review looks at pilot research of the last ten to fifteen years, concentrating, first, on research delineating the personality profile of the typical military pilot, described earlier by Fry and Reinhardt (1969) and Reinhardt (1970). Second, studies on personality inventories predicting a criterion are reviewed.

Research on the Personality Profile of Aviators.

One of the more often used personality scales in describing the aviator is the Edwards Personal Preference Schedule (EPPS), which has been used to study US Navy pilots, Royal Australian Air Force pilots, Australian commercial pilot trainees, and general American aviators.

As Edwards writes (cited in Graham and Lilly, 1984), the EPPS "was designed primarily as an instrument for research and counseling purposes, to provide quick and convenient measures of a number of relatively independent normal personality variables".

These personality variables were derived from Henry Murray's list of manifest needs, with several procedures for reducing the impact of social desirability in item responses. Unfortunately, as Graham and Lilly conclude, "Reviewers...are in clear agreement that there is not adequate evidence that the EPPS scales measure the constructs they were designed to measure or that the scales are useful in predicting important nontest variables" (p. 257-262)

An early study by Fry and Reinhardt (1969) found that the norms for Navy jet pilots were significantly different from the norms of both adult and college males. Following this work, Novello and Youssef (1974a) used Fry and Reinhardt's norms to compare civilian aviators to Navy pilots and to the general populace. They found, similar to Fry and Reinhardt, "a certain core of personality traits" (p. 187) common to both Navy pilots and general aviators. The pilots scored significantly higher on the five factors of Achievement, Exhibition, Dominance, Change, and Heterosexuality, and scored significantly lower on the seven factors of Deference, Order, Affiliation, Succorance, Abasement, and Nuturance. A brief description of each of the scales is listed below:

Achievement	to do one's best
Deference	follow instructions

Order	keep thing organized
Exhibition	to be the center of attention
Autonomy	independence in thought/action
Affiliation	attached to friends, groups
Intraception	anaylsis of motives, feelings, and behaviors
Succorance	to want help; sympathy
Dominance	to be a leader
Abasement	feeling guilt or blame
Nurturance	to show help, sympathy
Change	to experience novelty
Endurance	stay at a job until its finished
Heterosexuality	to do things with the opposite sex
Aggression	to be critical or attack others

In Novello and Youssef's (1974b) analysis of female general aviators, female pilots were found to have a distinctive personality profile that was more similar to that of male pilots than to that of the normative adult American woman. They also found that female pilots deviated in the same pattern from female norms as male pilots differed from male norms. Whether this pilot profile does, in fact, transcend sex distinctions, as Novello and Youssef maintain, is difficult to determine as later studies again focused on the male pilot.

Ashman and Telfer (1983) also found that Australian Air Force pilots and commercial pilots showed somewhat higher scores on Achievement, Exhibition, Dominance, Change, and Heterosexuality then the Australian community sample,

but only Achievement was significantly higher. Similarly, on the factors of Deference, Order, Affiliation, Succorance, Abasement, and Nuturance, the Australian pilots scored somewhat lower than the Australian community, but, the Air Force pilots scored significantly lower only on Affiliation and Nuturance, while the commercial pilot trainees scored significantly lower on Succorance and Nurturance.

Following Ashman and Telfer's interpretation of these data (1983), the current authors suggest that the scales of Nuturance, Affiliation, Succorance, and Achievement may distinguish pilots from the general populace, across cultures.

Descriptively, then, the typical pilot scores higher in doing his best and being successful (Achievement), but reports less attachment to groups and friends or desire to do things with friends (Affiliation). The typical pilot shows lower scores in need to have others provide help when in trouble (Succorance) or himself to be sympathetic or proffer help to other (Nurturance).

Recent work by Wichman and Ball (1983) found that general aviators were significantly more internal in their locus of control than the general U.S. population indicating that pilots perceive themselves to be more in control of what happens to them and less likely to believe that "luck" or "others" are the cause of their behavior. Dale and Bartram (Circa 1982) found that British Army Air corp candidates tended to fake in the direction of faking good, reflecting a possible self-serving bias. This is similar to Wichman

and Ball's (1983) other finding that pilots have strong self-serving biases regarding their skills and safety levels. It is to a pilot's advantage to believe in himself when he must make life or death decisions. However, as indicated by statistics on pilot error fatalities (Vail, 1985), the second highest cause for male pilot error fatalities is "attempted operation beyond experience/ability" (p. 315), so too much confidence and self-serving bias can detrimentally affect performance.

In summarizing the above studies, a few consistent findings emerge. The successful pilot or trainee scores high in achievement across cultures, shows an internal locus of control and tends toward extroversion or stable introversion. Both in the USA and Australia, military pilots score lower on nuturance and affiliation.

In the next section of this report entitled, Personality Profiles of Combat Ready Fighter Pilots, a more recent descriptive study of conbat-ready pilots is discussed in light of these previous findings.

Research on Personality Scales, Flight Safety and Training Success

Flight Safety. Recent studies have looked at a number of factors thought to be related to aviator accident rate. In general, accident rates correlate positively with pilots who are having troubled interpersonal relationships, demonstrate little sense of humor or humility about themselves or who have recently lost a loved one (Alkov and Borowski, 1980; Green, 1977). In other words, those persons, who either characteristically or situationally find themselves in unstable interpersonal relationships, are more likely to have accidents.

As part of their study on locus of control, Wichamn and Ball (1983) found that pilots with a higher internal locus of control were more likely to attend FAA safety clinics than those with a more external locus of control. Banta and Kosnosky (1978), reviewing the case of a pilot with a nonpsychotic obsessive-compulsive personality who crashed a plane during fight training, found the pilot showed perfectionistic tendencies associated with denial of errors and attributions of his problems to external causes.

These studies indicate the importance of a pilot perceiving himself as having control over his mistakes, the cockpit environment, and probably his personal life as well. However, this control needs to be modulated by a sense of humor or humility and a willingness to accept the responsibility of change.

Work done with the Swedish Air Force has focused specifically on the type and extent of defense mechanisms used by the pilot and flight safety. Using the Defense Mechanism Test originated by Kragh at the University of Lund, Swedish researchers have found that "counter-phobic" personality types are at very high risk for accidents. Counter-phobic is defined as personality defects that include "psychopathic tendencies, insufficient super-ego, aggressive self-assertiveness, antisocial attitudes, and a willful and irrational desire to prove oneself against all the odds" (Skelly, 1983 p. 11). Between 1967-71, the DMT identified 35 pilot candidates as poor prognosis, a diagnosis that was kept confidential. All of these were later eliminated from training, died in flying accidents, or were withdrawn from flying.

Two case studies reported by the Netherlands and Norwegian Air Forces involving pilots with flying problems found that, independent of knowledge about the pilots' case histories, the DMT confirmed poor prognosis for flying.

The DMT prognosis is based upon the type of psychological defenses the pilot uses. Projection and isolation, the more structured forms of defense, appear to be positively correlated with fighter pilot success, while more primitive, less structured defenses such as denial, reaction formation and repression appear to be negatively correlated to fighter pilot success. It would appear, then, that across several of the far northern European countries, aircraft accident rates are positively correlated with a certain counter-phobic pattern of behaviors and defenses. However, as Stoker and Kantor (1983) point out, the DMT has a 34% false positive rate, making it a very costly screening instrument.

What can be said about personality and accident rate based on these studies? Using very different methods from Americans, European researchers have found compatible results. The accident-prone pilot is one who, though perfectionistic, displays defenses that encourage denial of errors and responsibility for one's own contribution to a potentially fatal situation. Recalling that humor can be viewed as a complex, highly structured, adaptive defense, Green's finding that a sense of humor is positively related to flight safety supports the finding that fighter pilot success is correlated with the use of structured forms of defense such as projection and isolation. A discussion of the research implications of this work is found in section VI of this paper, Possible Future Approaches.

Flight Training Success. The other area to be reviewed in this section are post 1977 studies on personality inventories used to predict flight training outcome (Reviews of earlier studies can be found in Hunter, 1985; Rossanoer, 1980; Sells, 1956). Bartram and Dale (1982), using the Eysenck Personality Inventory (EPI), found that success in training for both air force and army aviators in Great Britain was positively correlated with both stability and extroversion. The stability measure is particularly important for introverts in that the neurotic or unstable introverts have very low pass rates.

Working with US Army student helicopter pilots, Roth found successful candidates to be significantly more (1) assertive and aggressive, (2) suspicious and dogmatic, and (3) practical and conventional, as measured by the 16 P.F.

The DMT, previously discussed in relationship to flight safety, has also been studied as a predictor of flight training success. Following Swedish administration and scoring methods, the Danish Air Force validated the DMT against two samples of student pilots (total N=191). They found that "87% of the poor scorers failed Basic Flying Training as compared to 31% of the good scorers" (Stoker and Kantor, 1983, p. 1; see also Skelly, 1983). The Royal Air Force, using a group administration, was unsuccessful in predicting flight training outcome.

Emerging from these studies is a pattern of the successful student pilot as one who (1) is emotionally stable, (2) uses more mature coping or defense

styles, (3) frequently demonstrates an extroverted or assertive approach, and yet, (4) is of a conventional or nonsociopathic orientation.

As can be seen by the above review, systematic study of pilots by the use of personality measures continues to be varied as regards to tests, methodology, and criteria used. A statement by Ellis and Conrad in 1948 remains almost as true today as then. "In contrast to their success in relation to the psychiatric criterion the military personality inventories proved generally ineffective for predicting performance measures such as successful completion of a training-course" (p. 421).

Ellis and Conrad mentioned the need for personality measures that are especially designed for the groups to which they will be applied. Many of the personality measures reviewed in this introduction have been used historically in one of two ways: first, as part of an extensive battery of tests to develop a clinically oriented, individual profile, or second, as a research instrument to specify differences between groups. What still needs to be developed is an instrument that is relatively quick and easy to administer, objective in scoring, and makes very fine individual distinctions within a highly select, and unusually mentally healthy group of subjects.

IV. TWO APPROACHES TO PILOT PERSONALITY RESEARCH

This section reports on two studies that are based on the two approaches that are discussed in Section I. The first study looks at the personality

profiles of combat ready fighter pilots across eight countries. The second study reviews preliminary analyses on an ongoing research battery attempting to predict flight training success for the USAF Undergraduate Pilot Training (UPT).

Personality Profiles of Combat Ready Fighter Pilots

The use of personality measures to improve the selection and training procedures of pilots, evaluate personnel, and predict combat effectiveness is not new, but historical findings have been inconsistent and unstable (North and Griffin 1977; Youngling, Levine, Mocharnuk, and Weston, 1977; Sanders, Hoffman and Neese 1976). However, because of the importance of personality factors in combat effectiveness, the search for stable and consistent measures of the relevant aspects of personality continues. One way to approach this problem is through the use of cross-cultural research as a way to identify dominant personality patterns in selected occupational roles. In this study, Cattell's Sixteen Personality Factor questionnaire (16PF) was chosen as a measure of personality.

The 16PF is an objectively scored personality test with sixteen scales that, according to Cattell (1972), are essentially independent as well as undimensional. Cattell also identified four second order factors which are derived from the sixteen primary factors. These scales contain high and low scores representing opposite characteristics (Graham and Lilly, 1984). In general, the 16PF is an adult level test designed for individuals sixteen years of age or older. The reasons for choosing the 16PF were, one, the

16PF was designed to make available in a practicable testing time, an objective, easily administered and scored instrument about primary personality factors (Cattell, Eber, and Tatsuoka, 1970), and secondly, there has been a great deal of research done on the 16PF, not only in the United States but also in other countries as well (Cattell, 1973; Golden, 1978).

Previous research relevant to the present study include studies looking at the equivalence of second order factors across cultures, the relationship of the 16PF to psychological defensiveness, and specific research on aviators and the 16PF. In his study, Golden (1978) found that Americans of Japanese ancestry appeared to have a significantly different factor structure from Americans with European ancestry. However, both Golden and Cattell (1973) found that the second order factor structure of extroversion and anxiety on the 16PF is basically equivalent for European or European ancestry cultures. Therefore, it would appear that cross-cultural comparisons across European or European ancestry groups can be made with some assurance of comparability of 16PF scores. Furthermore, Defense Mechanism Test (DMT) research has indicated that psychological defenses are important correlates of successful flying. A British study (Cooper and Kline, 1983) compared the 16PF to the Defense Mechanism Inventory (DMI) and found several factors that related to five defense mechanisms as measured by the DMI. The authors (Cooper and Kline, 1983) concluded that the 16PF can measure defenses hypothesized from psychoanalytic theory.

Of more direct relevance to flying, there have also been studies involving aviators and the 16PF. Sanders, Hoffman and Neese (1976), conducted a study attempting to cross validate an earlier study by Sanders and Hoffman (1975)

in which an individual scores on 3 bipolar factors from the 16PF (Group Dependent vs. Self Sufficient (Q2), Practical vs. Imaginative (M), Forthright vs. Shrewd (N)) were found to significantly discriminate between pilot accident and non-accident groups. Contrary to the earlier research, Sanders et al., (1976) found that on a different sample these 3 factors did not significantly discriminate between the pilot groups. These two studies show both the continued interest in the 16PF in distinguishing among pilots as well as the difficulty in finding consistent results. Futhermore, in a study by Roth (1980), the 16PF was used as part of a candidate selection battery for the United States Army's Initial Entry Rotary Wing Training (IERW). One hundred and ninety-eight eliminees and two hundred and twelve graduates revealed a factor pattern compatible with historical data on IERW students. Specifically, three of the sixteen primary factors (E,L,M) statistically differentiated between seventy-five eliminees and seventy-three control subjects. The graduates were found to be significantly more assertive and aggressive, suspicious, dogmatic, and irritable as well as more practical, conventional, and objective. In another study by De Vries (1975), et. al., scores on two factors (A - Reserved vs. Outgoing and Q_3 - Undisciplined vs. Controlled) were shown to significantly discriminate between successful and unsuccessful (eliminees) students attending undergraduate navigator training. The eliminees were more outgoing and controlled.

Overall, the following conclusions can be drawn from previous research. One, it is possible to compare 16PF scores across European or European ancestry countries, and two, tentative findings indicate that certain

factors on the 16PF may be able to discriminate between successful and unsuccessful pilot groups.

The purpose of this present study is to capitalize on the comparability of European and European ancestry scores and evaluate the psychological profiles of combat ready fighter pilots from eight North Atlantic Treaty Organization (NATO) countries as measured by Cattell's 16PF. The main objective of these comparisons was to gain a better overall understanding of the personality factors involved in pilot effectiveness.

METHOD

Subjects

The sample was comprised of 408 combat ready fighter pilots from eight NATO countries. Each pilot was chosen from an operational squadron and was considered "combat ready" by his respective Air Force standards. The number of pilots from each country were as follows: 39 from the United Kingdom, 31 from Canada, 70 from Germany, 69 from Belgium, 19 from the Netherlands, 30 from Norway, 10 from Denmark and 31 from the United States.

Instrument

Each of the countries administered the 16PF to their pilots, although the exact procedures that were followed in each country were not specified. The raw scores were then compiled and sent to the EURO-NATO Aircrew Selection Working Group (a NATO sponsored cooperative organization) who met in Brussels, January, 1985. The raw score means were then sent to the Air Force Human Resources Lab in San Antonio, Texas (Skelly, 1985). A description of the scales on the 16 PF can be found in Figure 3. It should

be noted that throughout the rest of this study the scales will be titled according to the higher end on each bipolar scale. This was done for ease of reference.

Analysis.

The analysis consisted of two parts. First, descriptive comparisons of raw scores across countries and 16PF factors were obtained. In this first analysis, common factors were operationally defined as those raw score means falling within a standard deviation and a half around the overall mean. Unique scores were operationally defined as raw score means falling outside of a standard deviation and a half around the overall mean on any factor. Second, American data were converted into sten scores. Sten scores are specialized standard scores that range from 1 to 10 and have a mean of 5.5 and a standard deviation of 2 (Graham and Lilly, 1984). The reason for the conversion of American data only into sten scores is that the necessary norms for the other countries were not available. In this conversion of raw scores to sten scores, numbers equal to five or greater were rounded upward. The resulting sten scores were then plotted on a profile and compared to the profile of the occupational group, airline pilots, found in the 16PF Handbook (Cattell, Ever, and Tatsuoka, 1970). This group was the most relevant for comparisons with American fighter pilots.

RESULTS AND CONCLUSIONS

An analysis of the raw score means was conducted to produce overall means and standard deviations on each personality factor, across all countries. Figure 1 indicates that all of the countries have in common the factors of

Conscientiousness (G) and Experimenting (Q_1). It should be noted that if the Germans' scores were not included, the factors of Abstract Thinking (B), Dominance (E), Suspiciousness (L), Imaginative (M) and Self Sufficiency (Q_2) would all be considered common factors (See Table 1). From this observation, it can be concluded that Germany's scores deviated more from the mean than any other country.

Furthermore, all of the countries had unique scores on some of the factors. Four countries; Norway, Denmark, the United States, and Canada each had unique scores on only one factor while three countries, the Netherlands, United Kingdom and Belgium each had unique scores on two factors (See Table 1). Germany scored higher than a standard deviation and a half on the factors of Abstract Thinking (B) and Shrewdness (N), but lower than a standard deviation and half on the factors of Dominance (E), Suspiciousness (L), Imaginative (M), and Self-sufficient (Q_2).

Looking specifically at the United States, the only factor in which the Americans scored lower than a standard deviation and a half was on the factor of Warmth (A). This was also the case on Figure 2, which compares Americans to the overall means of all other countries.

The conclusions that can be drawn from this first analysis are, one, there is more similarity than differences among the countries with respect to their scores on the 16PF. Two, each country has at least one unique raw score mean indicating cultural differences.

The second way to look at the data was to take the American data, convert it into sten scores, plot these scores on a profile, and then compare this profile to the profile of airline pilots. Figure 3 illustrates the fact that the two groups never scored more than two sten scores difference from each other. According to Graham and Lilly (1984), two sten scores equal one standard deviation. Therefore, these two groups scored within one standard deviation of each other on every factor. It should also be pointed out that neither group showed any extremely high or low sten scores, with the entire range for both groups being between 3 and 8 sten scores.

The general conclusion that can be drawn from this second analysis is that the two groups, fighter pilots and airline pilots, score similarly on the 16PF.

DISCUSSION

The results show that there are both cross cultural similarities and differences among pilots. Across all countries, the pilots were alike in their level of Conscientiousness (G) and Experimentation (Q_1). Putting aside Germany's results for a moment, the other NATO countries were similar in their level of Abstract Thinking (B), Dominance (E), Suspiciousness (L), Imaginativeness (M), and Self-Sufficiency (Q_2). Comparing these results to Roth's (1980) data, it can be seen that, in general, combat ready fighter pilots score similarly on the Factors of Dominance (E), Suspiciousness (L) and Imaginative (M), the same three factors that differentiated successful from unsuccessful pilots in training. One could speculate that to the

degree to which trainee pilots are similar to combat ready pilots, their likelihood of success in flight training is greater.

At the same time, the results clearly indicate that each country has its own unique national pattern (see Table 1). Looking at the American profile for which sten scores were available (Figure 3), one could note several interesting points. First, although the American fighter pilots are similar to the airline pilots, the fighter pilots scores are, in fact, even more like the successful IERW trainees (Roth 1980). Specifically, on the factors of Dominance (E) the mean sten scores for the three groups were: 6.0 for airline pilots, 7.0 for the American fighter pilots and 6.45 for the IERW graduates. On the Factor Suspiciousness (L) the mean sten scores were: 3.7 for the airline pilots and 6.0 for the American fighter pilots and 5.17 for the IERW graduates. Also on the Factor of Imaginative (M) the mean sten scores were: 3.7 for the airline pilots, 6.0 for the American fighter pilots, and 5.21 for the IERW graduates. This comparison lends further credence to the existence of an American military aviator profile that is measureable by the 16PF.

Pilots as a group are frequently described as being mentally healthy. Therefore, one would expect pilots to score in the direction of nondefensiveness on those personality factors that Cooper and Kline (1983) found related to defensiveness. In fact, this was true except on one measure. The defense mechanism entitled projection is measured on the 16PF by 3 factors, one of which is a low score on tendermindedness (I). It was on this factor that pilots scored low, that is, in the direction of

projection. To the extent that projection has been found to be an adaptive defense for pilots (Skelly, 1983), this profile again matches up with what one would expect of a successful pilot.

Several methodological issues limit interpretation of this study. First of all, in a cross-cultural study such as this, there is the problem of standardized administration. It is not known what specific procedures were followed in each country or what the meaning of the questions were after translation. This limitation was also pointed out in Golden's (1978) study.

Furthermore, there may be limitations within the 16PF itself. Graham and Lilly (1984) state that Cattell's data on the concept validity of the 16PF does not help one to understand or predict the relationship between scores on the 16PF and important nontest behaviors. In other words, this test may not enable one to predict performance based on the scores received on the test. These restrictions notwithstanding, the overall similar profiles of these pilots across various cultures indicate a homogeneous occupational group that transcends cultural boundaries. Additional research is needed on the predictive usefulness of this information as well as on the differences based on national norms.

Recommendations include more refined analyses of the data based upon the original data bank. Eysenck and Eysenck (1983) have discussed some of the methods by which personality assessments can be compared and these techniques might be usefully applied to the current data. Comparison of individual scores with flight safety or combat effectiveness as well as

other national data could provide knowledge on types of profiles correlated with aviator safety and effectiveness. Another possible avenue of research would involve comparing the 16PF data with the "Pilot Personality" based on Edwards Personal Preference Schedule (EPPS) as described by Fry and Reinhardt (1969) and refined by Novello and Youssef (1974). Combining or integrating these two profiles (one based on 16PF, the other on the EPPS) into a data base could provide a basis for future selection or development during training.

Longitudinal studies could address the issue of predictive validity. For example, using the 16PF profile derived from this study as a norm, student pilot profiles could be compared to flight outcome. A comparison between failures and passes then could be made based on their deviation from the normative pilot profile.

A Pilot Personality Inventory and Undergraduate Pilot Training Outcome

The importance of personality in accident prevention and success in flight training, though often discussed, is little understood. If one could accurately predict the role of personality in UPT outcome, one could reduce the cost of training accidents and failures. Theoretically, one would also be able reduce the likelihood of later accidents, combat ineffectiveness, or poor adaptation to stress.

In the 1940's and into the 1950's, clinically derived personality scales used to classify pilot trainees were useful for distinguishing psychiatric cases (Fulkerson, Freud, & Raynor, 19

Amber, 1957), but were not consistent across samples or different personality inventories in predicting pilot training success (Adamson, Mitchell, Crisp, & Stogdill, 1944; Barry, Sells, & Trites, 1954; Fulkerson, 1956). Subsequently, later studies focused on less psychiatrically oriented scales and more on pre-established personality inventories. Briefly summarizing the major significant findings relating personality functioning to UPT outcome, one finds (1) the importance of anxiety and subjective stress (Bucky and Spielberger, 1975; Green, 1963; Krahenbuhl, Marett, and King, 1977); (2) the positive effect of extroversion or stable introversion on UPT success (Bartram and Dale, 1982; Green, 1963; see also, Follett, 1976); (3) the role of defense mechanisms and characteristic perceptual biases; (Skelly, 1983; Stoker, 1984); (4) the use of the Personality Research Form in increasing the predictive validity of a battery of tests (Retzloff, 1985; Valentine, 1977); (5) and the role of assertiveness, suspiciousness, and imaginativeness in differentiating between attrition and nonattrition groups of student pilots, as measured by Cattell's 16PF questionnaire (Roth, 1980).

Given twenty-five years of research, the above findings appear meager, but, in fact, there have actually been very few, long-term, systematic studies. As mentioned earlier, almost all the studies quoted above have used well-known personality instruments that were designed primarily to distinguish differences among various normative groups, not to make very fine individual distinctions within a highly select and mentally healthy group of subjects such as pilot candidates. The Defense Mechanism Test is an exception to this criticism, having been developed especially for

determination of flight safety and training success. Researchers report extraordinarily high predictive validity rates, but the DMT does require at least 1/2 day's analysis by a trained psychologist per student, making it unfeasible to use in a large Air Force such as the USAF.

The USAF has chosen to develop a computer administered, objectively scored personality test based on both past empirical findings and current research. Theoretical roots lie not in a percept-genesis model, but more in the person-situation model of Mischel (1973).

The current study reports on the preliminary analyses of this objective, computer administered and scored, personality inventory, the Pilot Personality Inventory (PPI). The PPI is being developed to predict UPT outcome, and eventually, to aid in the selection of pilots for specialized flight training. Long term data collection will eventually allow researchers to correlate personality measures with accident rate and performance ratings.

METHOD

Subjects.

Group A was composed of 169 male USAF student pilots who took the Pilot Personality Inventory (PPI) prior to undergraduate pilot training as part of a battery of tests. Group B was composed of a second sample of 195 male USAF students who took the battery of tests at a later time.

Apparatus.

The USAF pilot selection and classification research program, through its AF Human Resources Laboratory, has supported the development of the Basic Attributes Test (BAT). The BAT consists of microcomputer - administered tests that evaluate a pilot candidate's characteristics in (1) information - processing capabilities, as well as (2) in the personality domain (Kantor, and Bordelon, 1985). The Pilot Personality Inventory originally consisted of a 202 item questionnaire consisting of 25 a priori scales thought to measure those personality qualities that the Clinical Psychology Section of the United States Air Force School of Aerospace Medicine had found useful in their work with pilots. (Patterson, 1985). Due to time restrictions, the 202 item version was reduced to 66 items (Retzloff, 1984), wherein 10 of the original 25 scales were retained.

Procedure.

Each subject completed the PPI as part of the Basic Attributes Test during his initial orientation as a student pilot. The data were kept confidential until after the student completed his 49 week-long undergraduate pilot training or was eliminated from training. Students' responses were then factor analyzed and correlated to UPT outcome. Three versions were analyzed: the original 202 item version; a statistically derived 66 item version (Retzloff, 1984) and an empirically determined 18 item scale.

RESULTS

A regression analysis of the 202 item questionnaire showed that none of the 25 a priori scales significantly correlated with UPT outcome (see Table 2).

A reliability analysis for the 25 scales revealed low level coefficients of reliability for all scales as measured by Cronbach's Alpha (see Table 3), indicating high within-scale heterogeneity.

An analysis of Retzloff's statistically derived 66 items, 10 scale version showed that none of the 10 scales were significantly correlated to UPT outcome (See Table 4). However, this version did show higher within-scale homogeneity, as measured by Cronbach's Alpha (See Table 5).

The eighteen items that most highly correlated with UPT outcome were combined to form an 18 item scale. Items with negative correlations were reverse scored. The total scale score was then derived, which was found to correlate significantly ($P \leq .01$) to UPT outcome ($r = .339$). A reliablity analysis showed high inter item heterogeneity (Cronbach's alpha = .183).

A varimax rotated factor analysis of this scale revealed three factors, the first two of which had eigenvalues over 1.00. The two factors with eigenvalues have been labeled: (1) extroverted social ease and (2) introversion/trusting others (see Table 6). However, these two factors only accounted for 13.6% and 10.2% of the total variance. Factor 1 describes someone who self reports that he does not hide feelings, feels comfortable speaking up in groups or in times of trouble, sees people as basically honest and non-argumentative, and is low on punitiveness. Factor 2 describes someone who self reports that he does not feel comfortable speaking up in groups, but who also sees people as basically honest and helpful.

AD-A166 176 UNITED STATES AIR FORCE SUMMER FACULTY RESEARCH PROGRAM 12/13
1985 TECHNICAL RE (U)UUNIVERSAL ENERGY SYSTEMS INC
DAYTON OH R C DARRAH ET AL. DEC 85 AFOSR-TR-86-0139
UNCLASSIFIED F49620-85-C-0013 F/G 5/9 NL

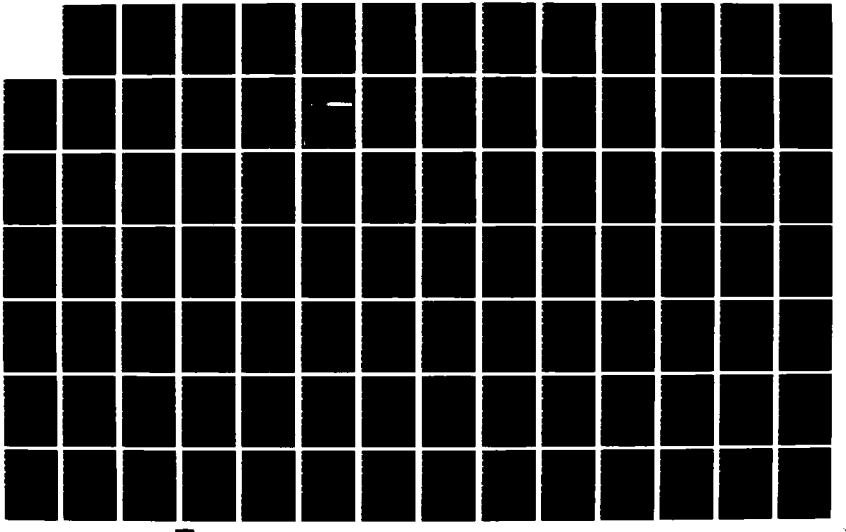

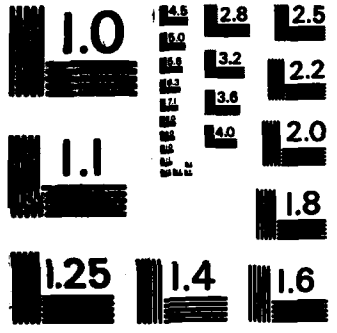

MICROCOPY RESOLUTION TEST CHART
NATIONAL BUREAU OF STANDARDS - 1963 - A

To test for test-retest reliability, two computer randomized subsamples of the 170 subject population were generated, one subsample being composed of 57 of the original population, the other being composed of 113 of the original population. UPT outcomes of these two subsamples were then correlated with the total 18 item scale score, resulting in a significant ($p \leq .05$) correlation of .307 for the subsample of 57 and .356 ($p \leq .01$) for the 113 subsample.

The 18 item scale derived from the analysis of scores of the first sample was then correlated to UPT outcome of a second sample of 190 student pilots. The total scale score correlated -.030 to UPT outcome, showing virtually no consistency in predictive ability across 2 samples.

Attempting to determine why there was so little consistency across the 2 samples, the means, standard deviations, and item to UPT outcome correlations were calculated. In addition, the samples were compared as to available demographic data: sex, age, hand preference, flight screening program, private pilots' license, and officer training school.

Comparing means of individual items across samples, six of the 18 items showed means lower for failures in the second sample, while these same items had means higher for failures in the original sample. Eight items of the 66 items showed significant correlations ($p \leq .05$) to UPT outcome in the second sample of 195, but only one of these, "I am easy to anger," ($r = -.166$) (also on the 18 item scale) was found predictive for the first sample. A comparison of demographic data showed no differences between the two samples.

A reliability analysis for the 25 scales revealed low level coefficients of reliability for all scales as measured by Cronbach's Alpha (see Table 3), indicating high within-scale heterogeneity.

An analysis of Retzloff's statistically derived 66 items, 10 scale version showed that none of the 10 scales were significantly correlated to UPT outcome (See Table 4). However, this version did show higher within-scale homogeneity, as measured by Cronbach's Alpha (See Table 5).

The eighteen items that most highly correlated with UPT outcome were combined to form an 18 item scale. Items with negative correlations were reverse scored. The total scale score was then derived, which was found to correlate significantly ($P \leq .01$) to UPT outcome ($r = .339$). A reliablity analysis showed high inter item heterogeneity (Cronbach's alpha = .183).

A varimax rotated factor analysis of this scale revealed three factors, the first two of which had eigenvalues over 1.00. The two factors with eigenvalues have been labeled: (1) extroverted social ease and (2) introversion/trusting others (see Table 6). However, these two factors only accounted for 13.6% and 10.2% of the total variance. Factor 1 describes someone who self reports that he does not hide feelings, feels comfortable speaking up in groups or in times of trouble, sees people as basically honest and non-argumentative, and is low on punitiveness. Factor 2 describes someone who self reports that he does not feel comfortable speaking up in groups, but who also sees people as basically honest and helpful.

From these results, it is concluded that the current inventory, in any of its forms, does not predict UPT outcome.

DISCUSSION

The results of this study did not support the use of the 202 or 66 item version of the PPI as a predictor of UPT outcome. The 18 item scale that was empirically derived did not show predictive validity in a second sample. Similar to previous studies, the current study did not find that pre-established scales distinguished successful from unsuccessful pilot trainees.

When one looks at the various items that did correlate with UPT outcome, one sees similarities to earlier finding that extroversion and stability are positively correlated with success in training, (Bartram and Dale, 1982).

In addition items associated with less social anxiety were significatnly related to successful UPT outcome reminding one that assertiveness and low anxiety (Roth, 1980; Bucky and Spielberger, 1973) previously have been associated with success in UPT.

These results underline several methodological and substantive issues in the use of personality variables to predict future behavior. Personality style as a predictor variable will be of utility only to the extent that the measure(s) is sensitive to (1) the variance among the subjects; (2) the particulars of the criterion variable, and (3) a clear definition of what is and is not included in that obscure and inconstant term "personality".

The particulars of the criterion variable need to be accurately assessed in determining which personality tests will be used. In this current study, the tests were selected because of their clinical utility in assessing mainly experienced pilots who, for medical reasons, are sent to the School of Aerospace Medicine (SAM) at Brooks Air Force Base for an evaluation. The problem lies in the possibility that instruments helpful in predicting clinical areas of interest in pilots who usually are experienced and older may not be helpful in predicting training outcome or combat effectiveness. A longitudinal study with the 202 item questionnaire may reveal that it successfully predicts medical problems 10-15 years later, even though it is of little use in predicting the current criterion variable, UPT outcome.

The idea that personality may play a bigger role in post training performance was noted 3 decades ago. Hunter (1985) cites Sells' (1956) comment, "... It has also been our thesis that the relative importance of ability and personality factors shifts after completion of training, the personality factors increasing in influence" (p. 446).

It is possible also that personality factors may be more important in level and type of performance than in predicting a pass/fail criterion. Successful students in UPT are classified by a board of instructors into Fighter-Attack-Reconnaissance (FAR) recommendation and non-FAR recommendation (Tankers, Transport, and Bombers (TTB)), dependent upon training performance. Those students who will become TTB pilots will be a part of flight crew, while fighter pilots primarily will fly alone. One speculates that the personality factors that are associated with being a

successful single-man, fighter pilot could be quite different from those associated with being a pilot who is part of a flight crew.

A methodological issue is the application of a linear model that sees training success as being uniformly correlated to either more or less of a certain personality attribute. It is possible that a nonlinear model might be more applicable. The inclusion of modulating variables should also be considered, as in the case of the successful introverted individual in which introversion is modulated by stability.

V. CONCLUSIONS

Several conclusions can be drawn from the reviews and reports contained herein. Looking first at the typical pilot, one sees a person who is physically and mentally healthy, a person who is a member of an cross-culturally homogeneous group. Based on the EPPS data, pilots, as a group, are high achievers, with below average needs in the areas of giving and receiving support from friends, or in needing strong attachments to friends. Results of the 16 PF study also show that pilots across countries are similar.

Attempts to assess individual differences among pilots, especially for the purpose of predicting some criterion have met with much less success than attempts to delineate the typical pilot profile. As both the current study and previous studies have shown, the usefulness of clinically based assessments is questionable, at best. Although one study may obtain

significant results, these results cannot be replicated across samples and different instruments. A notable exception to this is the DMT now being used in some NATO countries. Listed below are some ideas for future approaches that would seem to hold the greatest promise in developing a non-clinically based, objective instrument that could be used to predict criteria such as flight training outcome, stress tolerance, and effective performance. The DMT is then discussed in light of possible alternatives and recommendations.

VI. POSSIBLE FUTURE APPROACHES

The Pilot Personality Inventory as a criterion predictor

1. Continue to analyze the Pilot Personality Inventory on data now arriving at the Human Resources Laboratory, especially FAR/nonFAR recommendations.

2. Correlate the Pilot Personality Inventory with other BAT data now available to develop an overall personality measure or to look at increasing the predictive validity of these combined measures. Tests to be studied would be those measures on decisiveness, risk taking, and survivial attitudes.

3. Revise the current instrument to reflect the findings of previous studies. Possible sources of items are those reviewed in the literature as distinguishing among successful and unsuccessful pilots. These items could include questions from:

   a. scales of the EPPS (achievement, nurturance, succorance)

   b. state-trait anxiety scale

c. scales of the 16PF (submissiveness/assertiveness; trusting/suspiciousness; practical/imaginative)

d. stability of interpersonal relationships

e. scales on sense of humility and humor

f. the literature description of the successful pilot according to the DMT studies.

4. Revise the current instrument to also reflect the findings of ongoing research being done at Reese Air Force Base (Retzloff, 1985) and with the Royal Australian Air Force.

THE DEFENSE MECHANISM TEST

As discussed earlier in this paper, The Defense Mechanism Test (DMT) is being used extensively in the Scandinavian countries to screen out potentially accident-prone personality styles from pilot training. The question is, how can the USAF use these findings to produce a cost-effective instrument that assesses those qualities that appear to predict accident rate? Available options are:

1. Use the DMT as is.

2. Eliminate the DMT from consideration totally.

3. Use objective measures which have been found to have significant correlations with the DMT.

4. Develop objective questions which match the descriptions of the "poor" and good scorers.

Option 4 appears to offer the most promising approach to future USAF research with the DMT, given USAF restraints, and the advantages and disadvantages of each approach.

The development of objective measures could be accomplished by a combination of two methods. First, any previously developed scales or items could be compiled. Second, new items could be written from scratch, and then combined with previously developed questions to form a scale of maladaptive defensiveness. The poor scorer has been described as being "counter phobic, with psychopathic tendencies, insufficient super-ego or conscience, aggressive self-assertiveness, anti-social attitudes and a willful and irrational desire to prove oneself against all odds." (Skelly, p. 11). In addition to this description, there is available a complete catalogue of defense mechanisms that are measured by the DMT for which one could generate test items. For example, Skelly writes (1983, p. 10), "There is evidence from the Swedish research on the DMT that denial, reaction formation and repression are more highly correlated with maladaptation to the role of fast-jet pilot than are defense mechanisms such as projection and isolation."

Using these research findings as a guide, one could develop a scale which measures the extent to which a pilot used these defenses. Several objective scales already exist which purport to assess some of these defenses. Byrne's Repression-Sensitization scale could be used to assess the degree of repression and hypervigilance being used. At the same time, one would need to avoid those items which researchers have found to largely assess social desirability.

Work with the DMI and 16PF have shown that some of the factors on the 16PF (G, Q_3, C, I, L, and H) correlate with the defenses of projection, repression, reaction formation, denial, isolation and intellectualization (Cooper and Kline, 1983). Those scale items with the highest correlation to the above defenses also could be used as a source for generating a pilot defensiveness scale.

Or one could turn to Millon's Clinical Multiaxial Approach (Millon, 1985), wherein he defines the above terms in a way that would allow one to make up items based on these definitions. When reaction formation is defined as, "a tool that allows its users to display an image of reasonableness, maturity, and social acceptability when faced with circumstances that would normally evoke anger, dismay, or embarrassment," (p. 155) one is able to write items that would have socially desirable responses regardless of whether the respondent's answers are in the direction of reaction formation or not. Of course, one could use Millon's Clinical Multiaxial Inventory but it suffers from the problem of being a clinical inventory that would be used in a sophisticated, nonclinical population. Currently, one researcher is using Millon as a basis for a study on AF pilot trainees and results soon should be forthcoming (Retzloff, 1985).

TABLE 1

Standard Deviations of 16 P.F. Factor Scores Across Eight Countries

	Nether-lands	Nor-way	Den-mark	USA	U.K.	Can-ada	Ger-many	Bel-gium	Common to All	Common Except German
A	X	X	X	★	X	X	X	X		
B	X	X	X	X	X	X	★★	X		X
C	X	X	X	X	X	X	X	★		
D	X	X	X	X	X	X	★	X		
E	X	X	X	X	X	X	X	X		X
F	X	X	X	X	★★	X	X	X		
G	X	X	X	X	X	X	X	X	X	X
H	X	★	X	X	X	X	X	X		
I	X	X	★★	X	X	X	★	X		
L	X	X	X	X	X	X	★	X		X
M	X	X	X	X	X	X	★★	X		X
N	X	X	X	X	★	X	X	★★		
O	★	X	X	X	X	X	X	X	X	X
Q_1	X	X	X	X	X	X	★	X		X
Q_2	X	X	X	X	X	X	X	X		
Q_3	X	X	X	X	X	★★	X	X		
Q_4	★	X	X	X	X	X	X	X		

X = factor scores were within 1½ standard deviations
★ = factor scores were below 1½ standard deviations
★★ = factor scores were above 1½ standard deviations

46 0860
K·E 5 X 5 TO 1.2 INCH
KEUFFEL & ESSER CO

TABLE 2

CORRELATIONS OF 25 PERSONALITY SCALES
WITH UPT OUTCOME (202-item)

SCALE		CORRELATION w/ UPT OUTCOME
1	Inhibition of Aggression	-.14
2	Manifest Hostility	.004
3	Hostility	-.07
4	Trait Anger	.03
5	Disregard of Rights	.06
6	Acceptance of Aggression	.07
7	Frankness	.12
8	Need for Affection	.05
9	Denial of Social Anxiety	.11
10	Authority Problems	-.02
11	Social Imperturbability	.08
12	Naivete'	.08
13	Imperturbability	.04
14	Staid-Personal Rigidity	-.06
15	Distrust	-.003
16	Self Acceptance	-.001
17	Poignancy	.014
18	Brooding	-.004
19	Ego Inflation	-.06
20	Feeling Reactivity	.04
21	Value Flexibility	.09
22	Amorality	.03
23	Hypomania	.02
24	Speed and Impatience	.14
25	Hard Driving/Competitive	.12

TABLE 3

ALPHA RATING OF THE 25
SCALES OF THE 202 ITEM VERSION OF THE PPI

SCALE	N of ITEMS	CRONBACH'S ALPHA	MEAN (S.D.)	MEANS OF INTER-ITEM CORRELATIONS
1	7	.05	3.33 (1.06)	.008
2	15	.58	7.60 (2.56)	.08
3	37	.77	16.01 (5.47)	.08
4	4	.36	2.17 (.99)	.12
5	4	.50	1.94 (1.16)	.18
6	13	.12	6.96 (1.51)	.01
7	4	.39	2.15 (1.10)	.13
8	11	.49	6.75 (1.98)	.08
9	6	.74	3.92 (1.86)	.32
10	8	.22	3.21 (1.25)	.03
11	10	.54	7.22 (1.89)	.12
12	8	.53	4.79 (1.84)	.12
13	7	.17	4.20 (1.27)	.03
14	15	.63	4.26 (2.58)	.11
15	12	.44	6.14 (1.99)	.06
16	6	.30	2.49 (1.12)	.05
17	6	.26	2.18 (1.22)	.07

TABLE 4

CORRELATIONS OF 10 PERSONALITY
SCALES WITH UPT OUTCOME (66-item)

SCALE	CORRELATION WITH UPT OUTCOME	SCALE	CORRELATION WITH UPT OUTCOME
2	-.03	12	.08
3	-.04	14	-.03
4	.01	15	-.009
8	.04	18	-.05
9	.08	19	-.005

TABLE 5

ALPHA RATINGS OF THE 10
SCALES OF THE 66 ITEM VERSIONS OF THE PPI

SCALE	N of ITEMS	CRONBACH'S ALPHA	MEAN (S.D.)	MEANS OF INTER-ITEM CORRELATIONS
2	10	.63	3.92 (2.21)	.14
3	13	.73	5.46 (2.89)	.17
4	15	.66	6.72 (2.86)	.11
8	10	.60	5.69 (2.16)	.13
9	11	.78	7.67 (2.76)	.24
12	11	.68	6.56 (2.56)	.16
14	10	.68	3.41 (2.38)	.18
15	10	.47	4.46 (1.91)	.08
18	11	.74	3.46 (2.58)	.21
19	11	.73	3.36 (2.49)	.20

TABLE 6

FACTORS LOADINGS ON THE 18 ITEM SCALE

ITEM	FACTOR 1 LOADINGS	FACTOR 2 LOADINGS
* When I'm in a group. I have a hard time thinking of what to say.	.54	
* I hide my real feelings...s people don't know me well...don't know they hurt me	.46	
* Most people lie to stay out of trouble	.33	.41
Often people aren't what they seem to be.		-.34
I enjoy loud, fun parties		
* Sometimes people resent a good idea because they didn't come up with it.		
* People usually don't like to go out of their way to help somebody else.		.36
* It's really best for me to remain silent when I'm in trouble.	.38	
I am easy to anger but easy to forget		
I prefer others to speak to me before I speak to them.	-.34	
* Occasionally, I have used excuses like sickness to get out of something I don't want to do.		
It is hard for me to give a talk in front of a group of people.		.32
I don't mind being called on first to talk or give an opinion in a group.	.51	-.61
* When I am wronged, I feel I should retaliate as a matter of principle.	.38	
* Most people are honest because they fear being caught.		
* Reprimands and criticisms usually bother me.	.35	
* Discussion and argument are usually required to convince people of the truth.		
I enjoy being around people who appreciate practical jokes.		
Percent of variance	13.6	10.2

* ITEMS ARE REVERSED SCORED

K&E 5 X 5 TO 1/2 INCH • 7 X 10 INCHES
KEUFFEL & ESSER CO MADE IN U.S.A.

Figure 1

Range of 16 PF factor scores across eight countries (by standard deviations)

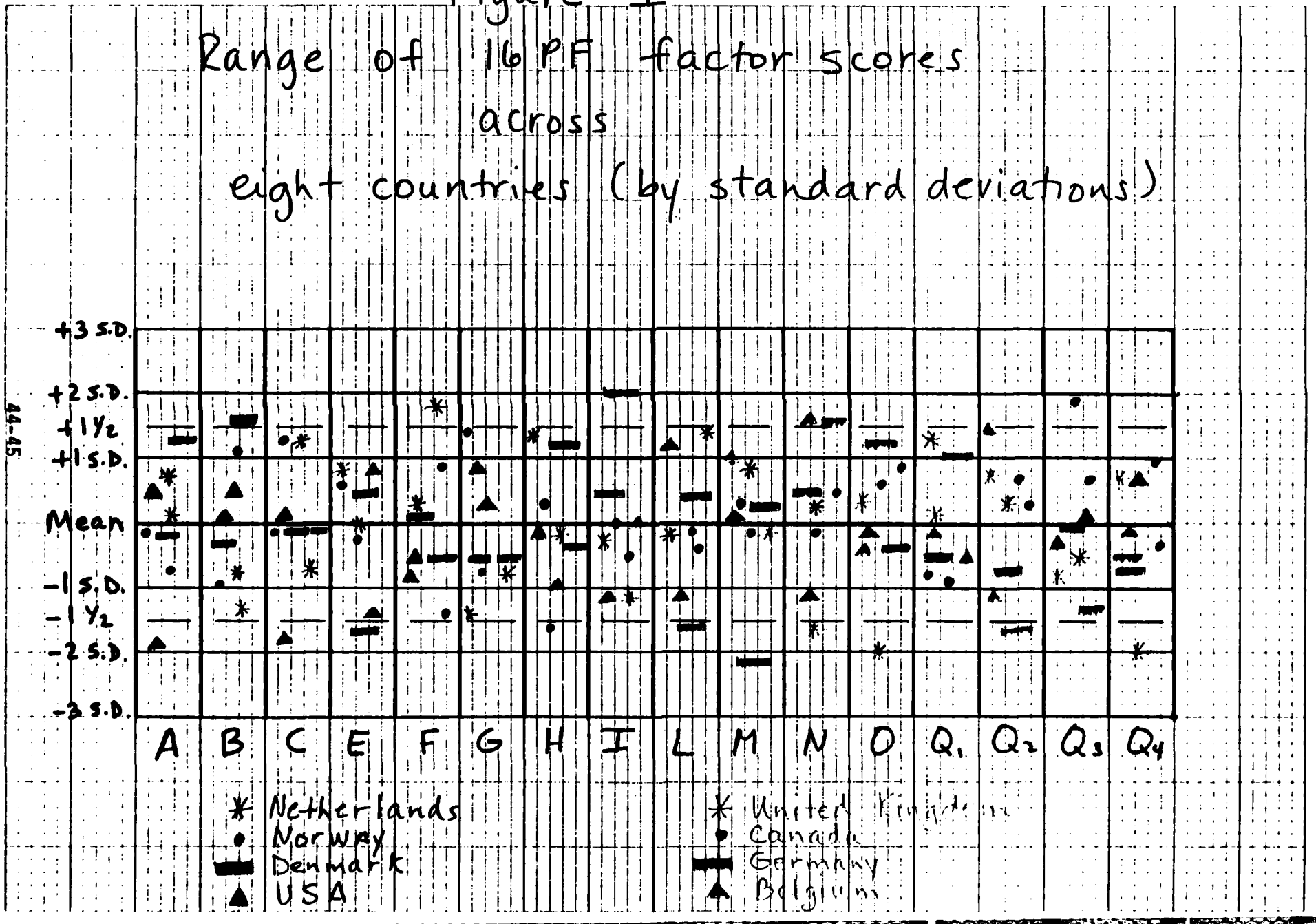

Figure 2

American Mean Scores Compared Against the Mean of all other countries.

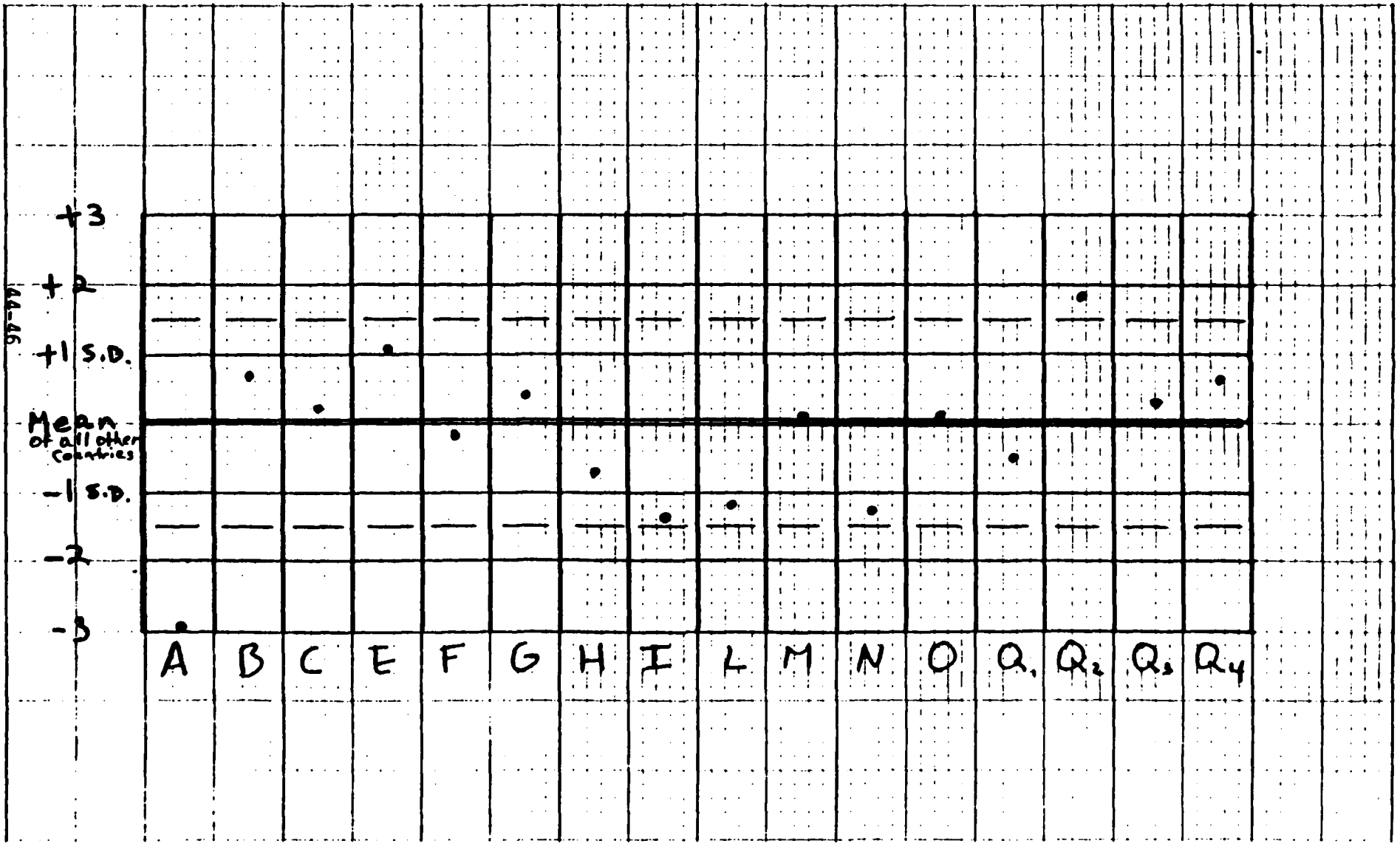

Airline Pilots

--- Airline Pilots

16PF TEST PROFILE

Figure 3
Profiles of American pilots and Airline Pilots

Sten Score
FB ____
FG ____

FACTOR	Raw Score Form A/C/E	Raw Score Form B/D	Raw Score Total	Standard Score	MEANING OF SCORE ON LEFT	MEANING OF SCORE ON RIGHT
A	6.77			4	**Cool**, Reserved, Impersonal, Detached, Formal, Aloof	**Warm**, Outgoing, Kindly, Easy-going, Participating, Likes People
B	7.39			7	**Concrete-thinking**, Less Intelligent	**Abstract-thinking**, More Intelligent, Bright
C	18.16			6	**Affected by Feelings**, Emotionally Less Stable, Easily Annoyed	**Emotionally Stable**, Mature, Faces Reality, Calm
E	16.25			7	**Submissive**, Humble, Mild, Easily Led, Accommodating	**Dominant**, Assertive, Aggressive, Stubborn, Competitive, Bossy
F	11.13			6	**Sober**, Restrained, Prudent, Taciturn, Serious	**Enthusiastic**, Impulsive, Heedless, Expressive, Cheerful
G	14.48			6	**Expedient**, Disregards Rules, Self-indulgent	**Conscientious**, Persistent, Moralistic, Staid, Rule-bound
H	14.87			6	**Shy**, Threat-sensitive, Timid, Hesitant, Intimidated	**Bold**, Venturesome, Uninhibited, Can Take Stress
I	11.97			3	**Tough-minded**, Self-reliant, No-nonsense, Rough, Realistic	**Tender-minded**, Sensitive, Over-protected, Intuitive, Refined
L	7.84			6	**Trusting**, Accepting Conditions, Easy to Get on with	**Suspicious**, Hard to Fool, Distrustful, Skeptical
M	13.03			6	**Practical**, Concerned with "Down to Earth" Issues, Steady	**Imaginative**, Absent-minded, Absorbed in Thought, Impractical
N	1.84			5	**Forthright**, Unpretentious, Open, Genuine, Artless	**Shrewd**, Polished, Socially Aware, Diplomatic, Calculating
O	7.06			4	**Self-assured**, Secure, Feels Free of Guilt, Untroubled, Self-satisfied	**Apprehensive**, Self blaming, Guilt prone, Insecure, Worrying
Q_1	9.90			6	**Conservative**, Respecting Traditional Ideas	**Experimenting**, Liberal, Critical, Open to Change
Q_2	12.58			7	**Group-oriented**, A "Joiner" and Sound Follower, Listens to Others	**Self-sufficient**, Resourceful, Prefers Own Decisions
Q_3	14.26			6	**Undisciplined Self-conflict**, Lax, Careless of Social Rules	**Controlled**, Self-respecting, Socially Precise, Compulsive
Q_4	10.39			5	**Relaxed**, Tranquil, Composed, Has Low Drive, Unfrustrated	**Tense**, Frustrated, Overwrought, Has High Drive

STANDARD TEN SCORE (STEN)

Average

1 2 3 4 5 6 7 8 9 10

Extraversion ____ Anxiety ____ Tough Poise ____ Independence ____

44-47

Second ____

Copyright © 1956, 1973, 1982 by the Institute for Personality and Ability Testing, Inc. P. O. Box 188, Champaign, Illinois

A sten of 1 2 3 4 5 6 7 8 9 10 is obtained

REFERENCES

Adamson, G.L., Mitchell, H.D., Crisp, A.G., & Stogdill, C.G. (1944). Report to subcommittee on personnel selection, associate committee on aviation medical research. National Research Council, Canada.

Alkov, R.A., & Borowsky, M.S. (1980). A questionnaire study of psychological background factors in US. Navy aircraft accidents. Aviation, Space, and Enviromental Medicine, 51(9), 860-863.

Ashman, A., & Telfer, R. (1983). Personality profiles of pilots. Aviation, Space and Enviromental Medicine, 54(10), 940-943.

Banta, G.R., & Kosnosky, D.P. (1978). Case report of an obsessive-compulsive personality: a precurser to accident proneness. Aviation, Space, and Enviromental Medicine, 49(6), 827-828.

Barry, J.R., Sells, S.B., & Trites, D.K. (1954). Psychiatric screening of flying personnel: Research on the Cornell Word Form. Project No. 21-0202-007, Report No. 7, United States Air Force, School of Aviation Medicine, Randolph Field, Texas.

Bartram, D., & Dale, H.C.A. (1982). The Eysenck Personality Inventory as a selection test for military pilots. Journal of Occupational Psychology, 55, 287-296.

Bartram, D., & Dale, H.C.A. (circa 1982). Personality and the selection of pilots in military aviation. Unpublished manuscript.

Bucky, S.F., & Spielberger, C.D. (1973). State and trait anxiety in voluntary withdrawal of student naval aviators from flight training. Psychological Reports, 33, 351-354.

Cattell, R.B., Eber, H.W., & Tatsuoka, M.M. (1970). Handbook for the 16PF. Illinois: Institute for Personality and Ability Testing.

Cattell, R.B. (1973). Personality and mood by questionnaire. San Francisco and London: Jossey-Bass.

Cooper, C., & Kline, P. (1983). A validation of the Defence Mechanism Inventory. Manuscript submitted for publication.

DeVries, P.B., Yakimo, R., Curtin, J.G., & McKenzie, J.F. (1975). Undergraduate navigator training attrition study (AFHRL-TR-75-62). Williams Air Force Base, AZ: Flying Training Division, Air Force Human Resources Laboratory.

Ellis, A., & Conrad, H.S. (1948). The validity of personality inventories in military practice. Psychological Bulletin, 45, 385-421.

Eysenck, H.J., & Eysenck, S.B.G. (1983). Recent advances in the cross-cultural study of personality. In J.N. Butcher & C.D. Spielberger (Ed.), Advances in Personality Assessment Volume 2 (pp. 41-69). Hillsdale, N.J.: Lawrence Erlbaum Associates.

Follett, S.C. (1976). Predicting performance in advanced radar intercept officer (R 10) training. Naval Postgraduate School, Monterey, California.

Fry, G.E., & Reinhardt, R.F. (1969). Personality characteristics of jet pilots as measured by the Edwards Personal Preference Schedule. Aerospace Medicine, 40(5), 484-486.

Fulkerson, S.C. (1956). Adaptibility screening of flying personnel: development of a preliminary screening battery. 56-84, School of Aviation Medicine, USAF, Randolph AFB, Texas.

Fulkerson, S.C., Freud, S.L., & Raynor, G.H. (1958). The use of the MMPI in the psychological evaluation of pilots. Aviation Medicine, 29, 122-129.

Golden, C. (1978). Cross-cultural second order factor structures of the 16PF. Journal of Personality Assessment, 42, 167-170.

Graham, J.R., & Lilly, R.S. (1984). Psychological Testing. New Jersey: Prentice Hall.

Green, L.R. (1963). An exploratory investigation of the relationship between four personality measures and voluntary resignation from aviation training. Project MR005. 13-5001, Subtask 1, Report No. 25, U.S. Naval School of Aviation Medicine, Pensacola, Florida.

Green, R.G. (1977). The psychologist and flying accidents. Aviation, Space, and Enviromental Medicine, 48(10), 922-923.

Hunter, D.R. (1985). Aircrew selection. Unpublished manuscript.

Jennings, S.L. (1948). Minnesota Multiphasic Personality Inventory: differentiation of psychologically good and poor combat risks among flying personnel. Aviation Medicine, 19(8), 222-226.

Kantor, J.E. & Bordelon, V.P. (1985). The USAF pilot selection and classification research program. Aviation, Space, and Enviromental Medicine, 56, 258-261.

Krahenbuhl, G.S., Marett, J.R., & King, N.W. (1977). Stress and performance in T-37 pilot training. Flying Training Division, Air Force Human Resources Laboratory, Williams Air Force Base, Arizona.

Millon, T., & Everly, G. (1985). Personality and its disorders. New York: John Wiley and Sons.

Mischel, W. (1973). Toward a cognitive social learning reconceptualization of personality. Psychological Review, 80, 252-283.

North, R.A., & Griffin, G.R. (1977). Aviation selection 1919-1977 (Special Report 77-2). Pensacola, FL: Naval Aerospace Medical Research Laboratory.

Novello, J.R., & Youssef, Z.I. (1974). Psycho-social studies in general aviation: 1. personality profile of male pilots. Aerospace Medicine, 45(2), 185-188.

Novello, J.R., & Youssef, Z.I. (1974b). Psycho-social studies in general aviation: 11. personality profile of female pilots. Aerospace Medicine, 45(6), 630-633.

Patterson, J. (1985). Private communication. School of Aerospace Medicine, Brooks Air Force Base, Texas.

Reinhardt, R.F. (1970). The outstanding jet pilot. American Journal of Psychiatry, 127(6), 32-36.

Retzloff, P. (1984). [Automated Aircrew Personality Profile]. Unpublished manuscript.

Retzloff, P. (1985). Private communication. Reese Air Force Base, Texas.

Rossander, P. (1980). Personality inventories and prediction of success in pilot training: The state of the art (Working Paper 80-10). Willowdale, Ontario: Canadian Forces Personnel Applied Research Unit.

Roth, J.T. (1980). Continuation of data collection on causes of attrition in initial entry rotary wing training. (Unnumbered report). Valencia, PA: Applied Science Associates.

Sanders, M.G., & Hoffman, M.A. (1975). Personality aspects of involvement in pilot-error accidents. Aviation, Space, and Enviromental Medicine, 46, 186-190.

Sanders, M.G., Hoffman, M.A., & Neese, T.A. (1976). Cross-validation study of the personality aspects of involvement in pilot-error accidents. Aviation, Space and Enviromental Medicine, 47, 177-179.

Sells, S.B. (1956). Further developments on adaptability screening of flying personnel. Journal of Aviation Medicine, 27, 440-451.

Skelly, G.B. (1983). [EURO-NATO aircrew selection working group meeting in the Hague, October 3-4, 1983, topic was the Defense Mechanism Test]. Unpublished manuscript.

Skelly, G.B. (1985). [EURO-NATO aircrew selection working group meeting at Brussels January 20-25, 1985. Update on 16PF study - Note by UK]. Unpublished raw data.

Stoker, P., & Kantor, J. (1983). Defense mechanism test research plan. Unpublished manuscript.

Stoker, P. (1984). Theoretical framework for personality deminsions relevant to capacity to cope with psychological stress in flying and flying training. Unpublished manuscript.

Vail, G.J. (1985). The social-psychological aspects of pilot error: male vs. female. In R.S. Jensen & J. Adrion (Ed.), Proceedings of the Third Symposium on Aviation Psychology. (pp. 309-319). Columbus, Ohio: Onio State University.

Valentine, L.D. (1977). Navigator-Observer Selection Research. (AFHRL-TR-77-36), Brooks Air Force Base, Texas, Personnel Research Divison, Air Force Human Resources.

Voas, R.B., Bair, J.T., & Amber, R.K. (1957). Validity of personaltiy inventories in the naval aviation selection program. Project NM16 01 11, Subtest 1, Report No. 13, U.S. Naval School of Aviation Medicine, Naval Air Station, Pensacola, Florida.

Wichman, H., & Ball, J. (1983). Locus of control, self-serving biases, and attitudes towards safety in general aviation pilots. Aviation, Space, and Enviromental Medicine, 54(6), 507-510.

Youngling, E.W., Levine, S.H., Mocharnuk, J.B., & Weston, L.M. (1977). Feasibility study to predict combat effectiveness for selected military roles: fighter pilot effectiveness (MDC E1634). St Louis, MO: McDonnel Douglas Astronautics Company.

1985 USAF-UES SUMMER FACULTY RESEARCH PROGRAM/

GRADUATE STUDENT SUMMER REPORT PROGRAM

Sponsored by the

AIR FORCE OFFICE OF SCIENTIFIC RESEARCH

Conducted by the

UNIVERSAL ENERGY SYSTEMS, INC.

FINAL REPORT

TRANSFER OF TRAINING BETWEEN ALTERNATIVE MOTION SIMULATORS

Prepared by:	John M. Flach
Academic Rank:	Assistant Professor
Department and	Institute of Aviation Department of Mechanical and Industrial Engineering Department of Psychology
University:	University of Illinois at Urbana-Champaign
Research Location:	Armstrong Aerospace Medical Research Laboratory Human Engineering Division Wright-Patterson, AFB, OH
USAF Research:	Dr. Rik Warren Dr. Grant McMillan
Date:	August 1985
Contract No:	F49620-85-C-0013

TRANSFER OF TRAINING BETWEEN ALTERNATIVE MOTION SIMULATORS

by

John M. Flach

ABSTRACT

The objective of this research project was to identify training strategies for increasing positive transfer in a roll-axis tracking task between the dynamic seat of the Advanced Low Cost G-Cuing System (ALCOGS) and the whole-body motion environment of the Roll-Axis Tracking Simulator. A mixed training procedure in which subjects were trained with a variety of cuing algorithms in the dynamic seat was tested and found to result in no more transfer than previous homogeneous training procedures. Recommendations are made that future studies should use a more difficult task to test transfer of training. The single dimension compensatory tracking task employed in this study may not be sensitive enough to provide a fair test of the utility of dynamic seat training.

ACKNOWLEDGMENTS

I wish to acknowledge the support of the Air Force Systems Command, Air Force Office of Scientific Research, and the Armstrong Aerospace Medical Research Laboratory for supporting this summer research. I am particularly in debt to Dr. Rik Warren for introducing me to the Summer Research Program, for sponsoring me as a graduate student in the summer of 1984, and for his continued support this summer. Working with Dr. Warren has been challenging, stimulating, and fun. I look forward to future associations and collaborations with Dr. Warren. During this past summer it was also my pleasure to work with Dr. Grant McMillan and Dr. Gary Riccio. Both have contributed to the research reported in this paper. The opportunity to collaborate with Dr. Warren, Dr. McMillan, and Dr. Riccio has made this summer well worth the time and effort.

I also wish to acknowledge the assistance of Melodie Snell, Matt Mittendorf, and the entire laboratory staff. It was a pleasure working with these people.

Finally, I wish to thank the staff at the University of Illinois who made it possible for me to be away for the summer. And most importantly to thank my wife who did double duty managing the home and family during my summer absence.

I. INTRODUCTION: A recent series of studies has investigated the utility of the dynamic seat (a subsystem of the Advanced Low Cost G-Cuing System---ALCOGS) for providing onset motion cues to the human operator in a roll-axis tracking task (Martin, 1985; Flach, McMillan, Warren, & Snell, 1985). The primary focus of these studies has been to identify an appropriate algorithm for driving the dynamic seat. Martin (1985) tested two algorithms for driving the dynamic seat---a position algorithm and a velocity algorithm. With the position algorithm, seat excursions were proportional to tracking error; with the velocity algorithm, seat excursions were proportional to tracking error rate. Martin (1985) found that RMS tracking error in a roll-axis control task was substantially reduced when dynamic seat motion cues were used in addition to the visual display. Performance was best with the velocity drive algorithm. Flach et al. (1985) found that tracking error could be further reduced, to a level comparable to that achieved by subjects in a whole-body motion environment, when a combination position/velocity algorithm was used to drive the dynamic seat. These studies demonstrated quite clearly that the dynamic seat is an effective cuing device.

How effective is the dynamic seat as a training device? In order to address this question, subjects in both the Martin (1985) and the Flach et al. (1985) studies were transferred to a whole-body motion roll-axis tracking

environment. In both studies subjects first received 20 sessions (four 3-minute trials per session) in the dynamic seat and were then transferred to an identical roll-axis tracking task in the Armstrong Aerospace Medical Research Laboratory's Roll-Axis Tracking Simulator (RATS), which provided whole-body motion cues. Results showed that only a minor, nonsignificant gain could be attributed to dynamic seat training. That is, subjects trained with the dynamic seat did no better than subjects who received only visual roll-axis training and only slightly better than subjects who received no previous roll-axis tracking experience.

The objectives of this summer's research were to explore methods for improving the transfer of training between the dynamic seat and the RATS for a roll-axis control task. I began working with the dynamic seat last summer when I participated in the Summer Research Program as a graduate student. The work last summer resulted in two papers which were presented at the Symposium on Aviation Psychology this past spring. A paper has also been submitted for a special issue of Ergonomics on Aviation Psychology. I am presently an Assistant Professor in the departments of Mechanical and Industrial Engineering, Psychology, and Aviation at the University of Illinois at Urbana-Champaign. My major area of research is Engineering Psychology with special interest in perceptual-motor skills.

II. OBJECTIVES OF THE RESEARCH EFFORT: The objectives of this research effort were to explore methods for improving the transfer of training between the dynamic seat and the RATS for a roll-axis control task. The fundamental hypothesis was that there is a subset of skills which are common to tracking in the dynamic seat and tracking in the RATS and that the training procedures used in previous studies (Martin, 1985; Flach et al., 1985) have not fully capitalized on these common skills.

Two training procedures were identified for examination---a "mixed" training procedure and an "alternating" training procedure. In the "mixed" training procedure subjects were exposed to a variety of cuing conditions during training with the dynamic seat. These conditions included visual only, motion only, visual plus motion using a position drive algorithm, and visual plus motion using a position/velocity drive algorithm. It was hoped that the variety of training conditions would increase the range of skills which were exercised during the training period. This wider range of skills would increase the likelihood that skills which are applicable to the RATS are developed during training. In addition, switching among various cuing conditions during training, may result in subjects who are better able to adapt to task variations. In a sense, the subjects may "learn-to-learn." The specific hypothesis for this study was that a variety of experiences

in the dynamic seat would better prepare subjects to learn the RATS, than did the homogeneous training routines employed in earlier studies. As a result, it was predicted that subjects in this training condition would learn the RATS at a faster rate than did subjects from previous studies (Martin, 1985; Flach et al., 1985).

The "alternating" training procedure was one in which subjects were to be trained with alternating training (dynamic seat) and criterion (RATS) sessions. It was hoped that this training procedure would enhance subjects' ability to focus on the subset of skills which are common to the two motion devices (dynamic seat and RATS). In previous studies subjects have had, at best, only a vague notion of the skills which would be required for criterion performance in the RATS. Under these circumstances it is likely that the most highly developed skills will be those which improve performance in the training task. These are not necessarily the same skills which are important for success in the criterion task. In an effort to bias subjects' attention toward the skills which are common to both the criterion and training task, subjects in this training condition were to receive periodic exposures to the criterion task. Also, in order to de-emphasize the importance of skills specific to the training task, feedback (in terms of error scores following a trial) was to be given only for criterion task

trials. Data from this training condition has not been collected at this time.

III. BACKGROUND: The measurement of what is learned during training has always been problematic. There is no direct way to measure learning. Learning can only be inferred form changes in performance. However, changes in performance can be the result of very different types of learning, from the development of very general skills as in learning-to-learn studies (Harlow, 1949; Meyer & Miles, 1953) to stimulus specific learning as in perceptual discrimination studies (Gibson, 1969). Inferring the combination of general and specific skills, or identifying which specific skills contribute to a particular performance change is quite difficult, especially when the task involves complex perceptual-motor skills. However, that is the task which must be accomplished in order to evaluate the utility of the dynamic seat for training flight control tasks.

Two performance indices have been examined for drawing inferences about learning in the dynamic seat---RMS error and frequency characteristics (describing functions) of the human operator. RMS error is a global measure of overall performance quality. Describing functions allow a finer grained analysis of performance that is thought to be more sensitive to changes in performance strategies than global error measures.

Through a subjective matching procedure, Flach et al. (1985) were able to choose a dynamic seat drive algorithm that resulted in both quantitative (RMS error) and qualitative (describing function) equivalence between performance measured in the dynamic seat and performance measured in the whole-body motion environment of the RATS. This equivalence suggested that subjects were performing at the same level and were using the same strategy for controlling the two devices. However, despite this performance similarity, there was no evidence for positive transfer from the dynamic seat to the RATS.

The failure to achieve positive transfer in the Flach et al. (1985) study seems to indicate that subjects are using specific skills in the dynamic seat which do not transfer to the RATS. Flach et al. (1985) have postulated that these skills may involve a strategy for distributing attentional resources across modalities. That is, the distribution of information across visual, tactual, kinesthetic, and vestibular modalities is likely to be different when tracking with the different motion systems. However, while optimal performance with a specific dynamic seat cuing algorithm may depend on different skills than optimal performance in the RATS, this does not rule out the possibility that skills relevant for learning the RATS can be taught using the dynamic seat. There may be general "learning-to-learn" type skills or even a subset of specific

skills relevant for performance in the RATS that can be taught using the dynamic seat. The challenge is in discovering the appropriate training procedure.

IV. METHODS: The first experiment used the mixed training procedure in which subjects were exposed to four different cuing conditions in the dynamic seat. The logic for this training procedure is described in sections II and III above.

A. Subjects. Six subjects were recruited from a paid subject pool. All subjects were right handed and had normal or corrected to normal vision. Subjects had no previous flight experience.

B. Apparatus. Two simulators were used. The dynamic seat, a subsystem of the ALCOGS, was used as the training device and the AAMRL's Roll-Axis Tracking Simulator (RATS) was used as the whole-body motion, criterion device.

The dynamic seat is a hydraulically actuated seat pan which can be driven in four degrees of freedom: longitudinal, heave, pitch, and roll. For this study, only the seat pan roll was used.

The RATS consists of a rotating seat frame, drive train, and control console. It is capable of 360 degree rolls, however was constrained to $\pm 90^{o}$ for this study. The axis of rotation is through the subjects' buttocks.

Both simulators were driven with an EAI 580 analog computer and a PDP 11/60 digital computer. The dynamics were representative of a fighter aircraft. This simulation operated at 100 Hz and included delays of only 75 msec in the visual and motion loops.

A TV monitor, mounted at the subjects' eye level was used to present visual information. Tracking error was displayed as angular deviations between a schematic plane and a horizontal reference line. The reference line subtended a visual angle of approximately 9 degrees.

Control inputs were made using a force sensitive control stick mounted at the right side of both the ALCOGS and the RATS.

C. Procedure. The primary experimental task was a roll-axis compensatory tracking task. The objective of this task is to maintain wings-level flight in the presence of a gust-like disturbance. The gust disturbance was composed of 13 sinusoids ranging in frequency from 0.2 to 32 rad/s. The amplitudes of the sinusoids were weighted to represent white noise passed through a low-pass filter with a double pole at 2 rad/s. The phases of the frequency components were randomized for each 3 min tracking trial, making the signal non-predictable.

Subjects participated in 20 training sessions in the dynamic seat and were then tested for an additional ten

sessions in the RATS. Each session consisted of four 3-minute trials.

During training each of the four trials used a different visual/motion cuing combination. The four combinations used were:

1. visual only
2. motion only (position drive)
3. visual + position seat drive
4. visual + position & velocity seat drive

The order in which cuing conditions were presented within a session was randomized.

At the end of each tracking trial subjects were asked to estimate the RMS error for that trial. Following this estimation the subjects' actual score was displayed on the visual monitor.

V. RESULTS: Figure 1 shows the RMS error across the twenty training sessions for each of the four cuing conditions. A nonparameteric test, the Wilcoxon Matched Pairs Signed Ranks Test, was used to compare the errors scores on the 1st, 5th, 10th, 15th, and 20th trials. The results from this test are summarized in Table 1. As can be seen in Table 1 and Figure 1, error was greatest for the visual only cuing condition. Error was least when the SIGMA (position/velocity) algorithm was used to drive the seat. These results are consistent with the results of Martin (1985) and Flach et al. (1985). There was no significant differences between the error

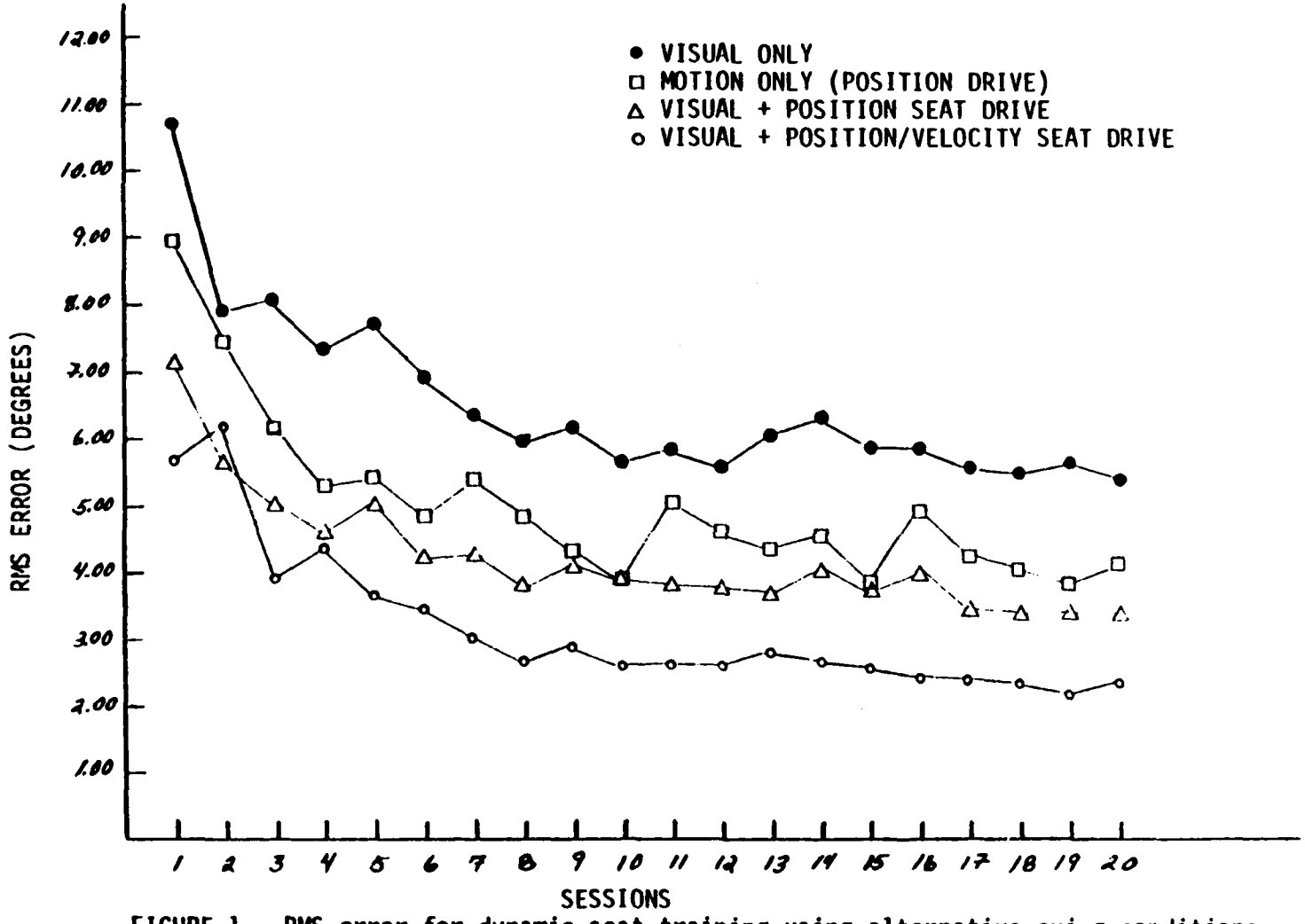

FIGURE 1. RMS error for dynamic seat training using alternative cuing conditions. Each data point represents a mean across six subjects.

TABLE 1

	TRIAL	MOTION	POSITION	SIGMA
VISUAL	1	=	<	<
	5	<	=	<
	10	<	<	<
	15	<	<	<
	20	=	<	<
MOTION	1		=	<
	5		=	=
	10		=	<
	15		=	<
	20		=	<
POSITION	1			<
	5			=
	10			<
	15			<
	20			<

TABLE 1. A comparison among RMS error scores achieved with various cuing conditions across the 20 training sessions. Comparisons were made on the 1st, 5th, 10th, 15th, and 20th trials using the Wilcoxon Matched-Pairs Signed Ranks Test. = indicates no significant difference. < indicates that RMS error was less for the column cuing condition than for the row condition.

levels for the motion only and visual + position motion algorithm. This is consistent with previous results reported by Snell, Flach, McMillan, and Warren (1985). This result suggests that much of the information used in this control task is available in the motion display.

The performance obtained in the first five sessions in the RATS was compared with the performance obtained previously by Martin (1985) and Flach et al. (1985) using the nonparametric Mann Whitney U test. The results indicated that there was no significant advantage for the mixed training procedure. Performance in the whole-body motion environment of the RATS was no better for the mixed training procedure than for homogeneous training procedures using no motion, a position algorithm, a velocity algorithm, or the position/velocity algorithm.

Subjective estimates of error scores were collected from subjects in order to make inferences about the subjective cost functional or error criterion which subjects are using while tracking. For example, a consistent overestimation of error scores upon transfer to the RATS might indicate that error is weighted more heavily in the whole-body motion environment than in the dynamic seat. These data have not been analyzed at the time of this report.

VI. CONCLUSIONS: The results indicate that for the specific roll-axis tracking task being used there is no advantage to mixed training over homogeneous training. Further, comparisons with no training control groups indicate that there is only a slight training benefit from training in the dynamic seat relevant to later performance in the RATS.

However, it is not clear at this point whether the nonsignificant results with regard to training indicate that the dynamic seat is not a good training device or whether they indicate that the particular single dimensional roll-axis tracking task is an insensitive task. Untrained subjects typically reach asymptote in the RATS within four or five sessions. Also, the sample sizes in this and previous studies which have examined dynamic seat training have been quite small (4 to 6 subjects). Thus, the statistical tests have not been very powerful.

McMillan, Martin, Flach, and Riccio (1985) report that significant positive transfer has been attained with both pilots and nonpilots when subjects were first trained in the RATS and then transferred to the dynamic seat. This may reflect an asymmetry of transfer between the two devices or it may simply be an artifact due to the slower base learning rates in the dynamic seat. Positive transfer from the dynamic seat to the RATS was also found when subjects were experienced pilots. Again this may reflect specific

abilities of pilots or it may simply be an artifact due to the homogeneity of the sample being tested. Thus, an important consideration before continuing research on dynamic seat training is how sensitive should the task be? The task currently being used appears to provide an extremely conservative test of dynamic seat training. Is this appropriate?

VII. RECOMMENDATIONS: The evidence from this study, together with evidence from Martin (1985) and Flach et al. (1985) indicates that the probability of finding a training benefit for the dynamic seat for this specific roll-axis control task is small. However, before any conclusions are drawn about the utility of the dynamic seat as a training device, tests should be made using a more complex or difficult task. Task complexity can be increased by using a multiple axis tracking task. However, this would require the availability of a multi-axis criterion device. An alternative to multi-axis control is to increase the difficulty of the single axis control task. This could be achieved by increasing the bandwidth of the forcing disturbance or by adding a secondary task.

My recommendation is to test several subjects in the RATS with a more difficult single axis control task (e.g. increase bandwidth of forcing function) before trying either

multi-axis control tasks or alternative training strategies such as the "alternating" training procedure described earlier in this report. If the learning rate is decreased or the time to asyptote is increased as a result of increasing difficulty, the the more difficult task should be used for future tests. Also, consideration should be given to repeating some earlier experiments using this more sensitive task.

REFERENCES

Flach, J.M., McMillan, G.R., Warren, R., & Snell, M.K. (April, 1985) The effects of psychophysical matching on the transfer of training between alternative motion simulators. Proceedings of the Third Symposium on Aviation Psychology. Columbus, OH.

Gibson, E.J. (1969). Principles of perceptual learning and development. New York: Appleton-Century-Crofts.

Harlow, H. F. (1949). The formation of learning sets. Psychological Review, 56, 51-65.

Martin, E.A. (April, 1985). An investigation regarding the use of a dynamic seat-pan display for training and as a device for communicating roll-axis motion information. Proceedings of the Third Symposium on Aviation Psychology. Columbus, OH.

McMillan, G.R., Martin, E.A., Flach, J.M., & Riccio, G.E. (1985,November). Advanced dynamic seats: An alternative to platform motion? Proceedings of the 7th Interservice/Industry Technical Equipment Conference.

Meyer, D.R. & Miles, R.C. (1953). Intralist-interlist relations in verbal learning. Journal of Experimental Psychology, 45, 109-115.

1985 USAF-UES SUMMER FACULTY RESEARCH PROGRAM/

GRADUATE STUDENT SUMMER SUPPORT PROGRAM

Sponsored by the

AIR FORCE OFFICE OF SCIENTIFIC RESEARCH

Conducted by the

UNIVERSAL ENERGY SYSTEMS, INC.

FINAL REPORT

CONTROL OF ADAPTIVE OPTICAL SYSTEMS

Prepared by:	John A. Fleming
Academic Rank:	Assistant Professor
Department and	Department of Electrical Engineering
University:	Texas A&M University
Research Location:	Rome Air Development Center
	Surveillance Division, Strategic Surveillance Branch
	Electro-Optics Section (RADC/OCSE)
USAF Researcher:	Dr. Richard J. Michalak
Date:	August 9, 1985
Contract No:	F49620-85-C-0013

CONTROL OF ADAPTIVE OPTICAL SYSTEMS

by

John A. Fleming

ABSTRACT

This final report describes several studies related to the use of large space-based adaptive optical systems for strategic surveillance. In particular we study several proposed procedures for control and estimation, including phase retrieval, calculation of point spread functions for synthetic aperture optical systems, and deconvolution for control of active mirrors. We first describe the phase retrieval problem and discuss several algorithms that we programmed, evaluated, and modified for improved performance. Next, we illustrate the Fast Fourier Transform (FFT) algorithm for two dimensional arrays. We derive sampling constraints so that the FFT can be used to provide the approximate point spread function and optical transfer function for arbitrary configurations and apodizations of synthetic apertures. Finally, we examine the use of deconvolution in the context of estimation and control of actuators for correction of wavefront errors in an active mirror experiment. The problem is one of least squares and we discuss the singular value decomposition for the solution of such problems. Recommendations and modifications of simulation software to include actual wavefront and actuator data (so that a closed loop control system is constructed) are outlined.

ACKNOWLEDGEMENTS

The author gratefully acknowledges the technical guidance provided by the members of the in-house group of the Electro-Optics Section (RADC/OCSE) and in particular by Dr. Richard Michalak. Their expertise and ongoing assistance was crucial to the selection, direction, and outcome of the resarch project. Working conditions and hospitality provided by the members of the Surveillence Division (RADC/OC), and in particular Mr. Thomas Pitts, chief of the Strategic Surveillence Branch, and Captain Patrick Nutz and then Mr. William Kaveney, chiefs of the Electro-optics section made the author's stay at Rome Air Development Center rewarding and enjoyable. Mr. John Ritz of the plans office (RADC/XP) coordinated the assignments of the summer faculty appointees, and arranged for housing, office space, presentation of seminars, etc..

The Summer Faculty Research Program is sponsored by the U. S. Air Force Systems Command, Air Force Office of Scientific Research, and was administered by Universal Energy Systems Incorporated. The author is grateful for the opportunity this worthwhile program provided, and appreciates the efficient management provided by these organizations.

I. INTRODUCTION

This report describes work completed while the author was a Summer Faculty Research Associate at the Optical Systems Engineering Laboratory in the Electro-Optics Section (RADC/OCSE) of the Strategic Surveillance Branch at Rome Air Development Center. The laboratory is concerned with large space-based optical systems for strategic surveillance. Of necessity (size, harshness of the space environment) these systems will be adaptive optical systems. Algorithms for estimation and control are required for experimentally evaluating such concepts as (a) using segmented mirrors to realize the large mirror size required for wide field of view optics, (b) using active mirrors to correct surface figure errors, and (c) optical phased arrays.

The author is an Assistant Professor of Electrical Engineering with research experience in control system theory, digital signal processing, and numerical analysis. Dr. Richard Michalak, laboratory director, described laboratory efforts, and these offerred an exciting opportunity for research. Although the author had no experience in optical system analysis and design, he was able to use the time before the summer period to read and study several recent laboratory reports.

II. OBJECTIVES OF THE RESEARCH EFFORT

The preliminary goals set forth for the research period included: (a) gaining familiarity with optical system analysis and design, (b) evaluating several proposed procedures for control and estimation, (c) development of tools for the analysis of system performance, and (d) studying the implementation and potential advantages of alternate strategies (e.g. adaptive Kalman filtering) for estimation and control. Specifically, procedures for phase retrieval were programmed, evaluated, and modified for improved performance; calculation of point spread function and optical transfer function for arbitrary configurations and apodizations of synthetic apertures was accomplished using two-dimensional fast Fourier transforms; singular value decomposition for the estimation of required actuator changes for correction of wavefront errors was studied, and modifications of simulation software to include actual wavefront and actuator data (so that a closed loop control system is constructed) were outlined.

III. PHASE RETRIEVAL

One proposed method for system control uses a wave front sensor. This sensor measures intensity distribution in the far field. Also known is the intensity

distribution at the aperture. The Fourier theory of Fraunhoffer diffraction 1,2 demonstrates that the (complex) amplitude distribution $A(x,y)$ at the aperture and (complex) amplitude distribution in the far field $A'(x',y')$ are related by Fourier transform and change of variables as in equation (1)

$$A'(x',y') = \int_{-\infty}^{-\infty}\int_{-\infty}^{-\infty} A(x,y)e^{-2\pi j(ux+vy)}\,dx\,dy \quad \Big| \quad u = \frac{x'}{\lambda f}, v = \frac{y'}{\lambda f}. \qquad (1)$$

Since the *magnitude* of a complex amplitude is the square root of its intensity, the measurements provide the magnitude of a function and the magnitude of its transform, but all phase information is lost. The phase retrieval problem is one of calculating the phase functions that go with the measured pair of magnitude functions [3,4,5]. Note that finding one of the phase functions automatically determines the other (Fourier transform pairs are unique).

For computational purposes the aperture plane and Fraunhoffer plane are discretized on an $N \times N$ grid and the phase retrieval problem is cast as one of finding the set of values $\theta(m,n)$ and $\phi(u,v)$ such that the discretized complex amplitude functions are legitimate discrete Fourier transform (DFT) pairs as in (2).

$$A'(u,v) = |A'(u,v)|\angle\phi(u,v) = DFT\{|A(m,n)|\angle\theta(m,n)\} \qquad (2)$$

Where the DFT of an $N \times N$ two-dimensional sequence $x(m,n)$ is a two-dimensional complex sequence $X(u,v)$ defined by the relation (3) and its inverse (4)

$$X(u,v) = DFT\{x(m,n)\} = \sum_{m=0}^{N-1}\sum_{n=0}^{N-1} x(m,n)e^{-2\pi j(um+vn)/N} \qquad (3)$$

$$x(m,n) = IDFT\{X(u,v)\} = \frac{1}{N^2}\sum_{u=0}^{N-1}\sum_{v=0}^{N-1} X(u,v)e^{+2\pi j(um+vn)/N} \qquad (4)$$

for $u,v, = 0,\ldots,N-1$ or $m,n = 0,\ldots,N-1$.

Since the laboratory computer system did not have a library routine for the Fast Fourier transform method of calculating the 2-D DFT, the first task was to write such a program and to make it flexible for use in other applications (for example Section IV of this report). The key observation is that the second relation in (3) shows that the 2-D DFT can be written as N 1-D DFT's to which the conventional 1-D FFT algorithm can be applied. Secondly, the form of (4) shows that the inverse transform can be calculated by conjugating the forward transform (equation (3)) of the conjugate of the sequence $X(u,v)$, and dividing by $N \times N$.

The solution of the phase retrieval problem is gotten by minimizing (over the $N \cdot N$ phase values at the grid points) the functional

$$B_k = \sum_u \sum_v (A'_k(u,v) - A'_{meas}(u,v))^2 \qquad (5)$$

using a functional minimization algorithm. This is a large optimization problem since resolution will require N to be at least 128 or 256. Three optimization methods (Gerchberg-Saxton [6], steepest descent [5], conjugate gradient [7]) were applied in order to compare computational efficiency and robustness.

The Gerchberg-Saxton method consists of repeated forward and inverse Fourier transforms (using the known magnitude data and updated phase information at each step). The steps of the algorithm are: (1) Given the measured aperture magnitude function and an estimate (guess) for the phase. Fourier transform this to obtain a corresponding magnitude and phase for the far field. (2) the magnitude function thus calculated will not match the known far field magnitude, so replace it by the measured magnitude, while keeping the calculated phase as an estimate of the correct phase. (3) inverse Fourier transform this function to obtain an estimate of the aperture function. (4) since this function will probably not have magnitude equal to the measured magnitude, use the measured magnitude (with the calculated phase as a new phase estimate) and redo the procedure. It can be shown that the iterative application of steps 1-4 will converge.

The steepest descent procedure is based on the fact that if one moves opposite the direction of the gradient, then (locally) along this path the cost functional is decreased faster than along any other direction. That is: Given a vector x_0 that has cost associated with it of $f(x_0)$, a point x_1 that has lower cost can be gotten by choosing $x_1 = x_0 - h \nabla f(x_0)$, where h is a step size, chosen so that $f(x_0 - h \nabla f(x_0))$, treated as a function of h, is as small as possible. (That is: go as far as possible in the negative gradient direction while making the function smaller). For the phase retrieval problem one must calculate the gradient of the cost function with respect to the phase values. After some algebra, this can be shown to be

$$\frac{\partial B_k}{\partial \theta} = -2|A(m,n)|\,|\mathcal{F}^{-1}\{A'(u,v)\}|\sin(\angle \mathcal{F}^{-1}\{A'(u,v)\} - \theta(m,n))$$

The computational procedure is therefore: (1) Given the measured magnitude at the aperture and an estimate of the phase, calculate the gradient by equation (6). This involves a forward transform. (2) pick a stepsize h that decreases the

cost, and update the estimate of the far field phase distribution. (3) inverse Fourier transform the function formed by the measured far field magnitude and new phase estimate. (4) replace the magnitude part of this result with the measured aperture magnitude, while keeping as the associated phase the value obtained by (3). Then repeat steps 1-4. It can be shown that as long as h is chosen so that there is a functional decrease (can always be done by taking h small), the steepest descent method will find a minimum.

The conjugate gradient method is based on the argument that a search along a descent direction which is (loosely speaking) orthogonal to the directions previously searched should find a minimum in fewer iterations. It had been observed that a zig-zag phenomenon often occurred in the behavior of the steepest descent algorithm. For the conjugate gradient method, instead of taking steps in the true negative gradient direction, the step direction is chosen so that each new direction is *conjugate* to all the others. In all other respects the steps of this method are as described for steepest descent. The formula for search direction d_k at iteration k is

$$d_k = -\nabla f(x_k) + \frac{\|\nabla f(x_k)\|^2}{\|\nabla f(x_{k-1})\|^2} d_{k-1} \tag{6}$$

Again the step size h is chosen so that the function is decreased.

Fienup in [4] and [5] derives strategies for choosing the step size. However, we found that in practice these procedures were not successful. Instead two alternative approaches common in numerical analysis were used. The first involves proposing a normalized step size of 2. If the function evaluated at the updated point is decreased, then the proposed stepsize is continually doubled and the function value retested until begins to increase. If the function was NOT decreased, the stepsize is continually halved until a decrease is found. (Since the gradient and conjugate gradient directions are each descent directions, a decrease in function can ALWAYS be found by making h small enough). The stepsize that decreases the function the most of those tested is chosen as the step for the iteration.

The second stepsize selection procedure is the quadratic approximation method suggested by Powell [8]. Here, the function is evaluated at three different stepsizes, a quadratic is passed through these points, and the minimum of the quadratic is found by formula and chosen as the optimal step.

We implemented each of the three phase retrieval methods and compared performance. No real image data was readily available, and so arrays of random numbers were chosen as examples. The results showed that the steepest descent

and the conjugate gradient methods outperformed the Gerchberg-Saxton method, and that unless one of the alternate stepsize procedures was used, convergence was rarely attained. Between the steepest descent and the conjugate gradient methods, no clear trend was seen. Between the first and second methods of stepsize selection, the quadratic approximation method was superior.

Faster convergence in minimization problems can usually be obtained by including either actual second derivative information, the Hessian matrix, (as in Newton's method) or an approximation to this matrix (as in the various quasi-Newton methods of which the Davidon, Fletcher, Powell (DFP) method is the most well known). It seemed promising to apply these ideas to the phase retrieval problem, and some effort was devoted to this. For the problem at hand, calculation of the Hessian by analytical formula is unwieldy. Likewise, use of finite differences poses computational problems since each entry involves taking a 2-D FFT. The quasi-Newton methods build up approximations to the Hessian using only gradient information and so these methods were considered. However, the futility of this becomes apparent when one realizes that for a 128x128 array of sensor data points, the Hessian matrix is (128x128) by (128x128), too large for the computer to store. Therefore, it seems that only first order methods are feasible for the phase retrieval problem.

IV. POINT SPREAD FUNCTION AND OPTICAL TRANSFER FUNCTION FOR SYNTHETIC APERTURE OPTICAL SYSTEMS

The point spread function $PSF(x,y)$ for an optical system is defined as the magnitude squared of the Fraunhoffer far field complex amplitude function. This in turn (by equation (1)) can be calculated by first Fourier transforming the aperture complex amplitude function, making a change of variable as in (1), and then squaring the magnitude of this complex function. Symbolically this is:

$$PSF(x,y) = |\{\mathcal{F}[A(x,y)] \mid u = \frac{x}{\lambda f}, v = \frac{y}{\lambda f}\}|^2 \qquad (7)$$

and the point spread function describes the intensity distribution in the Fraunhoffer plane, as a function of position in that plane.

The optical transfer function (OTF) is defined as the Fourier transform of the point spread function

$$OTF(u,v) = \mathcal{F}[PSF(x,y)]$$

where the arguments u and v are spatial frequencies. The OTF describes the filtering (in the spatial frequency sense) that the optical system performs on an

image. Small OTF magnitude at some spatial frequency (u, v) indicates that images with spatial frequency content at that value will have this content attenuated by the optics. The magnitude and phase of the OTF are given the names MTF (modulation transfer function) and PTF (phase transfer function), respectively.

The electro-optics section is interested in studying the synthetic aperture concept as a way of obviating the need for the large mirrors that would be necessary to obtain high resolution. Several smaller independent optical systems are combined in a phased array to produce a resolution that exceeds that produced by any single element. In order to aid in this work, computer procedures for the calculation and plotting of PSF and OTF for arbitrary locations and sizes of apertures were written. These rely on the 2-D Fast Fourier Transform program that was described in Section III. Also, closed form expressions for the point spread function for some regularly spaced arrays of identical circular apertures were calculated and plotted. These were used to observe the effects of various array configurations, aperture sizes and number of apertures, and also to evaluate the consistency of the numerical procedure. However, in order to study aberration effects, deliberate apodization, and what occurs when the apertures have irregular shapes, distributions, or sizes, the FFT based procedure is necessary since closed form solutions would be almost impossible to obtain.

For phased arrays consisting of apertures with pupil functions for which the individual Fourier transforms can be written in closed form (circles and rectangles, for example) the "time-delay" property of Fourier transform can be used to calculate the total transform as a sum of properly phase shifted individual transforms. This is the approach taken in [9] where several configurations of phased array were calculated. As part of the summer research, we first wrote a program to produce the total PSF for regularly spaced circular apertures, and compared results with [9]. Then the program was used to produce a series of PSF plots to illustrate the effects of number of individual apertures, and individual aperture diameters on the total PSF.

Closed form expressions for OTF can also be calculated for special cases by observing that the Fourier transform of a PSF is equivalent to the autocorrelation (with change of variable and scale as in equation (1)) of the pupil function. (More precisely, the pupil function and OTF are related by the autocorrelation function, but a change of variable $u' = -u$, $v' = -v$ is required because the definitions of both PSF and OTF are stated as forward Fourier transforms, not a forward/inverse pair).

In order to study more complicated phased arrays, a numerical procedure for calculating PSF and OTF, given arbitrary complex pupil function, is needed. The discrete Fourier transform can be interpreted as an approximation to the true Fourier transform provided several requirements relating to maximum sampling interval and minimum total record size are observed. First, in choosing a grid size for an approximation to the pupil function, the grid must be sufficiently dense so that the approximation is good (e.g. circles should look like circles). Second, an attempt should be made to choose the total number of grid points in the x or y direction so that these are less than or equal to 256 each. Otherwise the computational burden becomes staggering. Third, the total number of points in the x (or y) direction times the x (or y) interval size must be at least twice as large as the maximum width (or height) of the total pupil function. That is: the (x, y) region sampled must be at least two synthetic aperture diameters wide and high, where the diameter of the synthetic aperture is defined as the maximum dimension of the phased array. This is because an autocorrelation will have support equal twice the support of the original function. Fourth, the requirements of the sampling theorem [10] must be satisfied if aliasing is to be avoided. This requires that the grid interval in each dimension must be no larger than one-half the reciprocal of the ***highest frequency*** present in the transform. We note here that in going from pupil function to PSF, Fourier transformation is followed by a change of variable with the result that both pupil function and the PSF have distance variables (not spatial frequency) as their arguments. Thus the requirements are that

$$\Delta x < \frac{\lambda f}{2\, x_{PSFmax}} \qquad \Delta y < \frac{\lambda f}{2\, y_{PSFmax}}$$

Since the point spread function is not known in advance, and since the support of the transform of a function MUST be infinite when that function (the pupil function) is of finite size (Paley-Weiner Theorem), some aliasing is unavoidable. However, we can make a reasonable prediction of the support ("bandwidth") of the point spread function by noticing that the point spread function for circular apertures tends to be dominated by the term

$$\left[\frac{2J_1(\frac{2\pi ar}{\lambda f})}{(\frac{2\pi ar}{\lambda f})}\right]^2$$

where a is the radius of the smallest individual aperture. This term is less than .001 for all points outside of a radius

$$R = 3.7\frac{\lambda f}{2a}$$

Using this relation we can say that aliasing effects will be minor if the sampling interval for the pupil function is chosen no larger than $(a\ 3.7) = .2703a$.

When all sampling conditions hold, the relationship between Fourier transform and the discrete Fourier transform is expressed as:

$$\mathcal{F}\{f(x)\} \approx (\Delta x) DFT\{f(x_i)\} \tag{9}$$

Therefore, following sampling and DFT, the array of points that are obtained should be multiplied by the factor

$$\left[\frac{(\Delta x)(\Delta y)}{\lambda f}\right]^2$$

so that magnitude values will correspond.

Furthermore, in plotting a 2-D Fourier transform, one would normally place the frequency domain origin at the center of the plot. However, for DFT the "DC" value has index $(u, v) = (0, 0)$ while indices (u, v) with $u \geq N/2$ or $v \geq N/2$ correspond to negative frequencies. We therefore reordered the DFT array so that the origin would be placed at the center of the array — with higher spatial frequencies corresponding to radial distance from this center.

The PSF - OTF program takes as input a grid of magnitude and phase values which describe the complex amplitude function at the aperture plane. The cases for which we knew closed form solutions (no phase shift or apodization) had complex amplitude function given by

$$A(x, y) = \begin{cases} 1, & \text{if } (x, y) \text{ is a point within a subaperture;} \\ 0. & \text{otherwise.} \end{cases}$$

However, if one is interested in phasing or apodization effects, the function could be a complex valued function of position (x, y).

We generated, by the numerical procedure described above, PSF and OTF plots for several of the cases for which closed form solutions were known. The closeness of the results indicates the recommended procedure for calculation of step size and scaling factors is adequate in practice.

Although only textbook examples were run using the PSF and OTF computer programs, the goal is to use these procedures as an analysis tool for studying apodization, placement, tilt, and piston effects, and size tradeoffs that will allow the manufacturing advantage with high resolution of the synthetic aperture to be attained.

During the development of the PSF-OTF procedure we evaluated a technique that promised substantial payoff. Suppose one has a synthetic aperture made up of several identical subapertures centered at various points (x_i, y_i) in the aperture plane. By the "time-delay" property of the Fourier transform the PSF could be found by appropriately phase shifting and summing the canonical subaperture transform. Since the sample grid requirement to calculate the Fourier transform of a subaperture would be *less* than that required for the whole synthetic aperture, the DFT could be done with fewer grid points, saving computational effort. However, two observations indicate that the procedure is not desirable:

1. The resolution of the resulting PSF will be worse since there will be fewer grid points covering the same Fraunhoffer region. (The DFT of an $N \times N$ array is an $N \times N$ array and from the sampling theorem the "highest frequency" will need to be the same independent of the *number* of grid points).
2. In order to avoid aliasing in going from PSF to OTF it would be necessary to "sample" PSF on a narrower grid than the data provides.

Because of observation 1, the graph of PSF will not be as detailed as would be the case if the whole synthetic aperture were sampled. Observation 2 shows that in order to satisfy the sampling theorem the PSF data would have to be *interpolated* before the OTF could be attempted. *Analysis of the computational effort required* indicates that the savings in using subaperture pupil functions for PSF would be lost in the required 2-D interpolation step.

V. DECONVOLUTION

Large multi-mirror optical systems for wide field of view application will need to adaptively reconfigure themselves for figure error and misalignments. One estimation and control scheme for reconfiguration involves active mirrors [11,12]. Mirror figure errors are estimated from wave front sensor data, and control signals are sent to actuator motors that then deform the mirror surface to correct these errors. The calculation of the required actuator motion based on measured wave front data has been termed *deconvolution.*

It can be demonstrated (for the experimental deconvolution testbed) that deviations from planeness in wavefront data (an m-vector $\triangle \mathbf{z}$) and changes in actuator displacement (an n-vector $\triangle \mathbf{x}$) are approximately linearly related. That is

$$H \triangle \mathbf{x} \approx \triangle \mathbf{z}. \tag{10}$$

The $m \times n$ matrix H describes the relation, and since $m > n$ this is an overde-

termined set of linear equations. The goal of deconvolution is to infer from $\triangle \mathbf{z}$ the values of $\triangle \mathbf{x}$ that would cause the measured wavefront deviations, and then to subtract $\triangle \mathbf{x}$ from the present actuator position, thereby reconfiguring the optical system so that it should have smaller wavefront deviations (i.e. $\triangle \mathbf{z} \approx \mathbf{0}$).

If one knew H and $\triangle \mathbf{z}$ perfectly, then to minimize the cost functional

$$(H \triangle \mathbf{x} - \triangle \mathbf{z})^T (H \triangle \mathbf{x} - \triangle \mathbf{z}) = \mathbf{r}^T \mathbf{r}. \tag{11}$$

(i.e. the sum of the squares of the residuals $r_i = (H \triangle \mathbf{x} - \triangle \mathbf{z})_i$), the actuator settings would be given by

$$\triangle \mathbf{x} = H^{\dagger} \triangle \mathbf{z} \tag{12}$$

where $H^{\dagger}$ is the Moore-Penrose pseudoinverse (which is $H^{\dagger} = (H^T H)^{-1} H^T$ when H has full column rank, and can be calculated using the singular value decomposition even when H is rank deficient). The advantages of a singular value decomposition approach to the solution of least squares problems are:

(a) one never forms the matrix $H^T H$, whose condition number would be the square of the condition of H;

(b) the singular value decomposition is a numerically stable procedure. That is, one can expect that errors in results are of the same order as errors in the data being operated on; and,

(c) The condition number of H can be determined by taking the ratio of largest to smallest singular values. The rank of H is the number of non-zero singular values, and in the case where H is rank deficient (or approximately so), the pseudo-inverse is constructed by using only the "non-zero" singular values. Let the rank of H be r.

For any real (m by n) matrix H one can find *orthogonal* matrices U and V ($V^T V = I$ and $U^T U = I$) so that

$$U^T H V = S \qquad S = \begin{pmatrix} \Sigma_r & 0_{r \times (n-r)} \\ 0_{(m-r) \times r} & 0_{(m-r) \times (n-r)} \end{pmatrix} \tag{13}$$

with the square Σ_r matrix equal zero everywhere except on the diagonal. The real positive numbers s_i, $i = 1, \ldots, r$ on the diagonal are called the singular values of the matrix H.

The solution to the least squares problem is mathematically (not numerically) equivalent to solving the normal equations

$$(H^T H) \triangle \mathbf{x} = H^T \triangle \mathbf{z}. \tag{14}$$

Now suppose we have formed the singular value decomposition of $H = U S V^T$. Inserting this in (14) we have

$$(V S^T U^T U S V^T) \triangle \mathbf{x} = V S^T U^T \triangle \mathbf{z}. \tag{15}$$

and using the structure of S and orthogonality of U and V

$$\triangle \mathbf{x} = V \begin{pmatrix} \Sigma_r^{-1} & 0 \\ 0 & 0 \end{pmatrix} U^T \triangle \mathbf{z}. \tag{16}$$

We note that the matrix Σ_r^{-1} is diagonal with entries $1/s_i$ on the diagonal.

In summary, the least squares problem (11) can be solved by (a) forming the singular value decomposition (13), obtaining matrices U, V, and Σ_r and (b) performing the multiplication in (16).

Neither the relation (10) nor the value of $\triangle \mathbf{z}$ is exact due to measurement errors in the positioning of actuators and in the wavefront sensor; modeling errors, i.e. in the terms of the actuator influence matrix H, are another source of potential difficulty. There are several ways in which the problem statement of (11) can be modified to reflect these uncertainties [13].

Weighted Least Squares: Suppose the *measured* $\triangle \mathbf{z}$ and the *true* wavefront deviation vector $\triangle \mathbf{z}_{true}$ are related by

$$\triangle \mathbf{z} = \triangle \mathbf{z}_{true} + \mathbf{n}_z$$

where $\mathbf{n}_z$ is a vector of zero-mean, random variables describing wavefront sensor noise. Let the covariance matrix be denoted $\Sigma_{\mathbf{n}_z}$. The least squares criterion of (11) can be modified to

$$(H \triangle \mathbf{x} - \triangle \mathbf{z})^T \Sigma_{\mathbf{n}_z} (H \triangle \mathbf{x} - \triangle \mathbf{z}) = \mathbf{r}^T \Sigma_{\mathbf{n}_z} \mathbf{r}. \tag{17}$$

In particular, when the noise is uncorrelated so that $\Sigma_{\mathbf{n}_z}$ is diagonal, the cost functional becomes

$$\sum_{i=1}^{m} \frac{r_i^2}{\sigma_i^2}. \tag{18}$$

In minimization of (18), components of the measurement vector with small variance (i.e. reliable sensors) are weighted more heavily than other less reliable measurements.

The weighted least squares problem of (17) can be solved in a similar manner to that of (11) using the singular value decomposition. The covariance matrix may be

factored using Cholesky decomposition as $\Sigma_{n_z} = \Sigma^{\frac{1}{2}T}\Sigma^{\frac{1}{2}}$, and then cost functional (17) can be written

$$(H\triangle\mathbf{x} - \triangle\mathbf{z})^T \Sigma^{\frac{1}{2}T}\Sigma^{\frac{1}{2}} (H\triangle\mathbf{x} - \triangle\mathbf{z}) = (\Sigma^{\frac{1}{2}} H\triangle\mathbf{x} - \Sigma^{\frac{1}{2}}\triangle\mathbf{z})^T(\Sigma^{\frac{1}{2}} H\triangle\mathbf{x} - \Sigma^{\frac{1}{2}}\triangle\mathbf{z}).$$

By identifying $H = \Sigma^{\frac{1}{2}} H$ and $\triangle\mathbf{z} = \Sigma^{\frac{1}{2}}\triangle\mathbf{z}$ this is in the form of (11), and can be solved as described.

Note that the solution of the weighted least squares problem is different from the problem of (11) *only* when the variances of the elements of the measurement vector are not equal or when the measurements are correlated.

Damped Least Squares: Now suppose that the actuators can only be positioned as

$$\triangle\mathbf{x} = \triangle\mathbf{x}_{desired} - \mathbf{n}_x$$

where $\mathbf{n}_x$ is a zero-mean, random vector describing positioning accuracy limits. Denote as $\Sigma_{\mathbf{n}_x}$ the covariance matrix for $\mathbf{n}_x$.

Consider the problem of minimizing the cost functional

$$\|H\triangle\mathbf{x} - \triangle\mathbf{z}\|^2 + \lambda^2\|\triangle\mathbf{x}\|^2 \tag{19}$$

where the second term regularizes the problem so that a solution $\triangle\mathbf{x} \approx 0$ which makes the residuals small is sought. Relation (19) is

$$(H\triangle\mathbf{x} - \triangle\mathbf{z})^T(H\triangle\mathbf{x} - \triangle\mathbf{z}) + \lambda^2\triangle\mathbf{x}^T\triangle\mathbf{x} \tag{20}$$

and to find minimum with respect to $\triangle\mathbf{x}$ requires (by setting the gradient equal zero)

$$(H^TH + \lambda^2 I)\triangle\mathbf{x} = H^T\triangle\mathbf{z} \tag{21}$$

If we form the singular value decomposition of H as $H = USV^T$ and define $\mathbf{y} = V^T\triangle\mathbf{x}$, $\tilde{\mathbf{b}} = U^T\triangle\mathbf{z}$, then (21) is

$$(VS^TU^TUSV^T + \lambda^2 I)V\mathbf{y} = VS^TU^T\triangle\mathbf{z}$$

or

$$(S^TS + \lambda^2 I)\mathbf{y} = S^T\tilde{\mathbf{b}}. \tag{22}$$

Since S is diagonal with singular values s_i, $i = 1, \ldots, r$

$$y_i = \left(\frac{s_i\tilde{b}_i}{s_i^2 + \lambda^2}\right) \tag{23}$$

and then $\triangle \mathbf{x} = V\mathbf{y}$. Relation (23) shows the regularizing effect of the damped least squares problem. Even if some the singular values of H are small, the value of $\triangle \mathbf{x}$ will not fluctuate as wildly as would be the case in (11).

Since the solution to the problem posed in (19) depends on the value of λ^2, one can attempt to choose a *good* value for λ^2. We note that the first term of (19) has a covariance matrix $\Sigma_{\mathbf{n}_z}$ associated with it, while the second term has covariance matrix $\Sigma_{\mathbf{n}_x}$. In the special case when the elements of $\mathbf{n}_z$ are uncorrelated and of equal variance ($\sigma_z{}^2$), and the elements of $\mathbf{n}_x$ are likewise uncorrelated and of equal variance ($\sigma_x{}^2$), then

$$\Sigma_{\mathbf{n}_z} = \sigma_z{}^2 I, \qquad \Sigma_{\mathbf{n}_x} = \sigma_x{}^2 I. \tag{24}$$

Following the arguments put forth in the discussion of weighted least squares, to balance the requirements 1 and 2 of (19) one would choose as the cost function

$$\frac{\|H\triangle\mathbf{x} - \triangle\mathbf{z}\|^2}{\sigma_z{}^2} + \frac{\|\triangle\mathbf{x}\|^2}{\sigma_x{}^2} \tag{25}$$

or

$$\|H\triangle\mathbf{x} - \triangle\mathbf{z}\|^2 + (\frac{\sigma_z}{\sigma_x})^2\|\triangle\mathbf{x}\|^2 \tag{26}$$

That is: choose $\lambda = (\sigma_z/\sigma_x)$ in (19).

This choice of λ also results if one *conjectures* the form in (23), and then differentiates the resulting cost functional with respect to λ and sets it to zero in order to minimize with respect to λ. In several reports describing deconvolution procedures this was done, with no explanation as to why the form (23) is logical. This caused much confusion, and only by reconsidering the problem statement and deriving the results above was the author able to justify that step.

As has been discussed, the singular value decomposition provides a framework for solving the least squares problem that defines the deconvolution process in a numerically stable way. However, a variant to the SVD approach which, for the deconvolution testbed case ($m = 801$, $n = 37$) is more computationally efficient, is used in the reports that the author has come across. This variant first forms H^TH (which costs $\frac{m \cdot n^2}{2}$ operations) and then solves the normal equations (14 or 21) using the SVD of H^TH. The conditioning is worsened, but for the assumed test all singular values are such that this introduces neglegible error. The SVD for an $m \times n$ matrix takes on the order of $m \cdot n^2 + \frac{17}{3}n^3$ operations [14], while to decompose an $n \times n$ matrix requires approximately $\frac{20}{3}n^3$ operations. Since, for the

case studied, $m > n$, the extra work required in forming the $n \times n$ matrix $H^T H$ is justified.

Why, if the normal equations are to be formed, should not the more computationally efficient procedure of Cholesky decomposition be used in order to solve them? Cholesky decomposition of the normal equations (21) requires far fewer operations ($n^3/6$ vs $\frac{2}{3}n^3$) than does the SVD and this procedure is stable. The apparent answer is that if the procedure is to be iterated using an updated λ (which would change as estimates of σ_r change), the particular form of equation (23) allows one to update the estimate Δx *without* requiring a new decomposition, which would be computationally costly. Cholesky decomposition of the normal equations does not admit a simple dependence on λ as does (23). We note that, even with the re-decomposition necessary for each iteration, a method based on Cholesky still could be more efficient than one based on SVD. Also, it must be realized that the simple updating of (23) only holds for *uncorrelated* measurements and actuator errors. That assumption may be unreasonable; the author intends to investigate these questions further.

The contractor-supplied computer programs for deconvolution tested the concept. Later, at RADC the structure was modified to simulate the iterative nature of the planned three-flat deconvolution experiment. The experiment including sensor, actuator placement, and influence matrix noise terms has been simulated and shown to be a workable estimation scheme (this required some modifications in order for the programs to run correctly and consistently); next, the programs are to be made part of a closed loop control system for the actual three-flat optical hardware experiment. The measurement data will come from a wavefront sensor interfaced with the computer (method was outlined during the summer, although not yet tested due to the unavailability of the sensor), and the actuator influence matrix for the active mirrors will have been experimentally determined (work on the characterization of the active mirrors is underway). The framework for the control system software will be similar to that of the software simulation program with the following changes:

1. Experimentally determined influence matrix data will need to be supplied when subroutines INFLMAT and INFLNSE are called. The portions of the software that add noise to the influence matrix can be eliminated. Two approaches to the experimental determination of actuator influence are possible. The first examines the effect of unit displacement of each actuator in turn, and measures pathlength deviations at each of the surface points. The second approach uses

several "canonical" actuators (as a function of distance and angle from the center of the active mirror) and obtains data for the distribution of height deflection due to that actuator. Then any point on the mirror would be deflected an amount corresponding to the superposition of all the effects. An interpolation procedure would be necessary.

2. No noise generation is necessary since the measurements are already noisy. Programs NOISE, RANDOM, EIGSOL, and REIT should be thus modified. The file MEASURE.DAT supplied to EIGSOL by RANDOM should contain the measurements of wavefront deviation as obtained from the wavefront sensors.

VI. OTHER INVESTIGATIONS

In the course of the resarch period several other items were studied. A procedure for allowing the point spread function calculation to also calculate "power in the bucket" as a function of distance was derived, but is not yet programmed. Also, the Strehl ratio can be calculated from the two dimensional PSF data.

The eigenvalue-eigenfunction relation for 2-D functions is

$$\lambda g(x,y) = \int_{-\infty}^{+\infty}\int_{-\infty}^{+\infty} PSF(x-x',y-y')g(x',y')\,dx'\,dy'$$

and calculation of the eigenvalues and eigenfunctions would enable modal decomposition. By discretizing the (x,y) plane, approximate eigenvalue-eigenvector pairs λ and $g(x,y)$ would satisfy

$$\lambda\, g(x_i,y_j) = \sum_{\ell=0}^{N-1}\sum_{m=0}^{N-1} PSF(x_i-x_\ell,y_j-y_m)\; g(x_\ell,y_m)\;\Delta^2$$

for $i,j = 0,1,\ldots,N-1$. If one defines an $N^2 \times N^2$ matrix K describing the discretized PSF and a N^2 length vector $\mathbf{g}_k = g(x_i,y_j), \quad k = Ni+j$, then

$$K\mathbf{g} = \lambda\mathbf{g}$$

This is the eigenvalue-eigenvector calculation of matrix linear algebra for which good numerical techniques exist. However, examination of the size of the matrix K (which would be $128^2 \times 128^2$ for a 128 by 128 grid) shows that the calculation of the approximate eigenvalues and eigenvectors is not feasible. Two items for future research in this area are indicated. First, the special structure of K may make

possible some simplification of the eigenvalue computation. Second, an approach as follows might prove advantageous: (a) from the PSF array find a "closest" cubic spline on a reduced array of e.g. 64 nodes (i.e. use a much coarser grid); (b) perform the approximate eigen- calculation on this array; (c) Use a 2-D spline interpolation on the resulting approximate eigenfunction.

We also completed modifications of the large computer aided optical analysis and design program POLYPAGOS. This program now successfully runs on the Vax computer, and the modifications mostly consisted of using alternate subroutine calls, different COMMON areas, and conversion to double precision. Finally, a (rather awkward, but workable) scheme was devised for copying documents and APL workspaces from the Lonex or Multics systems repectively to the Vax.

VII. RECOMMENDATIONS

As has been discussed, much of the work during the summer period was in support of the OSEL laboratory in general, or the three-flat deconvolution experiment in particular. Instructions for use of the 2-D FFT and the PSF-OTF procedures have been left with the organization. The modifications necessary for the closed loop control of the three-flat experiment have been discussed with the engineer responsible for carrying out that task. Documents relating to changes to the POLYPAGOS code have been submitted for approval and further testing. No actual image data was tested in our studies of phase retrieval procedures. It will be necessary to evaluate the performance of the algorithms on such data.

The author intends to continue research in the general area to which he was exposed during the summer period. In particular, it appears that a study of the deconvolution procedure in the face of actuator or sensor degradation or failures is necessary. The actuator influence matrix will not be constant over time. In the near future we will perform simulations in order to demonstrate that an adaptive procedure will be required, and anticipate submitting a proposal for a mini-grant to support research into methods for identifying actuator or sensor failures and to *adaptively* estimate the data.

REFERENCES

1. Goodman, J. W., *Introduction to Fourier Optics*, McGraw-Hill, New York, 1968.
2. Nussbaum, A., and R. A. Phillips, *Contemporary Optics for Scientists and Engineers*, Prentice-Hall, Englewood Cliffs, NJ, 1976.
3. Baltes, H. P., *Inverse Source Problems in Optics*, Topics in Current Physics Series, Springer-Verlag, New York, 1978.
4. Fienup, J. R., "Reconstruction of an Object from the Modulus of its Fourier Transform", *Optics Letters*, Vol. 3, 27-29, 1978.
5. Fienup, J. R., "Phase Retrieval Algorithms: A Comparison", *Applied Optics*, Vol. 21, 2758-2769, 1982.
6. Gerschberg, R., and W. Saxton, "A Practical Algorithm for the Determination of Phase from Image and Diffraction Plane Pictures", *Optik*, Vol. 35, 237-246, 1972.
7. Dahlquist, G., A. Bjorck, N. Anderson, *Numerical Methods*, Prentice-Hall, Englewood Cliffs, NJ, 1974.
8. Powell, M. J. D., *Nonlinear Optimization*, Academic Press, New York, 1981.
9. Fender, J. S., "Synthetic Apertures: An Overview", *SPIE Proceedings*, 440, pp 1-7, 1984.
10. Shannon, C. E., "Communication in the Presence of Noise", *Proceedings of the IRE*, pp. 10-21, January 1949.
11. Watson, J. T., and D. C. Ehn, "Integrated Sensing and Control System for a Large, Deployable, Wide-Field Optical System", *SPIE Proceddings*, Vol. 228, Active Optical Devices and Applications, pp. 56-62,1980.
12. Michalak, R. J., "An Optical Platform for Testing Space-Based Optics Control Algorithms", *SPIE Proceedings*, 1984.
13. Lawson, C. L., and R. J. Hanson, *Solving Least Squares Problems*, Prentice-Hall, Englewood Cliffs, NJ, 1974.
14. Golub, G. H., and C. L. VanLoan, *Matrix Computations*, Johns Hopkins Univ. Press, Baltimore, MD, 1983.

1985 USAF-UES SUMMER FACULTY RESEARCH PROGRAM/

GRADUATE STUDENT SUMMER SUPPORT PROGRAM

Sponsored by the

AIR FORCE OFFICE OF SCIENTIFIC RESEARCH

Conducted by the

UNIVERSAL ENERGY SYSTEMS, INC.

FINAL REPORT

ELECTROCHEMICAL ANALYSIS OF THE DEGRADATION OF SYNTHETIC LUBRICANTS

Prepared by:	**Dr. Dennis R. Flentge**
Academic Rank:	**Assistant Professor**
Department and University:	**Department of Mathematics and Science Cedarville College**
Research Location:	**Aero Propulsion Laboratory, Fuels and Lubrication Division, Lubrication Branch, Wright-Patterson AFB, OH**
USAF Research:	**Phillip W. Centers**
Date:	**20 September 1985**
Contract No:	**F49620-85-C-0013**

ELECTROCHEMICAL ANALYSIS OF THE DEGRADATION OF SYNTHETIC LUBRICANTS

by

Dr. Dennis R. Flentge

ABSTRACT

Electrochemical properties of a lubricant provide useful information regarding the quality of the lubricant and, indirectly, regarding the condition of the turbine engine from which the lubricant was taken. The Complete Oil Breakdown Rate Analyzer, COBRA, and Cyclic Voltammetry have been used to examine several laboratory degraded lubricant formulations. Consumption of the additives PANA and DODPA were noted with only small increases in the COBRA values.

Acknowledgement

The author would like to thank the Air Force Systems Command, the Air Force Office of Scientific Research and Universal Energy Systems, Inc., for providing him with the opportunity to spend an interesting and profitable summer in the Lubrication Branch of the Aero Propulsion Laboratory at Wright-Patterson AFB, OH. He would also like to acknowledge the labroatory, particularly the Lubrication Branch, for its hospitality and excellent working conditions.

He would like to thank Phillip W. Centers for suggesting this area of research and for his helpful guidance throughout the project. He would like to acknowledge the excellent technical assistance provided by Chris Klenke.

I. INTRODUCTION:

The high performance demand on current turbine lubricants and an ultimate limit on the supply of materials from which these lubricants are synthesized present a need for careful monitoring of the quality of a lubricant during its use so as to maximize its lifetime without jeopardizing the engine which it is protecting. Such a monitoring system should be quick and simple to use, should give straightforward indication of lubricant degradation, should provide good reliability and should use only a small sample volume.

There are two techniques based on the electrochemical properties of the lubricant which satisfy these requirements. The Complete Oil Breakdown Rate Analyzer (COBRA) uses several drops of the lubricant and produces data which are easily interpreted. A rapid increase in the COBRA value or an excessively high value indicates that significant changes are taking place in the lubricant and that examination of the engine may be needed. The Air Force initiated a program using COBRA's following the failure to two engines in 1979.[1,2] Analysis of several lubrication samples from these engines showed COBRA values over 200. During the test period of May, 1980, through August, 1982, a total of 31 abnormal TF34-GE-100 engines were identified by COBRA monitoring.[1] Several design changes have been implemented to correct engine problems that were causing rapid lubricant degradation. A similar monitoring program was pursued using the J75-P-17 engine. Lubricant degradation was slow and no maintenance actions were reported which would cause high rates of lubricant degradation.

Cyclic voltammetry provides a second technique for evaluating the

change in the character of a lubricant. Anti-oxidant additives such as dioctyldiphenylamine (DODPA) and N-phenyl-1-naphthylamine (PANA) produce easily observed voltammograms and their presence can, therefore, be monitored using this technique. While the spectra are relatively easy to obtain, only small samples are needed for analysis and the spectra are not complicated, the technique has the disadvantage of requiring equipment that can be cumbersome and expensive. It is, then, a less desirable field technique than the COBRA. It should, however, be possible to examine lubricants from the same source with the two techniques and gain insights into the properties being measured by the COBRA. There is currently very little known about exactly which properties of the lubricant are being measured by the COBRA.

This researcher has a background in surface chemistry, spectroscopy, electrochemistry (from an SFRP experience) and lubricants. This background provided the basis for assignment to the project in the lubrication lab at Wright-Patterson AFB, OH.

II. OBJECTIVES OF THE RESEARCH EFFORT:

The overall goal for this project was the correlation of electrochemical information obtained using cyclic voltammetry with the data from the COBRA units. In order to achieve that goal several specific goals had to be met. They were:

(1) To determine laboratory degradation conditions that would produce samples acceptable for study;

(2) To identify products of oxidation of the additives which may contribute to the lifetime of the lubricant.

III. EXPERIMENTAL

The synthetic lubricant basestock was the ester, trimethylolpropane heptanoate (TMPH). Various formulations were prepared by adding p,p'-dioctyldiphenylamine, DODPA, (Vanlube 81, R. T. Vanderbilt Co.), or N-phenyl-1-naphthylamine, PANA, (DuPont), to TMPH. A concentration of 1% by weight of DODPA, PANA, and DODPA plus PANA (1% each) was used for the lubricant formulations. The degradation was accomplished using an Isothermal Test Bath from FLC Instruments, Inc. Air was bubbled through 50 mL samples of the lubricant at a rate of 10 L/hr. The temperature was fixed at 180°C. Degradation times varied from 8 hours up to 315 hours.

The cyclic voltammetry data were collected using an E. G. and G., Princeton Applied Research Model 175 Universal Programmer, Model 173 Potentiostat/Galvanostat and Model RE0089 X-Y Recorder. The working and counter electrodes were platinum and the reference electrode was $Ag/AgNO_3$ in acetonitrile. The electrolyte, lithium perchlorate, was dissolved in analytical grade acetone (Sargent-Welch). A Hewlett-Packard 1080B liquid chromatograph was used to analyze the composition of the samples.

The samples for the cyclic voltammetry measurements were prepared by dissolving 2.0 mL of the lubricant in 100 mL of a solution of 0.1M $LiClO_4$ in acetone. The sweep rate for the voltammograms was 500 mV/s. Five scans were recorded for each sample.

IV. VOLTAMMOGRAMS OF ANTIOXIDANT ADDITIVES:

The voltammograms were recorded in the range of +0.80 V to 0.0 V.

Figure 1 displays the voltammograms for the samples containing 1% DODPA, 1% PANA, and 1% DODPA/1% PANA. The DODPA sample displays an oxidation peak at 473 mV and a reduction peak at 385 mV. PANA has a pair of oxidation peaks at 351 and 513 mV and a reduction peak at 297 mV. The mixture contains all of these peaks plus one at 162 mV.

Figure 2 displays the spectra of the PANA sample after degradation for 41 hours (a) and 114 hours (b). There is some change in the intensities of the reduction peaks in the samples with shorter degradation times but the signal is almost completely removed at the 114-hour mark. HPLC analysis showed this sample to contain only 5.6% of the original amount of PANA. The COBRA value was 12.

The voltammograms for the DODPA sample showed similar behavior. The signal was essentially gone at 70 hours. The COBRA value was 13 at that time.

Figure 3 shows the voltammograms for the degraded mixture. The signal is gone at 99 hours (spectrum b). The COBRA value for this sample was 31.

V. HPLC ANALYSIS OF THE SAMPLES:

Analysis of the samples using high pressure liquid chromatography (HPLC) showed rapid decrease in the concentrations of the antioxidants (Figures 4 and 5). Also evident in the figures is the rise (and fall) in the concentrations of various products of the oxidation process. The concentrations of these new materials as plotted are relative to the maximum concentration achieved for each component. They were not all equal. Curves 3 and 4 in Figure 5 probably reach a maximum at some point

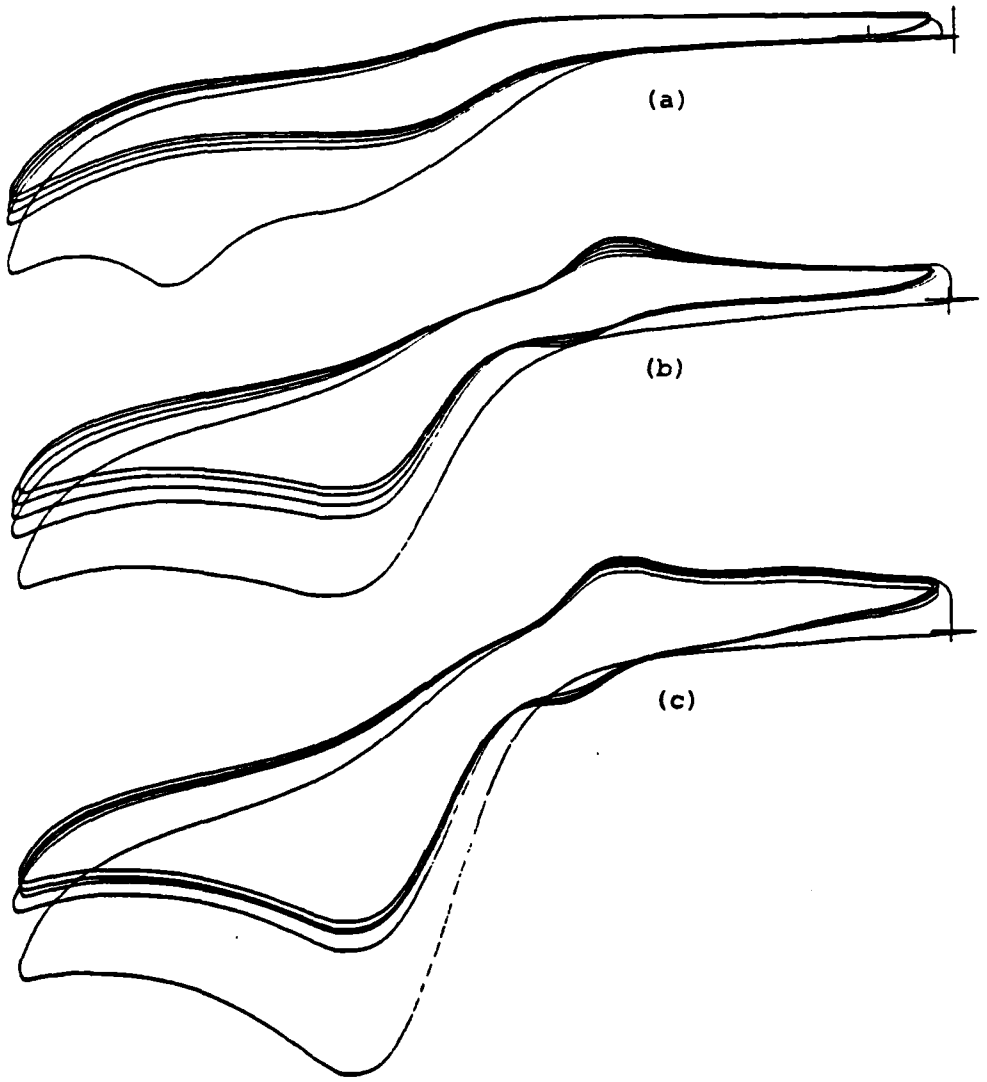

Figure 1. Cyclic voltammograms of TMPH containing (a) 1% DODPA, (b) 1% PANA, (c) 1% DODPA/1% PANA.

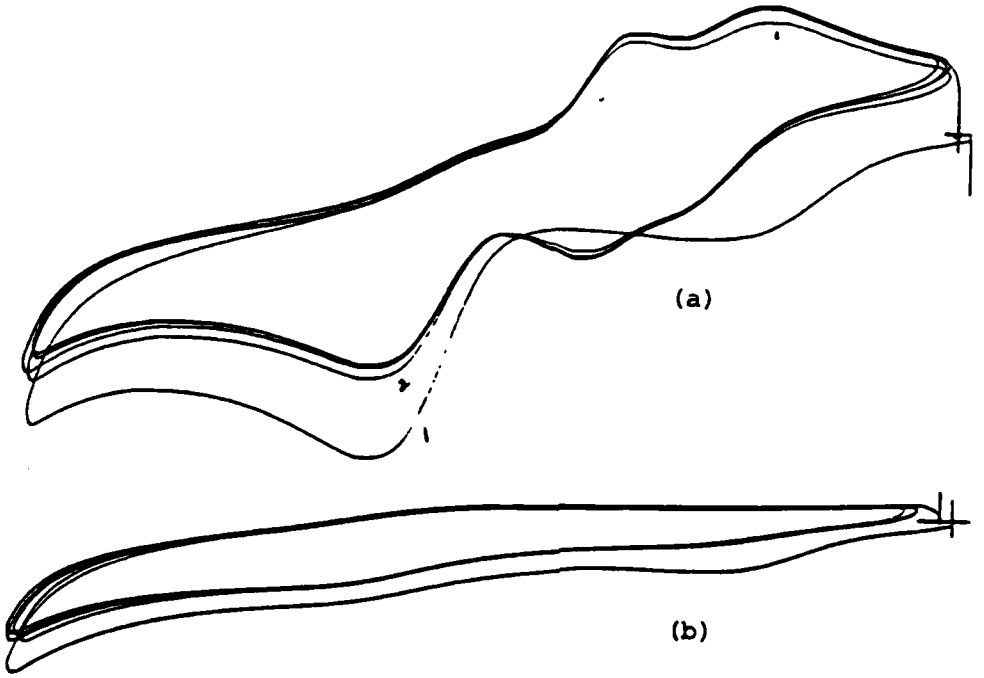

Figure 2. 1% PANA solution after degradation for (a) 41 hours, (b) 114 hours.

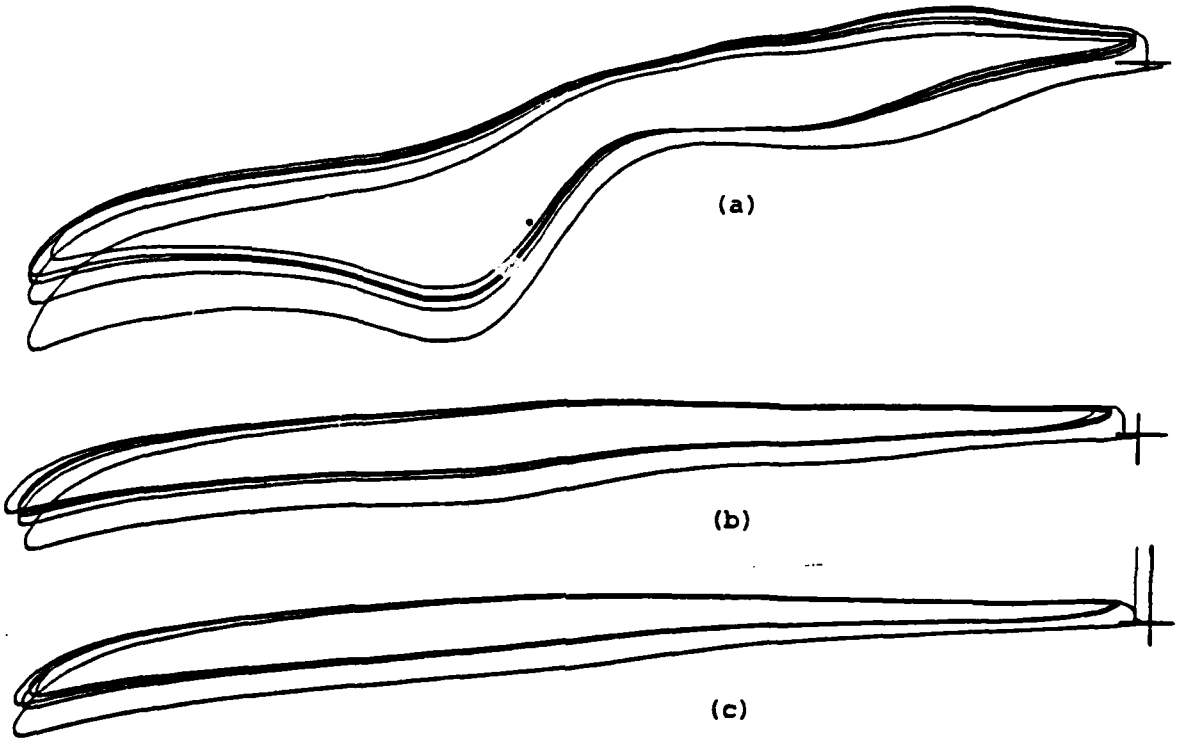

Figure 3. Mixture of 1% DODPA and 1% PANA degraded for (a) 24 hours, (b) 147 hours, (c) 315 hours.

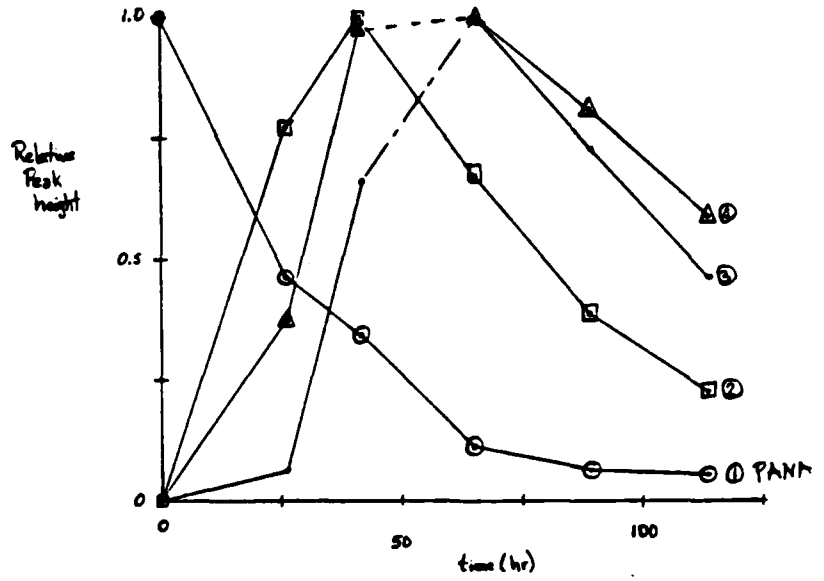

Figure 4. Relative concentrations of PANA and oxidation products as a function of time.

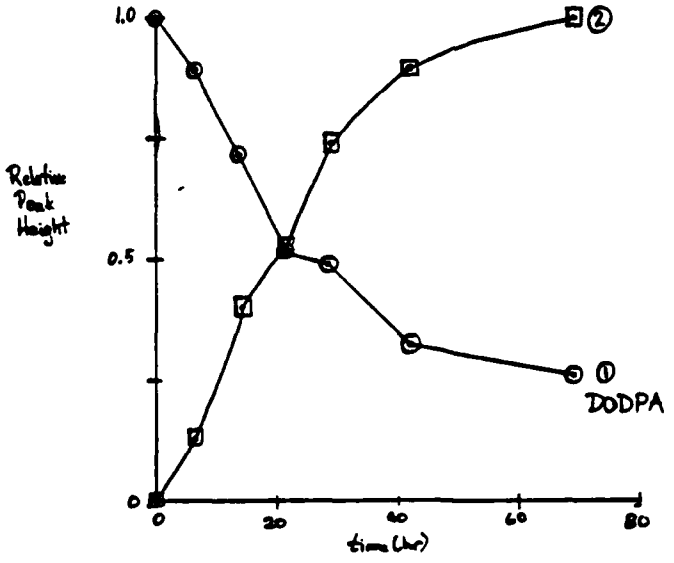

Figure 5. Relative concentrations of DODPA and oxidation product as a function of time.

between 40 and 60 hours degradation. Data points were not taken in this region so the dotted lines were drawn to indicate insufficient data. It is interesting to note that the concentrations of all the products in the decomposition of PANA were decreasing at the end of the run. The degradation that was carried to 315 hours showed these components disappearing before 150 hours of degradation.

Figure 6 shows the concentrations of PANA and DODPA compared with the COBRA values for the samples. A COBRA value of 150 for a degraded lubricant taken from an engine provides a cause for checking the engine for failure of a seal or other component.

VI. SUMMARY AND CONCLUSIONS:

The data show that the concentration of the additives decreases rapidly as the degradation proceedes. The concentrations are very low (less than 10%) at the end of the degradation but the COBRA values are not yet large enough to be noteworthy. The cyclic voltammograms show not appreciable signal for the antioxidants at this point. The conclusion that can be drawn relative to the major goal of gaining an understanding of COBRA data based on cyclic voltammetry data is that one cannot make a correlation. The COBRA values are measuring some electrochemical property which only becomes evident at the basestock itself begins to decompose.

VII. RECOMMENDATIONS:

Additional insight into the changes occurring within the lubricant systems discussed in this report could be obtained by pursuing the following activities:

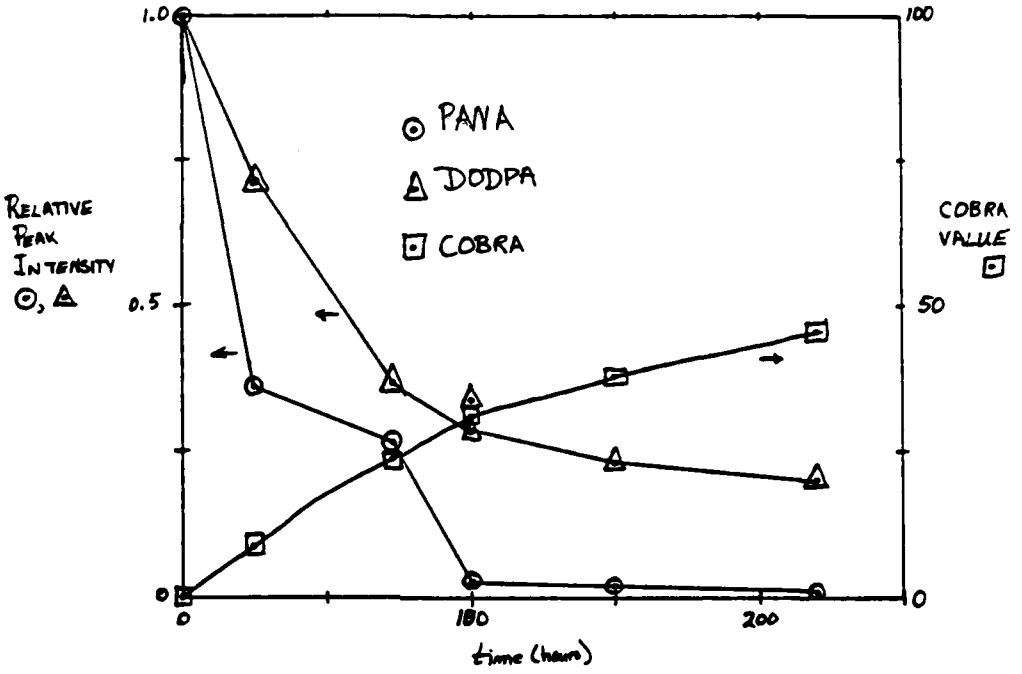

Figure 6. Comparison of concentrations of PANA and DODPA and COBRA values as a function of time.

(1) Examine the product distribution for the degradation reaction using HPLC, infrared spectroscopy and gas chromatography.

(2) Examine the effect of the antioxidant additives in various combinations.

(3) Use a series of potential products of the oxidation of PANA and DODPA as additives themselves.

REFERENCES

1. Smith, H. A., "Lubricant Monitoring Using the Complete Oil Breakdown Rate Analyzer (COBRA)," AFWAL Technical Report, AFWAL-TR-82-2109, March, 1983.

2. Smith, H. A., "Complete Oil Breakdown Rate Analyzer (COBRA) for Identifying Abnormal Operating Engines," JOAP International Symposium Proceedings, May, 1983.

3. Centers, P. W. and Smith, H. A., "COBRA Analysis of Laboratory Degraded Synthetic Turbine Engine Lubricants," Journal of Synthetic Lubricants Quarterly, Vol. 1, 1984, pp. 176-187.

1985 USAF-UES SUMMER FACULTY RESEARCH PROGRAM

GRADUATE STUDENT SUMMER SUPPORT PROGRAM

Sponsored by the

AIR FORCE OFFICE OF SCIENTIFIC RESEARCH

Conducted by the

UNIVERSAL ENERGY SYSTEMS, INC.

FINAL REPORT

INDUCED NUCLEAR RADIATION DOSE IN A SIMULATED STANDARD MAN WITH IMPLICATIONS ON AIRCREW SURVIVABILITY

Prepared by:	Dr. Bessie Ruth Foster
Academic Rank:	Professor
Department and University:	Department of Physics, Grambling State University, Grambling, LA
Research Location:	Air Force Weapons Laboratory, Kirtland Air Force Base, NM, Aircraft and Missile Division (NTA), Technology Branch (NTAT), Blast, Thermal, and Radiation Effects Section (NTATE)
USAF Research:	Lt. Alan Dooley
Date:	August 5, 1985
Contract No:	F49620-85-C-0013

INDUCED NUCLEAR RADIATION DOSE IN A SIMULATED STANDARD MAN WITH IMPLICATIONS ON AIRCREW SURVIVABILITY

by

Bessie Ruth Foster

ABSTRACT

An abbreviated report of a comprehensive research initiative is presented. The study involved computer modeling of a standard man both chemically and geometrically, and assessing whole body and organ depth dose in an induced nuclear gamma radiation environment. The phantom consists of hydrogen, carbon, nitrogen, oxygen, and trace elements, in proportions simulating standard man. A wide variety of tissue equivalent phantoms have been employed in depth dose studies conducted by different researchers previously. These models include slab, cylindrical, water bottle, plastic, and the like. The present study involves re-modeling a "more human" phantom using state-of-the-art graphic techniques to represent the asymmetry and compositional variations of the human body.

The Monte Carlo sampling method along with "Combinatorial Geometry" computer codes accessible at the Air Force Weapons Laboratory (AFWL) are employed to simulate the desired phantom and radiation environmental parameters, and to study radiation transport through material media.

A plausible explanation for radiosensitivity of the gastrointestinal tract is presented. Data indicated a biological anomaly in this organ; it exhibited a low mass density accompanied by high atomic density and atomicity.

The report consists of an introduction, objectives, research approach, results, discussion, and recommendations for implementing the results along with suggestions for follow-on research.

ACKNOWLEDGEMENTS

Research sponsored by the Air Force Office of Scientific Research/AFSC, United States Air Force, under Contract F49620-85-C-0013. The United States Government is authorized to reproduce and distribute reprints for governmental purposes not withstanding any copyright notation hereon.

The writer wishes to express her appreciation to the Technology Branch of the Aircraft and Missile Division at the Air Force Weapons Laboratory, Kirtland Air Force Base, New Mexico, for having selected her as a research associate; and to Lt. Alan Dooley of the Blast, Thermal, and Radiation Effects Section for his collaborative efforts with computer modeling and particle transport determinations which were germane in carrying out the research. I also wish to express my appreciation and gratitude to Dr. Jelle de Boer and to Mr. Harry Murphy for their amiable demeanors, and for their time-saving suggestions regarding the research approach, and to members of the staff of the Technical Library at AFWL for their invaluable assistance in conducting literature searches.

Lastly, I wish to thank Mr. Richard Griffith of the Lawrence Livermore National Laboratory, Livermore, California, for forwarding to me some essential base-line data regarding reference man which supplied the impetus for arriving at parameters basic to the research thrust.

I. INTRODUCTION:

A summer research assignment was afforded me in the Blast, Thermal, and Radiation Effects Section of the Technology Branch of the Aircraft and Missile Division at the Air Force Weapons Laboratory, New Mexico. Particular abilities which I possess that resulted in my being assigned to the laboratory include undergraduate training in science and mathematics, and graduate training, both at the master's and doctorate levels, in radiological science. My experiences in the areas of radiation effects and interactions of radiation with matter include: National Science Foundation fellow in a summer institute of radiology, Oak Ridge mobile isotope laboratory participant, student trainee at Brookhaven National Laboratory, participant in an extension course in radiation monitoring, faculty research associate at Argonne National Laboratory and Lawrence Livermore National Laboratory, and principal investigator on four federally funded research grants pertaining to radiation effects on cell population kinetics. My background in radiation dosimetry and radiobiology complement the "skill-mix" ratio in the Radiation Effects Section. Permanent and transient personnel of this section develop and apply computer models to predict the response of aeronautical systems, aircrews, and the environment to nuclear weapons effects; while my responsibility, as a visiting researcher, is to specify biological parameters required for "human" phantom modeling, and to make assessments as to aircrew survivability using results from depth dose determinations employing particle transport techniques.

Radiation dose and dose rate are required in diagnostic and therapeutic radiology, for workers exposed to radiation in industry, reactor operators, military personnel exposed in a radiation environment, such as in cruising aircraft and aircrews in space, and for personnel engaged in experimental and applied radiation research.

The present study involves assessing human tissue and organ dose in a simulated standard man due to induced nuclear gamma radiation in a tissue equivalent phantom. The phantom consists of hydrogen, carbon,

nitrogen, oxygen, and trace elements, in proportions simulating standard man, after the model of Auxier, Snyder, and Jones (Ref. 1) utilizing neutron irradiation, and that of Enz and Murphy (Ref. 2) employing gamma irradiation. Whereas, a cylindrical phantom was considered to approximate the standard man in the reports cited above, it is believed that a more realistic assessment of tissue and organ dose in a radiation environment can be made with a "more human" phantom. Thus, the present study involves remodeling the phantom, using state-of-the-art graphic techniques, to represent the assymmetry and the compositional variation of the human body. The Monte Carlo sampling method along with Combinatiorial Geometry (CG) computer codes accessible at AFWL are employed to simulate the phantom and radiation environment, study radiation transport through a material medium, and to calculate the dose in various critical body locations such as in the abdominal area.

Data are analyzed in respect to absorbed dose in rads/gamma ray/centimeter squared (cm^2) as a function of gamma ray energy, with an accompanying discussion on aircrew survivability in the radiation environment.

II. OBJECTIVES OF THE RESEARCH EFFORT:

Objectives of the research are to:

(1) review the literature on recent and current radiation research employing tissue equivalent phantoms, (2) determine the dimensions and composition of a standard man, (3) simulate the desired phantom using computer modeling, (4) solve the gamma ray transport equation in complex geometries of the human phantom based on the Monte Carlo technique, (5) compare the new model results versus cylindrical and other model results, and (6) make an assessment of human survivability in the induced nuclear radiation environment.

III. THE APPROACH TAKEN IN REACHING THE OBJECTIVES:

MATERIALS AND METHODS

A. Review of the Literature

The initial task undertaken in attaining the objectives was an in-depth review of the literature on radiation research and depth dose determinations in tissue equivalent phantoms; an overview of which is included in the section entitled "The Results." A large proportion of the information which was extracted from reports published in the open literature was obtained through the Technical Library at AFWL, as loans from other libraries, through telephone conversations with other investigators, and, on a small scale, consultation with researchers or former researchers employed at AFWL.

B. Mass, and Chemical Composition of Standard Man and Selected Organs

Information on mass and chemical composition of the phantom and selected organs was obtained from the Report of the Task Group on Reference Man (Ref. 3) prepared by the International Commission on Radiological Protection (ICRP). From these data, calculations were made based on the assumption that the fifteen most abundant elements comprising the human body are, for all practical purposes, "a standard man." The percentage composition of reference man and selected organs was re-computed based on the relative abundance of each of the fifteen elements and recorded in exponential notation for convenience with computer operations. A mass of 4.30E+4 grams, for example, reads "4.30×10^4 grams" or "43000 grams." Conversely, a mass of 2.90E-1 gram is read "2.90×10^{-1} gram" or "0.29 gram."

C. Mass, Atomic, and Electron Density

Mass density was computed by taking the density of a given organ as recommended by ICRP, and multiplying by the percentage composition of each element comprising the organ. This calculation resulted in the mass of each element/cm^3 of tissue. Atomic density was determined by multiplying the mass/cm^3 of an element, from the calculation above, by Avogadro's Number (6.02×10^{23}), and dividing by the mass number (atomic weight) of the element. This arithmetic manipulation resulted in the number of atoms of a given element/cm^3 of tissue. Lastly, electron density was determined by simply multiplying atoms/cm^3 by the atomic number of the element, which is also the number of electrons/atom. This calculation generated the number of electrons/cm^3. Arithmetic "summing" was performed in all three determinations in order to arrive at total mass, atomic, and electron densities of the human torso and selected organs.

D. Computer Modeling, Radiation Environment, and Particle Transport

Computer modeling of the phantom was carried out in a collaborative effort by Lt. Alan Dooley of AFWL/NTATE. The plotting code SLICE, was used to model the human phantom (Ref. 4). SLICE allows three-dimensional (3-D) as well as sectional views of input geometry. These views were used for confirming the phantom's geometric description.

Gamma ray transport determinations were made using the 3-D Monte Carlo transport code MORSE (Ref. 5). The "effect-of-interest," rads--tissue/gamma ray/cm^2, was calculated for each regional shape consisting of the appropriate chemical compositions. Photons were transported in an analog fashion using both a tracklength estimator and collision density estimator.

The depth dose was determined for 21 monoenergetic gamma sources for the DLC-31 cross-section energy group structure (Ref. 6). For the energy group structure used, together with effective average values for each region, refer to the section entitled "The Results." The source distribution was a planar source extending along the x- and z-axes with

the source output directed along the y-axis, in reference to the phantom. This configuration was chosen for consistency with the experimental source-to-phantom geometry employed by Enz and Murphy (Ref. 2). The resulting gamma fluences were collected in 21 energy bands. The number of photons transported for each source was determined by the criteria to achieve statistical errors of less than 10 percent for each regional element.

IV. THE RESULTS:

A. Literature Search

Radiation depth dose determinations involving human phantoms have followed numerous avenues of research, with variables embracing modeling techniques, nature of the radiation source, and orientation of the target material in space. An abbreviated overview of the literature follows.

In an early study published in 1965, Janni, Clark, Schneider, and Berger (Ref. 7) employed a phantom which was designed to simulate the true geometry of the human body and the body's interaction with all types of energetic ionizing radiation. However, a gross deviation was fabricated in the chemical composition of the phantom which reversed the carbon to oxygen ratio for reasons of stability. A later study reported by Auxier, et. al. in 1968 (Ref. 1) on neutron interactions and penetration in tissue, the Monte Carlo sampling method was used to estimate the dose in various regions of a homogeneous anthropomorphic phantom. The phantom was a right circular cylinder composed of oxygen, carbon, hydrogen, and nitrogen in proportions of standard man so that the density was approximately 1.0 gram/cm^3. It was divided into 150 volume elements, and the average dose/neutron/cm^2 in the incident beam was computed for each volume element. As reported by Auxier, et. al., there were no experimental results recorded in the literature, at that time (1968), with which to compare the calculated values directly.

A somewhat different approach to depth dose studies using the

Monte Carlo method in phantom models was reported in the literature extensively during the late nineteen "sixties" and early "seventies." Among the investigators were Snyder (Ref. 8), Berger (Ref. 9), and Snyder, Ford, and Warner (Ref. 10 and 11). Generally, the radiation source was placed in different "organs" including the total body, and results were analyzed in terms of the absorbed fraction. That is, the fraction of energy absorbed in the target organ of that emitted in the source organ.

Research was undertaken by Enz and Murphy which was published in 1973 (Ref. 2) to provide gamma fluence-to-gut dose information to complement Auxier's et. al. (Ref. 1) neutron results. Before the gamma ray problem was initiated, the geometry and source normalization were verified by running a neutron problem whose results agreed sufficiently with those of Auxier. Enz and Murphy used the SAMC Monte Carlo code to calculate the dose due to beams of monoenergetic gamma rays. Calculations were made for 12 source energies between 10 and 0.1 million electron volt (MeV) inclusive, and the dose was tabulated for each volume element of the middle layer of the phantom. The researchers concluded that their results may be used to compute the gamma ray dose within volume elements of a phantom when the external fluence is known.

In a relatively recent study (Ref. 12) published by Bauchinger, Kuhn, Dresp, Schmid, and Streng in 1983, depth dose measurements were made during the time human lymphocytes were irradiated in a tissue equivalent man phantom with 14.5 MeV neutrons. Human whole blood from a healthy male donor was irradiated in a flat nylon chamber. The chambers were placed in a water-filled plexiglass phantom at four different positions, and exposed in nine different irradiation experiments. The researchers reported that their results on depth dose measurements were in good agreement with Auxier's, et. al. results (Ref. 1), and a quality factor (QF) of approximately 7.30 was computed for all four exposure positions. QF is another name for a linear-energy-transfer dependent factor by which abosrbed doses are to be multiplied to account for the varying effectiveness of different

radiations.

From the overview of the literature search above, it is clear that sufficient comparative data exist in print with which results from the current study may be compared. In previous studies reviewed above, either the chemical composition of the phantom did not approximate standard man, or the geometry of the irradiated object did not compare optimally with the human body. Thus, the present study is undertaken to maximize state-of-the-art graphic techniques in studying radiation transport and depth dose measurements in tissue equivalent phantoms which simulate the human body both geometrically and chemically.

B. Mass, and Chemical Composition of Standard Man and Selected Organs

Data on the elemental composition of reference man and some selected organs are compiled in Table I. Here, too, the data presented are in abbreviated form because of the voluminous nature of the findings. From Table I, it is observed that the percentage of oxygen, for example, ranges from 75.8 in the lung, to 70.1 in the liver, to 61.3 in the "total body."

Inasmuch as the chemical composition of various organs differ widely from that of the "total body," which is an average, the need to simulate the phantom as a heterogeneous target is substantiated.

C. Mass, Atomic, and Electron Density

Mass, atomic, and electron densities are listed in summary form in Table II. The mass density ranged from a high of 1.07 grams/cm^3 in the "total body" to a low of 1.04 grams/cm^3 in the gastrointestinal (GI) tract. Atomic density, electron density, and atomicity or atoms/gram varied considerably from one organ to another. Again, the need for a heterogeneous target as opposed to one that is homogeneous is supported.

D. Computer Modeling, and Particle Transport

TABLE I

ELEMENTAL COMPOSITION OF REFERENCE MAN AND SOME SELECTED ORGANS BY MASS*

Chemical Element	Organism/Organ and Elemental Composition					
	Total Body		Lung		Liver	
	Mass (grams)	% of Mass	Mass (grams)	% of Mass	Mass (grams)	% of Mass
Oxygen	4.30E+4	6.13E+1	7.40E+2	7.58E+1	1.20E+3	7.01E+1
Carbon	1.60E+4	2.28E+1	1.00E+2	1.02E+1	2.60E+2	1.52E+1
Hydrogen	7.00E+3	9.98E+0	9.90E+1	1.01E+1	1.80E+2	1.05E+1
Nitrogen	1.80E+3	2.57E+0	2.80E+1	2.87E+0	5.10E+1	2.98E+0
Calcium	1.00E+3	1.43E+0	8.70E-2	9.00E-3	9.00E-2	5.00E-3
Phosphorus	7.80E+2	1.11E+0	7.80E-1	8.00E-2	4.70E+0	2.75E-1
Sulfur	1.40E+2	2.00E-1	2.20E+0	2.20E-1	5.20E+0	3.00E-1
Potassium	1.40E+2	2.00E-1	1.90E+0	1.90E-1	4.50E+0	2.60E-1
Sodium	1.00E+2	1.40E-1	1.80E+0	1.80E-1	1.80E+0	1.05E-1
Chlorine	9.50E+1	1.40E-1	2.60E+0	2.70E-1	3.60E+0	2.10E-1
Magnesium	1.90E+1	3.00E-2	7.10E-2	7.00E-3	3.10E-1	1.80E-2
Silicon	1.80E+1	2.00E-2	-	-	-	-
Iron	4.20E+0	6.00E-3	3.60E-1	3.70E-2	3.20E-1	1.90E-2
Fluorine	2.60E+0	4.00E-3	2.10E-3	2.00E-4	2.50E-3	1.50E-4
Zinc	2.30E+0	3.00E-3	1.10E-2	1.00E-3	8.50E-2	5.00E-3

*Data on mass taken from ICRP-23, 1975

TABLE II

MASS, ATOMIC, AND ELECTRON DENSITY; AND ATOMICITY IN STANDARD MAN

Target Material	Mass Density (grams/cm^3)	Atomic Density (atoms/cm^3) x 10^{20}	Electron Density (elet./cm^3) x 10^{20}	Atomicity (atoms/gram) x 10^{20}
Total Body	1.07	1031	3540	964
Lung	1.05	1009	3479	961
Liver	1.05	1038	3493	989
GI Tract	1.04	1047	3471	1007
Spleen	1.06	1028	3517	970
Average	1.05	1031	3500	978

A schematic of the phantom currently being modeled is presented in Figure 1. The computer modeling operations are in progress and only the energy group structure used, along with effective average energy values for each group are presented in Table III. The research undertaken is a comprehensive study which will require a far longer time-span than the 10-week Summer Faculty Research Program (SFRP). Thus, the final report covers mainly the literature search and base-line data on reference man rather than the results from particle transport determinations.

V. DISCUSSION:

The discussion which follows is generally a discourse on biological effectiveness of absorbed dose and radiation effects on aircrews. The bulk of the computer modeling and particle transport determinations remain to be processed, thus, precluding any explanation regarding the results at the time of this report. Comments on computer modeling and particle transport are expounded on in the section entitled "Recommendations."

The International Commission on Radiological Protection surmises that information on relative radiosensitivity of different parts of the body is limited, and that a common scale of "hurt or harmfulness" has not been developed. In general, the biological effectiveness of a given absorbed dose, D, depends on the quality of the radiation and on the irradiation conditions (Ref. 13). In radiation protection it is desirable to provide a quantity that specifies the presumed radiation risk. Thus, dose equivalent, H, as defined in the International Commission of Radiological Units (ICRU) Report 19, is an appropriate quantity for this purpose. The special unit of dose equivalent is the roentgen equivalent man (rem), which is defined as that radiation dose in man which will produce an effect equivalent to a dose of one roentgen in man. The rem is limited to radiation protection and should not be used for high level accidental exposures.

Casarett (Ref. 14), lists a number of biological factors which

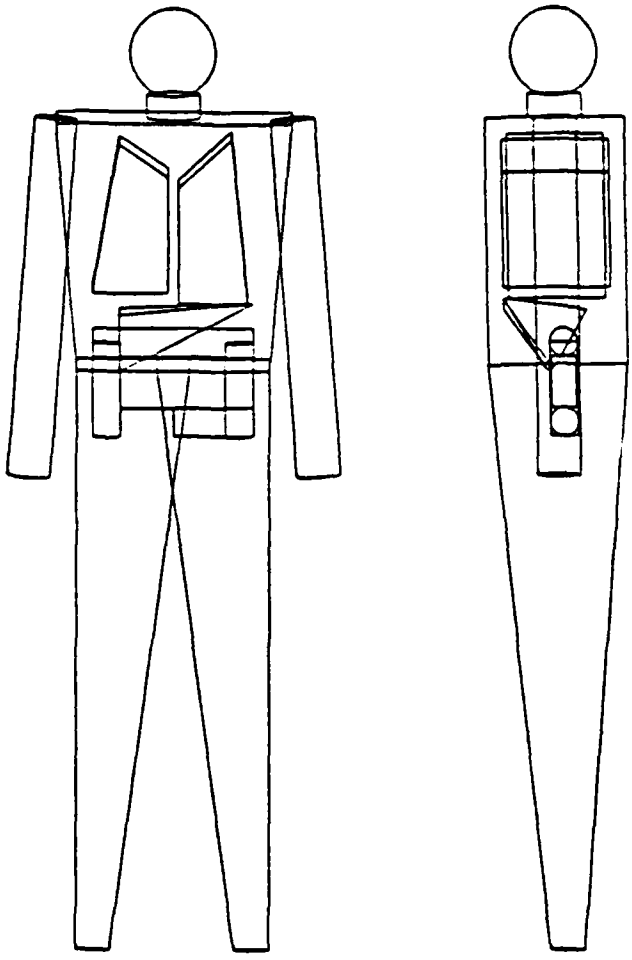

Figure 1. Schematic of the phantom (frontal and lateral views) showing the lung, stomach, and intestine as some of the selected organs under study.

TABLE III

GAMMA-RAY ENERGY BOUNDARIES FOR THE 37-21 COUPLED NEUTRON-GAMMA LIBRARY*

Group Number	Gamma Group (electron volts)	
	Energy	Effective Average
1	1.40+7**	1.20+7
2	1.00+7	9.00+6
3	8.00+6	7.50+6
4	7.00+6	6.50+6
5	6.00+6	5.50+6
6	5.00+6	4.50+6
7	4.00+6	3.50+6
8	3.00+6	2.75+6
9	2.50+6	2.25+6
10	2.00+6	1.75+6
11	1.50+6	1.25+6
12	1.00+6	8.50+5
13	7.50+5	5.75+5
14	4.50+5	3.75+5
15	3.00+5	2.25+5
16	1.50+5	1.25+5
17	1.00+5	8.50+4
18	7.00+4	5.75+4
19	4.50+4	3.75+4
20	3.00+4	2.50+4
21	2.00+4	1.50+4

*From RSIC Data Library Collection, DLC-31, ORNL, Radiation Shielding Information Center, Oak Ridge, Tennessee, Reviewed 7-26-79.

**Read as 1.40×10^7.

modify radiation response such as age, strain difference, sex of animal, health of animal, diet, endocrine status, oxygen concentration, and temperature. Probably the most effective biological means of modifying the radiation syndrome is by the production of hypoxia, that is, by a decrease in the oxygen concentration in the organism during irradiation (Ref. 14).

Mobley, Olson, and Lauritsen (Ref. 15) numerate several immediate and long-term effects of thermal and ionizing nuclear radiation on aircrews. Among them are flashblindness, retinal burn, skin burn, and radiation sickness. They reported that for radiation doses below 1000 rads, gastrointestinal and neuromuscular distress are the dominant responses of interest to aircrew performance. At doses above 1000 rads, cardiovascular and central nervous system (CNS) effects begin to dominate.

Of the organs comprising the human body, and among those selected for the current study, few can give rise to the acute and long-term sufferings as those manifested in the gastrointestinal (GI) viscera. The GI tract is regarded as one of the most radiosensitive compartments of the body. Its response under irradiation is attributed to its rapid "cell renewal" kinetics in accordance with the Law of Bergonie' and Tribondeau. They generalized that cells are radiosensitive if they have a high mitotic rate, long mitotic future, and of a primitive type. Exceptions to the "Law" are known, yet, the criteria still serve as a "rule of thumb" for predicting the relative radiosensitivity of cells (Ref. 14).

The most startling finding in the current study is the biological anomaly which exists in the GI tract. Refer to Table II. Data in the table reveal that even though the GI tract has the lowest mass density (1.04 grams/cm^3) among the organs under study, it also has the highest atomic density (atoms/cm^3) and greatest atomicity (atoms/gram) among these organs. The physical law governing density, mass, and volume holds that "the greater the density, the greater the number of atoms per unit volume." This law is reversed in the GI tract, and perhaps accounts for one of the reasons why the GI tract is so radiosensitive.

There is a greater number of target atoms per unit volume available for reaction, compared to other tissue which is relatively radioresistant.

Although the data are not presented in this report because of page-number constraints imposed by the contracting agency, it was observed that the GI tract exhibits a high percentage of oxygen in its chemical composition. The high oxygen content of the GI tract could also enhance its radiosensitivity. Hence, several new lines of research on radiosensitivity are recommended in the section which follows.

VI. RECOMMENDATIONS:

A. Guidance for Implementing the Results of Research

Because of the comprehensive nature of the research, a considerable portion of the study remains to be carried out. Recommendations to expand the current research are:

1. Include other vital organs of the human body (eyes, kidney, urinary bladder, etc.) to those selected for the current study, and carry out the same type of computer modeling and particle transport determinations for the additional organs as for those under investigation.
2. Study the possibility of converting the absorbed dose from rads/gamma ray/cm^2 to millirem (mrem) as in the report published by Kramer, Veit, and Drexler (Ref. 16).
3. Extend the current studies to irradiate the phantom in different positions such as in the chair, arc, and scanning positions as reported by Andrasi and Kotel (Ref. 17). Depth dose determinations in phantoms in different positions would be highly useful in assessing vulnerability to aircrews who often assume varying bodily orientations in air travel.
4. Re-model the phantom to include bone structures, etc. The value of employing a heterogeneous phantom is elaborated on by Hofmann, and Tschurlovits (Ref. 18). They assert that when multi-compartments are used, the transfer parameters may vary substantially and the use of a

mean value is not sufficient.

B. Suggestions for Follow-on Research

Follow-on research suggestions include the four recomendations for expansiion of the current study listed above, along with:

1. The development of a research plan to determine whether other highly radiosensitive organs of the body exhibit an anomalous relationship between mass density, and atomic density and atomicity as observed in the GI tract, and

2. The development of a research plan to determine whether other highly radiosensitive organs of the body exhibit high oxygen content in their chemical composition as observed in the GI tract.

Lastly, it is the intent of the writer to prepare and submit a follow-on mini-grant proposal to Universal Energy Systems, Inc. for possible funding to continue the current research. Whether the proposal is submitted depends on prior approval by appropriate personnel at AFWL.

REFERENCES

1. Auxier, J. A., Snyder, W. S., and Jones, T. D., "Neutron Interactions and Penetration in Tissue," In Radiation Dosimetry, Attix, F. H., Roesch, W. C., and Tochlin, E., (Ed.), 2nd Edition, Vol. I, New York: Academic Press, pp. 275-316, 1968.

2. Enz, R. W., and Murphy, H. M., "Gamma Ray Dose in a Cylindrical Phantom," Health Physics, 24: pp. 53-58, 1973.

3. ICRP, Report of the Task Group on Reference Man, International Commission of Radiological Protection, ICRP Publication 23, New York: Pergamon Press, 1975.

4. Vietch, L. R., Radke, G. E., Jr., and Philliber, N. P., "Satellite Vulnerability Code: User's Manual for Programs SLICE, MASS, OVERLAP," Air Force Weapons Laboratory, Kirtland AFB, NM, June, 1984.

5. Straker, E. A., Stevens, P. N., Irving, D. C., and Cain, V. R., "The Morse Code - A Multigroup Neutron and Gamma-Ray Monte Carlo Transport Code," ORNL-4585, Oak Ridge National Laboratory, September, 1970.

6. Radiation Shielding Information Center, "Defense Nuclear Agency 37 Neutron, 21 Gamma Ray Coupled, P_3, Multigroup Library in ANISN Format," RSIC Data Library Collection, ORNL, DLC-31, Oak Ridge, TN, Reviewed July 26, 1979.

7. Janni, J. F., Clark, B. C., Schneider, M. F., and Berger, P. S., A Dose-Equated Manikin for Space Radiation Research, AFWL TR-65-97, Air Force Weapons Laboratory, 1965.

8. Snyder, W. S., "Estimation of Absorbed Fraction of Energy from Photon Sources in Body Organs," Radiation Dosimetry, Vol. 1, Boris Kidric Institute of Nuclear Science, Beograd, p. 108, 1971.

9. Berger, M. J., "Energy Deposition in Water by Photons from Point Isotropic Sources," MIRD Pamphlet No. 2, J. Nuclear Med., Suppl. No. 1, p. 15, Februarv, 1968.

10. Snyder, W. S., Ford, M. R., and Warner, G. G., "Estimates of Absorbed Fractions for Photon Emitters Within the Body," Second European Congress on Radiation Protection, Budapest, Hungary, May 3-5, 1972.

11. Snyder, W. S., Ford, M. R., and Warner, G. G., "Estimates of Absorbed Fractions for Photon Emitters in the Body," ORNL-4811, p. 86, Health Physics Division Annual Report for Period Ending July 31, 1972.

12. Bauchinger, M., Kuhn, H., Dresp, J., Schmid, E., and Streng, S., "Dose-Effect Relationship for 14.5 MeV (d + T) Neutron-Induced Chromosome Aberrations in Human Lymphocytes Irradiated in a Man Phantom," Int. J. Radiat. Biol., Vol. 43, No. 5, pp. 571-578, 1983.

13. International Commission of Radiological Units, "Dose Equivalent," ICRU Supplement to ICRU Report 19, pp. 1-3, September 1, 1973.

14. Casarett, A. P., Radiation Biology, Englewood Cliffs: Prentice-Hall, Inc., 1968.

15. Mobley, T. S., Olson, C. T., and Lauritsen, T. N., The Effect of Thermal and Ionizing Nuclear Radiation on Aircrews, AFWL-TR-76-141, Air Force Weapons Laboratory, August, 1976.

16. Kramer, R., Veit, R., and Drexler, G., "Body Dose Conversion Factors for Computerized Tomography," Proceedings of an International Symposium jointly organized by IAEA and WHO, IAEA-SM-249/14, pp. 79-91, 27-31 October, 1980.

17. Andrasi, A., and Kotel, G., "Whole-Body Counter Efficiency Calculations for Distributed Sources in a Human Phantom," Hungarian Academy of Science, Report No. KFKI-72-30, Budapest, April, 1972.

18. Hofmann, W., and Tschurlovits, M., "On the Application of Monte Carlo Calculations in Environmental Modelling - Applicability and Limitations," Recent Developments and New Trends in Radiation Protection, XI Regional Congress of IRPA, Vienna, Austria, p. 110, September, 1983.

AD-A166 176 UNITED STATES AIR FORCE SUMMER FACULTY RESEARCH PROGRAM 13/13
1985 TECHNICAL RE (U)UNIVERSAL ENERGY SYSTEMS INC
DAYTON OH R C DARRAH ET AL DEC 85 AFOSR-TR-86-0139
UNCLASSIFIED F49620-85-C-0013 F/G 5/9 NL

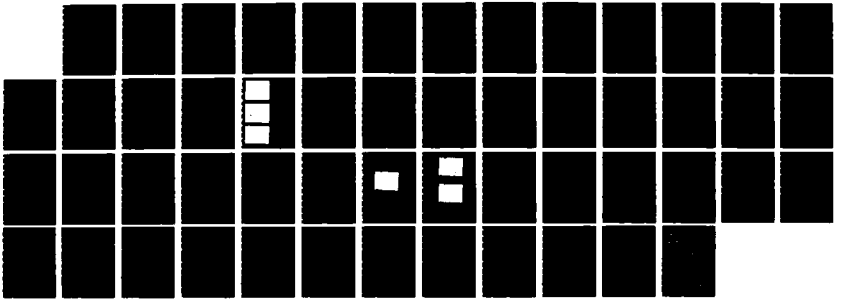

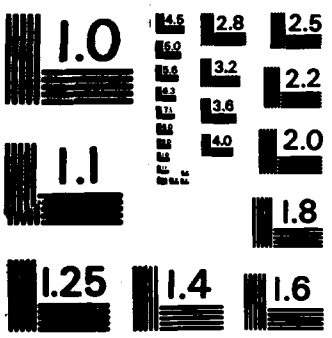

MICROCOPY RESOLUTION TEST CHART
NATIONAL BUREAU OF STANDARDS - 1963 - A

1985 USAF-UES SUMMER FACULTY RESEARCH PROGRAM/

GRADUATE STUDENT SUMMER SUPPORT PROGRAM

Sponsored by the

AIR FORCE OFFICE OF SCIENTIFIC RESEARCH

Conducted by the

UNIVERSAL ENERGY SYSTEMS, INC.

FINAL REPORT

Determination of Thermal Properties of Melanin Using Photoacoustic Techniques

Prepared by:	James M. Gallas
Academic Rank:	Asst. Prof. of Physics
Department and University:	Department of Earth and Physical Sciences, The University of Texas at San Antonio
Research Location:	Laser Laboratory, USAF School of Aerospace Medicine, Aerospace Medical Division, Brooks Air Force Base, Texas 78235
USAF Research:	Dr. Ralph Allen, Chief Scientist
Date:	19 August, 1985
Contract No:	F49620-85-C-0013

Determination of Thermal Properties of Melanin Using Photoacoustic Techniques

by

James M. Gallas

A photoacoustic detection apparatus was constructed to detect and measure both transient and time averaged pressure responses to pulsed radiation. Photoacoustic signals were recorded to analyze photothermal properties of melanin. Specifically, the thermal diffusivity of melanin was determined and compared with a value from the literature determined in a different manner. The dependence of pressure amplitudes upon laser pulse intensity and pulse frequency was also investigated. The thermal properties of melanin investigated here were then related to the general problem of laser induced retinal degradation and the possible role or roles played by melanin. A variety of experiments based upon the present work and which may lead to an elucidation of the retinal damage mechanism are suggested for future work.

I. INTRODUCTION:

In 1975 I entered the University of Houston to study physics problems relating to solar energy and to work on a Ph.D. dissertation in physics. At that time there was already a great deal of interest and activity in photothermal converters. Usually these converters were in the form of thin metallic coatings and films. Many of the physics graduate students were involved in solar energy projects producing many discussions relating to the optical and thermal transport properties of metal blacks. Several years later I began studying solar energy applications of melanin,

the pigment responsible for skin and hair coloration, as a natural black solar absorber. This led to considerations of the contrasting ways in which small metal particles and organic molecules degrade electromagnetic radiation to produce heat. In the case of melanin additional features were found to be provided by nature in the way in which the pigment interacted with light. As well as being an efficient (black) photothermal converter, the pigment also acts as a photostabilizer tosurrounding biological tissue, through its ability to stabilize normally reactive free radicals. The pigment thus functions as both a sunscreen and a photochemical free radical scavenger.

In 1979 I showed that melanin was fluorescent and subsequently was able to show that its weak fluorescence was related directly to the free radicals. My Ph.D. dissertation on the fluorescence of

melanin characterizes this fluorescence, investigates

the effect of various environmental parameters and shows that the melanin fluorophores are reactants in a chemical equilibrium involving

the free radicals as products. In the process I have acquired some expertise in a variety of spectroscopic areas including UV, visible, infrared, fluorescence and electron spin resonance spectroscopies. I have just finished a manuscript on fundamental characteristics of melanin fluorescence which I am submitting for publication.

Recently I have become interested in photoacoustic spectroscopy applied to melanin since this technique is concerned solely with radiationless transitions and thus provides an ideal way to separate the various de-excitation pathways following the absorption of light,only one of which is fluorescence.

The Air Force has been interested for quite some time, inthe role played by melanin in laser induced damage to the retina. It appears that there are three possible types of damage in the wavelength region between 400 and 1400nm. These are mechanical, thermal and photo- chemical. Melanin is believed to play a key role in all three types of damage(1). Further details of these possible mechanisms will be discussed in Section VI.

II. OBJECTIVES OF THE RESEARCH EFFORT:

The general objective in this work was to relate quantitatively the absorption of electromagnetic energy by melanin to transient acoustic pressure produced by the heated melanin.

The specific objectives were :

(1) to design and assemble an apparatus to measure pressure amplitude responses of melanin to a shuttered exposure froma cw laser;

(2) to characterize and describe the melanin photoacoustic signal.

III. MATERIALS AND METHODS

The general objective of describing the role of melanin in photo-induced retinal damage was partially achieved and bridged to the specific objectives through the photoacoustic determination of the thermal diffusivity. This is an important parameter in the thermal modeling of retinal damage and is obtained in this work as an example of the potential offered by the photoacoustic technique.

Synthetic suspensions of melanin from L-Dopa were prepared in water according to the method described by Felix (2). The suspensions were allowed to evaporate to produce concentrated stock melanin suspensions. Small strips of xerox paper (20 % cotton) of dimensions 10mm x 20mm x .1mm were weighed and then repeatedly dipped into the concentrated melanin suspensions. The melanin impregnated paper strips were then allowed to dry and weighed to determine the mass of melanin absorbed.

A diagram of the photoacoustic detection system is given in Figure 1. The photoacoustic cell was a pyrex cylinder with a closed pyrex bottom and open at the top. The paper strips were shaped to the curvature of the cylinder and inserted. An "O"-ring was placed around the circumference of a Realistic condenser microphone (model 33-1056A) which when inserted into the glass cylinder left a gas volume of approximately $1cm^3$. Approximately 20% of the incident light was reflected from the curved surface. The laser size was approximately 4 mm^2.

The laser source was a Spectra Physics argon ion laser. (model 171-09) The 514 nm line was used throughout the experiments. The beam was chopped by a Datalight optoacoustic chopper (model DLM-1V), triggered

by a Systron Donner 100C Pulse Generator which was able to control both the frequency and pulse width of the beam. The beam was then directed onto the acoustic cell containing the melanin impregnated paper strip. The signal from the microphone was fed into either an Ithaco391A phase lock-in amplifier or into a Nuclear Data ND100 signal averager which were trigerred by the chopper. Averaged transient respomnses were photograghed from the display trace. Theintensities of the laser pulses arriving at the cell before and after each signal average were measured with a Laser Precision Corp. photometer. In all cases the laser intensity variations were non significant.

Typical transient photoacoustic responses from the signal averager display are shown in Figure 2 for melanin (2a) and black silver halide coatings obtained from exposed photographs (2b). In addition a photograph of the laser trigger pulse was taken(1c). The pulse frequency was 12 Hz and in all experiments the pulse width was set at 1ms. In all cases the pulse frequencies were checked for accuracy with a Tektronix oscilloscope. The horizontal scale in Figure 1 is 250 ms full scale and the linear distance is 9 cm. Delay times between the excitation pulse and the acoustic pulsewere therefore estimated by measuring the distances from the leftmost marker to the peak of the acoustic pulse. The vertical scale of the Nuclear Data display was calibrated in millivolts/division to determine the pressure amplitudes. Alternatively, pressure signal amplitudes, phase and angles were read directly from the lock-in amplifier.

The thermal diffusivity can be determined by measuring the variation of the phase lag (as measured from the lock-in amplifier) with chopping frequency. Under the assumptions of one dimensional heatflow and

negligible lateral heat losses, it can be shown that

$$\Theta = \sin [\omega t - x(\omega/2a)^{1/2}] \qquad (1)$$

describes the relationship between the phase of the temperature wave at a distance x from the sample surface and the chopping frequency ω, and where a represents the thermal diffusivity(3).
The phase lag $\Delta\Theta$ is then given by

$$\Delta\Theta = x(\omega / 2a)^{1/2} \qquad (2)$$

It follows then that a plot of the phase lag, obtained from the lock-in amplifier, as a function of $\sqrt{\omega}$ will yield a straight line with a slope equal to $x / (2a)^{1/2}$.

IV. RESULTS

a. Thermal Diffussivity

Figure 3 is a graph of the signal phase as a function of $\sqrt{\omega}$. The data points indicate a straight line with a slope of 1.88. The thickness of themelanin films were determined to be approximately .01 cm with a micrometer, so that according to equation (2),

$$a = .01 / (1.88\sqrt{2}) \text{ cm}^2 / \text{s}$$

$$a = 3.7 \times 10^{-3} \text{ cm}^2 / \text{s}$$

It is interesting to compare this value with one obtained in the literature (4) based upon a knowledge of the thermal conductivity, k , specific heat, c , and mass density, ρ , for melannin. Interms of these parameters the thermal diffusivity is given by

$$a = k / (\rho c) \qquad (3)$$

$$= \frac{1.5 \times 10^{-3} \text{ cal/ s C cm}}{(1 \text{ cal/g C}) \text{ 1g/cm}^3}$$

$$= 1.5 \times 10^{-3} \text{ cm}^2/\text{s}$$

This relatively close agreement with the value obtained using photoacoustic techniques illustrates the potentialof photoacoustic methods in determining thermal properties of materials.

b. Pressure Amplitude Dependence Upon Laser Intensity

Figure 4 illustrates the dependence of the acoustic signal, measured in millivolts, upon the laser energy measured in microjoules. The dependence is not linear as one would have expected for a purely thermal response but instead has a slight sigmoid behavior. A linear dependence is expected provided an increase in laser intensity corresponds to a proportional increase in the rate of thermal energy produced at the sample surface, and that this in turn results in a proportional increase in the acoustical pressure amplitude. Possible explanations for the observed behavior are given in section V.

V. DISCUSSION OF RESULTS:

The photoacoustic effect is the result of light absorption followed by radiationless de-excitation. Resultant thermal energy is transferred to a thin layer of gas adjacent to the sample surface causing a pressure wave. When the process occurs periodically, as with a pulsed light source, a signal can be detected with a gas microphone and suitable instrumentation for signal amplification. Adequate theory has been developed to accurately describe and predict the acoustical responses (5) Application of the thermal diffusion equation to simple geometries with appropriate boundary conditions can lead to simple but important relationships such as equation (2) for the thermal diffusivity.

Figure 4 represents a departure from the expected behavior of a linear dependence of the pressure amplitude upon laser intensity. A possible clue to this departure comes from the hydrophilic properties of melanin. Up to fifty percent of its weight is in the form of both tightly and loosely boundwater. Thiswater canbe thermally desorbed and experiments (6) have shown that a sigmoidal behavior is associated with the water content and temperature (Figure 5). If the sigmoidal variation of pressure amplitude with laser intensity is related then to the (light induced) thermal desorption of lightly and tightly bound water , this would suggest that rather high local temperatures are reached as a result of the absorption of the laser pulses. This is valuable information which relates directly to retinal damage mechanisms. Also it should be emphasized that light enhanced thermally desorbed water may contribute to the

the photoacoustic signal and it may be necessary to account for this effect in future photoacoustic work involving melanin.

VI. RECOMMENDATIONS:

This work has shown that it is possible to use the photoacoustic effect to determine the thermal diffusivity of melanin, a quantity which has been shown to have particular significance in attempts to describe laser induced damage to the retina. This work has also shown that departures exist from the behavior expected for the dependence of the pressure amplitude upon laser intensity for of melanin and that these differences might be related to the particular hygroscopic properties of melanin. Rosencwaig and Pines studied the change in thermal diffusivity of rat stratum corneum with water content (7) and it would seem reasonable to do this for melanin.

But the role played by the water bound to the melanin may have still further significance if vaporization is involved in retinal damage. According to models for retinal damage in the literature it has been assumed that melanin granules do not contain water (8 .)However, current studies on the polyelectrolyte properties of melanin (9) shows that melanin does contain substantial water .

Photoacoustic studies could help elucidate the vaporization mechanism.

A more realistic experimental configuration would be achieved by placing a gelatinous materialdirectlyin frontof themelanin to mimic the vitreous humor mechanically. Because of the high transmission coefficient for an acoustic wave in going from solid (melanin) to solid (gelatin) it would be reasonable to use piezoelectric transducers to detect the photoacoustic signals. Furthermore these transducers have a very fast rise time (< usec) and therefore could respond to the very short signals anticipated.

My initial interest in photoacoustic techniques before working on this project was its complimentary role to my fluorescence work in which I related melanin fluorescence directly to the melanin free radical. It has been pointed out (1) that the melanin photo-induced free radical may play some role in the photochemical related damage to the retina. It might be helpful therefore to combine ESR, fluorescence and photoacoustic spectroscopy to study the overall role played by melanin in the light induced damage to retina.

REFERENCES

1. Ham, William,T., "The Nature of Retinal Radiation Damage", Vision Research, vol. 20, 1980,pp. 1105-1111.

2. Felix, C.C., et. al., Free Radicals in Biology, New York, Academic Press, 1980.

3. Adams, M. J. and Kirkbright, G.F., Thermal Diffusivity and Thickness Measurements for Solid Samples Utilizing the Opto-acoustic Effect," Analyst, vol. 102, 1977 pp. 678-682.

4. Hayes, J.R., and Wolbarsht, M.L., " Thermal Model For Retinal Damage Induced by Pulsed Lasers," Aereospace Medicine, May, 1968, pp. 474-480.

5. Rosencwaig, Allan, Photoacoustics and Photoacoustic Spectroscopy, New York, John Wiley & Sons, 1980.

6. Chio, Shiu-Shin, X-Ray Diffraction and ESR Studies on Amorphous Melanin, Ph.D. Dissertation, Univ. of Houston, 1977.

7. Rosencwaig, A. and Pines, E., Biochim. Biophys. Acta, vol. 493, 1977, pp. 10.

8. Welch, A.J. et. al., "Experimental Validation of Thermal Retinal Models of Damage From Laser Radiation", Report SAM-TR-79-9, USAF School of Aerospace Medicine, 1979.

9. Kirkpatrick, D.S. et. al.," Melanin-Water-Ion Dielectric Interactions", Pigment Cell, Vol. 4, 1979, pp. 257.

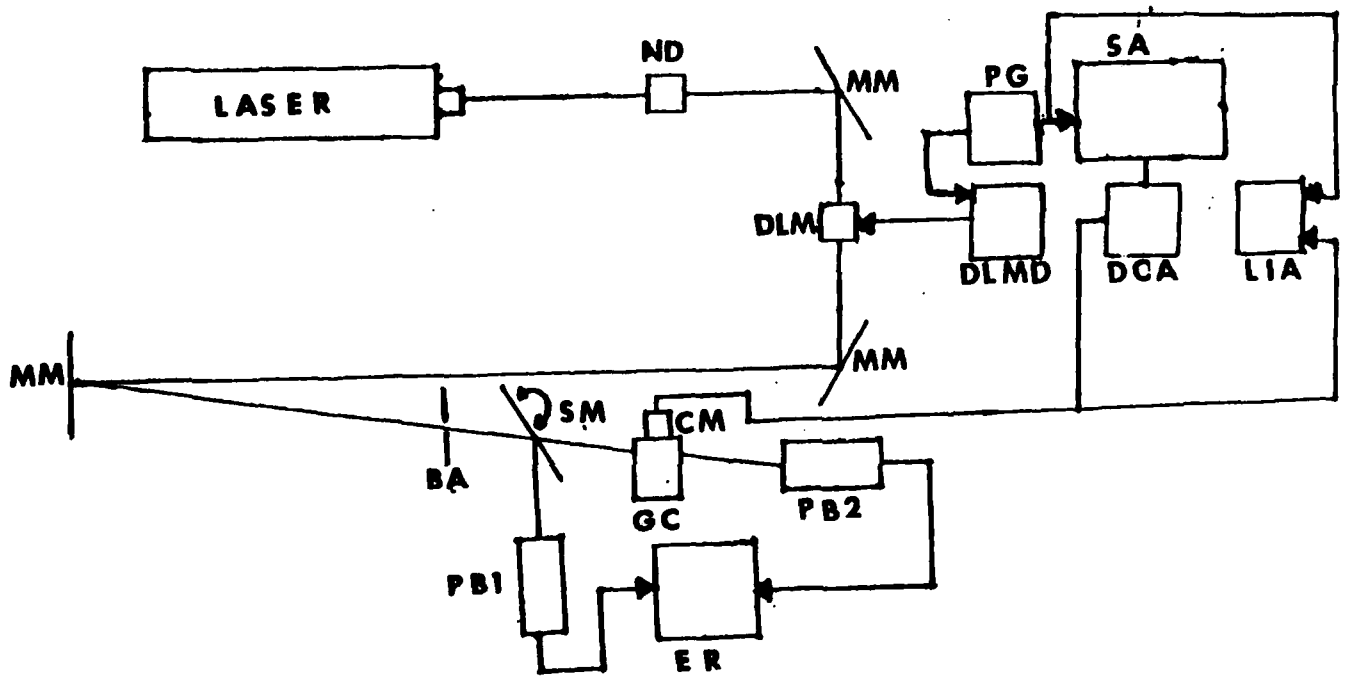

Figure 1

BA - Beam Aperture
CM - Condenser Microphone
DCA - D.C. Amplifier
DLM - Acoustic-optical Modulator
DLMD - Acoustic-optical Modulator Driver
ER - Energy Ratiometer
GC - Glass Cylinder
LASER - Spectra-Physics 171 Argon
LIA - Lock In Amplifier
MM - Mirror Mounts
ND - Filter Box
PB1 - Probe 1
PB2 - Probe 2
PG - Pulse Generator
SA - Signal Averager
SM - Swing Mirror

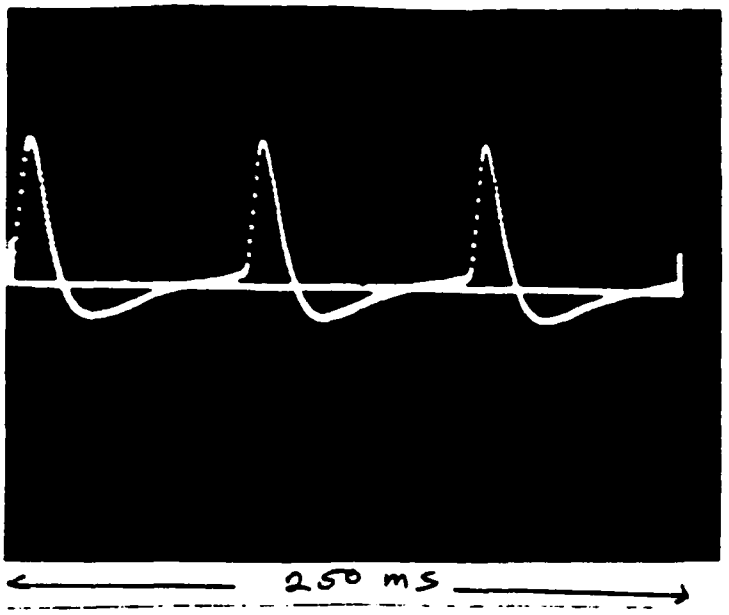

a) Melanin

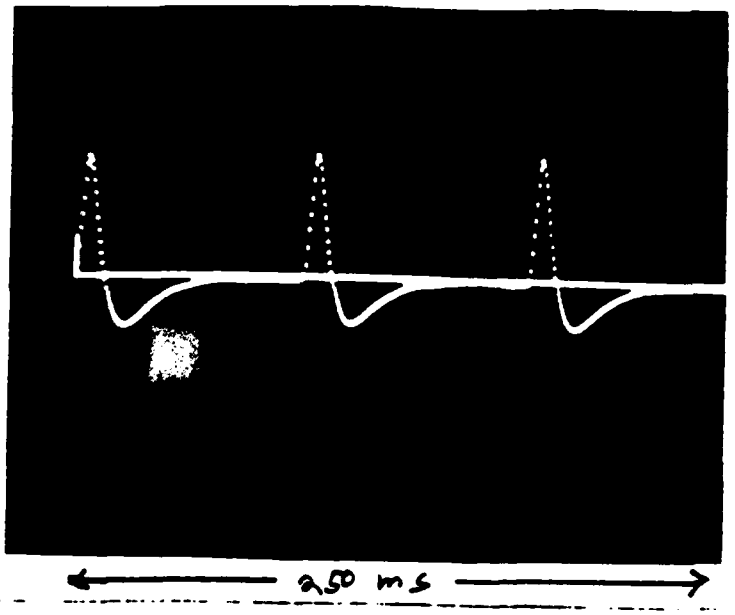

b) Silver Halide

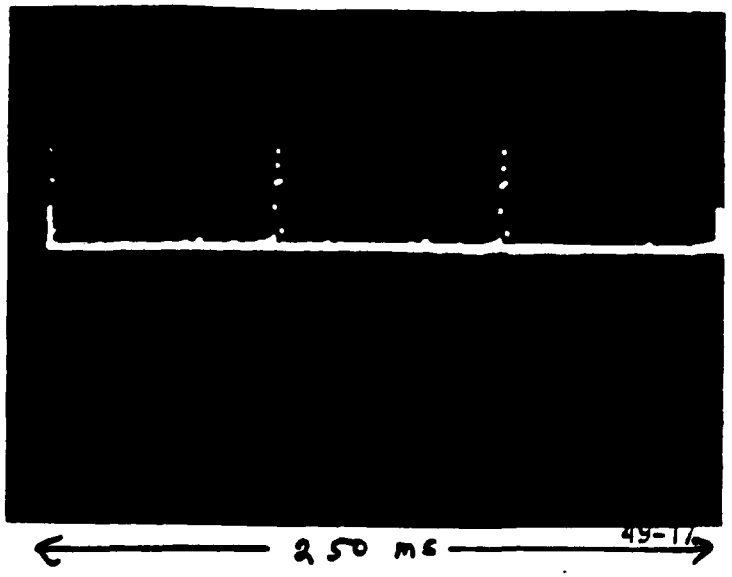

c) Laser signal
pulse width=
1 ms
pulse rep.
rate = 10 Hz

Figure 2:
Photoacoustic
Transient Signals

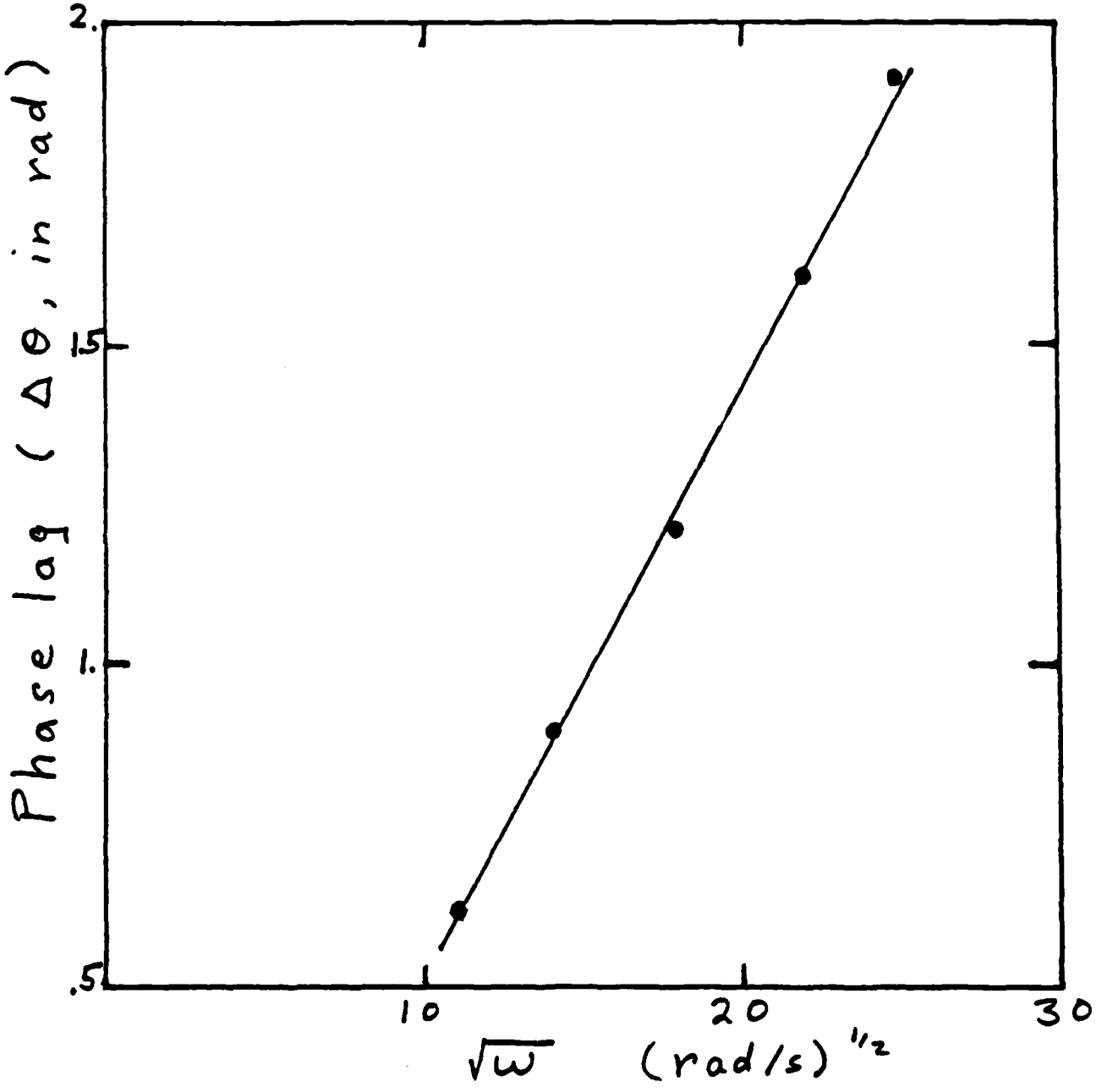

Figure 3: Graph of photoacoustic signal phase lag for melanin v.s. $\sqrt{\omega}$

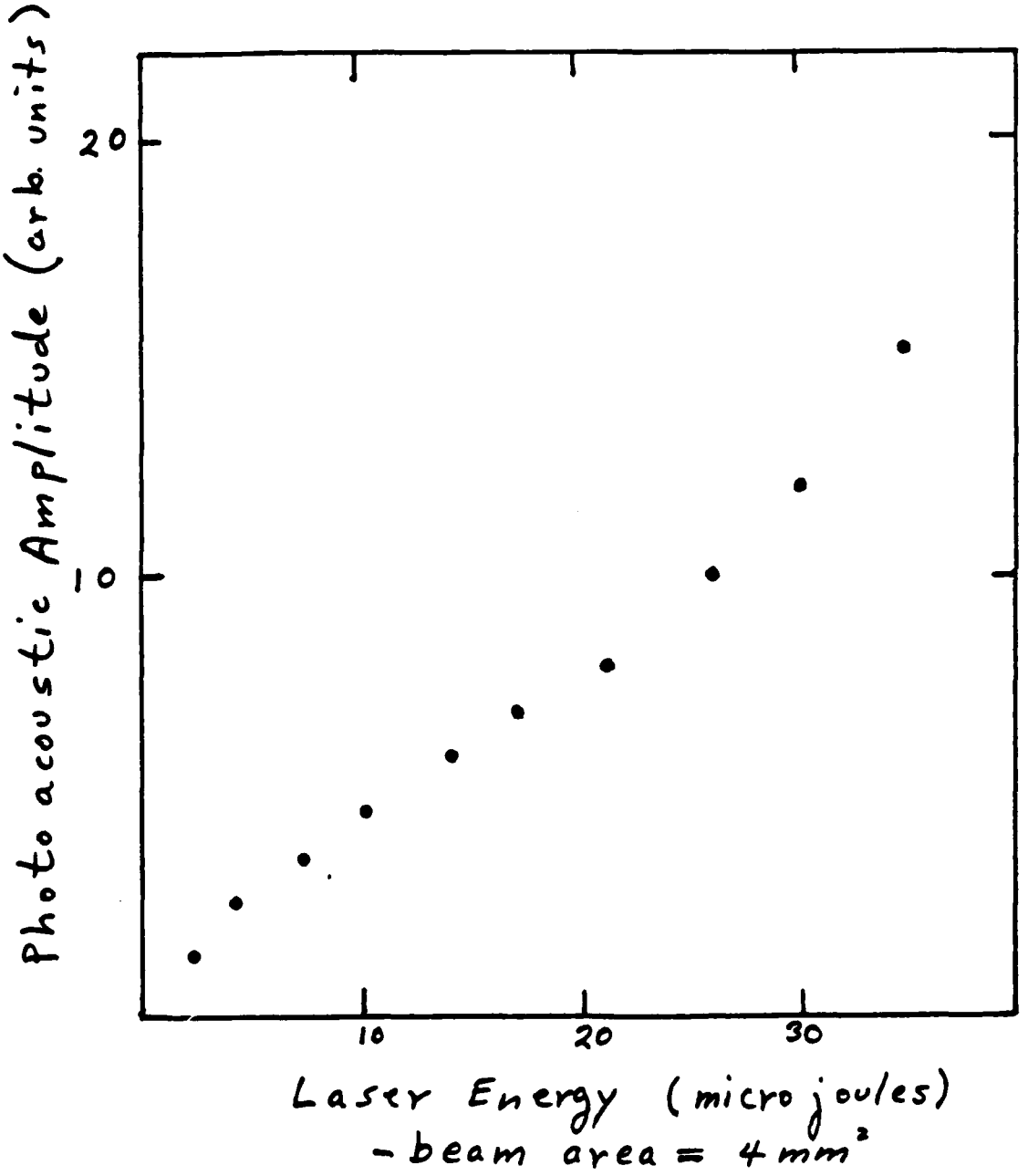

Figure 4 : Non linear Dependence of photoacoustic amplitude on Energy

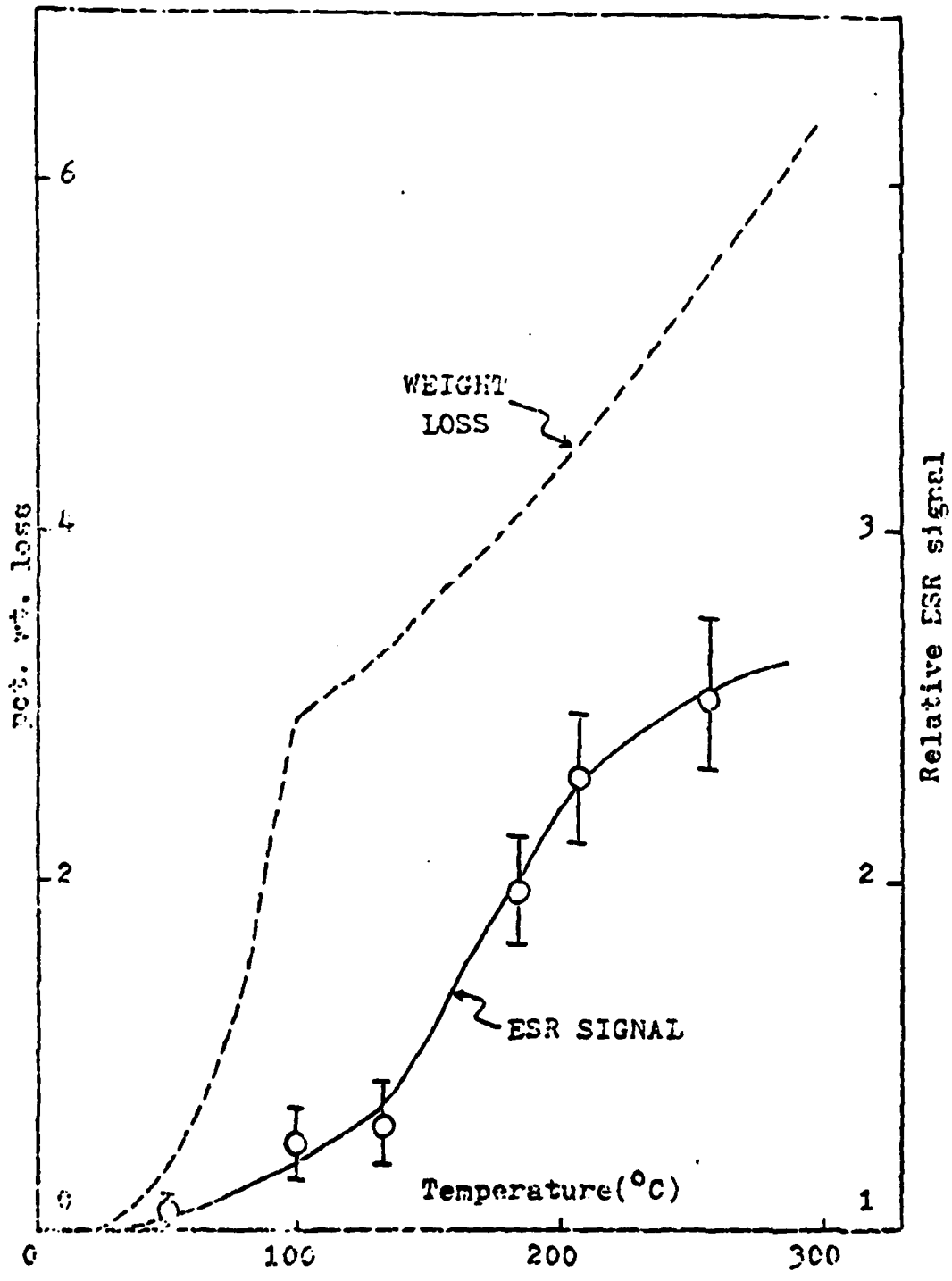

Figure 5: Percent weight loss of melanin with temperature due to thermal desorption of water

1985 USAF-UES SUMMER FACULTY RESEARCH PROGRAM/

GRADUATE STUDENT SUMMER SUPPORT PROGRAM

Sponsored by the

AIR FORCE OFFICE OF SCIENTIFIC RESEARCH

Conducted by the

UNIVERSAL ENERGY SYSTEMS, INC.

FINAL REPORT

Lidar Measurements of the Mesospheric Sodium Layer at the Air Force Geophysics Laboratory

Prepared by:	Chester S. Gardner
Academic Rank:	Professor
Department and	Electrical and Computer Engineering
University:	University of Illinois at Urbana-Champaign
Research Location:	Air Force Geophysics Laboratory, OPA, Lidar Group
USAF Research	C. Russel Philbrick
Date:	September 5, 1985
Contract No.	F49620-85-C-0013

Lidar Measurements of the Mesospheric Sodium Layer at the Air Force Geophysics Laboratory

by

Chester S. Gardner

Abstract

The AFGL Rayleigh scatter lidar system was modified to make measurements of the mesospheric sodium layer by adding a tunable dye laser, a laser wavelength monitor and an energy monitor. Sodium lidar measurements were obtained during several nights in July and August. Measurements were also obtained simultaneously at AFGL and at the University of Illinois during a two hour period in the early morning of August 29. These data are being analyzed for tidal and gravity wave effects. Additional simultaneous lidar measurements at AFGL and the University of Illinois have been planned for the Fall and Winter 1985-86.

Acknowledgements

The author would like to thank Dr. C. R. Philbrick for the invitation to participate in the Summer Faculty Research Program at AFGL and for his support and encouragement during the research period. The author also would like to acknowledge Dr. Dwight Sipler and Byron Dix of AFGL for their help in integrating the dye laser into the AFGL lidar system and Drs. Gil Davidson and Warren Moskowitz of Photometrics for their help in collecting the sodium lidar data.

The author gratefully acknowledges the sponsorship of the Air Force System Command, Air Force Office of Scientific Research and the Air Force Geophysics Laboratory.

I. Introduction

Gravity waves, tides and turbulence have a significant influence on the general circulation of the middle atmosphere[1,2]. Gravity waves are thought to be mainly responsible for the vertical transport of momentum into the mesosphere, and outside the tropics they are an important factor in determining the annual cycle of large-scale circulation. Among the numerous radio and optical techniques that have been developed for atmospheric research, lidar (light detection and ranging) has proven to be particularly effective for studying the influence of gravity waves and tides on the dynamics of the stratosphere and mesosphere[3-6]. Rayleigh scatter lidars are currently being used to measure atmospheric density and temperature up to about 80 km altitude and above 80 km, resonant scatter lidars are being used to study the metallic layers of Na, K, Li, Ca and Ca^+.

The mesospheric sodium layer is generally confined to an altitude range of 80-105 km with a peak density near 90 km of about 10^9 - 10^{10} m^{-3}. The layer was discovered in the late 1930's and is now believed to be of meteoric origin[7,8]. Before lidar systems became available, sodium layer measurements were largely restricted to studying resonantly-scattered sunlight. Ground-based measurements of this type were able to define seasonal variations in column abundance[9,10], but the sharp layer boundaries were not revealed until rocket-borne dayglow measurements were made[11]. Lidar observations of the vertical structure of the layer were first made in England[12]. Since then similar measurements have been reported from a variety of locations including France[13], Brazil[14], California[15], Illinois[16], and at the high latitude of Franz Joseph Land, USSR[5].

The development of the University of Illinois (UI) sodium lidar system was begun in 1975 by the author and Professor C. F. Sechrist, Jr. and the first sodium layer measurements were obtained in June 1976. The system currently consists of a large Fresnel lens telescope (1.2 m^2) and flashlamp pumped tunable dye laser (100 mj @ 10Hz). Professor Sechrist, the author and their students have also conducted steerable lidar measurements at the NASA-Goddard Space Flight Center, airborne lidar measurements at the NASA-Wallops Flight Facility, and correlative lidar-rocket measurements at the White Sands Missile Range. The author has been

primarily interested in studying the interaction of gravity waves with the sodium layer and in developing optimal signal processing algorithms for analyzing lidar photocount data. This research is summarized in References 16-19.

Rayleigh scatter lidars have also been used for many years to measure atmospheric density and temperature in the stratosphere and lower mesosphere. Rayleigh scatter lidars directly measure atmospheric density and temperature is inferred from the density measurements by using the equation of state and the hydrostatic equation. This technique was pioneered by Elterman in the early 1950's using a bistatic lidar system consisting of a search light modulated by a mechanical shutter and a telescope which scanned the search light beam[20]. More recently a number of groups including the Air Force Geophysics Laboratory (AFGL) at Hanscom AFB, MA, have used high energy YAG lasers in a monostatic lidar configuration to obtain density and temperature measurements up to 80 km altitude. These lidars have proven to be particularly useful for studying gravity wave effects on the stratosphere and lower mesosphere[6]. However, above 80 km the atmospheric density is so low that the scattered signals are too weak to permit accurate density and temperature measurement. Fortunately, because of the large resonant backscatter cross-section of the sodium atom, sodium lidars can be used for measurements from 80 to 105 km altitude.

The development of the AFGL lidar laboratory was begun in 1980 by Dr. C. R. Philbrick. By July 1985 the laboratory included a fixed large aperature (0.6 m^2) Rayleigh scatter lidar and a smaller (0.3 m^2) trailer mounted mobile lidar. Both lidars employ high energy YAG lasers (1-2J @ 10Hz) which operate at the doubled (532 nm) and tripled (355 nm) frequencies. In addition, a tunable dye laser was acquired in early 1985 for planned Na density and temperature measurements. Dr. Philbrick also has a strong research background in atmospheric dynamics and the AFGL lidar laboratory was developed in part for experimental research in this area. Thus the complementary research interests and backgrounds of Dr. Philbrick and the author and the excellent experimental facilities at AFGL and at UI provided a unique opportunity to develop a productive collaborative research program in lidar studies of the atmosphere.

II. Objectives of the Research Effort

The goals for the summer research period were:

(1) To integrate the new dye laser into the AFGL lidar system and to obtain the first measurements of the mesospheric sodium layer.
(2) To integrate the UI lidar software into the AFGL lidar data acquisition system.
(3) To obtain continuous measurements of the sodium layer profile simultaneously at AFGL and at UI during at least one night from sunset to sunrise. This experiment was designed to monitor tidal and gravity wave effects simultaneously at the two sites.
(4) To obtain continuous simultaneous measurements of the sodium layer profile and the atmospheric density profile using the AFGL sodium and Rayleigh scatter lidars during at least one night from sunset to sunrise. This experiment was designed to monitor gravity wave propagation from the stratosphere up through the mesosphere.

The objectives of goals (1) and (2) were to demonstrate the sodium measurement capabilities of the AFGL lidar system and to provide the AFGL lidar with the necessary signal processing capabilities to analyze the sodium lidar data. These two goals have been met. The objectives of goals (3) and (4) were to make scientifically interesting measurements of gravity waves and tidal effects which utilized the unique capabilities of the AFGL and UI lidar systems. Because of unfavorable weather, goals (3) and (4) were only partially realized. Sodium lidar measurements at AFGL and Urbana, IL and Rayleigh scatter lidar measurements at AFGL were obtained simultaneously during a two hour period on the morning of August 29. Additional measurements have been planned for the Fall and Winter 1985-86.

III. Sodium Lidar System Configuration

Figure 1 is a block diagram of the AFGL Na lidar system. The frequency doubled (532 nm) output of the Quantel YG482 YAG laser is used to pump the dye laser. Although the YAG laser is capable of generating 12 ns pulses with energies up to 800 mj/pulse @10Hz in the green, it is typically operated at energy levels between 100 and 400 mj. Higher energy levels can damage the optics in the dye laser (see Section VI). Two turning mirrors are used to elevate and deflect the pump beam into the Lambda-Physique FL2002EC dye laser. Because the doubler is less than 100% efficient, the YAG beam contains pulses at both the fundamental (1064 nm) and doubled (532 nm) frequencies. However, the dielectric turning mirrors have very low reflectivity at the YAG fundamental and therefore they act as a filter which removes most of the residual fundamental from the pump beam. The dye laser contains an oscillator, preamplifier and two power amplifiers. The oscillator is tuned using a diffraction grating and intracavity etalon. The linewidth is specified by the manufacturer at 1.4 pm. The efficiency of the dye laser depends upon the dye, operating wavelength, pump wavelength and alignment. We obtained efficiencies up to 17% using the Rhodamine 6G dye at the 589 nm Na resonance wavelength (Section VI). A glass flat is used to split off part of the dye laser output. This monitor beam is deflected to a photodetector and hollow cathode Na lamp (Section IV). The photodetector output is used during alignment to adjust the laser for maximum efficiency. The photodetector also triggers the data acquisition computer. The hollow cathode lamp signal is used to tune the dye laser to the Na resonance line. The dye laser output beam is deflected by a turning mirror to a steering mirror which aligns the beam with the telescope. The telescope has three UV (355 nm) and three green (532 nm) detectors to provide the required dynamic range for the Rayleigh scatter lidar. For Na measurements the most sensitive green detector is used by replacing the interference filter with a Na line filter (λ_c = 589 nm, $\Delta\lambda$ = 80 A FWHM). The photocount data are acquired using a LeCroy Model 6500 data acquisition system. The data are stored on floppy disks and ultimately transferred to a Zenith 100 computer for processing and analysis. The major system parameters of the AFGL Na lidar are listed in Table 1.

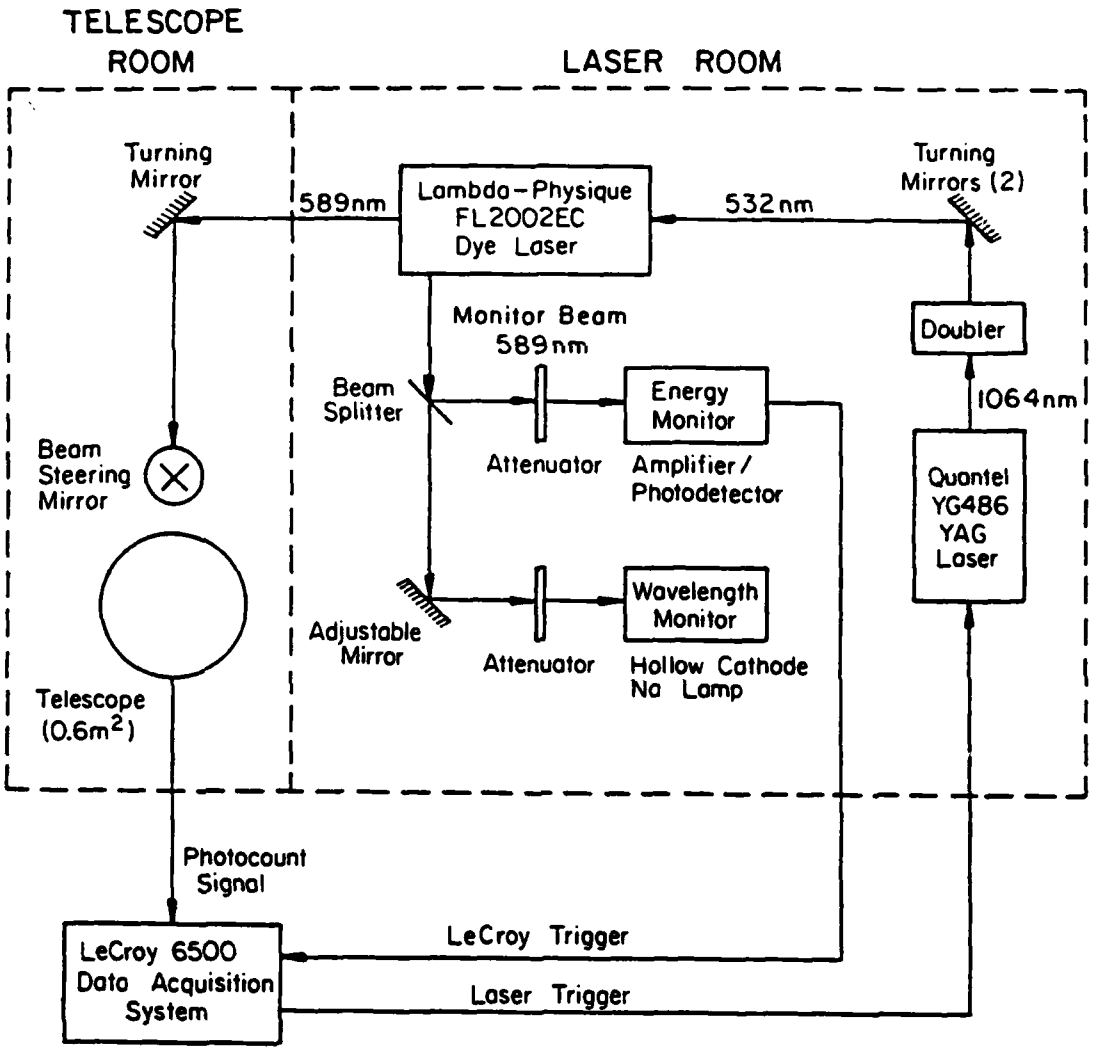

Figure 1. Block diagram of the AFGL sodium lidar system.

Table 1
AFGL Sodium Lidar System Parameters

Quantel Model YG482 YAG Pump Laser
- Wavelength = 532 nm
- Max Energy = 800 mj @ 10Hz
- Pulse Width = 12 ns

Lambda-Physique FL2002EC Dye Laser
- Wavelength = 589 nm
- Max Energy = 60 mj @ 10 Hz
- Pulse Width = 10 ns
- Divergence = 1 mrad

Telescope Area = 0.6 m^2
Planar FOV = 1 mrad
Bandwidth = 80 A FWHM
Detector Quantum Efficiency = 15%

IV. Laser Monitor Electronics

A photodetector power monitor and a hollow cathode Na lamp wavelength monitor were fabricated for the AFGL Na lidar. The devices are both mounted on a plate near the monitor beam port on the side of the dye laser. Figure 2 is a diagram showing the physical configuration of the monitor optics and electronics. Part of the monitor beam is deflected by a beam splitter to a series of neutral density (ND) filters and the photodetector. The detector is a Devar 529 integrated detector/amplifier. Because the detector has no gain control, the ND filters are used to adjust the dynamic range of the detector output. A ND filter, Na line interference filter and diffuser are mounted in the detector housing. The interference filter rejects most of the broadband amplified spontaneous emission (ASE) generated by the dye laser and facilitates adjustment of the laser to maximize the desired 589 nm output. Because even the weak monitor beam can damage the interference filter, a ND filter is permanently mounted in front of the interference filter to attenuate the beam. The diffuser minimizes signal fluctuations due to beam movement or changes in mode structure during alignment of the laser. The detector/amplifier is powered by two 9 volt batteries. Figure 3 contains the wiring diagram for the detector/amplifier. The detector output is switched through a junction box to an oscilloscope. Figure 4 is a typical oscilloscope trace of the detector output signal. The detector output also triggers the LeCroy data acquistion system. The required trigger pulse amplitude is approximately +3 volts peak into a 50 load.

The portion of the monitor beam passed by the beam splitter is deflected by an adjustable mirror through a series of ND filters and a Na line interference filter (to attenuate ASE) to a hollow cathode Na lamp. Figure 3 contains the circuit diagram of the lamp. The lamp is powered by a high voltage negative DC supply. The high voltage is adjusted so that the lamp current is in the range of 7-10 ma. The lamp is wired so that a current meter can be easily switched into the circuit. The lamp current should not exceed 12 ma. The mirror is adjusted so that the monitor beam passes through the center of the cathode. To minimize the photodiode effect, the beam illumination of the anode and cathode should be minimized. When the dye laser is tuned to the Na resonance line, the

opto-galvanic effect changes the lamp impedance and hence the voltage across the cathode and anode also changes. The lamp voltage is AC coupled through the junction box to an oscilloscope. Figure 5 shows typical oscilloscope traces with the laser tuned on and off the Na D_2 resonance line. The best signal-to-noise ratio is obtained with monitor beam attenuated to prevent saturation of the Na within the lamp and with the beam position adjusted to minimize the photodiode effect signal. The typical signal level with the laser tuned to the Na resonance wavelength is 10mv.

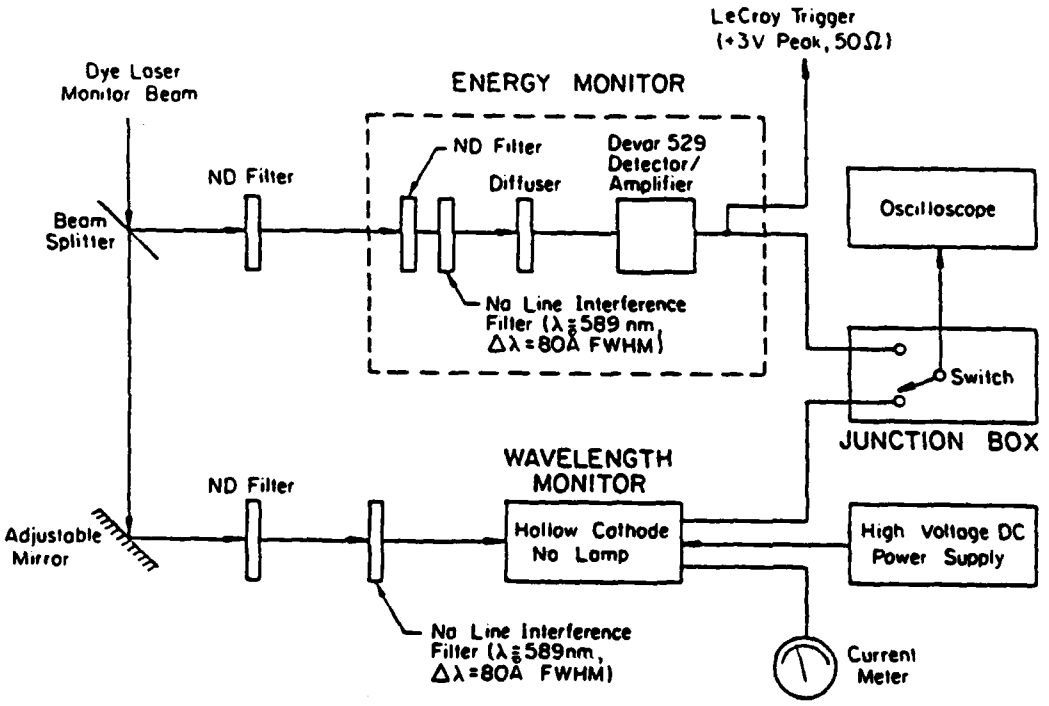

Figure 2 Optical and Electrical Configuration of the Dye Laser Energy and Wavelength Monitoring Circuits.

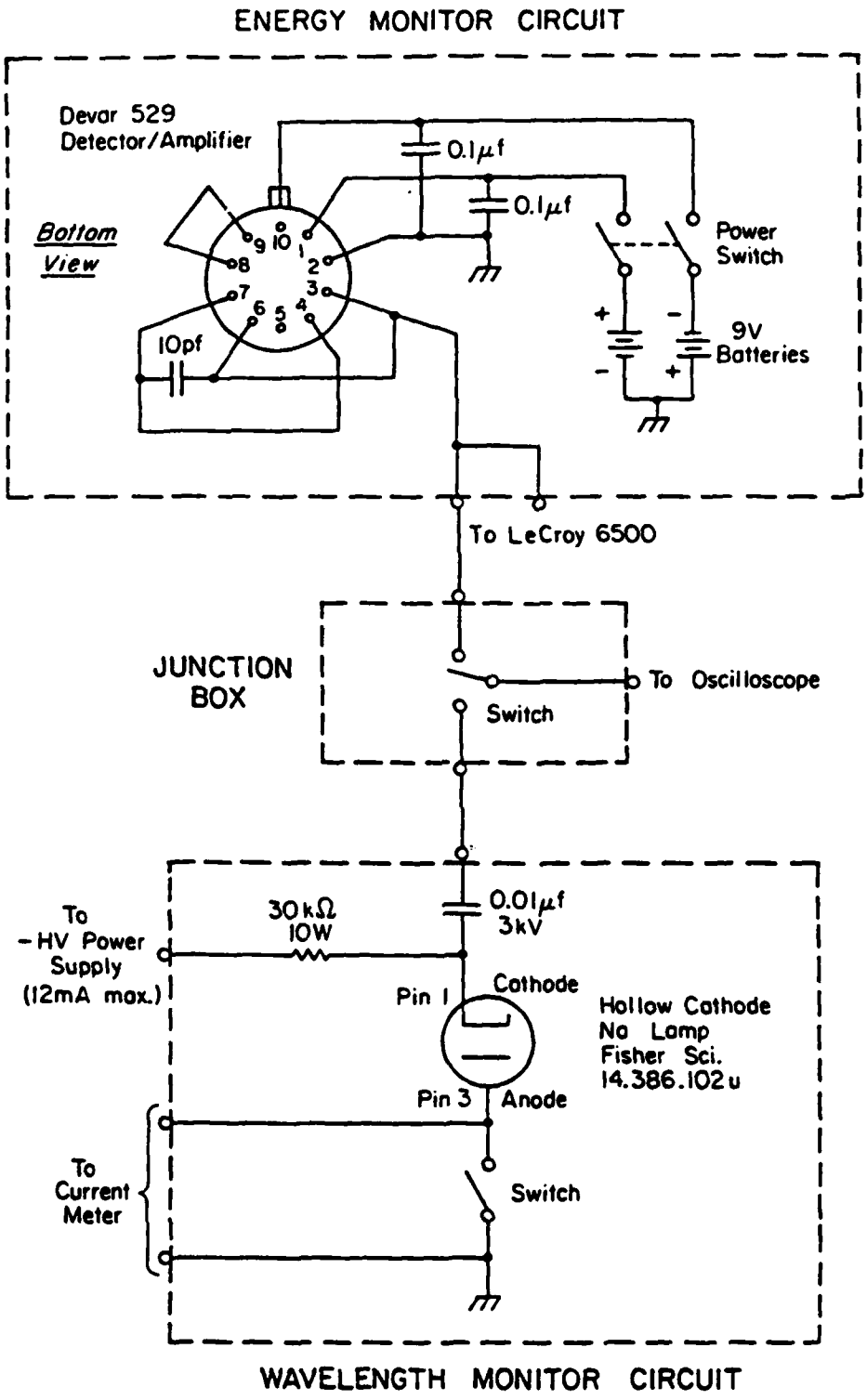

Figure 3 Wiring Diagram of the dye laser energy and wavelength monitors.

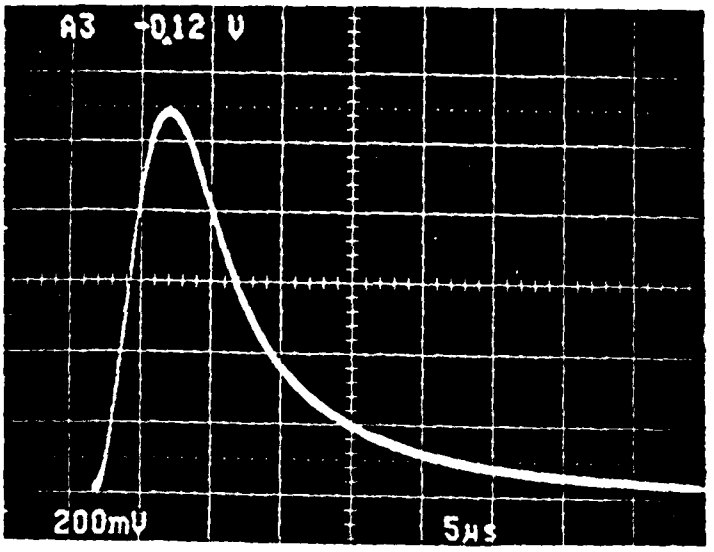

Figure 4 Typical oscilloscope trace of the energy monitor output.

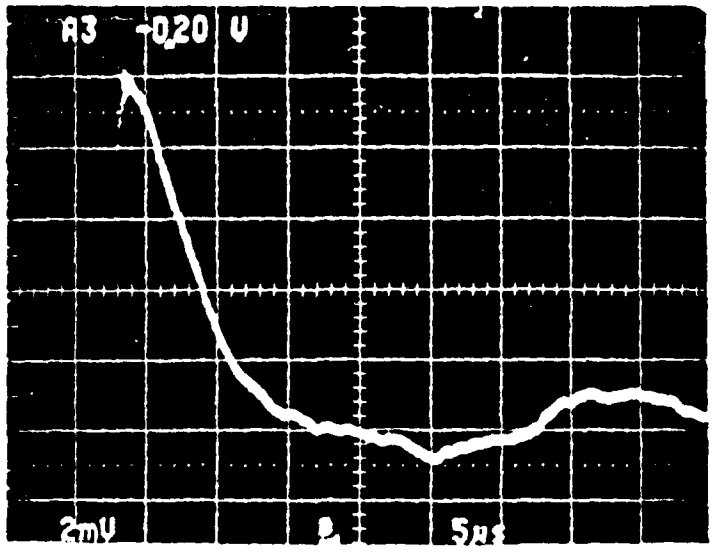

(a)

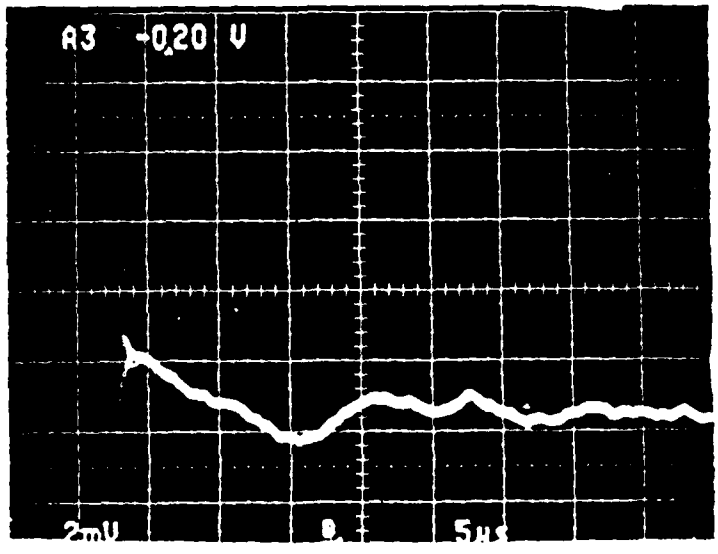

(b)

Figure 5 Typical oscilloscope traces of the hollow cathode Na lamp output. a) Dye laser tuned to the Na D_2 resonance line. b) Dye laser tuned off the Na D_2 resonance line.

V. Laser Alignment and Tuning

The dye laser consists of an oscillator, preamplifier and two power amplifiers. The laser alignment is described in detail in the operating manual. The most critical adjustments for each stage of the laser are the focus and vertical alignment of the pump beam and the alignment of the prism beam expander in the oscillator. To prevent damage to the dye laser, the initial alignment should be done with the pump energy below 100 mj/pulse. Because the vertical position of the pump beam can change if the focus position is changed, it is best to adjust the focus in small increments and then adjust the vertical position for maximum signal at each increment so that the optimum focus can be determined. The horizontal and rotation adjustments of the pump beam are less critical and usually do not require readjustment after the initial alignment. The pump beam should be positioned horizontally in the center of each cuvette so that it does not illuminate the edge seals. This is particularly critical in the power amplifier stages because the high pump energies can damage the seals. Alignment of the laser is greatly facilitated by using the energy monitor. The Na line filter in front of the energy monitor detector rejects much of the ASE so that when the laser is adjusted for maximum response of the energy monitor, the ASE will normally be minimized. After the initial alignment, it should only be necessary to adjust the

1) doubler crystal
2) oscillator prism beam expander
3) oscillator pump beam vertical position
4) preamplifier pump beam vertical position
5) first amplifier pump beam vertical position
6) final amplifier pump beam vertical position

in this order to maximize the laser output.

Alignment and tuning of the etalon and grating are also described in the laser manual. The most critical adjustment of the etalon is establishing the normal position. Once the laser and grating are aligned and tuned to the desired wavelength by the scanning computer, the oscillator output can be maximized by manually stepping the grating. Because the power amplifiers are operating near saturation, stability of the oscillator is more important than its output energy level. When

properly aligned, the total output energy of the laser is virtually the same with or without the etalon. Conversion efficiencies of 15 to 17% are relatively easy to obtain. Figure 6 is a plot of the measured YAG laser output energy at 532 nm and the dye laser output as a function of the flashlamp voltage in the YAG laser amplifier. The YAG oscillator flashlamp voltage was 1650 volts and the dye laser was tuned to 589 nm without the intracavity etalon. For these measurements the conversion efficiency at 1350 volts with the etalon installed was 100% x 21 mj/130 mj = 16.2%.

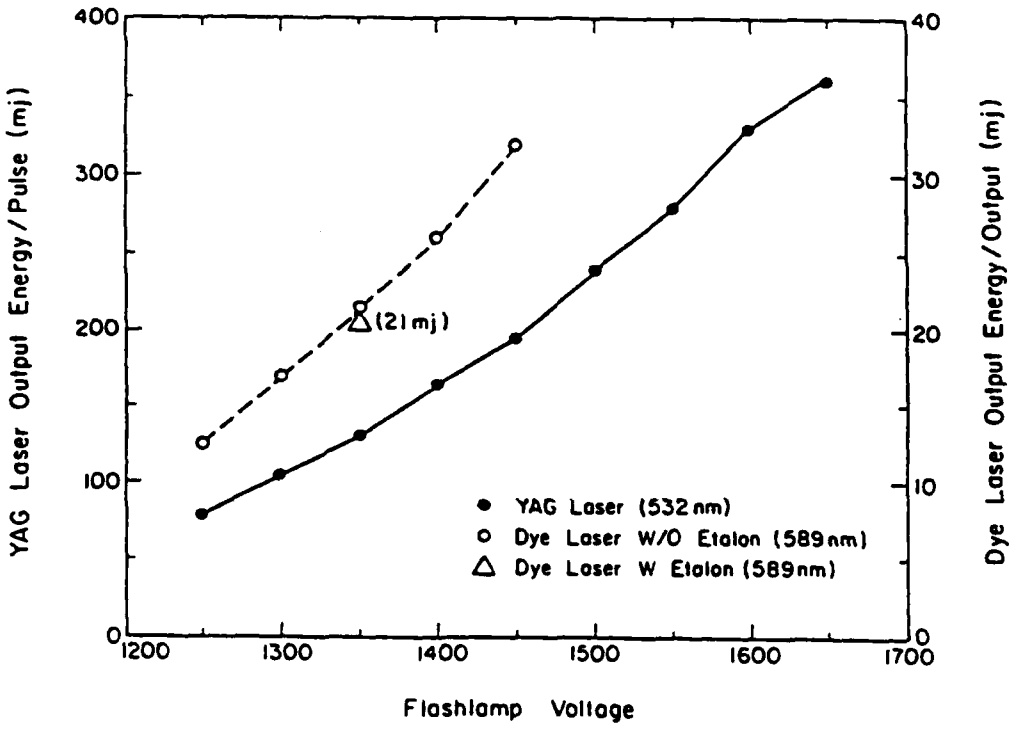

Figure 6 Plot of the YAG laser and dye laser output energies/pulse versus the flashlamp voltage in the YAG amplifier. The flashlamp voltage in the YAG oscillator was 1650 V.

VI. Sodium Lidar Data Processing and Analysis

Successful measurements of the mesospheric Na layer profile were made with the AFGL lidar during the nights of July 22, August 1, August 27 and August 28, 1985. Sodium lidar measurements were also obtained simultaneously at Urbana, IL during the nights of August 27 and 28. Plotted for comparison in Figure 7 are the profiles obtained at AFGL and Urbana, IL at 2:10A EST, August 29. Notice the similarity of the two profiles and in particular the very sharp bottomside of the layer. Gravity wave perturbations are clearly seen in both profiles. The August data from both sites are currently being processed and analyzed to determine gravity wave parameters and to determine if tidal effects are present. The results of these measurements and of additional measurements planned for the Fall and Winter 1985-86 will be summarized in a more extensive report and submitted for publication.

Tidal effects are most apparent in the column abundance variations of the sodium layer. To measure these variations accurately, the lidar data must be normalized and calibrated. The photocount in the k^{th} range bin is approximately

$$N_k = T^2 \frac{\eta A_R J \sigma \rho(z_k) \Delta z}{h\nu z_k^2} + N_B \qquad (1)$$

$$z_k = (k-1/2)\Delta z \qquad (2)$$

where T = one-way atmospheric transmission
η = lidar system efficiency
A_R = telescope aperture area (m^2)
J = total transmitted laser energy (joules)
σ = scattering cross-section (m^{-2})
Δz = range bin width (m)
$h\nu$ = photon energy (joules)
z_k = altitude of scatterers
$\rho(z)$ = density of scatterers (m^{-3})
N_B = background count/range bin

Variations in the laser energy and the atmospheric transmission can be compensated by normalizing the sodium photocounts by the Rayleigh photo-

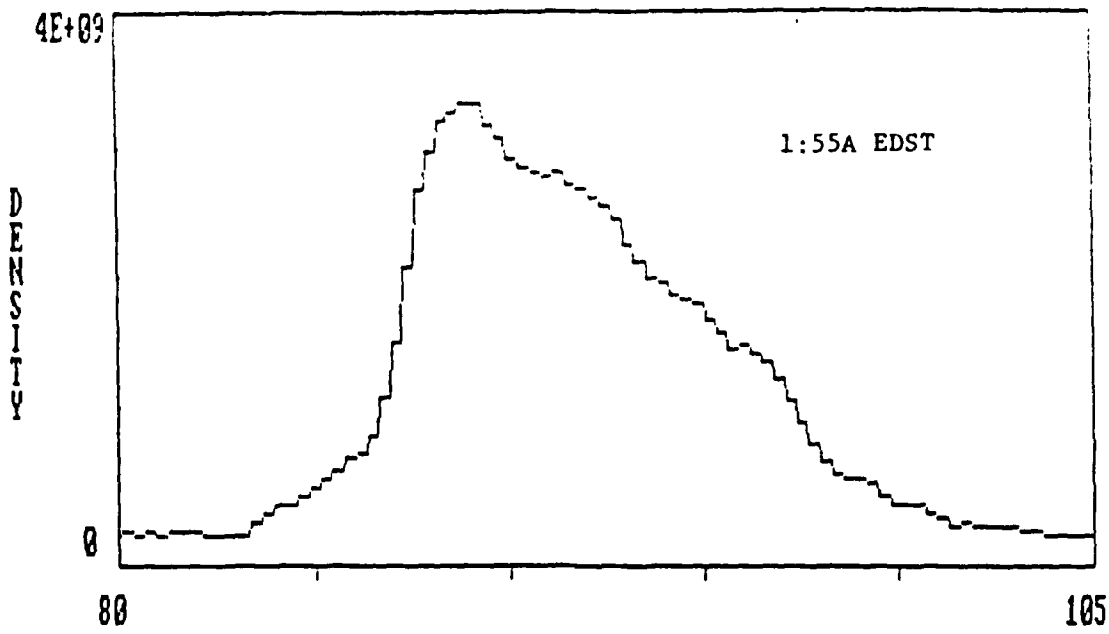

FILE: N5082926.ASC
TIME: 01:55:00
SNR: 3.535755
SHOTS: 2400

NA COL COUNT: 2.746665E+13
NA COUNTS/SHOT: 9.853318
BACKGROUND COUNT/BIN: 133.7647
CUTOFF WAVELENGTH: .6

a)

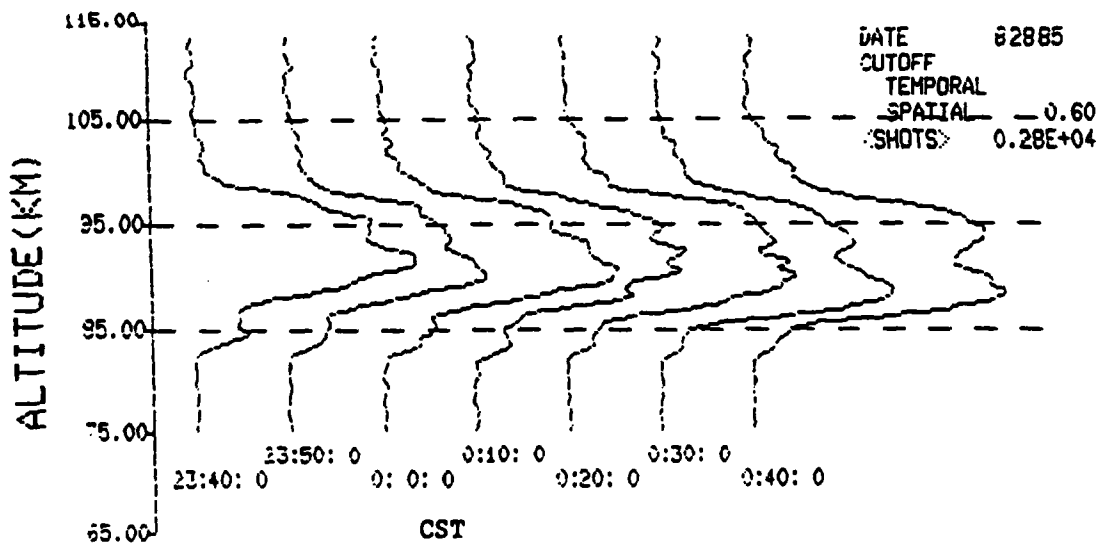

b)

Figure 7 Examples of the Na layer profiles measured on August 28-29, 1985 at the a) Air Force Geophysics Laboratory and b) University of Illinois. Note CST = EDST-2 hours.

count at an altitude free of aerosols. The Rayleigh photocount at 30 km altitude is typically used. Normalization and calibration is completed by first subtracting the expected background count from each range bin. The background count is estimated by averaging the photocount in the 65 to 75 and 105 to 115 km range bins. After subtracting the background count, the z^{-2} signal dependence is removed by multiplying the data by the square of the range bin height.

To minimize noise, the Rayleigh photocount at 30 km is estimated by averaging the range corrected data between 27 and 33 km. Because the atmospheric density decreases approximately exponentially with altitude, averaging is done by fitting an exponential curve to the data from 27-33 km. The sodium photocounts are then divided by the averaged Rayleigh photocount at 30 km altitude. The result is given by

$$\frac{z_k^{\,2}\,(N_k - N_B)}{(30\text{km})^2 (N_{30\text{km}} - N_B)} = \frac{\sigma_{Na}\ \rho_{Na}(z_k)}{\sigma_{Ray}\ \rho_{Ray}(30\text{km})} \tag{3}$$

where

N_{30km} = estimated Rayleigh photocount at 30 km

N_B = estimated background count/range bin.

The sodium density is therefore given by

$$\rho_{Na}(z_k) = \frac{\sigma_{Ray}\ \rho_{Ray}(30\text{km})}{\sigma_{Na}} \frac{z_k^{\,2}\,(N_k - N_B)}{(30\text{km})^2\,(N_{30\text{km}} - N_B)} \tag{4}$$

Near 30 km the product of the Rayleigh cross-section and atmospheric density is

$$\sigma_{Ray}\ \rho_{Ray} = 3.6 \times 10^{-31} \frac{P}{T\lambda^{4.0117}} \tag{5}$$

where

λ = wavelength (m)

T = temperature (K)

P = pressure (mb).

At 30 km altitude the 1976 U.S. Standard Atmosphere lists P = 11.718 mb

and T = 226.65 K. The Na cross-section depends on the laser lineshape and linewidth. Without the etalon the dye laser linewidth is 7 pm and $\sigma_{Na} \simeq 2.75 \times 10^{-16}$ m^{-2}. With the etalon, the dye laser linewidth is 1.4 pm and $\sigma_{Na} \simeq 6.7 \times 10^{-16}$ m^{-2}. These values were used to calibrate the AFGL Na lidar data.

VII. Recommendations

The AFGL Na lidar system can now obtain high quality measurements of the Na layer profile simultaneously with the UI Na lidar system and with the AFGL Rayleigh scatter lidar system. With this unique measurement capability, the propagation of gravity waves and tides from the stratosphere up through the mesosphere can be observed with excellent spatial and temporal resolution. In addition, gravity wave and tidal effects on the horizontal structure of the layer can be monitored. The measurements made this summer have demonstrated the technical feasibility of these experiments more extensive measurements are now required for a detailed scientific analysis of gravity wave and tidal effects. Therefore, it is recommended that additional simultaneous measurements be made at AFGL and UI during the Fall and Winter 1985-86. This will permit a more detailed study of similarities and differences in sodium layer dynamics at the two sites and will yield information on seasonal variations.

VIII. References

1. Geller, M. A., "Dynamics of the middle atmosphere," Space Sci. Rev., 34, 359-375, 1983.
2. Fritts, D. C., M. A. Geller, B. B. Balsley, M. L. Chanin, I. Hirota, J. H. Holton, S. Kato, R. S. Lindzen, M. R. Schoeberl, R. A. Vincent, and R. F. Woodman, "Research status and recommendations from the Alaska Workshop on gravity waves and turbulence in the middle atmosphere," Fairbanks, Alaska, 18-22 July 1983, Bull. Am. Meteorol. Soc., 65, 149-159, 1984.
3. Rowlett, J. R., C. S. Gardner, E. S. Richter, and C. F. Sechrist, Jr., "Lidar observations of wavelike structure in the atmospheric sodium layer," Geophys. Res. Lett., 5, 683-686, 1978.
4. Clemesha, B. R., V. W. J. H. Kirchhoff, D. M. Simonich, H. Takahashi, and P. P. Batista, "Spaced lidar and nightglow observations of an atmospheric sodium enhancement," J. Geophys. Res., 85, 3480-3484, 1980.
5. Juramy, P., M. L. Chanin, G. Megic, G. F. Toulinov, and Y. P. Doudoladov, "Lidar sounding of the mesospheric sodium layer at high latitudes," J. Atmos. Terr. Phys., 43, 209-215, 1981.
6. Chanin, M. L., and A. Hauchecorne, "Lidar observation of gravity and tidal waves in the stratosphere and mesosphere," J. Geophys. Res., 86, 9715-9721, 1981.
7. Gadsden, M., "Metallic atoms and ions in the upper atmosphere," Ann. Geophys., 26, 141-149, 1970.
8. Richter, E. S. and C. F. Sechrist, Jr., "A cluster ion chemistry for the mesospheric sodium layer," J. Atmos. Terr. Phys., 41, 579-586, 1979.
9. Blamont, J. E. and T. M. Donahue, "The dayglow of the sodium D lines," J. Geophys. Res., 66, 1407-1423, 1961.
10. Gadsden, M. and C. M. Purdy, "Observations of the sodium dayglow," Ann. Geophys., 26, 43-51, 1970.
11. Hunten, D. M. and L. Wallace, "Rocket measurements of the sodium dayglow," J. Geophys. Res., 72, 69-79, 1967.
12. Bowman, M. R., A. J. Gibson and M. C. W. Sandford, "Atmospheric sodium measured by a tuned laser radar," Nature, 221, 456-457, 1969.

13. Blamont, J. E., M. L. Chanin and G. Megie, "Vertical distribution and temperature profile of the night time atmospheric sodium layer obtained by laser backscatter," Ann. Geophys., 28, 833-838, 1972.
14. Batista, P. P., B. R. Clemesha, D. M. Simonich and V. W. J. H. Kirchhoff, "Tidal oscillations in the atmospheric sodium layer," J. Geophys. Res., 90, 3881-3888, April 20, 1985.
15. Hake, R. D., Jr., D. E. Arnold, D. W. Jackson, W. E. Evans, B. P. Ficklin and R. A. Long, "Dye-laser observations of the nighttime atomic sodium layer," J. Geophys. Res., 77, 6839-6848, 1972.
16. Gardner, C. S., J. D. Shelton, "Density response of neutral atmospheric layers to gravity wave perturbations," J. Geophys. Res., 90, 1745-1754, Feb. 1, 1985.
17. Shelton, J. D., C. S. Gardner and C. F. Sechrist, Jr., "Density response of the mesospheric sodium layer to gravity wave perturbations," Geophys. Res. Let., 7, 1069-1071, Dec. 1980.
18. Gardner, C. S. and J. D. Shelton, "Spatial and temporal filtering technique for processing lidar photocount data," Optics Letters, 6, 174-176, April 1981.
19. Gardner, C. S. and D. Voelz, "Lidar measurements of gravity wave saturation effects in the mesospheric sodium layer," to be published in Geophys. Res. Letts., 1985.
20. Elterman, L., "Seasonal trends of temperature, density, and pressure to 67.6 km obtained with searchlight probing technique," J. Geophys. Res., 59, 351-358, September 1954.

1985 USAF-UES SUMMER FACULTY RESEARCH PROGRAM

Sponsored by the

AIR FORCE OFFICE OF SCIENTIFIC RESEARCH

Conducted by the

UNIVERSAL ENERGY SYSTEMS, INC.

FINAL REPORT

AFWL HISTORY

Prepared by:	**Doris O. Ginn**
Academic Rank:	**Associate Professor**
Department and University:	**English and Modern Foreign Languages, Jackson State University**
Research Location:	**Air Force Weapons Laboratory/History Office Kirtland AFB, New Mexico 87117**
USAF Research:	**Dr. Robert W. Duffner**
Date:	**26 July 1985**
Contract Number:	**F49620-85-C-0013**

AFWL HISTORY

by

Doris O. Ginn

Abstract

The AFWL History is an annual project of the chief historian of the Air Force Weapons Laboratory (AFWL). My research pursuit was associated with that effort. The task assignments included a review of the secondary source material surrounding lasers, particle beams, nuclear weapon effects, and advanced weapons. Additionally, there was an open literature search of Air Force documents, New York Times Index, Los Angeles Times Index, and the Washington Post Index. Interviews of key program managers were conducted to gather data on select topics pertaining to the mission of AFWL for the historical narratives.

ACKNOWLEDGEMENTS

The researcher acknowledges with sincere appreciation the Air Force Systems Command, the Air Force Office of Scientific Research, and Universal Energy Systems, Incorporated for the sponsorship of this research effort.

This unique opportunity to experience a new horizon in research can be accredited with special acknowledgements to Kirtland Air Force Weapons Laboratory Chief Scientist, Dr. Arthur H. Guenther. My summer experience was enhanced by the hospitality of his office personnel and by the AFWL/UES Effort Focal Point, Craig Hammond.

Notable praise goes to the Weapons Laboratory Technical Library staff who made an enormous contribution to the success of this research. Without the attentive assistance of Ms. Donna Cromer and Ms. Janet Jourdain, the thoroughness and timeliness of my research tasks would have been impossible. I extol their proficiency and graciously acknowledge their effortless cooperation.

My special gratitude is extended to the Air Force Weapons Laboratory History Office Chief, Dr. Robert W. Duffner, for suggesting areas of research and for the stimulating discussions during our research collaboration. Many thanks to the competent and enthusiastic assistance of Sandra Contreras and Cheryl Brocksmith and, most cordially, to Mrs. Ida H. Houseknecht, Editorial Assistant, for her

diligent, impeccable skill in editing and typing research drafts and this final report.

I. INTRODUCTION

As an educator experienced in scientific research, trained in English and linguistics, and experienced in both areas as a writer and communicator, I found the nature of the U.S. Air Force research a complement to these assets.

My experience as a research associate at AFWL afforded opportunities to communicate with a variety of key personnel in informal situations regarding the administrative structure, function, and mission of the Weapons Laboratory and its relationship to Kirtland Air Force Base as a tenant organization. In formal interviews and teleconferences, my past experience as a communicator aided in securing the precise information needed.

The tasks of writing narratives, manuscripts, and reports could have been a fiasco had I not had intensive training as a linguist in the structure of the English language. The writing of historical documents required special skills exercising coherence, clarity, conciseness, and unity; the diversity of my experience in these writing conventions enhanced my ability to transfer these skills to the special writing structures and stylistics of the Air Force Weapons Laboratory History Office.

II. OBJECTIVES OF THE RESEARCH EFFORT

The goals established and accomplished were to research historical information pertinent to the mission of AFWL and to write historical narratives on selected AFWL programs assigned by the AFWL historian. Four specific objectives reinforced the manifestation of these goals:

1. Search the print media of all forms of mass communication for pertinent materials pertaining to the mission of the Weapons Laboratory.

2. Organize the collection of data from the print media into relevant sequences and categories of information.

3. Conduct interviews with chief AFWL program managers.

4. Prepare historical narrative on selected AFWL topics.

The unique experience in the Air Force Weapons Laboratory History Office was multifaceted in approaches. To ascertain the data for the history, the researcher used the most appropriate technique for the most comprehensive retrieval of information.

III. APPROACH I

In order to accomplish the general goals and the specific objectives set forth for this research, the researcher began with an indepth search of the literature using manual searches of journal indices: Aviation Week

and Space Technology, Applied Science and Technology, and Air University Review. These searches ranged from 1968 to 1984, with only approximately one-half of the indices appearing on microfilm.

IV. RESULTS OF THIS APPROACH

Information gathered from the indices of these periodicals provided a preliminary data base covering research and development activities during the span of 16 years (1968-1984) relevant to lasers, particle beams, nuclear weapon effects, advanced weapons, etc. Articles of special significance were photocopied and cataloged for quick reference in the History Office. The journals were considered key sources for their technological interest and highly respected for technology coverage and quality of reporting.

V. APPROACH II

This approach utilized a cross-referenced index approach on general information from 1968 to 1984 regarding technological advancement as it appeared in leading national newspapers. An indepth dialog and manual search was conducted of the New York Times, the Los Angeles Times, and the Washington Post. In addition to that search, a close search of the Congressional records covering the same timeframe was completed.

VI. RESULTS OF THIS APPROACH

The data retrieved was not as prolific as the journal findings, but the limited references were collated and cataloged alongside other documents of the print media.

VII. APPROACH III

The interview technique proved most beneficial for the retrieval of information regarding individuals and their accomplishments at AFWL. Each interview was taped, later transcribed, then drafted into a narrative. Interviews that were not completed in person were conducted via teleconference. The content of all interviews/teleconferences became an integral part of the historical documentation.

VIII. RESULTS OF THIS APPROACH

This technique of face-to-face communication and the recording of the same was invaluable for accuracy and completeness.

IX. RECOMMENDATIONS

This summer's effort represented a segment of a continuing effort to complete the annual history of the Air Force Weapons Laboratory History Office. The researcher would recommend:

1. Individuals expected to do SECRET documents be cleared prior to the first day of service.

2. The research effort of conducting interviews and literature searches be continued to develop a more comprehensive data base.

3. A system be organized to ensure a more timely and accurate retrieval of information.

END

DTIC

5-86